Handbook of
Food
Engineering
Practice

edited by

Kenneth J. Valentas
Enrique Rotstein
R. Paul Singh

CRC

CRC Press
Boca Raton   New York

The Editors

Enrique Rotstein, Ph.D., is Vice President of Process Technology of the Pillsbury Company, Minneapolis, Minnesota. He is responsible for corporate process development, serving all the different product lines of his company.

Dr. Rotstein received his bachelor's degree in Chemical Engineering from Universidad del Sur, Bahia Blanca, Argentina. He obtained his Ph.D. from Imperial College, University of London, London, U.K. He served successively as Assistant, Associate, and Full Professor of Chemical Engineering at Universidad del Sur. In this capacity he founded and directed PLAPIQUI, Planta Piloto de Ingenieria Quimica, one of the leading Chemical Engineering teaching and research institutes in Latin America. During his academic career he also taught at the University of Minnesota and at Imperial College, holding visiting professorships. He worked for DuPont, Argentina, and for Monsanto Chemical Co., Plastics Division. In 1987 he joined The Pillsbury Company as Director of Process Analysis and Director of Process Engineering. He assumed his present position in 1995.

Dr. Rotstein has been a member of the board of the Argentina National Science Council, a member of the executive editorial committee of the *Latin American Journal of Chemical Engineering and Applied Chemistry*, a member of the internal advisory board of Drying Technology, and a member of the editorial advisory boards of *Advances in Drying, Physico Chemical Hydrodynamics Journal*, and *Journal of Food Process Engineering*. Since 1991 he has been a member of the Food Engineering Advisory Council, University of California, Davis. He received the Jorge Magnin Prize from the Argentina National Science Council, was Hill Visiting Professor at the University of Minnesota Chemical Engineering and Materials Science Department, was keynote lecturer at a number of international technical conferences, and received the Excellence in Drying Award at the 1992 International Drying Symposium.

Dr. Rotstein is the author of nearly 100 papers and has authored or co-authored several books.

R. Paul Singh, Ph.D., is a Professor of Food Engineering, Department of Biological and Agricultural Engineering, Department of Food Science and Technology, University of California, Davis.

Dr. Singh graduated in 1970 from Punjab Agricultural University, Ludhiana, India, with a degree in Agricultural Engineering. He obtained an M.S. degree from the University of Wisconsin, Madison, and a Ph.D. degree from Michigan State University in 1974. Following a year of teaching at Michigan State University, he moved to the University of California, Davis, in 1975 as an Assistant Professor of Food Engineering. He was promoted to Associate Professor in 1979 and, again, to Professor in 1983.

Dr. Singh is a member of the Institute of Food Technologists, American Society of Agricultural Engineers, and Sigma Xi. He received the Samuel Cate Prescott Award for Research, Institute of Food Technologies, in 1982, and the A. W. Farrall Young Educator Award, American Society of Agricultural Engineers in 1986. He was a NATO Senior Guest Lecturer in Portugal in 1987 and 1993, and received the IFT International Award, Institute of Food Technologists, 1988, and the Distinguished Alumnus Award from Punjab Agricultural University in 1989, and the DFISA/FPEI Food Engineering Award in 1997.

Dr. Singh has authored and co-authored nine books and over 160 technical papers. He is a co-editor of the *Journal of Food Process Engineering.* His current research interests are in studying transport phenomena in foods as influenced by structural changes during processing.

Kenneth J. Valentas, Ph.D., is Director of the Bioprocess Technology Institute and Adjunct Professor of Chemical Engineering at the University of Minnesota. He received his B.S. in Chemical Engineering from the University of Illinois and his Ph.D. in Chemical Engineering from the University of Minnesota.

Dr. Valentas' career in the Food Processing Industry spans 24 years, with experience in Research and Development at General Mills and Pillsbury and as Vice President of Engineering at Pillsbury-Grand Met. He holds seven patents, is the author of several articles, and is co-author of *Food Processing Operations and Scale-Up.*

Dr. Valentas received the "Food, Pharmaceutical, and Bioengineering Division Award" from AIChE in 1990 for outstanding contributions to research and development in the food processing industry and exemplary leadership in the application of chemical engineering principles to food processing.

His current research interests include the application of biorefining principles to food processing wastes and production of amino acids via fermentation from thermal tolerant methlyotrophs.

Contributors

Ed Boehmer
StarchTech, Inc.
Golden Valley, Minnesota

David Bresnahan
Kraft Foods, Inc.
Tarrytown, New York

Chin Shu Chen
Citrus Research and Education Center
University of Florida
Lake Alfred, Florida

Julius Chu
The Pillsbury Company
Minneapolis, Minnesota

J. Peter Clark
Fluor Daniel, Inc.
Chicago, Illinois

Donald J. Cleland
Centre for Postharvest
  and Refrigeration Research
Massey University
Palmerston North, New Zealand

Guillermo H. Crapiste
PLAPIQUI
Universidad Nacional del Sur–CONICET
Bahia Blanca, Argentina

Brian E. Farkas
Department of Food Science
North Carolina State University
Raleigh, North Carolina

Daniel F. Farkas
Department of Food Science
  and Technology
Oregon State University
Corvallis, Oregon

Ernesto Hernandez
Food Protein Research
  and Development Center
Texas A & M University
College Station, Texas

Ruben J. Hernandez
School of Packaging
Michigan State University
East Lansing, Michigan

Theodore P. Labuza
Department of Food Science and Nutrition
University of Minnesota
St. Paul, Minnesota

Leon Levine
Leon Levine & Associates, Inc.
Plymouth, Minnesota

Jorge E. Lozano
PLAPIQUI
Universidad Nacional del Sur–CONICET
Bahia Blanca, Argentina

Jatal D. Mannapperuma
California Institute of Food and
  Agricultural Research
Department of Food Science and Technology
University of California, Davis
Davis, California

Martha Muehlenkamp
Department of Food Science and Nutrition
University of Minnesota
St. Paul, Minnesota

Hosahilli S. Ramaswamy
Department of Food Science
  and Agricultural Chemistry
MacDonald Campus of McGill University
Ste. Anne de Bellevue, Quebec
Canada

Enrique Rotstein
The Pillsbury Company
Minneapolis, Minnesota

I. Sam Saguy
Department of Biochemistry, Food Science,
  and Nutrition
Faculty of Agriculture
The Hebrew University of Jerusalem
Rehovot, Israel

Dale A. Seiberling
Seiberling Associates, Inc.
Roscoe, Illinois

R. Paul Singh
Department of Biological
  and Agricultural Engineering and
Department of Food Science and Technology
University of California, Davis
Davis, California

James F. Steffe
Department of Agricultural Engineering
  and Department of Food Science
  and Human Nutrition
Michigan State University
East Lansing, Michigan

Petros S. Taoukis
Department of Chemical Engineering
Laboratory of Food Chemistry
  and Technology
National Technical University of Athens
Athens, Greece

Martin J. Urbicain
PLAPIQUI
Universidad Nacional del Sur–CONICET
Bahia Blanca, Argentina

Kenneth J. Valentas
University of Minnesota
St. Paul, Minnesota

Joseph J. Warthesen
Department of Food Science
  and Nutrition
University of Minnesota
St. Paul, Minnesota

John Henry Wells
Department of Biological
  and Agricultural Engineering
Louisiana State University Agricultural
  Center
Baton Rouge, Louisiana

Preface

The food engineering discipline has been gaining increasing recognition in the food industry over the last three decades. Although food engineers formally graduated as such are relatively few, food engineering practitioners are an essential part of the food industry's workforce. The significant contribution of food engineers to the industry is documented in the constant stream of new food products and their manufacturing processes, the capital projects to implement these processes, and the growing number of patents and publications that span this emerging profession.

While a number of important food engineering books have been published over the years, the *Handbook of Food Engineering Practice* will stand alone for its emphasis on practical professional application. This handbook is written for the food engineer and food manufacturer. The very fact that this is a book for industrial application will make it a useful source for academic teaching and research.

A major segment of this handbook is devoted to some of the most common unit operations employed in the food industry. Each chapter is intended to provide terse, to-the-point descriptions of fundamentals, applications, example calculations, and, when appropriate, a review of economics.

- The introductory chapter addresses one of the key needs in any food industry namely the design of pumping systems. This chapter provides mathematical procedures appropriate to liquid foods with Newtonian and non-Newtonian flow characteristics. Following the ubiquitous topic of pumping, several food preservation operations are considered. The ability to mathematically determine a food sterilization process has been the foundation of the food canning industry. During the last two decades, several new approaches have appeared in the literature that provide improved calculation procedures for determining food sterilization processes.
- Chapter 2 provides an in-depth description of several recently developed methods with solved examples.
- Chapter 3 is a comprehensive treatment of food freezing operations. This chapter examines the phase change problem with appropriate mathematical procedures that have proven to be most successful in predicting freezing times in food. The drying process has been used for millennia to preserve foods, yet a quantitative description of the drying process remains a challenging exercise.
- Chapter 4 presents a detailed background on fundamentals that provide insight into some of the mechanisms involved in typical drying processes. Simplified mathematical approaches to designing food dryers are discussed. In the food industry, concentration of foods is most commonly carried out either with membranes or evaporator systems. During the last two decades, numerous developments have taken place in designing new types of membranes.
- Chapter 5 provides an overview of the most recent advances and key information useful in designing membrane systems for separation and concentration purposes.
- The design of evaporator systems is the subject of Chapter 6. The procedures given in this chapter are also useful in analyzing the performance of existing evaporators.
- One of the most common computations necessary in designing any evaporator is calculating the material and energy balance. Several illustrative approaches on how to conduct material and energy balances in food processing systems are presented in Chapter 7.

- After processing, foods must be packaged to minimize any deleterious changes in quality. A thorough understanding of the barrier properties of food packaging materials is essential for the proper selection and use of these materials in the design of packaging systems. A comprehensive review of commonly available packaging materials and their important properties is presented in Chapter 8.
- Packaged foods may remain for considerable time in transport and in wholesale and retail storage. Accelerated storage studies can be a useful tool in predicting the shelf life of a given food; procedures to design such studies are presented in Chapter 9.
- Among various environmental factors, temperature plays a major role in influencing the shelf life of foods. The temperature tolerance of foods during distribution must be known to minimize changes in quality deterioration. To address this issue, approaches to determine temperature effects on the shelf life of foods are given in Chapter 10.
- In designing and evaluating food processing operations, a food engineer relies on the knowledge of physical and rheological properties of foods. The published literature contains numerous studies that provide experimental data on food properties. In Chapter 11, a comprehensive resource is provided on predictive methods to estimate physical and rheological properties.
- The importance of physical and rheological properties in designing a food system is further illustrated in Chapter 12 for a dough processing system. Dough rheology is a complex subject; an engineer must rely on experimental, predictive, and mathematical approaches to design processing systems for manufacturing dough, as delineated in this chapter.

The last five chapters in this handbook provide supportive material that is applicable to any of the unit operations presented in the preceding chapters.

- For example, estimation of cost and profitability one of the key calculations that must be carried out in designing new processing systems. Chapter 13 provides useful methods for conducting cost/profit analyses along with illustrative examples.
- As computers have become more common in the workplace, use of simulations and optimization procedures are gaining considerable attention in the food industry. Procedures useful in simulation and optimization are presented in Chapter 14.
- In food processing, it is imperative that any design of a system adheres to a variety of sanitary guidelines. Chapter 15 includes a broad description of issues that must be considered to satisfy these important guidelines.
- The use of process controllers in food processing is becoming more prevalent as improved sensors appear in the market. Approaches to the design and implementation of process controllers in food processing applications are discussed in Chapter 16.
- Food engineers must rely on a number of basic sciences in dealing with problems at hand. An in-depth knowledge of food chemistry is generally regarded as one of the most critical. In Chapter 17, an overview of food chemistry with specific reference to the needs of engineers is provided.

It should be evident that this handbook assimilates many of the key food processing operations. Topics not covered in the current edition, such as food extrusion, microwave processing, and other emerging technologies, are left for future consideration. While we realize that this book covers new ground, we hope to hear from our readers, to benefit from their experience in future editions.

Enrique Rotstein
R. Paul Singh
Kenneth Valentas

Table of Contents

1 Pipeline Design Calculations for Newtonian and Non-Newtonian Fluids

James F. Steffe and R. Paul Singh

CONTENTS

1.1   INTRODUCTION

The purpose of this chapter is to provide the practical information necessary to predict pressure drop for non-time-dependent, homogeneous, non-Newtonian fluids in tube flow. The intended application of this material is pipeline design and pump selection. More information regarding pipe flow of time-dependent, viscoelastic, or multi-phase materials may be found in Grovier and Aziz (1972), and Brown and Heywood (1991). A complete discussion of pipeline design information for Newtonian fluids is available in Sakiadis (1984). Methods for evaluating the rheological properties of fluid foods are given in Steffe (1992) and typical values are provided in Tables 1.1, 1.2, and 1.3. Consult Rao and Steffe (1992) for additional information on advanced rheological techniques.

1.2   MECHANICAL ENERGY BALANCE

A rigorous derivation of the mechanical energy balance is lengthy and beyond the scope of this work but may be found in Bird et al. (1960). The equation is a very practical form of the conservation of energy equation (it can also be derived from the principle of conservation of momentum (Denn, 1980)) commonly called the "engineering Bernouli equation" (Denn, 1980; Brodkey and Hershey, 1988). Numerous assumptions are made in developing the equation: constant fluid density; the absence of thermal energy effects; single phase, uniform material properties; uniform equivalent pressure (ρ g h term over the cross-section of the pipe is negligible).

The mechanical energy balance for an incompressible fluid in a pipe may be written as

$$\left(\frac{\left(\overline{u}_2\right)^2}{\alpha_2} - \frac{\left(\overline{u}_1\right)^2}{\alpha_1} \right) + g\left(z_2 - z_1\right) + \frac{P_2 - P_1}{\rho} + \Sigma F + W = 0 \tag{1.1}$$

where ΣF, the summation of all friction losses is

$$\Sigma F = \Sigma \frac{2f\left(\overline{u}_1\right)^2 L}{D} + \Sigma \frac{k_f\left(\overline{u}\right)^2}{2} \tag{1.2}$$

and subscripts 1 and 2 refer to two specific locations in the system. The friction losses include those from pipes of different diameters and a contribution from each individual valve, fitting, etc. Pressure losses in other types of in-line equipment, such as strainers, should also be included in ΣF.

1.2.1   Fanning Friction Factor

In this section, friction factors for time-independent fluids in laminar and turbulent flow are discussed and criteria for determining the flow regime, laminar or turbulent, are presented. It is important to note that it is impossible to accurately predict transition from laminar to turbulent flow in actual processing systems and the equations given are guidelines to be used in conjunction with good judgment. Friction factor equations are only presented for smooth pipes, the rule for sanitary piping systems. Also, the discussion related to the turbulent flow of high yield stress materials has been limited for a number of reasons: (a) Friction factor equations and turbulence criteria have limited experimental verification for these materials; (b) It is very difficult (and economically impractical) to get fluids with a significant yield stress to flow under turbulent conditions; and (c) Rheological data for foods that have a high yield stress are very limited. Yield stress measurement in food materials remains a difficult task for rheologists and the problem is often complicated by the presence of time-dependent behavior (Steffe, 1992).

TABLE 1.1
Rheological Properties of Dairy, Fish, and Meat Products

Product	T (°C)	n (–)	K (Pa·s^n)	σ_o (Pa)	$\dot{\gamma}$ (s^{-1})
Cream, 10% fat	40	1.0	.00148	—	—
	60	1.0	.00107	—	—
	80	1.0	.00083	—	—
Cream, 20% fat	40	1.0	.00238	—	—
	60	1.0	.00171	—	—
	80	1.0	.00129	—	—
Cream, 30% fat	40	1.0	.00395	—	—
	60	1.0	.00289	—	—
	80	1.0	.00220	—	—
Cream, 40% fat	40	1.0	.00690	—	—
	60	1.0	.00510	—	—
	80	1.0	.00395	—	—
Minced fish paste	3–6	.91	8.55	1600.0	67–238
Raw, meat batters					
15[a] 13[b] 68.8[c]	15	.156	639.3	1.53	300–500
18.7 12.9 65.9	15	.104	858.0	.28	300–500
22.5 12.1 63.2	15	.209	429.5	0	300–500
30.0 10.4 57.5	15	.341	160.2	27.8	300–500
33.8 9.5 54.5	15	.390	103.3	17.9	300–500
45.0 6.9 45.9	15	.723	14.0	2.3	300–500
45.0 6.9 45.9	15	.685	17.9	27.6	300–500
67.3 28.9 1.8	15	.205	306.8	0	300–500
Milk, homogenized	20	1.0	.002000	—	—
	30	1.0	.001500	—	—
	40	1.0	.001100	—	—
	50	1.0	.000950	—	—
	60	1.0	.000775	—	—
	70	1.0	.00070	—	—
	80	1.0	.00060	—	—
Milk, raw	0	1.0	.00344	—	—
	5	1.0	.00305	—	—
	10	1.0	.00264	—	—
	20	1.0	.00199	—	—
	25	1.0	.00170	—	—
	30	1.0	.00149	—	—
	35	1.0	.00134	—	—
	40	1.0	.00123	—	—

[a] % Fat

[b] % Protein

[c] % Moisture Content

The Fanning friction factor (f) is proportional to the ratio of the wall shear stress in a pipe to the kinetic energy per unit volume:

$$f = \frac{2\sigma_w}{\left(\rho \bar{u}^2\right)} \tag{1.3}$$

TABLE 1.2
Rheological Properties of Oils and Miscellaneous Products

Product	% Total solids	T (°C)	n (–)	K (Pa·s^n)	σ_o (Pa)	$\dot{\gamma}$ (s^{-1})
Chocolate, melted		46.1	.574	.57	1.16	
Honey						
Buckwheat	18.6	24.8	1.0	3.86		
Golden Rod	19.4	24.3	1.0	2.93		
Sage	18.6	25.9	1.0	8.88		
Sweet Clover	17.0	24.7	1.0	7.20		
White Clover	18.2	25.2	1.0	4.80		
Mayonnaise		25	.55	6.4		30–1300
		25	.60	4.2		40–1100
Mustard		25	.39	18.5		30–1300
		25	.34	27.0		40–1100
Oils						
Castor		10	1.0	2.42		
		30	1.0	.451		
		40	1.0	.231		
		100	1.0	.0169		
Corn		38	1.0	.0317		
		25	1.0	.0565		
Cottonseed		20	1.0	.0704		
		38	1.0	.0306		
Linseed		50	1.0	.0176		
		90	1.0	.0071		
Olive		10	1.0	.1380		
		40	1.0	.0363		
		70	1.0	.0124		
Peanut		25.5	1.0	.0656		
		38.0	1.0	.0251		
		21.1	1.0	.0647		.32–64
		37.8	1.0	.0387		.32–64
		54.4	1.0	.0268		.32–64
Rapeseed		0.0	1.0	2.530		
		20.0	1.0	.163		
		30.0	1.0	.096		
Safflower		38.0	1.0	.0286		
		25.0	1.0	.0522		
Sesame		38.0	1.0	.0324		
Soybean		30.0	1.0	.0406		
		50.0	1.0	.0206		
		90.0	1.0	.0078		
Sunflower		38.0	1.0	.0311		

From Steffe, J. F. 1992. *Rheological Methods in Food Process Engineering*. Freeman Press, East Lansing, MI. With permission.

f can be considered in terms of pressure drop by substituting the definition of the shear stress at the wall:

$$f = \frac{(\delta P)R}{\rho L \bar{u}^2} = \frac{(\delta P)D}{2\rho L \bar{u}^2}$$

(1.4)

TABLE 1.3
Rheological Properties of Fruit and Vegetable Products

Product	Total solids (%)	T (°C)	n (–)	K (Pa·s^n)	$\dot{\gamma}$ (s^{-1})
Apple					
Pulp	—	25.0	.084	65.03	—
Sauce	11.6	27	.28	12.7	160–340
	11.0	30	.30	11.6	5–50
	11.0	82.2	.30	9.0	5–50
	10.5	26	.45	7.32	.78–1260
	9.6	26	.45	5.63	.78–1260
	8.5	26	.44	4.18	.78–1260
Apricots					
Puree	17.7	26.6	.29	5.4	—
	23.4	26.6	.35	11.2	—
	41.4	26.6	.35	54.0	—
	44.3	26.6	.37	56.0	.5–80
	51.4	26.6	.36	108.0	.5–80
	55.2	26.6	.34	152.0	.5–80
	59.3	26.6	.32	300.0	.5–80
Reliable, conc.					
Green	27.0	4.4	.25	170.0	3.3–137
	27.0	25	.22	141.0	3.3–137
Ripe	24.1	4.4	.25	67.0	3.3–137
	24.1	25	.22	54.0	3.3–137
Ripened	25.6	4.4	.24	85.0	3.3–137
	25.6	25	.26	71.0	3.3–137
Overripe	26.0	4.4	.27	90.0	3.3–137
	26.0	25	.30	67.0	3.3–137
Banana					
Puree A	—	23.8	.458	6.5	—
Puree B	—	23.8	.333	10.7	—
Puree (17.7 Brix)	—	22	.283	107.3	28–200
Blueberry, pie filling	—	20	.426	6.08	3.3–530
Carrot, Puree	—	25	.228	24.16	—
Green Bean, Puree	—	25	.246	16.91	—
Guava, Puree (10.3 Brix)	—	23.4	.494	39.98	15–400
Mango, Puree (9.3 Brix)	—	24.2	.334	20.58	15–1000
Orange Juice					
Concentrate					
Hamlin, early	—	25	.585	4.121	0–500
42.5 Brix	—	15	.602	5.973	0–500
	—	0	.676	9.157	0–500
	—	–10	.705	14.255	0–500
Hamlin, late	—	25	.725	1.930	0–500
41.1 Brix	—	15	.560	8.118	0–500
	—	0	.620	1.754	0–500
	—	–10	.708	13.875	0–500
Pineapple, early	—	25	.643	2.613	0–500
40.3 Brix	—	15	.587	5.887	0–500
	—	0	.681	8.938	0–500
	—	–10	.713	12.184	0–500

TABLE 1.3 (continued)
Rheological Properties of Fruit and Vegetable Products

Product	Total solids (%)	T (°C)	n (–)	K (Pa·s^n)	$\dot{\gamma}$ (s^{-1})
Pineapple, late	—	25	.532	8.564	0–500
41.8 Brix	—	15	.538	13.432	0–500
	—	0	.636	18.584	0–500
	—	–10	.629	36.414	0–500
Valencia, early	—	25	.583	5.059	0–500
43.0 Brix	—	15	.609	6.714	0–500
	—	–10	.619	27.16	0–500
Valencia, late	—	25	.538	8.417	0–500
41.9 Brix	—	15	.568	11.802	0–500
	—	0	.644	18.751	0–500
	—	–10	.628	41.412	0–500
Naval					
65.1 Brix	—	–18.5	.71	29.2	—
	—	–14.1	.76	14.6	—
	—	–9.3	.74	10.8	—
	—	–5.0	.72	7.9	—
	—	–0.7	.71	5.9	—
	—	10.1	.73	2.7	—
	—	29.9	.72	1.6	—
	—	29.5	.74	.9	—
Papaya, puree (7.3 Brix)	—	26.0	.528	9.09	20–450
Peach					
Pie Filling	—	20.0	.46	20.22	1–140
Puree	10.9	26.6	.44	.94	—
	17.0	26.6	.55	1.38	—
	21.9	26.6	.55	2.11	—
	26.0	26.6	.40	13.4	80–1000
	29.6	26.6	.40	18.0	80–1000
	37.5	26.6	.38	44.0	—
	40.1	26.6	.35	58.5	2–300
	49.8	26.6	.34	85.5	2–300
	58.4	26.6	.34	440.0	—
	11.7	30.0	.28	7.2	5–50
	11.7	82.2	.27	5.8	5–50
	10.0	27.0	.34	4.5	160–3200
Pear					
Puree	15.2	26.6	.35	4.25	—
	24.3	26.6	.39	5.75	—
	33.4	26.6	.38	38.5	80–1000
	37.6	26.6	.38	49.7	—
	39.5	26.6	.38	64.8	2–300
	47.6	26.6	.33	120.0	.5–1000
	49.3	26.6	.34	170.0	—
	51.3	26.6	.34	205.0	—
	45.8	32.2	.479	35.5	—
	45.8	48.8	.477	26.0	—
	45.8	65.5	.484	20.0	—
	45.8	82.2	.481	16.0	—
	14.0	30.0	.35	5.6	5–50
	14.0	82.2	.35	4.6	5–50

TABLE 1.3 (continued)
Rheological Properties of Fruit and Vegetable Products

Product	Total solids (%)	T (°C)	n (–)	K (Pa·s^n)	$\dot{\gamma}$ (s^{-1})
Plum					
Puree	14.0	30.0	.34	2.2	5–50
	14.0	82.2	.34	2.0	5–50
Squash					
Puree A	—	25	.149	20.65	—
Puree B	—	25	.281	11.42	—
Tomato					
Juice conc.	5.8	32.2	.59	.22	500–800
	5.8	38.8	.54	.27	500–800
	5.8	65.5	.47	.37	500–800
	12.8	32.2	.43	2.0	500–800
	12.8	48.8	.43	2.28	500–800
	12.8	65.5	.34	2.28	500–800
	12.8	82.2	.35	2.12	500–800
	16.0	32.2	.45	3.16	500–800
	16.0	48.8	.45	2.77	500–800
	16.0	65.5	.40	3.18	500–800
	16.0	82.2	.38	3.27	500–800
	25.0	32.2	.41	12.9	500–800
	25.0	48.8	.42	10.5	500–800
	25.0	65.5	.43	8.0	500–800
	25.0	82.2	.43	6.1	500–800
	30.0	32.2	.40	18.7	500–800
	30.0	48.8	.42	15.1	500–800
	30.0	65.5	.43	11.7	500–800
	30.0	82.2	.45	7.9	500–800

Simplification yields the energy loss per unit mass required in the mechanical energy balance:

$$\frac{(\delta P)}{\rho} = \frac{f 2 L \bar{u}^2}{D} \tag{1.5}$$

There are many mathematical models available to describe the behavior of fluid foods (Ofoli et al., 1987); only those most useful in pressure drop calculations have been included in the current work. The simplest model, which adequately describes the behavior of the food should be used; however, oversimplification can cause significant calculation errors (Steffe, 1984).

1.2.1.1 Newtonian Fluids

The volumetric average velocity for a Newtonian fluid ($\sigma = \mu\dot{\gamma}$ in laminar, tube flow is

$$\bar{u} = \frac{Q}{\pi R^2} = \frac{1}{\pi R^2}\left(\frac{\pi(\delta P)R^4}{8 L \mu}\right) = \frac{(\delta P)D^2}{32 L \mu} \tag{1.6}$$

Solving Equation 1.6 for the pressure drop per unit length gives

$$\frac{(\delta P)}{L} = \frac{32\bar{u}\mu}{D^2}$$ (1.7)

Inserting Equation 1.7 into the definition of the Fanning friction factor, Equation 1.4, yields

$$f = \left[\frac{(\delta P)}{L}\right]\left(\frac{D}{2\rho\bar{u}^2}\right) = \left[\frac{32\bar{u}\mu}{D^2}\right]\left(\frac{D}{2\rho\bar{u}^2}\right) = \frac{16}{N_{Re}}$$ (1.8)

which can be used to predict friction factors in the laminar flow regime, $N_{Re} < 2100$ where $N_{Re} = \rho D\,\bar{u}/\mu$. In turbulent flow, $N_{Re} > 4000$, the von Karman correlation is recommended (Brodkey and Hershey, 1988):

$$\frac{1}{\sqrt{f}} = 4.0 \log_{10}\left(N_{Re}\sqrt{f}\right) - 0.4$$ (1.9)

The friction factor in the transition range, approximately $2100 < N_{Re} < 4000$, cannot be predicted but the laminar and turbulent flow equations can be used to establish appropriate limits.

1.2.1.2 Power Law Fluids

The power law fluid model ($\sigma = K\,(\dot{\gamma})^n$) is one of the most useful in pipeline design work for non-Newtonian fluids. It has been studied extensively and accurately expresses the behavior of many fluid foods which commonly exhibit shear-thinning ($0 < n < 1$) behavior. The volumetric flow rate of a power law fluid in a tube may be calculated in terms of the average velocity:

$$\bar{u} = \frac{Q}{\pi R^2}\left[\pi\left(\frac{(\delta P)}{2LK}\right)^{\frac{1}{n}}\left(\frac{n}{3n+1}\right)R^{(3n+1)/n}\right]\left[\frac{1}{\pi R^2}\right]$$ (1.10)

meaning

$$\frac{(\delta P)}{L} = \frac{4\bar{u}^n K}{D^{1+n}}\left(\frac{2+6n}{n}\right)^n$$ (1.11)

which, when inserted into Equation 1.4, gives an expression analogous to Equation 1.8:

$$f = \left[\frac{\delta P}{L}\right]\left(\frac{D}{2\rho\bar{u}^2}\right) = \left[\left(\frac{4\bar{u}^n K}{D^{1+n}}\right)\left(\frac{2+6n}{n}\right)^n\right]\left(\frac{D}{2L\bar{u}^2}\right) = \frac{16}{N_{Re,PL}}$$ (1.12)

where the power law Reynolds number is defined as

$$N_{Re,PL} = \left(\frac{8D^n(\bar{u})^{2-n}\rho}{K}\right)\left(\frac{n}{2+6n}\right)^n = \left(\frac{D^n(\bar{u})^{2-n}\rho}{8^{n-1}K}\right)\left(\frac{4n}{3n+1}\right)^n$$ (1.13)

TABLE 1.4
Fanning Friction Factor Correlations for the Laminar Flow of Power-Law Food Products Using the Following Equation: $f = a\ (N_{Re,PL})^b$

Product(s)	a*	b*	Source
Ideal power law	16.0	–1.00	Theoretical prediction
Pineapple pulp	13.6	–1.00	Rozema and Beverloo (1974)
Apricot puree	12.4	–1.00	Rozema and Beverloo (1974)
Orange concentrate	14.2	–1.00	Rozema and Beverloo (1974)
Applesauce	11.7	–1.00	Rozema and Beverloo (1974)
Mustard	12.3	–1.00	Rozema and Beverloo (1974)
Mayonnaise	15.4	–1.00	Rozema and Beverloo (1974)
Applejuice concentrate	18.4	–1.00	Rozema and Beverloo (1974)
Combined data of tomato concentrate and apple puree	29.1	–.992	Lewicki and Skierkowski (1988)
Applesauce	14.14	–1.05	Steffe et al. (1984)

* a and b are dimensionless numbers.

Experimental data (Table 1.4) indicate that Equation 1.12 will tend to slightly overpredict the friction factor for many power law food materials. This may be due to wall slip or time-dependent changes in rheological properties which can develop in suspension and emulsion type food products.

Equation 1.12 is appropriate for laminar flow which occurs when the following inequality is satisfied (Grovier and Aziz, 1972):

$$N_{Re,PL} < \frac{6464n}{(1+3n)^2 \left(1/(2+n)\right)^{(2+n)/(1+n)}} = \left(N_{Re,PL}\right)_{critical} \tag{1.14}$$

The critical Reynolds number varies significantly with n (Figure 1.1) and reaches a maximum value around n = 0.4.

When Equation 1.14 is not satisfied, f can be predicted for turbulent flow conditions using the equation proposed by Dodge and Metzner (1959):

$$\frac{1}{\sqrt{f}} = \left(\frac{4}{n^{0.75}}\right)\log_{10}\left[\left(N_{Re,PL}\right)f^{(1-(n/2))}\right] - \left(\frac{0.4}{n^{1.2}}\right) \tag{1.15}$$

This equation is simple and gives good results in comparison to other prediction equations (Garcia and Steffe, 1987). The graphical solution (Figure 1.2) to Equation 1.15 illustrates the strong influence of the flow-behavior index on the friction factor.

1.2.1.3 Bingham Plastic Fluids

Taking an approach similar to that used for pseudoplastic fluids, the pressure drop per unit length of a Bingham plastic fluid ($\sigma = \mu_{pl}\dot\gamma = \sigma_o$) can be calculated from the volumetric flow rate equation:

$$\frac{(\delta P)}{L} = \left(\frac{8Q\mu_{pl}}{\pi R^4}\right)\left(\frac{1}{1-4c/3+c^4/3}\right) \tag{1.16}$$
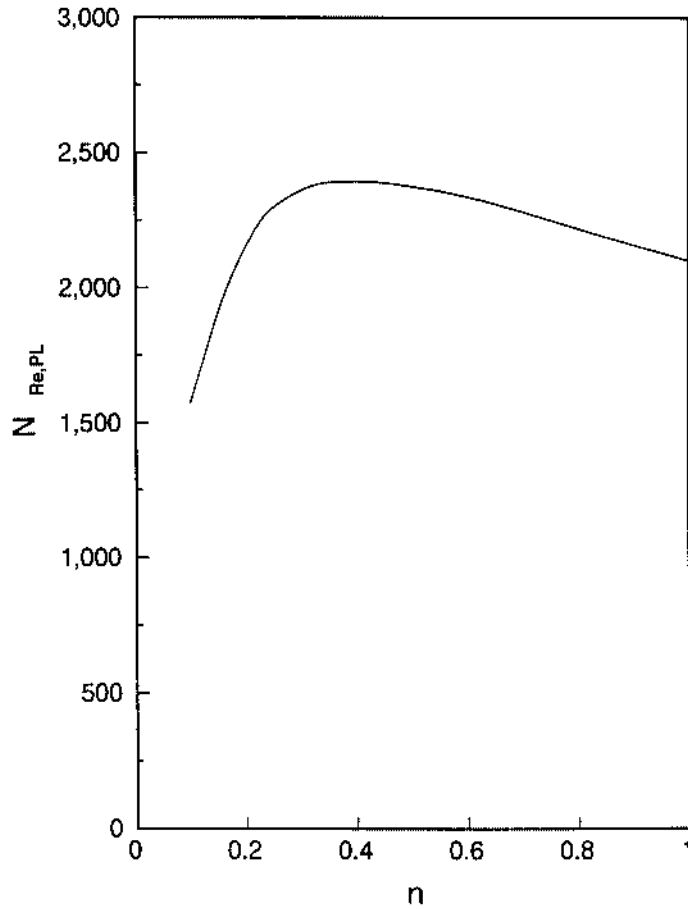
FIGURE 1.1 Critical value of the power-law Reynolds number ($N_{Re,PL}$) for different values of the flow-behavior index (n).

Written in terms of the average velocity, Equation 1.16 becomes

$$\frac{(\delta P)}{L} = \left(\frac{32\bar{u}\mu_{pl}}{D^2}\right)\left(\frac{1}{1-4c/3+c^4/3}\right) \tag{1.17}$$

which, when substituted into Equation 1.4, yields

$$f = \left[\frac{(\delta P)}{L}\right]\left(\frac{D}{2\rho(\bar{u})^2}\right) = \left[\left(\frac{32\bar{u}\mu_{pl}}{D^2}\right)\left(\frac{1}{1-4c/3+c^4/3}\right)\right]\left(\frac{D}{2\rho(\bar{u})^2}\right) = \frac{16\mu_{pl}}{Du-\rho}\left(\frac{1}{1-4c/3+c^4/3}\right) \tag{1.18}$$

where c is an implicit function of the friction factor

$$c = \frac{\sigma_o}{\sigma_w} = \frac{4L\sigma_o}{D\delta P} = \frac{2\sigma_o}{f\rho(\bar{u})^2} \tag{1.19}$$

The friction factor may also be written in terms of a Bingham Reynolds number ($N_{Re,B}$) and the Hedstrom Number (N_{He}), (Grovier and Aziz, 1972):
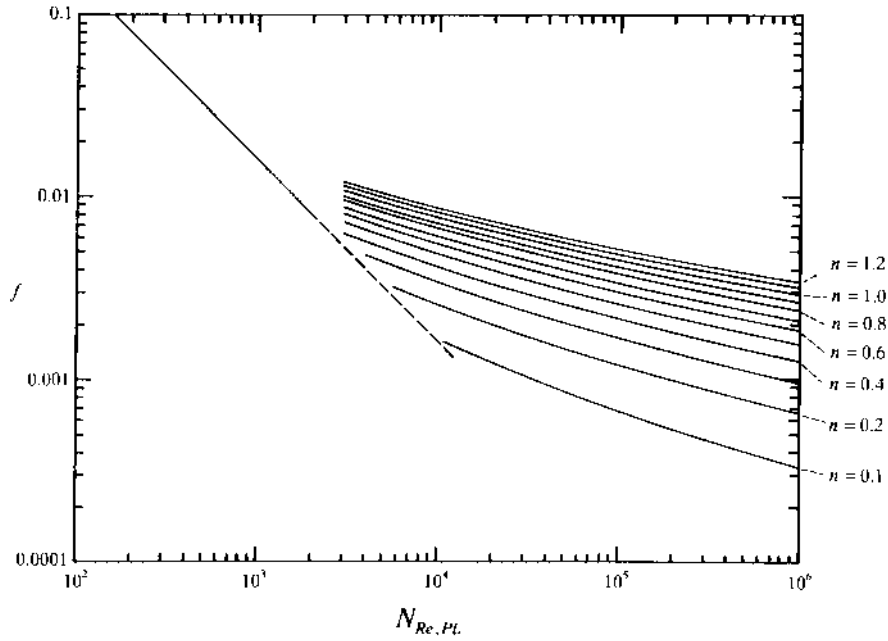
FIGURE 1.2 Fanning friction factor (f) for power-law fluids from the relationship of Dodge and Metzner (1959). (From Garcia, E. J. and Steffe, J. F. 1986, Special Report, Department of Agricultural Engineering, Michigan State University, East Lansing, MI.)

$$\frac{1}{N_{Re,B}} = \frac{f}{16} - \frac{N_{He}}{6\left(N_{Re,B}\right)^2} + \frac{\left(N_{He}\right)^4}{3f^3\left(N_{Re,B}\right)^8} \tag{1.20}$$

where

$$N_{He} = \frac{D^2 \sigma_o \rho}{\left(\mu_{pl}\right)^2} \tag{1.21}$$

and

$$N_{Re,B} = \frac{D \bar{u} \rho}{\mu_{pl}} \tag{1.22}$$

Equations 1.18 or 1.20 may be used for estimating f in steady-state laminar flow which occurs when the following inequality is satisfied (Hanks, 1963):

$$N_{Re,B} \leq \frac{N_{He}}{8c_c}\left(1 - \frac{4}{3}c_c + \frac{1}{3}c_c^4\right) = \left(N_{Re,B}\right)_{critical} \tag{1.23}$$

where c_c is the critical value of c defined as

$$\frac{c_c}{\left(1 - c_c\right)^3} = \frac{N_{He}}{16,800} \tag{1.24}$$
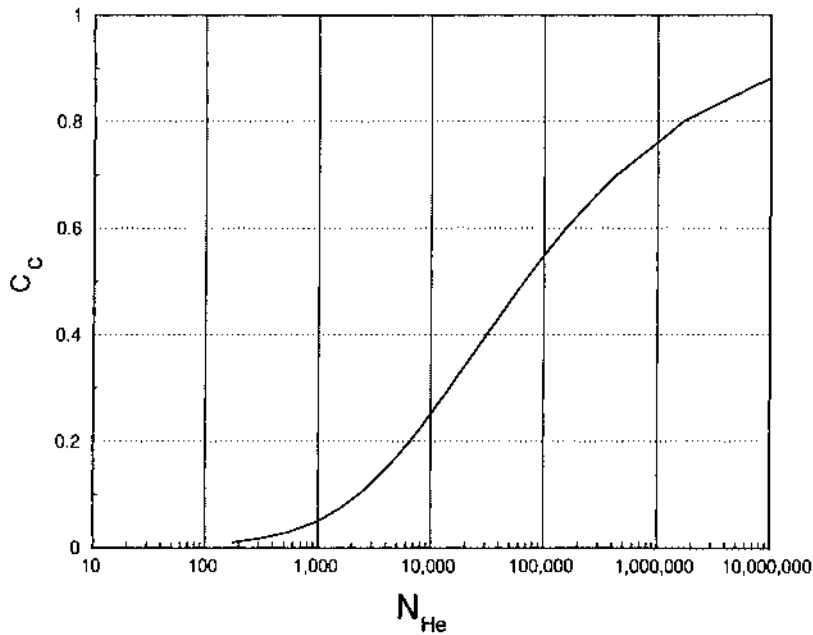
FIGURE 1.3. Variation of c_c with the Hedstrom number (N_{He}) for the laminar flow of Bingham plastic fluids. (From Steffe, J. F. 1992, *Rheological Methods in Food Process Engineering*, Freeman Press, East Lansing, MI. With permission.)
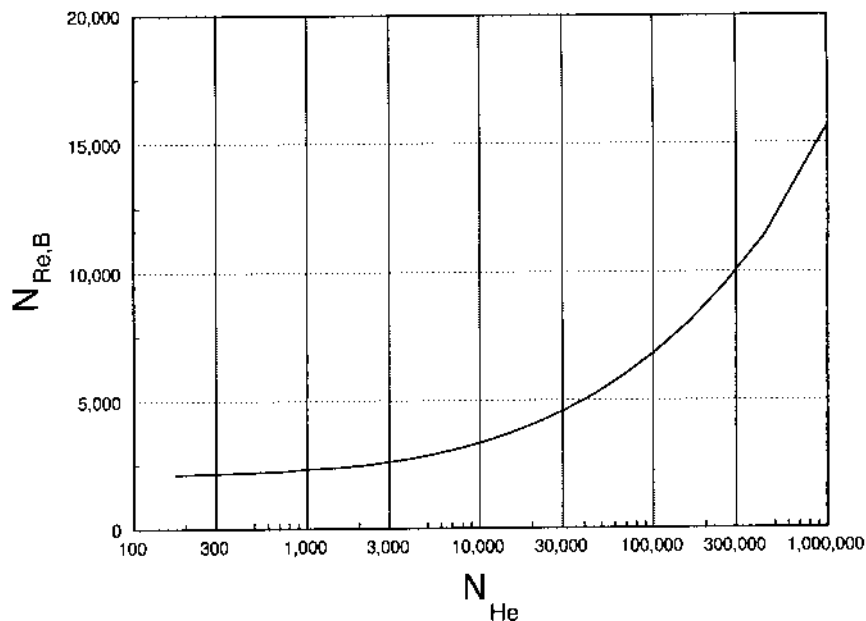
FIGURE 1.4. Variation of the critical Bingham Reynolds number ($N_{Re,B}$) with the Hedstrom number (N_{He}). (From Steffe, J. F. 1992, *Rheological Methods in Food Process Engineering*, Freeman Press, East Lansing, MI. With permission.)

c_c varies (Figure 1.3) from 0 to 1 and the critical value of the Bingham Reynolds number increases with increasing values of the Hedstrom number (Figure 1.4).

The friction factor for the turbulent flow of a Bingham plastic fluid can be considered a special case of the Herschel-Bulkley fluid using the relationship presented by Torrance (1963):
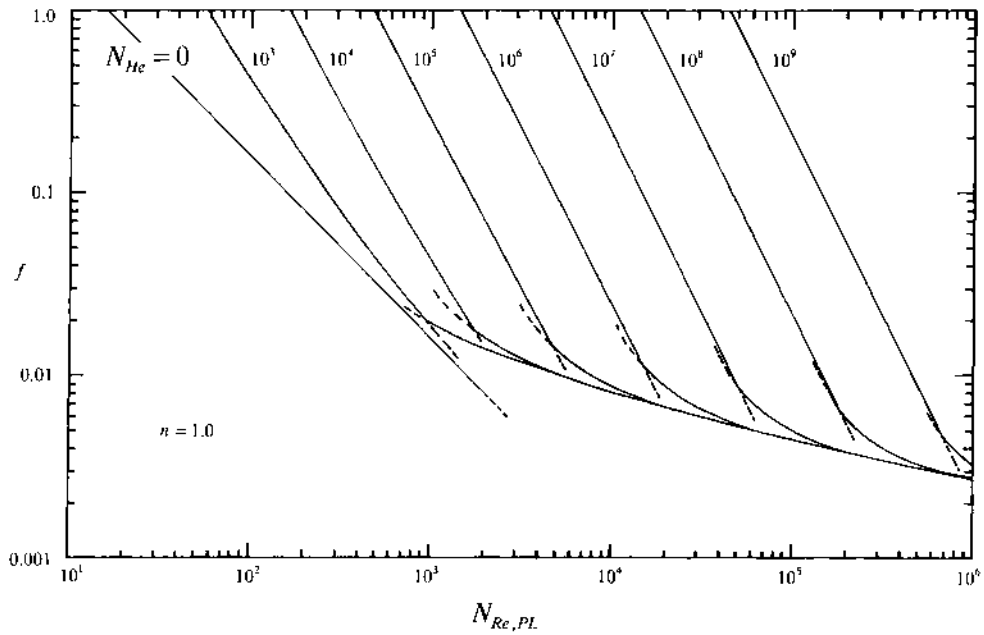
FIGURE 1.5 Fanning friction factor (f) for Bingham plastic fluids ($N_{Re,PL}$) from the relationship of Torrance (1963). (From Garcia, E. J. and Steffe, J. F. 1986, Special Report, Department of Agricultural Engineering, Michigan State University, East Lansing, MI.)

$$\frac{1}{\sqrt{f}} = 4.53 \log_{10}(1-c) + 4.53 \log_{10}\left(\left(N_{Re,B}\right)\sqrt{f}\right) - 2.3 \tag{1.25}$$

Increasing values of the yield stress will significantly increase the friction factor (Figure 1.5). In turbulent flow with very high pressure drops, c may be small simplifying Equation 1.25 to

$$\frac{1}{\sqrt{f}} = 4.53 \log_{10}\left(N_{Re,B}\sqrt{f}\right) - 2.3 \tag{1.26}$$

1.2.1.4 Herschel-Bulkley Fluids

The Fanning friction factor for the laminar flow of a Herschel-Bulkley fluid ($\sigma = K\,(\dot{\gamma}^n + \sigma_o)$ can be calculated from the equations provided by Hanks (1978) and summarized by Garcia and Steffe (1987):

$$f = \frac{16}{\Psi N_{Re,PL}} \tag{1.27}$$

where

$$\Psi = (1+3n)^n (1-c)^{1+n} \left[\frac{(1-c)^2}{(1+3n)} + \frac{2c(1-c)}{(1+2n)} + \frac{c^2}{(1+n)} \right]^n \tag{1.28}$$

c can be expressed as an implicit function of $N_{Re,PL}$ and a modified form of the Hedstrom number ($N_{He,M}$):
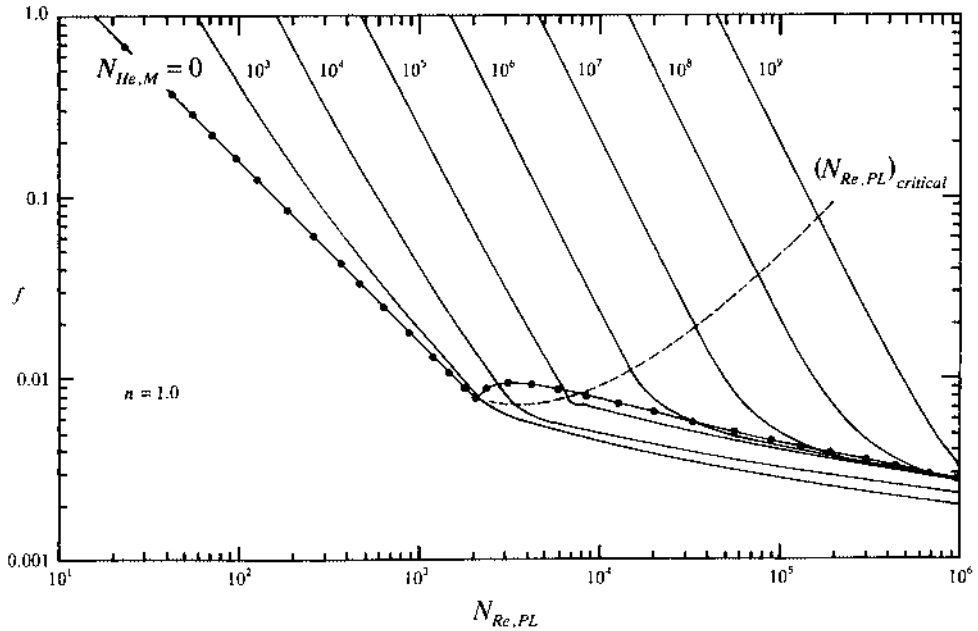
FIGURE 1.6 Fanning friction factor (f) for a Herschel-Bulkley fluid with n = 1.0, based on the relationship of Hanks (1978). (From Garcia, E. J. and Steffe, J. F. 1986, Special Report, Department of Agricultural Engineering, Michigan State University, East Lansing, MI.)

$$N_{Re,PL} = 2N_{He,M}\left(\frac{n}{1+3n}\right)^2\left(\frac{\Psi}{c}\right)^{\frac{2-n}{n}} \tag{1.29}$$

where

$$N_{Re,M} = \frac{D^2\rho}{K}\left(\frac{\sigma_o}{K}\right)^{\frac{2-n}{n}} \tag{1.30}$$

To find f for Herschel-Bulkley fluids, c is determined through an iteration of Equation 1.29 using Equation 1.28, then the friction factor may be directly computed from Equation 1.27. Graphical solutions (Figures 1.6 to 1.15) are useful to ease the computational problems associated with Herschel-Bulkley fluids. These figures indicate the value of the critical Reynolds number at different values of $N_{He,M}$ for a particular value of n. The critical Reynolds number is based on theoretical principles and has little experimental verification. Figure 1.6 (for n = 1) is also the solution for the special case of a Bingham plastic fluid and compares favorably with the Torrance (1963) solution presented in Figure 1.5.

1.2.1.5 Generalized Approach to Determine Pressure Drop in a Pipe

Metzner (1956) discusses a generalized approach to relate flow rate and pressure drop for time-independent fluids in laminar flow. The overall equation is written as

$$\frac{(\delta P)R}{2L} = K'\left(\frac{4Q}{\pi R^3}\right)^{n'} \tag{1.31}$$
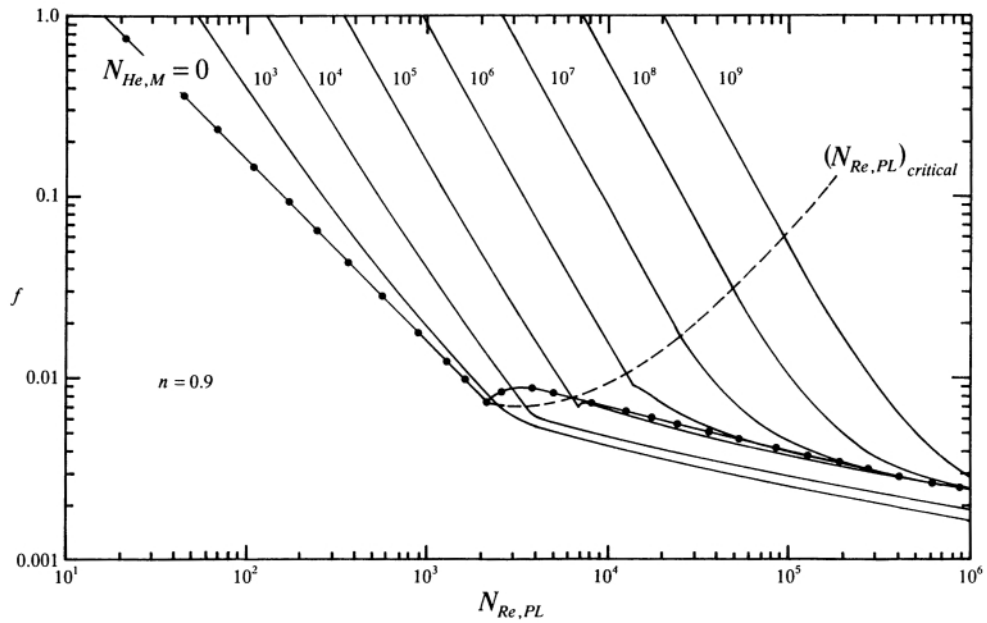
FIGURE 1.7 Fanning friction factor (f) for a Herschel-Bulkley fluid with n = 0.9, based on the relationship of Hanks (1978). (From Garcia, E. J. and Steffe, J. F. 1986, Special Report, Department of Agricultural Engineering, Michigan State University, East Lansing, MI.)
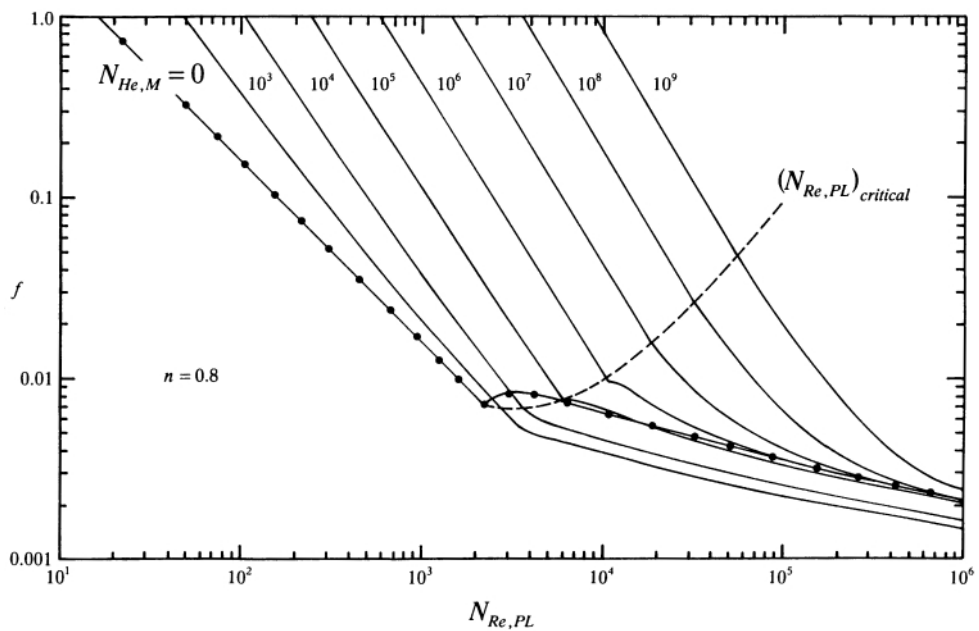
FIGURE 1.8 Fanning friction factor (f) for a Herschel-Bulkley fluid with n = 0.8, based on the relationship of Hanks (1978). (From Garcia, E. J. and Steffe, J. F. 1986, Special Report, Department of Agricultural Engineering, Michigan State University, East Lansing, MI.)

FIGURE 1.9 Fanning friction factor (f) for a Herschel-Bulkley fluid with n = 0.7, based on the relationship of Hanks (1978). (From Garcia, E. J. and Steffe, J. F. 1986, Special Report, Department of Agricultural Engineering, Michigan State University, East Lansing, MI.)

FIGURE 1.10 Fanning friction factor (f) for a Herschel-Bulkley fluid with n = 0.6, based on the relationship of Hanks (1978). (From Garcia, E. J. and Steffe, J. F. 1986, Special Report, Department of Agricultural Engineering, Michigan State University, East Lansing, MI.)
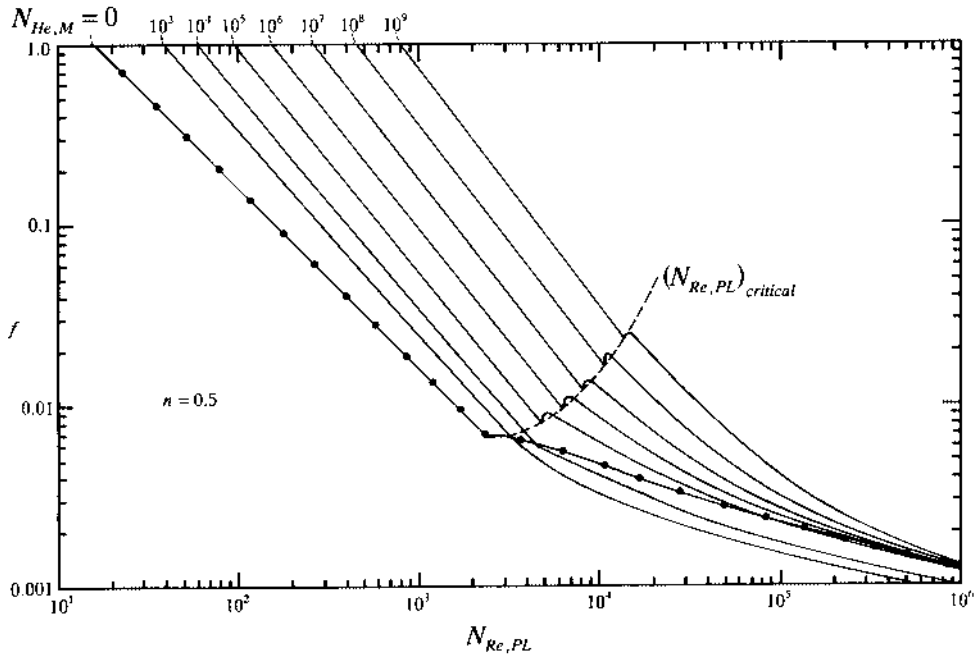
FIGURE 1.11 Fanning friction factor (f) for a Herschel-Bulkley fluid with n = 0.5, based on the relationship of Hanks (1978). (From Garcia, E. J. and Steffe, J. F. 1986, Special Report, Department of Agricultural Engineering, Michigan State University, East Lansing, MI.)
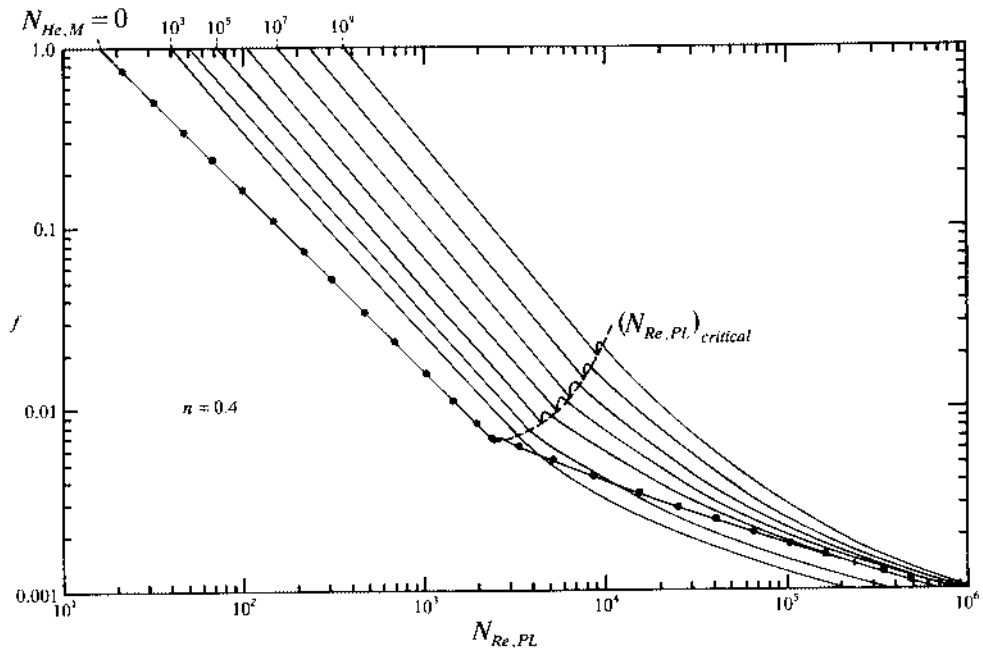
FIGURE 1.12 Fanning friction factor (f) for a Herschel-Bulkley fluid with n = 0.4, based on the relationship of Hanks (1978). (From Garcia, E. J. and Steffe, J. F. 1986, Special Report, Department of Agricultural Engineering, Michigan State University, East Lansing, MI.)
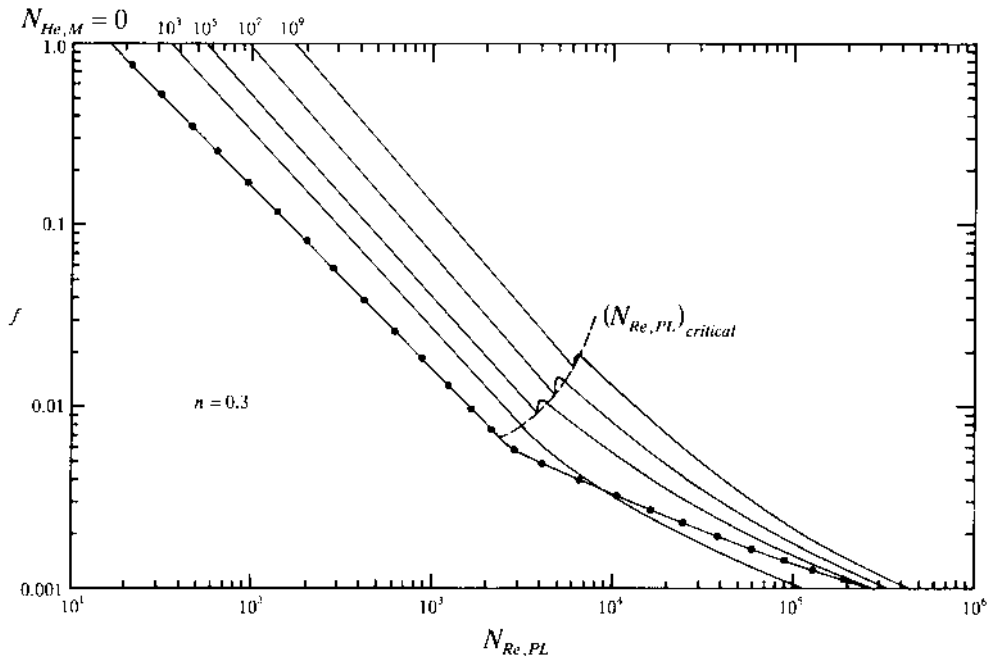
FIGURE 1.13 Fanning friction factor (f) for a Herschel-Bulkley fluid with n = 0.3, based on the relationship of Hanks (1978). (From Garcia, E. J. and Steffe, J. F. 1986, Special Report, Department of Agricultural Engineering, Michigan State University, East Lansing, MI.)
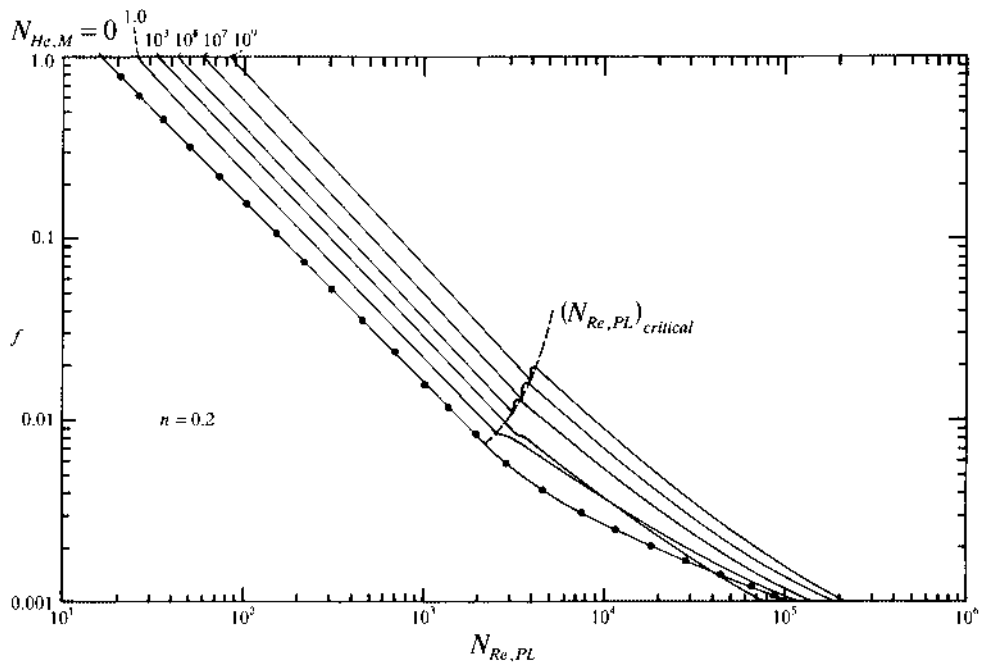
FIGURE 1.14 Fanning friction factor (f) for a Herschel-Bulkley fluid with n = 0.2, based on the relationship of Hanks (1978). (From Garcia, E. J. and Steffe, J. F. 1986, Special Report, Department of Agricultural Engineering, Michigan State University, East Lansing, MI.)
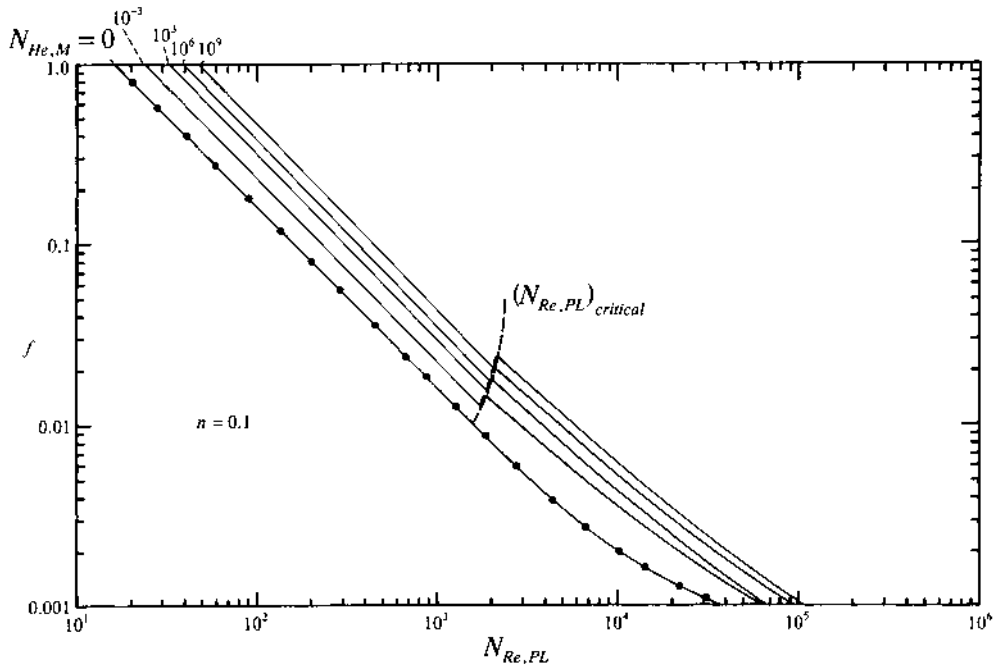
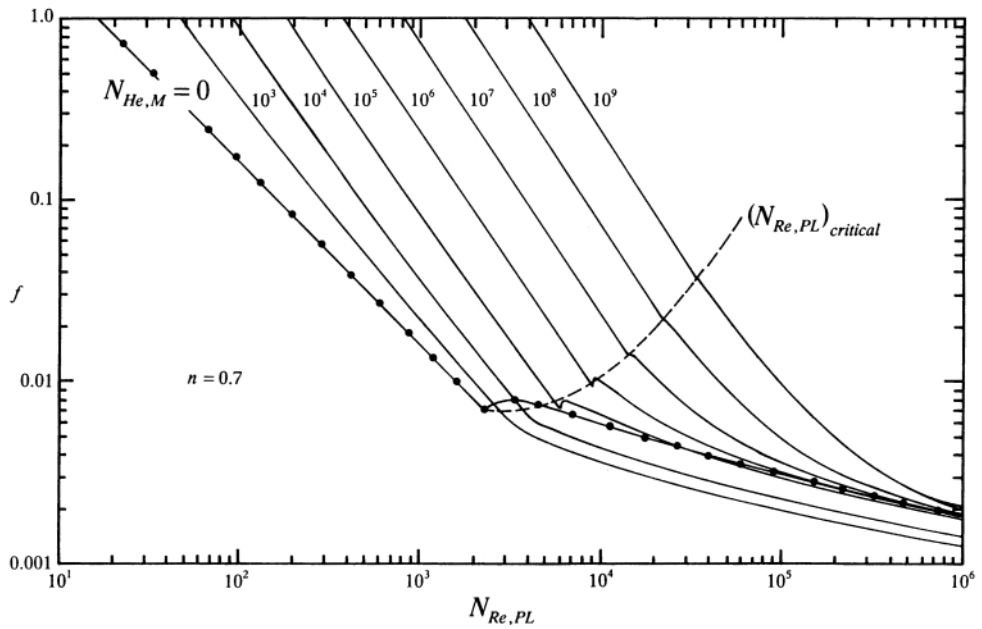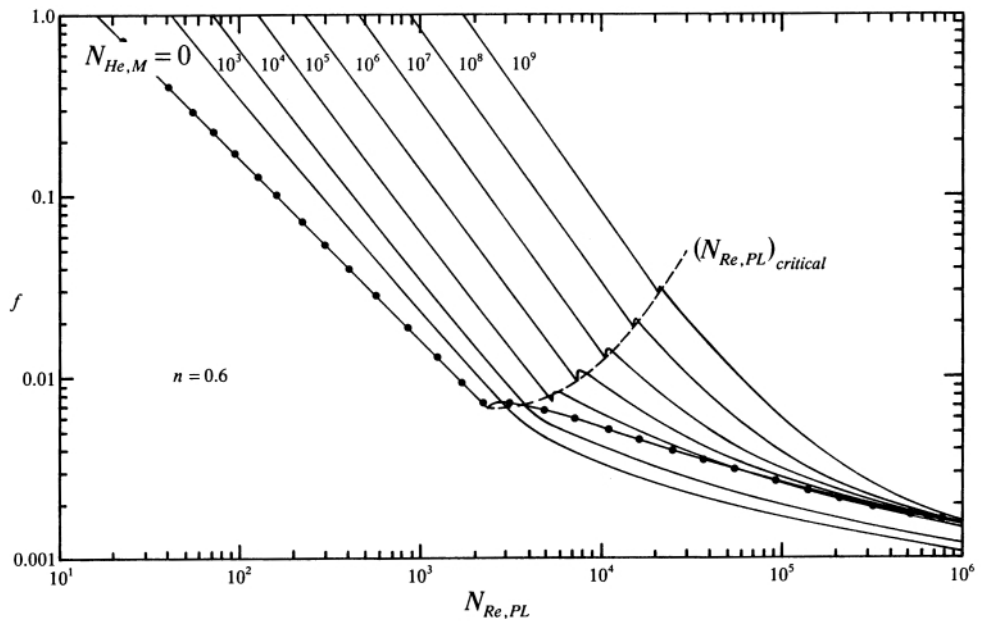**FIGURE 1.15** Fanning friction factor (f) for a Herschel-Bulkley fluid with n = 0.1, based on the relationship of Hanks (1978). (From Garcia, E. J. and Steffe, J. F. 1986, Special Report, Department of Agricultural Engineering, Michigan State University, East Lansing, MI.)

where

$$n' = \frac{d\ln\left((\delta P)R/(2L)\right)}{d\ln\left(4Q/\left(\pi R^3\right)\right)} \tag{1.32}$$

The relationship is similar to the power-law equation, Equation 1.10. In the case of the true power-law fluids

$$n' = n \quad \text{and} \quad K' = K\left(\frac{1+3n}{4n}\right)^n \tag{1.33}$$

In the general solution, n′ may vary with the shear stress at the wall and must be evaluated at each value of σ_w. Equation 1.31 has great practical value when considering direct scale-up from data taken with a small diameter tube viscometer or for cases where a well-defined rheological model (power law, Bingham plastic or Herschel-Bulkley) is not applicable. Lord et al. (1967) presented a similar method for scale-up problems involving the turbulent flow of time-independent fluids.

Time-dependent behavior and slip may also be involved in predicting pressure losses in pipes. One method of attacking this problem is to include these effects into the consistency coefficient. Houska et al. (1988) give an example of this technique for pumping minced meat where K incorporated property changes due to the aging of the meat and wall slip.

1.2.2 Kinetic Energy Evaluation

Kinetic energy (KE) is the energy present because of the translational rotational motion of the mass. KE, defined in the mechanical energy balance equation (Equation 1.1) as $\bar{u}^2/\alpha$, is the average KE per unit mass. It must be evaluated by integrating over the radius because velocity is not constant over the tube.

The KE of the unit mass of any fluid passing a given cross-section of a tube is determined by integrating the velocity over the radius of the tube (OSorio and Steffe, 1984):

$$KE = \left(\frac{1}{R^2 \bar{u}}\right) \int_0^R r u^3 \, dr \tag{1.34}$$

The solution to Equation 1.34 for the turbulent flow of any time-independent fluid is

$$KE = \frac{(\bar{u})^2}{2} \tag{1.35}$$

meaning $\alpha = 2$ for these cases. With Newtonian fluids in laminar flow, $KE = (\bar{u})^2$ with $\alpha = 1$. In the case of the laminar flow of power law fluids, α is a function of n:

$$KE = \frac{(\bar{u})^2}{\alpha} \tag{1.36}$$

where

$$\alpha = \frac{2(2n+1)(5n+3)}{3(3n+1)^2} \tag{1.37}$$

An approximate solution (within 2.5% of the true solution) for Bingham plastic fluids is (Metzner, 1956)

$$KE = \frac{(\bar{u})^2(2-c)}{2} \tag{1.38}$$

with $c = \sigma_o/\sigma_w$ and $\alpha = 2/(2-c)$. The kinetic energy correction factor for Herschel-Bulkley fluids is also available (Figure 1.16). It should be noted that this figure includes solutions for Newtonian, power-law, and Bingham plastic fluids as special cases of the Herschel-Bulkley fluid model. KE differences can be accurately calculated but are usually small and often neglected in pipeline design work.

1.2.3 Friction Losses: Contractions, Expansions, Valves, and Fittings

Experimental data are required to determine friction loss coefficients (k_f). Most published values are for the turbulent flow of water taken from Crane Co. (1982). These numbers are summarized in various engineering handbooks such as Sakiadis (1984). Laminar flow data are only available for a few limited geometries and specific fluids: Newtonian (Kittredge and Rowley, 1957), shear-thinning (Edwards et al., 1985; Lewicki and Skierkowski, 1988; Steffe et al., 1984), and shear-thickening (Griskey and Green, 1971). In general, the quantity of
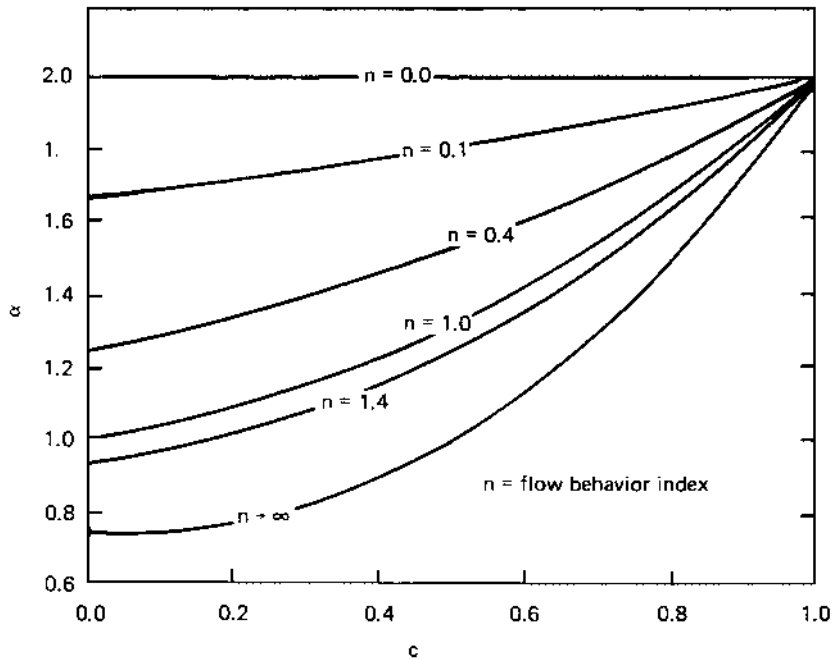
FIGURE 1.16 Kinetic energy correction factors (α) for Herschel-Bulkley fluids in laminar flow. (From Osorio, F. A. and Steffe, J. F. 1984, *J. Food Science*, 49(5):1295–1296, 1315. With permission.)

engineering data required to predict pressure losses in valves and fittings for fluids, particularly non-Newtonian fluids, in laminar flow is insufficient.

Friction loss coefficients for many valves and fittings are summarized in Tables 1.5 and 1.6. The k_f value for flow through a sudden contraction may be calculated at

$$k_f = .55\left(1 - \frac{A_2}{A_1}\right)\left(\frac{2}{\alpha}\right) \tag{1.39}$$

where A_1 equals the upstream cross-sectional and A_2 equals the downstream cross-sectional area. Losses for a sudden enlargement, or an exit, are found with the Borda-Carrot equation

$$k_f = \left(1 - \frac{A_1}{A_2}\right)^2\left(\frac{2}{\alpha}\right) \tag{1.40}$$

Equations 1.39 and 1.40 are for Newtonian fluids in turbulent flow. They are derived using a momentum balance and the mechanical-energy balance equations. It is assumed that losses are due to eddy currents in the control volume. In some cases (like Herschel-Bulkley fluids where α is a function of c), each section in the contraction, or expansion, will have a different value of α; however, they differ by little and it is not practical to determine them separately. The smallest α (yielding the larger k_f value) found for the upstream or downstream section is recommended.

After studying the available data for friction loss coefficients in laminar and turbulent flow, the following guidelines — conservative for shear thinning fluids — are proposed (Steffe, 1992) for estimating k_f values:

TABLE 1.5
Friction Loss Coefficients for the Turbulent Flow of Newtonian Fluids through Valves and Fittings

Type of Fitting or Valve	k_f
45° elbow, standard	0.35
45° elbow, long radius	0.2
90° elbow, standard	0.75
Long radius	0.45
Square or miter	1.3
180° bend, close return	1.5
Tee, standard, along run, branch blanked off	0.4
Used as elbow, entering run	1.0
Used as elbow, entering branch	1.0
Branching flow	1.0[a]
Coupling	0.04
Union	0.04
Gate, valve, open	0.17
3/4 Open[b]	0.9
1/2 Open[b]	4.5
1/4 Open[b]	24.0
Diaphragm valve, open	2.3
3/4 Open[b]	2.6
1/2 Open[b]	4.3
1/4 Open[b]	21.0
Globe valve, bevel seat, open	6.0
1/2 Open[b]	9.5
Composition seat, open	6.0
1/2 Open[b]	8.5
Plug disk, open	9.0
3/4 Open[b]	13.0
1/2 Open[b]	36.0
1/4 Open[b]	112.0
Angle valve, open[b]	2.0
Plug cock	
$\Theta = 0°$ (fully open)	0.0
$\Theta = 5°$	0.05
$\Theta = 10°$	0.29
$\Theta = 20°$	1.56
$\Theta = 40°$	17.3
$\Theta = 60°$	206.0
Butterfly valve	
$\Theta = 0°$ (fully open)	0.0
$\Theta = 5°$	0.24
$\Theta = 10°$	0.52
$\Theta = 20°$	1.54
$\Theta = 40°$	10.8
$\Theta = 60°$	118.0
Check valve, swing	2.0[c]
Disk	10.0[c]
Ball	70.0[c]

TABLE 1.5 (continued)
Friction Loss Coefficients for the Turbulent Flow
of Newtonian Fluids through Valves and Fittings

Type of Fitting or Valve	k_f

[a] This is pressure drop (including friction loss) between run and branch, based on velocity in the main stream before branching. Actual value depends on the flow split, ranging from 0.5 to 1.3 if main stream enters run and 0.7 to 1.5 if main stream enters branch.

[b] The fraction open is directly proportional to steam travel or turns of hand wheel. Flow direction through some types of valves has a small effect on pressure drop. For practical purposes this effect may be neglected.

[c] Values apply only when check valve is fully open, which is generally the case for velocities more than 3 ft/s for water.

Data from Sakiadis, B. C. 1984. Fluid and particle mechanics. In: Perry, R. H., Green, D. W., and Maloney, J. O. (ed.). *Perry's Chemical Engineers' Handbook*, 6th ed., Sect. 5. McGraw-Hill, New York.

TABLE 1.6
Friction Loss Coefficients (k_f Values)
for the Laminar Flow of Newtonian Fluids
through Valves and Fittings

	N_{Re} =		
Type of fitting or valve	1000	500	100
90° ell, short radius	0.9	1.0	7.5
Tee, standard, along run	0.4	0.5	2.5
Branch to line	1.5	1.8	4.9
Gate valve	1.2	1.7	9.9
Glove valve, composition disk	11	12	20
Plug	12	14	19
Angle valve	8	8.5	11
Check valve, swing	4	4.5	17

Data from Sakiadis, B. C. 1984. Fluid and particle mechanics. In: Perry, R. H., Green, D. W., and Maloney, J. O. (ed.). *Perry's Chemical Engineers' Handbook*, 6th ed., Sect. 5. McGraw-Hill, New York.

1. For Newtonian fluids in turbulent or laminar flow use the data of Sakiadis (1984) or Kittredge and Rowley (1957), respectively (Tables 1.5 and 1.6).
2. For non-Newtonian fluids above a Reynolds number of 500 (N_{Re}, $N_{Re,PL}$, or $N_{Re,B}$), use data for Newtonian fluids in turbulent flow (Table 1.5).
3. For non-Newtonian fluids in a Reynolds number of 20 to 500 use the following equation

TABLE 1.7
Values of β, for Equation 1.41

Type of fitting or valve	β	N_{Re}
90° Short curvature elbow, 1 and 2 inch	842	1–1000
Fully open gate valve, 1 and 2 inch	273	.1–100
Fully open square plug globe valve, 1 inch	1460	.1–10
Fully open circular plug globe valve, 1 inch	384	.1–10
Contraction, $A_2/A_1 = 0.445$	110	1–100
Contraction, $A_2/A_1 = 0.660$	59	1–100
Expansion, $A_2/A_1 = 1.52$	88	1–100
Expansion, $A_2/A_1 = 1.97$	139	1–100

Note: Values are determined from the data of Edwards, M. F., Jadallah, M. S. M., and Smith, R. 1985. *Chem. Eng. Res. Des.* 63:43–50.

$$k_f = \frac{\beta}{N} \tag{1.41}$$

where N is N_{Re}, $N_{Re,PL}$, or $N_{Re,B}$ depending on the type of fluid in question and β is found for a particular valve or fitting (or any related item such as a contraction) by multiplying the turbulent flow friction loss coefficient by 500:

$$\beta = \left(k_f\right)_{turbulent}(500) \tag{1.42}$$

Values of A for many standard items may be calculated from the k_f values provided in Table 1.5. Some A values can be determined (Table 1.7) from the work of Edwards et al. (1985) where experimental data were collected for elbows, valves, contractions, expansions, and orifice plates. The Edwards study considered five fluids: water, lubrication oil, glycerol-water mixtures, CMC-water mixtures (0.48 < n < 0.72, 0.45 < K < 11.8), and china clay-water mixtures (0.18 < n < 0.27, 3.25 < K < 29.8). Equations 1.41 and 1.42 are also acceptable for Newtonian fluids when $20 < N_{Re} < 500$.

The above guidelines are offered with caution and should only be used in the absence of actual experimental data. Many factors, such as high extensional viscosity, may significantly influence k_f values.

1.3 EXAMPLE CALCULATIONS

Consider the typical flow problem illustrated in Figure 1.17. The system has a 0.0348 m diameter pipe with a volumetric flow rate of 1.57×10^{-3} m³/s (1.97 kg/s) or an average velocity of 1.66 m/s. The density of the fluid is constant (ρ = 1250 kg/m³) and the pressure drop across the strainer is 100 kPa. Additional friction losses occur in the entrance, the plug valve, and in the three long radius elbows. Solving the mechanical energy balance, Equation 1.1, for work output yields
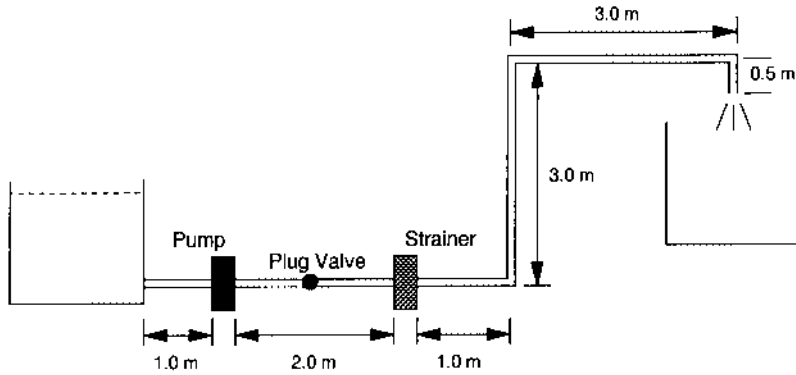
FIGURE 1.17 Typical pipeline system. (From Steffe, J. F. and Morgan, R. E. 1986, *Food Technol.*, 40(12):78–85. With permission.)

$$-W = \frac{\left(\bar{u}_2\right)^2}{\alpha_2} - \frac{\left(\bar{u}_1\right)^2}{\alpha_1} + g\left(z_2 - z_1\right) + \frac{P_2 - P_1}{\rho} + \Sigma F \tag{1.43}$$

Subscripts 1 and 2 refer to the level fluid in the tank and the exit point of the system, respectively. Assuming a near empty tank (as a worst case for pumping), $P_2 = P_1$ and $\bar{u}_1 = 0$, simplifies Equation 1.43 to

$$-W = g\left(z_2 - z_1\right) + \frac{\left(\bar{u}_2\right)^2}{\alpha_2} + \Sigma F \tag{1.44}$$

where (–W) represents the work input per unit mass and the friction loss term, Equation 1.2, includes the pressure drop over the strainer as a $\delta P/\rho$ added to the summation

$$\Sigma F = \frac{2f\bar{u}^2 L}{D} + \frac{\left(k_{f,entrance}\right)\bar{u}^2}{2} + \frac{\left(k_{f,valve}\right)\bar{u}^2}{2} + \frac{3\left(k_{f,elbow}\right)\bar{u}^2}{2} + \frac{100,000}{1,250} \tag{1.45}$$

or

$$\Sigma F = \frac{2f\bar{u}^2 L}{D} + \left(k_{f,entrance} + k_{f,valve} + 3\left(k_{f,elbow}\right)\right)\frac{\bar{u}^2}{2} + 80.0 \tag{1.46}$$

The pressure drop across the pump is

$$\left(\delta P\right)_p = \left(-W\right)\rho \tag{1.47}$$

In the following example problems, only the rheological properties of the fluids will be changed. All other elements of the problem, including the fluid density, remain constant.

1.3.1 CASE 1: NEWTONIAN FLUID IN LAMINAR FLOW

Assume, $\mu = 0.34$ Pa · s giving $N_{Re} = 212.4$ which is well within the laminar range of $N_{Re} < 2100$. Then, from Table 1.5, Equations 1.39, 1.41, and 1.42

$$k_{f,\text{entrance}} = \frac{(.55)(2.0/1.0)500}{212.4} = 2.59$$

$$k_{f,\text{valve}} = \frac{(9)(500)}{212.4} = 21.18$$

$$k_{f,\text{elbow}} = \frac{(.45)(500)}{212.4} = 1.06$$

The friction factor is calculated from Equation 1.8:

$$f = \frac{16}{212.4} = 0.0753$$

Then, the total friction losses are

$$\Sigma F = \frac{2(.0753)(1.66)^2(10.5)}{.0348} + \left(2.59 + 21.18 + 3(1.06)\right)\frac{(1.66)^2}{2} + 80.0 = 242.4 \, \text{J/kg}$$

and

$$-W = 9.81(2.5) + (1.66)^2 + 242.4 = 269.7 \, \text{J/kg}$$

$$(\delta P)_p = (269.7)(1250) = 337 \, \text{kPa}$$

1.3.2   CASE 2: NEWTONIAN FLUID IN TURBULENT FLOW

Assume, $\mu = 0.012$ Pa · s giving $N_{Re} = 6018$, a turbulent flow value of N_{Re}. Friction loss coefficients may be determined from Equation 1.39, and Table 1.2: $k_{f,\text{entrance}} = 0.55$; $k_{f,\text{valve}} = 9$; $k_{f,\text{elbow}} = 0.45$. The friction factor is determined by iteration of Equation 1.9:

$$\frac{1}{\sqrt{f}} = 4.0 \log_{10}\left(6018\sqrt{f}\right) - 0.4$$

giving a solution of $f = 0.0089$. Continuing,

$$\Sigma F = \frac{2(.0089)(1.66)^2(10.5)}{.348} + \left(.55 + 9 + 3(.45)\right)\frac{(1.66)^2}{2} + 80.0 = 109.8 \, \text{J/kg}$$

and

$$-W = 9.81(2.5) + \frac{(1.66)^2}{2} + 109.8 = 135.7 \, \text{J/kg}$$

$$(\delta P)_p = (135.7)(1250) = 170 \, \text{kPa}$$

1.3.3   CASE 3: POWER LAW FLUID IN LAMINAR FLOW

Assume, $K = 5.2$ Pa · s^n and $n = 0.45$ giving $N_{Re,PL} = 323.9$, a laminar flow value of $N_{Re,PL}$. Then, from Table 1.5, Equations 1.37, 1.41, and 1.42

$$k_{f,entrance} = \frac{(.55)(2/1.2)500}{323.9} = 1.42$$

$$k_{f,valve} = \frac{(9)(500)}{323.9} = 13.89$$

$$k_{f,elbow} = \frac{(.45)(500)}{323.9} = 0.69$$

The friction factor is calculated from Equation 1.12:

$$f = \frac{16}{323.9} = 0.0494$$

Then

$$\Sigma F = \frac{2(.0494)(1.66)^2(10.5)}{.0348} + (1.42 + 13.89 + 3(.69))\frac{(1.66)^2}{2} + 80.0 = 189.1 \text{ J/kg}$$

and, using Equations 1.37 to calculate α,

$$-W = 9.81(2.5) + \frac{(1.66)^2}{1.2} + 189.1 = 215.9 \text{ J/kg}$$

$$(\delta P)_p = (215.9)(1250) = 270 \text{ kPa}$$

1.3.4   CASE 4: POWER LAW FLUID IN TURBULENT FLOW

Assume, K = 0.25 Pa · s^n and n = 0.45 giving $N_{Re,PL}$ = 6736.6. The critical value of $N_{Re,PL}$ may be calculated as

$$\left(N_{Re,PL}\right)_{critical} = \frac{6464(.45)}{(1 + 3(.45))^2 \left(\frac{1}{2 + .45}\right)^{(2 + .45)/1 + .45}} = 2,394$$

meaning the flow is turbulent because 6736.6 > 2394. Friction loss coefficients are the same as those found for Case 2: $k_{f,entrance} = 0.5$; $k_{f,valve} = 9$; $k_{f,elbow} = 0.45$. The friction factor is found by iteration of Equation 1.15:

$$\frac{1}{\sqrt{f}} = \left(\frac{4}{(.45)^{0.75}}\right)\log_{10}\left[(6736.6)f^{(1-((.45)/2))}\right] - \left(\frac{0.4}{(.45)^{1.2}}\right)$$

yielding f = 0.0051. Then

$$\Sigma F = \frac{2(.0051)(1.66)^2(10.5)}{0.348} + (.55 + 9 + 3(.45))\frac{(1.66)^2}{2} + 80.0 = 103.5 \text{ J/kg}$$

and

$$-W = 9.81(2.5) + \frac{(1.66)^2}{2} + 103.5 = 129.4 \text{ J/kg}$$

$$(\delta P)_p = (129.4)(1250) = 162 \text{ kPa}$$

1.3.5 CASE 5: BINGHAM PLASTIC FLUID IN LAMINAR FLOW

Assume, $\mu_{pl} = 0.34$ Pa · s and $\sigma_o = 50$ Pa making $N_{Re,B} = 212.4$ and $N_{He} = 654.8$. To check the flow regime, c_c is calculated from Equation 1.24:

$$\frac{c_c}{(1 - c_c)^3} = \frac{654.8}{16,800}$$

giving $c_c = 0.035$. The critical value of $N_{Re,B}$ is determined from Equation 1.23:

$$\left(N_{Re,B}\right)_{critical} = \frac{654.8}{8(.035)}\left(1 - \frac{4}{3}(.035) + \frac{1}{3}(.035)^4\right) - 2,229$$

meaning the flow is laminar because 212.4 < 2229. Friction loss coefficients may be determined from Table 1.5, Equations 1.39, 1.41, and 1.42; however, in this particular problem, $N_{Re,B} = N_{Re,PL} = 212.4$, so the friction loss coefficients in this example are the same as those found in Case 1: $k_{f,entrance} = 2.59$; $k_{f,valve} = 21.18$; $k_{f,elbow} = 1.06$. α, a function of c (Figure 1.16), is taken as 1 (the worst case value) for the calculations. The friction factor is found by iteration of Equation 1.20:

$$\frac{1}{212.4} = \frac{f}{16} - \frac{654.8}{6(212.4)^2} + \frac{(654.8)^4}{3f^3(212.4)^8}$$

resulting in $f = 0.114$. Then,

$$\Sigma F = \frac{2(.114)(1.66)^2(10.5)}{0.348} + \left(2.59 + 21.18 + 3(1.06)\right)\frac{(1.66)^2}{2} + 80.0 = 306.7 \text{ J/kg}$$

and

$$-W = 9.81(2.5) + (1.66)^2 + 306.7 = 334.0 \text{ J/kg}$$

$$(\delta P)_p = (334.0)(1250) = 418 \text{ kPa}$$

1.3.6 CASE 6: HERSCHEL-BULKLEY FLUID IN LAMINAR FLOW

Assume, $K = 5.2$, $\sigma_o = 50$ Pa and $n = 0.45$ giving $N_{Re,PL} = 323.9$ and $N_{He,M} = 707.7$. Flow is laminar (Figure 1.11) and the friction loss coefficients are the same as those found for Case 3 because the Reynolds numbers are equal in each instance: $k_{f,entrance} = 0.83$; $k_{f,valve} = 13.89$; $k_{f,elbow} = 0.69$. Also, $\alpha = 1.2$ can be taken as the worst case (Figure 1.16). The friction factor is calculated by averaging the values found on Figures 1.11 and 1.12:

$$f = \frac{0.071 + 0.081}{2} = 0.076$$

Then

$$\Sigma F = \frac{2(.076)(1.66)^2(10.5)}{.0348} + \left(1.42 + 13.89 + 3(.69)\right)\frac{(1.66)^2}{2} + 80.0 = 230.3 \text{ J/kg}$$

and

$$-W = 9.81(2.5) + (1.66)^2 + 230.3 = 257.1 \text{ J/kg}$$

$$(\delta P)_p = (257.1)(1250) = 321 \text{ kPa}$$

1.4 VELOCITY PROFILES IN TUBE FLOW

1.4.1 LAMINAR FLOW

It is important to know the velocity profiles present in pipes for various reasons such as calculating the appropriate length of a hold tube for a thermal processing system. Expressions giving the velocity profiles in laminar flow are easily determined from the fundamental equations of motion. With a Newtonian fluid the result is

$$u = f(r) = \frac{(\delta P)}{4 L \mu}\left(R^2 - r^2\right) \tag{1.48}$$

and, for the case of a power law material,

$$u = f(r) = \left(\frac{(\delta P)}{2LK}\right)^{1/n}\left(\frac{n}{n+1}\right)\left[R^{\frac{n+1}{n}} - r^{\frac{n+1}{n}}\right] \tag{1.49}$$

By considering the volumetric flow rate, the relationship between the mean velocity ($\bar{u} = Q/\pi R^2$)) and maximum velocity (located at the center line where $r = 0$) may also be calculated:

$$\frac{\bar{u}}{u_{max}} = \frac{1+n}{1+3n} \tag{1.50}$$

In the case of a Bingham plastic fluid, the velocity profile equation is

$$u = f(r) = \frac{(\delta P)R^2}{4KL}\left[1 - \left(\frac{r}{R}\right)^2 - \frac{2r_o}{R}\left(1 - \frac{r}{R}\right)\right] \tag{1.51}$$

The velocity in the plug, at the center of the pipe, where $\sigma \leq \sigma_o$ for $r \leq r_o$ is

$$u = f(r) = \frac{(\delta P)R^2}{4KL}\left[\left(1 - \frac{r_o}{R}\right)^2\right] \tag{1.52}$$

where the value of the critical radius, r_o, is calculated from the yield stress:

$$r_o = \frac{\sigma_o 2L}{(\delta P)} \tag{1.53}$$

The velocity profile for a Herschel-Bulkley fluid may also be determined:

$$u = f(r) = \frac{2L}{(\delta P)\left(\frac{1}{n}+1\right)K^{\frac{1}{n}}}\left[\left(\sigma_w - \sigma_o\right)^{\frac{1}{n}+1} - \left(\frac{(\delta P)r}{2L} - \sigma_o\right)^{\frac{1}{n}+1}\right] \tag{1.54}$$

1.4.2   TURBULENT FLOW

It is difficult to predict velocity profiles for fluids in turbulent flow. Relationships for Newtonian fluids are reliable. Those for power-law fluids are available but they have not received adequate experimental verification for fluid foods.

1.4.2.1   Newtonian Fluids

Semi-theoretical prediction equations for the velocity profile of Newtonian fluids in turbulent flow, in smooth tubes, are well established and discussed in numerous textbooks (e.g., Brodkey and Hershey, 1988; Denn, 1980; Grovier and Aziz, 1972). The equations are presented in terms of three distinct regions of the pipe:

For the viscous sublayer

$$u^+ = y^+ \qquad\qquad y^+ \leq 5 \tag{1.55}$$

For the transition zone where turbulent fluctuations are generated

$$u^+ = -3.05 + 11.513 \log_{10}\left(y^+\right) \qquad 5 < y^+ < 30 \tag{1.56}$$

For the turbulent core

$$u^+ = 5.5 + 5.756 \log_{10}\left(y^+\right) \qquad 30 \leq y^+ \tag{1.57}$$

where

$$u^+ = \frac{u}{u*} \tag{1.58}$$

$$y^+ = \frac{yu*\rho}{\mu} \tag{1.59}$$

$$u* = \sqrt{\frac{\sigma_w}{\rho}} = \bar{u}\sqrt{\frac{f}{2}} \tag{1.60}$$

and, y, the distance from the pipe wall is

$$y = R - r \qquad (1.61)$$

The origin of the coordinate system is located at the wall, $r = R$; therefore, the velocity is zero at $r = R$ where $y = 0$ and a maximum at the center of the pipe where $r = 0$ and $y = R$. Combined, the above equations constitute the universal velocity profile.

A common problem facing the engineer in the food industry is to predict the maximum velocity found in a pipe. To illustrate an approach to this problem, consider the following example.

EXAMPLE 1.1

Assume: $\mu = 0.010$ Pa · s; $D = 0.0348$ m; $\bar{u} = 1.75$ m/s; $\rho = 1225$ kg/m³; $N_{Re} = 7460$; $f = 0.0084$. The velocity is maximum at the center line where $y = R$ and the friction velocity is

$$u^* = \bar{u} \sqrt{\frac{f}{2}} = 1.75 \sqrt{\frac{.0084}{2}} = 0.1134 \text{ m s}$$

The calculations proceed as

$$y^+ = \frac{yu^*\rho}{\mu} = \frac{(.0348/2)(.1134)1225}{.010} = 241.71$$

$$u^+ = 5.5 + 5.756 \log_{10}\left(y^+\right) = 5.5 + 5.756 \log_{10}(241.71) = 19.22$$

The maximum velocity may be calculated from the definition of the turbulent velocity, $u^+ = u/u^*$, as

$$u_{max} = u^+ u^* = (19.22).1134 = 2.18 \text{ m/s}$$

Once the maximum velocity has been determined, the ⅐ power-law equation may be used to approximate u/u_{max} at other locations:

$$\frac{u}{u_{max}} = \left(\frac{y}{R}\right)^{1/7} = \left(\frac{R-r}{R}\right)^{1/7} \qquad (1.62)$$

For example, the velocity halfway between the center line and the wall ($r = .5R$) would be calculated from

$$\frac{u}{u_{max}} = \left(\frac{R-r}{R}\right)^{1/7} = (.5)^{1/7} = 0.9067$$

making

$$u = (.9067)(2.18) = 1.98$$

The ⅐ power-law equation does a reasonable job of predicting velocity profiles in spite of the fact that it is independent of N_{Re}. Grovier and Aziz (1972) note that Equation 1.62 is most appropriate for $0.1 < y/R < 1.0$ and $3000 < N_{Re} < 100,000$. Also, the exponent may vary from ⅙ at $N_{Re} = 4000$ to ⅒ at $N_{Re} = 3,200,000$.

1.4.2.2 Power-Law Fluids

Dodge and Metzner (1959) derived equations to describe the velocity profile of power-law fluids in tube flow. Small errors were corrected by Skelland (1967) and the final equations were presented as

$$u^+ = \left(y^+\right)^{1/n} \tag{1.63}$$

for the laminar sublayer and

$$u^+ = \frac{5.66}{n^{.75}}\log_{10}\left(y^+\right) - \frac{0.566}{n^{1.2}} + \frac{3.475}{n^{.75}}\left[1.960 + 0.815n - 1.628n\log_{10}\left(3 + \frac{1}{n}\right)\right] \tag{1.64}$$

for the turbulent core, where y^+ incorporates the flow-behavior index needed for the consideration of power-law fluids:

$$y^+ = \frac{y^n\left(u*\right)^{2-n}\rho}{K} \tag{1.65}$$

Constants were obtained from friction-factor measurements so the thickness of the laminar sublayer was not obtained. The above equation can be used to predict the maximum velocity in a pipe. Consider the following example problem.

EXAMPLE 1.2

Assume: $K = 0.31$ Pa · s^n; $D = 0.0348$ m; $\bar{u} = 1.75$ m/s; $\rho = 1225$ kg/m^3; $n = 0.40$; $N_{Re, PL} = 7741$; $f = 0.0045$. The velocity is maximum at the center line where $y = R$. The friction velocity is

$$u* = \bar{u}\sqrt{\frac{f}{2}} = 1.75\sqrt{\frac{.0045}{2}} = 0.083 \text{ m s}$$

and

$$y^+ = \frac{y^n\left(u*\right)^{2-n}\rho}{K} = \frac{(.0348/2)^{.4}(.0838)^{2-.4}(1225)}{.31} = 14.6$$

$$u^+ = \frac{5.66}{(.4)^{.75}}\log_{10}(14.6) - \frac{0.566}{(.4)^{1.2}} + \frac{3.475}{(.4)^{.75}}\left[1.960 + 0.815(.4) - 1.628(.4)\log_{10}\left(3 + \frac{1}{.4}\right)\right] = 23.86$$

The maximum velocity may be calculated from the definition of the turbulent velocity, $u^+ = u/u*$, as

$$u_{max} = u^+u* = (23.86).083 = 1.98 \text{ m/s}$$

An alternative equation for predicting velocity in the turbulent core for power-law fluids was presented by Clapp (1961)

$$u^+ = \frac{2.78}{n}2.303\log_{10}\left(y^+\right) + \frac{3.80}{n} \tag{1.66}$$

This equation correlated well with experimental data for $0.698 < n < 0.813$ and $5480 < N_{Re,PL} < 42,800$.

1.5 SELECTION OF OPTIMUM ECONOMIC PIPE DIAMETER

The selection of pipe diameter for food processing systems is usually based on the requirements of the processing equipment such as inlet port size for a pump; however, optimum solutions can be used if sufficient economic data is available. Denn (1980) has discussed the solution for Newtonian fluids. In addition, Darby and Melson (1982) used dimensional analysis to develop graphs from which the optimum pipe diameter could be obtained directly for Newtonian, Bingham plastic, and power-law fluids. The problem has been solved for pumping Herschel-Bulkley fluids by Garcia and Steffe (1986a).

NOMENCLATURE

A_1	Upstream cross-sectional area, m^2
A_2	Downstream cross-sectional area, m^2
c	Yield stress/shear stress at the wall, σ_o/σ_w, dimensionless
c_c	Critical value of c, dimensionless
D	Pipe diameter, m
f	Fanning friction factor, dimensionless
g	Acceleration due to gravity, $9.81 \ m/s^2$
k_f	Friction-loss coefficient, dimensionless
K	Consistency coefficient, $Pa \cdot s^n$
KE	Kinetic energy per unit mass, J/kg
L	Length of pipe, m
N	Any dimensionless number
N_{He}	Hedstrom number for a Bingham plastic fluid, dimensionless
$N_{He,M}$	Modified Hedstrom number for a Herschel-Bulkley fluid, dimensionless
N_{Re}	Reynolds number for a Newtonian fluid, dimensionless
$N_{Re,B}$	Reynolds number for a Bingham plastic fluid, dimensionless
$(N_{Re,B})_{critical}$	Critical Reynolds number for Bingham plastic fluid, dimensionless
$N_{Re,PL}$	Reynolds number for a power-law fluid, dimensionless
$(N_{Re,PL})_{critical}$	Critical Reynolds number for a power-law fluid, dimensionless
n	Flow-behavior index, dimensionless
r_o	Critical radius, m
r	Radial coordinate, m
R	Pipe radius, m
Q	Volumetric flow rate in a pipe, m^3/s
u	Velocity, m/s
u^+	Turbulent velocity [u/u*], dimensionless
u^*	Friction velocity $\left[\sqrt{\sigma_w/\rho} = \bar{u}\sqrt{f/2}\right]$, m/s
$\bar{u}$	Volumetric average velocity $[Q/(\pi R^2)]$, m/s
u_{max}	Maximum velocity in the tube, m/s
W	Work output per unit mass, J/kg
y	Distance from pipe wall into fluid [R − r], m
y^+	Distance from the tube wall $[u^*\rho y/K]$, dimensionless
z	Height above a reference plane, m
α	Kinetic energy correction coefficient, dimensionless
β	Constant defined by Equation 1.42, dimensionless
δP	Pressure drop over a pipe of length, L, Pa
$(\delta P)_p$	Pressure drop across a pump, Pa
$\dot{\gamma}$	Shear rate, 1/s
μ	Newtonian viscosity, $Pa \cdot s$

μ_{pl}	Plastic viscosity of a Bingham fluid, Pa · s
ρ	Density, kg/m³
σ	Shear stress, Pa
σ_o	Yield stress, Pa
σ_w	Shear stress at the wall of a pipe $[(\delta PR)/(2L)]$, Pa

REFERENCES

Bird, R. B., Stewart, W. E., and Lightfoot, E. N., 1960, *Transport Phenomena*, John Wiley and Sons, New York.

Brodkey, R. S. and Hershey, H. C., 1988, *Transport Phenomena*, McGraw-Hill, New York.

Brown, N. P. and Heywood, N. I., Eds., 1991, *Slurry Handling: Design of Solid-Liquid Systems*, Elsevier, New York.

Clapp, R. M., 1961, Turbulent heat transfer in pseudoplastic non-Newtonian fluids, III.A. *Int. Dev. Heat Transfer*, ASME, Part III, Sec. A., 652–661.

Crane Co., 1982, Flow of fluids through valves, fittings and pipe, Technical Paper No. 410M, 21st printing, Crane Co., 300 Park Ave., New York.

Darby, R. and Melson, J. D., 1982, Direct determination of optimum economic pipe diameter for non-Newtonian fluids, *J. Pipelines* (2):11–21.

Denn, M. M., 1980, *Process Fluid Mechanics*, Prentice-Hall, Englewood Cliffs, NJ.

Dodge, D. W. and Metzner, A. B., 1959, Turbulent flow of non-Newtonian systems, *AIChE J* 5(7):189–204.

Edwards, M. F., Jadallah, M. S. M., and Smith, R., 1985, Head losses in pipe fittings at low Reynolds numbers, *Chem. Eng. Res. Des.* 63:43–50.

Garcia, E. J. and Steffe, J. F., 1986, Review of friction factor equations for non-Newtonian fluids in pipe flow, Special Report, Department of Agricultural Engineering, Michigan State University, East Lansing, MI.

Garcia, E. J. and Steffe, J. F., 1986a, Optimum economic pipe diameter for pumping Herschel-Bulkley fluids in Raminar flow, *J. Food Proc. Eng.* 8(2):117–136.

Garcia, E. J. and Steffe, J. F., 1987, Comparison of factor equations for non-Newtonian fluids in tube flow, *J. Food Proc. Eng.* 9(2):93–120.

Griskey, R. G. and Green, R. G., 1971, Flow of dilatant (shear-thickening) fluids, *IAIChE J* 17(3):725–728.

Grovier, G. W. and Aziz, K., 1972, *The Flow of Complex Mixtures in Pipes*, R. E. Krieger, Malabar, FL.

Hanks, R. W., 1963, Laminar-turbulent transition of fluids with a yield stress, *AIChE J* 9(3):306–309.

Hanks, R. W., 1978, Low Reynolds turbulent pipe flow of pseudohomogenous slurries, Paper C-2 in Proc. 5th Int. Conf. on Hydraulic Transport of Solids in Pipes (Hydrotransport 5), Hanover, Federal Republic of Germany, May 8–11, BHRA Fluid Engineering, Cranfield, Bedford, England.

Houska, M., Sesrák, J., Jeschke, J., Adam, M., and Prida, J., 1988, in *Progress and Trends in Rheology, II*, Giesekus, H., Ed., Proceedings of the Second Conference of European Rheologists, Prague, June 17–20, 1986, pp 460–463, Springer-Verlag, New York.

Kittredge, C. P. and Rowley, D. S., 1957, Resistance coefficients for laminar and turbulent flow through one-half inch valves and fittings, *Trans. ASME* 79:1759–1766.

Lewicki, P. P. and Skierkowski, K., 1988, Flow of fruit and vegetable purees through pipelines, in *Progress and Trends in Rheology, II*, Giesekus, H., Ed., Proceedings of the Second Conference of European Rheologists, Prague, June 17–20, 1986, pp 443–445, Springer-Verlag, New York.

Lord. D. L., Hulsey, B. W., and Melton, L. L., 1967, General turbulent pipe flow scale-up correlation for rheologically complex fluids, *Soc. Petrol. Engrs. J.* 7(3):252–258.

Metzner, A. B., 1956, Non-Newtonian technology: fluid mechanics, mixing, heat transfer, in *Advances in Chemical Engineering*, Vol. 1, Drew, T. B. and Hoopes, J. W., Eds., Academic Press, New York.

Ofoli, R. Y., Morgan, R. G., and Steffe, J. F., 1987, A generalized rheological model for inelastic fluid foods, *J. Texture Stud.* 18(3):213–230.

Osorio, F. A. and Steffe, J. F., 1984, Kinetic energy calculations for non-Newtonian fluids in circular tubes, *J. Food Sci.* 49(5):1295–1296, 1315.

Rao, M. A. and Steffe, J. F., Eds., 1992, *Viscoelastic Properties of Foods*, Chapman and Hall, New York.

Rozema, H. and Beverloo, W. A., 1974, Laminar isothermal flow of non-Newtonian fluids in circular pipe, *Lebensmitt. Wissenschaft und Technologie* 7:223–228.

Sakiadis, B. C., 1984, Fluid and particle mechanics, in *Perry's Chemical Engineers' Handbook*, 6th ed., Sec. 5. Perry, R. H., Green, D. W., and Maloney, J. D., Eds., McGraw-Hill, New York.

Skelland, A. P. H., 1967, *Non-Newtonian Flow and Heat Transfer*, John Wiley and Sons, New York.

Steffe, J. F., 1984, Problems in using apparent viscosity to select pumps for pseudoplastic fluids, *Trans. ASAE* 27(2):629–634.

Steffe, J. F., 1992, *Rheological Methods in Food Process Engineering*, Freeman Press, East Lansing, MI.

Steffe, J. F., Mohamed, I. O., and Ford, E. W., 1984, Pressure drop across valves and fittings for pseudoplastic fluids in laminar flow, *Trans. ASAE* 27(2):616–619.

Steffe, J. F. and Morgan, R. G., 1986, Pipeline design and pump selection for non-Newtonian fluid foods, *Food Technol.* 40(12):78–85. [Addendum: *Food Technol.* 41(7):32].

Torrance, B. McK., 1963, Friction factors for turbulent non-Newtonian fluid flow in circular pipes, *South African Mech. Engr.* 13:89–91.

2 Sterilization Process Engineering

Hosahalli S. Ramaswamy and R. Paul Singh

CONTENTS

2.1 INTRODUCTION

Conventional thermal processing generally involves heating of foods packaged in hermetically sealed containers for a predetermined time at a preselected temperature to eliminate the pathogenic microorganisms that endanger the public health as well as those microorganisms and enzymes that deteriorate the food during storage. The original concept of in-container

sterilization of foods has come a long way since Nicholas Appert first introduced the art of canning in 1810 (Lopez, 1987). Today, the consumer demands more than the production of safe and shelf-stable foods and insist on high quality foods with convenient end use. High temperature-short time (HTST) and ultra-high temperature (UHT) techniques have been developed to minimize the severity of heat treatment and promote product quality. Aseptic processing and packaging further minimize the heat severity by quick heating and cooling of the food under aseptic conditions prior to packaging. Thin profile, thermostable, micro-wavable packages have been developed for promoting faster heat-transfer rates which minimizes the heat damage to product quality while adding the convenience of package micro-wavability. Whatever the specific procedure employed, it is essential to design a process which will deliver the required heat treatment to the food. In this chapter, the principles of thermal processing are detailed emphasizing the use of process calculation methods for establishing thermal processes.

2.2 PRINCIPLES OF THERMAL PROCESSING

Generally, thermal processing is not designed to destroy all microorganisms in a packaged product. Such a process would result in low product quality due to the long heating required. Instead, the pathogenic microorganisms in a hermetically sealed container are destroyed and an environment is created inside the package which does not support the growth of spoilage type microorganisms. In order to determine the extent of heat treatment, several factors must be known (Fellows, 1988): (1) type and heat resistance of the target microorganism, spore, or enzyme present in the food; (2) pH of the food; (3) heating conditions; (4) thermo-physical properties of the food and the container shape and size; and (5) storage conditions following the process.

Foods have different microorganisms and/or enzymes that the thermal process is designed to destroy. In order to determine the type of microorganism on which the process should be based, several factors must be considered. In foods that are vacuum packaged in hermetically sealed containers, low oxygen levels are intentionally achieved. Therefore, the prevailing conditions are not conducive to the growth of microorganisms that require oxygen (obligate aerobes) to create food spoilage or public-health problems. Further, the spores of obligate aerobes are less heat resistant than the microbial spores that grow under anaerobic conditions (facultative or obligate anaerobes). The growth and activity of these anaerobic microorganisms are largely pH dependent. From a thermal-processing standpoint, foods are divided into three pH groups: (1) high-acid foods (pH < 3.7; e.g., apple, apple juice, apple cider, apple sauce, berries, cherry (red sour), cranberry juice, cranberry sauce, fruit jellies, grapefruit juice, grapefruit pulp, lemon juice, lime juice, orange juice, plum, pineapple juice, sour pickles, sauerkraut, vinegar); (2) acid or medium-acid foods (3.7 < pH < 4.5; e.g., fruit jams, fruit cocktail, grapes, tomato, tomato juice, peaches, pimento, pineapple slices, potato salad, prune juice, vegetable juice); and (3) low-acid foods (pH > 4.5; e.g., all meats, fish, vegetables, mixed entries, and most soups).

With reference to thermal processing, the most important distinction in the pH classification is the dividing line between acid and low acid foods. Most laboratories dealing with thermal processing devote special attention to *Clostridium botulinum* which is a highly heat-resistant, rod-shaped, spore-forming, anaerobic pathogen that produces the *botulism* toxin. It has been generally accepted that *C. botulinum* does not grow and produce toxins below a pH of 4.6. Hence, pH 4.5 is taken as the dividing line between the low acid and acid groups such that, with reference to processing of acid foods (pH < 4.5), one need not be concerned with *C. botulinum*. On the other hand, in the low acid foods (pH > 4.5), the most heat-resistant spore former that is likely to be present and survive the process is *C. botulinum* which can thrive comfortably under the anaerobic conditions that prevail inside a sealed container to

produce the potent exotoxin. There are other microorganisms, for example *Bacillus stearo-thermophilus*, *B. thermoacidurans,* and *C. thermosaccolyaticum*, which are more heat resistant than *C. botulinum*. These are generally *thermophilic* in nature (optimal growth temperature ~ 50–55°C) and hence are not of much concern if the processed cans are stored at temperatures below 30°C.

The phrase 'minimal thermal process' was introduced by the US Food and Drug Administration in 1977 and defined as "the application of heat to food, either before or after sealing in a hermetically sealed container, for a period of time and at a temperature scientifically determined to be adequate to ensure the destruction of microorganisms of public health concern (Lopez, 1987). *C. botulinum* is the microorganism of public health concern in the low-acid foods and due to its high-heat resistance, temperatures of 115–125°C are commonly employed for processing these foods. With reference to the acid and medium-acid foods, the process is usually based on the heat-resistant spoilage-type vegetative bacteria or enzyme which are easily destroyed even at temperatures below 100°C. The thermal processes for such foods are therefore normally carried out in boiling water.

2.3 THERMAL RESISTANCE OF MICROORGANISMS

The first step prior to establishing thermal processes is identification or designation of the most heat-resistant or target microorganism/enzyme on which the process should be based. This requires the microbiological history of the product and conditions under which it is subsequently stored rendering it somewhat product specific. The next step is evaluation of thermal resistance of the test microorganism which must be determined under the conditions that normally prevail in the container. In order to use thermal destruction data in process calculation, they must be characterized using an appropriate model. Further, since packaged foods cannot be heated to process temperatures instantaneously, data on the temperature dependence of microbial destruction rate is also needed to integrate the destruction effect through the temperature profile under processing conditions. The various procedures employed for experimental evaluation of thermal destruction kinetics of microorganisms are summarized in Stumbo (1973) and Pflug (1987).

2.3.1 SURVIVOR CURVE AND D VALUE

Published results on thermal destruction of microorganisms generally show that they follow a first-order reaction indicating a logarithmic order of death. In other words, the logarithm of the number of microorganisms surviving a given heat treatment at a particular temperature plotted against heating time (survivor curve) will give a straight line (Figure 2.1). The microbial destruction rate is generally defined in terms of a decimal reduction time (D value) which is the heating time in minutes at a given temperature required to result in one decimal reduction in the surviving microbial population. In other words, D value represents a heating time that results in 90% destruction of the existing microbial population. Graphically, this represents the time between which the survival curve passes through one logarithmic cycle (Figure 2.1).

Mathematically

$$D = \left(t_2 - t_1\right)/\left[\log(a) - \log(b)\right] \tag{2.1}$$

where a and b represent the survivor counts following heating for t_1 and t_2 min, respectively. The logarithmic nature of the survivor or destruction curve indicates that complete destruction of the microbial population is not a theoretical possibility, since a decimal fraction of the population should remain even after an infinite number of D values. In practice, calculated
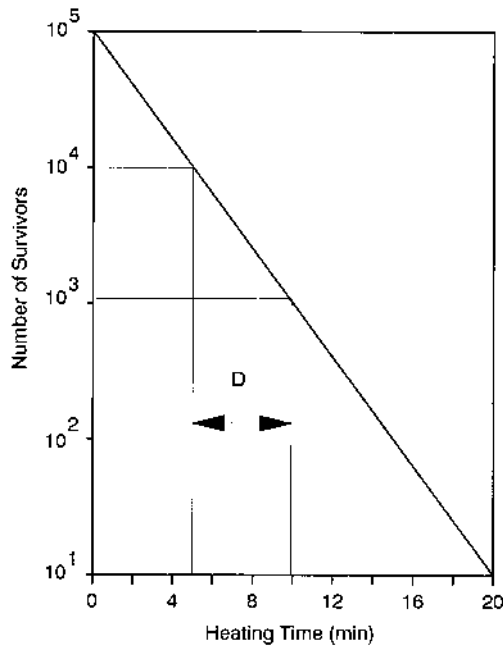
FIGURE 2.1 Typical survivor curve.

fractional survivors are treated by a probability approach; for example, a surviving population of 10^{-8}/unit would indicate one survivor in 10^8 units subjected to the heat treatment.

Traditionally, in thermal processing applications, survivor curves are plotted on specially constructed semilog papers for easy handling and interpretation of results. The survivor counts of microorganisms are plotted directly on the logarithmic ordinate against time on the linear abscissa. The time interval between which the straight line portion of the curve passes through a logarithmic cycle is taken as the D value. In engineering approaches, one can prepare a log N vs. t computer graph on spreadsheet and run a linear regression of log N on t in the range in which the points represent a reasonable straight line. The negative reciprocal slope of such a regression equation for the straight line gives the D value. Visual observation of data points prior to regression is desirable for proper selection of the regression range.

2.3.2 THERMAL DEATH TIME (TDT) AND D VALUE

In food microbiology, another term, namely thermal death time (TDT), is commonly employed which somewhat contradicts the logarithmic-destruction approach. TDT is the heating time required to cause complete destruction of a microbial population. Such data are obtained by subjecting a microbial population to a series of heat treatments at a given temperature and testing for survivors. TDT then represents a time below the shortest destruction and the longest survival times. The difference between the two are sequentially reduced and/or geometrically averaged to get an estimate of TDT. The "death" in this instance generally indicates the failure of a given microbial population, after the heat treatment, to show a positive growth in the subculture media. Comparing TDT approach with the decimal reduction approach, one can easily recognize that the TDT value depends on the initial microbial load (while D value does not). Further, if TDT is always measured with reference to a standard initial load or load reduction, it simply represents a certain multiple of D value. For example, if TDT represents the time to reduce the population from 10^9 to 10^{-3}, then TDT is a measure of 12 D values. In other words
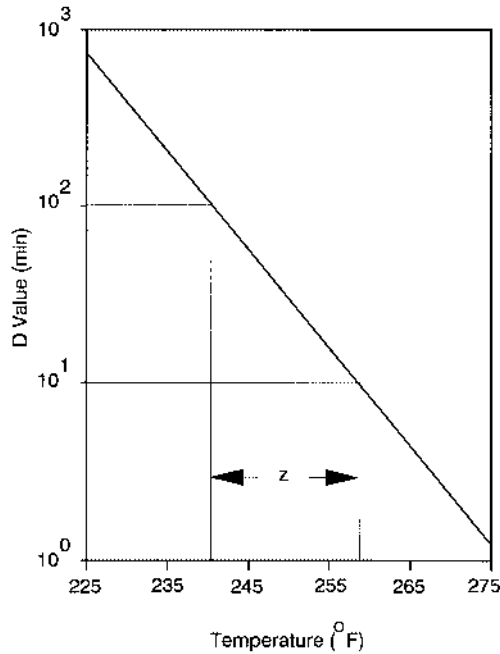
FIGURE 2.2   A typical thermal resistance curve.

$$TDT = n\,D \qquad\qquad (2.2)$$

where n is the number of decimal reductions.

It should be noted that there are several causes for deviations in the logarithmic behavior of the survivor curve. Generally, there is a lag at the start of the heating period when first-order behavior doesn't fit the observed data and frequently, deviation from first order also occurs at the tail end of the survivor curve referred to as "tailing". In his book *Thermobacteriology in Food Processing*, Stumbo (1973) has detailed several factors causing apparent deviations of the logarithmic order of microbial death showing typical survivor curves for each situation: (1) heat activation for spore germination; (2) mixed flora; (3) clumped cells; (4) flocculation during heating; (5) deflocculation during heating; (6) nature of the subculture medium; and (7) anaerobiosis. Stumbo (1973) has also summarized the various factors that influence the thermal resistance of bacteria: conditions present during sporulation (temperature, ionic environment, organic compounds, lipids, age, or phase of growth) and conditions present during heat treatment (pH and buffer components, ionic environment, water activity, composition of the medium).

2.3.3   TEMPERATURE DEPENDENCE AND z VALUE

The D value depends strongly on the temperature with higher temperatures resulting in smaller D values. The temperature sensitivity of D values at various temperatures is normally expressed as a thermal resistance curve with log D values plotted against temperature (Figure 2.2). The temperature sensitivity indicator is defined as z, a value which represents a temperature range which results in a ten-fold change in D values or, on a semilog graph, it represents the temperature range between which the D value curve passes through one logarithmic cycle. Using regression techniques, z value can be obtained as the negative reciprocal slope of the thermal resistance curve (regression of log D values vs. temperature).
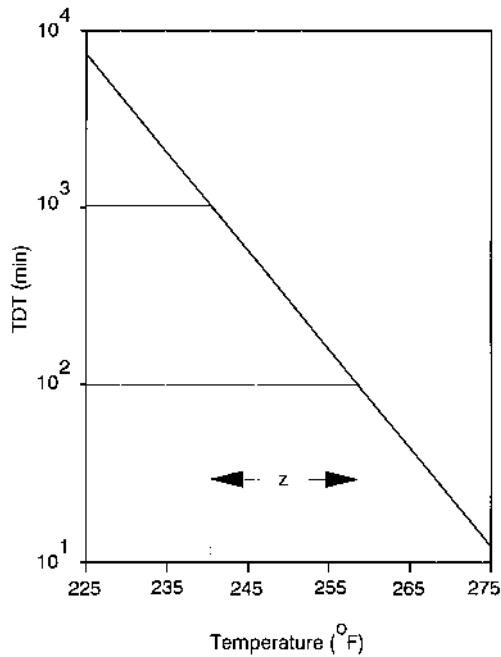
FIGURE 2.3 A typical TDT curve.

Mathematically

$$z = (T_2 - T_1) \big/ \big[\log(D_1) - \log(D_2)\big] \tag{2.3}$$

where D_1 and D_2 are D values at T_1 and T_2, respectively.

The D value at any given temperature can be obtained from a modified form of the above equation using a reference D value (D_o at a reference temperature, T_o, usually 250°F for thermal sterilization)

$$D = D_o \, 10^{(T_o - T)/z} \tag{2.4}$$

Equation 2.3 also can be written with reference to TDT values and the z value can be obtained from

$$z = (T_2 - T_1) \big/ \big[\log(TDT_1) - \log(TDT_2)\big] \tag{2.5}$$

where TDT_1 and TDT_2 are TDT values at T_1 and T_2, respectively. Graphically, as with the D value approach, the z value can be obtained as the negative reciprocal slope of log TDT vs. temperature curve (Figure 2.3; TDT curve). When using this approach, it is advisable to plot the longest survivor times and shortest destruction times (on logarithmic scale) vs. temperature (linear scale). The regression line could be based on the evaluated TDT as described earlier. As is noted in Pflug (1987) it will be necessary to make sure that the TDT curve is above all survivor data points (higher in temperature or longer in time). The TDT curve should be parallel to the general trend of the survival and destruction points.

2.3.4 Reaction Rate Constant (k) and Activation Energy (E_a)

The first-order rate thermal destruction of microorganisms is also sometimes expressed in terms of a reaction rate constant, k, obtained from the first-order model:

$$\log_e\left(N/N_o\right) = -kt \qquad (2.6)$$

which simplifies to

$$k = D/2.303 \qquad (2.7)$$

Several theories have suggested different models that relate the effect of temperature to reaction rates. The most well known and perhaps most frequently used theory in the area of biological engineering is that proposed by Arrhenius which is applicable to reactions in solutions and heterogeneous processes. Using a thermodynamic approach, Arrhenius suggested that in every system, at any instant of time there is a distribution of energy level among the molecules (Figure 2.4). For a molecule to enter into a reaction, it must possess a certain minimal amount of energy, which is called the activation energy (E_a). The mean of the frequency distribution of molecule energy levels is a function of temperature (Figure 2.4). The probability that a molecule will possess energy in excess of an amount, E_a, per mole at temperature T (absolute) is $e^{-E_a/RT}$ (where R = universal gas constant) (Figure 2.5). For a reaction to occur, molecules that are capable of reacting and have energy at or greater than E_a must encounter each other. Thus, according to Arrhenius, if the collision frequency of the molecule is given by k_o, the dependence of the reaction rate (k) on the absolute temperature (T) is

$$k = k_o e^{-E_a/RT} \qquad (2.8)$$

An Arrhenius plot is constructed by plotting the natural logarithm of reaction rate constant vs. the reciprocal of absolute temperature. A typical Arrhenius plot is shown in Figure 2.5 and the E_a can be calculated from such a plot as ($-$slope) $\times$ R. A frequent argument is made that the Arrhenius model is superior to the z-value model (Bigelow model) because the z value is temperature dependent where E_a is not. Comparisons probably cannot be made that simply, but it should be noted that while E_a is usually assumed to be constant, from absolute-rate and collision theory, we learn that the plot of lnk vs. 1/T will not always give a straight line. Several researchers have shown that either of the two methods can be used in thermal processing applications. Generally the z value is related to E_a using the equation

$$E_a = 2.303 RT^2/z \qquad (2.9)$$

where E_a is the activation energy, R is the universal gas constant, and T is the absolute temperature. However, caution should be exercised when converting z value to E_a or vice versa because it has been shown that errors associated with interconversion of E_a and z are functions of the selected reference temperature and the temperature range used (Ramaswamy et al. 1989). This discrepancy can be minimized by replacing T^2 with the product of the minimum (T_{min}) and maximum temperature (T_{max}) of the temperature range between which kinetic data were obtained (i.e., $T^2 = T_{min} \cdot T_{max}$).
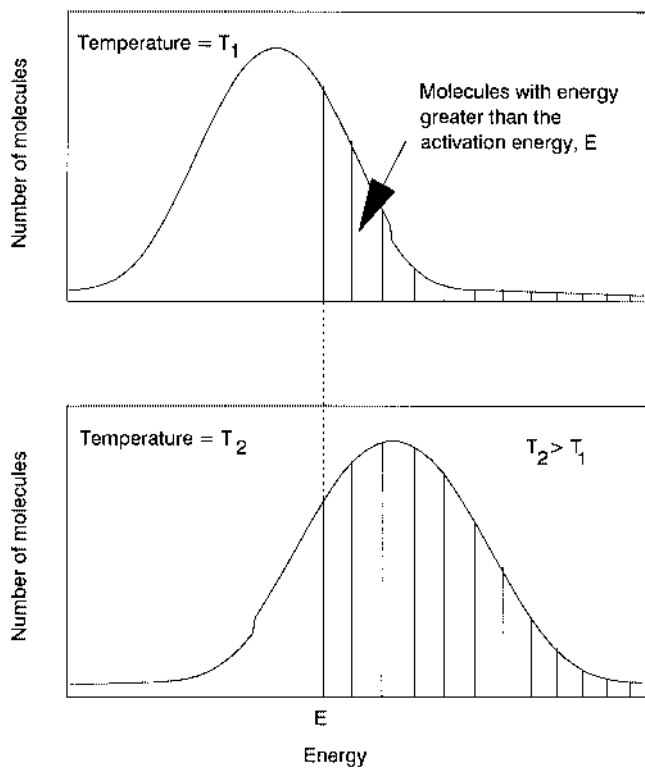
FIGURE 2.4 Energy distribution in a population of molecules.
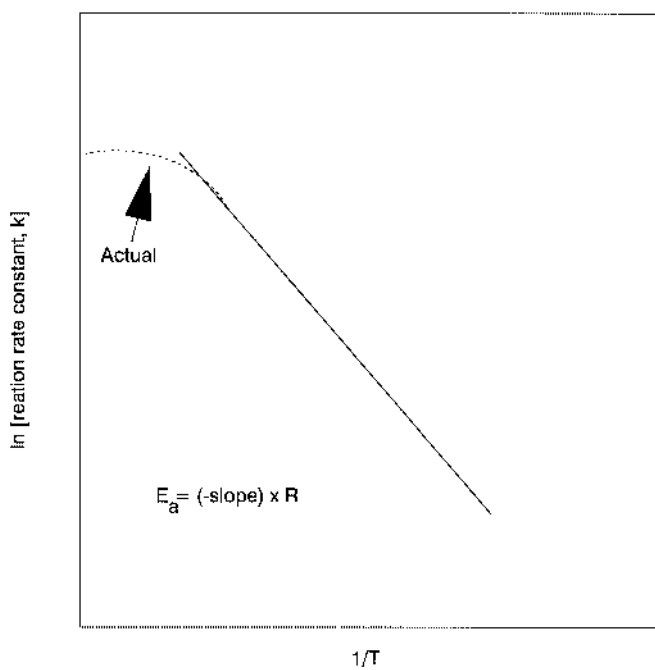
FIGURE 2.5 Typical Arrhenius plot: ln(k) vs. reciprocal absolute temperature.

2.3.5 LETHALITY CONCEPT

Lethality (F value) is a measure of the heat treatment or sterilization processes. In order to compare the relative sterilizing capacities of heat processes, a unit of lethality needs to be established. For convenience, this is defined as an equivalent heating of 1 min at a reference temperature, which is usually 250°F (121.1°C) for the sterilization processes. Thus, the F value would represent a certain multiple or fraction of D value depending on the type of microorganism; therefore, a relationship like Equation 2.5 also holds with reference to F value

$$F = F_o 10^{(T_o - T)/(1}$$ (2.10)

The F_o in this case will be the F value at the reference temperature (T_o). A reference (or phantom) TDT curve is defined as a curve parallel to the real TDT or thermal resistance curve (i.e., having the same z value) and having a TDT (F value) of 1 min at 250°F. With a phantom TDT curve so defined, it will be possible to express the lethal effects of any time-temperature combination in terms of equivalent minutes at 250°F or lethality.

$$\text{Lethality or } F_o = F \, 10^{(T - T_o)/z}$$ (2.11)

Thus, an F value of 10 min at 240°F is equivalent to an F_o of 2.78 min while the F value of 10 min at 260°F is equivalent to an F_o of 35.9 min when z = 18°F. In these situations, it is assumed that the heating to the appropriate temperatures and the subsequent cooling are instantaneous. For real processes where the food passes through a time-temperature profile, it should be possible to use this concept to integrate the lethal effects through the various time-temperature combinations. The combined lethality so obtained for a process is called the process lethality and is also represented by the symbol F_o. Further, with reference to the processing situation, the lethality can be expressed as related to a specific location (normally thermal center) or any other arbitrarily chosen location or a sum of lethality at all points inside a container. In terms of microbiological safety, the assurance of a minimal lethality at the thermal center is of utmost importance, while from a quality standpoint it is desirable to minimize the overall destruction throughout the container.

The criterion for the adequacy of a process must be based on two microbiological considerations: (1) destruction of the microbial population of public health significance; (2) reduction in the number of spoilage-causing bacteria. For low-acid foods, the microorganism of public health significance is *C. botulinum* and hence destruction of the spores of this organism is used as the minimal criterion for processing. Once again, it has been arbitrarily established that the minimum process should be at least as severe to reduce the population of *C. botulinum* through 12 decimal reductions (*bot cook*). Based on published information, a decimal reduction time of 0.21 min at 250°F (Stumbo, 1973) is normally assumed for *C. botulinum*. A twelve-decimal reduction would thus be equivalent to an F_o value of $12 \times 0.21 = 2.52$ min. The minimal process lethality (F_o) required is therefore 2.52 min. Several low-acid foods are processed beyond this minimum value. An F_o value of 5 min is perhaps more common for these foods. The reason for this is the occurrence of more heat-resistant spoilage-type microorganisms which are not of public health concern. The average D_o for these spoilage microorganisms may be as high as 1 min. An F_o value of 5 min would then be adequate only to achieve a 5 D process with reference to these spoilage microorganisms. It is therefore essential to control the raw-material quality to keep the initial count of these organisms below 100 per container on an average, if the spoilage rate were to be kept below one can in a thousand (10^2 to $10^{-3} = 5D$).

2.4 HEAT TRANSFER RELATED TO THERMAL PROCESSING

The rate of heating of an object or a product in a container is a function of the geometry of the object or container, its physical properties, and the heat-transfer characteristics of the object or the container. There are three possible mechanisms of heat transfer to a thermally processed food product: (a) conduction, (b) convection, or (c) broken heating (which is a sequential combination of conduction and convection or convection and conduction). The nature or consistency of a food or pharmaceutical product, the presence of particles, and the use of thickening agents and sugars in the covering liquid are some of the factors that determine whether the product heats by convection or by conduction.

When we heat or cool objects or products in containers, we are dealing with unsteady-state heat-transfer processes. Unsteady-steady state heat transfer is mathematically quite complex; however, once the equations have been derived or developed they can be simplified so their use is not difficult. Such simplification procedures that are extremely useful in dealing with heat-transfer processes in the food sterilization area have been developed and well documented (Ball and Olson, 1957). The following are brief mathematical analyses of both conduction and convection unsteady-state heat transfer conditions.

2.4.1 CONDUCTION HEAT TRANSFER

2.4.1.1 Steady-State Conduction

Fourier's law is the fundamental differential equation for heat transfer by conduction:

$$dQ/dt = -k\ A\ dt/dx \tag{2.12}$$

where dQ/dt is the rate of flow of heat, A is the area of cross section perpendicular to the direction of heat flow, and $-dT/dx$ is the rate of change of temperature with distance in the direction of the flow of heat, i.e., the temperature gradient. The factor, k, is the thermal conductivity and is a property of the material through which the heat is flowing.

For the steady flow of heat, the term dQ/dt is constant and may be replaced by q (rate of heat flow, BTU/h or W). If k and A are independent of temperature (T) and distance (x), the above equation becomes:

$$q = k\ A\ \Delta T/x \tag{2.13}$$

2.4.1.2 Unsteady-State Conduction

In unsteady-state conduction, temperature changes with time and solutions-to-heat transfer equations get more complicated. The governing partial-differential equation for unsteady-state conduction heating involving a three-dimensional (3D) body is given by

$$[\partial T/\partial t] = \alpha\left[\left(\partial^2 T/\partial x^2\right) + \left(\partial^2 T/\partial y^2\right) + \left(\partial^2 T/\partial z^2\right)\right] \tag{2.14}$$

where T is the product temperature, t is the time, x, y, and z are the distances in the x, y, and z directions, and α is the thermal diffusivity. The assumptions associated with the above equation are as follows: (1) the product temperature is uniform at the start of heating; (2) the surface temperature of the 3D body is constant after the start of heating; (3) the product thermal diffusivity α is constant with time, temperature, and position in the body. Examples of conduction-heated foods are tightly packaged solid products or highly viscous liquid/semi-solid foods such as vegetable puree, meat ball in gravy, etc.

2.4.1.3 Solution to Unsteady-State Heat Transfer Problem Using a Spherical Object as an Example

The partial differential equation involving a sphere in spherical coordinates is

$$[\partial T/\partial t] = \alpha\left[(\partial^2 T/\partial r^2) + (2/r)(\partial T/\partial r)\right] \tag{2.15}$$

where r represents the radius of the sphere. The solution for the spacial temperature in the form of an infinite summation series is given by

$$\left[(T_1 - T)/(T_1 - T_i)\right] =$$
$$\sum_{i=1}^{n}\left[2(\sin\beta_i - \beta_i\cos\beta_i)/(\beta_i - \sin\beta_i\cos\beta_i)\right]\left[\{\sin(\beta_i\,x/r)\}/(\beta_i\,x/r)\right]\exp\left[-\beta_i^2\alpha t/r^2\right] \tag{2.16}$$

where x represents the radial location and β_i is the ith root of the equation

$$Bi = 1 - \beta_i\cot\beta_i \tag{2.17}$$

It has been generally recognized that after a short heating time [i.e., Fourier number (F_o), $\alpha t/r^2 \geq 0.2$], the above series will rapidly converge to just the first term. Thus, the first term approximation can be written as

$$\left[(T_1 T)/(T_1 - T_i)\right] =$$
$$\left[2(\sin\beta_1 - \beta_1\cos\beta_1)/(\beta_1 - \sin\beta_1\cos\beta_1)\right]\left[\{\sin(\beta_1\,x/r)\}/(\beta_1\,x/r)\right]\exp\left[-\beta_1^2\,\alpha t/r^2\right] \tag{2.18}$$

and

$$Bi = 1 - \beta_1\cot\beta_1 \tag{2.19}$$

In most thermal processing applications, the heating behavior is characterized by a heating rate index, f_h, and a lag factor, j_{ch} (explained in detail in a later section). Representing f_h and j_{ch} by the following expressions (Equations 2.20 and 2.21), the equation for the temperature distribution in the sphere can be written as shown in Equation 2.22.

$$\left[(T_1 - T)/(T_1 - T_i)\right] = j_{ch}10^{-t/f_h} \tag{2.20}$$

$$j_{ch} = \left[2(\sin\beta_1 - \beta_1\cos\beta_1)/\beta_1 - \sin\beta_1\cos\beta_1\right]\left[\{\sin(\beta_1\,x/r)\}/(\beta_1\,x/r)\right] \tag{2.21}$$

$$f = \left[\beta_1^2\alpha/2.303\,r^2\right] \tag{2.22}$$

Details of the equations related to the other geometries can be found in Ball and Olson (1957).

2.4.2 Convection Heat Transfer

Convection heat transfer involves the transfer of heat from one location to the other through the actual movement or flow of a fluid. When the fluid flow involved is produced wholly by differences in fluid density as a result of changes in temperature, the heat transfer is called natural convection and if the fluid flow is aided by pumping/fan or some other type of mechanical device, the heat transfer is called forced convection. Since heat transfer by convection involves fluid flow and heat energy changes, to a great extent, it defies rigorous analysis. However, since convection heat transfer is extremely important in most processes, procedures for the engineering analysis and models have been developed by empirical methods.

2.4.2.1 Steady-State Convection Heat Transfer

There are many examples in the natural environment where heat transfer by convection takes place on a steady-state basis. In these systems, the rate of heat flow is constant and or quantity of heat flow is straight forward and simple compared to unsteady-state heat transfer.

2.4.2.2 Unsteady-State Convection Heat Transfer

In unsteady-state convection heat transfer in enclosed areas or confined volumes of fluid, the temperature at all locations changes with time. The rate of fluid flow inside the enclosed volume is determined by product characteristics including viscosity; however, the rate of heat transfer from or to an external source through the walls of the container will have a major effect on the rate of heating or cooling of the fluid inside the container. The thickness of the boundary layer between the flowing fluid and the wall is a critical factor in the heat transfer rate. This stagnant layer or transition velocity zone offers significant resistance to heat transfer. Therefore, in convection heat-transfer processes the wall-to-fluid film coefficient must be evaluated. Empirical expressions have been used for calculating the film coefficient for different fluids under different physical conditions. The equation that follows describes the rate of heat flow across the wall into or out of the container.

$$dQ/dt = UA(T_1 - T) \qquad (2.23)$$

where U is the overall heat transfer coefficient. In the heating of fluids in enclosures or confined volumes, the change in the quantity of heat in the fluid per unit of time is a function of the mass of the fluid (density, ρ, times volume, V), the specific heat (C_p), and the mean temperature, T. If we assume ideal thermal convection inside the container of product, these variables can be related using the following equation

$$dQ/dt = \rho \, C_p V \, dT/dt \qquad (2.24)$$

The solution to the unsteady-state convection heat-transfer problem is usually obtained from Newton's law: based on the assumption that the heat flowing into a container is absorbed by the contents, a temperature change of the product results. Combining Equations 2.23 and 2.24, we can write

$$U \, A(T_1 - T) = \rho \, C_p \, V \, dT/dt \qquad (2.25)$$

Separating the variables and integrating over temperature and time, we get

$$\left(T_1 - T\right)\big/\left(T_1 - T_i\right) = e^{-U\,A\,t/(\rho\,Cp\,V)} \tag{2.26}$$

or

$$\left(T_1 - T\right)\big/\left(T_1 - T_i\right) = 10^{-U\,A\,t/(2.303\,\rho\,Cp\,V)} \tag{2.27}$$

or, in terms of temperature and time

$$\left(T_1 - T\right)\big/\left(T_1 - T_i\right) = 10^{-[U\,A/(2.303\,\rho\,Cp\,V)]t} \tag{2.28}$$

Replacing the constant in the parentheses with $(1/f_h)$, we get the shortened form of the equation

$$\left(T_1 - T\right)\big/\left(T_1 - T_i\right) = 10^{-t/f_h} \tag{2.29}$$

which is similar to the one we obtained for conduction with $j_{ch} = 1.0$. It should be noted that Equation 2.29 was derived assuming that the system complies with Newton's Law of heating/cooling. Convection heating under these ideal conditions implies at time-zero a step change in the heating-medium temperature and an instantaneous surface response to the new temperature. Under ideal conditions, there will be no temperature gradients inside the body. These conditions occur only in a unit of infinitely small volume. The associated Biot number will be zero.

The heating characteristics in a container may be very different in agitated systems (forced convection) compared to nonagitating systems (natural convection). There is only slight deviation in heating characteristics of agitating systems compared to an idealized system. For practical purposes, in the agitated container, a flow pattern already exits at the time heating begins. All the resistance to heat transfer and the resulting temperature gradient is in the stagnant layer of the product adjacent to the wall. There is essentially no temperature gradient in the bulk contents. On the other hand, in the still (nonagitated) container, a finite time period is required for the establishment of the temperature-induced flow pattern. Temperature gradients continue to exist in the bulk of the fluid even after the flow pattern has been established. For these natural-convection systems the driving force for fluid flow decreases as the temperature gradient decreases and the system approaches heating-medium temperature. This phenomenon tends to cause the f_h-value to increase with heating time. This, in turn, may affect the intercept value of the heating curve, especially if data points collected at longer heating times are heavily weighed.

It has been generally recognized that it is convenient to treat experimental-heating or -cooling data using the f and j concept advocated by Ball (1923) and use it as a data fitting tool for both conduction and convection heating foods. This concept is explained in greater detail in the next section.

2.4.3 CHARACTERIZATION OF HEAT PENETRATION DATA

In order to establish thermal process schedules, information on the temperature history of the product going through the process is needed in addition to thermal resistance characteristics of the test microorganism (z and F_o). The temperature history of the product undergoing the process depends on several factors: (1) the heating process (sill vs. agitated cook; in-package vs. aseptic processing); (2) the heating medium (steam, water (immersion or spray) with or without air over pressure, steam/air mixtures); (3) the heating conditions (retort

temperature, initial temperature, loading pattern); (4) the product type (solid, semisolid, liquid, particulate liquid; thermophysical properties of the product); and (5) the container type, shape, and size.

Thermal processing may be applied to packaged foods as in the conventional way (canning for example) or foods may be heated and cooled, filled into sterile packages and sealed, all under aseptic conditions (aseptic processing). The latter permits rapid heating and cooling of the product as well as processing under HTST conditions, and, hence, generally offer a better quality product. Container agitation during processing promotes better mixing of the contents which results in a rapid and uniform heating of the product. Agitated processes therefore result in shorter process times and offer better quality retention. The principles of processing which follows this section is equally applicable for aseptically packaged foods as well as those processed in agitating retorts.

Although conduction is the mode of heat transfer in solids and convention in liquids, packaged foods heat neither by pure conduction nor by pure convection. The tightly packed solid foods and the heavy viscous type products, which exhibit after an initial lag, a semi-logarithmic straight-line heating curve, are commonly referred to as conduction-heating foods. These products do not move within the container during heating or cooling. Likewise, liquid products, light-consistency products, and liquid foods containing loosely packed particulates, which also exhibit semilogarithmic curves but generally of much steeper slope, are referred to as convection-heating foods. The products in this group are generally in continuous motion, characteristic of convection heating, during both heating and cooling. Between these two are those products which exhibit a broken-heating behavior; these foods generally heat by convection to start with and change to conduction type beyond a certain temperature. Products containing starch or other thickening agents typically exhibit this type of behavior due to gelatinization of starch at higher temperature.

In order to gather time-temperature data during heat processing, the thermocouple (the most common temperature measuring device) is generally placed at the geometric center of the cylindrical container for foods of the type heated by conduction and placed along the vertical axis about $\frac{1}{10}$ height from the bottom for the type heated by convection. Simple time-temperature curves during heating and cooling of conduction and convection heating type are shown in Figure 2.6. The General and Improved General methods of process calculation make use of this type of data. On the other hand, most Formula methods, make use of heat penetration data (f_h and j_{ch}) obtained from a plot of the logarithm of the temperature difference between the retort (T_r) and the product (T) [i.e., log ($T_r - T$)] vs. heating time (on linear abscissa) as shown in Figure 2.7. This can also be obtained by plotting the ($T_r - T$) data on a semilogarithmic paper (temperature difference on log scale and time on linear scale). The heating rate index, f_h, is then obtained as the time taken for the straight-line portion of the curve to pass through one log cycle and j_{ch} is obtained as the ratio of ($T_r - T_{pih}$) and ($T_r - T_i$). In thermal process calculations, this plotting has been further simplified by using a special plotting routine which permits the plotting of temperatures directly rather than the temperature difference as mentioned earlier. This is accomplished by rotating the semilog paper through 180° and setting the top line "one degree below the retort temperature", then plotting temperatures directly (this will result in the exact same semilogarithmic plot, but represented upside down).

A similar plot of log ($T - T_w$) which is the temperature difference between the product and the cooling water temperature vs. cooling time (Figure 2.8) is used to get the cooling parameters. For semilogarithmic plotting of the cooling curve, the semilog paper is kept in the normal position, and the bottom line is marked "one degree above the cooling water temperature" and the temperatures are plotted directly.
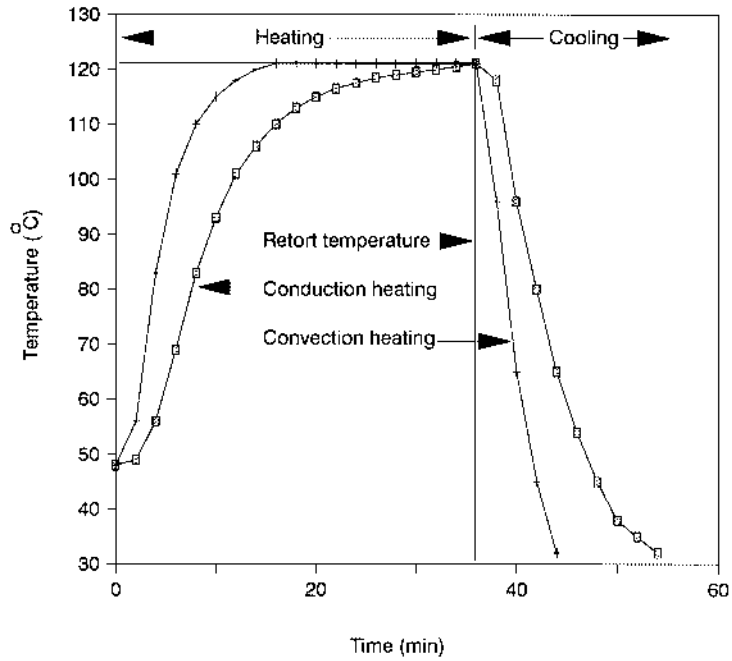
FIGURE 2.6 Heat penetration profiles of conduction and convection heating foods.
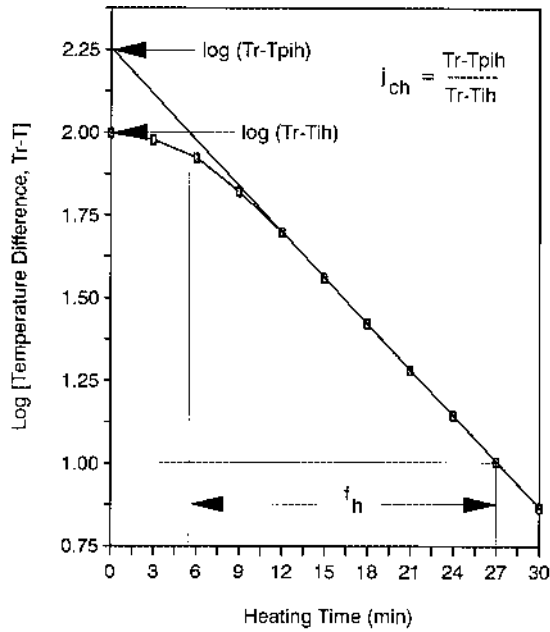
FIGURE 2.7 Heating curve and heating parameters.
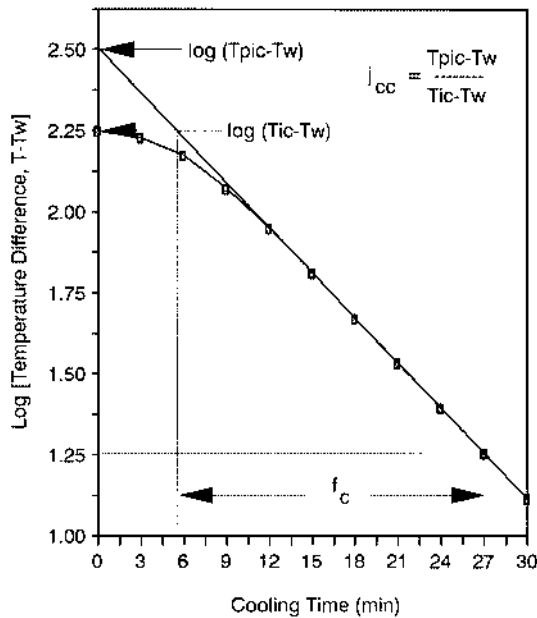
FIGURE 2.8 Cooling curve and cooling parameters.

2.4.4 HEAT PENETRATION PARAMETERS

The following data are normally obtained from the heat penetration curves and heating conditions for calculation purposes.

T_{ih} Initial food temperature when heating is started

T_{ic} Food temperature when cooling is started

T_r Retort temperature

T_w Cooling water temperature

I_h Difference between the retort temperature and food temperature at the start of the heating process $(T_r - T_{ih})$

I_c Difference between the cooling water temperature and food temperature at the start of the cooling process $(T_{ic} - T_w)$

g Difference between the retort temperature and food temperature (T) at time t, $(T_r - T)$

g_c The value of g at the end of heating or beginning of cooling $(T_r - T_{ic})$

f_h Heating rate index; the time required for the straight line portion of the heating curve (Figure 2.7) to pass through one log cycle; also the negative reciprocal slope of the heating rate curve

f_c Cooling rate index; the time required for the straight line portion of the cooling curve (Figure 2.8) to pass through one log cycle; also the negative reciprocal slope of the cooling rate curve

l Come-up period; in batch processing operations, the retort requires some time for reaching the operating condition; the time from steam to when the retort reached T_r is called the come-up period

$0.58\,l$ Effective beginning of the process; the retort come-up period varies from one process to the other and from one retort to the other; in process evaluation procedures, about 42% of this come-up period is generally considered as time at retort temperature because the product temperature increases even during this period; in order to accommodate this, the effective beginning of the process is moved left a distance "$0.42\,l$" from the time the retort reached T_r or moved right $0.58\,l$ from the time of steam.

T_{pih}	Pseudo-initial temperature during heating; temperature indicated by the intersection of the extension of the heating curve and the vertical line representing the effective beginning of the process (0.58 l)
T_{pic}	Pseudo-initial temperature during cooling; temperature indicated by the intersection of the extension of the cooling curve and the vertical line representing the start of cooling
j_{ch}	Heating rate lag factor; a factor which, when multiplied by I_h, locates the intersection of the extension of the straight-line portion of the semilog heating curve and the vertical line representing the effective beginning of the process (0.58 l) = $(T_r - T_{pih})/(T_r - T_{ih})$
j_{cc}	Cooling rate lag factor; a factor which when multiplied by I_c, locates the intersection of the extension of the straight-line portion of the semilog cooling curve and the vertical line representing start of the cooling process = $(T_w - T_{pic})/(T_w - T_{ic})$
B	Thermal process time; Ball-corrected for come-up period (steam on to steam off minus 0.58 l).
P_t	Operator's process time (time after come-up period; $P_t = B - 0.42\ l$)

2.4.5 THE RETORT COME-UP TIME

Autoclaves or retorts do not reach the specified operating temperature immediately after the steam is turned on, but require a measurable heating time until they reach operating temperature. The time measure from steam-on until the unit reaches the specified operating temperature is called the "come-up period" (differently denoted as l, CUT [come-up time], or t_c). In carrying out a heat penetration test and analyzing the resulting data, the come-up period of the heating equipment is an important parameter that must be recorded. It is used at a later time to establish the corrected zero of the test. The come-up time should always be as short as possible. However, the relative magnitude of CUT and f_h will determine if the measured f_h values are meaningful.

In processes where water is used as the heating medium, if CUT is long and the size of the container is small, meaningful f_h and j values for the product-container unit cannot always be obtained. To have the results of a heat penetration test yield meaningful f_h and j_{ch} values, the CUT should preferably be less than 0.5 f_h.

The objective of the heat penetration test is to obtain data for the product-container system that can be used to design a sterilization process. We can, to a large degree, eliminate the effect of CUT on the f_h value by noting when the autoclave or retort reaches the processing temperature and discounting the temperature data before drawing the f_h line. Correcting the j_{ch} value for the effect of CUT is more involved and requires the establishment of the effectiveness of the CUT or the corrected zero of the process.

Ball (1923) evaluated the effect of retort CUT in terms of time at the final operating temperature. Ball reported that 42% of the aggregate CUT could be considered as the time at the operating temperature. Although considered very conservative, especially while processing thin profile containers and other fast heating containers, the use of the above effectiveness is still the industry standard. Figure 2.9 shows an example in which the t_c is 5 min, of which only 2 min (42%) is taken as the time during which the retort is assumed to be operating at the normal operating temperature of 121°C.

The true j value of a product-container unit is for the ideal condition where at time zero, the retort is turned on and is immediately at the operating temperature. In our example, the autoclave reaches the operating temperature of 121°C after 5 min and remains at this temperature throughout the remainder of the process. The CUT correction indicates that 2 min of the 5-minute CUT can be considered time at the heating-medium temperature. The net result is replacement of the first 5 min, the CUT in this example, with $0.42 \times t_c$, which means neglecting the first $0.58 \times t_c$. Therefore, in this example, the corrected zero is 2 min before the time when the retort reached the operating temperature or at 3 min after turning on the steam.
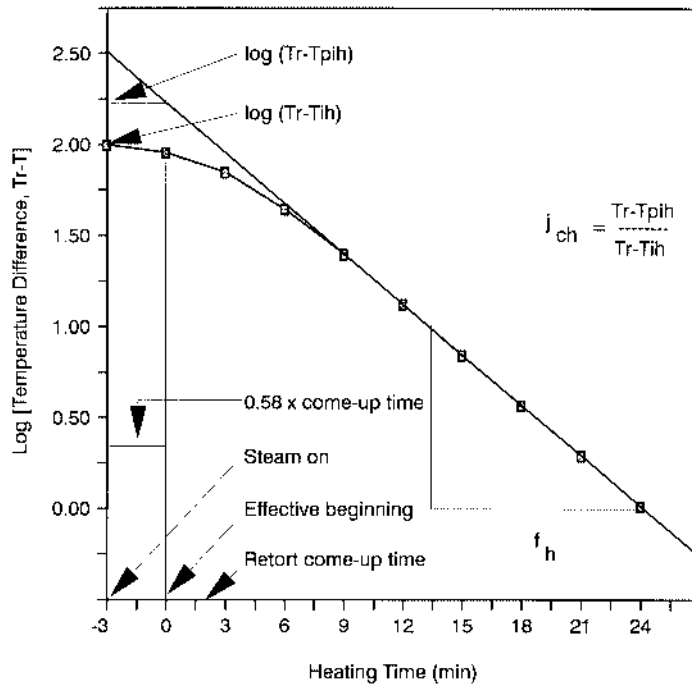
FIGURE 2.9 Semilogarithmic heating curve showing come-up time correction.

The value of $T_r - T_{pih}$ used in the j_h-value calculation is the intercept of the straight-line asymptote to the heating curve (f_h-value line) extended to zero time (or start of the process). In calculating the corrected j_h value, $T_r - T_{pih}$ should be obtained as the intercept at the corrected zero time as shown in Figure 2.10. As can be seen from the figure, f_h is not influenced by CUT as long as CUT is kept relatively short .

2.5 THERMAL PROCESS CALCULATIONS

The purpose of the thermal process calculations is to arrive at an appropriate process time under a given set of heating conditions to result in a given process lethality, or alternately to estimate the process lethality of a given process. The method used must accurately integrate the lethal effects of the transient temperature response of the food undergoing the thermal processes with respect to test microorganism of both public health and spoilage concern. The desired degree of lethality in terms of an equivalent time at a reference temperature (F_o) is generally pre-established and processes are designed to deliver a minimum of this preset value at the thermal center. The process calculation methods are broadly divided into two classes: (1) General methods and (2) Formula methods. The General methods integrate the lethal effects by a graphical or numerical integration procedure based on the time-temperature data obtained from test containers processed under actual commercial processing conditions. Formula methods, on the other hand, make use of parameters obtained from these heat-penetration data together with several mathematical procedures to integrate the lethal effects.

2.5.1 THE ORIGINAL GENERAL METHOD

This method originally described by Bigelow et al. (1920) is only of historical interest today. However, it has laid the foundation for all the subsequent process calculation methods. The method, as originally established, is a graphical procedure of integrating the lethal effects of
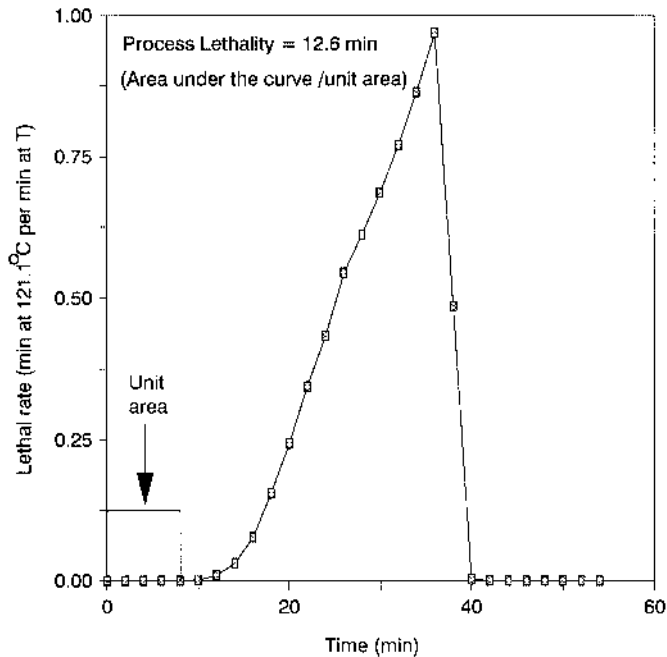
FIGURE 2.10 Lethal rate curve for calculating process lethality.

the time-temperature profile obtained from test products under processing conditions. Although not exactly the way it was originally employed, the following procedure will essentially describe the calculation procedure. The requirements are (1) kinetic data (a reference TDT value and z value) related to the target microorganism, (2) representative product heat penetration data, and (3) either the required sterilization value of the process (for calculating the process time) or process time (for calculating the sterilization value). The sterilization value is a measure of heat treatment severity. Bigelow defined the reciprocal of TDT as the lethal rate at the corresponding temperature. The product of lethal rate and the corresponding heating time gives the accomplished sterilization value. A unit sterilization value indicates that the heating time given is equivalent to the TDT at that temperature. While values higher than unity indicate overkill, sterilization values below 1.0 indicate inadequate processing. The Original General method is based on graphically integrating the lethal rate of product temperature profile over the entire heating time to arrive at the accomplished sterilization value. In order to get a target sterilization value the process time is appropriately increased or decreased as the case may be. The following example will describe the calculation procedure involved.

STEP 1   Kinetic data for the target microorganism
Example: TDT at 121.1°C is 2.52 min with a z value of 10°C
TDT at any other temperature is obtained from

$$\left[\mathrm{TDT_T}\right] = \left[\mathrm{TDT_{121.1}}\right]10^{(121.1-T)/10} \tag{2.30}$$

STEP 2   The product time-temperature data is tabulated in columns 1 and 2 (Table 2.1)
Column 1. Heating time.
Column 2. Temperature.
Column 3. Using Equation 2.30, TDT at each temperature in Column 2 is computed and the reciprocal of this value is entered in Column 3 (lethal rate).

TABLE 2.1
Process Calculation by General and Improved General Methods

Time (min)	Temperature (°C)	TDT (min)	TDT^{-1} (min^{-1})	L value
0	48	>1000	0.000	0.00
2	49	>1000	0.000	0.00
4	56	>1000	0.000	0.00
6	69	>1000	0.000	0.00
8	83	>1000	0.000	0.00
10	93	>1000	0.000	0.00
12	101	258	0.004	0.01
14	106	81.6	0.012	0.03
16	110	32.5	0.031	0.08
18	113	16.3	0.061	0.15
20	115	10.3	0.097	0.25
22	116.5	7.27	0.138	0.35
24	117.5	5.77	0.173	0.44
26	118.5	4.59	0.218	0.55
28	119.0	4.09	0.245	0.62
30	119.5	3.64	0.275	0.69
32	120	3.25	0.308	0.78
34	120.5	2.89	0.346	0.87
36	121.0	2.58	0.388	0.98
38	118	5.15	0.194	0.49
40	96	815	0.001	0.00
42	80	>1000	0.000	0.00
44	65	>1000	0.000	0.00
46	54	>1000	0.000	0.00
48	45	>1000	0.000	0.00
50	38	>1000	0.000	0.00
52	35	>1000	0.000	0.00
54	32	>1000	0.000	0.00
General method (Sterilization value) $\Sigma\,(1/TDT) \times \Delta t$			4.89	
Improved General method (F_o, min) $\Sigma\,(L\ value) \times \Delta t$				12.6

STEP 3   Calculation of the sterilization value

In the original method, a lethal-rate curve is drawn by plotting the lethal rate against heating time, the area under which integrates the lethal effects of all temperatures during heating and cooling. A unit sterilization value on the scale used for this curve will be equivalent to an area which results in the product of lethal rate × time equal to unity. The area under this curve in relation to the unit sterilization area will yield the sterilization value of the process. A sterilization value of unity is the minimal requirement with respect to the test microorganism. If the resulting sterilization value is greater or smaller than unity, the cooling curve is shifted manually to the left or right and the procedure is repeated to get the new sterilization value. This whole process is repeated until the desired sterilization value is obtained, and the corresponding process time is noted. This procedure is illustrated in the next section with the Improved General method.

The graphical procedure is rather tedious and cumbersome, and has gone through several modifications. A simple way of obtaining similar information is by numerical integration technique (Patashnik, 1953). If equal time intervals are used as shown in this example (Table 2.1), the lethal rates in Column 3 can be added (Σ TDT^{-1}) and multiplied by the time

interval (Δt) to get the sterilization value of the process ($\Sigma \, TDT^{-1} \times \Delta t$). If the logging time intervals are not the same, the above product could be obtained at the end of each time interval and are summed up later ($\Sigma TDT^{-1}\Delta t$). In the example, this gives a sterilization value of 4.89 which means that the given heat treatment is about five times what is needed to destroy the target microorganism. It should therefore be possible to reduce the process time.

2.5.2 THE IMPROVED GENERAL METHOD

The Improved General method employing a graphical approach was suggested by Ball (1923). The main improvement is the construction of a hypothetical thermal destruction curve as described earlier which is parallel to the thermal resistance curve of the test microorganism (i.e., with same z value) and having an F value of 1 min at 121.1°C (250°F). This designation permitted comparison of the different processes in terms of lethality achieved. Employing a thermal destruction curve as described above, the lethal rate (L) at any temperature can be obtained as (temperatures in °C)

$$L = 10^{(T-121.1)/z} \tag{2.31}$$

A plot of calculated L values against time (Figure 2.10) as suggested in the previous example for the Original General method will give a curve the area under which represents the equivalent minutes at 121.1°C (F_o). The area under the curve can be measured using a planimeter, by cutting and weighing, counting squares or by approximating to standard shapes (triangle, square, etc.). In the current example, the area under the curve is 12.6 cm^2. Each cm^2 on the graph represents an equivalent F_o value of 1 min [1 cm^2 on this curve indicates the product of lethal rate and time of 1 min; for example, the unit area indicated is the product of a lethal rate of 0.125 multiplied by 8 min = 1.0 min]. Therefore, the area under the curve, 12.6 cm^2, will yield an F_o value of 12.6 min. As mentioned earlier, the graphical procedure is tedious. Patashnik (1953) later employed a numerical integration technique to compute the process lethality by multiplying the lethal rate by the time interval and summing up the lethality values to get the accumulated lethality during the entire heating and cooling (12.6 min as shown in Table 2.1).

$$F_o = \int_0^t L \, dt \tag{2.32}$$

or

$$F_o = \sum_0^t L \, \Delta t \tag{2.33}$$

In order to obtain the appropriate process time to achieve a given F_o, a trial and error approach is needed. The usual practice is to carry out heat-processing tests at several process times. The results from several such tests are plotted as shown in Figure 2.11 and the achieved F_o values for each process time are determined. By plotting the areas under the curves or the achieved F_o value vs. process time (Figure 2.12), the required process time for achieving a target lethality can be obtained. For example, in order to get a target F_o of 10 min, the required process time will be about 33.5 min.

The General method of process calculation is the most accurate method for determining the sterilization value of a heat process. In the General method, the actual time-temperature data are used and the analysis is carried out using the z value of choice. The resulting F_o value is the true value for the specific data used. The measurement method used, be it graphical
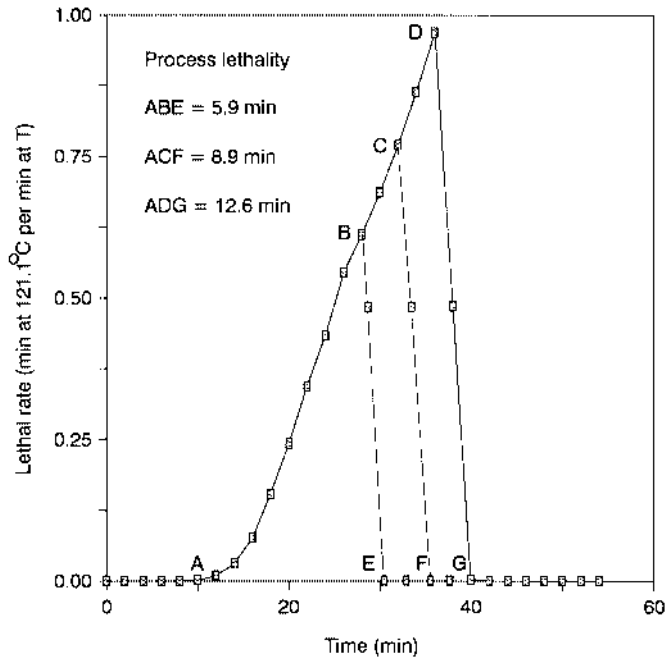
FIGURE 2.11 Lethal rate curves and process lethality for several process times.
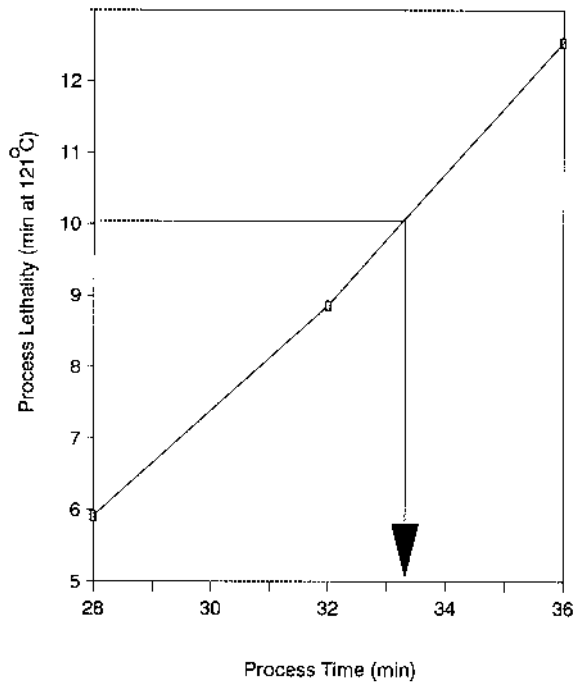
FIGURE 2.12 Process lethality vs. process time curve.

or numerical, by hand or using a calculator or computer will yield similar results. The General method is used as the basic method for calculating the F_o values to be used to compare the performance of the Formula methods. The results of the General method are very specific for the product under the conditions employed for testing. Extrapolation and generalization should be avoided or done with utmost caution.

2.5.3 THE BALL-FORMULA METHOD

The Ball-Formula method is the simplest and most widely used technique for process calculations. Several other Formula methods of heat-process analysis have evolved since the method was first published by Ball (1921). Attributes of this method are that: (1) it can be used to determine the process time if the target process lethality (F_o) value is known; (2) it can be used to calculate the delivered lethality of a given process; (3) since it uses heat penetration data in the parameter form (f_h and j values), new processes for the same product in many sizes of container can be calculated directly using available parameter conversion procedures; and (4) new processes can be directly calculated if there are changes in the heating-medium temperature (T_r) or the initial product temperature (T_i). Using Formula methods to evaluate a process is also considerably faster than using the General methods and has been very useful in studying the effects of processing variables.

It is based on the following equation derived from the heat penetration curve (using the same symbols as detailed earlier):

$$B = f_h \log\left(j_{ch} I_h / g_c\right) \tag{2.34}$$

B is the process time, f_h is the heating rate index, j_{ch} is the lag factor, I_h is the initial temperature difference ($T_r - T_i$) and g_c is the temperature difference at the end of the cook ($T_r - T$ at t = B), T_r is the retort temperature, T_{pih} is the pseudo-initial product temperature, and T_i is the initial product temperature.

Ball (1923) utilized the fact that the sterilization value of the heating portion of a heat process is a function of (1) slope of the heating curve, f_h, and (2) the difference between the final product temperature and the heating medium temperature at the end of the heating period ($T_r - T$). Ball used the term "g" to represent the temperature difference ($T_r - T$).

Based on the reference TDT curve concept, the TDT or F value at the retort temperature (denoted by U by Ball) is obtained as a product of the desired process lethality (F_o) and F_i which is the number of minutes at the retort temperature equivalent to 1 minute at 250°F. (All temperatures used in the following process calculation methods are given in °F.)

$$U = F_o F_i \tag{2.35}$$

and

$$Fi = 10^{(250 - T_r)/z} \tag{2.36}$$

The driving force for cooling is another factor that influences the lethality during cooling. Ball recognized that the heat penetration data were characterized by an initial hyperbolic heating lag, a logarithmic straight line, a hyperbolic cooling lag and a logarithmic straight line cooling. After examining numerous heating profiles, Ball concluded that the cooling lag factor may be approximated by an average j_{cc} value of 1.41. Ball provided the relationship between f_h/U and g in the form of a table as well as figure format. In deriving these

relationships, Ball also assumed that the f value of the heating curve is equal to the f value of the cooling curve ($f_h = f_c$) and further that the sterilization value of temperatures greater than 80°F below the heating-medium temperature is negligible. Ball also discovered that a given value of f_h/U has an associated value of g for a single value of z, and a single value of $T_r - T_w$ (180°F). It was found later that on the average a 10°F change in $T_r - T_w$ may result in a 1% difference in the calculated lethality (Stumbo, 1973).

Ball's Formula method has been the industry standard since it was first introduced. Some inaccuracies in the development of this method have been reported (Merson et al., 1978), but still it is the most widely used method in the food industry. One of the primary limitations of this method is the use of a constant cooling lag factor of 1.41 (j_{cc}). The calculation procedure makes use of experimentally evaluated heat penetration parameters (f_h and j_{ch}) and the operating conditions (T_r and T_i), and a table or a figure to compute the process time required to achieve a given process lethality (F_o) or vice versa. The American Can Company has developed more detailed tables, interpolating and extrapolating the tables that were originally published by Ball. These detailed tables are available in Lopez (1987).

Vinters et al. (1975) parameterized the data in the tables of Ball (1923) so that R in terms of g or log g could be obtained using a programmable calculator or computer. The equations developed by Vinters et al. are given:

- For calculating f_h/U

$$x = \log g$$

$$\text{If } x \leq -0.9542, \text{ then } f_h/U = 1/(0.71 - x)$$

$$\text{If } x > -0.9542, \text{ then } \log f_h/U = 0.072465\, x^5 + 0.06064\, x^4 + 0.071368\, x^3$$

$$+ 0.23426\, x^2 + 0.51548\, x + 0.12384 \qquad (2.37)$$

- For calculating log g

$$R = \log f_h/U$$

$$\text{If } f_h/U \leq 0.6, \text{ then } \log g = (0.71\, f_h/U - 1)/(f_h/U)$$

$$\text{If } f_h/U > 0.6, \text{ then } \log g = 0.042808\, R^5 - 0.35709\, R^4 + 1.1929\, R^3$$

$$- 2.1296\, R^2 + 2.4847\, R - 0.28274 \qquad (2.38)$$

Representative values of log g vs. f_h/U for Ball Method are shown in Table 2.2.

2.5.3.1 Come-Up Time Correction and the Ball-Process Time

The process time t_p (Operator's process time) is the time interval measured from the time the retort or autoclave reaches the design process temperature to the time the steam is turned off. As discussed in an earlier section, autoclaves do not reach the designed process temperatures immediately after the steam is turned on, but require a finite heating time (come-up time, CUT, or t_c) to come up to the operating temperature. It was also pointed out that the effectiveness of the come-up period has been established to be 42% and hence this value can be credited toward the process time. The corrected process time or Ball process time (t_B) includes the effective portion of the come-up time and hence, we can write:

TABLE 2.2
f_h/U vs. log g Values for the Ball Formula Method

f_h/U	log g	f_h/U	log g
0.350	−2.147	4.000	0.655
0.400	−1.790	4.500	0.702
0.450	−1.512	5.000	0.742
0.500	−1.290	5.500	0.776
0.550	−1.108	6.000	0.805
0.600	−0.949	7.000	0.854
0.650	−0.843	8.000	0.894
0.700	−0.736	9.000	0.927
0.750	−0.635	10.00	0.955
0.800	−0.544	15.00	1.052
0.850	−0.463	20.00	1.112
0.900	−0.392	25.00	1.155
0.950	−0.328	30.00	1.187
1.000	−0.273	35.00	1.214
1.100	−0.173	40.00	1.235
1.200	−0.090	45.00	1.254
1.300	−0.019	50.00	1.270
1.400	0.042	60.00	1.296
1.500	0.097	70.00	1.318
1.600	0.146	80.00	1.336
1.700	0.183	90.00	1.352
1.800	0.229	100.0	1.365
1.900	0.265	120.0	1.388
2.000	0.298	140.0	1.406
2.500	0.430	160.0	1.422
3.000	0.525	180.0	1.435
3.500	0.598	200.0	1.447

$$t_B = t_p + 0.42\, t_c \qquad (2.39)$$

The come-up time correction concept applies only to the Formula methods because in General methods the effect of the length of the CUT will be automatically included in the calculated lethality value because all temperatures used in the calculation will reflect the effect of the heat flowing into the product during the CUT. In calculating the process time for effecting a target F_o value by the Ball method, the result of the calculation will be t_B. If the calculated t_B-value is used as the recommended process time, t_p, the effect of CUT will be disregarded and the actual F_o value delivered to the product will be larger than initially specified. In this procedure, the CUT is assumed to be zero. This is perhaps the common practice in the industry. Neglecting the effect of CUT will make the process safer, but it may also represent a waste of capital, energy, product nutrients, and a loss in product quality.

When using the Formula methods for calculating the delivered lethality (Fo value), if t_p is used in the calculation instead of t_B, the calculated value will be lower. In calculating F_o values for deviant and or disputed processes, t_B is usually used (to account for a larger accomplished F_o value). Examples of using the Ball Formula method for process calculation are illustrated in Tables 2.3 and 2.4.

TABLE 2.3
Calculation of Process Time Using The Ball Method

1.	j_{ch}	2.0
2.	f_h	56 min
3.	Process lethality (F_o)	6.0 min
4.	Retort temperature (T_r)	248°F
5.	Initial temperature (T_i)	80°F
6.	$I_h = T_r - T_i$	168°F
7.	$j_{ch} \cdot I_h$	336
8.	$\log (j_{ch} \cdot I_h)$	2.526
9.	$z =$	18°F
10	$F_i = 10^{(250 - T_r)/z}$	1.282
11.	$f_h/U = f_h/(F_o \times F_i)$	7.224
12.	From Table 2.2, interpolate log g value	0.863
13.	$B = f_h [\log (j_{ch} \cdot I_h) - \log g]$	93.1 min.

TABLE 2.4
Calculation of Process Lethality Using the Ball Method

1.	j_{ch}	1.64
2.	f_h	30 min
3.	Process time	49 min
4.	Retort temperature (T_r)	260°F
5.	Initial temperature (T_i)	100°F
6.	$I_h = T_r - T_i$	160°F
7.	$j_{ch} \cdot I_h$	262.4
8.	$\log (j_{ch} \cdot I_h)$	2.42
9.	$z =$	18°F
10	$F_i = 10^{[(250 - T_r)/z]}$	0.28
11.	B/f_h	1.63
12.	$\log (g) = \log (j_{ch} \cdot I_h) - B/f_h$	0.79
13.	From Table 2.2, interpolate f_h/U	5.7
14.	$F_o = f_h/[(f_h/U) \times F_i]$	18.8 min

2.5.4 THE STUMBO FORMULA METHOD

Stumbo and Longley (1966) published several tables for process evaluation taking into account the variability of j_{cc} values. The Stumbo Formula method is essentially similar to the Ball Formula method except that it is somewhat more versatile in accounting for the thermal effects of cooling when the cooling lag factor (j_{cc}) differs from 1.41 as assumed by Ball. These original tables were obtained through planimeter measurements of hand-drawn temperature histories plotted on lethal rate papers and subsequent interpolation of the graphs. Revised tables were later developed (Purohit and Stumbo, 1971; Stumbo, 1973) through the use of computer integration of thermal histories generated from finite difference simulations of heat transfer equations. These tables have been reported to produce results which are often in better agreement with those obtained from General method calculation than do similar calculations using Ball's method (Smith and Tung, 1982). Typical tables for a z value of 10°F (typical of vegetative bacteria; pasteurization processes), 18°F (typical of *C. botulinum*; sterilization processes) and 40°F (typical of nutrients) are given in Tables 2.5 through 2.7.

Table 2.8 summarizes the procedure of calculating process times for a given lethality and Table 2.9 summarizes the same for calculating lethality of a process using the Stumbo method.

2.5.5 THE PHAM-FORMULA METHOD

Pham (1987) developed two sets of simple algebraic equations and simplified tables for thermal process calculations, one for $U/f_h > 1$ and the other for $U/f_h < 1$. Pham claims that his method provides values at least as accurate as Stumbo's and is more versatile because his one table substitutes for the 57 tables published by Stumbo. This method could also be used for mass-average lethality similar to Stumbo's method (1973). Recently Pham amended his equations to cover situations in which the heating and cooling rates differ, i.e., f_h not equal to f_c (Pham, 1990). The accuracy of the modified formulas was reported to be as good as the ones earlier reported for $f_h = f_c$ situations. Pham's equations and calculation procedures are summarized in Tables 2.10 and 2.11 as they are useful in computerized process calculations and yield results as accurate as Stumbo's method (Pham, 1987).

It is important to note that there is a large amount of published information available on the Formula method calculations and modifications to suit a variety of processing equipment, techniques and conditions especially in relation to the estimation of the thermal lags (Ball, 1923; Ball and Olson, 1957; Cleland and Robertson, 1985; Hayakawa, 1970, 1978; Larkin, 1989; Larkin and Berry, 1991; Merson et al., 1978; Steele and Board, 1979; Steele et al., 1979; Stumbo, 1973; Vinters et al., 1975.

Formula methods are widely used for process calculations because of the convenience, whereas the General method is accurate since no assumptions are made in relation to the nature of heating and cooling curves. The experimental data are taken directly, converted to lethal rates and integrated with respect to time. The major disadvantage of the General method is that the process time is specific for a given set of processing conditions. The mathematical methods have greater flexibility since there is no need to obtain experimental heat penetration data for each set of process conditions. One of the inherent problems in the mathematical method is that it is not easy to apply with products characterized by nonlinear heating curves.

TABLE 2.5
f_h/U Relationships when z = 10°F

	Values of g when j of cooling curve is								
f_h/U	0.40	0.60	0.80	1.00	1.20	1.40	1.60	1.80	2.00
0.20	2.68–05	2.78–05	2.88–05	2.98–05	3.07–05	3.17–05	3.27–05	3.36–05	3.46–05
0.30	8.40–04	9.39–04	1.04–03	1.14–03	1.24–03	1.34–03	1.43–03	1.53–03	1.63–03
0.40	5.84–03	6.51–03	7.18–03	7.85–03	8.53–03	9.20–03	9.87–03	1.05–02	1.12–02
0.50	2.01–02	2.21–02	2.40–02	2.60–02	2.79–02	2.99–02	3.18–02	3.38–02	3.57–02
0.60	4.73–02	5.11–02	5.49–02	5.87–02	6.25–02	6.63–02	7.01–02	7.39–02	7.77–02
0.70	8.85–02	9.44–02	1.00–01	1.06–01	1.12–01	1.18–01	1.24–01	1.30–01	1.36–01
0.80	0.143	0.151	0.159	0.167	0.175	0.183	0.191	0.199	0.207
0.90	0.208	0.218	0.228	0.238	0.248	0.258	0.268	0.278	0.288
1.00	0.282	0.294	0.305	0.317	0.329	0.340	0.352	0.364	0.376
2.00	1.14	1.17	1.19	1.21	1.24	1.26	1.29	1.31	1.33
3.00	1.83	1.88	1.92	1.97	2.01	2.05	2.10	2.14	2.19
4.00	2.33	2.41	2.48	2.55	2.63	2.70	2.77	2.85	2.92
5.00	2.71	2.81	2.92	3.03	3.14	3.24	3.35	3.46	3.57
6.00	3.01	3.15	3.29	3.43	3.57	3.72	3.86	4.00	4.14
7.00	3.25	3.43	3.61	3.78	3.96	4.13	4.31	4.49	4.66
8.00	3.47	3.68	3.89	4.10	4.30	4.51	4.72	4.93	5.14
9.00	3.67	3.90	4.14	4.38	4.62	4.85	5.09	5.33	5.57
10.00	3.84	4.11	4.38	4.64	4.91	5.17	5.44	5.70	5.97
15.00	4.60	4.97	5.35	5.72	6.09	6.47	6.84	7.21	7.59
20.00	5.22	5.67	6.12	6.57	7.01	7.46	7.91	8.35	8.80
25.00	5.78	6.27	6.77	7.27	7.77	8.27	8.76	9.26	9.76
30.00	6.27	6.81	7.34	7.88	8.41	8.95	9.48	10.02	10.55
35.00	6.72	7.29	7.85	8.41	8.98	9.54	10.10	10.67	11.23
40.00	7.14	7.72	8.31	8.89	9.48	10.06	10.65	11.23	11.82
45.00	7.52	8.12	8.72	9.33	9.93	10.53	11.13	11.73	12.33
50.00	7.87	8.49	9.10	9.72	10.34	10.95	11.57	12.18	12.80
60.00	8.51	9.15	9.78	10.42	11.06	11.69	12.33	12.97	13.60
70.00	9.07	9.72	10.37	11.02	11.68	12.33	12.98	13.63	14.28
80.00	9.56	10.23	10.89	11.55	12.22	12.88	13.55	14.21	14.88
90.00	10.0	10.7	11.4	12.0	12.7	13.4	14.1	14.7	15.4
100.00	10.4	11.1	11.8	12.5	13.1	13.8	14.5	15.2	15.9
150.00	11.9	12.6	13.4	14.1	14.8	15.5	16.3	17.0	17.7
200.00	13.0	13.7	14.5	15.2	16.0	16.8	17.5	18.3	19.0
250.00	13.7	14.5	15.3	16.1	16.9	17.7	18.5	19.3	20.1
300.00	14.3	15.2	16.0	16.8	17.7	18.5	19.3	20.1	21.0
350.00	14.8	15.7	16.5	17.4	18.3	19.1	20.0	20.9	21.7
400.00	15.2	16.1	17.0	17.9	18.8	19.7	20.6	21.5	22.4
450.00	15.5	16.5	17.4	18.3	19.3	20.2	21.1	22.1	23.0
500.00	15.8	16.8	17.8	18.7	19.7	20.6	21.6	22.6	23.5
600.00	16.3	17.4	18.4	19.4	20.4	21.4	22.4	23.4	24.5
700.00	16.8	17.8	18.9	19.9	21.0	22.1	23.1	24.2	25.3
800.00	17.1	18.2	19.3	20.4	21.5	22.6	23.7	24.8	25.9
900.00	17.4	18.5	19.7	20.8	22.0	23.1	24.3	25.4	26.6
999.99	17.7	18.8	20.0	21.2	22.4	23.6	24.7	25.9	27.1

From Stumbo, C.R. 1973. *Thermobacteriology in Food Processing.* 2nd ed. Academic Press, New York, p. 256. With permission.

TABLE 2.6
f_h/U Relationships when z = 18°F

f_h/U	Values of g when j of cooling curve is

f_h/U	0.40	0.60	0.80	1.00	1.20	1.40	1.60	1.80	2.00
0.20	4.09–05	4.42–05	4.76–05	5.09–05	5.43–05	5.76–05	6.10–05	6.44–05	6.77–05
0.30	2.01–03	2.14–03	2.27–03	2.40–03	2.53–03	2.66–03	2.79–03	2.93–03	3.06–03
0.40	1.33–02	1.43–02	1.52–02	1.62–02	1.71–02	1.80–02	1.90–02	1.99–02	2.09–02
0.50	4.11–02	4.42–02	4.74–02	5.06–02	5.38–02	5.70–02	6.02–02	6.34–02	6.65–02
0.60	8.70–02	9.43–02	1.02–01	1.09–01	1.16–01	1.23–01	1.31–01	1.38–01	1.45–01
0.70	0.150	0.163	0.176	0.189	0.202	0.215	0.228	0.241	0.255
0.80	0.226	0.246	0.267	0.287	0.308	0.328	0.349	0.369	0.390
0.90	0.313	0.342	0.371	0.400	0.429	0.458	0.487	0.516	0.545
1.00	0.408	0.447	0.485	0.523	0.561	0.600	0.638	0.676	0.715
2.00	1.53	1.66	1.80	1.93	2.07	2.21	2.34	2.48	2.61
3.00	2.63	2.84	3.05	3.26	3.47	3.68	3.89	4.10	4.31
4.00	3.61	3.87	4.14	4.41	4.68	4.94	5.21	5.48	5.75
5.00	4.44	4.76	5.08	5.40	5.71	6.03	6.35	6.67	6.99
6.00	5.15	5.52	5.88	6.25	6.61	6.98	7.34	7.71	8.07
7.00	5.77	6.18	6.59	7.00	7.41	7.82	8.23	8.64	9.05
8.00	6.29	6.75	7.20	7.66	8.11	8.56	9.02	9.47	9.93
9.00	6.76	7.26	7.75	8.25	8.74	9.24	9.74	10.23	10.73
10.00	7.17	7.71	8.24	8.78	9.32	9.86	10.39	10.93	11.47
15.00	8.73	9.44	10.16	10.88	11.59	12.31	13.02	13.74	14.45
20.00	9.83	10.69	11.55	12.40	13.26	14.11	14.97	15.82	16.68
25.00	10.7	11.7	12.7	13.6	14.6	15.6	16.5	17.5	18.4
30.00	11.5	12.5	13.6	14.6	15.7	16.8	17.8	18.9	19.9
35.00	12.1	13.3	14.4	15.5	16.7	17.8	18.9	20.0	21.2
40.00	12.8	13.9	15.1	16.3	17.5	18.7	19.9	21.1	22.3
45.00	13.3	14.6	15.8	17.0	18.3	19.5	20.8	22.0	23.2
50.00	13.8	15.1	16.4	17.7	19.0	20.3	21.6	22.8	24.1
60.00	14.8	16.1	17.5	18.9	20.2	21.6	22.9	24.3	25.7
70.00	15.6	17.0	18.4	19.9	21.3	22.7	24.1	25.6	27.0
80.00	16.3	17.8	19.3	20.8	22.2	23.7	25.2	26.7	28.1
90.00	17.0	18.5	20.1	21.6	23.1	24.6	26.1	27.6	29.2
100.00	17.6	19.2	20.8	22.3	23.9	25.4	27.0	28.5	30.1
150.00	20.1	21.8	23.5	25.2	26.8	28.5	30.2	31.9	33.6
200.00	21.7	23.5	25.3	27.1	28.9	30.7	32.5	34.3	36.2
250.00	22.9	24.8	26.7	28.6	30.5	32.4	34.3	36.2	38.1
300.00	23.8	25.8	27.8	29.8	31.8	33.7	35.7	37.7	39.7
350.00	24.5	26.6	28.6	30.7	32.8	34.9	37.0	39.0	41.1
400.00	25.1	27.2	29.4	31.5	33.7	35.9	38.0	40.2	42.3
450.00	25.6	27.8	30.0	32.3	34.5	36.7	38.9	41.2	43.4
500.00	26.0	28.3	30.6	32.9	35.2	37.5	39.8	42.1	44.4
600.00	26.8	29.2	31.6	34.0	36.4	38.8	41.2	43.6	46.0
700.00	27.5	30.0	32.5	35.0	37.5	39.9	42.4	44.9	47.4
800.00	28.1	30.7	33.3	35.8	38.4	40.9	43.5	46.0	48.6
900.00	28.7	31.3	34.0	36.6	39.2	41.8	44.4	47.0	49.7
999.99	29.3	31.9	34.6	37.3	39.9	42.6	45.3	47.9	50.6

From Stumbo, C.R. 1973. *Thermobacteriology in Food Processing.* 2nd ed. Academic Press, New York, p. 260. With permission.

TABLE 2.7
f_h/U Relationships when z = 40°F

f_h/U	Values of g when j of cooling curve is								
	0.40	**0.60**	**0.80**	**1.00**	**1.20**	**1.40**	**1.60**	**1.80**	**2.00**
0.20	8.58–05	9.64–05	1.07–04	1.18–04	1.28–04	1.39–04	1.49–04	1.60–04	1.70–04
0.30	3.98–03	4.47–03	4.96–03	5.46–03	5.95–03	6.44–03	6.93–03	7.43–03	7.92–03
0.40	2.72–02	3.06–02	3.39–02	3.73–02	4.07–02	4.40–02	4.74–02	5.08–02	5.42–02
0.50	8.67–02	9.72–02	1.08–01	1.18–01	1.29–01	1.39–01	1.50–01	1.61–01	1.71–01
0.60	0.188	0.211	0.234	0.256	0.279	0.302	0.324	0.347	0.370
0.70	0.329	0.368	0.408	0.447	0.487	0.527	0.566	0.606	0.645
0.80	0.501	0.562	0.622	0.682	0.743	0.803	0.864	0.924	0.984
0.90	0.698	0.782	0.867	0.952	1.036	1.121	1.205	1.290	1.374
1.00	0.912	1.023	1.135	1.246	1.357	1.469	1.580	1.691	1.802
2.00	3.30	3.72	4.13	4.55	4.96	5.38	5.79	6.21	6.62
3.00	5.46	6.15	6.84	7.53	8.22	8.91	9.60	10.29	10.98
4.00	7.25	8.18	9.11	10.04	10.97	11.90	12.83	13.77	14.70
5.00	8.75	9.89	11.04	12.18	13.32	14.46	15.61	16.75	17.89
6.00	10.1	11.4	12.7	14.0	15.4	16.7	18.0	19.3	20.7
7.00	11.2	12.7	14.2	15.7	17.1	18.6	20.1	21.6	23.1
8.00	12.2	13.8	15.5	17.1	18.7	20.4	22.0	23.6	25.2
9.00	13.1	14.9	16.6	18.4	20.2	21.9	23.7	25.4	27.2
10.00	14.0	15.8	17.7	19.6	21.5	23.3	25.2	27.1	29.0
15.00	17.3	19.6	22.0	24.3	26.7	29.0	31.4	33.8	36.1
20.00	19.8	22.5	25.2	27.8	30.5	33.2	35.9	38.6	41.3
25.00	21.8	24.8	27.7	30.6	33.6	36.5	39.4	42.4	45.3
30.00	23.5	26.6	29.8	32.9	36.1	39.2	42.4	45.6	48.7
35.00	24.9	28.3	31.6	34.9	38.2	41.5	44.9	48.2	51.5

From Stumbo, C.R. 1973. *Thermobacteriology in Food Processing.* 2nd ed. Academic Press, New York, p. 271. With permission.

TABLE 2.8
Calculation of Process Time
Using the Stumbo Method

1.	j_{ch}	1.3
2.	f_h	12.0 min
3.	Process lethality (F_o)	10 min
4.	Retort temperature (T_r)	255°F
5.	Initial temperature (T_i)	150°F
6.	$I_h = T_r - T_i$	105°F
7.	$j_{ch} \cdot I_h$	136.5
8.	$\log (j_{ch} \cdot I_h)$	2.14
9.	$z =$	18°F
10	$F_i = 10^{(250 - T_r)/z}$	0.53
11.	$f_h/U = f_h/(F_o \times F_i)$	2.27
12.	j_{cc}	1.6

From Table 2.6 for z = 18°F (j_{cc} = 1.6),
  obtain g value by interpolation

f_h/U	g value
2.0	2.34
3.0	3.89

Interpolate

2.27	2.76

13.	$B = f_h [\log (j_{ch} \cdot I_h/g)]$	20.3 min.

TABLE 2.9
Calculation of Process Lethality
Using the Stumbo Method

1.	j_{ch}	2.05
2.	f_h	34.9 min
3.	Process time	69.0 min
4.	Retort temperature (T_r)	245°F
5.	Initial temperature (T_i)	150°F
6.	$I_h = T_r - T_i$	95°F
7.	$j_{ch} \cdot I_h$	194.8
8.	$\log (j_{ch} \cdot I_h)$	2.29
9.	$z =$	18°F
10	$F_i = 10^{(250 - T_r)/z}$	1.90
11.	B/f_h	1.98
12.	$\log (g) = \log (j_{ch} \cdot I_h) - B/f_h$	0.31
13.	g	2.05
14.	j_{cc}	1.8

From Table 2.6 for z = 18°F (j_{cc} = 1.8),
  obtain f_h/U by interpolation

f_h/U	g value
1.0	0.586
2.0	2.15

Interpolate

1.94	2.05

15.	$F_o = f_h/[(f_h/U) \times F_i]$	9.50 min

TABLE 2.10
Pham's Method: The Related Equations and Coefficients

For high sterilizing values: $W > 1$

$\log (g/z) = -W + Aj - B/j + C$

$A = 0.088 + 0.107\ N_2$

$B = 0.102\ N_1$

$C = 0.074\ N_1 + 0.177\ N_2 - 0.653$

$W = U/f_h$

$N_1 = z/(T_r - T_i)$

$N_2 = z/(T_r - T_w)$

For low sterilizing values: $0.04 < W < 1.5$

$\log (a) = -W + A_1 + A_2 \exp (-2.7\ W^{0.5})$

$\log (b) = -W + B_1 + B_2 \exp (-2.7\ W^{0.5})$

$g = z\ (a + bj_{cc})$

$W = U/f_h$

$A_1 = -0.71 - 0.41(N_1/N_2) \exp (-0.58/N_2)$

$A_2 = 2.14\ (N_2)^2 + 0.6\ (N_2)^2/N_1 - 0.26\ (N_1)^2 - 1.24\ N_1 + 1.02$

$B_1 = 0.31\ (N_2/N_1)^{0.5} + 0.55\ (N_2)^{0.5} + 0.61\ (N_1)^{0.5} - 1.86$

$B_2 = (N_2/N_1)^{0.5}(0.91\ (N_1)^2 - 3.18\ N_1 - 0.755) - 1.38\ (N_1)^2 + 2.55\ N_1 + 1.52$

TABLE 2.11
An Example of Using Pham's Method

Steps 1 to 10 same as in Stumbo's Method (Table 9)

11. $f_h/U\ 2.27$
12. $W = U/f_h\ 0.44$

 $W < 1.5$

 $\log (a) = -W + A_1 + A_2 \exp (-2.7\ W^{0.5})$

 $\log (b) = -W + B_1 + B_2 \exp (-2.7\ W^{0.5})$

 $g\ = z\ (a + b\ j_{cc})$

 $W = 0.44$

 $A_1 = -0.71, \quad B_1 \quad = -1.20$

 $A_2 = 0.85, \quad B_2 \quad = 0.98$

 $a\ = 0.098 \quad \log (b) = 0.032$

 $g\ = 2.76$
13. $B\ = f_h\ [\log (j_{ch}.I_h/g)] = 20.5\ min$

REFERENCES

Ball, C.O., 1923, Thermal process time for canned food, Bull. 37. Vol. 7, Part 1. Nat'l. Res. Council, Washington, D.C.

Ball, C.O. and Olson, F.C.W., 1957, *Sterilization in Food Technology,* McGraw-Hill, New York.

Bigelow, W.D., Bohart, G.S., Richardson, A.C., and Ball, C.O., 1920, Heat penetration in processing canned foods, Nat'l. Canners Assoc. Bull., No. 16L.

Cleland, A.C. and Robertson, G.L., 1985, Determination of thermal processes to ensure commercial sterility of food in cans, in: *Developments in Food Preservation. 3.* Throne, S., Ed., Elsevier Applied Science, New York, 1.

Fellows, P., 1988, *Food Processing Technology: Principles and Practices,* Ellis Horwood, Chichester, England.

Hayakawa, K.-I., 1970, Experimental formulas for accurate estimation of transient temperature of food and their application to thermal process evaluation, *Food Technol.* 24(12):89.

Hayakawa, K.-I., 1978, A critical review of mathematical procedures for determining proper heat sterilization processes, *Food Technol.* 32(3):59.

Larkin, J.W., 1989, Use of a modified Ball's formula method to evaluate aseptic processing of liquid foods containing particulates, *Food Technol.* 43(3):124–131.

Larkin, J.W. and Berry, R.B., 1991. Estimating cooling process lethality for different cooling j values, *J. Food Sci.* 56(4):1063–67.

Lopez, A., 1987, *A Complete Course in Canning and Related Processes,* 12th ed. The Canning Trade, Baltimore, MD.

Merson, R.L., Singh, R.P., and Carroad, P.A., 1978, An evaluation of Ball's formula method of thermal process calculations, *Food Technol.* 32(3):66.

Patashnik, M., 1953, A simplified procedure for thermal process evaluation, *Food Technol.* 7(1):1.

Pflug, I.J., 1987, *Textbook for an Introductory Course in the Microbiology and Engineering of Sterilization Process,* Environmental Sterilization Laboratory, Minneapolis, MN.

Pham, Q.T., 1987. Calculation of thermal process lethality for conduction-heated canned foods, *J. Food Sci.* 52(4):967.

Pham, Q.T., 1990, Lethality calculation for thermal processes with different heating and cooling rates, *Int. J. Food Sci. Technol.* 25:148.

Purohit, K.S. and Stumbo, C.R., 1972, Computer calculated parameters for thermal process evaluations, Unpublished data; cited in Stumbo, C.R., 1972, *Thermobacteriology in Food Processing,* 2nd ed., Academic Press, New York.

Ramaswamy, H.S., van de Voort, F.R., and Ghazala, S., 1989, An analysis of TDT and Arrhenius methods for handling process and kinetic data, *J. Food Sci.* 54:1322.

Richardson, P.S. and Holdsworth, S.D. 1989. Mathematical modeling and control of sterilization processes, in: *Process Engineering in the Food Industry,* Field, R.W. and Howell, J.A., Eds., Elsevier Applied Science, New York, 169.

Smith, T. and Tung, M.A., 1982, Comparison of formula methods for calculating thermal process lethality, *J. Food Sci.* 47:626.

Steele, R.J. and Board, P.W., 1979, Thermal process calculations using sterilizing ratios, *J. Food Technol.* 14:227.

Steele, R.J., Board, P.W., Best, D.J., and Willcox, M.E., 1979, Revision of the formula method tables for thermal process evaluation, *J. Food Sci.,* 44:954.

Stumbo, C.R., 1973, *Thermobacteriology in Food Processing,* 2nd ed., Academic Press, New York.

Stumbo, C.R. and Longley, R.E., 1966, New parameters for process calculation, *Food Technol.* 20(3):341.

Vinters, J.E., Patel, R.H., and Halaby, G.A., 1975, Thermal process evaluation by programmable calculator, *Food Technol.* 29(3):42.

3 Prediction of Freezing Time and Design of Food Freezers

Donald J. Cleland and Kenneth J. Valentas

CONTENTS

3.1 INTRODUCTION TO FOOD FREEZER DESIGN AND OPERATION

Optimal design and operation of food freezers requires the classic economic compromise between capital expenditure and operating costs. The optimal freezer will completely freeze the product at the desired production rate with low weight loss and quality deterioration for low total cost.

3.1.1 FOOD QUALITY AND FREEZING RATE

The actual freezer design and operation must compromise between quality and cost criteria. Unfortunately the value of quality is difficult to quantify. Quality is usually considered to be related to freezing rate due to the latter's effect on ice crystal location and size and weight loss, but the relationship is ill-defined and very product specific (Rasmussen and Olson, 1972). Given that product size and packaging are usually fixed by marketing considerations, the type of freezer selected has a major influence on freezing rate. For most foods, as long as the freezing rate is "reasonably" fast, quality requirements become secondary to cost issues. Exceptions are usually very frost-sensitive or valuable foods. Given that many of the advantages of fast freezing can be lost during subsequent storage (Fennema, 1975), often too much emphasis is given to achieving the highest freezing rate in the process freezer. It is probably more critical that complete product freezing is achieved in the process freezer because rates of temperature reduction in frozen storage will be much lower and can lead to both significant loss of product quality and increased storage freezer refrigeration costs.

3.1.2 FREEZER DESIGN REQUIREMENTS

The initial stage in design of a freezer involves the following steps:

- Specification of product size, packaging, shape, production rate, and final storage temperature
- Selection of freezer type and level of automation based on overall economic strategy, desired rate of freezing for quality maintenance, and consistency with pre- and post-freezing processing operations
- Thermal design of the freezer and refrigeration system

The thermal freezer and refrigeration system design includes:

- Defining the size of the freezer and the product residence time
- Specifying the operating conditions, in particular, air velocity and temperature to achieve complete freezing within the residence time
- Sizing the fans, **evaporator coils**, compressors, and other refrigeration system components to match the freezer capacity
- Estimating the operating costs such as energy use and weight loss that are affected by the operating conditions

Lastly, the detailed mechanical design is completed.

The overall design process must be iterative to achieve the best economic compromise. The food engineer is normally not involved in mechanical design, but heavily involved in the earlier two stages. To perform this work the food engineer requires methods to predict freezing times and heat loads to ensure that both the freezer and the refrigeration system have sufficient **capacity**.

TABLE 3.1
Comparison of the Main Characteristics of Food Freezers

Characteristic	Still-air	Air-blast tunnel	Belt	Spiral	Fluidized bed	Plate	Immersion	Cryogenic
Capital cost	L	I	I	I/H	I	H	L	L
Fan/pump energy	L	I/H	I/H	I/H	I/H	L	L	L
Overall operating costs	L/I	I	I	I	I	L	L/I	H
Rate of freezing	L	L/I	I	I	I/H	H	H	H
Unwrapped weight loss	H	I/H	I	I	L/I	L	L	L
Relative size of facility	H	I/H	I	L/I	L	L	L	L
Product size	A	A	L/I	L/I	L	I/H	L/I	L/I
Product shape	A	A	U	A	U	R	A	A
Product types	A	A	FV,P,FH	A	FV,P	M,FH,P	M,C,PY,FH,P	A

Note: L = low, small; I = intermediate, medium; H = high, large; A = all; U = uniform; R = rectangular; M = meat; P = processed/prepared; FH = fish; FV = fruit and vegetables; PY = poultry; and C = canned.

3.1.3 FREEZER OPERATIONAL CONSIDERATIONS

After completion of the design, consideration must be given to plant operations. Plant operations are complicated by the fact that the freezer will not always be operating at the design production rate or other design conditions, yet once it is constructed, the only variables that can easily be changed are the operating conditions within the freezer. Changing operating conditions influence both the operating costs and the required capacity of the associated refrigeration system, so methods to quantify the effect of operating conditions are also required.

The following sections consider: types of food freezers, mathematical formulation of food freezing problems, prediction of food freezing times, determination of thermal properties and heat transfer coefficients, estimation of heat loads, characteristics and design of refrigeration system components, economic issues including capital costs, and operating costs such as weight loss and energy use. Worked examples of the proposed calculation techniques are presented.

3.2 TYPES OF FOOD FREEZING SYSTEMS

Industrial food-freezing systems can be divided into two broad groups — those using air as the cooling medium and those using other cooling mediums. Air-blast freezing systems can be further subdivided into still-air, blast-room or tunnel, belt, spiral-belt, and fluidized bed freezers. Other systems include plate, immersion, cryogenic freezers, and freezers for liquid foods. Table 3.1 compares these main freezer types.

3.2.1 AIR-BLAST FREEZERS

Air-blast freezers are the most common type of food freezer. Individual product items are placed in a recirculating air stream within a room or tunnel. The air is circulated by fans, which are often associated with the evaporator coils providing cooling. These freezers can be simple, operating in **batch** mode with manual loading and unloading of the product (Figures 3.1, 3.2), or more complex, with automated **continuous** operation (Figures 3.3, 3.4, 3.5). Continuous freezers are best suited to processing large volumes of product. They have
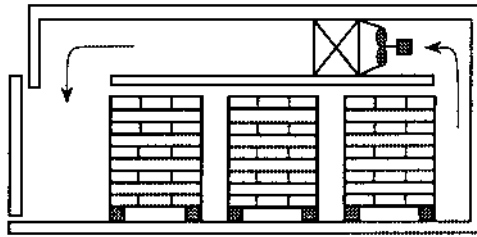
FIGURE 3.1 Schematic diagram of a batch air-blast tunnel freezer with racks of product and horizontal air flow.
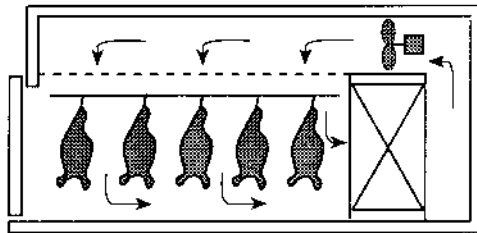
FIGURE 3.2 Schematic diagram of a batch air-blast carcass freezing room with vertical air flow through a distribution plenum.
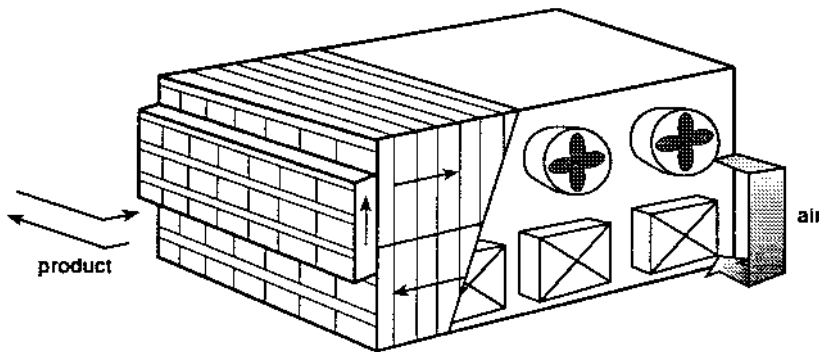
FIGURE 3.3 Schematic diagram of a continuous air-blast carton tunnel freezer with cross-flow of air.

lower labor costs, and generally provide more uniform freezing conditions, but are less flexible.

Many different air and product flow configurations can be used. Horizontal air flow is probably most common, but there are a number of designs using vertical air flow, often to avoid air bypassing the product (Figures 3.2, 3.5). In continuous systems, air and product flows can be cocurrent, countercurrent (Figure 3.5) or cross-flow (Figures 3.3, 3.4). The latter two configurations are most common as air temperature rise is small, so the temperature driving force for cooling and thus the rate of heat transfer are maximized. Methods to present the product to the air depend on the size, shape and packaging of the product, and include trays, racks, trolleys, hooks, conveyors, and belts. A wide range of product types, sizes, shapes, and packaging types can be handled by such freezers.
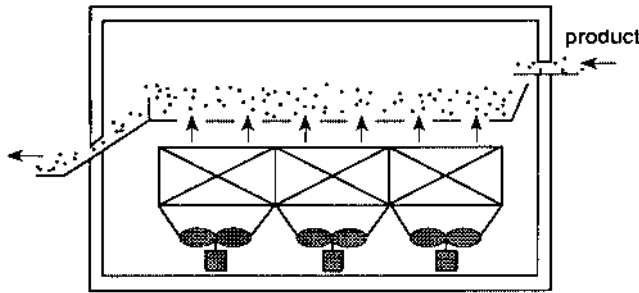
FIGURE 3.4 Schematic diagram of a continuous fluidized bed freezer. Belt freezers are similar but product is transported on a perforated conveyor belt.
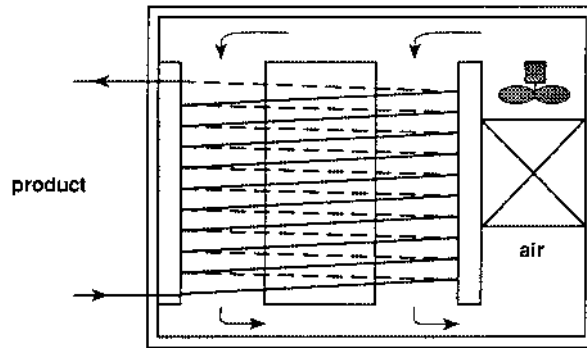
FIGURE 3.5 Schematic diagram of a continuous spiral belt freezer with vertical air flow.

The major advantages of air-blast freezers are their simplicity and flexibility. The disadvantages are that using air limits the rate of heat transfer at the product surface, requires the use of substantial fan energy, and to achieve uniform air distribution can be difficult. Also, further disadvantages are that: evaporative weight loss can be significant from unwrapped product; bulging of packaged product can occur; defrosting evaporator coils or another means of frost prevention is required which can disrupt freezer operation; and the refrigeration system must operate with a low suction condition due to the air-to-refrigerant heat exchange.

3.2.1.1 Still-Air Freezers

The simplest type of freezer is one in which the product is placed in a refrigerated room that is usually used to store frozen product. The process is historically referred to as sharp freezing. The shelves on which the product is placed within the room may be directly refrigerated, and the product may be bulk-stacked. Air flow over the product is minimal and the freezing rate is slow. Also, heat removal from the freezing product may cause undesirable temperature fluctuations in adjacent stored product.

3.2.1.2 Air-Blast Room and Tunnel Freezers

These freezers are commonly used for medium to large products where the rate of freezing is limited by the size of the product. The product does not need to be regular in shape. The product is placed on trays in racks or suspended so that air flow is possible around each individual product item. In continuous tunnel freezers, it is usual to have a mechanical system moving racks through the tunnel in a cyclic manner, automatic loading and unloading of the

racks, and product arriving and leaving on a conveyor system (Figure 3.3). For batch freezers, the racks are manually loaded and positioned in the room or tunnel (Figures 3.1, 3.2). In a tunnel system, the air is confined to flowing in the cross-section where the product is located. Also, the product is spaced evenly so that uniform air distribution and high air velocity is more easily achieved for a low total air flowrate and fan power. While most continuous tunnel freezers are restricted to one product size and shape in order to optimize the product loading configuration and air flow distribution, a range of products can be processed in the same tunnel if a variety of rack sizes and tray spacing are used. In a blast room there is often less strict control of the air flow pathway and bypassing of the air around the product can more easily occur.

3.2.1.3 Belt Freezers

Belt freezers involve the product passing continuously through a tunnel freezer on a perforated belt (Figure 3.4). The air flow is directed vertically up through the belt and product layer. There may be multiple belt passes. Such freezers are commonly used for small unwrapped products with uniform shape in which a free-flow individually quick frozen (IQF) product is desired. The air velocities are typically in the range 1 to 6 m/s and the layer of product can be partially fluidized. This creates high rates of heat transfer between the air and product. Even distribution of the product across the belt is important to achieve uniform air distribution and freezing rate. Product transfers from one belt to another and/or mechanical devices are sometimes installed to reduce clumping and to redistribute the product. The belt speed can be varied to cope with changing production rates but care must be taken to maintain a uniform thickness of product on the belt.

3.2.1.4 Spiral Belt Freezers

Spiral freezers are a specialized type of belt freezer in which a continuous belt is stacked in a spiral arrangement up to 50 or so tiers high (Figure 3.5). They allow very long belts (long product residence times) in a compact area as long as sufficient overhead space is available. Therefore, they are suitable for processing products with longer freezing times compared with other belt freezers (e.g., larger products and packaged products for which the packaging impedes heat transfer). The size of the product is limited by the distance between each spiral tier and the total height of the stack. Air flow can be either horizontal across or vertical through the belts. Recent design improvements have included self-stacking belts to reduce mechanical wear and maintenance, and cleaning-in-place of the belt and freezer.

3.2.1.5 Fluidized Bed Freezers

Fluidized bed freezers are only suitable for small unwrapped IQF products of uniform size and shape, such as fruits and vegetables for which the energy requirements for fluidization are not excessive. In a manner similar to belt freezers, air is directed up through a perforated plate and bed of the product but at a flowrate high enough to fluidize the product (Figure 3.4). The product is fed in at one end and overflows out of the freezer at the other. Fluidization achieves good distribution of the product and prevents clumping, even with very wet incoming product, and the surface heat transfer is significantly enhanced. The product moves by flowing within the fluidized bed, but this can be aided by vibrating and/or sloping the air distribution plate. Individual items reside for different periods depending on the flow pattern in the bed. The average residence time is fixed by the feed rate and the volume of the bed, which is controlled by the height of the overflow weir. Fluidized bed freezers can be very compact because the small product size and high rates of convective heat transfer keep freezing times short.
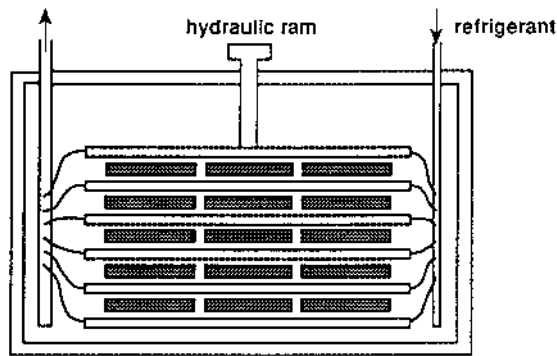
FIGURE 3.6 Schematic diagram of a batch horizontal plate freezer.

3.2.2 PLATE FREEZERS

Plate freezers consist of a series of parallel flat plates through which a coolant is circulated (Figure 3.6). The plates can be mounted either horizontally or vertically. A hydraulic system is used to both open the space between plates for loading and unloading, and to close the plates so that effective contact with the food product occurs during freezing. Spacers or limit stops between plates and a pressure relief valve in the hydraulic circuit can be used to prevent the product being crushed unevenly or excessively flattened during plate closure.

Vertical plate freezers are best suited to freezing unpackaged deformable products such as fish and meat. Blocks are formed by direct gravity feeding of the product between the plates. Plate heating and block ejection systems are required to remove the block at the end of the freezing process and cleaning may be required before reloading. Horizontal plate freezers are commonly used for either product packed into rectangular cartons or product formed into rectangular shapes by metal molds or trays. Although automated systems have been developed where individual plates are opened in order to facilitate simultaneous loading and unloading of rows of product from feed conveyors and continuous operation, plate freezers are more often manually loaded and operate in batch mode.

For efficient operation, uniform and effective contact between the plates and the food product surface is important. This can be achieved by a high packing density of the product (low void space) within the package and/or by application of a moderate pressure to the plates. For packaged products, design of carton dimensions ensuring low voidage and minimal head space is crucial for good heat transfer.

The major advantages of plate freezers are that: the rate of freezing is high even for packaged products; the product has very consistent size and shape and can be easily bulk stacked with high packing density and stability for subsequent transportation; they are very compact; infrequent defrosting of the plates is required; the total heat load and energy use are lower than for air systems (no fans and less infiltration and air interchange loads); and if evaporating refrigerant is used directly in the plates, the refrigeration system can operate at a higher **suction temperature**. The major disadvantages of plate freezers are the high capital cost, especially if they are automated to run continuously, and the limitation on product types that can be handled.

3.2.3 LIQUID IMMERSION FREEZERS

In immersion freezers the product is immersed directly in, or sprayed with, a cold liquid such as a brine or glycol. The product is usually packaged to prevent cross-contamination between the liquid and the product. Products with irregular shapes are easily handled. Although high rates of freezing can be achieved, these types of freezers are now seldom used except for
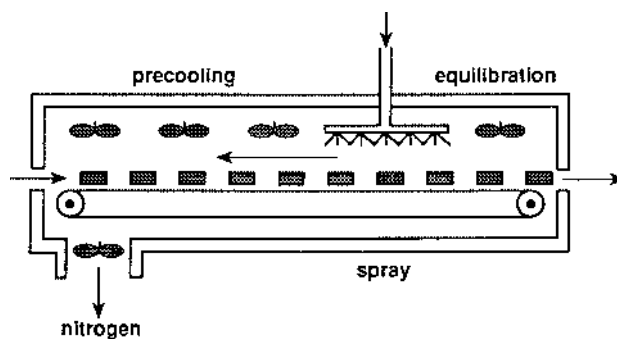
FIGURE 3.7 Schematic diagram of a typical continuous liquid nitrogen tunnel freezer.

some fish, meat, and poultry products. The liquid is refrigerated either by circulation through a heat exchanger or by cooling coils and/or a jacket built into the liquid tank.

3.2.4 CRYOGENIC FREEZERS

The most commonly used cryogens are liquid nitrogen (LN_2) and liquid carbon dioxide (LCO_2). Chlorofluorocarbons (CFCs) such as CFC-12 are no longer in use due to their ozone layer depletion effect. The cryogens have low boiling points, $-196°C$ for LN_2 and $-79°C$ for LCO_2, giving large temperature differences and high rates of heat transfer. Other important properties of such cryogens are that they are colorless, odorless, chemically inert, and nontoxic in normal concentrations. Therefore they are safe for direct contact with food. The product is either sprayed with, or immersed in, the cryogen at atmospheric pressure. Special care must be exercised with CO_2 because it forms a low density snow. Cryogenic freezers can operate continuously with the product being conveyed through a tunnel (Figure 3.7), but other configurations are also used.

Cryogenic freezers are generally only used for small to medium sized products because in larger products the rate of freezing is limited by heat transfer internal to the product. While the higher rate of freezing should lead to a higher quality product than using other freezer types, it is often forgotten that long-term storage negates these benefits. It has been shown that after about a month of conventional frozen storage, the quality of products was independent of the type of freezing system and rate of freezing used (Fennema, 1975).

LN_2 and LCO_2 are usually delivered as a high-pressure liquid, rather than being produced on-site, and are vented to the atmosphere after use. The cryogen storage system is a significant cost component. Effective insulation and/or refrigeration of the storage tank is necessary to prevent excess heat ingress and cryogenic loss. For LN_2, the system losses are typically up to 1% of stored volume per day. For LCO_2, the higher temperatures for the same storage pressure mean that a small supplemental mechanical refrigeration system can eliminate losses completely.

For efficient use of the cryogen, the product and cryogen flows are usually countercurrent and the cryogen vent temperature is kept reasonably close to ambient conditions ($-50°C$ to $0°C$). Because of the very high rates of heat transfer achieved, a product temperature equilibration stage is commonly included. Even then the product surface temperature will usually remain significantly colder than the center temperature at the freezer exit.

The main advantages of cryogenic freezers are: high rates of freezing achieved by the very cold temperatures and low refrigerant-to-product surface heat transfer resistance (resulting in lower weight loss and higher quality); ease of operation; compact size; low cost of the equipment; rapid installation and start-up; mechanical simplicity; and low maintenance cost. The main disadvantage is the high cost of the cryogens. The methods to predict freezing

times presented in Section 3.4 do not apply to the extremely low ambient temperatures (below –45°C) that can be achieved in cryogenic freezers.

Cryogenic freezing (or alternatively liquid immersion freezing) can be used for rapid crust freezing with completion of freezing in an air-blast freezer (often called combined cryomechanical systems). These systems aim to achieve the optimum balance between freezer operating costs and product moisture and quality loss. The principle is that most of the heat removal is performed by the mechanical system giving low operating costs while the initially rapid surface temperature pull-down minimizes product moisture and quality loss.

3.2.5 FREEZERS FOR LIQUIDS

Liquid products can be frozen in a wide variety of freezer types if packaged into suitable containers. The main specialist type is scraped-surface heat exchangers in which the liquid freezes onto the inside or outside of a refrigerated cylindrical surface scraped continuously by rotating blades. For example, ice cream mix is partially frozen on the inside surface of a cylindrical barrel (ice cream freezing is usually completed in air-blast hardening tunnels after the partially frozen liquid is poured into the final packaging). For pasty or particulate liquid foods, drum freezers can be used where freezing occurs on the outside of a refrigerated drum. The methods to predict freezing times presented in Section 3.4 do not apply to freezing of liquids in specialized liquid freezers.

3.3 FORMULATION OF FOOD FREEZING PROBLEMS

Food freezing, although conceptually simple, is difficult to rigorously model because of the physical complexity which arises when the freezing of the water fraction starts. The transient heat transfer then involves thermal properties that change rapidly with temperature, and mass transfer effects such as the onset of ice crystal nucleation can also be important.

3.3.1 FOOD FREEZING PHYSICS

Heat is removed at the surface of the food object by either a convective heat transfer medium (i.e., air or cryogens), or by conduction through contact with a refrigerated surface. As the object cools past the initial freezing point, phase change starts to occur in the aqueous phase. As water freezes to form essentially pure ice, the solutes in the food become more concentrated in the remaining water causing further depression of the freezing point. Thus there is no sharp freezing point as for pure water, but rather latent heat is removed over a range of temperatures. There must be supercooling of the food near the object surface to below the initial freezing temperature before ice crystal nucleation, the first step in the phase change process, is initiated.

Continued heat removal from the interior of the food requires conduction through the outer "frozen" portion. As the "freezing front" moves from the outside towards the **thermal center** its shape can change which further complicates the mathematics especially if the object geometry is not regular. Physical properties such as thermal conductivity and specific heat capacity change significantly with temperature as the change in phase of water occurs.

Further description of the freezing process is given in Section 3.5.3.1. Figure 3.8 shows typical measured temperature-time profiles for freezing of a food item in an air-blast freezer.

3.3.2 MATHEMATICAL MODELS

The two physical models commonly used to describe freezing of foods are the so-called heat conduction with temperature-variable thermal properties model and the unique phase-change front model (Cleland, 1990; Singh and Mannapperuma, 1990). For the simplest case of a one-dimensional infinite slab of thickness 2R that is symmetric about its center, the partial
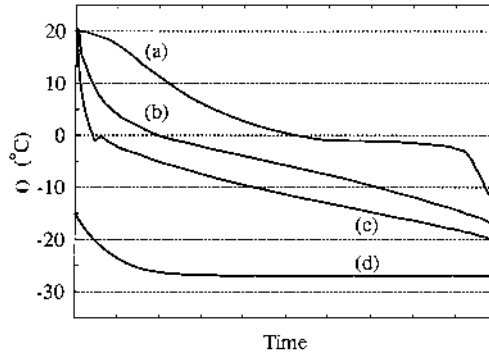
FIGURE 3.8 Typical temperature/time profiles for an object in a batch air-blast freezer (a) thermal center position, (b) position midpoint between the product center and surface, (c) product surface, (d) air.

differential equation for the more physically realistic heat conduction with temperature-variable thermal properties model can be stated as

$$\rho c(\theta) \frac{\partial \theta}{\partial t} = \frac{\partial}{\partial x}\left(k(\theta)\frac{\partial \theta}{\partial x}\right) \quad \text{for} \quad 0 < x < R \quad \text{and} \quad t > 0 \tag{3.1}$$

The unique phase-change front model assumes that all latent heat is released at a unique temperature at a sharp phase change front, that the thermal properties in the regions either side of the front are constant but different, and that change in density during freezing can be ignored. The governing equations representing conduction in the frozen and unfrozen regions and the movement of the phase change front for the symmetric one-dimensional object are

$$\rho c_f \frac{\partial \theta}{\partial t} = k_f \frac{\partial^2 \theta}{\partial x^2} \quad \text{for} \quad x_f < x < R \quad \text{and} \quad t > 0 \tag{3.2}$$

$$\rho c_u \frac{\partial \theta}{\partial t} = k_u \frac{\partial^2 \theta}{\partial x^2} \quad \text{for} \quad 0 < x < x_f \quad \text{and} \quad t > 0 \tag{3.3}$$

$$\rho L \frac{dx_f}{dt} = k_f \left[\frac{\partial \theta_f}{\partial x}\right]_{x_f^+} - k_u \left[\frac{\partial \theta_u}{\partial x}\right]_{x_f^-} \quad \text{for} \quad x = x_f \quad \text{and} \quad t > 0 \tag{3.4}$$

For both models, the initial condition is

$$\theta = \theta_i \quad \text{for} \quad 0 \le x \le R \quad \text{at} \quad t = 0 \tag{3.5}$$

and for the unique phase change front model only

$$x_f = R \quad \text{at} \quad t = 0 \tag{3.6}$$

In practice, heat transfer at the surface of an object being frozen can occur by a combination of all or some of convection, radiation, evaporation, and conduction. The most common modeling approach is to use Newton's law of cooling at the surface and to define an effective surface heat transfer coefficient to account for the net effect of all the actual mechanisms.

This approach is discussed further in Section 3.6. Using this approach for the symmetric one-dimensional object, the surface boundary condition is

$$k\frac{\partial\theta}{\partial x} = h(\theta_a - \theta) \quad \text{for} \quad x = R \quad \text{and} \quad t > 0 \tag{3.7}$$

while at the center of the object the symmetry boundary condition applies

$$\frac{\partial\theta}{\partial x} = 0 \quad \text{for} \quad x = 0 \quad \text{and} \quad t > 0 \tag{3.8}$$

3.4 FREEZING TIME PREDICTION

Methods to predict freezing times are of two main types — numerical methods and simple formulas.

3.4.1 NUMERICAL METHODS

If formulated and implemented appropriately, numerical methods such as finite differences and finite elements accurately predict freezing processes by approximating the partial differential equations for the temperature-variable thermal properties model (Equations 3.1, 3.5, 3.7, and 3.8) and are very versatile (Cleland, 1990; Cleland, 1991). They can be applied to a wide range of conditions including a variety of modes of surface heat transfer, time-variable conditions, and complex object geometries. They also predict full temperature-time profiles not just freezing time. The disadvantages of numerical methods are their complexity and high implementation costs (particularly for computer-program development and testing and data preparation, but to a lesser extent for computation time). Cleland (1990) and Singh and Mannapperuma (1990) review numerical methods and their application to food freezing time prediction.

3.4.2 SIMPLE FORMULAS

For engineering design purposes, a full numerical solution may not be warranted, especially in view of the likely uncertainty in thermal property data, and the imprecise control of freezing conditions that occurs in actual freezers. In these cases the overall accuracy of the predictions is determined less by the calculation precision than the data uncertainty. For this reason, simple prediction formulas derived by combining reasonable engineering assumptions (i.e., the use of the unique phase change model) with sound empiricism have been found to be nearly as accurate in many situations, and far simpler and less costly to use.

A large number of such prediction formulas have been proposed. These are reviewed by Heldman and Singh (1981), Cleland (1990), Singh and Mannapperuma (1990), and Cleland (1991). Most have their genesis in Plank's equation which is an analytical solution for a simplified version of the unique phase-change model.

3.4.2.1 Plank's Equation

Plank's equation for the one-dimensional infinite slab geometry is

$$t_f = \frac{\rho L}{(\theta_{if} - \theta_a)}\left[\frac{R}{h} + \frac{R^2}{2k_f}\right] \tag{3.9}$$

In addition to using the simplified unique phase-change front model, other assumptions inherent in Plank's equation are that the heat capacity of both the unfrozen and frozen regions

are negligible compared with the latent heat effect. Versions of Plank's equation have been derived analytically for infinite cylinders and spheres and for finite parallelopiped geometries but such an analytical approach is unlikely to be applied to more complex product shapes (Heldman and Singh, 1981; Cleland, 1990).

These assumptions mean that Plank's equation is not an accurate prediction method in itself. Its value is two-fold. First, it is the basis of the accurate empirical method given in Section 3.4.2.2, and second, it can show the relative effect of process variables. For actual freezer design, greater accuracy is required and terms to take account of sensible heat effects, the other limitations of the unique phase-change front model and a wider range of geometries, must be included.

3.4.2.2   Recommended Prediction Method

The freezing time prediction formula recommended, combines the modified Plank's equation for one-dimensional objects suggested by Pham (1986) with the modification for the effect of object shape proposed by Cleland (1991) and Hossain et al. (1992)

$$t_f = \frac{1}{E}\left[\frac{\Delta H_1}{\Delta T_1} + \frac{\Delta H_2}{\Delta T_2}\right]\left[\frac{R}{h} + \frac{R^2}{2k_f}\right]\tag{3.10}$$

where
$$\Delta H_1 = \rho c_u\,(\theta_i - \theta_{fm})$$

$$\Delta H_2 = \rho L + \rho c_f\,(\theta_{fm} - \theta_{fin})$$

$$\Delta\theta_1 = 0.5\,(\theta_i + \theta_{fm}) - \theta_a$$

$$\Delta\theta_2 = \theta_{fm} - \theta_a$$

$$\theta_{fm} = 1.8 + 0.263\,\theta_{fin} + 0.105\,\theta_a$$

This approach has been proven accurate by comparison with high-quality experimental data for high moisture products (>55% water) for a wide range of freezing conditions (Pham, 1986; Cleland, 1991). While differences of up to ±15% occurred, much of this was experimental error. It is often thought that it is possible to predict industrial freezing times very accurately. This is rarely true. In practice there are often large differences between the size and shape of product items, wide ranges in air velocities between different parts of air-blast freezers, and estimation of accurate thermal properties and heat transfer coefficients can be difficult. Hence, because of data uncertainties alone, freezing time estimates should be treated as being accurate to within about ±20% at best. Techniques to determine the data required to predict freezing times using Equation 3.10 are covered in the following sections.

3.4.3   CHARACTERISTIC HALF THICKNESS

The characteristic half thickness, R, is defined as the shortest distance from the thermal center (slowest point to cool) of the product to the product surface. Many products are symmetric, so the geometric center will be a good estimate of the thermal center. In this case the characteristic half thickness is half the smallest dimension of the product. For example, for a sphere R equals the radius, and for a rectangular carton R equals half the smallest side length.

3.4.4   SHAPE FACTOR

The exact way in which shape affects freezing is complex. In Equation 3.10 an approximate shape factor, the equivalent heat-transfer dimensionality, E, is used to describe the effect of shape of the product on freezing time.

3.4.4.1 Calculation of E

E is a measure of how much each of the three spatial dimensions contribute to heat transfer. E values are always between 1 and 3. A sphere is perfectly three dimensional so all three dimensions contribute fully and $E = 3$. An infinitely long cylinder has two fully contributing dimensions and one dimension with no contribution so $E = 2$. An infinite slab only has heat transfer in one dimension so $E = 1$. For other product shapes E can be estimated using (Cleland, 1991; Hossain et al., 1992)

$$E = 1 + \frac{\left(1 + \frac{2}{Bi}\right)}{\left(\beta_1^2 + \frac{2\beta_1}{Bi}\right)} + \frac{\left(1 + \frac{2}{Bi}\right)}{\left(\beta_2^2 + \frac{2\beta_2}{Bi}\right)} \tag{3.11}$$

β_1, β_2, and Bi are found using

$$\beta_1 = \frac{A}{\pi R^2} \tag{3.12}$$

$$\beta_2 = \frac{3V}{4\pi\beta_1 R^3} \tag{3.13}$$

$$Bi = \frac{hR}{k_f} \tag{3.14}$$

If V, the volume of the object, cannot easily be measured directly then it can be estimated using the weight of the object divided by the effective density of the product, ρ (Equations 3.18 and 3.25). A is the smallest cross-sectional area of the object measured through the thermal center. The cross-section should include the characteristic half thickness (that is, it should be possible to draw the characteristic half thickness on an outline of the cross-section).

For example, consider a whole fish. Looking from above, the fish is longer and deeper than it is wide. The characteristic half thickness is from the center of the body to the side (behind the gills where the fish is thickest). The smallest cross-section is found by cutting across the fish at this thickest part
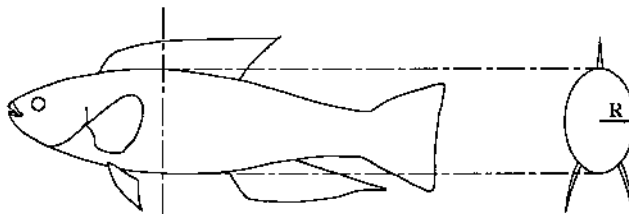
3.4.4.2 Experimental Estimation of E

The above formula to calculate E is most accurate for regular shapes such as rectangular bricks and finite cylinders. For less regular (naturally occurring shapes) there is more natural variability between product items and so measurement of R, V, and A becomes more difficult. Thus the final value for E may be less precise. Alternatively, if experimental data for freezing

an irregularly shaped product is available for one set of conditions then E can be back-calculated using Equation 3.10. Preferably a large number of experiments should be performed and the average E value calculated to account for any random variations in shape between the objects in the experiments. Examples of E for some irregular shapes measured in this way are (Cleland and Cleland, 1992):

Lamb (shoulder)	E = 1.4
Lamb (deep leg)	E = 2.0
Beef side (deep leg)	E = 1.3
Albacore tuna fish	E = 1.8

3.5   THERMAL PROPERTIES

In order to predict heat loads during freezing and product freezing times accurate thermal property data are essential. There are three alternatives — use of data from the literature, direct measurement, and prediction using simple methods based on composition information. There are many good general reviews of these areas including those of Mellor (1976, 1978, 1979, 1980), Jowitt et al. (1983), Sweat (1985b), Murakami and Okos (1989) and Heldman and Lund (1992).

3.5.1   LITERATURE DATA

Many sources of thermal property data are available but it is often difficult to assess the likely accuracy of the data. Some sources of data that may prove useful are Mohsenin (1980), Hayes (1987), ASHRAE (1989), Heldman and Lund (1992), Morley (1972) for meat and meat products, Sweat (1974) for fruits and vegetables, Sweat (1985a) for low and intermediate moisture food, and Rask (1989) for dough and bakery products. Care must be taken in using compendiums of data. For example, ASHRAE (1989) gives an extensive list of typical water contents, highest freezing temperatures, frozen and unfrozen specific heat capacities and latent heat values for foods. The specific heat capacity and latent heat are not measured data but have been calculated using some simple prediction formulas.

3.5.2   MEASUREMENT OF DATA

A large number of methods to measure thermal properties are reviewed by Mellor (1979), Kent et al. (1984) and Murakami and Okos (1989). Those considered most reliable and most commonly used are calorimetry to measure enthalpy and apparent specific heat capacity, and guarded hot-plate and line-source probes to measure thermal conductivity. Some laboratories provide thermal property measurement services.

3.5.3   PREDICTION OF THERMAL PROPERTIES

Prediction of thermal properties by simple equations from composition data is widely used. A major problem in measuring and estimating thermal property data is that many foods are very heterogeneous in composition and there can be large variation in composition from one item to another of nominally the same product. For these reasons, simple prediction methods based on basic compositional data are likely to be nearly as accurate as the best measured data, and perhaps more accurate than some of the poorer measured values. Use of the prediction methods outlined below is recommended if reliable measured thermal property data are not available. Fuller discussions of methods to predict thermal properties are given by Miles et al. (1983), Choi and Okos (1986), Murakami and Okos (1989) and Singh and Mannapperuma (1990).

3.5.3.1 Conceptual Model

The common basis of thermal property prediction methods is to consider the food as being homogenous but consisting of a number of components — water, fat, and solids other than fat

$$X_W + X_F + X_S = 1 \tag{3.15}$$

The solid other than fat component can also be subdivided further into carbohydrate, protein, and mineral fractions

$$X_S = X_C + X_P + X_M \tag{3.16}$$

but the following equations will use X_S only. If subdivision of the solid component is desired then terms containing X_S should be appropriately expanded.

Standard laboratory gravimetric techniques can be used to determine the component mass fractions. Alternatively publications such as Watt and Merrill (1975) and Holland et al. (1991) state typical compositions for a wide range of food materials and food products.

The change in thermal properties during freezing are dominated by the change in phase of the water component from liquid water to ice. The aqueous component is modeled as a mixture of ice and a solution of the nonaqueous components in the liquid water which causes freezing point depression. As water freezes into pure ice, the remaining solution becomes more concentrated, so freezing point depression increases. The net effects are that the initial freezing points for foods are below 0°C, and that latent heat of freezing is released over a range of temperatures and not at a unique temperature as for a pure substance. Finally, some of the water is loosely bound to the components (such as protein) and is never available to freeze, even at temperatures well below the initial freezing temperature. All these processes must be taken into account by the thermal properties estimation method.

The total water component is thus modeled as consisting of three fractions — liquid water, ice, and bound water

$$X_W = X_{LW} + X_I + X_B \tag{3.17}$$

In order to predict thermal properties, methods to estimate these fractions are required.

Phase change in the fat fraction can sometimes be important. The magnitude of the change and temperature at which it occurs depends on the fat constituents. Generally the fat latent heat effects are small compared to those for water. Therefore, an approach which includes an allowance for these latent heat effects in the specific heat capacity for the fat fraction is usually adequate.

3.5.3.2 Package Voidage and Porous Foods

Many food products contain significant internal voids (gas) space. The voids can be both within the food material if it is **porous** (e.g., apple flesh is typically 10 to 20% void space) and between items within a product (e.g., air voids within diced toppings on a pizza or air spaces between product items within a carton).

Air voids have a substantial effect on thermal properties. A common approach to evaluate the effect of voids is to calculate the properties of the nonporous, "solid" food material based on component mass fractions, and then to adjust this estimate for the presence of voids based on the void volume fraction (porosity), ε. Only density and thermal conductivity need to be modified as specific heat capacity and enthalpy use a weight basis and the voids have negligible mass. Density and thermal conductivity data from the literature will include the

effect of voids within porous materials but will not include the effect of voids created by combining food materials or items into a product package.

The porosity can be calculated from the overall weight and volume of the product, and the density of the nonporous food material

$$\varepsilon = 1 - \frac{W}{V\rho_{\varepsilon=0}} \tag{3.18}$$

3.5.3.3 Freezing Point Depression, Ice Fraction, and Bound Water

Assuming Raoults law of dilute solutions and the Claussius-Clapeyron relationship apply, it can be shown (Singh and Mannapperuma, 1990) that the relationship between freezing point depression and mass fractions for the food model is

$$\frac{1}{T} = \frac{1}{T_{0°C}} - \frac{R\,M_W}{L'} \ln\left(\frac{(X_W - X_I - X_B)/M_W}{(X_W - X_I - X_B)/M_W + (X_S + X_F)/M_E} \right) \tag{3.19}$$

The effective molecular weight of the nonwater components, M_E, which are assumed to all be soluble, can be estimated using this equation if the initial freezing point, θ_{if}, is known by substituting $X_I = 0$ and $T = \theta_{if} + T_{0°C}$. Alternatively, if the soluble solid components are well defined then the term $(X_S + X_F)/M_E$ can be calculated explicitly by summing X/M for each of the soluble components (Schwartzberg, 1976).

If θ_{if} is known, then using Equation 3.19, X_I can be related to temperature below θ_{if} by

$$X_I = (X_W - X_B)\left[1 - \frac{\exp\left(\frac{L'\,M_W}{R\,T_{if}}\right) - \exp\left(\frac{L'\,M_W}{R\,T_{0°C}}\right)}{\exp\left(\frac{L'\,M_W}{R\,T}\right) - \exp\left(\frac{L'\,M_W}{R\,T_{0°C}}\right)} \right] \tag{3.20}$$

Above θ_{if}

$$X_I = 0 \tag{3.21}$$

For dilute solutions, Schwartzberg (1976) showed that Equation 3.20 can be approximated with little loss of accuracy by

$$X_I = (X_W - X_B)\left(1 - \frac{\theta_{if}}{\theta} \right) \tag{3.22}$$

For X_I values calculated by Equations 3.20 or 3.22 to be accurate, precise data for θ_{if} is essential. Many of the sources of thermal property data include values of θ_{if} for the main food types and products but these data often are of dubious origin, have been significantly altered by rounding (especially when converting from Fahrenheit to Celsius or vice versa) and may not represent the midpoint of the range of variations in food products. For these reasons, literature values, of θ_{if} should be used with caution. Typical θ_{if} for fish, meats, fruits,

TABLE 3.2
Ranges for *b* for Some Food Systems

Food system	b Range
Meat, fish	0.14–0.32
Sucrose	0.30
Glucose	0.15–0.20
Egg	0.11
Bread	0.11–0.14
Orange juice	0
Vegetables	0.18–0.25

Data are from Schwartzberg (1976), Pham (1987a),
Murakami and Okos (1989).

and vegetables are in the range –2.0 to –0.5°C. For high moisture foods (>55% water), use of $\theta_{if} = -1.0°C$ is recommended as a first approximation if a better estimate is not available.

The bound water fraction must be known to estimate X_I. It is commonly related to the solids mass fraction

$$X_B = bX_S \qquad (3.23)$$

Some values of b evaluated for various food systems are given in Table 3.2. If better data are not available then use of b = 0.25 is suggested.

3.5.3.4 Density

The most commonly used model for density is

$$\frac{1}{\rho_{\varepsilon=0}} = \sum_j \frac{X_j}{\rho_j} \qquad (3.24)$$

Air voids affect the density in proportion to the porosity

$$\rho = \rho_{\varepsilon=0}(1-\varepsilon) \qquad (3.25)$$

3.5.3.5 Specific Heat Capacity

The most common approach employed to estimate c is to sum up the contributions from the components. Above θ_{if} the model recommended is

$$c = \sum_j X_j c_j \qquad (3.26)$$

Below θ_{if}, effects due to phase change by the water fraction must be added. A number of models have been developed (e.g., Schwartzberg, 1976; Miles et al., 1983). Differences between the various models for c arise from the selection of the method to predict ice fraction and from what approximations are made, particularly with respect to the thermodynamic

behavior of water, ice, and bound water at temperatures below θ_{if}. For most high moisture foods the differences between models are small and accurate prediction has been reported provided accurate data for θ_{if} and X_B are known. Schwartzberg (1976) developed one of the simplest models based on Equation 3.22 and assuming that component heat capacities are constant with temperature

$$c = c_u - \left(X_W - X_B\right)\left[\frac{L' \theta_{if}}{\theta^2} + \left(c_W - c_I\right)\right] \tag{3.27}$$

Singh and Mannapperuma (1990) proposed a more complex model using Equation 3.20 for ice fraction, and took into account variation in c_I and L' with temperature. Given the likely imprecision in values of θ_{if} and X_B for many foods, and the normal variability in composition of foods, use of more complex models than Equation 3.27 is difficult to justify.

3.5.3.6 Enthalpy and Latent Heat

Defining the datum, $H = 0$ at $\theta = \theta_{if}$, and assuming that the component c values and L' are constant with temperature, the corresponding enthalpy model derived from Equations 3.26 and 3.27 for $\theta > \theta_{if}$ is

$$H = \left(\theta - \theta_{if}\right)c_u = \left(\theta - \theta_{if}\right)\left(X_W c_W + X_F c_F + X_S c_S\right) \tag{3.28}$$

and for $\theta < \theta_{if}$ is

$$H = \left(\theta - \theta_{if}\right)\left(c_u - \left(X_W - X_B\right)\left[\frac{L'}{\theta} + \left(c_W - c_I\right)\right]\right) \tag{3.29}$$

The latent heat of freezing, L, results solely from the change in phase of water; the other components are merely cooled. A value of L can be estimated from the latent heat of water and the ice fraction at a temperature at which, for practical purposes, the material is fully frozen (for high moisture foods use of –25°C is recommended; see Section 3.5.4)

$$L = X_I L' \tag{3.30}$$

Figure 3.9(e) shows this method of estimation of L diagrammatically. Alternative freezing time prediction formulas to Equation 3.10 may use the enthalpy change during freezing (e.g., between θ_{if} and an endpoint temperature such as –10°C). In these cases, Equations 3.28 and 3.29 should be used to calculate the enthalpy change rather than Equation 3.30 which evaluates only the latent component.

3.5.3.7 Thermal Conductivity

A large number of physical models to predict thermal conductivity of foods have been proposed. Most models are based on volume rather than mass fractions. Volume fractions (excluding porosity) are calculated using

$$v_j = \frac{\rho_{\varepsilon=0} X_j}{\rho_j} \tag{3.31}$$
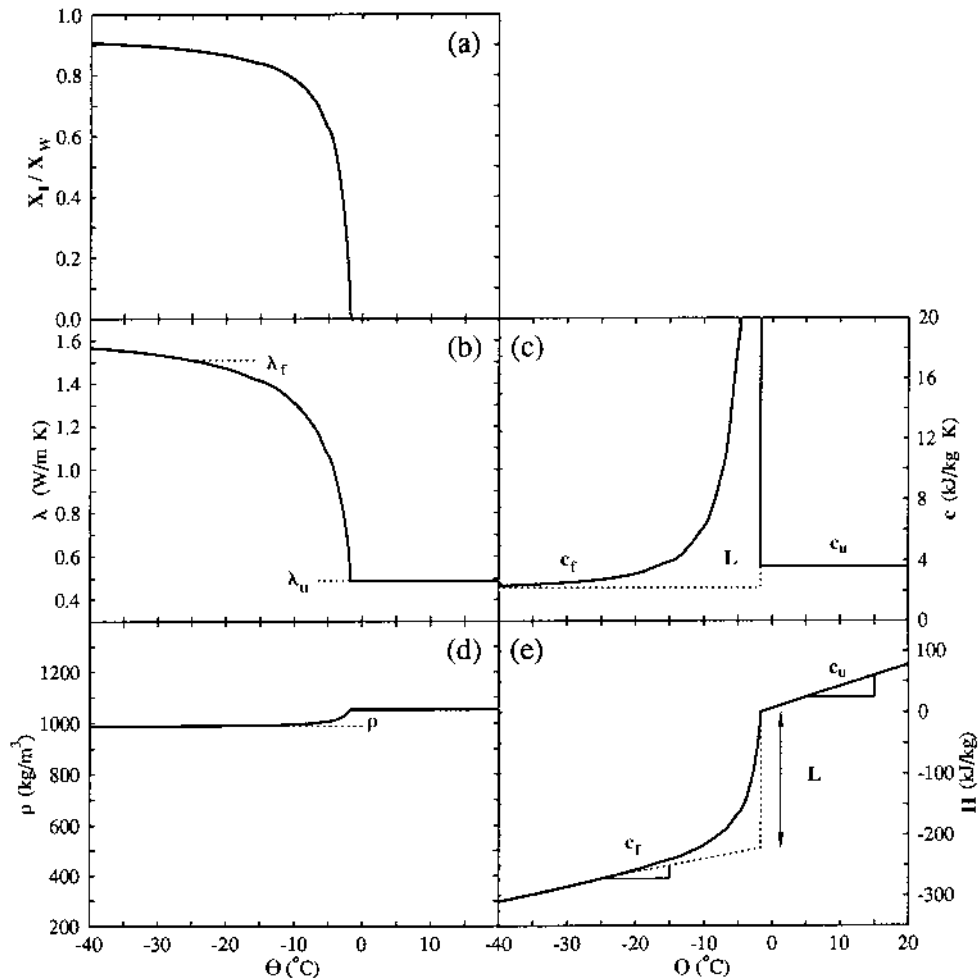
FIGURE 3.9 Typical change in thermal properties with temperature for a high moisture food: (a) fraction of water frozen (X_I/X_W), (b) thermal conductivity, (c) specific heat capacity, (d) density, (e) enthalpy.

Miles et al. (1983), Murakami and Okos (1989), and Pham (1990) give comprehensive reviews and evaluations of prediction models. Miles et al. (1983) recommended the use of the parallel-component heat transfer model for thermal conductivities of nonporous foods across the full temperature range. Murakami and Okos (1989) considered various models for a range of nonporous foods, both above and below their freezing points. Above the freezing point, the simple parallel model was confirmed as best. Below freezing, a combined parallel-series model (parallel nonliquid water components in series with liquid water) was suggested as being simple yet accurate.

For nonporous animal products only, Pham (1990) found that a modification to the Maxwell-Eucken model was most accurate. This model is more complex to use than other models, due to it being a two-phase model that must be applied consecutively to all of the components. The combined parallel-series model was not evaluated. In Pham's study there was less difference between models above θ_{if} than for frozen conditions and the parallel model was only slightly inferior to the modified Maxwell-Eucken model.

Thus, for unfrozen food the parallel model is recommended

$$k_{\varepsilon=0} = \sum_j v_j k_j = \rho_{\varepsilon=0} \sum_j \frac{X_j k_j}{\rho_j} \tag{3.32}$$

and below θ_{if} the combined parallel-series model is recommended as a compromise between accuracy and simplicity

$$\frac{1}{k_{\varepsilon=0}} = \frac{\left(v_{LW} + v_B\right)}{k_W} + \frac{\left(1 - v_{LW} - v_B\right)^2}{\sum\limits_{j \text{ not } LW,B} v_j k_j} \tag{3.33}$$

Unless comprehensive testing performed for a wider range of food products shows worthwhile accuracy improvements, especially below θ_{if}, use of more complex alternative models of similar accuracy is difficult to justify.

For porous foods of the type likely to be frozen industrially, there has been little systematic assessment of prediction methods for calculating k from $k_{\varepsilon=0}$ and ε. Based on a very limited comparison of methods, Miles et al. (1983) recommended the parallel model but found the Maxwell-Eucken equation to be of similar accuracy. Murakami and Okos (1989) evaluated nine models for porous foods. The best model involved 12 empirical constants, and was only applicable to and tested for, foods with $\varepsilon > 0.08$ and $X_W < 0.3$. This does not include the range important for food freezing. The Maxwell-Eucken model was one of the next best models.

Use of the relatively simple Maxwell-Eucken model to take account of porosity is recommended until systematic testing identifies a superior model for porous product of the type likely to be frozen. For porous foods the Maxwell-Eucken model is

$$k = k_{\varepsilon=0} \left[\frac{2k_{\varepsilon=0} + k_a - 2\varepsilon\left(k_{\varepsilon=0} - k_a\right)}{2k_{\varepsilon=0} + k_a + \varepsilon\left(k_{\varepsilon=0} - k_a\right)} \right] \tag{3.34}$$

This model assumes that the voids are evenly distributed throughout the product package and that the voids are sufficiently small so there is little natural convection of the air within the void. For some foods these conditions are not met so care should be taken in using the results. Alternative models that may be superior are a modification to Equation 3.34 due to Levy and the effective medium theory, both described by Pham (1990).

3.5.3.8 Component Thermal Properties

The above equations require data for the thermal properties of the components. Choi and Okos (1986) give equations for the component thermal properties in the range –40 to 150°C. Although the properties do change with temperature, for simplicity, average values are commonly used. Table 3.3 states typically used average values for the components of interest.

3.5.4 SIMPLIFIED THERMAL PROPERTY PREDICTION METHOD

Equations 3.15 to 3.34 can be used to predict properties across the full temperature range of interest for freezing as is required for numerical freezing time prediction methods. Figure 3.9 shows such predictions for a food with 76% water, 6.5% fat, 17.5% solids, $M_E = 359$, and $b = 0.23$.

The simple freezing time prediction method presented earlier requires specific data for both the unfrozen and fully frozen food. As Figure 3.9 shows, there is usually considerable

TABLE 3.3
Properties of Pure Components

j	ρ_j (kg/m³)	c_j (J/kg K)	k_j (W/m K)
LW,B	1000	4180	0.56
I	917	2110	2.22
a	1.3	1005	0.025
F	930	1900	0.18
S	1450	1600	0.22
P	1380	1900	0.20
C	1550	1500	0.245
M	2165	1100	0.26

Note: $L' = 334$ kJ/kg. (Data are from Miles et al. (1983), Choi and Okos (1986), and Pham (1990).

temperature-variability in properties especially below the initial freezing point. To calculate representative mean values, Equations 3.15 to 3.34 can be used with average component properties. For frozen properties, a temperature at which the food can be considered fully frozen must also be defined so that X_I can be evaluated. Use of –25°C is recommended as it is typical of the final food temperature in freezers and storage facilities, and for most high-moisture foods there are only small changes in X_I below –25°C.

Overall, the following procedure is recommended to estimate the properties required to predict freezing time from composition data as a reasonable compromise between complexity and accuracy:

1. Determine θ_{if} as suggested in Section 3.5.3.3
2. Calculate X_B using Equation 3.23
3. For fully frozen properties, calculate X_I and X_{LW} at –25°C using Equations 3.22 and 3.17, respectively; for unfrozen properties $X_I = 0$, and X_W is used instead of X_{LW} and X_B
4. Estimate $\rho_{\varepsilon=0}$, ε and ρ using Equations 3.24, 3.18, and 3.25 for fully frozen product
5. Use Equation 3.26 to estimate both c_u and c_f
6. Calculate $k_{f,\varepsilon=0}$ from Equation 3.33 at –25°C and k_f from Equation 3.34 for porous foods
7. Use Equation 3.30 to calculate L

The density change during freezing is sufficiently small and the other sources of imprecision sufficiently large that the effect of change of density on freezing-time prediction is unlikely to be significant. Use of the frozen material density calculated in Step 4 is recommended. This ensures that the calculation of ε is consistent with the methodology used to estimate the frozen thermal conductivity, k_f. Product dimensions and volumes should be measured in the frozen state to be consistent.

3.6 HEAT TRANSFER COEFFICIENTS

Heat transfer at the surface of an unwrapped product can occur by a number of mechanisms acting in parallel including convection, radiation, and evaporation. In addition, for wrapped products there can be the added heat-transfer resistance due to conduction across packaging

materials and trapped air gaps between product surface and packaging, but evaporation is usually insignificant. The most common approach is to estimate an effective heat-transfer coefficient, h, to account for all these mechanisms. Further, it is usually assumed that h is constant during the freezing process and uniform over the full product surface.

The normal additive rules for heat transfer resistances in series, and for heat transfer coefficients for parallel heat flow situations, then apply

$$\frac{1}{h} = \frac{1}{h_c} + \sum \frac{x_p}{k_p} + \frac{x_a}{k_a} \tag{3.35}$$

where

$$h_c = h_{con} + h_{rad} + h_{evap} \tag{3.36}$$

Expressed as pseudo-convection, the evaporative contribution is given by

$$h_{evap} = \frac{K(p_s - p_a)H_{lg}}{(\theta_s - \theta_a)} \tag{3.37}$$

This expression can seldom be used because of difficulties in estimating K (which includes the resistance of any skin or packaging layer as well as the resistance in the convective boundary layer), difficulties in measuring or estimating p_s as a function of θ_s (which requires a nonlinear function and also depends on the water activity of the product), and because there are large variations in θ_s, p_s, and hence h_{evap} with both time and surface position during freezing. It is often assumed that the evaporative contribution is relatively small compared to radiation and convection. For wrapped products this assumption is reasonable, but in other situations the evaporative contribution can be significant. Hallstrom et al. (1988) carried out an analysis assuming that K can be estimated from h_{con} using the heat/mass transfer analogy and that the product surface resistance is small. They showed that for unwrapped high moisture products h_{evap} can be greater than 20% of h_{con} for typical surface temperatures.

Assuming that the radiative source is at the same temperature as the cooling medium, the radiation pseudo-convection heat transfer coefficient is given by

$$h_{rad} = \sigma \, \varepsilon \, \Gamma\left(T_a^2 + T_s^2\right)\left(T_a + T_s\right) \tag{3.38}$$

Emissivity, ε, is about 0.9 for most foods and nonreflective packaging wraps (ASHRAE, 1989). Cooling medium temperatures are usually in the range –20 to –50°C and for most of the freezing process the surface temperature is typically below –5°C. For these conditions and the maximum Γ of 1.0, h_{rad} will be in the range 2 to 5 W/m²K, but is most likely to be about 3 W/m²K. In practice due to close stacking of product, Γ will be less than 1.0 and the radiation source temperature may be closer to the product surface temperature than the cooling medium temperature. Therefore, the radiation contribution is likely to be lower than the theoretical analysis suggests.

There are a large number of published data and correlations for convective heat transfer. For food freezing processes these are reviewed by Arce and Sweat (1980), Hallstrom et al. (1988) and ASHRAE (1989). Data and correlations tend to be medium and geometry specific. The correlations and values for h_c that follow have been found to be generally applicable for a wide range of freezing conditions and include allowance for typical radiative and evaporative components.

3.6.1 PLATE FREEZING

For plate freezing, h_c takes account of the resistance to heat transfer between the refrigerant and the plate, the resistance in the metal plates, and the resistance due to imperfect contact between the plates and the product (or packaging). If good distribution of refrigerant in the plates is achieved then the resistance due to imperfect contact dominates. For a plate freezer with poor contact, h_c may be as low as 50 to 100 W/m²K and a thin air layer may also be present (Cowell and Namor, 1974). For good contact h_c is typically in the range 200 to 500 W/m²K and there should not be an air layer trapped by the packaging (Creed and James, 1985). The degree of contact depends on plate pressure, ease of deformation of the product and packaging, packing density and use of spacers between plates. Proper package design should ensure a high packing density so that good contact is possible with minimum distortion of the package and at lower plate pressures.

3.6.2 AIR-BLAST FREEZING

For air-blast freezing, h_c is related to the rate of air movement and depends on the nature of the air flow pattern, the size and shape of the object and the orientation of the object in the air flow.

For natural convection (air velocity less than 0.4 m/s), a general correlation (Coulson and Richardson, 1977) is

$$h_{con} = 2.3\left(\theta_s - \theta_a\right)^{0.25} \tag{3.39}$$

For the usual temperature differences of 2 to 30°C and adding a radiation component of 3 to 4 W/m²K, Equation 3.39 and 3.36 predict that h_c is typically between 5 and 10 W/m²K for natural convection.

For forced convection (air movement by fans so that air velocity is greater than 1.0 m/s) over large product items with little interaction between items, the following approximations have been found to work well in a wide range of applications (Cleland and Cleland, 1992). For objects with planar surfaces

$$h_c = 7.3\, u_a^{0.8} \tag{3.40}$$

For oval objects

$$h_c = 12.5\, u_a^{0.6} \tag{3.41}$$

The correlations given by Pham and Willix (1986) for rectangular cartons in a cross-flow air-blast tunnel, Chavarria and Heldman (1984) for flow over flat plates, Flores and Mascheroni (1988) for beef hamburgers in a belt freezer, Mannapperuma et al. (1994a, 1994b) for air-blast freezing of chicken and turkey, and those summarized by Arce and Sweat (1980), ASHRAE (1989) and other heat transfer texts predict h_c values broadly consistent with the above simple equations.

For fluidized bed and belt freezers where the product items are generally small and where they interact with each other to form a porous bed, h_c values tend to be much higher than in air-blast freezing of larger individual product items. Vazquez and Calvelo (1980) and Khair-ullah and Singh (1991) provide some correlations. Typical values are in the range 120 to 200 W/m²K.

TABLE 3.4
Typical Thermal Conductivities for Food Packaging Materials

Packaging material	k_p Range (W/mK)	Typical k_p (W/mK)
Solid cardboard	0.06–0.08	0.065
Corrugated cardboard	0.04–0.065	0.048
Paper		0.13
Wood (soft)	0.1–0.2	0.12
High density polyethylene		0.48
Low density polyethylene		0.33
Polypropylene		0.12
Polytetrafluoroethylene		0.26
Air	0.021–0.027	0.025
Aluminium	200–270	220
Steel	40–50	45

Data are from Cowell and Namor (1974), Creed and James (1985), Hayes (1987), ASHRAE (1989), Singh and Mannapperuma (1990), Cleland and Cleland (1992).

3.6.3 LIQUID IMMERSION AND CRYOGENIC FREEZING

In liquid immersion systems only convective heat transfer is important. Values of h_c tend to be greater in liquid immersion than in air freezers for the same degree of fluid movement because of the greater density and thermal conductivities of the liquids compared to air. Typical h_c values for brine and glycol freezers are 300 to 600 W/m²K (Hayes, 1987; Singh and Mannapperuma, 1990).

Data relating h_c to $(\theta_s - \theta_a)$ for N_2 and CFC-12 freezers is summarized by Awonorin (1989) and Singh and Mannapperuma (1990). Likely values are in the range 150 to 250 W/m²K for sprayed N_2. There is little published information on h_c values during sublimation of CO_2 snow. Heat transfer coefficients may be lower than for a liquid cryogen due to poorer contact between the food and the CO_2 snow.

3.6.4 PACKAGING AND TRAPPED AIR

Packaging of product adds both the direct heat transfer resistance due to the packaging, plus the contact resistance and resistance of air trapped between multiple layers of packaging or the packaging and the product surface. These heat transfer resistances are additive (Cowell and Namor, 1974). Typical values of k_p for some packaging materials are given in Table 3.4.

Thicknesses of trapped air layers are not easy to measure or estimate but can have significant effect on the overall heat transfer coefficient. Equation 3.35 assumes that the air is stationary so in large gaps where natural convection can be significant the heat transfer resistance will be less than that predicted. For many cartoned products with high packing density (low porosity), air layer thicknesses in the range 0 to 3 mm and the assumption of still air are often appropriate. Due to product compaction, the gaps tend to be larger at the top and side surfaces than at bottom surfaces. For plate freezing, Creed and James (1985) report contact resistances between packaging layers in the range 0.0015 to 0.01 m²K/W with an applied pressure of 310 kPa corresponding to less than 0.3 mm nominal air gap.

TABLE 3.5
Typical Component Heat Load Percentages
for Well-Designed Food Freezers

Freezer type	Product	Fans/pumps	Pull-down	Defrost[a]	Other[b]
Batch air-blast	50–80%	10–40%	<10%	<5%	<5%
Continuous air-blast	50–80%	10–40%	0%	10–20%	5–10%
Plate	85–95%	5–10%	<5%	<5%	<5%
Cryogenic	85–95%	<10%	<5%	0%	<10%

[a] Assumes defrost is performed off-line for batch and plate freezers and on-line for continuous freezers.
[b] Insulation ingress, air interchange, equipment other than fans, storage vessel losses.

In some products the surface may be covered by a product component layer with significantly lower thermal conductivity than the rest of the product, e.g., a fat layer over a beef cut. Rather than adjusting the thermal properties to take account of this layer it may be better to treat it as an extra layer of packaging and adjust h instead.

For most freezing situations, the thermal capacity of the packaging is insignificant compared with the product and can be ignored with little loss of accuracy. Variations in numbers and thickness of packaging layers over the product surface should be averaged (e.g., for cartons, parts of some surfaces may have multiple layers and others single layers due to carton construction). The mean should be weighted so that the packaging on surfaces directly overlying the center of the product has greatest weighting. No quantitative guidelines have been proposed in the literature to aid the engineer in this area.

3.7 HEAT LOADS

The heat load during freezing is required to size the refrigeration system and to estimate energy costs. The heat load has two main components:

1. Product
2. Fans (pumps for plate or immersion freezers)

plus a number of what are generally smaller components including: insulation ingress, air infiltration, equipment other than fans or pumps (e.g., mechanical drives), defrost (if the freezer is defrosted while product is present), and freezer pull-down (batch operations only). Assuming that the freezer is well designed to keep the miscellaneous smaller load components minimal, typical contributions of the heat load components are given in Table 3.5. In many situations an allowance for all the smaller components of 10 to 25% of the product plus fan load is sufficiently accurate. However, any easily identifiable large components should be individually added, e.g., mechanical drives for product conveying systems.

3.7.1 PRODUCT

For a freezer with continuous product loading and unloading, product heat load will be essentially uniform with respect to time. For a batch freezer, the heat load will be highest at the start and will decrease as freezing progresses. The mean product heat load is given by

$$\phi_{pr} = \frac{W_{pr}}{t_{pr}} \left[c_u \left(\theta_i - \theta_{if} \right) + L + c_f \left(\theta_{if} - \theta_{out} \right) \right] \tag{3.42}$$

For a continuous freezer, W_{pr} is the amount of product resident in the freezer at any time and t_{pr} is the product residence time (W_{pr}/t_{pr} equals the production rate). For a batch process W_{pr} is the size of each batch and t_{pr} is the cycle time for each batch of product. It should be noted that at the end of the freezing process, there will be a temperature gradient from the center to the surface of the product and the outlet **mass-average temperature**, θ_{out}, will be lower than the final thermal center temperature, θ_{fin}, but higher than the cooling medium temperature, θ_a.

3.7.2 FANS OR PUMPS

The fan or pump heat load equals the energy use. For fans this is given by

$$\phi_{fan} = \frac{Q_a \Delta P_a}{\eta_{fan} \eta_m} \tag{3.43}$$

An analogous equation can be used for pumps. The difficulty in using Equation 3.43 is that the pressure difference is difficult to estimate from first principles for most air freezing systems. A large part of the pressure drop occurs through the air cooling evaporator coil. Coil manufacturers should supply data for this pressure drop, but the rate and effect of frost formation is seldom well known. For air-blast freezing systems there is often significant pressure drop in the product space due to the relatively small flow cross-sections and high air velocities that are used to promote air to product heat transfer. This pressure drop is commonly referred to by coil manufacturers as the external static pressure (ESP) that the fan must overcome. Calculation of ESP is difficult due to the complex flow geometries. Allowances of 100 to 250 Pa are commonly used but are very dependent on the type and configuration of the freezer.

The desired air flowrate is defined by the desired air velocity over the product and the cross-sectional area for air flow in the freezer, and this must be matched to the evaporator face area and face velocity. Fan efficiencies can be determined from manufacturers' data. For a fan well matched to the duty η_{fan} is typically 50 to 70%, and should not decline too severely as ΔP increases due to frosting. Similarly, motor efficiencies are usually in the range 85 to 95% depending on the quality of motor used.

The air velocity (fan speed) and fan power relationship is important for optimal freezer design

$$\phi_{fan} \propto u_a^{2-3} \tag{3.44}$$

Increasing air velocity may have beneficial effects on evaporator coil and product heat transfer performance but these are often small compared with the greatly increased fan energy and refrigeration costs. Examples 5 and 8 in Sections 3.9.5 and 3.9.8 illustrate this effect.

It is sometimes assumed that by mounting the fan motor outside the freezer the fan heat load is eliminated from the total heat load. This strategy is seldom worthwhile as it only eliminates the motor inefficiency component of the fan energy (<15% of total fan energy).

3.7.3 INSULATION INGRESS AND AIR INFILTRATION

Heat ingress through the insulated enclosure is generally a small load component. It is important that the insulation vapor barrier is complete and is properly maintained. Vapor barrier damage can lead to ice formation within the insulation. This can result in both greater rates of heat ingress and potential structural damage to the freezer enclosure.

Air infiltration loads are most important for freezers where loading and unloading occur during freezer operation. Adequate protection of the product entrances (e.g., minimization of

entrance size, strip curtains, vestibules) is essential to prevent infiltration. Excessive infiltration leads to problems of higher-than-expected heat load (higher air temperature) and rapid loss of evaporator coil performance due to frosting.

3.7.4 DEFROST

Defrost load is most important if it is desired to defrost during the freezing process without interruption to freezer operation (rather than defrost when the freezer is "off"). In this case, to maintain normal operating air temperature in the freezer it must be possible to sequentially isolate each coil for defrost. The refrigeration system must be sized to cope with the normal heat load, plus any extra instantaneous defrost heat load, while each coil is not in use. Alternatively, operation and control of the freezer must be flexible enough to either reduce or stop product throughput during defrost periods, thereby providing extra product residence time. This would ensure complete product freezing in spite of the lowered air velocities and higher air temperatures that will occur during defrost. This later option is often most desirable as normal breaks in production (e.g., sanitation and meal breaks) can be conveniently used for defrost.

Frost-free coils (e.g., using a glycol wash over the outside of the coil) are an option that avoids potential problems with defrost. Compared with conventional coils they have substantially higher capital cost and face air velocities must be limited to prevent liquid being blown off the coil.

3.7.5 PULL-DOWN

Heat load arising from pull-down of structures within the freezer can be important for batch freezing operations where significant heating occurs between batches and there is insufficient time for temperature pull-down prior to product entry (e.g., heating the freezer to above 0°C for comfort during manual loading, or sanitation washdown with hot water). Generally the room elements that represent the greatest thermal-mass and hence pull-down load are metal structures including the insulation lining and concrete floors (wearing slabs above the floor insulation).

3.7.6 PEAK HEAT LOADS

Typically in a batch freezer the peak heat load will be 2 to 4 times larger than the mean heat load, mainly due to the change in product load (Lovatt et al., 1993). The refrigeration system should have some capacity to cope with peaks greater than the expected mean heat load in worst case conditions, especially if control of the freezer to ensure optimal product quality and costs is desired. The degree of over capacity also depends on whether the system is dedicated to the freezer or serving a number of other applications. Sizing for the full peak, however, is seldom justified. Invariably, once installed, freezers are operated beyond their design capacity due to increases in production or other changes. Often this utilizes any excess capacity in the refrigeration system, so that freezer operation at full capacity is required at all times, thus leaving few options for process control to ensure product quality. The operating costs can then increase dramatically.

3.7.7 MINIMIZING HEAT LOADS

Minimizing the heat load reduces both operating costs and required refrigeration capacity. Common strategies include: defrosting when a freezer is not operating, keeping the product inlet temperature as low as possible, protecting product entrances to reduce air ingress,

preventing product reheat after freezing so θ_{fin} can be higher, and optimizing air flow design to reduce fan power.

3.8   ECONOMICS

3.8.1   CAPITAL COSTS

The main components of the capital cost of a freezer are the:

- Freezer insulated enclosure
- Product transfer and/or support systems (racks, conveyors, etc.)
- Evaporator coils and fans
- Refrigeration system or cryogen storage facilities associated with the freezer
- Control and monitoring systems

The relative costs of these components depend on the type of freezer utilized. The type of freezer is usually fixed by the available space, product type, and processing rate, the desired degree of automation, the need to match the freezer with other processing operations, and optimal balance between capital and operating costs for the business.

Both freezing time and heat load affect the capital cost. The freezing time affects capital cost as product residence time in the freezer determines the physical size of the freezer and product handling system. The size of the heat load mainly affects the capital cost of the refrigeration system associated with the freezer. The required size of the refrigeration system also depends on the operating conditions (particularly the cooling medium temperature, θ_a) and is therefore interrelated to the freezing time. Sometimes there are opportunities to reduce the heat load by increased capital investment (e.g., plate freezers eliminate fan load). This influences both the capital cost of the refrigeration system associated with the facility and the on-going operating costs, particularly energy.

3.8.1.1   Refrigeration System Capacity and Design

Design and sizing of the refrigeration system associated with a freezer is important as it often represents a large fraction of the capital cost and can have a large effect on operating costs. If the refrigeration system is dedicated to the freezer this gives flexibility because the freezer operation is independent of other refrigerated applications. However, compared with a refrigeration system that serves a number of applications, the dedicated system may require duplication of controls and other equipment. The benefits of economy of size and load sharing may not then be realized.

The refrigeration system could use any of a number of refrigerants, and could include use of any of a number of configurations such as single stage or two stage, and direct-expansion, flooded, or pump circulated refrigerant distribution. No refrigerant has any major thermodynamic advantage, but issues such as safety and manning levels can be influential. The ozone depletion issue has resulted in rapid changes in the availability of refrigerants for freezers. Currently, the main possibilities for new plants are ammonia (R-717), R-404A, R-410A, R-507 or HFC-134a, but systems using hydrocarbons, CO_2, and air are being developed. HCFC-22 and blends using HCFC refrigerants can still be used, but will be phased out in the near future. Some existing systems may still operate on R-502 or CFC-12, but supplies are becoming limited. For large multi-use plants, two stage ammonia with pump circulation has many advantages, whereas for independent and smaller installations, use of HCFC or HFC refrigerants and a simpler plant configuration (e.g., single stage and/or direct expansion) is likely to be more appropriate.

The following sections concentrate on the effect of design and operating conditions on refrigeration system capacity and hence capital cost.

3.8.1.2 Evaporator Coils and Fans

Evaporator coils for freezers are predominately of the plate fin type. Fans can be specified as part of the coil or separately. The evaporator coils and fans have dual roles:

- Heat removal from the freezer air to maintain air temperature
- Provision of the desired air movement through both the product and the evaporator coil

The size of the coil is affected by the freezer air flowrate design (the air flowrate through the coil must be consistent with the desired air velocity over the product). The ratio of coil face area to the cross-section area for air flow where the product is located is important. Standard coil face velocities are in the range 2.5 to 6 m/s. Standard fin pitches are 6.3 or 8.5 mm (3 or 4 fins/in) but for applications with high frosting potential wider spacings can be used. Variable fin spacing can also be used to reduce the effect of frost on coil performance. Coil costs are relatively low, so the final coil specification for a freezer often depends as much on the practical constraints of locating them within the freezer enclosure and achieving the desired air flow rates, as it does on heat transfer considerations.

A further constraint is that air flowrate must also be sufficiently high to ensure that the air temperature rise around the freezer is not excessive, although a large air temperature rise is less important if the product moves countercurrent to the air. For other product flow configurations, the freezer design is governed by the rate of freezing for the product in the warmest air returning to the coil. As a general rule, the greater the air temperature rise, the lower the evaporation temperature, θ_e, required for the same air-on temperature, θ_{on}, but the lower the fan power. For freezers with cross-flow air, temperature rise is typically less than 4°C. Special designs with efficient countercurrent contacting of product and air, such as vertical spiral freezers, may have rises as high as 10°C but also require specialized fan and coil designs.

Coils are generally rated on sensible heat removal performance for a fixed face velocity (air flowrate) in proportion to the refrigerant to air-on temperature difference (TD)

$$\phi_{tot} = UA_{on}\left(\theta_{on} - \theta_e\right) = Q_a \rho_a c_a \left(\theta_{on} - \theta_{off}\right) \tag{3.45}$$

Log-mean temperature difference taking into account drop in air temperature through the coil can also be used as the basis of ratings but the UA value will be correspondingly higher. As well as sensible heat, the coil will also achieve heat transfer via water vapor deposition as frost with consequential latent heat release to the coil refrigerant. For freezer conditions, the latent heat component is usually small and it is commonly assumed that the heat load is totally sensible heat to provide a slight safety factor in the coil sizing. Frosting has a significant effect, however, on the coil-sensible heat transfer performance by reducing air flow and hence reducing UA_{on}. Care must be taken that coil heat transfer and air flow ratings include allowance for typical frost loading, the likely ESP, and whether air-on or log-mean TD are used for rating purposes. A typical relationship between face velocity and coil rating is

$$UA_{on} \alpha \, u_a^{0.5-0.6} \tag{3.46}$$

The rating can also be affected by the refrigerant supply method used. Direct expansion coils are typically derated by 10 to 15% compared with the same-size coil in a flooded or pump
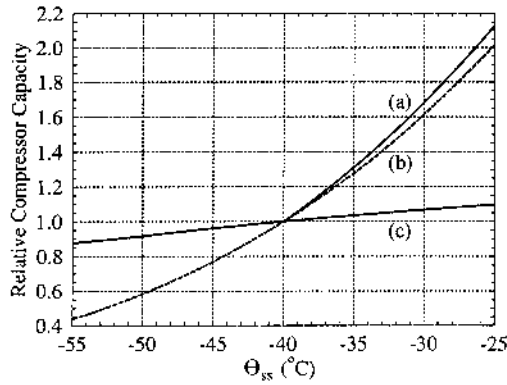
FIGURE 3.10 Effect of saturated suction temperature (θ_{ss}) on typical refrigeration system compressor capacity relative to that at –40°C: (a) single stage, (b) two stage boosters, (c) two stage high stage.

circulated system. Typical coil design TD are in the range 5 to 10°C which is a compromise between increased coil costs for low TD and increased energy costs due to lower θ_e for large TD.

3.8.1.3 Compressors, Condensers and Ancillaries

Compressors, condensers, and ancillaries, such as pumps, fans, vessels, piping, control systems, etc., represent a substantial capital cost as well as being the largest energy users for a freezing plant. Most of these refrigeration system components are selected on the basis of their capacity (usually heat load at the evaporator coil) for specified **saturated suction and discharge** conditions.

Figure 3.10 shows the typical relative capacity for single and two stage refrigeration systems for different suction temperatures. For two stage systems there are two curves representing low stage (booster) and high stage compressors separately. It is assumed that the high stage suction condition is held constant. The exact effect of the low stage suction condition on high stage capacity depends on the type of low stage compressors and the type of cooling used. High stage performance tends to be worse than that shown if the **booster compressors** do not have external cooling. The effect of condensation temperature on capacity is much smaller. There is approximately a 1% drop in capacity for high stage or single stage compressors per 1°C increase in condensation temperature.

The compressor saturated suction and discharge temperatures differ from the **evaporation and condensation** temperatures by the suction and discharge pipeline pressure drops, respectively. Typical design pressure drops are in the range 0.5 to 3.0°C **temperature equivalent** for both suction and discharge but vary widely depending on length of pipelines, etc.

Changes in pressure drop can be very influential when freezers operate at other than the design condition. For a fixed pipeline, the suction line pressure drop for the same heat load increases as θ_e decreases. The main reason is the increase in vapor velocity due to lower vapor density at the lower suction pressure. An approximate relationship is that each 1.0°C drop in θ_e increases pressure drop by about 7% (Cleland and Cleland, 1992)

$$\Delta P_2 = \Delta P_1 \, 1.07^{(\theta_{e1} - \theta_{e2})} \tag{3.47}$$

Similarly, as heat load increases the pressure drop increases due to the greater mass flowrate

$$\Delta P \propto \phi_{tot}^{1.8} \tag{3.48}$$

3.8.2   OPERATING COSTS

The main freezer operating costs are:

- Maintenance and labor
- Fan and refrigeration system energy use for mechanical refrigeration system or cryogenic use for cryogenic freezers
- Product evaporative weight loss

As for capital costs, the relative magnitude of these is highly influenced by the type of freezer, degree of automation, etc. In addition, the way in which the freezer is operated compared with its design conditions is also highly influential. Once the type of freezer is chosen, operating conditions are the main variables affecting energy costs and weight loss. Depending on the production rate the operating conditions also affect whether complete freezing is achieved, and therefore indirectly influence product quality.

In terms of operating costs, the heat load mainly affects the energy consumed by a mechanical refrigeration system or the rate of cryogen use for a cryogenic freezer. The freezing time and hence the required operating conditions significantly affect energy consumption.

3.8.2.1   Energy Use

For mechanical refrigeration systems the main energy users are the compressor and freezer fans but ancillary equipment, i.e., condenser coolant pumps, cooling tower fans, liquid refrigerant pumps, oil pumps, control systems, etc., are also important. Ancillary equipment are typically 10 to 15% of the compressor energy use and should be included in any calculation of energy costs. For fans and pumps the energy use is given by Equation 3.43. The relationship between heat load and compressor energy use is

$$\phi_{comp} = \frac{\phi_{tot}}{COP} \tag{3.49}$$

The **coefficient of performance** (COP) is a function of the refrigeration system design, the specific compressors and control methods used, and the condenser performance. The way in which these interact is complicated. Figure 3.11 shows typical COP for "good practice" industrial refrigeration systems as a function of saturated suction and condensation temperatures. For large freezers the use of two stage refrigeration systems is almost always justifiable and there will often be multiple compressors at each compression stage. For smaller freezers the extra capital expense for two staging may not be justified by savings in energy costs. Systems with economized compressors operate with an energy efficiency intermediate to single and two stage systems. Cleland (1988) and Cleland (1994) give a simple calculation method to estimate compressor energy use as a function of operating conditions for mechanical systems.

3.8.2.2   Cryogen Use

For a cryogenic freezer the main operating cost is the cryogen used. The rate of usage is given by

$$m_r = \frac{\phi_{tot}}{H_{out} - H_{in}} \tag{3.50}$$
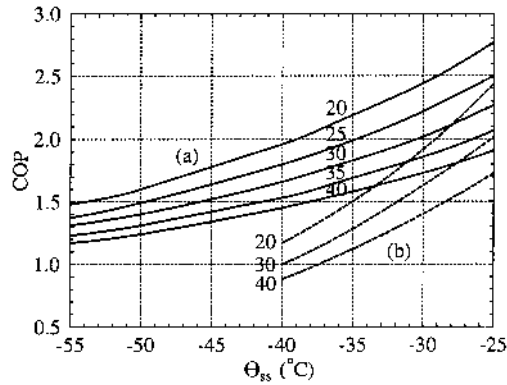
FIGURE 3.11 Effect of saturated suction (θ_{ss}) and condensation temperatures (°C) on typical refrigeration system energy efficiency (COP): (a) two stage, (b) single stage.

TABLE 3.6
Enthalpy of Nitrogen (N_2) and Carbon Dioxide (CO_2)

	N_2			CO_2	
Pressure (atm)	**Temperature (°C)**	**H_l or H_g (kJ/kg)**	**Pressure (atm)**	**Temperature (°C)**	**H_l or H_g (kJ/kg)**
1.0	27.0	462.1	1.0	37.8	405.2
1.0	−23.0	410.1	1.0	10.0	380.9
1.0	−73.0	358.0	1.0	−17.8	367.6
1.0	−123.0	305.8	1.0	−45.6	334.8
1.0	−173.0	253.0	1.0	−59.4	323.3
1.0	−195.8	228.7	1.0	−78.6	310.3
1.0	−195.8	29.4	5.11	−56.6	−31.9
1.35	−193.0	34.8	6.45	−51.1	−21.2
2.26	−188.0	45.2	8.05	−45.6	−10.7
3.55	−183.0	55.7	9.90	−40.0	0.0
5.33	−178.0	66.4	14.7	−28.9	21.4
7.67	−173.0	77.7	20.8	−17.8	43.7
10.7	−168.0	89.7	28.7	−6.7	68.8
14.5	−163.0	102.4	38.6	4.4	97.2
19.1	−158.0	116.2	50.9	15.6	129.6
24.9	−153.0	131.7	65.9	26.7	172.1
31.7	−148.0	154.6	73.0	31.1	225.9
33.5	−147.1	182.0			

Table 3.6 gives data to enable estimation of H_{out} and H_{in} for N_2 and CO_2 as a function of storage (inlet) and outlet conditions. ASHRAE (1989) gives more extensive data for a range of cryogens.

3.8.2.3 Product Evaporative Weight Loss

Product weight loss by evaporation from the surface during freezing can be both a major cost due to the loss of saleable product and can cause a significant loss in product quality

due to the dehydration effect. It also increases operating costs due to frosting of evaporator coils and the increased need to defrost to regain evaporator coil performance.

Weight loss is essentially mass transfer controlled drying. The basic equation for the rate of weight loss is

$$\frac{dW}{dt} = \int K(p_s - p_a)dA \qquad (3.51)$$

The mass transfer coefficient, K, includes the resistance of any packaging, the surface layer of the product, e.g., skin or fat layer, any resistance associate with the transition of water molecules from the solid or liquid phase to the gas state, plus the air boundary layer resistance. For the usual operating range for freezers the air boundary layer resistance is dominated by the other resistances. For packaged products the resistance of any packaging is usually so large that weight loss is effectively inhibited.

Difficulties in evaluating θ_s and hence p_s as functions of both time and position on the surface of products, and in estimating K, mean that use of Equation 3.51 to calculate weight loss during freezing processes is not practical without substantial experimental and computing resources. An expression for the maximum possible weight loss during freezing is given by Pham (1987b).

Some general principles to reduce weight loss can be identified. Any measure that will reduce θ_s and therefore p_s as quickly as possible will give the greatest reduction in weight loss. A direct reduction in product initial temperature is very effective in reducing weight loss as it minimizes the time the product spends with a large weight loss driving force. Lowering θ_a is also very effective, but has the disadvantage that freezer energy costs increase. Increasing air velocity increases h and hence reduces θ_s more quickly. This benefit is nearly always greater than the counteractive increase in K with air velocity. The overall benefit, however, may be small when the increase in fan operating costs is also considered. Increasing relative humidity of the air will have little effect on the rate of weight loss until the freezing process is almost complete. In general, the faster the freezing process the lower the weight loss.

Typical good-practice weight losses for unwrapped products are 0.1 to 1% for cryogenic freezing, 0.5 to 2.5% for air-blast freezing of large products, and 1.5 to 5% for air-blast freezing of small products. The more rapid reduction in θ_s is the main reason why cryogenic freezing processes generally give lower weight loss than air-blast systems. Although higher cryogen outlet temperatures reduce cryogen use, they do slow freezing and increase weight loss.

3.9 EXAMPLE CALCULATIONS

3.9.1 EXAMPLE 1: ESTIMATION OF THE SHAPE FACTOR E FOR A FINITE CYLINDER

Corn-on-the-cob is frozen under conditions so that Bi = 0.5. Each cob has about a 60 mm diameter and a 100 mm length. What is the shape factor, E?

The thermal center will be in the center of the cob, halfway along the length. The characteristic half thickness is half the diameter so R = 0.06/2 = 0.03 m. The smallest cross-section is circular, and the cross-sectional area and overall volume can be calculated by well-known geometric formulas

$$A = \pi \times 0.03^2 = 2.827 \times 10^{-3} \text{ m}^2 \quad V = \pi \times 0.03^2 \times 0.1 = 2.827 \times 10^{-4} \text{ m}^3$$

Using Equations 3.12 and 3.13

$$\beta_1 = 2.827 \times 10^{-3} / (\pi \times 0.03^2) = 1.0 \quad \beta_2 = 3 \times 2.827 \times 10^{-4} / (4\pi \times 1.0 \times 0.03^3) = 2.5$$

E is predicted using Equation 3.11

$$E = 1 + \frac{\left(1 + \dfrac{2}{0.5}\right)}{\left(1.0^2 + \dfrac{2 \times 1.0}{0.5}\right)} + \frac{\left(1 + \dfrac{2}{0.5}\right)}{\left(2.5^2 + \dfrac{2 \times 2.5}{0.5}\right)} = 1 + 1 + 0.308 = 2.31$$

3.9.2 EXAMPLE 2: PREDICTION OF THERMAL PROPERTIES FOR CARTONS OF FISH FILLETS

Fish fillets are packed into a carton with internal dimensions $58 \times 330 \times 650$ mm to a target weight of 10.2 kg. The fish is known to be 76% water and 6.5% fat and to have an initial freezing temperature of –1.7°C. What are the thermal properties of the fish product?

The prediction methodology described in Section 3.5 will be used.

1. θ_{if} is known to be –1.7°C, but it is necessary to calculate X_S. $X_W = 0.760$, $X_F = 0.065$. Using Equation 3.15: $X_S = 1 - 0.76 - 0.065 = 0.175$.
2. For fish products, Table 3.2 suggests an average b value of 0.23. The bound water is estimated using Equation 3.23: $X_B = 0.23 \times 0.175 = 0.040$.
3. The fully frozen ice fraction is calculated from Equation 3.22 for $\theta = -25$°C

$$X_I = (0.760 - 0.040)\left(1 - \frac{-1.7}{-25}\right) = 0.671$$

From Equation 3.17: $X_{LW} = 0.76 - 0.671 - 0.040 = 0.049$.
4. Equation 3.24 and the component densities from Table 3.3 are used to estimate the frozen material density, $\rho_{\epsilon=0}$

$$\frac{1}{\rho_{\epsilon=0}} = \frac{0.671}{917} + \frac{0.049}{1000} + \frac{0.04}{1000} + \frac{0.065}{930} + \frac{0.175}{1450}; \quad \rho_{\epsilon=0} = 989 \text{ kg/m}^3$$

The carton will contain significant air voids. It is likely that a high proportion are air gaps between the fish and the carton packaging. "Surface" voids of this type affect the surface heat transfer coefficient rather than the thermal properties and so should not be taken into account in the thermal properties. As a result the actual size of the fish fillet block will be smaller than the inside dimensions of the carton. Assuming that the air gaps were measured to be 2 mm on average for the top and side surfaces the porosity within the product can be estimated

$$M = 10.2 \text{ kg}$$

$$V = (0.058 - 0.002) \times (0.330 - 2 \times 0.002) \times (0.650 - 2 \times 0.002) = 0.01179 \text{ m}^3$$

$$\epsilon = 1 - \frac{10.2}{0.01179 \times 989} = 0.125$$

and from Equation 3.25

$$\rho = (1 - 0.125) \times 989 = 865 \text{ kg/m}^3$$

5. The frozen heat capacity is estimated using Equation 3.26 with the same mass fractions as in Step 4 and the component heat capacities from Table 3.3

$$c_f = (0.671 \times 2110) + ([0.049 + 0.040] \times 4180) + (0.065 \times 1900) + (0.175 \times 1600)$$

$$= 2191 \text{ J/kg K}$$

The unfrozen heat capacity is estimated using the mass fractions calculated in Step 1 in Equation 3.26

$$c_u = (0.76 \times 4180) + (0.065 \times 1900) + (0.175 \times 1600) = 3580 \text{ J/kg K}$$

6. The frozen volume fractions are calculated from Equation 3.31

$$v_I = \frac{989 \times 0.671}{917} = 0.724, \quad v_S = \frac{989 \times 0.175}{1450} = 0.119, \quad v_F = \frac{989 \times 0.065}{930} = 0.069$$

$$v_{LW} = \frac{989 \times 0.049}{1000} = 0.048, \quad v_B = \frac{989 \times 0.040}{1000} = 0.040$$

Using Equation 3.33 with the component thermal conductivities from Table 3.3

$$\frac{1}{k_{f,\varepsilon=0}} = \frac{(0.048 + 0.040)}{0.56} + \frac{(1 - 0.048 - 0.040)^2}{0.724 \times 2.22 + 0.119 \times 0.22 + 0.069 \times 0.18}$$

$$k_{f,\varepsilon=0} = 1.509 \text{ W/m K}$$

From Equation 3.34 with $k_a = 0.025$ W/mK (Table 3.3)

$$k_f = 1.509 \left[\frac{2 \times 1.509 + 0.025 - 2 \times 0.125 \times (1.509 - 0.025)}{2 \times 1.509 + 0.025 + 0.125 \times (1.509 - 0.025)} \right] = 1.25 \text{ W/m K}$$

In a carton of fillets the distribution of air voids may not be even and the distribution may vary from one carton to another. However, the voids will reduce the rate of heat transfer within the product so the above estimate is more realistic than using $k_{\varepsilon=0}$.

7. Using Equation 3.30 with $L' = 334 \times 10^3$ J/kg and the value of X_I for the fully frozen state

$$L = 0.671 \times 334 \times 10^3 = 224.1 \times 10^3 \text{ J/kg}$$

3.9.3 EXAMPLE 3: HEAT TRANSFER COEFFICIENT PREDICTION FOR CARTONS IN AN AIR-BLAST FREEZER

Air in a freezer flows at 2 m/s over the carton of fish fillets described in Example 2 (Section 3.9.2). The carton is a box and lid type with 1.8 mm thick walls of corrugated cardboard and lined with two layers of 0.2 mm thick LD polyethylene plastic. The larger top and bottom faces have a single cardboard layer and the sides have double or triple layers.

What is the best estimate of the heat transfer coefficient for the carton taking into account the assumed 2 mm air gaps between the product and carton on all but the bottom surface?

The six faces of the carton will each have different h values due to the different air gaps and cardboard layers. Either the cardboard and air gaps can be averaged or the final h values for the different faces can be averaged. The first option requires less calculation so it will be used.

The top and bottom surfaces represent 79% of the total carton surface area and are closest to the geometric center of the product. Judgment must then be applied, and decisions made are largely empirical and based on the experience of the engineer. Assigning the side faces half the weighting suggested by their surface area and assuming 3 layers of cardboard in the walls, an average cardboard thickness can be estimated by weighting in proportion to area

$$x_p = \frac{0.79 \times 1.8 + (1 - 0.79) \times 3 \times 1.8 \times 0.5}{0.79 + (1 - 0.79) \times 0.5} = 2.2 \text{ mm}$$

Similarly, a mean air gap can be estimated (noting the bottom surface has no air gap)

$$x_a = \frac{0.79 \times 0.5 \times 2.0 + 0.79 \times 0.5 \times 0 + (1 - 0.79) \times 2.0 \times 0.5}{0.79 + (1 - 0.79) \times 0.5} = 1.1 \text{ mm}$$

Using Equation 3.40 for an object with planar surfaces

$$h_c = 7.3 \times 2^{0.8} = 12.7 \text{ W/m}^2 \text{ K}$$

Taking $k_p = 0.048$ W/mK for the corrugated cardboard, $k_p = 0.33$ W/mK for the plastic and $k_a = 0.025$ W/mK (Table 3.4). Then using Equation 3.35

$$\frac{1}{h} = \frac{1}{12.7} + \frac{0.0022}{0.048} + \frac{2 \times 0.0002}{0.33} + \frac{0.0011}{0.025}$$

$$= 0.0787 + 0.0458 + 0.0012 + 0.0440 = 0.1697 \text{ K/m}^2 \text{W}$$

$$h = 5.9 \text{ W/m}^2 \text{ K}$$

The intermediate results in the example are important as they indicate the relative size of the component resistances to heat transfer. The air convection contributes 46% of the resistance (0.0787 out of 0.1697), the cardboard 27%, the plastic 1%, and the trapped air 26%. There is no obvious controlling resistance in this case; the net effect of the packaging (cardboard plus trapped air resistances) and the air convective resistances are similar in size. Normally, the greatest increase in h is achieved by reducing the controlling resistance. In this case, removing packaging (which may create product shape and handling problems), reducing external air resistance (by increasing air velocity), reducing the cardboard thickness, or increasing the packing density to eliminate air gaps are all worthwhile.

Alternatively in this example, separate h values could have been calculated for the top ($x_a = 2.0$ mm) and bottom ($x_a = 0$ mm) surfaces with an average cardboard thickness. Significantly higher h for the bottom surface would result, suggesting that the thermal center (last position to freeze) will be shifted above the geometric center of the carton. To use Equation 3.10 to predict freezing time the type of calculation discussed by Pham (1987c) and Mannapperuma et al. (1994b) must be applied. In this, either the h values must be averaged

or separate calculations performed both for freezing from the top down (lower h and smaller dimension), and for freezing from the bottom up (higher h and larger dimension), as well as for different thermal center positions, until agreement between the two estimates is reached.

3.9.4 EXAMPLE 4: PREDICTION OF FREEZING TIME FOR A PIZZA

Predict the time required to freeze pizza in an air-blast freezer with an air velocity of 3 m/s. The pizzas are 23 cm in diameter and have an average thickness of 1.58 cm (5/8"). The pizza has a composite thermal conductivity (frozen) of 1.5 W/mK and a density of 860 kg/m³. The specific heat capacity is 3.3 kJ/kg K unfrozen and 1.9 kJ/kg K frozen, and the latent heat of freezing is 180 kJ/kg. Cooling air is at –34°C, the pizza has an initial freezing point of –2°C, enters the freezer at 15.5°C and exits the freezer at –12°C. Summarizing the data

$$\theta_{if} = -2.0°C \qquad \theta_{a} = -34.0°C \qquad \theta_{i} = 15.5°C \qquad \theta_{fin} = -12.0°C$$

$$k_{f} = 1.5 \text{ W/m K} \qquad c_{u} = 3.3 \text{ kJ/kg K} \qquad c_{f} = 1.9 \text{ kJ/kg K} \qquad \rho = 860 \text{ kg/m}^{3}$$

$$L = 180 \text{ kJ/kg} \qquad u_{a} = 3 \text{ m/s} \qquad R = 0.0158/2 = 7.9 \times 10^{-3} \text{ m}$$

The heat transfer coefficient can be estimated directly from Equation 3.40 as there is only convective heat transfer

$$h = h_{c} = 7.3 \times 3^{0.8} = 17.6 \text{ W/m}^{2} \text{ K}$$

Using the same methodology as in Example 1, the shape factor, E, can be estimated to be 1.05. As expected, the pizza is very close to an infinite slab and the contribution of the edges to the heat transfer is very small. Equation 3.10 assumes the product is homogeneous whereas pizza is not, so when using Equation 3.10 to estimate t_f some uncertainty will result

$$\theta_{fm} = 1.8 + 0.263 \times (-12.0) + 0.105 \times (-34.0) = -4.93°C$$

$$\Delta H_{1} = 860 \times 3.3 \times 10^{3} \times (15.5 - -4.93) = 57.98 \times 10^{6} \text{ J/m}^{3}$$

$$\Delta \theta_{1} = 0.5 \times (15.5 + -4.93) - (-34.0) = 39.28°C$$

$$\Delta H_{2} = 860 \times 180 \times 10^{3} + 860 \times 1.9 \times 10^{3} \times (-4.93 - -12.0) = 166.66 \times 10^{6} \text{ J/m}^{3}$$

$$\Delta \theta_{2} = -4.93 - -34.0 = 29.07°C$$

$$t_{f} = \frac{1}{1.05} \left[\frac{57.98 \times 10^{6}}{39.28} + \frac{166.66 \times 10^{6}}{29.07} \right] \left[\frac{0.0079}{17.6} + \frac{0.0079^{2}}{2 \times 1.5} \right]$$

$$= \left[6.866 \times 10^{6} \right] \times \left[4.49 \times 10^{-4} + 2.08 \times 10^{-5} \right] = 3225 \text{ sec} = 53.8 \text{ min}$$

Note that heat transfer is controlled by the surface conditions (the first term in the second set of brackets is much larger than the first). Therefore, increasing the air velocity would be expected to give a significant reduction in freezing time. However, it is important to note that the uneven topography and heterogeneity of the pizza limit the applicability of Equation 3.10, introducing an error of unknown size. There is no quantitative guidance in the literature on what this error might be so experimental confirmation of freezing time may be desirable.

3.9.5 EXAMPLE 5: EFFECT OF PACKAGING ON FREEZING TIME (THERMAL RESISTANCES IN SERIES)

In the previous example, pizzas enter the freezer without any protective packaging layer. In such a situation there is evaporative moisture loss from the pizza, physical loss (blow-off) of expensive topping ingredients such as cheese and meat and rapid frost build-up on the coils from the moisture evaporating from the pizza. To eliminate these problems, the pizza could be protected by a shrink-wrap plastic film prior to freezing. This reduces the external convective heat transfer coefficient so air velocity will have to be increased to maintain the same production capacity. If the packaging film is 0.3 mm thick and has a thermal conductivity of 0.3 W/mK, what would the required air velocity be to maintain $t_f = 54$ min?

To maintain the same t_f the overall heat-transfer coefficient will need to remain at 17.6 W/m²K. A new h_c can be calculated from Equation 3.35 but an analysis will have to be performed to estimate the added thermal resistance of air trapped between the pizza surface and the plastic film. Since the thermal conductivity of air is very low (0.025 W/mK, Table 3.4) compared with the plastic film, the trapped air is likely to be the controlling resistance. Without physically examining the product, any estimate of the size of the new air gap will be as much a guess as a scientifically derived value, but for the sake of illustration, a 0.3 mm mean air layer thickness between the pizza and the film will be assumed. Using Equation 3.35

$$\frac{1}{17.6} = \frac{1}{h_c} + \frac{0.0003}{0.3} + \frac{0.0003}{0.025}$$

from which $h_c = 22.8$ W/m²K. From Equation 3.40

$$22.8 = 7.3\, u_a^{0.8} \quad \text{and} \quad u_a = 4.15 \text{ m/s}$$

Assuming that fan speed can be adjusted to deliver the new velocity, the relative increase in fan power can be estimated from Equation 3.44 using an exponent of 2.5 which is the midpoint of the range suggested in Section 3.7.2

$$\frac{\phi_{fan,\,new}}{\phi_{fan,\,old}} = \left(\frac{4.15}{3.0}\right)^{2.5} = 2.25$$

Only by comparison of the costs saved by retaining product moisture and reducing topping loss (yield gain) with the cost of the plastic wrap and the extra fan energy (125% increase) can the relative merit of the proposal be assessed. Since manufacturers often plastic wrap pizza after freezing, the cost of the wrapping may be irrelevant. It should be noted that the calculation is very sensitive to the thickness of the assumed air gap. Experimental data could be used to provide a better estimate of the air gap resistance. This would involve: measuring pizza freezing times in replicate both with and without shrink-wrap but otherwise under identical conditions; using Equation 3.10 to back-calculate the surface heat-transfer resistance 1/h for the mean of each case; and using Equation 3.35 to estimate the air gap heat transfer resistance and mean air gap size, from the difference in back-calculated resistances.

3.9.6 EXAMPLE 6: FREEZING TIME PREDICTION FOR A POROUS FOOD

Standard ice cream contains 50% entrapped air by volume. Product is sold by volume in half-gallon containers which are cylindrical with a diameter of 11 cm and a height of 16.5 cm. The container is a composite material 1 mm thick with a thermal conductivity of 0.2 W/mK.

The composition of the "solids" mix is 40% water, 35% fat, and 25% solids-not-fat. The ice cream mix is processed through a scraped-surface heat exchanger that incorporates 50% air by volume and reduces the temperature of the resulting foam to just below its initial freezing point of –4°C which results in partial freezing of the mix. This product is then filled into the half-gallon containers and transferred to an air-blast hardening tunnel with air at –34°C and at a velocity that gives a convective heat transfer coefficient of 20 W/m²K. What residence time is required in the hardening tunnel for the product center to reach –18°C?

In addition to being a porous food, this example has two features which will contribute to higher than usual uncertainty in the predicted freezing (hardening) time. First, Equation 3.10 assumes that the food is fully unfrozen when it enters the freezer. The extent of partial freezing by the scraped-surface heat exchanger is unknown so prediction of freezing time using the full latent heat of freezing for the mix is the simplest and most conservative approach. It means, however, that the predicted freezing time is likely to be an overestimate of that actually required. Second, Equation 3.10 was derived for and has only been tested for freezing of products with higher moisture content and therefore higher freezing temperatures and latent heat components than the ice cream mix. Its accuracy for products such as ice cream is unknown. Overall, the freezing (hardening) time predicted using Equation 3.10 should be interpreted as indicative only.

In such cases the prediction methodology would be expected to have greater value if it is used to find the relative effect of changes in operating conditions, because use of freezing time ratios may give some error cancellation. For example, if it is known that the hardening time is 2 hours with an air temperature of –34°C, then the ratio of predicted freezing times for –40 and –34°C could be used to scale this time to estimate the new hardening time with air at –40°C.

For illustrative purposes a full freezing time prediction will be undertaken but the limitations of the methodology for this situation must be noted. Using the methodology of Section 3.5 the solids properties can be estimated as

$$\theta_{if} = -4.0°C \qquad \rho = 1027 \text{ kg/m}^3 \qquad c_u = 2.74 \text{ kJ/kg K}$$

$$c_f = 2.17 \text{ kJ/kg K} \qquad L = 91.18 \text{ kJ/kg} \qquad k_{f,\varepsilon=0} = 0.84 \text{ W/m K}$$

Ice cream is an isotropic foam with air as the dispersed phase. In this case $\varepsilon = 0.5$, and the Maxwell-Eucken model, Equation 3.34, can be used to estimate the effective thermal conductivity

$$k_f = 0.84 \left[\frac{2 \times 0.84 + 0.025 - 2 \times 0.5 \times (0.84 - 0.025)}{2 \times 0.84 + 0.025 + 0.5 \times (0.84 - 0.025)} \right] = 0.35 \text{ W/m K}$$

Similarly, using Equation 3.25 the product density is

$$\rho = \rho_{\varepsilon=0}(1 - \varepsilon) = 1027 \times (1 - 0.5) = 519 \text{ kg/m}^3$$

In addition to the effect of incorporated air bubbles on product thermal conductivity, the insulation effect of the packaging material must also be taken into account. In this instance, since the product is filled as a semi-fluid it is reasonable to assume no additional air gap at the interface with the container. Using Equation 3.35

$$\frac{1}{h} = \frac{1}{20} + \frac{0.01}{0.2} = 0.05 + 0.05 = 0.1 \text{ K/m}^2 \text{ W}; \quad h = 10 \text{ W/m}^2 \text{ K}$$

The dimensions of the container are such that the heat transfer from the ends will be significant. The smallest dimension is the diameter so R is $0.11/2 = 0.055$ m. The methodology described in Section 3.4.4 was used to estimate E = 2.34. Finally, using Equation (3.10)

$$\theta_{fm} = 1.8 + 0.263 \times (-18.0) + 0.105 \times (-34.0) = -6.5°C$$

$$\Delta H_1 = 519 \times 2.74 \times 10^3 \times (-4.0 - -6.5) = 3.55 \times 10^6 \, J/m^3$$

$$\Delta \theta_1 = 0.5 \times (-4.0 + -6.5) - (-34.0) = 28.75°C$$

$$\Delta H_2 = 519 \times 91.18 \times 10^3 + 519 \times 2.17 \times 10^3 \times (-6.5 - -18.0) = 60.29 \times 10^6 \, J/m^3$$

$$\Delta \theta_2 = -6.5 - -34.0 = 27.5°C$$

$$t_f = \frac{1}{2.34}\left[\frac{3.55 \times 10^6}{28.75} + \frac{60.29 \times 10^6}{27.50}\right]\left[\frac{0.055}{10.0} + \frac{0.055^2}{2 \times 0.35}\right]$$

$$= \left[9.897 \times 10^5\right] \times \left[5.500 \times 10^{-3} + 4.321 \times 10^{-3}\right] = 9720 \, sec = 2.70 \, hours$$

The earlier warning with regard to accuracy of this result is reiterated.

3.9.7   EXAMPLE 7: AIR-BLAST AND PLATE FREEZER COMPARISON

Air-blast and plate freezers are being considered as two options to freeze 10 tons of fish fillets daily from 10 to –25°C. The fillets are packed into the 10 kg cartons described in Examples 2 and 3 over two 8 hour shifts each day. The proposed blast freezer design uses air at –30°C and 2 m/s while the plate freezer would use a plate temperature of –30°C. What are the required freezer and refrigeration system capacities and the relative energy costs of the two options?

The thermal properties for the fish in the 0.058 m × 0.330 m × 0.650 m carton were determined in Example 2 to be $\rho = 865 \, kg/m^3$, $c_u = 3580 \, J/kg \, K$, $c_f = 2191 \, J/kg \, K$, L = 224.1 kJ/kg, $k_f = 1.25 \, W/mK$ and $\theta_{if} = -1.7°C$. For both freezers $\theta_a = -30°C$, $\theta_i = 10°C$, and $\theta_{fin} = -25°C$.

3.9.7.1   Air-Blast Freezer

The average h was estimated to be 5.9 W/m²K in Example 3. The smallest dimension of the carton is 58 mm and there is a 2 mm air gap at the top but none at the bottom. Thus the product thickness is 0.056 m and the characteristic half thickness, R, is 0.028 m. The shape factor, E, is estimated using Equations 3.11 to 3.14 and data calculated in Examples 2 and 3

$$Bi = 5.9 \times 0.028/1.25 = 1.25 = 0.132 \quad V = 0.01179 \, m^3$$

$$A = 0.056 \times 0.326 = 0.018256 \, m^2 \, (\text{minimum cross-section through thermal centre})$$

$$\beta_1 = \frac{0.018256}{\pi \times 0.028^2} = 7.41 \qquad \beta_2 = \frac{3 \times 0.01179}{4\pi \times 7.41 \times 0.028^3} = 17.30$$

$$E = 1 + \frac{\left(1 + \dfrac{2}{0.132}\right)}{\left(7.41^2 + \dfrac{2 \times 7.41}{0.132}\right)} + \frac{\left(1 + \dfrac{2}{0.132}\right)}{\left(17.3^2 + \dfrac{2 \times 17.3}{0.132}\right)} = 1 + 0.097 + 0.028 = 1.13$$

Substituting into Equation 3.10 to calculate t_f

$$\theta_{fm} = 1.8 + 0.263 \times (-25.0) + 0.105 \times (-30.0) = -7.93°C$$

$$\Delta H_1 = 865 \times 3580 \times (10.0 - -7.93) = 55.52 \times 10^6 \text{ J/m}^3$$

$$\Delta \theta_1 = 0.5 \times (10.0 + -7.93) - (-30.0) = 31.04°C$$

$$\Delta H_2 = 865 \times 224100 + 865 \times 2191 \times (-7.93 - -25.0) = 226.20 \times 10^6 \text{ J/m}^3$$

$$\Delta \theta_2 = -7.93 - -30.0 = 22.07°C$$

$$t_f = \frac{1}{1.13} \left[\frac{55.52 \times 10^6}{31.04} + \frac{226.20 \times 10^6}{22.07} \right] \left[\frac{0.028}{5.9} + \frac{0.028^2}{2 \times 1.25} \right] = 53900 \text{ sec} = 15.0 \text{ hours}$$

A residence time of 16 hours will be used as the design basis. A management decision was made to use one batch freezer for each shift with product loading over each shift followed by a 16 hour freezing cycle. Each freezer would need to hold half the daily production (500 cartons). The refrigeration system would operate only intermittently during the loading period to keep the temperature low until the freeze cycle starts. The heat load in this period will be small so the refrigeration plant can be sized solely for the 16 hour freeze cycle. The product heat load can be estimated for each batch freezer by using Equation 3.42 but first θ_{out} must be found. θ_{out} will lie between the final center temperature, $-25°C$, and the air temperature, $-30°C$, and for simplicity, the mean of the two will be used. The error introduced by this approximation should be small.

$$W_{pr} = 5000 \text{ kg} \quad t_{pr} = 16 \text{ hours} = 57600 \text{ sec} \quad \theta_{out} = (-25.0 + -30.0)/2 = -27.5°C$$

$$\phi_{pr} = \frac{5000 \times [3580 \times (10.0 - -1.7) + 224100 + 2191 \times (-1.7 - -27.5)]}{57600 \times 1000} = 28.0 \text{ kW}$$

To keep the calculation simple other heat loads have not been estimated in detail. It is assumed that fan power is 20% of the total heat load and that other loads are 15% of the total load. These figures are consistent with the data in Table 3.5. The product load will be 65% of the total load so the total mean load for the two batch freezers and the fan power can be estimated

$$\phi_{tot} = (2 \times 28.0)/0.65 = 86.2 \text{ kW} \quad \phi_{fan} = \phi_{tot} \times 0.2 = 86.2 \times 0.2 = 17.2 \text{ kW}$$

Consideration then turns to the mechanical refrigeration system. If a sound engineering design has been performed the coil TD will be about 8°C and there might be 2°C equivalent suction line pressure drop. Thus for $-30°C$ air, $\theta_e = -38°C$ and $\theta_{ss} = -40°C$ might be expected. From Figure 3.11 for a two stage refrigeration plant with a typical condensation temperature of 35°C, COP = 1.53. Compressor energy is then estimated using Equation 3.49

$$\phi_{comp} = \frac{86.2}{1.53} = 56.3 \text{ kW}$$

Ancillary (pumps, etc.) energy use might be 8.4 kW (15% of ϕ_{comp}) so the total energy use (compressors, ancillaries, and fans) is 56.3 + 8.4 + 17.2 = 81.9 kW. This mean load includes both freezers and occurs for 16 hours daily.

3.9.7.2   Plate Freezer

Heat transfer in the plate freezer is effectively only through the large faces so $E = 1$. It is assumed that the fish thickness is 56 mm, accomplished by using 0.056 m spacers between the plates, so that the carton will be slightly crushed and the top air gap eliminated. The contact resistance, however, may still be significant. In this case, following the discussion of Section 3.6.1, for poor contact $h_c = 100$ W/m²K seems appropriate. The large faces have one 1.8 mm layer of cardboard and two layers of plastic film. Using Equation 3.35 and the other data used earlier in Example 3

$$\frac{1}{h} = \frac{1}{100} + \frac{0.0018}{0.048} + \frac{2 \times 0.0002}{0.33} = 0.0487 \text{ K/m}^2 \text{ W}; \quad h = 20.5 \text{ W/m}^2 \text{ K}$$

Only E and h have altered from the air-blast freezer prediction. Substituting into Equation 3.10 to calculate t_f

$$t_f = \frac{1}{1.0}\left[\frac{55.52 \times 10^6}{31.04} + \frac{226.20 \times 10^6}{22.07}\right]\left[\frac{0.028}{20.5} + \frac{0.028^2}{2 \times 1.25}\right] = 20200 \text{ sec} = 5.6 \text{ hours}$$

A single plate freezer processing the day's production in two 8 hour batch cycles starting at the end of each shift will be more than adequate. The freezer needs capacity to hold half the daily production (500 cartons). The mean product heat load over the 16 hours the plate freezer will operate will be the same as for the blast freezer option. Assuming that other loads are 10% of the total load (product load is 90% of the total, Table 3.5)

$$\phi_{tot} = 2 \times 28.0/0.9 = 62.2 \text{ kW}$$

There is no coil TD, so to achieve a plate temperature of –30°C, $\theta_e = -30$°C and $\theta_{ss} = -32$°C (assuming suction line pressure drop is the same as for the blast freezers). From Figure 3.11 for a two stage refrigeration plant with a typical condensation temperature of 35°C, COP = 1.79. Compressor energy is estimated from Equation 3.49

$$\phi_{comp} = \frac{62.2}{1.79} = 34.7 \text{ kW}$$

Allowing 5.2 kW (15% of ϕ_{comp}) for ancillaries, the total energy use (compressors, ancillaries, and fans) is $34.7 + 5.2 + 0 = 39.9$ kW and will occur for 16 hours daily.

3.9.7.3   Comparison of Freezer Options

A summary of the two freezer options is given in Table 3.7. The plate freezer refrigeration system only has to cope with 72% of the heat load and operates at a higher θ_{ss} where the same low stage and high stage compressors will have about 50 and 7% greater capacity, respectively, than for the blast freezer operating conditions (Figure 3.10). The net effect is that low stage and high stage compressors for the plate freezer option only need to be about 50% ($0.72/1.5 = 0.50$) and 67% ($0.72/1.07 = 0.67$), respectively, of the size of the compressors required for the blast freezer option. The plate freezer energy use will be about 50% of that for the blast freezer. The savings in energy and refrigeration system capital costs must be compared with the extra capital cost for the plate freezer compared with the blast freezer. The more regular shape of the carton produced by the plate freezer may also be important.

TABLE 3.7
Summary of the Comparison of Air-Blast and Plate Freezers for Example 7

	Air-blast freezer	Plate freezer
t_f (hours)	15.0	5.6
ϕ_{tot} (kW, 16 hour basis)	86.2	62.2
Energy use (kW)	81.9	39.9
θ_e (°C)	–38°C	–30°C
θ_{ss} (°C)	–40°C	–32°C
Relative compressor capacity at design	1.0 (low stage)	1.50 (low stage)
operating conditions (Figure 3.10)	1.0 (high stage)	1.07 (high stage)
Relative installed compressor size required	1.0 (low stage)	0.50 (low stage)
	1.0 (high stage)	0.67 (high stage)
Total freezer holding capacity (cartons)	1000	500

3.9.8 EXAMPLE 8: EFFECT OF AIR VELOCITY ON FREEZING TIME AND ENERGY USE

For the air-blast freezer of Example 7, if t_f can be reduced to less than 12 hours then a single 500 carton capacity freezer would be sufficient. Will a 50% increase in u_a to 3 m/s be sufficient and what will be the effect on overall energy use?

Using Equation 3.40 and 3.35: $h_c = 7.3 \times 3^{0.8} = 17.6$ W/m²K and h = 6.8 W/m²K. The increase in h is quite small, as the packaging and air gaps are significant resistances.

E will change slightly. Reworking the calculations in Example 7 the new values are: Bi = 0.152 and E = 1.12. Substituting directly into Equation 3.10 using the unchanged values of ΔH_1, $\Delta \theta_1$, ΔH_2, and $\Delta \theta_2$ from Example 7

$$t_f = \frac{1}{1.12 \times 3600}\left[\frac{55.52 \times 10^6}{31.04} + \frac{226.20 \times 10^6}{22.07}\right]\left[\frac{0.028}{6.8} + \frac{0.028^2}{2 \times 1.25}\right] = 13.2 \text{ hours}$$

If it is assumed that the same freezer air flow design is used, the new fan power can be estimated from Equation 3.44 using an exponent of 2.5 which is the midpoint of the suggested range

$$\phi_{fan} = 17.2 \times \left(\frac{3}{2}\right)^{2.5} = 47.4 \text{ kW}$$

The change in t_f is not enough to reduce the required freezer capacity unless a higher product outlet temperature can be tolerated. If $\theta_{fin} = -15$°C was acceptable, then it can be shown that t_f would reduce to 11.7 hours with $u_a = 3$ m/s and two 12 hour cycles might then be used in a single freezer. For this option, the mean product load over 24 hours can be estimated. The mass-average product outlet temperature is again approximated as the average of the final product center temperature and the air temperature

$$t_{pr} = 24 \text{ hours} = 86400 \text{ sec} \qquad \phi_{out} = (-15.0 + -30.0)/2 = -22.5°C$$

$$\phi_{pr} = \frac{10000 \times \left[3580 \times (10.0 - -1.7) + 224100 + 2191 \times (-1.7 - -22.5)\right]}{86400 \times 1000} = 36.1 \text{ kW}$$

For each of the freezers operating on the 16 hour cycle the miscellaneous loads were 6.5 kW (15% of the total load of 43.1 kW for each freezer). Assuming that miscellaneous loads will be similar for the freezer with higher air velocity, the new total heat load will be

$$\phi_{tot} = 36.1 + 47.4 + 6.5 = 90.0 \text{ kW}$$

Fans are now 53% of the total load. The mean load has only increased by 4% but occurs for 24 rather than 16 hours daily.

The performance of the evaporator coils will increase if the face velocity is higher. For the same freezer air flow design, coil face velocity will increase in proportion to the air velocity over the product. Equation 3.46 suggests an increase of about 25% in coil performance if air velocity is 50% higher ($1.5^{0.55} = 1.25$). Either, the evaporator coils can be smaller, or coil TD can be reduced and θ_e and θ_{ss} raised compared to the freezer operating at lower u_a. Assuming that a smaller coil is used so that θ_e and θ_{ss} are the same, COP will still be 1.53 and

$$\phi_{comp} = \frac{90.0}{1.53} = 58.8 \text{ kW}$$

Including ancillary power use of 8.8 kW (15% of ϕ_{comp}), overall power use is now 58.8 + 8.8 + 47.4 = 115.0 kW and it occurs for 24 hours daily. This is an 111% increase in energy use from the 81.9 kW for 16 hours daily that was estimated for the freezers operating with 2 m/s air velocity ($[115 \times 24]/[81.9 \times 16] = 2.11$).

In summary, for this example, increasing air velocity by 50% only achieves a 12% reduction in t_f which is sufficient to allow one 500 carton freezer to process the full daily production in two consecutive batches only if θ_{fin} is also increased to –15°C. The refrigeration system capacity required alters only slightly but energy use increases 111%. To fully assess this option, the increased energy cost plus the potentially poorer product quality due to higher θ_{fin}, need to be compared with the savings in capital for one rather than two freezers.

A better option might be to keep two freezers but reduce u_a below 2 m/s. As long as t_f is less than 24 hours the two 500 carton freezers will still cope with the full day's production. For example, reducing u_a to 1.0 m/s gives h = 4.4 W/m²K, E = 1.14, t_f = 19.6 hours, ϕ_{fan} = 3.0 kW, commensurate reductions in overall power use, and required refrigeration system capacity.

3.9.9   EXAMPLE 9: IMPACT OF CHANGES IN PRODUCTION RATE
ON FREEZER PERFORMANCE

A continuous air-blast freezer operates with θ_a = –30°C, θ_e = –38°C, and θ_{ss} = –40°C (8°C evaporator coil TD and 2°C equivalent pressure drop). The product load represents 75% of the total heat load. The freezer is serviced by a two stage refrigeration system. What are the effects of a 20% increase in production rate on freezer operation and performance if the same product outlet conditions must be maintained?

- t_f will need to reduce by 17% ($1.0/1.20 = 0.83$) to maintain the same outlet conditions with the 20% increase in throughput.
- Reducing θ_a is the simplest option to reduce t_f for an existing freezer. Equation 3.10 can be used to predict the new θ_a required. Using the product data in Example 7 it can be shown that θ_a will need to reduce from –30°C to about –35.2°C to achieve a 17% reduction in t_f. (If the form of Equation 3.10 is considered, it is apparent that the required reduction in θ_a for a constant fractional reduction in t_f is virtually independent of the product type and freezing conditions. Therefore, detailed knowledge of the

actual product and conditions, i.e., air velocity, are not essential to accurately predict fractional changes in t_f as θ_a changes.)

- The heat load will increase. The product load will increase in proportion to the increase in product throughput if the same product temperatures are maintained. Non-product loads will be unaffected by the increase in throughput but reduction in θ_a will have a small effect on ϕ_{tot} (e.g., higher ingress through insulation). The increase in ϕ_{tot} will be about 15% because the product component was 75% of the original total load ($1.2 \times 0.75 + 0.25 = 1.15$).
- The coil TD was 8°C. For a 15% increase in ϕ_{tot}, TD will increase by 15% to 9.2°C.
- To cool air at –35.2°C with a 9.2°C TD, the new $\theta_e = \theta_a - TD = -35.2 - 9.2 = -44.4$°C.
- To find the new θ_{ss}, the new pressure drop must be estimated. Pressure drop will be affected by both the increase in ϕ_{tot} and the reduction in θ_e. Using Equation 3.48 the effect of the 15% increase in ϕ_{tot} is approximately a 29% increase in pressure drop ($1.15^{1.8} = 1.29$).
- Using Equation 3.47 to estimate the fractional increase in ΔP due to the reduction in θ_e from –40.0 to –44.4°C

$$\frac{\Delta P_2}{\Delta P_1} = 1.07^{(-40.0 - -44.4)} = 1.35 \quad \text{(a 35\% increase)}$$

- The combined effect is an estimated 74% increase in ΔP ($1.29 \times 1.35 = 1.74$). The pressure drop will increase from 2.0 to about 3.5°C ($2.0 \times 1.74 = 3.5$).
- The new $\theta_{ss} = \theta_e - \Delta P = -44.4 - 3.5 = -47.9$°C.
- The lower θ_{ss} reduces the capacity of the refrigeration system. From Figure 3.10, the relative low and high stage compressor capacities at $\theta_{ss} = -47.9$°C will be about 66% and 94%, respectively, compared with operation with $\theta_{ss} = -40$°C.
- The overall increase in the required size of the low stage compressors due to higher ϕ_{tot} and lower θ_{ss} will be about 74% ($1.15/0.66 = 1.74$). Similarly the increase in size of the required high stage compressors will be about 22% ($1.15/0.94 = 1.22$).
- From Figure 3.11, for a two stage refrigeration system and 30°C condensation temperature, a typical COP for $\theta_{ss} = -40$°C is 1.66 and for $\theta_{ss} = -47.9$°C is 1.45. The energy use of the refrigeration system for the same load will increase by about 14% ($1.66/1.45 = 1.14$) due to the lower efficiency with a lower suction condition.
- Including the effect of the 15% increase in heat load the overall increase in compressor energy use will be about 31% ($1.15 \times 1.14 = 1.31$).

In summary, the 20% increase in production rate requires about 74% and 22% increases in installed low and high stage compressor sizes, respectively, and will increase energy use by about 31%. Unless there is a surplus of refrigeration capacity available it may be more cost effective to increase the size of the freezer so the original operating conditions and product residence times can be maintained at the higher production rate. Another alternative is to tolerate higher product outlet temperatures due to the reduced product residence time (but the impact on product quality may prevent this approach). The dangers of operating an existing plant beyond its design capacity are illustrated by this example. Ease of expansion is an important feature of any freezer and its associated refrigeration system.

3.9.10 EXAMPLE 10: COMPARISON OF CRYOGENIC AND MECHANICAL FREEZING SYSTEMS

Compare the costs of a liquid N_2 freezer and a mechanical air-blast freezer to freeze 1000 kg/hour of product from 20 to –20°C. The product is 60% water, 15% fat, has an initial

freezing temperature of –1.0°C, and is worth \$4/kg. Liquid N_2 costs \$0.11/kg while the composite electricity cost is \$0.05/kWh. The two stage mechanical refrigeration system is designed to operate with air at –35°C, a saturated suction temperature of –45°C and a condensation temperature of 30°C. Both freezers will operate for 4000 hours each year.

Using the techniques from Section 3.5, the thermal properties can be estimated to be

$$c_u = 3193\,\text{J/kg K} \quad c_f = 2115\,\text{J/kg K} \quad L = 174 \times 10^3\,\text{J/kg} \quad \theta_{if} = -1.0°\text{C}$$

The product heat load is given by Equation 3.42

$$W_{pr} = 1000\,\text{kg} \qquad t_{pr} = 3600\,\text{sec} \qquad \theta_{out} = -20.0°\text{C} \qquad \theta_i = 20.0°\text{C}$$

$$\phi_{pr} = \frac{1000 \times \left[3193 \times (20.0 - -1.0) + 174000 + 2115 \times (-1.0 - -20.0)\right]}{3600 \times 1000} = 77.5\,\text{kW}$$

Typical non-product component heat loads from Table 3.5 will be assumed.

3.9.10.1 Cryogenic Freezer

For the N_2 freezer, taking fans to be 4% and other components (including storage losses) to be 6% of the total load, the product load is assumed to be 90% of the total. Therefore

$$\phi_{tot} = 77.5/0.90 = 86.1\,\text{kW} \quad \phi_{fan} = \phi_{tot} \times 0.04 = 86.1 \times 0.04 = 3.4\,\text{kW}$$

Assuming the N_2 is stored at 20 bar (-157°C) and exits the freezer at -10°C (1.01 bar) the inlet and outlet N_2 enthalpies can be determined from Table 3.6

$$H_{in} = 120\,\text{kJ/kg} \quad H_{out} = 424\,\text{kJ/kg}$$

The rate of liquid N_2 use is estimated using Equation 3.50

$$m_r = \frac{86.1}{(424 - 120)} = 0.283\,\text{kg/s} = 1020\,\text{kg/hour}$$

The liquid nitrogen use is 1.02 kg N_2/kg of product. This is low compared with many other situations because the outlet gas temperature is high, and the product has lower moisture content than is often the case. The yearly N_2 cost is $4000 \times 1000 \times 1.02 \times 0.11 = \$448,800$. The annual fan operating costs will be $4000 \times 3.4 \times 0.05 = \$680$. There will also be the cost of weight loss. Typical weight loss for cryogenic freezing is in the range 0.1 to 1% as discussed in Section 3.8.2.3. Because the N_2 outlet temperature is quite high, the weight loss will be higher in the range; 0.75% was assumed. The annual cost of loss of product due to weight loss is $4000 \times 1000 \times 0.0075 \times 4.00 = \$120,000$. The estimated overall annual operating costs excluding labor, maintenance, and depreciation are \$569,500.

3.9.10.2 Air-Blast Freezer

For the air-blast freezer, taking fans to be 25% and other components 20% of the total load as suggested by Table 3.5, the product load is about 55% of the total and

$$\phi_{tot} = 77.5/0.55 = 140.9\,\text{kW} \qquad \phi_{fan} = \phi_{tot} \times 0.25 = 140.9 \times 0.25 = 35.0\,\text{kW}$$

From Figure 3.11, a two stage refrigeration system would operate with a COP of about 1.52

$$\phi_{comp} = 140.9/1.52 = 92.7 \text{ kW}$$

Allowing 13.9 kW (15% of ϕ_{comp}) for ancillaries, the total energy use is $92.7 + 13.9 + 35.0 = 141.6$ kW. The annual energy cost will be $4000 \times 141.6 \times 0.05 = \$28,300$. Allowing a weight loss of 2.5% (Section 3.8.2.3), the annual cost of loss of product due to weight loss is $4000 \times 1000 \times 0.025 \times 4.00 = \$400,000$. The estimated overall annual operating costs excluding labor, maintenance, and depreciation is $428,300.

3.9.10.3 Comparison of Freezer Options

In this example the extra operating costs ($141,200 annually) of using cryogenic refrigeration are significant, but may be offset by reductions in capital costs, decreased maintenance and labor, and/or product quality advantages. The relative operating cost is very sensitive to the cost of weight loss. In many cases reduction in weight loss does not give direct increases in sales revenue, as assumed in the example, but does have a quality cost benefit. Unfortunately, both quality benefits and total weight losses can be difficult to estimate accurately. Freezing trials in freezers similar to that envisaged can be helpful in assessing likely weight loss but can be expensive and difficult to perform. Nevertheless, they are probably essential to determine the optimum freezing option. Other possible processing options are use of a combined cryomechanical freezer, as discussed in Section 3.2.4, or use of a shrink wrap prior to the air-blast freezer to minimize evaporative weight loss.

3.10 FOR FURTHER INFORMATION

Major **technical organizations** providing information in refrigeration areas associated with the design and operation of freezers include the following.

1. American Society of Heating, Refrigerating, and Air-Conditioning Engineers (ASHRAE). ASHRAE is involved in a wide range of activities through its technical committee structure. Two conferences are held annually (published in *ASHRAE Trans.*) as well as specifically targeted technical meetings, seminars, symposia, and expositions. Other publications include the *ASHRAE Handbook* with one of 4 volumes updated and published each year, the *International Journal of HVAC&R Research*, the monthly magazine style *ASHRAE Journal* and *ASHRAE Insights*, plus standards and other books in the HVAC&R areas. Contact: ASHRAE, 1791 Tullie Circle, N.E., Atlanta, GA 30329. Phone: (404) 636-8400, Fax: (404) 321-5478. Web address: http://www.ashrae.org

2. International Institute of Refrigeration (IIR). The IIR is an intergovernmental organization divided into 11 commissions. Activities include regular commission meetings, a four yearly international congress, educational seminars, and courses. Publications include the bi-monthly abstract journal the *Bulletin of the IIR* (FRIG-INTER and FRIDOC are the equivalent electronic databases), the bi-monthly *International Journal of Refrigeration*, and proceedings of commission meetings (*Refrigeration Science & Technology*) and congresses. Contact: IIR, 177 Boulevarde Malesherbes, F75017, Paris, France. Phone: (1) 42-27-32-35. Fax: (1) 47-63-17-98. Web address: http://www.iifiir.org

3. Air-Conditioning and Refrigeration Institute (ARI). ARI is an association of mainly U.S. HVAC&R manufacturers. Refrigeration is one of four product sections. ARI

is involved in developing standards, equipment performance certification, monitoring regulatory issues, organization of lobby groups, and education and technology transfer activities. Publications include the monthly *Minuteman Bulletin* and *Koldfax* newsletter. Contact: ARI, 4301 North Fairfax Drive, Suite 425, Arlington, VA 22203. Phone: (703) 524-8800, Fax: (703) 528-3816.

Several **technical references** that provide further information in refrigeration design, cost, and operation include the following.

1. A good overview of prediction of freezing times by simple formula and numerical methods is presented in *Food Refrigeration Processes — Analysis, Design and Simulation* by Andrew C. Cleland (1990).
2. The outcomes of the European COST-90 program as reported in *Physical Properties of Foods,* edited by Jowitt et al. (1983) provide a good source of thermal property information. Other sources are listed in Section 3.5.
3. Good introductions to the practical design and operation of refrigeration systems are presented in *Industrial Refrigeration* by Wilbert F. Stoecker (1988) as well as the *ASHRAE Refrigeration and Fundamentals Handbooks* (ASHRAE, 1989, 1990).

A number of organizations, in addition to those listed above, operate regular **continuing education courses** in the area of industrial refrigeration. Those the authors are aware of follow.

1. International Institute of Ammonia Refrigeration (IIAR), 1101 Connecticut Avenue, Suite 700, Washington, D.C. 20036. Phone: (202) 857-1110.
2. Centre for Postharvest and Refrigeration Research, Massey University, Palmerston North, New Zealand. Phone: (6) 350-5240. Fax: (6) 350-5654.

GLOSSARY

Batch freezer: A freezer in which product is accumulated, loaded as a batch into the freezer which then operates for the required cycle time before unloading.

Booster compressor: Compressor operating on the low pressure suction of a two stage refrigeration system.

Capacity: The size of the heat load that the refrigeration system can handle.

Coefficient of Performance (COP): The ratio of the heat load removed to the compressor energy input for a refrigeration system.

Continuous freezer: A freezer in which product is continuously loaded and unloaded and the freezer operates continuously.

Evaporation or condensation temperature: Temperature at which the refrigerant evaporates or condenses in the evaporator coil or condenser of the refrigeration system.

Evaporator coils: Heat exchangers (generally of the finned tube type) in which refrigerant evaporates to cool air.

Mass-average temperature: The average temperature of the object using mass weighting. The temperature the object would equilibrate to if left in an adiabatic container.

Porous foods: Foods containing significant internal void space.

Saturated suction or discharge temperature: Condition at the refrigeration compressor suction or discharge expressed as the saturated temperature corresponding to the refrigerant pressure.

Temperature equivalent: The change in refrigerant saturated temperature equivalent to a pipeline pressure drop.

Thermal center: The slowest cooling position in the food object.

NOMENCLATURE

A   Area (m^2)
b   Ratio of bound water to solids mass fraction
Bi   Biot number
c   Specific heat capacity (J/kg K)
COP   Coefficient of performance for refrigeration system
E   Shape factor — equivalent heat transfer dimensionality
ESP   External static pressure (Pa)
h   Heat transfer coefficient (W/m^2K)
H   Enthalpy (J/kg)
k   Thermal conductivity (W/mK)
K   Mass transfer coefficient (s/m)
L   Latent heat of freezing (J/kg)
L′   Latent heat of freezing for water (J/kg)
m   Flow rate (kg/s)
M   Molecular weight
p   Partial pressure of water vapor (Pa)
Q   Flow rate (m^3/s)
R   Gas constant (J/kg mol K) (Equations 3.19 and 3.20 only)
R   Characteristic half thickness of object (m)
t   Time (s)
T   Temperature (K)
TD   Temperature difference — refrigerant to air (°C)
u   Velocity (m/s)
UA   Evaporator coil rating (W/K)
v   Volume fraction
V   Volume (m^3)
W   Product weight (kg)
x   Distance in x direction (m)
X   Mass fraction
β   Ratio of axes for equivalent ellipse
Γ   Radiation view factor
ε   Emissivity (Equation 3.38 only)
ε   Porosity
η   Efficiency
θ   Temperature (°C)
σ   Stefan-Boltzmann constant = 5.67×10^{-8} W/m^2K^4
ρ   Density (kg/m^3)
φ   Heat flow, heat load, or energy input (W)
ΔP   Difference in pressure (Pa or °C temperature equivalent for refrigerants)

Subscripts

a   Air or cooling medium
B   Bound water
c   Effective convective or contact
C   Carbohydrate
con   Convective
comp   Compressor
e   Evaporation
E   Effective
evap   Evaporative
f   Frozen
F   Fat
fan   Fan

fin	Final thermal center condition
fm	Mean freezing
g	In gaseous state
i	Initial
I	Ice
if	Initial freezing, highest freezing point
in	Inlet condition
j	Component j
l	In liquid state
lg	Phase transition from l to g
LW	Water in liquid state
m	Motor
M	Mineral
off	Air-off condition
on	Air-on condition
out	Outlet mass-average condition
p	Packaging
P	Protein
pr	Product
rad	Radiative
r	Refrigerant or cryogen
s	Surface
S	Solids-not-fat, solids other than fat
ss	Saturated suction
tot	Total
u	Unfrozen
W	H_2O
$\varepsilon=0$	For non-porous material
1	Case 1
2	Case 2

REFERENCES

Arce, J.A. and Sweat, V.E., 1980, Survey of published heat transfer coefficients encountered in food processes, *ASHRAE Trans.* 86(2):235–260.

ASHRAE, 1989, *ASHRAE Handbook — Fundamentals*, American Society of Heating, Refrigerating and Air-Conditioning Engineers, Atlanta.

ASHRAE, 1990, *ASHRAE Handbook — Refrigeration*, American Society of Heating, Refrigerating and Air-Conditioning Engineers, Atlanta.

Awonorin, S.O., 1989, A model for heat transfer in cryogenic food freezing, *Int. J. Food Sci. Technol.* 24:243–259.

Chavarria, V.M. and Heldman, D.R., 1984, Measurement of convective heat transfer coefficients during food freezing processes, *J. Food Sci.* 49:810–814.

Choi, Y. and Okos, M.R., 1986, Effects of temperature and composition on the thermal properties of foods, in *Food Engineering and Process Applications*, Le Mageur, M. and Jelen, P., Eds., Elsevier, London, 93–101.

Cleland, A.C., 1988, A rapid empirical method for estimation of energy savings from refrigeration plant alterations, *Refrig. Sci. and Technol.* 3:215–221.

Cleland, A.C., 1990, *Food Refrigeration Processes — Analysis, Design and Simulation*, Elsevier, London.

Cleland, D.J., 1991, A generally applicable simple method for prediction of food freezing and thawing times, *Proc. XVIII Int. Congr. Refrig.* 4:1874–1877.

Cleland, A.C., 1994, Polynomial curve-fits for refrigerant thermodynamic properties — extension to include R-134a, *Int. J. Refrig.* 17:245–249.

Cleland, A.C. and Cleland, D.J., 1992, *Cost-Effective Refrigeration*, Massey University, Palmerston North, New Zealand.

Cowell, N.D. and Namor, M.S.S., 1974, Heat transfer coefficients in plate freezing: the effect of packaging materials, *Refrig. Sci. and Technol.* 3:45–50.

Coulson, J.M. and Richardson, J.F., 1977, *Chemical Engineering,* Vol. 1, 3rd ed., Pergamon Press, London.

Creed, P.G. and James, S.J., 1985, Heat transfer during the freezing of liver in a plate freezer, *J. Food Sci.* 50:285–288,294.

Fennema, O.R., 1975, Freezing preservation, in *Principles of Food Science — Part II Physical Principles of Food Preservation*, Fennema, O.R., Ed., Marcel-Dekker, New York, 173–215.

Flores, E.S. and Mascheroni, R.H., 1988, Determination of heat transfer coefficients for continuous belt freezers, *J. Food Sci.* 53:1872–1876.

Hallstrom, B., Skjoldebrand, C., and Tragardh, C., 1988, *Heat Transfer and Food Products,* Elsevier, London.

Hayes, G.D., 1987, *Food Engineering Data Handbook,* Longman, London.

Heldman, D.R. and Lund, D.B., Ed., 1992, *Handbook of Food Engineering*, Marcel Dekker, New York.

Heldman, D.R. and Singh R.P., 1981, *Food Process Engineering*, 2nd ed., AVI Publishing, Westport, CT.

Holland, B., Welch, A.A., Unwin, I.D., Buss, D.H., Paul, A.A., and Southgate, D.A.T., 1991, *McCance and Widdowson's — The Composition of Foods*, 5th ed., Royal Society of Chemistry and Ministry of Agriculture, Fisheries and Food, Cambridge, U.K.

Hossain, Md.M., Cleland, D.J., and Cleland, A.C., 1992, Prediction of freezing and thawing times for foods of three-dimensional irregular shape by using a semi-analytical geometric factor, *Int. J. Refrig.* 15:241–246.

Jowitt, R., Escher, F., Hallstrom, B., Meffert, H.F.T., Spiess, W.E.L., and Vos, G., Eds., 1983, *Physical Properties of Foods,* Applied Science Publishers, London.

Kent, M.A., Christiansen, K., van Haneghem, I.A., Morley, M.J., Nesvadba, P., and Poulsen, K.P. 1984, COST90 collaborative measurements of thermal properties of foods, *J. Food Eng.* 3:117–150.

Khairullah, A. and Singh, R.P., 1991, Optimization of fixed and fluidized bed freezing processes, *Int. J. Refrig.* 14:176–181.

Lovatt, S.J., Pham, Q.T., Cleland, A.C., Loeffen, M.P.F., 1993, Prediction of product heat release as a function of time in food cooling. Part 2. Experimental testing, *J. Food Eng.* 18:37–62.

Mannapperuma, J.D., Singh, R.P., and Reid, D.S., 1994a, Effective heat transfer coefficients encountered in air blast freezing of whole chicken and chicken parts, individually and in packages, *Int. J. Refrig.* 17:263–272.

Mannapperuma, J.D., Singh, R.P., and Reid, D.S., 1994b, Effective heat transfer coefficients encountered in air blast freezing of single plastic wrapped whole turkey, *Int. J. Refrig.* 17:273–280.

Mellor, J.D., 1976, Thermophysical properties of foodstuffs. I. Introductory review, *Bull. Int. Inst. Refrig.* 56:551–563.

Mellor, J.D., 1978, Thermophysical properties of foodstuffs. II. Theoretical aspects, *Bull. Int. Inst. Refrig.* 58:569–584.

Mellor, J.D., 1979, Thermophysical properties of foodstuffs. III. Measurements, *Bull. Int. Inst. Refrig.* 59:551–563.

Mellor, J.D., 1980, Thermophysical properties of foodstuffs. IV. General Bibliography, *Bull. Int. Inst. Refrig.* 60:493–515.

Miles, C.A., van Beek, G., and Veerkamp, C.H., 1983, Calculation of thermophysical properties of foods, in *Physical Properties of Food*., Jowitt, R., Ed., Applied Science Publishers, London, 269–313.

Mohsenin, N.N., 1980, *Thermal Properties of Foods and Agricultural Materials*, Gordon and Breach, New York.

Morley, M.J., 1972, *Thermal Properties of Meats: Tabulated Data,* Meat Research Institute, Langford, U.K.

Murakami, E.G. and Okos, M.R. 1989, Measurement and prediction of thermal properties of foods. In *Food Properties and Computer Aided Engineering of Food Processing Systems*. Singh, R.P. and Medina, A.G., Eds., Kluwer Academic Publishing, Amsterdam, 3–48.

Pham, Q.T., 1986, Simplified equation for predicting the freezing time of foodstuffs, *J. Food Technol.* 21:209–219.

Pham, Q.T., 1987a, Calculation of bound water in frozen food, *J. Food Sci.* 52:210–212.

Pham, Q.T., 1987b, Moisture transfer due to temperature changes or fluctuations, *J. Food Eng.* 6:33–49.

Pham, Q.T., 1987c, A converging front model for the asymmetric freezing of slab-shaped food, *J. Food Sci.* 52:795–800.

Pham, Q.T., 1990, Prediction of thermal conductivity of meats and other animal products from composition data, in *Engineering and Food*, Vol. 1, Speiss, W.E.L. and Schubert, H., Eds., Elsevier, London, 408–423.

Pham, Q.T. and Willix, J., 1986, Heat transfer in the air blast freezing and thawing of cartons, Meat Research Institute of New Zealand, Report No. 845. Hamilton, New Zealand.

Rask, C., 1989, Thermal properties of dough and bakery products: a review of published data, *J. Food Eng.* 9:167–193.

Rasmussen, C.L. and Olson, R.L., 1972, Freezing methods as related to cost and quality, *Food Technol.* 26(12):32–47.

Schwartzberg, H.G., 1976, Effective heat capacities for the freezing and thawing of foods, *J. Food Sci.* 41:153–156.

Singh, R.P. and Mannapperuma, J.D., 1990, Developments in food freezing, in *Biotechnology and Food Process Engineering*. Schwartzberg, H.G. and Rao, M.A., Eds., Marcel Dekker, New York, 309–358.

Stoecker, W.F., 1988, *Industrial Refrigeration,* Business News Publishing, Troy, MI.

Sweat, V.E., 1974, Experimental values of thermal conductivities of selected fruit and vegetables, *J. Food Sci.* 39:1080–1083.

Sweat, V.E., 1985a, Thermal properties of low- and intermediate-moisture food, *ASHRAE Trans.* 91(2A):369–385.

Sweat, V.E., 1985b, Thermal conductivity of food; present state of the data, *ASHRAE Trans.* 91(2B):299–311.

Vazquez, A. and Calvelo, A., 1980, Gas particle heat transfer coefficient in fluidized pea beds, *J. Food Process Eng.* 4:53–70.

Watt, B.K. and Merrill, A.L., 1975, *Composition of Foods,* Agriculture Handbook No. 8, U.S. Department of Agriculture, Washington, D.C.

4 Design and Performance Evaluation of Dryers

Guillermo H. Crapiste and Enrique Rotstein

CONTENTS

4.1   INTRODUCTION

Drying or dehydration has been used worldwide for centuries to preserve different food and agricultural products. At present, the drying process is one of the major procedures of food preservation and an important unit operation in a wide variety of food industries. The basic

TABLE 4.1
Applications for Selected Dryers

Dryer type	Product applications
Tray or cabinet	Fruit, vegetables, meats, confectionery
Tunnel	Fruits, vegetables
Belt conveyor	Grains, vegetables, fruits, cereals, nuts
Rotary	Seeds, grains, starch, sugar crystals
Pneumatic or flash	Starch, pulps, crops, granules, powders
Fluid bed	Vegetables, granules, grains, peas
Spray	Milk, cream, coffee, tea, juices, eggs, extracts, syrups
Drum	Milk, soups, flakes, baby cereals, juices, purees
Foam mat	Fruit juices and purees
Puffing	Fruits and vegetables
Freeze	Flakes, juices, meat, shrimp, coffee, vegetables, extracts

objective of food dehydration is to remove water to a level at which microbial spoilage is minimized in order to extend the shelf-life of the product. In addition to this increase in stability, there is a significant reduction in weight and volume that also contributes to reduce the cost of packaging, handling, storing and distributing of foodstuffs. During drying, food materials undergo physical, chemical, and biological changes which can affect some natural attributes like texture, color, flavor, and nutritional value. Therefore, a second objective of drying should be to produce dried foods of good quality from a nutritional and organoleptic standpoint.

Dryers can be classified on the basis of method of supplying heat, type of drying equipment, method of transporting the product, nature and state of the feed, conditions of operation, and residence time. Due to the wide variety of material characteristics and the diversity of dried foodstuffs, many types of dryers are used in the food industry. Typical dryers and representative applications in food processing are summarized in Table 4.1.

For decades, industrial drying of foods was based on practical know-how rather than on solid engineering understanding. The operation is a highly complex means of processing foodstuffs to obtain dried products meeting several specifications and quality standards. The efficiency of the drying process and the quality of the final dried product depend upon physical and chemical properties of the raw material, dryer design, and operating conditions. A flow chart illustrating the steps needed to design and optimize a food dryer is given in Figure 4.1.

Several textbooks on drying principles and applications and dryer selection and design are available (Vanecek et al., 1966; Williams-Gardner, 1971; Perry and Chilton, 1973; Brooker et al., 1974; Keey, 1978, 1991; Masters, 1979; Mujumdar, 1987; Van't Land, 1991; Cook and DuMont, 1991). The classical book by Van Arsdel et al. (1973) and chapters of different texts on food engineering (Charm, 1971; Singh and Heldman, 1985; Fellows, 1988) deal specifically with the drying of foods. In addition, hundreds of papers and some exhaustive reviews on the fundamental aspects of the drying of food materials (Bruin and Luyben, 1980; Fortes and Okos, 1980; Bakker-Arkema, 1986; Crapiste et al., 1988; Okos et al. 1992) have been published in the past decades.

The objective of this chapter is to review current topics in food drying principles and technology, covering fundamentals as well as practical applications to design and performance evaluation of dryers.

DRYER DESIGN

MATERIAL AND PROCESS SPECIFICATION

MATERIAL CHARACTERISTICS
Psychometric properties
Equilibrium
Thermophysical properties
Heat / mass transfer coefficients
Drying kinetics
Chemical / structural changes

Literature data
Prediction
Lab. experiments

PROCESS KNOWLEDGE
Mass and energy balances
Experience
Equipment information
Small - escale tests

PROCESS SIMULATION
Kinetics
Heat and mass transfer
Boundary conditions
Numerical solution

RESULTS
Temperature and moisture profiles
Drying times
Main dimensions
Quality attributes

COSTS AND QUALITY ANALYSIS

DRYER OPTIMIZATION

FIGURE 4.1. Steps for dryer design and optimization.

4.2 FUNDAMENTALS

Drying calculations are based on knowledge of air and material properties. Air-water vapor relationships and psychrometric properties of moist air are commonly found in the literature in the form of psychrometric tables and charts (Perry and Chilton, 1973; Keey, 1978; Mujumdar, 1987), calculating equations (ASAE, 1982), or computer programs (Ratti et al., 1989). The moisture sorption characteristics and thermophysical properties of the product must be obtained in laboratory experiments or predicted by models. Thermophysical properties of food materials are reviewed in Chapter 11 of this book.

The drying process influences the quality of the final product. Changes in food material during drying and the most common degradation reactions have been reviewed by Bruin and Luyben (1980). Microbiological quality is one of the objectives of dehydration. Loss of nutritional quality is mainly due to the effect of temperature and dehydration on vitamins and proteins. Organoleptic quality is severely affected since texture, color, and flavor are significant attributes used in judging the quality of dried foods. Changes to the texture are associated with solubility and rehydration properties. Development of off-color, due to enzymatic and nonenzymatic browning, is one of the major problems occurring during processing

FIGURE 4.2. Schematic of the food drying phenomenon.

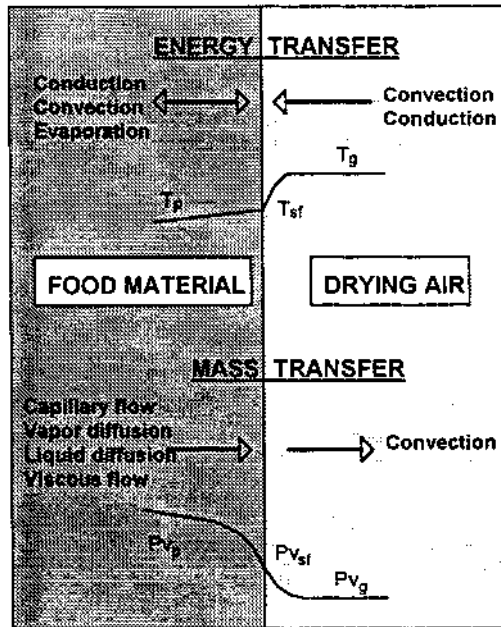and storage of dehydrated foods. Aroma losses and off-flavor development are important causes of quality deterioration. The kinetics of these phenomena, which are complex functions of temperatures and moisture content, should be known in order to simulate and optimize the drying process from a quality standpoint. However, there is both a lack of fundamental data and a scarcity of application to simulation. Thus, to relate drying conditions to product quality is still a difficult task (Bruin and Luyben, 1980; Mishkin et al., 1983; Lee and Pyun, 1993).

Drying kinetics is the most important information needed for dryer design. The drying rate equation is an integral part for the mass and energy balances used in modeling and simulation of a dryer. Drying kinetics of foods will be discussed in following sections.

4.2.1 MECHANISMS OF HEAT AND MASS TRANSFER

As it is sketched in Figure 4.2, two transport processes occur simultaneously during drying: (1) heat transfer from the external surroundings to the surface of the food material being dried combined with heat transmission within the material; and (2) mass transfer from inside to the surface of the material followed by external transport of moisture to the surroundings. Depending on food product and drying conditions, vaporization may occur either at the surface or inside the product.

Energy is transferred to the drying material by

- Convection, when the energy for evaporation is supplied by a stream of heated air flowing over or through the material. In most types of commercial drying processes, i.e., tray, belt-conveyor, flash, fluid-bed, and spray drying, heat is transferred mainly by convection.
- Conduction, when the material is in contact with a hot surface as is the case in tray, drum or rotary dryers.

Heat transmission inside the product occurs by conduction due to an internal gradient of temperature and to a less extent by convection due to moisture migration. Volumetric and

surface energy sources resulting from phase change (i.e., evaporation for free water, desorption for bonded water or sublimation in freeze drying, and energy absorption, particularly in dielectric or microwave drying), should be taken into account in modeling the process. Additional mechanisms of heat transfer (i.e., radiation) or energy source (i.e., chemical reactions) are less frequent in food drying applications.

Moisture movement in food materials can be caused by a combination of different transport mechanisms

- Capillary flow due to gradients of capillary suction pressure
- Liquid diffusion due to concentration gradients
- Vapor diffusion due to partial vapor-pressure gradients
- Viscous flow due to total pressure gradients, caused by external pressure or high temperatures

Other mechanisms like thermal diffusion, surface diffusion, and flow due to shrinkage pressure or gravity forces may have a minor contribution to mass transfer and are not taken into consideration in food drying.

Mass transfer from the product to the surroundings takes place mainly by convection, due to a difference in partial vapor pressure at the boundary layer in the air-product interface. Direct evaporation occurs when the vapor pressure on the surface is equal to the atmospheric pressure as in the case of vacuum drying and freeze drying.

Under convective drying, the boundary conditions for the heat flux, q_c, and the evaporation rate, n_w, should be of the following form:

$$\text{Heat transfer} \rightarrow q_c = h_g\left(T_{sf} - T_g\right) \tag{4.1}$$

$$\text{Mass transfer} \rightarrow n_w = k_g\left(p_{vsf} = p_{vg}\right) \tag{4.2}$$

where h_g and k_g represent the heat and mass transfer coefficients, T the temperature, and p_v the water vapor partial pressure. Vapor pressure at the product surface can be evaluated from the sorption isotherm $p_v = f(X,T)$.

Convective transfer coefficients are one of the most critical properties required for the analysis and simulation of the process. Heat transfer coefficients for different geometries and conditions can be found in the engineering literature (Bird et al., 1960; Bradshaw and Myers, 1963; Whitaker, 1972; Perry and Chilton, 1973) or can be calculated from drying experiments (Ratti and Crapiste, 1995). Several expressions for evaluating the convective heat transfer coefficients under drying conditions are presented in Table 4.2. Mass transfer coefficients can be derived from direct correlations (Bird et al., 1960; Treybal, 1980) or from the better-known heat transfer coefficients, using the mass and energy transfer analogies.

4.2.2 DRYING KINETICS OF FOODS

Data on drying of foods under industrial conditions are rather scarce and must be obtained experimentally or predicted by models. A typical drying behavior is qualitatively depicted in Figure 4.3. Experimental data are usually represented as drying curves (a plot of average moisture content, X_m, vs. time, t) or drying rate curves. The drying rate, n_w, is defined as:

$$n_w = -\frac{m_s}{A_s}\frac{dX_m}{dt} = -\frac{\rho_s}{a_v}\frac{dX_m}{dt} \tag{4.3}$$

TABLE 4.2
Correlations for Heat Transfer Coefficients

Correlation	Condition	Ref[a]
Single particles		
$Nu = 0.664\ Re^{1/2}\ Pr^{1/3}$	Flat sheet, $Re < 2 \times 10^5$	1,2
$Nu = 0.683\ Re^{0.466}\ Pr^{1/3}$	Cylinder, $Re < 4 \times 10^3$	2
$Nu = 2.0 + 0.6\ Re^{1/2}\ Pr^{1/3}$	Spheres, $Re < 5 \times 10^4$	1,2
$Nu = 0.036\ Re^{0.8}\ Pr^{1/3}$	Drying, $Re > 1.5 \times 10^5$	3
$Nu = 0.249\ Re^{0.64}$	Drying food particles	4
Packed beds		
$Nu = 1.95\ Re^{0.49}\ Pr^{1/3}$	$Re < 350$	1,2
$Nu = 1.064\ Re^{0.59}\ Pr^{1/3}$	$Re > 350$	1,2
$Nu_\varepsilon = (0.5\ Re_\varepsilon^{1/2} + 0.2\ Re_\varepsilon^{2/3})Pr^{1/3}$	$10 < Re_\varepsilon < 10^4$	5
$Nu_\varepsilon = 2.52\ Re_\varepsilon^{0.499}\ Pr^{1/3}$	$Re_\varepsilon < 3 \times 10^3$	6
Moving beds		
$Nu = 0.33\ Re^{0.6}$	Rotary dryers	7
$Nu = 0.024\ Re^{0.84}$	Fluidized beds	8
$Nu = 2.0 + 0.5–0.6\ Re^{1/2}\ Pr^{1/3}$	Spray dryers	9

Note: $Nu = h_g L_p/k$, $Re = L_p v_g \rho/\mu$, $Pr = C\mu/k$, $Nu_\varepsilon = h_g L_p \varepsilon/k(1 - \varepsilon)$, $Re_\varepsilon = L_p v_g \rho/\mu(1 - \varepsilon)$

[a] (1) Bird et al. (1960); (2) Perry and Chilton (1973); (3) Treybal (1980); (4) Ratti and Crapiste (1994); (5) Whitaker (1972); (6) Bradshaw and Myers (1963); (7) Bakker-Arkema (1986); (8) Vanecek et al. (1966); (9) Masters (1979).

where m_s and ρ_s represent the mass and density of dry solid while A_s and a_v are the external area and the area per unit volume, respectively.

The drying curve can be divided into different regions. Usually, there is an initial period in which evaporation may occur at the surface and the temperature evolves from the initial value to the wet bulb temperature. Traditional drying literature refers to the constant-rate period, an interval in which the surface contains free moisture and the material remains at the wet-bulb temperature. The process is externally controlled, the rate-controlling step of evaporation is the diffusion of water vapor through the boundary layer at the air-solid interface. All heat transferred from the air is used for the evaporation of water at the surface. Most food products do not exhibit a constant rate period. This can be explained in terms of shrinkage, the time needed to reach T_{wb} and the fact that the water is not always unbounded or the surface is not fully wetted. Due to these effects, a pseudo constant-rate period may be observed in some materials, the drying rate being lower than that of pure water and material dependent.

The point at which the falling-rate period starts is usually called the critical moisture content, X_{cr}. During this period the moisture content at the surface decreases and the surface temperature increases above the wet-bulb temperature, developing non-flat internal moisture and temperature profiles. The evaporation zone can move progressively from the surface into the material. Depending on drying conditions and material properties, both internal and external resistances can be important.

As the moisture content decreases, the internal resistance for mass transfer increases and may become the prevailing step while the product temperature approaches the dry bulb temperature. In this case, a second falling rate period may be observed. The controlling
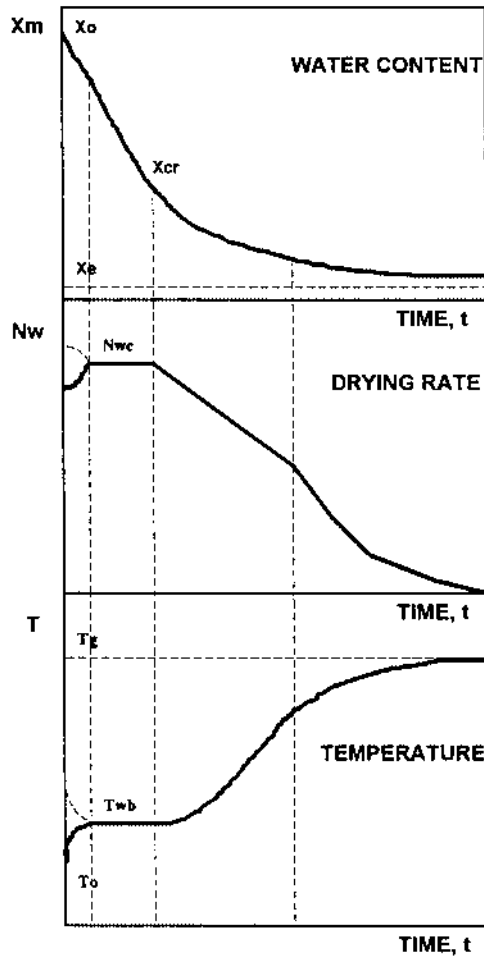
FIGURE 4.3. Characteristic behavior for convective drying.

mechanism is the rate at which moisture moves within the product, mainly by water vapor diffusion. The moisture content asymptotically reaches X_e, the equilibrium value at the relative humidity and temperature of the air.

As stated previously, the drying of individual food particles is a complex process involving simultaneous mass and energy transport in a hygroscopic shrinking system. Although extensive work has been done in developing theories of drying and significant progress has been made in understanding the process, knowledge of the mechanisms governing each stage during food dehydration is still limited. Due to the complexity of this problem, dependable theoretical models to predict experimental drying curves which can be used in engineering applications are scarce. The discussion will be limited to those models which can be of practical application in the design and evaluation of drying equipment.

4.2.3 EXTERNALLY CONTROLLED DRYING

Drying is externally controlled if both the heat and mass transfer resistances are located on the air side. In practice, external control is assumed when the Biot number is less than 0.1. Under these conditions, temperature and moisture profiles inside the product are flat. The process approximates free water evaporation from the surface of the solid and may be predicted by the following heat and mass transfer equations

$$m_s \frac{dX_m}{dt} = -k_g A_s \left(p_{vs} - p_{vg} \right) \qquad (4.4)$$

$$m_s C_p \frac{dT}{dt} = h_g A_s \left(T_g - T_s \right) - k_g \left(p_{vs} - p_{vg} \right) A_s \Delta H_v \qquad (4.5)$$

In Equation 4.5 C_p is the specific heat of the product on a dry basis and ΔH_v the heat of vaporization of water at the drying temperature.

When the wet-bulb conditions are reached, Equations 4.4 and 4.5 can be combined, resulting in the well-known equations for the wet-bulb thermometer

$$\frac{dX_m}{dt} = -\frac{k_g A_s \left(p_{vwp} - p_{vg} \right)}{m_s} = -\frac{h_g A_s \left(T_g - T_{wb} \right)}{m_s \Delta H_v} \qquad (4.6)$$

An initial stage of externally controlled drying occurs particularly with high moisture content food products. In this case, higher air temperatures can be used during this stage to improve the process rate, since the product is maintained around the wet-bulb temperature. Any intensification of convective heat and mass transfer by increasing air velocity or turbulence increases the evaporation velocity and reduces the drying time.

When case hardening (a hard impermeable skin is formed in the surface) or surface cracking should be avoided, as in the case of pasta or some fruits and vegetables, it is important to retard evaporation and maintain an external control. This can be achieved by decreasing the velocity or increasing the relative humidity of drying air.

In most practical situations the energy transport is not appreciably affected by the change in mass transfer control. Then, the temperature profile can be assumed to be flat and Equation 4.4 applies to the falling rate period, provided the corresponding expression for n_w is used.

4.2.4 DIFFUSIVE MODEL

For decades, and in spite of their physical validity, food engineers and scientists used the fact that diffusion equations can fit experimental drying curves for several foods. Crapiste et al. (1988) developed a complete theory of drying for cellular material based on water activity as the driving force and concluded that the above mechanisms of water migration can be lumped together into a diffusion-like equation:

$$\frac{\partial X}{\partial t} = \nabla_z \left(D_{eff} \nabla_z X \right) \qquad (4.7)$$

where D_{eff} represents an effective transport coefficient and z is a dimensionless coordinate following the shrinkage of the solid. This result explains those earlier simplified approaches to the problem which considered that Fick's law is applicable to the movement of water in foods regardless of the actual mechanisms of water transfer.

The dependence of the apparent or effective diffusion coefficient with temperature and moisture content is commonly represented by an Arrhenius type equation:

$$D_{eff} = D_o(X) \exp \left[\frac{\Delta E_d(X)}{RT} \right] \qquad (4.8)$$

where ΔE_d is the energy of activation for the diffusion process. Values of D_{eff} for several food materials at different moisture contents have been reviewed by Bruin and Luyben (1980) and Okos et al. (1992).

Analytical solutions of Equation 4.7 with different boundary conditions, valid for one-dimensional transport, regular geometries and constant diffusivity, are given by Crank (1967). Solutions for a slab are as follows:

• Internal mass transfer control

$$\frac{X_m - X_e}{X_0 - X_e} = \frac{8}{\pi^2} \sum_{i=0}^{\infty} \frac{1}{(2i+1)^2} \exp\left[-\frac{(2i+1)^2}{4L_p^2} \pi^2 D_{eff}(t - t_0)\right] \qquad (4.9)$$

• Internal and external resistances

$$\frac{X_m - X_e}{X_0 - X_e} = \sum_{i=0}^{\infty} \frac{2\,Bi^2}{\lambda_i^2 + Bi^2 + Bi} \exp\left[\frac{\lambda_i^2\,D_{eff}}{L_p^2}(t - t_0)\right] \qquad (4.10)$$

where L_p is the half thickness of the slab parameters λ_i are solutions of $\tan \lambda_i = Bi/\lambda_i$ and Bi represents the Biot number for mass transfer defined as

$$Bi = \frac{k_g L_p}{\rho_s D_{eff}(\partial X / \partial P_v)_t} \qquad (4.11)$$

It should be noted that, because of shrinkage and the dependence of D_{eff} with temperature and water content, use of these solutions to predict drying rates is limited to particular conditions. However, they are frecuently used to obtain approximations of the drying kinetics. Numerical methods must be used to solve the above partial differential equation for more exact calculations. For external mass transfer control the drying time required to reach a given water content is approximately proportional to the characteristic length of the particle. When the internal diffusion becomes important, the drying times vary with the square of the material thickness.

In the literature on drying of grains, a drying rate constant K_{eff} is used, instead of D_{eff}, to represent experimental data of dimensionless average water content of a particle in a packed or fluidized bed with time

$$\frac{X_m - X_e}{X_0 - X_e} = \exp(-K_{eff} t) \qquad (4.12)$$

This simplified approach along with other empirical equations used with these products are usually called "thin-layer" equations. Values of K_{eff} for different grains can be found in Brooker et al. (1974).

4.2.5 CHARACTERISTIC DRYING CURVE

Van Meel (1958), on the basis that it is possible to obtain a normalized drying curve for each material, developed a lumped parameter approach known as the characteristic drying curve. Keey (1972, 1978) and Keey and Suzuki (1974) discussed fundamentals and applications of
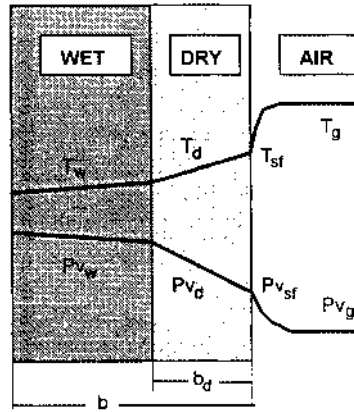
FIGURE 4.4. Scheme of the receding front model.

this formulation in detail. The model is based on a normalized evaporation rate f, characteristic for each product being dried, so that

$$n_w = f\left(\frac{X_m - X_e}{X_{cr} - X_e}\right)n_{wc} \tag{4.13}$$

Here n_{wc} represents the maximum evaporation rate, the flux that would be obtained during the constant rate period. The characteristic function f is independent of external drying conditions and depends only on the dimensionless moisture content.

The difficulty in applying this approach to food materials is that in many cases the constant rate period is absent and the critical moisture content X_{cr} is not defined. Fornell et al. (1980) suggested to use theoretical calculations for free evaporation to evaluate n_{wc}. Recently, Ratti and Crapiste (1992) extended those formulations to shrinking food systems and found the following expression for n_w

$$n_w = \frac{k_g\left[p_v - p_{vg}\right]}{\left[1 + \left(\theta/X_0\right)Bi\right]} \tag{4.14}$$

Theoretical formulations and experimental data demonstrated that the "generalized drying parameter" θ is independent of drying conditions, particle geometry, and food product being dried, and is only a function of water content.

4.2.6 RECEDING FRONT MODEL

Experimental observations indicate that during drying of some products evaporation takes place inside the material at a certain depth which divides the system into two regions, as shown in Figure 4.4. In the dry external region, moisture is in vapor phase only and, in the wet core, is in liquid or mixed form. As drying proceeds the evaporating front recedes increasing the ratio of dry to wet regions.

Modeling this problem, also called Stefan's problem, requires the simultaneous solution of coupled heat and mass transport equations in both regions. However, due to the resistance of the dry zone, temperature and moisture profiles in the wet zone can be neglected. In addition, the amount of moisture and energy stored in the dry region can be assumed negligible. Under these conditions, the following simplified heat and mass transfer equations result
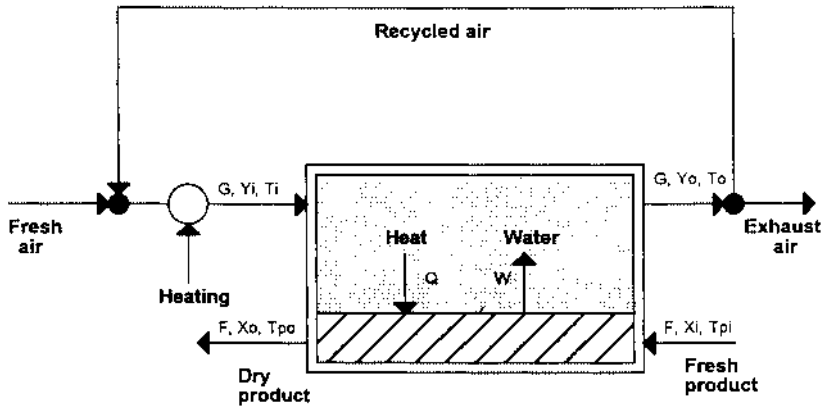
FIGURE 4.5. Scheme of a drying process.

$$m_s \frac{dX_m}{dt} = -K_g\, A_s \left(p_{vw} = p_{vg}\right) \tag{4.15}$$

$$m_s C_p \frac{dT}{dt} = U_g A_s \left(T_g - T_w\right) = K_g \left(p_{vw} - p_{vg}\right) A_s \Delta H_v \tag{4.16}$$

The overall mass and heat transfer coefficients are defined as

$$K_g = \frac{k_g}{1 + \dfrac{k_g b_d}{\rho_p \left(\partial X / \partial P_w\right) D_d}} \tag{4.17}$$

$$U = \frac{h_g}{\left[1 + h_g\, b_d / k_d\right.} \tag{4.18}$$

where D_d and k_d are the effective diffusivity and the thermal conductivity of the dry region, respectively.

The actual thickness of the dry zone may be related to moisture content as

$$\frac{b_d}{b} = 1 - \frac{\left(X_m - X_e\right)}{\left(X_0 - X_e\right)} \tag{4.19}$$

Receding front models can be successfully applied to freeze drying and spray drying of foods.

4.3 MASS AND ENERGY BALANCES

Application of overall mass and energy balances to the drying system usually gives important information on dryer performance and several parameters of dryer design. A simplified representation of the process is sketched in Figure 4.5. Although the illustration represents a continuous countercurrent system, the following analysis also applies to concurrent systems and to individual stages of a dryer.

For convenience, the practical use is to refer flowrates and compositions to a dry basis. Thus solid related variables are mass flowrate F (kg bone dry solid/s) and water content X (kg water/kg dry solid) while drying air variables are mass flowrate G (kg dry air/s) and moisture content Y (kg vapor/kg dry air). Neglecting loss of solids and leakages of air, both F and G remain constant through the drying process.

If W represents the total amount of water transferred from the foodstuffs to the air, the overall moisture balances give

$$\text{Solid} \qquad W = F\left(X_i - X_o\right) \qquad\qquad (4.20)$$

$$\text{Air} \qquad W = G\left(Y_o - Y_i\right) \qquad\qquad (4.21)$$

where subscripts i and o indicate inlet and outlet respectively.

The energy balances, after representing enthalpies in terms of temperatures and rearranging, yield

$$\text{Solid} \qquad Q = FC_{po}\left(T_{Po} - T_{Pi}\right) + W\left[\Delta H_v - C_w\left(T_{Pi} - T_r\right)\right] \qquad\qquad (4.22)$$

$$\text{Air} \qquad Q = GC_{hi}\left(T_{Gi} - T_{Go}\right) - WC_v\left(T_{Go} - T_r\right) \qquad\qquad (4.23)$$

where Q represents the net amount of energy transferred from the air to the solid, L_p the specific heat of the solid, and C_h the humid heat of moist air defined as

$$C_h = C_g + C_v Y \qquad\qquad (4.24)$$

In the above equations, ΔH_v represents the heat of vaporization of water at reference temperature T_r while C_w, C_g, and C_v are the specific heats of liquid water, dry air, and water vapor, respectively. For all practical purposes typical values of $\Delta H_v = 2,443$ kJ/kg at 25°C, $C_w = 4.197$ kJ/kgK, $C_g = 1.007$ kJ/kgK, and $C_v = 1.876$ kJ/kgK can be used. In deriving Equations 4.22 and 4.23 we approximated the total heat of desorption by ΔH_v and considered a linear dependence of C_p with moisture content, reasonable assumptions for engineering calculations.

Industrial operations will always depart from the theoretical energy balances given by Equations 4.22 and 4.23. An additional term Q_l accounting for heat losses should be added to the left-hand side of Equation 4.23. Thermal losses can be significant and will depend on properties of the wall material such as thermal conductivity and emissivity, dryer dimensions and operating conditions. Values for rough estimates of heat losses are given by Keey (1978). In practice, heat losses can be found through an energy balance around the dryer. The mechanical work done by the fans and the energy dissipated by the conveying system should also be considered. The fan work is usually small, even for through-circulating air, but can be significant in fluid bed or airlift dryers. In general, the power required to convey the solids in a continuous band dryer is relatively small although it can be important in rotary dryers.

4.3.1   EXAMPLE 4.1

A countercurrent dryer is used to dry 500 kg/h of potato slices from 78 to 8% moisture content on wet basis. Temperatures of product entering and leaving the dryer are 45 and 80°C

respectively. Air at 20°C and 30% relative humidity is heated to 90°C before entering the dryer at 28,000 kg/h. The specific heat of the dry product is 1.85 kJ/kg$_s$K. Calculate the conditions of the exhaust air.

The mass flowrate of dry solid is given by

$$F = 500 \times (1 - 0.78) = 110 \text{ kg}_s/\text{h}$$

and the water contents on dry basis result

$$X_i = 0.78/(1 - 0.78) = 3.545 \text{ kg}_w/\text{kg}_s$$

$$X_o = 0.08/(1 - 0.08) = 0.087 \text{ kg}_w/\text{kg}_s$$

From psychrometric calculations and assuming atmospheric pressure, it is found that the absolute humidity and the humid heat of the drying air are $Y_i = 0.0043$ kg$_v$/kg$_g$ and $C_h = 1.015$ kJ/kg$_g$K. The dry air flowrate is

$$G = 28,000/(1 + 0.0043) = 27,880 \text{ kg}_g/\text{h}$$

The heat required to raise the air temperature from 20 to 90°C is given by

$$Q_h = 27,880 \times 1.015 \times (90 - 20) = 1.839 \ 10^6 \text{ kJ/h}$$

The evaporation rate and the thermal load can be obtained from Equations 4.20 and 4.22

$$W = 110 \times (3.545 - 0.087) = 380.4 \text{ kg}_w/\text{h}$$

$$Q = 110 \times 1.85 \times (80 - 45) + 380.4 \times [2443 - 4.197 \times (45 - 25)]$$

$$= 7,121 + 897,006 = 904,127 \text{ kJ/h}$$

It can be seen that most of the heat transferred to the solid is used in evaporating the water and only 49% of the heat supplied to inlet air is used in the drying process.

From Equations 4.21 and 4.23 the outlet humidity and temperature result

$$Y_o = Y_i + W/G$$

$$= 0.0043 + 380.4/27,880 = 0.0179 \text{ kg}_v/\text{kg}_g$$

$$T_{Go} = (G \ C_{hi} \ T_{Gi} + W \ C_v \ T_r - Q)/(G \ C_{hi} + W \ C_v)$$

$$= (2,546,838 + 17,841 - 904.127)/(28,298 + 714)$$

$$= 57.2 \ ^\circ\text{C}$$

The corresponding relative humidity is 16.2%; a very low value, indicating that part of the exhaust air could be recycled to the intake air to optimize the process.
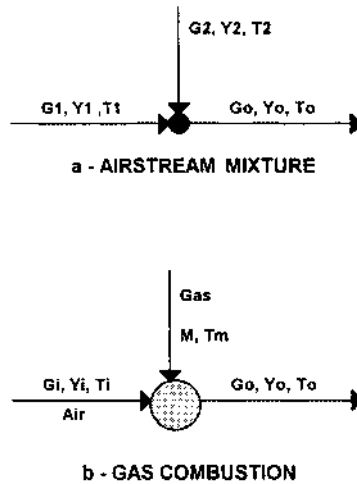
FIGURE 4.6. Mixing and combustion.

4.3.2 AIRSTREAM MIXTURES

Airstream mixtures are commonly found in drying installation because of the recycle. Consider two airstreams at different conditions that are mixed adiabatically (Figure 4.6a) to obtain a common outlet stream. Assuming that G_2 represents the recycle stream, the recycle ratio can be defined as $r = G_2/G_o$. In terms of r, mass and energy balances yields

$$\text{Dry gas} \qquad G_o = G_1 + G_2 \qquad\qquad (4.25)$$

$$\text{Humidity} \qquad Y_o = (1-r)Y_1 + rY_2 \qquad\qquad (4.26)$$

$$\text{Temperature} \quad T_o = \frac{(1-r)C_{h1}T_1 + rC_{h2}T_2}{C_{ho}} \qquad\qquad (4.27)$$

4.3.2.1 Example 4.2

Saturated air at 45°C is recycled and mixed with three parts of ambient air at 20°C and 30% relative humidity. Find the properties of the mixture.

The humidities of the airstream are $Y_1 = 0.0043$ kg$_v$/kg$_g$ and $Y_2 = 0.0649$ kg$_v$/kg$_g$, respectively. The recycle ratio results $r = 0.25$ and from Equation 4.26

$$Y_o = (0.75 \times 0.0043 + 0.25 \times 0.0649) = 0.0195 \text{ kg}_v/\text{kg}_g$$

Using Equation 4.24 we obtain $C_{h1} = 1.015$, $C_{h2} = 1.129$ and $C_{ho} = 1.043$ kJ/kg$_g$K. From Equation 4.27

$$T_o = (0.75 \times 1.015 \times 20 + 0.25 \times 1.129 \times 45)/1.043 = 26.8°C$$

The corresponding relative humidity of the mixture is 87.5%.

4.3.3 GAS COMBUSTION

Although heating of drying air can be achieved by indirect ways, e.g., electrical or steam heating, in most practical situations fuel combustion is used. In that case, flue hot combustion gases are put in direct contact with the product being dried. Natural gas is practically the only fuel used in the food industry because of its low price and its clean combustion. For engineering calculations it can be assumed that natural gas is 100% methane and the molar composition of dry air is 79% N_2 and 21% O_2. The combustion reaction is

$$CH_4 + 2\,O_2 \rightarrow CO_2 + 2\,H_2O.$$
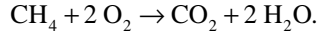
In practice combustion is carried out using moist air in excess of the stoichiometric requirement (17.13 kg dry air/kg methane) and passing the drying air through the burning system. For practical calculations of enthalpies and other psychrometric properties combustion gases can be considered as air (Keey, 1978).

Application of material and energy balances to the combustion process (Figure 4.6b) yields

$$\text{Dry gas} \qquad G_o = G_i - 1.25\,M \qquad\qquad (4.28)$$

$$\text{Humidity} \qquad Y_0 = \frac{\left(G_i Y_i + 2.25\,M\right)}{G_0} \qquad\qquad (4.29)$$

$$\text{Temperature} \quad T_o = T_i + \frac{M\left[\Delta H_c + C_m\left(T_m - T_r\right) - 2.96\left(T_i - T_r\right)\right] - Q_l}{G_o\,C_{ho}} \qquad (4.30)$$

The standard heat of combustion and the specific heat for methane at the reference temperature $T_r = 25°C$ are $\Delta H_c = 49{,}908$ kJ/kg and $C_m = 2.30$ kJ/kgK (Perry and Chilton, 1973). The heat Q_l in Equation 4.30 represents the thermal losses in the burning installation.

When the natural gas required to reach a given temperature has to be calculated, the energy balance can be used to obtain

$$M = \frac{G_i\,C_{hi}\left(T_o - T_i\right) + Q_l}{\left[\Delta H_c + C_m\left(T_m - T_r\right) - 2.96\left(T_o - T_r\right)\right]} \qquad (4.31)$$

4.3.3.1 Example 4.3

Ambient air at 20°C and 30% relative humidity ($Y_i = 0.0043$ kg$_v$/kg$_g$) has to be heated up to 90°C by direct burning of natural gas (methane). Evaluate the minimum requirement of methane and the composition of the resulting air. Assuming the methane temperature equal to 25°C and neglecting heat losses in the system Equation 4.31 gives

$$M/G_i = 1.015 \times (90 - 20)/\left[49{,}908 - 2.96 \times (90 - 25)\right]$$

$$= 0.00143 \text{ kg methane/kg dry air}$$

From Equations 4.29 and 4.30

$$G_o/G_i = 1 - 1.25 \times 0.00143 = 0.9982$$

$$Y_o = (0.0043 + 2.25 \times 0.00143)/0.9982 = 0.0075 \; kg_v/kg_g$$

There is a significant increase in air humidity due to the water produced by the combustion reaction. If direct heating is considered in Example 4.1 we obtain $M = 39.9 \; kg_m$ and the humidity of the outlet air $Y_o = 0.0211 \; kg_v/kg_g$.

4.3.4 AIR FLOW RATE

In theory, the minimum air flowrate corresponds to the situation where the outlet air is in equilibrium with the product (saturated for the case of free water). Thus, from Equations 4.20 and 4.21 the gas to solid ratio results

$$\frac{G_{min}}{F} = \frac{(X_i - X_o)}{(Y_o^* - Y_i)} = \frac{\Delta X}{\Delta Y^*} \tag{4.32}$$

However, in most typical situations of drying of foodstuffs the gas flowrate is determined by the thermal demand. By combining Equations 4.20 to 4.24 and neglecting secondary terms, a first estimate can be found as

$$\frac{G}{F} \approx \frac{\Delta H_v (X_i - X_o)}{C_g (T_{Gi} - T_{Go}^*)} = 2425 \frac{\Delta X}{\Delta T_G^*} \tag{4.33}$$

Since $\Delta X/\Delta T_G$ usually ranges between 0.01 and 0.1 the air flow results two to three orders of magnitude higher than the dry solid flow. In practice, process economy can be improved by: (1) recycling part of the exhaust air, (2) raising the temperature of the drying air; and (3) using a multistage dryer with internal heating and recirculation.

4.3.4.1 Example 4.4

For the drying situation presented in Example 4.1 different process strategies are analyzed.

1. *Calculate the minimum air flowrate required to dry the product* — It can be assumed that under ideal conditions the leaving streams are in thermal equilibrium with those entering the system, that means $T_{Po} = 90°C$ and $T_{Go} = 45°C$.

A rough estimate of the air can be obtained from Equation 4.33

$$G_{min} = 110 \times 2425 \times (3.545 - 0.087)/(90 - 45) = 20.499 \; kg_g/h$$

The energy balance given by Equation 4.23 can be used to find the minimum flowrate. From Equation 4.22 the thermal demand leads to

$$Q = 110 \times 1.85 \times (90 - 45) + 380.4 \times (2,442 - 4.197 \times (45 - 25))$$

$$= 906,164 \; kJ/h$$

so that

$$G_{min} = [Q + W \, C_v (T_{Go} - T_r)]/[C_{hi}(T_{Gi} - T_{Go})]$$

$$= (906,164 + 380.4 \times 1.876 \times 20)/(1.015 \times 45)$$

$$= 20,152 \; kg_g/h$$

TABLE 4.3
Calculations for Example 4.4

G_i	r	Q_h	M (kg$_m$/h)	T_o	Y_o
(kg$_g$/h)	(–)	(10^6 kJ/h)	)	(°C)	(kg$_v$/kg$_g$)
		Base case			
27,880	—	1.839	—	57.2	0.0179
27,880	—	—	39.9	57.2	0.0221
		Limit cases			
20,152	—	1.432	—	45.0	0.0233
20,116	—	—	28.5	45.0	0.0266
19,960	0.212	1.320	—	45.0	0.0285
19,728	0.371	1.235	—	45.0	0.0350
19,191	0.576	1.124	—	45.0	0.0510
18,749	0.665	1.080	—	45.0	0.0649
6,277	—	1.080	—	45.0	0.0649
7,103	—	—	22.2	45.0	0.0649

The outlet humidity is obtained using Equation 4.21

$$Y_o = 0.0043 + 380.4/20{,}152 = 0.0232 \text{ kg}_v/\text{kg}_g$$

The heat needed to raise the air temperature is

$$Q_h = 20{,}152 \times 1.015 \times (90 - 20) = 1.432 \; 10^6 \text{ kJ/h}$$

Note that the quantity of air used in Example 4.1 is only 39% higher than the minimum theoretical flow. Indirect heating has been considered in the above calculations. The results for direct combustion (see Example 4.3) are presented in Table 4.3.

The simplified approach given by Equation 4.33 overpredicts the flowrate by less than 2%. The final absolute humidities are far away from the saturation value at 45°C (0.0649 kg$_v$/kg$_g$) indicating that in this case the gas flowrate is determined by the thermal demand.

2. *Estimate the maximum amount of exhaust air that can be recycled* — Under ideal conditions the exhaust air leaves in equilibrium with the product feed, that means $T_{Go} = 45°C$ and $Y_o = 0.0649$ kg$_v$/kg$_g$ (provided the equilibrium water activity is nearly one).

Since the humidity of the air entering the dryer is unknown, Equation 4.23, after rearranging in terms of C_{ho}, is used to find the minimum flowrate of air as

$$G_{min} = \left[Q + W \, C_v \left(T_{Gi} - T_r \right) \right] / \left[C_{ho} \left(T_{Gi} - T_{Go} \right) \right]$$

$$= \left(906{,}164 + 380.4 \times 1.876 \times 65 \right) / \left(1.129 \times 45 \right)$$

$$= 18{,}749 \text{ kg}_g/\text{h}$$

and now the inlet humidity is obtained from Equation 4.21

$$Y_i = 0.0649 - 380.4/18{,}749 = 0.0446 \text{ kg}_v/\text{kg}_g$$

Note that the quantity of dry air is lower than in the previous case because of the higher humidity. The mass balances in the airstream mixture, Equation 4.26, allows us to calculate the recycle ratio

$$r = \left(Y_i - Y_1\right)/Y_2 - Y_1$$

$$= (0.0446 - 0.0043)/(0.0649 - 0.0043) = 0.665$$

From Equation 4.27 we can obtain the temperature of the mixture $T = 37.2°C$. Care must be taken since the resulting conditions correspond to oversaturated air, indicating that the airstream must be heated before mixing to avoid condensation.

The total heat requirement in this case is

$$Q_h = 18,749 \times \left[0.335 \times 1.015 \times 70 + 0.665 \times 1.129 \times 45\right]$$

$$= 1.08 \ 10^6 \ kJ/h$$

Theoretically, up to 66.5% of the exhaust air can be recycled to produce a 24.5% savings in the energy consumption. The results of the balances for different values of recycle ratio are shown in Table 4.3.

3. *Determine the minimum air flowrate if there are no constraints on the temperature of the drying air* — Assuming equilibrium, the air flowrate is obtained from Equation 4.32 as

$$G_{min} = F\left(X_i - X_o\right)/\left(Y_o - Y_i\right)$$

$$= 110 \times (3.545 - 0.087)/(0.0649 - 0.0043) = 6,277 \ kg/h$$

and the inlet temperature from Equation 4.23

$$T_{Gi} = 45 + (906,164 + 380.4 \times 1.876 \times 20)/(6,277 \times 1.015)$$

$$= 189.5°C$$

The heat needed to achieve the air temperature results

$$Q_h = 6,277 \times 1.015 \times (189.5 - 20) = 1.08 \ 10^6 \ kJ/h$$

Thus the inlet temperature at the minimum air flowrate must be 99.5°C higher to satisfy the same thermal demand. Note that recycling and overheating produce the same effect on the energy economy. However, in the first case there is a reduction in the driving force while in the second the inlet temperature is higher and the velocity of the air in the dryer is lower. The results of this section are also valid for the case of internal heating with the difference that part of the heat, approximately 59%, should be supplied with heaters placed inside the dryer. Again, these calculations are for indirect heating. Those corresponding to direct combustion, which require the simultaneous solution of the balances in the dryer and the burner, are given in Table 4.3.

Mass and energy balances around the dryer and the study of limit situations can be very useful tools in designing or improving the drying process. Obviously, the conditions discussed

in the example can only be reached in an ideal dryer (infinitely long and fully insulated). However, in a well-designed operation the heat losses and the final driving forces must be minimized.

In practice, part of the moist air can be recycled to improve the thermal economy of the dryer. As the recycle ratio r increases, the heat requirement or the gas consumption in the heater decreases. Since air humidity increases with r, recycling reduces the driving force in the dryer and larger equipment may be needed to obtain the same drying capacity. However, very frequently the residence times in food drying operations are defined mainly by the rate of internal water migration in the solid, allowing part of the exhaust air to be recirculated. In addition, recycling of humid air is restricted by the need to prevent condensation in cold sections.

Operation at higher temperatures, which also increases the thermal losses, is commonly constrained by the thermal sensitivity of most foodstuffs. In countercurrent flow, the food product may approach the temperature of the incoming hot air, resulting in thermal damage. In cocurrent flow, the final temperature and water content of the product are limited by the conditions of the air leaving the dryer. Thus, use of relatively high temperatures is only satisfactory in situations of very high evaporation rates or in cocurrent systems such as airlift dryers.

When possible, internal heating and recirculation or a multistage system appear to be the best solutions. This drying provides a more uniform process, a better temperature control and a considerable decrease in the energy consumption. In all cases, trade off between energy and capital costs, taking into account the product quality, has to be attained.

4.4   APPLICATIONS

This section is focused on applications of the above models and procedures to some common industrial drying systems: tray, belt, rotary, and pneumatic dryers. Since we emphasize the need for simulation and optimization in the design of dryers for the food industry, fully predictive models for simulation and design are presented. However, no attempt is made to present model solutions, which requires use of numerical methods and computers. Instead, some simplified example calculations and description of practical applications are provided.

4.4.1   TRAY OR CABINET DRYERS

A tray or cabinet dryer, as the unit illustrated in Figure 4.7, is the simplest drying equipment. It represents a typical batch operation. These dryers allow processing of different feed products, from slurries to piece-form solids, with a good control of the drying conditions. The material to be dried is placed in relatively thin layers (1 to 6 cm thick) on trays that are loaded into the drying cabinet. Air is heated and circulated between the trays (cross-flow) and less commonly through the material by using perforated trays (through-flow).

Modeling the batch drying is rather complex. A schematic view of the drying problem is sketched in Figure 4.8. For batch drying the solid bed is stationary. The conditions of product and air vary with both time and position because the drying air potential falls in the direction of the airflow. Simplified mass and energy balances over a differential volume in the bed yield the expressions

$$-\rho_s(1-\varepsilon)\frac{\partial X}{\partial t} = \rho_g \varepsilon v_g \frac{\partial Y}{\partial r} \tag{4.34}$$

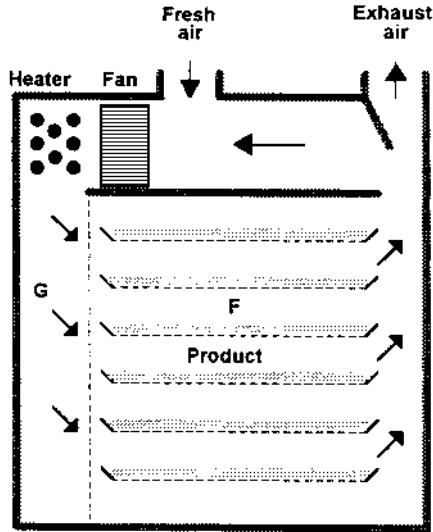$$-\rho_s(1-\varepsilon)\frac{\partial X}{\partial t} = n_w a_v \tag{4.35}$$

FIGURE 4.7. Cabinet tray dryer.

$$\rho_s(1-\epsilon)C_p\frac{\partial T_P}{\partial t} + n_w a_v \Delta H_v = -\rho_g \epsilon v_g C_h \frac{\partial T_G}{\partial r} \tag{4.36}$$

$$-\rho_g \epsilon v_g C_h \frac{\partial T_G}{\partial r} = h_g a_v \left(T_G - T_P\right) \tag{4.37}$$

where r represents the length in the direction of the airflow (the tray depth z for cross-flow and the bed thickness y for through-flow) and ϵ the volume fraction of air in the system (cross-flow) or the bed (through-flow). Depending on the material behavior, n_w can be estimated for one of the methods given in previous sections. Equations 4.34 through 4.37 along with the suitable expression for n_w constitute the drying simulation model that must be solved by numerical methods.

The average drying rate N_w by unit exposed surface A, also called the specific evaporation capacity of the dryer, can be determined by integration of the local value n_w over the entire solid volume

$$N_w = -\frac{F_t}{A}\frac{d\overline{X}}{dt} = \frac{1}{A}\int_{V_s} n_w a_v dV_s \tag{4.38}$$

Here F_t represents the total product load on a dry basis and X represents the average water content in the dryer at any time. Note that under uniform drying conditions inside the dryer, N_w is only a function of time and equals n_w for cross-flow and $n_w a_v b$ for through-flow. The drying time can be found by integration of Equation 4.38

$$\Delta t = \frac{F_t}{A}\int_{X_i}^{X_o}\frac{d\overline{X}}{N_w} \tag{4.39}$$

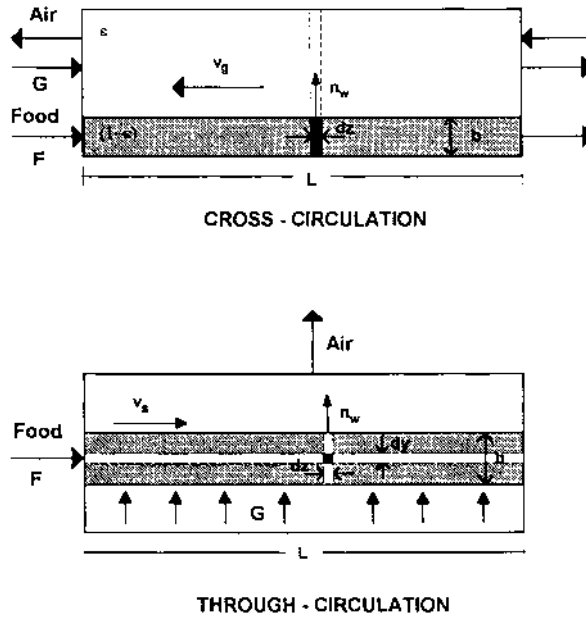On the other hand, overall mass and energy balances around the dryer yield

FIGURE 4.8. Schematic representation of the drying problem.

$$Y_o = Y_i + \frac{A \ N_w}{G} \tag{4.40}$$

$$T_{Go} \approx T_{Gi} + \frac{Q_h - A \ N_w \ \Delta H_v}{C_{hi} \ G} \tag{4.41}$$

where Q_h is the heat supplied by the heater in the cabinet. In deriving Equation 4.41 we have neglected the accumulation of energy by the product and the sensible heat of the evaporated moisture.

4.4.1.1 Example 4.5

A food product from filter cake has to be dried from $X_i = 0.45$ kg$_w$/kg$_s$ to $X_o = 0.12$ kg$_w$/kg$_s$ in a batch dryer. The bulk density of wet product is $\rho_b = 1{,}200$ kg/m^3. The dryer has 15 trays, 1.5 cm deep and 10 cm apart, of length $L = 0.75$ m by width $w = 1.2$ m. The total blowing capacity for cross-flow circulation is 3 m^3/s and the incoming air conditions are held constant at $T_g = 70°C$ and $T_{wb} = 30°C$. Estimate the total drying time.

Small-scale experiments show that the drying behavior of the product can be divided into three well-defined periods. Initially, from fresh product to a critical moisture content of $X_{cr} = 0.38$ kg$_w$/kg$_s$, a constant rate period is observed. In the second and third periods the diffusive model applies, resulting in $D_{eff} = 2.5 \times 10^{-9}$ m^2/s for the wet region and $D_{eff} = 5 \times 10^{-10}$ m^2/s for the dry region (for $X < 0.18$ kg$_w$/kg$_s$). From sorption isotherms it is found that equilibrium moisture content at air conditions is $X_e = 0.02$ kg$_w$/kg$_s$ and $(dX/dP_w)_T = 3.2 \times 10^{-2}$ kg$_w$/kg$_s$kPa as an average for the wet region. Shrinkage as a function of moisture content can be represented by $(b/b_0) = 0.6 + 0.4(X/X_0)$.

From dryer and tray dimensions the exposed area of product and the effective area for air cross-flow circulation are

$$A_p = n\, L\, w$$

$$= 15 \times 0.75 \times 1.2 = 13.5\ \text{m}^2$$

$$A_g = n\, b'w$$

$$= 15 \times (0.1 - 0.015) \times 1.2 = 1.53\ \text{m}^2$$

The batch size and the product load on dry basis are

$$L = \rho_b\, A_p\, b$$

$$= 1200 \times 13.5 \times 0.015 = 243\ \text{kg}$$

$$F_t = F' / (1 + X_i)$$

$$= 243/1.45 = 167.6\ \text{kg}_s$$

At the inlet air conditions the air properties result $Y_i = 0.0103\ \text{kg}_v/\text{kg}_g$, $\rho = 1.012\ \text{kg/m}^3$, $\eta = 2 \times 10^{-5}\ \text{m}^2/\text{s}$, $k = 3 \times 10^{-5}\ \text{kW/mK}$, $C_h = 1.026\ \text{kJ/kg}_g\text{K}$ and $Pr = 0.7$. The air flowrate on dry basis and the air velocity over the trays (assuming the air is evenly distributed) are

$$G = G' / \rho (1 + Y_i)$$

$$= 3 / (1.012 \times 1.0103) = 2.934\ \text{kg}_g/\text{s}$$

$$v_g = G' / A_g$$

$$= 3/1.53 = 1.96\ \text{m/s}$$

To determine the total time required to achieve the final moisture content, the evaporation rate and the drying time for each period must be predicted.

First drying period

Neglecting the induction period, the extent of which depends upon the initial temperature, there is a constant-rate period where n_w can be calculated from Equation 4.6

$$n_w = \frac{h_g (T_g - T_{wb})}{\Delta H_v}$$

Use of this result in Equation 4.39 with the assumption of constant conditions inside the cabinet, that means uniform drying, gives

$$\Delta t = \frac{F_t\, \Delta X}{A\, N_w} = \frac{F_t\, \Delta H_v}{A\, h_g (T_g - T_{wb})} (X_i - X_{cr})$$

The convective heat transfer coefficient can be evaluated from the expression for a flat sheet (Table 4.1) with $L_p = w = 0.75$ m. As an approximation, air properties at the dry bulb temperature are used.

$$Re = L\, v_g / \eta = 7.353\, 10^4$$

$$Nu = 0.664\, Re^{1/2}\, Pr^{1/3} = 150$$

$$h_g = Nu\, k/L = 0.0064\ kW/m^2K$$

On the basis of the above results we obtain

$$n_w = 0.0064 \times (70 - 30)/2{,}430 = 1.054\, 10^{-4}\ kg/m^2s$$

and

$$\Delta t_1 = 167.6 \times (0.45 - 0.38)/\left(13.5 \times 1.054\, 10^{-4}\right)$$

$$= 8{,}250\ s = 2.29\ h$$

From Equations 4.40 and 4.41 the exhaust moisture content and temperature result

$$Y_o = 0.0103 + 13.5 \times 1.054\, 10^{-4}/2.934 = 0.0108\ kg_v/kg_g$$

$$T_o = 70 - 13.5 \times 1.054\, 10^{-4} \times 2{,}430/(2.934 \times 1.026) = 68.85°C$$

Note that these calculations correspond to the maximum evaporation rate. The resulting values for Y_o and T_o indicate that the assumption of constant drying conditions is fairly good for this example. In other cases, or when part of the air is internally recycled and the flow across the product is $G/(1 - r)$, average values of temperature and moisture content have to be taken in order to recalculate the drying rate. For example, with a recycle ratio of $r = 0.95$ the fresh air flowrate reduces to $G = 0.147\ kg_g/s$ so that the outlet moisture content theoretically increases to $Y_o = 0.02\ kg_v/kg_g$. At the average air conditions ($Y = 0.0195\ kg_v/kg_g$ and $T = 69.4°C$) the wet bulb temperature results $T_{wb} = 34.1°C$. Under these circumstances, the driving force is decreased by about 12% and the drying time increases in the same proportion.

Second drying period

In the wet region both internal and external resistances may be important and Equation 4.10 should be applied. It can be proved that at sufficiently large times, usually higher than 10 to 15 min, the first term in the series expansion gives a good estimate of the solution, resulting in

$$\frac{X_m - X_e}{X_{cr} - X_e} = \frac{2\, Bi^2 \exp\left[-\dfrac{\lambda_1^2 D_{eff}}{b^2}\left(t - t_{cr}\right)\right]}{\lambda_1^2\left(\lambda_1^2 + Bi^2 + Bi\right)}$$

This equation can be derived to calculate dX_m/dt and obtain

$$n_w = -\frac{\rho_s \lambda_1^2 D_{eff}}{a_v b^2}\left(X_m - X_e\right.$$

Thus, from Equation 4.37 the drying time for the second period is given by

$$\Delta t = \frac{b^2}{\lambda_1^2 D_{eff}} \int_{X_d}^{X_{cr}} \frac{d\overline{X}}{(\overline{X} - X_e)} = \frac{b^2}{\lambda_1^2 D_{eff}} \ln\left[\frac{X_{cr} - X_e}{X_d - X_e}\right]$$

During this period the average moisture content is 0.28 kg_w/kg_s and the average thickness

$$b = 0.015 [0.6 + 0.4 x (0.28/0.45)] = 1.273 \times 10^{-2} \text{ m}$$

The mass transfer coefficient can be calculated from heat-mass transfer analogies, which for drying conditions yield

$$\frac{h_g}{k_g} = \frac{1.608 \, P_t C_h}{\beta (Pr/Sc)^{2/3}} \simeq 150 \frac{\text{kJ kPa}}{\text{kg K}}$$

allowing us to obtain k_g = 4.27 10^{-5} kg/(kPa·m²·s). Thus, the Biot number defined in Equation (4.11) is

$$Bi = 4.27 \, 10^{-5} \times 1.273 \, 10^2 / (828 \times 2.5 \, 10^{-9} \times 3.2 \, 10^{-2}) = 8.2$$

so that the first solution of $\tan\lambda = Bi/\lambda$ gives $\lambda_1 = 1.40$.
    Using these results the drying time is

$$\Delta t_2 = (1.273/1.4)^2 / 2.5 \, 10^{-5} \ln[(0.38 - 0.02)/(0.18 - 0.02)]$$

$$= 2.682 \, 10^4 \text{ s} = 7.45 \text{ h}$$

Third drying period
In general, since effective diffusivities for the dry zone are nearly one order of magnitude lower than those for the wet zone, internal mass transfer controls during the last period and Equation 4.9 can be used. Again, at sufficiently large times only the first term in the series expansion can be taken to obtain

$$\frac{X_m - X_e}{X_d - X_e} = \frac{8}{\pi^2} \exp\left[-\frac{\pi^2 D_{eff}}{4b^2}(t - t_d)\right]$$

From this expression n_w is evaluated as

$$n_w = \frac{\rho_s \pi^2 D_{eff}}{a_v 4b^2}(X_m - X_e)$$

and the drying time is given by

$$\Delta t = \frac{4b^2}{\pi^2 D_{eff}} \int_{X_o}^{X_d} \frac{d\overline{X}}{(\overline{X} - X_e)} = \frac{4b^2}{\pi^2 D_{eff}} \ln\left[\frac{X_d - X_e}{X_o - X_e}\right]$$

During this period the average moisture content is 0.15 kg_w/kg_s and the average thickness

$$b = 0.015\big[0.6 + 0.4 \times (0.15/0.45)\big] = 1.1\,10^2\ \text{m}$$

From these calculations the drying time is

$$\Delta t_3 = 4\,(1.1/\pi)^2 \big/ \big(2.5\,10^{-6}\big)\ln\big[(0.18 - 0.02)/(0.13 - 0.02)\big]$$

$$= 4.61\ 10^4\ \text{s} = 12.81\,\text{h}$$

Finally, the total drying time is the sum of the time for the three periods and becomes

$$\Delta t = \Delta t_1 + \Delta t_2 + \Delta t_3 = 22.55\,\text{h}$$

Tray dryers require high air flowrates to obtain a reasonable evaporation rate and to reduce uneven drying. Cross-flow operation needs higher air velocities, usually more than 1 to 1.5 m/s, while through-flow operation increases the evaporation rate and allows lower air velocities. The trays must be stacked close together to raise the air velocity; a clearance of 4 to 10 cm between trays is customary. The production in tray dryers is limited by the capacity of the cabinet and the relatively large drying cycles. For cross-flow, the drying rate is limited by the length in the direction of flow during the constant-rate period (due to the dependence of the transport coefficient with this dimension) and by the bed thickness during the falling-rate period. Therefore, a compromise between capacity and residence time is needed. The maximum specific evaporation capacity usually ranges between 0.1 and 1.0 kg/m²h. The higher values are obtained with through-flow operation and high temperatures.

Exhaust gas humidity and temperature vary with time, according to the evaporation rate. During an induction period, which depends upon initial conditions, they change rapidly and reach the critical situation: maximum Y_o and minimum T_o. Air conditions and recycle ratio must be selected to prevent saturation at this fastest evaporation rate. After a nearly constant period, Y_o continuously decreases while T_o gradually drops, both asymptotically, to the incoming conditions. To improve thermal efficiency, part of the air is recirculated and very often the recycle ratio is high, up to 80 to 95%. Under these conditions, the humidity of the inlet air varies during drying and the drying time increases, particularly in the initial stage.

4.4.2 TUNNEL AND CONVEYOR DRYERS

Tunnel and conveyor dryers are widely used for dehydration of food products, particularly fruits and vegetables. In these dryers, the product is spread in a fixed bed and dried by passing heated air across or through the bed. A typical tunnel dryer, which can be operated in concurrent or countercurrent flow, is sketched in Figure 4.9. The material is loaded in trays that are stacked in trucks. The trucks are introduced periodically into one end of the tunnel, advance through the tunnel and are removed at the other end. Although a tunnel dryer is operated with discontinuous loading it can be assumed semicontinuous in operation. A continuous single-stage belt conveyor drier is shown in Figure 4.10. Material to be dried, loaded in a relatively uniform and deep layer, is conveyed through the dryer on a slowly moving belt made of stainless steel screens or perforated plates. The load (5 to 15 cm thick and up to 25 cm thick in secondary stages) and the belt speed (1 to 15 m/h) are adjusted to the drying conditions.

Modeling continuous drying also requires solving the differential equations that represent the mass and energy transfer in the bed (see Figure 4.8). The conditions of product and air vary in the direction of flow. In this case, under steady-state conditions, the simplified mass and energy balances over an infinitesimally small section of the bed yield the following expressions
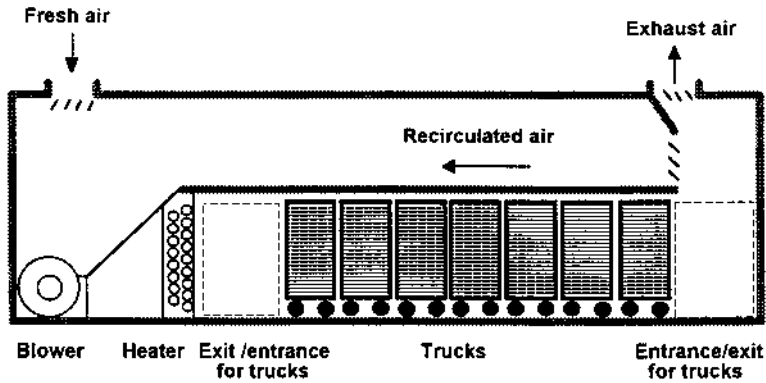
FIGURE 4.9. Diagram of a tunnel dryer.
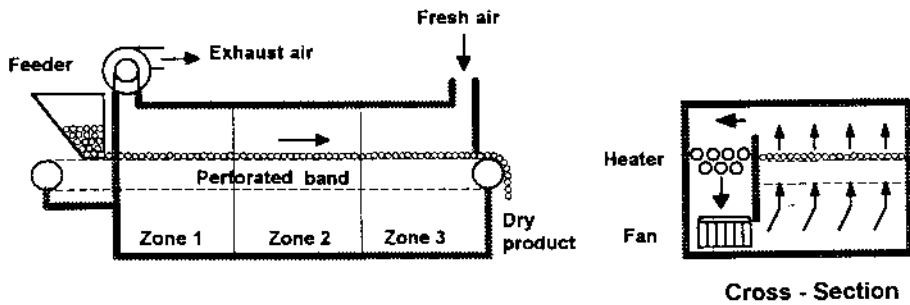
FIGURE 4.10. Illustration of a single conveyor dryer.

- For cross-circulation

$$-F\frac{\partial X}{\partial z} = \pm G\frac{dY}{dz} = n_w a_v A_l \tag{4.42}$$

$$FC_p\frac{\partial T_P}{\partial z} + n_w a_v A_l \Delta H_v = -\left(\pm GC_h\right)\frac{dT_G}{dz} = h_g a_v A_l\left(T_G - T_p\right) \tag{4.43}$$

where $A_l = w\,b$ is the bed cross-sectional area. In Equations 4.42 and 4.43 the positive sign is for countercurrent drying and the negative sign for concurrent drying.

- For through-circulation

$$-\rho_s(1-\varepsilon)v_s\frac{\partial X}{\partial z} = \rho_g\varepsilon v_g\frac{\partial Y}{\partial y} = n_w a_v \tag{4.44}$$

$$\rho_s(1-\varepsilon)C_p v_s\frac{\partial T_P}{\partial z} + n_w a_v \Delta H_v = -\rho_g\varepsilon v_g C_h\frac{\partial T_G}{\partial y} = h_g a_v\left(T_G - T_P\right) \tag{4.45}$$

These simulation models, also called the packed bed model, combined with the constitutive equation for n_w, have to be solved to predict the distribution of temperatures and moisture contents in the system.

As in the case of batch drying we can define an average evaporation rate by the unit exposed surface as

$$N_w = -\frac{F}{w}\frac{d\overline{X}}{dz} = \int_0^b n_w a_v dy \qquad (4.46)$$

Here F represents the product feed on a dry basis, w is the dryer width and $\overline{X}$ is the average water content at a given distance in the dryer. The dryer length required to obtain a desired reduction in moisture content, which is related to the drying time through the belt speed, is

$$\Delta z = -\frac{F}{w}\int_{X_i}^{X_o}\frac{d\overline{X}}{N_w} \qquad (4.47)$$

Overall mass and energy balances in a continuous dryer have been discussed in previous sections. On this basis, changes in air moisture content and temperature through the dryer can be modeled as

$$Y_z = Y_i + \frac{F\,\Delta X}{G} \qquad (4.48)$$

$$T_{Gz} = T_{Gi} - \frac{\left(F\,\Delta X\,\Delta H_v - F\,C_P\,\Delta T_P\right)}{G\,C_{hi}} \qquad (4.49)$$

where $\Delta X = (X_i - X_z)$, $\Delta T_P = (T_{Pi} - T_{Pz})$ for concurrent drying and $\Delta X = (X_z - X_o)$, $\Delta T_P = (T_{Pz} - T_{Po})$ for countercurrent drying. Accumulation of energy by the evaporated moisture, which represents less than 1% of the total heat transferred, has been neglected in Equation 4.49.

4.4.2.1 Example 4.6

A countercurrent dryer is to be designed for the drying of apple slices (average 5-cm diameter by 0.8-cm thickness). The required production is 735 kg/h of raw material with a moisture content $X_i = 6.35$ kg$_w$/kg$_s$ and temperature $T_i = 35°C$. A conveyor of 2-m width and having a speed of 5.5 m/h is to be used. The fresh air flowrate is 17,500 kg/h and 65% of the air is recycled. Average ambient air conditions are 20°C and 30% relative humidity while the incoming temperature is 75°C. Auxiliary fans are used to blow the air through the bed at a velocity of 1.2 m/s. Find the dryer length if the desired final water content is $X_o = 0.35$ kg$_w$/kg$_s$.

Bulk density and surface area per unit volume in the bed of fresh apple slices are $\rho_b = 620$ kg/m^3 and $a_v = 160$ m^2/m^3, respectively. It is found that small-scale experiments on drying of the product can be represented by the characteristic drying curve model with f = 0.97 for $X > X_{cr}$ and $f = 0.97\,((X - X_e)/(X_{cr} - X_e))^{1.1}$ for $X < X_{cr}$, being $X_{cr} = 5.5$ kg$_w$/kg$_s$ and $X_e = 0.03$ kg$_w$/kg$_s$.

The mass flowrate of dry solid and the initial bed depth are found as

$$F = 735 \times (1 + 6.35) = 100 \text{ kg}_s/\text{h}$$

$$b = 735/\left(\rho_b\,v_b\,w\right)$$

$$= 750/(620 \times 5.5 \times 2) = 0.108 \text{ m}$$

The mass flowrates of fresh air ($Y_a = 0.0043 \text{ kg}_v/\text{kg}_g$) and inlet air are

$$G_a = 17,500/(1+0.0043) = 17.425 \text{ kg}_g/\text{h}$$

$$G_i = 17,425/(1-0.65) = 49,786 \text{ kg}_g/\text{h}$$

From the overall mass balance, the outlet humidity is

$$Y_o = 0.0043 + 100(6.35 - 0.35)/17,425 = 0.0387 \text{ kg}_v/\text{kg}_g$$

and from Equation 4.26 the inlet air humidity is

$$Y_i = 0.35 \times 0.0043 + 0.65 \times 0.0387 = 0.0267 \text{ kg}_v/\text{kg}_g$$

The properties of the incoming air are $Y_i = 0.0103 \text{ kg}_v/\text{kg}_g$, $T_{wb} = 37.8°C$, $\rho = 0.972 \text{ kg/m}^3$, $\eta = 2 \times 10^{-5} \text{ m}^2/\text{s}$, $k = 3 \times 10^{-5} \text{ kW/mK}$, $C_h = 1.057 \text{ kJ/kg}_g\text{K}$ and $Pr = 0.7$.

The convective transport coefficients are evaluated from the correlation for packed beds (Table 4.2) using the equivalent particle diameter $D_p = 1.82$ cm.

$$Re = D_p v_g/\eta = 1.092 \; 10^3$$

$$Nu = 1.064 \; Re^{0.59} \; Pr^{1/3} = 58.6$$

$$h_g = Nu \; k/D_p = 0.0966 \text{ kW/m}^2\text{K}$$

The drying rate is found using the characteristic drying curve model, Equation 4.13, expressed as

$$n_w = f \; n_w^o = f \frac{h_g(T_g - T_{wb})}{\Delta H_v}$$

where for this case the value of parameter f is obtained from

$$f = 0.97, X \geq 5.5 \quad \text{and} \quad f = 0.97 \left[\frac{(X-0.03)}{5.47} \right]^{1.1}, \; X < 5.5$$

The air temperature and moisture content are evaluated from Equations 4.46 and 4.47. A first estimate of the product temperature through the dryer can be obtained from (Keey, 1978)

$$T_P = fT_{wb} + (1-f)T_{db}$$

We assume that the air velocity is high enough to neglect variations of n_w in the y direction. On the other hand, although a_v increases and b decreases with water content we consider the product $a_v b$ constant during drying. Thus the evaporation rate is given by

$$N_w = n_w \; a_v \; b = 17.25 \; n_w$$

TABLE 4.4
A Twelve-Step Discretization to Solve Example 4.6

Step	X (kg$_w$/kg$_s$)	Y (kg$_v$/kg$_g$)	f (–)	T$_P$ (°C)	T$_G$ (°C)	N$_w$ (kg/m²h)	Δz (m)
0	6.35	0.0387	0.970	35.0	47.1	22.14	0
1	5.85	0.0377	0.970	38.9	49.5	27.86	1.00
2	5.35	0.0367	0.941	40.0	51.8	32.33	0.831
3	4.85	0.0357	0.844	43.6	54.1	33.77	0.756
4	4.35	0.0347	0.748	47.2	56.4	34.16	0.736
5	3.85	0.0337	0.654	50.7	58.8	33.53	0.739
6	3.35	0.0327	0.560	54.2	61.1	32.03	0.763
7	2.85	0.0317	0.468	57.6	64.4	29.41	0.814
8	2.35	0.0307	0.378	60.9	65.7	25.86	0.905
9	1.85	0.0297	0.289	64.2	68.0	21.43	1.057
10	1.35	0.0287	0.203	67.4	70.4	16.25	1.326
11	0.85	0.0277	0.120	70.5	72.7	10.30	1.883
12	0.35	0.0267	0.043	73.4	75.0	3.90	3.520

Finally, the dryer length can be determined from Equation 4.47. Results for a twelve-step discretization, taking an average N$_w$ for each step, are presented in Table 4.4. From these calculations it follows

$$L = 14.33 \text{ m}$$

Tunnel and conveyor dryers can be operated in cocurrent or countercurrent flow, the arrangement depending mainly on the sensitivity of the product to temperature. Countercurrent systems, which use lower air temperatures and flowrates, appear to be more efficient in energy usage than concurrent systems. However, in cocurrent drying the dry product is exposed to lower temperatures, decreasing the possibility of quality damage. In practice, air flow is a combination of cross and through circulation, which increases significantly the evaporation rate. Typical through-bed velocities vary between 0.5 and 1.5 m/s. Recirculation of air is in the range of 50 to 80%.

Most industrial conveyor dryers have more than one stage. Each stage contains only one conveyor but usually has different sections, 1.5 to 3 m long each. The belts can be from 3 to 20 m in length and 1 to 4 m in width. Typical installations can be divided into air-up and air-down zones and a cooling zone. The flow direction is reversed to allow uniform drying. Usually the airflow is down in the last zone to prevent the small dry particles from being blown out. Temperature, humidity, and air velocity can be controlled in each section to maintain optimum conditions. Multistage systems, with two or more conveyors at different speeds arranged in series, produce mixing and reloading in a deeper bed to improve uniformity of drying and to increase residence times. Multiple pass conveyors, which result in more compact and efficient installations, are also used in the food industry.

4.4.3 ROTARY DRYERS

A cocurrent flow cascading rotary dryer is shown in Figure 4.11. The product is transported along a slightly inclined cylinder while it is dried with heated air in concurrent or countercurrent flow. The shell rotates slowly and is fitted internally with a set of flights to lift the particles through the air stream.
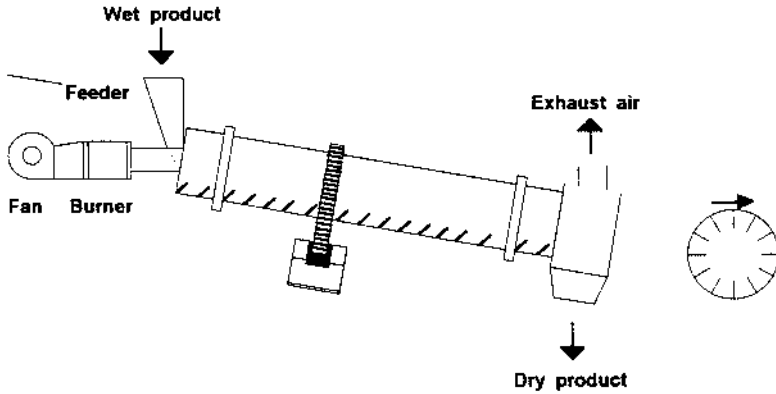
FIGURE 4.11.   A concurrent flow rotary dryer.

Modeling the cascading rotary dryer requires the simultaneous solution of a set equations representing the heat and mass transfer in the system and the movement of the particles through the drum. The differential equations are basically the same as those presented for cross-circulated packed beds, given by Equations 4.42 and 4.43. The main problems are the complicated particle dynamic in the dryer, which is expressed as residence time models, and a suitable expression for the heat transfer coefficient. Residence time and convective coefficients will depend on properties of product and air, dryer dimensions, number and design of flights, and rotational speed. Several expressions have been developed to predict residence times in rotary dryers but none is universally applicable. The following equation has been recommended to evaluate the residence time in minutes

$$\tau = \frac{0.23\,L}{D\,N^{0.9}\,\tan\alpha} \pm \frac{10\,D_p^{-0.5}\,L\,G}{F} \tag{4.50}$$

where the positive sign is for countercurrent flow and the negative sign for concurrent flow. In this equation, L and D represent the length and diameter of the dryer, α the drum slope, N the rotational dryer speed in rpm, G and F the mass flowrate of gas and product, respectively.

On the other hand, by considering the drying as a volumetric heat transfer problem, the following expression has been presented for design purposes

$$Q_t = 2.8\,D\,L\,G_a^{0.67}\,\Delta T_m \tag{4.51}$$

where Q_t represents the total heat transferred, G_a is the mass flowrate of gas per unit cross-sectional area and ΔT_m is the mean temperature difference between air and product defined as

$$\Delta T_m = \frac{\left(T_G - T_P\right)_i - \left(T_G - T_P\right)_o}{\ln\left[\dfrac{\left(T_G - T_P\right)_i}{\left(T_G - T_P\right)_o}\right]} \tag{4.52}$$

However, although the above equations are of practical application, their confidence for fundamental design procedures is still limited.

4.4.3.1 Example 4.7

A cascading cocurrent rotary dryer is to be used to dry 3,000 kg/h of seed with an initial moisture content of 22%. The dryer is 1.25 m in diameter and 10 m long, with a 1° slope and a rotational speed of 3 rpm. It is proposed to use 4,250 m³/h of ambient air (20°C and 30% relative humidity) heated up to 180°C by direct combustion of natural gas. Estimate the output conditions. Some seed properties are average particle diameter D_p = 3 mm, density ρ_p = 1100 kg/m³, equilibrium moisture content X_e = 0.025 kg$_w$/kg$_s$, and effective diffusivity D_{eff} = 5 × 10⁻¹¹ m²/s.

The initial moisture content and the product flowrate on dry basis are

$$F = 3,000 \times (1 - 0.22) = 2,340 \text{ kg}_s/\text{h}$$

$$X_i = 0.22/(1 - 0.22) = 0.282 \text{ kg}_w/\text{kg}_s$$

The fresh air properties are Y = 0.0043 kg$_v$/kg$_g$, ρ = 1.201 kg/m³ and C_h = 1.015 kJ/kg$_g$K and the dry air flowrate results

$$G = 4,250 \times 1.201/(1 + 0.0043) = 5,082 \text{ kg/h}$$

Mass and energy balances in the combustion system give

$$M = 5,082 \times 1.015 \times 160/(49,908 - 2.96 \times 155) = 16.7 \text{ kg}_{methane}/\text{h}$$

$$G_i = 5,082 - 1.25 \times 16.7 = 5,061 \text{ kg}_g/\text{h}$$

$$Y_i = 0.0043 + 2.25 \times 16.7/5,082 = 0.0117 \text{ kg}_v/\text{kg}_g$$

The properties of the incoming air result T_{wb} = 46.1°C, ρ = 0.774 kg/m³ and C_h = 1.029 kJ/kg$_g$K. From dryer dimensions the cross-sectional area and the volume are A = 1.227 m² and V = 12.27 m³.

Residence time is calculated from Equation 4.50

$$t = 0.23 \times 10/(0.0157 \times 3^{0.9} \times 1.25) - 0.01 \times 10 \times 5,061/\left[2,340 \times \left(2 \ 10^{-3}\right)^{0.5}\right]$$

$$= 43.60 - 3.95 = 39.65 \text{ min}$$

$$= 2,379 \text{ s}$$

From this result the volumetric load and the holdup of product in the dryer are

$$V_P = 3,000 \text{ x } t/\rho_p = 1.811 \text{ m}$$

$$H = V_P/V = 0.148$$

Because of the agitation and the high air velocities, in most practical cases of rotary drying the external resistance to mass transfer is negligible. Assuming that there is no shrinkage and the effective diffusivity is constant, drying of spherical particles is given by (Crank, 1967)

$$\frac{X - X_e}{X_i - X_e} = \frac{6}{\pi^2} \sum \frac{1}{n^2} \exp\left[-\frac{n^2 \, D_{eff}}{R_p^2} t\right]$$

Considering that all particles dry to the same extent and taking the first term in the series, an assumption that is valid for sufficiently high times, the final moisture content is

$$X_o = 0.025 + (0.282 - 0.025)6/\pi^2 \exp\left[-5 \ 10^{-11} \times 2{,}379/2.25 \ 10^{-6}\right]$$

$$= 0.173 \ kg_w/kg_s$$

From the overall mass and energy balances, the outlet humidity and temperature result

$$Y_o = 0.0117 + 2{,}340 \times (0.282 - 0.173)/5{,}061$$

$$= 0.0621 \ kg_v/kg_g$$

$$T_o = 180 - 2{,}340 \times (0.282 - 0.173) \times 2{,}443/(5{,}061 \times 1.029)$$

$$= 60.3°C$$

where the thermal load has been approximated by

$$Q = 2{,}340 \times (0.282 - 0.173) \times 2{,}443 = 6.23 \ 10^{-5} \ kJ/h$$

Note that the total heat that may be transferred by convection from the air to the product can be expressed as

$$Q_t = h_g \, a_v \, V \, (\Delta T)_m$$

Air properties taken at at the average conditions ($T_{ave} = 120°C$ and $Y_{ave} = 0.0369 \ kg_v/kg_g$) are $\rho = 0.879 \ kg/m^3$, $\eta = 2.6 \times 10^{-5} \ m^2/s$, $k = 3.4 \times 10^{-2}$ W/mK and Pr = 0.7. Thus, the air velocity

$$v = G(1 + X)/[\rho(1 - H)A]$$

$$= 5{,}061 \times 1.0369/(0.879 \times 0.852 \times 1.227 \times 3{,}600) = 1.59 \ m/s$$

The factor (1 – H) accounts for the effect of flights and product on the cross-sectional area. The average heat transfer coefficient is found as (Table 4.2)

$$Re = D_p \, v_g/\eta = 183$$

$$Nu = 0.33 \, Re^{0.6} = 7.52$$

$$h_g = Nu \, k/D_p = 0.0852 \ kW/m^2K$$

Assuming the product is at the wet bulb temperature we obtain

$$(\Delta T)_m = (133.9 - 14.2)/\ln(133.9/14.2) = 53.3°C$$

The total heat obtained in this way is very much higher than that required to evaporate the water, indicating that the heat transfer is not the controlling resistance. Finally, application of Equation 4.51 to this example gives $Q_t = 5.63 \times 10^5$ kJ/h, approximately 10% lower than the thermal load obtained above.

Rotary dryers are particularly suitable for products that tend to stick together. The agitation and the high exposed area provide relatively high evaporation rates and uniform drying. However, their use is restricted because of damage to the food caused by impact and abrasion in the drum. Typical dryer dimensions are 0.5 to 3 m in diameter and 5 to 10 times the diameter in length. The shell is inclined with a slope of 0 to 5° to the horizontal. The peripheral speed of rotation is usually 0.25 to 0.4 m/s. Particle size may range from 100 to 200 μm to centimeters. A practical product holdup in the dryer of 10 to 15% is customary. Air flowrates of 1 to 3 kg/m²s, giving gas velocities of 0.5 to 2.5 m/s, are used.

4.4.4 FLASH OR PNEUMATIC DRYERS

In flash or pneumatic dryers the food, in the form of powders or particles, is continuously dried in a vertical duct while being conveyed by the heated airstream, usually air plus combustion gases. After very short drying times, in the order of seconds, one or more cyclones are used to separate the dried material from the exhaust air. A typical pneumatic dryer configuration is shown schematically in Figure 4.12. Short contact times, small particle sizes (lower than 2 mm), and concurrent operation allow the use of relatively high air temperatures without overheating the product.

The heat and mass transfer equations which model the process are similar to those proposed for cross-circulated beds in concurrent flow, represented by Equations 4.42 and 4.43. Usually, the air velocity should be adjusted to lift and classify the particles. Two limit velocities are important in fluidization and pneumatic transport of solids. The incipient fluidization velocity v_f is the minimum air velocity required to achieve fluidization, that means to suspend the particles with the airstream. The entrainment or terminal velocity v_t is the minimum air velocity needed to convey or transport the particles with the airstream. For spherical particles of diameter D_p they can be found by

$$v_f = \frac{g\, D_p^2\, \varepsilon^3 (\rho_w - \rho)}{180\, \mu (1 - \varepsilon)} \tag{4.53}$$

$$v_e = \frac{g\, D_p^2 (\rho_s - \rho)}{18\, \mu} \tag{4.54}$$

where ρ_s and ρ are the densities of the solid and the air respectively, g is the acceleration due to gravity, μ the viscosity of the fluid, and ε the voidage of the bed. To use this information in selecting the air velocity, the particles must have a rather regular shape and a narrow size distribution.

When the feed has a broad particle size distribution $E(D_p)$, small and less humid particles are dried and conveyed faster than heavier particles, which are suspended in a fluid bed until a given drying is obtained. Thus, there is a distribution of residences times and the average moisture content of the material leaving the dryer can be evaluated as
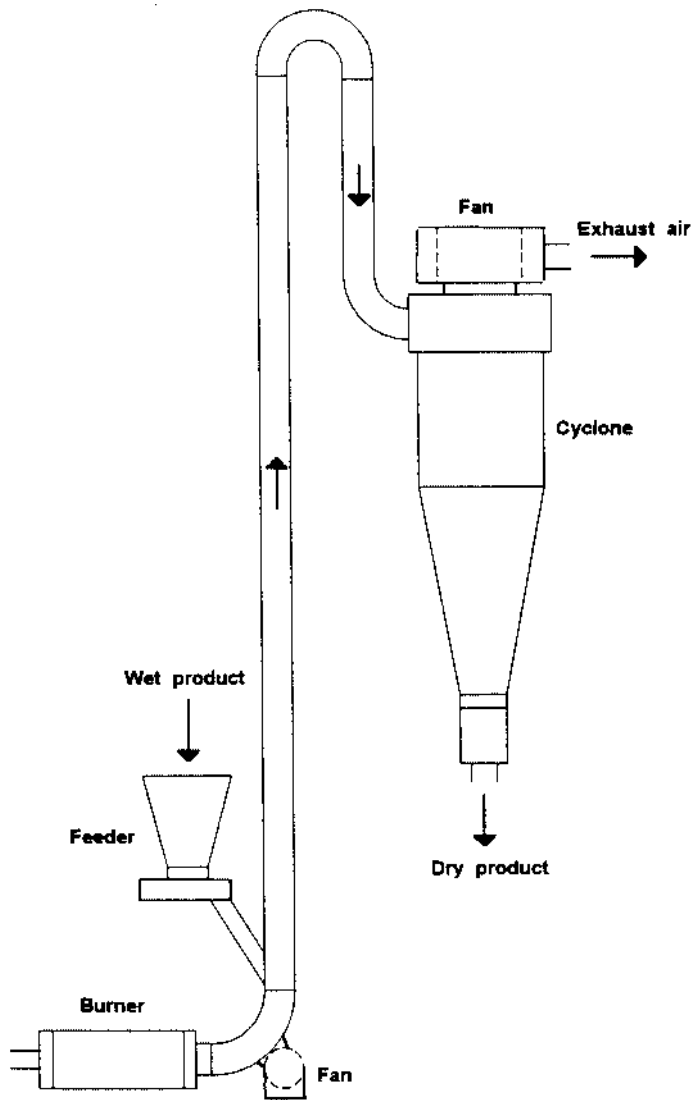
FIGURE 4.12 Scheme of a pneumatic dryer.

$$X_m = \int\limits_0^\infty E\left(D_p\right) X\left(D_p\right) dD_p \qquad (4.55)$$

where $X(D_p)$ is the moisture content of the particle after drying during the residence time.

4.4.4.1 Example 4.8

A flash dryer is to be designed to dry 7,500 kg/h of potato granules from 28 to 13% moisture content on a wet basis. Ambient air (T = 20°C and Y = 0.0043 kg_v/kg_g) is heated by direct combustion of natural gas. The initial temperature is 60°C and the recommended temperatures for the air entering and leaving the dryer are 220 and 75°C, respectively. Calculate the amount of air required and estimate the main dimensions of the dryer.

Main properties of potato granules are average particle diameter D_p = 0.3 mm, density ρ_p = 1,250 kg/m³, specific heat C_p = 1.85 kJ/kg_sK, thermal conductivity k_d = 0.21 × 10⁻³

W/mK and effective diffusivity $D_d = 2.5 \times 10^{-10}$ m²/s. From sorption isotherms it is found that $X_e = 0.045$ kg$_w$/kg$_s$, $Y_e = 0.203$ kg$_v$/kg$_g$, and $(dX/dP)_T = 1.3 \times 10^{-2}$ at the outlet conditions.

The product flowrate, and initial and final moisture content on dry basis are

$$F = 7,500 \times (1 - 0.28) = 5,400 \text{ kg}_s/\text{h}$$

$$X_i = 0.28/(1 - 0.28) = 0.389 \text{ kg}_w/\text{kg}_s$$

$$X_o = 0.13/(1 - 0.13) = 0.149 \text{ kg}_w/\text{kg}_s$$

Mass and energy balances in the burner, Equations 4.28 through 4.31, give

$$Y_i = 0.0136 \text{ kg}_v/\text{kg}_g$$

The properties of the drying air are $T_{wb} = 50.2°C$, $\rho = 0.710$ kg/m³, $\eta = 3.8 \times 10^{-5}$ m²/s and $C_h = 1.032$ kJ/kg$_g$K.

The entrainment velocity is found by using Equation 4.54

$$v_t = 9.81 \times 0.3^2 \ 10^{-6} \times (1,250/0.71 - 1)/(18 \times 3.8 \ 10^{-5}) = 2.27 \text{ m/s}$$

Thus the minimum air flowrate to convey the particles is given by

$$G_{min} = \rho \ v_t \ A/(1 + Y)$$

Assuming typical dryer diameters of 0.5 to 1.2 m we obtain G_{min} in the range 1,100 to 6,500 kg$_g$/h. Although v_t increases as the air temperature decreases, these calculations are rather conservative because of the decrease in D_p due to shrinkage during drying.

On the other hand, and using mass transfer considerations, from Equation 4.32 the minimum air flowrate becomes

$$G_{min} = 5,400 \times (0.389 - 0.149)/(0.203 - 0.0136) = 6,840 \text{ kg}_g/\text{h}$$

Finally, taking into account the thermal load G_{min} can be estimated from Equation 4.33

$$G_{min} = 2,425 \times 5,400 \times (0.389 - 0.149)/220 - 75 = 21,675 \text{ kg}_g/\text{h}$$

The minimum air flowrate is determined by the thermal demand, suggesting that part of the air should be recycled, and it is sufficient for the pneumatic transport of the granules.

The drying of the product can be modeled using the receding front model, Equations 4.15 and 4.16, where the overall heat and mass transfer coefficients for spherical geometry are expressed as

$$U = \frac{h_g}{1 + \dfrac{h_g \ \Delta R}{k_d \left(1 - \Delta R/R_p\right)}}$$

$$K_g = \frac{k_g}{1 + \dfrac{k_g \ \Delta R}{\rho_s (\partial X/\partial P) D_d \left(1 - \Delta R/R_p\right)}}$$

TABLE 4.5
Solution of Example 4.8

Step	W (%)	Y (kg$_v$/kg$_g$)	T$_P$ (°C)	T$_G$ (°C)	v$_g$ (m/s)	ΔP (kPa)	ΔX/Δt (kg/kgs)	Δt (s)
0	28	0.0136	60.0	220.0	19.7	16.75	1.415	0
1	27	0.0183	54.2	211.5	19.4	11.52	0.703	0.0191
2	26	0.0228	57.6	199.2	19.2	13.52	0.639	0.0278
3	25	0.0272	60.0	187.7	18.8	15.02	0.574	0.0294
4	24	0.0315	62.3	176.5	18.5	16.16	0.514	0.0328
5	23	0.0357	63.9	165.9	18.3	17.07	0.461	0.0334
6	22	0.0398	64.9	155.7	18.0	17.62	0.410	0.0380
7	21	0.0438	65.7	146.0	17.7	17.64	0.358	0.0418
8	20	0.0477	66.3	136.5	17.4	17.69	0.315	0.0468
9	19	0.0515	66.3	127.5	17.1	17.54	0.276	0.0520
10	18	0.0552	66.2	118.9	16.8	16.76	0.235	0.0588
11	17	0.0588	65.8	110.5	16.6	15.75	0.196	0.0676
12	16	0.0624	65.2	102.4	16.3	14.74	0.164	0.0786
13	15	0.0657	64.3	94.7	16.0	13.38	0.133	0.0938
14	14	0.0691	63.2	87.2	15.7	11.79	0.105	0.1146
15	13	0.0724	62.8	80.1	15.5	10.02	0.080	0.1444

In this case the thickness of the dry region is given by

$$K_g = \frac{g}{1 + \dfrac{k_g\,\Delta R}{\rho_s(\partial X/\partial P)D_d\left(1\right.}}$$

The convective transport coefficients are obtained from the correlation for a sphere (Table 4.2) using the terminal velocity

$$Re = D_p\,v_t/\eta$$

$$Nu = 2.0 + 0.6\,Re^{1/2}\,Pr^{1/3}$$

$$h_g = Nu\,k/D_p$$

$$k_g = 150/h_g$$

The air temperature and moisture content are evaluated from Equations 4.46 and 4.47. Solution of the problem using a fifteen-step discretization, and taking average coefficients and driving forces for each step, is presented in Table 4.5. A gas flowrate of 22,000 kg$_g$/h and constant particle size have been considered. Note that the most intensive drying occurs in the first meters of the dryer. The dryer capacity depends on the diameter and length of the lifting duct. The dryer length is calculated from

$$L = \left(v_g - v_t\right)t$$

For a diameter of 0.75 m, which gives the air velocities shown in Table 4.5, it becomes L = 13.4 m.

TABLE 4.6
Characteristics of Selected Dryers

Dryer type	Evaporation capacity (kg$_w$/m²h)	Energy consumption (kJ/kg$_w$)	Thermal efficiency (%)	Residence time (s,min,h)
Tray or cabinet	0.1–1	3000–4500	50–80	2–24 h
Tunnel and conveyor	5–18	4000–6000	35–60	10–180 m
Rotary	30–120[a]	3500–6000	40–70	10–60 m
Fluid bed	30–90	3100–6000	40–80	5–30 m
Pneumatic	10–100[a]	3500–5000	50–75	2–15 s
Spray	1–30[a]	4000–5000	50–60	5–120 s
Drum	4–30	3000–3500	70–85	10–30 s
Vacuum and freeze	1–7	>7500	—	1–24 h

[a] in kg$_w$/m³h

In pneumatic transport, heat and mass transfer take place mainly by convection. The high temperature-short time process provides a very high evaporation rate, particularly at the entry point where unbound moisture evaporation is practically instantaneous. A narrow particle-size distribution, the maximum particle size being 1 to 2 mm, is required to avoid overheating of small particles and insufficient drying of larger particles. The gas velocity depends on the particle size but usually is in the range 10 to 30 m/s. Typical dryer dimensions vary between 0.6 to 1.1 m in diameter and 12 to 30 m in length. Pneumatic dryers are frequently combined with a secondary dryer to achieve the final moisture content.

4.5 DRYER SELECTION

Drying equipment for food processing has to be selected and designed on the basis of

- Characteristics of the raw material
- Quality requirements on the dry product
- Economic analysis or cost estimation
- Safety and environmental considerations

Applications and some characteristics of the most widely used types of dryers for foods are summarized in Tables 4.1 and 4.6, respectively. Information for selection and performance evaluation of common industrial dryers can be found in Perry and Chilton (1973), Van't Land (1991) and Keey (1991). Applications to drying of foods have been reviewed elsewhere (van Arsdel et al., 1973; Sokhansanj and Jayas, 1987; Fellows, 1988; Jayaraman and Das Gupta, 1992; Okos et al. 1992).

Batch tray or cabinet dryers are flexible to process different feed products. However, their use and capacity are restricted by the large drying cycles and the nonuniform drying at different locations within the chamber. The main advantages are the low capital and maintenance costs and a straightforward scaling-up from small-scale tests. Commercial use of cabinet dryers is restricted to relatively low productions. Drying of nonsticky particulate solids at high production rates often requires tunnel or belt conveyor dryers. Conveyor dryers provide a better control of drying conditions and the most uniform quality. Belt through and vibrated bed give a more uniform drying and a more efficient energy usage but increase the investment cost.

Rotary dryers are suitable for products that tend to stick, providing for very high drying rates and a uniformly dried product. As indicated earlier, possible damage of the food product

by impact and abrasion is a concern. Flash or pneumatic dryers are very useful for drying powders and granular material. Frequently, flash dryers must be integrated with a secondary dryer to obtain the required final moisture. Fluid bed dryers are limited to medium and coarse particulate foods, usually exceeding 0.1 mm, which fluidize uniformly without mechanical damage. Pneumatic and fluid bed dryers have high drying rates and thermal efficiencies and close control of drying conditions. Additionally, because of their simple design with low moving parts, capital and maintenance costs are low. Spray dryers are used for dehydrating several fluid or semifluid foods, i.e., solutions, suspensions, and pastas. These dryers can handle large production rates but demand high capital and energy costs. Drum dryers are suitable for drying liquids, slurries, and pasta with high drying rates and high energy efficiencies, but require relatively high capital and maintenance costs. Their use is being limited because of the damage to heat sensitive foods.

Conventional atmospheric air drying and drum drying usually yield products that tend to have an excessive damage and rehydrate or reconstitute slowly. Fluid bed, flash, and spray dryers cause less heat damage and yield products which rehydrate more satisfactorily. Foam mat and explosion puffing increase costs of traditional methods but improve quality of products that rehydrate rapidly. Foam mat is restricted to small productions and is only used with liquid foods that can form stabilized foams. Explosion puffing is still limited to some fruits and vegetables. Vacuum drying and freeze drying are very expensive methods of dehydration. Since the drying is done at lower temperatures, thermal damage is minimized and the product quality is very high. Their application is restricted to extremely high heat sensitive material or highly valued foods.

4.5.1 COST ESTIMATION

Drying is an individual operation. More often than not, the economic analysis of drying has to be taken in the broader context of the overall manufacturing process. Chapter 13 provides useful insights on Cost and Profitability Estimation. Peters and Timmerhaus (1991) gave a thorough foundation for the general subject of cost estimation. They reviewed cash flow, factors affecting investment and production costs, capital investment estimates, cost updating indexes and the like.

As a first approximation, industrial dryers installed range between \$1,000 and \$25,000/m^2. The wide variation reflects both the changes in size and type of dryers. Tray and tunnel dryers have the lowest prices. Conveyor dryers cost between \$1,500 and \$3,000/m^2. Belt-through and vibrated-bed systems increase the investment costs. Flue-gas rotary dryers cost between \$2,500 and \$3,300/m^2, for areas between 120 and 10 m^2. Steam-tube rotary dryers range between 1,500 and 9,500/m^2 for transfer areas between 1000 and 30 m^2. Drum dryers have a higher unit cost. Double drum atmospheric dryers range between \$2,600 and \$15,000/m^2 (50 to 5 m^2). Single drum vacuum dryers may have an installation cost between \$20,000 and \$25,000/m^2 for areas ranging between 15 and 1 m^2. Approximate costs of typical dryers are shown in Popper (1970), Perry and Chilton (1973), Peters and Timmerhaus (1991) and Van't Land (1991).

The above numbers suggest that cost per square meter decreases as scale of production increases. This is reflected in the well-established six-tenths factor rule

$$\frac{C_1}{C_2} = \left(\frac{A_1}{A_2}\right)^{r_c} \tag{4.56}$$

were C_1 and C_2 are purchased dryer costs corresponding to production capacities A_1 and A_2, respectively, and r_c is the extrapolating factor. The rule of thumb value $r_c = 0.6$ can be replaced by better approximations from publications on commercial data. For instance, Popper (1970) shows r_c values of 0.45, 0.38, and 0.45 for drum, pan, and rotary vacuum dryers, respectively.

Peters and Timmerhaus (1991) recommend $r_c = 0.40$ for single drum atmospheric driers and $r_c = 0.76$ for single drum vacuum dryers. Van't Land (1991) presents an r_c value of 0.424 for direct heat rotary dryers and linear relationships between costs and capacities for flash and spray dryers, which suggest $r_c = 0.35$ and $r_c = 0.47$, respectively. In general, these extrapolations are reasonably safe for a ten-fold or less increase in capacity. Equation 4.56 can be used in terms of specific cost $S = C/A$. Then

$$\frac{S_1}{S_2} = \left(\frac{A_2}{A_1}\right)^{1-r_c} \tag{4.57}$$

Cost estimation is used as a first approximation, together with all the technical considerations leading to select one or more dryers. The next step to obtain an accurate cost assessment is to work with vendors. The large variety of drying equipment and the complexity of scaling up its performance has resulted in a number of specialized equipment suppliers. In dealing with vendors, the user is quite frequently analyzing both cost and expected performance. Ideally, the vendor should guarantee both. In many instances there is need to carry out equipment trials. Many vendors have representative pilot equipment and an established scaling up procedure. With complex food materials it is important to be aware that auxiliary systems, such as feeders, dust collectors and the like, may be key to the performance of the equipment being tested. Insuring test material representativity and integrity is an essential requisite for trials (Moyers, 1992).

When equipment cost is evaluated, the entire drying system must be considered, taking into account all needed auxiliary systems as ducts, conveyors, fans, motors, heaters, cyclones, and dust collectors. To obtain the final investment cost, the installation costs (including engineering, buildings, foundation, piping, instrumentation, and auxiliary services) must also be considered. As a rule of thumb, Van't Land (1991) suggests to multiply the equipment cost by a factor of 2.25 to 2.75 to obtain the total installed costs. This average figure applies to different dryers (conveyor, spray, flash, rotary and fluid-bed) manufactured of stainless steel and carbon steel, respectively.

Operating cost must be evaluated and incorporated into the decision-making process. Food dehydration is one of the most energy-intensive processes and the energy consumption constitutes the main factor in the total manufacturing cost. The energy cost is determined by initial and final moisture contents, drying conditions, the scale of the process and the type of system (forced-air, drum, freeze, and vacuum drying). Energy consumption in different food drying installations has been discussed by Flink (1977) and Tragardh (1981). Strumillo and Lopez-Cacicedo (1987) reviewed the main topics on energy in drying and discussed strategies to optimize energy use. Typical energy consumptions and efficiencies (energy actually used to evaporate the water over total energy available for evaporation) for different dryers are summarized in Table 4.6. For an existing operation, Cook and DuMont (1991) have reviewed four basic strategies: (1) improve efficiency or otherwise reduce evaporation load, (2) optimize heating temperatures and air moisture contents, (3) reduce heat losses, and (4) identify alternative means of providing heat. The authors discuss practical implementation examples.

Cabinet and tunnel dryers have relatively high labor costs involved in handling the product. Automatic loading and conveying simplify the process and reduce labor costs. In addition, maintenance costs per year average about 5 to 6% of the total investment cost. This figure can be as low as 3% for simple dryers (tray, tunnel, and flash dryers) but can reach 10% of the installed costs for mechanically complicated systems (rotary, drum, and vacuum dryers).

In general, air drying in cabinet or tunnel dryers would show the lowest cost. Drying in conveyor, drum, and pneumatic systems are of relatively low cost. Fluid bed and spray drying are more costly and can reach twice the cost of forced air drying. The use of vacuum increases significantly the cost of drying. Freeze drying is the most expensive way of food dehydration,

TABLE 4.7
Some N.F.P.A. Codes Relevant to Drying

Subject	Reference
Fire and dust explosions in facilities manufacturing and handling starch — 1989	61A, Vol. 2
Fire and dust explosions in the milling of agricultural commodities for human consumption — 1989	61D, Vol. 2
Ovens and furnaces: design, location, and equipment — 1990	86, Vol. 4
Industrial furnaces using vacuum as an atmosphere — 1990	86D, Vol. 4
Installation of exhaust systems for air conveying of materials — 1992	91, Vol. 4
Pneumatic conveying systems for handling combustible materials — 1990	650, Vol. 7

up to 4 to 5 times higher than conventional air drying. As an example, Sapakie and Renshaw (1984) discussed the equipment and operating cost of several dryers and concentration equipment at different evaporation rates. The total fixed cost of forced air, drum, fluid bed, spray, continuous vacuum, and freeze dryers showed the first four as being fairly close and the last two increasingly expensive. The same grouping applied in terms of manufacturing cost.

Final selection of a dryer cannot be based only on investment and operating costs. Quality of the resulting product is a significant consideration. Product quality and cost are usually competing factors. In each particular application the designer looks for a favorable combination of cost, energy efficiency, quality, and price of the final product.

4.5.2 Hazards in Drying

Fires and explosions are the main hazards in a drying operation. Fires can result from combustion of the material being dried, volatiles evolving from it, or accidents related to the fuel being used. The more common type of explosion associated with drying is dust explosion. It may occur in the drier itself or in auxiliary equipment associated with the operation, in particular dust collectors.

Combustible dust is an explosion risk. The risk increases as the material is dried. Most drying systems, from raw material feed to packaging, are interconnected. Therefore, risk assessment must consider the operation in broad terms. Collectors and their connecting ducts are likely areas for explosion. The source, such as overheated material, may come from the dryer or auxiliary equipment. Another likely source is a spark or static electricity. A particular area of concern is driers where the wall temperature is much higher than the product temperature, leading to risk conditions during cycle interruptions. The subject has been discussed by several authors (Cook and DuMont, 1991; Keey, 1991; Van't Land, 1991).

The National Fire Codes, published by the National Fire Protection Association (NFPA) are particularly useful in building accident prevention in the design, construction, and operation of drying systems. The complete set of Codes contains the codes, standards, and guides developed by the technical committees of the NFPA. Table 4.7 provides reference numbers of some of the material relevant to drying of foods. The National Fire Codes Subscription Service (NFPA, 1992) includes 13 volumes: the first 8 contain Codes and Standards; Volumes 9 through 11 contain Recommended Practices, Manuals, and Guides; Volume 12 contains Formal Interpretations, Tentative Interim Amendments, and Errata. There is an additional volume containing the Master Index, which allows quick identification of specific references.

NFPA 650, Standard for Pneumatic Conveying Systems for Handling Combustible Materials (NFPA, 1993), indicates that a dust explosion has four requirements: (1) a combustible dust, (2) the dust dispersed in air or oxygen at or exceeding the minimum explosion concentration, (3) an ignition source, and (4) confinement. Different standards elaborate on equipment requirements, explosion relief and venting, dust control, and other practices. The standard specifies evaluation tests for combustible dusts.

REFERENCES

Abbott, J.A., 1990, *Prevention of Fires and Explosions in Dryers — A User Guide*, 2nd ed., Institute of Chemical Engineering, Rugby, U.K.

American Society of Agricultural Engineers, 1982, *Agricultural Engineers Yearbook*, ASAE, St. Joseph, MI.

Bakker-Arkema, F.W., 1986, Heat and mass transfer aspects and modeling of dryers — a critical review, in *Concentration and Drying of Foods*, MacCarthy, D., Ed., Elsevier, London, 165–202

Bird, R.B., Stewart, W.E., and Lightfoot, E.N., 1960, *Transport Phenomena*, John Wiley, New York.

Bradshaw, R.D. and Myers, J.E., 1963, Heat and mass transfer in fixed and fluidized beds of large particles, *AIChE J.* 9:590–598.

Brooker, D.B., Baker-Arkema, F.W., and Hall, C.W., 1974, *Drying Cereal Grains*, AVI Publishing, Westport, CT.

Bruin, S. and Luyben, K.Ch.A.M., 1980, Drying of food materials: a review of recent developments, in *Advances in Drying*, Vol. 1, Mujumdar, A.S., Ed., Hemisphere, Washington, D.C., 155–215.

Charm, S.E., 1971, *The Fundamentals of Food Engineering*, 2nd ed. Avi Publishing, Westport, CT.

Cook, E.M. and DuMont, J.D., 1991, *Process Drying Practice*, McGraw-Hill, New York.

Crank, J., 1967, *The Mathematics of Diffusion*, Oxford University Press, London.

Crapiste, G.H., Whitaker, S., and Rotstein, E., 1988, Drying of cellular material. I. A mass transfer theory. II. Experimental and numerical results, *Chem. Eng. Sci.* 43(11):2919–2936.

Fellows, P., 1988, *Food Processing Technology: Principles and Practice,* Ellis Horwood, Chichester, U.K.

Flink, J.M., 1977, Energy analysis in dehydration processes, *Food Technol.* (3):77–84.

Fornell, A., Bimbenet, J.J., and Amin, Y., 1980, Experimental study and modelization for air drying of vegetable products, *Lebensm.-Wiss U.-Tecnol.* 14:96–100.

Fortes, M. and Okos, M.R., 1980, Drying theories: their bases and limitations as applied to food and grains, in *Advances in Drying*, Vol. 1, Mujumdar, A.S., Ed., Hemisphere, Washington, D.C., 119–154.

Jayaraman, J.S. and Das Gupta D.K., 1992, Dehydration of fruits and vegetables — recent developments in principles and techniques, *Drying Technol.* 10(1):1–50.

Keey, R.B., 1972, *Drying Principles and Practice*, Pergamon Press, Oxford.

Keey, R.B., 1978, *Introduction to Industrial Drying Operations*, Pergamon Press, Oxford.

Keey, R.B., 1991, *Drying of Loose and Particulate Materials*, Hemisphere, New York.

Keey, R.B. and Suzuki, M., 1974, On the characteristic drying curve, *Int. J. Heat Mass Transfer* 17:1455–1464.

Lee, D.S. and Pyun, Y.R., 1993, Optimization of operating conditions in tunnel drying of food, *Drying Technol.* 11(5):1025–1052.

Masters, K., 1979, *Spray Drying Handbook*, George Godwin Ltd., London.

Mishkin, M., Saguy, I., and Karel, M., 1983, Dynamic optimization of dehydration processes: minimizing browning in dehydration of potatoes. *J. Food Sci.* 48:1617–1621.

Moyers, C.G., 1992, Don't let dryer problems put you through the wringer, *Chem. Eng. Process* 88(12):34–40.

Mujumdar, A.S., 1987, *Handbook of Industrial Drying*, Marcel Dekker, New York.

N.F.P.A., 1992, *National Fire Codes Subscription Service*, Vols. 1–12 and Master Index. National Fire Protection Association, Quincy, MA.

Okos, M.R., Narsimhan, G., Singh, R.K., and Weitnauer, A.C., 1992, Food dehydration, in *Handbook of Food Engineering*, Heldman, D.R. and Lund, D.B., Eds., Marcel Dekker, Inc., New York, 437–562.

Perry, R.H. and Chilton, C.H., 1973, *Chemical Engineers' Handbook*, 5th ed., McGraw-Hill Kogakusha, Tokyo.

Peters, M.S. and Timmerhaus, K.D., 1991, *Plant Design and Economics for Chemical Engineering*, 4th ed., McGraw-Hill, New York.

Popper, H., 1970, *Modern Cost Engineering Techniques*, McGraw-Hill, New York.

Ratti, C. and Crapiste, G.H., 1992, A generalized drying curve for shrinking food materials, in *Drying'92*, Mujumdar, A.S., Ed., Elsevier, New York, 864–873.

Ratti, C. and Crapiste, G.H., 1995, Determination of heat transfer coefficients during drying of foodstuffs, *J. Food Proc. Eng.,* 18:41–53.

Ratti, C., Crapiste, G.H., and Rotstein, E., 1989, Psychr: a computer program to calculate psychrometric properties, *Drying Technology*, 7(3):575–580.

Sapakie, S.F. and Renshaw, T.A., 1986, Economics of drying and concentration of foods, in Engineering and Food, Vol. 2, Processing Applications, McKenna, R.M., Ed., Elsevier Applied Sci., 937–938.

Singh, R.P. and Heldman, D.R., 1985, *Introduction to Food Engineering*, Academic Press, New York.

Sokhansanj, S. and Jayas, D.S., 1987, Drying of foodstuffs, in *Handbook of Industrial Drying*, Mujumdar, A.S., Ed., Marcel Dekker, New York, 517–554.

Strumillo, C. and Lopez-Cacicedo, C., 1987, Energy aspects in drying, in *Handbook of Industrial Drying*, Mujumdar, A.S., Ed., Marcel Dekker, New York, 823–862.

Tragardh, C., 1981, Energy and energy analysis in some food processing industries, *Lebensm.-Wiss. Technol.* 14:213–217.

Treybal, R.E., 1980, *Mass-Transfer Operations*, 3rd ed., McGraw-Hill, New York.

Van Arsdel, W.B., Copley, M.J., and Morgan, A.I., 1973, *Food Dehydration*, 2nd ed., AVI Publishing, Westport, CT.

Van Meel, D.A., 1958, Adiabatic convection batch drying with recirculation of air, *Chem. Eng. Sci.* 9:36–44.

Vanecek, V., Markvart, M., and Drbohlav, R., 1966, *Fluidized Bed Drying*, Leonard Hill Books, London.

Van't Land, C.M., 1991, *Industrial Drying Equipment*, Marcel Dekker, New York.

Whitaker, S., 1972, Forced convection heat transfer correlations for flow in pipes, past flat plates, single cylinders, single spheres, and for flow in packed beds and tube bundles, *AICHE J.* 18(2):361–371.

Williams-Gardner, A., 1971, *Industrial Drying*, Leonard Hill, London.

5 Design and Performance Evaluation of Membrane Systems

Jatal D. Mannapperuma

CONTENTS

5.1   INTRODUCTION

Membrane is an interface between two bulk phases which are liquid and solute mixtures. The membrane controls the mass exchange between the bulk phases by being selective to some species of the mixture with respect to other species. A membrane process allows the selective transfer of some species of a mixture from one bulk phase to the other bulk phase separated by a membrane.

This definition of membrane processes includes a wide range of unit operations from sieving to reverse osmosis. The scope of this chapter is limited to a narrower branch of membrane-based unit operations better described as cross-flow filtration. Filtration of coarse particles down to micron range can be done by conventional **dead-end filtration**. Particles retained by the filter in dead-end filtration build up with time as a cake layer which results in increased resistance to filtration. This requires frequent cleaning or replacement of filters.

In **cross-flow filtration** the bulk phase under pressure is forced to flow along the surface of the membrane, sweeping the retained particles so that the cake layer remains relatively thin and the resistance to filtration remains low. This allows relatively high fluxes to be maintained over long periods of time. Figure 5.1 illustrates the difference between these two modes of filtration.

5.1.1   MEMBRANE FILTRATION SPECTRUM

Cross-flow membrane filtration is used to separate particles which are about 10 μm to solute molecules that are a few Angstroms. The membrane filtration spectrum is divided into four narrower ranges based on the particle size. Figure 5.2 is an illustration of the filtration spectrum in relation to food processing applications.

Microfiltration is the coarsest of the membrane filtration classes. Its applications are to separate small particles suspended in liquids. Microfiltration membranes are classified by **pore diameter cut off** which is the diameter of the smallest particles that are retained by it, typically in the range of 0.1 to 10 μm. Microfiltration requires lowest operating pressures of all, usually in the range of 10 to 50 psi.
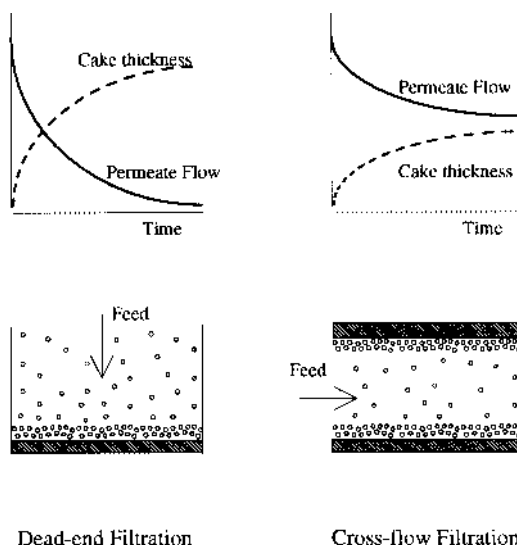
FIGURE 5.1   Dead-end and cross-flow filtration.

Ultrafiltration is used for the separation of large macromolecules such as proteins and starches. Ultrafiltration membranes are classified by the **molecular weight cut-off** which is defined as the molecular weight of the smallest molecule, 90% of which is retained by the membrane. Ultrafiltration range spans from 1,000 to 500,000 molecular weight cut-off. Ultrafiltration requires somewhat higher operating pressures compared to microfiltration, usually in the range of 20 to 200 psi.

Nanofiltration membranes retain solute molecules ranging from 100 to 1000 molecular weight. Nanofiltration membranes are classified by the molecular weight cut-off like ultra-filtration membranes or by percentage sodium chloride rejection like reverse osmosis membranes. Nanofiltration uses operating pressures in the range of 100 to 500 psi.

Reverse osmosis involves the tightest membranes which are capable of separating even the smallest solute molecules. Reverse osmosis membranes are classified by **percentage rejection** of sodium chloride in an aqueous solution under specified conditions and ranges from 99.5 to 95%. High pressures in the range of 200 to 1500 psi are required to overcome the high osmotic pressure of solutions of small molecules.

The membrane processes discussed in this chapter are pressure driven and separate solutes primarily based on size. Electrodialysis and pervaporation are membrane separation processes with applications in food processing industry. However, these are not pressure-driven processes and the separations are not based on size of solutes. These processes are not discussed in this chapter.

5.1.2   MEMBRANE MATERIALS AND STRUCTURES

Membranes are manufactured with a wide variety of materials which include sintered metals, ceramics, and polymers. The manufacturing processes result is a number of different membrane structures such as, microporous, asymmetric, composite, etc. Figure 5.3 illustrates some of these structures through photomicrographs.

Metal, metal oxide, ceramic, and polymer particles are sintered to produce **microporous** membranes typically with pore diameter of 0.1 μm or larger. These membranes are usually symmetric but asymmetric membranes are also made by layers of porous material of decreasing size applied in stages. Ceramic materials have been successful in extending the pore-size
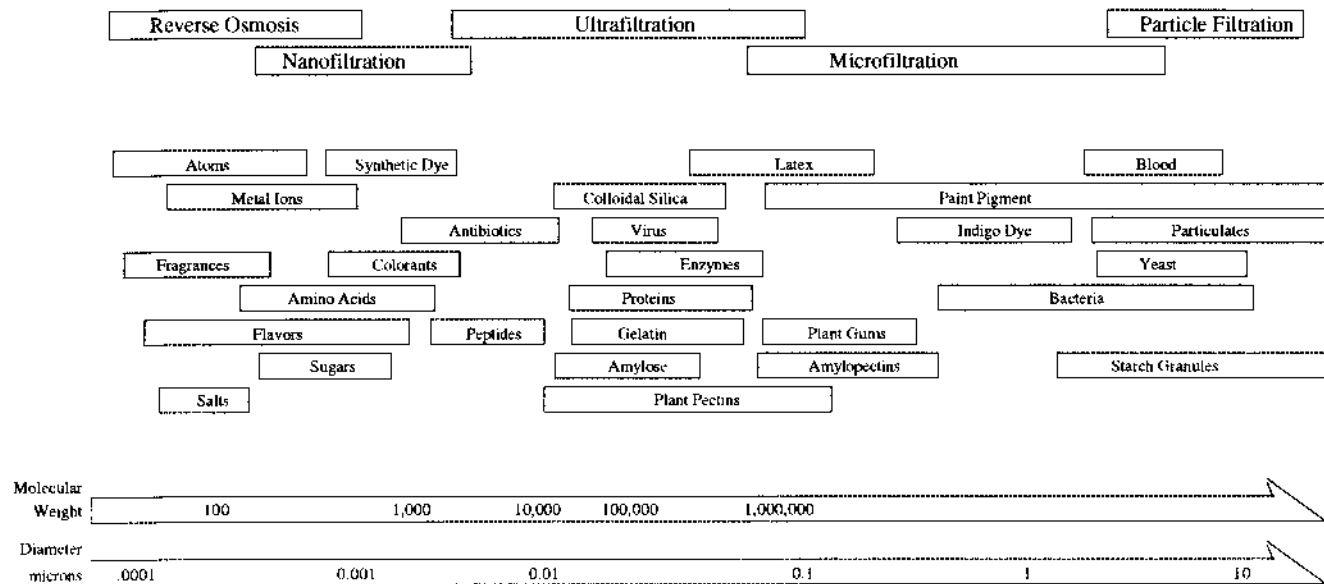
FIGURE 5.2 Membrane filtration spectrum.
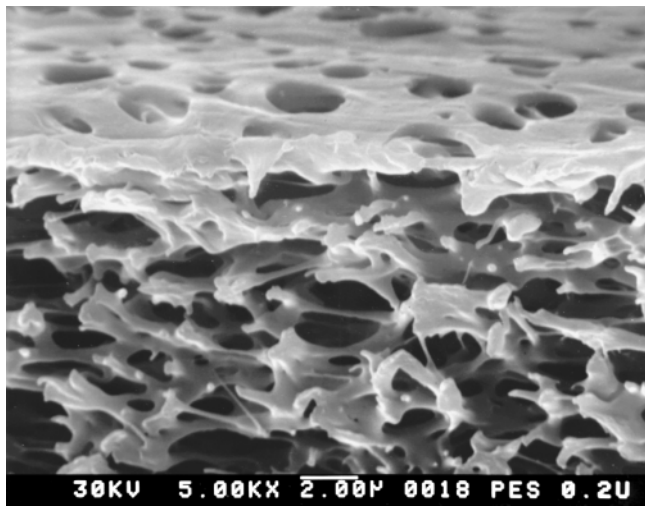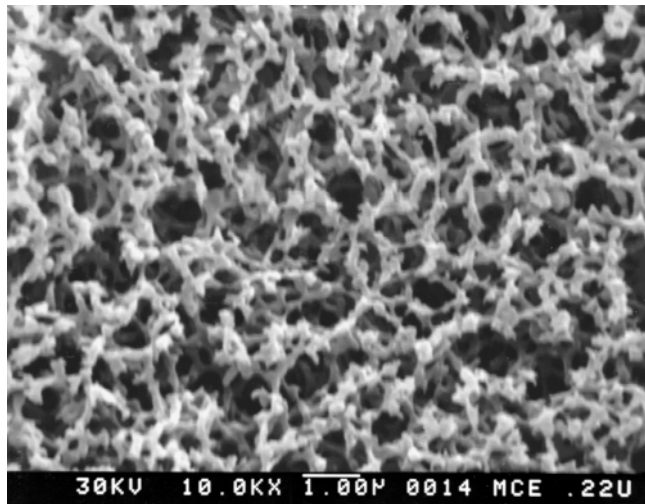
FIGURE 5.3 Membrane structure. (a) Symmetric microporous membrane (cross-section); mixed cellulose ester with a 2 μm nominal pore size. (b) Asymmetric microporous membrane (surface view and cross-section); polyethersulfone with a 0.2 μm nominal pore size. Samples courtesy of Poretics.

range down to 20 nm. Sol-gel process has been successful in production of nanofiltration membranes using ceramic materials.

Track-etch membranes are made by exposing a polymeric film to a radiation source to breakdown the polymer chains and then etching in a chemical bath which selectively dissolves the damaged regions. This process produces membranes with cylindrical pores having a narrow pore-size distribution. Track-etched membranes fall in the microfiltration range. Polycarbonate and polyester are common materials used for track-etch membranes.

Symmetrical phase inversion polymeric membranes constitute the bulk of the microfiltration membranes in the market. A solution of the polymer in a solvent is prepared, spread as a thin film and precipitated by the addition of a nonsolvent or lowering temperature. Finally, the solvent is washed out to produce the porous structure.

Asymmetric phase inversion membranes are important across the whole filtration spectrum. The production process involves a quenching step to form a thin skin with small pores that functions as the separating layer. The skin is supported by the rest of the membrane
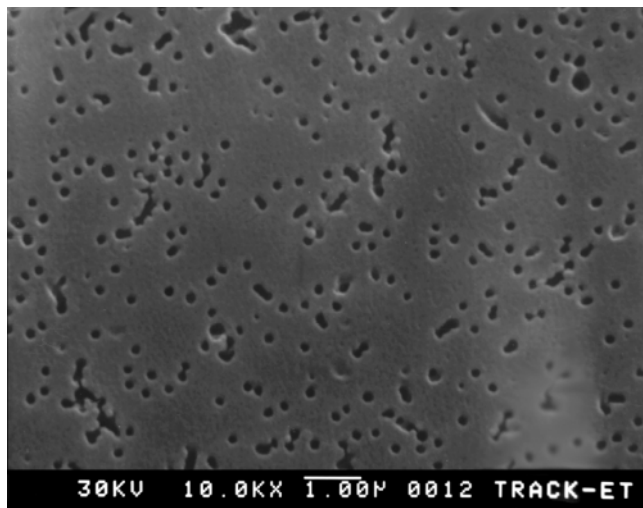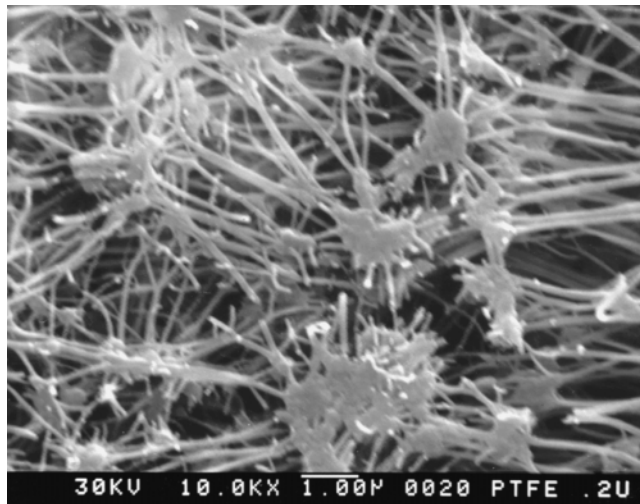
FIGURE 5.3 cont. (c) Stretched microporous membrane (surface view); PTFE with a 0.2 μm nominal pore size. (d) Track-etch microfiltration membrane (surface view); polycarbonate with a 0.1 μm nominal pore size. Samples courtesy of Poretics.

which is thicker and has larger pores to reduce resistance to liquid flow. Asymmetric cellulose acetate membranes are typically 100 μm thick and the skin layer is about 0.3 μm. Asymmetric aromatic polyamide membranes are spun into fine fibers with a 42-μm internal diameter and 85-μm external diameter.

An extremely fine layer of a hydrophilic polymer is formed on a microporous backing material to produce thin film **composite** reverse osmosis membranes. **Interfacial polymerization** at the surface of the porous support film is the technique used to form these membranes and polysulfone is usually the support material. Thickness of the skin layer in thin film composites ranging from 0.03 to 0.2 μm have been reported.

Membrane materials and their surface characteristics play an important role in the performance of the membrane. Hydrophlic materials like cellulose acetate are less prone to surface fouling by oily compounds than hydrophobic materials like polysulfone. Polyacrylonitrile is a highly hydrophilic material used in ultrafiltration and microfiltration membranes.
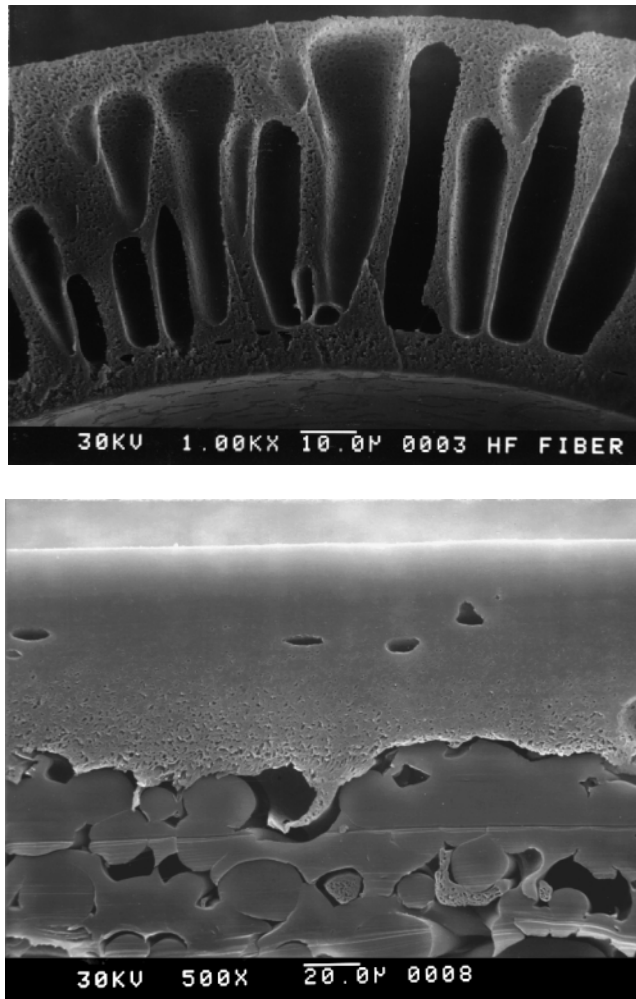
FIGURE 5.3 cont. (e) Hollow fiber membrane (cross-section); polysulfone with 500,000 nominal molecular weight cutoff (courtesy of Romicon). (f) Composite membrane (cross-section); polyvinyl-alcohol nanofiltration (courtesy of Hydranautics).

Membranes with a surface charge are extremely effective in separating colloidal solutions which contain oppositely charged particles. Special purpose membranes are made by application of specific functional groups by techniques, i.e., chemical grafting, plasma polymerization, and sputtering. Self-cleaning membranes have been produced by attaching enzymes to the membrane surface (Drioli et al., 1990).

5.1.3 MEMBRANE MODULES

Membranes are assembled as modules that are easily integrated into systems containing hydraulic components. Primary objectives of module design are to accommodate large membrane areas in a small volume, to withstand the pressures required in filtration, and cross-flow velocities required to maintain a clean membrane surface. Flat plate, tubular, hollow fiber, hollow fine fiber, and spiral are common module configurations. Figure 5.4 illustrates these module designs.

In **flat plate** modules two flat sheets of membranes are separated by a support plate which also contains the permeate channels. These membrane sandwiches are separated by a spacer
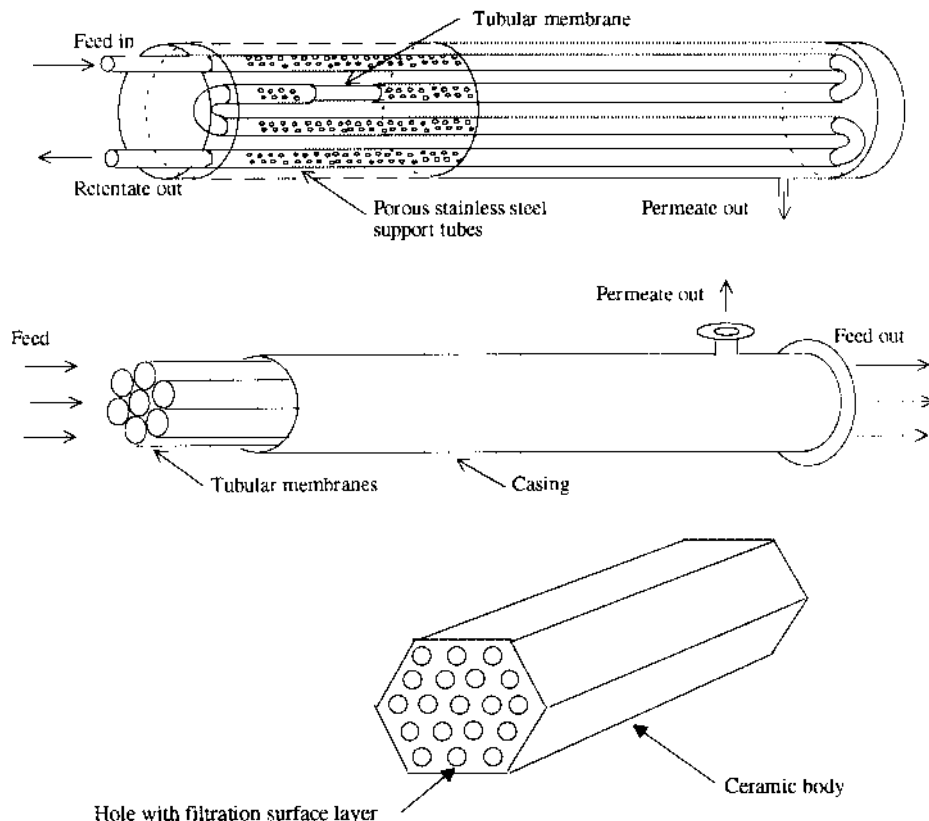
FIGURE 5.4 Membrane modules: (a) tubular (externally supported) membrane module; (b) tubular (self supported) membrane module; (c) tubular (monolithic) membrane module.

plate which also has the feed-flow channels. Alternate layers of membrane sandwiches and spacer plates are assembled and held together by bolts. This module can withstand high pressures but is susceptible to fouling by suspended particles.

Tubular modules consist of membranes formed inside tubes, typically 6 to 25 mm in diameter, and are of three basic types. **Self supporting tubular** modules consists of several membrane tubes held together as a pack and connected to common headers and permeate vessels. Typical modules have 1, 7, or 19 tubes. This type is limited by its structural strength to low-pressure applications. **Externally supported tubular** membrane modules consist of tubular membranes held inside individual porous support tubes. Several such tubes are assembled to common headers and permeate vessels to form a module. This type can withstand high pressures and is therefore used in reverse-osmosis applications. In **monolithic tubular** modules several tubular channels are formed in a porous block of material and the membrane layer is formed inside the tubes. All types of tubular modules can accommodate suspended particles.

Hollow fiber modules consist of bundles of hollow fibers typically 0.5 to 3 mm in diameter sealed into plastic headers and assembled in permeate casings. The feed passes through the central bore and permeate collects in the outer casing. Hollow fibers are self supporting hence these modules are for use in low-pressure applications only. These can accommodate moderate levels of suspended particles.

Hollow fine fiber modules contain strands of fine fiber about 50 to 100 μm in diameter. A bundle of fibers is formed into U shape and the ends are formed into a single header and the U bundle is placed in a tube. The feed liquid is outside the fibers while the permeate
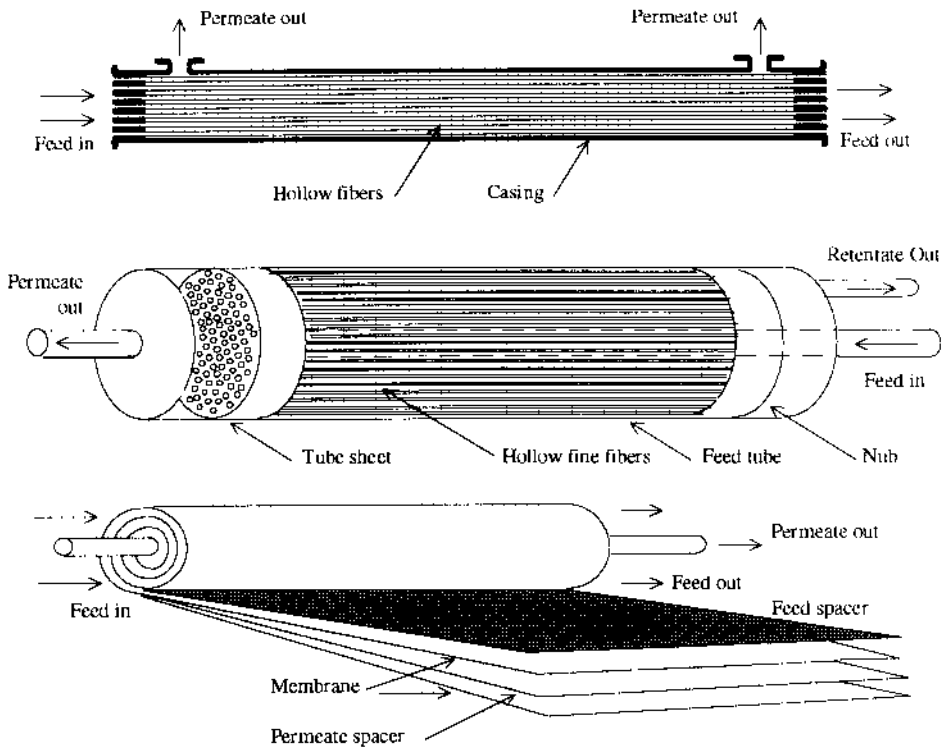
FIGURE 5.4 cont. (d) Hollow fiber membrane module; (e) hollow fine fiber membrane module; (f) spiral membrane module.

flows into the fibers. This arrangement can withstand high pressures but it is extremely susceptible to fouling by suspended particles.

Spiral modules are made by placing a plastic mesh which acts as the permeate channel between two membrane layers and sealing three sides. Fourth side of this sandwich is attached to the permeate tube, another plastic mesh which acts as the feed channel is laid over it and the assembly is wrapped around the central permeate tube. This module also can withstand high pressures but is susceptible to fouling by suspended particles.

The range of materials and modules present a large number of combinations for membrane processes. Table 5.1 is a summary of these combinations for widely used membrane materials and modules. The first challenge in membrane process design is the selection of the proper combination.

In addition to five common membrane modules described earlier, there are several less common and special-purpose membrane modules. The tubular configuration with membrane layer on the outside of the tube has the advantage of better structural strength, ease of observation, and physical cleaning of the fouling layers. Transverse flow module consists of hollow fibers with the filtering layer outside of the fiber and retentate flow perpendicular to the fibers. The fibers themselves act as turbulence promoters. Compressed gases are also used as a back flush in these modules. A rotary module consisting of concentric cylinders and circular discs is introduced to process high fouling liquids. Flat plate module mounted on a torsionally vibrating pad is also used in similar applications.

5.2   PRINCIPLES OF MEMBRANE FILTRATION

Cross-flow filtration is a pressure driven process. A mixture of liquid and solids is brought into contact with a membrane to force the liquid to flow through the membrane. The retained

TABLE 5.1
Membrane Materials, Structures, Modules, and Filtration Ranges

Membrane Material	Structure							Module						Range			
	Symmetric microporous	Asymmetric microporous	Stretched microporous	Track etch	Symmetric phase inversion	Asymmetric phase inversion	Composite	Flat plate	Tubular	Monolithic	Hollow fiber	Hollow fine fiber	Spiral	Microfiltration	Ultrafiltration	Nanofiltration	Reverse osmosis
Polymers																	
Cellulose acetate CA					x	x		x	x			x	x			x	x
Polyamide PA							x	x	x			x	x			x	x
Sulfonated polysulfone							x	x	x				x		x	x	x
Polysulfone					x	x		x	x					x	x	x	
Polyethersulfone					x	x		x						x	x	x	
Polyvinilidenefluoride					x	x		x	x		x			x	x	x	
Polytetrafluoroethylene			x					x	x					x	x		
Polypropylene					x			x			x			x			
Polyacrylonitrile					x	x		x			x			x	x	x	
Polycarbonate				x										x			
Polyester			x	x										x			
Ceramics/Metallic																	
Alumina	x									x				x			
Zirconia/alumina	x	x								x				x	x		
Zirconia/metal		x									x			x			
Zirconia/carbon		x									x			x			
Silica	x									x							
Silicon carbide	x										x			x			
Titanium oxide/metal		x									x			x			
Sintered steel	x							x	x					x			
Sintered alloys	x							x	x					x			

solids are swept along the surface of the membrane by the flow of the liquid-solid mixture. A small amount of solids also flow through the membrane.

Flow of the **liquid through the membrane** is driven by hydraulic pressure gradient. In case of reverse osmosis and nanofiltration osmotic pressure of the solution opposes the hydraulic pressure. In ultrafiltration and microfiltration the osmotic pressure is negligible due to high molecular weight of the solutes.

In reverse osmosis and nanofiltration, flow of the **solute through the membrane** is by diffusion driven by concentration gradient. There are some models that allow for solute transport through oversize pores in the membrane. In ultrafiltration and microfiltration the solutes flow through oversized membrane pores. Because the solutes are macromolecules and particulates, this flow is usually considered negligible.

The solute that is rejected at the membrane accumulates in a thin boundary layer near the membrane surface and establishes a concentration gradient in the direction opposite to the permeation. The **solute diffuses across the boundary layer** to the bulk phase driven by the concentration gradient. This phenomenon termed **concentration polarization** plays a

major role in all branches of cross-flow filtration but the mechanism of diffusion varies with the solute.

Accumulation of rejected solute in the boundary layer creates a resistance to flow of liquid. This resistance is small in reverse osmosis and nanofiltration. In ultrafiltration and microfiltration, the hydraulic resistance of the boundary layer is appreciable and often exceeds the resistance of the membrane. In addition, macromolecules and particulates reach saturation at the membrane surface and form gel layers which offer additional resistance.

The performance of a membrane filtration system is measured in terms of its ability to produce large volumes of filtrate in a short period of time and the degree of purity of the filtrate with respect to the solute concentration. **Permeate flux** and **solute rejection** are the two parameters used for this purpose universally. Permeate flux "J" is defined as the volume of permeate that flows through a unit area of membrane in a unit time period. Two common unit combinations used to report permeate flux are liters per square meter per hour (lmh) and gallons per square foot per day (gfd).

$$\text{Permeate Flux 'J'} = \frac{\text{Permeate Volume}}{\text{Membrane Area} \times \text{Time}} \qquad (5.1)$$

Solute rejection is defined as the solute retained by the membrane as a fraction of the solute in the original feed stream and usually expressed as a percentage.

$$\text{Solute rejection} = \left[1 - \frac{\text{Solute concentration in the permeate}}{\text{Solute concentration in the feed}} \right] \times 100\% \qquad (5.2)$$

A mathematical model of the cross-flow filtration involves two transport equations for the liquid and solute transport through the membrane, two transport equations for the liquid and solute transport through the boundary layer, and a continuity equation. A generalized mathematical model can describe the broad range of cross flow filtration processes. However, the transport phenomena in the reverse osmosis end of the filtration spectrum are fundamentally different from those in the microfiltration end of the spectrum. Therefore, characterization of membrane filtration is done using two models for the two ends of the spectrum.

5.2.1 Reverse Osmosis and Nanofiltration Processes

When a solution is separated into pure solvent by a semipermeable membrane that is permeable to the solvent but not to the solute, the solvent passes through the membrane to the solution. This phenomenon is called osmosis and the driving force that causes the solvent transfer is called osmotic pressure. Separating pure solvent from the solution by reverse osmosis involves driving the solvent through a semipermeable membrane by exerting pressure. This process is opposed by the osmotic pressure of the solution. Therefore, pressures in excess of osmotic pressure is required in reverse osmosis.

Osmotic pressure is a colligative thermodynamic property of solutions that depends on the number of solute particles in the solution. Same weight of a solute with a low molecular weight like sodium chloride has a higher osmotic pressure than a solute with a higher molecular weight like protein. Therefore, reverse osmosis involves higher pressures than ultrafiltration.

5.2.1.1 Transport Model

Reverse osmosis and nanofiltration involve solutions of small molecules like salts and sugars where the osmotic pressure becomes significant compared to the hydraulic pressure required
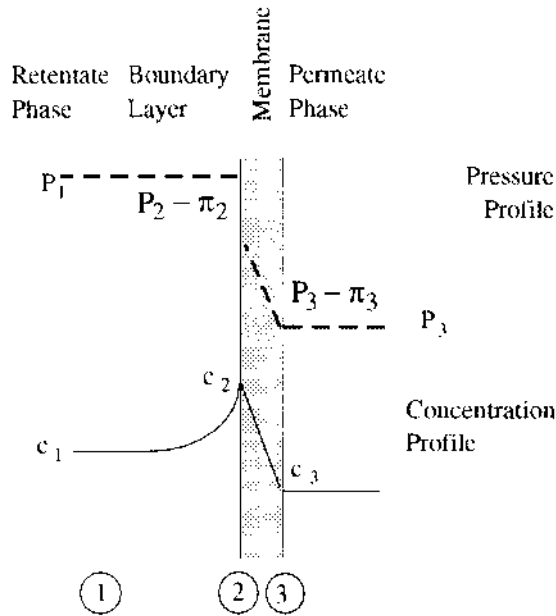
FIGURE 5.5 Transport model of reverse osmosis process.

to induce flow of the liquid. The hydraulic resistance of the boundary layer for convective flow of the liquid becomes negligible hence the transport equation for flow of liquid through the boundary layer is not invoked. Figure 5.5 illustrates the flows and profiles in reverse osmosis process.

Flow of the liquid through the membrane is caused by the hydraulic pressure difference in excess of the osmotic-pressure difference across the membrane. The flow has to overcome the hydraulic resistance of the membrane. Equation 5.3 describes this process.

$$J = \frac{1}{r_m}\left\{\left(P_1 - P_3\right) - \left(\Pi_2 - \Pi_3\right)\right\}$$ (5.3)

Flow of solute through the membrane is caused by the concentration difference across the membrane and it has to overcome the diffusive resistance of the membrane. It is customary to express this resistance as a conductance as in Equation 5.4.

$$S = k_m\left(c_2 - c_3\right)$$ (5.4)

The solute is transported across the boundary layer towards the membrane by the liquid flow while rejected solute is transported away from the membrane by ordinary diffusion. This diffusive flow is represented by Equation 5.5.

$$S = -D\frac{dc}{dy}$$ (5.5)

The solute flow due to liquid flow in the opposite direction is equated to the diffusive flow of the solute as in Equation 5.6.

$$D\frac{dc}{dy} = J(c - c_3) \tag{5.6}$$

Equation 5.6 is integrated over the thickness of the boundary layer δ to obtain Equation 5.7.

$$J = \frac{D}{\delta} \ln \frac{c_2 - c_3}{c_1 c_3} \tag{5.7}$$

Since the boundary layer thickness δ is not easily defined or determined, the practice is to replace D/δ by h_b which is the mass transfer coefficient of the concentration boundary layer (Equation 5.8).

$$J = h_b \ln \frac{c_2 - c_3}{c_1 - c_3} \tag{5.8}$$

The continuity condition provides an additional relationship between liquid and solute fluxes as expressed in Equation 5.9.

$$S = J c_3 \tag{5.9}$$

Equations 5.3, 5.4, 5.8 and 5.9 represent liquid and solute transport through the membrane and the boundary layer in reverse-osmosis process. This simple model consists of four equations with 12 entities that comprise three solute concentrations, two hydraulic pressures, two osmotic pressures, three transport properties, and two fluxes.

The model can be used to determine four of the 12 entities if the other 8 are known. Ideally, two fluxes, J, and S, and two concentrations, c_2 and c_3, are determined while all other parameters are known. However, the nature of the model and interdependency of the parameters makes this task difficult. The equations cannot be solved explicitly for the fluxes and concentrations in terms of other parameters. The nonlinear relationship between Π_2 and c_2, and the logarithmic nature of flux-concentration relation (Equation 5.7) are the reasons for this difficulty.

5.2.1.2 Estimation of Model Parameters

A substantial body of literature is available on the determination of parameters contained in the transport model. These involve the dependence of transport properties on operating variables such as pressure, concentration, temperature, and cross-flow velocity. Basic relations describing these dependencies form an important part of the model.

Osmotic Pressure is a thermodynamic property of solutions that manifests itself in the presence of a semipermeable membrane. In dilute solutions osmotic pressure can be determined by van't Hoff model (Equation 5.10) while Gibb's Model (Equation 5.11) can be used at higher concentrations. Table 5.2 shows a comparison of predictions by the two models with experimental data.

- van't Hoff model

$$\Pi = cRT \tag{5.10}$$

- Gibb's Model

$$\Pi = -\frac{RT}{V} \ln x \tag{5.11}$$

TABLE 5.2
Osmotic Pressure of Aqueous Sucrose
Solutions at 25°C

Sugar content (% by weight)	Osmotic pressure (atm)		
	Experimental	Van't Hoff	Gibbs
3.31	2.65	2.39	2.46
6.41	5.19	4.68	4.99
9.31	7.79	6.88	7.53
12.04	10.38	8.99	10.13
14.61	13.05	11.03	12.75
17.03	15.76	12.98	15.43
19.32	18.59	14.86	18.18
21.49	21.44	16.68	20.94
23.55	24.34	18.42	23.77
25.50	27.29	20.11	26.68
40.63	58.6[a]	35.92	58.25
50.66	95.8[a]	46.87	94.66
57.78	141.2[a]	55.30	134.74
63.11	193.0[a]	61.98	177.55

[a] At 30°C.

Osmotic pressure variation with concentration of solute is approximately linear in the low-concentration range which is of interest in most practical applications. This can be used to rewrite Equation 5.3 as equate 5.12.

$$J = \frac{1}{r_m}\left\{(P_1 - P_3) - a(c_2 - c_3)\right\} \tag{5.12}$$

Boundary Layer Mass Transfer Coefficient, h_b is a hydrodynamic property and can be predicted with reasonable accuracy for simple geometries using nondimensional mass-transfer correlations found in literature (Kulkani et al., 1992) relating Sherwood number ($Sh = kd_h/D$) with Reynolds number ($Re = Ud_h/\nu$) and Schmidt number ($Sc = \nu/D$).

• Developing laminar flow

$$Sh = 0.664\, Re^{0.5}\, Sc^{0.33}\left[\frac{d_h}{L}\right]^{0.5} \tag{5.13}$$

• Fully developed laminar flow

$$Sh = 1.62\, Re^{0.33}\, Sc^{0.33}\left[\frac{d_h}{L}\right]^{0.33} \tag{5.14}$$

• Turbulent flow

$$Sh = 0.023\, Re^{0.8}\, Sc^{0.33} \tag{5.15}$$

These correlations require: the solution properties, diffusivity (D) and viscosity (ν); system parameters, hydraulic diameter (d_h) and channel length (L); and the cross-flow velocity of the liquid U. Diffusivity and viscosity data are available for a limited number of solutes. Sourirajan (1970) contains these properties for aqueous solutions of several inorganic salts and sucrose over a wide range of concentrations.

Membrane transport properties.   The resistance of the membrane for liquid transport (r_m) and the conductivity of the membrane for solute transport (k_m) are determined through experimentation. Literature contains values for experimental membranes but rarely for commercially available membranes. The industry practice is to provide permeate flux and solute rejection at specified values of pressure, temperature, and concentration. Sodium chloride is the standard solute for reverse osmosis membranes while magnesium sulfate, glucose, and sucrose are used as standard solutes for nanofiltration membranes.

5.2.1.3   Performance Characteristics

Mathematical models of reverse osmosis process are rarely used to predict permeate and solute fluxes due to unavailability of parameters required by the models. However, the models provide valuable insight of the process through the prediction of parametric dependence of membrane performance. The performance of a reverse osmosis system is quantified by permeate flux and solute rejection. These two parameters are influenced primarily by concentration, pressure, velocity, and temperature of the feed.

Existence of the concentration boundary layer creates an ambiguity in the definition of solute rejection. The apparent rejection is defined in relation to the bulk concentration (Equation 5.16) while the intrinsic rejection is defined in relation to concentration at the membrane surface (Equation 5.17). In this chapter, rejection is used to denote apparent solute rejection.

$$\text{Apparent solute rejection} = 1 - \frac{c_3}{c_1} \qquad (5.16)$$

$$\text{Intrinsic solute rejection} = 1 - \frac{c_3}{c_2} \qquad (5.17)$$

Permeate flux increases with feed pressure but the osmotic pressure at the membrane surface also increases. This opposes the flux increase and tends to moderate it. The solute flux is not affected directly by the feed pressure since it is not driven by pressure. Therefore, solute rejection increases with the increase in pressure. However, increase in concentration at the membrane surface indirectly increases the solute flux thus moderating the increase in rejection.

Temperature increases both permeate flux and solute flux. Increase in permeate flux is attributed to decrease in viscosity which is related to the inverse of absolute temperature. The increase in solute flux is attributed to increase in diffusivity and solubility of the solute in the membrane. In general, solute flux increases more rapidly with temperature than the permeate flux resulting in a decrease in solute rejection with increase in temperature.

Concentration of solute in the feed decreases the permeate flux due to increase in osmotic pressure. Solute flux increases with concentration. Decrease in permeate flux complements this effect and causes rapid increase in solute concentration in permeate. The net effect is a rapid decrease in solute rejection with an increase in solute concentration in the feed.

Cross-flow velocity of the feed influences the membrane performance through its effect on boundary-layer mass-transfer coefficient h_b. This coefficient increases with cross-flow velocity raised to a fractional power index which depends on the flow regime and other
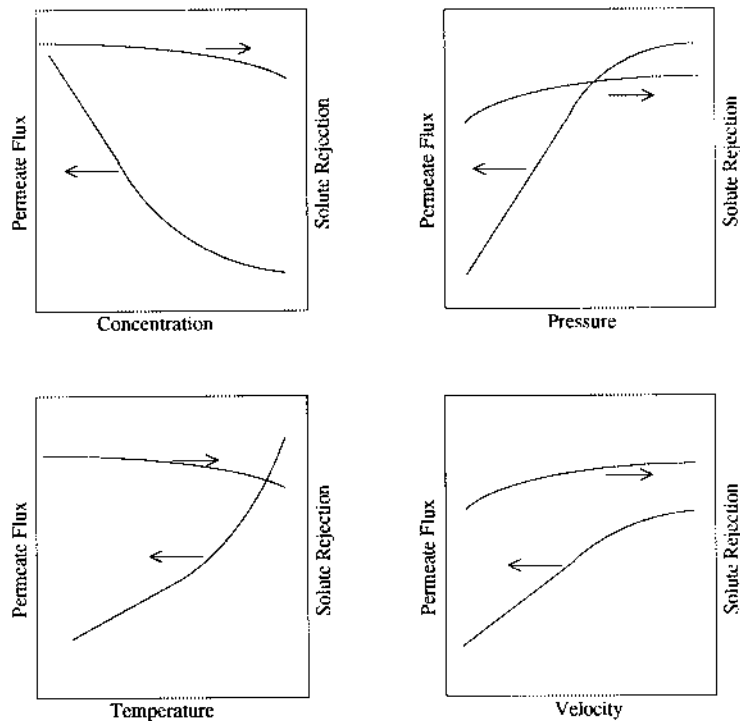
FIGURE 5.6 Performance characteristics of reverse osmosis.

hydrodynamic characteristics. This index is around 0.3 for laminar flow and 0.8 for turbulent flow. Increase in h_b increases the permeate flux and the increase is moderated by osmotic pressure increase. The solute rejection increases with increase in velocity and is moderated similar to its variation with pressure.

The other major feed parameter that affects membrane performance is pH. The effect of pH on permeate flux and solute rejection depends on ionic properties of the solute and the membrane. Therefore, it is not possible to present general performance characteristics for pH dependence. Figure 5.6 illustrates the dependence of permeate flux and solute rejection on the operating variables during reverse osmosis process.

5.2.2 MICROFILTRATION PROCESSES

Microfiltration involves separation of small particles in the micron size range, usually from about 0.1 to 10 μm. Microfiltration is a sieving process where particles are physically retained by the membrane which has pores smaller than the particles. The osmotic pressure becomes insignificant since the particles are relatively large and their number density is small. The leakage of particles through the membrane is insignificant. Rejected particles accumulate at the membrane surface and build up a cake layer. The hydraulic resistance of this layer for convective flow of the liquid becomes significant. Figure 5.7 illustrates the flows and profiles in microfiltration process.

5.2.2.1 Transport Model

The transport model for microfiltration involves equations for the flow of liquid through the membrane (Equation 5.18), the flow of liquid through the cake layer (Equation 5.19), and for the transport of solute through the boundary layer (Equation 5.5). Since solute does not flow through the membrane, an equation for this flow and the continuity equation are not invoked.
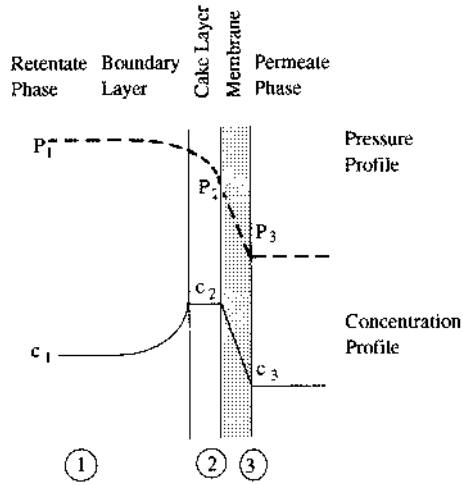
FIGURE 5.7 Transport model of microfiltration process.

$$J = \frac{1}{r_m}\left(P_2 - P_3\right) \tag{5.18}$$

$$J = \frac{1}{r_b}\left(P_1 - P_2\right) \tag{5.19}$$

The diffusive flow of solute across any plane in the boundary layer given by Equation 5.5 is equated to the solute flow due to bulk flow in the opposite direction and integrated over the thickness of the boundary layer δ to arrive at Equation 5.20.

$$J = \frac{D}{\delta}\ln\left(\frac{c_1}{c_2}\right) \tag{5.20}$$

Since the boundary layer thickness δ is not easily defined or determined, the practice is to replace D/δ by h_b which is the mass transfer coefficient (Equation 5.21)

$$J = h_b\ln\left(\frac{c_2}{c_1}\right) \tag{5.21}$$

The concentration of rejected particles at the membrane surface reaches saturation level very early in conditions encountered in microfiltration. When this condition is met, c_2 is replaced by a constant c_c which is the cake layer concentration resulting in Equation 5.22.

$$J = h_b\ln\left(\frac{c_c}{c_1}\right) \tag{5.22}$$

It is also customary to add Equations 5.18 and 5.19 to eliminate P_2 resulting in Equation 5.23.

$$J = \frac{1}{r_b + r_m}\left(P_1 - P_3\right) \tag{5.23}$$

Equations 5.23 with Equation 5.21 or 5.22 constitute the transport model of microfiltration process. Equation 5.21 is valid before cake-layer formation while Equation 5.22 is valid after cake-layer formation. This model contains only one property of the membrane but three properties of the boundary/cake layer. The only membrane property r_m also becomes insignificant compared to r_b in practical situations. Therefore, microfiltration process is controlled almost entirely by the boundary/cake layer.

5.2.2.2 Estimation of Model Parameters

The transport model contains four parameters, r_m, r_b, h_b and c_c, that need to be determined in order to predict permeate flux using the model. A substantial amount of work has been done towards achieving this objective.

Membrane resistance, r_m, can be determined easily by conducting an experiment using pure water and calculating the slope of the flux pressure relation. It can also be predicted if the pore size distribution is known using Hagen-Poiseuille equation for capillary flow (Equation 5.24).

$$r_m = \frac{128\,\mu b}{\pi \sum \left[n_p\, d_p^4 \right]} \tag{5.24}$$

Hydraulic resistance of the cake, r_b, can be determined when the cake is incompressible by the Carmen-Cozeny relation given by Equation 5.25. The void fraction ε of a randomly packed cake is about 0.4 while the specific surface area S_c is $3/r_s$ for rigid spheres. The coefficient K has a value of about 5.

$$r_c = \frac{K(1-\varepsilon)^3\, S_c^2\, \delta_c}{\varepsilon^3} \tag{5.25}$$

Mass transfer coefficient of the boundary layer, h_b, can be estimated using Leveque solution for analogous heat transfer problem in laminar flow in tubes. (Zydney and Colton, 1986). The expression for h_b averaged over tube length L in developing laminar flow is given by Equation 5.26.

$$h_b = 0.807 \left(\frac{\gamma_w D^2}{L} \right)^{1/3} \tag{5.26}$$

Diffusivity of the solute D that should be used in Equation 5.26 has been a subject of controversy. Brownian diffusivity expressed by Stokes-Einstein equation has consistently underpredicted the mass transfer coefficient hence the permeate flux (Porter, 1972; Zydney and Colton, 1986). Shear augmented diffusivity (Equation 5.27) has been reported to produce much closer agreement with experimental data (Zydney and Colton, 1986).

$$D = 0.0075\, d_p^2\, \gamma_w \tag{5.27}$$

The mass transfer coefficient using shear augmented diffusivity is expressed by Equation 5.28. This equation predicts a strong linear relation compared to the ⅓ power relation resulting from Brownian diffusivity, hence, it results in better correlation with experimental data.

TABLE 5.3
Parameters of Selected
Particulate Suspensions

Suspension	c_c (% v/v)	r_s (micron)
Bovine blood	95	3.0
Whole blood	95	4.2
Platelets	90	1.5
Bacteria	69	1.0/0.6
Electroprimer	70	1.0
Clay	70	5.0/0.6
Latex spheres	75	0.25

Data from Zydney, A.L. and Colton, C.K., *Chem. Eng. Commun.,* 47, 21, 1986.

$$h_b = 0.078 \left(\frac{d_p^4 \, \gamma_w^3}{16 \, L} \right)^{1/3} \qquad (5.28)$$

Cake layer concentration, c_c, has a theoretical maximum value of 0.74 for hexagonally packed rigid spheres. However, values as high as 0.9 have been observed for flexible particles such as red blood cells. Mixtures of nonuniform size particles also can produce higher values. Macromolecular solutions such as proteins and starches have lower values in the range of 0.2 to 0.4. Table 5.3 lists cake layer concentrations of some particles frequently met with in microfiltration practice.

5.2.2.3 Performance Characteristics

The mathematical model of microfiltration cannot be used easily for prediction of permeation flux due to difficulty in estimating model parameters accurately. However, the model can be used to analyze the performance characteristics which are extremely useful in understanding the microfiltration process.

Permeate flux in microfiltration increases with pressure but boundary layer resistance, r_b, also increases resulting in a nonlinear trend. The concentration of rejected solutes at membrane surface, c_2, also increases with flux until formation of cake layer begins. Any further increase in pressure simply increases the thickness of the saturated cake layer and its hydraulic resistance, r_b, balancing each other and resulting in the same flux.

Permeate flux decreases with increase in feed concentration, c_1. The solute concentration at membrane surface, c_2, also increases simultaneously until cake layer formation begins. At this point, c_2 becomes constant at c_c and the flux reduction becomes a logarithmic function of the single variable c_1. Figure 5.8 illustrates the pressure and concentration dependence of permeate flux in the microfiltration process.

5.2.3 Ultrafiltration Process

Ultrafiltration involves separation of macromolecules and colloidal suspensions. It spans the molecular weights from 1,000 to about 500,000 and pore sizes from several nanometers to
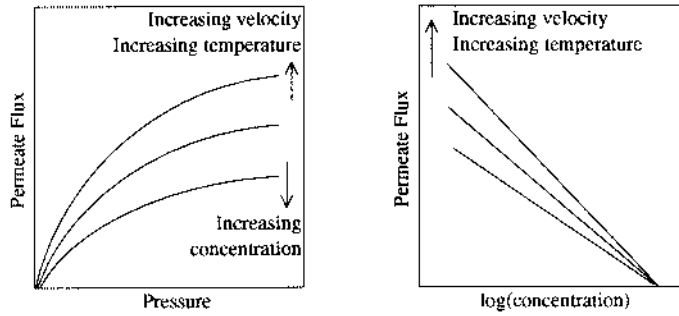
FIGURE 5.8 Performance characteristics of microfiltration.

0.1 μm. The basic separating mechanism is sieving action that holds molecules and particles bigger than the pore size of the membrane similar to microfiltration. However, the membranes used in ultrafiltration evolved from reverse osmosis membranes and not from microfiltration membranes. This is because the resistance of pores which varies inversely with the fourth power of the pore diameter demands ultrafiltration membranes to be several folds thinner than microfiltration membranes to achieve similar permeate fluxes.

5.2.3.1 Transport Model

The transport model for ultrafiltration consists of Equations 5.21, 5.22 and 5.23 derived for microfiltration process. The pressure and concentration profiles and the mathematical model of ultrafiltration are similar to those of microfiltration. However, the osmotic pressure becomes somewhat more significant since the particles are relatively smaller and their number density is higher. Therefore, the pressure dependence of the permeate flux in ultrafiltration is represented by two alternative models known as the resistance model and the osmotic pressure model.

The resistance model (Cheryan, 1986a) hypothesizes that the increase in pressure increases the flux which compacts the boundary layer. The increases in hydraulic resistance of the boundary layer caused by compaction opposes further increase in flux. Mathematical expression of this model assumes that the hydraulic resistance of the boundary layer increases proportionately with pressure difference as given by Equation 5.29.

$$r_b = \phi\left(P_1 - P_3\right) \tag{5.29}$$

Equation 5.29 is substituted in Equation 5.23 and rearranged to obtain a relationship for the pressure dependence of flux.

$$J = \frac{\left(P_1 - P_3\right)}{r_m + \phi\left(P_1 - P_3\right)} \tag{5.30}$$

The osmotic pressure model neglects the hydraulic resistance of the boundary layer completely. It hypothesizes that the increase in pressure increases the concentration of solute at the membrane surface hence the osmotic pressure. This opposes the increase in flux. Equation 5.3 in the reverse osmosis model is modified by neglecting the osmotic pressure of the permeate ($\Pi_3 = 0$). Osmotic pressure at the membrane surface Π_2 is assumed to be a function of concentration c_2, and Equation 5.21 is used to substitute for c_2.

$$J = \frac{(P_1 - P_3) - f\{c_1 \exp[J/h_b]\}}{r_m} \tag{5.31}$$

Both the resistance model (Equation 5.30) and the osmotic pressure model (Equation 5.31) correctly emulate the experimentally observed flux pressure behavior. The actual reason may be a combination of both hydraulic resistance and osmotic pressure buildup due to concentration polarization.

5.2.3.2 Estimation of Parameters

The transport model of ultrafiltration also contains four parameters, r_m, r_b, h_b, and c_c that need to be determined in order to predict permeate flux using the model. Estimation of these parameters has been the subject of several studies.

Membrane resistance, r_m, can be determined by an experiment using water or be predicted if the pore size distribution is known using Equation 5.24 like in microfiltration.

Hydraulic resistance of the cake, r_b, for macromolecular compounds is best found by experimentation. Equation 5.30 can be rearranged to produce a linear relation between $1/J$ and $1/(P_1 - P_2)$ which can be used to determine ϕ which relates r_b to the pressure difference.

Mass transfer coefficient of the boundary layer, h_b, can be estimated using Equations 5.13, 5.14 or 5.15 depending on the flow regime. In the turbulent flow regime the predictions by Equation 5.13 agree well with experimental data. In the laminar flow regime Equations 5.14 and 5.15 underpredict experimental data by 15 to 30% for macromolecular solutions. In case of colloidal suspensions in laminar flow the agreement is extremely poor. The predicted fluxes are lower than the experimental fluxes by a factor of 15 or more (Porter, 1972).

Viscosity and diffusivity of solutions are required for the use of Equations 5.13, 5.14 and 5.15. Viscosity of a solution can be determined easily in a laboratory. However, diffusivity of solutes is not easily determined in laboratories. Brownian diffusivity expressed by Stokes-Einstein relation (Equation 5.32) has produced acceptable results for macromolecular solutions.

$$D = \frac{kT}{3\pi\mu d_p} \tag{5.32}$$

Brownian diffusivity (Equation 5.32) decreases with increasing particle size. This translates to a decrease in flux with increasing particle size which agrees with experimental observations for macromolecular solutions. In case of colloidal suspensions the flux is observed to increase with particle size (Porter, 1972). This dictates that a mechanism other than Brownian diffusivity is responsible for counter transport of solute in colloidal suspensions.

Tubular finch effect which moves particles laterally across the streamlines away from the wall of a tube towards its center has been proposed as the mechanism of counter transport in the boundary layer in colloidal suspensions. This mechanism predicts fluxes increasing with particle size as experimentally observed. Shear augmented diffusivity proposed by Zydney and Colton (1986) for microfiltration of particulates also predicts fluxes increasing with particle size. However, extension of this model to ultrafiltration has not been reported.

Cake layer concentration, c_c, for macromolecular solutions such as proteins and starches have values in the range of 0.2 to 0.4 while colloidal suspensions have higher values. Table 5.4 lists cake layer concentrations of some food systems frequently met with in ultrafiltration practice.

TABLE 5.4
Transport Parameters of Selected Food Systems

	c_c (% protein)	Molecular weight	Diffusivity (10^{-12} m²/s)/ temperature (°C)
Skim milk	20–25		
Whole milk	9–11		
Soybean extract	10		
Whey	20–30		
Gelatin	20–30		
Egg white	40		
α-Lactalbumin		16,000	74.0/20
β-Lactoglobulin		18,000	64.0/25
Casein		24,000	14.0/25
Collagen		345,000	11.6/20
Soy protein 7 S		180,000	38.5/20
Soy protein 11 S		350,000	29.1–33.0/20

Data from Cheryan, M., *Ultrafiltration Handbook,* Technomic Publishing, Lancaster, PA, 1986.

5.3   DESIGN OF MEMBRANE SYSTEMS

Cross-flow filtration uses pressure to drive the liquid through the membrane and velocity to keep the retained solutes from building up at the membrane surface. The membrane manufacture deals with the development of high flux and high rejection membranes while the module and system design deals with pressures and velocities. Maintaining high cross-flow velocity to reduce the thickness hence the resistance of the boundary layer to achieve economical permeate fluxes gets a high priority in membrane system design.

Batch, feed and bleed, and single pass are the three common design configurations. Several variations of these configurations and some specialized designs such as diafiltration and cocurrent permeate flow design constitute the range of membrane system configurations found in food industry applications. Concentration ratio and recovery are two terms that are used frequently in discussions of membrane systems.

Concentration, fractionation, clarification, and filtration are some common terms used for membrane applications. These names identify the intended use of the final product which is either permeate, retentate, or both. However, from a mathematical point of view all of these can be treated as concentration of solute in a feed volume through the removal of solvent as permeate. **Concentration ratio** and **volume ratio** are two terms used to measure degree of concentration.

When a volume of a solution V is reduced by dV to increase its concentration from C by dC, using a membrane having a rejection σ, the following relationship holds for the new concentration.

$$C - dC = \frac{CV - C(1-\sigma)dV}{V - dV} \tag{5.33}$$

This equation reduces to following simpler form upon simplification.

$$\frac{dC}{C} = -\sigma \frac{dV}{V} \tag{5.34}$$

This equation can be integrated when rejection σ is a simple function of concentration. When rejection remains constant irrespective of concentration, Equation 5.35 relating volume ratio to concentration ratio is obtained.

$$\frac{C}{C_0} = \left(\frac{V_0}{V}\right)^{\sigma} \tag{5.35}$$

Equation 5.35 is applicable to batch concentration systems but it can be modified by replacing volumes (V and V_0) by flow rates (Q and Q_0) and used for continuous systems.

Recovery is the volume of permeate recovered from a given volume of feed expressed as a percentage. In the case of continuous membrane processes, recovery is expressed in terms of the permeate flow rate and the feed flow rate.

$$\text{Recovery} = \frac{\text{Permeate Volume (or Flow Rate)}}{\text{Feed Volume (or Flow Rate)}} \times 100\% \tag{5.36}$$

5.3.1 BATCH SYSTEMS

Batch processing systems are the simplest in design and they require the least membrane area to achieve a given concentration in a given time. However, it requires buffer storage capacity to become part of a continuous production plant. Also this configuration has the highest retention time.

Batch system with total recycle (Figure 5.9a) uses only one pump to feed the system and also to maintain the cross-flow velocity. This is the optimal configuration for low pressure operation where operating pressure is in the same range as the pressure drop along the membrane module. This situation occurs in microfiltration systems.

In ultrafiltration applications where the system pressure is significantly higher than the pressure drop along the module it is more economical to use a separate recirculation pump. This is the batch processing system with partial recycle (Figure 5.9b).

The mathematical description of batch process involves two differential mass balances which equate rate of change of liquid volume and solute mass to the rates of their permeation through the membrane area.

$$\frac{dV}{dt} = -J A \tag{5.37}$$

$$\frac{d(VC)}{dt} = -J C_p A \tag{5.38}$$

In these two equations J and C_p are functions of C. The functional dependence is given implicitly by the set of Equations 5.3, 5.4, 5.8 and 5.9 for reverse osmosis. The combined system of equations for batch concentration by reverse osmosis cannot be solved explicitly. Only numerical solutions are possible.

In microfiltration and ultrafiltration where solute leakage is negligible, Equation 5.38 drops out of the system. The functional dependence of J on C is given by Equation 5.22. Relationship between V and C is obtained by setting $\sigma = 1$ in Equation 5.35. These equations
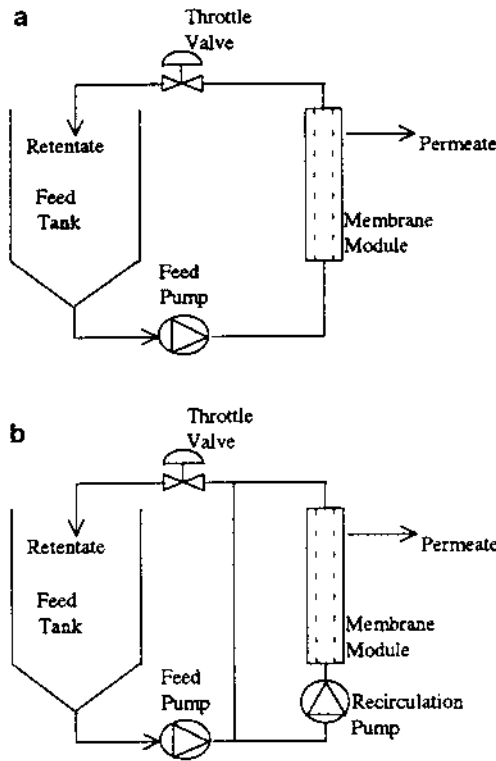
FIGURE 5.9 Batch processing systems: (a) total recycle; (b) partial recycle.

can be substituted in Equation 5.37 to obtain a simple relationship for rate of change of concentration C with time.

$$\frac{dC}{dt} = \frac{h_c\,A}{C_0\,V_0}C^2\ln\frac{C_B}{C} \tag{5.39}$$

Unfortunately, even this seemingly simple equation does not have a closed form solution. Most of the apparent arbitrariness of membrane system design stems from these mathematical difficulties. Simple numerical procedures can be used to design batch concentration systems and to calculate operating parameters.

5.3.2 FEED AND BLEED SYSTEMS

In this scheme the feed gets concentrated in the recirculation loop and a part of it is bled off continuously. Fresh feed is pumped into the loop to balance the retentate bleed and permeation rate (Figure 5.10a). Since the system is fed and bled continuously, feed and bleed systems are continuous processing systems. The mathematical description of feed and bleed operation involves two mass balances which equate the liquid and solute permeation rates to the difference between feed and bleed rates. Equations 5.40 and 5.41 are the mass balances of a single-stage system or the first stage of a multistage system.

$$Q_1 = Q_0 = A_1 J_1 \tag{5.40}$$

$$Q_1 C_1 - Q_0 C_0 = A_1 J_1 C_{p1} \tag{5.41}$$
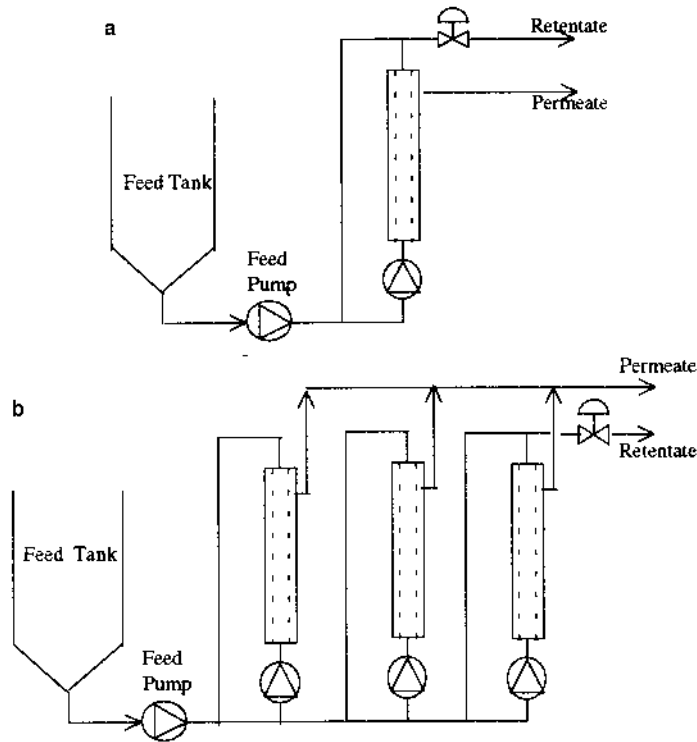
FIGURE 5.10 Feed and bleed systems: (a) single-loop system; (b) multi-loop system.

In feed and bleed configuration the membrane always encounters the highest concentration which generally corresponds to the lowest flux. Therefore, it has the highest possible membrane area. It also has a wide distribution of residence times. The multistage feed and bleed configuration which consists of several feed and bleed loops (Figure 5.10b) in series reduces the membrane area drastically. Three or four loop feed and bleed design has a membrane area very close to the batch configuration.

Multiloop feed and bleed design with a common manifold is the most common configuration in food processing applications. This design has the advantage of maintaining the cross-flow velocity irrespective of other system parameters which can vary with time or feed composition. It is invariably the most expensive of all the design configurations.

The leakage of retentate from one loop to another in the common manifold results in a wider variation of retention times than the single loop design. A valve between loops is incorporated for use during flushing of the system to reduce flushing time.

5.3.3 SINGLE PASS SYSTEM

In single pass design the feed enters from one end and exits from the other end having achieved the desired concentration ratio or the permeate recovery. This is the most economical of all membrane system configurations due to low membrane area, lack of recirculation pumps and simplicity of design. The mathematical description of single pass configuration is similar to the model for batch configuration where area along the membrane system in the direction of flow is used as the independent variable instead of time.

$$\frac{dQ}{dA} = -J \tag{5.42}$$
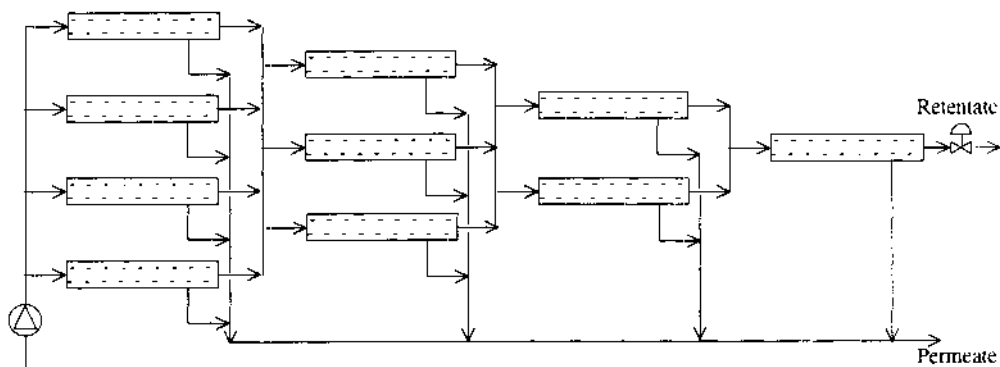
FIGURE 5.11 Single pass system.

$$\frac{d(QC)}{dA} = -J\, C_p \tag{5.43}$$

In these two equations J and C_p are functions of C while C is a function of Q. Equation 5.35 with flow rates in place of flow volumes represent the relationship between Q and C. The functional dependence between J and C_p with C is given by the Equations 5.3, 5.4, 5.8 and 5.9 for reverse osmosis. The combined system of equations for single pass concentration by reverse osmosis also cannot be solved explicitly. Only numerical solutions are possible.

In microfiltration and ultrafiltration where solute leakage is negligible, Equation 5.43 drops out of the system. The functional dependence of J on C is given by Equation 5.22. Relationship between V and C is obtained by setting $\sigma = 1$ in Equation 5.35. These equations can be substituted in Equation 5.42 to obtain a simple relationship for change of concentration along the system.

$$\frac{dC}{dA} = \frac{h_b}{C_0\, Q_0} C^2 \ln \frac{C_B}{C} \tag{5.44}$$

It should be noted that h_b is a strong function of cross-flow velocity which varies along the system as Q decreases due to permeation. This equation also cannot be solved explicitly even for the case of constant h_b. Numerical solution is possible with allowance for variation of h_b with Q and other parameters.

The permeate recovery in a single pass through a membrane module depends on the ratio of permeate flux to cross-flow velocity and very low in practice. Therefore, this design is restricted to situations with low concentration polarization that does not require high cross-flow velocities. Reverse osmosis of brackish water and high purity water production are common applications.

Pressure vessels containing several spiral membrane modules are the norm in single pass systems. The cross-flow velocity decreases as feed passes through the membranes due to feed volume reduction through permeation. This is compensated by the tapered or "Christmas Tree" configuration where several stages with progressively decreasing number of pressure vessels in parallel are arranged in series (Figure 5.11). The feed pressure also decreases as the retentate progresses through the system. This is compensated by having booster pumps.

The design of single-pass tapered systems is done using computer programs made available by leading membrane manufacturers to systems manufacturers. These programs are based on numerical procedures. Examples of the use of these programs is found in the literature (e.g., Bradley, 1993; Ko and Guy, 1988)
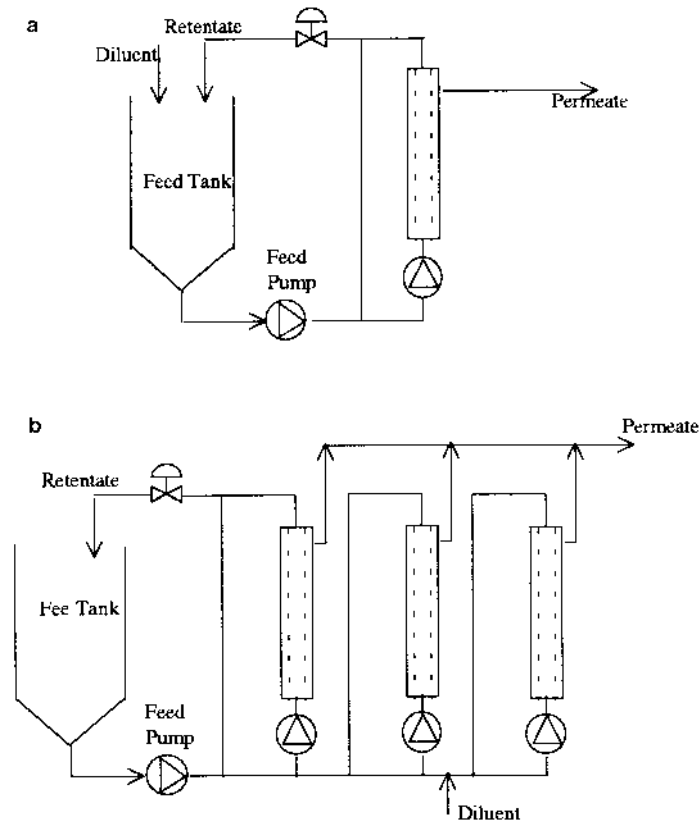
FIGURE 5.12 Diafiltration systems: (a) single-loop system; (b) multi-loop system.

Single pass configuration allows the addition of pressure vessels in parallel without adding pumps when the production falls below design levels. This is because reduction of permeate flow automatically increases the cross flow. This adds a degree of flexibility when membrane flux declines with time.

Single pass design has the lowest retention time. This is an advantage in food processing since many food components have a tendency to deteriorate with time and also due to increase in microbial growth with time. Unfortunately, this advantage has not been exploited by systems manufacturers to date. The only known food process application using single pass design is the reverse osmosis treatment of evaporator condensate to produce boiler feed water.

5.3.4 DIAFILTRATION SYSTEMS

Diafiltration involves the addition of solvent (diluent) to the retentate and removing it as permeate together with more solute. Its objective may be the increased recovery of solute or a retentate with a higher level of purity. Diafiltration can be done in any filtration range from microfiltration to reverse osmosis. Batch systems as well as continuous systems can be operated in diafiltration mode (Figure 5.12).

Diafiltration can be done sequentially by alternating concentration and dilution several times. Diafiltration can also be done continuously by adding diluent to makeup for the permeate volume that is being removed. In sequential diafiltration the concentration of a given solute in the retentate after n stages is given in terms of volume reduction ratio ρ and apparent solute rejection σ by

$$C = C_0 \, \rho^{n(\sigma-1)+1} \tag{5.45}$$
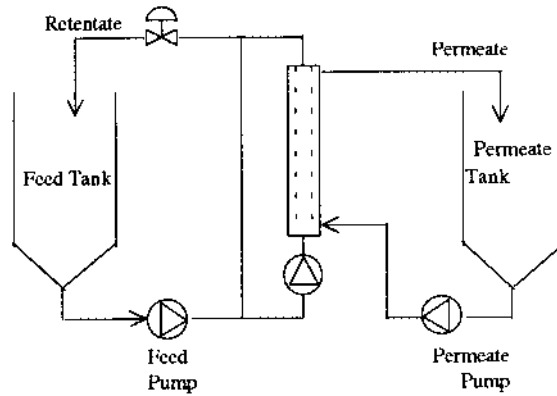
FIGURE 5.13 Cocurrent permeate flow system.

In continuous diafiltration the concentration of the solute in the retentate after m times the initial volume is removed as permeate is given by

$$C = C_0 \, e^{-m(1-\sigma)} \tag{5.46}$$

Diafiltration at low concentrations produces high fluxes but the volume that has to be removed is also large. At high concentrations permeate fluxes are low but the volume to be removed is also low. There is an intermediate optimum concentration for continuous diafiltration that results in the lowest time to remove a given volume of permeate. The optimum concentration in the gel layer controlled ultrafiltration or microfiltration is a unique function of the gel layer concentration (Ng et al., 1976) and is given by

$$C_{opt} = \frac{C_c}{e} \tag{5.47}$$

The optimum concentration being a function only of C_c, is independent of other factors like temperature and velocity that affect permeate flux in the gel layer controlled region.

5.3.5 COCURRENT PERMEATE FLOW SYSTEM

Microfiltration frequently requires operation at high cross-flow velocities to reduce the thickness of the concentration boundary layer and at low transmembrane pressure differences to reduce compaction of the cake layer. However, when high cross-flow velocities are maintained, the pressure drop along the membrane reaches high levels far exceeding optimum transmembrane pressure drop. Under these conditions, transmembrane pressure drop is high at the inlet of the module and low at the outlet end. This results in high fouling at the inlet end and low utilization of the outlet end.

Cocurrent permeate flow system (Bhave, 1991) incorporates a permeate pumping loop parallel to the retentate pumping loop so that the pressure profile in the permeate closely simulates the profile in the retentate loop. This results in a virtually uniform pressure drop along the length of the membrane module. Figure 5.13 is a flow diagram of a cocurrent permeate flow system.

Ceramic microfiltration systems incorporating this design have reported permeate fluxes in the range of 300 to 1000 lmh in food, dairy, and beverage applications. These fluxes are several folds higher compared to alternative designs.

5.3.6 PILOT PLANT TRIALS

The primary objective of the membrane system design is to estimate the surface area of membranes required to concentrate a given volume or a flowrate by a given concentration ratio. The variation of permeate flux and solute rejection with solute concentration from initial to final concentration is required as input. The prediction of the flux-rejection-concentration relation from first principles is rarely attempted due to lack of properties and mathematical difficulties. Instead they are obtained by experiments conducted using pilot plants.

Basic pilot plant is a small membrane system consisting of feed and recirculation pumps, pressure vessels or membrane modules, feed and clean-in-place tank, flow and pressure control valves, flowmeters, pressure gauges, and temperature gauges. All the components are mounted on a compact skid for easy transport.

The primary objective of pilot trials is to obtain the permeate flux and solute rejection as a function of solute concentration. This is obtained by a batch concentration trial better known as 'concentration scan'. The results of a concentration scan are dependent on other operating parameters such as pressure, temperature, and cross-flow velocity. These dependencies can be studied by pressure scans, velocity scans, and temperature scans.

Ideally, each of these scans consists of several points where only one parameter is varied while all other variables are held constant. Even if each scan consists of only a few points, obtaining a comprehensive set of 'scans' becomes a formidable task. Another difficulty in conducting a broad set of scans is the irreversibility of fouling phenomena. The first pressure scan may establish a cake layer on the membrane that does not disappear upon returning to zero pressure. This requires a chemical cleanup which is time consuming.

Therefore, the parametric relations are used judiciously to reduce the experimental work. Temperature scans are almost never conducted. Instead, corrections based on property variations are used. In reverse osmosis trials a 3% increase in flux per degree Celsius rise in temperature is used as the standard correction. This correction is based on the viscosity-temperature relation. Pressure and velocity scans at initial and final concentrations are required as a minimum to determine suitable operating points.

5.3.7 SAMPLE DESIGN CALCULATIONS

Numerical schemes have to be used to design even the simplest membrane system due to mathematical difficulties described earlier. Fortunately, these numerical schemes can be implemented on spread sheets on desktop computers. An example of numerical schemes that can be used in the design of several configurations are presented in this section.

The variation of permeate flux and solute rejection with solute concentration from initial to final concentration, under expected operating conditions is required as input for the design procedure.

These relations are obtained by a pilot scale concentration scan. This example uses the flux and rejection characteristics shown in Equations 5.48 and 5.49.

$$J = 28.3 \ln \frac{37}{c} \tag{5.48}$$

$$\sigma = 0.43 \tag{5.49}$$

Rejection is assumed to be a constant at 0.43 for simplicity. This value is selected so that a fivefold volume reduction corresponds to a twofold increase in concentration. The parameters of Equations 5.48 and 5.49 correspond closely with experimental results reported by Cheryan (1986c) for the ultrafiltration of skim milk using hollow fiber module of polysulfone

TABLE 5.5
Design of Batch Processing System

c (%)	J (Lmh)	V (L)	Area (m²)
10	37.0	5000	
11	34.3	4007	27.8
12	31.9	3274	22.1
13	29.6	2719	18.1
14	27.5	2289	15.1
15	25.6	1950	12.8
16	23.7	1679	11.0
17	22.0	1458	9.6
18	20.4	1277	8.6
19	18.9	1126	7.7
20	17.4	1000	7.0
Total area			139.7

membrane with 50,000 molecular weight cut off. The experimental conditions are at 60°C temperature and 1.11 m/s cross-flow velocity. The examples determine the membrane area required to concentrate 5000 L of skim milk with 10% solid content five-fold in 1 h operation producing 1000 L of product with 20% solids.

5.3.7.1 Batch System

The concentration range from 10 to 20% solids is divided into smaller increments. The volume at each concentration level is calculated using Equation 5.37 with $\sigma = 0.43$. Area required for volume reduction in each increment is calculated by dividing the volume reduction by average flux over the increment. Table 5.5 illustrates this procedure for 10 increments.

5.3.7.2 Feed and Bleed System

In single-stage feed and bleed system the membrane always sees the liquid at the final concentration which has the lowest flux. The membrane area requirement for this system can be determined easily by first calculating the flux at the final concentration using Equation 5.24 and dividing the total permeate volume by the flux.

Permeate flux at final concentration	$= 28.3 \ln (37/20)$	$= 17.4$ L/m²-h
Total permeate volume	$= 5,000–1,000$	$= 4,000$ L/h
Membrane area	$= 4000/17.4$	$= 229.8$ m²

5.3.7.3 Continuous System

In continuous or multiloop feed and bleed system loops can have different membrane areas. However, this introduces too many degrees of freedom and a unique design does not exist. All the loops having the same membrane areas is the most practical design from constructional and operating perspective. This restriction also results in a unique design.

The last loop operates at the final concentration irrespective of the number of loops. Therefore, the numerical procedure for the system design begins with the final stage. The set of equations for final stage are

TABLE 5.6
Design of Multiloop Processing System

	Three-loop system			Five-loop system	
Stage	Q (L/h)	C (%)	Stage	Q (L/h)	C (%)
3	1000	20.0	5	1000	20.0
2	1931	15.1	4	1527	16.7
1	3292	12.0	3	2210	14.2
0	5000	10.0	2	3029	12.4
			1	3965	11.1
			0	5000	10.0

$$Q_{n-1} = Q_n + h_b \, A \ln \frac{C_c}{C_n} \tag{5.50}$$

$$\frac{C_n}{C_{n-1}} = \left[\frac{Q_{n-1}}{Q_n} \right]^{\sigma} \tag{5.51}$$

An initial value for A is assumed and Equation 5.50 is solved for Q_{n-1}. This value is used in Equation 5.51 and solved for C_{n-1}. The procedure is repeated sequentially backwards for each stage until stage 1 is solved for Q_0 and C_0. The value of A is adjusted until Q_0 and C_0 become equal to the required values. Table 5.6 illustrates the results of this solution procedure for three- and four-loop systems.

The membrane area per loop that produces these results was 53.5 and 30.3 m^2 for three-loop and five-loop systems, respectively. Therefore, total membrane area of three and five loop systems are 160.5 and 151.5 m^2, respectively. These values are between the areas required for batch system and single stage system. The system areas for all the designs are summarized below.

Batch system	= 139.7 m^2
Five-loop recycle system	= 151.5 m^2
Three-loop recycle system	= 160.5 m^2
Single-loop feed and bleed system	= 229.8 m^2

5.3.8 SANITARY MEMBRANE SYSTEMS

Dairy applications require that the membrane systems meet the sanitary standards recommended by the U.S. Public Health and Dairy Industry Committee (Anon., 1967) also known as 3-A standards. All piping, vessels, valves, etc., are to be of 316 stainless steel with minimum # 4 mill finish. Diaphragm-type transducers are used for sensing pressure and temperature. Stagnant areas should be avoided in piping. Materials for gaskets, membranes, and other module components should meet Code of Federal Regulations (Anon., 1982).

A spiral membrane module was specially developed for dairy applications. This module eliminates the brine seal and the fiberglass wrap found in standard spiral module. One or two layers of feeder spacer is wrapped around the module to adjust its diameter to suit the internal diameter of the pressure vessel. The adhesives and other plastic components used in sanitary spiral module manufacture do not leak chemicals under anticipated operating conditions.

5.4 OPERATION OF MEMBRANE SYSTEMS

Operation of membrane systems involves maintaining permeate flux and solute rejection within specific limits that meet the product and process specifications. The permeate flux during processing of a solution is much lower than the pure water flux. The different transport properties of the solution, different membrane response, concentration polarization, and membrane fouling are responsible for this reduction in flux. Understanding and controlling these mechanisms is the basis of proper operation of membrane systems.

5.4.1 FOULING PHENOMENA

The primary challenge in membrane applications is the decline in flux with time that is loosely termed fouling. In the strict sense fouling is the gradual decline in flux with time when all operating parameters, i.e., pressure, temperature, concentration, velocity, etc., are held constant (Cheryan, 1986b).

The first and easiest to diagnose form of fouling occurs in the membrane modules. When dealing with liquids with suspended solids using hollow fiber modules, larger particles can block the entrance to the fibers. In spiral membrane modules particles get trapped in the feed spacer mesh in addition to blocking the entrances. These events are accompanied by a decrease in flux as well as an increase in pressure drop along the module hence easy to recognize.

Within the first few seconds of the start-up of a membrane operation a concentration polarization layer sets up on the surface of the membrane. This is an inevitable transport phenomenon. It is also reversible. The initial decline in flux due to concentration polarization can be reduced by decreasing the pressure, increasing the velocity, or decreasing the concentration. Therefore, this phenomenon is not considered a form of fouling.

The second form of fouling that occurs on the surface of the membrane is a consequence of concentration polarization. Solutes that accumulate on the membrane surface undergo irreversible changes over time and form resistant layers on the membrane surface. The mechanism of fouling-layer formation is governed by surface-chemistry, membrane-solute and solute-solute interactions. Macromolecules like proteins, pectins and starches are common surface foulants in ultrafiltration. Inorganic compounds like calcium sulfate, calcium phosphate, and calcium carbonate precipitate on the membrane surface during reverse osmosis.

The third form of fouling is pore plugging. Solutes that are small enough to enter a membrane pore could get trapped in narrow or tortuous sections of the pore. Tortuous pore microporous microfiltration membranes are susceptible to this type of fouling. Capillary pore (track-etch) membranes are generally free from pore lugging due to uniform cross-section of pores. Asymmetric membranes are also less prone to pore plugging due to divergent profile of pores.

Solute absorption is the fourth form of fouling. Adsorption makes all pores smaller. Even a small reduction in the diameter of the pore reduces the flux significantly because flow is proportional to the fourth power of the pore diameter (Equation 5.24). Absorption of proteins on pore walls is recognized as a primary fouling mechanism in ultrafiltration. Ceramic microfiltration of sugar water solutions has shown that membrane-sugar interactions cause drastic reduction in flux (Padilla-Zakour and McLellan, 1993).

5.4.2 PRETREATMENT

Fouling of feeder channels and by suspended materials has to be controlled by physical elimination through pretreatment. This is crucial in spiral membrane modules which have the strongest tendency for this type of fouling. Suspended materials that settle within about 1 h and particles that are bigger than one-tenth the feeder channel width are considered detrimental for these modules. Spiral membrane modules are produced with several standard

spacers. The common spacer widths are 24, 30, 45, 60, and 80 mil. Therefore, particles larger than 3 mil or 75 μm should be removed when the commonest 30 mil spacer is being used.

The commonest form of pretreatment is the prefiltration by coarse filters. Wedge-wire filters, vibratory sieves, rotary sieves, pressure parabolic screens are some of the coarse filters used in practice. Centrifuging is also used to separate fine cheese particles left over in whey before ultrafiltration.

Hollow fiber and tubular modules require less rigorous screening compared to spiral modules. However, hollow fine fiber modules require much finer prefiltration. Fruit juice that is concentrated using hollow fine fiber modules are pretreated by ultrafiltration.

Chemical pretreatment of feed streams is necessary for the removal of chemically active foulants. In reverse osmosis pH adjustment by addition of acids is used to prevent carbonate scaling while sequestrants are used to prevent sulfate scaling. Flocculation of colloidal suspensions by treating with polyelectrolytes is also common in reverse osmosis. When thin film composite membranes with low chlorine resistant membranes are used, dechlorination through addition of sodium bisulfite or activated carbon treatment is employed.

Pectin is a major foulant in fruit juice clarification and concentration. Depectinization using enzymes helps alleviate membrane fouling and also increases juice yield. High temperature helps reduce fouling in applications involving hydrocolloids like gelatinized starch and gelatin. High temperature also increases permeate fluxes by reducing the viscosity.

5.4.3   MEMBRANE CLEANING

Improvements to membranes, modules, systems, operating procedures, and pretreatments can reduce fouling drastically. However, prolonged operation of membranes will eventually require some form of cleaning. Membrane cleaning utilizes mechanical, hydraulic, and chemical methods.

Mechanical cleaning in large diameter tubular systems is done by passing oversize sponge balls through the tube. Hydraulic cleaning is done by several methods. Periodic back washing and back pulsing of the permeate is used in tubular and monolithic membrane systems. These methods cannot be used with thin film membranes due to tendency for delamination. Reversing the flow direction is used as a means of cleaning hollow fiber membranes which tend to get fouled mostly at the outlet end. Pressurizing the permeate is used with microfiltration systems as an operating method rather than as a method of cleaning.

Chemical cleaning by far is the most important method of membrane cleaning. It has developed into a specialized and lucrative market by itself. Acids (nitric, phosphoric, citric) are used to clean inorganic fouling. Examples are calcium phosphate in dairy applications and calcium carbonate in desalination applications. Caustic cleaning is the most effective method when fouling is organic in nature. Proteins and fats that cause fouling in dairy applications are cleaned using caustics or chlorine.

Chemical cleaning of reverse osmosis membranes requires close attention to chemical compatibility of the membranes. Composite membranes have very limited chlorine tolerance but broader pH tolerance. Hence, they can be cleaned by relatively strong acids and caustics. Asymmetric cellulose acetate membranes have better chlorine tolerance but narrower pH tolerance. Most materials used in microfiltration and ultrafiltration have high tolerance for both chlorine and pH limits.

5.4.4   MEMBRANE SYSTEM CONTROL

The objective of membrane system control is to maintain required flow rate and quality of a process stream in relation to variations in input stream and the processing system. Gradual decline in flux with time due to fouling is the major problem that control systems have to address. The primary control variable in a membrane system is the pressure.

TABLE 5.7
Membrane Applications in Food Industry

Industry	Application	Range	Module	Membrane
Dairy	Milk concentration	RO	Spiral	CA, TFC
	Whey concentration	RO	Spiral	CA, TFC
	Whey fractionation	UF	Spiral	PS, PVDF, PES
	Lactose concentration	RO	Spiral	CA, TFC
	Milk pasteurization	MF	Tubular	Ceramic
	Desalting	NF	Spiral	TFC
Juice	Clarification	MF	Tubular	Ceramic
		MF	Hollow fiber	PS, PE
		UF	HF	PS
		MF/UF	Tubular	PVDF, PS
	Concentration	RO/NF	Spiral	TFC
		RO/NF	Tubular	TFC
		RO/NF	HFF	TFC
	Caustic recovery	MF	Tubular	Ceramic
Gelatin	Concentration	UF	Spiral	PS
Corn Sweetener	Dextrose clarification	MF	Spiral	PS/PES
Sugar	Clarification	MF/UF	Tubular	Ceramic
	Preconcentration	RO	Spiral	TFC

Note: RO = reverse osmosis; UF = ultrafiltration; MF = microfiltration; NF = nanofiltration; CA = cellulose acetate; TFC = thin film composite; PS = polysulfone; PVDF = polyvinylidine difluoride; PES = polyethersulfone; PE = polyester.

The control system adjusts the pressure as permeate flux changes due to fouling or variation of concentration of input. Pressure is controlled by a pneumatically actuated back pressure valve. The quality of the output stream is controlled by maintaining a given ratio between flowrates of output stream and the input stream. When variable frequency driven pumps are used the speed of the pump motor is controlled to maintain the required ratio. In case of multistage centrifugal pumps, a control valve on the output side of the pump is employed for flow control.

Typically a membrane system in a food processing plants starts operation at a low pressure in the morning. The pressure is gradually increased throughout the day to maintain the required production rate as flux declines due to fouling. In dairy applications, the system design with about 20 h of operation allows 4 h for daily cleanup. This scheme fits well with mandatory cleanup of other equipment in the plant. In fruit juice processing two daily cleanings is common. Some membrane systems are designed to introduce additional membrane banks as the demand increases or the fluxes decrease.

5.5 MEMBRANE APPLICATIONS IN THE FOOD INDUSTRY

Membranes have made rapid advances in food industry from a modest beginning in early 1960s. This is a remarkable achievement in an industry that is universally viewed as conservative. The range of membrane applications that are commercialized, span the complete spectrum from microfiltration to reverse osmosis. These applications are spread over several sectors of the industry including, dairy, fruit and vegetables, beverages, grain processing, and sugar industries. Table 5.7 is a summary of important membrane applications in the food industry.

5.5.1 Dairy

Concentration of milk by reverse osmosis prior to evaporation and cheese making has proven to be viable in membrane applications. The concentration factor is limited by the calcium phosphate precipitation to about three- to fourfold. Membrane systems are less capital intensive to purchase and more economical and energy efficient to operate compared to competitive technology. (Cheryan and Alvarez, 1995). Spiral modules of cellulose acetate and thin film membranes are used for these applications.

Production of cheese leaves about 85% of the milk as whey which contains whey proteins, lactose, and salts in solution. Whey concentration by reverse osmosis and whey fractionation by ultrafiltration have become the largest membrane applications in the food industry today. Whey concentration by reverse osmosis reduces transport costs while whey fractionation produces a whey protein concentrate which is a valuable byproduct.

Microfiltration of milk using monolithic ceramic systems has become viable since the introduction of cocurrent permeate flow design. This process is said to result in more stable pasteurized and refrigerated milk products.

Nanofiltration and electrodialysis are used as alternatives to ion exchange in the desalting of whey. Production of low-sodium and low-lactose dairy food products is an area of intense interest that involves membrane applications.

5.5.2 Fruit and Vegetable Juice

Production of single strength fruit juices involves several filtration operations to remove suspended and colloidal particles. Traditionally this is done in rotary vacuum filters and pressure leaf filters using filter aids and fining agents. Ultrafiltration has advantages over media filtration due to increased recovery, elimination of filter media, better product quality, and reduced waste disposal costs.

Fruit juices are concentrated from original 10 to 16% sugar content to about 60% for long-term storage and transport. Concentration of juices is done typically in multi-effect evaporators. Reverse osmosis has the advantage of lower costs and energy compared to evaporators. However, these advantages are limited to the low concentration range typically up to about 24%. Another advantage of reverse osmosis is that it produces a better quality concentrate due to lack of thermal damage. Higher concentrations up to 60% are achieved in specially designed multistage systems but not with economic advantages. Concentration of cloudy or unclarified juices is done using tubular modules while clear clarified juices are concentrated in spiral systems.

Tomato juice is concentrated from 5% solids content to about 30% solids content using thermal evaporation. High suspended solids content and non-Newtonian nature of tomato juice makes it a challenge to membrane systems designers. Tubular modules are used to concentrate tomato juice to 8% solids level (Merry, 1994) for the production of a sauce.

5.5.3 Sugar

Cane and beet sugar processes involve clarification of juice to remove suspended and colloidal particles. Ultrafiltration has been introduced for this application. Thin juice concentration using reverse osmosis has also been done successfully. Maple syrup preconcentration is one of the early reverse osmosis applications to be commercialized.

5.5.4 Corn Sweetener

Corn sweeteners are produced by the acid or enzyme hydrolysis of corn starch. This process involves several clarification, fractionation, and concentration operations. Diatomaceous earth

filters used in dextrose clarification are being replaced by spiral microfiltration systems. Glucose-Oligo separation is done using spiral nanofiltration membranes. Fructose preconcentration can be done using reverse osmosis. About 2 to 3 million ft^2 of membranes are used in commercial applications in this industry (Lee, 1994).

5.5.5   WINE AND BREWERY

In wine making, diatomaceous earth filters and pad filters are being replaced by tubular and hollow fiber microfiltration membranes in the clarification process. Ultrafiltration has been effective in replacing fining to a limited scale. Concentration of wines using reverse osmosis accelerates the tartrate precipitation process in cold stabilization. Reverse osmosis is used to produce low alcohol wine.

Microfiltration through ceramic membranes is used to produce cold sterilized beer. Reverse osmosis is used to produce low alcohol beer. Vapors leaving beer stills are condensed and treated by reverse osmosis membranes to reduce air pollution and to recover thermal energy.

5.5.6   ANIMAL PRODUCTS

Blood is a high volume waste product of abattoirs. Byproduct recovery from waste blood using membranes include separation and purification of blood cells by ultrafiltration, concentration of plasma by ultrafiltration, and concentration of homogenized blood. These applications employ tubular, spiral, and flat plate modules.

Gelatin is an animal byproduct containing colloidal proteins formed by hydrolysis of collagen. The hydrolysate containing 3 to 15% solids is concentrated and dried to produce gelatin powder. The traditional method involved steam evaporation and drum drying. Ultrafiltration was found to be superior to steam evaporation due to less thermal damage and lower cost. Ultrafiltration also allows leakage of salts thus producing a superior product. In clarification of gelatin, diatomaceous earth filters have been replaced by tubular microfiltration systems.

5.5.7   PROCESS EFFLUENTS

Food processing plants discharge large volumes of water containing suspended and dissolved solids. Increasing effluent disposal costs in urban areas have forced food processors to look for advanced effluent treatment technology. When the effluents disposal problem is related to dissolved organic matter or salts, reverse osmosis becomes the technology of choice. The brining and pickling industry has employed microfiltration to clarify brines for reuse and reverse osmosis for concentration of brining waste for alternative disposal.

5.6   ECONOMIC ASSESSMENTS

Economic assessment of membrane applications involves evaluation of costs associated with the application with the resulting benefits in comparison to competitive technology or other non-technological alternatives. The costs of membrane applications include capital amortization, membrane replacement, energy use, cleaning chemicals, and operating labor. The benefits in process applications include reduced operating costs relative to competitive technology, saving of product, recovery of byproducts, savings of water, energy, chemicals, etc. In effluent reduction applications savings in disposal costs become important.

5.6.1   MEMBRANE AND MEMBRANE SYSTEM COSTS

The cost of a membrane depends on its type while the cost of membrane systems depend on type, size, and degree of automation of the design. A comparison of current costs of six of

TABLE 5.8
Membrane and Membrane Systems Costs

	Spiral polymeric RO[a]	Spiral polymeric UF[a]	Hollow fiber polymeric UF[b]	Tubular-ES polymeric RO[c]	Tubular-SS polymeric UF[c]	Tubular-ML ceramic MF[d]
Base System Parameters						
Area (m^2)	600	600	147	520	250	37
Power (kW)	125	45	40	120	80	67
Base System Costs						
Membrane Membranes ($)	32,000	32,000	36,000	100,000	60,000	75,000
Membrane System ($)	196,000	162,000	110,000	750,000	350,000	300,000
Specific Costs and Power						
Electric Power (W/m^2)	212	77	272	230	320	1,810
Membrane Modules ($/m^2)	55	55	245	192	240	2,030
Membrane System ($/m^2)	334	276	750	1440	1400	8,100

Note: ES — Externally supported; SS — self supported; ML — monolithic.

[a] Courtesy of Dr. Bala Raghunath, Membrane System Specialists, Wisconsin Rapids, Wisconsin.

[b] Courtesy of Mr. C. Russel Davis, Koch Membrane Systems, Saint Charles, Illinois.

[c] Courtesy of Mr. Peter Allen, PCI Membrane Systems, Santa Rosa, California.

[d] Courtesy of Mr. Mike Grigas, Niro Hudson, Inc., Hudson, Wisconsin.

the most common types of membrane systems in the food industry is presented in Table 5.8. These costs are based on budgetary quotations provided by systems manufacturers in 1996.

The spiral membrane and system costs are for concentration of whey from 6 to 12% solids by reverse osmosis and for manufacture of 35% whey protein concentrate by ultrafiltration using 4-in modules with 30-mil spacer elements. Wider spacers will have less area per module and hence higher costs. Larger diameter modules cost less while smaller modules cost more. The hollow fiber system costs are based on 5-in modules of 1.1-mm diameter polysulfone fibers. Larger diameter fibers would increase the costs considerably. Tubular system is based on 12.7-mm diameter tubes. Ceramic system is based on 4-mm diameter tubes.

The cost of the membrane system alone cannot be used in the decision making process. Permeate fluxes for the same feed differ significantly among different systems. Spiral systems which are extremely cost effective have little tolerance for suspended solids hence require elaborate and costly pretreatment. Hollow fiber and tubular systems can accommodate more suspended solids and particulates. Polymeric systems have limited chemical tolerance compared to ceramic systems. These factors should be considered before comparing costs.

Membrane systems are modular in nature. Therefore, the capital cost of membrane systems increases almost linearly with size. System size scale factors for seawater and brackish water desalination applications are reported to be around 0.85 to 0.95 (Ray, 1992).

5.6.2 ENERGY COSTS

Cross-flow filtration is driven by pressure and assisted by velocity. Both pressure and velocity are generated by pumps driven by electrical energy. In high-pressure applications like reverse osmosis of seawater, the feed pump is the primary energy user. In low pressure applications like ultrafiltration and microfiltration the recirculation pumps use more energy than the feed pump.

Membrane filtration is one of most energy efficient means of separating solutes like salt and sugar from water. The minimum free energy requirement for desalting saline water is a

function of salt concentration, recovery, and temperature, increasing with the increase of each parameter (Dresner and Johnson, 1980). The minimum free energy requirement for desalting seawater with 3.5% salt content with 50% recovery at 25°C is about 1.04 kWh/m^3. Energy consumption in seawater desalting systems ranges from 4 to 10 kWh/m^3 while in brackish water and softening systems consume about 0.5 to 2 kWh/m^3.

The energy consumption in optimally designed ultrafiltration systems is about 50 W/m^2 of membrane area (Eycamp, 1995). When the overall efficiency is 50% and the average permeate flux is 20 lmh, the energy consumption in an optimally designed system is about 5 kWh/m^3.

5.6.3 OTHER COSTS

Membrane replacement, cleaning chemicals, and labor are the other costs associated with membrane systems. The cost of membrane replacement is inversely proportional to membrane life. In dairy applications where severe cleaning protocols are used daily, the membrane life is about 12 to 18 months. Hollow fiber ultrafiltration membranes have been used for about 4 years in vinegar clarification. Ceramic membranes have extra long life span extending beyond 8 years.

The cost of cleaning is highly variable, depending strongly on severity of fouling. Specific cleaning cost of $0.10/m^2-year has been reported for fermentation broth clarification in a 4000 h/yr operation (Bemberis and Neely, 1986). Membrane cleaning is more effective at high temperatures. Steam, gas, or electricity can be used to heat water depending on availability. This is a relatively minor operating cost but capital cost of steam or gas pipework can be significant. In general, cleaning costs range from 10 to 20% of the total operating costs of a membrane system. Membrane systems do not require full-time operators. Most of the regular labor requirement is during startup and cleaning. About 2 h/d is a typical labor requirement.

5.6.4 ECONOMIC ASSESSMENT OF WHEY PROTEIN CONCENTRATION

Whey protein concentration is the best established membrane application in the food industry. Early difficulties with capacity, flux stability, cleanability, and membrane durability have been overcome in time to make this a standard unit operation in cheese processing plants. A steady decrease in the cost of dairy membrane modules in the recent past has also helped this trend.

The sample economic assessment presented in Table 5.9 is based on the information provided by a leading membrane system manufacturer (Braun, 1995). This whey protein concentration system uses 4″ sanitary spiral polysulfone membrane modules. A three-loop recirculation system where each loop consists of 10 vessels each holding 5 modules providing 150 modules with a 1000 m^2 of total membrane area is the basis of the estimate.

The plant processes 460,000 L/d (1,000,000 lb) of whey with 6.2% total solids and produces 81,500 L (178,600 lb) of 35% (dry basis) whey protein concentrate containing 10.4% total solids. This amounts to a 5.6-fold concentration of the original feed.

A whey processing plant requires, in addition to the ultrafiltration system, a clarifier for solids separation, a heat exchanger for pasteurization and cooling, storage tanks, piping, etc. It may also require augmentation of utilities such as electricity, steam, water, and refrigeration. The capital and operating costs of these facilities should be included in an overall economic assessment. Alternatives to whey processing are hauling to farms for animal feed or disposal for treatment as wastewater which are far less attractive.

5.6.5 ECONOMIC ASSESSMENT OF JUICE CLARIFICATION

Juice clarification involves separation of suspended particles and colloidal matter that cause cloudiness. Centrifugation is the technology of choice to separate large particles but it

TABLE 5.9
Economic Assessment of Whey Protein Concentration

System Parameters	
Whey feed volume (L/d)	456,000
Whey protein concentrate (L/d)	81,500
Whey protein concentrate (dry kg/d)	8,500
Permeate volume (L/d)	374,500
Permeate flux (Lmh)	19.5
Operating hours per day	20
Operating days per year	312
Membrane area (m^2)	1,000
Capital investment ($)	300,000
Electric power (kW)	60
Expenses ($/year)	
Amortization of capital ($300,000 @ 0.149)	44,700
Energy cost (374,400 kWh @ $0.075)	28,100
Membrane replacement ($75,000 per 18 mos.)	50,000
Cleaning (lump sum)	24,000
Operating Labor (lump sum)	12,000
Total expenses	158,800

becomes increasingly expensive when particles are smaller and when density difference is smaller. Filtration is relatively less sensitive to these factors. Media filters of rotary vacuum and pressure leaf type dominate the technology for fine filtration. However, membrane filtration is more attractive than media filtration under most circumstances.

A cost comparison between ultrafiltration and media filtration for fermentation broth clarification based on the example presented by Bemberis and Neely (1986) is shown in Table 5.10. This table compares a hollow fiber ultrafiltration system with a rotary drum media filter. The comparison in Table 5.10 shows that even though the capital cost of ultrafiltration system is over four times the cost of the media filter, its total operating expenses are 35% lower. The cost of filter aid dominates the economics of media filtration. The cost of disposal of spent filter aid and possibility of increased recovery through ultrafiltration (about 2% reported by Bembiris and Neely, 1985) also favor ultrafiltration over media filtration.

5.6.6 ECONOMIC ASSESSMENT OF JUICE CONCENTRATION

Membrane systems have to compete with thermal evaporation for juice concentration. The economics of evaporation depend on the type of the evaporator and the cost of energy. A sample comparison between an evaporator and a reverse osmosis system for tomato juice preconcentration from 4.5 to 8.5 Brix (Anon., 1984) is presented in Table 5.11. A three effect forced circulation type evaporator with a steam economy of 2.78 was used in the comparison.

This assessment includes only energy and membrane replacement costs. Other costs can be considered comparable for both systems. The results indicate the great economic advantage of reverse osmosis relative to evaporation. Preconcentration from 4.5 to 8.5 Brix removes about half the water that has to be removed in the paste-making process. It is considered technically feasible to concentrate up to about 15 Brix by reverse osmosis. Membrane preconcentration has further advantages of less heat damage to the product and lower air pollution.

5.6.7 ECONOMIC FEASIBILITY OF EFFLUENT REDUCTION

Economic feasibility of membrane applications for effluent reduction is strongly dependent on the avoided cost of effluent disposal. This varies widely among communities. Disposal of

TABLE 5.10
Comparison of Membrane and Media Clarification

	Ultrafiltration	Media filtration
System Parameters		
Permeate volume (L/d)	300,000	300,000
Permeate flux (Lmh)	17	410
Membrane area (m²)	1,070	46
Membrane life (yr)	1	—
Filter aid consumption (kg/m³ filtrate)	—	24
Operating hours per day	16	16
Operating days per year	250	250
Labor (h/d)	2	8
Capital investment ($)	856,000	207,000
Electric power (kW)	150	50
Expenses ($/year)		
Amortization of capital (Investment @ 0.149)	127,540	30,840
Energy cost($0.075/kWh)	45,000	15,000
Membrane replacement ($150/m²)	160,500	—
Filter aid (1,800,000 kg @$0.26/kg)	—	468,000
Cleaning ($0.10/m²/d)	26,750	
Maintenance (lump sum)	3,000	10,000
Operating Labor ($20/h)	10,000	40,000
Total expenses	372,790	573,480

TABLE 5.11
Preconcentration of Tomato Juice

	Reverse osmosis	Evaporation
System parameters		
Feed flow rate (L/h)	40,000	40,000
Water removal rate (L/h)	18,820	18,820
Membrane area (m²)	429	—
Electric power	180	32
Steam consumption (kg/h)	—	6,775
Operating hours per day	24	24
Operating days per year	50	50
Expenses ($/year)		
Electricity cost ($0.04/kWh)	8,640	1,536
Steam cost ($0.18/kg)	—	146,247
Membrane replacement (lump sum)	14,112	—
Total expenses	22,772	147,783

the concentrate is a major concern. Animal feed and land application are the common disposal options. Short length of the operating season is also a disadvantage in fruit and vegetable processing plants.

In general, membrane applications cannot be justified on savings on disposal costs alone. Recovery of byproducts, chemicals, and heat can complement the benefits and make the application cost effective. Recovery of sugars from rinse waters, recovery of chemicals from

cleaning water, and recovery of heat from blanching waters are some examples where membrane systems have found to be economically feasible.

Effluent containing dissolved organic matter is treated biologically. Aerobic treatment is the best choice for dilute effluents while anaerobic treatment is better suited for more concentrated effluents. Membrane treatment can be used to concentrate the dilute effluents for anaerobic treatment with the added benefit of water recovery.

NOMENCLATURE

A   Membrane area of the system (m^2)
b   Membrane thickness (m)
c   Concentration of solute (kg/m^3)
C   Concentration of solute in the retentate (kg/m^3)
C_p Concentration of solute in the permeate (kg/m^3)
D   Diffusivity of solute in solution (m^2/s)
d_h Hydraulic diameter (m)
d_p Diameter of pores/particles (m)
h_b Mass transfer coefficient in the boundary layer (m/s)
J   Solvent flux ($m^3/m^2/s$)
k   Boltzmann's constant (1.381×10^{-23} J/K)
k_m Conductance of membrane to solute flow (m/s)
L   Channel length (m)
P   Pressure (Pa)
R   Universal gas constant (J/mol/K)
r_b Resistance of boundary layer to solvent flow (Pa-s/m)
r_m Resistance of membrane to solvent flow (Pa-s/m)
r_s Radius of a spherical particle (m)
S   Solute flux ($kg/m^2/s$)
S_c Surface area of solids per unit volume of cake layer (1/m)
T   Absolute temperature (K)
V   Partial molar volume of the solvent
V   Volume of the batch (m^3)
x   Molar fraction of solvent
y   Distance perpendicular to membrane surface (m)
α Proportionality coefficient between osmotic pressure and concentration (Pa-m^3/kg)
δ Concentration boundary layer thickness (m)
δ_c Cake layer thickness (m)
ϵ Void fraction in the cake layer
ϕ Proportionality coefficient between cake layer resistance and pressure (s/m)
γ_w Shear rate at the wall (1/s)
μ Dynamic viscosity (Pa-s)
ν Kinemetic viscosity (m^2/s)
π Osmotic pressure (Pa)
ρ Volume reduction ratio
σ Solute rejection

BIBLIOGRAPHY

Effective Industrial Membrane Processes: Benefits and Opportunities, 1991, Turner, M. K., Ed., Elsevier Applied Science, London.
Handbook of Industrial Membrane Technology, 1990, Potter, M.C., Noyes Publications, Park Ridge, NJ.
Inorganic Membranes, Synthesis, Characteristics and Applications, 1991, Bhave, R.R., Ed., Van Nostrand Reinhold, New York.
Membrane Filtration: Handbook. Selection Guide, 1993, Merlo, C.A., Rose, W.W., and Ewing, N.L., National Food Processors Association, Dublin, CA.

Membrane Handbook, 1992, Ho, W.S.W. and Sirkar, K.K., Ed., Van Nostrand Reinhold, New York.

Membrane Separations Technology, Principles and Applications, 1995, Noble, R.D. and Stern, S.A., Eds., Elsevier Applied Science, London.

Reverse Osmosis, 1970, Sourirajan, S., Academic Press, New York.

Ultrafiltration Handbook, 1986, Cheryan, M., Technomic Publishing, Lancaster, PA.

REFERENCES

Agrawal, J.P. and Sourirajan, S., 1969, Specification, selectivity and performance of cellulose acetate membranes in reverse osmosis, *Ind. Eng. Chem., Process Des. Dev.,* 8(4):439.

Anon., 1967, 3-A, Accepted Practice for Permanently Installed Sanitary Product-Pipelines and Cleaning Systems, 605-02, U.S. Public Health Service and the Dairy Industry Committee, International Association of Milk, Food and Environmental Sanitarians. 1966, Revised 1967.

Anon. 1982. Code of Federal Regulations. Title 21- Food and Drugs. Parts 175.300,177.2600.

Anon. 1984. Reverse Osmosis Concentration of Tomato Juice. Patterson Candy International Limited.

Bemberis, I. and Neely, K. 1986. Ultrafiltration as a competitive unit process, *Chem. Eng. Prog.,* 82(11):29

Bhave, R.R. 1991. Liquid filtration and separation with inorganic membranes, in *Inorganic Membranes, Synthesis, Characteristics and Applications,* Bhave, R.R., Ed., Van Nostrand Reinhold, New York, 129.

Bradley, R., 1993, Design consideration for reverse osmosis systems, in *Reverse Osmosis, Membrane Technology, Water Chemistry, and Industrial Applications*, Amjad, Z., Ed., Van Nostrand Reinhold, New York, 104.

Braun, M., 1994, Review of Commercial dairy applications. Practical Short Course on Membrane Separations in Food Processing, Food Protein Research and Development Center, Texas A&M University, College Station, Texas.

Cheryan, M., 1986a, *Ultrafiltration Handbook,* Technomic Publishing, Lancaster, PA, 89.

Cheryan, M., 1986b, *Ultrafiltration Handbook,* Technomic Publishing, Lancaster, PA, 171.

Cheryan, M., 1986c, *Ultrafiltration Handbook,* Technomic Publishing, Lancaster, PA, 214.

Cheryan, M. and Alvarez, J.R., 1995, Food and beverage industry applications, in *Membrane Separations Technology, Principles and Applications,* Noble, R.D. and Stern, S.A., Eds., Elsevier Applied Science, London, 415.

Dresner, L. and Johnson, J.S., 1980, Hyperfiltration, in *Principles of Desalination*, Spiegler, K.S. and Laird, A.D.K., Eds., Academic Press, New York, 401.

Drioli, E., Iorio, G., and Cetapano, G., 1990, Enzyme membrane reactors and membrane fermentors, in *Handbook of Industrial Membrane Technology,* Potter, M.C., Ed., Noyes Publications, Park Ridge, NJ.

Eycamp, W., 1995, Microfiltration and ultrafiltration, in *Membrane Separations Technology, Principles and Applications,* Noble, R.D. and Stern, S.A., Ed., Elsevier, London, 415.

Ko, A. and Guy, D.B., 1988, Brackish and seawater desalting, in *Reverse Osmosis Technology: Applications for High Purity Water Production,* Parekh, B.S., Marcel Dekker, New York.

Kulkani, S.S., Funk, E.W., and Li, N.N., 1992, Ultrafiltration: theory and mechanistic concepts, in *Membrane Handbook*, Ho, W.S.W. and Sirkar, K.K., Eds., Van Nostrand Reinhold, New York, 398.

Lee, C.H., 1994, Membrane applications in corn sweetener production, Practical Short Course on Membrane Separations in Food Processing, Food Protein Research and Development Center, Texas A&M University, College Station, Texas.

Merry, A., 1994, Reverse osmosis and applications of reverse osmosis in food processing. Practical Short Course on Membrane Separations in Food Processing, Food Protein Research and Development Center, Texas A&M University, College Station, Texas.

Ng, P., Lungblad, J., and Mitra, C., 1976, *Sep. Sci.,* 11(3):234.

Padilla-Zakour, O. and McLellan, M.R., 1993, Optimization and modeling of apple juice cross flow microfiltration with a ceramic membrane, *J. Food Sci.*, 58(2): 369.

Porter, M.C., 1972, Concentration polarization with membrane ultrafiltration, *Ind. Eng. Chem., Prod. Res. Dev.*, 11(3):234

Ray, R.J., 1992, Reverse osmosis: cost estimates, in *Membrane Handbook,* Ho, W.S.W. and Sirkar, K.K., Eds., Van Nostrand Reinhold, New York, 355.

Sourirajan, S., 1970, *Reverse Osmosis.* Academic Press, New York, 552.

Zydney, A.L. and Colton, C.K., 1986, A concentration polarization model for the filtrate flux in cross flow microfiltration of particulate suspensions, Chem. Eng. Commun., 47:21.

6 Design and Performance Evaluation of Evaporation

Chin Shu Chen and Ernesto Hernandez

CONTENTS

6.1   GENERAL PRINCIPLES

Evaporation is a separation of a volatile liquid from a nonvolatile solid based on the principle of vaporization. When the water is present in a large amount, i.e., liquid foods, its removal is usually carried out by evaporation. The foodstuff may contain flavor compounds more volatile than water or it may be so viscous that it will hardly flow. It may deposit scale on the heating surface, it may precipitate crystals, it may tend to foam, or it may have a relative high boiling point. This wide variety of liquid-food characteristics has led to considerable variation in the types of evaporators used in the food industry. Practical considerations and experiences have greatly influenced the design and operation of evaporators for the various food processing industries.

Evaporative concentration is usually to produce a concentrate containing the desired solids in the solution or sometimes to remove the pollutants from waste streams. The primary objectives of liquid-food evaporation are to reduce the weight and volume of products and thereby reduce packaging, transportation, and storage costs; reduce energy consumption during subsequent drying; and reduce water activity (a_w) to enhance storage stability.

6.1.1   VAPORIZATION

Vaporization is a natural phenomenon of phase change from a liquid to a vapor. Imagine a closed vessel which is thermally insulated. The vessel is partially filled with a liquid and the air is evacuated. The liquid evaporates into the evacuated air space contained in the vessel, thereby a pressure is developed; ultimately, the space reaches saturation at which time as many molecules return to the liquid in any given time interval as leave it. That is an equilibrium condition at which a constant vapor pressure is reached at a given temperature and the net evaporation is zero. However, if the vapor is evacuated from the vessel, that is, the molecules leaving the liquid are removed continuously with no opportunity to return to the liquid layer, the evaporation will continue but the rate of evaporation will decrease as the liquid temperature will fall as a result of evaporation.

Conversely, if a steady supply of heat is transmitted to the vessel to maintain the liquid at the boiling temperature, the rate of evaporation will be maintained at a high level. It follows that for evaporation to proceed continuously, two conditions must be met: (1) the heat necessary for the vaporization of the liquid must be supplied and (2) the liquid molecules, as they escape through the boundary layer, must constantly be removed (Badger and Banchero, 1955).

6.1.2   TERMINOLOGY

An evaporator is a device wherein liquid is evaporated from a thin (low density) feed material in order to produce a more dense or thick product (concentrate). The feed may be a solution, slurry, or suspension of solid materials in a liquid. The heat necessary for vaporization is supplied through heat transfer across metallic surfaces by condensing steam. Thus, evaporator operations basically involve energy transfer (heat for vaporization and condensation), mass transfer (moisture removal), and fluid flow (feed and vapor flows).

Evaporators applied in the food and dairy industries are mostly operated under high vacuum. A vacuum evaporator consists of three principal elements: heat exchanger which transfers heat from steam to the food, vapor-liquid separator, and vacuum producer by a

mechanical pump or steam ejector. The equipment system units in which heat transfer takes place are called heating units or calandrias. The vapor-liquid separators are called bodies, vapor heads, or flash chambers. The term body is also referred to as the basic building module of an evaporator which consists of one heating element and one flash chamber. An effect is one or more bodies boiling at the same pressure. It is used to indicate the sequence of vapor or steam flow through the evaporator. A stage is used to indicate the sequence of product flow as it travels through the evaporator. A multiple-effect evaporator is an evaporator system in which the vapor from one effect is used as the heating medium for a subsequent effect for boiling at a lower temperature. The numbers for the effect and the stage in a multiple-effect evaporator need not be the same.

Evaporators may be rated on two bases, steam economy or evaporation capacity (Standiford, 1973). The steam economy of an evaporator may be measured in the number of kilograms of water evaporated per kilogram of steam supplied and evaporation capacity may be measured by the number of kilograms of water evaporated per hour (or per square meters per hour). The economy of evaporators operated under vacuum is in the order of 0.75 to 0.95 N where N is the number of effect. For example, in a single-effect evaporator, the economy is about 0.75 to 0.95; and a six-effect evaporator is in the range of 4.5 to 5.7. Variations of steam economy are due to many factors such as feed temperature, insulation, venting, vacuum leakage, age of evaporator, with or without heat recovery design, and so on. The steam consumption, in kilograms per hour, is also an important measure. It equals the capacity divided by the economy.

6.1.3   LIQUID CHARACTERISTICS

Liquid food characteristics are major factors affecting the selection of a particular type of evaporator. Some of the most important properties of liquid foods are as follows.

6.1.3.1   Concentrative Properties

Thermal and rheological properties of most liquid foods change with both temperature and solids content (Okos, 1986). In general, the specific heat of liquid foods decreases with higher solids content. A typical equation of specific heat for sugar-containing solutions was presented by Chen (1993):

$$cp = 4.187\left\{1 - x_s\left[.57 - .0018(T - 20)\right]\right\} \tag{6.1}$$

where c_p = the specific heat (kJ/kg°C), T = temperature (°C) and X_s = weight fraction of soluble solids.

The specific gravity or density of liquid foods increases with solids content. Several scales have been developed to relate the measured specific gravity or density to the concentration of various solutions. For example, the Quevenne scale is an abbreviated specific gravity scale used primarily by the milk industry; the Brix scale is being used by the fruit-juice industry in determining the sucrose equivalent of soluble solids in the juice. The term "Brix" or "degrees Brix (°B)" is being used interchangeably with the percent sucrose or the soluble solids by weight in fruit juices and is determined by using density measurements.

The viscosity of most liquid foods such as fruit and vegetable juices increases drastically with solids content at lower temperatures (Chen, in Nagy et al., 1993). High viscosity affects not only the rate of heat transfer but also may become too viscous for flow. Adequate feed flow is a necessity in achieving complete coverage of the heat transfer surface during evaporation to prevent local burn-on or localized overheating of the product.

The vapor pressure of most aqueous solutions is less than that of water at the same temperature. Consequently, for a given pressure the boiling point of the solutions is higher

than that of pure water. The increase in boiling point over that of water is known as the boiling point rise (BPR) of the solution (McCabe and Smith, 1976). The boiling point of liquid foods may also rise considerably as the solid content increases. The boiling point rise must be subtracted from the temperature drop that is predicted from the steam tables in design calculations.

6.1.3.2 Temperature-Time Effects

Most desirable food-quality attributes such as flavors, colors, nutrients, etc., are heat sensitive which may be degraded when heated to moderate temperatures for relatively short residence times. Optimum quality is obtained when processing times and temperatures are kept as low as possible during concentration of the products. In general, a high temperature short time (HTST) vacuum evaporator system is favored over the traditional low temperature long residence time vacuum evaporator system.

6.1.3.3 Foaming

Some materials, especially protein-containing liquid foods, may foam during agitation and vaporization. A stable foam accompanies the vapor out of the evaporator, causing heavy entrainment. In extreme cases, the entire mass of liquid may boil over into the vapor outlet and be lost. Use of antifoam agents can be of some value, but their choice is limited to those acceptable for food use.

6.1.3.4 Scale

Some solutions deposit scale on the heating surfaces of evaporators. The overall heat transfer coefficient then steadily diminishes until the evaporator must be shut down and the heating surfaces cleaned. Scale may also be a result of local burn-on due to improper operation; and when the scale is hard and insoluble, the cleaning is difficult and expensive.

6.1.3.5 Fouling

Fouling may be defined as the formation of deposits on heat transfer surfaces which impede the transfer of heat and increase the resistance to fluid flow. Fouling of heat transfer surfaces by biological fluids is a complex phenomenon. In many instances, chemical kinetics are involved as well as solubility characteristics and corrosion properties. Cleaning schedules must be formulated and maintained to restore the desired evaporator performance.

6.1.4 QUALITY AND FLAVOR RECOVERY

In food applications, the liquid being evaporated usually contains flavorful heat-sensitive materials in a large amount of water. The water and volatile flavors are removed by the addition of heat through the condensing steam. During the process of evaporation, many of the natural flavor or odor components are removed with the water. However, the loss of volatiles during evaporation of most liquid foods, i.e., coffee or fruit juices, in most cases, are undesirable. Therefore, various systems have been developed for the recovery of volatiles during evaporation processes. The volatiles recovered during the manufacture of fruit juice concentrate are referred to as essence. An essence recovery unit is a combination of stripping, rectification, steam distillation, and solvent extraction occurring simultaneously (Redd and Hendrix, 1993).

In concentration of most fruit juices, the recovery of aroma of volatiles generated in the first effect of a multiple-effect system is accomplished. This vapor fraction is then passed to a recovery system such as fractional distillation. In fractional distillation, the diluted aroma

compounds are passed through a distillation column where the aroma compounds are concentrated 100- to 200-fold, which can be added back to the concentrate produced in the last effect. The term "fold" is referred to as the ratio of volume reduction, for example, a five-fold concentrate has had its volume reduced by 80%. To prevent heat damage and oxidation of the diluted aroma compounds, a separation process is carried out under vacuum and desirable vapors are condensed at low temperatures.

Volatile recovery system is not always needed in food applications. The removal of unpleasant volatile substances, e.g., during evaporation of milk, may be an advantage.

6.2 EVAPORATOR SYSTEMS AND APPLICATIONS

6.2.1 Evaporator Systems: Single-Effect or Multiple-Effect

An evaporator may be designed for use as a single-effect system or several evaporator bodies connected to form a multiple-effect system. They may be operated as once-through or as recirculation units. The circulation may be induced by natural convection or by mechanical forces.

Multiple-effect evaporators are widely used in large operation and the principles are well known. Two or more single-effect evaporators may be connected so that the vapor from one effect serves as the heating medium for the next effect and so on. A condenser and air ejector establish a vacuum in the last effect and withdraw noncondensible from the system. The first effect of a multiple-effect evaporator is the effect to which the live steam is fed and in which the vapor pressure is the highest. In this manner, the pressure difference between the steam and the condenser is spread across two or more effects in the multiple-effect system. The pressure in each effect is lower than in the effect from which it receives steam and above that of the effect to which it supplies vapor.

The temperature of the steam is determined by measuring the pressure in the steam space and calculating the temperature by the use of steam tables. The temperature of the boiling liquid is determined by measuring the pressure in the vapor space and calculating the corresponding temperature of the liquid from the steam tables. The difference of these two is known as the apparent temperature drops.

6.2.2 Evaporator Types

There is no single type of evaporator which is satisfactory for all conditions or all kinds of liquid-food materials. Quality, heat transfer property, energy, and cost factors determine the choice of various types of evaporators for a particular application. Both tubular and plate-type steam-heated heat exchangers have been used. Major manufacturers for evaporators are APV Crepaco, Inc. (Chicago, IL), Alfa-Laval, Inc. (Fort Lee, NJ), Cook Machinery (Dunedin, FL), Dedert Corp. (Olympia, IL), FMC (San Jose, CA), GEA Food and Process Systems Corp. (Columbia, MD), Niro Evaporators, Inc. (Columbia, MD), Signal Swenson Div. (Harvey, IL), Tito Manzini & Figi S.P.A. (Parma, Italy), etc. Some common types of evaporators (Milton, 1986; McCabe and Smith, 1976; Standiford, 1973) are described.

6.2.2.1 Short-Tube Evaporator

This is one of the first evaporators ever developed and is often called short-tube evaporator or calandria evaporator (Figure 6.1). It operates at higher temperatures and is used with products that are not sensitive to heat such as sugar solutions. They are usually used in multiple-effect systems. It consists of a vertical body with an array of tube bundles 2.5 to 3.5 m long and 33 to 46 mm inside diameter (ID). The liquid is fed into the lower part of the calandria where it starts to be heated and boils as it rises to the top of the evaporator, the
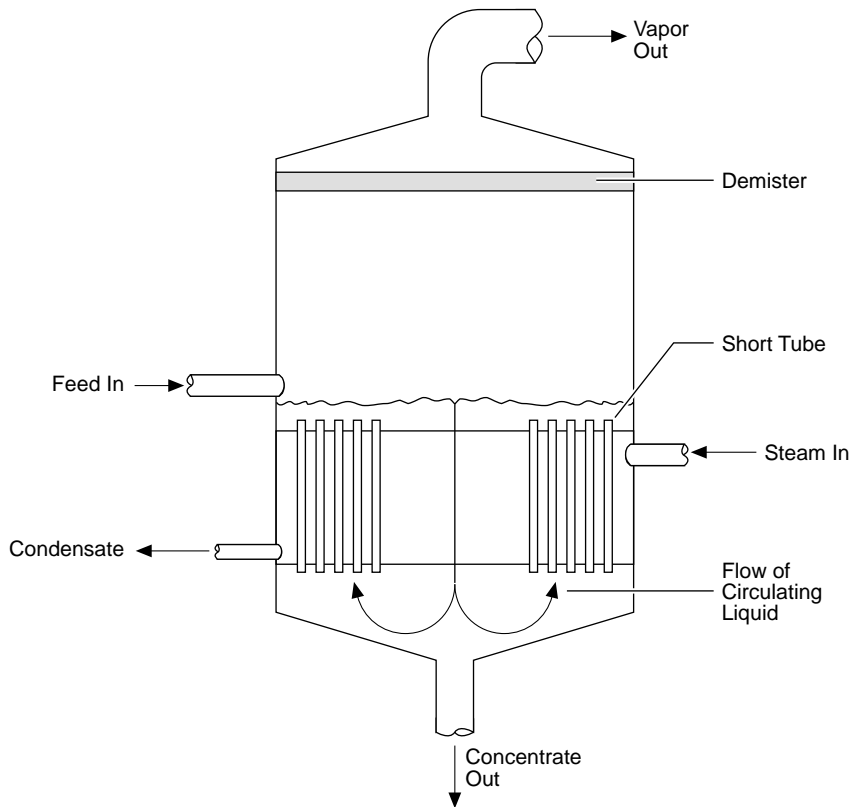
FIGURE 6.1 A schematic diagram of a typical vertical short-tube evaporator (Swenson Evaporator Co.) (From Milton, P.E., 1986, *Handbook of Evaporation Technology,* Noyes Publications, Fairview, NJ. With permission.)

vapor produced escapes to the top of the dome where a deflector separates any entrained liquid in the vapor. The concentrate exits down the central well and is either recirculated or fed to a subsequent effect. High residence times (10 to 20 min) in these types of systems make them less suitable for heat sensitive liquid food. Most of the concentration of cane sugar solutions use this type of evaporator. Overall heat transfer coefficients ranging from 1000 to 1500 W/m^{2}K are commonly found.

6.2.2.2 Falling Film Evaporator

The long-tube vertical (LTV) evaporator is commonly found in the food industry. This type of evaporator is used for heat sensitive products. The tubes are typically 3.5 to 12 m long with 25 to 50 mm ID. In a falling film type (Figure 6.2), the liquid is fed into the top of the tubes and falls down as a film in the inside walls. As liquid enters the top of a falling film evaporator, a liquid film formed by gravity flows down the heat transfer surface. During evaporation, vapor fills the center of the channel and as the momentum of the vapor accelerates the downward movement, the film becomes thinner. The holdup times are usually small (0.5 to 2.0 min) and the boiling temperature is basically the same as the vapor head. A common problem encountered with this type of evaporator is plugging of the distribution system by suspended or undissolved solids and it requires systematic and efficient cleaning. Problems of feed distribution on the walls of the tubes where evaporation is taking place can be overcome with the use of spray nozzles to feed the liquid into each of the tubes. Another alternative is the use of a perforated plate on top of the tubes with orifices at the inlet of each tube.

FIGURE 6.2   A schematic diagram of a typical falling film type evaporator. (From Milton, P.E., 1986, *Handbook of Evaporation Technology,* Noyes Publications, Fairview, NJ. With permission.)

Overall heat transfer coefficients of 2500 W/m²K are commonly found in the first effect and values of 1000 W/m²K are typical in the last effect of a multiple-effect system. This evaporation system is commonly used in the concentration of milk and fruit juices.

6.2.2.3   Forced-Circulation Evaporator

This type of evaporator (Figure 6.3) is used for viscous liquids or for products with suspended solids and shows less fouling, scaling, or salting than natural recirculation evaporators. The liquid can be pumped through the heating element at a constant rate regardless of the evaporation rate; this makes it easier to analyze and control. Fluid velocities in the tubes can exceed 5 m/s. This system is usually designed so that the liquid recirculates through the heating element under pressure; no boiling takes place until the product reaches the separating chamber where vapor flashing occurs. The heating element can be external or internal and vertical or horizontal depending on the intended use. Viscous liquid foods, i.e., tomato products, are commonly evaporated with this type of system. Average heat transfer coefficients above 2000 W/m²K have been reported. Forced circulation evaporators normally are more expensive than film evaporators because of the need for large bore circulating pipework and large recirculating pumps. Operating costs of such a unit also are considerably higher.
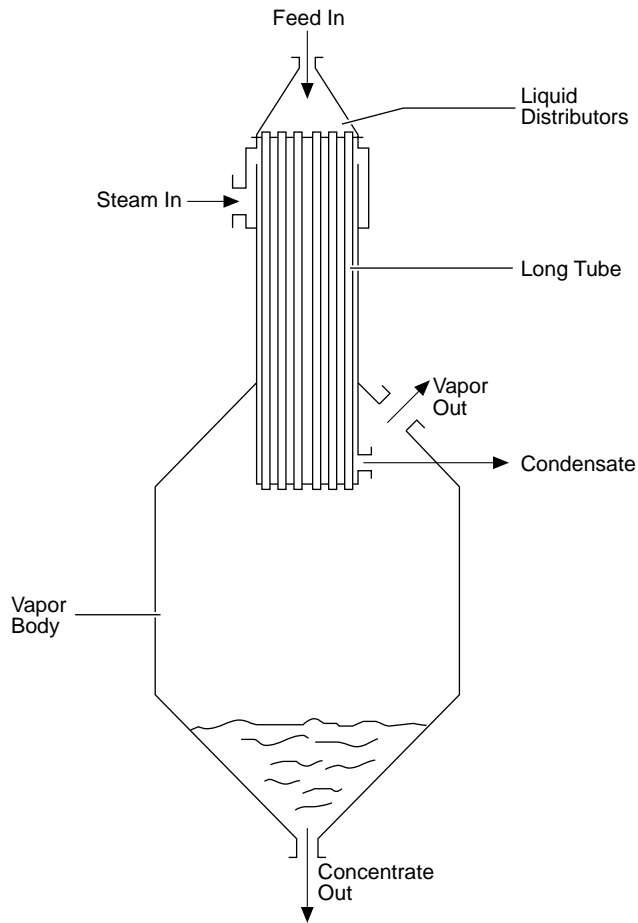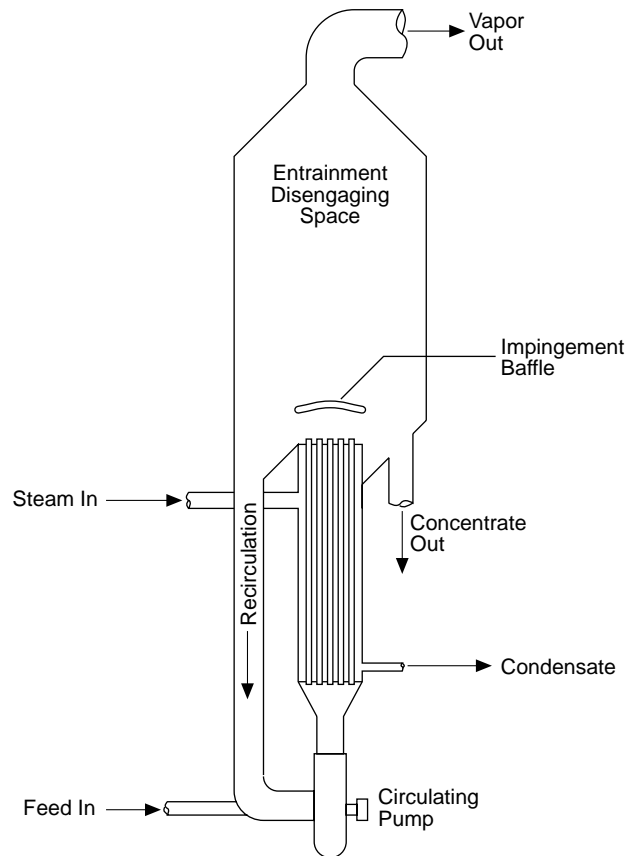
FIGURE 6.3 A schematic diagram of a forced long-tube type evaporator (Swenson Evaporator Co.) (From Milton, P.E., 1986, *Handbook of Evaporation Technology,* Noyes Publications, Fairview, NJ. With permission.)

6.2.2.4 Rising Film Evaporator

These evaporators are also long-tube type and operate at high vacuum (Figure 6.4). They can be used in recirculation or single pass systems and in single- or multiple-effect modes. They are commonly used for the evaporation of tomato and fruit juices. Typical evaporators have vertical stainless steel tubes 6 to 12 m long. In this system, the liquid is pumped to the bottom of the evaporator and rises through the tubes under vacuum. Two zones are identified in the tubes, a liquid zone where the feed is rising and a boiling zone at the top of the evaporator where a two-phase flow takes place. Therefore, temperature differences and overall heat transfer coefficients can be quite different at the bottom and top of the evaporator. Because static head and pressure drop boiling points increase at the bottom of the evaporator by 5 to 10°C and holdup times vary between 2 to 3 min. Average heat transfer coefficients of up to 1800 W/m^{2}K have been reported.

6.2.2.5 Mechanically Assisted Evaporator

Agitated film evaporators such as the scraped surface type are used to concentrate liquids that are heat sensitive and viscous and where foaming of the evaporating liquid can be a problem. It consists of a large-diameter steam-jacketed tube, usually vertical. The liquid is normally fed to the top and is spread on the walls into a thin film by rotating blades. The

FIGURE 6.4 A schematic diagram of a typical vertical long-tube evaporator (Swenson Evaporator Co.) (From Milton, P.E., 1986, *Handbook of Evaporation Technology,* Noyes Publications, Fairview, NJ. With permission.)
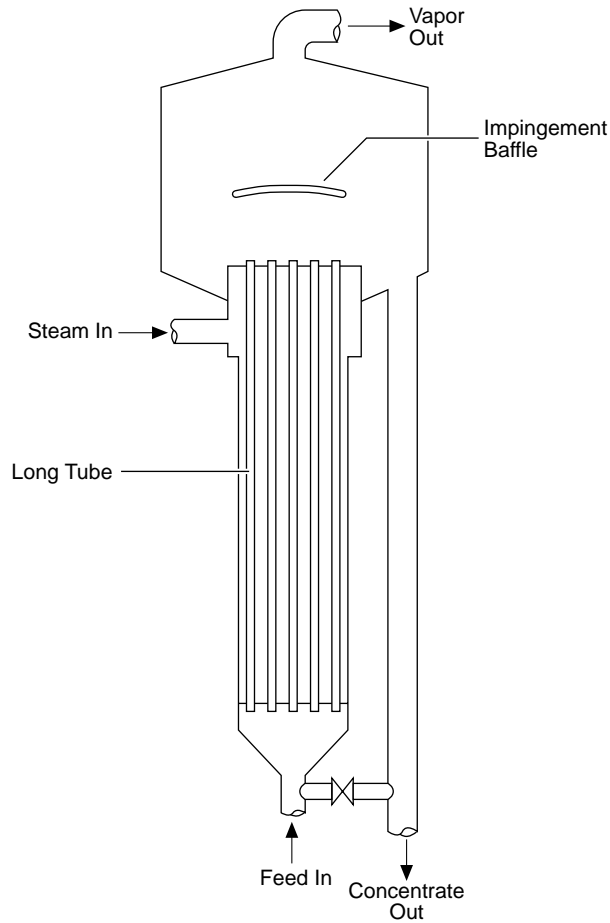
concentrated product exits at the bottom of the evaporators into a separating chamber fitted with a deflector where the vapor is separated from the concentrated product and flows into a condenser. Rotor speeds in the order of 10 to 15 m/s are normally found. Residence times of only a few seconds permit the use of high temperature differences. This type of evaporator is usually operated in a single-effect mode. The expensive construction and high maintenance cost reduce the use of this type of evaporator to a few applications for concentration of heat sensitive liquids. This evaporator is used to concentrate heat sensitive liquid foods with suspended solids with viscosities of up to 20,000 mPa·s. Overall heat transfer coefficients of up to 4000 W/m^{2}K have been reported.

6.2.2.6   Plate-Type Evaporator

Other variations of the units described above are used in the food industry such as the plate evaporators where the feed is force-circulated through a plate heat exchanger and then is flashed into a separation chamber. Plate evaporators initially were developed by APV in 1957 to provide an alternative to the tubular systems. The plate evaporator can provide flexible capacity merely by adding more plate units and a more compact design with low headroom requirements.

6.2.3 ENERGY CONSERVATION AND VAPOR RECOMPRESSION

Evaporation consumes a large amount of energy in liquid food processing industries (Schwartzberg, 1977). Approximately 3.5 kJ are spent in generating 1 kJ of electrical energy and the amount of energy required to evaporate 1 kg of water can be estimated from the latent heat of vaporization of water (2257.1 kJ/kg at 100°C). The conversion of fuel into steam usually takes place at approximately 80% efficiency due to energy losses. To prevent thermal degradation of liquid foods and reduce energy requirements, a vacuum is drawn on the equipment for lowering the boiling point which enables one to reuse the vapor for conserving the heat energy necessary for evaporation by using a multiple-effect design. For intermediate to large size evaporator applications, it is common to choose a multiple-effect system — usually one with two to seven effects.

The vapor exiting the evaporator contains significant heating value as latent heat of vaporization. This energy can be recovered by heat-recovery techniques, i.e., incorporating interstage preheaters and reheaters in the design of a multiple-effect multiple stage system (Chen, 1982a). The other methods for reusing a fraction of this vapor are by vapor recompression (Anon., 1977):

- Thermal vapor recompression (TVR)
- Mechanical vapor recompression (MVR)

Of the two vapor-recompression methods, TVR requires less capital but yields lower heat recovery than does MVR. The addition of a thermal compressor will provide an improved steam economy approximately equivalent to the addition of one extra effect but at a considerably lower cost. A steam-jet ejector is used to compress a fraction of the vapor leaving the evaporator so that the pressure and temperature are raised. TVR is normally applied to the first effect on existing evaporators or where the conditions are right for the application in single-effect units.

In most mechanical compression operations, all the vapor leaving the evaporator is compressed. Compression raises the pressure and saturation temperature of the vapor so that it may be returned to the evaporator system chest to be used as heating steam. Under optimum conditions, the equivalent of up to 20 effects can be achieved by MVR. This high energy recovery must be balanced against the capital, maintenance, and electrical energy costs for the compressor. The vapor leaving the compressor is super heated, but this usually has no appreciable effect on heat transfer rates.

6.2.4 APPLICATIONS

Evaporators with tubular heating surfaces are the most widely utilized in food fields. Stainless steel surfaces are used for food contact almost exclusively. The feed may be single pass or recirculated. Circulation of the liquid past the surface may be induced by boiling (natural circulation) or by mechanical methods (forced circulation). In forced circulation, boiling may or may not occur on the heating surface.

In some situations, it is convenient to use a combination of the evaporators just described. For example, for the production of tomato paste, it is common to use a recirculation evaporator to concentrate to about 20% solids followed by mechanical agitation to produce tomato paste over 30% solids.

The fruit juice processing industry is one of the world's major agro-based businesses. The modern development of fruit juice processing industries has evolved with the production of fruit juice and essence concentrates as valuable semifinished products (Nagy et al., 1993). World trade in fruit juice concentrates increased nearly four-fold between 1977 and 1988, reaching US $4 billion (Olesen, 1990). Orange juice concentrate produced by evaporation is

the dominant fruit juice concentrate traded worldwide. Evaporator installations in the citrus processing industry are very large; five to seven effect evaporators are commonly installed.

A special type of evaporator, which incorporates a section of heat exchanger for pasteurization prior to evaporation and also includes a distillation unit for essence recovery from evaporated vapor in a complete system design, was developed in the early 1960s and commercially installed in the citrus processing industry (Chen, 1982b). These evaporators employ the HTST principles with either tubular or plate heat surfaces. The highest juice temperature regime in the evaporator system is in the range of 95 to 105°C for 10 sec. with the residence time of 6 to 10 min.

The most commonly used citrus evaporator is called TASTE which is an acronym for Thermally Accelerated Short Time Evaporator. The TASTE system can be generally described as a continuous, single pass, LTV falling film type, multiple-effect multiple stages, high vacuum no vapor recompression, HTST evaporator. The TASTE systems are developed by R. W. Cook of Cook Machinery in FL (Dunedin, Florida) and are assembled in stacks and installed without covered structure. A typical TASTE system installed in a citrus processing plant is shown in Figure 6.5. Evaporation capacity of an average citrus concentrate plant is approximately 40 to 50 ton/h with two to three evaporators installed.

A new HTST evaporator system for citrus juice concentration was introduced in Brazil in 1990 by GEA Food and Process Systems Corp. (Columbia, MD). This new system is known as GEA Wiegand evaporator (Wiegand, 1992). A typical 5-effect unit with TVR is shown in Figure 6.6. Its capacity is approximately 26,500 kg/h water evaporating rate for the production of a 65°B (i.e., % soluble solids by weight) juice concentrate at an hourly output rate of 4500 kg/h and its steam economy is 6.44:1 which is equivalent to a conventional 7-effect TASTE evaporator without vapor recompression. The GEA Wiegand TVR evaporator can be generally described as a continuous, single pass, LTV falling film type, multiple-effect multiple stages, high vacuum with TVR, HTST evaporator.

6.2.5 STABILITY AND CONTROL

Multiple-effect evaporator systems are sensitive to changes in operating conditions, that is why most of them are difficult to control. Various control strategies from simple feedback to more complex feed forward controls have been applied to control evaporator systems (Shinskey, 1978). The main goal of evaporator control is one of adjusting the heat load to achieve a desired product concentration despite changes in input variables or equipment efficiency. There is a measurable residence time between thin feed entering and thick product leaving the evaporator. This lag complicates the control problem using standard techniques, as does the fact that mass transfer responds much more quickly to demand changes than does energy transfer. Feedback control techniques have been applied to control commercial multiple-effect citrus evaporator systems (Chen et al., 1981).

6.2.6 SELECTION OF EVAPORATORS

Evaporator systems are major pieces of process equipment and are often purchased on a total responsibility basis. The purchaser's task is to define the process, quality, and mechanical limitations accurately to enable the vendors to engineer economical and suitable systems for the intended duty.

The selection and comparing vendor's offerings of an evaporator should include the following considerations (Minton, 1986)

1. Compare initial capital cost and operating cost
2. Check to see that specifications have been met. Some important specification considerations are

FIGURE 6.5 Typical citrus TASTE evaporator showing stacked design (Courtesy of Alcoma Packing Co., Lake Wales, FL).

    a. Operation capacity

    b. Product viscosity, suspended solids and density (i.e., as percent of solids content by weight

    c. Temperature-time profile as related to product quality

    d. Cooling water temperatures
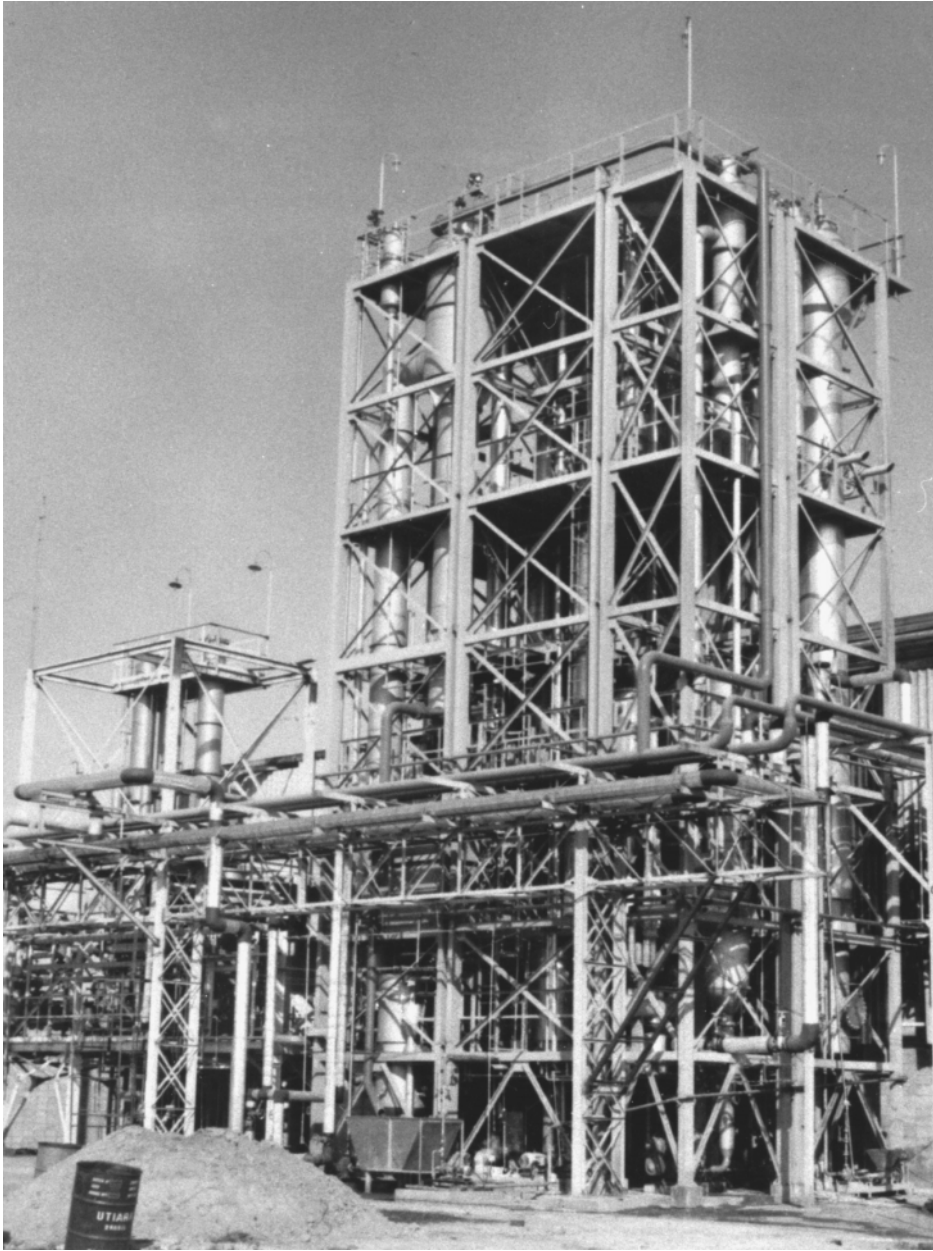
FIGURE 6.6 GEA Wiegand citrus evaporator — a thermal vapor recompression (TVR) evaporator. (GEA Food and Process Systems, Columbia, MD) (From Nagy, S., Chen, C.S., and Shaw, P.E., Eds., 1993, *Fruit Juice Processing Technology,* Agscience, Auburndale, FL. With permission.)

    e. Steam levels and requirements
    f. Materials of construction
    g. Condenser type
    h. The volatile recovery requirements
    i. Headroom requirements (e.g., indoor or outdoor)
    j. Any special requirements
  3. Maintenance considerations
    a. Manual vs. automatic control

b. Reliability and simplicity of operation
c. Sanitation, ease of cleaning, and cleaning cycle
d. Safety requirements
4. Service after sale and guarantees
a. Start up assistance
b. Spare parts availability
c. Engineering expertise and response to problems
d. Personnel training

Typical types of evaporators used in the food industry are listed in Table 6.1 and may be used as a guide for selection (Dinnage, 1972).

6.3 HEAT TRANSFER COEFFICIENTS IN EVAPORATORS

6.3.1 OVERALL HEAT TRANSFER COEFFICIENT

A practical presentation of the fundamental heat transfer principles underlying basic evaporation method and equipment has been given by Badger and Banchero (1955). The general equation describing heat transferred from the heating steam through the metal wall to the product being evaporated is

$$Q = V_o \, \lambda_s = UA(T_s - T) = UA\Delta T \tag{6.2}$$

where Q = rate of heat transfer, V_o = condensed steam rate, λ_s = the latent heat of vaporization of steam at condensing temperature, U = overall heat transfer coefficient, A = heating surface area, T_s = condensing steam temperature, T = product evaporating temperature, $\Delta T = T_s - T$, temperature drop.

The overall heat transfer coefficient for condensing steam through a heating surface to liquid foods may be written as

$$1/UA = 1/h_s \, A_s + x/kA_m + 1/h_f \, A_f \tag{6.3}$$

where A_m = the mean area for the steam and product sides of the heat exchange surface, A_s = steam-side heat transfer area, h_s = steam-side heat transfer coefficient, k = thermal conductivity of the wall material, x = thickness of the wall, h_f = liquid-side heat transfer coefficient, and A_f = liquid-side heat transfer area. In the calculation of commercial heat transfer equipment, the question often arises as to whether the inside, the outside, or the mean surface area of the tube should be used as a basis for design. It is suggested that Equation 6.3 be used to calculate the total length of the tube required. For tubular evaporators, Equation 6.3 becomes:

$$\frac{1}{U_o} = \frac{1}{h_s} + \frac{d_o}{2k \, \ln(d_o/d_i)} + \frac{d_o}{h_f d_f} \tag{6.4}$$

where d_o = outside heat transfer tube diameter and d_i = inside heat transfer tube diameter.

Local heat transfer coefficients are generally expressed as dimensionless parameters, $h^* = hd/k$, usually in function of the Reynolds (Re) and Prandtl (Pr) numbers,

$$h^* = a \, Re^b \, Pr^c \tag{6.5}$$

where a, b, and c = experimental constants.

TABLE 6.1
Types of Evaporators Employed in Concentrating Liquid Foods

Evaporator type	Circulation assisted	Typical residence time (min)	Applicable to multiple effect	Can handle suspended solids	Viscosity capability approx (cps)	Heat transfer rate	Capital cost
Calandria (short-long tube)	Natural	40	Yes	Yes	100	Good	Low
Calandria	Assisted	40	Yes	Yes	600	Good	Medium
Calandria	Forced	60	Yes, but limited	Yes	600	Poor	Medium
Falling film tube	None	0.5	Yes	Limited	2,000	Excellent	Low-Medium
Rising-falling film tube	None	1.5	Yes	Limited	2,000	Good	Low-Medium
Rising film	None	1.0	Yes	Yes	1,000	Good	Low-Medium
Mechanically agitated film	None	1.5	No	Yes	20,000	Good	High
Rising-falling film plate	None	0.5	Yes	Limited	2,000	Good	Low-Medium
Paravap	None or Medium	0.1	No	Yes	10,000	Excellent	Medium

Adapted from Dinnage, D.F., *Proc. 20th Annu. Nat. Dairy Eng. Conf.,* MSU, East Lansing, MI, 1972.

TABLE 6.2
Local Heat Transfer Coefficients

$$h_s^* = 1.13 \left(\frac{\rho^2 g \lambda L^3}{\mu_c k_c (T_s - T_w)} \right)^{1/4}$$

Condensing steam on vertical tubes, laminar flow, Re < 1800 (McAdams, 1954)

$$h_s^* = 0.007 \frac{(\rho^2 g L^3)}{\mu_c^2} Re^{0.4}$$

Condensing steam on vertical tubes, turbulent regime, Re > 1800 (McAdams, 1954)

Condensing steam on horizontal tubes (McAdams, 1954)

$$h_s^* = 0.725 \left(\frac{\rho^2 g \lambda D^3}{N \mu_c k_1 (T_s - T_w)} \right)^{1/4}$$

$h^* = 0.0086 \, Re^{0.8} \, Pr^{0.6} \, (\sigma_f/\sigma)$ — Natural circulation evaporators (Piret and Isbin, 1954)

$h^* = 0.023 \, Re^{0.8} \, Pr^{0.4}$ — Forced circulation evaporators (Coulson and Richardson, 1978)

$h^* = 0.042 \, Re^{0.17} \, Pr^{0.53}$ — Free falling film, turbulent range, Re < 10^4 (Muddawar and El-Masri, 1986)

$h^* = 8.5 \, Re^{0.2} \, Pr^{1/3} \, (V_s/V_f)^{2/3}$ — For climbing film evaporators (Burgois and Le Maguer, 1987)

$h^* = 3103 \, Re_f^{-0.98} \, Re_R^{0.40} B^{-0.326} We^{0.494}$ — For scraped surface heat exchangers (Skoczylas, 1970)

Note:

a   Experimental constant
B   Number of blades in scraped surface evaporator
D   Tube diameter, m
h   Heat transfer coefficient, W/m²K
h* Dimensionless heat transfer coefficient
L   Tube length, m
N   Number of tubes
Re Reynolds number
Pr Prandtl number
We Webber number
g   Acceleration of gravity, m/s²
k   Thermal conductivity, W/mK
T   Temperature, °C
V   Vapor flow rate, kg/h

Greek letters

μ   Viscosity, mPa·s
λ   Latent heat of vaporization, kJ/kg
ρ   Density, kg/m³
σ   Surface tension

Subscripts

c   Condensate
f   Feed
l   liquid
R   Rotor
s   Steam side
w   Wall side

Table 6.2 shows some equations for h^* for different applications and types of evaporators.

In most cases, in food applications, the middle term on the right hand side of Equation 6.3 is too small to be of practical significance. Furthermore, the steam-side heat transfer coefficient is so much higher than the liquid-side heat transfer coefficient that the latter is essentially equal to the overall heat transfer coefficient. In such cases, reasoning based on the overall heat transfer coefficient is nearly as satisfactory as if the liquid-side heat transfer coefficient itself were available. Thus, in practice, the overall heat transfer coefficient is used

TABLE 6.3
Typical Heat Transfer Coefficients for Evaporative Concentration of Liquid Foods

Product	Concentration (%)	Product temperature (°C)	ΔT (°C)	Evaporator type[a]	U (W/m²·°C)	Tube length (m)
Dextrose	27–35	93	28	FF SP	1136	6.1–8.5
	49–78	57	22	FF SP	795	6.1–8.5
Corn syrup	35–43	57	22	FF SP	568	6.1–8.5
	57–82	93	28	FF SP	1022	6.1–8.5
Skim milk	88–212	68	14	RF SP	2158	3.0
	21.2–44	46	22	RF SP	988	3.0
Corn steep liquor	7.7	104	17	FF REC	1420	6.1–8.5
	50	57	19	FC	1022	—
Sugar	67	57	11	CAL	1476	0.6
	33	57	11	CAL	3407	0.6
	19	100	21	RF REC	2726	6.1
	50	43	19	RF REC	636	6.1
	39.5–67	93	22	FF SP PAN	943–477	2.4
	39.5–67	93	22	FF REC PAN	1124–676	2.4
Tomato paste	5–8.7	93	28	RF REC	1408	—
	8.7–20	77	17	FC	1022	—
	20.7–28	54	22	FC	721	—
	8	108	34	FC	3009	—
	12.5	87	18	FC	2413	—
	30	53	33	RF REC	823	—
Gelatin	2.75–4	92–104	7.38–9.7	RF SP	1959–2129	6.4
	4–6.4	78–95	8.9–13.3	RF SP	852–1334	6.4
	6.4–19.5	44–52	30.6–43.3	RF SP	159–244	6.4
Stick water	2–35	43–96	25–27.8	FF SP	909	6.1

Note: FF = Falling film; RF = Rising film or thermosyphon; FC = Forced-circulation; SP = Single pass; REC = Recirculating; PAN = Panel-type heat exchange surface; CAL = Calandria.

From Schwartzberg, 1977, *Food Tech.,* Mar: 67–76. With permission.

in design calculation. Table 6.3 shows typical heat transfer coefficients for evaporative concentration of liquid foods (Schwartzberg, 1977).

6.3.2 BOILING-POINT RISE

The BPR caused by a nonvolatile solid in food solutions follows the well-known solution theory. For food solutions, the BPR can be predicted by the following relationship (Chen, 1993)

$$\Delta T_b(°K) = -\left(K_v/M_w\right) \ln a_w \tag{6.6}$$

where $\Delta T_b = T - T_b$, boiling-point rise; T_b = boiling point of water, T = boiling temperature of the liquid; $K_v = 512$ kg K/kg-mol, a constant for boiling-point rise; $M_w = 18$, molecular weight of water; a_w = water activity of food solutions ($0 \le a_w \ge 1$) which is a function of soluble solids content. An empirical equation for the BPR of sugar solutions expressed as a function of solids content is given as

$$\Delta T_b(°C) = 0.33 \exp\left(4 X_s\right) \quad ; \quad 0.1 \le X_s \ge 0. \tag{6.7}$$

where X_s = weight fraction of soluble solids.

Duhring charts are commonly used to estimate boiling-point rise due to dissolved solutes and work fairly well for simple solutions of sugar and salts (McCabe and Smith, 1976).

6.3.3 THE EFFECT OF FOULING

One of the problems in the food evaporative process is the effect of fouling or scale formation on the rate of heat transfer. Fouling of evaporator tubes by heat sensitive food materials is observed whenever viscous liquids receive heat while flowing inside evaporator tubes. Production rates and product quality can be affected markedly by the accumulation of denatured material on the surface of the tubes. The effect of fouling on the rate of heat transfer with time is represented by the equation (Kern, 1950)

$$1/U^2 = a + b\,\Theta \tag{6.8}$$

where U = the heat transfer coefficient at any time, Θ = time (hours) in operation, a and b = constants. The effect of fouling can also be expressed as a fouling induced resistance as

$$R_f = \frac{1}{U} + \frac{1}{U_o} \tag{6.9}$$

where R_f = the fouling resistance, U_o = the overall heat transfer coefficient for a clean tube.

6.4 DESIGN CALCULATION OF EVAPORATORS

Evaporator calculations and analysis are often required in design and in evaluating evaporator performance. The conditions under which evaporation is carried out in practice are widely varied. Two types of analysis may be performed on an evaporator system: dynamic and steady-state analysis. The dynamic analysis can lead to the development of models for predicting the dynamic behavior of the system to an upset in any of the operating variables which is useful in unsteady state operation. However, a steady-state condition is normally reached within a short period of time in evaporator operations. When a multiple-effect evaporator system is in steady state operation, the pressure (and therefore the temperature) of the steam to the first effect can be set, and the pressure (and therefore the temperature) of the vapor leaving the last effect is determined by the available cooling water temperature. Thus, the available ΔT is practically fixed at a predetermined range. It is important to recognize the fact that there is no external control of the distribution of temperature between effects. Steady state analyses are widely used in evaporator calculations which are described in this section (Kern, 1950; Holland, 1975).

6.4.1 THE MATERIAL AND ENERGY BALANCES

A schematic diagram of a typical single-effect evaporator illustrating the energy and material flows is shown in Figure 6.7. The rate of steam flow and of condensate is V kg/h; that of the feed (thin liquor) is F kg/h; and that of the concentrate (thick liquor) is L kg/h. The rate of vapor flow to the condenser, assuming that no solids precipitate from the liquor, is V = (F – L) kg/h. Also, let T_s be the condensing temperature of the steam, T the boiling temperature of the liquid in the evaporator, and T_f the temperature of the feed, all in degrees Centigrade.

The material and energy balances may be developed for describing this single-effect evaporator in the following manner. Component material balances on the solute (solids) and the solvent (water) are

$$FX_f = LX_p \tag{6.10}$$

and

$$F(1 - X_f) = V + L(1 - X_p) \tag{6.11}$$

where X_f = weight fraction of the solute in the feed and X_p = weight fraction of the solute in the thick liquor. A total material balance is given by

$$F = V + L \tag{6.12}$$

The calculation of the amount of evaporation is fundamental in any evaporation problem and it is easy to demonstrate that the amount of evaporation in concentrating a solution from 5 up to 10% total solids is the same as concentrating a solution from 30 to 60%. A formula for this calculation can be derived from Equations 6.11 and 6.12

Evaporation rate

$$V = F(1 - X_f/X_p) \tag{6.13}$$

Feed rate

$$F = V/(1 - X_f/X_p) \tag{6.14}$$

Table 6.4 gives the amount of evaporation for kilograms of water evaporated per 1000 kg of feed at varying percent compositions when concentrated to higher densities.

The energy balance may be written in terms of latent heat of vaporization and specific heat as follows

$$Q = V_o \lambda_s = (F - L)\lambda + Fc_p(T - T_f) \tag{6.15}$$

where V_o = steam rate (kg/h) and c_p = specific heat of feed. Thus, the steam requirement is

$$V_o = [(F - L)\lambda + Fc_p(T - T_f)]/\lambda_s \tag{6.16}$$

The steam economy (E) is

$$E = \text{kg evaporation/kg steam} = V/V_o \tag{6.17}$$

Equation 6.13 can be extended to a multiple-effect evaporator for sensitivity analysis of product concentration variation due to steam or feed fluctuation (Shinskey, 1978) as follows

$$\Sigma V_i = F(1 - X_f/X_n) \tag{6.18}$$

where i = 1,2,…,n effects. This equation may be solved for product quality

$$x_n = x_f/(1 - \Sigma V_i/F) \tag{6.19}$$

TABLE 6.4
Evaporation Table: kg Water Evaporated/1000 kg Feed

°Bin feed juice	°Bin Juice Concentrate (% soluble solids by wt)																
	10	12	14	16	18	20	25	30	35	40	45	50	55	60	65	70	75
1	900	917	929	938	944	950	960	967	971	975	978	980	982	983	985	986	987
2	800	833	857	875	889	900	920	933	943	950	956	960	964	967	969	971	973
3	700	750	786	813	833	850	880	900	914	925	933	940	945	950	954	957	960
4	600	667	714	750	778	800	840	867	886	900	911	920	927	933	938	943	947
5	500	583	643	688	722	750	800	833	857	875	889	900	909	917	923	929	933
6	400	500	571	625	667	700	760	800	829	850	867	880	891	900	908	914	920
7	300	417	500	563	611	650	720	767	800	825	844	860	873	883	892	900	907
8	200	333	429	500	556	600	680	733	771	800	822	840	855	867	877	886	893
9	100	250	357	438	500	550	640	700	743	775	800	820	836	850	862	871	880
10		167	286	375	444	500	600	667	714	750	778	800	818	833	846	857	867
11		83	214	313	389	450	560	633	686	725	756	780	800	817	831	843	853
12			143	250	333	400	520	600	657	700	733	760	782	800	815	829	840
13			71	188	278	350	480	567	629	675	711	740	764	783	800	814	827
14				125	222	300	440	533	600	650	689	720	745	767	785	800	813
15				63	167	250	400	500	571	625	667	700	727	750	769	786	800
16					111	200	360	467	543	600	644	680	709	733	754	771	787
17					56	150	320	433	514	575	622	660	691	717	738	757	773
18						100	280	400	486	550	600	640	673	700	723	743	760
19						50	240	367	457	525	578	620	655	683	708	729	747
20							200	333	429	500	556	600	636	667	692	714	733
21							160	300	400	475	533	580	618	650	677	700	720
22							120	267	371	450	511	560	600	633	662	686	707
23							80	233	343	425	489	540	582	617	646	671	693
24							40	200	314	400	467	520	564	600	631	657	680
25								167	286	375	444	500	545	583	615	643	667

Differentiating with respect to $\Sigma V_i/F$ will yield the sensitivity of product concentration to the steam-feed ratio

$$dX_n \big/ d\big(\Sigma V_i/F\big) = X_f \big/ \big(1 - \Sigma V_i/F\big)^2 = X_n^2 \big/ X_f \qquad (6.20)$$

Equation 6.20 facilitates comparison of sensitivities for various operating conditions. An additional relationship is to convert the denominator into a fractional steam-feed ratio. Rearranging Equation 6.18 yields

$$\Sigma V_i/F = \big(X_n - X_f\big)\big/X_n \qquad (6.21)$$

From equations 6.20 and 6.21, one can obtain

$$dX_n \Big/ \big[d\big(\Sigma V_i/F\big)\big/\big(\Sigma V_i/F\big)\big] = \big[X_n\big(X_n - X_f\big)\big]\big/X_f \qquad (6.22)$$

Specific heats for sugar solutions and latent heats of vaporization of saturated steam are widely available. The specific heat values of orange juice are presented in Table 6.5 that may also be used for most fruit and vegetable juices. The latent heats of vaporization of saturated

TABLE 6.5
Specific Heat of Orange Juice at Temperatures of 0–80°C

°B	Temperature (°C)							
(% by wt)	0	5	10	15	20	40	60	80
0	4.186	4.186	4.186	4.186	4.186	4.186	4.186	4.186
5	4.045	4.046	4.048	4.050	4.052	4.060	4.067	4.075
10	3.903	3.907	3.911	3.914	3.918	3.933	3.948	3.963
15	3.762	3.767	3.773	3.778	3.784	3.807	3.829	3.852
20	3.620	3.628	3.635	3.643	3.650	3.680	3.710	3.741
25	3.479	3.488	3.497	3.507	3.516	3.554	3.592	3.629
30	3.337	3.348	3.360	3.371	3.382	3.427	3.473	3.518
35	3.196	3.209	3.222	3.235	3.248	3.301	3.354	3.407
40	3.054	3.069	3.084	3.099	3.114	3.175	3.235	3.295
45	2.913	2.930	2.947	2.963	2.980	3.048	3.116	3.184
50	2.771	2.790	2.809	2.828	2.846	2.922	2.997	3.073
55	2.630	2.650	2.671	2.692	2.713	2.795	2.878	2.961
60	2.488	2.511	2.533	2.556	2.579	2.669	2.759	2.850
65	2.347	2.371	2.396	2.420	2.445	2.543	2.641	2.738

Note: Specific heat in kJ/kgK or kJ/kg°C.

From Chen, C.S., 1993 in *Fruit Juice Processing Technology,* Nagy, S., Chen, C.S., and Shaw, P.E., Eds., Agscience, Auburndale, FL. With permission.

steam at various temperatures calculated from Steam Tables (Keenan et al., 1969) are presented in Table 6.6.

EXAMPLE 6.1

An evaporator concentrates a feed of 10% solids to 70%. Calculate the effect of 1% change in steam flow or feed rate on product concentration.

Solution

$$dX_n \Big/ \Big[d\big(\Sigma V_i/F\big)/\big(\Sigma V_i/F\big)\Big] = \big[0.7(0.7-0.1)/0.1\big] = 4.2$$

A change of 1% in either steam or feed rate can cause product concentration to deviate ± 4.2% from the 70% specification.

6.4.2 TEMPERATURE-TIME RELATIONSHIP

To prevent degradation of heat-sensitive materials during processing, it has long been recognized that a low operating temperature and a short residence time are essential. The residence time achieved in any evaporator can be calculated from the equation below (Milton, 1986):

$$E_f = 1 - Exp(-\theta/r) \tag{6.23}$$

where F_f = fraction of feed removed, θ = residence time, and r = ratio of holding volume to discharge rate (time).

It has been recognized that the time factor is more important than the temperature level in the time-temperature relation, and so the earlier emphasis on maintaining low operating

TABLE 6.6
Latent Heat of Vaporization of Saturated Steam

Temperature °C	Vapor pressure (kPa)	Latent heat (kJ/kg)	Temperature (°C)	Vapor pressure (kPa)	Latent heat (kJ/kg)
10	1.2	2477.8	100	101.3	2257.1
12	1.3	2473.1	102	108.7	2251.8
14	1.5	2468.4	104	116.6	2246.5
16	1.7	2463.7	106	125.0	2241.1
18	2.0	2458.9	108	133.9	2235.7
20	2.3	2454.2	110	143.3	2230.3
22	2.6	2449.5	112	153.2	2224.8
24	3.0	2444.8	114	163.6	2219.4
26	3.4	2440.0	116	174.7	2213.8
28	3.8	2435.3	118	186.3	2208.3
30	4.3	2430.5	120	198.6	2202.7
32	4.8	2425.8	122	211.5	2197.1
34	5.4	2421.0	124	225.1	2191.4
36	6.0	2416.3	126	239.4	2185.7
38	6.7	2411.5	128	254.4	2180.0
40	7.5	2406.7	130	270.2	2174.2
42	8.3	2402.0	132	286.7	2168.4
44	9.2	2397.2	134	304.1	2162.6
46	10.2	2392.4	136	322.3	2156.7
48	11.3	2387.5	138	341.4	2150.8
50	12.5	2382.7	140	361.4	2144.8
52	13.7	2377.9	142	382.3	2138.8
54	15.1	2373.1	144	404.1	2132.7
56	16.6	2368.2	146	427.0	2136.6
58	18.2	2363.3	148	450.9	2120.5
60	20.0	2358.4	150	475.9	2114.3
62	21.9	2353.6	152	501.9	2108.0
64	24.0	2348.6	154	529.1	2101.7
66	26.2	2343.7	156	557.4	2095.4
68	28.6	2338.8	158	586.9	2089.0
70	31.2	2333.8	160	617.7	2082.6
72	34.0	2328.9	162	649.8	2076.1
74	37.0	2323.9	164	683.1	2069.5
76	40.2	2318.9	166	717.9	2062.9
78	43.6	2313.8	168	754.0	2056.2
80	47.3	2308.8	170	791.5	2049.5
82	51.3	2303.7	172	830.5	2042.7
84	55.5	2298.6	174	871.1	2035.9
86	60.1	2293.5	176	913.2	2029.0
88	64.9	2288.4	178	956.9	2022.1
90	70.0	2283.2	180	1002.2	2015.1
92	75.5	2278.1	182	1049.2	2008.0
94	81.4	2272.9	184	1098.0	2000.8
96	87.6	2267.6	186	1148.6	1993.6
98	94.2	2262.4	188	1200.9	1986.4

Calculated from Keenan et al. (1969).
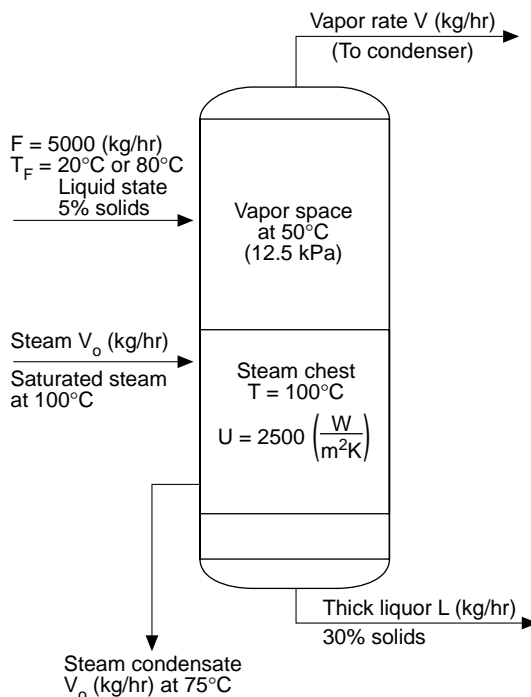
FIGURE 6.7 A schematic diagram of a typical single-effect evaporator showing energy and material flows.

temperatures in evaporators has shifted towards accurate control of low residence times and relatively higher operating temperatures (Chen, 1982b; Chen et al., 1981). This has resulted not only in better products but also lower investment and operating costs.

6.4.3 SINGLE-EFFECT EVAPORATOR

One of the simplest evaporators is a steam-jacketed kettle having its vapor outlet connected to a condenser, with or without vacuum equipment. Its use is limited to batch or semi-batch operations with viscous products such as jam, jelly, and various syrups. Even in these applications, however, it is gradually being replaced by continuous single-effect evaporators.

EXAMPLE 6.2

It is desired to preconcentrate a sugar-containing solution from 5 to 30% solids in a single-effect evaporator (see Figure 6.7). Steam is available at atmospheric pressure (100°C). A vacuum of 12.5 kPa is to be maintained in the vapor space and this pressure corresponds to steam at 50°C. The feed to the evaporator is 5000 kg/h. The condensate leaves the evaporator at 75°C and the solution has a negligible elevation in boiling point. Calculate the steam requirement and steam economy if the temperature of the feed is (a) 20°C and (b) 80°C.

Solution

a. Feed solution enters at 20°C — the material balance is

$$\text{Evaporation rate} = 5000(1 - 0.05/0.30) = 4166.7 \text{ kg/h}$$

From Steam Table (Table 6.6),

$$\lambda_s = 2257.1 \text{ kJ/kg @ }100°C$$

$$\lambda = 2382.7 \text{ kJ/kg @ } 50°C$$

The specific heat of sugar-containing solutions may be calculated from Equation 6.1 or Table 6.5

$$c_p = 4.05 \text{ kJ/kg°C}$$

The heat balance is:

$$2257.1 \ V_o = 4166.7 \times 2382.7 + 5000 \times 4.05(50 - 20)$$

The steam requirement is

$$V_o = 4667.3 \text{ kg steam/hr}$$

The steam economy is:

$$E = V/V_o = 4166.7/4667.3 = 0.89 \text{ kg water evaporated/kg steam}$$

b. Feed solution enters at 80°C — The material balance is unchanged. The heat balance is:

$$2257.1 \ V_o = 4166.7 \times 2382.7 + 5000 \times 4.05(50 - 80)$$

The steam requirement is

$$V_o = 4129 \text{ kg steam/hr}$$

The steam economy is

$$E = V/V_o = 4166.7/4129 = 1.01 \text{ kg water evaporated/kg steam}$$

Discussion

In Part a, the temperature of the thin liquor fed to the evaporator is less than the boiling temperature so part of the steam energy is used to heat the feed to the boiling temperature. This amount of heat is the heating load. In Part b, the temperature of the feed is greater than the boiling temperature. The steam requirement is reduced since some heat is brought in by the feed above its boiling point in the evaporator. This quantity of heat is the flash evaporation.

EXAMPLE 6.3

Calculate the heating surface areas for Example 6.2 if the apparent overall heat transfer coefficient can be taken as 3000 W/m²°C.

Solution

Heating surface — This is calculated by Equation 6.2, a rate equation.

$$A = Q/U\Delta T = 2257.1 \times 4667.3 / \left[3000(100 - 50)\right] :$$

(a) $\ A = 2257.1 \times 4667.3 / \left[3000(100 - 50)\right] = 70.2 \text{ m}^2$

(b) $\ A = 2257.1 \times 4129 / \left[3000(100 - 50)\right] = 62.1 \text{ m}^2$

Discussion

One of the problems that arises in the use of the rate equation is in the value to be used for Δ T. In Example 6.2, steam condenses at 100°C and the condensate leaves at 75°C. The liquid is fed at 20°C and is being preheated to the boiling point at 50°C. The heat gives up 2257.1 kJ/kg
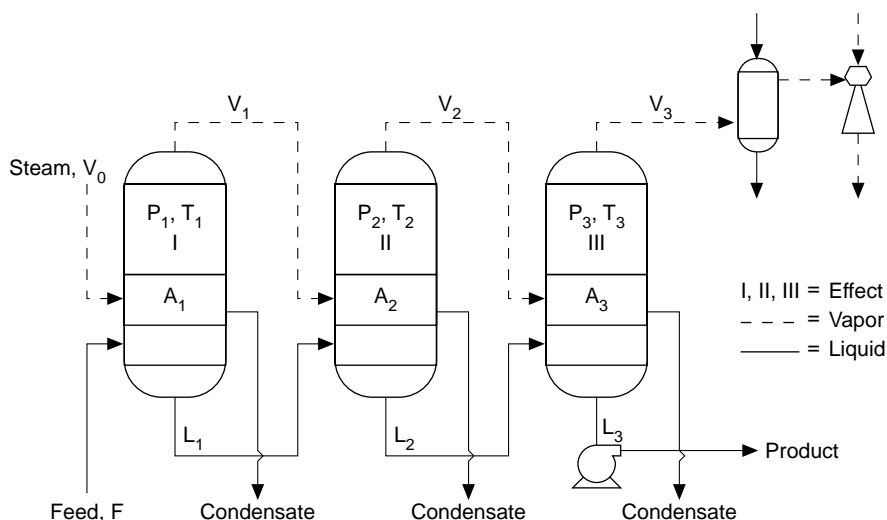
FIGURE 6.8 A schematic diagram of a simple triple-effect evaporator with forward feed.

in condensing at 100°C and $4.187 \times (100 - 75)$ kJ/kg in cooling to 75°C. The heat given up in condensing is so large in comparison to the heat given up in cooling condensate that the latter quantity is usually omitted in calculating temperature drops. In evaporator design, the heat transfer surface areas are calculated by using the temperature difference between condensing steam and boiling liquid.

6.4.4 MULTIPLE-EFFECT EVAPORATORS

A multiple-effect evaporator may be operated with forward feed, backward feed, or mixed feed. Comparisons of different feeding schemes have been presented by Coulson and Richardson (1978).

A schematic of a simple triple-effect evaporator with forward flow is shown in Figure 6.8. The flow of vapor removed in the first effect is related to the steam flow to the first effect and its steam economy, E

$$V_1 \Delta H_1 = E V_o \Delta H_o \tag{6.24}$$

Similarly, the vapor removed from the second effect is related to first-effect vapor rate

$$V_2 \Delta H_2 = E V_1 \Delta H_1 = E^2 V_o \Delta H_o \tag{6.25}$$

The sequence can be continued to n-effects and then the individual vapor flows summed

$$\Sigma V_i = V_o \Delta H_o \left[E/\Delta H_1 + E^2/\Delta H_2 + \ldots + E^n/\Delta H_n \right] \tag{6.26}$$

Equation 6.26 can be used to calculate vapor-steam ratios vs. number of effects for a given E value and the conditions of evaporator pressure and temperatures (Shinskey, 1978).

The enthalpy ΔH_i gained by the vapor boiling in a given effect is not exactly equal to its latent heat of vaporization. In forward feed, the solution coming from an upstream effect will be above its boiling point due to the reduction in pressure. However, the vapor driven from each effect is super heated by the boiling-point elevation of the solution. From the standpoint

of an overall heat balance, these factors are usually neglected. If latent heats are used for each ΔH in Equation 6.26, the vapor-steam ratio can be readily calculated for any evaporator.

EXAMPLE 6.4

Calculate the vapor-steam ratio for a triple-effect evaporator for the temperature difference between 25 and 100°C, beginning with 25°C in the last effect, and assuming a temperature difference of 25°C per effect and E = 0.92.

Solution

From Steam Table 6.6

$$\text{From Steam Table 6, } \lambda_o = 2$$

$$\lambda_1 = 2$$

$$\lambda_2 = 2$$

$$\lambda_3 = 2$$

The vapor-steam ratio for a triple-effect evaporator in terms of the latent heat of vaporization is:

$$\Sigma V_i / V_o = \lambda_o \left[E/\lambda_1 + E^2/\lambda_2 + E^3/\lambda_3 \right]$$

$$= 2257.1 \left[0.92/2285.8 + (0.92)^2/2382.7 \right]$$

$$+ (0.92)^3/[2442.4]$$

$$= 2.43$$

The calculations in Example 6.2 demonstrate three sources of heat can be reused or recovered for improving energy efficiency. The vapor may be reused in heating the liquid at a lower boiling temperature under a partial vacuum, the feed may be preheated in an interstage preheater and the heat in the condensate may be recovered by flashing to a lower temperature. These potential energy savings have been incorporated in the design calculations of modern multiple-effect evaporators as discussed by Chen (1982a).

For heat sensitive foods, forward feed operation is the most commonly used. Here the feed is introduced into the first effect and flows into the next effect parallel to the flow of steam. Preheating is usually necessary with this type of operation and higher vacuum is required at the last stage since the temperature of the last effect is the lowest in the system.

In backward feed operation, the feed is introduced at the last effect and is discharged at the first unit where the highest temperature of evaporation takes place. This system is commonly used with viscous liquid foods or where a cooked flavor, such as in tomato paste, is desired.

EXAMPLE 6.5   THE CALCULATION OF MECHANICAL RECOMPRESSION

It is desirable to increase the heating capacity of vapor by mechanical recompression for a single-effect evaporator (see Figure 6.9) that is concentrating sugar-containing solutions from 10 to 55% solids. Given

$$\text{Feed} = F = 5040 \text{ kg/hr} \quad \text{Product} = F_1 = 2240 \text{ kg/hr}$$

$$cp_f = 3.95 \text{ kJ/kg°C} \quad cp_1 = 2.78 \text{ kJ/kg°C} \ (\text{Table 5})$$
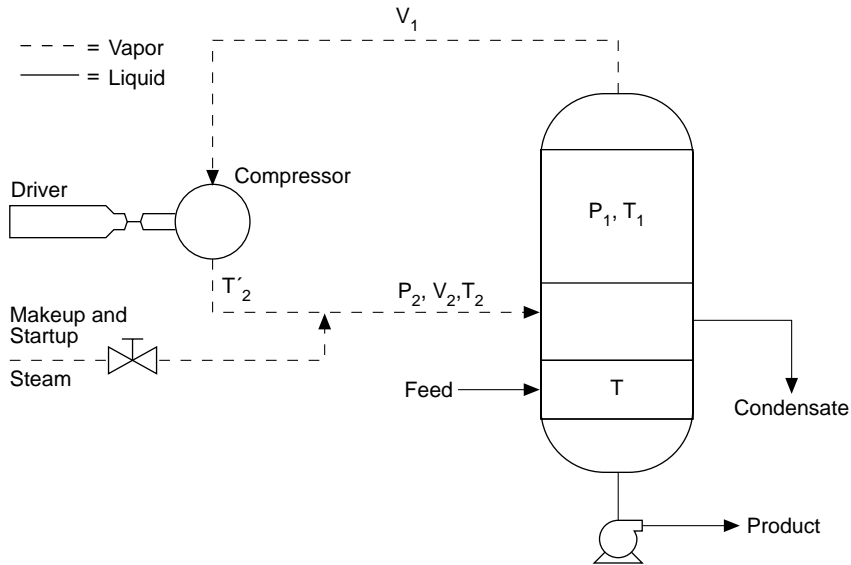
FIGURE 6.9 A schematic diagram of a single-effect evaporator with a mechanical recompressor.

Vapor from the evaporator

$$V_1 = 2800 \, \text{kg/hr}, \; T_f = 100°C, \; P_1 = 101.3 \, \text{kPa}$$

It is required to compress it to $P_2 = 150$ kPa. If saturated steam at 120°C is available for makeup (assume compression efficiency of 78%), calculate (a) compression work and (b) makeup steam required.

Solution

Steam compressed to a higher pressure becomes super-heated. Theoretically the amount of energy required to compress the vapor is equal to the difference between the enthalpy (H) at the suction and discharge points, at a constant vapor entropy (S).

Change in entropy for isoentropic compression can be found from a steam table (Keenan et al. 1969)

$$H_1 = 2676 \, \text{kJ/kg} \; (\text{for sat. steam at } 100°C)$$

$$S_1 = S_2 = 7.355 \, \text{kJ/(kg.K)}$$

$$H_2 = 2744 \, \text{kJ/kg} \; (\text{from super-heated Steam Tables for } S_2)$$

Energy per kg steam required for compression

$$W = (H_2 - H_1)/0.78 = (2744 - 2676)/0.78 = 87.18 \, \text{kJ/kg}$$

a. Compression work = (87.18 kJ/kg)(2800 kg/h) = 2.441×10^5 kJ/h. Overall heat balance in evaporator

$$F cp_f(T_f - 0) + V_s H_s + W V_1 = F_1 cp_1(T_1 - 0) + (V_s + V_1) h_c$$

where V_s is makeup steam; H_s is enthalpy of saturated makeup steam; h_c is enthalpy of steam condensate.

$$(5040)(3.95)(70-0) + V_s(2706) + (87.18)(2800) = (2240)(2.78)(100-0) + (V_s + 2800)(419)$$

b. Makeup steam required $= V_s = 69$ kg/h

6.5 PERFORMANCE EVALUATION OF A COMMERCIAL CITRUS EVAPORATOR

The concentration of citrus juices is a typical application of evaporator technology in the food processing industry. In commercial operations, the average juice yield from oranges varies from 43 to 55% and the solids content are from 9 to 15% which are concentrated to 60 to 65% by evaporation. The most popular design of citrus evaporators is known as the TASTE evaporator. Several field tests on citrus TASTE evaporators have been reported. A field test of a typical early design of commercial multiple-effect citrus evaporator was presented by Chen (1982a). Heat and mass balance calculations for commercial citrus evaporator systems are fairly complex. In many cases, the design information is lacking and some estimates have to be made for heat and mass balance calculations for field performance evaluation.

EXAMPLE 6.6   FIELD EVALUATION OF A COMMERCIAL CITRUS EVAPORATOR

A typical TASTE evaporator, 4 effect, 7 stage, designed for 18,144 kg/h evaporation capacity and upgraded to 5 effect 8 stage, is schematically shown in Figure 6.10. For multiple-effect evaporators, an analysis of the existing system can be carried out by imposing a heat balance across each effect individually and a mass balance for the whole system. Heat losses to the environment and energy losses due to the venting of steam to remove noncondensibles were assumed to be negligible. Referring to Figure 6.10, the heat and mass balance equations can be written in terms of specific heat and latent heat of vaporization basis (approximate from enthalpy basis) as follows

1st Effect-2nd Stage
Heat balance

$$V_o\lambda_o - Q_6 + F_1C_1(T_{f6} - T_2) = V_2\,\lambda_2 \tag{6.27a}$$

$$Q_6 = F_1C_1(T_{f6} = T_{f5}) \tag{6.27b}$$

Mass balance

$$V_2 = F_1(1 - X_1/X_2) \tag{6.27c}$$
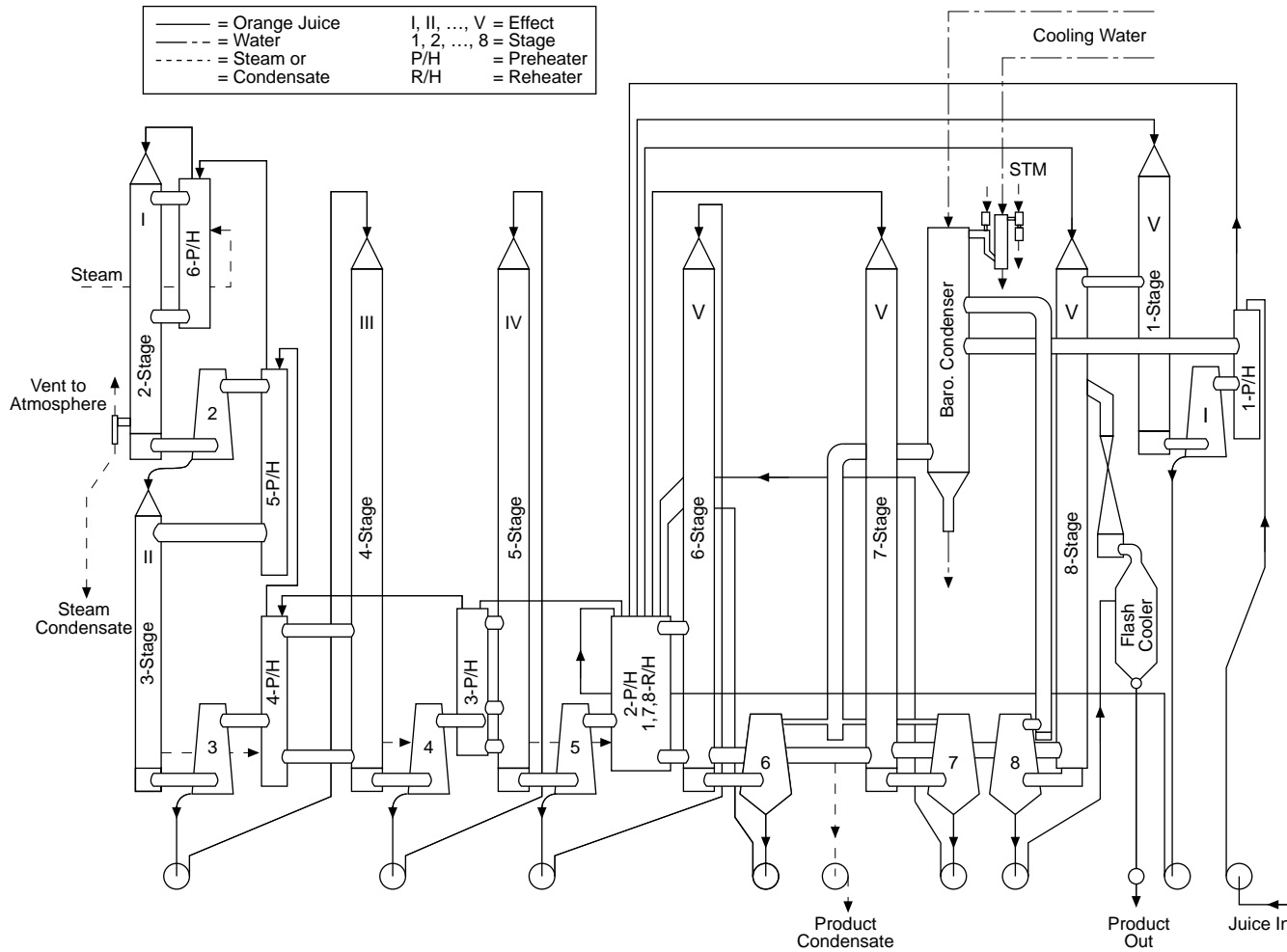
Heat transfer coefficients
For evaporation

$$U_2 = (V_oH_o - Q_6)/(A_2 \times (T_s - T_2 - B_2)) \tag{6.27d}$$

For preheater (#6)

$$U_6^* = Q_6/(A_6^* \times LMTD) \tag{6.27e}$$

FIGURE 6.10 A schematic diagram of a typical 5-effect 8-stage citrus TASTE evaporator system. (Gulf Machinery Corp, Dunedin, FL.) (From Nagy, S., Chen, C.S., and Shaw, P.E., Eds., *Fruit Juice Processing Technology,* Agscience, Auburndale, FL. With permission.)

2nd Effect-3rd Stage
Heat balance

$$V_2\,\lambda_2 = Q_5\big(F_1 - V_2\big)C_2\big(T_2 - T_3\big) = V_3\,\lambda_3 \tag{6.28a}$$

$$Q_5 = F_1 C_1\big(T_{f5} - T_{f4}\big) \tag{6.28b}$$

Mass balance

$$V_3 = \big(F_1 - V_2\big)\big(1 - x_2/x_3\big) \tag{6.28c}$$

Heat transfer coefficients
  For evaporator

$$U_3 = \big(V_2\,\lambda_2 - Q_5\big)\big/\big(A_3 \times \big(T_2 - T_3 - B_3\big)\big) \tag{6.28d}$$

  For preheater (#5)

$$U_5^* = Q_5\big/\big(A_5^* \times LMTD\big) \tag{6.28e}$$

3rd Effect-4th Stage
Heat balance

$$V_3\,\lambda_3 = Q_4 + \big(F_1 - V_2 - V_3\big)C_3\big(T_3 - T_4\big) + V_2 C\big(T_3 - T_4\big) = V_4\,\lambda_4 \tag{6.29a}$$

$$Q_4 = F_1 C_1\big(T_{f4} - T_{f3}\big) \tag{6.29b}$$

Mass balance

$$V_4 = \big(F_1 - V_2 - V_3\big)\big(1 - X_3/X_4\big) \tag{6.29c}$$

Heat transfer coefficients
  For evaporator

$$U_4 = \big(V_3\,\lambda_3 - Q_4\big)\big/\big(A_4 \times \big(T_3 - T_4 B_4\big)\big) \tag{6.29d}$$

  For preheater (#4)

$$U_4^* = Q_4\big/\big(A_4^* \times LMTD\big) \tag{6.29e}$$

4th Effect-5th Stage
Heat balance

$$V_4\,\lambda_4 - Q_3 + \big(F_1 - V_2 - V_3 - V_4\big)C_4\big(T_4 - T_5\big) + \big(V_2 + V_3\big)C\big(T_4 - T_5\big) = V_5\,\lambda_5 \tag{6.30a}$$

$$Q_3 = F_1 C_1\big(T_{f3} - T_{f2}\big) \tag{6.30b}$$

Mass balance

$$V_5 = (F_1 - V_2 - V_3 - V_4)(1 - X_4/X_5) \tag{6.30c}$$

Heat transfer coefficients
  For evaporator

$$U_5 = (V_4 \lambda_4 - Q_3)\Big/\big(A_5 \times (T_4 - T_5 - B_5)\big) \tag{6.30d}$$

  For preheater (#3)

$$U_3^* = Q_3\Big/\big(A_3^* \times LMTD\big) \tag{6.30e}$$

5th Effect-6th Stage
Heat balance

$$M_1 \times V_5 \lambda_5 - Q_2 - Q_{r1} - Q_{r8} + (F_1 - V_2 - V_3 - V_4 - V_5)C_5$$
$$(T_5 - T_6) + (V_2 + V_3 + V_4)C(T_5 - T_6) = V_6 \lambda_6 \tag{6.31a}$$

$$Q_2 = F_1 C_1 (T_{f2} - T_{r1}) \tag{6.31b}$$

$$Q_{r1} = F_o C_o (T_{r1} - T_{f1}) \tag{6.31c}$$

$$Q_{r7} = (F_1 - V_2 - V_3 - V_4 - V_5 - V_6)C_6(T_6 - T_{r7}) \tag{6.31d}$$

$$Q_{r8} = (F_1 - V_2 - V_3 - V_4 - V_5 - V_6 - V_7)C_7(T_7 - T_{r8}) \tag{6.31e}$$

Mass balance

$$V_6 = (F_1 - V_2 - V_3 - V_4 - V_5)(1 - X_5/X_6) \tag{6.31f}$$

Heat transfer coefficients
  For evaporator

$$U_6 = (M_1 \times V_5 \lambda_5 - Q_2 - Q_{r1} - Q_{r7} - Q_{r8})\Big/\big(A_6 \times (T_5 - T_6 - B_6)\big) \tag{6.31g}$$

  For preheater #2

$$U_2^* = Q_2\Big/\big(A_2^* \times LMTD\big) \tag{6.31h}$$

  For reheater for Stage 1

$$U_1^* = Q_{r1}\Big/\big(A_1^* \times LMTD\big) \tag{6.31i}$$

For reheater for Stage 7

$$U_7^* = Q_{r7}\Big/\left(A_7^* \times \text{LMTD}\right) \qquad (6.31j)$$

For reheater for Stage 8

$$U_8^* = Q_{r8}\Big/\left(A_8^* \times \text{LMTD}\right) \qquad (6.31k)$$

5th Effect-7th Stage
Heat balance

$$M_2 \times V_5\, \lambda_5 + \left(F_1 - V_2 - V_3 - V_4 - V_5 - V_6\right)C_6\left(T_{r7} - T_7\right) = V_7\, \lambda_7 \qquad (6.32a)$$

Mass balance

$$V_7 = \left(F_1 - V_2 - V_3 - V_4 - V_5 - V_6\right)\left(1 - X_6/X_7\right) \qquad (6.32b)$$

Heat transfer coefficient
   For evaporator

$$U_7 = \left(M_2 \times V_5\, \lambda_5\right)\Big/\left(A_7 \times \left(T_5 - T_7 - B_7\right)\right) \qquad (6.32c)$$

5th Effect-8th Stage
Heat balance

$$M_3 \times V_5\, \lambda_5 + \left(F_1 - V_2 - V_3 - V_4 - V_5 - V_6 - V_7\right)C_7\left(T_{r8} - T_8\right) = V_8\, \lambda_8 \qquad (6.33a)$$

Mass balance

$$V_8 = \left(F_1 - V_2 - V_3 - V_4 - V_5 - V_6 - V_7\right)\left(1 - X_7/X_8\right) \qquad (6.33b)$$

Heat transfer coefficient
   For evaporator

$$U_8 = \left(M_3 \times V_5\, \lambda_5\right)\Big/\left(A_8 \times \left(T_5 - T_8 - B_8\right)\right) \qquad (6.33c)$$

5th Effect-1st Stage
Heat balance

$$M_4 \times V_4\, \lambda_5 + F_o C_o\left(T_{r1} - T_1\right) = V_1\, \lambda_1 \qquad (6.34a)$$

Mass balance

$$V_1 = F_o\left(1 - X_o/X_1\right) = F_o - F_1 \qquad (6.34b)$$

$$M_1 + M_2 + M_3 + M_4 = 1 \tag{6.34c}$$

Heat transfer coefficient
  For evaporator

$$U_1 = \left(M_4 \times V_5\,\lambda_5\right)\big/\left(A_1 \times \left(T_5 - T_1 - B_1\right)\right) \tag{6.34d}$$

Heat recovery from exhaust of effect 5

$$Q_1 = F_o C_o \left(T_{f1} - T_{fo}\right) \tag{6.35a}$$

Heat transfer coefficient
  For preheater (#1)

$$U_1^* = Q_1 \big/ \left(A_1^* \times LMTD\right) \tag{6.35b}$$

Overall mass balance

$$V = V_1 + V_2 + \ldots + V_8 \tag{6.36}$$

Feed requirement

$$F_o = V \big/ \left(1 - X_o/X_8\right) \tag{6.37}$$

Flash cooler

$$V_9 = \left(F_o - V\right)C_8 \left(T_9 - T_9\right)\big/\lambda_9 \tag{6.38}$$

The above equations were used for calculating the heat and mass balances.

Calculation Procedures

Since there are 50 variables and 27 equations for the heat and mass balances calculation, 23 of the variables must be specified to solve the equations to obtain the remaining variables. There are 17 variables and 17 equations for heat transfer coefficients; they can be solved readily.

   The following 23 variables were measured and used in the calculation: T_s, T_{rl}, T_{fo}, T_{r7}, T_{r8}, T_{f1} through T_{f6}, T_1 through T_8, V_o, F_o, X_o, and X_8. An additional seven variables were also measured and used to estimate the energy loss and to check the validity of the computed results. They were X_3 through X_7, X_9, and T_9.

Latent heat of vaporization was calculated from the steam table by the following equation

$$\lambda = 2499\,\mathrm{Exp}\left(-0.001016\,T\right) \tag{6.39}$$

Specific heat was calculated from Equation 6.1

$$C = C_p = 4.187\left\{1 - X_s\left[.57 - .0018(T - 20)\right]\right\} \tag{6.40}$$

Boiling-point rise was calculated from the empirical BPR equation for sucrose solutions

$$B = 0.33 \, \text{Exp}\!\left(4X_s\right) \tag{6.41}$$

The value of X_s is the weight fraction of soluble solids and T and B in Celsius in Equations 6.39 through 6.41.

Expected steam economy was calculated from the measured temperature profile and Brix data by assuming no heat loss. The actual economy was calculated using the measured steam rate. The difference between the two methods of calculation was attributed to lumped heat loss.

Experimental results during normal operation in a processing plant along with an analysis of heat and mass balances for the 5-effect 8-stage TASTE evaporator are shown in Table 6.7. This unit was an old design of citrus TASTE evaporator. At the designed evaporation capacity, the steam efficiency was found to be 0.74N where N is the number of effects. A large percentage energy loss was found mainly due to air leakage and/or excessive steam venting to the atmosphere. Thus, it is important to maintain air-tight in a high vacuum multiple-effect system and avoid excessive steam venting.

The steam efficiencies of similar citrus TASTE systems and comparable plate-type citrus evaporators of newer design were found to be 0.85N and 0.82N, respectively (Filho et al., 1984).

6.6 ECONOMICS

Evaporation is one of the high capital cost and energy intensive unit operations. During the era of low energy costs, the major selection criterion was based on the low initial equipment cost. However, in the past two decades, energy costs have increased radically in comparison to initial equipment costs. By far, energy is the major cost in evaporator operations (Standiford, 1963). As a result, more energy-efficient designs have gained favor for new installations.

6.6.1 COST AND OPTIMIZATION

The installed cost of a multiple-effect evaporation system is usually related to the heat transfer area of evaporation raised to a power m (King, 1980):

$$\text{Installed cost} \;=\; K\!\left(A_1^m + A_2^m + \ldots + A_N^m\right) \tag{6.42}$$

where A is heat transfer area of evaporator; m is a constant depending on the type of evaporator usually <1; K is cost per unit area.

The calculation of the optimum number of effects involves balancing between operating costs and capital equipment costs. Operating costs include steam and maintenance cost. Capital equipment involves initial equipment cost and annual fixed charges.

When the heat transfer areas are the same for all effects, the following simplified expression can be used to estimate the optimum number effects

$$\text{Steam cost} = C_s V_T / NE \tag{6.43}$$

$$\text{Fixed cost} = C_e N A^m \tag{6.44}$$

$$\text{Total cost} = \frac{C_s V_T}{NE} + C_e N A^m \tag{6.45}$$

where C_s is cost of steam per kilogram; V_T is total kilograms of steam; N is number of effect; E is steam economy; C_e is evaporator unit cost; V_s is kilograms of live steam. Differentiating Equation 6.44 and equating to zero, we can obtain the optimum number effects (N_{opt})

$$N_{opt} = \left[\left(C_s / C_e \right) \left(V_s / A^m \right) \right]^{1/2} \qquad (6.46)$$

In general, the optimum number effects will increase with the steam cost, heat transfer coefficients, and temperature differences and will decrease with higher evaporator costs. The above equation is no longer valid when the heat transfer areas of the effects are not equal. As a result, the determination of N_{opt} becomes an optimization problem. Other factors should be considered in the fixed cost such as depreciation and interest rates. The determination of the steam cost should also take into account the type of feed utilized, i.e, the steam economy of forward feed is generally assumed to be 10% lower than for backward feed.

The steams used in evaporation are predominantly generated by using either fuel oils or natural gases. The costs of steam increase with the rise in the prices of fuels (Rebeck, 1976).

EXAMPLE 7. CALCULATION OF STEAM COST

Boiler Costs — Basis and assumptions
560 kW boiler = $95,000.00 installed including piping, slab, room, etc.
Boiler fuel = 3256 kJ/kg water evaporated
Yearly operating hours = 4000 h/yr
Maintenance and compounds = $2500.00/yr

Operating Costs
Depreciation
   $95,000 @ 5 yr × 4000 h/yr $ 4.75/h
Maintenance and compounds
   $2500.00/4000 h $ 0.63/h
Electricity
   18.8 kW × $0.055/kWh $ 1.03/h
Fuel (Bunker C)
   $\dfrac{6{,}800 \text{ kg/h} \times 3{,}130 \text{ kJ/kg} \times \$120/m^3}{40{,}000{,}000 \text{ kJ/m}}$ $63.85/h
TOTAL $70.26/h

Steam Costs

$$\frac{70.26 \ \$/hr \times 1000}{6{,}800 \ kg/hr} = \$10.33/1000 \ kg \ steam$$

Not including salaries, taxes, interest, etc.

6.6.2 METHODS FOR ENERGY SAVINGS

Many existing evaporator systems were designed with minimization of capital costs during the era of low energy costs. As a result of escalating high oil prices, considerable economic benefits can be gained in upgrading the existing evaporator systems to reduce energy costs for evaporation. There are three general areas for modifying existing evaporators for energy savings (Anon., 1977)

1. **Fine tuning existing evaporator**. These low-investment improvements do not change the basic evaporator layout (e.g., improvements in venting and additional

TABLE 6.7
Heat and Mass Balances of a 5-Effect 8-Stage Citrus Taste Evaporator

Stage		1	2	3	4	5	6	7	8	P/O
Steam rate	kg/h		4792							
Feed rate	kg/h	22122								
Steam temp	°C	47.7	100.0	88.2	78.3	68.2	47.7	47.7	47.7	
Conc. temp in	°C	46.7	96.4	88.9	79.1	69.3	49.9	44.5	43.3	39.4
Conc. temp out	°C	43.3	88.9	79.1	69.3	49.9	41.3	39.4	39.4	15.6
BPR	°C	0.6	0.6	0.8	1.1	2.3	2.9	3.3	3.7	4.0
Latent heat	kJ/kg	2391	2283	2306	2329	2375	2396	2400	2400	2459
Specific heat	kJ/kg °C	3.98	3.94	3.88	3.78	3.62	3.19	3.03	2.96	2.86
Conc. flow out	kg/h	20042	16232	12624	9116	5619	5002	4730	4468	4344
Evap. rate	kg/h	2080	3809	3608	3508	3497	617	271	262	124
Brix out (calc.)	°Br	13.5	16.6	21.4	29.6	48.0	54.0	57.1	60.4	62.1
Brix out (expt.)	°Br	13.2		21.5	29.9	48.2	53.7	56.8	60.4	
Heat balance										
Available heat	kJ/kg	1326	3005	2440	2377	2482	784	163	163	
Preheat	kJ/kg	257.0	279.0	277.0	213.0	328.0	79.0	0.0		
Sensible heat	kJ/kg	81.0	166.0	172.0	129.0	178.0	43.0	21.0	15.0	

Heat loss	%	2.0	15.8	1.0	1.0	1.0	2.0	2.0	2.0
Heat for evap	kJ/kg	1381	2416	2311	2269	2307	411	181	175
Heat transfer	kJ/kg	1300	2250	2139	2140	2129	368	160	160
Evaporator									
Δ T	°C	4.3	11.1	9.2	8.9	18.3	6.4	8.2	8.2
Area	m^2	132.8	119.9	132.8	149.9	149.9	107.5	65.2	33.5
U	W/m^2 °C	2262	1690	1759	1598	775	536	298	580
Heat flux	W/m^2	9803	18785	16128	14299	14224	3425	2450	4771
Evaporation	%	11.8	21.6	20.4	19.9	19.8	3.5	1.5	1.5
Preheater or reheater		1	6	5	4	3	2	R/H 1	R/H 8
Juice temp out	°C	34.7	96.4	83.8	71.3	61.7	46.9	46.7	43.3
Juice temp in	°C	24.2	83.8	71.3	61.7	46.9	43.3	34.7	39.4
Heater ΔT	°C	9.0	8.3	9.3	11.1	12.5	2.1	4.7	6.1
Heater area	m^2	9.1	7.8	7.8	7.8	7.8	7.8	9.1	6.8
Preheater U	W/m^2 °C	3805	2453	3356	4850	6927	3675	3139	4276

Note: Material = orange juice; feed °Brix = 12.2 °Brix; product °Brix = 60.4 °Brix; product rate = 4468 kg/h; product solids = 2699 kg/h; evaporation rate = 7654 kg/h; steam economy = 3.68 kg H_2O removed/kg steam; heat requirement = 613 kj/kg H_2O.

From Chen, 1982b. *Evaporation in the Citrus Industry.* Paper presented at AICHE, Orlando, FL.

TABLE 6.8
Typical Energy Savings by Various Methods

Method	Capital requirement	Achievable energy savings (%)
Venting and thermal insulation	Low	5
Improved maintenance	Low	5
Heat-recovery exchangers	Low	10
Condensate reuse	Low	5
Thermal recompression	Medium	45
Mechanical recompression	High	70–90
Additional effects	High	$\left[1-\left(\dfrac{N}{N+n}\right)\right]100\%$

Note: N = original number of effects; n = number of added effects.

Example: The savings for increasing a three-effect evaporator to four effects is

equal to $\left[1-\left(\dfrac{3}{3+1}\right)\right]100\% = 25\%$, approximately.

From Anon. (1977).

insulation, improved maintenance, and increased attention to preventing water or vacuum leakage).

2. **Modifying auxiliary hardware**. These moderate-investment changes normally can be authorized at the plant level (e.g., improved heat recovery from condensates and product streams).

3. **Major hardware modifications**. These high-investment changes normally require approval at the corporate level (e.g., installing additional effects or adding a vapor-recompression unit).

Typical energy savings by various methods are shown in Table 6.8. The actual energy savings and operating cost reductions will depend on the operating conditions of the existing evaporator system.

6.6.3 ECONOMIC EFFECTS OF ENERGY SAVINGS

Since the energy crisis in the late 1970s, considerable efforts have been made in food processing industries to identify leading unit operations for energy consumption in processing plants and to find ways for energy savings. Evaporation is one of the most energy-intensive unit operations used by the food processing industry (Anon., 1977). Various energy saving options for evaporation have been evaluated and demonstrated.

Specific examples of energy savings by adding effect and automatic control have been reported. It was determined that the energy consumption in a 4-effect, 7-stage TASTE evaporator with a capacity of evaporation of 18,140 kg H_2O/h, to be between 836 and 1000 kJ/kg of water evaporated. By adding one effect, i.e., one stage after the fourth-stage, the energy consumption was reduced to the range of 565 to 640 kJ/kg of water evaporated (Chen et al., 1979).
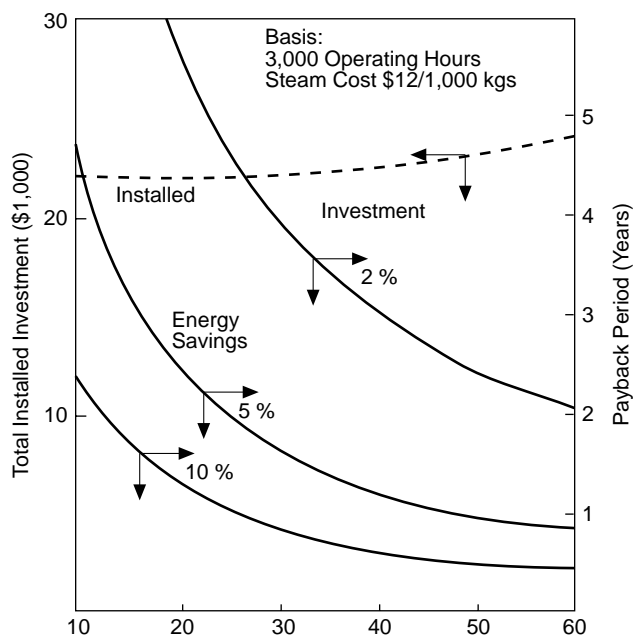
FIGURE 6.11 Investment and payback period for computer control of a 5-effect citrus TASTE evaporator (Data from Chen, C.S. et al. 1981, Trans. Citrus Eng. Conf. Fla, Sec. ASME, 27:58–80.)

Computer-aided techniques have been applied in automatic control of evaporators to improve energy efficiency of evaporator operations. For example, the traditional control system for the multiple-effect TASTE evaporators consists of two pneumatic control valves, one to control steam and the other to control feed juice flow. Under manual operation the steam flow is usually set at constant pressure and the feed flow is adjusted manually according to the desired solids concentration of the product (pump-out Brix value). The steam at atmospheric pressure is varied with the altitude; the pressure of the vapor leaving the last effect is determined by the cooling water. When the system is in operation, a distribution of temperature among effects is established, and a steady operation is reached after a certain elapsed time. This steady-state condition to produce the desired pump-out is the target of evaporator operators. Unfortunately, the desired pump-out Brix can increase or decrease several degrees within a few minutes without changing any operating settings due to fluctuation in feed Brix, feed rate, steam rate, or change in environmental conditions, i.e., temperatures, wind speeds, or rain falls, etc., but any attempt to correct the deviation may require several changes of feed rate and/or steam rate by trial-and-error methods. Prolonged deviation from the desired value may result not only in an off-specification product but also in loss of useful energy. The loss of energy may be due to excess steam venting to the atmosphere. Energy savings may be achieved by converting manual to computer-assisted automatic control. It has been demonstrated that the steam economy ratios of a six-effect TASTE evaporator were 4.63 and 4.94 for manual and automatic control, respectively, showing that energy savings achievable by automatic control techniques were approximately 6.7% for this particular system.

Reduction of energy consumption for evaporation depends on several factors, such as evaporation capacity, number of effects, operation efficiency, and annual operation hours. Cost savings and payback depend upon control system cost against fuel cost and energy savings. Estimates of investment and payback period for automatic control of a five-effect evaporator in 1980 are shown in Figure 6.11 (Chen et al., 1981).

NOMENCLATURE

A, A_i	Evaporator heat transfer area (m²)
a_w	Water activity
$B, B_i, \Delta T_b$	Boiling-point rise (°C)
C_e	Evaporator unit cost ($)
C_s	Cost of steam per kg ($/kg)
C, C_i, c_p	Specific heat of feed or concentrate (kJ/kg°C)
d	Heat transfer tube diameter (m)
E	Steam economy
F, F_i	Feed flow rate (kg/h)
$H, H_i, \Delta H$	Enthalpy (kJ/kg)
h	Heat transfer coefficient (W/m²K)
K	Cost per unit heat transfer area ($/m²)
K_v	A constant for boiling-point rise (kg K/kg-mol)
k	Thermal conductivity (W/mK)
L, L_i	Liquid flow rate (kg/h)
M_j	Fraction of vapor distribution in parallel stages
N, n	Number of effects
P, p	Pressure (Pa)
Q	Rate of heat transfer (kJ/h)
Q_i	Rate of heat for preheating (kJ/h)
Q_{ri}	Rate of heat for reheating (kJ/h)
S	Entropy (kJ/kg.K)
T	Temperature; liquid temperature (°C)
T_i	Boiling temperature of liquid in stages 1 to n (°C)
T_s	Steam temperature (°C)
T_{fo}	Initial feed temperature (°C)
T_{fi}	Feed temperature at exit of the ith preheater (°C)
T_{ri}	Feed temperature at exit of the reheater (°C)
U, U_i	Overall coefficient of heat transfer for the ith stage (W/m²/°C)
V	Total water removed; total evaporation rate (kg/h)
V_o	Steam rate (kg/h)
V_i	Vapor flow rate (kg/h)
V_s	Kilogram of live steam (kg)
V_T	Total kgs of steam (kg)
W	Compression work per kg of steam (kJ/kg)
X_i	Solids content (°Brix)
X_s	Weight fraction of soluble solids; solids content (°Brix)
λ	Latent heat of vaporization (kJ/kg)
Θ	Residence time (h)
Σ	Summation

ABBREVIATIONS

BPR	Boiling-point rise (°C)
LMTD	Log mean temperature difference (°C)
P/H	Preheater
R/H	Reheater

SUBSCRIPTS

b	Boiling
f	Liquid
i or j	1,2,3, …n, Number of effects or stages or preheater number; inside
m	Mean

o	Initial; steam; outside
p	Product
s	Steam-side; steam; soluble solids
v	Vapor

SUPERSCRIPTS

| * | Preheater |
| ** | Reheater |

ROMAN NUMERALS

I, II, III,… 1st Effect, 2nd effect, 3rd effect,…

ACKNOWLEDGMENT

REFERENCES

Anon., 1977, *Upgrading Existing Evaporators to Reduce Energy Consumptions,* ERDA, U.S. Dept. of Commerce, Virginia.

Badger, W.L. and Banchero, 1955, *Introduction to Chemical Engineering,* McGraw-Hill, New York.

Burgois, J. and Le Maguer, M., 1987, *J. Food Eng.,* 3:39–50.

Chen, C.S., 1982a, *Trans. ASAE,* 25(5):1457–1463.

Chen, C.S., 1982b, Evaporation in the citrus industry, presented at AICHE, Orlando, FL.

Chen, C.S., 1993, in *Fruit Juice Processing Technology,* Nagy, S., Chen, C.S., and Shaw, P.E., Eds., Agscience, FL.

Chen, C.S. et al., 1979, in *Changing Energy Use Futures,* Vol. 4, Fazzolare and Smith, Eds., Pergamon Press, Elmsford, NY.

Chen, C.S. et al., 1981, *Trans. Citrus Eng. Conf. Fla, Sec. ASME* 27:58–80.

Coulson, J.M. and Richardson, J.F., 1978, *Chemical Engineering,* Vol. 2, Pergamon Press, New York.

Dinnage, D.F., 1972, *Proc. 20th Annu. Nat. Dairy Eng. Conf.,* MSU, East Lansing, MI.

Filho, G. et al., 1984, *J. Food Process Eng.,* 7:77–89.

Holland, C.D., 1975, *Fundamentals and Modeling of Separation Processes,* Prentice-Hall, Englewood Cliffs, New Jersey.

Keenan, J.H., Keyes, F.G., Hill, P.G. and Moore, J.G., 1969, *Steam Tables-Metric Units,* John Wiley & Sons, New York.

Kern, D.Q., 1950, *Process Heat Transfer,* McGraw-Hill, New York.

King, C.J., 1980, *Separation Processes,* McGraw-Hill, New York.

Matthews, R.F., Ed., 1976, *Heat Transfer in Food Processing,* University of Florida, Gainesville, FL.

McAdams, W.H., 1954, *Heat Transmission,* McGraw-Hill, New York.

McCabe, W.L. and Smith, J.C., 1976, *Unit Operations of Chemical Engineering,* 3rd ed., McGraw-Hill, New York.

Milton, P.E., 1986, *Handbook of Evaporation Technology,* Noyes Publishing, Fairview, NJ.

Muddawar, I.A. and El-Masri, 1986, *Int. J. Multiphase Flow,* 12(5):771–790.

Nagy, S., Chen, C.S., and Shaw, P.E., Eds., 1993, *Fruit Juice Processing Technology,* AgScience, Auburndale, FL.

Okos, M.R., Ed., 1986, *Physical and Chemical Properties of Food,* ASAE, St. Joseph, MI.

Olesen, R.K., 1990, *Int. Trade Forum,* 26(4):12–17.

Piret, E.L. and Isbin, H.S., 1986, *Chem. Eng. Progr.,* 50(6):305.

Rebeck, H., 1976, in *Heat Transfer in Food Procesing,* Matthews, ??, Ed., University of Florida, Gainesville, FL.

Redd, J.B. and Hendrix, C.M., Jr., 1993, in *Fruit Juice Processing Technology,* Nagy, Chen, C.S., and Shaw, Eds., AgScience, Auburndale, FL.

Schwartzberg, H.G., 1977, *Food Tech.,* Mar:67–76.

Shinskey, F.G., 1978, *Energy Conservation through Control,* Academic Press, New York.

Skoczylas, A., 1970, *Br. Chem. Eng.,* 15(2):221–222.

Standiford, F.C., 1963, *Chem. Eng.,* 70(25):164–170.

Standiford, F.C., 1973, Evaporation, in *Perry's Chemical Engineers' Handbook,* 5th ed., Perry Chilton, Eds., McGraw-Hill, New York.

Wiegand, B.W.H., 1992, *Trans. Citru. Eng. Conf. Fla. Sec. ASME,* 38:64–78.

7 Material and Energy Balances

Brian E. Farkas and Daniel F. Farkas

CONTENTS

7.1 INTRODUCTION TO MATERIAL AND ENERGY BALANCES IN THE FOOD PROCESSING INDUSTRY

7.1.1 SCOPE

The material and energy balance is one of the most useful tools an engineer possesses. Material and energy balances are fundamental in the "engineering approach" to designing

new processes or analyzing the results of in-plant tests. Material and energy balances play an important role in process streamlining, economic analysis of alternate technologies, waste reduction, and selecting process modifications to increase yield. For example, the practicing engineer may choose to reduce waste output or energy consumption in an effort to increase the profitability of a process. Waste reduction may be accomplished by increasing the desired product and decreasing the byproduct material or by utilizing the byproduct to form a useful product. Reduction of energy consumption requires that the engineer know how, why, and where energy is being consumed and the minimum energy requirement for the process.

Food processing operations differ from the processing of other materials in that raw materials entering the process generally consist of plant or animal tissue which can include both living and nonliving cells. The processing of these materials can result in simultaneous loss of soluble cell materials and gain of water, e.g., when vegetables are heated in hot water, a process known as blanching. This chapter is presented to help the practicing food engineer handle the special material and energy balance requirements of the food processing industry.

In their book, *Plant Design and Economics for Chemical Engineers,* Peters and Timmerhaus (1980) list eight requirements which must be determined within narrow limits if a successful plant design is to be obtained. The first requirement is to determine the process. The next requirement is to complete, for the entire process, material and energy balances around each unit operation or unit process. Simply stated, the food engineer must be able to present in quantitative terms the flows of product, byproduct, waste, effluent, and energy across a boundary defining each unit operation.

Realistic material and energy balances are essential to the design of an economically viable process to deliver safe and nutritious food products meeting all quality specifications. Material and energy balances are the basis for cost effective and environmentally sound processes and plants. Ultimately they form the basis for computer-aided manufacturing by helping determine marketable product delivered to the warehouse, byproduct flows, schedules for just-in-time delivered ingredients, and schedules for labor, utilities, cleaning, and maintenance.

Material and energy balances are essential to process development in the food processing industry. They can be used for the selection and sizing of processes and equipment, or for the determination of economic alternatives. However, it may be challenging for process engineers with limited food engineering experience to perform realistic material and energy balances with food processing equipment and typical food ingredients. Unlike chemical process plants, most food processing operations do not involve the reaction of chemicals of known purity. Food processing is the conversion of living plant and animal tissue to edible foods. Chapter 7 is written to help the practicing food engineer develop reasonably good material and energy balances around the common unit operations and processes used to convert raw plant and animal materials to edible food products ready for distribution.

Chapter 7 will not cover several areas of material and energy balances normally covered in chemical engineering texts. Stoichiometry, the analysis of material balances around reactions of pure chemicals will not be covered. Processes which generate large amounts of energy through combustion or exothermic reactions will not be covered. The reader is referred to one or more references dealing with stoichiometry provided in Further Reading at the end of this chapter.

Food processing operations differ from conventional chemical processing operations in that raw materials used as feedstocks usually start as whole or parts of living plants or animals. These masses of cells may be refined to yield pure compounds as in the production of pure sucrose from sugar cane or sugar beets. Alternatively a portion of a plant or animal may be washed, trimmed of inedible tissue, and preserved by heat or refrigeration as with seafood, poultry, or various common fruits or vegetables preserved by refrigeration, canning, or freezing. The composition of raw plant and animal feed stocks may be highly variable. Thus the accuracy of material and energy balances used in the analysis of processes for the

preparation of these raw materials for further processing may require data based on representative samples of the raw material to be processed. These data may be taken on a representative pilot plant processing line or from tests on an existing process line. The food engineer must be aware of the variability of raw material feed stocks due to seasonal changes, country or region of origin, varietal, and growing factors.

Food processing operations may be grouped into four broad categories for the purpose of material and energy balance calculations. Category I and II operations reflect minimum mass transfer, but may require heat transfer. They can be handled with relatively straight forward calculations using handbook data. Category III and IV operations are less amenable to the use of handbook data. Results must be confirmed with pilot plant or process line tests. This is mainly due to the complex nature of food materials and their range of compositions due to biological variation.

Category I operations include the assembly and mixing of ingredients, with or without heating, to produce a food product with a proprietary formulation. This category also includes such unit operations as emulsifying, foaming, and coating. Material balances are straight forward and often can be determined from handbook data.

Category II operations deal primarily with energy balances related to preserving packaged foods by heating or cooling. This category also includes energy balances involving ionizing radiation, ultrahigh pressure, and other preservation means using a minimum of heat. The product is generally packaged before treatment. Energy balances generally can be determined from handbook data.

Category III operations include those which convert living plant and animal tissues to food ingredients by mechanical treatments such as washing, peeling, size grading, size reduction, inspection and defect removal, and mechanical transport. Some diffusional mass transfer may take place due to incidental soluble solids loss by process water leaching. For most Category III operations mass transfer is a minimum. Mass balances can reflect the yield of edible material, byproduct, and waste.

Category IV operations involve complex simultaneous heat and mass transfer. This category includes blanching, baking, drying, evaporation, distillation, heating by steam injection, extrusion, and evaporative or vacuum methods for cooling. Material and energy balances almost always require actual tests to confirm assumptions and calculations based on handbook data.

In general, Category I and II material and energy balances will be easier to complete, can be more accurately estimated, and can be made with fewer assumptions than those in Category III and IV since they are less dependent on the composition of the material being processed. For example, very accurate data on the heating rate and heat requirements for the heat sterilization of various sizes of canned pumpkin puree, a Category II operation, are available from handbooks (NFPA, 1995) and from computer simulations (Singh, 1996). By contrast it is difficult to determine the yield, energy requirements, byproduct flow, the composition of waste streams, and the finished product associated with the production of pumpkin puree from field run pumpkins. This process involves a series of Category III and IV operations. The method of heating the pumpkin, such as direct steam vs. immersion in water, would have a major effect on material and energy balances (Bomben et al., 1975). Factors such as leaching of solubles and absorption of water are difficult to predict and therefore must be determined by actual tests.

7.1.2 MATERIAL AND ENERGY BALANCES AROUND CATEGORY I OPERATIONS

Category I operations include the mixing of ingredients to produce a specific food product. The mixing of flavors, sugar, color, and water to make a juice drink is a typical example. Material balances around Category I operations usually can be calculated with a fair degree

of accuracy using handbook data for ingredient composition, physical, and thermophysical properties. Equation 7.1 provides an estimate for the specific heat (c_p) of a food based on its composition while Equation 7.2 allows estimates of the specific heat of meat products with water contents above 26% and fruit juices with water contents above 50% (Singh and Heldman, 1993).

$$c_p[kJ/kg°C] = 1.424\, m_c + 1.549\, m_p + 1.675\, m_f + 0.837\, m_a + 4.187\, m_m \qquad (7.1)$$

where m is the mass fraction of each component with subscripts: c, carbohydrate; p, protein; f, fat; a, ash; and m, moisture.

$$cp[kJ/kg°C] = 1.675 + 0.025\, w \qquad (7.2)$$

where w is water content (%). Both equations show that moisture content is a primary determinate of specific heat.

The following example will illustrate how a material and energy balance, using handbook data, could be used to estimate the yield, energy, and utility requirements for the manufacture of cans of a vegetable juice product, prepared from concentrated vegetable juices using the equations shown.

EXAMPLE 7.1   PRODUCTION OF A CANNED VEGETABLE JUICE

A company wishes to introduce a canned vegetable juice product containing carrot, tomato, and sweet red pepper juices with added salt, sugar, citric, and ascorbic acid. The composition of 100 units of the product is: salt 0.05, sugar 0.10, citric 0.05, ascorbic acid*, carrot concentrate 16.70, tomato concentrate 16.70, red pepper concentrate 16.70, water 49.70. The soluble solids (carbohydrate) of the final mix is found to be 20%.

Carrot and sweet red pepper juice ingredients are to be supplied in frozen concentrate form. Tomato concentrate is to be supplied in 300-gal aseptic bulk cartons. Juice concentrates are all purchased at 30% soluble solids concentration. Other ingredients (salt, color, flavor, sugar, citric, and ascorbic acid) are purchased in dry form. The finished product is to be filled in 46 oz. (1.36 l) cans at a minimum temperature of 200°F (93°C). The production rate is to be 300 cans/min for two 4-h shifts/d.

An abbreviated flow sheet for the process for mixing, heating, can filling, sealing, and cooling is shown:
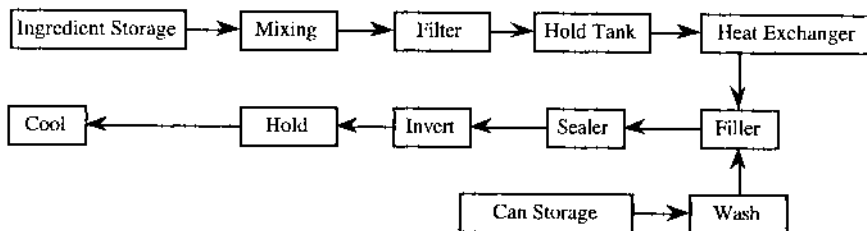
The basis for the material and energy balance is 1 h of operation. The first use of the material and energy balance could be to estimate the size of the processing equipment needed for each operation.

The information supplied indicates that the finished product will be packaged in cans holding 46 fluid oz (No. 3 cylinder, 404 × 700), however, the weight of the can contents was not given thus the mass flow of the product must be estimated from the specific gravity of the product. The net weight of a can of juice having 20% soluble solids and holding 46 fluid oz can be

---

* Ascorbic acid is to be present at a concentration of 100 mg per serving. A typical serving is 10 oz or 300 mL.

estimated from published specific gravity values for similar fruit and vegetable juice products (*The Almanac*, 1990). A value of 1.09 is representative of the specific gravity based on a soluble solids content of 20%. This value is equal to a label weight of 1460 g (51.5 oz). The mass flow per hour is then:

$$(300 \text{ cans/min})(60 \text{ min/hr})(1.460 \text{ kg/can}) = 26,280 \text{ kg/hr} \left(57,885 \text{ lb}_m / \text{hr}\right)$$

The specific heat of the juice may be estimated from Equation 7.2 to be 3.7 kJ/kg°C (0.9 Btu/lb$_m$°F). This data, plus the weight and heat capacity of the steel cans, will allow the calculation of the feed rate each hour for each ingredient and the energy per hour needed to heat the juice mix from its hold tank temperature to the sterilization process temperature. Additionally, cooling water flows can be estimated based on a cooled can temperature of 32°C (90°F) for the cans entering the labeling operation.

This example illustrates how data may be obtained for estimating material and energy balances when the composition of ingredients can be specified. Often a simple plot of moisture content or density against corresponding thermophysical properties for the foods of interest will provide a useful estimate of the desired value.

7.1.3 Material and Energy Balances around Category II Operations

Category II operations treat packaged food products which must undergo one or more heating or cooling steps or other preservation treatments, i.e., exposure to radiation, ultrahigh pressure, or capacitance discharge prior to storage and distribution. Heating or cooling is performed to preserve the packaged food by heat inactivating microbes or by cooling to a temperature where microbial growth is slowed or inhibited. Storage at temperatures below –18°C (0°F) will effectively inhibit the growth of all food spoilage microbes. Reactions causing loss of flavor and color may take place at –18°C due to active enzymes or the presence of oxygen.

EXAMPLE 7.2 ESTIMATION OF ENERGY REQUIREMENTS IN CANNED PRODUCT COOLING

Example 7.1 can be used to illustrate a simple Category II energy balance. In this case filled and sealed cans of juice are to be cooled from 93°C (200°F) to 32°C (90°F) prior to labeling. The weight of the can (No. 3 cylinder 404×700) must be determined by actual weighing since the can specifications were not provided. An average can weight was found to be 170 g. At a production rate of 300 cans/min 18,000 cans will be produced each hour and the total weight of the cans will be 3060 kg. The heat capacity (c_p) of steel is found to be 0.46 kJ/kg°C. The energy needed to be removed from the cans of juice per hour when cooling from 93 to 32°C is the total of the mass of juice times the heat capacity of the juice and the mass of steel times the heat capacity of the steel times the temperature difference.

$$m_{juice} = 26,280 \text{ kg} \qquad c_{p,steel} = 0.46 \text{ kJ/kg°C}$$

$$c_{p,juice} = 3.7 \text{ kJ/kg°C} \qquad T_0 = 93°C$$

$$m_{steel} = 3060 \text{ kg} \qquad T_f = 32°C$$

Energy removed per hour from the steel cans

$$Q_{cans} = (3060 \text{ kg/hr})(0.46 \text{ kJ/kg°C})(93°C - 32°C) = 85,864 \text{ kJ/hr}$$

Energy removed per hour from the juice

$$Q_{juice} = (26,280 \text{ kg/hr})(3.7 \text{ kJ/kg°C})(93°C - 32°C) = 5,931,400 \text{ kJ/hr}$$

Total cooling energy required

$$Q_{total} = Q_{cans} + Q_{juice} = 6,017,264 \text{ kJ/hr}$$

It should be noted that the cooling energy required for the cans is only about 1.5% of the total cooling requirement.

Heating of sealed cans in steam, to insure the complete inactivation of microbes, may involve a more complex energy balance calculation depending on the equipment used. For example, steam may be used to purge air (known as venting) from still retorts to insure that an atmosphere of pure steam surrounds each package. Steam requirements for venting must be determined from operating experience or from manufacturers data. Lopez (1987) provides steam consumption estimates for several canned fruit and vegetable products and for the flow of steam through holes of different sizes.

7.1.4 MATERIAL AND ENERGY BALANCES AROUND CATEGORY III PROCESSES

The profitability of processing raw plants and animals to ingredients for direct consumption by consumers or for further processing depends on the overall yield of edible product. Estimates of the yield of edible material from raw plants and animals are available in the literature. *The Almanac* (1990) lists yields of vegetables per acre and farm and processed weight equivalents, that is the mass yield of processed commodity from a unit mass of farm-weight raw material. For example, 1 kg of frozen apples is shown to require 1.67 kg of tree run fruit. This indicates an overall yield of 60%. This figure would be a useful first estimate for an overall material balance for an apple processing line producing frozen slices and could be useful for estimating energy requirements for freezing the processed product. Overall, vegetable yields are found to range from a low of 27% for sweet corn to a high of 92 and 95% for shelled peas and lima beans, respectively. Agriculture Handbook No. 8, (Watt and Merrill, 1963) can be used to estimate processing losses by consulting the tables listing edible portions of 1 lb of food as purchased. The 1963 revision, Table 2, contains a column entitled "Refuse" which provides data on the percent waste generated in obtaining an edible portion. The nature of the refuse is indicated, thus this reference is particularly useful.

Published overall yield figures are only approximate and most food processors can achieve higher overall yields. Overall yield is the result of the product of individual material balance yields for each unit operation used to convert the raw product to the finished processed product. The literature on food processing contains numerous references to studies seeking to increase the yield of useable material of various commodities from unit operations such as washing, peeling, size reduction, sorting, and handling. Major losses can result from peeling and size reduction. Sizing of raw materials having a wide range of sizes to obtain a narrow fraction can generate large amounts of under- and oversized byproduct. The utilization of sort-outs, and out-of-specification material generated in sizing operations can play an important role in the profitability of a raw product processing line.

7.1.5 MATERIAL AND ENERGY BALANCES
AROUND CATEGORY IV OPERATIONS

Unit operations and processes which include simultaneous heat and mass transfer are included in this category. These are represented by blanching, various methods of dehydration including frying, air drying, pervaporation, freeze drying, distillation, and concentration by evaporation.

TABLE 7.1
Yield and Solids Loss During Steam
Blanching for Various Vegetables

Material	Yield (%)	Solids Loss (%)
Carrots	95.0	2.0
Peas	89.0	2.5
Green Beans	93.0	1.7
Lima Beans	97.0	0.5
Broccoli	98.0	1.9
Cauliflower	97.0	2.1
Brussels Sprouts	101.8[a]	1.16

[a] Increased weight due to water pickup

Procedures for the accurate estimation of material and energy balances involving simultaneous or coupled heat and mass transfer are presented in Section 7.4. The classic blanching studies of Bomben et al. (1975), serve to illustrate the complexity of mass and energy balances when water uptake, tissue breakdown due to heating, and leaching losses occur simultaneously. The yield of seven commonly frozen vegetables blanched using steam was determined in this study where the three aforementioned changes occur simultaneously during the blanching operation. Their individual contributions to overall yield, soluble solids concentration in the liquid waste stream, and final product composition require a complete analysis of all product streams to obtain an accurate estimate of the true yield of product in terms of product solids. Yield and solids loss are given in Table 7.1

Even with this data, the true yield of water soluble vitamins and flavors may need to be determined independently as leaching rates for any selected water soluble vitamin may not be related to soluble solids loss by leaching. Accurate estimates of the nutritional composition of food ingredients must be known to meet nutritional labeling data requirements.

Careful material balance studies are needed when water is used in the transport, heating, cooling, and washing of raw plant and animal tissue or in the osmotic concentration of plant and animal tissue. During osmotic concentration water is removed by immersing the food in a syrup containing 60% or more sucrose (Lewicki and Lenart, 1992). The rate of weight loss is a function of piece size, temperature, syrup concentration, syrup flow rate, and composition. The composition of the final product will represent a balance between the loss of water and soluble nutrients, and the uptake of syrup solids. Chipoletti et al. (1977) carried out a similar analysis on the uptake of salt and ethanol in vegetables frozen at 20°F (–7°C) using a mixture of 15% ethanol and 15% sodium chloride as the coolant.

7.1.6 DEFINING TERMS

Before developing a material or energy balance around a process it is necessary to first identify the type of process under consideration. Unit operations may be classified according to the type of throughput, as **batch**, **semibatch**, or **continuous** processes.

1. Batch — A batch process is fed a charge of material which is then processed and discharged. During processing no material enters or exits the operation. (Example:
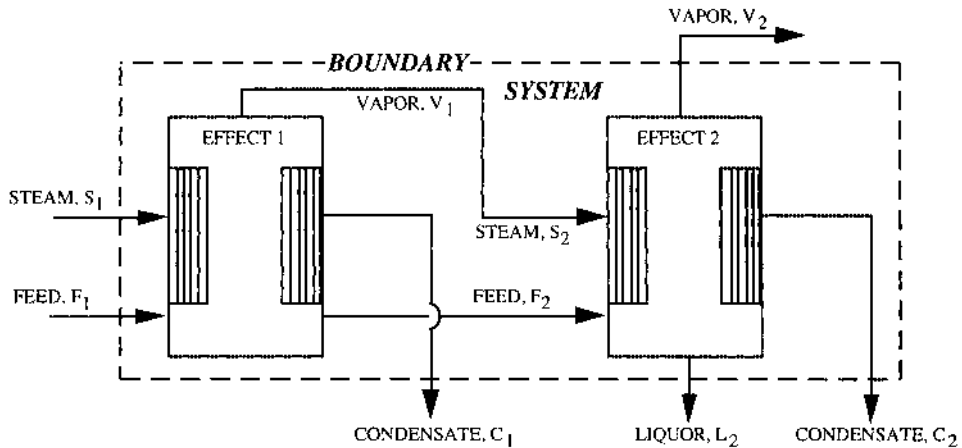
FIGURE 7.1 Example of a flowchart with a defined system and boundary for a double-effect forward feed evaporator.

In freeze-dehydration a chamber is loaded with frozen material, the material dried, and the chamber unloaded.)

2. Semibatch — A semibatch process (or semicontinuous process) is characterized by the continuous feed and discharge of discrete packs of material. (Example: In tunnel drying trucks containing product on trays are introduced at one end of the tunnel and removed at the other end, thus the semibatch process. Note that the air may flow concurrent or countercurrent to the direction of the trucks.)

3. Continuous — During a continuous process the input and output are introduced and removed continuously throughout the process. (Example: In the continuous production of aseptically processed juices, fluid is pumped through a heat-hold-cool cycle and packaged in a continuous fashion.)

Steady state and **transient** are used to describe the relationship between various process variables (such as temperature, flow rate, or pressure) and time. If these variables are independent of time the process is known as steady state, if they change with time the process is transient. Typically, continuous processes may be assumed to be steady state in operation and batch/semibatch operations are transient.

Material and energy balance calculations are developed around a defined **system** which may consist of a complete processing line, one unit operation in the line, or a portion of that unit operation. Regardless, the system is defined by a **boundary** which is drawn around it during the construction of a **flowchart** of the process. These are shown in Figure 7.1.

The system may be **open** or **closed** according to whether material crosses the boundary during the period of time of interest. The system is closed if no mass crosses the boundary and is open otherwise. By definition, semibatch and continuous processes are treated as open systems while a batch process may be open or closed.

A **basis of calculation** is used to simplify process scale up or down. A basis may be a unit of time (1 s, min, or h), mass (1 kg, 1 lb_m), or mass flow rate (1 kg/s, 1 lb_m/h). If a mass or mass flow rate is specified in the problem, it is often most convenient to use this quantity as a basis of calculation. If no mass amount or flow rate is given, it is then necessary to assume one.

It is rare to have pure substances to work with, especially in the food industry. Consequently it becomes necessary to define the amount of various components which combine to form the entire material. One of the most frequently used methods is that of **mass fraction** or x_i^j where "i" refers to the specific stream carrying the compound and "j" designates the

compound. Mass fraction is calculated as the mass of the compound over the total mass of the material. Thus, if a material is composed of 4 kg oil, 13 kg starch, and 1 kg water then the mass fraction of oil would be 0.22.
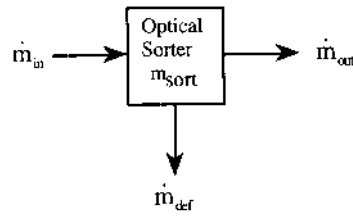
FIGURE 7.2 Flowchart defining the unit operation of optical sorting. m_{in} = Feed material (kg/s); m_{out} = discharged inspected material (kg/s); m_{def} = defective material (kg/s); m_{sort} = material in sorter (kg).

7.2 MATERIAL BALANCES

Section 7.2 focuses on material balances using a Category III operation, sorting, as an example. Material balances for Category IV operations such as frying, drying, steam injection heating, and evaporative cooling will be treated in Section 7.4.

7.2.1 GENERAL MASS BALANCE

The sum of the mass balances around each unit operation will yield the mass balance around an entire process. In order to perform a mass balance, it is necessary to identify and specify all material flows within narrow limits. The principle of mass conservation forms the basis for the calculation of the general mass balance. This principle requires that, in a given time interval, all mass entering or leaving a system across a defined boundary surrounding the system must be counted together with the mass already in the system. Thus

$$\begin{matrix} \text{total mass} \\ \text{into the system} \end{matrix} - \begin{matrix} \text{total mass} \\ \text{out of the system} \end{matrix} = \begin{matrix} \text{total mass accumulated} \\ \text{in the system} \end{matrix} \tag{7.3}$$

The unit operation of sorting can be used to illustrate a simple mass balance. Defective materials are removed from a flow of washed, cut, and sized product prior to unit operations used for preservation. One method of sorting uses high speed optical inspection of each piece of food. Pieces enter the sorter and are subject to an intense light while passing under an array of diodes. These optical transducers record the spectrum of light energy reflected from the material and send the signals to a computer which compares the spectrum to a standard for acceptable color. Pieces with spectrum differing from the standard by a preset amount are removed from the main flow of material by mechanical means. A flowchart for the process is given in Figure 7.2. For a general case, the flow rate of product to the sorter is $d\dot{m}_{in}/dt$, the flow rate leaving the sorter is $d\dot{m}_{out}/dt$, and the rate of flow of defective material is $d\dot{m}_{def}/dt$. The mass of product in the sorter at any time is identified as $d\dot{m}_{sort}/dt$.

In this example the feed to the sorter will be assumed to be either zero (shut down status) or a constant value (operating status) equal to $\dot{m}_{in}$ (kg/s). For constant feed rate conditions, m_{sort} (kg) will be a constant proportional to $\dot{m}_{in}$ since the sorter is not designed to accumulate product. If all product is acceptable, then $\dot{m}_{out}$ will be constant and equal to the feed rate. If defective product is present in the feed then the sum of the flows of $\dot{m}_{out}$ and $\dot{m}_{def}$ will be

equal to the feed rate. This condition would represent normal sorter operation. Flow rates of defective material are generally a small percentage of the entering feed.

Equation (7.4) summarizes the conditions noted above and illustrates the principle of mass conservation. The notation accounts for the rate of flow of 1 to L streams into the sorter (m_{in}) and 1 to M streams out (m_{out}) plus 1 to N defective streams out ($\dot{m}_{def}$). The mass of material in the system at any instant is m_{sort} and is assumed to be constant. Note that multiple defective streams may be used for production of "value-added" products from various grades of waste material.

$$\sum_{i=1}^{i=L} \dot{m}_{in,i} - \left(\sum_{j=1}^{i=M} \dot{m}_{out,j} + \sum_{k=1}^{i=N} \dot{m}_{def,k} \right) = 0 \qquad (7.4)$$

7.2.2 APPLICATION OF MASS BALANCES TO THE PROCESSING OF RAW PLANT AND ANIMAL MATERIALS

Mass flow rates and material balances for the design of processing plants, to convert raw plant materials to ingredients, are required to determine equipment capacity, labor needs, water supplies, and waste handling capabilities. The yield of finished packaged product per ton of raw plant tissue harvested (overall yield) is the mass balance information of primary importance in the design of a processing line to treat seasonal fruits and vegetables. Handbook data are available (Jones, 1990) for converting farm weights of fruits and vegetables to cases of canned or frozen fruit and vegetable commodities. These values are useful as a first approximation in checking the yields calculated from a material balance for any proposed process line. The amounts of byproduct and waste can be estimated from these data.

Yield of edible materials often forms the basis of payment for raw materials. For example, apple size and extent of bruising directly affects the yield and value of fresh apples when used for canned apple slices and sauce. Quantitative correlations have been developed in a classic set of studies by Johnson et al. (1959). These studies show the relationship between apple size and bruise level on case yield and labor requirements to prepare slices or sauce. Equations were developed to link raw material quality with raw material prices to insure that processing lines could operate at their design capacity and maintain a desired return on investment. Farkas (1967) demonstrated how the ratio of seed size to pod diameter could be used to predict processed snap bean quality and yield and hence form the basis for estimating raw material value.

7.2.2.1 Peeling

The following will illustrate the application of material balances around unit operations for peeling plant products, i.e., fruits, vegetables, and grains. Several methods can be used to remove the outer layer of cells constituting the peel which protects the inner edible tissue. These include high pressure steam, freezing, alkali solutions, i.e., sodium hydroxide, and mechanical means, i.e., cutting, abrasion, or grinding.

Milling of wheat, to obtain a flour containing almost pure endosperm, a mixture of starch and protein largely free of bran and equal to about 75% of the weight of a wheat kernel, is accomplished by mechanically rubbing the bran layer of cells of the wheat berry to remove them from the soft endosperm (Matz, 1991). This is accomplished by first conditioning the bran cell layer with moisture to make it plastic. The grain then passes through a series of paired break rolls machined with horizontal teeth running the length of the rolls. The opposing rolls run at slightly different speeds so as to shear the wheat kernel as it passes through the nip of the rolls. A series of these rolls with progressively closer nip settings is used to rub

the bran layer from the endosperm. Sifting occurs between each set of break rolls to remove the bran fraction from the flour. Since a mill may produce up to 500 ton flour/d, improvements in the yield of flour in the second decimal place can be significant. Rice milling requires a similar understanding of the material balance around each milling operation (Matz, 1991).
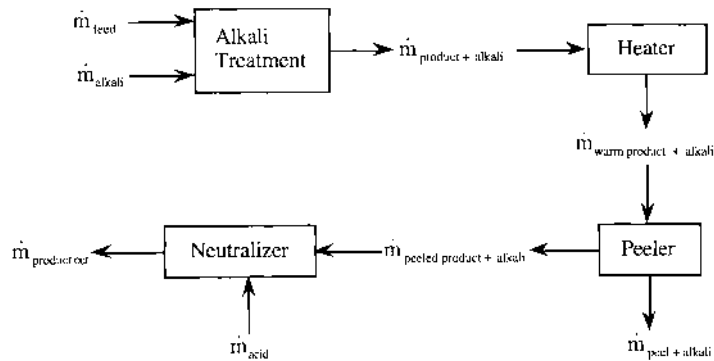
FIGURE 7.3 Flowchart for chemical peeling of fruits and vegetables where $\dot{m}$ = mass flow rate (kg/s) and subscripts refer to specific stream.

Chemical peeling is based on the use of alkali materials, i.e., sodium- or potassium hydroxide solutions of controlled strength and temperature. The product to be peeled, e.g., potatoes, beets, carrots, or tomatoes, is immersed in the caustic solution for a controlled length of time. The caustic diffuses through the peel layer to the layer of cells connecting the peel to the edible material. Diffusion may be enhanced by the use of a wetting agent to facilitate the penetration of the caustic through a natural waxy layer usually present on the surface of plant materials. The connective cells are partially digested by the caustic and thus the peel is released from the edible tissue. The released peel can be removed by mechanical brushes and washing. The exposed edible tissue layer is dipped in acid to neutralize any residual caustic. The alkali containing peel and wash water form a slurry which, after neutralization by addition of acid or by a lactic acid fermentation, can be used as animal feed.

The process of chemical peeling described above includes four separate unit operations, Figure 7.3. The first unit operation is that of alkali treatment of the material to be peeled. The system has flows of product and alkali entering a tank of alkali and a flow of product containing alkali leaving the tank.

For Figure 7.3 it is assumed that the food material to be peeled and the tank of alkali are at room temperature. The reader is referred to the work of Graham et al. (1969) on the dry caustic peeling of potatoes for a detailed analysis of the chemistry of peeling. The second unit operation is one of heat transfer to warm the product to a temperature where the alkali will rapidly diffuse and digest the cells connecting the peel to the edible portion. The third unit operation is mechanical peel removal while the fourth unit operation is a neutralization step. Steps one and two are often accomplished in a single unit using heated alkali. Similarly, Steps three and four can be combined in a single peel removal machine with the use of a neutralizing spray just before discharge of the peeled material from the machine. Assuming steady state operation, general material balance equations may be written and applied to each unit operation or combination of unit operations. These general equations consist of a total balance and component balance as follows.

Total mass balance

$$\sum_{i=1}^{i=N} \dot{m}_i = \sum_{j=1}^{j=M} \dot{m}j \qquad (7.5)$$

where N is the number of streams entering the process and M is the number of streams exiting the process. Again, Equation 7.5 may be applied to any system operating at steady state.

Component mass balance

$$\sum_{i=1}^{i=N} x_i^k \dot{m}_i = \sum_{j=1}^{j=M} x_j^k \dot{m}_j \qquad (7.6)$$

where k is a specific component of the streams i and j. Simply, Equation 7.6 states that the mass of a component entering the system must equal the mass exiting the system.

The maximization of yield of edible product is the usual goal of a successful process design. Thus each of the four unit operations in the peeling process must be optimized in terms of delivering a high ratio of $\dot{m}_{product}/\dot{m}_{feed}$. Process optimization can be achieved by

1. Breaking down a process into its individual unit operations
2. Drawing a boundary around each unit operation to define the system
3. Inspecting the boundary of the system to determine all *entering* materials and their mass flow rates
4. Inspecting the boundary of the system to determine all the *exiting* materials and their mass flow rates
5. During steady state operation, determining the mass of material inside the system boundary

For the unit operation designed to contact product with alkali, for any given constant flow rate of product into the contacting system, the mass flow of alkali will be proportional to the amount absorbed or adhering to the product. A higher concentration and/or a longer contact time is likely to increase the uptake of alkali. For a fixed flow of product, the only way a longer hold time can be achieved is to increase the size of the contacting equipment. This will result in a larger mass in the system. The rate which the alkali penetrates into the product by diffusion will be influenced by numerous factors including: physical properties of the product, surface concentration, hold time, mechanical agitation, and temperature.

In addition to maximizing yield of edible tissue by minimizing excess peel removal, the caustic peeling process must minimize the use of alkali. The process should provide precise control of alkali diffusion by coating the product to be peeled with a controlled amount of alkali. In a four-step process, the cold alkali coated product is exposed to heat to raise the surface temperature quickly while concentrating the surface alkali by evaporation. At the precise moment when the cells holding the peel have been digested, the peel can be removed mechanically from the edible tissue. Finally, a small amount of water containing an edible acid can be brushed on the product to neutralize any remaining alkali. The peel-alkali mix is removed as a concentrated slurry (hence the name of the four-step process "dry caustic peeling") and can be fermented to animal feed or used as a source of fermentable carbohydrate through a enzymatic saccharification step.

The high cost of sodium hydroxide plus the problems of disposing high concentrations of sodium in alkali-containing wastes has provided an incentive for the use of high pressure steam for peeling. High temperatures will soften the cells holding the peel to the edible flesh of potatoes, other root vegetables, and tomatoes in a manner analogous to chemical peeling.

A brief exposure to saturated steam at temperatures up to 150°C will loosen the peel sufficiently to allow mechanical removal. A small amount of wash water combined with mechanical scrubbing will remove any residual peel tissue. The removed peel and wash water can be pumped to storage and used for animal feed without further treatment.
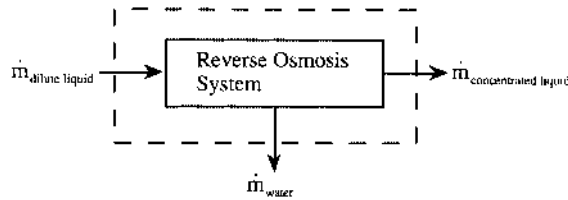
FIGURE 7.4   Material balances for reverse osmosis of dilute liquid foods.
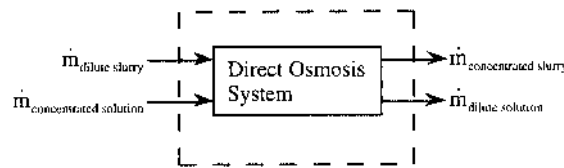
FIGURE 7.5   Material balances for direct osmosis concentration of dilute liquid food slurries.

Peeling using steam, radiant heat, or direct flames for heat transfer consists of two unit operations. The first involves an energy balance. This will be discussed in Section 7.3. The second unit operation is the mechanical removal of the loosened peel. This is similar to the peeling operation used for chemically peeled product. No acid wash is required.

7.2.2.2   Membrane Separations and Countercurrent Extraction

Membranes can be used to concentrate dilute liquid foods and to recover dilute soluble and suspended food components, i.e., starches, sugars, and proteins. Alternate methods have been developed to remove water and other low molecular weight compounds and ions from dilute liquid foods. Examples range from the desalinization of sea water by reverse osmosis to the removal of alcohol from wine or beer to obtain a low alcohol product (Boulton et al., 1996). A dilute food can be concentrated by reverse osmosis by pushing the water in the food through a membrane designed to retain all compounds with a molecular weight (molecular size) slightly larger than water. The liquid is pumped into an array of membranes of a given area. At a pressure slightly greater than the osmotic pressure of the system, which is a function of the chemical composition and concentration of the system, water will start to flow from the low pressure side of the membrane. The rate of flow will be a function of the concentration of the system and will be reduced by any chemical or mechanical changes in the membrane caused by the food. A thorough analysis of membrane concentration operations can be found in King (1980). As the system becomes more concentrated, higher pressures are required to maintain a constant rate of water passage (flux) through the membrane area.

Alternatively, a membrane with a dilute liquid on one side, can be exposed to a concentrated solution on the other. Thus the water dissolving or diffusing into the membrane on the dilute side will be osmotically absorbed by the concentrated solution on the other side. This process, which is called direct osmosis, is useful for the concentration of dilute food slurries which could foul reverse osmosis membranes and which could present excessively high pumping pressures in reverse osmosis systems. Solutions of sugar or salt are used as the concentrated solution. These can be reconcentrated by standard means for evaporative con-

centration. Figures 7.4 and 7.5 show a material balance around a reverse osmosis and direct osmosis system, respectively.

Continuous counter current extraction and batch extraction operations are used for the separation of a soluble food fraction from an insoluble matrix. The extraction medium is usually water, but alcohol may be used for flavor extraction, hexane can be used for vegetable oil extraction, and super critical gases, i.e., carbon dioxide, can be used to remove caffeine from coffee and tea or hop aroma from dry hops.
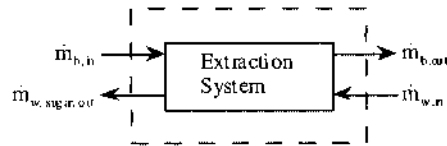
FIGURE 7.6 Material balance around a system defined as cut sugar beets during the first stage of counter current extraction of sugar.

Sugar beets contain up to 20% sucrose at harvest. The sucrose can be extracted by flowing the sugar beet, sliced to maximize surface area while minimizing cell damage, in a counter current manner against a stream of pure water (Avlani et al., 1976). As the sugar beet moves against the water flow, the water becomes enriched in sugar and the beet tissue becomes enriched in water. A material balance on the system, defined as the insoluble cut sugar beet mass, at any point in the counter current extraction process, will show two materials entering the system and two materials leaving. Figure 7.6 illustrates the material balance around the insoluble beet slices during initial mixing and separation.

This process can be repeated many times until the desired level of sucrose is extracted from the beet pulp. The concentration of the sucrose in the water leaving the extractor will be at a lower value then the concentration of the sugar in the fresh beet slices. However, a simple material balance on the counter current extractor system as a whole can provide the overall ratio of water to beet slices. Assume 100 units of beet slice enters the extractor each hour. If 100 units of pure water enter the opposite end of the extractor each hour and if the beet slices are fully extracted of sucrose, then the concentration of sucrose in the water leaving the extractor is

$$x_{w,out}^{sugar} = \frac{\text{Mass of sugar in extraction liquid}}{\text{Total mass of extraction liquid}} = \frac{x_{b,in}^{sugar}\ \dot{m}_{b,\ in}}{x_{b,\ in}^{sugar}\ \dot{m}_{b,\ in} + \dot{m}_{w,\ in}}$$

thus

$$x_{w,out}^{sugar} = \frac{(0.20)(100 \text{ units beets})}{(0.20)(100 \text{ units beets}) + (100 \text{ units water})} = 0.167$$

Thus, for an efficient counter current sugar beet extractor, the concentration of the sugar in the final stage extraction water may reach 16.7%, if the beet slices do not gain water during extraction. The actual amount of water held by the beet slices can be determined by analysis. If significant water is held by the beet slices then a mechanical pressing operation can be used to return the pure water to the system. The pressed beet slices would be available for feed or conversion to byproducts.

Casimir (1983) designed an unique countercurrent extractor for the preparation of fruit and vegetable juices from fresh apples, pears, cranberries, tomatoes, and other fruits and vegetables. The system employed a perforated screw conveyor to move the product against

a flow of warm water in a jacketed trough. The screw conveyor was driven by a motor which could be programmed to turn the screw N turns forward and then N-1 turns in reverse. This invention prevented the thinly sliced tissue being extracted from riding along with the screw. Food materials have a tendency to stick to the screw conveyor in conventional single or double screw counter current extractors. The reversing motion creates a stirred reactor in each flight of the screw and gives extremely high contacting efficiency for the volume of the equipment.

A counter current extractor has considerable material holdup. The holdup requirements are in proportion to the rate of diffusion of soluble material from the food pieces. As with reverse or direct osmosis processes, the rate of diffusion is influenced by piece thickness, temperature, agitation, and concentration (Gunasekaran et al., 1989).

7.2.3 CONCLUSIONS

This section has illustrated a range of material balances from those carried out around simple mixing processes to those depending on diffusion controlled processes. The simplicity of the material balance underlines its usefulness in the analysis of product flows to and from any defined unit operation. The examples used in this section were selected to emphasize the need for care in defining the boundary of the system in which the mass flows are to take place. In some cases, it may be desirable to separate the material balance from the energy balance around the system in order to understand any transport phenomena which may control the **rate** of the operation. Again, it should be noted that material and energy balances do not deal with the mechanisms of heat or mass transfer. They are used to measure the amount of energy or material or rate of material or energy flowing in a given time across a boundary. When these values are known, then the actual process equipment can be sized based on a detailed knowledge of reaction rates, i.e., rate of inactivation of a heat resistant pathogen or the rate of diffusion of sugar from a slice of fruit.

7.3 ENERGY BALANCES

The driving force behind performing material and energy balances is to understand the flow of mass and energy in a system and identify potential areas for conservation or increased yield. Energy balances are written to account for the flow of energy into and out of a given process. This information, when used in conjunction with a material balance, leads to determining the overall energy required by the system. Typical processes involving energy balances are

1. Freezing/thawing — Energy required to freeze/thaw an amount of material from an initial to final temperature;
2. Blanching — Energy required to blanch broccoli at a desired rate
3. Pumping — Pump size needed to pump 300 l/min of a fluid from a holding tank to a packing line
4. Refrigeration — Required refrigeration capacity needed to maintain a frozen storage facility

These and many other practical questions may be answered through energy balances.

7.3.1 DEFINING TERMS

As discussed in Section 7.1.6, a system is defined as a region in space or quantity of matter. The interface between the system and its surroundings is known as the boundary. The boundary may be real, i.e., the walls of a blancher, or the boundary may be imaginary,

containing a blancher and freezer. The system may also be defined as open or closed. An open system allows exchange of mass with the surroundings while a closed system allows none.

Properties of the system may be described as **intensive** (i.e., pressure, density, or temperature) or **extensive** (i.e., volume, mass, or moles). Intensive properties are independent of the quantity of material in the system, extensive properties are dependent on the quantity of material in the system. The condition of the system or its components is called the **state** and is related to the intensive properties, i.e., temperature, pressure, phase, and composition.

Energy balances are based on conservation of energy or the **first law of thermodynamics** which states that energy can neither be created nor destroyed. This is in parallel to the conservation of mass given in the previous section and therefore yields a similar equation known as the **general energy balance**

$$
\begin{array}{c}\text{total energy} \\ \text{into the system}\end{array} - \begin{array}{c}\text{total energy} \\ \text{out of the system}\end{array} = \begin{array}{c}\text{total energy accumulated} \\ \text{in the system}\end{array} \tag{7.7}
$$

Note that if the system is in a steady state, total energy accumulated is zero, thus:

$$
\begin{array}{c}\text{total energy} \\ \text{into the system}\end{array} = \begin{array}{c}\text{total energy} \\ \text{out of the system}\end{array} \tag{7.8}
$$

A system may consist of energy in three forms: **kinetic** energy (KE), **potential** energy (PE), and **internal** energy (U). Kinetic energy is due to the motion of the system, such as flowing water through a pipe and is calculated as:

$$
KE = \frac{mv^2}{2} \tag{7.9}
$$

Potential energy is sometimes known as stored energy and is due to the position of the system (water in a tank on stilts possesses potential energy) or is due to a conformation of the system relative to its equilibrium state (a wound rubber band). Potential energy is calculated as

$$
PE = mgh \tag{7.10}
$$

Finally, internal energy is due to the random motion of molecules in the material under consideration. This motion may result from thermal, chemical, molecular, or nuclear sources. The sum of these three forms is the **total energy** of the system (E) which may accumulate.

Energy in transit, across the system boundary, is not a property of the system. **Heat** (Q) and **work** (W) constitute this type of energy. Heat transfer is the result of a temperature difference between the system and its surroundings and may be in the form of conduction, convection, and/or radiation. Work, by definition, is positive when done by the system on the surroundings.

If the Subscript 1 is used to denote initial (or entrance) conditions and Subscript 2 to denote final (or exit) conditions a total energy balance on a system may be written as (Felder and Rousseau, 1986)

$$
Q + W + U_1 + KE_1 + PE_1 = U_2 + KE_2 + PE_2 \tag{7.11}
$$

Note that Q is positive when heat is added to the system and W is positive if work is done on the surroundings and negative if work is done on the system. Equation 7.11 may be rewritten for the change in energy of the system as

$$Q + W = \Delta U + \Delta KE + \Delta PE \tag{7.12}$$

Equation 7.12 is the basic form for the first law of thermodynamics. It is important to note that in a closed system work is accomplished through the movement of the system boundary against an opposing force, i.e., a piston in a chamber (work resulting from changes in pressure or volume) or shaft turning a mixing blade (work resulting from friction and molecular motion), or by generation of an electrical or radiative current which passes through the system boundary. If these do not exist then W = 0. An open system, by definition, allows mass to pass through the system boundary leading to the production of **shaft work** (W_s) and **flow work** (W_f). Shaft work is that imparted to a fluid in the system by a mechanical means, i.e., a turbine. The difference between the work performed on a fluid at its entrance to a system and its exit is the flow work (Felder and Rousseau, 1986):

$$W_f = P_1 \dot{V}_1 - P_2 \dot{V}_2 = \Delta \left(P \dot{V} \right) \tag{7.13}$$

where P = pressure, $\dot{V}$ = volumetric flow rate, and Subscripts 1 and 2 denote entrance and exit position, respectively. Thus, work in an open system is expressed as $W = W_s + W_f$. This leads to

$$Q + W_s + W_f = \Delta U + \Delta KE + \Delta PE \tag{7.14}$$

or

$$Q + W_s + \Delta \left(P \dot{V} \right) = \Delta U + \Delta KE + \Delta PE \tag{7.15}$$

The **enthalpy** (H) of a system is defined as (Singh and Heldman, 1993):

$$H = U + PV \tag{7.16}$$

or

$$\Delta H = \Delta U + \Delta \left(PV \right) \tag{7.17}$$

Substitution of Equation 7.17 into 7.15 yields the starting point for most energy balance calculations on open, steady state systems.

$$Q + W_s = \Delta H + \Delta KE + \Delta PE \tag{7.18}$$

If the process under consideration does not involve changes in kinetic and potential energy and has no shaft work Equation 7.18 reduces to (Singh and Heldman, 1993)

$$Q = \Delta H \tag{7.19}$$

This will be the starting point for most energy balance calculations addressed in this chapter. Processes involving flow (and thus shaftwork) potential, and kinetic energy, are addressed in Chapter 1.

7.3.2 ENTHALPY

It is not possible to measure the absolute value of enthalpy, H, of a material but rather the change in enthalpy is measured corresponding to a change of state in the process material. Therefore, a **reference state** is required and the change in enthalpy between the reference state and state of interest is determined. The reference state is chosen arbitrarily, often depending on available data and ease of calculation.

In considering Equation 7.19 it is seen that a change in enthalpy is simply a change in heat content. Two types of change in heat content are typically found in food processing, sensible heat and latent heat. Sensible heating involves the increase in temperature of the material in the system (Singh and Heldman, 1993)
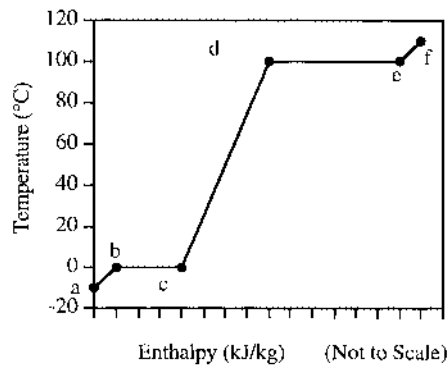
FIGURE 7.7 Temperature vs. enthalpy plot for the conversion of ice to superheated steam. (Adapted from Singh, R.P. and Heldman, D.R., 1993, *Introduction to Food Engineering*, 2nd ed., Academic Press, New York.)

$$\Delta H = Q = m \int_{T_1}^{T_2} c_p dT \qquad (7.20)$$

where m = mass of material, kg; T_1 and T_2 = initial and final temperature, respectively, °C; and c_p = the **specific heat** of material, kJ/kg°C. Assuming a constant c_p over the temperature range, integration of Equation 7.20 yields

$$\Delta H = Q = mc_p \left(T_2 - T_1\right) \qquad (7.21)$$

where c_p is the specific heat of the material over the specified temperature range. Enthalpy changes involving latent heat are due to a change in phase of a material, i.e., the melting of ice, at a constant temperature. Latent heat of fusion (ΔH_f) is found in melting and latent heat of vaporization (ΔH_v) is found in evaporation.

EXAMPLE 7.3

Write a general equation for the total change in enthalpy for heating a mass of ice to steam for the process shown in Figure 7.7. Based on Figure 7.7 it is clear that the process may be broken down into five distinct stages consisting of either sensible heating (ab, cd, and ef) or absorbtion

of latent heat (bc and de). The sum of the energy required in each of these stages is the total energy required for the process. This is given as

$$\Delta H_t = mc_{p,ice}\left(T_b - T_a\right) + m\Delta H_{bc,fus} + mc_{p,water}\left(T_d - T_c\right) + m\Delta H_{de,vaor}\left(T_f - T_e\right)$$

This approach may also be used with food materials if the required property data is known. Once again, the reader is referred to Chapter 11 which covers physical and thermal properties for a variety of materials.

7.3.3 PERFORMING ENERGY BALANCES: GENERAL METHOD

An energy balance may be performed on an existing process to determine the energy throughput of unknown streams and process efficiency or on a theoretical process to aid in the design and sizing of energy sources, i.e., boilers, steam lines, or electrical wiring. Regardless, the process may be broken down into a stepwise method, similar to that found in material balances. This method is outlined in the following example.
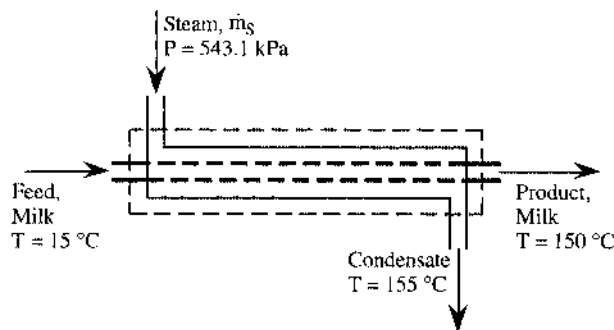
FIGURE 7.8 Concurrent flow tubular heat exchanger.

EXAMPLE 7.4 INDIRECT STEAM HEATING: OPERATION OF A CONCURRENT TUBULAR HEAT EXCHANGER

Milk is to undergo UHT (ultra high temperature) processing with a concurrent tubular heat exchanger being used as the method of heating. UHT lowfat (2%) fluid milk is to be produced at 5000 kg/h with a desired time/temperature of 2 seconds at 150°C. Milk with an initial temperature of 15°C is fed to the heat exchanger and steam at 543.1 kPa and 100% quality is used as the heating media. Condensate at 155°C flows from the steam trap. What is the required flow rate of steam to the heat exchanger? The composition of 2% lowfat milk is given as: 89.2% moisture; 3.3% protein; 2% fat; 4.8% carbohydrate; 0.7% ash.

The following solution outlines a stepwise approach which may be used in most energy balance calculations:

1. Construction and Labeling of a Process Flowchart. Figure 7.8

Construct a block diagram of the process, whether it is in the design phase or operational, and draw a boundary (dashed line) identifying the system and surroundings. The flowchart should be labeled with all known and unknown material and energy streams entering and exiting the system. The labels should reflect the phase (solid, liquid, or vapor) of the material, for example $H_2O(s)$ for ice or $H_2O(v)$ for vapor, if it is unclear.

2. Determine the Specific Enthalpy of Each Stream and Stream Components (If Needed): Reference State: Water at 0°C.

Energy in:

Milk:

$$\Delta H_{M,I} = \dot{m}_M c_{p,M} \left(T_M - T_{ref} \right)$$

From Equation 7.1 the specific heat is found as

$$c_p = (1.424 \ kJ/kg°C)(0.048) + (1.549 \ kJ/kg°C)(0.033) + (1.675 \ kJ/kg°C)(0.020) +$$

$$(0.837 \ kJ/kg°C)(0.007) + (4.187 \ kJ/kg°C)(0.892) = 3.894 \ kJ/kg°C$$

$$\Delta H_{M,I} = (5000 \ kg/h)(3.894 \ kJ/kg°C)(15°C - 0°C) = 292,050 \ kJ/h$$

Steam

$$\Delta H_S = \dot{m}_S H_v$$

From the steam tables the enthalpy of steam (H_v) is found to be 2746.5 kJ/kg thus

$$\Delta H_S = (\dot{m}_S)(2746.5 \ kJ/kg)$$

Energy Out

Milk

$$\Delta H_{M,O} = (5000 \ kg/h)(3.894 \ kJ/kg°C)(150°C - 0°C) = 2,920,500 \ kJ/h$$

Condensate

$$\Delta H_C = (\dot{m}_C)(4.18 \ kJ/kg°C)(150°C - 0°C) = (\dot{m}_C)(627 \ kJ/kg)$$

3. Write the appropriate energy balance equations and solve for the desired quantities

$$\Delta H_{M,I} + \Delta H_S = \Delta H_{M,O} + \Delta H_C$$

or

$$292,050 \ kJ/h + (\dot{m}_S)(2746.5 \ kJ/kg) = 2,929,500 \ kJ/h + (\dot{m}_C)(627 \ kJ/kg)$$

Using $\dot{m}_S = m_C$ and solving for m_S yields

$$\dot{m}_S = 1240 \ kg/h$$

Therefore, 1240 kg/h steam will be required to heat 5000 kg/h fluid milk. Note that the condensate exits the heat exchanger at 155°C contains considerable energy which may be utilized.

7.3.4 EXAMPLES OF UNIT OPERATIONS AND SOURCES OF ENERGY

The following are a series of examples which reflect a variety of energy balance problems the practicing engineer might encounter. Although it is clearly not possible to cover all possible unit operations the following examples contain many of the same calculations and may be applied to a wide variety of scenarios even though the process or product may be different.

EXAMPLE 7.5 SENSIBLE HEATING PROCESS: BATCH RETORTING

A retort and 2000 cans of tuna fish have been heated to a uniform temperature of 116°C. It is desired to cool the cans to 35°C before removing them from the retort. How much cooling water is required if it enters the retort at 20°C and leaves at 30°C?

Given
Specific heat of Tuna fish (c_p) = 3.65 kJ/kg°C
Specific heat of can wall (c_p) = 0.46 kJ/kg°C
Specific heat of water (c_p) = 4.18 kJ/kg°C
Mass of tuna fish/can = 450 g
Mass of can wall/can = 55 g
Energy required to cool retort = 75,000 kJ
Assume negligible heat loss through retort walls

Solution
1. Construct and label a process flowchart. In this case the problem is very simple, this is reflected in the flowchart of Figure 7.9.
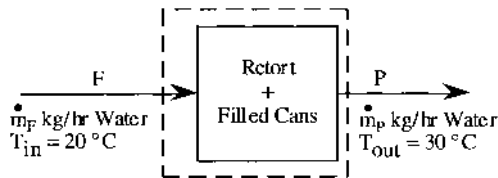

FIGURE 7.9   Retorting of canned tuna fish.

2. Determine the enthalpy of each stream

$$\Delta H_F = Q_F = \dot{m}c_p\left(T_{in} - T_{ref}\right)$$

$$\Delta H_P = Q_P = \dot{m}c_p\left(T_{out} - T_{ref}\right)$$

Total change in enthalpy of water

$$\Delta H_{water} = Q_{water} = \Delta H_P - \Delta H_F = \dot{m}_{water}c_{p,water}\left(T_{out} - T_{in}\right)$$

or

$$Q_{water} = \dot{m}_{water}\left(4.18\frac{kJ}{kg°C}\right)(30°C - 20°C)$$

Determine the heat lost by the retort, cans, and tuna fish

$$Q_{retort} = 75,000 \text{ kJ}$$

$$Q_{cans} = m_{can} c_{p,can} \left(T_{initial} - T_{final} \right)$$

$$Q_{tunafish} = m_{tunafish} c_{p,tunafish} \left(T_{initial} - T_{final} \right)$$

Total heat lost by system (retort, cans, and tunafish)

$$Q_{sys} = 75,000 \text{ kJ} + m_{can} c_{p,can} \left(T_{initial} - T_{final} \right) + m_{tunafish} c_{p,tunafish} \left(T_{initial} - T_{final} \right)$$

or

$$Q_{sys} = 75,000 \text{ kJ} + \left(55 \frac{g}{can} \right) (2000 \text{ cans}) \left(\frac{1 \text{ kg}}{1000 \text{ g}} \right) \left(0.46 \frac{kJ}{kg°C} \right) (116°C - 35°C)$$

$$+ \left(450 \frac{g}{can} \right) (2000 \text{ cans}) \left(\frac{1 \text{ kg}}{1000 \text{ g}} \right) \left(3.65 \frac{kJ}{kg°C} \right) (116°C - 35°C)$$

$$Q_{sys} = 345,183.6 \text{ kJ}$$

Solve for the mass of water required by equating Q_{water} and Q_{sys}

$$Q_{water} = Q_{sys}$$

$$\dot{m}_{water} \left(4.18 \frac{kJ}{kg°C} \right) (30°C - 20°C) = 345,183.6 \text{ kJ}$$

$$\dot{m}_{water} = 8,258 \text{ kg}$$

Note that while the energy balance gives a total quantity of water required for cooling it does not give an indication as to the time required for the process. An approximation of this time may be determined through the use of unsteady state heat transfer calculations (Singh and Heldman, 1993).

EXAMPLE 7.6 SENSIBLE HEATING PROCESS: CONTINUOUS BLANCHING

A tunnel blancher is designed to process 5000 kg/h of cut broccoli using steam at atmospheric pressure. Determine the theoretical steam consumption.

Given
Input temperature of broccoli = 15°C
Output temperature of broccoli = 100°C
Specific heat of broccoli (c_p) = 3.8 kJ/kg°C
Assume 100% efficiency for theoretical calculation

Solution
1. Construct and label a process flowchart, Figure 7.10
2. Determine the enthalpy of each stream
   Reference state: water at 0°C

$$\Delta H_F = Q_F = \dot{m}_F c_{p,F} \left(T_{in} - T_{ref} \right)$$

$$\Delta H_P = Q_P = \dot{m}_P c_{p,P} \left(T_{out} - T_{ref} \right)$$

$$\Delta H_s = \dot{m}_s \Delta H_{vap}$$

Note that only the latent heat of vaporization is considered as the condensate stream exits at 100°C and therefore does not lose sensible heat to the system.
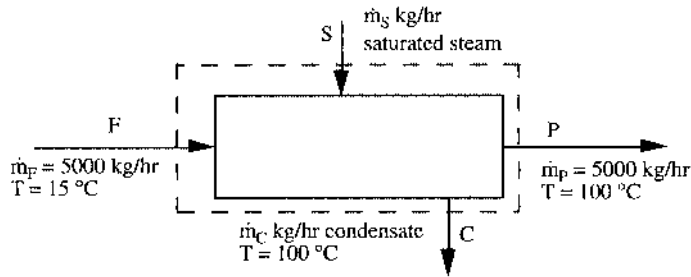

FIGURE 7.10 Blanching broccoli.

3. Determine theoretical steam required by equating enthalpies

$$\Delta H_P - \Delta H_F = \Delta H_S$$

$$\dot{m}_F c_{p,F} \left(T_{out} - T_{in} \right) = \dot{m}_s \Delta H_{vap}$$

$$\left(5000 \frac{kg}{hr} \right) \left(3.8 \frac{kJ}{kg°C} \right) (100°C - 15°C) = \dot{m}_s \left(2257 \frac{kJ}{kg} \right)$$

$$\dot{m}_s = 716 \ kg/hr$$

It is important to note that in this example the steam required was calculated assuming 100% efficiency. Many blanchers are typically only 10 to 30% efficient and the reader is referred to Singh (1986) for further discussion on energy monitoring in the food industry.

EXAMPLE 7.7 LATENT HEAT PROCESS: THAWING AND EVAPORATION

Determine the heat required to thaw 200 kg of frozen tomato juice, bring it to the boiling point, and evaporate 50 kg of water from the juice. The process takes place at atmospheric pressure, assume no freezing point depression or boiling point elevation.

Given
Initial temperature of frozen juice = –10°C
Freezing point of juice = 0°C
Boiling point of juice = 100°C
Specific heat of frozen juice (c_p) = 2.01 kJ/kg°C
Specific heat of liquid juice (c_p) = 3.98 kJ/kg°C
Latent heat of fusion (ΔH_{fus}) = 333.2 kJ/kg
Latent heat of vaporization (ΔH_{vap}) = 2257 kJ/kg

Solution

1. Construct and label a process flowchart. In this case it is more useful to diagram the heating process rather than an actual unit operation.

    Step 1: Sensible heat from –10 to 0°C
    Step 2: Latent heat of fusion at 0°C (thawing)
    Step 3: Sensible heat from 0 to 100°C
    Step 4: Latent heat of vaporization at 100°C (boiling)

2. Determine the energy (Q) required at each step.

    Step 1: $Q_1 = m_1 c_{p,1} (T_{final} - T_{initial})$
    Step 2: $Q_2 = m_2 \Delta H_{fus}$
    Step 3: $Q_3 = m_3 c_{p,3} (T_{final} - T_{initial})$
    Step 4: $Q_4 = m_4 \Delta H_{vap}$

3. Determine the total energy required by summing all steps.

$$
\begin{aligned}
Q_{tot} &= Q_1 + Q_2 + Q_3 + Q_4 \\
&= m_1 c_{p,1}\left(T_{final} - T_{initial}\right) + m_2 \Delta H_{fus} + m_3 c_{p,3}\left(T_{final} - T_{initial}\right) + m_4 \Delta H_{vap} \\
&= (200\ kg)\left(2.01\frac{kJ}{kg°C}\right)\left(0°C -^- 10°C\right) + (200\ kg)\left(333.2\frac{kJ}{kg}\right) \\
&\quad + (200\ kg)\left(3.98\frac{kJ}{kg°C}\right)(100°C - 0°C) + (50\ kg)\left(2257\frac{kJ}{kg}\right) \\
&= 263,110\ kJ
\end{aligned}
$$

Again note that the balance does not give any information on heating time and that the energy calculated is for an idealized process. While the above calculation is a good method of determining an order of magnitude approximation for energy requirements, a more accurate calculation would include losses to the environment, freezing point depression, and boiling point elevation which are discussed by Toledo (1991).

EXAMPLE 7.8   MIXING STREAMS OF DIFFERENT TEMPERATURE

A hot gas composed of nitrogen and oxygen, with mole fractions of 0.79 and 0.21, respectively, is used to heat water in a steady state flow heat exchanger. The liquid water enters at a rate of 10 kg/s, 15°C, and atmospheric pressure and exits as steam at 200°C and 1553.8 kPa. The gas stream enters at 300°C, 1 atm, and exits at 150°C, 1 atm. Determine the mass flow rate of hot gas required for the process. Assume 100% efficiency.

1. Construct and label a process flowchart, Figure 7.11.

    Stream A, Gas In: $x_1 = 0.79\ N_2$, $x_2 = 0.21\ O_2$, $T_A = 300°C$
    Stream B, Gas Out: $x_1 = 0.79\ N_2$, $x_2 = 0.21\ O_2$, $T_B = 150°C$
    Stream C, Water In: 10 kg/s, $T_C = 15°C$
    Stream D, Steam Out: 10 kg/s, $T_D = 200°C$

FIGURE 7.11   Mixing of streams; steam generation.

2. Write the appropriate energy balance equations for the enthalpy of each stream.
Energy lost by cooling of heating media, sensible heat:

$$\Delta H_{AB} = \dot{m}_G c_p \left(T_A - T_B \right)$$

Energy gained by water stream may be determined using steam table values:

$$\Delta H_{CD} = \dot{m}_W \left(\Delta H_{vap}^{200} - \Delta H_{lip}^{15} \right)$$

3. Solve for the desired quantities.
   I. Determine the change in enthalpy of the water.

$$\Delta H_{CD} = \left(10 \ \text{kg/s} \right) \left(2793.22 \ \text{kJ/kg} - 62.99 \ \text{kJ/kg} \right) = 27,302 \ \text{kJ/s}$$

   II. Find the c_p of the gas (Felder and Rousseau, 1986) at 300°C using:

$$c_p^T = \sum_{i=2}^{n} x_i c_{pi}^T \quad \text{and} \quad \bar{c}_p = \frac{1}{n} \sum_{i=2}^{n} c_{pi}^{T_i}$$

$$c_p^{300} = \left(0.79 \right) \left(29.52 \ \text{kJ/mol°C} \right) + \left(0.21 \right) \left(42.10 \ \text{kJ/mol°C} \right)$$

$$c_p^{300} = 32.16 \ \text{kJ/mol°C}$$

$$c_p^{150} = \left(0.79 \right) \left(29.26 \ \text{kJ/mol°C} \right) + \left(0.21 \right) \left(39.50 \ \text{kJ/mol°C} \right)$$

$$c_p^{150} = 31.41 \ \text{kJ/mol°C}$$

$$\bar{c}_p = \left(\frac{32.16 + 31.41}{2} \right) \frac{\text{kJ}}{\text{mol°C}} = 31.79 \ \frac{\text{kJ}}{\text{mol°C}}$$

$$\bar{c}_p = \left(31.79 \ \frac{\text{kJ}}{\text{mol°C}} \right) \left(31.373 \ \frac{\text{kg}}{\text{mol}} \right)^{-1} = 1.01 \ \frac{\text{kJ}}{\text{kg°C}}$$

   III. Solve for the mass flow rate of the gas stream using $\Delta H_{AB} = \Delta H_{CD}$

$$\left(\dot{m}_G \right) \left(1.01 \ \text{kJ/kg°C} \right) \left(300°C - 150°C \right) = 27,302 \ \text{kJ/s}$$

$$\dot{m}_G = 180 \ \text{kg/s}$$

7.4   COUPLED MATERIAL AND ENERGY BALANCES

The coupling of mass and energy balances adds an additional difficulty to the calculations yet the coupled balance problem is one of the most common and useful problems. The coupled balance problem allows the linking of material feed and exit rates with process energy consumption. Clearly, this becomes a powerful tool in the determination of process efficiency. Any processes involving simultaneous energy, mass, and/or momentum transfer will require the use of coupled material balances. Examples of such processes are drying, evaporation, and flash cooling. Development and solution of coupled mass and energy problems involves

a procedure similar to that outlined in previous sections on non-coupled problems. This procedure is outlined in the following example for a single effect evaporator.

EXAMPLE 7.9   SINGLE-EFFECT EVAPORATION OF JUICE

A juice at 20°C with 8% total solids is being concentrated in a single-effect evaporator. The evaporator is being operated at a sufficient vacuum to allow the product moisture to evaporate at 70°C, while steam at 95% quality is being supplied at 84.55 kPa. (See Chapter 6 for a discussion on steam quality.) The feed material enters the evaporator at a rate of 7000 kg/h. A small amount of energy, 2000 kJ/h, leaves the evaporator as losses to the surrounding environment. Calculate the product, vapor, steam, and condensate flow rates and the steam economy for the process, when the condensate is released at 70°C. The specific heat of the feed is 4.0 kJ/kg°C, and of concentrated product is 3.2 kJ/kg°C. Ignore any effects due to boiling point elevation of the juice as it condenses. These are discussed by Toledo (1991).

Solution

1. Construct and label a process flowchart (Figure 7.12).
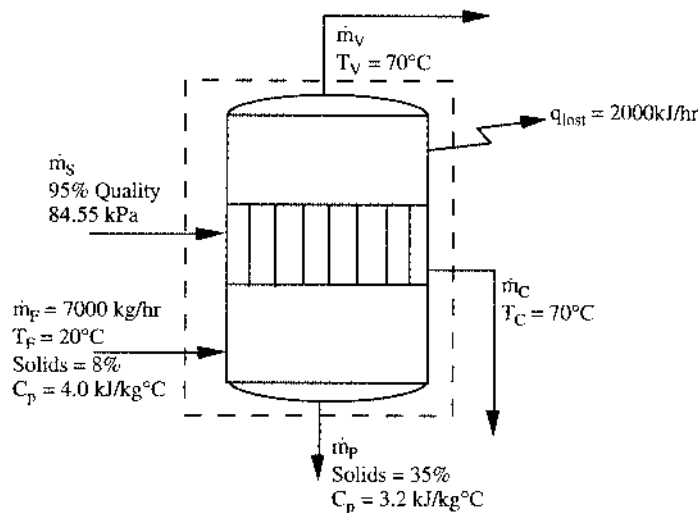
FIGURE 7.12   Single effect evaporator.

2. Develop general mass and energy balance equations around the process.
    Total mass balance, mass in = mass out

$$\dot{m}_F + \dot{m}_S = \dot{m}_V + \dot{m}_P + \dot{m}_C$$

and

$$\dot{m}_S = \dot{m}_C$$

so

$$\dot{m}_F = \dot{m}_V + \dot{m}_P$$

Solids mass balance, solids in = solids out

$$x_F^S \, \dot{m}_F = x_P^S \, \dot{m}_P$$

Total energy balance, energy in = energy out

$$q_F + q_S = q_V + q_P + q_C + q_{lost}$$

3. Determine the enthalpy of each stream.
Reference state: water at 0°C

$$q_F = \dot{m}_F c_p \left(T_F - T_{ref} \right)$$

$$= \left(7000 \text{ kg/hr} \right) \left(4.0 \text{ kJ/kg°C} \right) \left(20°C - 0°C \right) = 560,000 \text{ kJ/hr}$$

$$q_S = \dot{m}_S \left(\Delta H_c^{110} + 0.95 \left(\Delta H_v^{110} - \Delta H_c^{110} \right) \right)$$

$$= \dot{m}_S \left(461.3 \text{ kJ/kg} + 0.95 \left(2691.5 \text{ kJ/kg} - 461.3 \text{ kJ/kg} \right) \right) = \dot{m}_S \left(2578 \text{ kJ/kg} \right)$$

$$q_V = \dot{m}_V \Delta H_v^{70}$$

$$= \left(5400 \text{ kg/hr} \right) \left(2626.8 \text{ kJ/kg} \right) = 14,184,720 \text{ kJ/hr}$$

$$q_P = \dot{m}_P c_p \left(T_P - T_{ref} \right)$$

$$= \left(1600 \text{ kg/hr} \right) \left(3.2 \text{ kJ/kg°C} \right) \left(70°C - 0°C \right) = 358,400 \text{ kJ/hr}$$

$$q_C = \dot{m}_C \Delta H_c^{70}$$

$$= \dot{m}_C \left(292.98 \text{ kJ/kg} \right)$$
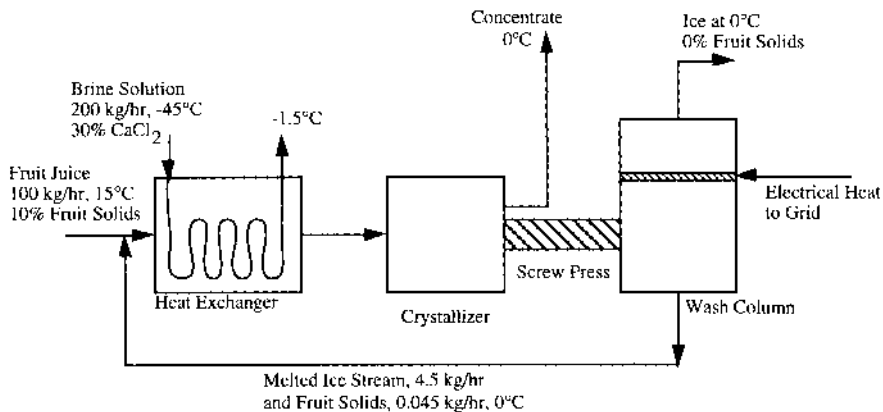
$$q_{lost} = 2000 \text{ kJ/hr}$$

FIGURE 7.13 Concentration of fruit juice.

4. Write the appropriate energy balance equations and solve for the desired quantities.

$$560,000 \text{ kJ/hr} + \dot{m}_S \left(2578 \text{ kJ/kg} \right) = 14,184,720 \text{ kJ/hr} + 358,400 \text{ kJ/l}$$

$$+ \dot{m}_C \left(292.98 \text{ kJ/kg} \right) + 2000 \text{ kJ/}$$

Recalling that $m_S = m_C$ and solving for m_S yields

$$\dot{m}_S = \dot{m}_C = 6120 \text{ kg/hr}$$

Steam economy $= \dot{m}_V/\dot{m}_S = 5400 \text{ kg/h}/6120 \text{ kg/h} = 0.882$

Evaporation is used extensively in the food industry for production of pastes and sauces, including orange juice, maple syrup, and tomato paste. These have a greatly reduced weight and volume from the raw material and are hence less expensive to transport. Advantages to evaporation include high efficiency, especially when multiple effects and vapor recompression are used, and high material throughput. Holland and Liapis (1983) cover the mechanics of evaporation and utilize numerical simulation for analysis of efficiency, throughput, and flow configuration.

Removal of water from a raw or partially processed material is one of the principle methods of preservation. In the previous example evaporation was used to examine a case in which both mass and energy balances were needed to find the required information. Other forms of moisture removal include many types of drying, membrane separation, and freeze concentration. The following example uses the process of freeze concentration to demonstrate coupled mass and energy balances in which a solid-liquid phase change is involved.

EXAMPLE 7.10 FREEZE CONCENTRATION OF FRUIT JUICE

Fruit juice may be concentrated by removing water in the form of ice as shown in Figure 7.13. Refrigeration is provided by a 30% $CaCl_2$ brine solution and heat exchanger. Ice crystals from the crystallizer are pressed into the wash column where 4.5 kg/h of ice are melted and used to wash solids off the surface of the other crystals before being recycled to the feed. *Note:* Heat is in the form of an electric resistance heating grid.

Assuming 1960 kJ/h leaks into the system due to poor insulation, calculate the concentration of solids which may be achieved in the concentrate stream.
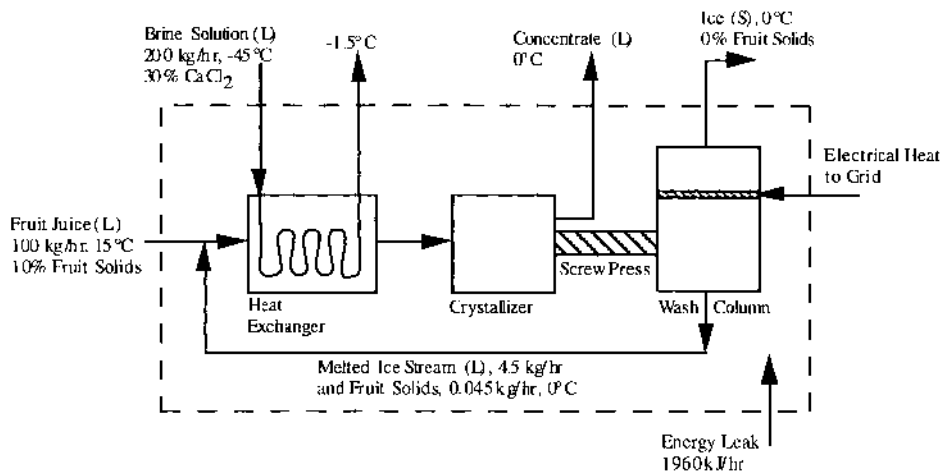
FIGURE 7.14 Concentration of fruit juice.

1. Construction and labeling of a process flowchart: Figure 7.14.
   Draw a flow diagram of the process with a boundary (dashed line) identifying the system and surroundings. The flowchart should be labeled with all known and unknown material and energy streams entering and exiting the system. The labels should reflect the phase (solid, liquid, or vapor) of the material, for example $H_2O(S)$ for ice or $H_2O(V)$ for vapor, if it is unclear. Note that it may be necessary to first perform a material balance to determine the mass flow rate of one or more streams.

2. Determine the specific enthalpy of each stream and the stream components. Reference state: 0°C (ice)

Energy in:
Feed

$$c_p = 1.675 \text{ kJ}/\text{kg}°C + [0.025 \text{ kJ}/\text{kg}°C][90\%] = 3.925 \text{ kJ}/\text{kg}°C$$

$$\Delta H_f = (100 \text{ kg}/\text{hr})(3.925 \text{ kJ}/\text{kg}°C)(15°C - 0°C) + (90 \text{ kg}/\text{hr}(333.22 \text{ kJ}/\text{kg}) = 35,877.3 \text{ kJ}/\text{h}$$

Brine

$$c_p = 1.675 \text{ kJ}/\text{kg}°C + [0.025 \text{ kJ}/\text{kg}°C][70\%] = 3.425 \text{ kJ}/\text{kg}°C$$

$$\Delta H_b = (200 \text{ kg}/\text{hr})(3.425 \text{ kJ}/\text{kg}°C)(-45°C - 0°C) + (140 \text{ kg}/\text{hr}(333.22 \text{ kJ}/\text{kg}) = 15,825.8 \text{ kJ}/\text{h}$$

Leak

$$\Delta H_l = 1960 \text{ kJ}/\text{hr}$$

Heater

$$\Delta H_h = (4.5 \text{ kg}/\text{hr})(333.22 \text{ kJ}/\text{kg}) = 1,499.5 \text{ kJ}/\text{h}$$

Energy Out:
Brine

$$\Delta H_b = (200 \text{ kg}/\text{hr})(3.425 \text{ kJ}/\text{kg}°C)(-1.5°C - 0°C) +$$
$$(140 \text{ kg}/\text{hr})(333.22 \text{ kJ}/\text{kg}) = 45,623.3 \text{ kJ}/\text{h}$$

Concentrate
Let m_w = mass of water in concentrate stream

$$\Delta H_c = (m_w \text{ kg}/\text{hr})(333.22 \text{ kJ}/\text{kg})$$

Ice

$$\Delta H_i = 0 \text{ kJ}/\text{hr}$$

3. Write the appropriate mass and energy balance equations and solve for the desired quantities.

$$\Delta H_f + \Delta H_{b,in} + \Delta H_l + \Delta H_h = \Delta H_{b,out} + \Delta H_c + \Delta H_i$$

or

$$35,877.3 \text{ kJ/hr} + 15,825.8 \text{ kJ/hr} + 1960 \text{ kJ/hr} + 1,499.5 \text{ kJ/h}$$

$$45,623.3 \text{ kJ/hr} + \left(m_w \text{ kg/hr}\right)\left(333.22 \text{ kJ/kg}\right) + 0 \text{ kJ/hr}$$

Solving for m_w yields

$$m_w = 28.63 \text{ kg/hr}$$

therefore

$$x_s = \frac{10 \text{ kg solids/hr}}{38.63 \text{ kg total/hr}} = 0.259$$

Thermal processing of foods requires that a food be heated to a target temperature and held for a prescribed period of time, e.g., retorting and pasteurization. Following application of the thermal treatment it is desired to cool the product as quickly as possible to minimize losses in quality and nutrient content. Cooling may be accomplished by several means and selection of the best method is largely dependent on the material/package to be cooled. For example, water immersion with air over pressure is most common in retorting of canned products. In this process, one is limited by the need to prevent cans containing a food material at temperatures above 100°C from rupturing. Cooling of pumpable foods in a continuous process may be accomplished in a wide variety of heat exchangers, by flash cooling, or by addition of a cold ingredient. In the following example a fruit puree is to be cooled through the addition of ice. The quantity of ice must be determined based on the flow rate and thermal properties of the incoming liquid, and the desired end temperature of the product.
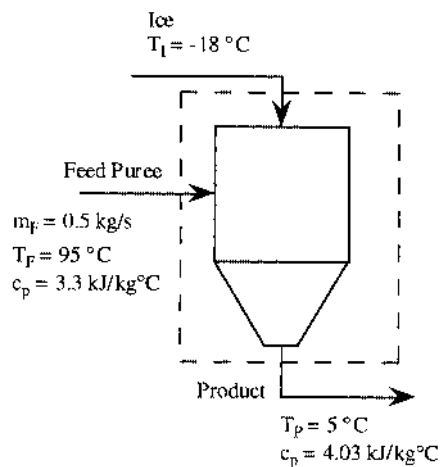
FIGURE 7.15 Cooling of fruit puree.

EXAMPLE 7.11   COOLING OF HOT LIQUID WITH ADDITION OF ICE

Fruit puree at 95°C is to be cooled on a continuous basis to 5°C by the addition of ice, initially at –18°C. The puree, with a specific heat of 3.3 kJ/kg°C, is pumped into an insulated continuous flow stirred tank reactor with the required mass flow rate of ice. The juice which exits has a

specific heat of 4.03 kJ/kg°C. Determine the flow rate of ice into the reactor if puree is pumped in at 0.5 kg/s.

Mass balance

$$\dot{m}_F + \dot{m}_I = \dot{m}_P$$

Energy balance, reference state: 0°C (liquid)

$$q_F + q_I = q_P$$

$$q_F = \dot{m}_F c_{p,F}\left(T_F - T_{ref}\right) = \left(0.5 \text{ kg/s}\right)\left(3.3 \text{ kJ/kg°C}\right)\left(95°C - 0°C\right) = 156.74 \text{ kJ/s}$$

$$q_I = \dot{m}_I c_{p,I}\left(T_I - T_{ref}\right) + \dot{m}_I \Delta H_{fus}$$

$$= \dot{m}_I\left(c_{p,I}\left(T_I - T_{ref}\right) + \Delta H_{fus}\right) = m_I\left((2.02 \text{ kJ/kg°C})\left(-18°C - 0°C\right) - 333.22 \text{ kJ/kg}\right)$$

$$= \dot{m}_I\left(-369.58 \text{ kJ/kg}\right)$$

$$q_P = \dot{m}_P c_{p,P}\left(T_P - T_{ref}\right) = \dot{m}_P\left(4.03 \text{ kJ/kg°C}\right)\left(5°C - 0°C\right)$$

$$= \dot{m}_P\left(20.15 \text{ kJ/kg}\right)$$

Solve for the mass flow rate of ice using mass and energy balance equations:

Mass balance

$$\dot{m}_P = 0.5 \ \text{kg/s} + \dot{m}_I$$

Energy balance

$$156.75 \ \text{kJ/s} + \dot{m}_I\left(369.58 \ \text{kJ/kg}\right) = \dot{m}_P\left(20.15 \ \text{kJ/kg}\right)$$

to yield:

$$\dot{m}_P = 0.38 \ \text{kg/s}$$

7.5 ECONOMICS OF MATERIAL AND ENERGY BALANCES AND CONCLUSIONS

Material and energy balances form the basis for optimizing the design or modification of a food processing facility. Virtually all costs, types, and sizes of equipment, labor, and staffing requirements, utility inputs, and waste streams are determined from material and energy flows. Additionally, raw material availability and delivery schedules, daily and weekly operating schedules, finished product shipping schedules, and inventories are all determined by the flow of material and energy through the plant. The material and energy balance for the overall plant and each individual unit operation must be studied on a regular basis to insure that maximum recovery of raw materials is being achieved with the minimum use of energy and water. Changes in raw material composition, waste disposal costs, or labor can justify an analysis of current unit operations with the objective of justifying the installation of new equipment, new waste management procedures, or improving the productivity of plant personnel. For example, the availability of efficient electronic sorting and defect detection

equipment has reduced the need for hand sorting of a wide variety of fruit and vegetable commodities. A justification for the purchase of this equipment can be developed by an analysis of material flows and level of defect removal per worker.

In the following example the decision to purchase a continuous cooker is based on the combination of material and energy balances, and economic analysis.

EXAMPLE 7.12   THERMAL PROCESSING OF CRABS: PURCHASE OF BATCH OR CONTINUOUS COOKER

Background

Crabs are a valuable seafood commodity along the coastal regions of the U.S. A portion of the harvest is sold live while the remaining is thermally processed, the edible portion separated, or "picked", and sold to the food service industry and retail stores. The process is highly labor intensive from the harvest and sorting of live crabs to the picking of meat from the body and claws of the cooked product. Cooking is done by either boiling or retort processing in saturated steam.

Problem

The newly formed ABC Crab Co. is trying to determine whether to purchase a still retort (a batch process) or a continuous cooker to thermally process their crabs. It has been brought to their attention that the use of a continuous cooker may save them money while at the same time increasing product quality, throughput, and safety. Unfortunately a "turn-key" continuous cooker is approximately $100,000 while a still retort is $15,000. Due to the high quality and price of the product and desire to take the market "by storm" they decide to proceed with a numerical comparison of the two processes. Some of the factors which must be considered are throughput, energy efficiency, product quality, labor required, capital investment, etc. One of the most important factors is the yield of edible meat. Yield is typically low, in the 10 to 12% range, and small increases in the yield are significant due to the high price of the product (*Note:* This is for Blue crabs but we will extrapolate to all crab types for this example).

Background — Batch Process

A basket containing 1000 kg of crabs is loaded into a retort which is then closed and steam introduced while venting air out. The process runs with a slight overpressure to maintain a flow from the bleed vents. When the retort temperature reaches 100°C the cook cycle is started and continues for 14 min. It is known that the ideal process time is 8 min, but due to inefficiency in the steam distribution an extended period is required to fully process crabs at the center of the retort. When cooking is complete the retort is opened, the hot loaded basket is taken out for cooling, and a new load introduced. A total turn-around time of 20 min is standard and an average of 3000 kg/h is processed. The still retort requires four operators and uses approximately 0.25 kg steam/kg crab.

Background — Continuous Process

The continuous cooker is comprised of a belt on which the raw material is loaded at one end and removed from at the opposing end. The belt moves the product through a saturated steam cooking chamber at a constant speed. The unit has a rated capacity of 5000 kg crabs/h but may be operated as low as 1000 kg crabs/h with little decrease in efficiency. Due to a high level of control and continuous nature, cook times are 10 min. In addition, the unit requires two operators and uses 0.20 kg steam/kg crab.

Additional Information

Hourly labor for operating either cooker is paid $6.00/h and pickers are paid by the pound at an average of $3.63/kg of meat picked. Live crabs are purchased at $0.77/kg.

Solution

This problem is typical of those commonly found in small to medium sized processing operations. The question of whether or not to by a piece of equipment, hire more personnel, implement

a new process, or schedule a shut-down for maintenance are problems that engineers and plant managers face almost daily. In this problem the need to spend an additional $85,000 for the purchase of a continuous cooker is questioned. Tangible factors, i.e., labor, throughput, and yield, must be considered but other intangibles, i.e., the ability to control throughput, increase production above immediate requirements, and process alternative products, are more difficult to quantify. The solution comes in the form of a simple economic balance most easily solved on a spread sheet such as Microsoft Excel™.

A general flow diagram which represents both processes may be drawn:
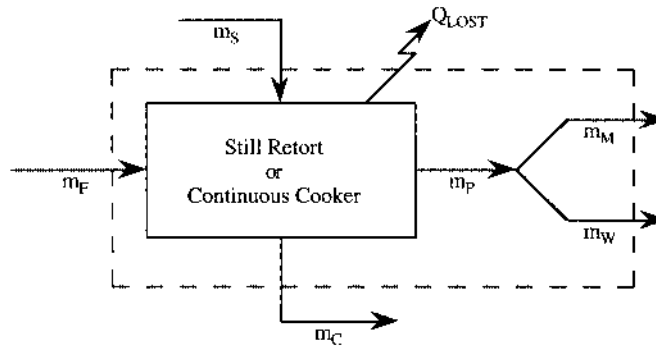
where m_F is mass of feed, m_S is mass of steam, m_C is mass of condensate, m_P is mass of product, m_M is mass of salable (edible) meat, m_W is mass of waste, and Q_{LOST} is the quantity of energy lost to the environment. In this type of analysis we are concerned with determining each of these quantities and how they are manifested in the economics of the operation. In addition, the influence of these variables on other factors of economic importance, i.e., labor, must be determined.

The basis of calculation for this problem is 1 h. The continuous process has the ability to produce a higher throughput than the still retort, therefore the production rate is set at 3000 kg/h for ease of comparison. It has been shown that the optimum retort cook time for (Dungeness) crab is approximately 8 min and that each minute over this time leads to a 0.6% reduction in yield of salable meat (Crapo and Crawford, 1991). Due to inefficiencies the still retort requires 14 min and the continuous process 10 min for sufficient thermal processing. The maximum yield of edible meat is approximately 12% but due to losses in processing the actual yield is lower. Finally, the continuous process requires two fewer personnel for operation and is slightly more efficient in steam usage. Based on this information the following data and equations are given for implementation on a spread sheet.

Mass balance:

$$m_F + m_S = m_P + m_C$$

using

$$m_F + m_S = m_P +$$

yields

$$m_F + m_S = m_M + m_W + m_C$$

Energy balance:

$$m_F c_{p,F}\left(T_F - T_{REF}\right) + m_S \Delta H_S = m_M c_{p,M}\left(T_M - T_{REF}\right) + m_W c_{p,W}\left(T_W - T_{REF}\right) + m_C \Delta H_C - Q_{LOST}$$

Yield:

$$\text{Yield of edible meat} = \ Y_F = \left(m_M / m_F\right) \times (100) \tag{7.22}$$

Neither of these processes has been installed therefore it is not possible to actually determine the mass of edible meat produced, m_M, in each process. Therefore, using the empirical correlation given by Crapo and Crawford (1991) for yield leads to:

$$Y_F = Y_{MAX} - 0.6\left(t_A - t_o\right) \tag{7.23}$$

where Y_F is the final yield of salable meat, %; Y_{MAX} is the maximum yield of salable meat, %; t_A is the actual process time, min; and t_O is the optimal process time, min. Using this empirical relationship allows the output of the two processes to be compared on a theoretical level. It should be noted that actual yields may be quite different. Once Y_F is obtained using Equation 7.23 the kilograms of salable meat produced, m_M, may be determined using Equation 7.22. An example of the tie between mass and energy balances and economic calculations is as follows.

Calculations show that the batch process produces 252 kg of picked meat per hour while the continuous process produces 324 kg/h due to a shorter process time (Equations 7.22 and 7.23). In addition, the continuous process uses 150 kg/h less steam than the batch process. This example will use only raw material and labor costs to illustrate the link between material balances and economic returns. Table 7.3 compares differences between batch and continuous processing costs on an hourly basis.

TABLE 7.3
Cost Per Hour for Batch and Continuous Processing of Crab

Cost item[a]	Batch	Continuous
Raw crab, $0.77/kg	$2310	$2310
Picked meat, $3.63/kg	$915	$1176
Equipment operator, $6/h	$24	$12
Steam cost[b]	—	—
Total cost per hour	$3249	$3498
Value of product, $26.40/kg	$6653	$8554
Increase in value[c]	$3404	$5056
Difference in value per hour between continuous and batch	$1652	

[a] Basis is 1 h of operation using 3000 kg of raw crab with yields of 252 kg for the batch process and 324 kg for the continuous process.
[b] Steam cost is neglected for this example.
[c] Increase in value = value of product – total cost per hour.

This very limited analysis favors the purchase of a continuous system since the yield increase is significant and the value of the processed product high. The capital cost of the continuous system was $85,000 higher than the batch system. Based on this preliminary analysis the number of operating hours needed to return $85,000 is estimated to be:

$$\$85,000 / \$1652 / \mathrm{hr} = 52 \mathrm{\ hr}$$

This operating period represents less than 2 weeks of single shift operation and clearly favors the use of continuous equipment. This example also illustrates the effect of yield on operating costs for foods with a high sales value. In general, the purchase of improved process technology to achieve higher yields favors meat products of all kinds and a limited number of fruit and vegetable products.

Food processing plants which operate year round and produce a variety of products provide an additional challenge in terms of optimizing the use of raw products, processing equipment, utilities, and labor to deliver finished packaged food products at the lowest cost. Least costs must be determined not only for each product, but for each product in relation to each other. In this case, the lowest cost for any single product may not be the least overall operating cost or most profitable operating mode for the plant as a whole. Consideration must be given to electric rates throughout the day, premiums for certain labor shifts, change-over costs, cleaning schedules, and availability of seasonal raw materials. The need to stop production to clean a process line between different products must be considered when scheduling a series of products for manufacture on a single line. For example, a flavored milk would be processed after an unflavored milk to avoid the need to clean the line between product runs.

Computerized simulations are available to help in the optimization of a processing plant. Simulations are based on material and energy balances for a given set of products, a defined set of unit operations, and a set of delivery schedules. Programs are available (Balint and Okos, 1990) to help determine the sequence, length of operation, and time of day to run several products on single or parallel lines. These programs take into account the cost factors outlined above and, based on the shipping requirements for each product, determine the most cost effective process schedule.

The optimization of any plant and its individual unit operations must be ongoing even when the plant appears to be running efficiently based on standards developed by product development, industrial engineering, and accounting personnel. Value engineering is the process for reducing the overall cost of an individual product through ingredient substitution, package, or process modification. For food processing operations, any modification to the product formulation, package specifications, or process conditions is almost certain to have an effect on the product as a whole. For example, a new ingredient may allow a faster line speed. This in turn may affect the accuracy of packaging filling. Any modifications, no matter how small or insignificant they may seem, should be tested by performing actual material and energy balances on the process line to insure that; recoveries are equal to or better than previous standards; that labor, waste and utility costs have not increased; and that consumer perception of the quality of the product has not changed.

Food products often are defined by a complex set of consumer quality attributes which are based on flavor, appearance, and structure. The process engineer must be aware of the effects of changes in product quality by cost reduction through value engineering. It is difficult to estimate changes in product quality, as perceived by the consumer, from a material and energy balance. Any changes made in the process should be evaluated through consumer quality tests as a final check. Cost reduction on a product that no longer can generate sales in the market place is not a desirable outcome of careful material and energy balances in conjunction with product value engineering.

GLOSSARY

Basis (of calculation): Used to simplify process scale up or down. May consist of a unit time or mass.

Batch: A batch process is fed a charge of material which is then processed and discharged. During processing no material enters or exits the operation. Example: Freeze-dehydration — A chamber is loaded with frozen material, the material dried and the chamber unloaded.

Boundary: A dashed line which defines surrounds and the system.

Closed System: The system is closed if no mass crosses the boundary. Note that a batch process may be open or closed.

Continuous: During a continuous process the input and output are introduced continuously throughout the process. Example: The continuous production of aseptically processed juices in which fluid is pumped through a heat-hold-cool cycle and packaged in a continuous fashion.

Flowchart: A block diagram which depicts the process under consideration.

Mass Fraction x_i^j: The mass of a compound in a body over the mass of the body. Where "i" refers to the specific stream carrying the compound and "j" designates the compound

Open System: The system is open if mass crosses the boundary. By definition, semibatch and continuous processes are treated as open systems.

Semibatch: A semibatch process (or semicontinuous process) is characterized by the continuous feed and discharge of discrete packs of material. (Example: Tunnel drying. Trucks containing product on trays are introduced at one end of the tunnel and removed at the other end, thus the semibatch process. Note that the air may flow concurrent or countercurrent to the direction of the trucks.)

Steady State Flow: Used to describe the relationship between various process variables such as temperature, flow rate, or pressure and time. If these variables are independent of time the process is known as steady state.

System: A process which is defined by a boundary. A system may vary in size ranging from a single cell to a production facility. It may consist of a complete processing line, one unit operation in the line, or a portion of that unit operation.

Transient Flow: Used to describe the relationship between various process variables such as temperature, flow rate, or pressure and time. If these variables change with time the process is transient.

FURTHER READING

Stoichiometry: Felder, R.M. and Rousseau, R.W., 1986, 1986, *Elementary Principles of Chemical Processes,* 2nd ed., Wiley, New York. 1986.

REFERENCES

Avlani, P.K., Singh, R.P., and Chancellor, W.J., 1976, Energy consumption in sugar beet production and processing in California, in *Energy and Agriculture;* CNV 271. Dept. of Agricultural Engineering, University of California, Davis.

Balint, A. and Okos, M.R., 1990, Simulation of multi-product food processing operations using batches, in *Food Processing Automation,* ASAE Publication 02-90, American Society of Agricultural Engineers, St. Joseph, MI, U.S.A.

Bomben, J.L., Dietrich, W.C., Hudson, J.S., Hamilton, H.K., and Farkas, D.F., 1975, Yields and solids loss in steam blanching, cooling and freezing vegetables, *J. Food Sci.* 40:660–664.

Boulton, R.B., Singleton, V.L., Bisson, L.F., and Kunkee, R.E., 1996, *Principles and Practices of Winemaking,* Chapman and Hall, New York.

Casimir, D.J., 1983, Counter Current Extraction. *CSIRO Food Res. Q.,* 43:38–43.

Chipoletti, J.C., Robertson, G.H., and Farkas, D.F., 1977, Freezing of vegetables by direct contact with aqueous solutions of ethanol and sodium chloride, J. Food Sci. 42:911–916.

Crapo, C.A. and Crawford, D.L., 1991, Influence of polyphosphate soak and cooking procedures on yield and quality of Dungeness crab meat, *J. Food Sci.,* 56(3):657–659, 664.

Farkas, D., 1967, Use of seed sizes for controlling snap bean quality for processing. Food Tech. 21(5):789–791.

Felder, R.M. and Rousseau, R.W., 1986, *Elementary principles of chemical processes,* 2nd ed., Wiley & Sons, New York.

Graham, R.P., Huxsoll, C.C., Hart, M.R., Weaver, M.L., and Morgan, A.I., Jr., 1969, "Dry" caustic peeling of potatoes, *Food Tech.* 23(2):195–197, 199, 221.

Gunasekaran, S., Fisher, R.J., and Casimir, D.J., 1989. Predicting soluble solids extraction from fruits in a reversing, single screw counter current diffusion extractor, *J. Food Sci.* 54(5):1261–1265.

Holland, C.D. and Liapis, A.I., 1983, *Computer Methods for Solving Dynamic Separation Problems,* McGraw-Hill, New York.

Johnson, J.M., Lopez, A., Wood, C.B., and Moser, R.E., 1959, Relationships of apple grade and size to apple value in processing of apple slices, *Food Tech.* 13(7):385–390.

The Almanac of the Canning, Freezing, Preserving Industries, 1990, 75th ed., Edward E. Jones & Sons, Westminster, MD.

Juliano, B.O., Ed., 1985, *Rice: Chemistry and Technology,* 2nd ed., American Association of Cereal Chemists, St. Paul, MN.

King, C.J., 1980, *Separation Processes,* 2nd ed., McGraw-Hill, New York.

Lewicki, P. and Lenart, A., 1992, Energy consumption during osmo-convection drying of fruits and vegetables, in *Drying of Solids,* Mujumdar, A.S., Ed., International Science, New York, 354–366.

Lopez, A., 1987, Vol. 3, 12th ed., The Canning Trade, Baltimore, MD.

Lorenz, K.J. and Kulp, K., Eds., 1991, *Handbook of Cereal Science and Technology,* Marcel Dekker, New York.

Matz, S. A., 1991, The chemistry and technology of cereals as food and feed, 2nd ed., Van Nostrand Reinhold, New York.

Mohsenin, N., 1984, *Electromagnetic Radiation Properties of Foods and Agricultural Products,* Gordon and Breach, New York.

National Food Processors Association, 1995, Thermal Processes for Low-Acid Foods in Metal Containers, 13 ed., Bulletin 26-L.

National Food Processors Association, 1991, Thermal Processes for Low-Acid Foods in Glass Containers, 6 ed., Bulletin 30-L.

Perry, R.H. and Chilton, C.H., Eds., 1984, *Chemical Engineers' Handbook,* 6th ed., McGraw-Hill, New York.

Peters, M.S. and Timmerhaus, K.D., 1980, *Plant Design and Economics for Chemical Engineers,* 3 ed., McGraw-Hill, New York.

Singh, R.P., Ed., 1986, *Energy in food processing,* Elsevier; New York.

Singh, R.P., 1996, *Computer Applications in Food Technology,* Academic Press, San Diego.

Singh, R.P. and Heldman, D.R., 1993, *Introduction to Food Engineering,* 2nd ed., Academic Press, San Diego.

Toledo, R.T., 1991, Fundamentals of Food Process Engineering, 2nd ed., Van Nostrand Reinhold, New York

Urbaniec, K., 1989, *Modern Energy Economy in Beet Sugar Factories,* Elsevier, New York.

Watt, B.K. and Merrill, A.L., 1963, *Composition of Foods, Raw, Processed, Prepared,* Agricultural Handbook No. 8, United States Department of Agriculture, Washington, D.C.

8 Food Packaging Materials, Barrier Properties, and Selection

Ruben J. Hernandez

CONTENTS

8.1   INTRODUCTION

The share of plastics in the packaging market has been growing at remarkable pace, partially replacing paper, glass, and metal. Because of their unique combination of properties, plastics have expanded the packaging industry to sophisticated levels. Plastic containers are light weight, breakage resistant, transparent, flexible, squeezable, moldable in complex shapes, easily colored and printed, retortable, sterilizable, reusable, and recyclable. Plastics have many positive tradeoffs within their array of versatile properties, including easy processing, good mechanical properties, large range of processing temperatures, lowest density among packaging materials, and (for better or worse) they are pemeable materials. In addition, plastics are economically competitive in cost with paper, glass, steel, and aluminum. A brief cost analysis of plastic packaging is now presented.

Comparative costs of resins between 1980 and 1996 are presented in Table 8.1. Although the price of resins fluctuates up to 40% within a short period of time, compared with 1980 prices they have remained quite stable. Demand for resins between 1993 and 1988 is presented in Table 8.2.

8.1.1   Main Economic Factors of Plastic Packages

The prices of packaging containers depend on the type of material and desired shape of container. Complex conversion processes (e.g., blow molding, coating, and laminations) add to the cost of the finished package. Price of packaging products are affected by the costs of raw materials, technology competition, vertical integration, and opportunities in material substitution. Prices are affected by domestic economic conditions, recessions result in over-supply, and growth cycles strain production capacity. The international demand for goods and packaging materials also affects prices. Packages can be produced in house, or purchased directly from molders and converters or from independent distributors. While a container may be obtained from any of these sources, one is rarely able to obtain all packaging components from a single source. Normally, bottles, caps, films, labels, pallets, and stretch-wrap are produced by independent sources.

TABLE 8.1
**Comparative Price of General Purpose Resins
(Truckload Quantities) in 1980 and 1996**

		$/lb	
Plastic	Density (g/ml)	1980	1996
Acrylic		0.65	0.92
Nylon 6,	1.120–1.140	1.30	1.42
Polycarbonate		1.30	1.90
HDPE, blow molding	0.940–0.965	0.47	0.52
LDPE, extrusion	0.915–0.942	0.47	0.55
LLDPE, extrusion	0.918–0.940		0.46
Polypropylene	0.895–0.910	0.45	0.46
HIPS		0.55	0.57
Polystyrene	1.05–1.06	0.54	0.55
PET	1.35–1.41		0.64
PVC homopolymer	1.220–1.400	0.33	0.55
PVC compounds		0.50	0.41

Note: Resin prices can fluctuate as much as ± 40% of the given price. HDPE = high density polyethylene; LDPE = low density polyethylene; LLDPE = linear LDPE; HIPS = high impact polystyrene; PET = polyethylene terephthalate; PVC = polyvinyl chloride.

8.1.1.1 Development Costs

According to Leonard (1980), the main factors determining the cost of a package can be classified as follows.

1. Identification of package characteristics that takes into account the nature of the product, FDA requirements, and customer's needs.
2. Concept search; when several types of packaging material can equally serve the same goal, at least two different packages must be considered.
3. Design to provide the best combination of material, shape, size, appearance, color, special features, and product's shelf-life.
4. Preparation of package models to provide a basis for evaluation and even customer research.
5. Fabrication of samples to test the package in real situations.
6. A sample evaluation program may be necessary to assess extreme processes and market conditions, i.e., rough handling or high temperatures.
7. Preparation of cost analysis and specifications taking into account results of the sampling program.
8. Test marketing to evaluate on a small-scale the whole development plan from package production to logistics and consumer satisfaction.
9. Design and specification refinements that may be necessary to improve the original concept.
10. Tooling for production including, but not limited to, molds, litho plates for caps, and containers.

TABLE 8.2
Plastics Demands in Flexible and Rigid Containers

Resin	Flexible Packaging		Rigid Packaging	
	Demand (%)[a]	Growth (%)[b]	Demand (%)[a]	Growth (%)[b]
LDPE	38.3	0.5	0.6	–2.6
LLDPE	25.7	9.9	3.3	8.4
PP	8.7	2.9	10.7	4.3
HDPE	12.2	6.7	43.9	3.6
PVC	2.3	–2.1	1.4	–3.6
PS	3.2	4.7	15.5	2.7
TP polyesters	4.1	9.8	19.3	9.0
EVA	0.9	2.4	—	—
Nylon	0.9	3.3	—	—
PVA	0.7	5.4	—	—
Polyurethanes	—	—	1.2	3.9
Other	3.0	3.5	4.1	3.9
Total	100.0	4.0	100.0	4.4
Total resin demand, in Mkg	4426 [c]		5707 [c]	

Note: LDPE = low density polyethylene; LLDPE = linear LDPE; PP = polypropylene; HDPE = high density polyethylene; PVC = polyvinyl chloride; PS = polystyrene; EVA = ethylene vinyl acetate; PVA = polyvinyl acetate.

[a] Demand percent between 1993 and 1988.

[b] Expected annual average growth rate between 1993 and 1988.

[c] Expected total demand in 1988.

Adapted from Shroeder, G. O., *Modern Plastic Encyclopedia*, McGraw-Hill, NY, 1995, A-35.

11. A quality control program to regulate quality requirements, attributes, and allowable limits.
12. Startup costs that will occur at the starting of production.

8.1.1.2 One-Time Costs

One-time costs are the expenditures that are made only once during the expected time of the package.

1. Machines to make the containers, which may include, e.g., a bag former or blow molder.
2. Supplier molds or dies for the packages, caps, secondary packages.
3. Printing plates, dies, or cylinders.
4. Packaging line equipment or replacement parts.
5. Equipment installation.

8.1.1.3 Package Material Costs

1. Resins or films to make the container.
   The cost of resin is, in many cases, the main package cost component, and its price can be used as an estimation of the container's price. Numerical factors relating the price of resin to the cost of containers may be useful guides to the food engineer in estimating packaging costs.

2. Packaging for inbound shipment
3. Inbound freight
4. Storage and handling the package material from the supplier to the packer's filling lines
5. Waste factor from damage and loss during container production, filling, or printing
6. Sampling and inspection

8.1.1.4 Packaging Machinery Costs Other Than One-Time

1. Rental or lease of equipment and machines
2. Services and maintenance
3. Amortization of purchased machines, auxiliary equipment
4. Energy and utilities

8.1.1.5 Packaging Process Costs

1. Direct labor
2. Indirect labor
3. Overhead
4. Incidental materials

8.1.1.6 Distribution Costs

1. Storage handling and warehousing.
2. Outbound freight.

8.1.2 COST ANALYSIS OF PLASTIC RIGID CONTAINERS

Food-grade resins are more expensive than the general-purpose grade since they require sanitary process conditions, US Food and Drug Administration (FDA) additives, and limitations in the use of scrap and reworked conditions. In the case of polyvinyl chloride (PVC), the addition of heat stabilizer, color, and plasticizer almost double the price of the raw resin.

Resin density directly affects the cost of a plastic container. For a given container, the cost of the material in a container, C_m, is

$$Cm = A \cdot \ell \cdot d \cdot r = W \cdot r$$

where A is the package area, l is its average thickness, d is the resin density, and r is the resin cost per unit of mass.

If the container can be made of two different resins having prices r_1 and r_2 when the container's thickness is kept constant, the cost of container 1 is related to container 2 by their densities values

$$Cm_1 = X \cdot Cm_2$$

where $X = d_1 r_1 / d_2 r_2$, and d_1 and d_2 are the respective density of the resins. Example: if $d_2 = 0.953$ g/cm^3, $r_2 = \$0.385$, $d_1 = 1.257$, and $r_1 = \$0.63$, then $X = 2.157$, that is, the container made of resin 1 will cost 2.157 as much as resin 2.

8.1.2.1 Injection Molding (IM)

IM is used for producing containers and parts, i.e., closures, that require high precision in their dimensions. A rule of thumb for large production runs and simple product geometry is that the cost of a container or part is twice as much the cost of the resin — the resin is 50% of the container cost — (Leonard, 1980). For example, 1000 closures of polypropylene (PP) costing \$0.46/lb. and weighing 10 g each will have a producing cost of approximately C = $2 \times 1000 \times 10 \times 0.46/454 = \$20.2/1000$ pieces. Main cost components of injection molded pieces are

1. Plastic resin(s)
2. Mold and cavities; the mold cost is amortized over a million pieces
3. Molding processes (labor, energy, and overhead)
4. Scrap discarded or grounded for re-use
5. Assembling, finishing, and/or decorating

Therefore, the simpler the molded piece, the lower its cost.

For example, simple injection-molded closures, i.e., snap-ons, are made on two-piece molds and follow the 50% rule.

More complex molding operations are required for the linerless threaded screw cap used for glass bottles. In this case, the thread prevents the cap from being removed from the mold by a simple push, like the snap-ons. This requires a mold that costs twice as much as the snap-on mold. The actual impact in the cost of the cap is hard to estimate since there are many variables, i.e., number of frames, cavities, tooling, and cycling time, that affect the design and operation of the mold. The linerless thread cap may cost about 3.4 times the cost of the resin. If a liner made of fiberboard and plastic layer is incorporated into the cap, it may increase the cost by 25 to 30% over the unlined cap.

Dispenser caps for detergent bottles and aerosol push-up button caps are made of several parts. This requires the combination of multi molding and assembly making the cost of these pieces much higher than indicated by the 50% rule. Some factors increasing the cost include:

1. Complexity of the molded piece
2. Multipart pieces requiring additional manual assembling
3. The inventory practice of the proprietary molder (A custom molder that manufactures based on existing purchase orders has lower costs than a molder that stocks an inventory, and maintains a warehouse.)
4. Lot size of several million pieces will be more cost-effective than smaller runs of several ten thousands
5. Mold ownership (If the container maker is the owner of the mold, the injection-molder sells the pieces as stock items rather than using a customer's mold.)

8.1.2.2 Blow Molding

As indicated in Table 8.2 the most common resins for blow-molded containers are: high density polyethylene (HDPE), thermoplastic polyesters, polystyrene, and PP. They make up 90% of the market. Rigid blow-molded containers, primarily bottles, are widely used in beverages, food, medicinal products, cleaning products, and many other applications.

Compared to glass containers, the cost ratio of polyolefin resins to glass is 1.4 to 1. But plastic containers' lower weight reduces transportation costs, and can more than equalize the raw material cost between polyolefins and glass containers. As a rule of thumb, the price of bulk shipment in large boxes of blow-molded bottles of natural HDPE is about 3.2 times the

price of the resin at the molder's plant. Smaller containers, 12 oz (360 ml) have a slightly higher factor while larger containers of 1 gal (3.75 l) are lower. Colored containers cost more depending on the formulation and number of pieces produced.

Major manufacturers of blow molded containers in North America are: Constar International, Inc. (Atlanta, GA); Johnson Controls, Inc., Plastic Containers Division (Manchester, MI), Owens-Brockway Plastic Products (Toledo, OH); Graham Packaging, Co., (York, PA); Plastipak Packaging, Inc. (Plymouth, MI); Continental PET Technologies, Inc. (Florence, KY); Continental Plastic Containers, Inc. (Norwalk, CT); Silgan Plastic Corp. (Chesterfield, MO); Wheaton Plastic Products (Millville, NJ); and Southeastern Container, Inc. (Enka, NC).

Table 8.3 illustrates a cost analysis for producing injection blow molded polyethylene terephthalate (PET) containers (Albrant, 1996).

8.1.2.3 Thermoforming

Thermoformed packages are made from sheets of thermoplastic materials. Polyethylene, PVC, Ionomers, PETG, polystyrene, and cellulose acetate are common plastics used for thermoformed packages. The sheets are prepared by extrusion-casting or calendering.

Many variations of thermoforming processes are available, among the most important are (Gruenwald, 1987) billow, cavity vacuum, drape vacuum forming, plug-assisted forming, billow drape forming, snap-back forming, reverse draw, trapped sheet pressure forming, twin sheet forming, mechanically thermoformed, matched-mold forming, and rubber pad and fluid pressure. The cost of thermoformed packages includes:

1. Cost of resin
2. Cost of fabricating the sheet
3. Alternatively, price of purchasing the sheet
4. Thermoforming equipment, mold, and trimming tools (Thermoforming molds are less expensive than blow molding and injection molds.)
5. Thermoforming operations that include heating of sheet, forming the container, and trimming it off
6. In the case of a blister package, heat sealing the blister to a paperboard, normally 0.015 in thick (380 μm)
7. Other costs associated with waste handling, e.g., regrinding and re-extrusion (Laminated structures are eliminated or included as reground layer; scrapless thermoforming substantially reduces the waste.)
8. Post-forming costs including stacking, packing, and shipment

8.1.2.4 Flexible Packaging

Versatile flexible, or nonrigid, containers, are made from plastic films and multilayer structures combining plastic, paper, foil, and aluminum-oxide, silica-coated or metallized films. A structure can be transparent, opaque, colored, or metallized in appearance. These materials are formed into bags, stand-up pouches, liners, and wrappers. Almost any requirement can be achieved by combining the appropriate material in a flexible web. Flexible packaging can be used for many products, a variety of filling methods are available, and diverse delivery methods exist to remove the product from the bag. Solids, liquids, powders, food, chemicals, and drugs can be packaged under vacuum, or special atmosphere conditions. Flexible packages can be frozen, retorted, boiled, heated or irradiated. With the new polyolefin plastomers (POP), higher values in O_2 and CO_2 permeability can be achieved facilitating the packaging of fresh-cut produce (Young, 1996). On the other hand, ultra-high oxygen barrier structures are manufactured for oxygen-sensitive products. Flexible packaging can be presented with high quality surfaces printed by flexo, gravure, offset, or letterpress processes. Since there

TABLE 8.3
Cost Analysis of PET Bottles

Container type		0.5 l	1.0 l
Net weight	Gram	24	30
Type of resin		PET	PET
Resin cost[a]	$/lb	1.10	1.10
Scrap loss	Percent	1.0	1.0
Machine type		RBU-225[b]	RBU-225[b]
Number of cavities		2	4
Cycle time	Seconds	3	3.3
Blow molder efficiency	Percent	59	95
Container per hour		2280	4145
Depreciation term	Years	7	7
Blow molder	Cost	$511,250.00	$511,250.00
Mold/tool	Cost	$30,000.00	$30,000.00
Auxiliary equipment	Cost	$163,620.00	$ 163,620.00
Installation	Cost	$ 5,000.00	$ 5,000.00
Misc. fixed costs	Cost	$0.00	$0.00
Interest terms	Month	84	84
Interest annual	Rate %	8.0	8.0
Direct labor cost	$/h	$7.50	$7.50
Operators (0.5)	$/h	$5.00	$5.00
Inspectors/Pack (0.5)	$/h	$2.50	$2.50
Utilities	$/h	$0.00	$0.00
Paletize (0.5)	$/h	$0.00	$0.00
Indirect Labor Cost	$/h	$0.00	$0.00
Overhead cost	$/h	$5.00	$5.00
Miscellaneous hourly cost	$/h	$0.00	$0.00
Energy cost auxiliary		$0.07	$0.07
Energy consumption	kW/h	85	85
Energy cost		$0.07	$0.07
Operating hours/year		6000	6000
Production per year		**13,680,000**	**13,680,000**
Fixed Costs	Total	$188,060.75	$188,060.75
Depr. blow molder		$73,035.71	$73,035.71
Depr. mold tool		$4,285.71	$4,285.71
Depr. auxilliary equip.		$714.29	$714.29
Depr. miscellaneous fixed cost		$0.00	$0.00
Annual interest		$71,313.25	$71,313.25
Prevent maintenance/parts		$15,337.50	$15,337.50
Hourly Costs	**Total**	**$75,000.00**	**$75,000.00**
Direct labor		$45,000.00	$45,000.00
Indirect labor		$0.00	$0.00
Overhead		$30,000.00	$30,000.00
Miscellaneous hourly cost		$0.00	$0.00
Energy cost	Total	$35,700.00	$35,700.00
Resin cost	Total	$804,152.38	$804,152.38
Total mfg costs		**$1,102,913.13**	**$1,102,913.13**
Cost per 1000 containers		$80.62	$95.38

*Not*e: PET = polyethylene terephthalate.

[a] Resin cost = cost of purchasing preforms.

[b] Supplier is Bekum American Corporation (Williamston, MI)

are several plastic materials that can be combined with foil, paper, and a variety of surface treatments, the number of flexible structures is very large.

Total investment for manufacturing the web of material including the printing is very high. From the standpoint of using a flexible structure, the material cost is related to the flexible structure composition, which in turn is determined by the product characteristics, storage and transportation conditions, and shelf-life requirements. The cost of flexible packaging materials is usually expressed per area of structure, m^2 or 1000 in^2. The cost can be expressed by unit of package or "repeat."

One of the less expensive flexible packages is an unprinted polyethylene bag. The cost of the material for a bag made of a simple polymer is given by

$$Cm = A \cdot \ell \cdot d \cdot r / 454$$

where A is the area, l thickness, d density, and r price of resin per pound. For instance, an unprinted 50 cm × 30 cm heavy-duty bag made of HDPE (density = 0.95 g/cm^3) with total area of 3000 cm^2 (465 in^2) and 125 μm (5 mils) thick has a material cost of

$$Cm = 3,000 \times 125 \times 10^{-4} \times 0.95 \times 0.47 / 454 = \$0.004.8138$$

with an estimated 60% increase for blowing into film and 50% for converting it into a bag, the final cost is approximately $0.14 per bag.

In the converting operation, the cost of a multilayer structure is built up from the elements combined in it. Consider the fabrication of a laminate for ground coffee bag. As an illustration of cost analysis, a possible structure can be made by combining a 100% reverse-printed 0.6-mil Mylar laminated to 0.0003 in aluminum foil and extrusion-coated to a blend of 50% low-density polyethylene (LDPE) and 50% metallocene. Table 8.4 shows the main cost components of this structure.

Major manufacturers of film and sheet in North America are: DuPont Co. (Wilmington, DE); Mobile Chemical Co. (Pittsford, NY); Bemis Co. (Minneapolis, MN); First Brand Co. (Danbury, CT); Cryovac Division (Duncan, SC); American National Can Co. (Chicago, IL); Printpack, Inc. (Atlanta, GA); Huntsman Packaging Co. (Salt Lake City, UT); ICI Americas, Inc. (Wilmington, DE); and James River Co., Packaging Business (Milford, OH).

8.2 PLASTICS IN FOOD PACKAGING

Synthetic or natural polymers are macromolecules made from the repetition of one or more species or group of atoms called mer and linked to each other by covalent bonds. The smaller chemical unit that completely describes the main polymer structure is called the constitutional unit. For instance, the constitutional unit of polyethylene is CH_2. The peculiar properties of polymers are determined by the large number of constitutional units in the molecule. The effect of the large number of mer are such that the polymer's properties do not vary markedly with the addition or removal of a few hundred constitutional units. In the field of engineering and related areas thermoplastic polymers are referred to as plastics. We will briefly review the most important properties that characterize a plastic material commonly used in the design, evaluation, specification, and fabrication of food plastic containers.

8.2.1 PROPERTIES OF PLASTIC RESINS

Composition — The final composition of a plastic resin includes the macromolecules made of a particular monomer (or monomers) as well as additives that are incorporated during processing. For example, PP is based on propylene and PVC results from the polymerization

TABLE 8.4
Cost Analysis of a High Barrier Lamination for Coffee

Foil lined coffee pouch			Cost ($/m²)
Material costs			
0.6-mil Mylar film, 20 g/m²	$3.00/lb	$0.00661/g	0.130
Ink, 1.5 g/m² (30% solid)[a]	$2.50/lb	$0.00551/g	0.030
Adhesive acrylic, 5 g/m² (50% solid)	$2.00/lb	$0.00441/g	0.040
0.3-mil Aluminum foil, 21 g/m²	$2.25/lb	$0.00496/g	0.100
Extrusion coating 16 g/m² of	$0.63/lb	$0.00138/g	0.020
50% LDPE	$0.40/lb	$0.00088/g	
50% Metallocene	$0.85/lb	$0.00187/g	
Subtotal material cost			0.330
Waste 10%			0.030
Total material cost			**0.360**
Conversion costs			
Hourly printing[b] rate	$200.00	96,000 m²/h	0.022
Hourly laminate rate	$600.00	96,000 m²/h	0.066
Total converting cost			**0.088**
Flexible material cost			0.448
Gross margin 18%			0.081
Total flexible material cost			0.529

Note: LDPE = low density polyethylene.

[a] White ink @ 100% coverage.

[b] Reverse printed with 8 color press.

vinylchloride monomer. PP resins contain antioxidants, and plasticizers are added to PVC as processing aids.

Molecular Weight — Unlike low-molecular-weight compounds made of the same type of molecules, a polymer is made of macromolecules having different lengths. For this reason the molecular weight of a polymer is actually a distribution of molecular weights. The molecular weight distribution of polymers is defined by the average molecular weight and its broadness. Two average molecular weights are commonly employed: number average molecular weight, $\overline{M}n$; and weight average molecular weight, $\overline{M}w$. The broadness of the molecular weight distribution (MWD) is given by the ratio $\overline{M}w/\overline{M}n$. This is called the dispersity index (DI). For most commercial polymers DI falls between 2 and 8. A low DI value indicates narrow distribution of the polymer, while large DI indicates a broad distribution, (Progelhof and Throne, 1993). $\overline{M}n$, $\overline{M}w$, and MWD determine properties such as strength, melting temperature, and heat sealing temperatures. A popular method to determine Mn, Mw, and MWD, is gel permeation chromatography which is described in the standard ASTM (American Society for Testing and Materials) D 3593.

Melting Temperature, T_m — The melting temperature marks the maximum temperature at which a plastic can be heated before it becomes a melt. Most crystalline and semicrystalline polymers have their melting temperature given as a temperature range which depends on their MWD and composition. Plastics show T_m as low as 275 K for polyisobutylene, and as high as 728 K in the case of PET (Van Krevelen, 1990). Semicrystalline plastics become soft

before reaching their melting temperature. Most noticeable, amorphous plastic such as polystyrene do not show a melting temperature range but rather they soften as temperature increases, especially above the glass transition temperature. Methods for measuring T_m are described in ASTM D 2117 and ASTM D 3418.

Glass Transition Temperature T_g — T_g is associated with the onset of the rotation and mobility of chain segments involving a small number of monomers. The concept of glass transition is important because below T_g a polymer is stiff and glassy and above T_g it has a plastic and rubbery behavior (Progelhof and Throne, 1993). In food packaging, T_m and T_g determine the temperature range of application of a container. For instance, a PP container may become brittle at a freezing temperature if its T_g is near 0°C, and polystyrene is brittle at room temperature because it has a T_g about 80°C and does not contain plasticizer. On the other hand, a polymer with low T_m value such as polyethylene cannot be steam sterilized. Differential thermal analysis (DTA) and differential scanning calorimetry (DSC) are used to determine T_m and T_g. These methods are described in ASTM D 3418.

Melt Flow INdex, MFI — MFI gives information about the extrusion characteristics of a resin and is used primarily in quality control. MFI is expressed in grams of extrudate per 10 min according to ASTM D 1238.

Mechanical Properties — These properties of plastics measure the strength, elongation, stiffness, tensile strength at break, elongation at break, tensile yield strength, tensile modulus, force/area, which are described in ASTM D 638. Other properties of interest are listed below. The respective ASTM standard methods are in parentheses.

- Methods for conditioning plastics (D 618)
- Coefficient of linear thermal expansion (D 696)
- Thermoforming heat deflection temperature (D 648)
- Thermal conductivity (C 177)
- Flammability (D 1433)

8.2.2 PROPERTIES OF SHEETS AND FILMS FOR FLEXIBLE PACKAGING

Thickness — The unit in the SI system is the micrometer, µm (10^{-6} m). The customary unit used in the U.S. is mil (equals to 0.001 inch), gauge is 0.01 mil (TAPPI [Technical Association of the Pulp and Paper Industry] 411).

Area Factor — Also referred to as yield, this gives the area of the film per unit of mass, m^2/kg. Area factor is calculated as the inverse of density times thickness in coherent units (ASTM D 4321).

Tensile Characteristics — Stress-strain tensile characteristics of a flexible structure include ultimate tensile strength to determine the maximum tensile stress the material can sustain, elongation, and modulus of elasticity to determine the force required to deform the structure. Modulus of elasticity or Young's modulus, is a measure of the material stiffness in N/m^2 (ASTM D 882). The area under the stress-strain curve also gives the toughness of a material.

Density — The density of a plastic is proportional to its crystallinity. The standard ASTM D 1505 describes the "density gradient" method to evaluate the density of films and resins; the units are kg/m^3.

Bursting Strength — This is the hydrostatic pressure required to produce rupture of the material when the pressure is applied at a controlled increased rate through a rubber diaphragm to a circular area of 30.48 mm (1.2 in) in diameter. "Points bursting strength" is the pressure in pounds per square inch. This is the same test used for the bursting strength of paper and paper products, ASTM D 774. Free falling dart method is described in ASTM D 1709.

Impact Strength — Impact strength is the energy required to puncture a flexible structure to shock loading. This gives a measure of the toughness. The test is described in the ASTM D 3420 and ASTM D1709.

Tear Strength — The measurement of tear strength takes into account the energy absorbed by the film sample in propagating a tear. Two standard methods are available: ASTM standard D 1004 describes the measurement for initial tear resistance, and ASTM D 1922 refers to the energy absorbed by a test specimen in propagating the tear that has already been initiated by cutting a small hole in the sample. The value of tear strength in one film may vary widely depending on the degree of orientation such as oriented PP, and whether the measurement is performed in the machine direction or cross machine direction. This is described by ASTM D 1938.

Pinhole Flex Test — Pinhole flex resistance is the ability of a film to avoid the formation of pinholes during repeated folding. A film that has a low value of pinhole flex resistance will generate pinholes, at the folding line, following repeated flexing (ASTM F 456). A related test is the folding endurance.

Folding Endurance — This test measures the resistance of the material to flexure or creasing. The ASTM recommended procedure is described in the standard D 2176 which is used to determine the number of folds necessary to break a sample film.

Heat sealing Temperature — Important properties for wrapping, bag making, or sealing a flexible structure is the heat sealability characteristic of the material. To evaluate the seal, two values are normally measured: the peel strength (ASTM F 88), and the hot tack strength. As previously indicated, the absolute temperature and range of temperature must be considered. The polymer's average molecular weight determines the temperature level and the MWD determines its range.

Coefficient of Friction — The coefficient of friction (COF) is a measurement of the friction force between two surfaces. Cases in which friction is important include films passing over free-running rolls, bag forming, wrapping film around a product, and bag stacking. Speed, temperature, static, humidity, blocking, and surface smoothness affect the COF (TAPPI T 503 and ASTM D 1894).

Blocking — This is the tendency of two films to stick together when they are contacting each other. This effect is enhanced by a smooth surface and when the films are left under pressure, as is the case of stacked sheets or compacted rolls of film. Blocking can be measured by the force needed to separate two sheets when force is applied perpendicular to them, (ASTM D 1893 and D 3354, or Packaging Institute Procedure T 3629).

Haze — Haze is the percentage of transmitted light that, in passing through the sample, deviates by more than 2.5° from an incident parallel beam. The appearance of haze is caused by light being scattered by surface imperfections and nonhomogenous materials, (ASTM D 1003).

Gloss — Gloss is the percentage of incident light that is reflected at an angle equal to the angle of incidence (normally 45°). It is a measure of the ability of a surface to reflect the incident light. High gloss produces a sharp image of any light source and gives a pleasing sparkle, (ASTM D 2457).

Transparency and Opacity — A transparent material has a transmittance above 90%. Transmittance is the percent of incident light that passes through a material sample and is determined by the effectiveness of the absorption and scattering of light by the material. In most polymers light absorption is insignificant, therefore, scattering controls the light transmission. The scattering of power of a polymer results from morphological inhomogeneities and/or the presence of crystal and fillers. The less crystalline a polymer is, the more transparent it is. Amorphous homogeneous polymer, such as "crystal" polystyrene, showing little or no scattering power, is transparent. A highly crystalline polymer as HDPE will be mostly opaque. Transmittance is measured according to ASTM D 1003.

Dimensional Stability — Dimensional stability refers to the capability of a structure to maintain its dimensions under changing conditions of temperature and humidity. Machine and transverse directions may produce different changes in dimensional stability. Dimensional stability is important in any flexible material converting process particularly in printing, since even small changes in dimensions during printing may lead to serious problems in holding a print pattern (ASTM D 1204).

Permeability — The barrier properties of a plastic material is commonly expressed by its permeability coefficient value P. As the permeability increases, the barrier value decreases. But the permeability coefficient actually depends on the combined effect of the diffusion and solubility process. The well known relationship $P = DS$ where D is the diffusion coefficient and S is the Henry's law solubility applies well to relatively low concentration values of permeant, which is the case found in many food systems. Several factors affect D, S, and P of polymers: (1) chemical composition of polymer and permeant; (2) polymer crystallinity; the diffusion and sorption occur mainly through the polymer's amorphous phase; (3) temperature, as temperature increases permeation increases; and (4) presence of plasticizers and fillers in the polymer. In food systems, the values of permeability of water, gases as well as aromas and flavor components. ASTM 1434 describes the standard method for measuring gas permeability of plastic film and sheeting. The oxygen permeability of films using a coulometric sensor is described in ASTM D 3985, and for packages in ASTM F 1307. Water vapor permeability method for flexible barrier materials is describe in ASTM 372, for film/sheeting using infrared sensor in F 1249, and for packages in ASTM D 895, D 1251, and D 3079. Water vapor transmission rate (WVTR) for pressure sensitive tapes is in ASMT D 3833. Permeability of organic compounds, flavors, and aroma are described by Hernandez et al. (1986).

Chemical Resistance — The evaluation of plastics resistance to chemicals is as follows: for acids, ASTM D 543; for alkalis, ASTM D 543; greases and oils, ASTM D 722; solvents, ASTM D 543; and sunlight, ASTM D 1435.

Wettability — Adhesion and printing operations to a plastic surface depend on the value of the plastic surface tension. A measure of a material's surface tension is given by the wettability (ASTM D2578).

8.2.3 PLASTICS AND THE FDA

Food packaging manufacturers are concerned with components that, originally contained in the packaging material, may come in contact with food by a migration process. When these

components are found in the food they are called indirect additives. Therefore, all plastic packaging for indirect contact with foods are required to be FDA-sanctioned. It is worth noting that the use of components are made in compliance or in accordance with "sanctioned" or "certified" ingredients rather than "FDA-approved."

Title 21 of the Code of Federal Regulations (CFR) covers all indirect additives as well as direct additives. Part 174 considers general aspects of indirect additives in food in relation with good manufacturing practice. Part 175 includes a long list of sanctioned indirect additives in adhesives and components of coatings, Part 176 is for paper and paperboard components, Part 177 covers polymers, and Part 178, adjuvants, production aids, and sanitizers. Since all ingredients in the packaging material must comply with the CFR, the packaging manufacturer should inform the food packer of that. For instance, a heat induction foil innerseal for rigid containers is a lamination containing Aluminum foil, PP film, paperboard, and adhesive as main components. The FDA status for all the components, in reference to 21CFR, is as follows: 175.105 for the adhesives, 175.300 for resinous and polymeric coatings, 175.320 for coatings of polyolefin films, 176.170 for paper and paperboard components in contact with aqueous and fatty foods, 176.180 for paper and paperboard components in contact with dry foods, 176.300 for fungicides, 177.1210 for closures with sealing gaskets, 177.1520 polyolefins. Aluminum foil is regulated in Section 409 of the Food Additives amendment of the Federal Food, Drug and Cosmetic Act.

8.3   MAJOR PLASTICS

8.3.1   POLYOLEFINS

Olefin, which means oil-forming, is an old synonym for alkenes. Originally, the term olefin was the name given to ethylene. Alkenes are hydrocarbons containing a carbon-carbon double bond, i.e., ethylene and propylene. In the plastic industry, olefin is a common term that refers to the family of plastics based on ethylene and propylene. The term polyolefin should strictly apply to polymers made of alkenes, whether a homopolymer or copolymer. This includes the family of polyethylene, and the family of polypropylene.

Polyethylene, the first useful olefinic polymer in food packaging, was introduced in the 1940s. Low-density polyethylene was first produced by free-radical polymerization at extremely high pressures and temperatures. The structure of this polymer was quite randomly branched. Better polyolefins, linear polymer chains (e.g., HDPE), became possible by the development of low-pressure polymerization process based on multi-sited Ziegler-Natta catalysts in the 1960s. Multi-sited catalysts procedure polymers having short, medium, and long molecules, and wide range of comonomer branches. These resins then, are characterized by wide MWD and wide composition distributions. An improvement in chain linearity came in 1970s with the solution- and gas-phase technology to produce linear low density polymer. Today, new and sophisticated polyolefins are being produced by the process based on the single-site metallocene catalysts known as metallocene catalyzed polymers. Unlike the multi-site catalyzed resins, metallocene polyolefins have a much narrower MWD and composition distribution.

Branched and linear polyethylenes are described in Section 8.3.1.1 and metallocenes are described in Section 8.3.1.3.

8.3.1.1   Polyethylene

General information — Polyethylene (PE) is a family of addition polymers based on ethylene (CH_2=CH_2). PE can be linear or branched, homopolymer or copolymer. In the case of a copolymer, the other comonomer can be an alkene, i.e., propene, butene, hexene, or octene, or a compound having a polar functional group, i.e., vinyl acetate (VA), acrylic acid (AA),
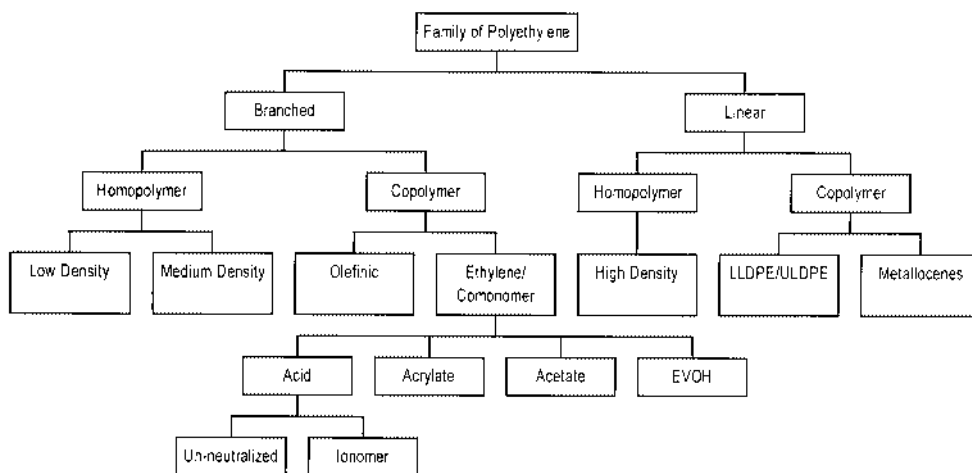
FIGURE 8.1 Family of polyethylene. EVOH = ethylene vinyl alcohol; LLDPE = linear low density polyethylene; ULDPE = ultra low density polyethylene.

ethyl acrylate (EA), methyl acrylate (MA), or vinyl alcohol (VOH). If the molar percent or the comonomer is less than 10% the polymer can be classified as either a copolymer or homopolymer. Figure 8.1 illustrates a diagram of the family of PE. PE resins are used as films, molded containers, closures, and in multilayer laminations. They are available in a large range of composition and MWD that determine a wide range of values in strength; toughness; thermal, heat-sealing, and barrier properties; and processing conditions.

Linear and branched polyethylene — Linear PE implies long chains of the ethylene monomer linked without major branching. The long range stereo-regularity of the linear molecule tends to yield highly crystalline PE. For this reason, linear PE has a crystallinity between 70 to 90%. On the other hand, the major effect of branches in the backbone chain is to limit the formation of PE crystals and produce amorphous or "loosely packed" PE. Since crystalline regions are denser than amorphous regions, linear PE is more dense than the branched PE. Linear low density PE combines the main features of both HDPE and LDPE.

Branched PE typically has a crystallinity of 40 to 60% and the density ranges from 0.910 to 0.950 g/cm^3. In contrast, HDPE will have a density of about 0.950 to 0.970 g/cm^3.

By the addition of comonomers, such as propylene and hexene, the number and the length of the branches in PE can be controlled. A wide variety of branched PE are commercially available depending on the reaction conditions and on the type and amount of comonomer.

Linear PE can be produced as a homopolymer HDPE, or copolymer linear low density polyethylene (LLDPE) and ultra low density polyethylene (ULDPE). Copolymers are produced with butene, hexene, or octene. The controlled placement of the comonomer in the polymer chain during the polymerization process, produces a rather linear polymer with very short strands and low density. LLDPE is characterized by a relatively narrow molecular weight and MWD, and a linear structure with very short branches due to the presence of butene, hexene, or octene.

The FDA has cleared the use of polyolefin resins for direct food contact as specified in 21 CFR, Section 177.1520.

8.3.1.1.1   Low density polyethylene

Properties — LDPE is a branched homopolymer. The branching of the chains yields a polymer with low percent of crystallinity on properties such as clarity, flexibility, sealability, and ease of processing. The actual values of these properties depend on the balance of the molecular weight, MWD, and branching.

TABLE 8.5
LDPE Branched Film and Resin Properties

Melting temperature	98–115°C	208–239°F
Glass transition temperature	–25°C	–13°F
Specific gravity	0.917–0.942	—
Tensile strength at break	8.3–31.8 kPa	1.2–4.6 kpsi
Tensile modules, stiffness	172–283 kPa	25–41 kpsi
Flexural modulus, 23°C	242–331 kPa	35–48 kpsi
Bursting strength, mil (Mullen)	10–12	10–12
Initial tearing strength	25.1–222 kN/m	65–575 g/mil
Propagating tearing strength	87.5–52.5 kN/m	50–300 lb/in
Permeability		
Water, at 37.8°C	66–99[a]	17–25.5[c]
Oxygen, at 25°C	1940[b]	500[d]
CO_2, at 25°C	10490[b]	2700[d]
N_2, at 25°C	700[b]	180[d]
Resistance to		
Acids	Good	
Alkali	Good	
Grease and Oil	Poor	
Water	Good	

Note: LDPE = low density polyethylene.

[a] Units in g·μm/m²·d·kPa.

[b] Units in cc(STP)·μm/m²·d·kpa.

[c] Units in g·mil/100 in²·d·atm.

[d] Units in cc(STP)·mil/100 in²·d·atm.

Adapted from *Modern Plastic, Guide to Plastics*, 1987, McGraw-Hill, New York.

Applications — LDPE is very versatile with respect to processing mode. Diverse processing techniques common to thermoplastic materials, i.e., blown film, cast film, extrusion coating, extrusion molding and blow molding, are available to LDPE.

Compared with other plastics, LDPE is one of the higher barriers to water but one of the lower to oxygen, CO_2, organic vapors, and flavors.

Film is the single largest production form of LDPE. In the U.S., 55% of the total volume is made into films with thickness less than 300 μm (12 mils). Products made of LDPE include containers and bags for food (i.e., packaging bakery items, snacks, and produce), clothing, industrial liners, agricultural films, household products, shrink- and stretch-wrap films. Selected properties of LDPE are presented in Table 8.5.

Medium density polyethylene (MDPE), 0.925 to 0.950, is more crystalline and therefore somewhat stronger, stiffer, and less permeable than LDPE. MDPE processes similarly to LDPE, though usually at a slightly higher temperature.

A major competitor material of LDPE is LLDPE which provides superior strength at equivalent densities. However, LDPE is still preferred in applications demanding high clarity or for coating a substrate. Table 8.6 presents trends in properties of PE resins.

Branched copolymers of PE — Other branched PEs are produced by copolymerizing ethylene with either alkene compounds or monomers containing polar functional groups, i.e., VA, AA, and VOH. The inclusion of polar monomers in the main chain produces branched ethylene copolymers with lower crystallinity, more flexibility, wider range of heat sealing

TABLE 8.6
Properties Trends in Polyethylene

As average molecular weight increases

Tensile strength,	Increases
Impact strength	Increases
Clarity	Increases
Ultimate elongation,	Increases
Melt strength,	Increases
Tear resistance,	Decreases
Melting temperature	Increases

As molecular weight distribution broadens

Ultimate elongation,	Decreases
Tear impact,	Decreases
Impact strength,	Decreases
Melt pressure,	Decreases
Melt strength,	Increases
Heat seal range	Increases

As density increases

Tensile strength,	Increases
Melting temperature,	Increases
Clarity,	Decreases
Ultimate elongation,	Decreases
Tear resistance,	Decreases
Impact strength,	Decreases
Blocking,	Decreases
Gas permeability,	Decreases

temperatures, and denser materials. Some of these copolymers, like EVOH, have substantially different barrier properties than the original homopolymer.

The content of VA in the copolymer ranges from 5 to 50% and are commercially available, although for optimal food applications primary copolymers with ranges from 5 to 20% are recommended. Ethylene vinyl acetate (EVA) resins are mainly recognized by their flexibility, toughness, and heat sealability in extruded coatings. The physical properties of available LDPE vary widely by the choice of reaction conditions and by the type and amount of comonomer.

8.3.1.1.2   Ethylene vinyl acetate

Properties — EVA is a random copolymer whose properties depend on the content of VA (CH_2=CHOCOCH$_3$) and the molecular weight. As the content of the VA increases, the crystallinity decreases; however, in contrast with LDPE, the density increases at the same time. As the VA content increases, clarity improves, flexibility is better at low temperatures, an increase in the impact strength is expected, and the material is tougher. EVA is totally amorphous (transparent) when the content of VA reaches 50%. Since the acetate group is polar, as the VA content increases so does the polarity of the resin. As polarity increases there is an increase in adhesion strength and tackiness. As the molecular weight increases, the viscosity, toughness, heat seal strength, hot tack, and flexibility all increase.

Applications — Because of its excellent adhesion and ease in processing, EVA is available as film, useful as heat sealing layer in coextrusion, and it blends well with homopolymer PE. As a heat sealing layer, EVA is used in extrusion coating with PET, cellophane, and biaxially oriented PP packaging films for applications such as cheese wrap and medical films. EVA is a good choice when toughness is required at low temperatures such as in the case of ice bags

and stretch wrap for meat and poultry (Landvatter; 1994). FDA has cleared the use of EVA copolymers for direct food contact as specified in 21 CFR, Section 177.1350.

8.3.1.1.3 Ethylene acrylic acid

The copolymerization of ethylene with acrylic acid (CH_2=CHCOOH) produces copolymers containing carboxyl groups along the main and side chains of the molecule. These copolymers are known as EAA.

Properties — As the content of AA increases, the crystallinity decreases, which implies that clarity also increases. Similarly, adhesion strength increases because of the increase in polarity, and the heat seal temperature decreases due to the decrease of crystallinity. EAA copolymers are flexible thermoplastics having chemical resistance, and barrier properties similar to LDPE. EAA is superior to LDPE in strength, toughness, hot tack, and adhesion, with two major uses as blister packaging and as an extrusion-coating tie layer between aluminum foil and other polymers.

Applications — Films of EAA are used in flexible packaging of meat, cheese, snack foods, medical products, in skin packaging and adhesive lamination. Extrusion coating applications include condiment and food packages, coated paperboard, aseptic cartons, composite cans and toothpaste tubes. The FDA has cleared the use of EAA copolymers for direct food contact as specified in 21 CFR, Section 177.1320. Up to 25% of AA for copolymers of ethylene in food direct contact is permitted by FDA (Mergenhagen; 1992).

Suppliers of branched PE — American Polymers (Worcester, MA); Bamberger Polymers, Inc. (Lake Success, NY); Chevron Chemical Co. (Houston, TX): Down Plastics (Midland, MI); DuPont Co. (Wilmington, DE); Eastman Chemical Co. (Kingsport, TN); Exxon Chemical Americas (Houston, TX); Mobil Polymers (Norwalk, CT); Monmouth Plastics, Inc. (Asbury Park, NJ); Novacor Chemicals, Ltd. (Calgary, AB, Canada); Quantum Chemical Corp. (Cincinnati, OH): Rexene (Dallas, TX); Union Carbide Corp. (Danbury, CT); Washington Penn Plastic Co. (Washington, PA); and Westlake Plastics PVC Corp. (Houston, TX).

8.3.1.1.4 Ionomers

Neutralization of EAA or EMAA (ethylene methyl acrylate), with a cation such as Na^+, Zn^{++}, of Li^+, produces a material that shows even better transparency, toughness, and higher melt strength than the un-neutralized copolymer. These materials are called ionomers because they combine covalent and ionic bonds in the polymer chain. Surlyn® is the DuPont's trade name for ionomers.

Properties — Ionomers are used in packaging where formability, toughness, and visual appearance are important. They are used in combination with nylon, PET, LDPE, polyvinylidene chloride (PVDC), paperboard, and aluminum foil to form a heat seal layer in films and multilayer structures. Ionomers improve the pinhole and flexing resistance of the structure. Coextrusion lamination and extrusion coating are the most common techniques for processing ionomers. With normal processing temperatures in the range of 175 to 290°C, ionomers can resist the impact at temperatures as low as –90°C (lower than for LDPE) (Reed and Vaughan; 1965). Barrier properties of Ionomers are rather poor, but when combined with PVDC produce a composed material that is an excellent barrier. There are more than 50 commercial grades of ionomer with a wide range of properties. In general, sodium ion types are better in optical, hot tack, and oil resistance. Zinc ionomers are more inert to water, have better adhesion properties in coextrusion and for extrusion in coating foil (Statz; 1994).

Applications — Ionomers are used in composite films for fresh and processed meats such as hotdogs. Other applications of ionomers include frozen foods (fish and poultry), cheese, snack foods, fruit juice, wine, water, oil, margarine, nuts, and pharmaceuticals. Ionomers are highly resistant to oils and aggressive products, and provide reliable seals over a broad range

TABLE 8.7
LLDPE Film and Resin Properties

Melting temperature	122–124°C	252–255°F
Glass transition temperature	°C	°F
Specific gravity	0.910–0.940	
Tensile strength at break	13–27.6 MPa	1.9–4.0 kpsi
Tensile modules, stiffness	262–518 MPa	38–75 kpsi
Flexural strength	–kPa	–kpsi
Flexural modulus, 23°C	276–725 MPa	40–105 kpsi

Note: LLDPE = linear low density polyethylene.

Adapted from *Modern Plastic, Guide to Plastics*, 1987, McGraw-Hill, New York.

of temperatures. FDA has cleared the use of ionomeric resins for direct food contact as specified in 21 CFR, Section 177.1330.

Producers of Ionomer — DuPont and Exxon.

8.3.1.1.5   Ultra low density polyethylene

ULDPE is a copolymer of both ethylene and octene. It has density between 0.880 and 0.915 g/cm^3. ULDPE copolymers show a good combination strength, sealability, flexibility, and optical properties. They are superior to LLDPE in tear strength, puncture resistance, impact strength, and transparency. Their oxygen permeability is higher than other PEs, yet similar to that of EVAs. However, the WVTR values of ULDPE are similar to those of PEs.

8.3.1.1.6   Linear low density polyethylene

Properties — Physical properties of LLDPE are controlled by its molecular weight and density (0.916 to 0.940). Due to the linearity of its molecules, LLDPE is more crystalline and therefore stiffer than LDPE. This results in an increase of 10 to 15°C in the melting point of LLDPE as compared to LDPE. LLDPE has higher tensile strength, puncture resistance, tear properties, and elongation than LDPE. However, LDPE has better clarity than LLDPE. The haze and gloss of LLDPE is worse than LDPE due to its higher crystallinity.

Applications — Common uses of LLDPE include stretch/cling film, grocery sacks and heavy duty shipping sacks. A summary of LLDPE is presented in Table 8.7.

8.3.1.1.7   High density polyethylene

Properties — HDPE is a milky-white nonpolar, linear thermoplastic. The molecular chains of HDPE homopolymers are long and straight with little branching. HDPE forms large fractions of ordered, crystalline regions as it cools below its T_m. This close molecular packing produces HDPE with a crystallinity of 65 to 90% and contributes to HDPE's good moisture-barrier properties, its chemical resistance, and its opacity. Its density ranges from 0.940 to 0.965. It is a versatile polymer, and, together with LDPE, is one of the most common plastics in the packaging industry. Table 8.8 presents HDPE film and resin properties. Table 8.9 shows the relation between PE density, and oxygen and water permeability.

Applications — Containers for milk, detergent, bleach, juice, water, and industrial chemical drums are made by blow molding. Buckets, thin walled dairy containers and closures are made by injection mold, while cosmetic containers, pharmaceutical bottles, and shampoo and deodorant containers are made by injection blow molding. Blown and cast films are utilized in feasible packaging applications. HDPE replaces glassine for cereal, crackers, and snack

TABLE 8.8
HDPE Film and Resin Properties

Melting temperature	130–137°C	266–276°F
Glass transition temperature	–100°C	–148°F
Specific gravity	0.940–0.965	—
Tensile strength at break	22–31 kPa	3.2–4.5 kpsi
Tensile modules, stiffness	1070–1090 kPa	155–158 kpsi
Flexural modulus, 23°C	1000–1550 kPa	145–225 kpsi
Propagating tearing strength	2.6–52.5 kN/m	15–300 lb/in
Permeability		
Water, at 37.8°C	16–94[a]	4–23.5[c]
Oxygen, at 25°C	390–1750[b]	100–450[d]
CO2, at 25°C	2300[b]	590[d]
N_2, at 25°C	160[b]	42[d]
Resistance to		
Acids	Good	—
Alkali	Good	—
Grease and oil	Good	—
Water	Good	—

Note: HDPE = high density polyethylene.

[a] Units in g·µm/m^2·d·kPa.

[b] Units in cc(STP) ·µm/m^2·d·kPa.

[c] Units in g·mil/100 in^2·d·atm.

[d] Units in cc(STP) ·mil/100 in^2·d·atm.

Adapted from *Modern Plastic, Guide to Plastics,* 1987, McGraw-Hill, New York.

TABLE 8.9
Effect of Density on the Permeability of Oxygen and Water in Polyethylene

Density of polyethylene	Water permeability (g·µm/m^2·d·kPa)	Oxygen permeability (g·µm/m^2·d·kPa)
0.910	94	1750
0.915	84	1630
0.920	74	1440
0.925	63	1280
0.930	50	1050
0.935	40	880
0.940	30	660
0.945	26	580
0.950	23	490
0.955	20	450
0.960	16	390

Adapted from Smith, M. A., 1986, in *Wiley Encyclopedia of Packaging Technology*, Bakker, M., Ed., John Wiley & Sons, New York.

food packaging. It is used for wrapping delicatessen products and to produce bags. FDA has cleared the use of PE for direct food contact as specified in 21 CFR Section 177.1520.

Producers of linear PE and HDPE — In addition to the ones listed as producers of branched PE, the following companies are also manufacturers: Federal Plastics Co. (Cranford, NJ); Hoechst Celanese Corp. (Chatham, NJ); Novacor Chemicals Ltd. (Calgary, AB, Canada); Paxon Polymers Co. (Baton Rouge, LA); Shulman, Inc. (Akron, OH); and Solvay Polymers, Inc. (Houston, TX).

8.3.1.2   Polypropylene

PP is a group of thermoplastic polymers based on the polymerization of propylene monomer (CH_2=$CHCH_3$). PP is commercially available as a PP homopolymer, and PP random copolymer. The latter is produced by the addition of a small amount of ethylene (2 to 5%) during the polymerization process. Thermoplastic PP polymers are characterized by their low density (0.89 to 0.92 g/cc) and good resistance to chemical and mechanical fatigue. Applications of PP in packaging include film, cups, trays, closures, and other containers. Manufacturers of PP continuously are offering PP grades with improved or modified properties. FDA has cleared the use PP resins for direct food contact as specified in 21 CFR, Section 177.1520.

8.3.1.2.1   PP homopolymer

General — Depending on the type of catalyst and polymerization conditions, the molecular structure of the resulting polymer consists of the three different types of stereo-configurations for vinyl polymers: isostatic (stereo-regular), syndiotactic (alternating stereo-regular) and atactic (random configuration) (McCrum et al.; 1988). Industrial processes are designed to minimize the production of the atactic PP, a lower-value, noncrystalline, tacking byproduct that is used mainly in adhesives. Metallocene polypropylene (mPP) is a new generation of PP for which a controlled balance between isotacticity and atacticity, type of comonomer, mean molecular weight, molecular distribution, are truly controlled. Containers with a PP have much thinner walls but keeping the same stiffness with very high melt flow index values.

The isostatic PP (iso-PP) is the most common commercial form of a PP homopolymer. The placement of the methyl groups all on the same side of polymer backbone provides a structure which readily yields a highly crystalline material. The crystalline nature of the iso-PP gives its good chemical and heat resistance, but is not transparent. Compared with LDPE and HDPE, PP has a lower density, higher melting point temperature and higher stiffness (higher tensile modulus). These properties determine the different types of application for PP homopolymer. For example, higher value of stiffness and ease of orientation make PP homopolymers suitable for stretched application, while their higher heat resistance allow a container made of this material to be autoclavable.

Properties — Compared with PE, iso-PP is more sensitive to oxidative degradation due to heat and light. Oxidative degradation may produce chain scission which reduces the average molecular weight and chemically degrades the polymer. To control this process, antioxidants are added during processing. Other processing additives for PP include antistatic agents, commonly used in packaging to dissipate static charge (see section 8.4). Properties of PP are summarized in Table 8.10.

Orientation of PP films improves strength, clarity, and gloss over the nonoriented PP films, see Table 8.11. Oriented PP (OPP) film is a very versatile material. It can be metallized, coextruded, laminated, coated, and even silica- and aluminum-oxide coated to meet specific applications.

Applications — Acrylic-coated OPP is available for candy, cookie, and snack packaging, where good machinability, low coefficients of friction (0.2 to 0.3), attractive appearance, and

TABLE 8.10
Polypropylene, Biaxially Oriented (BOPP) Film and Resin Properties

Melting temperature	160–175°C	194–347°F
Glass transition temperature	–20°C	–4°F
Specific gravity	0.895–0.910	
Tensile strength at break	31–42 MPa	4.5–6.0 kpsi
Tensile modules, stiffness	1140–1550 MPa	165–225 kpsi
Flexural strength	42–55 MPa	6.0–8.0 kpsi
Flexural modulus, 23°C	1170–1725 MPa	170–250 kpsi
Initial tearing strength	386–579 kN/m	1000–1500 g/mil
Propagating tearing strength	0.53–1.75 kN/m	3–10 lb/in
Permeability		
Water, at 37.8°C	16.5–26[a]	4.3–6.8[c]
Oxygen, at 25°C	622[b]	160[d]
CO_2, at 25°C	2100[b]	540[d]
N_2, at 25°C	78[b]	20[d]
Resistance to		
Acids	Good	
Alkali	Good	
Grease and oil	Good	
Water	Excellent	

[a] Units in g·μm/m²·d·kPa.
[b] Units in cc(STP)·μm/m²·d·kPa.
[c] Units in g·mil/100 in²·d·atm.
[d] Units in cc(STP).mil/100 in²·d·atm.

Adapted from *Modern Plastic Encyclopedia* (1987).

TABLE 8.11
Effect of Chain Orientation on PP Film Properties

	Nonoriented PP	Oriented PP
Water permeability, g·μm/m²·d·kPa, 37°C	60	25
Stiffness	Very low	High, similar to cellophane
Propagated tear strength	High	Very low CD; very high MD
Heat sealability	Yes, 350–450°F	No, film distorts
Density	0.902	No change
Optics	Good	Excellent
Surface adhesivity to inks, etc.	Low	Low
Oxygen permeability, cc(STP)·μm/m²·d·kPa at 25°C	930	620

Note: PP = polypropylene; CD = cross direction ; MD = machine direction.

cost-effectiveness are essential. For flavor protection and odor sensitive products, e.g., chocolate bars, a PVDC coated OPP can be selected. A higher barrier metallized OPP will extend the shelf-life of oxygen-sensitive products, e.g., low fat chips, nuts, and dried fruits. For applications in bag-in-box, e.g., cereal, crackers, soup mix packaging, stand up pouches, OPP

TABLE 8.12
Values of Heat Sealing Temperature, T$_g$, and Heat Deflection Temperature in PP-Containing Ethylene

Weight percent ethylene	Maximum heat sealing temperature[a] (°C)	T$_g$ (°C)	Heat deflection temperature[b] (°C)
0	163	6	115
2	152	2.5	95
4	143	–2	80
6	138	–6	64
8	125	–9	46
9	120	–11	40

[a] Melting temperature.
[b] AT 66 psi.

Adapted from Davis, D. S., 1992, *J. Plastic Film Sheeting* 8(4):101–108.

is a well-suited material (Rice; 1995). PP has a melting point of 163°C (325°F), therefore, microwave applications are limited to reheating. PP is also an excellent material for injection-molded closures for HDPE, PET, and glass beverage bottles. Plastic-lug®, Double-lok®, and Drip-lok® from Alcoa are examples of closure application so for PP, (Alcoa, 1993). Two-sided acrylic coated biaxially oriented PP (BOPP) films are heat sealable, highly transparent, highly glossy, and flavor barrier. Heat sealing temperature ranges from 93°C (200°F) to 145°C (293°F) with high hot-tack values. The films also show low COF and enhanced stiffness. OPP uses include shrink wrap for records, toys, games, hardware items, frozen foods, and cigarettes (Mobil, 1994).

8.3.1.2.2   PP random copolymer

Properties — PP copolymers show markedly different thermal properties as compared to PP homopolymer. As indicated in Table 8.12, the copolymers have lower heat sealing temperature, lower heat deflection temperature for thermoforming, and resist better subzero storage conditions. Random copolymer PP typically contains 1.5 to 7% ethylene, by weight, as comonomer. The addition of ethylene placed randomly in the chain backbone decreases the high crystallinity of iso-PP. Low crystallinity results in improved clarity and flexibility, and lower melting point (up to 152°F with 7% ethylene). The density is also lower 0.89 to 0.90 g/cc, showing that random copolymer is slightly lighter than homopolymer. Random PP has good toughness and lower temperature impact than homopolymer PP. These copolymers show good chemical resistance to acids, alkalies, alcohols, and to low-boiling hydrocarbons (no aromatic hydrocarbons).

Applications — PP random copolymers are used as films, blow, and injected parts. Applications include medical and food packaging, bakery products, and produce. The 7% ethylene copolymer is used as heat-seal layer in food packaging. Unoriented films are soft and are easy to heat seal.

Coextruded thermoformed containers — Thermoformed containers from multilayer cast sheet are used for shelf-stable and retortable single food packaging, e.g., microwaveable meals, prepared puddings, microwaveable baby foods, single-service apple sauce, nutritional supplements for the elderly, and even high-end pet foods. Other applications include modified atmosphere packaging (MAP) for meat, medical, and pharmaceutical products.

Typically, the coextruded structures are made of 5, 7, or 9 layers. They contain a symmetrical arrangement of polyolefin/regrind/tie layer/barrier layer/tie layer/regrind/polyolefin. The barrier layer is normally EVOH, PVDC, of Nylon. For MAP structures, it may include formed PS/tie layer/EVOH/PE or EVA with one regrind layer.

Suppliers of PP — American Polymers (Worcester, MA); Amoco Chemicals (Chicago, IL); Aristech Chem Corp. (Pittsburgh, PA); Bamberger Polymer, Inc. (Success, NY); ComAlloy International Co. (Nashville, TN); Exxon Chemical (Houston, TX); Federal Plastics Co. (Cranford, NJ); Fina Oil & Chemical Co. (Dallas, TX); Monmouth Plastics, Inc. (Asbury Park, NJ); Montell Polyolefins (Wilmington, DE); Phillips Chemical Co. (Bartlesville, TX); Quantum Chemical Corp. (Cincinnati, OH); Rexene (Dallas, TX); A. Shulman, Inc. (Akron, OH); Shell Chemical (Houston, TX); Solvay Polymers, Inc. (Houston, TX); and Washington Penn Plastic Co. (Washington, PA).

8.3.1.3 Metallocenes

As indicated in Section 8.2.1, single-site catalyst (SSC) polymers are characterized by narrow MWD and composition distributions. This means that the polymers molecules all have a similar number of side branches of comonomers at the same place along the polymer chain. In 1992, Exxon introduced metallocene plastomers (under the name EXACT®) with a range of density of 0.860 to 0.915 and a molecular weight ranging from 40,000 to 120,000. Polyolefin plastomers are being produced by Dow Chemical using SSC under the name of AFFINITY®. These plastomers are available as copolymers of propylene, butene, hexene, or octene, as well as terpolymers. The main characteristics of metallocenes are (Simon, 1994)

1. Low-molecular weight components which impart the resins with high extractable fraction are eliminated. This has the benefit of being a much purer resin for food contact applications. It also reduces odor and off-taste flavor.
2. Initiation seal temperatures are lower and sealing initiation temperatures are wider than HDPE. Strong hot-tack strength, and seal strength are shown by these resins so they can be used as a coextruded and/or blended heat seal layer.
3. Mechanical properties like puncture resistance, spencer impact, and blocking are improved with respect to resins produced by Ziegler-Natta catalysts. Haze and gloss are improved due to the absence of high-molecular weight fraction in the metallocene resins.
4. New metallocene PEs are expected to replace some PVC and produce new stretch films, sealant shipping bags and have application in taste-sensitive packaging (Manders; 1995). Other applications include meat, poultry, and fish requiring low sealing temperatures; coextruded structures for cereal and cake mix liners; and coffee pouch laminations. SSC resins can be blended with LDPE and HDPE.

8.3.2 POLYVINYL CHLORIDE

8.3.2.1 General

PVC is a homopolymer of vinyl chloride (CH_2=CHCl). Of commercial PVC in packaging, 80% is produced by an addition polymerization reaction in a liquid suspension; other methods included emulsion and solution. Rigid PVC (used for making pipes) has a $T_g = 180°F$ (82°C) and is very difficult to process. Flexible PVC material used in packaging is obtained by incorporating plasticizers. Plasticizers are additives that by a "lubricating" action at a molecular level, soften rigid polymers making them more flexible. Plasticizers decrease T_g and processing temperatures of a polymer. The addition of a liquid plasticizer to PVC then, permits the production of a flexible film with a moderate oxygen permeability.

TABLE 8.13
PVC Plasticized* Film and Resin Properties

	°C	°F
Melting temperature		
Glass transition temperature	75–105°C	167–221°F
Specific gravity	1.22–1.40	
Tensile strength at break	9.7–2.4 kPa	1.4–3.5 kpsi
Bursting strength, mil (Mullen)	20	20
Initial tearing strength	42.4–112 kN/m	210–290 g/mil
Propagating tearing strength	10.5–175 kN/m	60–1000 lb/in
Seal temperature	143–160°C	277–320°F
Permeability		
Water, at 37.8°C	330–2000[a]	85–510[c]
Oxygen, at 25°C	389–3900[b]	100–1000[d]
CO_2, at 25°C	1170–2330	300–6000[d]
Resistance to		
Acids	Good	
Alkali	Good	
Grease and oil	Fair	
Water	Excellent	

* Calendared and extruded.
[a] Units in g·μm/m²·d·kPa.
[b] Units in cc(STP)·μm/m²·d·kPa.
[c] Units in g·mil/100 in²·d·atm.
[d] Units in cc(STP)·mil/100 in²·d·atm.

Adapted from *Modern Plastic Encyclopedia* (1987).

PVC blow molded bottles are produced with plasticized PVC. The manufacture of a wide variety of packaging materials from PVC is possible because of the miscibility of the polymer with a range of plasticizers. Formulations to produce specific products made of PVC are mostly proprietary, for direct food contact, however, the additives need to be FDA sanctioned. DOA [di(2-ethyl hexyl)adipate] is the most common plasticizer used for PVC. Stabilizers such as Ca/Zn salts, which avoid the decomposition of PVC and the corresponding product of HCl, are also incorporated in PVC during compounding. The processing of PVC is carried out by conventional methods, e.g., injection molding, extrusion, blow film and blow molding.

8.3.2.2 Properties

PVC shows good clarity, good barrier properties, puncture resistance, and good sealability. PVC films provide good toughness and resilience. Properties of PVC are shown in Table 8.13.

8.3.2.3 Applications

Most PVC films are used for packaging food products particularly red and fresh meat. The oxygen permeability of PVC film is well suited to maintain the necessary oxygen requirements of the meat. This is necessary to keep the red color of the meat and its appearance of freshness. PVC is also used to wrap fresh fruits and vegetables. Almost all poultry producers in the U.S. use PVC stretch films for chilled, tray-packed poultry parts. PVC is available as stretch-wrap film. Examples of PVC packaging application include: bottles for milk, dairy products, edible oil, cosmetics, detergents, liquors, food wrap butter, and margarine; box lid for fresh, frozen, and cured meat; and, blister packaging fish, produce, and pharmaceutical products. PVC is also used for blood and intravenous-solutions tubing and bags.

8.3.2.4 PVC Concerns and the FDA

In the polymerization process of PVC slightly less than 100% of vinyl chloride monomer (VCM) is converted to polymer. This means that relatively high values of VCM may remain unreacted and trapped in the resin. The resin is subsequently submitted to a process in which VCM is removed. By repeated applications of vacuum, VCM is eliminated from the resin to reach concentration values of less than 1 ppm in the resin.

PVC is used extensively in food contact applications such as meat, oil, and water. The FDA has never banned or limited the use of PVC, but in the mid 1970s had expressed concern regarding its use in food due to the discovery of residual VCM in PVC. The FDA has not cleared VCM for food contact because VCM is a carcinogen in large doses, at least in laboratory animals. Currently, the industry produces PVC with extremely low levels of VCM in the resin, and the amount of VCM that might migrate to food is well below the sensitivity of analytical methods. It can be said that the concentration of VCM in food, by the action of migration from PVC containers, is sufficiently low and should not generate concern.

In the 1990s, PVC is now the center of a different controversy. Several European countries have banned the use of any PVC packaging because of the fear that during incineration of solids waste, HCl gases and chlorinated organic compounds (in which dioxins can be found) are generated and emitted into the environment. This increases the impact of the acid rain and poses health risks to humans. Japan, where a large portion of the solids waste is incinerated, has developed technology that prevents the emission of such unwanted compounds. However, some European countries maintain the ban on PVC.

8.3.2.5 Suppliers of PVC (Flexible Unfilled)

Alpha Gary Co. (Leominster, MA); Borden, Inc. (Andover, MA); Colorite Plastics Co. (Rigefield, NJ); Novatec Plastics & Chemicals Co., Inc. (Eatontown, NJ); A. Shulman, Inc. (Akron, OH); Shintech, Inc. (Houston, TX); Synergistics Industries, Inc. (Farmingdale, NJ); Teknor Apex Co. (Pawtucket, RI); Union Carbide Corp. (Danbury, CT); Vi-Chem Corp. (Grand Rapids, MI); and Vista Chemical Co. (Houston, TX).

8.3.3 VINYLIDENE CHLORIDE COPOLYMERS

8.3.3.1 General

Vinylidene chloride copolymers, known as Saran® or PVDC, were developed by the Dow Chemical Co. during the 1930s. These polymers result from the copolymerization of vinylidene chloride (VDC) ($CH_2=CCl_2$) with vinyl chloride, methyl acrylate, or acrylonitriles. Many commercial Saran polymers contain two or more comonomers. VDC homopolymer has a melting point of 198°C to 205°C, but it decomposes at 210°C. These conditions make VDC homopolymer, or PVDC, difficult to process. By copolymerization the melting point of the copolymers are decreased to a range of 140 to 175°C, making the melt-processing feasible. Saran polymer contains 2 to 10% plasticizer (e.g., dibutyl sebacate or diisobutyl adipate), and heat stabilizers. The most notable attribute of Saran copolymers are their extremely low permeability to gases and liquids and chemical resistance, which are comparable to EVOH resins.

8.3.3.2 Forms of Saran®

Saran is available in the following forms: F-Resins (with acrylonitrile as copolymer) used as solvent-soluble polymer for barrier coating; aqueous emulsion latexes for barrier coatings; and extrusion resins which are melt processable in rigid multilayer coextruded containers, extrusion of films, and sheets.

F-resins include F-239, and F-278 types. These resins are used to coat plastic films such as cellophane and polyester to give water permeability values ranging from 2.0 to 1.3 g·μm/m²·d·kPa, and oxygen permeability around 0.09 cc·μm/m²·d·kPa. Resin F-310 is used for paper coating. Heat sealing temperature of F-resins are in the 100 to 130°C range, (Dow Chemical Co. Form 190-305-1084).

Latexes are applied to coat paper, paperboard, and plastics films such as PP and PE. Also PET, PVC, PS, and PE rigid containers can be coated with latexes. Barrier properties of latexes are similar to those of F-Resins, (Dow Chemical Co. Form 190-309-1084).

Extrusion resins are used for flexible packaging in monolayer, and multilayer (coextruded or laminated) structures for meat and other food applications. For nonrefrigerated foods in rigid containers, extrusion resins can be coextruded with PP or PS resins. Extrusion resins are poorer barrier that F-Resins or latexes, (Dow Chemical Co. Form 190-320-1084). Saran HB Films (with vinyl chloride as comonomer) are a better barrier than F-Resins having an oxygen permeability of 0.04 cc·μm/m²·d·kPa, (Dow Chemical Co. Form 500-1083-586).

8.3.3.3 Applications

As indicated, different processing methods are available to Saran resins including extrusion, coextrusion, laminating resin, and latex coating to meet specific packaging requirements. Also injection molding, blown-film extrusion film and cast film are common industry processes for the resins. The main applications of Saran resins are in food packaging as barrier materials to moisture, gases, flavors, and odors. Monolayer films are widely used in household wrap.

Multilayer films, generally coextrusions with polyolefins are used to package meat, cheese and other moisture or gas-sensitive foods. The structures usually contain 10 to 20% of VDC copolymer and are commonly used as shrinkable films to provide a tight barrier around the food product. PVDC can be used as barrier layer in thermoformed containers made of a coextruded multilayer for shelf-stable and retortable single food packaging.

Industrial applications of monolayer films include laminations unit dose packaging drum and pack liners for moisture, oxygen and solvent-sensitive products in pharmaceutical and cosmetic packaging. FDA has cleared the use PVDC copolymer resins for direct food contact as specified in 21 CFR Sections 175.105 for adhesives, 175.320 for coating polyolefins, 176.170 for paper in contact with aqueous and fatty foods, 176.180 for contact with dry foods, and 177.1990 for resins.

Suppliers of PVDC include: Dow Plastics (Midland, MI).

8.3.4 POLYSTYRENE

As other polymeric materials, polymers based on the polymerization of styrene, ($CH_2{=}CHC_6H_5$) are being produced by new technologies. New copolymerization methods, additives, rubber-modification and blending make polystyrene (PS) a very versatile packaging material. PS is hydrophobic, nonhygroscopic, easily extruded and a thermoformed material. Three types of PS are available: general purpose, impact, and Foams.

8.3.4.1 General Purpose Polystyrene (GPPS)

Although referred to as crystal PS, these are totally amorphous materials with no melting temperature, highly transparent, and with excellent optical properties. "Crystal" PS linear polymer has a T_g value ranging from 74 to 105°C, which makes it brittle and stiff at room temperature. There are three grades of GPPS: high heat, medium flow, and high flow (or easy flow). High heat resins have high molecular weight, contain few or no additives, and are brittle. They are used as extruded foams and thermoformed materials for electronic packaging, injection molded jewel box, high quality cosmetic containers and CD jewel boxes.

TABLE 8.14
Polystyrene Oriented Film and Resin Properties

	Amorphous °C	°F
Melting temperature		
Glass transition temperature	74–105°C	165–221°F
Specific gravity	1.05–1.06	
Tensile strength at break	14–70 MPa	2–10 kpsi
Tensile modules, stiffness	2280–3280 MPa	330–475 kpsi
Flexural strength	69–100 MPa	10–14.6 kpsi
Flexural modulus, 23°C	2620–3380 MPa	380–490 kpsi
Bursting strength, mil (Mullen)		16–35
Initial tearing strength	104–191 kN/m	270–495 g/mil
Propagating tearing strength	0.9 kN/m	5 lb/in
Permeability		
Water, at 37.8°C	460–660[a]	120–170[c]
Oxygen, at 25°C	970–1260[b]	250–350[d]
CO_2, at 25°C	3500	900[d]
Resistance to		
Acids	Good	—
Alkali	Good	—
Grease and oil	Poor	—
Water	Good	—

[a] Units in g·μm/m²·d·kPa.

[b] Units in cc(STP)·μm/m²·d·kPa.

[c] Units in g·mil/100 in²·d·atm.

[d] Units in cc(STP)·mil/100 in²·d·atm.

Adapted from *Modern Plastic Encyclopedia* (1987).

High flow resins have a low molecular weight and usually contain 3 to 4% mineral oil as additive. This makes crystal PS more flexible (less brittle) with lower distortion temperature. Typical applications include disposable medical ware, dinner ware, and coextruded sheets for thermoformed packaging.

Medium flow resins have an intermediate molecular weight, with 1 to 2% mineral oil as additive. These resins are used in blow molded bottles and coextruded materials for food and pharmaceutical packaging.

8.3.4.2 High Impact Polystyrene

High impact polystyrene (HIPS) contains particulates of rubber which are added to enhance the impact resistance. This produces an opaque material easy to process that can be thermoformed. Typical food packaging application are tubs for refrigerated dairy products, serving-size cups, lids, plates, and bowls. Limiting factors for HIPS are heat resistance, oxygen permeability, UV light stability, and resistance to oil and chemicals. According to Toebe et al. (1990) containers made of HIPS have an intense flavor scalping action on foods.

8.3.4.3 Expandable PS

Foam is a form of crystal PS supplied as a partially expanded bead. Expandable PS (EPS) foam has good shock absorbing and heat insulation characteristics. Application in food packaging includes egg cartons and meat trays.

Selected properties of PS are presented in Table 8.14. FDA has cleared the use of PS resins for direct food contact as specified in 21 CFR Section 177.1640.

8.3.4.4   Suppliers of Homopolymer PS

A. E. Plastics, Inc. (Elk Grove Village, IL), American Polymers (Worcester, MA); Amoco Chemical Co. (Chicago, IL); Bamberger Polymer Inc. (Success, NY); BASF Corp. (Wyandotte, MI); Chevron Chemical Co. (Houston, TX); Dow Plastics (Midland, MI); Federal Plastics Co. (Cranford, NJ); Fina Oil & Chemical Co. (Houston, TX); Hutsman Chemical Co. (Chesapeake, VA); RTP Co. (Winona, MN); A. Shulman, Inc. (Akron, OH); and Washington Penn Plastic Co. (Washington, PA).

8.3.5   ETHYLENE VINYL ALCOHOL

8.3.5.1   General

Introduced in 1970 in Japan, EVOH is produced by a controlled hydrolysis of EVA copolymer. The hydrolytic process transforms the VA group in VOH, (CH_2=CHOH). The presence of OH in the backbone chain substituting a certain number of H atoms in PE has several profound effects on the polymer properties. First, the OH group is highly polar which increases the intermolecular forces, and at the same time becomes more hydrophilic than PE. Second, the OH group is small enough to give the polymer chain enough estereoregularity to form a polymer with high percent of crystallinity; even if it is randomly distributed in the chain it provides an excellent barrier to permeants. If the percent of OH in the olefinic backbone is zero, the product is PE, and at 100% VA the product becomes polyvinyl alcohol (PVOH).

Contrary to PE, PVOH has exceptionally high gas and odor barrier properties (the lowest of any polymers available), but is difficult to process, and is water soluble. When the percent of VOH in EVOH ranges from 52 to 70%, the ethylene-VOH copolymers obtained combine the processability and water resistance of PE and the gas and odors barrier characteristic of PVOH. EVOH copolymers are highly crystalline and their processing and barrier properties vary with respect to the equivalent percent of ethylene. When the ethylene percent is about 30%, gas and organic vapor barrier are exceptionally high but process conditions become more difficult. When ethylene content increases the water barrier and processability improve.

8.3.5.2   Properties

The most important characteristic of EVOH is the outstanding O_2 and odor barrier properties. Packaging structures with EVOH provides high retention of flavors and quality associated with oxygen reaction with the food product. EVOH also provides a very high resistance to oils and organic vapors. This resistance decreases somehow as the polarity of the penetrating compound increases. For example, the resistance to linear and aromatic hydrocarbons is outstanding, yet for ethanol and methanol it is low. It may, therefore, absorb up to about 12% of ethanol.

As indicated, the hydroxyl group OH makes the polymer hydrophilic, attracting of water molecules. The presence of water has a depressing effect in the oxygen barrier property. This poses an interesting challenge to the design of high barrier packages since external non-hydrophilic layers are necessary to protect the EVOH oxygen barrier characteristics. Selected properties for two EVOH copolymers are presented in Table 8.15.

8.3.5.3   Applications

EVOH can be coextruded in numerous combinations with PE or PP, and laminated or coated to several substrates including PET, PE, nylons, etc. EVOH can also be extruded in films, and processed in blow molding, injection molding, and coextrusion blow molding. Selected structures are listed in Table 8.16.

TABLE 8.15
Selected Properties of EVOH copolymers

Property	EVOH (32% ethylene)	EVOH (44% ethylene)
Density, g/cc	1.19	1.14
Ultimate tensile strength, MPA	80	59
Tear strength, N/mm	154	193
T_m, (T_g) in °C	181, (70)	164, (55)
Heat seal temperature, °C	179–238	177–238
Oxygen permeability, cc·μm/m²·d·kPa	0.03 (0% RH)	0.15 (0% RH)
	0.2 (65% RH)	0.3 (65% RH)
WVTR, g·μm/m²·d·kPa at 38°C	250	92

Note: EVOH = ethylene vinyl alcohol; WVTR = water vapor transmissin rate; RH = relative humidity.

Adapted from EVAL Company of America.

TABLE 8.16
EVOH Applications for Selected Structures

Application	Structure
Processed meats, cheese, snacks	PET/EVOH/EVA Nylon/EVA/Nylon/Ionomer OPP/EVA/EVOH/EVA
Dairy, meat, coffee, condiments	Onylon 6/EVOH/Onylon 6
Red meat	LLDPE/EVOH/LLDPE
Tea, condiments	OPP/EVOH/LDPE
Aseptic packaging	LDPE/paperboard/ EVOH/PP/Ionomer
Yogurt	PP/EVOH/PP
Ketchup	PET/EVOH/PET
Cosmetics	LDPE/EVOH/LDPE
Pharmaceuticals	EVOH/LDPE

Note: PET = polyethylene terephthalate, EVOH = ethylene vinyl alcohol; EVA = ethylene vinyl acetate; PP = polypropylene; OPP = oriented polypropylene; LDPE = low density polyethylene; LLDPE = linear LDPE.

Adapted from Foster, R., 1986, *The Wiley Encyclopedia of Packaging Technology*, Bakker, M., Ed., John Wiley & Sons, New York, 270–275.

FDA has cleared the use of EVOH resins for direct food contact as specified in 21 CFR, Section 177.1360 up to 80% of VOH. Application in packaging include flexible and rigid containers. Typical applications are ketchup and barbecue sauce bottles, jelly preserves, vegetable juice, mayonnaise containers, and meat packages. Non-food applications include packaging of solvent and chemicals.

8.3.5.4 Suppliers

Eval Company of America (Lisle, IL); Nippon Goshei (Japan), and Kurary Co. (Japan).

8.3.6 NYLON

8.3.6.1 General

Nylons are a family of condensation, linear, thermoplastic polyamides that contain the amide group (–CONH–) as a recurring part of the chain. Polyamides can be produced by the reaction of diacid with a diamine or by the polymerization of single amino acids such as ε-caprolactam to produce nylon 6, Kohan (1973).

8.3.6.2 Properties

In general nylons are clear, thermoformable, very strong, and tough materials over a broad range of temperatures. They are a good barrier to gas, oil, and aromas (see properties in Table 8.17). Nylons are polymers with strong intermolecular forces taking place by the presence of H-bonding between the –C=O and HN– groups of different chains. These high intermolecular forces are combined with crystallinity to yield tough high-melting thermoplastic materials. For instance, Nylon 6,6 has a melting point of 269°C (516°F). In addition, nylons have good puncture resistance, impact strength, and temperature stability. Furthermore, the flexibility of the aliphatic portion in the chain permits film orientation that enhances strength. By reacting comonomers (for example, 2 different di-acids), amorphous nylons can be produced, e.g., 6I/6T (Selar®, PA, trade mark from DuPont). 6I/6T is a copolymer of hexamethylene adipamine and isophthalic and terephthalic acids (Blatz, 1989).

Since the amide group is polar, nylons are moisture sensitive or hydrophilic. Left in its normal environmental conditions at 65 to 80% RH (relative humidity), nylons can easily absorb 6 to 8% of its weight of water, depending on their chemical composition. Complete sorption isotherms of Nylon 6 and amorphous nylon 6I/6T at three temperatures are given by Hernandez (1994). The amount of water in a nylon sample can be described as a function of relative humidity by a sorption isotherm curve.

Oxygen permeability in nylons is affected by their moisture content. As indicated in Figures 8.2 and 8.3, in the case of semicrystalline nylons such as nylon 6, oxygen permeability increases above an equilibrium RH of 30 to 40%, while in amorphous 6I/6T it stays constant after a decrease from 0%, (Hernandez, 1994).

8.3.6.3 Applications

Nylons are melt-processable using conventional extrusion. Film manufacture can be produced by either cast-film process or blown film process. During film production, diverse degrees of crystallinity are obtained depending on the temperature quenching rate. When the cooling rate is increased, a less crystalline nylon is obtained since the polymer was not given sufficient time to form crystals. The biaxial orientation of nylon (BON) films provides increased transparency, crack resistance, mechanical properties, and barrier characteristics. The increase in amorphousness produces improved transparency and thermoformable film.

Nylons are used in coextrusion with other plastic materials providing strength and toughness to the structure. Polyolefins are commonly used in nylon coextrusions to provide heat sealability, moisture, and low cost. Nylon is used to extrusion coat paperboard to obtain heavy duty paperboard.

Blow molding process is used with nylon resins to produce industrial containers. Thermoformed nylons are employed for disposable medical devises, meat and cheese packaging and are in thermoform/fill/seal packaging.

Important attributes of nylons for packaging are their excellent thermoformability, flex-crack resistance, abrasion resistance, grease, and odor barrier, mechanical strength (tensile, burst and impact) up to above 200°C.

TABLE 8.17
Nylon 6 Film and Resin Properties

Melting temperature	210–220°C	410–428°F
Glass transition temperature	°C	°F
Specific gravity	1.12–1.14	—
Tensile strength at break[a]	41.4–166 MPa	6–24 kpsi
Tensile modules, stiffness[a,b]	690–1700 kPa	100–247 kpsi
Flexural strength[a,b]	400 kPa	58 kpsi
Flexural modulus, 23°C[a,b]	966 kPa	140 kpsi
Initial tearing strength	386–463 kN/m	1000–1200[a] g/mil
Propagating tearing strength	2.8–4.9 kN/m	16–28[c] lb/in
Folding endurance[a]	250,000	—
Permeability		
Water, at 37.8°C	660–620[d]	170–187[h]
Oxygen, at 25°C	10.0[e,f]–5.1[e,h]	2.6[f,g]–1.3[g,h]
CO_2, at 25°C	39–47	10–12[f,g]
N_2, at 25°C	3.5	0.9 [f,g]
Resistance to		
Acids	Poor	—
Alkali	Fair	—
Grease and oil	Excellent	—
Water	Poor–Good	—

[a] Molding and extrusion compound.

[b] As conditioned to equilibrium at 50% RH.

[c] Units in g·mil/100 in²·d·atm.

[d] Units in g·µm/m²·d·kPa.

[e] Units in cc(STP)·µm/m²·d·kPa.

[f] Cast.

[g] Units in cc(STP)·mil/100 in²·d·atm.

[h] Biaxially oriented.

Adapted from *Modern Plastic Encyclopedia* (1987).

The most common nylons used in food packaging is nylon 6 and nylon 6,6. FDA has cleared the use of nylon resins for direct food contact as specified in 21 CFR, Section 177.1500. For most applications nylons are combined with other materials that add moisture barrier and heat sealability, e.g., LDPE, ionomer, EVA. Multilayer films containing a nylon layer are used principally in vacuum-packing bacon, cheese, bologna, hot dogs, and other processed meats. Coextrusion such as nylon 6/EVOH/nylon 6 provides a unique combination of mechanical and barrier properties. PVDC copolymer coating on nylons are available for an improved oxygen, moisture vapor, grease barrier properties. Nylon based structures are used in MAP involving CO_2 flushing for poultry, fish, and fresh meat.

8.3.6.4 Suppliers of Nylon 6

The following are suppliers of Nylon 6 (molding and extrusion compound): Adell, Inc. (Baltimore, MD); Allied Signal, Inc. (Morristown, NJ); ALM Co. (Wayne, NJ); Ashley Polymers, Inc. (Brooklyn, NY); BASF Co. (Wyandotte, MI); Bamberger Polymers, Inc. (Success, NY); Bayer co. (Pittsburgh, PA); Com Alloy International Co. (Nashville, TN); Custom Resins Division of Bemis Co. (Henderson, KY); DuPont Co. (Wilmington, DE); EMS, Inc. (Sumter, SC); Hoechst Celanese Co. (Chatham, NJ); Nylon Corporation of American
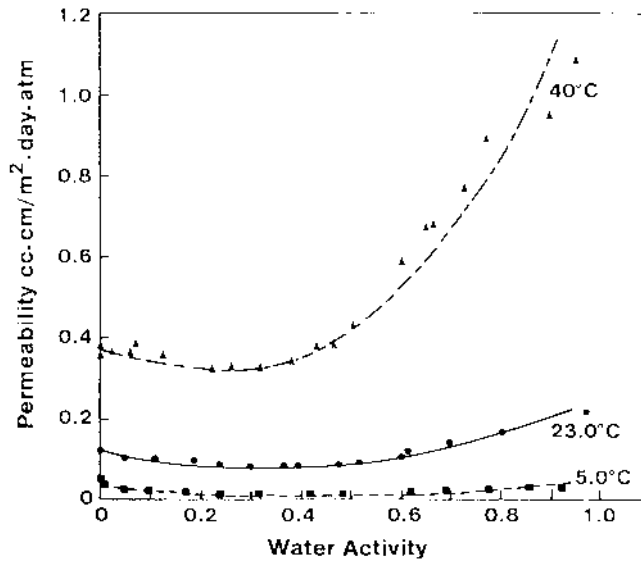
FIGURE 8.2 Oxygen permeability of Nylon 6. (From Hernandez, R. J., 1994, *J. Food Eng.,* 22:502. With permission.)
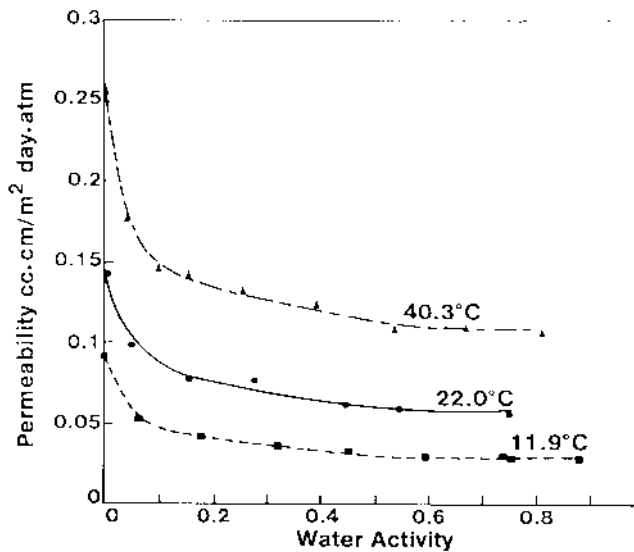
FIGURE 8.3 Oxygen permeability of Nylon 6I/6T. (From Hernandez, R. J., 1994, *J. Food Eng.,* 22:502. With permission.)

(Manchester, NH); Polymer Resources (Farmington, CT); Polymers International, Inc. (Spartanburg, SC); A. Shulman, Inc. (Akron, OH); Texapol Co. (Bethlehem, PA); and Thermofil, Inc. (Brighton, MI).

8.3.7 POLYETHYLENE TEREPHTHALATE

8.3.7.1 General

PET is a linear, thermoplastic polyester produced by the esterification reaction of glycol and terephthalic acid. Due to the step-wise type of reaction which imparts high steroregularity to

TABLE 8.18
PET Film and Resin Properties

Melting temperature	212–265°C	413–509°F
Glass transition temperature	70–80°C	158–176°F
Specific gravity	1.35–1.41	
Tensile strength at break	48.3–72.5 MPa	7–10.5 kpsi
Tensile modules, stiffness	2760–4140 MPa	400–600 kpsi
Flexural strength	83–124 MPa	12–18 kpsi
Flexural modulus, 23°C	2400–3100 MPa	350–450 kpsi
Bursting strength, mil (Mullen)	55–80	—
Initial tearing strength	79.3–116 kN/m	50–300 g/mil
Propagating tearing strength	175–525 kN/m	1000–3000 lb/in
Folding endurance[a]		>100,000
Permeability		
Water, at 37.8°C	66–86[a]	17–22[c]
Oxygen, at 25°C	11.6–23.3[b]	3.0–6.0[d]
CO_2, at 25°C	58.3–97.1[b]	75–25[d]
N_2, at 25°C	2.7–3.9[b]	0.7–1.0[d]
Resistance to		
Acids	Good	
Alkali	Poor	
Grease and oil	Good	
Water	Good	

Note: PET = polyethylene terephthalate.

[a] Units in $g \cdot \mu m/m^2 \cdot d \cdot kPa$.

[b] Units in $cc(STP) \cdot \mu m/m^2 \cdot d \cdot kPa$.

[c] Units in $g \cdot mil/100 \ in^2 \cdot d \cdot atm$.

[d] Units in $cc(STP) \cdot mil/100 \ in^2 \cdot d \cdot atm$.

From *Modern Plastic Encyclopedia* (1987).

the polymer chain, PET is a semicrystalline polymer. Homopolymer PET has become a very important packaging material in food packaging films and carbonated beverage bottles. Copolymerization with other monomers produces polyester resins of different degrees of crystallinity, including an amorphous material, which are used for containers and trays.

8.3.7.2 Properties

The great acceptance of PET as a carbonated beverage packaging material is due to its toughness and clarity, capability of being oriented, reasonable cost, and the development of high speed bottle processing technology. PET containers are lightweight, shatter-resistant, good barriers, and recyclable. PET is produced by the condensation of a diacid and a dialcohol. Oriented PET has good strength, toughness, and clarity. It resists weak acids, bases, and many solvents. See Table 8.18.

The presence of moisture during the extrusion of PET reverts the condensation reaction and produces some degree of depolymerization. Before extrusion then, PET must be dried to remove water molecules. Moisture content should be less than 0.005% to minimize hydrolytic breakdown and loss of properties. Films can be produced using chill roll. Injection molding is used to produce bottles. Molding material should be free from contamination to comply with FDA regulations.

8.3.7.3 Applications

PET is used for packaging food, distilled spirits, carbonated soft drinks, noncarbonated beverages, and toiletries. FDA has cleared the use of PET resins for direct food contact as specified in 21 CFR, Section 177.1315. Typical food products include, e.g., mustard, pickled foods, peanut butter, spices, edible oil, syrups, and cocktail mixers. PET is extensively used for extrusion coating and extrusion into film and sheet. Its crystalline form (CPET) is the basic material for oven-ware containers. Biaxially oriented PET is used in meat and cheese packaging. Thermoforming is a common operation applied to PET sheets. Other applications include ovenable boards, boil-in-bag, and sterilizable pouches. As the food processors continue to refine their technologies of low acid, high-particular entrees, aseptic packaging could become an important market for multilayer barrier containers such as PET/EVOH/PET.

Since FDA has accepted the use of regenerated PET (reclaimed PET that has undergone a rigorous chemical or mechanical recycling process to assure clean liners), it is expected that the use of this material in multilayer food packaging may reduce the cost of producing the thermoformable sheets. Under development is a three-layer amorphous PET sheet structure with a core layer of 60 to 70% regrind. The intended use of this structure is for bakery and refrigerated products. Since PET resists higher retort temperatures 127 to 135°C than copolymer PP, 121°C, the three-layer amorphous sheet could be used in retortable, aseptic packaging (Toensmeier, 1995).

8.3.7.4 Thermoplastic Copolyesters

The name copolyesters is applied to those polyesters whose synthesis is carried out by using more than one glycol and/or more than one diacid. The copolyester chain is less regular than homopolymer and the degree of crystallinity is lower, some of those are amorphous. PCTA is a polymer of cyclohexanedimethanol (CHDM) and terephthalic/isophthalic acids. This is an amorphous polyester, designed primarily for film forming and sheeting in food, pharmaceutical, and, in general, blister packaging applications. PETG is made with CHDH and glycol plus terephthalic acid. PETG, with a T_g of about 81°C, is a glossy, transparent, tough, sterilizable with gamma rays, and recyclable.

8.3.7.5 Polyethylene Naphthalate

Polyethylene naphthalate (PEN) is the last addition to the polyester family. Its packaging application has been directed to the beverage industry. PEN is a clear material, although less than PET, with enhanced gas-barrier characteristics. The oxygen permeability constant of PEN is five times lower than for PET. It has a T_g near 120°C (43° higher than for PET), and is stronger and stiffer than PET. These properties make PEN well suitable for hot fillings and an excellent material for carbonated beverages. Because of its absorbance of UV radiation, PEN may provide an extra protection to UV-sensitive products. PEN resins, presently more expensive than PET, can be processed by blow molding, injection molding, and extrusion molding. Containers made with this resin are returnable, refillable, and recyclable.

8.3.7.6 Suppliers

Suppliers of PET and copolyesters unfilled include: DuPont Co. (Wilmington, DE); Eastman Chemical Co. (Kingsport, TN); Hoechst Celanese Co. (Chatham, NJ); A. Shulman, Inc. (Akron, OH); Shell Chemical Oil Co. (Houston, TX); and Texapol Co. (Bethlehem, PA).

8.3.8 POLYCARBONATE

Polycarbonate (PC) is a glassy, amorphous thermoplastic material. It has excellent balance of toughness and clarity. It has a heat deflection temperature of about 130°C and a glass

transition temperature of 149°C. PC has major applications in the automobile industry and appliances markets and has good potential for packaging applications.

Commonly, PC is produced by the reaction of bisphenol-A and carbonyl chloride.

Toughness is the most impressive property of PC. For instance, PC is the material of choice for school window and sports equipment. Being tough and clear makes PC a material well suited for reusable bottles, particularly 19-l (5-gal.) water bottles or 1-gal milk bottles. Systems with washing stations have been developed for reusable PC bottles. PC films are odorless, have no taste, and do not become stained through normal contact with natural or synthetic coloring agents.

PC has good resistance to fruit juices, aliphatic hydrocarbons, and aqueous solutions of ethanol but is attacked by some solvents such as acetone and dimethyl ethyl ketone. Since PC is FDA approved, food-contact applications include microwave, ovenware, and food storage containers.

In Europe, most food applications include prebaked bread, biscuits, confectionery, meat, and processed cheese. Other emerging applications include hot fillings, modified atmospheric packaging, rigid packaging to substitute PVC, high gloss for paper, and barriers for fruit juice cartons.

PC finds application in medical-device packaging. It can be sterilized by commercial sterilization techniques such as ethylene oxide, autoclave sterilization, and gamma sterilization.

PC can be processed by injection molding, extrusion, coextrusion, and blow molding. Coextrusions with EVOH or polyamides are carried out with the help of adhesives. PC can be laminated or coextruded to PP, PE, PET, PVC, and PVDC. PC is a hydrophilic polymer and at ambient conditions can reach moisture levels of 0.35%.

8.3.8.1 Suppliers

Suppliers of PC include: Albis Co. (Rosenberg, TX); American Polymers (Worcester, MA); Ashley Polymers, Inc. (Brooklyn, NY); Bamberger Polymers, Inc. (Success, NY); Bayer Co. (Pittsburgh, PA); Dow Plastics (Midland, MI); Federal Plastics, Inc. (Cranford, NJ); General Electric Plastics (Pittsfield, MA); MRC Polymers, Polymer Resources (Farmington, CT); Progressive Polymers, Inc. (Jacksonville, TX); RTP Co. (Winona, MN); and Shuman (Charlotte, NC).

8.3.9 SILICA-COATED AND ALUMINUM-COATED FILMS

Silicon oxide (SiO_x) deposition on polymer substrates have been applied to packaging to provide a high barrier to gases and vapors. PET coated with silicon oxide has proved to acquire excellent barrier properties for water and oxygen. Its barrier properties are slightly affected by temperature variations but it maintains its transparency and is retortable and microwaveable. Three vacuum deposition processes (evaporation, sputtering, and plasma-based) are used to coat PET, LDPE, BOPP, and BON (Felts, 1993). Results showed that the SiO_x coatings made by plasma-enhanced chemical vapor deposition (PECVD) yielded the best oxygen barrier properties. Oxygen permeability values are much lower than those of EVOH. Silica-coated films are produced by Airco Coating Technology (Concord, CA). The permeation of organic vapors through silica-coated PET films have been measured by Sajaki and Giacin (1993).

Aluminum oxide (AlO_x) coatings produced by Flex Products (Santa Rosa, CA) and by A.D. Tech (Taunton, MA) are close rivals of silicon-oxide coatings. Aluminacoated films are also excellent barriers to gases and vapors, optically transparent, and microwaveable.

8.4 PLASTIC ADDITIVES

Pure resins are rarely processed into final products without the addition of highly selected compounds, called additives, that are incorporated during the process of extrusion and molding of a plastic resin or applied externally on the formed material. There are several reasons

for the addition of these compounds into the formulation of the final product: to improve the processing conditions; to increase the resin's stability to oxidation; to obtain a better impact resistance; to increase or decrease hardness; to control surface tension; to facilitate the extrusion and molding; to control blocking; to reduce cost; to increase flame resistance, etc.

The number and amount of additives incorporated in the compounding process of a resin vary greatly with the type of resin and application. In the case of PE, for instance, an antioxidant may be the only additive incorporated. In the case of PVC, several plasticizers, a filler, heat stabilizer, and colorant are normally incorporated. Many options are available to the manufacturer. In most cases the final formulation is considered proprietary information.

Additives are incorporated by the resin manufacturer and/or by the packaging converter. The presence of additives in packaging applications always raises the question of additive migration. Most of the additives diffuse within the polymer and tend to go to the surface of the material. When the packaged product is in direct contact with a compounded polymer there will be a transfer of the additive to the product. The additive transfer is controlled by the system's mass transfer coefficients and thermodynamics. Selected additives relevant to food packaging are reviewed.

8.4.1 ANTIFOGGING AGENTS

When condensation of water molecules takes place on the internal surface of the headspace of a package, a continuous thin layer of small droplets of water can be formed. On transparent films and structures, the layer of droplets of water produces the refraction of light in many directions. This phenomenon, called fogging, makes the film or structure appear opaque. This is not only aesthetically poor but also may produce damage in the packaged product. The droplets are formed when the polymer surface tension is lower than the surface tension of water, which prevents the formation of a continuous layer of water.

Antifogging additives function by increasing the critical surface tension of the polymer surface and allowing the molecules of water to wet the polymer surface.

Common antifogging agents are: fatty acid esters, such as, glycerol and sorbitol stearate, fatty alcohols and ethyloxylates of nonyl phenols. Antifogging agents are incorporated in the resin in levels ranging from 0.5 to 4%. Several factors are involved in the selection and use of these additives, e.g., polymer type (LDPE, LLDPE, PVC, EVA, PP, and PET), thickness of the structure or film, performance life, and whether the product is a food. In the latter case, FDA clearance is necessary for its application. Antifogging compounds can be applied on the surface of the material or compounded internally in the packaging material.

8.4.2 ANTIBLOCKING

Blocking is the tendency of two adjacent layers of polymer films to stick to each other by simple physical contact. Blocking is mainly determined by the smoothness of the surfaces. To reduce blocking the smoothness of the surfaces must be altered by the presence of tiny particulates imbibed within the polymer. Solid particulates, antiblocking agents are usually incorporated into polymers films to reduce the area of flat contact.

According to Radosta (1991), diatomaceus earth of 2 to 4 μm has been employed to reduce blocking in PE films, but talc also has important commercial use as an antiblock agent for LLDPE and LDPE. Diatomaceus earth is a class of compact, granular, or amorphous mineral composed of hydrated silica formed of fossil diatoms. Talc is a soft mineral of fine colloid particles with soapy feel, made of hydrated magnesium silicate, $4SIO_2$-$3MgO$-H_2O. The advantages of talc over diatomaceus earth include platelet morphology, particle size distribution, and the possibility of being coated to make it more compatible with PE. Its level range is between 0.1 to 0.5% of the resin.

When antiblocking agents are incorporated to PE films other important properties of the polymer are also affected. This includes an increase in stiffness, a decrease in the COF, and an increase of haze.

8.4.3 ANTIMICROBIALS

Antimicrobial agents preserve compounded polymeric materials from attack by microorganisms, i.e., bacteria, fungi, or mildews.

Most synthetic polymers in their pure state are not attacked by microorganisms, they are in general nonbiodegradable. However, when various low molecular additives are compounded within the polymer, conditions for microorganism attack are created.

The presence of plasticizers, lubricants, or heat stabilizers in the polymeric matrix are the target of the microbial activity. It has to be said, however, that different additives pose different resistance to be biodegraded. If the expected value of the shelf-life of a package is in the order of the time required for the package material to develop microbial attack it will be necessary to consider the use of an antimicrobial agent.

One of the most compounded polymers available in packaging is PVC which may contain an appreciable amount of plasticizers and lubricants (40 to 50% in weight percent). Among the most common preservatives used for polymers are 2-n-octyl-4 isothiazolin-3 and copper-8-quinoleate, the use level ranges from 0.1 to 1%. Antimicrobial agents for polymers are considered pesticides by the Environmental Protection Agency under the Federal Insecticide, Fungicide and Rodenticide Act (FIFRA).

8.4.4 ANTIOXIDANTS

Polymeric materials chemically deteriorate during fabrication, processing, and storage due to a series of complex chemical oxidation reactions using atmospheric oxygen. Several factors promote the oxidation reactions, among them are high temperature during processing, ionizing radiation, mechanical stress, chemical attack, or simple storage. In an oxidative degradation process such as one generated in the extrusion process, covalent bonds in the polymer chain are broken and free radicals are formed. This process goes to a propagation and the termination process.

The oxidative degradation may considerably damage the polymer by chain scission and cross-linking. Usually, the average molecular weight changes and the MWD broadens. To prevent the damage on the polymer generated by the oxidative degradation, chemical additives called antioxidants are incorporated to the polymer during processing.

Two main types of antioxidants (AO) are available commercially, primary AO and secondary AO. Primary AO work by inhibiting the propagation of oxidation process. Examples of primary AO include hindered phenols, e.g., butylated hydroxy toluene (BHT), and secondary arylamines.

The secondary AOs work by decomposing the peroxide molecule into nonradical stable products. Examples of a secondary AO are phosphites and sulfur compounds. Because the role of primary and secondary AO differ in their mechanism of attack to prevent oxidative degradation, in practice both types of AO are used together to obtain the best results.

Saturated polymers containing tertiary carbon off the backbone, such as PP, are more susceptible to oxidation than saturated linear polymer containing only secondary carbon in the backbone, such as PE.

In packaging, three resins consume most of the AO produced: PP, PE, and HIPS. For PP a combination of hindered phenol and phosphite AO is commonly used and the total concentration is normally from 0.08 to 1%, depending on formulation and end use. For LDPE, 50 to 500 ppm of BHT is normally incorporated. There is a tendency, however, to employ less volatile additives to prevent its migration from the resin. For HDPE and LLDPE, AO is

less volatile than BHT. Polyphenols at a higher concentration are normally used in combination with phosphites. For HIPS hindered phenols are used in combination with UV absorbers.

Evaluation of the use of α-tocopherol, or vitamin E, as an AO for polyolefins is discussed by Laermer and Zambetti (1992).

In the case of PVC the degradation is mostly ionic. PVC breakdown occurs through dehydrochlorination. The reaction is autocatalyzed by HCl byproduct and further accelerated by oxygen. Organometallic compounds and salts derived from lead, cadmium, barium, zinc and tin, as well as epoxides and phosphites, are the most common stabilizers used for PVC.

8.4.5 ANTISTATICS

In general, static electricity is generated on a polymer surface by friction or by rubbing it against another surface, and this may include a solid or just air. Accumulation of electricity is favored by the low conductivity of the polymers. In packaging, the fast moving film, whether in a continuous converting operation or in a form-fill-seal processing line for instance, promotes the generation of static electricity on the film.

Static can adversely affect a manufacturing operation or process by introducing uncontrolled electrical forces that may result in, e.g., folding and sticking surfaces. It may also create dangerous conditions such as spark formation, leading to vapor explosions. In most polymers, electric charges are accumulated on the surface because polymers have high resistivity which makes the surface able to conduct electrons and ions.

Polymer surface static is controlled by the presence of antistatic agents that make the surface more conductive, or less resistive. For example, the presence of water within a hydrophilic polymer, such as polyamides, which is in equilibrium with air at 65% RH will act as an antistatic agent and will prevent the static buildup. This action is not seen at low RH values. Since most polymers used in packaging are not hydrophilic, antistatic agents must be used to control static. These agents are, in general, cationic, ionic, or nonionic surfactants.

A common group of cationic antistatics is alkyl quaternary ammonium salts that are mostly employed in polar substrates such as PVC and styrenic polymers. Other types include alkyl phosphonium and alkyl sulfonium salts. Flexible PVC may have a content of up to 7% of these antistatics which are not cleared by the FDA. Sodium alkyl sulfonates, similar to common detergent, have gained wide acceptance as an anionic antistatic that also are used in PVC and styrenic polymers. Other anionic antistats include alkyl phosphonic, dithiocarbamic, and carboxylic acids.

For nonpolar polyolefins, nonionic antistatics are the most commonly used. Nonionic antistatics include ethoxylated fatty amines, fatty acid esters, ethanolamides, and PE glycolesters. Dosages for LDPE is around 0.05%. Antistatic can be applied internally or externally. Internal antistatics are compounded with the resin and they act once they migrate to the surface of the polymer. External antistatics are applied directly to the surface by spraying or eventually by dipping the polymer in a solution of the antistatic. Testing of antistats are described by ASTM D 257 and measures the electric resistivity; or Federal Test Method Standard 101C Method 4046 that measures the generation or decay of static electricity.

8.4.6 COLORANTS

The use of colorants in plastics is almost exclusively driven by product appearance to influence consumers and by marketing considerations. Colorants do not add mechanical strength nor improve mass barrier properties. They may give an opaque appearance that can contribute to protection from light for a packaged product. Selecting, combining, and matching colors is a complicated art that only well-trained individuals are able to perform correctly. There are hundreds of different colorants used in the plastic industry, and there are as many types of colorants as there are different applications for plastics.

The present tendency of the plastic industry is to move away from toxic colorants, specially those based on heavy metals, i.e., chromium, cadmium, and lead. Similar to measuring optical properties of papers and paperboard, the characterization of a color for plastics is based on the measurement of color (hue), brightness, and opacity. Other important variables to be considered include dispersability in the plastic, migration, toxicity, light stability, and chemical resistance.

There is a world-wide movement to eliminate heavy metal colorants. The European Union had considered banning them in 1995. In 1993, in the U.S. there were 22 states that restricted or banned the use of heavy metal colorants. The use of organic colorants, or heavy-metal-free (HMF) colorants, is continuously increasing, and many colorant producer companies are replacing all heavy-metal-containing colorants. Colorants incorporated in plastic containers are in direct contact with food and have to be cleared by FDA.

There are several more important types of colorants used in plastics (Dick, 1987). These will be discussed.

8.4.6.1 Dyes

Dye is a colorant that is soluble in the plastic. Normally, dyes are low-molecular-weight organic compounds. They impart great transparency to the plastic, but migrate easily from it. Their tendency to migrate is the reason dyes have limited use in the plastic industry. Some dyes are very toxic and their use is regulated by U.S. Occupational Safety and Health Association (OSHA). Dyes include azo, diazo, pirazalones, anthraquinones, quiniphthalones, and quinolines dyes.

8.4.6.2 Organic Pigments

Organic pigments, unlike dyes, are insoluble in the plastic matrix. They are produced in the form of very fine particles which give the plastic an opaque appearance. Organic pigments tend to migrate less than dyes and similarly, some are very toxic. While handling these pigments OSHA directives must be followed. Examples of organic pigments include

    Benzimidalones (yellow, red, orange)
    Phthalocyanines (blue, green)
    Quinacridones (violet, red, orange)
    Dioxazines (violet)
    Disazos (yellow, red)
    Pyrazalones (orange, red)

8.4.6.3 Inorganic Pigments

Widely used in the plastic industry, inorganic pigments have neither the brightness nor the intensity of color that characterize organic pigments, however, they are less expensive, more opaque, and more stable to high temperature. Since they are very insoluble in the polymers, their migration tendency is less than the organic pigments. Many of the inorganic pigments are extremely toxic since they are oxides of heavy metals, such as chromium, lead, cadmium, or nickel. When manipulating these colorant OSHA guidelines must be followed. Example of inorganic pigments include

    Titanium oxide (white)
    Lead chromates (yellow, orange)
    Zinc chromate (yellow)
    Nickel titanate (yellow)

Chrome titanate (yellow)
Chromium oxide (green)
Iron oxides (brown, red, yellow, black)
Cadmium sulfoselenides (maroon, red, orange)
Cobalt alumate (blue)
Lead molybdate (orange)
Cadmium sulfide (orange)
Iron chromite (black, infrared reflective)

8.4.6.4   Lake Pigments

Lake pigments consist of a dye associated with an inorganic support such as alumina hydrate. They are used in packaging for visual effects.

8.4.6.5   Pearlescent Colorants

Pearlescent colorants impart a special pearly luster and provide iridescent effects. Titanium oxide-coated mice and ferric oxide-coated mice are the major pearlescents in use. They form thin platelets of high refractive index, which both reflect and transmit the incident light.

8.4.6.6   Colorants and the FDA

Besides economic factors, the use of colorants in plastic packaging requires both health and safety considerations. As indicated in Section 8.1.3, the FDA has made public a list of sanctioned colorants. Colorants for polymers are considered in Title 21 of CFR §178.3297. Colorants listed there "may be safely used as colorants in the manufacture of articles or components of articles intended for use in producing, manufacturing, packing, processing, preparing, treating, packaging, transporting, or holding food." There are also some provisions related to definition of colorant, migration to food, and conformation under Section 409 of the Federal Food, Drug and Cosmetic Act that should be reviewed when dealing with this subject.

Inorganic colorants listed in 21CFR §178.3297 includes aluminum, aluminum hydrate, aluminum and potassium silicate, aluminum silicate, barium sulfate, bentonite, calcium carbonate, calcium silicate, calcium sulfate, carbon black (channel process, prepared by the impingement process from stripped natural gas), chromium oxide green (Cr_2O_3), cobalt aluminate (with restrictions), diatomaceous earth, iron oxides, (kaolin-modified for use in olefin polymers up to 40%), magnesium oxides, magnesium silicate (talc), Sienna, silica, titanium dioxide, titanium dioxide-barium sulfate, ultramarines, zinc carbonate (limited use), zinc chromate (less than 10%), zinc oxide (limited use), and zinc sulfide (less than 10%).

Partial listing of organic colorants from 21CFR §178.3297 include all FD&C certified colors, C.I. Pigment Blue 15, C.I. Pigment Violet 19, C.I. Pigment Red 38, C.I. Pigment Orange 64, C.I. Pigment Yellow 95, C.I. Pigment Yellow 138, and C.I. Pigment Red 177. In recent years, the FDA has sanctioned few new colorants for food-packaging or extended the use of others. Some of them have limited thermal stability which probably make them unsuitable for use with high-heat resins like nylons and polycarbonate (Lachance, 1996). A final decision on colorants as with other additives for food-contact packaging should be done in accordance with the FDA regulations.

8.4.7   Heat Stabilizers

The major disadvantage of PVC is its poor thermal stability. Products made with PVC such as films and bottles degrade when they are heated at moderately high temperatures or subjected to gamma rays sterilization or even UV radiation, unless proper additives are present. Compounds classified as heat stabilizers can effectively hinder and reduce the degradation process

which makes the PVC become progressively yellow, to amber, to reddish brown, and finally black. The best way to control the degradation of PVC is to carefully select the correct heat stabilizer for a specific PVC application. PVC stabilizers are inorganic, organometallic compounds and organic compounds. Barium-cadmium, organotin and organolead compounds account for more than 90% of type total heat stabilizers used in the U.S. One of the most common organotin stabilizers is dibutyltin.

The additives in PVC bottles like dibutyltin, calcium-zinc compounds and methyltin for cooking oil and other food products must have FDA clearance. For flexible packaging materials the most common stabilizers are the mixed metals such as barium-zinc and calcium-zinc that are replacing the cadmium-zinc formulations. For rigid blow-molded containers and calendared sheets organotin formulations are the most commonly employed.

8.4.8 PLASTICIZERS

A plasticizer is a substance that is incorporated into a rigid plastic to increase its flexibility, workability, and distensibility. By reducing the glass transition temperature and increasing chain lubricity, plasticizers also improve processing and extrusion characteristics, reduce the minimum required processing temperature, reduce the plastic's hardness and improve low temperature flexibility.

Not all plastics require the use of a plasticizer, but for certain plastics, such as PVC, the use of an appropriate plasticizer is essential for the desired end use. Indeed, PVC applications depend on the level of the plasticizer.

Without plasticizers, PVC is a semicrystalline, brittle polymer very difficult to process. At low levels of concentration the plasticizer helps to reduce the processing temperature. This prevents thermal degradation of the polymer.

At higher levels besides improving processing conditions, it reduces hardness and increases flexibility of the final product. PVC is a polymer well suited for plasticization and accounts for more than 80% of the total production of plasticizer. In order for a plasticizer to work it has to have a correct balance of different functional groups to fully compatibilize with the polymer. Normally they have a slightly to strong polar functionality for compatibility with polymer polar groups and nonpolar groups (hydrocarbon) for internal lubrication. Different ratios of polar/nonpolar groups make a plasticizer more suitable for one application than for another. To improve processing conditions at high temperatures a more polar plasticizer is preferred, such as dibuthyl phthalate. To improve application at low temperatures, that is, make the PVC more flexible by depressing T_g, a nonpolar plasticizer is better, such as dioctyl sebacate.

Common plasticizers are the phthalates and among them, diethylhexyl phthalate (COP) is the most widely used. Safety concerns of DOP were raised in the 1980s but never fully clarified. To date, no action has been taken to regulate the production or use of DOP. Both in the U.S. and Europe it appears that DOP is making something of a comeback.

8.4.9 UV STABILIZERS

UV radiation from outdoor or from gamma radiation used for sterilization of medical and biomedical products can cause photo-oxidation in PS, polyolefins (especially PP), PVC, and other polymers. Highly energetic, UV photons are easily captured by a polymeric chain resulting in the breaking of covalent bonds and the producing of free radicals. Although the particular response to UV varies with each polymer due to different sensitivity, the global effect may be destructive of the polymer. Change of color, loss of flexibility and gloss, and degradation are some of the effects that can be seen by photo-oxidation. (UV radiation has similar deteriorative effects when reaching the human skin). To protect polymers from the destructive action of UV radiation, different approaches have been adopted.

One of them is to use "screen protector" agents that absorb the harmful UV radiation and emit a radiation of larger wavelength and lower energy. An example of this type is hydrobenzophenone used with PVC, PE, PP, cellulosics, and PET. The family of Tinuvin P, based on benzotriazoles, are commonly used although not as effective in polyolefins as the hydrogenzophenones. Pascall et al., 1995, described the decreasing lipid oxidation of soybean oil when an UV absorber, Tinuvin 326, is incorporated in the packaging material.

A second group of stabilizers may act by "quenching" a polymeric chain that has been excited by the UV photon to higher level of energy. An example is an organosalt of nickel used in PP and PE.

Finally, a third approach may be when the stabilizer acts by accepting free radicals, i.e., a free-radical scavenger. The highly efficient family of hindered amine light stabilizers (HALS) belongs to this group. HALS, contrary to phenolic and phosphite antioxidants, provide a regenerative radical trapping process. In this way several free radicals are eliminated before they are converted into inert derivatives. Applications of HALS include pigmented polymers, and radiation stabilizers for PP in biomedical products. The growing concern in the use of ethylene oxide in sterilization has increase the acceptance of gamma radiation in the sterilization of medical supplies. This requires that UV stabilizers must protect the polymeric materials used in this process. HALS have become very important UV stabilizers. In the market, there are many formulations of HALS and the correct selection must be a function of the polymer and the intended application. Combining different stabilizers trigger a synergistic effect and provide excellent protection to the polymer.

Carbon black is an inexpensive material that offers UV protection to polymers even at low concentrations. It can be used in PVC, PE, and PP.

8.4.10 OTHER ADDITIVES

Other additives may be incorporated into polymers, although they are not very important in packaging. The following types of additives may be found: flame retardants, fillers, coupling agents, mold-release agents, and processing aids. Blowing agents although not truly additives, are used to form plastic foams. Blowing agents can be chemical blowing agents (CBA) or physical blowing agents (PBA). CBA refers to the decomposition of organic compounds to generate the blowing gas; In PBAs, compressed gases are used and no change in chemical composition is involved. Fluorocarbons were widely used in the recent past as PBA, but they have been eliminated due to problems with the ozone layer. Expanded PS is fabricated with pentane. Expanded PE does not contain a blowing agent. Currently, expanded PET, PP, and PVC foams are produced by using endothermic CBS that produces a lesser amount of evolving gases. As indicated in Section 8.2.3, any additive used in food-contact packaging must comply with FDA regulations.

8.5 MASS TRANSFER IN PACKAGING SYSTEMS

Mass transfer in packaging systems is controlled by the type of packaging materials and the physical integrity of the package. Mass transfer through a package can occur in:

1. Package discontinuities, e.g., micro holes and cracks in the package walls and sealed areas and in closures; see Section 8.5.1
2. Permeation through the package wall, section 8.5.2
3. Partition equilibrium (covered elsewhere in this handbook)

8.5.1 MASS TRANSFER THROUGH MICRO HOLES

Micro holes and cracks not only allow mass transfer between the interior of a package and the outside environment, but also may permit microbe penetration into the package. Some bacteria can penetrate holes as small as 0.4 μm in diameter (Axelson and Cavlin, 1991).

Modeling mass flow through package pores is relevant in packaging integrity testing, and in the use of perforated films for modified atmospheric packages.

Nondestructive package integrity tests are in general based on leak detection of gas through the packaging material. The change in pressure between the package headspace and the environment can be detected by a variety of methods (Floros and Gnanasekharan, 1992). Nondestructive testing methods can be classified in the following categories: visual optical, acoustic, pressure difference, and others. The gas exchange through micro holes in MAP increases the transfer rate of gases such as CO_2 and O_2.

Other package discontinuities may exist in bottles between the finish and the cap. To secure a good seal, the use of cap liners and adequate applied cap torque are necessary.

8.5.1.1 Diffusion through a Micro Hole in a Barrier Membrane

The barrier membrane can be a flexible material, a rigid container wall, a thermoformed blister package, or the seal line formed in a pouch by heat sealing or adhesion. The molecular transport through the pore comprises the diffusion due to concentration differences (Knudsen diffusion), and the hydrodynamic flow as a result of a pressure difference (Poiseuille flow).

Consider a cylindrical capillary pore of diameter d and length *l* equal to the wall thickness of the packages. The wall separates two gas mixtures, that inside of the package and that in the outside environment. Assume the inside pressure to be p_i and total external pressure is p_o. If the radius of the pore is smaller than the molecular mean free path λ of the diffusant gas, a particular molecule will more often collide with the pore walls rather than with another molecule (see Example 8.2). The value of d/λ can be less than 0.2, larger than 20, or in between. When $d/\lambda < 0.2$ the rate of diffusion is governed by the collisions of the gas molecules with the pore walls and follows Knudsen's law (Treybal, 1980).

8.5.1.2 Knudsen Diffusion

The flux of a gas, A, controlled by Knudsen diffusion is given by the following equation (Youngquist, 1970)

$$N_A = -D_{KA} \frac{dc_A}{dx} \tag{8.1}$$

where N_A is the molar flux of A in mol/m²s, D_{KA} is the Knudsen diffusion coefficient in m²/s, c_A is the concentration of A in mol/l, x is the axial distance in the porous. From the kinetic theory of gas D_{KA} is given by

$$D_{KA} = \frac{d}{3} \overline{v_A} \tag{8.2}$$

where $\overline{v_A}$ is the mean molecular velocity in m/s given by

$$\overline{v_A} = \left(\frac{8}{\pi} \frac{RT}{M} \right)^{1/2} \tag{8.3}$$

where R is the gas constant = 8314 N m/kg mol K; T is the temperature in Kelvin degrees; and M_A is the mass of one mole of gas, Kg-mol.

EXAMPLE 8.1

Calculate the velocity of a CO_2 molecule in a Knudsen diffusion process at 0°C.

TABLE 8.19

Values of $\overline{v_A}$ **for Selected Gases**

Gas	Molecular weight	Temperature 0°	15°C	25°C
O_2	32	425.1	436.6	444
N_2	28	454.5	466.8	474.8
He	4	1202.0	1256	1256.2
CO_2	44	362.5	372.4	378.8
G_2O	18	566.8	582.1	592.1
Air	28.8	448.1	460.2	468.1

Note: Values given in meters per second.

Solution

From Equation 8.3 and knowing that M = 44 kg·mol.

$$\overline{v_{CO_2}} = \left(\frac{8}{\pi} \frac{8.614 \times 273.15}{44} \right)^{1/2} = 362.5 \text{ m/s}$$

From Equation 8.3 we have

$$\frac{\overline{v_A}}{v_B} = \left(\frac{M_B}{M_A} \right)^{1/2} \tag{8.4}$$

and

$$\frac{\overline{v_1}}{v_2} = \left(\frac{T_1}{T_2} \right)^{1/2} \tag{8.5}$$

From Equation 8.4 it can be seen that the lighter molecule has a higher velocity and therefore will be transferred faster than the heavier one. Values of $\overline{v_A}$ for selected gases are presented in Table 8.19.

At steady state, the Knudsen flux N (in mol/m²s) through a pore of area A, is obtained by integrating Equation 8.1.

$$N = A \frac{D_{KA}}{R \ell T} \left(p_i - p_o \right) \tag{8.6}$$

or

$$J = 706 \ d^3 \overline{v_A} \left(p_i - p_o \right) / \ell T \tag{8.7}$$

where J is the gas flow through the pore in ml(STP)/s; d is the porous diameter, in m; $D_{K\ell}$ is the velocity of the molecule from Equation 8.3 (or Table 8.19) in m/s; T is temperature in Kelvin; l is the thickness of the package wall in m; and p_i and p_o are the pressures inside and outside, respectively, in Pa. STP conditions are 0°C and 1 standard atmosphere.

TABLE 8.20
Molecular Mean Free Path for Selected Gases
at 25°C and Pore Diameter for Knudsen Flow

Gas	$\sigma \times 10^{10}$ m	Pressure	λ μm	d = 0.2 λ μm
CO_2	3.34	0.2 atm	0.4	0.08
O_2	2.98	0.2 atm	0.5	0.1
N_2	3.15	0.8 atm	0.1	0.02
He	1.9	0.01 atm	24.9	5.0

8.5.1.2.1   Mean free path

Knudsen flow takes place in a pore when the pore diameter, d, is smaller than one fifth of the molecular mean free path λ. The mean path can be estimated from the following equation (Cunningham and Williams, 1980)

$$\lambda = \frac{k_B T}{\left(\pi\sqrt{2}\sigma^2 p\right)} \tag{8.8}$$

where k_B is Boltzmann's constant = 1.38×10^{-23} J/K; and σ^2 is the collision diameter of diffusing molecule. Equation 8.8, indicates that the molecular mean free path increases with temperature and decreases with the gas pressure. For most packaging situations T = 25°C = 298.7K and the pressure is 1 atm or less.

EXAMPLE 8.2

Calculate λ for O_2 at 25°C and p = 0.2 atm.

Solution
From Equation 8.8

$$\sigma = 2.98 \times 10^{-10} \text{m (CRC Handbook, 64th Ed.)}$$

$$p = 0.2 \times 1.013 \times 10^5 \text{ Pa}$$

$$\lambda = \frac{1.38 \times 10^{-23} \times 293.15}{\pi\sqrt{2} \times \left(2.98 \times 10^{-10} \times 0.2 \times 1.013 \times 10^5\right)} = 5 \times 10^{-7} \text{m}$$

Other values of λ are presented in Table 8.20.

The Knudsen flow can be calculated through a pore in a package wall by applying Equation 8.7.

EXAMPLE 8.3

Calculate the Knudsen flow of oxygen O_2 throughout a 0.1×10^{-6} m diameter pore in a package wall of 100×10^{-6} m thick, assuming the $p_i - p_o$ is 0.2 atm (2.0265×10^4 Pa) at 25°C.

Solution
Applying Equation 8.7 for d = 0.1×10^{-6} m; $(p_i - p_o) = 2.0265 \times 10^4$ Pa; T = 298.15 K; l = 10^{-4} m. The value of $\bar{v}$ is given in Table 8.19.

$$J = 706 \times \left(1 \times 10^{-7}\right)^3 \times 444 \times 2.0265 \times 10^4 \big/ \left(298.15 \times 1 \times 10^{-4}\right)$$

$$J = 2.1 \times 10^{-10} \, \text{mL}\,(\text{STP})/\text{s} \quad \text{for each pore.}$$

The total gas volume V transferred through 1000 pores during 100 days is

$$V = 2.1 \times 10^{-10} \times 1000 \times 100 \times 86400 = 1.8 \, \text{mL of O}_2 \text{ at STP.}$$

EXAMPLE 8.4

Calculate the Knudsen flow of helium throughout 100 pores of 5×10^{-6} m diameter in a package 100 μm thick if $p_i - p_o = 0.01$ atm (1.013×10^3 Pa) and at 25°C

Solution

Applying Equation 8.7 for $d = 5 \times 10^{-6}$ m; $(p_i - p_o) = 1.013 \times 10^3$ Pa; T = 298.15 K; $l = 1 \times 10^{-4}$ m. The value of $\bar{v}$ is given in Table 8.19.

$$J = 706 \times \left(5 \times 10^{-6}\right)^3 \times 1256 \times 1.013 \times 10^3 \big/ \left(298.15 \times 1 \times 10^{-4}\right)$$

$$J = 3.8 \times 10^{-4} \, \text{mL}\,(\text{STP})/\text{s for each pore}$$

This type of flow may be significant in leak detection methods.

8.5.1.3 Flow in an Intermediate Pore

For d/λ in the range of 0.2 to about 20, a transition flow consisting of both molecular and Knudsen diffusion, take place in the pore. This flow is given by the following equation (Treybal, 1980)

$$N_A = \frac{N_A}{N_A + N_B} \frac{D_{AB,\text{eff}}\, p_t}{R\ell T} \ln \frac{\dfrac{N_A}{N_A + N_B}\left(1 + \dfrac{D_{AB,\text{eff}}}{D_{K,A,\text{eff}}}\right) - y_{A,o}}{\dfrac{N_A}{N_A + N_B}\left(1 + \dfrac{D_{AB,\text{eff}}}{D_{K,A,\text{eff}}}\right) - y_{A,i}} \tag{8.9}$$

where A and B are the diffusing molecules; N_A and N_B are the flux in mole/area time; D_{AB} is the molecular diffusion coefficient of A through B; $D_{AB,\text{eff}}$ is the effective diffusion coefficient which reflects the effect of the pore structure; $D_{K,A}$ is the Knudsen diffusion coefficient of A; and $D_{K,A,\text{eff}}$ is the effective Knudsen diffusion coefficient of A. Equation 8.9 shows that the flux does not depend on the diameter of the pore, d.

The effective diffusion coefficient is a measure of the tortuous path through the holes. For porous material this value generally is not known. However in packaging material, we can assume that the length of the pinhole is equal to the thickness of the package wall, i.e., no tortuous path. In this case the molecular diffusion coefficient D_{AB} and the effective diffusion coefficient $D_{AB,\text{eff}}$ can be considered no different.

8.5.1.4 Flow through Large Pores

When the ratio d/λ is greater than 20, ordinary molecular diffusion predominates and the equation describing steady state flow is (Treybal, 1980; Youngquist, 1970)

$$N_A = \frac{N_A}{N_A + N_B} \frac{D_{AB,\,eff} P_t}{R\ell T} \ln \frac{N_A/(N_A + N_B) - y_{Ao}}{N_A/(N_A + N_B) - y_{Ai}} \qquad (8.10)$$

where $Y_A = p_A/p_t$ is the mole fraction; p_A is the partial of component A; and p_t is the total pressure. Subscripts o and i indicate outside and inside the package. Also

$$D_{AB} \propto \frac{T^{3/2}}{p} \qquad (8.11)$$

For binary mixtures we have (Treybal, 1980)

$$\frac{N_A}{N_B} = -\left(\frac{M_A}{M_B}\right)^{1/2} \qquad (8.12)$$

where M is the molecular weight.

EXAMPLE 8.5 (SMALL PORES)

Calculate the transition flow of oxygen, throughout a 2.0 µm diameter pore in a package seal of 1×10^{-4} m thick and with an external partial pressure of 0.21 atm and 0 atm inside the package. Nitrogen is 1 atm inside and 0.79 atm outside. Total pressure is 1 atm. Additional information includes

$$\frac{d}{\lambda} = \frac{2 \times 10^{-6}}{0.5 \times 10^{-6}} = 4$$

The dissusivity of the O_2–N_2 system at O°C is given by Treybal (1980).

$$D_{O_2 - N_2} = 1.81 \times 10^{-5}\, m^2/s$$

from Equation 8.2, and Tables 8.15 and 8.16.

$$D_{K, O_2} = \frac{d}{3} v_A = \frac{1 \times 10^{-7}}{3} \times 444 = 1.5 \times 10^{-5}\, m^2/s$$

Solution

From Equation 8.11, the dissusivity at 25°C and 1 atm is

$$D_{O_2 - N_2} = 1.81 \times 10^{-5} \times \left(\frac{298}{273}\right)^{3/2} = 2.06 \times 10^{-5}\, m^2/s$$

From Equation 8.4

$$\frac{N_{N_2}}{N_{O_2}} = -\frac{N_{O_2}}{N_{N_2}} = -\left(\frac{32}{28.02}\right)^{1/2} = -1.069$$

Applying Equation 8.9 for the following condition,

$$y_{O_2,o} = 0.21 \text{ atm} \quad y_{O_2,i} = 0 \quad p_t = 1.01325 \times 10^5 \text{ N/m}^2 \quad \ell = 10^{-4} \text{ m}$$

$$\frac{N_{O_2}}{N_{O_2} + N_{N_2}} = \frac{1}{1 + \dfrac{N_{N_2}}{N_{O_2}}} = 14.49 \quad \frac{D}{}$$

Substituting value, Equation 8.9 finally becomes

Substituting values

$$N_{O_2} = \frac{-14.49 \times 1.81 \times 10^{-5} \times 1.013 \times 10^5}{8314(29.8) \times 10^{-4}} \, \ell n \, \frac{-14.49(1+1.2) - 0}{-14.49(1+1.2) - 1.21}$$

$$N_{O_2} = 7.0 \times 10^{-4} \text{ kmol/m}^2 \cdot \text{s}$$

$$J = N_{O_2} \times \text{pore Area} \times 22,414 \times 10^3 = 7 \times 10^{-4} \times \frac{\pi}{4} \times \left(2 \times 10^{-6}\right)^2 \times 22,414 \times 10^3$$

$$J = 5.1 \times 10^{-3} \text{ mL/s}$$

which is the flow per pore 2 μm in diameter.

EXAMPLE 8.6 (LARGE PORES)

For the same condition as the previous example, assume that the pore diameter is now 40 μm

$$\frac{d}{\lambda} = \frac{40 \times 10^{-6}}{0.5 \times 10^{-6}} = 80$$

Solution
Applying Equation 8.10

$p_t = 1 \text{ atm} = 1.012 \times 10^5 \text{ Pa}$

$$\frac{N_{O_2}}{N_{O_2} + N_{N_2}} = -14.49, \quad \ell = 10^{-4} \text{ m}, \quad T = 298 \text{ K}, \quad y_{O_2,o} = 0.21 \text{ atm}, \quad y_{O_2,i} = 0$$

$$N_{O_2} = \frac{-14.49 \times 1.81 \times 10^{-5} \times 1.013 \times 10^5}{8314 \times (298) \times 10^{-4}} \ln \frac{-14.49 - 0}{-14.49 - 0.2}$$

$$N_{O_2} = 1.47 \times 10^{-3} \text{ kmol/m}^2 \cdot \text{s}$$

$$J = N_{O_2} \times \text{pore area} \times 22414 \times 10^3 = 1.47 \times 10^{-3} \times \frac{\pi}{4}\left(40 \times 10^{-6}\right)^2 \times 22414 \times 10$$

$$J = 4.1 \times 10^{-5} \text{ mL/s per por 40 } \mu\text{m in diameter}$$

8.5.1.5 Hydrodynamic Flow of Gas (Poiseuille's Flow)

When there is a difference in absolute pressure across the porous solid, such as by action of a vacuum pump, a hydrodynamic flow through the straight capillary tube will occur. For a single gas obeying the ideal gas law and for relatively small velocities (Reynolds number <2100), the flow can be described by Poiseuille's Law (Treybal, 1980) where

$$J = \frac{\pi \, d^4 \left(p_i - P_2\right)}{128 \, \mu \ell} \tag{8.13}$$

where J is the flow in m³/s through the pore; d is the pore diameter, $(d/\lambda > 20)$, m²; $p_i - p_2$ is the pressure differential in Pa; μ is the viscosity of gas in N·s/m² = kg/m²s; and l is the capillary length, equal to the package's wall thickness.

EXAMPLE 8.7 POISEUILLE'S FLOW

Assume that a package containing a processed meat with a headspace atmosphere composition of 80% N_2 and 20% of CO_2, is tested for seal integrity by a vacuum nondestructive test (Jensen, 1994).

Assume that the test lasts 24 s and is desired to reach a maximum level leak of 300 ppm of CO_2 in the vacuum chamber having a volume of 0.013 m³. The thickness of the package is 62 μm. The inside pressure of the package p_i = 1 atm and the outside vacuum is 0.6 atm. The temperature of testing is 25°C. Estimate the size of the pore allowing this leak.

Solution

The viscosity of the mixture μ = (0.8 × 0.180 + 0.2 × 0.15) × 10^{-4} = 0.174 × 10^{-4} Pa·s (Perry and Green, 1984). With these values J can be calculated.

$$J = \frac{0.013 \times 300 \times 10^{-6}}{24 \times 0.2} = 8.125 \times 10^{-7} \text{ m}^3/\text{sec}$$

If μ = 0.174 × 10^{-4} Pa·s and $p_1 - p_2$ = 0.4 × 1.01325 Pa, solving for d in Equation 8.13

$$d = \left[\frac{128 \, \mu \ell \, J}{\pi \left(p_1 - p_2\right)}\right]^{1/4} = \left[\frac{128 \times 0.174 \times 10^{-4} \times 62 \times 10^{-6} \times 8.125 \times 10^{-7}}{\pi \times 0.4 \times 1.01325 \times 10^5}\right]$$

$$d = 30.6 \times 10^{-6} \text{ m}$$

8.5.1.5.1 Leak detection

Test equipment for leak detection based on the measurement of trace gas can provide good information on the package integrity. However, calculating the size of an ideal pinhole is less certain because several factors are unknown. These factors include the real geometry of the leak and more importantly the number of the leak points. Other factors related to the test apparatus (such as sensitivity and sample procedure) may also affect the result. If more than one pinhole is present in the package, Equation 8.12 can be written as

$$J = \frac{\pi(p_1 - p_2)}{128\,\mu\ell} \sum_i^n d_i^4 \tag{8.14}$$

where n is the number of pinholes and d_i is the average diameter of each pinhole. However, a single pinhole having an equivalent flow to the n pinholes will have a diameter,

$$d^4 = \sum_i^n d_i^4$$

If the pores are considered all the same size

$$d_i = \frac{d}{n^{1/4}} \tag{8.15}$$

where d_e is the diameter of the equivalent pinhole. Equation 8.14 indicates that the flow J in Example 8.7 could also be produced by, for instance, 100 pores 9.5 µm in diameter.

8.5.2 PERMEABILITY

The concept of permeability is normally associated with the quantitative evaluation of the "barrier" property of a material. A material that is a good barrier has low permeability value.

Polymers unlike metals, glass, and ceramic, are permeable materials. The phenomenon of permeability takes place when a polymer wall separates two fluid phases that contain low molecular weight species having different values of activity in each of the phases. The molecules at the high side concentration, or activity, tend to diffuse through the polymer structure and reach the other side to eventually equalize concentration at both phases.

8.5.2.1 Barrier Material

The barrier property of a plastic structure is the physical resistance that it opposes to the passage of any molecule or compound able to diffuse through the polymer: oxygen, carbon dioxide, water, and odors from air or headspace; flavors, aromas, and components from food; and external compounds contained either in secondary packages (e.g., corrugated boxes), board components (like vanillin and o-vanillin), or remains of solvents. In packaging design, it is very important to know the barrier characteristics of a package. An optimum package design results from balancing the packaging material properties, product protection requirements, environmental and transport conditions, and cost considerations. The barrier characteristics of the polymeric material relates mainly to its chemical structure. A polymeric structure can be polar or nonpolar, and a polar polymer can be hydrophilic or not. Polar hydrophilic polymers are good gas and organic vapor barriers when dry but are poor gas barriers when wet (e.g., nylons and EVOH). Conversely, the barrier properties of polar nonhydrophilic polymers containing groups such as nitrile, chlorine, or fluorine, are not dependent on the presence of water molecules. Similarly nonpolar polymers, e.g., polyolefins, are not affected by the presence of water, but they are not as good a barrier as the polar polymer, except against a polar water molecule itself. We also may say that like permeates like.

8.5.2.2 Permeation Mechanism

Figure 8.4 illustrates the sorption and diffusion mechanisms that take place through a package film or sheet structure surrounded by two fluid phases, to determine a permeation process.
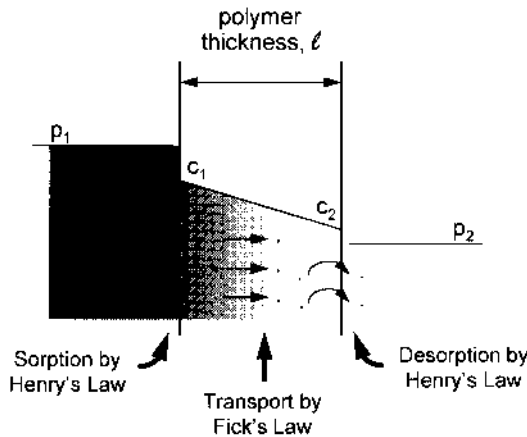
FIGURE 8.4 Permeation mechanism.

The permeation process involves three steps. (1) The permeant molecule from the contracting fluid phase at a partial pressure, p_1, penetrates the polymer surface. For pressure below one atmosphere, the value of the permeant concentration at the polymer interphase follows Henry's Law. (2) The permeant diffuses within the polymer film from the side of high concentration toward the side of low concentration according to Fick's laws. (3) The permeant leaves the opposite polymer interphase to diffuse in the adjacent continuous phase (liquid or gas phase) at a pressure p_2.

8.5.2.3 Permeability, WVTR, and Gas Transmission Rate

The solution of the diffusion equation through a nonporous polymer film at steady state is given by

$$F = -D\frac{\Delta c}{\ell} \tag{8.16}$$

where F is the flux through the film [or gas transmission rate (GTR)], Δc is the permeant concentration in the polymer/gas phase interphase, $c_1 - c_2$ and D is the diffusion coefficient. The value of c can be related to the partial pressure p through Henry's law of equilibrium

$$c = Sp \tag{8.17}$$

where S is the solubility coefficient in kg permeant/m³ polymer · Pa. Where D is concentration-independent and the sorption equilibrium between the permeant and polymer follows Henry's law, Equations 8.16 and 8.17 can be combined to give

$$F = DS\frac{\Delta p}{\ell} = \frac{q}{At} \tag{8.18}$$

and

$$F\frac{\ell}{\Delta p} = P = DS \tag{8.19}$$

TABLE 8.21
Units of permeability, permeance, and Gas Transmission Rate

		Common Units	SI	Fundamental dimension	
Amount of mass	q	g, cm^3(STP), mol	kg	M	Mass
Thickness	l	cm/ mil	m	L	Length
Time	t	h, d	s	θ	Time
Area	A	cm^2, in^2	m^2	L^2	Length
Partial pressure	p	atm, psi, mmHg	Pa	F/L^2	Force/length

where P = permeability and coefficient; t = time, during which the permeation process takes place; l = thickness of the material with permeability P; Δp = difference of pressure at both sides of the film where P is the permeability coefficient; A = area of the package exposed to the permeation process with the same permeability value; and q = total quantity of the permeant throughout the exposed area during time t. A dimensional analysis of P indicates that the fundamental unit of P is time if the solubility coefficient is expressed in Kg/m^2 · Pa

$$[P] = [D][S] = \left[\frac{L^2}{\theta}\right]\left[\frac{\theta^2}{L^2}\right] = [\theta] \text{ or sec in the SI}$$

Combining Equations 8.18 and 8.19 gives the well-known relation for P

$$P = \frac{q \cdot \ell}{t \cdot A \cdot \Delta p} \tag{8.20}$$

Tables 8.21 and 8.22 present units for Equation 8.20 and common conversion factors for permeability units, respectively. Permeability can be expressed in seconds or, most commonly, in any combination of the above units.

The relationship between water vapor transmission rate (WVTR), GTR, Permeance, normalized WVTR, and permeability coefficient P is indicated in Figure 8.5.

EXAMPLE 8.8

The gas transmission rate of oxygen through a film of PE, 1 mil thick is GTR = F = 3.5 ×

$10^{-2} \dfrac{g}{h \cdot m^2}$ and the differential in partial pressure through the film Δp = 30 mmHg. Calculate permeance and permeability coefficient.

Solution

$$\text{Permeance} = \text{GTR.} \quad \frac{1}{\Delta p}$$

$$\frac{1}{\Delta p} = \frac{3.5 \times 10^{-2} \text{ g}}{30 \text{ h} \cdot m^2 \text{ mmHg}} = 1.17 \times 10^{-3} \frac{g}{h \cdot m^2 \cdot mmHg}$$

$$\text{Permeance} = \frac{\text{GTR}}{\Delta p} \times \text{thickness} =$$

$$\frac{1.17 \times 10^{-3} \text{ g} \times 2.54 \times 10^{-3} cm}{h \cdot m^2 \cdot mmHg} = 2.96 \times 10^{-6} \frac{g - cm}{h \cdot m^2 \cdot mmHg}$$

TABLE 8.22
Permeability Units Conversion Table

Convert from	Convert to	Multiplier
s	as	1×1^{-18}
s	$\dfrac{kg \cdot m}{m^2 \cdot s \cdot Pa}$	1
$\dfrac{kg \cdot m}{m^2 \cdot s \cdot Pa}$	$\dfrac{kg \cdot \mu m}{m^2 \cdot d \cdot kPa}$	8.64×10^{13}
$\dfrac{g \cdot mil}{m^2 \cdot d}$ at 100°F and 90% RH	$\dfrac{g \cdot \mu m}{m^2 \cdot d \cdot kPa}$	4.264
$\dfrac{kg \cdot \mu m}{m^2 \cdot d \cdot kPa}$	$\dfrac{g \cdot mil}{m^2 \cdot d \text{ at}}$	3.989×10^3
$\dfrac{kg \cdot m}{m^2 \cdot s \cdot Pa}$	$\dfrac{g \cdot mil}{100 \text{ in}^2 \cdot d \text{ at}}$	2.224×10^{16}
$\dfrac{g \cdot mil}{100 \text{ in}^2 \cdot d}$ at 100°F and 90% RH	$\dfrac{g \cdot \mu m}{m^2 \cdot d \cdot kPa}$	66.09
$\dfrac{kg \cdot m}{m^2 \cdot s \cdot Pa}$	$\dfrac{m^3(STP) \cdot m}{m^2 \cdot s \cdot Pa}$	$\dfrac{22.414}{MW}$
$\dfrac{m^3(STP) \cdot m}{m^2 \cdot s \cdot Pa}$	$\dfrac{cc(STP) \cdot mil}{100 \text{ in}^2 \cdot d \cdot atm}$	2.2237×10^{19}
$\dfrac{cc(STP) \cdot mil}{100 \text{ in}^2 \cdot d \cdot atm}$	$\dfrac{cc(STP) \cdot \mu m}{m^2 \cdot d \cdot kPa}$	3.883
$\dfrac{cc(STP) \cdot mil}{100 \text{ in}^2 \cdot d \cdot at}$	$\dfrac{cc(STP) \cdot mil}{m^2 \cdot d \cdot at}$	15.5
as	$\dfrac{cc(STP) \cdot mil}{m^2 \cdot d \cdot at}$	$\dfrac{1936.57}{MW}$
as	$\dfrac{cc(STP) \cdot mil}{100 \text{ in}^2 \cdot d \cdot atm}$	$\dfrac{498.47}{MW}$

* as = 1 atto sec = 1×10^{-18} sec; MW = molecular weight of permeant; RH = relative humidity. STR = standard temperature and pressure (0°C; 1 atm)
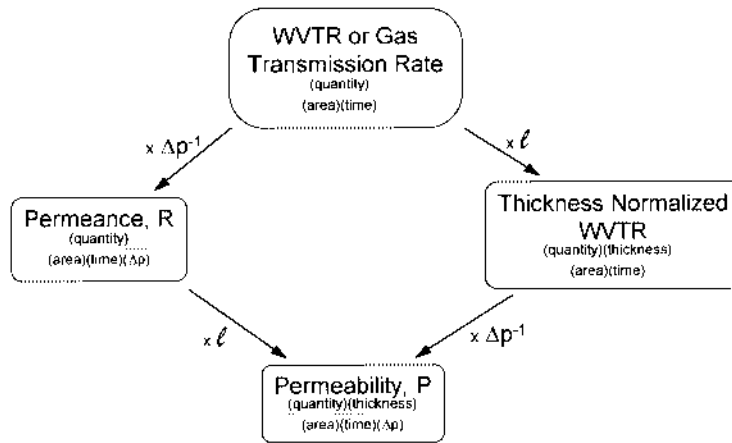
EXAMPLE 8.9

Calculate the water permeability coefficient of a polymer film 38.1 μm thick (1.5 mil) having a WVTR value of 0.1 g/dm^2 at 38°C (100°F) and 90% RH (ASTM conditions).

Solution

To calculate P, we need to multiply WVTR by the thickness over the pressure differential across the film.

$$P = WVTR \times \frac{1}{\Delta p}$$

FIGURE 8.5 Relation between water vapor transmission rate (WVTR), gas transmission rate, permeance, thickness normalized WVTR, and permeability coefficient.

since

$$RH = \frac{p}{ps} \times 100$$

where p^s is the saturation vapor pressure of water,

$$p = \frac{p^s}{100} RH$$

therefore

$$\Delta p = p_o - p_i = \frac{p^s}{100}\left(RH_o - RH_i\right)$$

According to ASTM E 96 test $p_i = 0$ because it is in equilibrium with the desiccant. From Perry's Handbook page 3-45 (Perry and Green, 1984), p^s at 38°C: 49.7 mmHg

$$\Delta p = \frac{49.7}{100} \times 90 = 44.73 \text{ mmHg} = 5.88 \times 10^{-2} \text{atm} = 5.964 \text{ Pa}$$

$$P = \frac{WVTR \cdot \ell}{\Delta p} = \frac{0.1 \times 10^{-3} \times 38.1 \times 10^{-6}}{5964 \times 3600 \times 24} = 7.40 \times 10^{-18} \frac{\text{kg} \cdot \text{m}}{\text{m}^2 \cdot \text{s} \cdot \text{Pa}} = 9.8 \text{ as}$$

8.5.2.4 Variables Affecting Permeability

1. The chemical structure of the polymer and the permeant, determines the particular level of interaction. There is a value of permeability for each pair of polymer/permeant.
2. Polymer morphology; an increase in polymer crystallinity (density), orientation, or cross-linking, decreases permeability.

3. Humidity increases or decreases permeability (especially in hydrophilic polymers). Oxygen permeability increases with relative humidity for EVOH and Nylon 6. However, oxygen permeability decreases in amorphous nylon.
4. An increase in temperature increases permeability.
5. Fillers generally decrease permeability, however, the effect is complicated by the type, shape, and amount of filler and the interaction with permeant.
6. Concentration of the permeant, in general, is found to have no effect at low and moderate pressure for gases, and low-activity values for organic compounds in the range of Henry's Law. Strong effects can be found for organic compounds at high values of activity (Liu et al., 1991).
7. Plasticizers, usually, but not always, increase the permeability.
8. Film thickness does not affect, in principle, the permeability, the diffusion coefficient, or the solubility. However, film of different thicknesses may have different morphologies generated, e.g., by having different cooling characteristics during processing.
9. Molecular weight of a polymer has been found to have little effect on the permeability of a polymer except in the very low range of molecular weight.

8.5.2.4.1   *Effect of temperature*

The change in permeability with temperature is given by the following equation

$$P = P_o e^{-\frac{E_P}{RT}} \tag{8.21}$$

where E_p is the activation energy, R the gas constant, P_o is a pre-exponential term and T is temperature in Kelvin.

If a value of permeability P_1 is given at temperature T_1, the value of the permeability P_2 at T_2 can be calculated if E_p is known.

$$P_2 = P_1 \cdot \exp \frac{E_p}{R}\left(\frac{1}{T_1} - \frac{1}{T_2}\right) \tag{8.22}$$

That can be written as

$$P_2 = P_i \cdot f \tag{8.23}$$

where

$$f = \exp \frac{E_P}{R}\left(\frac{1}{T_1} - \frac{1}{T_2}\right) \tag{8.24}$$

EXAMPLE 8.10

The permeability of oxygen in PET at 25°C is

$$P = 22 \frac{cc \cdot \mu m}{m^2 \cdot d \cdot kPa}$$

Calculate the value of permeability of PET at 50°C. Temperature = 25°C = 25 + 273.15 = 298.15 K.

Solution

From Table 8.23 is E_p = 32 KJ/mol = 7.6 kcal/mol

$$\frac{Ep}{R} = \frac{7600}{1.987} = 3{,}849 \text{ K}$$

$$\frac{1}{T_1} - \frac{1}{T_2} = \frac{1}{25+273} - \frac{1}{50+273} = .0002597 \text{ K}$$

From Equation 8.25

$$f = \frac{E_p}{e^p}\left(\frac{1}{T_1} - \frac{1}{T_2}\right) = e^{3.849 \times 0.0002597} = 0.09996 = 2$$

Substituting in Equation 8.23

$$P_2 \cdot f = P_2 = P_1 \times 2.74 = 22 \times 2.74 = 60.3 \frac{cc \cdot \mu m}{m^2 \cdot d \cdot kPa}$$

Values of f are given in Table 8.20 and plotted in Figure 8.6 for values of P_1 at 25°C and from 0 to 50°C. E_p varies between 3 and 20 kcal/mol

EXAMPLE 8.11

For the above example calculate f from Table 8.24.

Solution

$$Ep = 7.6 \text{ kcal}$$

$$T_2 = 50°C$$

$$f = 2.7 \text{ (interpolated between 2.49 and 2.84)}$$

8.5.2.5 Measuring Permeability

Determination of WVTR is described in ASTM E96. Determination of permeability of O_2 and CO_2 is covered by ASTM D1434. For organic compounds there is not an ASTM standard, however, continuous and quasi-isostatic methods are discussed by Hernandez, et al. (1986).

A consistency analysis to measure the permeability based on the experimental data for the continuous flow method is discussed by Hernandez and Gavara, (1993).

8.5.2.6 Multilayer Structures

The permeability of a packaging wall made of a multilayer structure is given by the following equation

$$P_T = \frac{L_T}{\displaystyle\sum_i^n \frac{\ell_i}{P_i}} \tag{8.25}$$

where P_T is the total permeability coefficient of the structure; L_T total thickness, $L_T = \Sigma l_i$; n is the number of layers, and, l_i, and P_i are the thickness and permeability coefficient of each layer.

8.5.2.6.1 Permeance

The ratio $\dfrac{P_i}{\ell_i} = R$ is permeance. Equation 8.25 can then be written as

$$R_r = \left(\sum \frac{1}{R_i} \right)^{-1} \tag{8.26}$$

where R_T is the total permeance of the structure and R_i is the permeance of each layer.

8.5.2.6.2 WVTR
Similarly for WVTR

$$\frac{\Delta P_T}{(WVTR)_T} = \sum_{i}^{n} \left(\frac{\Delta p}{WVTR} \right)_i \tag{8.27}$$

or

$$(WVTR)_T = \frac{\Delta P_T}{\displaystyle\sum_{i}^{n} \left(\frac{\Delta P}{WVTR} \right)_i} \tag{8.28}$$

EXAMPLE 8.12

Calculate the total oxygen permeability of the following multilayer structure (units in cc $\mu m/m^2 \cdot d \cdot kPa$)

Solution
From Equation 8.25

$$\frac{L_T}{P_T} = \sum_{1}^{3} \frac{\ell_i}{P_i}$$

$$P_T = \frac{L_T}{\displaystyle\sum_{1}^{3} \frac{\ell_i}{P_i}}$$

$$L_T = 18 + 10 + 20 = 48 \ \mu m$$

$$\sum_{1}^{3} \frac{\ell_i}{P_i} = \frac{\ell_1}{P_1} + \frac{\ell_2}{P_2} + \frac{\ell_3}{P_3} = \frac{18}{1900} + \frac{20}{25} + \frac{20}{620} = 0.4417 \frac{m^2 \cdot d \ kPa}{cc}$$

$$P_T = \frac{48}{0.4417} = 109 \, \frac{cc \cdot \mu m}{m^2 \cdot d \cdot kPa}$$

The effect of temperature on the permeability of a multilayer structure is

$$P_T = \frac{L_T}{\displaystyle\sum_1^i \frac{\ell_i}{P_{1,i} \, f_i}} \qquad (8.29)$$

where f_i is given by Equation 8.24 and can be obtained from Table 8.20 or Figure 8.6 for each layer, and $P_{1,i}$ is the permeability at temperature 1 for each layer i of the structure. Equation 8.29 can be written as

$$\left(\frac{P_T}{L_T}\right)^{-1} = \sum_1^i \frac{\ell_i}{P_{2i} \, f_i} \qquad (8.30)$$

EXAMPLE 8.13

Calculate the total oxygen permeability P_T for the following structure at 40°C. Values of P were obtained at 25°C.

$f_1 = 2.29$, $f_2 = 2.34$, and $f_3 = 2.53$, obtained from Table 8.20.

$$L_T = \ell_1 + \ell_2 + \ell_3 = 48 \, \mu m$$

Applying Equation 8.30

$$P_T = \left(\frac{18}{1,900 \times 2.29} + \frac{10}{25 \times 2.34} + \frac{20}{1,500 \times 2.53}\right)^{-1} 48$$

$$P_T = 266 \, \frac{cc \cdot \mu m}{m^2 \cdot d \cdot kPa}$$

Note: If this calculation were based only on the barrier layer, Nylon 6, neglecting the barrier contribution of both LDPE and PP, we would obtain

$$P_T = 280 \, \frac{cc \cdot \mu m}{m^2 \cdot d \cdot kPa}$$

8.5.2.7 Application of Permeability to Material Section and Shelf-Life Estimation

Gas permeability values presented in Figures 8.7 and 8.8 for easy comparison. Permeability values of organic compounds have been compiled by Hernandez and Giacin (1996).

Equation 8.20 is a simple but useful design equation for packages. It provides a basic relationship among the main variables associated with a packaging system: quantity of permeant transferred, thickness of the package, area, storage conditions (temperature and humidity), shelf-life, and permeability. More elaborate model can be found in the works of Labuza et al., (1972), Karel (1974), Kim (1992), and Pocas (1995).

Equation 8.20 is valid for steady state value. Also, it is assumed that the container does not have any pinholes or cracks. Besides its limitations, Equation 8.20 can be a first approx-

TABLE 8.23
Permeability, Diffusion and Solubility Coefficients

|	Temperatures (°C)	P	Ep	S × E3	D × E10
Polyethylene LDPE (d = 0.914 g/cc)					
H_2	25	6.4E + 03		1.6E + 00	4.7E − 01
He	25	3.2E + 03	3.5E + 01	5.0E − 02	6.8E + 00
O_2	25	1.9E + 03	4.3E + 01	4.7E − 01	4.6E − 01
CO_2	25	7.0E + 02	3.9E + 01	2.5E + 00	3.7E − 01
N_2	25	6.3E + 02	4.9E + 01	2.3E − 01	3.2E − 01
CH_4	25	1.9E + 03	4.7E + 01	1.lE + 00	1.9E − 01
H_2O	25	5.9E + 04	3.4E + 01		
HDPE (d = 0.964 g/cc)					
He	25	7.4E + 02	3.0E + 01	2.8E − 02	3.1E + 00
O_2	25	2.6E + 02	3.5E + 01	1.8E − 01	1.7E − 01
CO_2	25	2.3E + 02	3.0E + 01	2.2E − 01	1.2E − 01
N_2	25	9.5E + 01	4.0E + 01	1.5E − 01	9.3E − 02
CH_4	25	2.5E + 02	4.lE + 01	5.lE − 01	5.7E − 02
H_2O	25	7.8E + 03			
Polypropylene (d = 0.907 g/cc) 50% crystallinity					
He	20	2.4E + 02	3.2E + 01		2.0E + 01
O_2	25	6.2E + 02	4.8E + 01		
CO_2	25	2.lE + 03	3.8E + 01		
N_2	25	8.0E + 01	5.6E + 01		
H_2O	30	4.4E + 04	4.2E + 01		
Poly (ethylene-co-propylene) 40/60 amorphous					
N_2	24.1	3.5E + 03	4.2E + 01	4.4E − 01	9.4E − 01
Polystyrene, biaxially oriented					
He	25	1.2E + 04			
O_2	25	1.lE + 03			
CO_2	25	3.5E + 03			
N_2	25	5.2E + 02			
H_2O	25	7.3E + 05	−8.0E + 00		
Polyacrylonitrile(Barex)					
O_2	25	3.5E + 00			
CO_2	25	1.0E + 01			
H_2O	25	4.2E + 05			
Polyvinyl acetate					
He	30	8.2E + 03	1.3E + 01	7.8E − 02	6.5E + 00
O_2	30	3.lE + 02	5.6E + 01	6.4E − 01	5.6E − 02
CH_4	25	2.0E + 01	8.3E + 01	1.4E + 00	1.7E − 03
Ethylene vinyl alcohol (E 32%)					
O_2 (0% RH)	25	3.0E − 02			
O_2 (65% RH)	25	2.0E − 01			
H_2O	25	3.1E + 05			
Ethylene Vinyl Alcohol (E 44%)					
O_2 (0% RH)	25	1.5E − 01			
O_2 (65% RH)	25	3.0E − 01			
H_2O	25	1.lE + 05			
PVC, unplasticized					
O_2	25	2.9E + 01	5.6E + 01	2.9E − 01	1.2E − 02
CO_2	25	1.0E + 02	5.7E + 01	4.7E − 00	2.5E − 03
N_2	25	7.7E + 00	6.9E + 01	2.3E − 01	3.8E − 03
CH_4	25	1.8E + 01	6.6E + 01	1.7E + 00	1.3E − 03
H_2O	25	1.8E + 05	2.3E + 01	8.7E + 02	2.4E − 02
O_2 (plasticized)	25	3.2E + 03			

TABLE 8.23 (continued)
Permeability, Diffusion and Solubility Coefficients

	Temperatures (°C)	P	Ep	S × E3	D × E10
Polyvinylidene chloride (Saran)					
O_2	30	3.3E + 00	6.7E + 01		
CO_2	30	1.9E + 01	5.2E + 01		
N_2	30	6.0E + 01	7.0E + 01		
H_2O	25	6.0E + 03	4.6E + 01		
H_2S	30	2.3E + 01	7.5E + 01		
Polytetrafluorethylene (Teflon)					
O_2	25	2.8E + 03	1.9E + 01	2.1E + 00	1.5E – 01
CO_2	25	6.5E + 03	1.4E + 01		
N_2	25	8.6E + 02	2.4E + 01	1.2E + 00	8.8E – 02
CH_4	90	3.3E + 03	3.4E + 01	1.7E + 00	2.2E – 01
Polyisoprene, rubber					
O_2	25	1.5E + 04	2.9E + 01	1.0E + 00	1.7E + 00
CO_2	25	9.9E + 04	2.2E + 01	9.2E + 00	1.3E + 00
N_2	25	6.1E + 03	3.6E + 01	6.1E – 01	1.2E + 00
H_2O	25	1.5E + 06			
CH_4	25	2.0E + 04	3.1E + 01	2.6E + 00	8.9E – 01
PET 40% crystallinity					
O_2	25	2.2E + 01	3.2E + 01	7.2E – 01	3.5E – 03
CO_2	25	8.0E + 01	1.8E + 01	2.0E + 01	6.0E – 04
N_2	25	3.9E + 01	3.3E + 01	4.5E – 01	1.3E – 03
H_2O	25	8.5E + 04	2.9E + 00		
CH_4					
PET amorphous					
O_2	25	3.8E + 01	3.8E + 01	9.8E – 01	4.5E – 03
CO_2	25	2.0E + 02	2.8E + 01	2.8E + 01	8.0E – 04
Polycarbonate(lexan)					
O_2	25	9.1E + 02	1.9E + 01	5.0E + 00	2.1E – 02
CO_2	25	5.2E + 03	1.6E + 01	1.2E + 01	4.8E – 03
N_2	25	1.9E + 02	2.5E + 01		

TABLE 8.23 (continued)
Permeability, Diffusion and Solubility Coefficients

	Temperatures (°C)	P	Ep	S × E3	D × E10
H_2O	25	9.lE + 05			6.8E − 01
Nylon 6					
O_2 (100% RH)	25	2.5E + 01	4.4E + 01		
CO_2	25	5.0E + 01	4.lE + 01		
N_2	25	3.5E + 00	4.7E + 01		
H_2O	25	1.2E + 02			
Nylon 6,6 drawn					
CO_2	25	4.5E + 01		1.5E + 01	
Nylon 11					
CO_2	40	6.5E + 02	3.4E + 01	4.9E − 01	1.9E − 02
Cellophane					
O_2(0% RH)	25	1.4E + 00			
O_2(76% RH)	25	5.7E + 00			
CO_2(0% RH)	25	3.0E + 00			
CO_2(76% RH)	25	4.7E + 01			
N_2(0% RH)	25	2.lE + 00			
N_3(76% RH)	25	4.8E + 00			
H_2O	25	1.6E + 07			

Note: These values are provided as a general guide. P = cc(STP) μm/m²·d·kPa; D = m²/s; S = cc(STP)/cc·kPa; E_p = kJ/mol; LDPE = low density polyethylene; HDPE = high density polyethylene; PET = polyethylene terephthalate; PVC = polyvinyl chloride; RH = relative humidity.
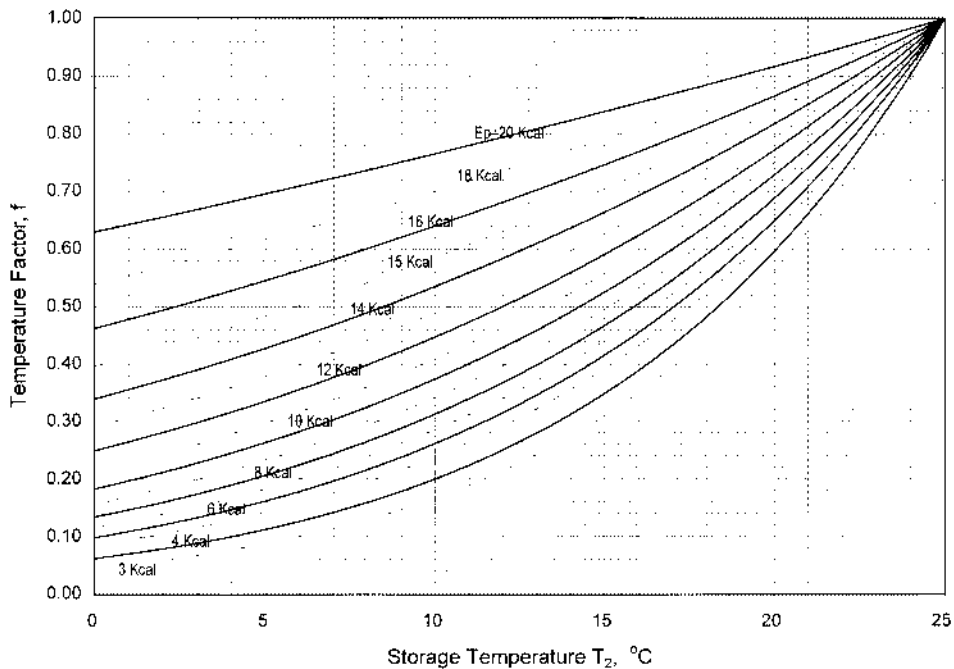
FIGURE 8.6a Values of f (Equation 8.23) for $0 < T_1 < 25°C$
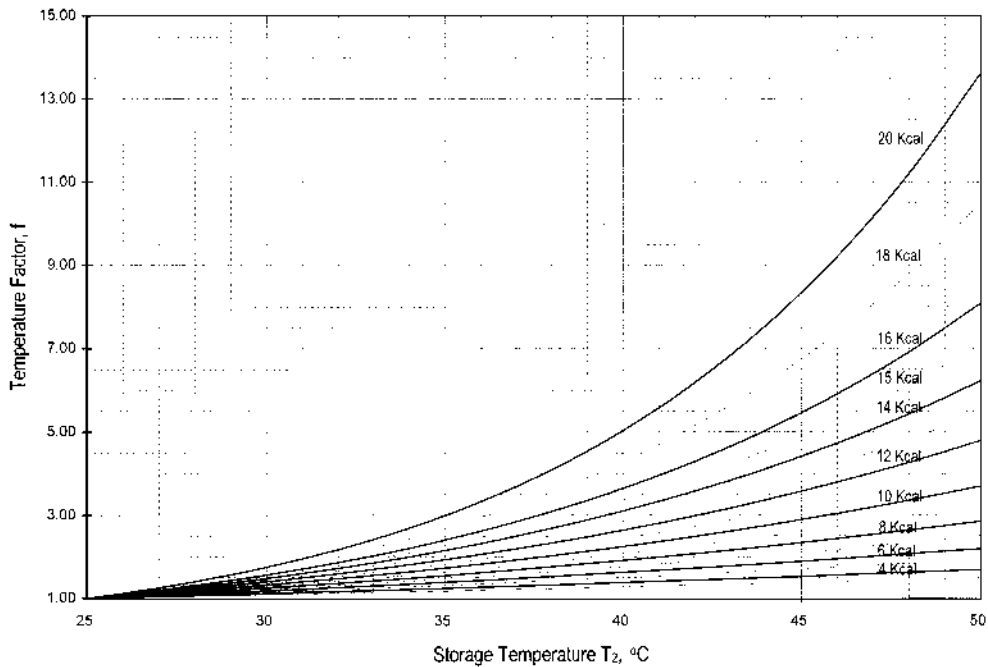
FIGURE 8.6b Values of f (Equation 8.23) for 25°C $<T_1<$50°C

imation designing tool in the selection of important package parameters. A careful analysis of the assumption and limitations however, must be practiced. Consider two cases, Δp constant and Δp variable. The simplest case in Equation 8.20 is when Δp can be considered constant. Consider the case of an oxygen-sensitive product for which the kinetic and type-of-product failure is known. Since the product reacts with any entering oxygen molecule the oxygen headspace concentration always is assumed to be zero.

EXAMPLE 8.14

Calculate the minimum packaging thickness for protection and loss of product. A water-based product has a compound that reacts with oxygen, producing unwanted effects. Analysis has shown that when the product reacts with an amount of oxygen equivalent to 0.005% (wt/vol), i.e., 50 ppm of oxygen, it is no longer acceptable for sale. Also, assume that PET is the packaging material and that the product volume is 500 ml. Further, the area of the package is around 400 cm^2 and it is expected that the package will be stored at 25°C and around 60% RH. Estimate the minimum thickness of the package to protect the product from oxygen for 6 months. In addition, for the calculated thickness, estimate the loss of water during the 6-month period.

Solution

From Equation 8.20 the thickness of the package is

$$\ell = \frac{PtA\,\Delta p}{q}$$
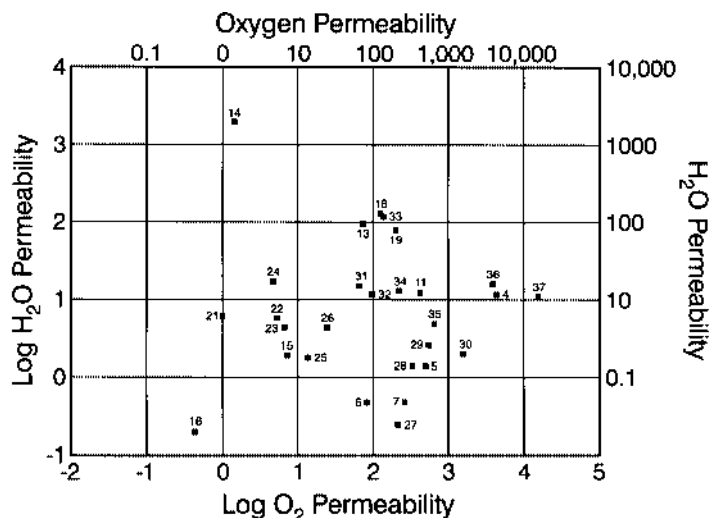
From Table 8.19 the permeability of PET at 25°C,

TABLE 8.24
Values of f (Equation 23)

| T$_2$ (°C) | E$_p$ (Kcal/mol) |
	3	4	5	6	7	8	9	10	11	12	13	14	15	16	18	20
0	0.629	0.538	0.461	0.395	0.338	0.290	0.248	0.213	0.182	0.156	0.134	0.115	0.098	0.084	0.062	0.045
2	0.654	0.568	0.493	0.428	0.372	0.323	0.280	0.243	0.211	0.183	0.159	0.138	0.120	0.104	0.078	0.059
4	0.681	0.599	0.527	0.463	0.408	0.359	0.315	0.278	0.244	0.215	0.189	0.166	0.146	0.129	0.100	0.077
6	0.708	0.631	0.562	0.501	0.447	0.398	0.355	0.316	0.282	0.251	0.224	0.199	0.178	0.158	0.126	0.100
8	0.736	0.664	0.599	0.541	0.488	0.441	0.398	0.359	0.324	0.293	0.264	0.239	0.215	0.194	0.158	0.129
10	0.764	0.699	0.639	0.584	0.534	0.488	0.446	0.408	0.373	0.341	0.312	0.285	0.260	0.238	0.199	0.166
12	0.793	0.734	0.680	0.629	0.582	0.539	0.499	0.462	0.428	0.396	0.366	0.339	0.314	0.291	0.249	0.213
14	0.823	0.771	0.723	0.677	0.635	0.595	0.557	0.522	0.489	0.459	0.430	0.403	0.378	0.354	0.311	0.273
16	0.853	0.810	0.768	0.728	0.691	0.655	0.622	0.590	0.559	0.531	0.503	0.477	0.453	0.429	0.386	0.348
18	0.885	0.849	0.815	0.783	0.751	0.721	0.692	0.665	0.638	0.612	0.588	0.564	0.542	0.520	0.479	0.442
20	0.916	0.890	0.865	0.840	0.816	0.792	0.770	0.748	0.726	0.705	0.685	0.666	0.647	0.628	0.593	0.559
22	0.949	0.933	0.916	0.901	0.885	0.870	0.855	0.840	0.825	0.811	0.797	0.783	0.770	0.757	0.731	0.706
24	0.982	0.976	0.971	0.965	0.959	0.953	0.948	0.942	0.937	0.931	0.925	0.920	0.914	0.909	0.898	0.888
25	1.000	1.000	1.000	1.000	1.000	1.000	1.000	1.000	1.000	1.000	1.000	1.000	1.000	1.000	1.000	1.000
26	1.016	1.022	1.027	1.033	1.038	1.044	1.049	1.055	1.061	1.066	1.072	1.078	1.084	1.090	1.101	1.113
28	1.051	1.068	1.086	1.104	1.123	1.141	1.160	1.180	1.199	1.219	1.240	1.260	1.281	1.303	1.347	1.392
30	1.086	1.117	1.148	1.180	1.213	1.247	1.281	1.317	1.354	1.392	1.431	1.471	1.512	1.554	1.642	1.735
32	1.122	1.166	1.212	1.259	1.309	1.360	1.413	1.469	1.526	1.586	1.648	1.713	1.780	1.850	1.997	2.157
34	1.159	1.217	1.279	1.343	1.411	1.482	1.557	1.635	1.718	1.804	1.895	1.991	2.091	2.196	2.423	2.674
36	1.196	1.270	1.348	1.431	1.520	1.613	1.713	1.818	1.930	2.049	2.175	2.309	2.451	2.602	2.933	3.305
38	1.235	1.324	1.421	1.524	1.635	1.754	1.882	2.019	2.166	2.323	2.492	2.673	2.868	3.077	3.541	4.075
40	1.273	1.380	1.496	1.622	1.758	1.905	2.065	2.238	2.426	2.630	2.850	3.089	3.349	3.630	4.264	5.010
42	1.313	1.438	1.574	1.724	_1.888	2.067	2.264	2.479	2.714	2.972	3.254	3.564	3.902	4.273	5.124	6.144
44	1.353	1.497	1.656	1.831	2.026	2.241	2.478	2.741	3.032	3.354	3.710	4.103	4.539	5.020	6.142	7.514
46	1.394	1.558	1.740	1.944	2.172	2.426	2.710	3.028	3.383	3.779	4.222	4.716	5.269	5.886	7.346	9.168
48	1.436	1.620	1.828	2.062	2.326	2.624	2.961	3.340	3.768	4.252	4.796	5.411	6.105	6.887	8.766	11.158
50	1.478	1.684	1.918	2.185	2.490	2.836	3.231	3.681	4.193	4.776	5.441	6.198	7.061	8.044	10.438	13.546

	Polymer	Thickness (µm)	P$_i$ at 25°C	Ep (kcal/mol)
Layer 1	LDPE	18	1,900	10.2
Layer 2	Nylon 6	10	25.0	10.5
Layer 3	PP	20	620	11.5

Layer no.	Polymer type	Thickness (µm)	P$_i$ at 25°C $\left(\dfrac{cc \cdot \mu m}{m^2 \cdot d \cdot kPa}\right)$	Ep (kcal/mol) From Table
1	PE	18	1,900	10.3
2	Nylon 6	10	25.0	10.5
3	PP	20	1,500	11.5

FIGURE 8.7 Oxygen and water vapor permeability chart. List of polymers: (1) Poly (1,3-butadiene); (2) gutta percha; (3) poly (chloroprene); (4) polyisoprene; (5) polyethylene (PE) d = 0.914; (6) PE, d = 0.964; (7) polypropylene; (8) poly (ethyl methacrylate); (9) poly (acrylonitrile); (10) poly (methacrylonitrile); (11) polystyrene; (12) poly (tetrafluoroethylene); (13) polyvinyl acetate; (14) polyvinyl alcohol; (15) polyvinyl chloride; (16) polyvinylidene chloride; (17) cellulose; (18) cellulose acetate; (19) cellulose nitrate; (20) ethyl acetate; (21) Barex; (22) Nylon 6.9/6.10; (23) phenoxy; (24) Nylon 6.6; (25) polyvinyl fluoride; (26) Nylon; (27) polytetrafluorethylene; (28) polybutene; (29) Surlyn; (30) butyl rubber; (31) SAN; (32) ABS; (33) polyurethane; (34) polycarbonate; (35) neoprene; (36) polybutadene; (37) silicone.

FIGURE 8.8 Oxygen and CO_2 permeability chart. List of polymers: (1) Poly (1,3-butadiene); (2) gutta percha; (3) poly (chloroprene); (4) polyisoprene; (5) polyethylene (PE) d = 0.914; (6) PE, d = 0.964; (7) polypropylene; (8) poly (ethyl methacrylate); (9) poly (acrylonitrile); (10) poly (methacrylonitrile); (11) polystyrene; (12) poly (tetrafluoroethylene); (13) polyvinyl acetate; (14) polyvinyl alcohol; (15) polyvinyl chloride; (16) polyvinylidene chloride; (17) cellulose; (18) cellulose acetate; (19) cellulose nitrate; (20) ethyl acetate; (21) Barex; (22) Nylon 6.6; (23) phenoxy; (24) Nylon 6/6.6; (25) polyvinyl fluoride; (26) Nylon; (27) polytetrafluoroethylene; (28) polybutene; (29) Surlyn; (30) butyl rubber; (31) SAN; (32) ABS; (33) polyurethane; (34) polycarbonate; (35) neoprene; (36) polybutadene; (37) silicone.

$$t = 6 \text{ months} = 180 \text{ d}$$

$$A = 400 \text{ cm}^2 = 0.04 \text{ m}^2$$

$$\Delta p = 0.21 \text{ at} = 21.27 \text{ k Pa (assume } p_i = 0 \text{ inside the package)}$$

$$q = \frac{500}{32} \times \frac{0.005}{100} \times 22,414 = 17.5 \text{ cc(STP) of oxygen}$$

$$\ell = \frac{22 \times 180 \times 0.04 \times 22.27}{17.5} = 193 \,\mu\text{m} \left(7.6 \text{ mil}\right)$$

The same equation can be used to calculate the loss of water. Since Δp is constant, there is enough water (inside the package) to keep the water activity unchanged during the package's shelf life. Solving for q

$$q = \frac{PtA \,\Delta p}{\ell}$$

$$P_{H_2O} = 8.5 \times 10^4 \frac{\text{cc(STP)}\mu\text{m}}{\text{m}^2 \cdot \text{d} \cdot \text{kPa}} \quad \text{(from Table 8.19)}$$

$$t = 180 \text{ da}$$

$$A = 0.04 \text{ m}^2$$

$$\Delta p = p^s \times \left(\frac{100 - 60}{100}\right) = 1.267 \text{ kPa}$$

$$p^s = 23.76 \text{ mmHg} = 3.17 \text{ kPa}$$

$$q = \frac{8.5 \times 10^4 \times 180 \times 0.04 \times 1.267}{193} = 4,017 \text{ cc(STP)} = 3.20 \text{ g of water}$$

Equation 8.20 cannot be used if Δp changes during the shelf-life of the product. This is the case of moisture-sensitive products showing sorption isotherm curves. In simplified calculation, hysterisis of the sorption isotherms are not considered. However, the product's sorption isotherm needs to be known. The book by Iglesias and Chirife (1982) provides a valuable source of information on sorption isotherms.

For moisture-sensitive products the moisture content of the product varies with the relative humidity at which it is in equilibrium and vice versa. The relationship between the product moisture content and the relative humidity of the headspace is given by the product sorption isotherm. Assuming that the relative humidity outside the package (relative humidity of storage conditions, p_o) is constant, the Δp change through the shelf-life period is a function of the product moisture content, $\Delta p = p_o - p_i(M)$, where M is the product moisture content on a dry basis. A differential quantity dq of water exchanged through the package is equal

to the differential moisture content times the dry weight of the product W, dq = WdM. For moisture-sensitive products, the shelf-life can be written as

$$t = \frac{\ell\,W}{AP} \int_{M_i}^{M_2} \frac{dM}{p_o - p_i(M)} \tag{8.31}$$

where the limits M_1 and M_2 refer to the product's initial and final moisture content values, respectively. This equation estimates the value of the product's shelf-life which is defined as the time during which a packaged moisture-sensitive product remains in an acceptable or saleable condition under specific conditions of storage. Equation 8.31 relates the product's shelf-life with the area, thickness, mass of the product, and storage conditions. The validity of the above equations are subject but not limited to the following conditions.

1. There is a fast equilibrium between the product and the packages internal conditions.
2. The delay in reaching steady state condition of permeability through the package material is neglected
3. The temperature and external humidity are constant through the shelf-life period, t.
4. P is not affected by any other permeant.

For nonlinear isotherms, Equation 8.31 needs to be numerically integrated to solve for time t. Simplified solutions to Equation 8.31 can be obtained. For instance, if the portion of the sorption isotherm of interest can be linearized as

$$Y = a + bM$$

where Y is the relative humidity, the integration of 8.31 yields

$$t = \frac{\ell\,W}{PA\,p^s\,b} \ln \frac{Y_o - Y_{i,t=o}}{Y_o - Y_{i,t}}$$

where Y_o is the outside relative humidity; and Y_i is the headspace relative humidity.

EXAMPLE 8.15

A product with a dry weight W = 80 g and a b-value = 9.0 kg product/kg H_2O, will be stored at 23°C and 85% RH.

The initial equilibrium RH of the product $Y_{i,t=0} = 20\%$. The final equilibrium RH of the product $Y_{i,t} = 70\%$. The permeability of the package material is

$$P = 4 \times 10^{-2} \frac{kg\,\mu m}{m^2 \cdot d \cdot kPa}$$

For a package thickness of 53 μm, calculate the maximum package area to maintain the RH_i equilibrium of the product at or below 70% during 100 d.

Solution

l = 53 μm
W = 80 g = 0.08 kg
P = 4 × 10⁻² kg μm/m² d kPa
p^s = 21.07 mmHg = 2.81 kPa
b = 9.0

$$\ln \frac{Y_o - Y_{i,t=o}}{Y_o - Y_{i,t}} = \frac{85-20}{85-70} = 1.466$$

$$A = \frac{53 \times 0.08}{4 \times 10^{-2} \times 100 \times 2.81 \times 9} \times 1.466 = 6.14 \times 10^{-2} \ m^2$$

8.6   CONCLUDING REMARKS

In this chapter, we have reviewed: (1) the economics of plastic containers; (2) major plastics used in food packaging and their properties; (3) main additives incorporated into plastics during processing; and (4) mass transfer applications of plastics in food packaging systems. Because of their unique combination of properties, technologies, and economics, plastics are versatile materials from which the food industry will continue to benefit.

REFERENCES

Albrant, P. D., 1996, Personal communication, Bekum America Co., Williamston, MI.

Alcoa, 1990, Form 992-100-6093, Crawfordville, IN.

Axelson, L. and Cavlin, S., 1991, Aseptic integrity and microhole determination of packages by gas leakages detection, *Pack. Tech. Sci.* 4:9–20.

Bezigian, T., 1996, Personal communication.

Blatz, P., 1989, Properties of films from blends of amorphous and crystalline nylons, AlChE Nat. Conf. April 2–6.

Brown, W. E., 1992, *Plastics in Food Packaging*, Dekker, New York.

Chirife, J. and Iglesias, H. A., 1982, *Handbook of Food Isotherms: Water Sorption Parameters for Food and Food Components*, Academic Press, NY.

CRC Handbook of Chemistry and Physics, 1983, 64th ed., CRC Press, Boca Raton, FL, F162.

Cunningham, R. E. and Williams, R. J., 1980, *Diffusion in Gases and Porous Media*, Plenum Press, New York.

Davis, D. S., 1992, Ethylene incorporation in polypropylene: effect on thermal-related properties, *J. Plastic Film Sheeting*, 8(4):101–108.

Dick, J. S., 1987, *Compounding Materials for the Polymer Industry*, Noyes Publications, NJ.

Felts, J. T., 1993, Transparent barrier coatings update: flexible substrates, *J. Plastic Film Sheeting* 9:201.

Fish, M., 1992, *Modern Plastic Encyclopedia*, 146.

Floros, J. D. and Gnanasekharan, V., 1992, Principles, technology and application of destructive and non-destructive package integrity testing, in *Advances in Aseptic Processing Technology*, Singh, R. K. and Nelson, P. E., Ed., Elsevier, London, ch.7.

Foster, R., 1986, Ethylene-vinyl alcohol copolymers (EVOH), in *The Wiley Encyclopedia of Packaging Technology*, Bakker, M., Ed., John Wiley & Sons, New York, 270–275.

Gibbs, D. S. and Wessling, R. A., 1983, Vinylidene chloride and poly(vinylidene chloride), in *Kirk-Othmer: Encyclopedia of Chemical Technology*, Interscience Publishers, New York, vol. 23, 764–798.

Gruenwald, G., 1987, *Thermoforming, A Plastic Processing Guide*, Technomics, Lancaster, PA.

Hernandez, R. J., 1994, Effects of water vapor on the transport properties of oxygen through polyamides packaging materials. *J. Food Eng.* 22:495–507.

Hernandez, R. J., Giacin, J. R., and Baner, A. L., 1986, The evaluation of the aroma barrier properties of polymer films, *J. Plastic Film Sheeting* 2(July):187–211.

Hernandez, R. J. and Gavara, R., 1993, Consistency test for continuous flow permeability experimental data, *J. Plastic Film Sheeting* 6(April):126–138.

Hernandez, R. J. and Giacin, J. R., 1996, Factors affecting permeation, sorption, and migration processes in packaging-product systems, Taub, I. and Singh, P. R., Eds., ACS Monograph Series,

Jensen, P. H., 1994, Testing of package integrity based on CO_2 on a trace gas, IAPRI Symposium, 9–12 October, Reims, France.

Karel, M., 1974, Packaging protection for oxygen-sensitive products, *Food Res.* 14:340.

Kim, J. N., 1992, An Application of the Finite Difference Method to Estimate the Shelf-Life of a Packaged Moisture Sensitive Pharmaceutical Tablet, M.S. Thesis, School of Packaging, Michigan State University, Ann Arbor, MI.

Kohan, M. I., Ed., 1973, *Nylon Plastics*, John Wiley & Sons, New York.

Kroschiwitz, J., Ed., 1987, *Polymers An Encyclopedic Sourcebook of Engineering Properties*, Encyclopedia Reprint Series, John Wiley, NY.

Labuza, T. P., Mizrahi, S., and Karel, M., 1972, Mathematical model for optimization of flexible film packaging of food for storage, *Trans. ASAE* 15:150.

Lachance, K., 1966, Meeting FDA regulations for food packaging made clear, *Packag. Technol. Eng.* 7:44.

Laermer, S. F. and Zambetti, F. F., 1992, Alpha-tocopherol (vitamin E)-the natural antioxidant for polyolefins, *J. Plastic Film Sheeting* 8:228–248.

Landvatter, G. R., 1994, Ethylene-vinyl acetate (EVA), in *Modern Plastics Encyclopedia Handbook*, McGraw-Hill, New York, 39.

Leonard, E. A., 1980, *Packaging Economics*, Books for Industry, New York.

Liu, K. I., Hernandez, R. J., and Giacin, J. R., 1991, The effect of water activity and vapor activity on the permeation of toluene vapor through a two-side PVDC coated oriented polypropylene film, *J. Plastic Film Sheeting* 7:56–67.

Manders, P. W., 1995, Polyethylene: new branches of the polymer family extend into specialized applications, *Modern Plastic Encyclopedia*, (Nov):B3-B6.

Mergenhagen, L. K., 1992, Ethylene acid copolymer in *Modern Plastics Encyclopedia*, McGraw-Hill, New York, 64.

Mobil, 1994, *Mobil OPP Films, Product Characteristics*, Mobil Chemical Company, Chadds Ford, PA.

Modern Plastic, Guide to Plastics, 1987, McGraw-Hill, New York.

McCrum, N. G., Bucley, C. P., and Bucknall, C. B., 1988, *Principle of Polymer Engineering*, Oxford University Press, New York.

Perry, R. H. and Green, D. W., 1984, *Perry's Chemical Engineers' Handbook,* 6th ed., McGraw-Hill, NY, 3–247.

Pascall, M. A., Harte, B., Giacin, J., and Gray, I., 1995, Decreasing lipid oxidation in soybean oil by a UV absorber in the packaging material. *J. Food Sci.,* 60(5):1116–1118.

Pocas, M. F., 1995, Modeling the moisture transfer of two-component food products in a flexible package, M.S. Thesis, School of Packaging, Michigan State University, Ann Arbor, MI.

Progelhof, R. C. and Throne, J. L., 1993, *Polymer Engineering Principles*, Hanser Publisher, New York.

Radosta, J. A., 1991, Talc anti-blocks for maximized LLDPE blown film performance, *J. Plastic Film Sheeting* 7:81–189.

Reed, R. W. and Vaughan, D., 1965, Surlyn A ionomer. I. The effect of ionic bonding on polymer structure. II. The effect of ionic bonding on solid state and melt properties, *Polymer Preprints* 1(1).

Rice, J., 1995, Opting for OPP, *Food Process.* Jan:71–73.

Sajaki, T. and Giacin, J. R., 1993, Permeation of ethyl acetate vapor through silica deposited PET films and composite structures, *J. Plastic Films Sheeting* 9:97.

Simon, D. F., 1994, Single-site catalysts produce tailor-made consistent resins, *Packaging Tech. Eng.,* April: 34–37.

Smith, M. A., 1986, High density polyethylene, in *The Wiley Encyclopedia of Packaging Technology*, Bakker, M., Ed., John Wiley & Sons, New York, 514–523.

Statz, R. J., 1994, Ionomer, in *Modern Plastics Encyclopedia Handbook*, McGraw-Hill, New York, 41–42.

Toebe, J. M., Hoojjat, H., Hernandez, R. J., Giacin, J. R., and Harte, B. R., 1990, Interaction of flavour components from an onion/garlic sour cream with HIPS, *Packag. Technol. Sci.* 3:133–140.

Toensmeier, P. A., 1995, *Modern Plastics*, Feb:44z–47.

Treybal, R. E., 1980, *Mass Transfer Operations*, 3rd ed., McGraw-Hill, New York, ch.2.

Van Drumpt, J., 1992, *Modern Plastic Encyclopedia*, Oct:150–154.

Van Krevelen, D. W., 1990, *Properties of Polymers*, 3rd ed., Elsevier, New York.

Young, G., 1966, New materials transform fresh-produce packaging, *Convert. Mag.* (July):78–79.

Youngquist, G. R., 1970, Diffusion flow of gases in porous solids, *Ind. Eng. Chem.* 62(8):52–63.

9 Kinetics of Food Deterioration and Shelf-Life Prediction

Petros S. Taoukis, Theodore P. Labuza, and I. Sam Saguy

CONTENTS

9.1 INTRODUCTION

Quality is an attribute of food, on which understandably a lot of consideration is focused. *Food quality* can be defined as the assemblage of properties which differentiate individual units and influence the degree of acceptability of the food by the consumer or user (Kramer and Twigg, 1968). Due to the nature of foods as physicochemically and -biologically active systems, food quality is a dynamic state continuously moving to reduced levels (with the notable exception of the cases of maturation and aging). Therefore, for each particular food, there is a finite length of time after production it will retain a required level of organoleptic and safety qualities under stated conditions of storage. This period of time can be generally defined as the *shelf-life* of the food product. There is no established, uniformly applicable definition of shelf-life. The definition of shelf-life and the criteria for the determination of the end of shelf-life are dependent on specific commodities and on the definition's intended use (i.e., for regulatory vs. marketing purposes). Food related authorities have proposed various definitions that can serve as guidelines. The International Institute of Refrigeration

(IIR) recommends two different definitions for frozen food (IIR, 1972). *High quality life* (HQL) is the time from freezing of the product to the development of a just noticeable sensory difference (70 to 80% correct answers in a triangular sensory test). Another type of shelf-life definition that can be extended to other types of food products is the *practical storage life* (PSL). PSL is the period of proper (frozen) storage after processing (freezing) of an initially high quality product during which the organoleptic quality remains suitable for consumption or for the process intended. PSL is usually in the order of two to three times longer than HQL. *Time of minimum durability*, introduced by the European Economic Community (EEC) directive on food labeling, (89/395) and defined as the time during which the foodstuff retains its specific properties when properly stored is different in principle from the aforementioned ones, in that it relates to properties of the product itself and not to considerations of its use. It is a working definition for the food scientist satisfying the often made fundamental assumption that the highest quality product is the freshly processed (or harvested) one. However, since characteristic properties are overlaid, a decision has to be made at what level the change in a certain characteristic or the development of an undesirable one can be detected by the consumer. For example, if having a specific flavor means the absence of off flavors, it has to be decided at what intensity levels these flavors are detectable by the consumer. Thus, this definition is closely related to the HQL definition.

For any definition to be used as a working tool it has to be followed by further guidelines, i.e., the meaning of organoleptic quality has to be accurately defined and appropriate methods of measuring it and criteria for setting acceptability limits must be discussed.

Sensory evaluation by a trained panel, whereby the food is graded on a "standardized" hedonic scale, usually best approximates the overall quality state of the food (Labuza and Schmidl, 1988). This approach is not without problems. There are considerable difficulties in establishing a meaningful scale for each food product. An expert panel is not necessarily representative of consumers, let alone different consumer segments (Mackie et al., 1985). Even if that assumption can be made, a cut-off level of acceptability has to be decided. The time at which a large (but preset) percentage of panelists judge the food as being at or beyond that level is the end of shelf-life (PSL). A criterion like that includes an indication of the proportion of the consumers to whom the product must be acceptable till the end of shelf-life, another variable to which reference or agreement is required. Other problems with the sensory approach are the high cost that is involved with large testing panels and the questions connected with tasting spoiled or potentially hazardous samples. In some cases microbial growth or nutrient degradation could reach unacceptable levels while the food is still judged organoleptically acceptable. Sensory data are not "objective" enough for regulatory purposes and in cases of legal action or dispute. Sometimes consumers can be "trained" to accept lower standard products by being exposed to products of gradually slipping quality. That makes the need of alternative ways of assessing quality apparent (Herborg, 1985).

Chemical, microbiological, and physical tests are being used widely in the study of food quality. Characteristics used by the consumer for evaluation of a product, such as flavor, color, and textural properties can be measured instrumentally or chemically. The study of the chemical and biological reactions and physical changes that occur in the food during and after processing allows the recognition of the ones that are most important to its safety, integrity, and overall quality. Physicochemical or microbiological parameters can be used to quantitatively assess quality. The values of these parameters can be correlated to sensory results for the same food and a limit that corresponds to the lowest acceptable organoleptic quality can be set. However, caution should be drawn to the fact that correlation of values of individual chemical parameters to sensory data is often not straightforward because overall organoleptic quality is a composite of a number of changing factors (Trant et al., 1981). The relative contribution of each factor to the overall quality may vary at different levels of quality or at different storage conditions.

Despite the discussed difficulties in defining and evaluating quality and determining shelf-life of a food, a lot of progress has been made towards a scientific and generally accepted approach. It is an area of continuous and extensive research. An in-depth study of the different deteriorative mechanisms that occur in a food system and systematic analysis and interpretation of the results lead to more meaningful and objectively measurable ways of assessing food quality and determining shelf-life. Proper application of chemical kinetic principles to food quality loss is essential for efficiently designing appropriate tests and analyzing the obtained results.

9.2   KINETICS OF FOOD DETERIORATION

9.2.1   Reaction Modeling Principles

Applying fundamental chemical kinetic principles, the rate of food quality change may in general be expressed as a function of composition and environmental factors (Saguy and Karel, 1980):

$$\frac{dQ}{dt} = \mathbf{F}\left(C_i, E_j\right) \tag{9.1}$$

where C_i are composition factors, such as concentration of reactive compounds, inorganic catalysts, enzymes, reaction inhibitors, pH, water activity, as well as microbial populations and E_j are environmental factors, such as temperature, relative humidity, total pressure and partial pressure of different gases, light and mechanical stresses. What the food kineticist is thus faced with, is a physicochemical system of high complexity involving numerous physical and chemical variables and coefficients which in most cases are imposible or impractical to quantitatively define. Even if the system could be explicitly expressed in terms of measurable parameters, an analytical solution is usually nonexistent and exact numerical solutions are too complicated and laborious to be useful as working tools.

The established methodology consists of first identifying the chemical and biological reactions that influence the quality and the safety of the food. Then, through a careful study of the food components and the process, the reactions judged to have the most critical impact on the deterioration rate, are determined (Labuza, 1985). Excluding the effect of the environmental factors, E_j, by assuming them constant, at the most probable level or judging it negligible within their expected variation, a simplified reaction scheme that expresses the effect of the concentration of the reactants is developed. The ultimate objective is to model the change of the concentrations of constituents connected to food quality, as functions of time. Molecular, irreversible reactions are typically expressed as

$$\mu_1 A_1 + \mu_2 A_2 + \mu_3 A_3 + \ldots + \mu_m A_m \xrightarrow{\ k_f\ } P \tag{9.2}$$
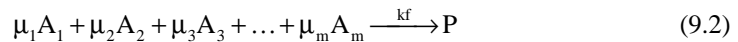
where A_j = the reactant species, μ_j = the respective stoichiometric coefficients ($j = 1,2\ldots m$), P = the products and k_f the forward reaction rate constant. For such a scheme the reaction rate, r, is given by (Hills and Grieger-Block, 1980)

$$r = -\frac{1}{\mu_j}\frac{d\left[A_j\right]}{dt} = k_f\left[A_1\right]^{n_1}\left[A_2\right]^{n_2}\ldots\left[A_m\right]^{n_m} \tag{9.3}$$

where n_j = the order of the reaction with respect to species A_j. For a true molecular reaction, it holds that: $n_j = \mu_j$. More often than not, the degradation of important components to undesirable

products is a complex multistep reaction for which the limiting reaction and intermediate products are difficult to identify. A lot of reactions are actually reversible having the form

$$\alpha\, A + \beta\, B \underset{k_b}{\overset{k_f}{\rightleftharpoons}} \gamma\, C + \delta\, D \tag{9.4}$$

In this case A reacts with B to form products C and D which can back react with a rate constant of k_b. The reaction rate in this case would be

$$r = \frac{-d[A]}{\alpha\, dt} = \frac{-d[B]}{\beta\, dt} = \frac{+d[C]}{\gamma\, dt} = \frac{+d[D]}{\delta\, dt} = k_f[A]^\alpha\,[B]^\beta - k_b[C]^\gamma\,[D]^\delta \tag{9.5}$$

For the majority of food degradation systems either k_b is negligible compared to k_f, or for the time period of practical interest they are distant from equilibrium, i.e., [C] and [D] are very small, allowing us to treat it as an irreversible reaction. In most cases, the concentration of the reactant that primarily affects overall quality is limiting, the concentrations of the other species being relatively in large excess so that their change with time is negligible (Labuza, 1984). That allows the quality loss rate equation to be expressed in terms of specific reactants

$$r = \frac{-d[A]}{dt} = k_f'[A]^\alpha \tag{9.6}$$

where α is an apparent or pseudo order of the reaction of component A and k_f' is the apparent rate constant. Another case that can lead to a rate equation similar to Equation 9.6 is when the reactants in Reaction 9.2 are in stoichiometric ratios (Hills, 1977). Then from Equation 9.3 we have

$$r = k_f \prod_i^m [A_i]^{n_i} = k_f \left(\prod_i^m \mu_i^{n_i} \right) \left[\frac{A_1}{n_1} \right]^{\sum n_i} \tag{9.7}$$

or

$$r = \frac{-d[A]}{dt} = k_f'[A]^\alpha \tag{9.8}$$

where $A = A_1$ and $\alpha = \Sigma n_i$, an overall reaction order.

Based on the aforementioned analysis and recognizing the complexity of food systems, food degradation and shelf-life loss is, in practice, represented by the loss of desirable quality factors A (e.g., nutrients, characteristic flavors) or the formation of undesirable factors B (e.g., off flavors, discoloration). The rates of loss of A and of the formation of B are expressed as in Equation 9.6, namely:

$$r_A = \frac{-d[A]}{dt} = k[A]^m \tag{9.9}$$

$$r_B = \frac{d[B]}{dt} = k'[B]^{m'} \tag{9.10}$$

The quality factors [A] and [B] are usually quantifiable chemical, physical, microbiological, or sensory parameters characteristic of the particular food system. Both k and k′ are the apparent reaction rate constants and m and m′ the reaction orders. It should be again stressed that Equations 9.9 and 9.10 do not represent true reaction mechanisms and m and m′ are not necessarily true reaction orders with respect to the species A and B but rather apparent or pseudo orders. The apparent reaction orders and constants are determined by fitting the change with time of the experimentally measured values of [A] or [B] to Equations 9.9 or 9.10. The techniques used for the solution can be generally classified into two categories: (a) differential methods and (b) integral methods (Hills and Grieger-Block, 1980).

In experimental kinetic studies, it is impossible to measure the reaction rate itself. Instead, the concentration of A or B is measured (directly or indirectly) as a function of time. If these concentrations are plotted against time and smooth curves are fitted either graphically or using a statistical fitting method (e.g., polynomial regression) the reaction rates may be obtained by graphical or numerical differentiation of the curves. By taking the logarithm of both sides of Equation 9.9 and 9.10, the following linear expressions are obtained:

$$\log r_A = \log k + m \log [A] \qquad (9.11)$$

$$\log r_B = \log k' + m' \log [B] \qquad (9.12)$$

Data can be fitted to these equations by the method of least squares to determine values of the constants.

Two differential approaches can be alternatively used. The first involves differentiation of data obtained from a single experimental run. It requires measurement of A or B concentrations with time, to at least 50% conversion. The second is differentiation of data from initial rate measurements. In this approach, measurements of concentrations are carried out to very small conversions (e.g., 5%). This is repeated for a number of initial reactant concentrations. Thus, each estimated rate corresponds to a different initial reactant concentration and involves a separate experimental run. Another difficulty often faced with this method is in fitting data from kinetic experiments in which the rate changes rapidly even within the low conversions that are used (e.g., in case of enzymatic reactions). One has to obtain an initial slope from a set of data points with a rapid change in slope and also inevitable scatter from experimental errors. The usual methods of least square fitting of a polynomial may give erratic estimates of the initial slope. A flexible mathematical method to overcome this problem is the use of spline functions (Wold, 1971). The major advantage of the spline function method is that it uses all the data to estimate the initial rate, but is not unduly influenced by experimental error in individual data points. In general, the differential methods involve two statistical fittings, thus being more sensitive to experimental scattering and requiring a large number of data points for a dependable parameter estimate.

In the integral method, variables in Equations 9.9 and 9.10 are separated and integration is carried out. For example, for Equation 9.9, we have

$$-\int_{A_o}^{A} \frac{d[A]}{[A]^m} = kt \qquad (9.13)$$

Regardless of the value of m, Equation 9.13 can be expressed in the form:

$$Q(A) = kt \qquad (9.14)$$

where the expression Q(A) is defined as the quality function of the food.

TABLE 9.1
Quality Function Form and Half-Life Times
for Different Order Reactions

Apparent reaction order	Quality function $Q(A)_t$	Half-life time $(t_{1/2})$
0	$A_o - A_t$	$A_o/(2k_o)$
1	$\ln(A_o/A_t)$	$\ln 2/k_1$
2	$1/A_t - 1/A_o$	$1/(k_2 A_o)$
$m\,(m \neq 1)$	$\dfrac{1}{m-1}\left(A_t^{1-m} - A_o^{1-m}\right)$	$\dfrac{2^{m-1}-1}{k_m(m-1)}A_o^{1-m}$

TABLE 9.2
Important Quality Loss Reactions that
Follow Zero- or First-Order Kinetics

Zero order	Overall quality of frozen foods
	Nonenzymatic browning
First order	Vitamin loss
	Microbial death/growth
	Oxidative color loss
	Texture loss in heat processing

The form of the quality function of the food for an apparent zero, 1st, 2nd and mth order reaction can be derived from Equation 9.13 and 9.14 and is shown in the following Table 9.1. The half-life time of the reaction, i.e., the time for the concentration of the quality index A to reduce to half its inital value is also included.

To determine the quality function one assumes different values of m (0, 1, or other) and tries a graphical or a least square linear fit to the corresponding equations (Table 9.1) of the experimental data. If the experiment has been carried out to at least 50% conversion and preferably 75%, it is usually easy to determine which reaction order and equation gives the best fit, either graphically or by using statistical goodness of fit criteria. The coefficient of determination (R^2) of the linear regression is in most cases a sufficient criterion. The value of the R^2, for a least square fit in general, is given by the following equation:

$$R^2 = 1 - \left(\sum_{i=1}^{N} \left(y_i - \hat{y}_i\right)^2 \middle/ \sum_{i=1}^{N} \left(y_i - \bar{y}\right)^2 \right) \tag{9.15}$$

where y_i the experimentally observed values of the measured parameter (i = 1 to N), $\hat{y}_i$ the value predicted from the regression equation, $\bar{y}$ = the average of the observed values, and N = the number of measurements (Ott, 1984). The correct apparent order is that for which the R^2 is closer to unity. The overwhelming majority of the food reactions that have been studied have been characterized as pseudo zero or pseudo first order (Labuza, 1984). Characteristic examples are listed in Table 9.2.
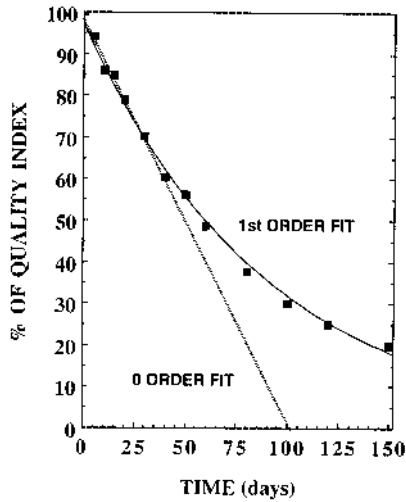
FIGURE 9.1 Loss of food quality as a function of time with display of difference between zero and first order reaction.
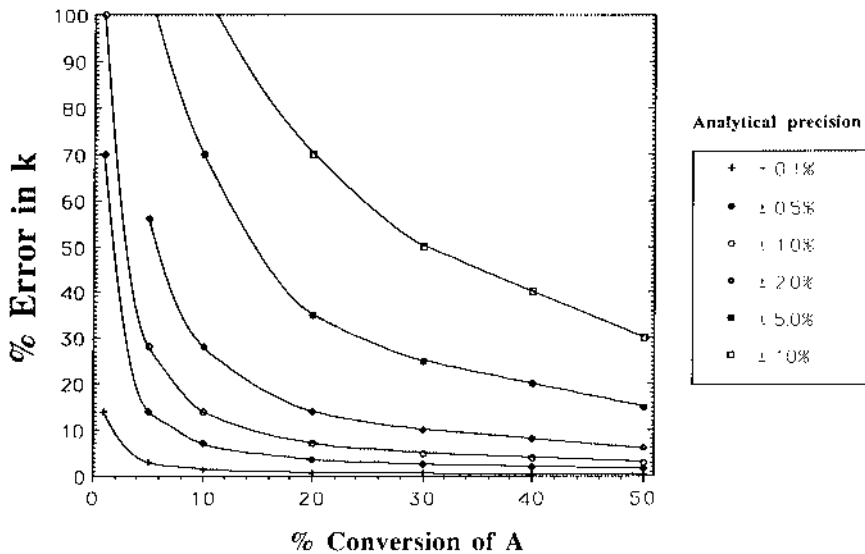
FIGURE 9.2 Effect of the analytical precision on the accuracy of the estimated reaction rate constant (k). (Based on data from Benson, 1960).

Caution is advised in deciding the appropriate apparent order and quality function, as noted by Labuza (1984). For example, when the reaction is not carried far enough (<50% conversion) both zero and first order might be indistinguishable from a goodness or fit point of view as is illustrated in Figure 9.1. On the other hand, if the end of shelf-life is within less than 20% conversion, for practical purposes either model is sufficient.

Additionally, the worse the precision of the method of measuring the quality factor A the larger the extent of change to which the experiment should be performed to obtain an acceptably accurate estimate of the reaction rate constant as illustrated in Figure 9.2. It should be noted here that most measurements in complex foods typically involve an error of 5% or worse.

Erroneous results are often obtained this way, especially if the data are used to extrapolate to longer times. Unfortunately, this has often occurred in the literature. Studies of reaction systems involved in food quality loss are not followed to sufficient reaction extent, resulting in inaccurate reaction rate constants and undeterminable reaction orders. A lot of valuable data cannot be utilized to their fullest extent and databases of food reaction kinetic parameters contain a lot of uncertainties.

Another problem that scattered data can cause are values of R^2 obtained by the zero-order and first order fit that are practically indistinguishable. In the case of the first-order reaction the logarithms of the measured quantities are used (semilog plot) thus the R^2 is calculated for $\ln y_i$ and $\ln y$ rather than y_i and y (Equation 9.15). This, in effect, tends to give a larger R^2, especially if the larger scatter is at the larger values (Boyle et al., 1974). This bias in the criterion might lead to a skewed preference to the first-order model. In these cases it is advisable to use additional criteria for goodness of fit, like residual plots. Alternatively, instead of the logarithmic equation for the first order reaction (Table 9.1) the exponential form can be used, where:

$$A = A_o \exp(-kt)$$

and a nonlinear least square fitting computed, for determination of the k parameter. The R^2 for this fit is given by Equation 9.15 and is directly comparable to the R^2 from the linear regression for the zero-order model.

A final pitfall that should be avoided when determining the apparent order, concerns reactions that exhibit a lag period. During a typical lag period there is a buildup of a critical intermediate concentration. The rate of the reaction during the buildup period is normally slower. In some cases, the reaction is not detectable due to analytical limitation as in the case of the formation of brown pigments monitored at 420 nm during a nonenzymatic Maillard type reaction. The most common approach for dealing with a lag period, is to draw each data point and to look for the time where a distinct change in the reaction rate occurred. Obviously, this approach calls for special attention as a change in the reaction mechanism may also take place. Typical reactions where lag period is observed are nonenzymatic browning (Labuza, 1982; Saguy, et al., 1979) and microbial growth.

Once the apparent order of the quality deterioration reaction has been decided, further statistical analysis and statistical evaluation of the parameter k, the rate constant, is required to get an estimate of the error in the determination of k (Labuza and Kamman, 1983). If a linear regression method is used to estimate the parameters, their 95% confidence limits can be calculated using the Student t distribution. In addition to the confidence limits, a list of standarized residuals and a residual plot is a useful statistical tool that allows evaluation of how well the chosen equation can model the data and also permits the recognition of extreme or outlier values that may be the result of experimental errors or other extraneous effects and should be excluded from the calculations (Arabshasi and Lund, 1985). The standardized residuals should be randomly distributed around zero and usually within –2 and +2. Any data that generate standard residuals outside this range are possible outliers.

An alternative procedure to linear regression for the calculation of k is the point-by-point or long interval method (Margerison, 1969; Lund, 1983) in which each data point is an independent experiment with respect to zero time. The value of k is calculated as the average of the n individual slopes. Labuza (1984) showed that one gets similar value ranges for k from the two methods. A minimum of eight data points is recommended by Labuza and Kamman (1983) for reasonably narrow confidence limits in k within the practical and economic limits of most experimentation.

In some cases higher- or fractional-order models are clearly indicated by the experimental data. To determine the apparent order m, two methods can be alternatively used. As mentioned

before, different values for m can be assumed and the fit of the quality function for $m \neq 1$ (Table 9.1), tested. A second method is to allow m as a parameter and run a nonlinear least square regression on the equation to determine the order that best conforms with the experimental data. For example, it was found that second order kinetics best described the oxidation of extractable color pigments from chili pepper (Chen and Gutmanis, 1968). Autoxidation of fatty acids in the presence of excess oxygen is best described with a half-order model with respect to the fatty acid concentration (Labuza, 1971), whereas hexanal production from lipid oxidation is shown to theoretically fit a cubic model (Koelsch and Labuza, 1992).

As has been explained before, the developed food quality loss functions are based on the stated assumptions and do not necessarily reflect true reaction mechanisms. In a case for which the assumptions are not applicable or the actual mechanism is very complex due to side reactions or limiting intermediate steps, Equations 9.9 and 9.10 may not sufficiently model the measured changes. One approach in this case is to develop a semiempirical kinetic/mathematical model that effectively represents the experimental data. Preferably the model would still have the general form of the quality function of Equation 9.14, where Q(A) can obtain any form other than the typical ones of Table 9.1. The steps for building such a model are described by Saguy and Karel (1980). Multivariable linear models, polynomial equations, or nonlinear models can be defined and their fit to the data can be tested with computer-aided multiple-linear, polynomial, or nonlinear regressions. Empirical equations modeling the effect of different composition or process parameters can be derived from statistical experimental designs like the surface response methods (Thompson, 1983).

A special category of reactions important in foods, the enzymatic reactions, are usually modeled by the Michaelis-Menten equation. This is a reaction rate function based on the steady-state enzyme kinetics approach (Engel, 1981). For an enzymatic system, with no inhibition, the rate equation has the form

$$r_A = \frac{k[A]}{K_m + [A]} \tag{9.16}$$

where A is the substrate, $k = k_o(e)$ is proportional to the enzyme (e) concentration (k is usually called v_{max} in biochemical terminology) and K_m is a constant ($r_A = 0.5\,k$ for $[A] = K_m$). When $(A) \gg K_m$, the equation reduces to a zero order reaction, $r_A = k$. This is often the case in foods with uniformly distributed substrate in excess and with small amounts of enzyme, e.g., lipolysis of milk fat. When $K_m \gg (A)$, the equation reduces to first order, $r_A = (k/K_m)\,[A]$. This occurs in foods where the enzymes are highly compartmentalized and have limited access to the substrate or where generally the substrate limits the reaction, e.g., browning of fruit and vegetable tissue due to polyphenolase activity. Thus, a large portion of enzymatic reactions in foods can be handled as zero or first order systems. When a Michaelis-Menten rate equation has to be used, the Lineweaver-Burk transformation is used that allows the estimation of the parameters by linear regression

$$\frac{1}{r_A} = \frac{K_m}{k}\frac{1}{[A]} + \frac{1}{k} \tag{9.17}$$

The described initial rate measurement differential method is usually applied for the kinetic analysis of enzymatic reactions.

When one of the quality deterioration models previously described is used its applicability usually is limited to the particular food system that was studied. Since the model often does not correspond to the true mechanism of the reaction, a compositional change in the system may have an effect in the rate of loss of the quality parameter that cannot be predicted by it.

Thus, any extrapolation of kinetic results to similar systems should be done very cautiously. In certain cases, an in-depth kinetic study of specific reactions important to food quality is desirable, so that the effect of compositional changes can be studied. In these cases the actual mechanism of the reactions is sought to be revealed if possible. Such studies are usually done in model systems, rather than in actual foods, so that the composition and the relative concentrations of the components are closely controlled and monitored. They are particularly useful in cases where the toxicological or nutritional impact of the accumulation of breakdown products, including intermediate or side step reactions, is examined. Examples of such studies are the multistep breakdown of the sweetener aspartame (Stamp, 1990) and the two step reversible isomerization of β-carotene (Pecek et al., 1990). In the first case a complex statistical analysis using a nonlinear multiresponse method was employed where all the reaction steps for the true reaction mechanism are expressed in the form of a linear system of differential equations. With this method, all the experimental data is utilized simultaneously to determine the kinetic parameters for each degradation step by a multidimensional nonlinear regression analysis of the system of differential equations. These parameters can be used to predict the concentration of each degradation product as a function of time at any temperature.

9.2.2 EFFECT OF ENVIRONMENTAL FACTORS

9.2.2.1 Temperature

The hitherto outlined approaches to kinetically define a food system include the underlying assumption that the environmental conditions are constant. A shelf-life loss kinetic model is characteristic not only of the studied food but equally important to the set of environmental conditions of the experiment. These conditions can determine the reaction rates and have to be defined and monitored during kinetic experiments.

Since most enviromental factors do not remain constant, the next logical step would be to expand the models to include them as variables especially the ones that strongly affect the reaction rates and are more prone to variations during the life of the food. The practical approach is to model the effect into the apparent reaction rate constant, i.e., expressing k of Equation 9.9 as a function of E_j: $k = k(E_j)$.

Of the aforementioned environmental factors namely temperature, relative humidity, total and partial pressure of different gases, light, and mechanical stresses, the factor most often considered and studied is temperature. This is justifiable because temperature not only strongly affects reaction rates but is also directly imposed on the food externally (direct effect of the environment), the other factors are at least to some extent controlled by the food packaging.

The history of the fundamental thermodynamic reasoning in developing models of temperature effect on reactions (Van't Hoff, 1884, Hood, 1885, and Arrhenius, 1889) has been reviewed by Bunher (1974). The most prevalent and widely used model is the Arrhenius relation, derived from thermodynamic laws as well as statistical mechanics principles where

$$\frac{\partial \ln K_{eq}}{\partial (1/T)} = -\frac{\Delta E^o}{R} \qquad (9.18)$$

The Arrhenius relation, developed theoretically for reversible molecular chemical reactions, has been experimentally shown to hold empirically for a number of more complex chemical and physical phenomena (e.g., viscosity, diffusion, sorption). Food quality loss reactions described by the aforementioned kinetic models have also been shown to follow an Arrhenius behavior with temperature. For m^{th} order systems shown in Table 9.1 the reaction rate constant is a function of temperature (with the remaining E_j factors assumed constant) given by the following equation, directly obtainable from Equation 9.18 with k in place of K_{eq}

$$k = k_A \exp\left(-\frac{E_A}{RT}\right) \tag{9.19}$$

with k_A the Arrhenius equation constant and E_A the excess energy barrier that factor A needs to overcome to proceed to degradation products (or B to form), generally referred to as *activation energy*. In practical terms it means that if values of k are available at different temperatures and lnk is plotted against the reciprocal absolute temperature, $1/T$, a straight line is obtained with a slope of $-E_A/R$.

$$\ln k = \ln k_A - \frac{E_A}{R}\left(\frac{1}{T}\right) \tag{9.20}$$

If the rate constants k_2, and k_1 at two temperatures T_2 and T_1 are known, the Arrhenius parameters can be calculated by the equations

$$E_A = \ln\left(\frac{k_2}{k_1}\right)\frac{R\,T_1\,T_2}{T_2 - T_1} \tag{9.21}$$

and

$$k_A = k_1^{\left(\frac{T_1}{T_1 - T_2}\right)} k_2^{\left(\frac{T_2}{T_2 - T_1}\right)} \tag{9.22}$$

In practice, since there is experimental error involved in the determination of the values of k calculations of E_A from only two points will give a substantial error. The precision of activation energy calculated from Equation 9.21 is examined by Hills and Grieger-Block (1980). Usually, the reaction rate is determined at three or more temperatures and k vs. $1/T$ is plotted in a semilog graph or a linear regression fit and Equation 9.20 is employed.

It should be pointed out that there is no explicit reference temperature for the Arrhenius function as expressed in Equation 9.19. The temperature 0K, at which k would be equal to k_A is implied. Alternatively to Equation 9.19 it is often recommended that a reference temperature is chosen corresponding to an average of the temperature range characteristic of the described process. For most storage applications, 300K is such a typical temperature, whereas for thermal processes 373.15K (100.0°C) is usually the choice. The modified Arrhenius equation would then be written as

$$k = k_{ref} \exp\left(-\frac{E_A}{R}\left[\frac{1}{T} - \frac{1}{T_{ref}}\right]\right) \tag{9.23}$$

where k_{ref} the rate constant at the reference temperature T_{ref}. Respectively, Equation 9.20 is modified to

$$\ln k = \ln k_{ref} - \frac{E_A}{R}\left[\frac{1}{T} - \frac{1}{T_{ref}}\right] \tag{9.24}$$

The above transformation is critical for enhanced stability during numerical integration and parameter estimation. Additionally, by using a reference reaction rate constant, besides

giving the constant a relevant physical meaning, one signals the applicability of the equation within a finite range of temperatures enclosing the reference temperature and corresponding to the range of interest. Indeed, as it will be discussed further in this section the Arrhenius equation may not be uniformly applicable below or above certain temperatures, usually connected with transition phenomena.

When applying regression techniques statistical analysis is again used to determine the 95% confidence limits of the Arrhenius parameters. If only three k values are available, the confidence range is usually wide. To obtain meaningfully narrow confidence limits in E_A and k_A estimation, rates at more temperatures are required. An optimization scheme to estimate the number of experiments to get the most accuracy for the least possible amount of work was proposed by Lenz and Lund (1980). They concluded that five or six experimental temperatures are the practical optimum. If one is limited to three experimental temperatures a point-by-point method or a linear regression with the 95% confidence limit values of the reaction rates included will give narrower confidence limits for the Arrhenius parameters (Labuza and Kamman, 1983).

Alternatively, a multiple linear regression fit to all concentration vs. time data for all tested temperatures, by eliminating the need to estimate a separate A_o for each experiment and thus increasing the degrees of freedom, results in a more accurate estimation of k at each temperature (Haralampu et al., 1985). Since it is also followed by a linear regression of lnk vs. 1/T, it is a two-step method as the previous ones.

One step methods require nonlinear regression of the equation that results by substitution of Equations 9.19 or 9.23 in the equations of Table 9.1. For example, for the first order model the following equations are derived

$$A = A_o \exp\left[-k_A\, t \exp\left(\frac{-E_A}{RT}\right)\right]$$
(9.25)

or

$$A = A_o \exp\left\{-k_{ref}\, t \exp\left(-\frac{E_A}{R}\left[\frac{1}{T} - \frac{1}{T_{ref}}\right]\right)\right\}$$
(9.26)

These equations have as variables both time and temperature, the nonlinear regression gives simultaneous estimates of A_o, k_A (or k_{ref}) and E_A/R (Haralampu et al., 1985; Arabshahi and Lund, 1985). Experimental data of concentration vs. time for all tested temperatures are used, substantially increasing the degrees of freedom and hence giving much narrower confidence intervals for the estimated parameters. The use and the statistical benefits of employing a one step method were demonstrated for computer simulated food degradation data, following first order kinetics by Haralampu et al. (1985) and for actual data for nonenzymatic browning of whey powder (zero order model) and for thiamin loss in an intermediate moisture model system (first order model) by Cohen and Saguy (1985). In this method, the Arrhenius parameter's estimates were judged on the size of the joint confidence region at 90%. The joint confidence region is an ellipsoid in which the true parameters probably exist together at a specified confidence level. The extremes of the 90% confidence ellipsoid region do not correspond to the 95% confidence intervals (derived from a t-test) for the individual parameters. Since experience shows that E_A and lnk_{ref} are highly correlated, the ellipsoid is thus a more accurate representation of the confidence region (Draper and Smith, 1981).

The confidence region may be constrtucted by considering both the variance and covariance of the parameters' estimates, and by assuming that the estimates are from a bivariate normal distribution. The confidence contours for a nonlinear regression creates a deformed

ellipsoid. The complexity of the computation hampers its application as a routine statistical test. However, the appropriate extreme points of the confidence region could be derived using a computer program (Draper and Smith, 1981) which incorporates approximation for a nonlinear regression

$$S = \left\{ 1 + \frac{N_p}{n - N_p} \mathbf{F}\left[N_p, n - N_p, (1-q)\right] \right\} SS \tag{9.27}$$

where f is the fitted nonlinear model, SS is the nonlinear least square estimate of the fitted model, i.e., $SS = \Sigma(A_i - f)^2$ for i = 1 to n, n is the number of data points, N_p the number of parameters derived from the nonlinear least squares, $100(1 - q)\%$ the confidence level and **F** the F-statistics. This method allows a reliable derivation of the confidence limits of the determined parameters that can affect the application of the kinetic data for shelf-life prediction and product design and demonstrates the caution that should be exercised when kinetic data is compared. Its main disadvantage is the complexity of calculations and the need for special software.

In case there are large differences in the calculated confidence intervals for the reaction rates at the different temperatures, this variability can be incorporated into the linear regression of lnk vs. 1/T by using weighted regression analysis. Arabshahi and Lund (1985) proposed appropriate regression weight factors that can be used in this case. A weighted nonlinear least squares method was developed that involves weighing of all the individual concentration measurements (Cohen and Saguy, 1985). This method requires a large increase in the number of calculations and it was concluded that its use was not justified, except in the case of substantial skewness of the standardized residuals obtained from the unweighted nonlinear least squares method.

Estimation of the Arrhenius parameters as described hitherto, requires isothermal kinetic experiments at least at three temperatures. Alternatively, a single nonisothermal experiment can be conducted. During this experiment the temperature is changed according to a predetermined function, T(t), such as a linear function. From Equations 9.9 and 9.19

$$r_A = k_A \exp\left[\frac{-E_A}{R} \frac{1}{T(t)}\right][A]^m \quad \text{or} \quad \ln r_A = \ln k_A + m \ln[A] - \frac{E_A}{R} \frac{1}{T(t)} \tag{9.28}$$

The rate r_A is determined by the differential method and the parameters k_A, m, and E_A through a multiple linear regression. Usually m is set as either zero or one. The second approach uses a nonlinear regression on the integrated form of Equation 9.28, which for a first order reaction is:

$$A = A_o \exp\left[-k_A \int_0^t \exp\left[\frac{-E_A}{R} \frac{1}{T(t)}\right] dt\right] \tag{9.29}$$

The integral is calculated numerically (Nelson, 1983). The nonisothermal approach requires very good temperature control and small experimental error in the concentration measurements. Yoshioka et al. (1987) in a statistical evaluation showed that a larger number of samples need to be measured to a higher reactant conversion than the isothermal method. The nonisothermal approach is very sensitive to experimental error in concentration measurements. Even at the precision level of 2%, the one step isothermal method with experiments at three temperatures gave better accuracy in the estimation of the Arrhenius parameters than

TABLE 9.3
Q_{10} Dependence on E_A and Temperature

E_A (kJ/mol)	Q_{10} at 4°C	at 21°C	at 35°C	Reactions in E_A range
50	2.13	1.96	1.85	Enzymic, hydrolytic
100	4.54	3.84	3.41	Nutrient loss, lipid oxidation
150	9.66	7.52	6.30	Nonenzymatic browning

the nonisothermal method with a linearly increasing temperature in the same range and for the same total number of data points. Another usually overlooked factor is the nonuniform temperature within the samples due to the unsteady state heat transfer occurring during the nonisothermal experiment (Labuza, 1984). The nonisothermal method also does not allow for recognition of possible deviation of the reaction from an Arrhenius behavior above or below a certain temperature that sometimes occurs in foods.

Temperature dependence has been traditionally expressed in the food industry and the food science and biochemistry literature as Q_{10} the ratio of the reaction rate constants at temperatures differing by 10°C or the change of shelf-life θ_s when the food is stored at a temperature higher by 10°C. The majority of the earlier food literature reports endpoint data rather than complete kinetic modeling of quality loss. The Q_{10} approach in essence introduces a temperature dependence equation of the form

$$k(T) = k_o\, e^{bT} \quad \text{or} \quad \ln k = \ln k_o + bT \tag{9.30}$$

which implies that if $\ln k$ is plotted vs. temperature (instead of $1/T$ of the Arrhenius equation) a straight line is obtained. Equivalently, $\ln\theta_s$ can be plotted vs. temperature. Such plots are often called shelf-life plots, where b is the slope of the shelf-life plot and k_o is the intercept. The *shelf-life plots* are true straight lines only for narrow temperature ranges of 10 to 20°C (Labuza, 1982). For such a narrow interval, data from an Arrhenius plot will give a relatively straight line in a shelf-life plot, i.e., Q_{10} and b are functions of temperature

$$\ln Q_{10} = 10\,b = \frac{E_A}{R}\frac{10}{T\,(T+10)} \tag{9.31}$$

The variation of Q_{10} with temperature for reactions of different activation energies is shown in Table 9.3.

Similarly to Q_{10} the term Q_A is sometimes used. The definition of Q_A is the same as Q_{10} with 10°C replaced by A°C

$$Q_A = Q_{10}^{A/10} \tag{9.32}$$

Another term used for temperature dependence of microbial inactivation kinetics in canning and sometimes of food quality loss (Hayakawa, 1973) is the z-value. The value of *z* is the temperature change that causes a 10-fold change in the reaction rate constant. As in the case of Q_{10}, *z* depends on the reference temperature (Ramaswamy et al., 1989). It is related to b and E_A by the following equation

$$z = \frac{\ln 10}{b} = \frac{(\ln 10)\, R\, T^2}{E_A} \tag{9.33}$$

Other forms of the k(T) function have been proposed (Kwolek and Bookwalter, 1971) like linear, power, and hyperbolic equations, but over a wide range of temperatures, the Arrhenius equation gave as good or better correlation.

Eyring's equation was utilized in the pharmaceutical industry (Kirkwood, 1977)

$$\ln k = \ln(k_B/h) + S/R - H/RT + \ln T \tag{9.34}$$

where H is the heat of activation, h is the Planck constant, k_B is the Boltzmann constant and S is the entropy.

Eyring's equation was applied to calculate the enthalpy/entropy compensation in food reactions (Labuza, 1980a). Theoretical equations based on the collision theory and the activated complex theory that introduce an additional temperature term to the Arrhenius relation were also discussed by Labuza (1980a). An example of such an equation is:

$$k = k'\, T^n \exp\!\left(-\frac{E_A}{RT}\right) \tag{9.35}$$

where k' the preexponential factor and n a constant with a value between 0 and 1. It was concluded that the contribution of these terms is negligible at the temperatures relevant to food processing and storage.

Nevertheless, there are factors relevant to food and food quality loss reactions that can cause significant deviations from an Arrhenius behavior with temperature (Labuza and Riboh, 1982). Phase changes are often involved. Fats may change to the liquid state contributing to the mobilization of organic reactants or vice-versa (Templeman et al., 1977). In frozen foods the effect of phase change of the water of the food is very pronounced in the immediate subfreezing temperature range. Generally, as freezing proceeds and the temperature is lowered, the reaction rate in nonenzymatic frozen systems follows a common pattern: (a) just below the initial freezing point the rate increases (in an almost discontinuous fashion) to values well above those obtained in the supercooled state at the same temperature; (b) passes through a maximum; and (c) finally declines at lower temperatures (Fennema et al., 1973). This behavior is shown schematically in an Arrhenius plot in Figure 9.3. The rate increase is especially notable for reactants of low initial concentration. The rate enhancement induced by freezing is related basically to the freeze-concentration effect. This enhancement is prominent in the temperature zone of maximum ice formation. The width of this zone will depend on the type of food but generally will be in the range of –1 to –10°C. Experimental studies showing this negative temperature effect were reviewed by Singh and Wang (1977). A dramatic demonstration of the described pattern was shown by Poulsen and Lindelov (1975) who studied the reaction rate between myosin and malonaldehyde in the range of 45 to –40°C. Enzymatic reactions also deviate from the Arrhenius behavior in the immediate subfreezing range.

Other phase change phenomena are also important. Carbohydrates in the amorphous state may crystallize at lower temperatures, creating more free water for other reactions but reducing the amount of available sugars for reaction (Kim et al., 1981). A characteristic case is the phenomenon of staling of bread (Zobel, 1973). Retrogradation of the amylopectin and a redistribution of moisture between starch and gluten have been implicated in staling. Staling shows a negative temperature effect between 4 and 40°C, having the maximum rate at 4°C. A number of studies, using a variety of textural indices, were reviewed by Labuza (1982).
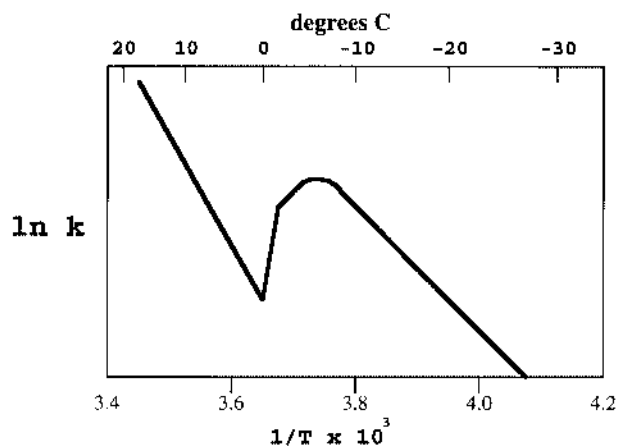
FIGURE 9.3 Anomalies in Arrhenius behavior. Typical effect of subfreezing temperatures to reaction rates.
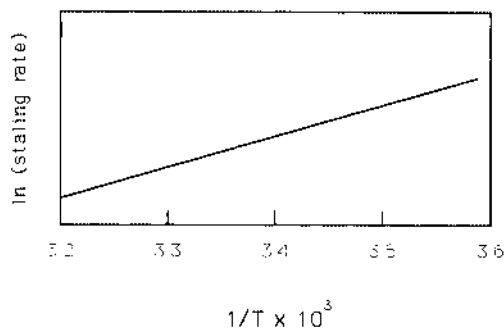
FIGURE 9.4 Anomalies in Arrhenius behavior. Effect of temperature on rate of bread staling.

A typical bread staling Arrhenius plot is shown in Figure 9.4 with an average "negative E_A" of –9 kcal/mol.

Glass transition phenomena are also implicated in systems that, at certain temperature ranges, deviate significantly from an Arrhenius behavior. Certain processing conditions or drastic changes in storage conditions, such as rapid cooling and solvent removal, result in formation of metastable glasses, especially in carbohydrate-containing foods (MacKenzie, 1977; Roos and Karel, 1990; Levine and Slade, 1988). Examples of such foods include spray dried milk (Bushill et al., 1965), boiled sweets (White and Cakebread, 1969), frozen solutions (MacKennzie, 1977), whey powder and dehydrated vegetables (Buera and Karel, 1993).

Glass transition theory applicable to amorphous polymers has been used for food polymers and compounds of smaller molecular weight. Amorphous glasses undergo a glass to rubber transition at a temperature T_g. Above the glass transition temperature, T_g, there is a drastic decrease in the viscosity (from an order of 10^{12} to 10^3 Pa.s) (Ferry, 1980) and a substantial increase in the free volume, i.e., the space which is not taken by polymer chains themselves. This results in a greater polymer chain mobility and faster reactant diffusion. Often the dependence of the rate of a food reaction on temperature, when Tg is crossed, cannot be described with a single Arrhenius equation. A change of slope (i.e., in activation energy) is observed at T_g. Furthermore, above T_g, in the rubbery state, the activation energy may exhibit a temperature dependency, expressed as a gradually changing slope in the Arrhenius plot. Williams, Landel, and Ferry (1955) introduced the WLF equation to empir-

ically model the temperature dependence of mechanical and dielectric relaxations within the rubbery state. It has been proposed (Slade et al., 1989) that the same equation may describe the temperature dependence of chemical reaction rates within amorphous food matrices above T_g. In diffusion controlled systems where diffusion is free volume dependent, reaction rate constants can be expressed as functions of temperature by the WLF equation (Sapru and Labuza, 1992):

$$\log\left(\frac{k_{ref}}{k}\right) = \frac{C_1\left(T - T_{ref}\right)}{C_2 + \left(T - T_{ref}\right)} \tag{9.36}$$

where k_{ref} the rate constant at the reference temperature T_{ref} ($T_{ref} > T_g$) and C_1, C_2 are system-dependent coefficients. Williams et al. (1955), for $T_{ref} = T_g$, using experimental data for different polymers, estimated average values of the coefficients: $C_1 = -17.44$ and $C_2 = 51.6$. In various studies these are used as universal values to establish the applicability of WLF equation for different systems. This approach can be misleading (Ferry,1980; Peleg, 1992; Buera and Karel, 1993) and effort should be made to obtain and use system specific values.

Alternative approaches for accessing the applicability of the WLF model and calculating the values of C_1 and C_2 have been evaluated (Nelson, 1993; Buera and Karel, 1993). Equation 9.36 can be rearranged into an equation of a straight line. Thus the plot of $\left[\log\dfrac{k_{ref}}{k}\right]^{-1}$ vs. $\dfrac{1}{T - T_{ref}}$ is a straight line with a slope equal to C_2/C_1 and an intercept of $1/C_1$. If T_g is known, the WLF constants at T_g can be calculated (Peleg, 1992)

$$C_{1g} = \frac{C_1 C_2}{C_2 + T_g - T_{ref}} \quad \text{and} \quad C_{2g} = C_2 + T_g - T_{ref} \tag{9.37}$$

These values can be compared to the aforementioned average WLF coefficients.

When Tg and reaction rate data at many higher temperatures are available, k_g, C_1, and C_2 can be estimated from Equation 9.36 using nonlinear regression methodology.

Ferry (1980) proposed an additional approach for verifying the WLF equation and determining the coefficients. A temperature T_∞, at which the rate of the reaction is practically zero, is used. T_∞ can be approximated by the difference between T_{ref} and C_2, i.e., $T_\infty = T_{ref} - C_2$. Rearranging Equation 9.36

$$\log\left(\frac{k_{ref}}{k}\right) = \frac{C_1\left(T - T_{ref}\right)}{T - T_\infty} \tag{9.38}$$

i.e., if T_∞ is chosen correctly, a plot of $\log(k/k_{ref})$ vs. $(T - T_{ref})/(T - T_\infty)$ is linear through the origin with slope equal to C_1. $T_g - 50°C$ was proposed as a good initial estimate of T. Buera and Karel (1993) used this approach to test the applicability of WLF equation in modeling the effect of temperature on the rate of nonenzymatic browning, within several dehydrated foods and carbohydrate model systems. Table 9.4 gives the calculated values of the coefficients of the WLF equation for the different systems at the used reference temperature as well as at T_g, for different moisture contents.

A number of recent publications debate the relative validity of the Arrhenius and WLF equations in the rubbery state namely in the range 10 to 100°C above T_g. This dilemma may very well be an oversimplification (Karel,1993). As mentioned above, processes affecting food quality that depend on viscosity changes (e.g., crystallization, textural changes) fit the WLF model. However, chemical reactions may be either kinetically limited, when $k \ll \alpha D$

TABLE 9.4
WLF Coefficients Determined for Several Foods and Model Systems

System	T_∞	T_{ref} (°C)	T_g (°C)	Moisture (g H_2O/g solid)	C_1	C_2	C_{1g}	C_{2g}
Apple	$T_g - 50$	55	22	0.014	8.79	83	14.59	50
			2	0.022	8.79	103	18.05	50
			–7	0.050	8.79	112	19.69	50
			–13	0.087	8.70	118	20.73	50
			–24	0.011	8.79	129	22.68	50
			–38	0.017	8.79	143	25.14	50
Cabbage	T_g-50	45	15	0.014	7.82	80	12.5	50
			5	0.021	7.82	90	14.07	50
			1	0.032	7.82	94	14.7	50
			–8	0.056	7.82	103	16.1	50
			–29	0.089	7.82	115	17.98	50
			–26	0.117	7.82	121	18.92	50
			–58	0.179	7.82	153	23.93	50
Carrot	$T_g - 50$	43	–5	0.054	7.44	98	14.58	50
			–20	0.062	7.44	103	15.33	50
			–15	0.080	7.44	108	16.07	50
Nonfat dried milk	$T_g - 100$	90	101	0.000	8.1	89	7.2	100
			65	0.012	8.1	125	10.14	100
			44	0.059	8.1	146	11.83	100
Nonfat dried milk	$T_g - 100$	90	50	0.030	6.8	140	9.52	100
			45	0.040	6.8	145	9.86	100
			40	0.050	6.8	150	10.2	100
Onion	$T_g - 50$	30	–8	0.056	8.8	88	15.9	50
			–20	0.089	8.8	100	18.1	50
			–58	0.189	8.8	138	24.5	50
Potato	$T_g - 65$	50	30	0.049	7.92	85	10.4	65
			20	0.094	7.92	95	11.6	65
			–5	0.150	7.92	120	14.6	65
			–15	0.200	7.92	130	15.84	65
Whey powder	$T_g - 100$	35	29	0.059	8.4	106	9.0	100
			18	0.080	8.4	117	9.9	100
Model sys1[a]	T_g-90	45	45	0.059	8.3	90	8.3	90
Model sys2[b]	T_g-10	55	40	0.073	6.93	135	7.8	120

Note: WLF = Williams, Landel, and Ferry. Data are reported at a reference temperature (C_1 and C_2) and transformed to correspond to $T_{ref} = T_g$ (C_{1g} and C_{2g})

[a] Composition: 99% poly(vinyl pyrrolidone), 0.5% glucose, 0.5% glycine.

[b] Composition: 98% poly(vinyl pyrrolidone), 1% xylose, 0.5% lysine.

Adapted from Buera, P. and Karel, M., 1993, *J. Food Proc. Preserv.* 17:13–41.

(where D the diffusion coefficient and α a constant independent of T), diffusion limited when $k \gg \alpha D$, or dependent on both when k and αD are of the same order of magnitude. In the latter case the effective reaction rate constant can be expressed as $\dfrac{k}{1 + k/\alpha D}$. k in most cases exibits an Arrhenius type temperature dependence and D has been shown in many studies to either follow the Arrhenius equation with a change in slope at T_g or to follow the WLF equation in the rubbery state and especially in the range 10 to 100°C above T_g. The value of
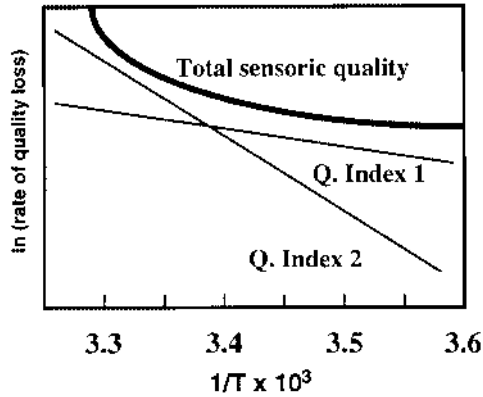
FIGURE 9.5 Typical temperature dependence of quality loss when reactions of different E_A contribute to total sensoric quality.
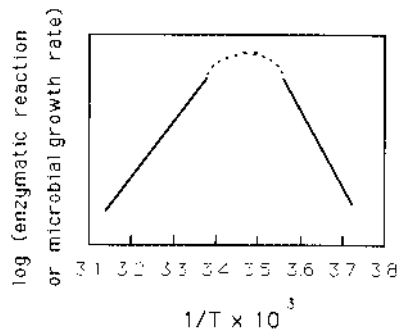
FIGURE 9.6 Typical temperature dependence curve of an enzymatic reaction or microbial growth.

the ratio $k/\alpha D$ defines the relative influence of k and D and determines whether the deteriorative reaction can be successfully modeled: (a) by a single Arrhenius equation for the whole temperature range of interest; (b) with an Arrenhius equation with a break in slope that occurs at T_g with a practically constant slope above T_g or (c) with a changing slope, in which case the WLF equation will be used for the range 10 to 100°C above T_g. In complex systems where multiple phases and reaction steps can occur, a successful fit to either model has to be considered as an empirical formula for practical use and not an equation explaining the mechanism or phenomenon.

When several reactions with different E_A are important to food quality, it is possible that each of them will predominantly define quality for a different temperature range. Thus, for example, if quality is measured by an overall flavor score, the quality change rate vs. $1/T$ will have a different slope in each of these regions. This is shown schematically in Figure 9.5. A typical example of such a behavior is quality loss of dehydrated potatoes where lipid oxidation and loss of fat soluble vitamins predominates up to 31°C and nonenzymatic browning and lysine loss above 31°C (Labuza, 1982).

The behavior of proteins at high enough temperatures whereby they denature and thus increase or decrease their susceptibility to chemical reactions depending upon the stereochemical factors that affect these reactions, is another factor that can cause non-Arrhenius behavior. For reactions that involve enzymatic activity or microbial growth the temperature dependence

plot shows a maximum rate at an optimum temperature, below and above which an Arrhenius type behavior is exhibited. This is demonstrated in Figure 9.6.

The study of the temperature dependence of microbial growth has lately been an area of increased activity. The described kinetic principles are applied to compile the necessary data for modeling growth behavior, in a multidisciplinary field coded *predictive microbiology* (Buchanan, 1993; McClure et al., 1994; McMeekin et al., 1993). For a temperature range below the optimum growth temperature either of the two simple equations, Arrhenius and square root, sufficiently model the dependence for all practical purposes (Labuza et al., 1991). The two-parameter empirical square root model, proposed by Ratkowsky et al. (1982) has the form

$$\sqrt{k} = b\left(T - T_{min}\right) \tag{9.39}$$

where k is growth rate, *b* is slope of the regression line of $\sqrt{k}$ vs. temperature, and T_{min} is the hypothetical growth temperature where the regression line cuts the T axis at $\sqrt{k} = 0$. The relation between Q_{10} and this expression is

$$Q_{10} = \left(\frac{T - T_{min} + 10}{T - T_{min}}\right)^2 \tag{9.40}$$

Equations with more parameters to model growth (and lag phase) dependence through the whole biokinetic range were also introduced either based on the square root model (Ratkowsky et al., 1983) or the Arrhenius equation (Mohr and Krawiek, 1980; Scoolfield et al., 1981; Adair et al., 1989). They were reviewed and experimentally evaluated by Zwietering et al. (1991).

Traditionally the mathematical models relating the numbers of microorganisms to temperature have been divided into two main groups (Whiting and Buchanan, 1994). Those describing propagation or growth primarily refer to the lower temperature range, and those describing thermal destruction at lethal temperature range. Recently, a combined approach utilizing a single mathematical formula to describe both the propagation and destruction rate constant over the entire temperature range, from growth (k(T) > 0) to lethality was proposed (Peleg, 1995). The main applicability of such a model is to account for changes that take place at a temperature range where transition from growth to lethality occurs.

Finally, temperature can have an additional indirect effect by affecting other reaction determining factors, which will be discussed in the next section. A temperature increase, increases the water activity at the same moisture level or enhances the moisture exchange with the environment in cases of permeable packaging affecting the reaction rate. Reactions that are pH-dependent can be additionally affected by temperature change, since for many solute systems pH is a function of temperature (Bates, 1973). Solubility of gases, especially of oxygen, changes with temperature (25% decrease with every 10°C increase for O_2 in water) thus affecting oxidation reactions where the oxygen is limiting.

9.2.2.2 Effects of Other Environmental Factors

Moisture content and water activity (a_w) are the most important E_j factors besides temperature that affect the rate of food deterioration reactions. Water activity describes the degree of boundness of the water contained in the food and its availability to act as a solvent and participate in chemical reactions (Labuza, 1980b).
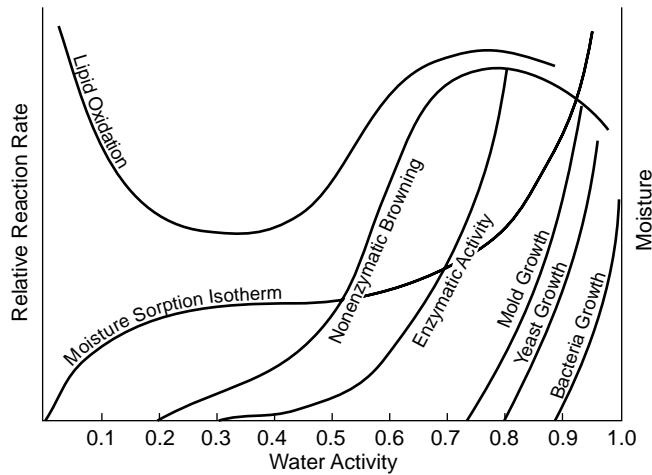
FIGURE 9.7 Global food stability map (Adapted from Labuza et al., 1969).

Critical levels of a_w can be recognized above which undesirable deterioration of food occurs. Controlling the a_w is the basis for preservation of dry and intermediate moisture foods (IMF). Minimum a_w values for growth can be defined for different microbial species. For example, the most tolerant pathogenic bacterium is *Staphylococcus aureus,* which can grow at a low a_w of 0.85 to 0.86. This is often used as the critical level of pathogenicity in foods. Beuchat (1981) gives minimum a_w values for a number of commonly encountered microorganisms of public health significance.

Textural quality is also greatly affected by moisture content and water activity. Dry, crisp foods (e.g., potato chips, crackers) become texturally unacceptable upon gaining moisture above the 0.35 to 0.5 a_w range (Katz and Labuza, 1981). IMF-like dried fruits and bakery goods, upon losing moisture below 0.5 to 0.7 a_w become unacceptably hard (Kochhar and Rossel, 1982). Recrystallization phenomena of dry amorphous sugars caused by reaching an a_w of 0.35 to 0.4 affect texture and quality loss reaction rates, as already mentioned.

Besides the specific critical a_w limits, a_w has a pronounced effect on chemical reactions. This effect plays a very important role in the preservation of IMF and dry foods. Generally, the ability of water to act as a solvent, reaction medium, and reactant increases with increasing a_w. As a result, many deteriorative reactions increase exponentially in rate with increasing a_w above the value corresponding to the monolayer moisture. This can be represented schematically in a global food stability map (Figure 9.7).

The critical a_w limits for microbial growth and the relative rates of reactions important to food preservation such as lipid oxidation and nonenzymatic browning can be seen in Figure 9.7. The underlying reasons for this behavior have been the subject of several studies (e.g., Taoukis et al., 1988a). Most reactions have minimal rates up to the monolayer value. Lipid oxidation shows the peculiarity of a minimum at the monolayer (m_o) with increased rates below and above it (Labuza, 1975; Quast et al., 1972).

The proposed theories that attempt to explain the effect of a_w on food deterioration reaction as well as ways to systematically approach and model this effect are discussed by Labuza (1980b). The moisture content and a_w can influence the kinetic parameters (k_A, E_A), the concentrations of the reactants, and, in some cases, even the apparent reaction order, n. Most relevant studies have modeled either k_A as a function of a_w (Labuza, 1980b) related to the change of mobility of reactants due to a_w dependent changes of viscosity, or E_A as a function of a_w (Mizrahi et al., 1970 a, b). The inverse relationship of E_A with a_w (increase in a_w decreases E_A and vice versa) could be theoretically explained by the proposed phenomenon of enthalpy-

entropy compensation. The applicability of this theory and data that support it have been discussed by Labuza (1980a).

Additionally, moisture content and a_w directly affect the T_g of the system. With increasing a_w, T_g decreases. As was discussed in the previous section, transverse of T_g and change into the rubbery state has pronounced effects, especially in texture and viscosity depended phenomena but also in reaction rates and their temperature dependence. It has been proposed for dehydrated systems that a critical moisture content/a_w alternative to the monolayer value of the BET sorption theory, is the value at which the dehydrated system has a T_g of 25°C (Roos, 1993). Consideration of these critical values contributes to explanations of textural changes occurring at distinct a_w and ambient temperatures (e.g., loss of crispness of snack foods above 0.3 to 0.5 or unacceptable hardness of IMF foods below 0.7 to 0.5) but their practical significance in a_w dependent chemical reactions is not straightforward and cannot be viewed isolated. Nelson and Labuza (1994) reviewed cases where the fundamental assumption that reaction rates within the rubbery state were dramatically higher than in the "stable" glassy state was not verified. In complex systems, matrix porosity, molecular size, and phenomena such as collapse and crystallization occurring in the rubbery state result in more complicated behavior. Both water activity and glass transition theory contribute to explain the relationship between moisture content and deteriorative reaction rates. It should be stressed though, that in contrast to the well-established moisture isotherm determination, i.e., the moisture-a_w relation, accurate determination of T_g as a function of moisture in a real food system is a difficult task and an area where much more work is needed. Furthermore, caution should be exercised when extrapolating state of the art knowledge to matters of safety. Water activity, used as an index of microbial stability, is a well-established and practical tool in the context of hurdle technology. Additional criteria related to T_g should be considered only after careful challenge and sufficient experimental evidence (Chirife and Buera, 1994).

Mathematical models that incorporate the effect of a_w as an additional parameter can be used for shelf-life predictions of moisture sensitive foods (Mizrahi et al., 1970a; Cardoso and Labuza, 1983; Nakabayashi et al., 1981). Such predictions can be applied to packaged foods in conjunction with moisture transfer models developed based on the properties of the food and the packaging materials (Taoukis et al., 1988b). Also accelerated shelf-life testing (ASLT) methods have been used to predict shelf-life at normal conditions based on data collected at high temperature and high humidity conditions (Mizrahi et al., 1970b).

The pH of the food system is another determining factor. The effect of pH on different microbial, enzymatic, and protein reactions has been studied in model biochemical or food systems. Enzymatic and microbial activity exhibits an optimum pH range and limits above and below which activity ceases, much like the response to temperature (Figure 9.6). The functionality and solubility of proteins depend strongly on pH, with the solubility usually being at a minimum near the isoelectric point (Cheftel et al., 1985), having a direct effect on their behavior in reactions.

Examples of important acid-base catalyzed reactions are nonenzymatic browning and aspartame decomposition. Nonenzymatic browning of proteins shows a minimum near pH = 3 to 4 and high rates in the near neutral-alkaline range (Feeney et al., 1975; Feeney and Whitaker, 1982). Aspartame degradation is reported at a minimum at pH = 4.5 (Holmer, 1984), although the buffering capacity of the system and the specific ions present have significant effect (Tsoumbeli and Labuza, 1991). Unfortunately very few studies consider the interaction between pH and other factors, e.g., temperature. Such studies (Bell and Labuza, 1991, 1994a; Weismann et al., 1993) show the significance of these interactions and the need for such information for the design and optimization of real systems. Significant progress in elucidating and modeling the combined effect to microbial growth of factors such as T, pH, a_w, or salt concentration has been achieved in the field of predictive microbiology (Ross and McMeekin, 1994; Rosso et al., 1995)

Gas composition also affects certain quality loss reactions. Oxygen affects both the rate and apparent order of oxidative reactions, based on its presence in limiting or excess amounts (Labuza, 1971). Exclusion or limitation of O_2 by nitrogen flushing or vacuum packaging reduces redox potential and slows down undesirable reactions. Further, the presence and relative amount of other gases, especially carbon dioxide, and second ethylene and CO, strongly affects biological and microbial reactions in fresh meat, fruit, and vegetables. The mode of action of CO_2 is partly connected to surface acidification (Parkin and Brown, 1982) but additional mechanisms, not clearly established, are in action. Quantitative modeling of the combined effect on microbial growth of temperature is an area of current research (Willcox et al., 1993). Different systems require different O_2:CO_2:N_2 ratios to achieve maximum shelf-life extension. Often excess CO_2 can be detrimental. Alternatively, hypobaric storage, whereby total pressure is reduced, has been studied. Comprehensive reviews of controlled and modified atmosphere packaging (CAP/MAP) technology are given by Kader (1986), Labuza and Breene (1989), and Farber (1991). Labuza et al. (1992) reviewed the efforts that have focused on kinetically modeling the CAP/MAP systems.

Currently experiments with very high pressure technology (1,000 to 10,000 atm) are being conducted. This hydrostatic pressure, applied via a pressure-transfering medium, acts without time delay and is independent of product size and geometry. It can be effective at ambient temperatures (Hoover, 1993). Key effects sought from high pressure technology include (Knorr, 1993): (a) inactivation of microorganisms; (b) modification of biopolymers (protein denaturation, enzyme inactivation or activation, degradation); (c) increased product functionality (e.g., density, freezing temperatures, texture), and (d) quality retention (e.g., color, flavor due to the fact that only nonvalent bonds are affected by pressure). Kinetic studies of changes occurring during high pressure processing and their effects on shelf-life of the foods are very limited and further research will be needed for this technology to be fully utilized.

To express the above-discussed effect of different factors in a simple mathematical form, the concept of the quality function can be used in a more general approach. Assuming that the quality of the food depends on i different quantifiable deterioration modes (quality factors), A_i, respective quality functions can be defined in analogy to Equation 9.14.

$$Q_i(A_i) = k_i \, t \qquad (9.41)$$

The rate constant k_i of each particular deterioration mode is a function of the aforementioned factors, namely

$$k_i = f_i\left(T, a_w, pH, P_{O_2}, P_{CO_2} \ldots\right) \qquad (9.42)$$

the values of which are, in turn, time dependent

$$T = T(t), a_w = a_w(t), pH = pH(t), P_{O_2} = P_{O_2}(t), P_{CO_2} = P_{CO_2}(t) \qquad (9.43)$$

The functions of Equation 9.42 incorporate the effects of storage conditions, packaging method and materials and biological activity of the system. Thus for variable conditions the rate constant is overall a function of time, i.e., $k_i = k_i(t)$. In that case the quality function value at a certain time is given by the expression

$$Q_i(A_i) = \int_0^t k_i \, dt \qquad (9.44)$$

If the lower acceptable value of the quality parameter A_i, noted as A_m, is known, then at time t the consumed quality fraction, Φ_{c_i}, and the remaining quality fraction, Φ_{r_i}, are defined as:

$$\Phi_{c_i} = \frac{Q_i(A_i) - Q_i(A_o)}{Q_i(A_m) - Q_i(A_i)} \tag{9.45}$$

$$\Phi_{r_i} = \frac{Q_i(A_m) - Q_i(A_i)}{Q_i(A_m) - Q_i(A_o)} \tag{9.46}$$

Knowledge of the value of Φ_{r_i} for the different deterioration modes allows the calculation of the *remaining shelf-life* of the food, θ_r, from the expression

$$\theta_r = \min\left[\Phi_{r_i}/k_i\right] \tag{9.47}$$

where the rate constants k_i are calculated for an assumed set of "remaining" constant conditions.

The above analysis sets the foundations of shelf-life prediction of a complex system under variable conditions. The major tasks in a scheme like this are recognition of the major deterioration modes, determination of the corresponding quality functions and estimation of Equation 9.42, i.e., the effects of different factors on the rate constant. The latter is a difficult task for real food systems. Most actual studies concern the effect of temperature and variable temperature conditions, with the expressed (or implied) assumption that the other factors are constant. Controlled temperature functions like square, sine, and linear (spike) wave temperature fluctuations can be applied to verify the Arrhenius model, developed from several constant-temperature shelf-life experiments. Labuza (1984) gives analytical expressions for Equation 9.44 for the above temperature functions using the Q_{10} approach. Similarly solutions can be given using the Arrhenius or square root models.

To systematically approach the effect of variable temperature conditions the concept of effective temperature, T_{eff}, can be introduced. T_{eff} is a constant temperature that results in the same quality change as the variable temperature distribution over the same period of time. T_{eff} is characteristic of the temperature distribution and the kinetic temperature dependence of the system. The rate constant at T_{eff} is analogously termed effective rate constant, and $Q_i(A_i)$ of Equation 9.44 is equal to $k_{eff} \, t$. If T_m and k_m are the mean of the temperature distribution and the corresponding rate constant, respectively, the ratio Γ is also characteristic of the temperature distribution and the specific system, where

$$\Gamma = \frac{k_{eff}}{k_m} \tag{9.48}$$

For some known characteristic temperature functions shown in Figure 9.8 analytical expressions for the Q_{10} and Arrhenius models are tabulated in Table 9.5.

From Γ of a variable temperature distribution the effective reaction rate and temperatures, k_{eff} and T_{eff}, and the value of the quality function for the particular deterioration mode are calculated. Comparison of this value to the experimentally obtained quality value, for variable temperature functions covering the range of practical interest is the ultimate validation of the developed kinetic models. This methodology was applied by Labuza and coworkers for various food reaction systems and then assessed for agreement or deviation from predicted
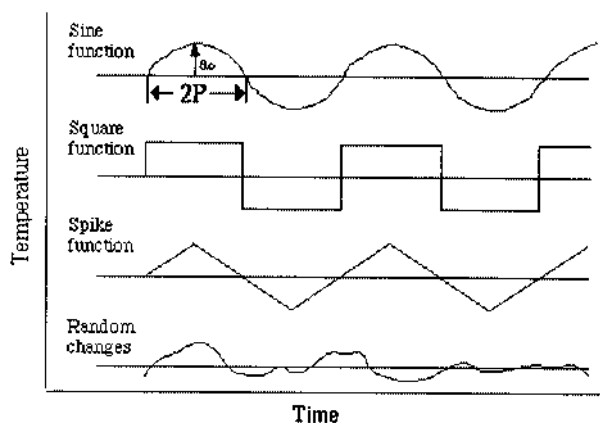
FIGURE 9.8 Characteristic fluctuating temperature distributions used to verify validity of kinetic models. a_o is the amplitude of the sine, square, and spike wave functions.

TABLE 9.5
Analytical Expressions for Calculation of Γ for Different Temperature Functions

Function	Q_{10} Approach	Arrhenius approach
Sine wave	$\Gamma = I_o(a_o b)$	$\Gamma \approx I_o\left[\dfrac{E_a a_o}{RT_m \langle T_m + a_o \rangle}\right]$
Square wave	$\Gamma = \dfrac{1}{2}\left[e^{a_o b} + e^{-a_o b}\right]$	$\Gamma = \dfrac{1}{2}\exp\left[\dfrac{E_A a_o}{RT_m(T_m + a_o)}\right] + \dfrac{1}{2}\exp\left[\dfrac{-E_A a_o}{RT_m(T_m - a_o)}\right]$
Spike wave	$\Gamma = \dfrac{e^{a_o b} - e^{-a_o b}}{2 a_o b}$	$\Gamma = \dfrac{\exp\left[\dfrac{E_A a_o}{RT_m(T_m + a_o)}\right] - \exp\left[\dfrac{-E_A a_o}{RT_m(T_m - a_o)}\right]}{2\dfrac{E_A a_o}{RT_m(T_m + a_o)}}$
Random	$\Gamma = \dfrac{\sum\limits_{j=0}^{n} e^{b T_j}\Delta t_j}{e^{b T_m}}$	$\Gamma = \dfrac{\sum\limits_{j=0}^{n} \exp\left(\dfrac{-E_A}{RT_j}\right)\Delta t_j}{\exp\left(\dfrac{-E_A}{RT_m}\right)}$

Note: $I_o(x)$ is a modified Bessel function of zero order. Its values can be calculated from an infinite series expansion, $I_o(x) = 1 + \dfrac{x^2}{2^{2+}}\dfrac{x^4}{2^2 4^2} + \dfrac{x^6}{2^2 4^2 6^2} + \ldots$, or found in mathematical handbooks (e.g., Tuma, 1988).

kinetic behavior (Berquist and Labuza, 1983; Kamman et al., 1981; Labuza et al., 1982; Riboh and Labuza, 1982; Saltmarch and Labuza, 1982; Taoukis and Labuza, 1989).

Alternatively the effect of variable temperature distribution can be expressed through an equivalent time (t_{eq}), defined as the time at which a reference temperature is resulting in the same quality change (i.e., same value of quality function) as the variable temperature. The

practicality of t_{eq} is that if the chosen T_{ref} is the suggested keeping temperature, e.g., 4°C for chilled products, it will directly give the remaining shelf-life at that temperature. Note that if the mean temperature is chosen as the reference temperature, $T_{ref} = T_m$, then $t_{eq}/t = \Gamma$.

Further a short mention of the equivalent point method is relevant. This approach has been used for evaluation and modeling of thermal processes (Nunes and Swartzel, 1990) and the response of time temperature indicators (TTI) (Fu and Labuza, 1993). The same methodology would apply for quality loss during the shelf-life of foods. Using the expression of the quality function

$$Q(A) = k_A \exp\left(-\frac{E_A}{RT}\right)t \qquad (9.49)$$

and if $Y = Q(A)/k_A$ then the above equation can be written as

$$\ln Y = \frac{-1}{RT}E_A + \ln t \qquad (9.50)$$

i.e., a plot of lnY vs. E_A of different food systems gives a straight line. For a particular variable time-temperature distribution it is proposed that a unique point (T_e, t_e) is defined from the slope and intercept of Equation 9.50. This would allow calculation of the quality change in a food system of known E_A from the measured change of two (at least) other food systems (or TTI) subjected to the same time-temperature conditions. It has been recently argued that this approach is only valid for isothermal conditions (Maesmans et al., 1995).

9.3 APPLICATION OF FOOD KINETICS IN SHELF-LIFE PREDICTION AND CONTROL

9.3.1 ACCELERATED SHELF-LIFE TESTING

Taking into account the described limitations and the possible sources of deviation, the Arrhenius equation can be used to model food degradation for a range of temperatures. This model can be used to predict reaction rates and shelf-life of the food at any temperature within the range, without actual testing. Equally important it allows the use of the concept of accelerated shelf-life testing (ASLT).

ASLT involves the use of higher testing temperatures in food quality loss and shelf-life experiments and extrapolation of the results to regular storage conditions through the use of the Arrhenius equation. That very substantially cuts down the testing time. A reaction of an average E_A of 90 kJ/mol may be accelerated by 9 to 13 times with a 20°C increase in the testing temperature, depending on the temperature zone. Thus an experiment that would take a year can be completed in about a month. This principle and the methodology in conducting effective ASLT are described by Labuza (1985), Labuza and Schmidl (1985), and in a publication by the Institute of Food Science and Technology, U.K. (IFST, 1993).

Designing a shelf-life test is a synthetic approach that requires sufficient understanding of all food-related disciplines, namely food engineering, food chemistry, food microbiology, analytical chemistry, physical chemistry, polymer science, and food regulations. The following steps outline the ASLT procedure:

1. Evaluate the microbiological safety factors for the proposed food product and process. Use of the Hazard Analysis Critical Control Point (HACCP) principles is a good approach to be followed from the design stage. If major potential problems

exist at this stage (i.e., CCPs exist that are difficult to control), the formula or process should be changed.

2. Determine from a thorough analysis of the food constituents, the process and the intended storage conditions, which biological and physicochemical reactions will significantly affect shelf-life and hence can be used as quality loss indices. A good knowledge of the system, previous experience and a thorough literature search are the tools to fulfill this step. If from this analysis it seems likely, without actual testing, that required shelf-life is not likely to be achieved because of serious quality loss potential, product design improvement must be considered.

3. Select the package to be used for the shelf-life test. Frozen, chilled, and canned foods can be packaged in the actual product packaging. Dry products should be stored in sealed glass containers or impermeable pouches at the product's specified moisture and a_w.

4. Define the test's storage temperatures. The following Table can be used a guideline.

Product type	Test temperatures (°C)	Control (°C)
Canned	25, 30, 35, 40	4
Dehydrated	25, 30, 35, 40, 45	−18
Chilled	5, 10, 15, 20	0
Frozen	−5, −10, −15	<−40

5. From the desired shelf-life at the expected storage and handling temperatures, and based on available information on the most likely Q_{10}, calculate testing time at each selected temperature. If no information is available on the expected Q_{10} value, minimum three testing temperatures should be used.

6. Decide the type and frequency of tests to be conducted at each temperature. A useful formula to determine the minimum frequency of testing at all temperatures based on the testing protocol at the highest temperature

$$f_2 = f_1 \, Q_{10}^{\Delta T/10} \tag{9.51}$$

where f_1 is the time between tests (e.g., days, weeks) at highest test temperature T_1; f_2 is the time between tests at any lower temperature T_2; and ΔT is the difference in degrees Celsius between T_1 and T_2. Thus, if a canned product is held at 40°C and tested once a month, then at 35°C (i.e., $\Delta T = 5$) and a Q_{10} of 3, the product should be tested at least every 1.73 months. Usually, more frequent testing is recommended, especially if the Q_{10} is not accurately known. Use of too long intervals may result in an inaccurate determination of shelf-life and invalidate the experiment. At each storage condition, at least six data points are required to minimize statistical errors; otherwise, the statistical confidence in the obtained shelf-life value is significantly reduced.

7. Plot the data as it is collected to determine the reaction order and to decide whether test frequency should be altered. It is common practice for the data not to be analyzed until the experiment is over and then it is recognized that changes in the testing protocol, affected early on, would have added significantly to the reliability of the results.

8. From each test storage condition, determine reaction order and rate, make the appropriate Arrhenius plot, and predict the shelf-life at the desired actual storage condition. Product can also be stored at the final condition, to determine its shelf-

life and test the validity of the prediction. However, in industry this is uncommon because of time and cost constraints. It is a much more effective and realistic practice to test the obtained predictive shelf-life model by conducting an additional test at a controlled variable temperature. The results will be compared to the predicted values according to Table 9.5.

Mathematical models that incorporate the effect of a_w as an additional parameter can be used for shelf-life predictions of moisture sensitive foods. Such predictions can be applied to packaged foods in conjunction with moisture transfer models developed based on the properties of the food and the packaging materials (Taoukis et al., 1988b). Also ASLT methods have been used to predict shelf-life at normal conditions based on data collected at high temperature and high humidity conditions (Mizrahi et al., 1970b). Weissman et al. (1993) propose a novel approach for ASLT whereby not only external conditions but concentration of selected reactants or catalysts are used to accelerate the storage test. When this is feasible high acceleration ratios can be achieved and testing times can be reduced significantly.

9.3.2 USE OF TIME TEMPERATURE INDICATORS AS SHELF-LIFE MONITORS

Generally a TTI can be defined as a simple, inexpensive device that can show an easily measurable, time-temperature dependent change that reflects the full or partial temperature history of a (food) product to which it is attached. TTI operation is based on mechanical, chemical, enzymatic, or microbiological systems that change irreversibly from the time of their activation. The rate of change is temperature dependent, increasing at higher temperatures in a manner similar to most physicochemical reactions. The change is usually expressed as a visible response, in the form of mechanical deformation, color development, or color movement. The visible reading thus obtained gives some information on the storage conditions that have preceded it. The ability of TTI to function as cumulative recorders of temperature history from their activation time to the time each response measurement is taken, make them useful for two types of applications.

TTI can be used to monitor the temperature exposure of individual food packages, cartons, or pallet loads during distribution up to the time they are displayed at the supermarket. By being attached to individual cases or pallets they can give a measure of the preceding temperature conditions at each receiving point. These points would serve as information gathering and decision making centers. The information gathered from all stations could be used for overall monitoring of the distribution system, thus allowing for recognition and possible correction of the more problematic links.

The second type of TTI application involves their use as quality monitors. With quality loss being a function of temperature history and with TTI giving a measure of that history, their response can presumably be correlated to the quality level of the food. If that can be achieved, TTI can be used in either (or both) of two ways. The first would be as an inventory management and stock rotation tool at the retail level. The approach used presently is the first in first out (FIFO) system according to which, products received first and/or with the closest expiration date on the label are displayed and sold first. This approach aims in establishing a "steady state" with all products being sold at the same quality level. The assumption is that all products have gone through uniform handling, thus quality is basically a function of time. The use of the indicators can help establish a system that does not depend on this unrealistic assumption. The objective will again be the reaching of a "steady state" situation with the least remaining shelf-life products being sold first. This approach could be coded LSFO (least shelf-life first out) (Labuza and Taoukis, 1990). The LSFO system could theoretically (although not proven) reduce rejected products and eliminate consumer dissatisfaction since the fraction of product with unacceptable quality sent into the distribution

system would be eliminated. Second, TTI attached on individual packaged products, can serve as dynamic or active shelf-life labeling instead of (or in conjunction with) open date labeling. The TTI would assure the consumers that the products were properly handled and would indicate remaining shelf-life. Use of TTI as "consumer indicators" is the ultimate goal of these systems.

A variety of TTI based on different physicochemical principles have been described by Byrne (1976) and Taoukis et al. (1991). Statistical correlations of TTI performance and product quality characteristics have been reported for a variety of perishable and frozen foods (Tinker et al., 1985; Chen and Zall, 1987; Wells and Singh, 1988). A general approach that allows the correlation of the response of a TTI to the quality changes of a food product of known deterioration modes, without actual simultaneous testing of the indicator and the food, was developed by Taoukis and Labuza (1989a). Three types of TTI commercially available were mathematically modeled using Arrhenius kinetics. One type is based on a time-temperature dependent diffusion of a dye along a wick, the second on a change of color due to a controlled enzymatic reaction and the third on development of color based on a solid state polymerization. A scheme was introduced that allows the correlation of the TTI response, X, to the quality index A of the food. X can be expressed as a function of time

$$F(X)_t = k\, t = k_I \exp\left(-E_A/RT\right)t \qquad (9.52)$$

where F(X) is the response function of the TTI, t is the time, and k the response rate constant; the constant k_I and the activation energy E_A are the Arrhenius parameters. For a TTI going through the same temperature distribution, T(t), as the monitored food, the value of $F(X)_t$ is known from the response X; T_{eff} can then be calculated from Equation 9.52 for $T = T_{eff}$. T_{eff} and knowledge of the kinetic parameters of deterioration of the food allows the evaluation of Q(A) and hence the quality loss of the product. The reliability of the TTI under variable temperature conditions was also assessed (Taoukis and Labuza, 1989b), using the relations of Table 9.5, and in general was judged satisfactory.

9.4 EXAMPLES OF APPLICATION OF KINETIC MODELING

9.4.1 KINETIC CALCULATIONS

Two highlighted examples are based on simulated model systems (Saguy and Cohen, 1990) describing a nonenzymatic browning reaction (Table 9.6; Figure 9.9) and thiamin retention (Table 9.7; Figure 9.10). The data was generated assuming the values of the energy of activation, E_A/R, the rate constant defined at a reference temperature, k_{ref} and the initial concentration A_o. A random error of ±5% was introduced to account for realistic experimental conditions and error. It is worth noting that in both examples, the reference temperature, T_{ref}, was chosen as 300 K. As pointed out previously, this transformation is important for improving the stability during numerical integration and for nonlinear parameter estimation. The transformation is also recommended since the parameters are highly colinear and are not easily directly regressed (Cohen and Saguy, 1985; Haralampu et al., 1985; Nelson, 1983).

Linear and nonlinear subroutines were utilized to derive the regression coefficients and analyses (BMDP1R and BMDPAR; Dixon, 1989).

1. Two-step method — The most common method to estimate the Arrhenius parameters is the classic successive two-steps ordinary linear least squares fit. The first step is the regression of the quality function (Table 9.1; i.e., A_o for zero-order, or $\ln(A_t/A_o)$ for a first-order reaction) vs. time, at each temperature, to estimate the rate constant k, and the initial concentration A_o. The estimation of A_o avoids bias

TABLE 9.6
Simulated Nonenzymatic Browning Data
as a Function of Storage Temperature

Time (days)	Nonenzymatic browning (OD/g solid) for temperatures			
	25°C	35°C	45°C	55°C
1			0.102	0.111
2				0.121
3				0.131
4				0.139
5	0.103	0.104	0.110	0.152
8				0.177
9				0.190
10			0.124	
11				0.238
15			0.137	
20	0.101	0.112	0.148	
25			0.158	
30	0.101	0.114	0.169	
40		0.123	0.194	
50		0.127	0.244	
60	0.106	0.133		
90	0.107	0.148		
105		0.155		
120	0.110			
135		0.160		
150	0.114			
180		0.175		
200	0.117			
275	0.127			
350	0.130			

Adapted from Saguy, I.S. and Cohen, E., 1990, Shelf-life prediction course notes.

in the determination, and provides an additional criterion of the adequacy of the model to describe the experimental data. A significant discrepancy between the estimated and experimental A_o suggests that a problem exists. The problem may be due to an inadequate kinetic model, large experimental error, insufficient number of data, etc. The second step is regression of $\ln(k)$ vs. $(1/T - 1/T_{ref})$ to obtain the estimated k_{ref} and E_A/R.

2. Non-linear least squares (one step method) — The nonlinear regression performs a single regression an all of the data points ($i = 1,...,n$), to estimate E_A/R, k_{ref} and A_o, without calculating the rates for each temperature.

3. Results — The Arrhenius parameters and the initial concentration derived using the two regression methods are summarized in Table 9.8 for nonenzymatic browning (zero order) and thiamin (first order) kinetics. The results show no substantial differences among the derived values of E_A/R and k_{ref} when Methods 1 and 2 were applied. Nevertheless, the values derived by Method 2 are closer to the actual values used for the simulation.
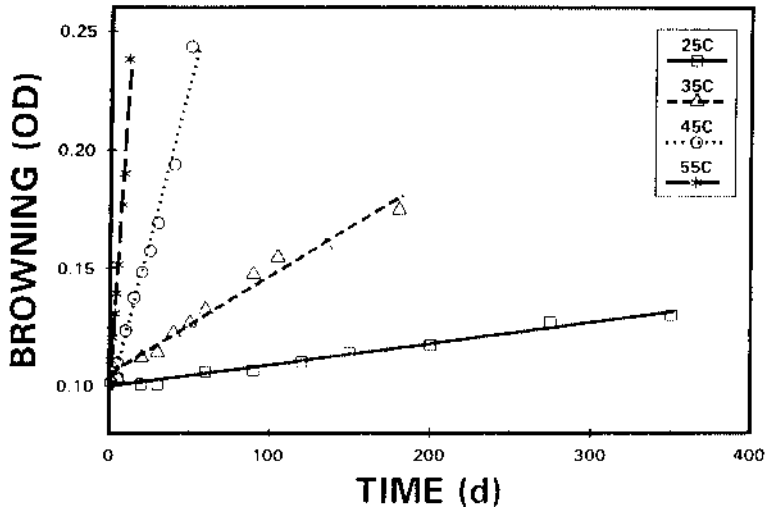
FIGURE 9.9 Nonenzymatic browning of a model system as a function of storage temperature (zero order reaction).

4. Confidence Contour — As mentioned before the confidence contour for E_A/R and k_{ref} can be derived using a computer program (Draper and Smith, 1981) which incorporates approximation for a nonlinear regression of Equation 9.27 (see page 375) where f is ???????? The values used for deriving the confidence contour for the nonlinear regression of the nonenzymatic browning data were as follows (see Table 9.8):

$$E_A/R = 15, 796, \; K_{ref} = 0.1.22, \; A_o = 0.97 \text{ from which}$$
$$SS = 1.331 \times 10^{-3} \text{ and } F(3.34, 90\%) = 2.27.$$

The fitted model, f, in Eq. 9.27, is replaced with the appropriate model based on the reaction order

zero-order

$$f = A_o \pm t \, k_{ref} \exp\left[-\frac{E_A}{R} \left(\frac{1}{T} - \frac{1}{T_{ref}} \right) \right] \tag{9.53}$$

first order

$$f = \exp\left\{ \ln(A_o) \pm t \, k_{ref} \exp\left[-\frac{E_A}{R} \left(\frac{1}{T} - \frac{1}{T_{ref}} \right) \right] \right\} \tag{9.54}$$

n-order ($n \neq 1$)

$$f = \left\{ A_o^{(n-1)} \pm (1-n) t \, k_{ref} \exp\left[-\frac{E_A}{R} \left(\frac{1}{T} - \frac{1}{T_{ref}} \right) \right] \right\}^{(1/(1-n))} \tag{9.55}$$

TABLE 9.7
Simulated Thiamin Retention for a Model System
as a Function of Storage Temperature
(First-Order Reaction)

Time (days)	Thiamin concentration (mg/g solid) for temperatures			
	25°C	35°C	45°C	55°C
1			96.70	93.40
2				85.47
5	98.22	0.104	89.44	69.92
8				54.60
10			80.98	47.50
12				42.29
15			72.36	33.43
20	98.16	0.112	66.72	
25			59.91	14.80
30	94.80	0.114	51.93	
40		0.123	44.11	
50		0.127		
60	92.56	0.133	28.62	
90	88.61	0.148		
105		0.155		
120	85.84			
135		0.160		
150	81.27			
180		0.175		
197	76.29			
257	70.55			
300	67.15			

Adapted from Saguy, I.S. and Cohen, E., 1990, Shelf-life prediction course notes.

The appropriate sign $\pm$ in the above equations should be chosen. For a reaction where concentration increases a positive should be used. For a depletion reaction the negative sign should be utilized.

The algorithm implemented to derive the confidence region is as follows:

1. Initial concentration is assumed constant and the estimated value derived by the nonlinear regression is utilized.
2. The confidence contour is derived by choosing values of E_A/R and k_{ref} which fulfill the equality expressed in Equation 9.27. Obviously, the value of E_A/R and k_{ref} are varied within the range of values that satisfies the inequality listed in Equation 9.27, i.e. $S \leq \{1 + \dfrac{N_p}{n - N_p} F[N_p, n-N_p, (1-q)]\}SS$. This trial and error procedure is normally carried out on a computer.
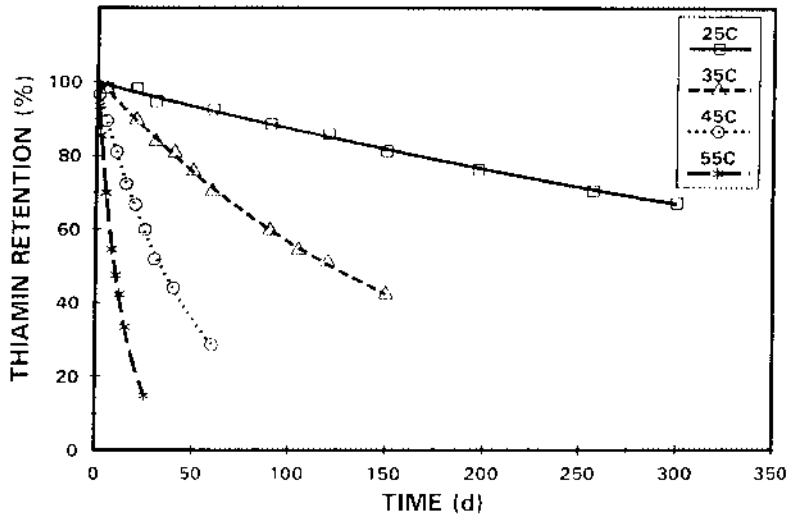
FIGURE 9.10 Thiamin retention of a model system as a function of storage temperature (first-order reaction).

TABLE 9.8
Effect of the Regression Method on the Arrhenius Parameters Derived for Nonenzymatic Browning (Zero-Order) and Thiamin Retention (First-Order Reaction)

Regression method	df[a]	$k \times 100$[b]				E_A/R	k_{ref}[c]	Ao[d]				Aoavr[e]
		25°C	35°C	45°C	55°C			25°C	35°C	45°C	55°C	
Nonenzymatic Browning												
						15000	0.135					0.100
Two steps	1	9.1	41.6	270.2	1157.9	16067	0.117	0.100	0.105	0.095	0.098	0.098
Nonlinear	19	—	—	—	—	15796	0.122	—	—	—	—	0.099
Thiamin retention												
						13000	0.00178					100.0
Two steps	2	0.133	0.580	2.065	7.588	13125	0.00175	99.7	100.4	99.2	101.5	100.2
Nonlinear	16	—	—	—	—	12985	0.00182	—	—	—	—	99.8

[a] Degrees of freedom.

[b] Reaction rate constant: OD/g/d or d^{-1} for a zero and first order reaction, respectively

[c] Units of k_{ref} at 300 K as in b.

[d] Derived initial concentration: OD/g or mg/g thiamin for a zero- and first-order reaction, respectively.

[e] Average of the derived initial concentration. Units as in d.

The derived confidence contour is depicted in Figure 9.11. It shows the span in the calculated values of E_A/R and k_{ref}. When comparing the confidence regions derived by the two regression methods, the nonlinear regression yields typically a smaller confidence region. This means that a better estimation of shelf-life prediction and simulation is possible (Cohen and Saguy, 1985; Haralampu et al., 1985).
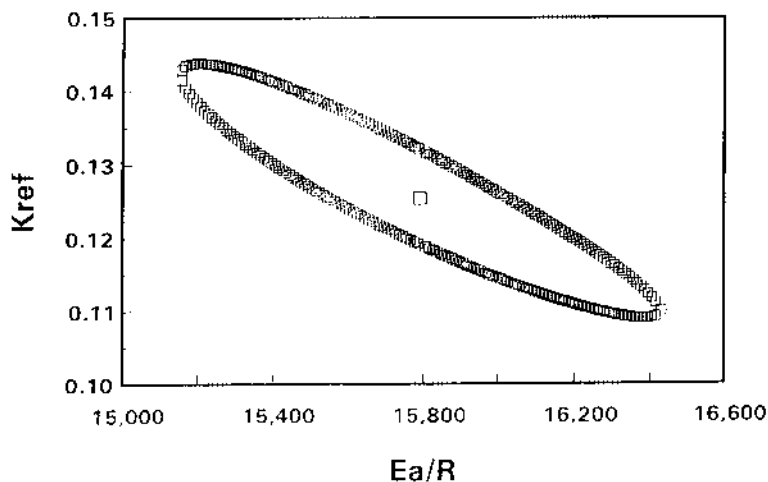
FIGURE 9.11 Joint confidence contour (90%) for E_A/R and k_{ref} derived by one-step nonlinear least squares method, for nonenzymatic browning.

9.4.2 EXAMPLES OF SHELF-LIFE MODELING OF FOOD PRODUCTS

The preceding kinetic calculation cases show how judiciously we should use the kinetic parameters we obtain from shelf-life experiments. In most practical cases the two step method is used due to its simplicity and convenience. The results should be understood as mean values with possibly large confidence limits, and treated as such. Nevertheless, the information obtained from carefully designed shelf-life testing, at three or more temperatures, is usually sufficient to allow derivation of satisfactory shelf-life predictive models. Further, two examples illustrate the use of ASLT principles and kinetic modeling. The first, a commercially sterilized, flavored dairy beverage, sweetened with the sweetener aspartame, is a case of straightforward use of these principles, as the quality function of the food is defined by a dominant, quantifiable quality index, aspartame. In contrast, the second example, of a complex food system of many antagonizing quality deterioration modes illustrates the multidisciplinary approach and the deep knowledge of the system required for effective shelf-life testing.

9.4.2.1 Aspartame Sweetened Chocolate Drink

This practical example is based on experimental data generated in studies by Bell and Labuza (1994b) and Bell et al. (1994). These studies were intended to evaluate the aspartame stability in commercially sterilized skim milk beverages of various compositions. There is a steadily growing market for nutritious, low calorie dairy products, and aspartame as a high intensity sweetener, without the controversy surrounding saccharin, can be a very desirable ingredient. However, at the inherent pH of milk (6.6) the rate of aspartame degradation is very high, reducing significantly the sensory shelf-life of the product. Quantifying and modeling the behavior of this dominant quality index would allow optimization of the product formulation and extension of shelf-life, possibly by slight alteration of the pH. For that purpose different commercially sterilized skim milks, sweetened with 200 ppm of aspartame and slightly buffered with citrates or phosphates to pH ranging from 6.38 to 6.67 were studied with regard to the aspartame degradation. Samples were stored at 5 temperatures from 0 to 30°C and triplicate samples were analyzed by high performance liquid chromotography (HPLC), at appropriately spaced time intervals (based on Equation 9.51) and an average Q_{10} value of 4 from the literature). Results of these experiments (at pH 6.67 with .008 M citrate) are listed in Table 9.9.

TABLE 9.9

Aspartame Degradation in a pH 6.67 Aseptic Dairy System

Time (h)	Aspartame concentration (ppm) for temperatures				
	30°C	20°C	10°C	4°C	0°C
10	181				
10	175				
10	182				
23	168	186			
23	166	172			
23	171	181			
38	130				
38	127				
38	141				
48	120	152			
48	101	160			
48	108	162			
78		172			
78		154			
78		153			
95			175		
95			173		
95			175		
121			168	189	198
121			168	180	195
121			167	186	194
143		146			
143		129			
143		150			
262		63	140	165	
262		73	134	165	
262		94	160	167	
455			114	132	159
455			96	117	152
455			118	121	155
599			93	110	136
599			87	104	136
599			91	88	134
694				80	130
694				95	119
694				86	113
767					115
767					109
767					103

In Figure 9.12a aspartame concentration (APM or A) is plotted vs. time at the 5 temperatures. The best linear fit of the form $Q(A) = kt$ was achieved for $Q(A) = \ln(A/A_o)$, i.e., first order kinetics (Figure 9.12b). All measurements were included in the statistical analysis (no averaging of the 3 samples per time) to increase the degrees of freedom and include the measurement spread in the model. Calculated rate constants and 95% C.I. are given in Table 9.10.
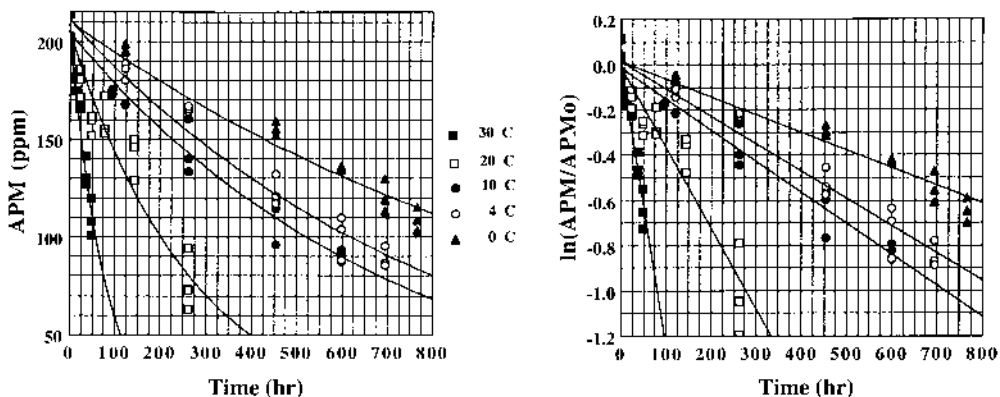
FIGURE 9.12 Plots of aspartame degradation and $Q(A)$ vs. at 5 temperatures in a 6.67 pH dairy system.

TABLE 9.10
Aspartame Degradation Reaction Rate Constants with
Confidence Intervals at Five Temperatures

Rate constant	30°C	20°C	10°C	4°C	0°C
$-k$ (h^{-1})	0.0125	0.00356	0.00138	0.00121	0.000790
±95% C.I.	±0.0013	±0.00046	±0.00010	±0.00009	±0.000062

To determine the Arrhenius parameters, $-k$ is plotted in a semilogarithmic scale vs. the inverse of absolute temperature (or $\ln(-k)$ vs. $1/T$). To increase the degrees of freedom and get a narrower confidence interval for the calculated parameters, the 95% C.I. for k is included (Figure 9.13). The Arrhenius plot gives by linear regression the values of $k_A = 3.163 \times 10^8$ h^{-1} and activation energy $E_A = 14,560$ cal/mol. The coefficient of determination, R^2, is 0.952 and the 95% CI 1,830 cal/mol.
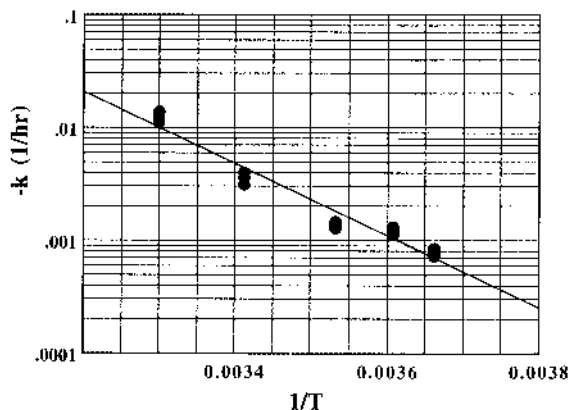
FIGURE 9.13 Arrhenius plot for aspartame degradation in a 6.67 pH dairy system.

The obtained kinetic information allows the prediction of aspartame degradation and thus the shelf-life of the product for any keeping temperature. Thus, if one assumes that the product is overcompensated with aspartame at 0 time to allow for acceptable product sweetness up to the point that half of the sweetener is degraded, the shelf-life at 4°C is approximately 4 weeks (670 h). Remaining shelf-life can also be calculated after exposure at any known temperature conditions. As an example, it is assumed that the aseptic milk product is exposed for 10 d to the temperature conditions shown in Figure 9.14. It is a nonspecific variable distribution with a mean temperature, T_m, of 7.1°C. The total aspartame degradation at the end of the 10 d can be calculated by integration. The value of ratio Γ (Equation 9.48 and Table 9.5 for random T) is determined as 1.0437. At T_m after 10 d, the remaining aspartame is 71.7% (Equation 9.25). Thus the actual aspartame level is calculated as 68.7%. This can be further translated to remaining shelf-life at constant 4°C of 307 h (12.8 d) (Equations 9.46 and 9.47). Note that if the product was assumed to have remained at 4°C at the first 10 d, the remaining shelf-life would be 18 d.
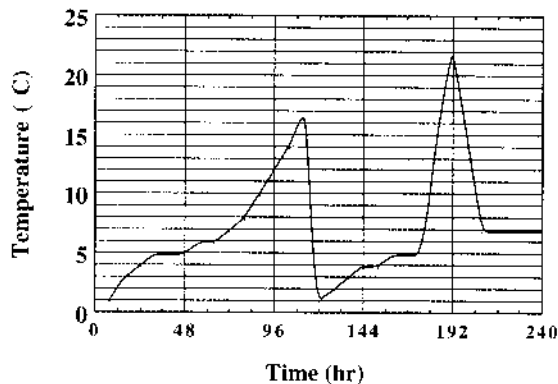
FIGURE 9.14 Variable temperature distribution of exposure of the aspartame sweetened product for the first ten d.

The practical value of the described analysis is that it allows a systematic approach to shelf-life prediction and optimization. Indeed similar results at the other studied pHs showed activation energies in the range of 14 to 18 kcal/mol and shelf-lifes that reached 60 d at the lower end of pH range of 6.38. This is a valuable indication of the approach to follow to increase shelf-life of a product under development. Note that although the experiments were conducted also at low temperatures, the satisfactory Arrhenius fit indicates that the alternative formulations can be studied only at the high temperatures, according to ASLT principles reducing the needed test time down to 200 h.

9.4.2.2   Case of Complex Food System

The preceding example is very helpful in illustrating the systematic approach for shelf-life prediction in foods where dominant and easily quantifiable quality indices can be recognized. In multicomponent complex food products the situation might be more difficult to put in quantifiable terms. Nevertheless, a careful approach of evaluating all the possible modes of deterioration, estimating the importance of their contribution under the expected conditions and the availability of methodology for measuring them, and finally using a judiciously developed testing protocol based on the principles developed in this chapter. The "ultimate" example of food where such an approach is needed is frozen pizza. All the aspects affecting the quality of this product were detailed by Labuza and Schmidl, 1985 and Labuza, 1985. Systems to be considered for monitoring chemical changes in pizza during frozen storage

include: total free fatty acids, specific volatile free fatty acids by gas chromatography (GC), peroxides, oxidative volatiles (e.g., hexanal) by GC, spice volatiles by GC, lysine, color (decrease in red color or increase in brown), sensory properties: taste and flavor, and nutrient loss such as vitamins A and C. Physical changes such as loss of crust crispness, loss of cheese functionality and meltability and development of in-package ice must also be considered. Finally, microbiological changes cannot be neglected, especially under abusive scenarios.

Detailed analysis of the relative contribution of the above factors and a proposed testing protocol can be found in the referenced sources.

REFERENCES

Arabshahi, A., 1982, Effect and interaction of environmental and composition variables on the stability of thiamin in intermediate moisture model systems, Ph.D. Thesis, University of Wisconsin, Madison, Wisconsin.

Arabshashi, A. and Lund, D.B., 1985, Considerations in calculating kinetic parameters from experimental data, *J. Food Proc. Engi.* 7:239-251.

Bates, R.G., 1973, *Determination of pH: Theory and Practice,* 2nd ed., John Wiley & Sons, New York, NY.

Bell, L.N. and Labuza, T.P., 1991, Aspartame degradation kinetics as affected by pH in intermediate and low moisture food systems, *J. Food Sci.* 56:17-20.

Bell, L.N. and Labuza, T.P., 1994a, Influence of the low-moisture state on pH and its implications for reaction kinetics, *J. Food Eng.* 22:291-312.

Bell, L.N. and Labuza, T.P., 1994b, Aspartame stability in commercially sterilized flavored dairy beverages, *J. Dairy Sci.* 77:34-38.

Bell, L.N., Shoeman, D., Tsoubeli, M., and Labuza, T.P., 1994, Kinetics of aspartame degradation in liquid dairy beverages, in: *Developments in Food Engineering*, Proceedings of the 6th Int. Congress on Engineering and Food, (Yano, T., Matsuno, R., Nakamura K. Eds.) Blackie Academic and Professional, London, 489-491.

Benson, S.W., 1960, *Foundations of Chemical Kinetics*, McGraw-Hill, New York.

Bergquist, S., and Labuza, T.P., 1983, Kinetics of peroxide formation in potato chips undergoing a sine wave temperature fluctuation, *J. Food Sci.* 43:712.

Beuchat, L.R., 1981, Microbial stability as affected by water activity, *Cereal Foods World* 26: 345-349.

Boyle, W.C., Berthouex, P.M., and Rooney, T.C., 1974, Pitfalls in parameter estimation for oxygen transfer data, *J. Environ. Eng.*, 100:391-408.

Buchanan, R.L., 1993, Predictive food microbiology, *Trends Food Sci. Technol.* 4:6-11.

Bunher, D., 1974, Simple kinetic models from Arrhenius to computer, *Accts. Chem. Res.* 7:195.

Bushill, J.H., Wright, W.B., Fuller, C.H.F., and Bell, A.V., 1965, The crystallization of lactose with particular reference to its occurrence in milk powders, *J. Sci. Food Agr.* 16:622.

Buera, P. and Karel, M., 1993, Application of the WLF equation to describe the combined effects of moisture, temperature and physical changes on non-enzymatic browning rates in food systems, *J. Food Proc. Preserv.* 17:31-47.

Byrne, C.H., 1976, Temperature indicators — the state of the art, *Food Technol.* 30(6):66-68.

Cardoso, G., and Labuza, T.P., 1983, Effect of temperature and humidity on moisture transport for pasta packaging material, *Br. J. Food Technol.* 18:587.

Cheftel, J.C., Cuq, J., and Lorient, D., 1985, Aminoacids, peptides and proteins, in *Food Chemistry*, Fennema, O.R., Ed., Marcel Dekker, New York.

Chen, S.L. and Gutmanis, F., 1968, Auto-oxidation of extractable color pigments in chili pepper with special reference to ethoxyquin treatment, *J. Food Sci.*, 33, 274-280.

Chen J.H. and Zall, R.R., 1987, Packaged milk, cream and cottage cheese can be monitored for freshness using polymer indicator labels, *Dairy Food Sanitation* 7(8):402.

Chirife, J. and Buera, P., 1994, Water activity, glass transition and microbial stability in concentrated/semimoist food systems, *J. Food Sci.* 59:921-927.

Cohen, E. and Saguy, I., 1982, The effect of water activity and moisture content on the stability of beet powder pigments, *J. Food Sci.* 48:703-707.

Cohen, E. and Saguy, I., 1985, Statistical evaluation of Arrhenius model and its applicability in prediction of food quality losses, *J. Food Proc. Pres.* 9:273-290.

Davey, K.R., 1989, A predictive model for combined temperature and water activity on microbial growth during the growth phase, *J. Appl. Bacteriol.* 67:483-488.

Dixon, W.J., Ed., 1989, *BMDP — Statistical Software,* University of California Press, Berkley, CA.

Draper, N. and Smith, H., 1981, *Applied Regression Analysis,* 2nd ed., Wiley, New York, NY.

Engel, 1981, *Enzyme kinetics. The steady-state approach,* 2nd ed., Chapman and Hall, New York.

Feeney, R.E., Blackenhorn, G., Dixon, H.B.F., 1975, Carbohydrate-amine reactions in protein chemistry, *Adv. Protein Chem.* 29:135-203.

Feeney, R.E., Whitaker, J.R., 1982, The Maillard reaction and its preservation, in *Food Protein Deterioration, Mechanisms and Functionality,* ACS Symposium Series 206, Cerry, J.P. Ed., ACS, Washington, D.C., 201-229.

Fennema, O., Powrie, W.D., Marth, E.H., 1973, *Low-Temperature Preservation of Foods and Living Matter,* Marcel-Dekker, New York.

Ferry, J.D., 1980, *Viscoelastic Properties of Polymers*, 3rd ed., Wiley, New York.

Fogler, H.S., 1986, *Elements of Chemical Reaction Engineering,* Prentice Hall, Englewood Cliffs, NJ, 63.

Fu B. and Labuza, T.P., 1993, Shelf-life prediction: theory and application, *Food Control* 4:125-133.

Fu, B., Taoukis, P.S., and Labuza, T.P., 1991, Predictive microbiology for monitoring spoilage of dairy products with time temperature indicators, *J. Food Sci.* 56:1209-1215.

Guadagni, D.G., 1968, Cold storage life of frozen fruits and vegetables as a function of temperature and time, in *Low Temperature Biology of Foodstuffs* (Hawthorne, J., and Rolfe, E.J., Eds., Pergamon Press, New York.

Haralampu, S.G., Saguy, I., and Karel, M., 1985, Estimation of Arrhenius model parameters using three least squares methods, *J. Food Proc. Pres.* 9:129-143.

Hayakawa, K., 1973, New procedure for calculating parametric values for evaluating cooling treatments applied to fresh foods, *Can. Inst. Food Sci. Technol.* 6(3):197.

Hendel, C.E., Silveira, V.G., and Harrington, W.O., 1955, Rates of nonenzymatic browning of white potato during dehydration, *Food Technol.* 9, 433.

Herborg, L., 1985, Shelf-life quality: a question of relativity, *I.I.F. - I.I.R. — (Commissions C2, D3) 1985-4*, International Institute of Refrigeration, Paris, p. 39-43.

Hills, C.G. Jr., 1977, *An Introduction to Chemical Engineering Kinetics and Reactor Design,* John Wiley & Sons, New York.

Hills, C.G. Jr., Grieger-Block, R.A., 1980, Kinetic data: generation, interpretation, and use, *Food Technol.* 34:56-66.

Holmer, B., 1984, Properties and stability of aspartame, *Food Technol.* 38:50.

Hong Y.C., Koelsch, C.M., and Labuza, T.P., 1991, Using the L number to predict the efficacy of moisture barrier properties of edible food coating materials, *J. Food Proc. Pres.* 15:45-62.

Hoover D.G., 1993, Pressure effects on biological systems, *Food Technol.* 47(6):150-155.

Institute of Food Science and Technology (UK), 1993, *Shelf-Life of Foods — Guidelines for Its Determination and Prediction.* IFST, London.

Kader, A.A., 1986, Biochemical and physiological basis for effects of controlled and modified atmospheres on fruits and vegetables, *Food Technol.,* 40(5):99.

Kamman, J.F., Labuza, T.P., and Warthesen, J.J., 1981, Kinetics of thiamin loss in pasta as a function of constant and variable storage conditions, *J. Food Sci.,* 46(5):1457.

Karel, M., 1985, Effects of water activity and water content on mobility of food components, and their effects on phase transitions in food systems, in *Properties of Water in Foods,* Simatos, D. and Multon, J.L., Eds., Martinusm, Nijhoff, Dordrecht, 153-169.

Karel, M., 1993, Temperature-dependence of food deterioration processes (Letter to the editor), *J. Food Sci.* 58(6):ii.

Karel, M. and Saguy, I., 1993, Effect of water on diffusion in food systems, in *Water relation in Foods,* (Levine, H. and Slade, L., Eds., Plenum Press, NY, 157-181.

Katz, E.E. and Labuza, T.P., 1981, Effect of water activity on the sensory crispness and mechanical deformation of snack food products, *J. Food Sci.,* 46, 403.

Kim, M.N., Saltmarch, M., and Labuza, T.P., 1981, Nonenzymatic browning of hygroscopic whey powders in open vs. sealed pouches, *J. Food Proc. Preserv.* 5:49.

Kirkwood, T.B.L., 1977, Predicting the stability of biological standards and products, *Biometrics* 33, 736.

Knorr D., 1993, Effects of high-hydrostatic-pressure processes on food safety and quality, *Food Technol.* 47(6):155-161.

Kochhar, S.P. and Rossel, J.B., 1982, A vegetable oiling agent for dried fruits, *J. Food Technol.* 17, 661.

Koelsch, C.M., Downes, T.W., and Labuza, T.P., 1991, Hexanol formation via lipid oxidation as a function of oxygen concentration: Measurement and kinetics. *J. Food Sci.* 56:816–820.

Kramer, A., 1974, Storage retention of nutrients, *Food Technol.* 28:5.

Kramer, A. and Twigg, B., 1968, Measure of frozen food quality and quality changes, in *The Freezing Preservation of Foods,* Vol. 2, 4th ed., Tressler, D.K., Ed., AVI Publishing, Westport, Conn.

Kwolek, W.F. and Bookwalter, G.N., 1971, Predicting storage stability from time-temperature data, *Food Technol.* 25(10):51.

Labuza, T.P., 1971, Kinetics of lipid oxidation of foods, *C.R.C. Rev. Food Technol.* 2:355.

Labuza, T.P., 1975, Oxidative changes in foods at low and intermediate moisture levels, in *Water Relations of Foods*, Duckworth, R., Ed., Academic Press, New York, 455.

Labuza, T.P., 1979, A theoretical comparison of losses in foods under fluctuating temperature sequences, *J. Food Sci.* 44:1162.

Labuza, T.P., 1980a, Temperature/enthalpy/entropy compensation in food reactions, *Food Technol.* 34(2):67.

Labuza, T.P., 1980b, The effect of water activity on reaction kinetics of food deterioration, *Food Technol.* 34:36.

Labuza, T.P., 1982, *Shelf-Life Dating of Foods.* Food & Nutrition Press, Westport, CT.

Labuza, T.P., 1984, Application of chemical kinetics to deterioration of foods, *J. Chem. Educ.* 61:348-358.

Labuza, T.P., 1985, An integrated approach to food chemistry: Illustrative cases, in *Food Chemistry,* ed. 2, O.R. Fennema, Ed., Marcel Dekker, New York, 913–938.

Labuza, T.P. and Breene, W.M., 1989, Applications of "active packaging" for improvement of shelf-life and nutritional quality of fresh and extended shelf-life refrigerated foods, *J. Food Process. Pres.* 13:1-69.

Labuza, T.P. and Contreras-Medellin, R., 1981, Prediction of moisture protection requirements for foods, *Cereal Foods World* 26:335-343.

Labuza, T.P. and Kamman, J., 1983, Reaction kinetics and accelerated tests simulation as a function of temperature, in *Applications of Computers in Food Research,* Saguy, I., Ed., Marcel Dekker, New York, chap. 4.

Labuza, T.P. and Ragnarsson, J.O., 1985, Kinetic history effect on lipid oxidation of methyl linoleate in model system, *J. Food Sci.* 50(1):145.

Labuza, T.P. and Riboh, D., 1982, Theory and application of Arrhenius kinetics to the prediction of nutrient losses in food, *Food Technol.* 36:66-74.

Labuza, T.P. and Schmidl, M.K., 1985, Accelerated shelf-life testing of foods, *Food Technol.,* 39(9):57-62, 64.

Labuza, T.P. and Schmidl, M.K., 1988, Use of sensory data in the shelf-life testing of foods: principles and graphical methods for evaluation, *Cereal Foods World* 33(2):193-206.

Labuza, T.P. and Taoukis, P.S., 1990, The relationship between processing and shelf life in *Foods for the 90's* Birch, G.G., Campbell-Platt, G., and Lindley, M.G., Eds., Developments Series, Elsevier Applied Science, London, 73-105

Labuza, T.P., Bohnsack, K., and Kim, M.N., 1982, Kinetics of protein quality loss stored under constant and square wave temperature distributions, *Cereal Chem.* 59:142.

Labuza, T.P., Fu, B., and Taoukis, P.S., 1992, Prediction for shelf-life and safety minimally processed CAP/MAP chilled foods, *J. Food Protection* 55:741-750.

Labuza, T.P., Mizrahi, S., and Karel, M., 1972, Mathematical models for optimization of flexible film packaging of foods for storage, *Trans. Am. Soc. Agric. Eng.* 15:150.

Labuza, T.P., Tannenbaum, S.R., and Kavel, M., 1969, Water content and stability of low-moisture and intermediate-moisture foods. *Food Tech.,* 24, 35–39.

Lenz, M.K. and Lund, D.B., 1980, Experimental procedures for determining destruction kinetics of food components, *Food Technol.* 34(2):51.

Levine, H. and Slade, L., 1988, Collapse phenomena — a unifying concept for interpreting the behavior of low moisture foods, in *Food Structure- Its Creation and Evaluation,* Blanshard, J.M.V. and Mitchell, J.R., Eds., Butterworths, London, 149-180.

Lund, D.B., 1983, Considerations in modeling food processes, *Food Technol.* 37(1), 92.

MacKenzie, A.P., 1977, Non-equilibrium freezing behavior of aqueous systems, *Phil. Trans. R. Soc. Lond. B.* 278:167-189.

Mackie, I.M., Howgate, P., Laird, W.M., Ritchie, A.H., 1985, Acceptability of frozen stored consumer fish products, I.I.F. — I.I.R. (Commissions C2, D3) 1985-4, 161-167.

Maesmans, G., Hendrickx, M., De Cordt, S., Tobback, P., 1995, Theoretical consideration of the general validity of the equivalent point method in thermal process evaluation, *J. Food Eng.* 24:225-248.

Margerison, D., 1969, The treatment of experimental data, in *Comprehensive Chemical Kinetics, The Practice of Kinetics,* Banford, C.H. and Tipper, C.F.H., Eds., Elsevier, New York.

McClure, P.J., Blackburn, C. de W., Cole, M.B., Curtis, P.S., Jones, J.E., Legan, J.D., Ogden, I.D., Peck, M.W., Roberts, T.A., Sutherland, J.P., and Walker, S.J., 1994, Modeling the growth, survival and death of microorganisms in foods: the U.K. foodmodel approach, *Int. J. of Food Microbiol.* 23:265-275.

McKekin, T.A., Olley, J.N., Ross, T., and Ratkowsky, D.A., 1993, *Predictive Microbiogy: Theory and Application.* Research Studies Press, Somerset, U.K.

Mizrahi, S., Labuza, T.P., and Karel, M., 1970a, Computer aided predictions of food storage stability, *J. Food Sci.* 35:799-803.

Mizrahi, S., Labuza, T.P., and Karel, M., 1970b, Feasibility of accelerated tests for browning in dehydrated cabbage, *J. Food Sci.* 35:804-807.

Mohr, P.W. and Krawiec, S., 1980, Temperature characteristics and Arrhenius plots for nominal psychrophiles, mesophiles and thermophiles, *J. Gen. Microbiol.* 121, 311-317.

Nakabayashi, K., Shimamoto, T., and Mina, H., 1981, Stability of package solid dosage forms, *Chem. Pharm.* 28(4):1090; 29(7):2027; 2051; 2057.

Nelson, R.R., 1983, Stability prediction using the Arrhenius model, *Comput. Program Biomed.* 16:55-60.

Nelson, K., 1993, Reaction Kinetics of Food Stability: Comparison of Glass Transition and Classical Models for Temperature and Moisture Dependence, Ph.D. Thesis, Univ. of Minnesota, St. Paul, MN.

Nelson, K. and Labuza, T.P., 1994, Water activity and food polymer science: implications of state on Arrhenius and WLF models in predicting shelf-life, *J. Food Eng.* 22:271-290.

Norwig, J.F. and Thompson, D.R., 1986, Microbial population, enzyme and protein changes during processing, in *Physical and Chemical Properties of Foods,* Okos, M.R., Ed., Am. Soc. Agric. Eng., St. Joseph, MI.

Nunes, R.V. and Swartzel, K.R., 1990, Modeling thermal processes using the equivalent point method. *J. Food Eng.,* 11, 107–117.

Ott, L., 1984, *An Introduction to Statistical Methods and Data Analysis,* 2nd ed., PWS Publishers, Boston, MA.

Parkin, K.L. and Brown, W.D., 1982, Preservation of seafood with modified atmospheres, in *Chemistry and Biochemistry of Marine Food Products,* Martin, E. et al., Eds., AVI Publishing, Westport, CT, 453-465.

Pecek, C., Warthesen, J., and Taoukis, P., 1990, A kinetic model for the equilibration of isomeric β-carotenes, *J. Food Agric. Chem.* 38:41-45.

Peleg, M., 1992, On the use of WLF model in polymers and foods, *Crit. Rev. Food Sci. Nutr.* 32:59-66.

Peleg, M., 1995, A model of temperature effects on microbial populations from growth to lethality, *J. Sci. Food Agri.* 68:83-89.

Poulsen, K.P. and Lindelov, F., 1975, Stability of frozen systems and frozen foods, Food Technology Laboratory, DtH, DK 2800 Lyngby, Denmark.

Quast, D.G. and Karel, M., 1972, Computer simulation of storage life of foods undergoing spoilage by two interactive mechanisms, *J. Food Sci.* 37:679.

Quast, D.G., Karel, M., and Rand, W., 1972, Development of a mathematical model for oxidation of potato chips as a function of oxygen pressure, extent of oxidation and equilibrium relative humidity, *J. Food Sci.,* 37:679.

Ramaswamy, H.S., Van de Voort, F.R., and Ghazala, S., 1989, An analysis of TDT and Arrhenius methods for handling process and kinetic data, *J. Food Sci.* 54:1322-1326.

Ratkowsky, D.A., Olley, J., McMeekin, T.A., and Ball, A., 1982, Relationship between temperature and growth rate of bacterial cultures, *J. Bacteriol.* 149:1-5.

Ratkowsky, D.A., Lowry, R.K., McMeekin, T.A., Stokes, A.N., and Chandler, R.E., 1983, Model for bacterial culture growth rate throughout the entire biokinetic temperature range, *J. Bacteriol.* 154:1222- 1226.

Riboh, D.K. and Labuza, T.P., 1982, Kinetics of thiamine loss in pasta stored in a sine wave temperature condition, *J. Food Proc. Pres.* 6(4):253.

Roos Y.H., 1993, Water activity and physical state effects on amorphous food stability, *J. Food Proc. Pres.* 16:433-452.

Roos, Y.H. and Karel, M., 1990, Differential scanning calorimetry study of phase transitions affecting quality of dehydrated materials, *Biotechnol. Prog.* 6:159-163.

Roos, Y. and Karel, M., 1991, Plasticizing effect of water on thermal behavior and crystallization of amorphous food models, *J. Food Sci.* 56:38-43.

Ross, T. and McMeekin, T.A., 1994, Predictive microbiology, *Int. J. Food Micro.* 23:242-264.

Rosso, L., Lobry, J.R., Bajard, S., and Flandrois, J.P., 1995, Convenient model to describe the combined effects of temperature and pH on microbial growth, *Appl. Envir. Micro.* 61:610-616.

Saguy, I.S. and Cohen, E., 1990, Shelf-life prediction course notes, Course #71917, The Hebrew University of Jerusalem, Faculty of Agriculture, Rebovot, Israel.

Saguy, I., and Karel, M., 1980, Modeling of quality deterioration during food processing and storage, *Food Technol.* 34(2), 78-85.

Saguy, I., Kopelman, I.J., and Mizrahi, S., 1979, Extent of nonenzymatic browning in grapefruit juice during thermal and concentration processes: kinetics and prediction, *J. Food Process. Pres.,* 2:175.

Saltmarch, M. and Labuza, T.P., 1982, Kinetics of browning and protein quality loss in sweet whey powders under steady and non-steady state storage conditions, *J. Food Sci.* 47:92.

Sapers, G.M., 1970, Flavor quality in explosion puffed dehydrated potato, *J. Food Sci.* 35:731.

Sapru, V. and Labuza, T.P., 1992, Glassy state in bacterial spores predicted by glass transition theory, *J.Food Sci.* 58:445-448.

Simon, I., Labuza, T.P., and Karel, M., 1971, Computer aided prediction of food storage stability: oxidation of a shrimp food product, *J. Food Sci.* 36:280.

Singh, R.P. and Wang, C.Y., 1977, Quality of frozen foods — a review, *J. Food Proc. Eng.* 1:97-127.

Singh, R.P. and Wells, J.H., 1986, Keeping track of time and temperature: new improved indicators may become industry standards, *Meat process.,* 25(5):41-42, 46-47.

Shoolfield, R.M., Sharpe, P.J.H., and Magnuson, C.E., 1981, Non-linear regression of biological temperature-dependent rate models based on absolute reaction-rate theory, *J. Theor. Biol.* 88, 719-731.

Slade, L., Levine, H., and Finey, J., 1989, Protein-water interactions: water as a plasticizer of gluten and other protein polymers, in *Protein Quality and the Effects of Processing,* Phillips, R.D. and Finlay, J.W., Eds., Marcel Dekker, New York, 9-123.

Stamp, J.A., 1990, Kinetics and Analysis of Aspartame Decomposition Mechanisms in Aqueous Solutions using Multiresponse Methods, Ph.D. Thesis, Univ. of Minnesota, St. Paul, MN.

Stamp, J.A. and Labuza, T.P., 1989, An ion-pair high performance liquid chromatographic method for the determination of aspartame and its decomposition products, *J. Food Sci.* 54:1043.

Taoukis P.S., Breene, W.M., and Labuza, T.P., 1988a, Intermediate-moisture foods, in *Advances in Cereal Science and Technology*, Vol. 9, Pomeranz, Y., Ed., American Association of Cereal Chemists, 91-128.

Taoukis, P.S., El Meskine, A., and Labuza, T.P., 1988b, Moisture transfer and shelf life of packaged foods, in *Food and Packaging Interactions*, Hotchkiss, J.H., Ed., ACS Symposium Series, No. 365, 243-261.

Taoukis, P.S. and Labuza, T.P., 1989a, Applicability of time-temperature indicators as shelf-life monitors of food products, *J. Food Sci.* 54:783-788.

Taoukis, P.S. and Labuza, T.P., 1989b, Reliability of time-temperature indicators as food quality monitors under non isothermal conditions, *J. Food Sci.* 54:789-792.

Taoukis, P.S., Reineccius, G.A., and Labuza, T.P., 1990, Application of time-temperature indicators to monitor quality of flavors and flavored products, in *Flavors and Off-Flavors '89,* Charalambus, G., Ed., Elsevier, London, 385-398.

Taoukis, P.S., Fu, B., and Labuza, T.P., 1991, Time-temperature indicators, *Food Technol.* 45(10):70-82.

Templeman, G., Sholl, J.J., Labuza, T.P., 1977, Evaluation of several pulsed NMR techniques for solids in fat determination in commercial fats, *J. Food Sci.* 42, 432.

Thompson, D., 1983, Response surface experimentation, *J. Food Proc. Preserv.,* 6, 155-188.

Tinker, J.H., Slavin, J.W., Learson, R.J. and Empola., V.G., 1985, Evaluation of automated time-temperature monitoring system in measuring the freshness of chilled fish, *IIF-IIR Commissions C2, D3 4,* 1985, 286.

Trant, A.S., Pangborn, R.M., and Little, A.C., 1981, Potential fallacy of correlating hedonic responses with physical and chemical measurements, *J. Food Sci.,* 41, 583.

Tsoumbeli, M.N. and Labuza, T.P., 1991, Accelerated kinetic study of aspartame degradation in the neutral pH range, *J. Food Sci.* 56:1671-1675.

Tuma, J.J., 1988, *Engineering Mathematics Handbook,* 3rd ed., McGraw-Hill, New York.

Weissman, I., Ramon, O., Kopelman, I.J., and Mizrahi, S., 1993, A kinetic model for accelerated tests of Maillard browning in a liquid model system, *J. Food Proc. Pres.* 17:455-470.

Wells, J.H. and Singh, R.P., 1988, Application of time-temperature indicators in monitoring changes in quality attributes of perishable and semi-perishable foods, *J. Food Sci.,* 53(1), 148.

White G.W. and Cakebread, S.H., 1966, The glassy state in certain sugar containing food products, *J. Food Tech.,* 1, 73.

Whiting, R.C. and Buchanan, R.L., 1994, Microbial modeling, *Food Tech.* 48:113-120.

Williams, M.L., Landel, R.F., and Ferry, J.D., 1955, The temperature dependence of relaxation mechanisms in amorphous polymers and other glass-forming liquids, *J. Chem. Eng.* 77:3701-3707.

Willcox, F., Mercier, M., Hendrick, M., and Tobback, P., 1993, Modelling the influence of temperature and carbon dioxide upon the growth of *Pseudomonas fluorescens*, *Food Micro.* 10:159-173.

Wold, S., 1971, Analysis of kinetic data by means of spline functions, *Chem. Scripta*, 1:97.

Yoshioka, S., Aso, Y., and Uchiyama, M., 1987, Statistical evaluation of nonisothermal prediction of drug stability, *J. Pharmaceutical Sci.,* 76(10):794-798.

Zobel, H.F., 1973, A review of bread staling, *Baker's Dig.* 47(5):52.

Zwietering, M.H., De Koos, J., Hasenack, B.E., DeWilt, J.C., and Van't Riet, K., 1991, Modeling of bacterial growth as a function of temperature, *Appl. Environ. Microbiol.* 57:1094-1101.

10 Temperature Tolerance of Foods during Distribution

John Henry Wells and R. Paul Singh

CONTENTS

10.1 INTRODUCTION

All food products regardless of preservation technique will eventually deteriorate. In particular, frozen and refrigerated foods are sensitive to the environmental conditions in which they are stored. Fruits and vegetables that are marketed as fresh products require refrigerated conditions to limit the biological functions of respiration and avoid a proliferation of resident microorganisms (Wills et al., 1981). Meat, fish, and poultry products preserved by freezing need controlled temperature conditions to retard biochemical changes that result from chemical and enzymatic activity (Desrosier and Tressler, 1977).

Freezing is one of the most satisfactory methods available for long-term preservation of foods (Fennema et al., 1973). Proper freezing and frozen storage can effectively retain flavor, color, and nutritive value of food and is moderately effective for preservation of texture. Freezing invariably produces some detrimental effects during long-term storage, with the severity depending on the product, the freezing process, and the temperature history during frozen storage (Singh and Wang, 1977).

Four factors principally affect end-product quality of any given frozen food: (1) the initial quality of the original foodstuff, (2) the processing and packaging of the product, (3) the temperature of storage, and (4) the duration of storage (Van Arsdel et al., 1969). Among these factors, the temperature history (the cumulative effect of storage time and temperature) is perhaps the most important determinate in keeping quality of the frozen food (Labuza, 1982; Jul, 1984). For most frozen products, storage temperature higher than recommended adversely affects keeping quality. While it is understood that properly controlled temperatures during storage and distribution are essential in order to maintain the quality of frozen food, the temperature to which frozen products are exposed are often beyond precise control (Taoukis et al., 1991).

10.2 FROZEN FOOD QUALITY

10.2.1 PERISHABLE NATURE OF FOOD

Perishable food quality is a complex topic that must include the considerations of consumptive safety, product composition, and physical properties, chemical and enzymatic activity, and microbiological interaction and growth. A consumer perspective of quality can be referenced to specific and/or predominate characteristics or attributes that are inherent to a food, thereby allowing a product's quality to be expressed in terms of expectations or preferences for individual product *qualities* (Schutz et al., 1972). Such quality attributes (or product *qualities*) can then be quantified in terms of the presence of desirable (or absence of undesirable) characteristics. Thus, an item with a greater degree of desirable characteristics would be perceived to be of higher quality, whereas an item with a lesser degree of the same characteristics would be considered of lower quality. Food perishes through deteriorative and spoilage processes by virtue of developing undesirable combinations of quality attributes relating to sensorial properties, nutritional value, safety, and/or aesthetic appeal of that product.

10.2.2 QUALITY EVALUATION TECHNIQUES

Physical, chemical, enzymatic, and microbial changes that contribute to perceptions of frozen food quality can be detected by instrumental and sensory evaluations. For example, the lipid oxidation in meats and fish can be expressed in the development of rancid off-flavors as observed during sensory evaluation or through analytically monitoring levels of chemical byproducts that result from oxidation reactions. Accordingly, frozen food quality (and a criterion of acceptability by a consumer) may be contemplated as a combination of many distinctive chemical or sensory attributes. One or more of these attributes may change during

storage, and the resulting change can eventually lead to consumer rejection of the product. Identification and quantitative definition of quality attributes during a controlled storage study can provide a means to monitor the influence of temperature history on changes in quality. It must be noted that sensory techniques must be augmented with an objective means of microbiological and toxicity testing for proof of food safety.

Sample preparation is one of the most important factors in obtaining valid results from a frozen-food storage study. A detailed repeatable procedure must be devised to assure that product handling during sample selection and specimen preparation does not negate, overshadow, or enhance any product quality changes which have resulted due to experimental treatment conditions. Sensory analysis of frozen products may require development of extraordinary experimental procedures to maintain product quality during preparation (Dolan et al., 1985). Optimally, the researcher would like any quality changes perceived by sensory or instrumental measurement to be only a result of treatment effects.

10.2.2.1 Sensory Difference Methods

Difference testing procedures such as paired comparisons or triangle testing do not provide information about either the rate or extent to which the quality change proceeds. The results of storage studies that use difference techniques produce useful information as to the expected length of time a product can be stored (an endpoint measure), but are of limited value in determining the way a quality change proceeds (a kinetic measure). Sensory methods to monitor changes in frozen food quality should include procedures to measure the rate and extent of changes while at the same time remaining sensitive to "noticeable changes" that could have an economic impact on the industry.

10.2.2.2 Sensory Rating Methods

A sensory rating methodology uses panelists trained to recognize specific product characteristic. As applied in a frozen storage study, rating methods can be used to determine quality attribute change and the extent of changes when products are subjected to treatments of differing storage temperatures and times. Rating methodologies allow the changes in product characteristic (i.e., product attribute) to be quantified as a prelude to quality loss modeling.

The product characteristics measured using sensory rating must be defined in advance of a storage study. To accomplish this, preliminary descriptive analysis can be conducted in combination with a literature search for reports of analogous research and product evaluations. The descriptive session might involve analysis of products that have undergone either accelerated temperature exposure or long-term isothermal exposure (Meilgaard et al. 1991). Either approach should be designed to bring about sensory changes in excess of those expected during the nominal shelf-life. A freshly manufactured product can then be compared to the product with advanced deterioration by individuals experienced in sensory techniques. Such a descriptive analysis session should include a solicitation of comments on the method of determining specific characteristics as well an open discussion following product evaluation to characterize the differences, in descriptive terms, chosen by the judges. From the information obtained during the descriptive session, the sensory attributes for the sensory rating study can be selected and specific analysis instructions can be developed. The temperature treatments for a frozen storage study and timing of the sensory evaluation session should be established according to the guidelines listed in Table 10.1.

10.2.2.3 Example: Measuring Frozen Foods Quality Changes

In a frozen food study by Singh et al. (1984) six frozen foods (strawberries, peas, bologna, hamburger, ice cream, and salmon) were examined using a deviation-from-reference with sensory rating techniques. For each product, evaluation sessions were held every 3 weeks

TABLE 10.1
Guidelines for Establishing the Temperature Treatments and Timing
of Deviation-from-Reference Evaluation Sessions

An initial session should be conducted on the same day as products are placed into treatment storage to establish a day zero observation.

At least 4 to 6 evaluations should be scheduled during the anticipated length of the study.

The study should extend to minimum length of time for the expected product PSL for all experimental temperature treatments.

The interval of time between sessions should not be excessively long to miss the point in time at which attribute differences become significantly different.

Products stored at –35°C or lower should be designated as reference.

Temperature treatments should include the range of conditions recommended for storage and one condition considered mildly abusive.

A minimum of three temperature treatments should be considered (e.g., reference, recommended and abusive).

All treatment conditions should be evaluated simultaneously during each session.

```
                              R
  |_____|_____|

  Less than the                         More than the
  Reference                               Reference
```
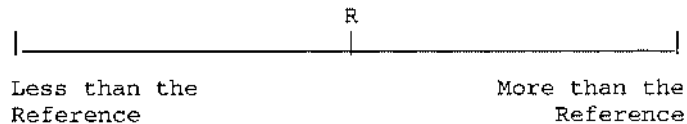
FIGURE 10.1 Deviation-from-reference scale used to measure sensory changes in specific quality attributes during frozen storage. R indicates score to which identified reference sample should be assigned.

during the study period and evaluations were conducted by 15 volunteer judges. To ensure unbiased results, the judges were not made aware of the purpose of the experiment or of any experimental details. The data of judges participating in less than half of the scheduled sessions were not included in the analyses. Samples stored under the three experimental conditions (reference, recommended, and abusive temperatures) were presented in random order, together with an identified reference sample. The identified reference was labeled with an "R" and each randomized sample was coded with a four-digit random number. Flavor and texture attributes were evaluated in duplicate in individual booths under red light while samples evaluated for appearance attributes were displayed on trays or individual holders under white light.

Sensory analysis, using deviation-from-reference scaling, rates (scores) each sample according to how much it deviated from a reference product on a 10-cm unstructured scale, anchored at the ends by the terms less or more than reference. The midpoint of the scale is marked to indicate the attribute intensity of the reference and changes in attribute intensity can be scored more or less than the reference (Figure 10.1). For a frozen storage study, product stored at –35°C can be designated as a reference since it is generally accepted that only slight quality changes occur at this temperature (Jul, 1984).

Prior to the beginning of the series of evaluation sessions, the judges participated in a training session conducted in the same manner as succeeding sessions. The product samples presented at this training session had been previously stored under treatment conditions for not more than 2 weeks. The purpose of the training session was to acquaint the panelists with the score sheets, the type of scaling and the manner of presentation of the samples. There is a strong body of evidence that precision of sensory evaluation increases with increased panelists' training (Amerine et al., 1965).

FIGURE 10.2 Changes in mean sensory scores for hamburger rancidity during frozen storage.

For a frozen storage study utilizing a deviation-from-reference rating technique, differences between storage treatments at the beginning of a study should not be significant. However, with longer storage times (especially at higher storage temperature), the differences between reference sample and experimental samples will become significant (Figure 10.2). Additionally, over continued storage time and at subsequent sensory evaluation sessions, the differences will remain significant such that during the course of the storage study there will be a point in time when the sensory differences between treatment samples are judged to be consistently and significantly different. The hypothesis of this analysis is that the storage time, when product samples first begin to show consistent significant differences, is correlated to a shelf-life criterion. A sensory rating methodology may be used to define a shelf-life criterion as well as monitor sensory changes for use in obtaining parameters for quality prediction.

10.2.3 PRODUCT SHELF-LIFE

The loss of a desirable food quality attribute (i.e., an undesirable change in product quality) can be measured using sensory, empirical, or analytical techniques. For example, analysis of chemical components that contribute to changes in the perception of a desirable characteristic would constitute a typical analytical technique. Time-dependent studies of changes in frozen food quality has been aimed at identifying the length of time necessary for quality changes to result in an unacceptable product. These frozen food storage studies have been the basis for establishing criteria to define the shelf-life of foods (Dethmers, 1979).

10.2.3.1 Strategies to Determine Shelf-Life

A trilevel investigation strategy has been proposed for predicting sensory acceptance of foods held in frozen storage (ABMPS, 1982). The methodology proposed included the use of difference testing, attribute rating, and consumer evaluations on frozen products that have relatively long storage life. A quality change threshold would be determined with sensory difference testing, and after that point in time when a significant difference was found (threshold achieved), attribute rating and acceptance evaluations would begin. This type of

storage study investigation is appropriate when examining subsistence products with a relatively long frozen storage shelf-life.

Many frozen products cannot be stored for extended periods of time without loss of quality. Products of this nature may develop detectable quality loss in a period of time as short as a few months, especially in the absence of proper temperature control needed to maintain the highest quality possible. For storage studies with these products the use of difference testing may be inappropriate since discrimination methods do not measure a progression of quality change. Because the quality change in certain types of frozen product may be very rapid, difference methods may unreasonably conclude a longer storage time to significant difference than is actually true. An alternative approach would be to use attribute rating techniques for the onset of the investigation, perhaps including the use of single or multiple standard samples (Tarver and Schenck, 1958).

10.2.3.2 Shelf-Life Criterion

The keeping quality of frozen foods during storage is contemplated in terms of an estimated product shelf-life. Such estimates assume: (1) that the original products are of an initial high quality state, and (2) that a recommended, uniform storage temperature is maintained throughout all phases of storage and distribution (Wells and Singh, 1989). A high quality state, both in terms of high levels of desirable (or low levels of undesirable) quality characteristics is maintained during product manufacturing through careful selection of raw materials and attention to process control.

Product shelf-life is estimated by: (1) measuring changes in food quality characteristics in response to known external vectors (e.g., temperature, humidity, packaging, etc.), and (2) defining a shelf-life failure criteria based on some noticeable quality difference between experimental and control samples. During a storage study the external vectors are controlled to act uniformly upon the product and the failure criteria is based on sensory or analytical examination. When quality differences between experimental and control samples can be routinely detected at a statistically significant level (either a predetermined number of trained sensory panelists or magnitude of instrumental change) the product is declared to have reached the end of shelf-life (Van Arsdel et al., 1969). The level of statistical significance can be specified such that it would call attention to a noticeable difference that may be of commercial significance if the product has been introduced in commerce.

Popular definitions of shelf-life for frozen foods include: just noticeable difference (JND), high quality life (HQL) and practical storage life (PSL). These definitions employ sensory difference testing and a strict statistical criteria for shelf-life failure. Typically, statistical criteria (or other comparative analyses) are imposed on measurements of time dependent changes of a product's quality attributes such that a shelf-life can be defined in terms of an expectation that a product has or has not perished. Thus the shelf-life of a product becomes a binary measure of the suitability (or lack of suitability) of a product for consumption or other intended purpose.

10.2.3.3 Example: Determining Frozen Food Shelf-Life

The results from frozen storage studies conducted by Singh et al. (1984) have been disseminated into the general food science literature (Dolan et al., 1985, 1986, 1987). The range of shelf-life times as determined by the deviation-from-reference rating technique (Singh et al., 1984) are compared with those determined by sensory difference methods (Van Arsdel et al., 1969) are presented in Table 10.2. The shelf-life data documented by Van Arsdel et al. (1969) had been determined using difference testing and reported sensory analysis to determined the storage time required to bring about noticeable quality differences at different temperatures. Noticeable differences reported were for the product as a whole and were not described as

TABLE 10.2
**Summary and Comparison of Storage Stability Data for
Selected Frozen Producs as Stored in Isothermal Conditions**

	Temperature (°C)	JND[1] (d)	Significant difference[b] (d)[c]
Hamburger[d]	–18	120	—[e]
	–12	80	82–103
			(Rancidity)
Peas	–18	265	—[e]
	–12	120	130–148
			(Sweetness)
Salmon	–18	60–90	—[e]
	–12	—[f]	—[e]
Strawberries	–18	360	—[e]
	–12	60	42–65
			(Darkness of red color)

Note: Sensory attribute indicated parenthetically.

[a] Just Noticeable Difference as judged by sensory difference test (Van Arsdel et al., 1969).

[b] Significant Difference as determined by Deviation-From-Reference test (Singh et al., 1984); $p<.05$.

[c] Range of days specified represent the last nonsignificantly different session and first consistent significantly different session between samples stored at –12 and –35°C.

[d] Hamburger with 20% granular soy added.

[e] No consistently significantly different sessions observed during study.

[f] Comparative data not available.

specific product attributes. Since the work documented by Van Arsdel et al. (1969) occurred over several years, compared with the less than 7-month storage studies reported by Singh et al. (1984), only comparison of storage study results for –12°C storage are appropriate.

Shelf-life measurements from the storage studies by Singh et al. (1984) are reported as a range because the researchers used a nominal 3-week interval between evaluations. Additionally, slight discrepancies in the comparison [e.g., peas 120 d (Van Arsdel et al., 1969) vs. 130 to 148 d (Singh et al., 1984)] may be accounted for by considering that Singh et al. (1984) compared product at –12°C to product at –35°C, where as Van Arsdel et al. (1969) did not report this exact condition. Also, it must be realized that although the rate of quality change is slight at –35°C, perceptible changes in quality may occur after a period of time. Overall, these results imply sensory rating methods can be used to determine shelf-life criteria during a frozen food storage study. In addition to satisfactorily estimating shelf-life, rating methods provide a means of gathering data for kinetic analysis and quality change predictions if used in conjunction with a well-planned, statistically sound experimental design.

10.3 MODELING FROZEN FOOD QUALITY CHANGES

10.3.1 TEMPERATURE HISTORY EFFECTS

In general, the shelf-life of frozen foods increases with colder temperatures in an approximately exponential relationship. That is when the time to reach the end of a product's shelf-

FIGURE 10.3 Comparison of acceptability times for various frozen foot products.

life is plotted on semilog paper against storage temperature, the points fall roughly on a straight line for the range of temperatures important in commercial storage (Figure 10.3). This finding has been the basis for the observations that: (1) for every frozen product there exists a relationship between storage temperature and the time it takes at this temperature for the product to undergo a certain loss of quality; and (2) time/temperature influences resulting in quality loss are cumulative and irreversible over the entire storage life of the product.

A few exceptions to the above general rules include: (1) emulsions and colloidal products that undergo repeated warming to near the melting point (in such cases deterioration is not strictly an arithmetic accumulation); (2) storage conditions that create wide temperature fluctuations (thus causing large internal temperature gradients) that result in a higher degree of desiccation (i.e., freezer burn); (3) prolonged storage of frozen products at temperatures warmer than the minimum required for microbial growth (around –10°C), and (4) products that exhibit reverse and neutral stability (observed phenomena that colder temperatures during storage result in a shorter shelf-life or no change in shelf-life, respectively).

The books by Van Arsdel et al. (1969) and Jul (1984) reviewed the results of storage investigations on the keeping quality of frozen foods. A similar type of comprehensive review for the keeping quality of fresh fruits and vegetables, dairy products, and other refrigerated foods is available in a book by Labuza (1982). Significant factors contributing to the keeping quality of perishable foods are storage temperature, initial product composition and quality, processing techniques, and the packaging materials and processes (Fennema et al., 1973; Goodenough and Atkin, 1981).

10.3.2 KINETIC MODELING APPROACHES

Earliest interest in the mathematical modeling of food quality loss was motivated by the observation that frozen foods stored at fluctuating temperatures did not have the same shelf-life as products stored at constant temperature conditions, even though the two storage environments had the same mean temperature (Hicks, 1944; Schwimmer et al., 1955). Recent interpretations of the relationship between temperature history (the combined effect of time and temperature) and quality have been discussed under the loosely defined heading of "shelf-life kinetics." Included in these interpretations are models using the Arrhenius equation

(Heldman and Lai, 1983), an approach analogous to thermal death time (Labuza, 1979), and Q-value technique (Schubert, 1977). A graphical representation of the temperature history/quality relationship was developed utilizing time-temperature indicators in monitoring temperature-history related quality changes in frozen foods (Wells et al., 1987).

The chemical kinetic approach in food quality modeling had been advocated by Kwolek and Brookwalter (1971) as the most general and widely applicable mathematical model to describe the temperature influence on the rate of quality loss. The primary characteristic of the kinetic approach is that the rate of quality loss is an exponential function of the reciprocal of absolute temperature (the Arrhenius relationship). Saguy and Karel (1980) concurred with the recommendation of the kinetic model in food quality modeling, but other researchers have applied alternative or modified forms of the Arrhenius model to successfully describe temperature dependent changes in food quality (Moreno, 1984; Zhao et al., 1992).

10.3.2.1 Mathematical Structure of the Kinetic Model

The general form of the kinetic model to describe time- and temperature-dependent losses of a predominate quality attribute, Q, is

$$-\frac{dQ}{dt} = k_o \exp\left(-\frac{E_A}{R_g}\frac{1}{T}\right) Q^n \tag{10.1}$$

The kinetic model has three unknown parameters (n, k_o, and E_A) which must be determined from experimental data. The reaction order, n, is an empirical constant (generally assumed to be an integer value) manipulated to best fit the experimental data; the pre-exponential factor, k_o, represents a theoretical rate of change in quality attribute per unit time; and the temperature characteristic term (activation energy), E_A, indicates the temperature sensitivity of the observed quality change. Quality changes in most foods have been observed to follow either a zero-order ($n = 0$) or a first-order ($n = 1$) reaction (Labuza, 1982).

For an isothermal storage treatment, the mathematical notation for the zero- ($n = 0$) or first-order ($n = 1$) kinetic model is

$$-\frac{dQ}{dt} = k \tag{10.2a}$$

$$-\frac{dQ}{dt} = k\,Q \tag{10.2b}$$

where Equations 10.2a and 10.2b denote a zero- ($n = 0$) or first-order ($n = 1$) reaction, respectively, and k is the specific reaction rate constant for a particular isothermal condition. The analytical solution for Equations 10.2a and 10.2b may be found by separation of variables, integrated over the time interval 0 to t . The resulting equations:

$$Q = Q_o - k\,t \tag{10.3a}$$

$$\ln(Q) = \ln(Q_o) - k\,t \tag{10.3b}$$

are in the form of a simple linear model with the initial level of the quality attribute denoted as Q_o. Equations 10.3a or 10.3b may be used in regression analysis of food quality measurements [Q or $\ln(Q)$] vs. time to obtain an estimate of the specific reaction rate constant.

The influence of temperature on the specific reaction rate can be described with the Arrhenius relationship. The linear form of the Arrhenius equation is:

$$\ln(k) = \ln(k_o) - \frac{E_A}{R_g}\frac{1}{T} \qquad (10.4)$$

The parameters E_a and k_o may be determined (indirectly from $\ln k_o$ and E_A/R_g) by regression analysis of the natural logarithm of isothermal reaction rate against the reciprocal of the corresponding absolute temperatures (the Arrhenius plot). Specific rate constants from three or more isothermal conditions are desirable to properly conduct the regression analysis for the Arrhenius expression.

Two-step linear and nonlinear regression approaches to predicting kinetic parameters have been compared by Arabshahi and Lund (1985), Cohen and Saguy, (1985), and Haralampu et al. (1985). Lai and Heldman (1982) derived a methodology to determine the value of the activation energy of food quality losses from shelf-life data at known storage temperatures. Lai and Heldman documented the values of activation energy for the quality changes in a number of frozen foods. The activation energies for quality changes in various refrigerated and semiperishable foods has also been published (Labuza, 1982).

10.3.3 COMPUTER SIMULATION ALGORITHMS

Previous investigators have used computer algorithms to predict changes in food quality for time varying temperature conditions during storage (Singh, 1976; Saguy and Karel, 1980; Labuza, 1979). A typical algorithm structure is denoted in the flow chart shown in Figure 10.4. Singh (1976) presented a computer algorithm to predict changes in frozen food quality based on a simulated temperature history during storage. The Arrhenius relationship provided a means to estimate the rate of quality change for a small calculation step in the prediction algorithm. Later, Singh and Heldman (1983) discussed the need of obtaining kinetic information about frozen food quality changes. They proposed the use of sensory rating methods and specifically the deviation-from-reference technique as a possible method of gathering kinetic information. Wells (1987) developed a computer program to predict changes in food quality for user-defined temperature conditions as part of a computer-based inventory management system.

10.4 LOGISTICAL INVENTORY CONTROL

10.4.1 STOCKPILE ACCUMULATION

An inventory is an accumulation resulting from a net difference in the flux of items received (i.e., an order quantity) and items dispersed (i.e., a demand quantity) within a stockpile. Often the quantity in a stockpile (i.e., the on-hand inventory) is considered to be an amount of stored product necessary to meet dynamic demand quantities of various purchasers (Nahmias, 1982). Inventory management theory has been discussed within the management science and operations research literature. The order in which items are dispersed from a stockpile (inventory) has been considered in the classic *inventory depletion problem*, and the procedure by which the shipment decision is made is governed by the *inventory issue policy*.

Perishable inventories familiar in the food industry include refrigerated products such as fruits, vegetables and other produce, meats, and bakery items — products that require some means of temperature reduction to deter spoilage. Other perishable inventories that one may not readily consider as such include photographic film (since color fading can occur prior to exposure), batteries (because charge capacity decays during storage), and pharmaceuticals

INPUT
Kinetic Parameters
k_o and E_A

INPUT
Initial Quality Level and Time Values
$Q = Q_o$ and $t = 0$

OUTPUT
Plot Q vs. t

Increment Quality and Time Values
$Q_n = Q$ and $t = t + \Delta t_n$

Look-up Temperature History for Time Step
$T = T(\Delta t_n)$

Calculate Specific Reaction Rate
$k = k_o \exp\left(-\frac{E_A}{R_g}\frac{1}{T}\right)$

Calculate Quality Change During Time Step
$Q = Q_n - k\ \Delta t_n$
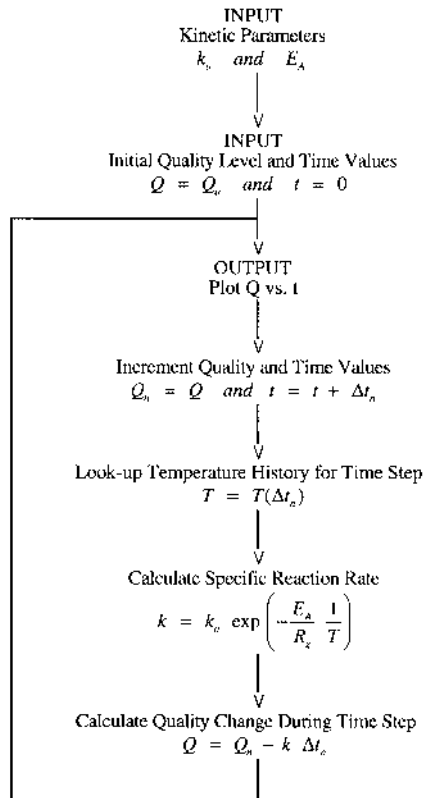
FIGURE 10.4 Flow chart representing general structure of a computer simulation algorithm to predict frozen food quality changes based on the zero-order kinetic model. The algorithm shown facilitates quality calculations based on actual temperature history data in a lookup table of Δt_n and $T(\Delta t_n)$.

and blood (where loss of biochemical efficacy/compatibility can occur over time) (Nahmias, 1982; Prastacos, 1984). Another important perishable commodity is currency, as observed in the case where the value of currencies vary day-to-day in international commerce. All perishable inventories require some management strategy to extend, preserve, and deliver items from a stockpile accumulation to the end users with the perishable benefits (quality attributes) optimally still intact. Inasmuch as deterioration of frozen foods proceeds even at recommended storage temperatures (and is accelerated as a result of temperature fluctuation), frozen foods are unquestionably perishable inventories.

10.4.2 PERISHABLE INVENTORY MANAGEMENT

Frozen inventories move via a distribution chain (a transportation and storage network) that may encompass temporary storage within a manufacturing plant, shipment to one or more centralized warehouses, and final transport to multiple points of retail sale (Figure 10.5). The varied movement of products within the distribution chain result in the potential for different temperature exposures. Generally, frozen foods stored at lower (colder) temperatures exhibit a longer shelf-life compared with products stored at a higher (warmer) temperature (Jul, 1984). Thus the products stored at colder temperatures appear less perishable. If nonuniform temperature variations occur during storage or distribution, the quality levels and future shelf-life expectations of the various stockpile items will be different even if items have the same age. For those familiar to the industry, it is easy to envision that frozen products experience different temperature histories as they move from manufacture to consumption.
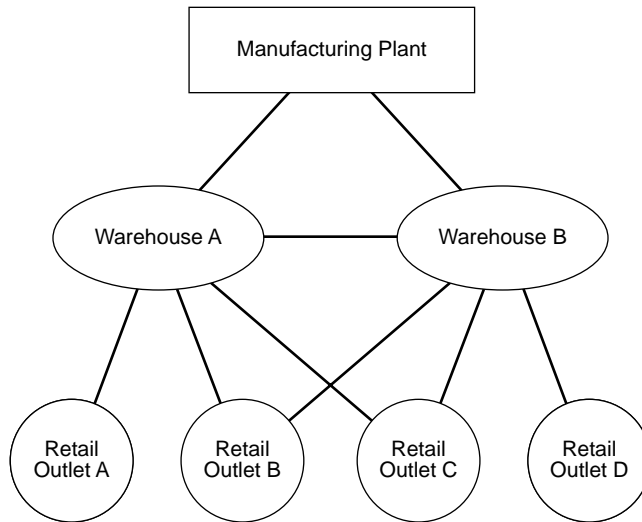
FIGURE 10.5 Possible movement of products with a frozen food distribution chain. (From Wells, J.H., 1987).

Since stockpile items typically are received and dispersed in unequal quantities and at different times, logistical tracking of the movement of items in and out of a stockpile is important. Product tracking can be used to determine available stock on-hand and to establish schedules for stockpile replenishment and issue priority. Development of an appropriate criteria (an inventory issue policy) to determine which items should be selected from the stockpile to fulfill needed demand quantities can be a serious problem in the frozen food industry.

10.4.2.1 Inventory Issue Policies

Three classes of inventory issue policies exist for the management of perishable inventories: (1) convenience-based policies, (2) time-based policies, and (3) quality-based policies. Each is briefly explained.

10.4.2.1.1 Convenience-based policies

Convenience-based policies have convenience (including economic convenience) as the sole consideration for warehouse logistics. The goal of such policy could be simply to minimize the "bother" associated with locating any priority item within the stockpile. Alternatively, the management goal could reflect least-cost considerations relating to labor utilization to fulfill issue demand. Possible convenience-based inventory issue policies include: (1) haphazard or random stockpile selections (implying there is no policy or no priority for issue) and (2) closest-to-the-door stockpile selections (implying a management priority relating to labor/economic productivity). In practice, convenience often motivates decisions regarding food inventory management, especially if a stockpile has high turnover volume.

10.4.2.1.2 Time-based policies

Time-based policies use product age either in terms of time since manufacture (i.e., product age) or time held in the stockpile (i.e., age of stockpiled product) to establish stockpile issue priority. Under uniform manufacture and delivery schedules, time since manufacture will closely relate to time held in the stockpile, thus usually no distinction is made in how product age is measured. Two policies for time-based inventory issue policies relating to the length of time a product is held in the stockpile include: (1) first-in first-out (FIFO) selection (implying that priority is given to the oldest or longest held product in the stockpile) and (2) last-in first-out selection (LIFO) (implying that priority is given to the youngest or most

recently acquired product in the stockpile). Time-based issue policies use time (age) measurements alone to establish criteria for logistical control of an inventory.

10.4.2.1.3   Quality-based policies

Quality-based policies use a measure (or expected measure) of product quality as the consideration for warehouse management. Such inventory policies consider the priority of demand quantity in terms of minimizing product variability. Two quality-based inventory management philosophies include: (1) just-in-time (JIT) inventory management and (2) shortest remaining shelf-life (SRSL) stockpile selection. The use of a quality-based management philosophy has become increasingly popular in industrial manufacturing settings (Japan Management Association, 1993). Such a philosophy implies fulfillment of product (or product component) demand at the time that they are needed and at an expected level of quality. For example, a JIT strategy minimizes (or eliminates) the requirement of a stockpile altogether through fulfilling order quantities from an industrial consumer by directing the needed amount straight from the manufacturer to the consumer (i.e., prompt delivery of a manufacture quantity to precisely fulfill an order quantity at the time it is needed). Such procedures rely on a manufacturer's ability to minimize product defects that could lead to product rejection (a product's perished state), creating situations that interfere with overall consumption schedules. Generally, quality-based inventory issue policies implicitly recognize ties between inventory scheduling and economic productivity of an industry.

10.4.2.2   Example: Comparison of Various Issue Policies

While FIFO concepts are fundamentally understood and used in the frozen food industry, the presumed intent of such a management strategy (i.e., delivery of the highest quality product to the consumer) is incorrect (Derman and Klein, 1958; Bomberger, 1961; Pierskalls and Roach, 1972). Instead application of FIFO practices to uniformly deteriorating perishable inventory minimizes variability among instances of product issue. The objective of an FIFO inventory policy is to improve quality consistency of issued products, even at the sacrifice of overall average quality of perishable products issued from the stockpile. The implementation of an LIFO inventory issue policy optimally provides the highest quality product to be issued. However, this is accomplished without regard for quality variation or ultimate obsolescence of a perpetual inventory within the stockpile. With food products, obsolescence ultimately increases product waste and overall operating costs. Temperature fluctuations and abuse experienced by products prior to entering the stockpile confound quality and quality consistency objectives of time-based inventory issue policies.

Quality-based inventory issue policies have become feasible as a result of methodologies to quantify the rate and extent of food quality change with storage temperature (Labuza, 1984). Additionally, logistic managers can use temperature history monitors for the prediction of food quality change, which in turn can estimate a product's remaining shelf-life assuming a future recommended storage temperature (Wells and Singh, 1988). Based on the expected measure of remaining shelf-life, frozen inventories can be scheduled for issue in sequence from shortest to longest remaining shelf-life (Wells, 1987). Simulation studies of frozen broccoli have shown the SRSL policy to improve quality consistency of issued products compared with time-based policies (Wells and Singh, 1989). The SRLS issue policy has also been reported in the literature as least shelf-life first out (LSFO) inventory issue policy (Taoukis et al., 1991).

10.4.3   QUALITY-BASED INVENTORY CONTROL

A lack of temperature control during frozen storage and distribution should not be equated with a lack of logistical control of an inventory of frozen food. While the importance of temperature control within the domain of storage and distribution logistics is acknowledged,

the management strategies offered to the industry to promote quality and consistency of frozen food focus exclusively on product manipulation within the manufacturing environment. In practice, there is only limited methodology for inventory control beyond control of temperature to which a frozen inventory is exposed.

Food manufacturers use various quality control management strategies for manufacture and delivery of consistently high quality products. Important management strategies for the frozen food industry include: (1) quality assurance standards along with the implementation of statistical quality control procedures during manufacture, (2) temperature control during storage, and (3) special handling procedures and controlled logistical scheduling of frozen inventories.

Central to statistical quality control is routine attribute measurement of some sample population (Hubbard, 1990). Typically, attribute measurements are summarized in terms of the sample central tendency and the sample dispersion. The summarized measurements of the mean and range (or other variance measure) are separately plotted on time sequence, quality control charts (e.g., mean and range charts). When such quality control techniques are used in a manufacturing setting, machine operators (or managers) have an immediate indication if a process (or process management policy) has achieved both targeted level and consistency goals.

Because logistical convenience often compels frozen food inventory issue decisions, there is strong motivation to adopt some means of statistical inventory control. Through the simple technique of developing time series plots for product remaining shelf-life (pull date less the product age), management can have an objective measure of the effectiveness of present inventory issue policies. This combined with periodic product inspection, random temperature monitoring, or tracking consumer comments provides diagnostic tools for assessing the need to implement quality-based inventory management practices.

10.4.3.1 Remaining Shelf-Life Prediction

The objective of an inventory issue policy is to maximize the total life of an inventory stockpile. In the case of a perishable food inventory, maximizing the life of a stockpile at a centralized site will yield increased distribution flexibility for deliveries to satellite storage locations, and could provide increased demand satisfaction among multiple shipment locations. In large stores of frozen foods, stock replenishment may either be periodic, for food items which are processed throughout the year, or irregular, for items which are produced seasonally. However, from a myopic point of view, a warehousing operation which stores more than one stock keeping unit (product "lot") may be considered a stockpile.

The remaining shelf-life of a stockpile item may be expressed mathematically in terms of the difference between current level of estimated quality and an intolerable quality threshold. Since shelf-life data are available in the literature, quality threshold values can be determined for an arbitrary value of initial product. Thus for an initial value of Q_o (say $Q_o = 100$), a level threshold quality, Q_{TH}, can be calculated for a reference storage temperature, T_{REF}. Estimated levels of food quality may be predicted using a kinetic quality change model for known (or expected) temperature history. Accordingly stockpile items which have undergone a differing amount of quality deterioration (based on differing temperature histories) can be compared to one another in terms of remaining shelf-life expectations assuming that products will experience the same future temperature history exposure (T_{REF}).

Assuming that food quality change is satisfactorily modeled with a zero-order reaction kinetics, the relationship for remaining shelf-life is given by:

$$L(Q_n) = \frac{Q_n - Q_{TH}}{k_o \exp\left(-\frac{E_A}{R_g}\frac{1}{T_{REF}}\right)}$$

(10.5)

where $L(Q_n)$ = maximum remaining shelf-life of a product stored at the constant temperature (T_{REF}); Q_{TH} = threshold quality level; Q_n = current quality level; and T_{REF} = recommended storage temperature. The current quality level, Q_n, can be obtained from actual quality level measurements, known temperature history data and a computer simulation algorithm, or correlation of food quality change with time-temperature indicators (Wells and Singh, 1988).

For situations where logistics of delivery require lengthy travel time, an appropriate distribution constraint would be:

$$L(Q_n) > L(d_j) \qquad\qquad (10.6)$$

where $L(d_j)$ = the length of time required to deliver a shipment to some distant location. Equation 10.6 implies that the remaining shelf-life of a product must be greater than the length of time it takes to travel the distance to destination "j." This would become an especially important distribution constraint for situations of long over-land or over-sea transport. While several items may meet the constraint given in Equation 10.6, additional criteria based on remaining shelf-life expectations could be used to specify the order in which items are to be issued from an inventory stockpile. It is suggested that the most appropriate basis for decisions regarding perishable inventory issue priority be shortest-remaining shelf-life, subject to the distribution constraint placed on the remaining shelf-life by transport logistics.

10.4.4 ECONOMIC IMPLICATIONS OF INVENTORY CONTROL

The best example of research weighing the economic implications of perishable inventory issue policy has been conducted in the pulp wood industry (Springer, 1979; Schmidt, 1990). Turpentine and tall oil are valuable byproducts recovered during the process of pulping wood chips. However, the amount of these compounds deteriorates during stockpile storage of wood chips. Regarding the economics of compound deterioration as influenced by stockpile (inventory) management, Springer (1979) reported minimum losses with a policy approximating JIT, and Schmidt (1990) found that a policy combining both LIFO and FIFO (a mixed policy) minimized losses and provided delivery of products with the most consistent levels of desired compounds. The implication of these studies is that quality-based inventory management strategies minimized economic losses for perishable products that are valued based on the level of component compounds (component quality attributes) within the product. To date the economic value of food products are not valued according to component compounds. However, imposing a penalty cost for disposal or sundry operations associated with items that fail to meet quality threshold standards or shelf-life expectations could alter the classical view of inventory management policy.

NOMENCLATURE

d_j Distance from stockpile location to distribution destination (miles or km)

E_A Temperature characteristic term expressed as an activation energy (cal/mol)

k Specific reaction rate for an isothermal condition (sensory rating score/day or instrumental measurement/day)

k_o Pre-exponential factor expressed as rate of change per unit time (sensory rating score/day or instrumental measurement/day)

$L(d_j)$ Length of time to travel from stockpile location to distribution destination "j" (d)

$L(Q_n)$ Remaining shelf-life expectation for product stored at T_{REF} and current quality level Q_n (d)

n Reaction order usually an integer value (dimensionless)

Q Quality attribute level (sensory rating score or instrumental measurement value)

Q_n Current quality level in remaining shelf-life prediction (sensory rating score or instrumental measurement value)

Q_o Initial quality level (sensory rating score or instrumental measurement value)

Q_{TH} Threshold quality level corresponding to end of shelf-life (sensory rating score or instrumental measure value)

R_g Universal gas constant (1.987 cal/mol K)

t   Time (d)

T   Absolute temperature (K)

T_{REF} Reference or recommended storage absolute temperature (K)

GLOSSARY

Just Noticeable Difference (JND)   Or First Noticeable Difference (FND), defines how long product can be stored before people notice product differences. JND occurs at the earliest time that a trained sensory panel can detect a noticeable difference between experimental and control samples using sensory difference test. Differences are evaluated considering all things and are not referenced to a specific quality attribute.

High Quality Life (HQL)   "…The elapsed time between freezing of an initially high quality product and the moment when 70% of experienced tasters successfully distinguish the product from the control (which has been maintained at a very cold temperature, –40°C or colder) in a triangle or duo-trio test." (International Institute of Refrigeration, 1972)

Practical Storage Life (PSL)   "…The practical storage life is the period of frozen storage after freezing of an initially high quality product during which the organoleptic quality remains suitable for consumption or for the process intended." (International Institute of Refrigeration, 1972)

FURTHER INFORMATION AND RESOURCES

American Frozen Food Institute
1764 Old Meadow Ln., Suite 350
McLean, VA 22102
(703) 821-0770

Canadian Association of Warehousing and Distribution Services
P.O. Box 125
Oshawa, ON, CANADA L1H 7L1
(416) 436-8801

Chilled Foods Association
5775 Peachtree-Dunwoody Rd.,
Atlanta, GA 30342
(404) 252-3663

Food Institute of Canada
130 Albert St. Suite 1409
Ottawa, ON, CANADA K1P 5G4
(613) 233-4049

Frozen Vegetable Council
1838 E. Camino Real,
Burlingame, CA 94010
(415) 697-6835

International Association of Refrigerated Warehouses
7315 Wisconsin Ave., #1200N
Bethesda, MD 20814
(301) 652-5674

International Ice Cream Association
888 16 St. NW
Washington, D.C. 20006
(202) 296-4250

National Food Processors Association
1401 New York Ave. NW
Washington, D.C. 20005
(202) 639-5900

National Frozen Food Association, Inc.
4755 Linglestown Rd., Ste. 300
Harrisburg, Pa 17112
(717) 657-8601

United Fresh Fruit & Vegetable Association
727 N. Washington St.
Alexandria, VA 22314
(703) 836-3410

REFERENCES

ABMPS, 1982. Predicting acceptance of frozen foods stored for extended periods, Report No. 126, Prepared by Committee on Plant Products, Advisory Board on Military Personnel Supplies, Commission on Engineering and Technical Systems, National Research Council, National Academy Press, Washington, D.C.

Amerine, M.A., Pangborn, R.M., and Roessler, E.B., 1965. *Principles of Sensory Evaluation of Food*, Academic Press, New York.

Arabshahi, A. and Lund D.B., 1985, Considerations in calculating kinetic parameters from experimental data, *J. Food Process Eng.* 7(1985):239-251.

Bomberger, E.E., 1961, Optimal inventory depletion policies, *Manage. Sci.* 7:294-303.

Cohen, E. and Saguy, I., 1985, Statistical evaluations of Arrhenius model and its applicability in prediction of food quality losses, *J. Food Process. Preservat.* 9(1985):273-290.

Derman, C. and Klein, M., 1958, Inventory depletion management, *Manage. Sci.* 4:450-456.

Desrosier, N.W. and Tressler, D.K., 1977. *Fundamentals of Food Freezing*, AVI Publishing, Westport, CT.

Dethmers, A.E., 1979, Utilizing sensory evaluation to determine product shelf-life, *Food Technol.* 34(11):40-42.

Dolan, K.D., Singh, R.P., and Wells, J.H., 1985, Evaluation of time-temperature related quality changes in ice cream during storage. *J. Food Process. Preservat.* 9(1985):253-271.

Fennema, O.R., Powrie, W.D., and Marth, E.H., 1973, *Low Temperature Preservation of Foods and Living Matter,* Marcel Dekker, New York.

Goodenough, P.W. and Atkin, R.K., 1981, *Quality in Stored and Processed Vegetables and Fruits*, Academic Press, London.

Haralampu, S.G., Saguy, I., and Karel, M., 1985, Estimation of Arrhenius parameters using three least squares methods, *J. Food Process. Preservat.* 9(1985):129-143.

Heldman, D.R. and Lai, D., 1983, A model for prediction of shelf-life of frozen foods. IIR, Commission C2 Preprints, 16th International Congress of Refrigeration, 427-433.

Hicks, E.W., 1944, Note on the estimation of the effect of diurnal temperature fluctuation on reaction rates in stored foodstuffs and other materials. J. Counc. Sci. Ind. Res., Aust. 17:111-114.

Hubbard, M.R., 1990, *Statistical Quality Control for the Food Industry.* Van Nostrand Reinhold, New York.

International Institute of Refrigeration, 1972, *Recommendations for the Procession and Handling of Frozen Foods,* 2nd., International Institute of Refrigeration, Paris.

Japan Management Association, 1993, *Kanban Just-In-Time at Toyota: Management Begins at the Workplace*, rev. ed., D.J. Lu, trans., Japan Management Association, Tokyo.

Jul, M., 1984, *The Quality of Frozen Foods,* Academic Press, New York.

Kwolek, W.F. and Brookwalter, G.N., 1971, Prediction storage stability from time-temperature data, *Food Technol.* 25(10):1025.

Labuza, T.P., 1979, A theoretical comparison of losses in food under fluctuating temperature sequences, *J. Food Sci.* 44(4):1162-1168.

Labuza, T.P., 1982, *Shelf-Life Dating of Foods* Food and Nutrition Press, Westport, CT.

Labuza, T.P., 1984, Application of chemical kinetics to deterioration of food, *J. Chem. Educ.* 61(4):348-358.

Lai, D. and Heldman, D.R., 1982. Analysis of kinetics of quality change in frozen foods, *J. Food Process Eng.* 6(1982):179-200.

Meilgaard, M., Civille, G.V., and Carr, B.T., 1991, *Sensory Evaluation Techniques*, 2nd ed., CRC Press, Boca Raton, FL.

Moreno, J., 1984, Quality deterioration of refrigerated foods and its time-temperature mathematical relationships, Int. J. Refrig., 7(6):371-376.

Nahmias, S. 1982. Perishable inventory theory: a review, *Operat. Res.* 30:680-708.

Pierskalls, W.P. and Roach, C.D., 1972, Optimal issuing policy for perishable inventory, *Manage. Sci.* 18:603-614.

Prastacos, G.P., 1984, Blood inventory management: an overview of theory and practice, Manage. Sci. 30:777-800.

Saguy, I. and Karel, M., 1980. Modeling of quality deterioration during food processing and storage, *Food Technol.* 34(2):78-85.

Schmidt, R.L., 1990, The effect of wood chip inventory rotation policies on storage cost, chip quality, and chip variability, *TAPPI J.* 73(11):211-216.

Schubert, H., 1977, Criteria for the application of T-TI indicators to quality control of deep frozen products, *Sci. Techn. Froid IIF-IIR* 1977-1:407-423.

Schutz, H.C., Damrell, J.D., and Locke, B.H., 1972, Predicting hedonic rating of raw carrot texture by sensory analysis, *J. Texture Stud.* 3(1972):227-232.

Schwimmer, S., Ingraham, L.L., and Hughes, H.M., 1955, Temperature tolerance in frozen food processing: effective temperatures in thermal fluctuating systems, *Ind. Eng. Chem.* 47(6):1149-1151.

Singh, R.P., 1976, Computer simulation of food quality during frozen food storage. *Int. Instit. Refrig. Bull. Supp.* 1976-1:197-204.

Singh, R.P. and Heldman, D.R., 1983, Quality changes in frozen foods. Presented at the 1983 Winter Meeting of the American Society of Agricultural Engineers, Chicago, ASAE Paper No. 83-6510.

Singh, R.P. and Wang, C.Y., 1977, Quality of frozen foods – a review, *J. Food Process Eng.* 1:97-127.

Singh, R.P. and Wells, J.H., 1985, Use of time-temperature indicators to monitor quality of frozen hamburger, *Food Technol.,* 39(12):42-50.

Singh, R.P. and Wells, J.H., 1986, Keeping track of time and temperature, *Meat Process.* 25(5):41-42, 46-47.

Singh, R.P. and Wells, J.H., 1987, Monitoring quality changes in stored frozen strawberries with time-temperature indicators, *Int. J. Refrig.* 10(5):296-300.

Singh, R.P., Wells, J.H., Dolan, K.D., Gonnet, E.J., and Muñoz, A.M., 1984, Critical evaluation of time temperature indicators for monitoring quality changes in stored subsistence, Report prepared for United States Army Natick Research & Development Center, Natick, MA.

Springer, E.L., 1979, An economic comparison of chip storage methods, *TAAPI J.* 62(9):39-42.

Taoukis, P.S., Fu, B., and Labuza, T.P., 1991, Time-temperature indicators, *Food Technol.* 45(10):70-82.

Tarver, M. and Schenck, A.M., 1958, Statistical development of objective quality scores for evaluation the quality of food products, *Food Technol.* 12(3):127-131.

Van Arsdel, W.B., Coply, M.J., and Olson, R.L., 1969, *Quality and Stability of Frozen Foods*, Wiley-Interscience, New York.

Wells, J.H., 1987, A computer-based inventory management system for perishable foods, Eng. D. dissertation. University of California, Davis, CA.

Wells, J.H. and Singh, R.P., 1988, A kinetic approach to food quality prediction using full-history time-temperature indicators, *J. Food Sci.* 53(6):1866-1871, 1893.

Wells, J.H. and Singh, R.P., 1989, A quality-based inventory issue policy for perishable foods, *J. Food Process. Preservat.* 12:271-292.

Wells, J.H., Singh, R.P., and Noble, A.C., 1987, A graphical interpretation of time-temperature related quality changes in frozen food, *J. Food Sci.* 52(2):436-439, 444.

Wills, R.B.H., Lee, T.H., Graham, D., McGlasson, W.B., and Hall, E.G., 1981, *Postharvest,* AVI Publishing, Westport, CT.

Zhao, Y., Wells, J.H., and Marshall, D.L., 1992, Description of log phase growth for selected microorganisms during modified atmosphere storage, *J. Food Process Eng.* 15(1992):299-317.

11 Thermal and Rheological Properties of Foodstuffs

Martin J. Urbicain and Jorge E. Lozano

CONTENTS

11.1   INTRODUCTION

Physical properties are those characteristics of the matter capable of being measured by physical means. They depend upon the matter composition, its physical state and the conditions under which the measurement is performed.

A natural edible product is usually processed in order to preserve it, to enhance its hedonic acceptance, to increase its nutritional value, and/or make it easier to consume. In any case, physical properties play an important role in defining the manufacturing procedure, but they are not always available to the design engineer. Finding relevant data is usually the controlling step in the design of a given operation, and considering the broad set of materials that make up the food category, the best solution is frequently the experimental determination. Among those properties, thermophysical and rheological are the most relevant groups.

11.2   THERMOPHYSICAL PROPERTIES

Thermophysical properties of any material are those which control the thermal energy transport and/or storage within it, as well as the transformations undergone by the material under the action of heat. Foods are no exception to this general rule. Typically, thermal conductivity, thermal diffusivity, specific heat, and density or specific gravity are regarded as thermophysical properties. They are dependent on the temperature and the material chemical composition and physical structure. Since foodstuffs are composite materials, it is apparent that the relevant information is the average or effective value. This value is clearly some function of those of the components. Hence, the generation of predictive models requires a physical representation of the material under study. In this sense foodstuff materials can be regarded as complex substances, showing three different levels of complexity.

First, in the lowest level, what eventually looks like a continuous and homogenous single phase, is in fact composed of different chemical compounds. These compounds could be considered the most elemental *species* regarding the thermal property calculation. When continuous, any model proposed for the prediction of a given property must consider the individual contribution of the *species*, namely proteins, carbohydrates, fats, fiber, water, and minor components. This is done by means of some weighing factor accounting for the proportion in which they are present.

Second, some food materials can be considered a solid matrix of the continuous factors described and a disperse phase of gas or liquid, usually air or water, respectively. This description typically refers to porous foods, suspensions, flours, powders, and dusts. In this case, both the volumetric fraction and the spatial distribution of each phase are to be considered, which is done by means of distribution factors.

Finally, the third level is attained when quite different materials are processed together to give place to composite materials. This group includes all kinds of canned and packed foods, pastry, confectionery, and a wide variety of prepared foods. Again, modeling requires the information of the mean or effective values of the components together with the representation of the physical structure.

The value of the thermophysical property will be a function of the temperature through the dependence of the components and porosity or water content for porous or composite foodstuffs. Since water can be either liquid or solid, particular attention is paid to frozen foods.

Though available information is only partial, it is also true that there is a fairly large amount of data on some particular foods. These data sometimes are contradictory due to the different conditions at which they were gathered, as well as to the differences among the same foods of different origin, composition, and structure. Hence, this chapter is oriented, whenever possible, to the presentation of correlating expressions more than to the tabulation of punctual data, in order to provide prediction tools of a more general nature, together with the description of the accepted measuring techniques. Efforts have been made to include the most recent data and correlations whenever possible.

The chapter will focus on theory and measuring techniques as well as predictive correlations as a function of relevant parameters such as temperature, moisture content, and porosity whenever applicable.

11.2.1 THERMAL CONDUCTIVITY

In this section, theoretical and semiempirical models for the prediction of thermal conductivity are presented.

Heat has been defined as "energy in transit" through a given medium. When a temperature difference is established between two points located within that medium, a heat flux vector is generated, proportional to the value of the temperature gradient between the points. The thermal conductivity is the proportionality constant between both vectors, as expressed by the well known Fourier's Equation 11.1

$$q = -k\frac{dT}{dz} \qquad (11.1)$$

where k is the thermal conductivity, q the heat flux, T the local temperature, and z the distance measured in the direction of the flux vector. The minus sign accounts for the fact that both vectors have opposite directions, that is, heat flows in the direction of the decreasing temperature.

Physically, it is a measure of how much heat travels through a unit surface in a unit time, under the driving force imposed by a unit temperature difference, and it is an intrinsic property of the material.

11.2.1.1 Theoretical and Semiempirical Models for Thermal Conductivity of Foods

The prediction of the thermal conductivity has been based on methods developed for composite materials other than foods, such as soils, ceramics, polymers, and the like, which have the same physical characteristics. Consideration is paid to the heat flux direction in relation to the geometrical arrangement if the medium is anisotropic, as fibrous materials with fibers oriented in a main direction, (meat, some vegetables, suspensions, etc.).

Both theoretical and empirical models have been developed to predict thermal conductivities of composite materials. Empirical relationships of k as a function of temperature and composition will be given below for many products. Theoretical models are more general in nature but they need to assume a description of the topology of the matter, that is, the spatial distribution of different constituents. Also some models derived from theoretical considerations are actually semiempirical as they have parameters which are to be fitted for particular products from measured values.

The most elementary models are those assuming that different components are arranged in layers either parallel or normal to the heat flow, resulting in the following expressions based on the electric analogy of heat transmission, where the effective property is noted simply as k:

Series Model — In this model, layers of components placed normal to the heat flow, in a serial arrangement of resistances and the effective thermal conductivity, k, can be calculated as follows

$$k = \frac{1}{\sum\limits_{i=1}^{N} \dfrac{\phi_i}{k_i}} \tag{11.2}$$

where k_i = individual thermal conductivity of each constituent, also known as the intrinsic thermal conductivity, and ϕ_i = volume fraction of each constituent. Series model as been recommended by Andrieu et al. (1987) as giving the best prediction for quasihomogeneous foodstuffs, such as proteins, gels, meat, and tofu in both the frozen and unfrozen state.

Parallel model — In this model, layers of components are placed in the direction of the heat flow, in parallel arrangements of resistances: The effective thermal conductivity is given by

$$k = \sum_{i=1}^{N} k_i \phi_i \tag{11.3}$$

Randomly distributed models — These models are more general in nature, as they do not have the geometrical restriction of the above-mentioned. They consider that there is a continuous phase with a discontinuous phase dispersed within the former one, as particles of various shapes in either regular or irregular array. They were developed for electrical conductivity but have been applied successfully to thermal conductivity of heterogenous materials like foodstuffs.

There are several theoretical and semiempirical equations in literature which can be successfully applied to a given pair of constituents and given conditions, but no one represents

TABLE 11.1
Coefficients to Calculate Parameters of A_i of Equation 11.5

	A_1	A_2	A_3	A_4
a	0.44735	–2.22601	–1.83405	–0.394814
b	0.873233	14.3434	–0.619566	–5.44528
c	–0.43634	–25.5292	75.18500	53.41450
d	2.18646	9.22053	53.01440	–41.87700

From Murakami, E. G. and Okos, M. R., 1986, Predicting the thermal conductivity of dry porous foods, ASAE Paper No. 86-6538. With permission.

all systems. Some of them are described below to provide a basic insight on the subject, but application should be confirmed by experimental data.

Keey's (1972) model with variable distribution factor, combines series and parallel models to predict the effective thermal conductivity in powders, flours, and dusts, by assuming that in a heterogenous material, such as porous foodstuffs, the solid and the pores are arranged in a random fashion which can be represented by a linear combination of normal and parallel arrangements:

$$\frac{1}{k} = \frac{1-f}{(1-\varepsilon)\,k_s + \varepsilon\,k_g} + f\left[\frac{1-\varepsilon}{k_s} + \frac{\varepsilon}{k_g}\right] \tag{11.4}$$

where $k_s = \Sigma \omega_i k_i$, for i = 1… N – 1 (air not included), w_i = mass fraction of component i, ε = povosicity, $k_g = k_{air}$ and f = distribution factor which accounts for the spatial distribution of pores and solid material. If a parallel arrangement is assumed, f = 0, and for pure normal arrangement f = 1. All the intermediate values corresponding to the contribution of each arrangement to the heat conduction mechanism in the actual spatial distribution are calculated using Equation 11.4. Murakami and Okos, (1986) calculated the factor f in Equation 11.4 by a third degree polynomial in ε, the coefficients of the polynomial being in turn another polynomial in moisture content as follows:

$$f = A_1 + A_2(\varepsilon - 0.4) + A_3(\varepsilon - 0.4)^2 + A_4(\varepsilon - 0.4)^3 \tag{11.5}$$

and

$$A_i = a + b\,\xi + c\,\xi 2 + d\,\xi 3$$

where ξ = X for i = 1 and 2, ξ = (X – 0.25) for i = 3 and ξ = (X – 0.1627) for i = 4, a, b, c, and d depend on the particular A_i. Their values are given in Table 11.1.

Choi and Okos (1986) correlated experimental data of different thermophysical properties, like thermal conductivity, specific gravity, and specific heat, using models based on the mass fraction of the major components (protein, fat, carbohydrate, fiber, ash, and water), and developed group models as quadratic and linear functions of the temperatures for those substances. Thermal conductivity and diffusivity depend upon the spatial structure of the material. Consequently the models use the volume fraction ϕ_i to estimate the value of the

property for the composite material. Mass fractions are easier to measure than volumetric ones, hence, those are calculated from the mass fractions, w_i, and densities, ρ_i. Density and specific heat are intensive properties which depend directly on the mass fractions. Hence, volume fractions in Equation 11.3 are calculated by means of Equation 11.6 as functions of mass fractions w_i and intrinsic densities ρ_i.

Volume fraction

$$\phi_i = \frac{\dfrac{w_i}{\rho_i}}{\sum \dfrac{w_i}{\rho_i}} \qquad (11.6)$$

Thermal diffusivity

$$\alpha = \sum \alpha_i w_i \qquad (11.7)$$

Density

$$\rho = \frac{1}{\sum \dfrac{w_i}{\rho_i}} \qquad (11.8)$$

Specific heat

$$C_p = \sum C_{p_i} w_i \qquad (11.9)$$

Unfrozen water fraction

$$\frac{\lambda}{R}\left[\frac{1}{T_o} \frac{1}{T_i}\right] = \ln\left[\frac{\dfrac{w_w}{M_w}}{\dfrac{w_w}{M_w} + \sum \dfrac{w_i}{M_i}}\right] \qquad (11.10)$$

Equations able to estimate the thermal conductivity, thermal diffusivity, density, and specific heat for basic constituents of food as proposed by Choi and Okos, are given in Table 11.2.

One of the simplest is that of Woodside and Messmer (1961), who proposed a model based on the weighed geometric mean of the constituents, using the volume fraction as the weighing factor. It is easy to use and is valid for a broad set of conditions, since its formulation represents the chaotic nature of randomly distributed media.

$$k = \prod k_i^{\phi_i} \qquad (11.11)$$

Among these models, that of Lewis and Nielsen (1970) was found suitable to correlate the thermal conductivity of tomato paste with varying moisture content by Rivero (1982). It is represented by Equation 11.12.

TABLE 11.2
Thermal Properties of Major Components of Foods
as Functions of Temperature

Thermal	Main component	Equation
k (W/m°C)	Carbohydrate	$k = 0.20141 + 1.3874 \cdot 10^{-3}\, T - 4.3312 \cdot 10^{-6}\, T^2$
	Ash	$k = 0.32962 + 1.4011 \cdot 10^{-3}\, T - 2.9069 \cdot 10^{-6}\, T^2$
	Fiber	$k = 0.18331 + 1.2497 \cdot 10^{-3}\, T - 3.1683 \cdot 10^{-6}\, T^2$
	Fat	$k = 0.18071 + 2.7604 \cdot 10^{-4}\, T - 1.7749 \cdot 10^{-7}\, T^2$
	Protein	$k = 0.17881 + 1.1958 \cdot 10^{-3}\, T - 2.7178 \cdot 10^{-6}\, T^2$
	Water	$k_A = 0.57109 + 1.7625 \cdot 10^{-3}\, T - 6.7036 \cdot 10^{-6}\, T^2$
	Ice	$k_H = 2.2196 - 6.2489 \cdot 10^{-3}\, T + 1.0154 \cdot 10^{-4}\, T^2$
α (m²/s) × 10⁶	Carbohydrate	$\alpha = 8.0842 \cdot 10^{-2} + 5.3052 \cdot 10^{-4}\, T - 2.3218 \cdot 10^{-6}\, T^2$
	Ash	$\alpha = 1.2461 \cdot 10^{-1} + 3.7321 \cdot 10^{-4}\, T - 1.2244 \cdot 10^{-6}\, T^2$
	Fiber	$\alpha = 7.3976 \cdot 10^{-2} + 5.1902 \cdot 10^{-4}\, T - 2.2202 \cdot 10^{-6}\, T^2$
	Fat	$\alpha = 9.8777 \cdot 10^{-2} + 1.2569 \cdot 10^{-4}\, T - 3.8286 \cdot 10^{-8}\, T^2$
	Protein	$\alpha = 6.8714 \cdot 10^{-2} + 4.7578 \cdot 10^{-4}\, T - 1.4646 \cdot 10^{-6}\, T^2$
	Water	$\alpha_A = 0.1317 + 6.2477 \cdot 10^{-4}\, T - 2.4022 \cdot 10^{-6}\, T^2$
	Ice	$\alpha_H = 1.1756 - 6.0833 \cdot 10^{-3}\, T + 9.5037 \cdot 10^{5}\, T^2$
ρ (kg/m³)	Carbohydrate	$\rho = 1.5991 \cdot 10^3 - 0.31046\, T$
	Ash	$\rho = 2.4238 \cdot 10^3 - 0.28063\, T$
	Fiber	$\rho = 1.3115 \cdot 10^3 - 0.36589\, T$
	Fat	$\rho = 9.2559 \cdot 10^2 - 0.41757\, T$
	Protein	$\rho = 1.3299 \cdot 10^3 - 0.51840\, T$
	Water	$\rho = 997.18 + 3.1439 \cdot 10^{-3}\, T - 3.7574 \cdot 10^{-3}\, T^2$
	Ice	$\rho = 916.89 - 0.13071\, T$
C_p (kJ/kg°C)	Carbohydrate	$C_p = 1.5488 + 1.9625 \cdot 10^{-3}\, T - 5.9399 \cdot 10^{-6}\, T^2$
	Ash	$C_p = 1.0926 + 1.8896 \cdot 10^{-3}\, T - 3.6817 \cdot 10^{-6}\, T^2$
	Fiber	$C_p = 1.8459 + 1.8306 \cdot 10^{-3}\, T - 4.6509 \cdot 10^{-6}\, T^2$
	Fat	$C_p = 1.9842 + 1.4733 \cdot 10^{-3}\, T - 4.8008 \cdot 10^{-6}\, T^2$
	Protein	$C_p = 2.0082 + 1.2089 \cdot 10^{-3}\, T - 1.3129 \cdot 10^{-6}\, T^2$
	Water	$C_{p1} = 4.0817 - 5.3062 \cdot 10^{-3}\, T + 9.9516 \cdot 10^{-4}\, T^2$ (−40 < T < 0°C)
		$C_{p2} = 4.1762 - 9.0864 \cdot 10^{-5}\, T + 5.4731 \cdot 10^{-6}\, T^2$ (0 < T < 150°C)
	Ice	$C_p = 2.0623 + 6.0769 \cdot 10^{-3}\, T$

From Choi, Y. and Okos, M. R., 1986, Effects of Temperature and composition on the thermal properties of foods, *Food Engineering and Process Applications.* Vol. 1, *Transport Phenomena,* LeMaguer, M. and Jelen, P., Eds., Elsevier, New York. With permission.

(11.12)

$$k = k_c \frac{1 + A\, B\, \phi}{1 - B\, \phi\, \psi}$$

where B and Ψ are parameters which depend on water content and are given by

$$B = \frac{k_d - k_c}{k_d + A\, k_c}$$

(11.13)

TABLE 11.3
Values of A and Ξ_m in Lewis and Nielsen's Equation for Different Shapes and Packing of Dispersed Particles in a Suspension

Shape of dispersed phase	Heat flow direction	Packing type	A	χ_m
Cubes	Any		2.0	
Spheres	Any		1.5	
		Hexagonal		0.740
		Faces centered cubic		0.740
		Bodies centered cubic		0.6
		Simple cubic		0.524
		Random compact		0.601
Random cylinders				
L/D = 2	Any		1.58	
L/D = 4	Any		2.08	
L/D = 6	Any		2.8	
L/D = 10	Any		4.93	
L/D = 15	Any		8.38	
One direction oriented	Parallel		2 L/D	
	Normal		0.5	
Cylinders or fibers		Hexagonal compact		0.907
		Simple cubic		0.785
		Random in one direction		0.82
		Random in three directions		0.52

From Lewis, T. and Nielsen, L., 1970, Dynamic mechanical properties of particulate-filled polymers, *J. Appl. Polym. Sci.,* 14. With permission.

A and χ_m are empirical constants which take into account type, shape, and orientation of dispersed particles, tabulated for different products by the cited authors and shown in Table 11.3.

Maxwell (1904) derived the following theoretical relationship for a composite material consisting of a continuous medium into which a dispersed one is randomly distributed

$$k = k_c \frac{k_d + 2 k_c - 2 \phi_d (k_c - k_d)}{k_d + 2 k_c + \phi_d (k_c - k_d)} \tag{11.14}$$

where k_c and k_d are the thermal conductivities of the continuous and dispersed phases, respectively, and ϕ_d is the volume fraction of the dispersed phase. In a foodstuff, the cellular material can be regarded as the continuous phase, while air and/or water forms the dispersed phase. For a multiphase system, with N dispersed phases of known particle shapes in a continuous matrix, Equation 11.14 becomes

$$k = k_c \frac{1 - \sum_1^N \frac{\phi_i (S_i - 1)(k_c - k_i)}{k_i + (S_i - 1) k_i}}{1 + \sum_1^N \frac{\phi_i (k_c - k_i)}{k_i + (S_i - 1) k_i}} \tag{11.15}$$

where S_i is the particle shape factor $= 3/\Psi$, Ψ being the sphericity (1 for spheres) and k_i and ϕ_i are as defined.

Behrens (1968) proposed a theoretical model for a two-phase system assuming it is composed of cylinders in a square network, which gives k as a function of the volume fraction of the dispersed phase, and the ratio between individual thermal conductivities, $p = k_d/k_c$

$$k = k_c \frac{(p+1)+(p-1)\phi}{(p+1)-(p-1)\phi} \qquad (11.16)$$

which for spheres cubic symmetry reduces to the Maxwell equation. The reader will find additional references in *For Further Information* in this chapter.

Mattea et al. (1986, 1989) have developed two theoretical models of statistical nature which have been applied to vegetables and similar materials. The first model by Mattea et al. (1986) is based on the so-called Effective Medium Theory, which considers an heterogenous medium as represented by a virtual homogenous one with the same properties. The derived equation is

$$\sum_{i=1}^{n} \phi_i \frac{k - k_i}{k_i - 2k} = 0 \qquad (11.17)$$

where ϕ_i and k_i are the volume fraction and the thermal conductivity of constituent i, respectively.

For a two-component continuous medium, such as vegetable tissues, powders, and other porous materials, Equation 11.17 becomes

$$k = k_p \left(b + \sqrt{b^2 + 2m} \right) \qquad (11.18)$$

where k_p is the thermal conductivity of the pores, usually air, $m = k_{cells}/k_p$ and b is given by

$$b = 3\varepsilon - 1 + \left[3(1-\varepsilon) - \right] \qquad (11.19)$$

ε being the total porosity, i.e., the volume fraction of pores in the product.

Equations 11.17 to 11.19 were applied to potatoes and pears at different moisture contents, by Mattea et al. (1986) with $k_{cell} = k_{water}$, $k_p = k_{air}$ and experimental values of ε given by Lozano et al. (1983). They found very good agreement with directly measured values of thermal conductivities of the products being dried.

The second model by Mattea et al. (1989) is based on the simulation of the food tissue by means of a geometrical representation named Voronoi tessellation. This refers to the subdivision of the sample into polygons representing the cells and the pores. The theory, when applied to the prediction of the thermal conductivity of pears and apples as a function of the moisture content showed good agreement with experimental values obtained by the same authors, showing that the geometrical representation fits the physical structure of those products.

Obviously, whatever the model, the individual or intrinsic values of the property is to be known for it to be applied. Hence it must be either calculated by means of a suitable predictive equation, or measured with any of the well-known techniques, which will be outlined.

Alternatively, the property of the composite material can be either calculated by a predictive equation or measured. However, measured values are not always available, and the models presented so far are sometimes the only way to estimate the value of the property, with the additional advantage that collected components data can be used for predicting other properties by models based on individual contributions.

11.2.1.2 Experimental Measurement of Thermal Conductivity

Several experimental methods have been devised to measure the thermal conductivity of composite materials which are suitable for foodstuffs. They can be divided into two main groups: steady state and transient techniques.

11.2.1.2.1 Steady State Methods

The steady state methods are based on the measurement of the constant heat flux in a sample of known thickness and flow area under a constant imposed temperature gradient applied to the sample boundaries. Under these conditions, temperatures within the sample are functions of the position only. Among these methods the most known is the hot guarded plates, named for the isolated isothermal plates bounding the sample.

In general, these methods are not suitable for foodstuffs, because they require fairly sophisticated and expensive equipment, and the experiments take relatively long times, which introduces a source of error due to convection effects, water migration, and composition changes during the measurement. Further, only moderate temperatures are allowed, as the higher the temperature, the larger the magnitude of those errors. Hence, no further attention is to be paid to these methods in this chapter.

11.2.1.2.2 Transient Techniques

In contrast, transient methods are fast, cheap, and reliable. All of them are based on the fact that any material submitted to a constant strength heat source of a given geometry in a given position, undergoes a transient thermal behavior, that is, the temperature of a given point changes with time in accordance to the material's physical characteristics and its thermal conductivity. The analysis of the temperature history gives the value of the thermal conductivity, under certain restrictions that will be discussed. These methods are also used in the measurement of thermal diffusivity.

Depending on the heat source geometry and operation, there are methods based on either the line-source, like the thermal probe and the hot wire, or the pulse (or flash) theory. The former is the most widely used and therefore will be more extensively presented here. The theory has been discussed extensively by several authors. Some of the most recent are Moshenin (1980), who made a detailed discussion of the errors introduced by the sample finite dimensions and the water migration into the value measured; Casada and Walton (1989), who presented a new model for the temperature rise when a thermal probe is used in an infinite medium, to account for the finite diameter and specific heat of the probe; and Kent et al. (1984) who discussed methods of measurement of different properties and is an excellent reference for all models.

The theory can be summarized as follows. A nonmaterial line heat source imbedded in a given medium provokes a temperature field governed by Equation 11.20

$$T(r, t) - \frac{q}{2\pi k} \int_{\beta}^{\infty} \frac{\exp\left(-\beta^2\right)}{\beta} \, d\beta \qquad (11.20)$$

where q = line-source strength (W/m); k = thermal conductivity (W/m/°C); $\beta = r^2/(4\alpha t)$; t = time elapsed since t_0; t_0 = initial time at which the constant q is initiated; α = thermal diffusivity (m²/s); and r = distance from the line source.

The integral in Equation 11.20 can be solved and T(r,t) results

$$T(r, t) = \frac{q}{2\,k}\left[-0.\frac{57721}{2} - \ln\beta + \frac{\beta}{2} - \frac{\beta^2}{4} + \ldots\right] \qquad (11.21)$$

Nix et al. (1967) found that the first 40 terms of the above equation are to be evaluated to ensure convergence. However, for values of $0 < \beta < 0.16$, the residual error is made if only the first two terms within brackets are taken. That is a condition easily attained if the probe and the point where the temperature is measured are closely located and the time is large (order of minutes).

If the experience is performed such that at two times t_1 and t_2 two temperatures T_1 and T_2 are recorded, Equation 11.21 becomes

$$T_2\,T_1 = \frac{q}{2\,\pi\,k}\ln\left(\frac{t_2}{t_1}\right) \qquad (11.22)$$

These are the theoretical values of T at a given pair of times t_1 and t_2. The expression is independent of the radius, provided the restriction on β holds, which means that no special care is to be taken in mounting the probe, which in turn means an additional advantage in using this type of setup. In practice, the thermocouple is either attached or inside the source so the temperature recorded is actually that of the probe itself. It is apparent that if values of T and t are collected together, and q is known from electrical measurements, k can be easily calculated, in a clean, fast experiment which requires only a device simulating a linear source, which does not interfere with the sample.

However, experiments show deviations from values predicted by Equation 11.21, due to several factors: the finite dimensions of both the source radius and the sample; the contact resistance between them; and the difference between their thermal properties. Hooper and Leeper (1950) showed that those effects can be accounted for by means of a constant subtractive time term t_0, such that Equation 11.22 becomes

$$T_2\,T_1 = \frac{q}{2\,\pi\,k}\ln\left(\frac{t_2 - t_0}{t_1 - t_0}\right) \qquad (11.23)$$

Term t_0 has a clear physical significance. It is the time required for the temperature rise to be a linear function of the logarithm of time.

The current practice is to make a linear regression of an experimental pair of values T, t (Urbicain and Elustondo, 1975) by repeating the calculations with a decreasing number of pairs. Each calculation yields increasing values of the slope as the points at lower times are discarded because they lie above the theoretical line. When two successive calculations produce the same slope, it is the theoretical value, as it means that only points lying on the straight line have been left. The method was successfully applied to the measurement of thermal conductivity of apples at different water contents and of tomato paste at different concentrations by Lozano et al. (1979) and Rivero (1978), and were expressed by Correlations 11.65 and 11.39, respectively.

11.2.1.3 Measuring Devices

As mentioned, the most popular devices are the hot wire and the thermal probe, because of their simplicity and reliability. Both techniques allow the use of the theory of the heat-line source.

In both techniques a small diameter wire capable of being heated is located within the sample. Constant electrical power is applied to the wire and its temperature recorded as a function of time by means of a thermocouple attached to it. The response is a function of the input energy and the material thermal conductivity only, the temperature of the wire is the only variable to be measured.

The heated wire is mounted vertically along the geometrical axis of a vessel into which the material to be tested is poured. It is recommended for liquids, pastes, and powders. Upper and lower leads provide DC current and a thermocouple soldered to the wire allows the temperature recording.

The probe, which is more popular than the heating wire, is usually built into a hypodermic needle, introducing the heating resistance while the thermocouple is either mounted with the power leads or stuck to the surface. Different designs have been discussed by Sweat (1974), Hayashi et al. (1974), Woodside and Messmer (1961), and by Choi and Okos (1983). The measurements are carried out by simply introducing the needle in the sample, switching the current, recording times and temperatures for a few minutes depending on the material type. Urbicain and Elustondo (1975) modified the device so that the heating wire becomes the probe. It is 0.0005 m in diameter, covered with an epoxy resin as isolation, and is sharply bent onto itself to become a needle. The thermocouple is glued to the probe. It proved to be much simpler to build and repair, and once tested in pure substances of known thermal conductivity, as water with 0.5% of agar gel to avoid convective currents, showed to have an accuracy of ±2% as referred to tabulated values. The probe is widely used with liquids and soft solids, as well as powders. The main practical problem with soft solids is the small air gap built up between the probe and the material after puncture. Convective currents are a source of errors in liquids, but they can be avoided if the liquid is mixed with a small proportion of gelling agents.

Elustondo and Urbicain (1993) modified the design to get a device that has the features of both the heating wire and the thermal probe. Figure 11.1 shows a diagram of the system. The probe is also the heating device, which, once located into the metallic piece at the bottom, closes the electrical circuit and works as a heating wire. The temperature increase in the probe is measured by the thermocouple located inside the tube and recorded with a personal computer. A simple program performs the control of the experiment as well as the calculations rendering the value of the thermal conductivity.

11.2.2 THERMAL DIFFUSIVITY

Thermal diffusivity (α) is closely related to thermal conductivity, as it is the transport parameter in the energy transport equation, which states that the enthalpy balance in an isotropic elemental volume bounded by an elemental surface, across which there are heat fluxes in the three coordinate directions, can be expressed by Equation 11.24

$$c_p \, \rho \, \frac{\partial T}{\partial t} - k \, \nabla^2 T \qquad (11.24)$$

where the left hand side is the unsteady state enthalpy change with time and $\nabla^2 T$ is the flux gradient along the three axes, written in terms of the temperatures when fluxes are expressed by Equation 11.1 If physical properties are grouped, the well-known Laplace's equation is obtained.

TC

St. St. OD = 1.5 m/m ID = 1.5 m/m

⊙ DC

SILICON OIL

SPECIMEN

O RING

⊖ DC
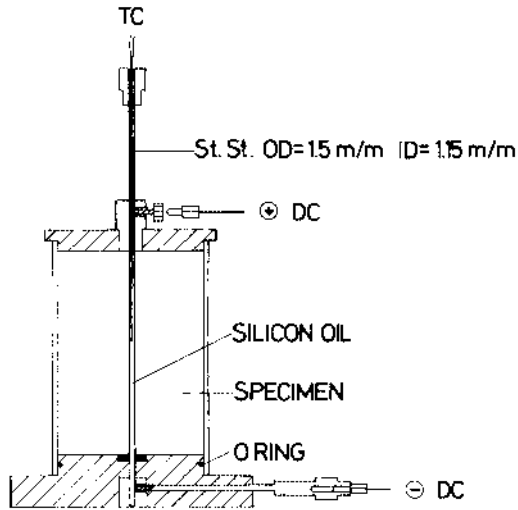
FIGURE 11.1 Sketch of thermal probe as designed by Elustondo and Urbicain (1993).

$$\frac{\partial T}{\partial t} = \alpha \, \nabla^2 T \tag{11.25}$$

where the new constant α is equal to

$$\alpha = \frac{k}{c_p \, \rho} \tag{11.26}$$

Lord Kelvin called α the thermal diffusivity of the material and Maxwell called it the thermometric conductivity. Physically, it is the change of temperature produced in a unit volume of unit surface and unit thickness, containing ρ grams of matter, by heat flowing in the unit time through the unit face, under the unit temperature difference between opposite faces.

11.2.2.1   Measurement of the Thermal Diffusivity

Usually it is a byproduct of the thermal conductivity, specific heat, and density measurements by application of Equation 11.26. Alternatively, it is measured by the same techniques used for thermal conductivity, in particular the thermal probe.

More recently, Andrieu et al. (1986) presented the pulse method applied to foodstuffs. The sample, shaped as a slab or disk, with parallel faces is submitted to an energy pulse on one of its faces, for a very short time, by means of a flash lamp, capable of delivering about 800 J in .01 s. The temperature rise of the opposite face is recorded. Thermograms of reduced temperatures vs. times give parameters which lead to the calculation of α by simple relationships. Verma et al. (1990) suggest an alternative technique for the determination of the thermal diffusivity using the theory of the line heat source.

Fitch (1935) proposed a method consisting of imposing a known constant flux of heat on one face of a slab of the tested material, while temperature in the opposite face is recorded as time elapses. The solution of the Fourier equation leads to a linear relationship between

the logarithm of the recorded temperature and time, the slope being a function of thermal conductivity. The main disadvantage of the method is that reliability increases as sample thickness decreases, making the experiment more difficult. More details on the method can be found in Mohsenin (1980) and in Zuritz et al. (1987).

The reader will find some useful references in *For Further Information*.

11.2.3 SPECIFIC HEAT

Specific heat is the amount of heat required to increase the temperature of 1 kg of material 1°C at a given temperature. The specification of the interval is needed, as it changes with temperature. If the increase is a certain ΔT as a consequence of the action of an amount Q of heat on a given mass W, the calculated specific heat is the average one, that is

$$C_{avg} = \frac{Q}{m \, \Delta T} \tag{11.27}$$

If ΔT is small, and q = Q/W, Equation 11.27 gives the instantaneous value of C

$$C = \lim_{\Delta T \to 0} \left(\frac{q}{\Delta T} \right)_T = \left(\frac{dq}{dT} \right)_T \tag{11.28}$$

The specific heat of a gas depends on whether the heat transfer takes place under constant volume or pressure, and correspondingly two different parameters, C_v and C_p, are defined for those conditions. Specific heat of solids and liquids depends upon temperature but are not sensitive to pressure, as they are incompressible to all practical purposes. However it is common to use the constant pressure specific heat, C_p. Foodstuffs are not an exception, as all processes involving them are carried out at that condition. The relevant parameters in calculating C_p are temperature, moisture content, and porosity for porous materials.

The units of C_p are, in accordance with its definition, kJ/kg °C, but also Kcal/kg °C are commonly used. It must be recalled that, given the definitions of calorie and British thermal unit in metric and English systems, respectively, C_p value is numerically the same in both systems.

11.2.3.1 Specific Heat Measurement

Specific heat has been traditionally measured in calorimeters, consisting in an isolated Dewar flask in which W_{ref} grams of a reference liquid of known specific heat $C_{p,ref}$ and temperature $T_{i,ref}$ is put in contact with W_s grams of the testing sample at a different temperature $T_{i,s}$ allowing them to reach a final equilibrium temperature T_{eq}. A simple enthalpy balance, if losses are neglected, allows the calculation of the sample C_p by Equation 11.29

$$C_p = \frac{C_{p,ref} \, W_{ref} \left(T_{i,ref} - T_{eq} \right)}{W_s \left(T_{eq} - T_{i,s} \right)} \tag{11.29}$$

The reference substance is usually water or oil, depending on the sample nature.

The modern method to measure C_p is by means of a Differential Scanning Calorimeter (DSC). It is easy to use and much more accurate because it is a direct measure of the property as it is defined. The only problem is that it requires a bit more sophisticated piece of equipment. The basic function of the apparatus is to measure the amount of heat required to raise the temperature of the sample at a predetermined rate within a given interval.

Measurements include the previous determination of a baseline with no samples present, only the aluminum pans which hold the sample and a reference substance during the measurement. The plot is the "calorimetric equivalent", that is the energy required to heat the ancillary elements, from which the actual recording is to be subtracted.

The measurement is made by comparison with an external standard, the specific heat of which is already known. This makes the operation easier and more reliable. The equation governing the measurement is as follows

$$C_p = \frac{W_{ref}}{W} \frac{d}{d_{ref}} C_{p,ref} \qquad (11.30)$$

where $C_{p,ref}$, W_{ref}, and d_{ref} are, respectively, the specific heat, the mass, and the deflection from the base line of the reference standard, and C, W, and d the corresponding values of the tested material.

All DSC units are commercial. They are manufactured by well-known companies in the field and are provided with all the information necessary to operate the equipment.

11.2.4 Density and Specific Gravity

Density is the mass of the unit volume, and is measured in kg_m/m^3. Specific gravity is the relative density, that is the ratio between the actual density and that of a reference substance taken as a unit (water for liquids and solids), making specific gravity a dimensionless magnitude. Specific weight is the weight of the unit volume, measured in Kg_f/m^3.

11.2.4.1 Measurement

There are two main procedures for measuring density of liquids: hydrometric and pycnometric techniques.

The first one is based in the Archimedes principle, and consists of measuring the loss in weight of a solid body of known volume when it is immersed in the liquid, which requires the density of the solid to be higher than that of the liquid. It can be easily shown that ρ, the liquid density, is equal to

$$\rho = \frac{P_0 - P_s}{m_b} \rho_b \frac{g}{g_c} \qquad (11.31)$$

where P_0 and $P_s (kg_f)$ are the weights of the body in the air and in the liquid, respectively, and m_b (kg_m) and ρ_b (kg_m/m^3) are the body mass and density, respectively. The quotient g/g_c accounts for the difference in dimensions of P and m, making the equation dimensionally homogeneous without changing the numerical result, as it is equal to 1 for all practical purposes. In fact, mass and weight are numerically the same, 1 kg_f is the weight of 1 kg_m, then the numerical value of density in kg_m/m^3 is the same as that in kg_f/m^3.

The pycnometer is essentially a calibrated flask which allows the weighing of an exact known volume of liquid, which in turn gives the density $\rho = W/V$. To set the experimental temperature, the picnometer is immersed in a constant temperature bath and filled with the sample. The weight is determined by difference from the empty flask. For further information on the techniques described, the reader is referred to ASTM standard test methods D 368, D 891, and D 1298 for hydrometers and modified ASTM D 369 and D 891 for pycnometers, where all details of the procedures are provided.

A recommended procedure for meats is to add a known mass (approx. 5 g) of sample to a calibrated 60 mL flask, completing the volume with distilled water at 22°C, calculating density by means of Equation 11.32:

$$\rho = \frac{w}{V_s} = \frac{w}{60 - V_w}$$

(11.32)

where w and V_s are the mass and volume of the sample, respectively, calculated from the added water volume V_w.

11.2.5   PREDICTIVE EQUATIONS

There are several very comprehensive works on thermophysical properties of foods, which collect punctual values for a given product at given conditions, as well as predicting correlations for a particular set of foodstuffs, generally as functions of temperature and, eventually, water content or porosity. But it should be stated, as a general remark, that in spite of the intense work devoted by hundreds of researchers to the development of predictive equations, they are approximations of variable accuracy and should be dealt with accordingly. Foods can be regarded as "living" matter, with differences within the same sample. All information must be handled as a first estimation and, if more accuracy is required, experimental data for the particular system is to be obtained by means of the different methods previously explained. The reader is referred to *For Further Information* where very good sources of information on this topic are cited.

A rule of thumb, regarding densities of major food components, states that values of fats, proteins, and carbohydrates fall within narrow ranges; consequently average values of 0.92, 1.25, and 1.55 g/cm³ can be taken for most of the calculations.

Out of the many correlations already published, this section presents those selected for one or more of the following characteristics (with no order of priority)

1. More reliable, as claimed by authors
2. Easier to apply
3. Wider range of variables
4. Representing more realistic physical models

The information will be presented by product or set of similar products.

11.2.5.1   Liquids, Solutions, and Suspensions

As mentioned above, a very attractive approach is that of Choi and Okos (1986), who presented the correlations of properties of major components of foods as functions of temperature which, by means of additive models as represented by Equations 11.6 to 11.10 allow the calculation of the property for the composed food. The correlations are those in Table 11.2. The application ranges are 40 to 150°C for suspensions with solids content from 0 to 95% and the predicted values are claimed to be within 3.9% error of the literature values of liquid foods and 4.7% of evaporated milk, orange juice, and bratwurst sausage.

11.2.5.1.1   Juices

Among liquids, juices are relevant examples of useful correlations. Assuming juices are sugar solutions, Riedel (1951) proposed the following correlation for thermal conductivity.

$$k = \left(565.22 + 1.8\,T - 0.006\,T^2\right)\left(0.46 + 0.0054\,M\right) \times 10^{-3}$$

(11.33)

For different properties of clarified apple juice, Constenla et al. (1989) found

$$\rho = 0.82780 + 0.34708 \exp\left(0.01\,Bx\right) - 5.479 \times 10^{-4}\,T \tag{11.34}$$

where Bx is concentration in °Brix and T is in K. By deriving a theoretical expression of ρ in terms of density of water ρ_w, the influence of temperature was implicitly considered, giving place to Equation 11.35

$$\rho \frac{\rho_w}{0.992417 - 3.739 \times 10^{-3}\,Bx} \tag{11.35}$$

An analogous analysis for thermal conductivity, leads to Equations 11.36 and 11.37, respectively

$$k = 0.27928 - 3.5722 \times 10^{-3}\,Bx + 1.1357 \times 10^{-3}\,T \tag{11.36}$$

$$k = \frac{k_{wo}\,\rho}{\rho_w\left(0.9789 - 0.007719\,Bx\right)} \tag{11.37}$$

For specific heat of clarified apple juice the same authors found

$$C_p - 0.80380 - 4.3416 \times 10^{-3}\,B + 5.6063 \times 10^{-4}\,T \tag{11.38}$$

For tomato paste thermal conductivity is (Rivero, 1982)

$$k = 0.647 - 0.276 \exp\left(-0.5927\,X\right) \tag{11.39}$$

Specific heat for fruit juices with water content greater than 50% (Dickerson, 1968)

$$Cp = 1674.7 + 25.12\,M \tag{11.40}$$

Alvarado and Romero (1989) presented a general correlation for density of fruit juices which they claim agrees with values calculated from the Choi and Okos model and fits experimental values obtained for 30 different juices. It is valid for temperatures above freezing and for soluble solids concentration up to 30°Bx

$$\rho = \left(1002 + 4.61\,B\right) - 0.460\,T + 7.001 \times 10^{-3}\,T^2 - 9.175 \times 10^{-6}\,T^3 \tag{11.41}$$

Bayindirli and Ozsan (1992b) present correlations for density and viscosity of sour cherry, apple, and grape juices as a function of temperature and concentration. Sour cherry juice

$$\rho = 0.79 + 0.35 \exp\left(0.0108\,Bx\right) - 5.41 \times 10^{-4}\,T\,(K) \tag{11.42}$$

$$\ln\left(\frac{\mu}{\mu_w}\right) \frac{\left(-0.3 + \dfrac{920}{T}\right)Bx}{100 - \left(1.83 - 3.55 \times 10^{-3}\,T\right)Bx} \tag{11.43}$$

where μ_{wo} is the water viscosity at the same temperature, temperatures are measured in Kelvin and concentrations in degrees Brix.

Bayindirli and Ozsan (1992a) based on the previous work of Constenla et al. (1989) proposed for apple juice

$$\rho = 0.83 + 0.35 \exp\left(0.01\, Bx\right) - 5.64 \times 10^{-4}\, T\,(K) \tag{11.44}$$

and

$$\ln\left(\frac{\mu}{\mu_w}\right) = \frac{\left(-0.24 + \dfrac{918}{T}\right) Bx}{100 - \left(2.03 - 2.67 \times 10^{-3}\, T\right) Bx} \tag{11.45}$$

For grape juice, the same properties were found.

$$\rho = 0.74 + 0.43 \exp\left(0.01\, Bx\right) - 5.55 \times 10^{-4}\, T\,(K) \tag{11.46}$$

$$\ln\left(\frac{\mu}{\mu_w}\right) = \frac{\left(-0.24 + \dfrac{1821}{T}\right) Bx}{100 - \left(0.86 - 4.41 \times 10^{-3}\, T\right) Bx} \tag{11.47}$$

Fernández-Martín and Montes (1972) developed a model to predict thermal conductivity of different types of milk for temperatures from 5 to 75°C and solids content, S, up to 40%.

$$k = a_o + a_1\, S + \left(a_2 + a_3\, S\right) T + \left(a_4 + a_5\, S\right) T^2 \tag{11.48}$$

the coefficients, a_i, are listed in Table 11.4.

Fernández-Martín and Montes (1977) reported on cream, for T measured in °C.

$$k = 912.63 + 0.051\, T - 0.000175\, T^2 \cdot \left[1 - \left(0.0843 + 0.0019\, T\right)\phi_f\right] \times 4.18 \times 10^{-} \tag{11.49}$$

where ϕ_f is fat volume fraction.

Dairy products and margarine thermal conductivities were correlated by Sweat and Parmellee (1978) by means of a linear equation in water mass fraction w_w.

$$k = 0.141 + 0.412\, w_w \tag{11.50}$$

11.2.5.2 Meats

Sanz et al. (1987, 1989) present a list of the most appropriate equations for the calculation of thermal conductivity, thermal diffusivity, enthalpy, apparent specific heat, and density of meats and meat products, as well as freezing points and bound water in frozen products. The reader is referred to those works for punctual values at different temperature ranges and for predictive correlations as they are two of the most comprehensive available sources in literature of meat thermal properties.

Bazán and Mascheroni (1984) give, for frozen lamb meat, the following correlations for thermal properties. Density ρ as a function of densities of unfrozen meat, ρ_o, water, ρ_w, ice ρ_h and water fraction on wet basis Y, and fraction frozen w_h

$$\rho_f = \frac{\rho_o}{1 + \dfrac{Y \, w_h \, \rho_o}{\rho_a}\left(\dfrac{\rho_o}{\rho_h} - 1\right)} \tag{11.51}$$

in turn w_h is given as a function of temperatures by

$$w_h = 0.9418 + \frac{0.8597}{T} \tag{11.52}$$

Thermal conductivity in three different temperature regions is

$$k = 0.48534 + 1.0627 \times 10^{-3} \, T \quad \text{for} \quad T \geq -0.9113\,°C$$

$$k = 0.48436 + 3.7590 \times 10^{-4} \, w_i \quad \text{for} \quad -1.15°C \leq T \leq -0.913°$$

$$k = 1.3598 + \frac{0.97069}{T} \quad \text{for} \quad T \leq -1.15°C \tag{11.53}$$

For specific heat calculated above the initial freezing temperature T_0, they recommended the equation by Levy (1975).

$$C_{p_0} = 0.979 + 3.1754 \, Y \tag{11.54}$$

Also, for temperatures below T_0

$$C_{p_0} = \frac{C_2}{\left(C_1 - T\right)^2} \quad \text{for} \quad T \geq T_g$$

$$C_{p_0} = \frac{C_3 \, T}{\left(C_1 - T\right)^2} \quad \text{for} \quad T < T_g \tag{11.55}$$

where T_g is a temperature at which the enthalpic gradient changes. Regression of the experimental points allowed the calculation of C_i and T_g for 3 different water contents, and when extrapolated to the usual values of Y in lamb meat, the resulting values were used as constants for that product, since the differences were smaller than the experimental errors. All those values are shown in Table 11.5.

TABLE 11.5
Coefficients of Equation 11.55 for
Calculation of C_p of Frozen Meats

%Water	C_1	C_2	C_3	T_g
4.4	1.69	280.35	42.65	−6.7
52.5	1.37	349.22	46.90	−7.0
64.9	0.87	377.52	48.57	−7.0
74–76	0.46	385.00	48.20	−8.0

From Bazán, H. C. and Mascheroni, R. H., 1984 Transferencia de calor con simultáneo cambio de fase en la congelación de carnes ovinas, *Rev. Lat. Transf. Cal. Mat.* 8:55–76. With permission.

Sweat (1975) proposed correlations for thermal conductivity of meats (beef, poultry, and fish) as being the best among six other correlations (standard deviations lower than 10%). A simple one based in water content only

$$k = 0.080 + 0.0052\,M \qquad (11.56)$$

for temperatures above freezing point and up to 60°C and M = 60 to 80%, and

$$k = -0.28 + 0.019 - 0.0092\,T \qquad (11.57)$$

for T between –40 and –5°C and M = 65 to 85%.

11.2.5.3 Porous Foods

Porous foods are typical examples of composite materials discussed above, to which two phase media models have been applied, such as those represented by Equations 11.4, 11.11, 11.12, and 11.14 to 11.17. Fruits, vegetables, grains, flours, and powders are typical examples of this type of foods.

For fruits and vegetables, Sweat (1974) recommends

$$k = 0.148 + 0.493\,M \qquad (11.58)$$

which is valid up to M = 60% but not to be used with porous and low density fruits.

Ramaswamy and Tung (1981) give correlations of k, C_p, and α from pooled experimental data for Golden Delicious and Granny Smith apples above and below the freezing point. The experimental values of k and C_p were determined by the heated probe method and by DSC, respectively. Thermal diffusivities were in turn calculated from k, C_p, and ρ. In the following equations M and T_f are water content on percent wet basis and freezing temperature in degrees Celsius respectively.

Thermal conductivity

$$k = 0.0159\,M + 0.0025\,T - 0.994 \quad \text{for} \quad T > T_f$$

$$k = 0.133\,M + 0.0103\,T - 10.3 \quad \text{for} \quad T \le T_f \qquad (11.59)$$

Specific heat of Granny Smith as a function of temperature.

$$Cp = 3.40 + 0.0049\,T \quad \text{for} \quad -1 < T < 60°C$$

$$Cp = 2.65 - 1.42\,T \quad \text{for} \quad -10 < T < -1°C$$

$$Cp = 2.49 + 0.760\,T \quad \text{for} \quad -25 < T < -10°C$$

$$Cp = 2.50 + 0.0118\,T \quad \text{for} \quad T \leq -25°C \tag{11.60}$$

Specific heat of Golden Delicious as a function of temperature.

$$Cp = 3.36 + 0.0075\,T \quad \text{for} \quad -1 < T < 60°C$$

$$Cp = 2.18 - 1.48\,T \quad \text{for} \quad -10 < T < -1°C$$

$$Cp = 2.44 + 0.791\,T \quad \text{for} \quad -25 < T < -10°C$$

$$Cp = 2.89 + 0.0138\,T \quad \text{for} \quad T \leq -25°C \tag{11.61}$$

The thermal diffusivity for a range of temperatures from below freezing up to 60°C for Golden Delicious

$$\alpha = (-0.187\,T - 1.22) \times 10^{-7} \quad \text{for} \quad -25 < T \leq -10°C$$

$$\alpha = (0.437\,T - 4.37) \times 10^{-7} \quad \text{for} \quad -10°C < T \leq T_f$$

$$\alpha = (-0.00278\,T - 1.39) \times 10^{-7} \quad \text{for} \quad T > T_f \tag{11.62}$$

for Granny Smith

$$\alpha = (-0.123\,T - 0.603) \times 10^{-7} \quad \text{for} \quad -25 < T \leq 10°C$$

$$\alpha = (-0.399\,T - 3.66) \times 10^{-7} \quad \text{for} \quad -10 < T \leq T_f$$

$$\alpha = (-0.00556\,T - 1.31) \times 10^{-7} \quad \text{for} \quad T > T_f \tag{11.63}$$

Lozano et al. (1979) measured and correlated density and thermal conductivity of apples as a function of water content for the whole range of full turgor down to dry-bone and obtained the following equations for density and thermal conductivity, respectively.

$$\rho = 0.636 + 0.102 \ln(X) \left(r^2 = 0.978 \right) \tag{11.64}$$

$$k = 0.489 - 0.443 \exp(-0.206\,X) \left(r^2 = 0.967 \right) \tag{11.65}$$

where X = g water/g of dry matter.

Mattea et al. (1986), correlated experimental results of thermal conductivity of potatoes and pears as functions of water content fraction on dry basis, X, and obtained the following.

Potatoes

$$k = 0.5963 - \frac{0.1931}{X} + \frac{0.0301}{X^2} \qquad (11.66)$$

and pears

$$k = 0.4875 - \frac{0.0566}{X} + 0.0227 \ln(X) \qquad (11.67)$$

valid for X/Xo from 0.1 to 1, with $r^2 = 0.95$. Xo corresponds to fresh product water content. Mattea et al. (1989) proposed Equations 11.68 and 11.69 as the best fit of calculated values by a computer model for apples and pears, respectively.

$$k = 0.605 - 0.529 \exp(-0.121\,X)\left(r^2 = 0.99\right) \qquad (11.68)$$

$$k = 0.493 - 0.359 \exp(-1.033\,X)\left(r^2 = 0.96\right) \qquad (11.69)$$

Alagusundaram et al. (1991) give correlations of thermal conductivity for bulk barley, lentils and peas, claiming mean relative percent errors around 2% for all three seed types in the explored ranges of $-29 < T < 29°C$ and $9 < M < 23\%$.

Barley

$$k = 0.173 + 7.51 \times 10^{-4}\,T + 1.51 \times 10^{-3}\,M \qquad (11.70)$$

Lentils

$$k = 0.193 + 10^{-3}\,T + 1.51 \times 10^{-3}\,M \qquad (11.71)$$

Peas

$$k = 0.168 + 8.4 \times 10^{-4}\,T + 3.05 \times 10^{-3}\,M \qquad (11.72)$$

For potatoes, Yamada (1970) gives specific heat as a function of water content for two ranges expressed as a fraction on wet basis.

$$Cp = (0.216 + 0.78\,Y)4.1868\;\text{kJ kg}^{-1}\,\text{K}^{-1} \quad \text{for} \qquad (11.73)$$

and

$$Cp = (0.393 + 0.437\,Y)4.1868\;\text{kJ kg}^{-1}\,\text{K}^{-1} \quad \text{for} \quad 0.5 \qquad (11.74)$$

From tabulated data of Rice et al. (1988), linear fitting equations for k, α, ρ, and C_p with temperature in degrees Celsius, and with errors ranging from 2 to 5% were found.

$$\alpha \times 107 = \left(1.263 + 8.286 \times 10^{-4}\right. \tag{11.75}$$

$$k = 0.296 + 3.057 \times 10^{-3}\ T \tag{11.76}$$

$$\rho = 1.300 + 2.517 \times 10^{-3}\ T \tag{11.77}$$

$$Cp = 1.793 + 2.544 \times 10^{-3}\ T \tag{11.78}$$

Wang and Brennan (1993) measured C_p of potatoes by DSC technique, between 40 and 70°C and from 0 to 80% moisture content on wet basis and correlating the experimental data by Equation 11.79

$$Cp = 0.406 + 0.00146\ T + 0.203\ M - 0.0249\ M^2 \tag{11.79}$$

with a main relative percentage deviation of 3.36%, which the authors claim to be in good agreement with experimental data.

For gelatinized starches, Marouilis et al. (1991) proposed:

$$k = 0.210 + 0.410 \times 10^{-3}\ T(K) \quad \text{for } 303\ K < T < 343\ K \tag{11.80}$$

Califano and Calvelo (1991) measured thermal conductivity of potatoes between 50 and 100°C, obtaining a quadratic equation, which fitted experimental values within a mean absolute deviation of 2.3%, with $r^2 = .985$ from 23 points.

$$k = 1.05 - 1.96 \times 10^{-2}\ T + 1.90 \times 10^{-4}\ T^2 \tag{11.81}$$

For pistachio with water contents ranging from 5 to 40% on wet basis Hsu et al. (1991) gave a bulk density of

$$\rho = 439 + 5.003\ M \quad \left(r^2 = 0.959\right) \tag{11.82}$$

Specific gravity

$$\gamma = 1.289 - 3.375 \times 10^{-3}\ M \left(r^2 = .975\right) \text{(inverse with M)} \tag{11.83}$$

Specific heat

$$Cp = 1074 + 27.79\ M \quad \left(r^2 = 0.920\right) \tag{11.84}$$

Thermal conductivity

$$k = 0.0866 - 0.2817 \times 10^{-3}\ M \quad \left(r^2 = 0.963\right) \tag{11.85}$$

TABLE 11.6
Coefficients of Equation 11.88 to Calculate Densities of Vegetables

Foodstuff	Density	h	m	p	q	r^2
Carrot	Bulk	0.984	0	0.224	1.80	0.97
	Particle	1.497	–0.294	–0.253	39.793	0.96
	Particle (true por.)	1.497	–0.294	0.033	36.820	0.97
Pear	Bulk	1.251	–0.153	–0.107	1.33×10^{-6}	0.97
	Particle	0.832	0.220	0.632	2.775	0.97
Potato	Bulk	1.202	–0.148	0.259	15.507	0.96
	Particle	1.234	–0.117	0.085	19.040	0.97
Sweet potato	Bulk	1.266	–0.219	–0.319	6.700	0.96
	Bulk (whole piece)	3.260	1.172	–2.325	–0.395	0.96
Garlic	Bulk (sliced)	1.130	–0.567	0.187	–0.866	0.95
	Particle	2.694	0	–1.316	–0.1638	0.95

From Lozano, J. E., Urbicain, M. J., and Rotstein, E., 1983, Shrinkage, porosity and bulk density of foodstuffs at changing moisture content, *J. Food Sci.,* 48:1497–1502, 1553. With permission.

Bulk thermal conductivity

$$0.0260 + 0.4113 \times 10^{-3} \, M \left(r^2 = 0.992 \right) \tag{11.86}$$

Thermal diffusivity

$$\alpha = 51.1 \times 10^{-9} - 0.568 \times 10^{-9} \, M \left(r^2 = 0.983 \right) (\text{inverse with M}) \tag{11.87}$$

Lozano et al. (1983) measured bulk and particle density of several vegetables and found that they can be correlated with an equation of the form

$$\rho = h^+ m \frac{X}{X_o} + p \exp \left(-q \frac{X}{X_o} \right) \tag{11.88}$$

the values of parameters h, m, p, and q, are listed in Table 11.6. Equation 11.88 proved not to be suitable for particle density of sweet potato. Therefore, Equation 11.89 has been proposed ($r^2 = 0.97$).

$$\rho_{sp} = 1.553 - 4.954 \frac{X}{X_o} + 4.630 \left(\frac{X}{X_o} \right)^{1.051} \tag{11.89}$$

11.2.5.4   Cereals, Flours, Pasta, and Bakery

In terms of the specific heat of bread, Christenson et al. (1989) assumed that dependence with moisture follows a mass fraction model.

$$C_p = C_p(\text{water}) \times M + C_p(\text{dry solid})(1 - M) \tag{11.90}$$

where C_p of dry solid is given by

$$C_{p,dry} = 0.098 + 0049\,T\,(K) \quad for \quad 298\,K < T < 358\,K \tag{11.91}$$

They also proposed the thermal conductivity:

$$\ln k = -4.12 - 17.8\,M + 0.0031\,T + 0.065\,M.T \tag{11.92}$$

For pasta, Andrieu et al. (1989) found

$$k = 0.23\,Y_w + 0.308 \quad at\ 20°C \tag{11.93}$$

and

$$k = 0.30\,Y_w + 0.302 \quad at\ 60°C \tag{11.94}$$

but since the temperature dependence is not strong, both equations can be arithmetically averaged to give a single expression for the whole range of 20 to 60°C

$$k = 0.285\,Y_w + 0.305 \tag{11.95}$$

with an error in the order of 1% in the extreme temperatures.

Applying the series model, with intrinsic values of k for starch, gelatin, sucrose, and gluten of 0.39, 0.34, 0.30, and 0.29 $Wm^{-1}K^{-1}$, respectively, they obtained the best accordance with experimental models of gels with those constituents. This means that those values are useful in determining the effective thermal conductivity of foodstuffs like durum wheat pasta.

For thermal diffusivity of pasta, α, Andrieu et al. (1989) gave, as a function of water content, M (% wet basis)

$$\alpha = 1.91 - 2.76\,M + 3.19\,M^2 \quad at\ 20°C \tag{11.96}$$

$$\alpha = 1.71 - 1.81\,M + 1.93\,M^2 \quad at\ 40°C \tag{11.97}$$

$$\alpha = 1.47 - 0.74\,M + 0.62\,M^2 \quad at\ 60°C \tag{11.98}$$

a general relationship involving Y and T was given, claiming a mean error of 4%

$$\alpha = (1.73 - 0.9\,M - 0.003\,T)\,10^{-7} \tag{11.99}$$

Pasta density was measured by pycnometry with ethanol as the solvent and, as a function of moisture content M, was correlated by Equation 11.97

$$1/\rho = (3.02\,M + 6.46)\,10^{-4} \tag{11.100}$$

Specific heats were correlated for starch

$$C_p = 5.737\,T + 1328 \tag{11.101}$$

and gluten

$$C_p = 6.329\,T + 1465 \tag{11.102}$$

Applying the additive model (Equation 11.8), the specific heat of pasta can be calculated.

From data tabulated by Wallapapan et al. (1983), relationships for thermal diffusivity of two products have been derived. For corn, yellow dent, thermal diffusivity

$$\alpha = 1.05 \times 10^{-3} - 1.739 \times 10^{-5}\,M + 4.36 \times 10^{-7}\,M^2 \quad \text{for} \quad 8.7 < T < 23.3°C \tag{11.103}$$

and for wheat soft white

$$\alpha = 9.56 \times 10^{-4} - 1.83 \times 10^{-6}\,M + 4.36 \times 10^{-7}\,M^2 \quad \text{for} \quad 8.7 < T < 23.3°C \tag{11.104}$$

with errors lower than 1 and 4%, respectively. Wallapapan et al. (1983) recommend (when no other data are available and only for estimation purposes of specific heat of food materials) using the equations reported by ASHRAE as proposed by Seibel (1892).

$$Cp = 0.200 + 0.008\,M\;(\text{for above free} \tag{11.105}$$

$$Cp = 0.200 + 0.003\,M\quad(\text{for below free} \tag{11.106}$$

Miles et al. (1983) report that for density of porous foodstuffs, where ε is the porosity, and w_i and ρ_i are the mass fraction and density of component i, respectively, Equation 11.107 represents Keey's model for a porous material.

$$\rho = (1 - \varepsilon)\frac{1}{\sum \dfrac{x_i}{\rho_i}} \tag{11.107}$$

11.2.5.5 Frozen Foods

A very important parameter when dealing with frozen foods is the initial freezing temperature, since it is the value which separates two regions of different thermal behavior, below which the water will be partially or wholly ice. Then specific heat and enthalpy calculations differ at both sides.

Miles et a. (1983) report an equation to calculate the initial freezing temperature, $T_f(°C)$, from Riedel (1978)

$$\left(d\,T_f^3 + c\,T_f^2 + a\right)\cdot\left(x_w - 1\right) + T_f\left[b\left(x_w - 1\right) + 1\right] = 0 \tag{11.108}$$

where x_w is the water mole fraction and fitting constants a, b, c, and d are tabulated for different foodstuffs in Table 11.7. The same constants can be used to calculate the amount of ice formed from the water contained in a given foodstuff, as given by the following equations:

$$Y_{ice} = \frac{s + Y_w - 1}{s} \qquad (11.109)$$

where

$$s = \frac{T}{a + bT + cT^2 + dT^3} \qquad (11.110)$$

Enthalpy changes provoked by heating or cooling the product can be conveniently calculated by integration of the product $C_p \, dT$, taking C_p as constant over the temperature interval, provided there are no phase changes in the interval.

$$\Delta H = \int_{T_1}^{T_2} C_p \, dT \tag{11.111}$$

11.2.5.6 Fats and Oils

Latyshev and Ozerova (1976), give C_p for fats

$$C_f = A + B\,T + \sum_{i=1}^{n} \frac{A_i}{1 + \dfrac{B_i}{A_i}\left(T - T_i\right)^2} \tag{11.112}$$

where the values of the constants are given in Table 11.8.

Noureddini et al. (1992a) give the correlation parameters c and m of equations of the type

$$\rho = c + m\,T\,(°C) \tag{11.113}$$

for seven oils (Crambe, Rapeseed, Corn, Soybean, Milkweed, Coconut, and Lesquerella) and eight fatty acids (Nonanoic, Capric, Lauric, Myristic, Palmitic, Stearic, Oleic, and Erucic).

Viscosities of the same products were correlated by Noureddini (1992b)

$$\ln \mu = A + \frac{B}{T} + \frac{C}{T^2} \tag{11.114}$$

and

$$\ln \mu = A + \frac{B}{T} + C\,T \tag{11.115}$$

where μ is in centipoise, T is in K, and the constants A, B, and C are tabulated in the cited work.

11.2.5.7 Miscellaneous

Shafiur Rahman (1992) correlated thermal conductivity experimental values of four food materials in a single equation as a function of porosity and water content and initial value (fresh product) of the property. Since it is a ratio, the influence of temperature is discarded.

$$\frac{k_d}{k_o}\left(\frac{1}{1-\varepsilon}\right) - 1.82 - 1.66 \exp\left(-0.85\,\frac{w_w}{w_{wo}}\right) \tag{11.116}$$

where k_o and k_d are conductivities of fresh and dried food, and w_{wo} and w_w are water mass fraction of fresh and dried material, respectively. Equation 11.116 is the best fitting of 122 reference points from the literature on apple, beef, pear, potato, and squid meat.

TABLE 11.9
Rheological Classification of Materials

Rheological behavior	Denomination	Governing equation	Additional comments
Solids			
Rigid solid	Euclidian	$\gamma = 0$	
Elastic solid	Hookean	$\tau = G\gamma$	G = Young's module
	Non-Hookean	$\tau = G(\gamma)\,\gamma$	Nonlinear
Viscoelastics			
Nonviscous fluid	Pascalian	$\tau = 0$	
Viscous fluid (linear)	Newtonian	$\tau = \mu\,\dot{\gamma}$	μ = viscosity
Viscous fluid (nonlinear)	Non-Newtonian	$\tau = \eta(\dot{\gamma},t)\,\dot{\gamma}$	η = apparent viscosity
Semisolids	Maxwell model	$\sigma + \lambda d\sigma/dt = \eta d\gamma/dt$	$\lambda = \eta/G$ (relaxation time)
	Kelvin model	$d\gamma/dt + \sigma/\lambda = \sigma/\eta$	

11.3 RHEOLOGICAL PROPERTIES

Rheology can be stated as the science dealing with the deformation and flow of bodies (Fredrickson, 1964). All materials ideally possess all the rheological properties, both as solid or fluid. However, from a practical point of view and under a given set of conditions, the scheme of classification listed in Table 11.9 can be adopted. Flow pertains to liquid matter, e.g., fruit juice, and deformation pertains to solids, e.g., hard cheese. Materials that are not solids or liquids but possess both properties are considered viscoelastics, e.g., yogurt. Measurement or prediction of the rheological properties of foods is very important in the design, operation, and optimization of processes, as well as the control of quality of food products.

11.3.1 FUNDAMENTAL CONCEPTS AND NOMENCLATURE

Definitions of quantities like stress, strain, rate of strain, etc. must be given to make a proper description of the kinematics of deformation and flow. For those involved in the analysis of the stress-strain response, a knowledge of the tensors method is essential. Some simple cases of deformation and flow are given to point out the physical meaning of strain and stress. Precise definitions of these quantities can be obtained from the well-known books by Bird et al. (1960) and Fredrickson (1964).

Consider a volume element with the shape of a unit cube and let us consider the response of the material to an applied external force. Under this condition an internal force acting upon unit area (F/A), called stress, will develop. Stress is then a function of the direction and magnitude of the applied force and the plane of action. Therefore, a tensor with nine components will completely define a stress in a three-dimensional space. There are two basic types of stresses that can be exerted on any material in this volume element.

Normal stresses (σ) which act perpendicular to the face of the cube
Shear stresses (τ) which act tangential to the faces of the cube

The stress tensor at a given point in a body will have nine components as it is specified by the following (3×3) matrix

$$\sigma_{ij} = \begin{bmatrix} \sigma_{xx} & \tau_{xy} & \tau_{xz} \\ \tau_{xy} & \sigma_{yy} & \tau_{yz} \\ \tau_{zx} & \tau_{zy} & \sigma_{zz} \end{bmatrix} \tag{11.117}$$

where σ_{ii} and τ_{ij} are the normal and shear stresses along the x, y, and z Cartesian coordinates, respectively. For a body that is isotropic, homogeneous and continuous the τ_{ij} are not independent and the stress components acting on opposite faces of the imaginary cube are identical, so that $\tau_{yx} = \tau_{xy}$, $\tau_{zx} = \tau_{xz}$, $\tau_{zy} = \tau_{yz}$. When a body is subjected to an isotropic pressure acting as normal stress it may be deformed thereby altering its volume but not its shape. Such deformations are called compression (the volume decrease) or dilatation (the volume increase). Strain is the relative change in dimension of a body subjected to stress. Different stresses give different strains. Normal (σ) and shear (τ) stresses will produce normal (ε) and shear (γ) strains, respectively. The strain tensor also has six components for an isotropic, homogeneous, and continuous body.

$$\varepsilon_{ij} = \begin{bmatrix} \varepsilon_{xx} & \dfrac{\gamma_{xy}}{2} & \dfrac{\gamma_{xz}}{2} \\ 0 & \varepsilon_{yy} & \dfrac{\gamma_{yx}}{2} \\ 0 & 0 & \varepsilon_{zz} \end{bmatrix} \tag{11.118}$$

In ideal elastic solids the strain occurs and disappears instantaneously if the stress is removed and the original geometry is regained. There is a linear relationship between stress and strain. They are called Hookean solids and they are rheologically represented by a spring with a constant, or modulus, defined as the ratio of the stress to the strain (Rao, 1992).

$$\begin{aligned} \text{Young's modulus}: &\quad E = \sigma/\varepsilon = \sigma_{xx}/\varepsilon_{xx} \\ \text{Rigidity modulus}: &\quad G = \tau/\gamma = \tau_{xy}/\gamma_{xy} \\ \text{Bulk modulus}: &\quad K = \sigma/\varepsilon = (\delta F/A)/(\delta V/V) \end{aligned} \tag{11.119}$$

The latter (K) is practically a hydrostatic state of stress, when the force is isotopically applied from all directions and the body reduces its volume but the shape is not altered. When the cube is stretched in only one direction, e.g., the x axis, the stress tensor results: $\tau_{ij} = \tau_{xx}$. Extension in the x plane is accompanied by contraction in the y and z planes. Under this condition the strain tensor is given by

$$\varepsilon_{ij} = \begin{bmatrix} \varepsilon_{xx} & 0 & 0 \\ 0 & -\mu\varepsilon_{xx} & 0 \\ 0 & 0 & -\mu\varepsilon_{xx} \end{bmatrix} \tag{11.120}$$

where

$$\mu = \frac{\varepsilon_{yy}}{\varepsilon_{xx}} = -\frac{\varepsilon_{zz}}{\varepsilon_{xx}} = \frac{-(\delta D/D)}{\delta L/L} \tag{11.121}$$

is the well-known Poisson's ratio, which equals ½ if the material volume remains unchanged after the simple tension. In Equation 11.121 δD and δL are the lateral contraction and longitudinal elongation, respectively. Relationships between the moduli, applied to elastic, homogeneous, and isotropic bodies were presented by Rao (1992)
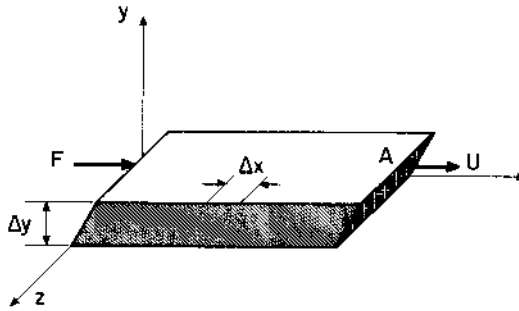
FIGURE 11.2 Simple shear.

$$G = E/2(1 + \mu)$$

$$E = 3K(1 - 2\mu) \tag{11.122}$$

$$K = EG/(9G - 3E)$$

Consider now that a tangential force (F) is applied to the upper surface so that all the points of the cube, except the base, are displaced from the original position. During this simple shear, the displacement γ is equal to the angle of shear and only the components $\varepsilon_{xy} = \gamma/2$ will be nonzero.

11.3.2 FLUID AND SEMISOLID FOODS

Fluid and semisolid foods exhibit a variety of rheological behaviors ranging from Newtonian to time dependent and viscoelastic. Whereas an ideal elastic solid produces an elastic displacement when shear stress is applied, a fluid produces viscous flow. Figure 11.2 illustrates what happens when a simple shear stress (τ) is applied to a liquid. As the figure shows, a liquid is held between two parallel infinite plates and the top plate moves at a velocity U (length/time) relative to the bottom plate. The force required to maintain this motion will produce a viscous flow and a velocity gradient, which is equivalent to the shear rate ($\dot\gamma = dU/dx$) will develop. Under this condition

$$\dot\gamma = \tau/\eta_{app} \tag{11.123}$$

where η_{app} is called the apparent viscosity and is constant only for this one value of $\dot\gamma$. If η_{app} is a constant at different values of $\dot\gamma$ then

$$\tau = \mu\,\gamma \tag{11.124}$$

where μ is the Newtonian viscosity of the fluid.

11.3.3 NEWTONIAN FOODS

Newtonian behaviors indicate that the viscosity of the food is shear-independent (Figure 11.2). Newtonian flow is exhibited by water, sugar solutions, and vegetable oils. Viscosity of Newtonian foods has the units Pascal-seconds or poises = 1 g/cm·s. The following definitions are of interest in the rheological study of foodstuffs in general and food suspensions and macromolecular solutions in particular.

Kinematic viscosity

$$\nu = \mu/\rho \ (cm^2/s, \ stoke)$$

where ρ = density

Relative viscosity

$$\mu_r = \mu/\mu_o$$

the ratio of solute to solvent viscosity at equal temperatures

Specific viscosity

$$\mu_{sp} = \mu_r - 1$$

Reduced viscosity

$$\mu_{red} = \mu_{sp}/c$$

where c = concentration of solute

Intrinsic viscosity

$$[\mu] = \mathscr{L}(ln\mu_r/c)_{[c \to o]}$$

also called limiting viscosity number, are usually correlated with molecular weight.

11.3.4 NON-NEWTONIAN FOODS

Most of the foodstuffs of interest show a more complicated relationship between shear rate and shear stress. It is no longer feasible to talk in terms of viscosity, since η varies with the rate of shear. As Table 11.9 shows, for non-Newtonian fluids η may or not be a function of the time of duration of shear (t) and they are usually divided into three general classes: (1) those whose properties are independent of time of duration of shear; (2) those whose properties are dependent of time of shear; and (3) those which exhibit many characteristics of a solid.

11.3.4.1 Non-Newtonian, Time-Independent Foods

Most of the foods are time-independent, and can be classified as follows.

Bingham plastic foods — They differ from Newtonian fluids only in that the linear relationship between $\dot{\gamma}$ and τ does not go through the origin (curve A, Figure 11.3). The τ value at $\dot{\gamma} = 0$ is the yield value or yield stress (τ_y). Foods which show this behavior are called ideal plastic material or Bingham bodies. Chocolate toppings were found to show Bingham flow.

Pseudoplastic foods — They include most of non-Newtonian foods. Curve B in Figure 11.3 shows the shape of flow curve for this type of liquid food. When a food is pseudoplastic, above yield stress is also known as mixed type plastic. Pseudoplastic flows are exhibited by fruit purees, condensed milk, ketchup, and other shear sensitive foodstuffs.

Dilatant foods — Their rheological behavior are opposite to the pseudoplastic, as curve C (Figure 11.3) shows, in which $\dot{\gamma}$ decreases as τ increases.
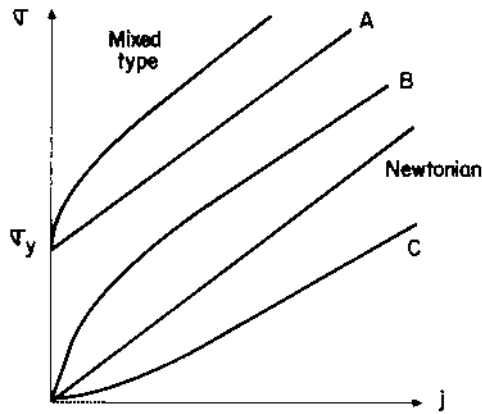
FIGURE 11.3 Shear diagram.
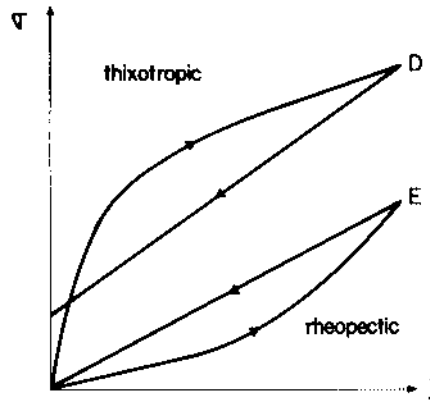
FIGURE 11.4 Time dependent fluids.

11.3.4.2   Non-Newtonian; Time-Dependent Foods

Time-dependent non-Newtonian foods are generally classified as

Thixotropic foods — This group includes those foods which possess a structure whose breakdown is function both of time and $\dot{\gamma}$. At constant shear rate the shear stress value decreases with time while the structure collapses. A typical diagram of a thixotropic fluid is given in Figure 11.4.

Rheopectic materials — Includes those few materials which are able to buildup (or setup) while submitted to a shear stress at constant $\dot{\gamma}$. No food was found to follow this behavior. However, some materials associated with the food processing, like bentonite solids were observed to behave as rheopectic. Rheopectic behavior is also plotted in Figure 11.4.

11.3.5   Semisolid Foods

Many foodstuffs (e.g., cheese) show both solid (elasticity) and fluid (viscosity) behavior when they are subjected to a sudden, instantaneous, constant shear stress, when sufficient time is allowed for the test, and the stress is large enough to prevent the food showing pure elasticity. In the flow of these fluids normal stresses σ are built up, giving rise to unusual phenomena,
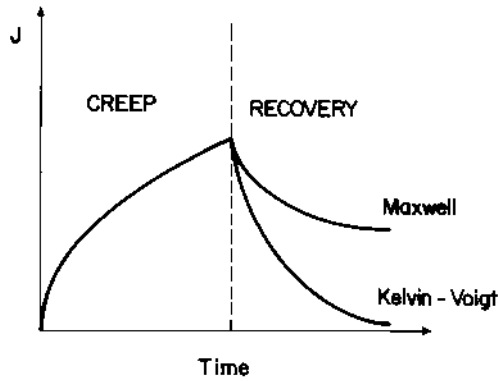
FIGURE 11.5 Typical creep curve.

such as the Weissemberg effect (Fredrickson, 1964) in which the fluid has a tendency to climb up a shaft rotating in the fluid. In the linear viscoelastic foods the stress-strain ratio depends on time, only. For non-linear viscoelastic foods this ratio is also a function of stress. In most rheological studies of semisolid foods a linear behavior is assumed. The viscoelastic behavior of foodstuffs is commonly explained by two basic tests: stress relaxation and creep.

11.3.5.1 Creep Compliance

The increase of strain with time in semisolids is called *creep*, and the ratio of the strain to the constant stress is the *creep compliance*.

$$J(t) = \gamma/\tau \tag{11.125}$$

Creep compliance-time curves are very useful in the study of linear viscoelastic behaviors. After steady state has been achieved, the strain and, thus, the creep compliance, becomes linear with time. A typical creep-compliance curve (Figure 11.5) can be divided into three principal regions (Sherman, 1970):

1. A region (A-B) of *instantaneous compliance* J_O in which the bonds between the different structural units are stretched elastically. In this region the structure of the sample will recover completely after removing the applied stress.

$$J_o = 1/E_o = \gamma_o/\tau \tag{11.126}$$

   where, E_O is the instantaneous elastic modulus and γ_O the strain at $t = 0$.
2. B-C interval in Figure 11.4 is the region where the bonds break and reform but all of them do not break and reform at the same rate. It was defined as the *time-dependent retarded elastic region*. A simple expression for the compliance in this region, J_R is:

$$J_R = J_m\left[1 - \exp\left(-t/\tau_m\right)\right] \tag{11.127}$$

   In Equation 11.127 J_m is the mean compliance of all the bonds and τ_m is the mean retardation time; τ_m equals $J_m\eta_m$, where η_m is the mean viscosity. A more detailed relationship can also be found in Sherman (1970).

3. The last region (C-D) was identified as a *linear region of Newtonian compliance* in which the compliance, J_m, and the viscosity are related by

$$J_N = t/\eta_N = \gamma_N/\tau \qquad (11.128)$$

where γ_N is the strain in this linear region.

Once the stress is removed at point D, there is an elastic recovery (D-E) of the stressed body, followed by a retarded elastic recovery (E-F). It can be observed that the initial structure is not completely recovered. Dealy (1982) called recoverable shear the maximal value of strain recovered after the application of the stress.

$$S_r = \tau J_{ec} \qquad (11.129)$$

where τ is the applied stress and J_{ec} is the value of the straight-line portion of the creep-compliance extrapolated to zero time. The sum of Equations 11.126, 11.127, and 11.128 gives an approximation to the whole creep compliance-time curve of Figure 11.4. A shear modulus, G_r was also defined (Dealy, 1982) as the reciprocal of the steady-state compliance, J_{eo}.

Viscoelastic bodies are usually represented by a mechanical model. The basic elements of these models are the spring (Hooke's law) and the dashpot. When both elements are in series, they form the Maxwell model. A spring and dashpot in parallel form a Kelvin-Voigt body. Linear viscoelastic behavior can be approximately represented for example, by using one spring in series with a Kelvin-Voigt body and a dashpot.

11.3.5.2   Stress Relaxation

If the strain is kept constant while the stress decreases with time, the rheological study is called *stress relaxation*. When a Maxwell body is deformed at a constant rate, the stress, at any time is given by

$$\tau(t) = \tau_o \exp\left(-t\,G/\eta\right) \qquad (11.130)$$

where the modulus G was given in Equation 11.122. Other stress-relaxation models to represent more complex viscoelastic behaviors can be found in the literature (Sherman, 1970; Rao, 1992).

11.3.6   DYNAMIC PROPERTIES OF FOODS

All the test modes discussed so far involve subjecting the foodstuff to a step change in γ (or τ) and measuring the stress (or strain) as a function of time. A useful procedure in the study of food rheology is to subject the same to a periodic deformation. If the rheological behavior is studied through a dynamic test, the stress or the strain is made to vary sinusoidally with time at a determined frequency (ω). The use of dynamic tests in foods coincides with the development of relatively low-cost commercial dynamic rheometers. Oscillation is a nondestructive technique for investigating the structure of foods. It is an ideal method for measuring structural changes (e.g., gelling or thixotropic recovery). Like creep, it also provides information on viscoelastic behavior. Figure 11.6 shows a typical sinusoidal variation in stress and strain. From the application of this technique, which is especially valuable for small values of times, several rheological parameters were defined (Rao, 1978; Bistany and Kokini, 1983a,b)
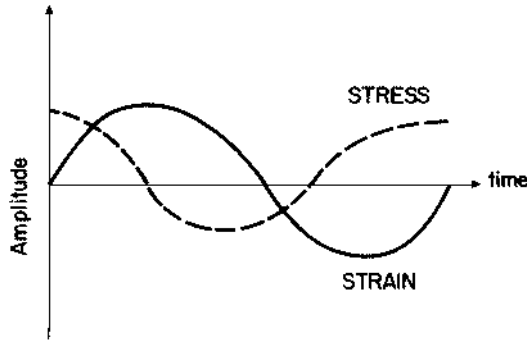
FIGURE 11.6 Dynamic test response.

$$\gamma^* = \gamma_o \sin(\omega t) \qquad (11.131)$$

where (γ^*) is the complex strain. If the strain amplitude γ_o is sufficiently small, the shear stress can be written as

$$\tau^* \tau o \sin(\omega t + \delta) \qquad (11.132)$$

where τ^* is the complex stress; τ_O is the amplitude of the shear stress and δ is the phase shift relative to the strain. Equations 11.131 and 11.132 are used to calculate functions with a more obvious physical significance. In this way, τ^* may be written as a sum of in-phase and out-of-phase terms.

$$\tau^* = \gamma o \left[G' \sin(\omega t) + G'' \cos(\omega t) \right] \qquad (11.133)$$

$$\tau^* = \gamma o \left[n' \sin(\omega t) + \eta'' \cos(\omega t) \right] \qquad (11.134)$$

where G' and G'' in Equation 11.133 are called the storage and loss modulus, respectively. In Equation 11.134 $\eta' = G''/\omega$ is the ratio of stress in phase with the strain to the rate of strain; and $\eta'' = G''/\omega$ is the stress 90° out of phase with the strain, divided by the rate of strain. The absolute magnitude of the complex viscosity is

$$\eta^* = \left(\eta' + \eta'' \right)^{1/2} \qquad (11.135)$$

Equations 11.132 and 11.133 can be combined to give

$$G'(\omega) = \left(\tau_o/\gamma_o \right) \cos \delta \qquad (11.136)$$

$$G''(\omega) = \left(\tau_o/\gamma_o \right) \sin \delta \qquad (11.137)$$

A complex modulus can also be defined.

$$|G^*| = \left(G'^2 + G''^2 \right)^{1/2} \qquad (11.138)$$

Finally, the complex compliance is defined as

$$J^* = J' - i\,J''$$
(11.139)

where J' is called storage compliance, a measure of the energy stored and recovered per cycle, and J'' is the loss compliance, a measure of the energy dissipated as heat per cycle (Sherman, 1970).

Variation of G' and G'' with ω was used to study gel properties (Ross-Murphy, 1984; Doublier et al., 1992). If $G' \gg G''$ the food behaves like a solid; if $G'' \gg G'$ the energy used to deform the food dissipates viscously. For additional details on the flow behavior of viscoelastic substances, see Rao and Steffe (1992).

11.4 PREDICTION AND CORRELATION OF RHEOLOGICAL PROPERTIES

In the absence of reliable experimental rheological property data, empirical models can provide accurate estimations for many engineering applications. Foodstuffs are, in general, complex systems and factors such as water content and chemical and biochemical reactions which influence the rheological properties. Models developed for nonfood materials should be revised before applying them to foodstuffs.

11.4.1 NEWTONIAN FOODS

In the case of Newtonian foods, viscosity (μ) completely describes the rheological behavior. Liquid foods that obey this simple rheological relationship include sugar solutions, milk, beer, fruit juices (without pulp), vegetable oils, molten fats, and some honeys among others. Newtonian fluids can be described over the entire range of $\dot{\gamma}$ at a constant temperature by the relation

$$\mu = \tau/\gamma$$
(11.140)

11.4.2 VISCOSITY OF SOLUTION AND PARTICULATE FOOD SYSTEMS

A particulate system, like food emulsions and dispersions is a diluted particle-liquid mixture so that it can be transported in laminar flow (Heldman and Singh, 1981). Considering that particles are spherical, uncharged, and large in comparison to the liquid molecules, and that neither particles slip nor liquid turbulence is present, simple expressions as the often-cited Einstein relationship (Metzner, 1985) can be applied.

$$\mu_s = \mu_l(1 + 2.5\,X)$$
(11.141)

where μ_s = viscosity of the particulate system; μ_l = viscosity of the liquid; and X = concentration of particles. Mooney (1951) developed the following semitheoretical expression to evaluate the relative viscosity (ratio of the viscosity μ to that of the suspending fluid μ_w) of concentrated solutions.

$$\ln\frac{\mu}{\mu_w} = 2.5\frac{\phi}{1 - K\phi}$$
(11.142)

where ϕ denotes the volume fraction of solids and K is a coefficient which takes into account the interactions between particles. This equation reduces to the classic Einstein's equation for an infinitely dilute suspension of spheres and K usually varies from 1 to 1.9 for mono-disperse systems (Mooney, 1951; Perry and Chilton, 1973). Krieger (1983) and Rao (1987) reviewed several theories for the most important types of particulate systems (emulsions, dispersions, gels, and foams) applicable to foodstuffs.

11.4.3 NON-NEWTONIAN FOODS

11.4.3.1 Time-Independent Models

The Ostwald-de Waele, or power-law, rheological equation has been widely used to describe the rheological behavior in the absence of yield stress (τ_y).

$$\tau = k \, \dot{\gamma}^n \tag{11.143}$$

where k = consistency index; and n = flow behavior index. When n < 1 the food behaves as a pseudoplastic; when n > 1 the food behaves as a dilatant. It can be verified that $\eta = k \cdot \dot{\gamma}^{n-1}$. The following restrictions apply: (1) if $n \to 0$ and $\dot{\gamma} \to 0$; then $\eta \to \infty$; and (2) if $n \to \infty$ and $\dot{\gamma} \to 0$; then $\eta \to 0$.

When $\dot{\gamma}$ remains below the yield stress value, the strained food can move only as a solid body or remain at rest. Several models take into account this phenomenon. The simplest for this category of liquids are the Bingham-Schwedoff (Equation 11.144), Herschel-Bulkley (Equation 11.145), and the Casson's (Equation 11.146) equations (Bourne, 1982).

$$\tau = \tau_y + \eta \, \gamma \quad \left(\tau > \tau_y \right) \tag{11.144}$$

$$\tau = \tau_y + K \, \dot{\gamma}^n \tag{11.145}$$

$$\tau^{1/2} \tau_y^{1/2} + K \tag{11.146}$$

The literature is also abundant with many other models like the Mizrahi-Berk (1972) model

$$\tau^{1/2} = \tau_y^{1/2} + K_M \, \gamma^n \tag{11.147}$$

which was used to characterize concentrated orange juice, or the Vocadlo and Young (1969) equation

$$\tau = \left(\tau^{1/n} + K \, \gamma \right)^n \tag{11.148}$$

for the description of rheological properties of fats.

11.4.3.2 Time-Dependent Models

The characterization of the complex time-dependent flow properties of liquid and semisolid foods were considered by different authors (Hahn et al., 1959; Tiu and Boger, 1974; Figoni and Shoemaker, 1981; Shoemaker and Figoni, 1984). For thixotropic liquid foods that vary

in apparent viscosity with time and become more fluid with time of shearing, some sufficiently accurate rheological models are available. Elliot and Green (1972) described the thixotropic behavior of several food systems in terms of a modified Bingham body, which followed a first-order kinetic equation, represented as

$$\tau = \tau_e + \left(\tau_o - \tau_e\right) \exp\left(-K\,t\right) \tag{11.149}$$

where τ is the shear stress τ_e is the equilibrium value of τ which is reached after a sufficient long shear time (Pa); τ_o is the initial shear stress (Pa); K is a parameter to be determined (s^{-1}) and t is the time of shearing(s). The models of Hahn et al. (1959) (Equation 11.150) and Tiu and Boger (1974) were also used to describe time-dependent rheological behaviors.

$$\log\left(\tau - \tau_e\right) = A_1 - B_2\,t \tag{11.150}$$

where coefficients A_1 and A_2 are constants to be determined. In the Tiu-Boger model (Equation 11.151), λ is a time dependent structural parameter to be determined experimentally.

$$\tau = \lambda\left(\tau_y + k\,\dot{\gamma}^{1/2}\right) \tag{11.151}$$

Equation 11.151 was proposed for the description of rheological properties of mayonnaise.

11.4.4 SEMISOLID FOODS

Use of previous rheological models were based on the fact that all deformations in the considered foods are unrecoverable, in other words, they do not present elastic behavior. Semisolid foods like cheese and flour doughs are not purely viscous in nature, and their viscoelastic behavior can be described mechanically by the combination of elastic springs (elastic behavior) and dashpots (pure viscous flow). These two elements in series constitute a Maxwell body, Equation 11.152 and when in parallel a Kelvin-Voigt body, Equation 11.153.

$$\sigma + \lambda\,\frac{d\sigma}{dt} = \eta\,\frac{d\gamma}{dt} \tag{11.152}$$

$$\frac{d\gamma}{dt} + \frac{\sigma}{\lambda} = \frac{\sigma}{\eta} \tag{11.153}$$

It must be emphasized that the use of these models and their combinations is applicable only within the linear viscoelastic range. A practical equation to analyze stress-decay curves was proposed by Peleg (1977).

$$t\,\sigma_o \big/ \left(\sigma_o - \sigma(t)\right) = k_1 + k_2\,t \tag{11.154}$$

where σ_o is the value of the stress at the beginning of relaxation and k_1, k_2 are fitting parameters. Other common mechanical models useful in representing the viscoelastic behavior of specific foods can be found in the literature (Lerchental and Muller, 1967; Brennan, 1980; Shama and Sherman, 1966, Rao and Steffe, 1992).

Creep and relaxation continue to be an area of interest to food scientists and numerous experiments have been carried out for many foodstuffs. Bistany and Kokini (1982) and Mills

and Kokini (1984) compared rheological parameters obtained from steady shear and dynamic viscoelastic properties of foods. The so-called Cox-Merz rule, which states that equal magnitudes of η_a and η^* are obtained at equal values of $\dot{\gamma}$ and ω, respectively, was obeyed by some biopolymer dispersions but failed with aggregates and complex food systems (Rao and Cooley, 1992). Complete definitions of small-amplitude oscillatory properties as well as the values of dynamic parameters of foods were also published by Kokini (1992). Mason et al. (1982) developed a model to simulate transient shear stress growth in semisolid foods based on an earlier model developed by Leider and Bird (1974)

$$\tau = k\dot{\gamma}^n \left[1 + b_o \dot{\gamma}^{(t-1)}\right] \frac{\sum b_i \exp\left(-\dfrac{t}{\lambda_i}\right)}{\sum b_i} \qquad (11.155)$$

where k and n are the power-law parameters; λ_i are time constants and b_o and b_i are constants. Useful relationships between η^*, η' and (steady) η viscosities are also available for different foodstuffs (Bistany and Kokini, 1983a,b).

11.4.5 FOOD GELS

Food gels consist of polymeric molecules, mainly polysaccharides and proteins, cross-linked to form a tangled, interconnected network immersed in water in excess. Gelation of food components arises mostly from physical cross-linking through polymer-polymer interactions. These gels exhibit solid-like properties which were recently reviewed by Doublier et al. (1992). They concluded that both transient and dynamic measurements are required for a complete rheological characterization of these gels. A linear model that fit the relaxation curve of pectin gels is (Gross et al., 1980)

$$\sigma(t) = \sigma_1 \exp\left(-t/\tau_1\right) + \sigma_2 \exp\left(-t/\tau_2\right) \qquad (11.156)$$

where σ_1, σ_2 are the values of the stress at time $t = 0$ in a model made with two Maxwell units in parallel.

11.4.6 TEMPERATURE AND PRESSURE DEPENDENCE OF FOODSTUFFS RHEOLOGICAL PARAMETERS

Viscosity-temperature dependence is frequently represented by the Arrhenius type equation.

$$\ln \eta = A + \frac{\Delta E_\eta}{R\,T} \qquad (11.157)$$

where A is a constant, ΔE_η is the activation energy of flow, and R is the gas constant. Other equations like the empirical (Utracki, 1975)

$$\ln \eta = A' + \frac{B'}{T - T_0} \qquad (11.158)$$

where A', B', and T_o are constants, are also applicable.

During food processing operations in which foodstuffs are submitted to high pressures (e.g., extrusion), viscosity may be related to pressure (P) by
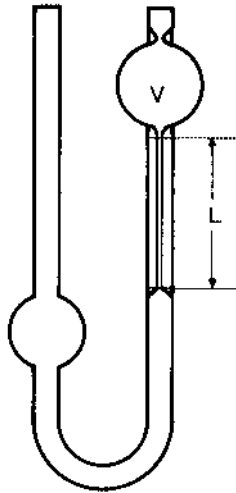
FIGURE 11.7 Ostwald viscometer.

$$\mu = \mu_0 \, e^{a\,P} \tag{11.159}$$

where μ_o is the viscosity at reference pressure and a is a parameter for the sample food. For non-Newtonian foods, either τ or $\dot{\gamma}$ must be specified as a parameter.

11.5 VISCOMETRY AND RHEOMETRY

In this section the experimental methods which are used to determine the properties of viscoelastic fluids are considered. In particular, methods of viscometry (measurement of apparent viscosity) are described in detail. Viscometers are based on the measurement of either the resistance to flow in a capillary tube, or the torque produced by the movement of an element through the fluid. There are three main categories of commercially available viscometers applicable to foodstuffs: capillary, falling ball, and rotational viscometers. More recently, rheometers are available at a relative low cost, can measure wide ranges of shear behavior, and perform complete rheograms including thixotropic recovery, stress relaxation, or oscillatory experiment at a programmed temperature sweep.

For Newtonian liquid food it is sufficient to measure μ as the ratio $\tau/\dot{\gamma}$. Besides the ratio of shear stress and rate of shear, the properties required to describe a non-Newtonian material can be measured by (a) *compression* (force-deformation relationship); (b) means of the *creep test* (stress vs strain as a function of time); (c) *stress relaxation* (stress required to maintain a constant strain; or (d) a *dynamic test* (deformation by a time variable stress, generally oscillatory stress).

11.5.1 CAPILLARY TUBE VISCOMETERS

Figure 11.7 shows schematically a capillary tube viscometer. The fluid to be tested is stored in the upper reservoir (V) from where it is discharged through a capillary tube (L) as a result of a driving force (gravity, gas pressure, a descending piston, or partial vacuum at the exit). Table 11.10 lists some of the principal capillary viscometer characteristics, and their principles of operation, applications and limitations. Johnson et al. (1975) presented a complete description of nine different glass capillary viscometers. Orifice type viscometers, such as the Zhan viscometer, which basically consist of a cup with a hole in the bottom (Bourne, 1982) can also be considered capillary viscometers.

TABLE 11.10
Capillary Tube Viscometers

Type	Governing equations	Principles of operation	Applications and limitations
Glass	$\mu = \pi\, PR^4/8LQ$	A fixed volume of sample flows	Suitable for measuring
I-Ostwald	$\eta = \pi\, R^4 g\sigma/[8Lk(dQ/dP+,$	from a reservoir bulb to a	Newtonian liquid foods,
II-Cannon-Fenske	$Pd^2Q/4dP^2)]$	receiver bulb located at a lower	at low shear stress only;
III-Ubbelohde	$\gamma = 4Q/\pi R^3$	level (I) in the other arm or (II)	Cannon-Fenske design
	$\tau = PR/2L$	in the same arm; Ubbelohde (III)	reduces error due to bad
	$\tau y = P_o\, g\rho R/2L$	viscometer has an additional arm	alignment
Variable pressure	Same as above	There are a variety of methods of	Valid for measurement of
		varying pressure (compressed	viscosities on Newtonian
		gases, pumps, etc.); in capillary	and non-Newtonian foods
		rheometers the fluid is forced	in the range of 0.01–$5 \times$
		through a capillary tube	10^6 mPa, up to very high
		recording the pressure required	shear stresses; precision
		to have constant flow rate	good to moderate

Note: P = pressure; L = capillary length; Q = flow, cm^3/s; R = capillary radius; ρ = density; k = constant; $P_o = P_{p-o}$.
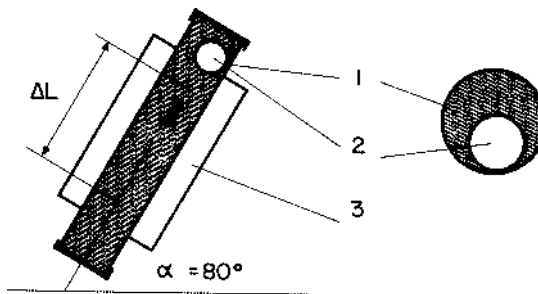
FIGURE 11.8 Falling-ball viscometer.

11.5.2 FALLING-BALL VISCOMETERS

Falling-ball viscometers (Figure 11.8) operate on the principle of measuring the time for a ball to fall through a liquid under the influence of gravity. The falling ball reaches a limiting velocity when the acceleration due to the force of gravity is exactly compensated by the friction of the fluid on the ball. A variation of this type of viscometers is the rolling-ball viscometer in which the ball falls through a tube tilted at given angle. A summary of characteristics of falling-ball viscometers is given in Table 11.11.

11.5.3 ROTATIONAL VISCOMETERS

This instruments can determine the viscosity of Newtonian and non-Newtonian fluids contained between two coaxial cylinders (Figure 11.9), or a cone and plate geometry (Figure 11.10) by measuring the drag of the fluid on a mobile member (cylinder or cone) while the other member (cylinder or plate) remains stationary. From the earlier works of Couette (1890) several detained analyses of both coaxial cylinders and cone and plate viscometers were published (Slattery, 1961; Van Waser et al., 1963). Table 11.12 shows

TABLE 11.11
Falling Ball Viscometer

Governing equations	Principles of Operation	Applications and limitations
$\eta = K(\rho_1 - \rho_2)t$ $\dot{\gamma}_{max} = 3\mu/2R$	Consists of a vertical or inclined glass tube (1) where a ball (2) is allowed to slide; the falling time of the ball between two marks separated a fixed distance (ΔL) is measured	Useful for the measurement of viscosity of transparent Newtonian foods; different balls with densities ranging from that of glass (approx. 2 g/cm³) to stainless steel (approx. 8 g/cm³) are used; it is also convenient to thermostatize the viscometer The measuring range of viscosity is from 20 mPa·s to 85,000 mPa·s

Note: $\dot{\gamma}_{max}$ = Shear rate with tilted angle at 90°; K = calibration constant; ρ_1 = ball density; ρ_2 = liquid density; t = falling time, μ = ball speed, cm³/s and R = tube radius.
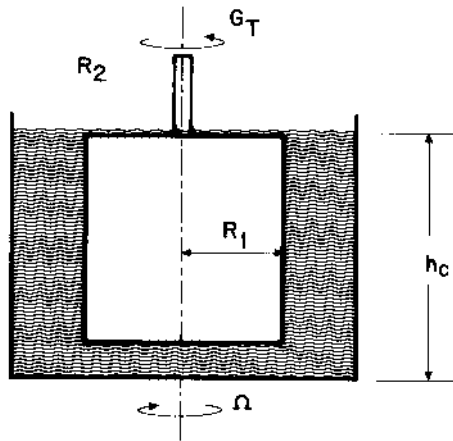
FIGURE 11.9   Sketch of coaxial cylinders viscometer.
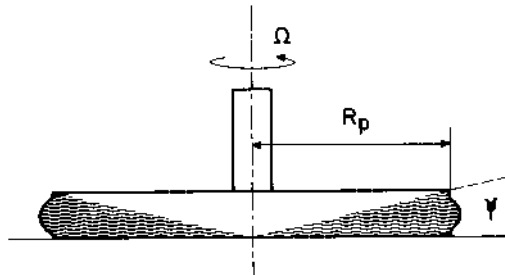
FIGURE 11.10   Sketch of cone and plate viscometer.

equations used to calculate the rheological parameters with rotational viscometers, as well as other operational characteristics and limitations. Some other empirical rotational viscometers widely used in the industry as Bravender Viscocorder, Brookfield Viscometer, and FMC Consistometer are basically used for quality control purposes and rigorous mathematical analysis is not available nor is it necessary.

TABLE 11.12
Rotational Viscometers

Type	Governing equations	Principles of operation	Applications and limitation
Coaxial cylinders	$\mu = G_T(1/R_1^2 - 1/R_2^2)/4\pi h_c\,\Omega$ $\eta = (\mu\pi M/G_T) - (D/\Omega)\ln(R_2/R_1)$ $\dot{\gamma}_{min} = 2\Omega R_1^2/(R_2^2 - R_1^2)$ $\dot{\gamma}_{max} = 2\Omega R_2^2/(R_2^2 - R_1^2)$ $\tau = (1/R_1^2 - 1/R_2^2)/4\,\pi h_c$ $\tau_y = \tau G(\Omega \to 0)/\ln(R_2/R_1)$	Basically consists of a pair of coaxial cylinders, so that one can be rotated whereas the other is held fixed; in the Searle type viscometer the inner cylinder is the rotor; in the Coutte type viscometer the external cylinder rotates; the torque (G_T) necessary to maintain the rotor at a fixed rotational speed (Ω) (Searle), or fixed inner cylinder (Coutte), is a measure of the shear stress (τ); the rotational speed (Ω) is a measure of the rate of shear ($\dot{\gamma}$); in Stormer type viscometer $\dot{\gamma}$ is measured at constant G_T; in McMichael type instrument, G_T is measured at Ω constant	Newtonian and non-Newtonian viscosities can be measured; some commercial instruments show end and edge effects; with appropriate modifications creep compliance-time responses, stress relaxation, and dynamic rheological properties of semisolid can be measured
Cone-plate	For small ψ $\mu = 3G_T\psi/(2\pi R_p^3\varsigma)$ $\dot{\gamma} = \Omega/\psi$ $\tau = 3G_T/(2\pi R_p^3)$ $\tau_y = \tau G(\Omega \to 0)$	In this type of viscometer the fluid to be tested is sheared between a rotating cone and a fixed plate; $\dot{\gamma}$ and τ are the result of the measurement of G_T and Ω, respectively; it can be used for oscillatory testing (η^*); if the instrument is capable of measuring normal stresses it is called rheogoniometer; on the other hand, rheometers can also measure dynamic strain when the sample is subjected to oscillating rotation	Suitable for measuring Newtonian and non-Newtonian fluid foods, at high rate of shear but with danger of heating by friction; end effects practically negligible; applicable for time-dependent liquids; particulate fluid foods require careful selection of cone angle and gap

Note: G_T = torque; R_1 = internal cylinder radius; R_2 = external cylinder radius; hc = external cylinder length; ς = angular velocity of rotating member; ψ = cone angle.

11.5.4 RHEOMETERS

These instruments are easily configurable for specialized testing applications such as elevated temperature or pressure as well as semisolid testing. The measuring principle is based in a very low inertia torque motor and drive shaft bearing systems which practically ensures a frictionless transmission of the applied stress to the test food. The sensor system geometries normally include cone plates, parallel plates, and coaxial cylinders of different sizes and materials. Automatic gap adjustment, normal force measurement, forced oscillation test, and complete multiprocessor computer control are the principal features of these sophisticated rheometers.

11.5.5 COMMERCIALLY AVAILABLE APPARATUS

Table 11.13 shows some commercial viscometers and rheogoniometers commonly used in food science and technology. In most cases the information has been taken from catalogues; in some cases the data was supplied by the manufacturer. The Ranges column consists of

figures that are intended as a general guide and readers must approach manufacturers for further details. Information provided in Table 11.13 is required for preliminary consideration of instruments for a particular study.

11.6 RHEOLOGICAL PROPERTIES OF FOODSTUFFS

11.6.1 NEWTONIAN FOODS

Most beverages and liquid foods such as wines, beer, tea, coffee, clarified fruit juice, soda and cola drinks, vegetable oils, milk, etc. exhibit Newtonian behavior. Several empirical or semiempirical equations relating liquid food viscosity with both soluble solids and temperature were published (e.g., Rao, 1977). However, most of the liquid foods have mainly water, salts, and sugars in solution, different vegetable oils and fat in suspension, and insoluble high-molecular weight carbohydrates and proteins. As an early approximation viscosity of Newtonian liquid foods can be estimated as the viscosity of water (μ_w) and that of the principal soluble solids. The viscosity of water can be calculated by the formula (Berstch and Cerf, 1983)

$$\ln \mu_w = 0.266 - 2.02 \times 10^{-2}\ T + 4.4 \times 10^{-5}\ T^2 \qquad (11.160)$$

where t = temperature, °C. On the other hand, viscosity of sucrose solutions may be calculated from Kubota et al. (1980) equation

$$\mu = a \exp\left(b/T^n\right) \qquad (11.161)$$

where

$$\log a = 0.00458\ X^{1.15} - 3.05$$

and

$$b = 9.90 \times 10^4\ X^{1.51} + 6.1 \times 10^7$$

The ranges of validity of Equation 11.161 are temperature (T) = 283.2 to 323.2 K and concentration (X) = 0 to 40° B. Rao et al. (1984) reported that the effect of concentration on viscosity of fruit juices at a constant temperature can be represented by an exponential-type relationship. When the effect of temperature must also be evaluated, very complex expressions for E_η resulted. Constenla et al. (1989) modified the Mooney (1951) equation (Equation 11.162) in order to express the concentration on a weight basis (X), as °Brix, and to take into account the effect of temperature.

$$\ln \frac{\mu}{\mu_w} = \frac{A\ X}{100 - B\ X} \qquad (11.162)$$

where the coefficients A and B are functions of temperature. The resulting coefficients of the above equation for apple juice and different sugars are presented in Table 11.14. Viscosity values of salt solution (NaCl), another major ingredient in foodstuffs, can also be calculated as (Kubota et al.; 1980)

TABLE 11.13

Some Commercial Viscometers and Rheogoniometers Commonly Used in Food Science and Technology

Name and manufacturer	Type	$\dot{\gamma}$, s^{-1}	Overall τ (Pa)	Ranges $\eta(\mu)$ (mPa·s)	T (°C)	Other characteristics
BOHLIN Instruments	Viscometers Coax. cylin.	$4-10^{-4}$		$3.8-10^6$	$-20/150$	Torque: Min: 0.001 mN Max: 50 mNm
Metric Group Ltd	Rheometers Cone plate	$0.1-10^5$	$0.01-10^4$		$-15/250$	Speed: 320 rad/sec
Love lane,	Paral. plate Coax. cylin.					Freq: $10^{-3}-50$ Hz
Cirencester,						Automat. creep recovery test
GLOUCESTER SHIRE,						
GL71YG; ENGLAND						
BROOKFIELD	Coax. cylin.	$0.6-122$		$1-64 \times 10^6$	$-10/100$	Automatic speed scanning
Brookfield Engn. Lab. Inc.	Rotary spindles Cone-plate	$0.6-750$				
Stoughton, MA						
02072, US						
CANNON®	Glass capillary viscometer			$0.3-10^5$		
Cannon Instrument Co.						
P.O. Box 16						
State College, PA						
16801, US						
Ferranti-Shirley	Cone-plate	$0.18-1800$	$44-1.1 \times 10^5$	$0.024-62 \times 10^3$	200	Automatic speed scanning
Ferranti Ltd.	Coax. cylin.	$0.3-950$	$0.8-6.100$	$8 \times 10^{-4}-2 \times 10^4$		Stress relax. capability
Moston, England						
Gilmont Instrument	Falling ball			$0.25-300$		
401 Great Neck Road,						
Great Neck, NY						
11021, US						

Company	Type					Notes
HAAKE	Searle	0.01–4×10^5		2–10^{-9}		Automatic speed scanning
Gebruder Haake	Couette	0.06–1000		0.5–10^{-4}		
Dieselstrasse 4 D75	Falling ball			0.2–10		P up to 1000 bars
Karlsruhe 41;	Rheometers		0.04–$24,000$			Automat. gap setting
Germany	Cone/plate	min:1.5	0.05–$30,000$			
	Paral. plate	min:1.05	0.01–$19,000$	1.0–10^{-9}	$-50/950$	Torque
	Coax. cylin.	min:1.29				Min 10^{-6} Nm
						Max 0.05 Nm
						Min. angle 10^{-6} rad
INSTRON	Capillary and rotary	0.4–1.1×10^{-4};	570–4.3×10^6;	5×10^{-2}–1×10^7	40/350	Pressure range
INSTRON Ltd.	rheometers	2×10^{-6}–2.6×10^4	0.9–9.6×10^5	3.5×10^{-5}–1.2×10^{11}	400	3×10^5–3.8×10^x
Coronation Rd.						$\omega = 10^{-5}$–100 Hz
High Wycombe						
Bucks HP123SY						
Great Britain						
PARR PHYSICA	Rheometers					Fully automatic
Meβtchnik GmbH	Several geometries					Creep and oscillation tests
Vor dem Lauch 6						
D70567 STUTTGART						
GERMANY						
FAX: (49) 7117291						
Rheomat	Cone-plate	0.05–1000	0.2–4×10^3		30/100	$\omega = 3 \times 10^{-5}$–$20$ Hz
Contraves AG Zurick	Coax. cylin.					
Schaffhauserstrasse						
580 Zurich,						
Switzerland						
Rheometrics	Mechanical spectrometer	10^3–10^4	1.6–3200	1×10^{-3}–1×10^{10}	$-150/400$	
RHEOMETRICS Inc.	Cone-plate		0.1–1×10^7			
spectrometer						
Piscateway, NJ, US						

TABLE 11.13 (continued)

Some Commercial Viscometers and Rheogoniometers Commonly Used in Food Science and Technology

Name and manufacturer	Type	$\dot{\gamma}$, s^{-1}	Overall τ (Pa)	Ranges $\eta(\mu)$ (mPa·s)	T (°C)	Other characteristics
Rheotron Brabender OHG Duisburg D-4100 Duisburg 1 Kulturstraße 51-55, GERMANY	Coaxial cylinder Cone-plate	$5–2 \times 10^4$	$0.1–10^5$	$0.5–10^9$	–30/300	Automatic scanning $\omega = 0.01–100$ rad/s
Schott GERÄTE GmbH Postfach 1130 D-6570 Hofheim GERMANY	Glass capillary Ubelohde Reverse flow Cannon-Fenske Ostwald	$0.35–3 \times 10^5$			–80/150	Fully automatic Digital optoelectric IR detector meniscus
TA Instrument Ltd. Leatherhead, Surrey KT227UQ. ENGLAND	Rheometer (Carri-Med) Different geometries Autogap setting Inertia correction				–30/150	Torque: Min: 0.0001 nNm Max: 50 nNm $\omega = 10^{-4}–50$ Hz Angle, m 2.5 μ
Weissenberg Sangamo Schlumberger North Bersted, B. Regis, W. Sussex PO 22 9B5, ENGLAND	Rheogoniometer Cone-plate Paral. Plate Coax. cylin.	$7 \times 10^3–9 \times 10^3$	$1.9 \times 10^{-3}–9 \times 10^3$	$1 \times 10^{-4}–5 \times 10^6$	–50/400	$\omega = 3.1 \times 10^{-4}–50$ Hz

$$\mu = a\, e^{\frac{b}{T^n}} \qquad (11.163)$$

where

$$\log a = 0.00359\, X^{1.33} - 2.00$$

and

$$b = 3.09 \times 10^5\, X^{1.59} + 6.1 \times 10^7$$

In this equation the validity ranges are temperature (T) = 283.2 to 323.2 K and concentration X = 0 to 24 wt%.

TABLE 11.14
Values of Coefficients A and B in Equation 11.27 for Evaluating Viscosity

Coefficient	Sucrose	Glucose	Fructose	Apple juice
A	2.6122	2.5617	2.4153	2.5289
B	1.0381	0.9725	0.9807	1.0052

Note: T = 20°C.

From Constenla, D. T., Lozano, J. E., and Crapiste, G. H., 1989, Thermophysical properties of clarified juice and their concentrates, *J. Food Eng.,* 6:257. With permission.

11.6.2 NON-NEWTONIAN FOODS

Most foodstuffs are non-Newtonian in nature. Viscoelastic and semisolid foods have been the topic of extensive study in recent years. Rheological characterizations of non-Newtonian foods have been in the form of τ vs $\dot{\gamma}$ curves, dynamic characteristic, time effect on η at constant $\dot{\gamma}$ etc. Values of these parameters were compiled by different authors (e.g., Rao, 1977; Kokini, 1992). Shawa and Sherman (1966) proposed the following creep compliance vs time equation for the description of the rheological behavior of ice cream

$$J(t) = J_0 + J_1\left(1 - e^{-t\,\tau_1}\right) + J_2\left(1 - e^{-t\,\tau_2}\right) + \frac{\tau}{\eta} \qquad (11.164)$$

where J_0 is the instantaneous elastic compliance; J_1 and J_2 are the compliances associated with retarded elastic behavior; τ_1 and τ_2 are retardation times, associated with retarded elasticity; and η is the viscosity associated with Newtonian flow. Equation 11.164 is a representative example of a model for description of the viscoelastic behavior of semisolid foods. Typical values of the rheological parameters for frozen ice cream (–11°C) are given by Equation 11.165.

$$J(t) = 10^{-5} + 2.2 \times 10^{-5}\left(1 - e^{1866\,t}\right) + 8.9 \times 10^{-6}\left(1 - e^{-144\,t}\right) + \frac{t}{6} \times 10^8 \qquad (11.165)$$

TABLE 11.15
Viscosity and Other Rheological Parameters for Selected Foodstuffs at Room Temperature

Foodstuff	μ or $\eta(\dot{\gamma})$ (mPa·s)	n[a]	K[a] (Pa·s[n])	τ_y[b] (Pa)	Additional parameters
Apple Sauce		0.15–0.24	40.6–76.9	18.4–50.7	
Butter		0.042	417.0	1.16	n = 0.037[a]
Chocolate, melted (46°C)		0.574	0.57		K = 15,800
Egg (whole	6.4				E_η = 5.89 kcal/gmol
Egg Yolk		0.88	0.32		
Ketchup		0.107	79.4		n = 0.160
					K = 851
Mayonnaise		0.050	260		n = 0.090
					K = 637
Meat (fat = 30%; protein = 10.4%)	254	0.341	160.2	27.8	
Milk (condensed)		0.834	36.0		
Pear juice (70°B)	1.15				Ea = 8.2 kcal/gmol
Pectin, 0.5 (wt%)	4.5 (500s[1])				
Tomato concentrate (30 wt%)		0.40	187		
Tomato paste (30°B)	serum: 4.3–140	0.28	139–252	78–212	
Oil-water emulsions, 0.32–0.62 volume fraction		1.06–1.2	0.014–0.071		
Yogurt	43	0.46	1.31	3.97	

Data adapted from Harper and El Sahrigi, 1965; Rao, 1977; Steffe, 1986; Qiu and Rao, 1988; Ibarz and Sintes, 1989; Bistani and Kokini, 1983; Ramaswamy and Basak, 1992; Da Silva et al., 1992.

[a] n and K are the power law parameters for η vs. Ω.
[b] τ is the yield stress.

Doublier et al. (1992) proposed the following equation to fit creep under constant stress σ_0

$$\frac{\gamma}{\sigma_0} = \frac{1}{G_0} + \frac{t}{\eta_\infty} + \sum_{i=1}^{n} \frac{\left(1 - e^{-t/\tau_i}\right)}{G_i} \qquad (11.166)$$

where $\tau_i = \eta_i/G_i$, given in shear or its equivalent form in compression. Equation 11.166 with n = 1 was used for agar and pectin gels. Values of n = 2 or n = 3 were also used to fit the data from other food gels.

In Table 11.15 selected experimental data of viscosity and values of power law and other rheometric parameters for different foodstuffs are listed. Additionally, Table 11.16 shows rheological tests applied to typical foodstuffs together with the measuring conditions and used equations.

11.6.3 FOOD TEXTURE

Texture is one of the main quality factors in foodstuffs and it is related to the response of the tactile senses to physical stimuli which results from the contact between the body (mouth, hands, etc.) and the food. Although texture is difficult to define, since it consists of a number of different physical sensations, Bourne (1982) arrived at the following definition:

"The textural properties of a food are the group of physical characteristics that arise from the structural elements of the food, are sensed by the feeling of touch, are related to the deformation, disintegration and flow of the food under a force, and are measured objectively by functions of mass, time and distance".

Texture properties are associated with rheological properties. However rheological parameters do not cover all the factors that constitute the texture of a food. Szczesniak (1963) classifies texture-measuring instruments into three groups: fundamental, empirical, and imitative tests. Fundamental texture determinations are objective tests that measure real rheometric properties of foods and include Young's modulus (E); G modulus; viscosity (μ); and Poisson's ratio (P = change in width per change in length). The fundamental tests have the advantage that the parameters are physically well defined in known units and the experiences can be reproduced.

In addition, empirical and imitative tests, which can be classified as nonfundamentals, are specific to a limited number of foodstuffs and give nonconvertible data, but they are capable of correlating with the sensory methods, simple to perform, and widely used in the food industry.

11.6.4   TEXTURE MEASUREMENT BY NON-FUNDAMENTAL METHODS

These mechanisms include those designed to imitate a specific human operation (e.g., chewing) and only few apparatuses have been reported, as the denturometer (Proctor et al., 1955); and the empirical instrument which applies a sequence or combination of stresses and the response of the food is analyzed. The most common instruments used to measure texture of foodstuffs by these nonfundamental methods in which a rigorous theoretical analysis is not possible, are the force and the distance measuring instruments. Some of the many instruments which are based on empirical principles are classified in Table 11.17. However, in some cases a single texture measuring system (e.g., Instron Universal Testing Machine and Kramer Shear Press) can perform several empirical and imitative tests by using a variety of probes and cells, and readers are encouraged to approach manufacturers for further details and quotations.

TABLE 11.16
Typical Rheological Properties of Foodstuffs: Measuring Instruments and Related Equations

Foodstuff	Rheological instrument	Used equations	Measured variables	Measuring conditions	Ref.
Apple juice	Capillary visc.	11.8, 11.10	$\mu(X,T)$	$X = 10–75\ °B$ $T = 10–80°C$	Constenla et al., 1989
Applesauce	Cone-plate	11.13, 11.14, 11.15	τ_y	Pulp content 86–96% $X = 17\ °B, T = 25°C$	Qiu and Rao, 1988
Butter, cheese, cream, etc.	Mechanical Spectrometer cone-plate	Dynamic properties	η^* G' G''	$f = 0.04$ rad; $R = 1.25$ cm gap $= 50\ \mu m; T = 25°C$	Bistany and Kokini, 1983
Honey	Falling ball	11.8	$\mu(X,T)$	$X = 10–75\ °B$ $T = 20–70°C$	Munro et al., 1943
Fruit juice and purees	Contraves Rheomat	11.8, 11.15, 11.22	$\mu(T,X)$ $\eta(T,X)$	$X = 10–75\ °Brix$ $T = 20–70°C$	Saravacos, 1970
Fruit pulps	Rheometrics Cone-Plate	11.8, 11.13, 11.17	$\tau(\dot{\gamma}, t, T)$	$X = 26–34\ °B$ $T = 30–55°C$ $f = 0.1$ rad; $R = 25$ mm	Ibarz and Lozano, 1992
Gums	Rheometrics Fluids Rheometer Cone-Plate		η^*, η', η''	$X = 0.5–3.0\%; T = 24°C$ $f = 0.0196$ rad $R = 2.5$ cm; gap $= 50\ \mu m$	Mills and Kokini, 1984
Mayonnaise	Weissemberg Rheogoniometer	11.16	$\tau(\dot{\gamma})$ $\eta(t)$	$f = 1°23'; T = 19.5°C$ $R = 3.75$ cm; $0.41 < \dot{\gamma} < 205$	Tiu and Boger, 1974
Oil-water	Tube viscometer	11.13	$\eta\ (\phi,X)$		Suzuki et al., 1991

Orange juice	Haake RV12	11.8	$\tau(\dot{\gamma})$	Pulp content: 2–12% T = –5°C	Crandall et al., 1990
Pectin, citrus	Parallel cylinders	Viscoelastic properties	$\tau(\dot{\gamma})$, G, J*	Pectin = 0.42% Saccharose = 60% T = 20°C; R_1 = 8–15 mm R_2 = 11–18 mm; h_0 = 10–30 mm	Dahme, A., 1984
Pectin/fructose	Carri-med rheometer Cone-plate	Dynamic test	η^*, G′, G″	Pectin: 0.5–1.0% Fructose: 60% f = 2°; R = 2 cm; T = 10–50°C	Rao et al., 1993
Pectin and locust bean gum	Carri-med Rheometer Cone-plate	Eq.	$\eta(\dot{\gamma})$	f = 3.97°; R = 2.5 cm gap = 118 μ T = 25°C	Lopes Silva et al., 1992
Potato starch	Coaxial cylinders	11.13 modified	$\eta(\tau)$, τ_y		Janas, 1991
Starch suspension	Couette	11.8, 11.13	η, G′, G″	v = 0.002–2.5Hz; T = 6 f = 2°; X = 1–10 (wt%)	Evans & Haisman, 1980
Skim milk	Capillary	11.8	$\mu(X,T)$	X = 0–15 (wt%) T = 10–50°C	Kubota et al., 1980
Tomato conc.	Coaxial cylinders	11.8	$\eta(X,T)$ $\tau(\dot{\gamma})$	R_1 = 38 mm; h_c = 150 mm gap = 0.25–2.0 mm X = 5.8–30, wt% T = 32–82°C	Harper and El Sahrigi, 1965 Rao et al., 1981
Tomato pastes	Haake RV2 Carri-Med Cone-plate	11.8, 11.14 Dynamic test	$\tau(\dot{\gamma})$ η^*, G′, G″	X = 25.5–34.4°B; f = 2°; R = 2 cm v = 1–10 Hz; T = 40°C	Rao and Cooley, 1992
Yogurt	Haake RV20	11.13	η, $\tau(\dot{\gamma})$ T = 10°C	Pectin 0–0.5%	Ramaswamy and Basak, 1992

TABLE 11.17
Classification of the Principal Nonfundamental Tests for Food Texture Measurement

Mode of operation	Principle	Device and manufacturer	Examples of application
Puncture and penetration	The force required to penetrate a probe into a semisolid food, causing irreversible changes in the structure (yield point) is measured; it was found to be proportional to the area and the perimeter of the probe	Magness-Taylor Pressure Tester D. Ballauf Co. 619 H Street N.W. Washington D.C. US	Fruits and vegetables, butter, margarine, solid fats, meats
		Bloom Gelometer G.C.A. Precision Scientific Group 3737 W. Cortland St. Chicago IL 60647 US	
Shear	The force necessary to shear through a food; one or multiple blades; or the force to extrude a food through an outlet of defined shape and area; results involve complex combinations of stresses and cannot be expressed in terms of shear moduli	Kramer Shear Cell Food Technology Co. 12300 Parklawn Drive Rockville, MD 20852 US	Fruit and vegetables, meat, cheese, baked goods
		Instron Universal Testing Machine Instron Corporation 2500 Washington St. Canton, MA 02021 US	
		O.T.M.S. Canners Machinery Ltd. PO Box 190 Simcoe, Ontario N3Y 4LI, CANADA	
Flow device	Time to flow food through a vessel of known dimensions	Adams Consistometer National Manufacturing Co. PO BOX 30226 Lincoln, NE 68503 US	Comminuted fruits and vegetables (purees, catsup, etc.), jellies, cream
		Bostwick Consistometer Central Scientific Co. 2600 South Kostner Ave. Chicago, IL 60623 US	
Mixing device	Torque developed by the mixing of pastes	Farinograph C. W. Brabender Instrument 50E Wesley St. South Hackensack, NJ 07606 US	Flour, bread dough

Data from Bourne (1982) and Brennan (1980).

GLOSSARY

Calorimeters: Laboratory apparatus for determining the heat capacity of substances, based on the conservation of energy principle

Intrinsic: Individual value, in terms of any component of the food product, or its property

Line source: Infinitely long linear heat source of virtual thickness that provokes a concentric temperature field when heated

Species: Chemical component of a foodstuff, in generic terms

Temperature gradient: Difference of temperature between two points provoking a heat flux

Thermocouple: Device for measuring temperatures, consisting of a junction of two wires of different metals which produce an electric tension when heated

NOMENCLATURE

b	Parameter in Equation 11.15
Bx	Soluble solids concentration (°Brix)
C_p	Constant pressure specific heat (kJ/kg °C and Kcal/kg °C)
E	Young's modulus (Pa)
ΔE_η	Flow activation energy ($Jkmol^{-1}$)
G	Rigidity modulus (Pa)
f	Distribution factor (Equation 11.4)
g	Acceleration of gravity (m/s^2)
G	Young's modulus (Pa)
G''	Loss shear modulus (Pa)
G'	Storage shear modulus (Pa)
G^*	Complex shear modulus (Pa)
g_c	Conversion factor (9.81 N/Kg_f)
G_T	Torque (N·m)
H	Enthalpy (J/kg)
J''	Loss compliance
J'	Storage compliance
J^*	Complex compliance
J_o	Instantaneous compliance
J_R	Retarded compliance
J_m	Mean compliance
J_N	Newtonian compliance
K	Bulk modulus (Pa)
k	Consistency coefficient ($Pa·s^n$)
k	Thermal conductivity (W/m·K)
M	Molecular weight (g/mol) and moisture content on wet basis (g/100 g wet material)
n	Flow behavior index
N	Number of components of a composite material
p	Thermal conductivities ratio k_d/k_c
q	Heat flux (w/m^3)
r	Radial distance from linear heat source axis (m)
R	Gas constant ($J·K^{-1}kmol^{-1}$)
R_i	Radius (m)
t	Time (s)
T	Temperature (°C or K)
V	Volume (m^3)
w	Mass fraction
W	Mass (g or kg)
x	Mole fraction
X	Moisture content on dry basis (g/g dry matter) and concentration (%)
Y	Fraction of water on wet basis (M/100)
z	Distance (m)

SUBSCRIPTS

c	Continuous phase
d	Disperse phase and dry
eff	Effective
eq	Equilibrium
f	Freezing temperature
g	Gaseous phase
h	Ice
i	Generic component in a mixture or composite material
o	Fresh or initial state
r	Relative
red	Reduced
ref	Reference substance
s	Sample
sp	Specific
w	Water

GREEK LETTERS

α	Thermal Diffusivity (m^2/s)
β	Integration variable in Equation 11.17
γ	Strain
$\dot{\gamma}$	Rate of shear (s^{-1})
$\gamma\dot{}$	Complex strain
ε	Strain (normal)
ε	Porosity
η	Apparent viscosity (Pa·s^n)
η''	Elastic component of the dynamic viscosity (Pa·s)
η'	Viscous component of the dynamic viscosity (Pa·s)
η^*	Complex dynamic viscosity (Pa·s)
λ	Water heat of diffusion (J/kg)
$\boldsymbol{\mu}$	Poisson's ratio
μ	Viscosity (Kg/m·s) and (C$_p$)
ρ	Specific gravity and density (kg/m^3)
σ	Normal stress (Pa)
σ	Stress (Pa)
τ	Shear stress (Pa)
τ	Shear stress time derivative (Pa/s)
$\tau\dot{}$	Complex stress (Pa)
τ_y	Yield stress (Pa)
ν	Kinematic viscosity (stokes)
ϕ	Volume fraction
χ	Viscometer cone angle (rad)
ω	Dynamic frequency (rad/s)
Ω	Angular speed (rad/s)
$[\mu]$	Intrinsic viscosity

FOR FURTHER INFORMATION

Progelhof et al. (1976) have made a comprehensive review of different predictive methods. The paper has 87 references. Assuming a given space distribution as well as shape (sphere, rods, etc.) of the space, several correlations of the effective property, k_{eff}, have been proposed as a function of k_c, k_d, and ϕ_d. The reader is referred to that paper as a very comprehensive source.

Rehman, S. (1995). *Food Properties Handbook,* CRC Press, Boca Raton, Florida. This is a most comprehensive handbook devoted to the subject. It covers sorption, thermophysical and transport properties, and includes both extensive experimental data and predictive models. More than 600 references are cited.

Reidy and Rippen (1969) presented a comprehensive study of different methods to measure thermal conductivity in foods. The study has 56 references.

Nesvadba (1982a) gives a very good critical review of the methods for the measurement of both thermal conductivity and diffusivity. He presents a summary of different measuring techniques for α and k, with sketches describing the apparatus used and the equations to calculate the properties from the experimental measurements. It is a work of great practical value.

Miles et al. (1983) collected a very comprehensive list of predictive equations of thermophysical properties of foods. Some of them are derived from theoretical considerations, but most are the result of fitting experimental data.

Polley et al. (1980) is a very comprehensive list of values of all thermal properties of a large amount of food products under given conditions.

Reidel (1975) devoted several chapters to physical properties of foodstuffs, and provide excellent information.

Kent et al. (1984), though particularly devoted to measurement techniques, provides many punctual values of thermal properties of different foodstuffs.

Witte et al. (1976) is a good compilation of individual product values and provides 41 references.

Lewin (1962) reported punctual values of pH for many different foods.

Cuevas and Cheryan (1978) reviewed thermal conductivity of liquid foods and discussed measuring techniques as well as predictive models. They cited 48 references. Their work is very interesting.

Sanz et al. (1987) completed a very comprehensive review of thermal properties for meat products. They collected experimental values of k, α, ρ, Cp, and enthalpy, for temperatures above and below initial freezing points from 78 references. The same authors, in 1989, reviewed equations to predict thermal properties; 41 references are cited.

Sherman (1979) presents a multidisciplinary approach including the psychophysics of the sensory evaluation and measuring of textural properties, the food processing aspects of food rheology, and the relationship between structure and rheological properties of foodstuffs like gels, chocolate, dough, and dairy products.

Voisey and deMan (1976) and then Bourne (1982) gave a survey of instruments for the determination of food texture. These authors summarize instrument applications in a general way and give sources of the many details.

The Journal of Texture Studies, published quarterly by Food and Nutrition Press, 1 Trinity Square, Westport, Connecticut 06880, is one of the best sources of information on developments in the field of food rheology and texture. The instrumental and theoretical aspects as well as the actual results of the rheological characteristics of liquids and semiliquid foods have been widely reviewed and discussed in the following books.

Kramer, A. and Szczesniac, S., 1973, *Texture Measurements of Foods,* Reidel Publisher, Dordrech, Netherlands.

Peleg, M. and Bagley, E. B., 1983, *I.F.T. Basic Symposium Series,* AVI Publishing, Westport, Connecticut.

REFERENCES

Alagusundaram, K., Jayas, D. S., Muir, W. E., and White, N. D. G., 1991, Thermal conductivity of bulk barley, lentils and peas, *Trans. ASAE* Vol. 34, No. 6, 1784–1788.

Alvarado, J. D. and Romero, C. H., 1989, Physical properties of fruits. I, II, Density and viscosity of juices as functions of soluble solids content and temperature, *Lat. Am. App. Res.* 19:15–21.

Andrieu, J., Gonnet, E., and Laurent, M., 1986, Pulse method applied to foodstuffs: thermal diffusivity determinations, in *Food Engineering and Procedural Applications* Vol. 1, *Transport Phenomena,* Le Maguer and Jelen, Eds., Elsevier App. Sci., London, U.K. 103–122.

Andrieu, J., Gonnet, E., and Laurent, M., 1987, Intrinsic thermal conductivities of basic food components, *High Temp. High Press.* 19:323–330.

Andrieu, J., Gonnet, E., and Laurent, M., 1989, Thermal conductivity and diffusivity of extruded Durum Wheat Pasta, *Lebensm.-Wiss. u.-Technol.* 22:6–10.

Bayindirli, L., 1992, Mathematical analysis of variation of density and viscosity of apple juice with temperature and concentration, *J. Food Proc. Press.* 16:23–28.

Bayindirli, L. and Özsan, O., 1992, Modeling the thermophysical properties of sour cherry juice, *GIDA* 17(6):405–407.

Bazán, H. C. and Mascheroni, R. H., 1984, Transferencia de calor con simultáneo cambio de fase en la congelación de carnes ovinas, *Rev. Lat. Transf. Cal. Mat.* 8:55–76.

Behrens, E., 1968, Thermal conductivities of composite materials, *J. Comp. Mater.* 2(Jan):2, 2(Oct):521.

Bird, R. B., Stewart, W. E., and Lightfoot, E. N., 1960, *Transport Phenomena,* Wiley, New York.

Bistany, K. L. and Kokini, J. L., 1983a, Dynamic viscoelastic properties of foods in texture control, *J. Rheol.* 27:605–620.

Bistany, K. L. and Kokini, J. L., 1983b, Comparison of steady shear rheological properties and small amplitude dynamic viscoelastic properties of fluid food materials, *J. Texture Studies,* 14:113–124.

Bourne, M. C., 1982, *Food Texture and Viscosity: Concept and Measurement,* Academic Press, New York.

Brennan, J. G., 1980, Food texture measurement, in *Developments in Food Analysis Techniques-2,* King, R. D., Ed., Applied Science Publishers, London, 56–63.

Califano, A. N. and Calvelo, A., 1991, Thermal conductivity of potato between 50 and 100°C, *J. Food Sci.* 56(2):586–587, 589.

Casada, M. E. and Walton, L. R., 1989, New model for determining thermal diffusivity with the thermal probe, *ASAE,* 32(3):973–976.

Casson, N., 1959, A flow equation for pigment-oil suspensions of the printing ink type, in *Rheology of Disperse Systems,* Mill, C. C., Ed., Pergamon Press, New York, 82–104.

Choi, Y. and Okos, M. R., 1983, The thermal properties of tomato juice concentrates, *Trans. ASAE.* Vol. 26, 305–311.

Choi, Y. and Okos, M. R., 1986, Effects of temperature and composition on the thermal properties of foods, in *Food Engineering and Process Applications,* Vol. 1, *Transport Phenomena,* Maguer, M. Le and Jelen, P., Eds., Elsevier, London, 93–101.

Christenson, M. E., Tong, C. H., and Lund, D. B., 1989, Physical properties of baked products as functions of moisture and temperature, *J. Food Proc. Preserv.* 13:201–217.

Constenla, D. M., Lozano, J. E., and Crapiste, G. H., 1989, Thermophysical properties of clarified apple juice as a function of concentration and temperature, *J. Food Sci.* 54: 663–668.

Couette, M. M., 1890, Ettudes sur le frottement des liquides, *Ann. Chim. Phys.* 21, 433–510.

Cuevas, R. and Cheryan, M., 1978, Thermal conductivity of liquid foods — a review, *J. Food Proc. Eng.* 2:283–306.

Dealy, J. M., 1982, *Rheometers for Molten Polymers,* Van Nostrand Reinhold, New York.

DeMan, J. M., Voisey, P. W., Rasper, V. F., and Stanley, D. W., 1976, *Rheology and Texture in Food Quality,* AVI Publishing, Wesport, Connecticut.

Dickerson, Jr., R. W., 1968, Thermal properties of foods, in *The Freezing Preservation of Foods,* Vol. 2, 4th ed., AVI Publishing, ch. 2.

Doublier, J. L., Caunay, B., and Cuvelier, G., 1992, Viscolastic properties of food gels, in *Viscolastic Properties of Foods,* Rao, M. A. and Steffe, J. F., Eds., Elsevier Applied Science, London, U.K.

Elustondo, M. and Urbicain, M. J., 1993, Modified design of the thermal probe to measure thermal conductivities of foods, Unpublished.

Eucken, A., 1940, Forsch. Gebiete Ingenieur, Ausgabe A, 19, 1, 6.

Fernández-Martín, F. and Montes, F., 1972, Influence of temperature and composition on some physical properties of milk and milk concentrates. III, Thermal conductivity, *Milchwissenschaft* 27(12):772–776.

Fernández-Martín, F. and Montes, F., 1977, Thermal conductivity of creams, *J. Dairy Res.* 44:103–109.

Figoni, P. I. and Shoemaker, C. F., 1981, Review paper: characterization of structure breakdown of foods from their flow properties, *J. Texture Studies,* 12:287–305.

Fitch, D. L., 1935, A new thermal conductivity apparatus, *Am. Physics Teacher,* 3(3):135–136.

Fredrickson, A. G., 1964, *Principles and Applications of Rheology,* Prentice-Hall, Englewood Cliffs, NJ.

Gross, M. O., Rao, V. N. M., and Smit, C. J. B., 1980, Rheological characterization of low methoxly pectin gel by normal creep and relaxation, *J. Texture Studies,* 11, 27–29.

Hahn, S. J., Ree, T., and Eyring, H., 1959, Flow mechanism of thixotropic substances, *Ind. Eng. Chem.,* 51:856.

Harper, J. C., 1972, *Elements of Food Engineering,* University of California, Davis, California.

Harper, J. U. C. and El Sahrigi, A. F., 1965, Viscometric behavior of tomato concentrates, *J. Food Sci.,* 30:470–476.

Hayashi, K., Nishikawa, T., and Vei, I., 1974, Studies on thermal conductivity measurements of granular materials in systems of solid–fluid mixture, *Yogyo-Kyokay Shi,* 82, 26.

Heldman, D. R. and Singh, R. P., 1981, *Food Process Engineering,* AVI Publishing, Westport, CT.

Hooper, F. C. and Lepper, F. R., 1950, Transient heat flow apparatus for the determination of thermal conductivities, *ASHV Trans.* 56:309–324.

Hsu, M.-H., Mannapperuma, J. D., and Singh, R. P., 1991, Physical and thermal properties of pistachios, *J. Agric. Eng. Res.* 49:311–321.

Ibarz, A. and Sintes, J., 1989, Rheology of egg yolk, *J. Texture Stud.* 20:161–167.

Janas, P., 1991, Rheological studies on potato starch pastes at low concentrations. IV, *Starch/stärke,* 43:172–175.

Johnson, J. F., Martin, J. R., and Porter, R. S., 1975, Determination of viscosity of food systems, in *Theory, Determination and Control of Physical Properties of Food Materials,* Rha, C., Ed., D. Reidel Publishing, Dordrecht, Holland, 25–38.

Jowitt, R., Eseher, F., Kent, M., McKenna, R., and Roqnes, M., 1983, *Physical Properties of Foods, 1 and 2,* Elsevier Applied Science Publishers.

Keey, R. B., 1972, *Drying: Principles and Practice,* Pergamon Press, NY.

Kent, M., Christiansen, K., van Hanehem, I. A., Holtz, E., Morley, M. J., and Nesvadba, P., and Poulsen, K. P., 1984, Cost 90 collaborative measurements of thermal properties of foods, *J. Food Eng.* 3:117–150.

Kokini, J. L., 1992, Rheological properties of foods, in *Handbook of Food Engineering,* Heldman, D. R. and Lund, D. B., Eds., Marcel Dekker, New York, 1–39.

Krieger, I. M., 1983, Rheology of emulsions and dispersions, in *Physical Properties of Foods,* Peleg, M. and Bagley, E. B., AVI Publishing, Westport, CT.

Kubota, K., Matsumoto, T., Kurisu, S., Suzuki, K., and Hosaka, H., 1980, The equation regarding temperature and concentration of the density and viscosity of sugar, salt and skim milk solutions, *J. Fac. Appl. Biol. Sci.* 19:133–145.

Latyshev, V. P. and Ozerova, T. M., 1976, *Kholoid Tekn,* 5:37.

Leider, P. J. and Bird, R. B., 1974, Squeezing flow between parallel disks. I. Theoretical analysis, *Indust. Eng. Chem. Fund.* 13:336–341.

Lerchental, C. H. and Muller, H. G., 1967, Research in dough rheology at the Israel Institute of Technology, *Cereal Sci. Today,* 12:190–192.

Levy, F. L., 1975, Calculating time-temperature and weight loss diagrams of chilling and freezing meats. Freezing, frozen storage and free drying of biological materials and foodstuffs, *I.I.R. Paris,* 325–340.

Lewin, H., 1962, Plant handbook data — FE special report, *Food Eng.,* March 89–99.

Lewis, T. and Nielsen, D., 1970, Dynamic mechanical properties of particulate-filled polymers, *J. Appl. Polym. Sci.* 14:1449.

Lopes da Silva, J. A., Gonçalve, M. P., and Rao, M. A., 1992, Rheological properties of high-methoxil pectin and locust bean gum solutions in steady shear, *J. Food Sci.* 57:443.

Lozano, J. E., Urbicain, M. J., and Rotstein, E., 1979, Thermal conductivity of apples as a function of moisture content, *J. Food Sci.* 14(1):198–199.

Lozano, J. E., Urbicain, M. J., and Rotstein, E., 1983, Shrinkage, porosity and bulk density of foodstuffs at changing moisture content, *J. Food Sci.* 48:1497–1502, 1553.

Marouilis, Z. B., Shah, K. K., and Saravacos, G. D., 1991, Thermal conductivity of gelatinized starches, *J. Food Sci.* 56(3):773–776.

Mattea, M., Urbicain, M. J., and Rotstein, E. R., 1986, Prediction of thermal conductivity of vegetable foods by the effective medium theory, *J. Food Sci.* 51(1):113–115, 134.

Mattea, M., Urbicain, M. J., and Rotstein, E. R., 1989, Effective thermal conductivity of cellular tissues during drying: prediction by a computer assisted model, *J. Food Sci.* 54(1):194–197, 204.

Mattea, M., Urbicain, M. J., and Rotstein, E. R., 1990, Prediction of thermal conductivity of cellular tissues during dehydration by a computer model, *Chem. Eng. Sci.* 45(11):3227–3232.

Maxwell, J. C., 1904, *A Treatise on Electricity and Magnetism,* 3rd ed., The Claredon Press, Oxford, 1, 440.

Metzner, A. B., 1985, Rheology of suspensions in polymeric liquids, *J. Rheol.* 29:739–744.

Miles, C. A., van Beek, G., and Veerkamp, C. H., 1983, Calculation of thermophysical properties of foods, in *Physical Properties of Foods,* Jowitt, R., Escher, F., Hallstrom, B., Meffert, H. F. Th., Spiess, W. E. L., and Vos, G., Eds., Applied Science, London, 281.

Mills, P. and Kokini, J. L., 1984, Comparison of steady shear and dynamic viscoelastic properties of guar and karaya gums, *J. Food Sci.* 49:1–4.

Mizrahi, S. and Berk, Z., 1972, Flow behaviour of concentrated orange juice: Mathematical Treatment, *J. Texture Studies,* 3:68–79.

Mohsenin, N., 1980, *Thermal Properties of Food and Agricultural Materials,* 2nd Ed. Gordon and Breach Science Publishers, New York.

Mooney, M., 1951, The viscosity of concentrated suspensions of spherical particles, *J. Colloid Sci.* 6:162.

Murakami, E. G. and Okos, M. R., 1986, Predicting the thermal conductivity of dry porous foods, ASAE Paper No. 86-6538.

Nesvadba, P., 1982a, Methods for the measurement of thermal conductivity and diffusivity of foodstuffs, *J. Food Eng.* 1:93–113.

Nesvadba, P., 1982b, A new transient method for the measurement of temperature dependent thermal diffusivity, *J. Phys. D. Appl. Phys.* 15:725–738.

Nix, G. H., Lowery, G. W., Vachon, R. I., and Tanger, G. E., 1967, Direct determination of thermal diffusivity and conductivity with a refined line-source technique, in *Progress in Aeronautics and Astronautics,* Vol. 23, G. R. Heuer, Ed., Academic Press, New York, 865–878.

Noureddini, H., Teoh, B. C., and Davis Clements, L., 1992a, Densities of vegetable oils and fatty acids, *JAOCS,* 69(12):1189–1191.

Noureddini, H., Teoh, B. C., and Davis Clements, L., 1992b, Densities of vegetable oils and fatty acids, *JAOCS,* 69(12):1184–1188.

Peleg, M., 1977, Contact and fracture elements as components of the rheological memory of solids foods, *J. Food Sci.* 44:277–281.

Perry, R. H. and Chilton, C. H., 1973, *Chemical Engineers' Handbook,* 5th ed., McGraw-Hill, New York.

Polley, S. L., Snyder, O. P., and Kotnour, P. A., 1980, Compilation of thermal properties of foods, *Food Technol.,* Nov. 76–94.

Proctor, B. E., Davison, S., Malecki, G. J., and Welch, M., 1955, A recording strain-gage denture tenderometer for foods. 1. Instrument evaluation and initial tests, *Food Technol.* 9:471–479.

Progelhof, R. C., Throne, J. L., and Ruetsch, R. R., 1976, Methods for predicting the thermal conductivity of composite systems: a review, *Polymer Eng. Sci.* 16(9):615–625.

Qiu, C. G. and Rao, M. A., 1988, Role of pulp content and particle size in yield stress of apple sauce, *J. Food Sci.* 53:1165–1170.

Ramaswamy, H. S. and Basak, S., 1992, Pectin and raspberry concentrate effects on the rheology of stirred commercial yogurt, *J. Food Sci.* 57:357–360.

Ramaswamy, H. S. and Tung, M. A., 1981, Thermophysical properties of apples in relation to freezing, *J. Food Sci.* 46:724–728.

Rao, M. A., 1971, Rheology of liquid foods, J. Texture Studies, (8):135–168.

Rao, M. A., 1978, Measurement of flow properties of fluid foods. Developments, limitations, and interpretation of phenomena, *J. Texture Stud.* 8:257–282.

Rao, M. A., 1987, Predicting the flow properties of food suspensions of plant origin, *Food Technol.* 41:85–88.

Rao, M. A. and Cooley, H. J., 1992, Rheological behavior of tomato pastes in steady and dynamic shear, *J. Texture Stud.* 23:415–425.

Rao, M. A., Cooley, H. J., and Vitali, A. A., 1984, Flow properties of concentrated juices at low temperatures, *Food Technol.* 38:113–118.

Rao, M. A. and Steffe, J. F., 1992, in *Viscoelastic Properties of Foods,* Elsevier, London.

Rao, V. N. M., 1992, Viscolastic properties of solid foods, in *Viscolastic Properties of Foods,* Eds., Rao, M. A. and Steffe, J. F., Elsevier Applied Science, London, U.K.

Rha, Chokyun, 1975, Thermal properties of food materials, in *Chemie Microbiologie.*

Rice, P., Selman, J. D., and Abdul-Rezzak, R. K., 1988, Effect of temperatures on thermal properties of 'record' potatoes, *Int. J. Food Sci. Tech.* 23:281–286.

Riedel, L., 1978, Chemie mikrobiologie technologie der lebensmittel, *Chemie Microbiologie* 1982 5(5):129–133.

Rivero, S., 1982, Conductividad Térmica de Concentrados de Jugo de Tomates, M.Sc. Thesis, Universidad Nacional del Sur, Argentina.

Ross-Murphy, S. B., 1984, Rheological methods, in *Biophysical Methods in Food Research,* Blackwell Scientific, London.

Sanz, P. D., Alonso, M. D., and Mascheroni, R. H., 1987, Thermophysical properties of meat products: general bibliography and experimental values, *ASAE* 30(1):283–289/296.

Sanz, P. D., Alonso, M. D., and Mascheroni, R. H., 1989, Equations for the prediction of thermophysical properties of meat products, *Latin Am. Appl. Res.* 19:155–163.

Seibel, E., 1892, Specific heats of various products, *Ice and Refrigeration,* 2:256–257.

Shafiur Rahman, Md., 1992, Thermal conductivity of four food materials as a single function of porosity and water content, *J. Food Eng.* 25:261–268.

Shama, F. and Sherman, P., 1966, The texture of ice-cream. 2. Rheological properties of frozen ice-cream, *J. Food Sci.* 31:699–706.

Sherman, P., 1970, *Industrial Rheology with Particular Reference to Foods, Pharmaceuticals, and Cosmetics,* Academic Press, New York.

Sherman, P., 1979, *Food Texture and Rheology,* Academic Press, New York.

Shoemaker, C. F. and Figoni, P. I., 1984, Time-dependent rheological behavior of foods, *Food Technol.* 38:110–112.

Slattery, J. C., 1961, Analysis of the cone-plate viscometer, *J. Colloid Sc.* 16:431–437.

Suzuki, K., Maeda, T., Matsuoka, K., and Kubota, K., 1991, Effect of constituent concentration on rheological properties of corn oil-in-water emulsions, *J. Food Sci.* 56:796–798.

Sweat, V. E., 1974, Experimental values of thermal conductivity of selected fruits and vegetables, *J. Food Sci.* 39:1080–1083.

Sweat, V. E., Modelling the thermal conductivity of meats, *Trans. ASAE,* Vol. 18, No. 3, 564–568.

Sweat, V. E., and Parmellee, 1978, Measurement of thermal conductivity of dairy products and margerines, *J. Food Process Eng.,* 2, 187.

Szczesniak, A. S., 1963, Classification of textural characteristics, *J. Food Sci.* 28:385–389.

Szczesniak, A. S., 1983, Physical properties of foods: What they are and their relation to other food properties, in *Physical Properties of Foods,* Peleg, M. and Bagley, E. B., Eds., AVI Publishing, Westport, CT, 16.

Tiu, C. and Boger, D. V., 1974, Complete rheological characterization of time-dependent food products, *J. Texture Stud.* 5:329–338.

Urbicain, M. J. and Elustondo, M. P., 1975, Conductividad térmica de alimentos: método del sensor, 1er. Simposio Nacional Sobre Tecnologia de Carne Bovina, Bahía Blanca, Argentina, Dec. 1975.

Utracki, L. A., 1974, Temperature dependence of liquid viscosity, *J. Macromol. Sci.-Phys.* (3):477–505.

Van Waser, J. R., Lyons, J. W., Kim, K. Y., and Colwell, R. E., 1963, *Viscosity and Flow Measurement,* Interscience, New York.

Verma, L. S., Shrotriya, A. K., Singh, R., and Singh, U., 1990, An alternative approach for the thermal diffusivity calculation by parallel wire method, *Nat. Acad. Sci. Lett. (India),* 13(8):321–323.

Vocadlo, J. J. and Young, M., 1969, Rheological properties of some commercially available fats, *Can. Inst. Food Technol. J.* 2:137–140.

Voisey, P. W. and deMan, J. M., 1976, Application of instruments for measuring food texture, in *Rheology and Texture in Food Quality,* AVI Publishing, Westport, CT.

Wallapapan, K., Sweat, V. E., Diehl, K. C., and Engler, C. R., 1983, Thermal properties of porous foods, ASAE paper No. 83-6515.

Wang, N. and Brennan, J. G., 1993, The influence of moisture content and temperature on the specific heat of potato measured by DSC, *J. Food Eng.* 19:303–310.

Witte, L. C., Cheng, Y. T. E., and Cox, J. E., 1976, Thermophysical properties of foodstuffs, ASME paper 76-HT-59.

Woodams, E. E. and Nowrey, J. E., 1968, Literature values of thermal conductivities of foods, *Food Technol.* 22(4):150–158.

Woodside, W. and Messmer, J. H., 1961, Thermal conductivity of porous media. 1. Unconsolidated sands, *J. Appl. Phys.* 32(9):1688–1699.

Yamada, T., 1970, Thermal properties of potatoes, *Nippon Nogei Kagaku, Kaishi,* 44:587–590.

Zuritz, C. A., Sastry, S. K., McCoy, S., Konanayakan, M., and Crawford, J., 1987, A revised theory for improvement of the Fitch method of thermal conductivity measurement, ASAE Paper 97-6540, Winter meeting of the ASAE, Chicago, Dec. 15–18, 1987.

12 Dough Processing Systems

Leon Levine and Ed Boehmer

CONTENTS

12.1 INTRODUCTION

The processing and handling of doughs and dough-like materials play an important role in the food processing industries, particularly the bakery, pasta, ready-to-eat cereal, and snack-food business. Unfortunately, little is available in either the process engineering literature or the food science literature to assist the food engineer in performing design tasks. It is the intent of this chapter to provide introductory material that will aid in the understanding of some of the underlying principals associated with dough processing.

12.1.1 WHAT IS A DOUGH?

There is no formal definition of what constitutes a dough. The dictionary simply defines a dough as a moistened mass of material, usually made of flour, water, and other ingredients. This does not really provide us with any working description of a dough. Discussions with those who work with these kinds of materials will give a definition something like, "I know a dough when I see a dough." However, when questioned about the difference between a

dough and a simple paste, these individuals will readily differentiate between the two by stating that a dough is more "solid-like" and/or has viscoelastic properties. We will not attempt a more detailed definition than this but will trust that the reader also "knows a dough when they see it".

12.1.2 Types of Dough

There are several types of doughs that the engineer is likely to encounter in the food industry. We find that these fall into three basic types. These are:

1. Doughs that are primarily held together by the interaction between the protein fraction of the dough and water. In particular, we are talking about those doughs whose structure and properties are controlled by the "development" of the particular kind of protein known as gluten. This last term normally applies to the protein found in wheat flours. These protein structured doughs are the basis for most bakery products and the pasta industry.
2. Doughs that are primarily held together by the action of the starch fraction of the dough, require that the starch be cooked to some minimal degree. The best examples of these doughs are found in the cereal and snack food industries. The most common examples of products made with dough that fall into this category are corn-masa based snacks, such as tortilla chips and fabricated potato chips made from dehydrated potatoes.
3. The third type of dough are those which often have a higher fat content, and have a limited level of water available to hydrate the raw materials. The limited water prevents the gluten from developing. These doughs are more putty-like in consistency. This type of character is often described by bakers as being "short". The most common use of these doughs is found in the production of cookies and pie doughs.

Most of the food- and cereal-science literature concerns itself with the handling of the first type, gluten-based doughs, and this chapter too will be concentrating on this area. First a definition of the widely used term "development" is needed.

The "development" of a dough is the term used by cereal chemists and bakers to describe the physical changes that are observable as the dough is mixed and the gluten molecules within the dough are hydrated and aligned. The formation of a developed dough is associated with the conversion of the initially wet sticky paste of water and flour into a stiffer, less sticky, more viscous mass. Bakers and cereal chemists commonly use two other terms to describe the physical characteristics of dough developed in this manner. Doughs that develop a very stiff, viscous, character are sometimes called "bucky". Doughs that do not develop a very stiff, viscous, character are called "slack". The optimal consistency for handling doughs is somewhere between these two extremes. The optimal material resists extension (stretching), has a memory (tends to "snap back" after deformation), and exhibits the ability to be stretched into very thin films without tearing or breaking. The film's properties are controlled by the composition of the dough, the source of wheat flour used, and the degree of mixing that has been imparted to the dough. The ability to form these films is a unique property of wheat flour doughs. It is this property that allows the dough to hold gas (rise) when carbon dioxide is formed by the action of yeasts or chemical leavenings, or when water vapor is formed during heating. Yeasts form carbon dioxide by the action of fermentation of sugars within the dough. Chemical leavenings form carbon dioxide by the decomposition of bicarbonate salts.

Bakers and cereal chemists (Pyler, 1988) describe the progression of dough development in five distinct stages

- Blending is the first stage of dough mixing. This is a short period where the various ingredients are brought into contact.
- Pickup is the second stage of dough mixing. This is simply the point at which all the ingredients are uniformly mixed. At this point the dough appears to be a sticky paste with little or no elastic properties.
- Cleanup is the third stage of mixing. At this stage the dough begins to exhibit significant viscoelasticity and the ingredients begin to pull away cleanly from the sides of the mixer.
- Development is the fourth stage of mixing. This is the period when the viscosity and elasticity of the dough continue to increase. At the point of maximum development the stiffness, or apparent viscosity, of the dough is maximized. This is the point at which the dough has its maximum, or nearly maximum, gas holding potential. Therefore, this is normally the goal of dough mixing.
- Breakdown is the fifth stage of mixing. At this stage the dough stiffness, or apparent viscosity, begins to decrease. The dough becomes less elastic, stickier, and loses gas holding properties. This is usually called "overdevelopment". This is believed to occur as a result of the breakage of intermolecular disulfide bonds that were formed during the earlier mixing stages.

This process can be observed in commercial mixers but is often studied in a laboratory device known as a Farinograph (C.W. Brabender Co., Figure 12.1), which is a small double sigma blade mixer used to study the mixing process and the properties of different flours. The device described by D'Appolonia and Kunerth (1984), measures apparent viscosity, or stiffness, by recording the mixer torque (reported as Brabender units) as mixing progresses. An example output from a Farinograph is illustrated in Figure 12.2 (D'Appolonia and Kunerth, 1984). Another type of device that has been used to study the development phenomenon is the Mixograph (National Manufacturing Corp.).

One question that needs to be asked is, "How do we describe the degree of mixing that leads to development?." In the polymer industries (e.g., see Mana-Zloczower and Tadmor, 1994) which the engineer may be familiar with, the degree of mixing of highly viscous materials is usually quantified by the imposition of strain on the paste by the action of shear and stretching. In the cereal literature, the degree of mixing is usually measured by the total quantity of work imparted to the material being mixed. It then falls upon the design and/or operations engineer to insure that in addition to producing a dough at the correct formula and temperature, that the correct amount of work, or degree of development, has been imparted to the dough.

12.2 TYPES OF MIXERS

Most dough mixers are operated in a batch mode. Batch mixers fall into several different categories. It is convenient to place the mixers into three categories: vertical, horizontal, and high speed.

The vertical mixers are perhaps the most familiar to the reader. Similar devices may be found on a small scale in a well-equipped home kitchen. These mixers are often multifunctional and limited in capacity. There are two basic types: the dough hook/paddle mixer manufactured by The Hobart Co. and AMF, Inc. is illustrated in Figure 12.3. These have a maximum dough capacity of approximately 110 kg. The spiral type has a rotating bowl, and may have one or two agitators (manufactured by Rykaart Inc., Rademacher Inc., The Moline Co., The Hobart Co., CMC America Inc., and VMI, Inc.). These are illustrated in Figures 12.4 and 5. The capacity of the single spiral mixer is limited to approximately 300 kg, while the double spiral design can have a capacity up to 350 kg. Table 12.1 gives typical capacities
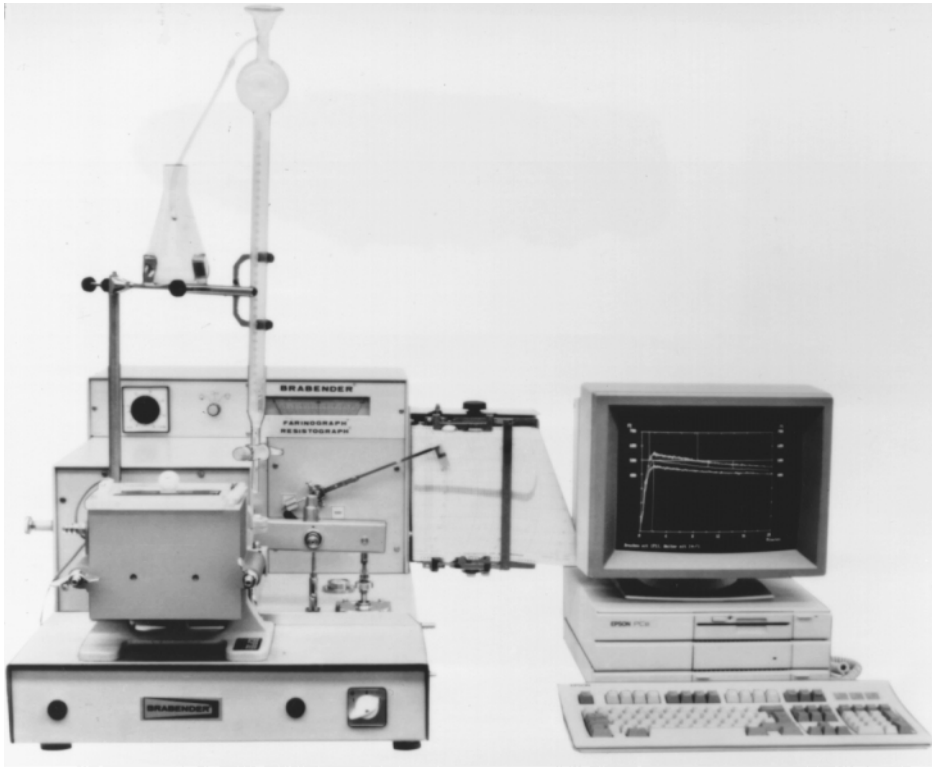
FIGURE 12.1 A Farinograph (Courtesy of C.W. Brabender, Lincoln, NE).
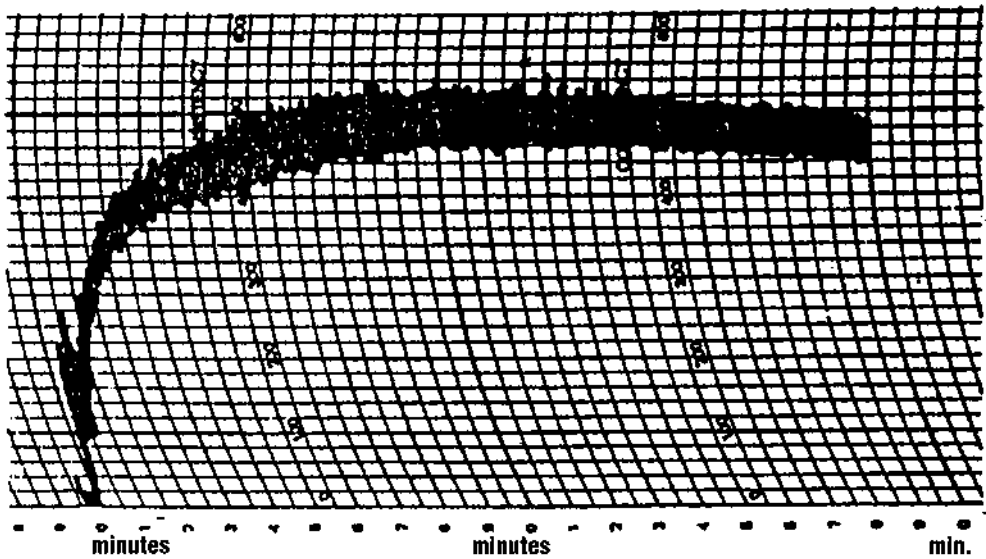
FIGURE 12.2 A Farinograph curve: Brabender units vs. time.

FIGURE 12.3 A dough hook. (Courtesy of The Hobart Co., Troy, OH.)

FIGURE 12.4 A single spiral mixer. (Courtesy of Rykaart, Inc., Hamilton, OH.)

TABLE 12.1
Capacity and Motor Size for
Hobart Dough Hook Mixers

Capacity (qt)	Capacity (kg)	Motor size (kw)
30	25	0.9
60	50	1.5
80	65	2.2
140	110	3.7

TABLE 12.2
Capacity and Motor Size for Rykaart
Single Spiral Vertical Mixers

Capacity (l)	Capacity (kg)	Motor size (kw)
80	65	3.5
165	125	5.0
250	190	6.5
300	250	8.5
390	300	13.0

TABLE 12.3
Capacity and Motor Size for VMI
Double Spiral Vertical Mixer

Capacity (l)	Capacity (kg)	Motor size (kw)
100	48	3.7
170	80	6.0
220	120	9.0
280	180	11.7
400	250	14.6
550	360	22.4

and motor powers for a dough hook mixer (Hobart, Anonymous). Tables 12.2 (Rykaart, Anonymous (1994a) and 12.3 (VMI, Anonymous, 1994) give typical capacities and motor powers for single and double spiral type mixers. The mixers are not normally jacketed, so removal of the heat generated by viscous dissipation is generally not possible with this type of mixer.

Note that the dough hook mixer manufacturer has kept the ratio of power:capacity approximately constant at a value of 0.035 kW/kg. It is apparent that they are cognizant of keeping energy per unit mass constant. Larger motor sizes are available for very stiff doughs,

FIGURE 12.5 A double spiral mixer. (Courtesy of VMI, Inc., Cranberry, NJ.)

such as pizza or bagel doughs. These have power:capacity ratios of approximately 0.045 kW/kg. Adaptor bowls (Figure 12.6), available from National Manufacturing Inc., are intended to emulate the mixing action of a Mixograph, or the horizontal bar mixer described.

Note that the single spiral mixer manufacturer has kept the ratio of power:capacity approximately constant at a value of 0.04 kW/kg.

The double spiral mixer manufacturer keeps the ratio of motor size to capacity constant for mixers capacity below 180 kg at about .075 kW/kg. For the larger mixers the ratio drops to about 0.05 kW/kg, in an attempt to keep energy per unit mass constant.

One manufacturer (Cooper, 1994) does not recommend the single spiral for very stiff doughs such as those encountered in pizza or bagel production, while another (Moline, 1994) specifies that stiff doughs can be processed in these mixers. This is accomplished by reducing the speed and the size of the mixer load to reduce the torque on the mixer shafts. If one assumes that a fixed energy input is required to develop a dough, this means that a longer mix time may be required for this mixing situation.

A specialized form of vertical mixer is sometimes used to mix pie dough and the like. This mixer has two clawlike arms, which gently lift and mix the dough, in emulation of a home cook's use of common forks, and is illustrated in Figure 12.7. The capacity of this type of mixer is limited to approximately 200 kg of dough (CMC America, 1994a).

Horizontal mixers are perhaps the workhorse devices of large bakeries. There are several types of horizontal mixers. The most common is the horizontal bar mixer illustrated in Figure 12.8. These mixers are manufactured by APV Baker Inc., Peerless Machinery Inc., Champion Inc., among others. In this kind of mixer the dough is stretched, squeezed, and sheared by the action of multiple rollers mounted on a moving "spider". In addition, there is a stationary bar, called the breaker bar. This bar "picks" the dough off the spider, preventing the motion of the dough as a solid mass. This allows the rollers to then knead a continuously refreshed supply of dough against the wall of the mixer. These mixers come in many sizes up to a capacity of approximately 3000 lb of dough. They are jacketed for refrigerant
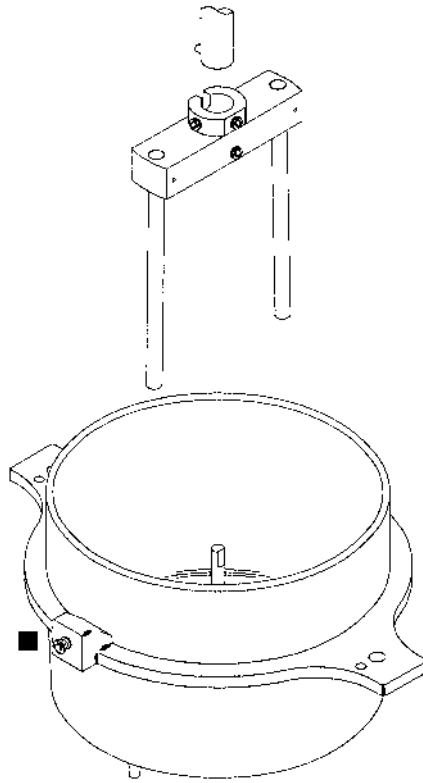
FIGURE 12.6 A McDuffy bowl. (Courtesy of National Manufacturing, Lincoln, NE.)

circulation, normally can be run at two speeds, have tilt bowls to ease dough discharge, and can be fully automated. The capacity and horsepower data for two different manufacturers are provided in Tables 12.4 (APV, 1994) and 12.5 (Peerless, 1985). Both manufacturers normally design their mixers to operate at 35 or 70 rpm.

The energy input/unit mass for the two designs are held roughly constant at .04 hp/lb (.065 kW/kg) and 0.05 hp/lb (.08 kW/kg), respectively, across the mixer sizes. These energy input capabilities are significantly greater than those of spiral mixers, even though spiral mixers operate at high speeds. This indicates that these horizontal bar mixers can develop considerably more torque per unit mass, suggesting that they can handle a wider range of products (stiffer doughs), or may be capable of developing doughs more rapidly.

The other type of horizontal mixer commonly encountered is a single arm spiral mixer, described in Figure 12.9. These are often used for cookie doughs, or other "short" dough products, and tilt for easy dough discharge and are jacketed for cooling. They usually operate at low speeds (approx. 25 rpm). Table 12.6 (CMC America, 1994a) provides one manufacturer's information on this type of mixer.

Note that the ratio of energy input rate to capacity of these machines is about 0.01 hp/lb, which is considerably less than for either the vertical spiral or horizontal bar mixers. The short doughs processed in these mixers do not have the elastic nature encountered in gluten-based doughs. This is because these doughs have insufficient water and levels of "strong" protein available to develop the dough and the doughs contain large amounts of sugars and, most importantly, fat, which make them less elastic and more putty-like than developed doughs.

FIGURE 12.7 A double-arm pie-dough mixer. (Courtesy of CMC America, Joliet, IL.)

FIGURE 12.8 A horizontal dough mixer. (Courtesy of Peerless Manufacturing Corp., Sydney, OH.)

TABLE 12.4
Capacity and Motor Size for APV
Baker Horizontal Bar Mixers

Max capacity (lb)	Min capacity (lb)	Motor size (hp)
1600	800	60
2000	1000	75
2500	1000	100

TABLE 12.5
Capacity and Motor Size for
Peerless Horizontal Bar Mixers

Capacity (lb)	Motor size (hp)
1300	60
1600	75
2000	100
2400	125

FIGURE 12.9   A single spiral mixer. (Courtesy of Peerless Manufacturing Corp., Sydney, OH.)

TABLE 12.6
Capacity and Motor Size
for Champion Sigma Mixers

Capacity (lb)	Motor size (hp)
500	5
750	7.5

FIGURE 12.10 A high speed mixer. (Courtesy of Stephan, Columbus, OH.)

12.2.1 HIGH SPEED MIXERS

High speed mixers were developed in the 1960s at Chorleywood, England (APV, 1995) to improve the efficiency of bakery operations. These mixers have high speed agitators (300 to 1200 rpm), and hold small batches to develop dough rapidly. It has also been reported (APV, 1995; Andrews et. al, 1989) that these mixers can produce good dough at higher moisture levels than conventional batch mixers and produce smaller cell sizes in the raised product. There are several different manufacturers of this type of mixer. Some of the manufacturers are Tweedy (APV Baker, Inc.), Stephan Machinery Corp., Rykaart Inc., and Peerless Machinery Corp. Figures 12.10 and 12.11 illustrate examples of this type of mixer. Some operate under partial vacuum, which reduces the number and size of air bubbles in the dough. This is probably why a finer, more uniform, pore structure is produced with this type of mixer. Although the mixers are often provided with cooling jackets, the mixing time is so short that it is difficult to remove significant heat through the jackets.

Tables 12.7 (APV) and Table 12.8 (Rykaart, 1994a) provide manufacturer's information for a mixer that might be used in a high capacity bakery and a smaller bakery.

Note that the gross energy available per unit mass for the Tweedy mixer is roughly constant at 19 Wh/kg. The manufacturer states that the process design calls for a net energy input of 11 Wh/kg. The process will produce 14 batches per hour with a 3-min mixing time
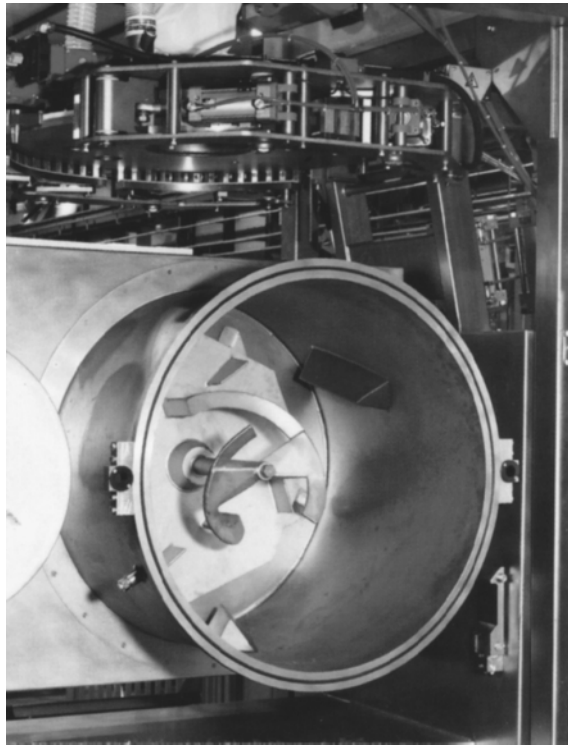
FIGURE 12.11   A Tweedy high speed mixer. (Courtesy of APV Baker, Inc., Peterborough, England.)

TABLE 12.7
Characteristics of Tweedy Mixers

Batch size (kg)	Output (kg/h)	Motor size (kw)
220	3000	55
275	3850	75
340	4700	90
385	5400	110

TABLE 12.8
Characteristics of High Speed Rykaart Mixers

Batch size (kg)	Output (kg/h)	Motor size (hp)
80	1200	20
110	1800	30
160	2400	40

per batch. Note that the design basis of 11 Wh/kg is the same as reported for the Chorleywood process (Kilborn and Tipples, 1972a,b). This number should be used as a guideline only. There are several reports in the literature (Kilborn and Tipples, 1972a,b; Mitchell, 1984; Wilson, 1992; Wooding et al. 1994) that clearly state that the required energy input can vary significantly from that normally stated for the Chorleywood process (Skeggs and Kingswood, 1981). The actual energy required to produce optimal doughs is a function of the composition of the wheat, which is influenced by the variety and growth conditions. Actual reported work inputs vary from approximately 5 Wh/kg to as high as 20 Wh/kg.

The information given in Table 12.8 appears to size the motor for a gross work input rate of 12 Wh/kg, which is the above-given mixer.

12.2.2 CONTINUOUS MIXERS

Continuous mixers have not found wide spread acceptance in the U.S. In the 1950s two systems (AMF Inc. and J. C. Baker Inc.) were sold to continuously mix dough. These systems are described in the literature (Matz, 1992; Doerry, 1995). Their performance is discussed by Bushuk et al. (1965). The products manufactured by this process tended to have a very fine grain that some have compared to styrofoam. In addition, the mixers seemed to have limited capabilities beyond the production of white breads. Neither system is sold any longer.

In recent years continuous dough mixing has found acceptance, particularly in Europe. Some of the manufacturers of the this equipment are Werner and Pfleiderer Corp. (illustrated in Figure 12.12), Reimelt Inc., Rykaart, Inc., and Buss Inc. There is little, or nothing, in the literature about the performance of these devices. The Reimelt and Werner and Pfleiderer systems are based upon twin-screw extruder technology. The Buss is a special type of single screw extruder that is known as a Ko-Kneader in the polymer industry (White, 1990), and the Paramelt (Rykaart) continuous kneading device is based upon the input of work with high speed paddles. Table 12.9 (Werner and Pfleiderer, 1993) provides some data for the mixing of wheat doughs on a Werner and Pfleiderer system.

There is considerable variation reported for the capacities of these machines. For example, Werner and Pfleiderer (Werner and Pfleiderer, 1993) reports values that the 120 mm machine may produce as much as 700 kg/h of other wheat doughs. The lower maximum speeds and powers of the larger mixers is probably a reflection of the fact that there is reduced heat transfer area per unit volume in the larger mixers. This makes temperature control for larger mixers much more difficult. As a consequence, lower power and capacity per unit mixer volume are necessary for larger machines.

12.3 ENGINEERING ASPECTS OF MIXER PERFORMANCE AND DESIGN

12.3.1 ENERGY BALANCES AROUND DOUGH MIXERS

One of the key issues that must be resolved when engineering dough-mixing systems is clear resolution of the energy balance around the system. Energy input is specified according to the requirements of dough development. In addition further dough property requirements specify the final temperature of the dough exiting the mixer. There are several items that must be considered when performing the heat balance calculations. A total energy balance is given by

$$\sum_{\text{ingredients}} M_i \cdot \Delta h_i = M_{\text{flour}} \cdot \Delta h_w + M \cdot E_m - Q_j \tag{12.1}$$
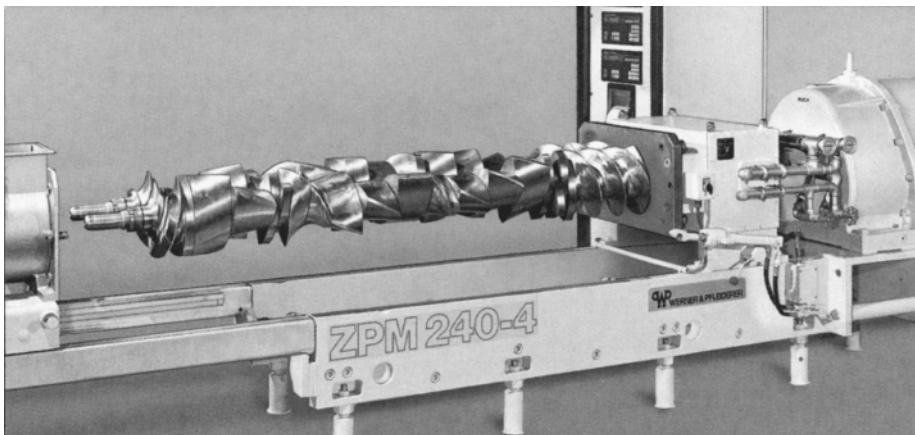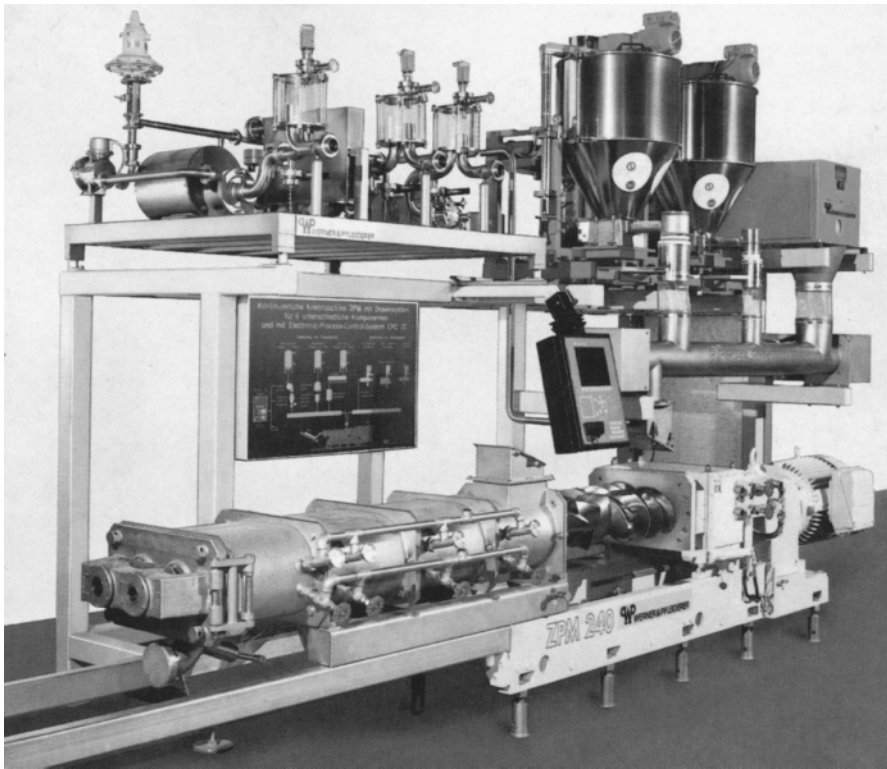
FIGURE 12.12 A continuous dough mixer. (Courtesy of Werner and Pfleiderer, Stuttgart, Germany.)

The heat input on the right hand side of this equation comes from two sources: the positive heat input as a result of mechanical energy, roughly 10 Wh/kg and the negative value heat input (heat removal) by the jacket through conduction and convection. In addition, there is a small quantity of heat that can be considered as heat input, which is associated with the heat of wetting of the flour. The approximate heat of wetting of flour is (Pyler, 1988),

$$\Delta h_w = 15.1 \cdot \frac{kj}{kg} \qquad (12.2)$$

TABLE 12.9
Characteristics of Werner and Pfleiderer
ZPM Dough Mixing Systems

Screw diameter (mm)	Output (kg/h)	Max motor size (kw)	Max screw speed (rpm)
120	400	35	130
240	1500	80	100
320	2700	100	100

TABLE 12.10
Heat Capacity of Dough Components

Temp (°C)	Heat Capacity (kJ/kg·K)				
	Water	Protein	Fat	Carbohydrates	Ash
20	4.180	1.711	1.928	1.547	0.908
30	4.172	1.765	1.953	1.586	0.937
40	4.174	1.775	1.981	1.626	0.947

The enthalpies of the inlet streams are determined from the physical properties of the various components of the raw materials. One must remember that water can, and often is, introduced as ice, to take advantage of the extra energy removal associated with melting of ice. The heat of fusion of water is approximately 334 kJ/kg. This technique is often used during the summer to overcome the problem of warm flour being received from storage. Ice may also be used on a year-round basis to control the temperature of doughs which are very viscous. High viscosity doughs cause high energy input rates as a result of viscous dissipation.

In order to calculate the enthalpy, or heat content of the various components, various sources can be used. For example, Rask (1989) reports values of the heat capacity of various doughs between 2.62 kJ/kg·K and 3.16 kJ/kg·K, with an average value of 2.88 kJ/kg·K. This data was for doughs containing between 42 and 46% moisture. Pyler (1988) suggests a flour heat capacity of 1.76 kJ/kg·K. Mohsenin (1980) gives several methods for estimating the heat capacity of food products and provides equations and graphs of the heat capacity of wheat at various moistures and temperatures. The most versatile data to use are given by Okos and Choi (1986). These data give heat capacities of various dough components as a function of temperature. The data is summarized in Table 12.10.

The value of heat capacity for a mixture is obtained by simply mass averaging the heat capacity values of the individual components. The heat capacity given for fat assumes that no melting or crystallization of fat is occurring. The heat of fusion of fat solids is between 20 and 44 cal/g of melted fat solids (Formo, 1979). To be rigorous, the energy associated with melting the solid fraction of the fat should be included. Realistically, the change in temperature (percent solids) and heat of fusion are small, so ignoring the heat of fusion of fat components will not prove significant.

There is limited data available about convective heat transfer coefficients for mixing viscous materials such as these. Uhl and Gray (1967) report overall heat transfer coefficients

for similar paste mixers in the range of 225 to 450 W/m²·K. Pyler (1988) reports an estimate of a maximum of 400 W/m²·K for horizontal bar mixers. Yacu (1985) reports a value of 500 W/m²·K for twin screw extruders, which are not unlike the Werner and Pfleiderer continuous mixers. For single screw extruders, Levine and Rockwood (1985) report values of 200 to 480 W/m²·K, and Harper (1985) reports a value of 225 W/m²·K. Assuming a value of about 225 W/m²·K certainly seems reasonable.

EXAMPLE 12.1

The use of the data given above is probably best illustrated by the following problem.

Assumptions

Assume the flour has the following approximate composition

Water	14%
Ash	1%
Protein	12%
Fat	1%
Carbohydrate	72%

Using the data in Table 12.10, the heat capacity is estimated to be 1.93 kJ/kg·F. The dough is made of 0.65 kg water/kg flour. The heat capacity of water from Table 12.10 is approximately 4.18 kJ/kg·C.

Assume that the total energy delivered to develop the dough is 10 Wh/kg and that this energy is delivered over a 12-min mixing period.

The mixer holds 700 kg, and the jacket area is 3.5 m². The coolant temperature is assumed to be –5°C. Assume a heat transfer coefficient of 225 W/m²·K.

Assuming that the water and flour are delivered at 20°C, what will be the final temperature of the dough?

Solution

The heat balance is performed as follows:

First calculate the apparent initial temperature of the mixture of ingredients added to the mixer.

$$\sum_{\text{ingredients}} M_i \cdot \Delta h_i = M_{\text{flour}} \cdot \Delta h_w \tag{12.3}$$

Calculate the heat input due to flour wetting

$$M_{\text{flour}} \cdot \Delta h_w = 1.78 \cdot \text{kwhr} \tag{12.4}$$

The enthalpy changes of the flour and water are

$$\Delta h_{\text{water}} = Cp_{\text{water}} \cdot (T - 20°C) \tag{12.5}$$

$$\Delta h_{\text{flour}} = Cp_{\text{flour}} \cdot (T - 20°C) \tag{12.6}$$

Equations 12.3, 12.4, 12.5, and 12.6 may be combined to solve for the temperature obtained when all the ingredients are combined. This is the apparent initial mixing temperature. This initial temperature is found to be approximately 23.3°C.

The heat removed by the jacket during the mixing process is given by

$$Q_j = uAt\Delta T_{LM} \tag{12.7}$$

The enthalpy balance for the mixing period is

$$\sum_{ingredients} M_i \cdot \Delta h_i = M_{flour} \cdot \Delta h_w + M \cdot E_m = Q_j \tag{12.8}$$

Combining Equations 12.5 and 12.6 with 12.7 and 12.8 provides an equation for finding the final temperature of the dough through the use of a trial and error procedure. The final dough temperature is found to be approximately 27.3°C.

If it is desired to maintain the dough temperature below 20°C, how much ice must be used?

The heat balance for mixing the ingredients together to obtain the initial mixing temperature is

$$\sum_{ingredients} M_i \cdot \Delta h_i = M_{flour} \cdot \Delta h_w \tag{12.9}$$

The enthalpy change associated with melting ice is given by

$$\Delta h_{ice} = Cp_{water} \cdot (20C - 0C) - 334 \cdot \frac{kj}{kg} \tag{12.10}$$

Calculation of the enthalpy changes for water and flour are given above in Equations 12.5 and 12.6. One must remember that the ratio of water and ice to flour is still 0.65 kg/kg.

During the mixing period the enthalpy balance is

$$\sum_{ingredients} M_i \cdot \Delta h_i = M_{flour} \cdot \Delta h_w + M \cdot E_m = Q_j \tag{12.11}$$

The heat removal by the jacket is again given by Equation 12.7.

The two enthalpy balances, Equations 12.9 and 12.11, must be solved simultaneously, for the unknown apparent initial mix temperature and the required quantity of ice. Again a trial and error solution is required. The initial mix temperature is found to be approximately 13.4°C, and the required ice addition to keep the final dough at 20°C is approximately 46.3 kg, so about one sixth of the formula water must be introduced in the form of ice.

12.3.2   SOME ASPECTS OF MIXER DESIGN AND SCALE UP

Different mixer designs have different geometries and operating speeds. This has led to some confusion about mechanical energy requirements of dough mixing. For example, Bloksma and Bushuk (1988) report that for old mixer designs, the energy required to develop a dough was between 10 and 15 kJ/kg using a mixing time of about 30 min. More modern mixers, probably corresponding to today's horizontal bar mixers, require about 25 kJ/kg in about 12 min, and the Chorleywood process, which uses high-speed mixers requires 40 kJ/kg with a mixing time of about 3 min. It was earlier suggested that the values for the Chorleywood Process may vary significantly (Kilborn and Tipples, 1972a; Wilson, 1992; Wooding et al. 1994). No data is available to quantify the variation that may be expected for required work input for horizontal bar mixers. One would expect that the variation could be as large as that observed for the Chorleywood process (energy varies by a factor of approximately four). Nonetheless we can use the numbers reported by Bloksma and Bushuk to come up with an

estimate of the rate of power dissipation for these different mixer types. This allows the engineer to make an estimate of the motor sizes required for the various mixer designs.

TABLE 12.11

Element type	Required Wh/kg
Triangle	7.8
Star	9.2
Dumbbell	13.4
Eccentric cylinder	17.4

For example, the older, slower, mixer would draw an *average* motor load of about 0.007 kW/kg. The modern horizontal bar mixer would draw an *average* motor load of about 0.035 kW/kg. The high speed mixers used in the Chorleywood process would draw an *average* load of about 0.22 kW/kg. Remember, this is an average power draw. For a Tweedy mixer, the average draw and the maximum draw are roughly equivalent, since the mixer normally operates at or near maximum power load (Russell-Eggitt, 1975; Kilborn and Tipples, 1981). Not surprisingly then, using the number given for power draw requirements of a Tweedy mixer, closely follows the manufacturers' motor power numbers given in Tables 12.7 and 12.8. For a horizontal mixer the peak power consumption will be significantly larger than the average power consumption. Using a factor of maximum to average power of approximately 1.25, one obtains motor sizes very close to those given above for horizontal bar mixers (Tables 12.4 and 12.5) and reasonable estimates for the powers recommended for the single spiral mixers (Table 12.2).

There are several sources (Valentas et al. 1991; Wooding and Walker, 1992; Fortman et al. 1964; Hazelton and Walker, 1994) that point out that the geometry of the mixer, within a mixer type may significantly affect rate of development and energy requirments.

Wooding and Walker (1992) tested the effect of Mixograph bowl size. Geometric similarity was approximately maintained for two Mixographs having capacities of 35 and 10 g. It was found that the time required to peak remained approximately the same for both mixers. This suggests that, if the total energy input determines the degree of dough development, then the rate of energy input per unit mass of dough is the same for both of these mixers. This is consistent with Valentas et al. (1991) where it is demonstrated that if geometry similarity is maintained across mixer sizes, then the rate of work input is independent of mixer scale. As a consequence, one obtains the same work input at the same mixing time, and presumably, the same degree of dough development.

Fortman et al. (1964) tested a high speed dough mixing system that incorporated a figure-eight shaped mixing chamber with two intermeshing mixing elements. They found that the energy required to develop dough was a strong function of the design of the mixing elements. Their data are summarized in Table 12.11.

Given the results presented in Table 12.11, it is not surprising that the reported energy input requirements for different mixer designs vary widely.

Hazelton and Walker (1994) also explored varying the pin geometry on a Mixograph. Not surprisingly they found that as pin diameter increased, the rate of dough development increased, resulting in decreased mix-time requirements. Over a range of bowl pin diameters of ⅛ to ¼ in. in a 35-g capacity bowl, maximum torque developed by the mixer increased by a factor of about 10%, work input to peak increased about 15%, and the required mix time decreased by about 15%. This is explained by the authors as a direct consequence of the fact that increasing pin diameter reduces pin-to-pin clearance, which increases shear rate. We might point out that increasing pin diameter not only increases the shear rate by decreasing

clearance, but also increases the surface area over which power is dissipated. One would therefore expect that the clearance between moving and nonmoving surfaces, such as one finds between roller and wall and roller and stationary bar in a horizontal bar mixer is a critical issue in mixer performance. A similar statement can be made about the surface area (diameter) of the rollers. When testing on small scale mixers, the engineer should pay particular attention to the manufacturer's maintenance of geometric similarity.

Varying geometries, by considering different mixer types was recently studied by Mani et al. (1992) and Kilborn and Tipples (1973). They found that over a wide range of mixer designs (dough hook, spiral, Mixograph, Farinograph) each mixer type dissipated energy at different rates and required different total energy inputs and mix times to obtain optimal quality dough. Fortunately, the different methods produced equal quality dough despite approaching the development via different routes. This seems to suggest that there is no "best" mixer type, but rather that almost any mixer type should be capable of producing acceptable products. The choice of mixer must be based on cost, efficiency, sanitation, flexibility, space requirements, etc.

Increasing mixer speed should increase the rate of energy input. The rheology of doughs is quite complex. However, as a first approximation, doughs can be considered as a shear thinning fluid that can be described by the power law below

$$\tau = m \cdot \left| \frac{dv}{dy} \right|^{(n-1)} \frac{dv}{dy} \qquad (12.12)$$

One can easily show (Valentas et al., 1991) that power consumption increases with rpm to the power of $1 + n$. When measuring mixer torques, one sees the torque increase with rpm to the power of n. A number of estimates for the flow index, n, can be found in the literature. Most values are in the range of 0.25 to 0.5. For example, Hlynka (1962) estimated the flow index to be 0.5, by measuring the effect of mixer speed on torque in a Farinograph. Launay and Bure (1973) used cone and plate viscometry and measured flow indices between 0.3 and 0.5. Levine (1983) estimates a value of 0.5 for a "sweet" dough through the use of a cone and plate viscometer. Levine (1995) reports a value of 0.28 for a starch-based dough. This was determined by measuring the forces on a sheeting roll. Menjuivar (1990a) performed rheological measurements of the viscosity of cookie doughs. From those measurements, Levine and Boehmer (1992) estimated the flow index to be about 0.42. In addition, Levine estimated the value of the flow index of 0.41 for a hard wheat flour dough. Harper (1981) reports a value of 0.5 for semolina doughs. Hazelton and Walker (1994) cite earlier work of Vidal-Quintanar and Walker (1994) which reported changes in Mixograph peak heights for bread doughs as a function of Mixograph speed. Over a speed change from 76 to 100 rpm, peak height (torque) changes from 40.5 to 44.3%. This can easily be converted to a flow index estimate by plotting the data on log-log paper, which results in a flow index of 0.33.

Recently, Contamine et al. (1995) considered the effect of speed on the energy input of biscuit mixers. They state that the power consumption of a mixer is proportional to the square of mixer speed. This conclusion is not valid since it incorrectly assumes that the doughs do not shear thin, and may be approximated as a Newtonian fluid (flow index = 1).

12.3.3 CONTROL AND MONITORING OF MIXING

Process control of mixers is critical to determine the specific (optimum) mix times that optimize dough development. There are two basic methods for monitoring dough development and controlling uniformity and consistency of quality: total work input and peak development.

The first method uses some sort of power measuring device, usually electric, to measure the total work put into the dough. Kilborn and Tipples (1972a,b), Mani et al. (1992), and Contamine et al. (1995) discuss the use of mixing to at least a minimum total energy to

achieve dough development. Russell-Eggitt (1975) suggests a method for using total energy at a specific mixing speed to measure work input and the use of water addition to correct the dough formulation for optimum development.

TABLE 12.12
Effect of Repeat Sheeting on Energy Input and Loaf Volume

Number of sheetings	Energy input (Wh/lb)	Loaf volume (cc)
12	0.07	770
22	0.17	875
32	0.25	925
42	0.39	935
62	0.47	910
82	0.61	880

The second method is to use a power measuring device to determine the maximum or peak development. Measuring the maximum torque or power developed by the motor, determines the degree of dough development. Mitchell (1984) discusses the use of this method to determine peak dough development. Wilson (1992) and Kilborn and Tipples (1981) discuss other devices as a means of measuring peak dough development. Instead of measuring motor behavior, these techniques use a more direct method of measuring dough rheology.

12.4 INTRODUCTION TO DOUGH SHEETING AND LAMINATING

The sheeting and laminating of doughs are very important parts of dough processing operations. Sheeting is simply the act of reducing a dough from a large mass, or thick slab, to a thin slab. Laminating is the act of creating multiple layers of dough, which may be interspersed with a separating agent, usually shortening, but sometimes a "dusting" flour.

Sheeting is the method of choice for producing most thin products. It is clearly the commercial descendant of the rolling pin. There are many examples of products produced by sheeting. It is commonly used in the production of cookies, crackers, pizza, thin breads (such as pita breads and matzos), pastry doughs, pie doughs, and ethnic specialties (such as tacos and tortillas). Sheeting used to be the preferred method for producing pasta shapes such as ravioli, tortellini, egg noodles, and bows (butterflies). It is still used to produce egg noodles destined for canned noodle soups, and for the production of oriental (Ramen) style noodles. The snack industry makes wide use of sheeting for producing corn chips, fabricated potato chips, and the like.

Lamination, or layering of doughs is utilized for several reasons. The most important reason is to produce a layered structure of fat and dough. This layered structure is what gives pastries their unique tender structure and crackers their flaky texture. In addition, doughs are often laminated in order to reduce the elastic stresses in dough that have accumulated in previous processing operations.

There is some information in the literature about the effect of sheeting on the properties of dough. The work of Kilborn and Tipples (1974) illustrates that the work input of sheeting operations produces development and overdevelopment of doughs in a similar fashion to that observed for dough mixing. They reported that multiple passes through a sheeter produced the same effects as mixing, i.e., undermixing, optimal mixing, and overmixing. They dem-

onstrated this by measuring the gas holding capacities of doughs made into breads after subjecting the dough to repeated sheeting. Table 12.12 illustrates their results.
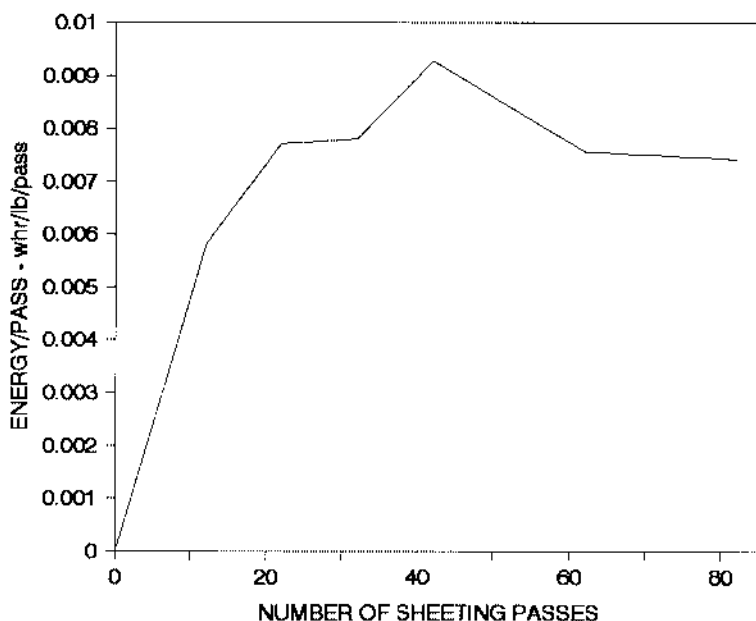
FIGURE 12.13   Development of dough through rolls.

Obviously, the loaf volume data indicates that the dough is underdeveloped for 32 or less sheetings, is near optimal after about 42 sheetings, and is overdeveloped, or beginning to breakdown with more than about 42 sheetings. This behavior is similar to what is observed when one traces loaf volume vs. mixing time. What is particularly interesting about these results is the sensitivity of dough character to sheeting work input. Kilborn and Tipples (1974) found that the energy required to optimally develop dough by sheeting was only 10 to 15% the amount of work required by a dough mixer. This illustrates that sheeting may have a dramatic effect on dough quality.

Levine and Drew (1990) reexamined the data of Kilborn and Tipples. Their analysis, which is illustrated in Figure 12.13, reinforces the idea that sheeting develops dough. The abscissa of the graph (energy/pass) is directly proportional to the torque, or Brabender units, obtained with the Farinograph test previously described. The ordinate (number of sheeting passes) is analogous to the time of mixing. The similarity between Figure 12.13 and the Farinograph curve, illustrated in Figure 12.2, is striking.

There are a number of other measurements that have been reported that support the observation that the sheeting process stresses and orients gluten proteins in a way that is similar to the mixing process. Durum wheat doughs used for pasta (Feillet et al., 1977) and soft wheat doughs used for oriental noodles (Watanabe and Nagasawa, 1968) exhibited alignment of protein. For the durum wheat doughs, the extractability of gluten, which is a measure of gluten cohesiveness, was reduced by repeated sheeting. This effect was attributed to scission of the intermolecular disulfide bonds. Microscopic studies of durum wheat dough revealed that sheeting breaks down the structure of the protein network. The alignment of protein is probably the source of the nonisotropic character of sheeted doughs.

Related observations are reported by Moss (1980) and Oh et al. (1985). The former reported that the sheeting of dough resulted in less extensibility (maximum strain before tearing) and reduced resistance (elasticity). It was suggested that stronger doughs are needed when they are going to be subjected to multiple sheetings, such as is done in the production

of multilayer pastries. The latter demonstrated that conditions used to sheet soft wheat doughs for ramen noodles had a significant effect on final noodle texture.

FIGURE 12.14 A trough type feeder. (Courtesy of T.L. Green, Indianapolis, IN.)

In a similar vein, Menjuivar (1990b) has indicated that the failure of the strength of gluten doughs appears to be related to the accumulation of shear strain. Sheeters operate by applying shear stresses to doughs, so shear strain must accumulate during sheeting operations.

Several authors (Stenvert et al., 1979; Matz, 1992; Pyler, 1988) point out that sheeting expels gas from the dough. It is known that entrained air bubbles act as nuclei for the growth of bubbles as a result of carbon dioxide evolution by yeasts and chemical leavenings, and the evolution of water vapor during baking. As a result, sheeting produces finer grained baked products. This is probably one reason why some bread doughs are "molded" (rolled) into loaves prior to proofing and baking.

Levine (1991) points out that excessive reduction of a dough in one pass through a sheeting roll, introduces a circulation pattern that may disrupt the laminar structure that is sought. This phenomenon will be discussed later.

All of these observations illustrate that much care must be taken in the specification, design, and operation of sheeting lines.

12.4.1 SHEETING EQUIPMENT

Sheeting is accomplished in a number of ways. One method of forming a crude sheet is by placing the mixed dough in a trough whose bottom is a slowly moving belt. At the discharge end of the trough, the dough is squeezed between a large, low speed, roller that is usually corrugated to increase friction between the dough and the roll. The thick dough slab formed is then fed to additional pairs of sheeting/laminating operations to achieve the final desired

thickness and number of laminations. Figure 12.14 illustrates a dough being dumped into the forming trough.

Another method for starting a dough down a sheeting line is to feed "chunks" of dough to the three or four roll sheeters, illustrated in Figures 12.15 and 16.
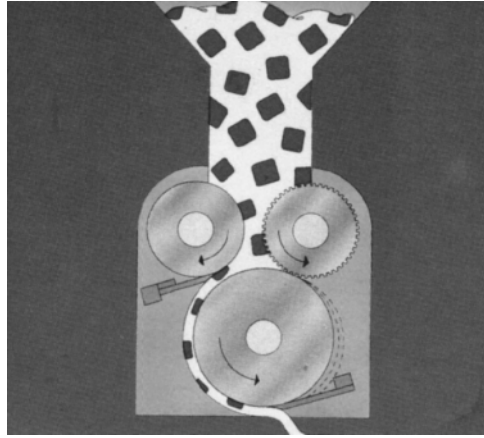
FIGURE 12.15   A three roll sheeter. (Courtesy of Rykaart, Inc., Hamilton, OH.)
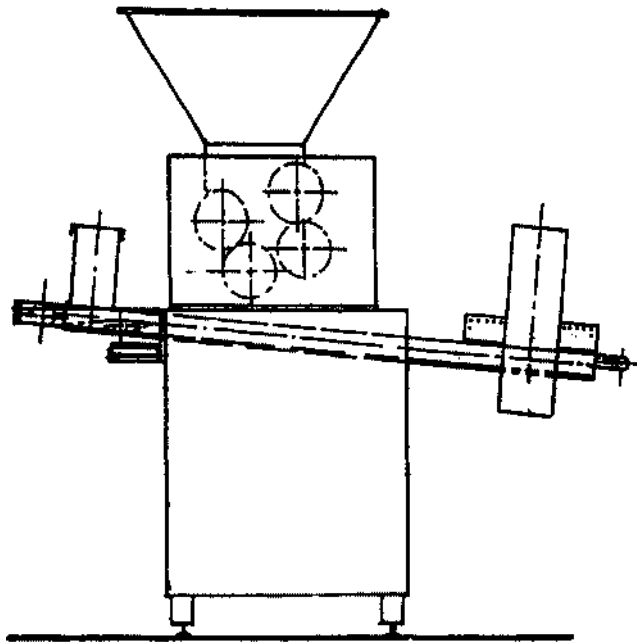
FIGURE 12.16   A four roll sheeter. (Courtesy of Rademacher, Inc., Hudson, OH.)

A crude sheet of dough is sometimes created through the use of a single, or multiscrew, extruder equipped with a slit die at its discharge. An example of this is illustrated in Figure 12.17.

Multiple reductions are usually required to produce doughs of the desired final thickness and properties. The simplest low capacity devices used for this are small table-top sheeters (Figure 12.18), or reversible sheeters (Figure 12.19). Reversible sheeters operate by placing
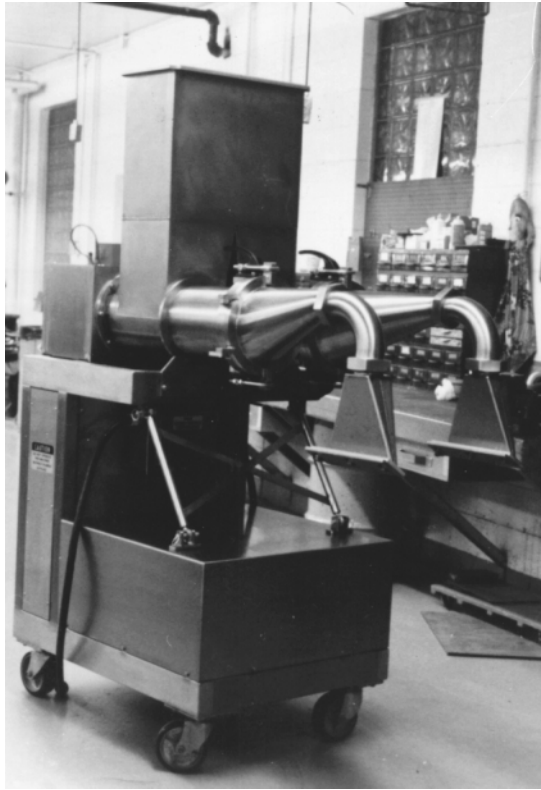
FIGURE 12.17 A dough extruder. (Courtesy of Moline, Duluth, MN.)

the dough on a belt which feeds a pair of rollers. The discharge from the rollers is collected on another belt, the gap is reduced, and direction of movement of the belts and rollers is reversed. Multiple reductions on a table top sheeter is accomplished by manually refeeding a dough that has previous passed through the sheeter. These types of sheeters are used primarily in small retail bakery operations.
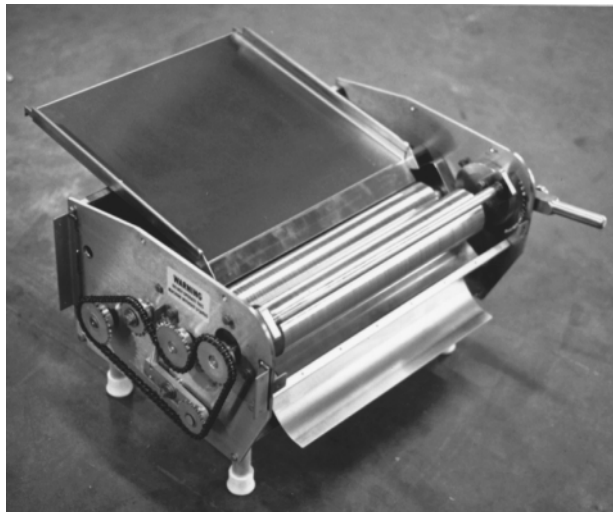
FIGURE 12.18 A table top sheeter. (Courtesy of Moline, Duluth, MN.)
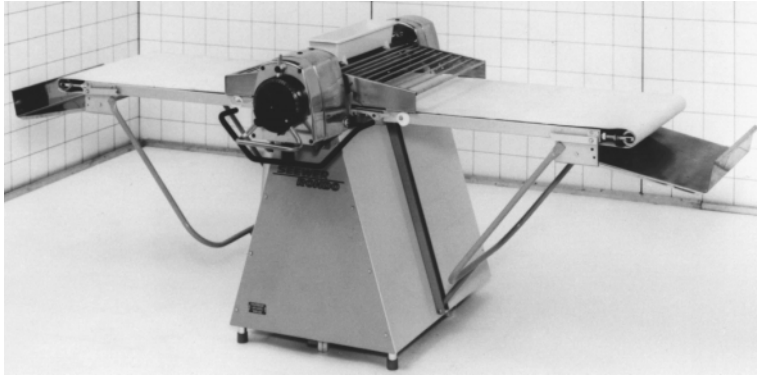
FIGURE 12.19 A reversible sheeter. (Courtesy of Rondo, Hackensack, NJ.)

Traditional operations use multiple pairs of sheeting rolls in series. Figure 12.20 illustrates a roll stand with four pairs of rollers. The dough is usually conveyed between pairs of rolls by a belt or series of rollers, but gravity conveying is also used in certain configurations.

FIGURE 12.20 A four roll stand. (Courtesy of T.L. Green, Indianapolis, IN.)

An alternative approach is incorporated in stretcher (Figure 12.21) or multiroller (Figure 12.22) designs. The former uses a multiplicity of small rollers acting against a dough that is lying on a series of belts. The latter uses a carousel of small rollers acting against a dough that is lying on a large roll. These devices are claimed to reduce the stress and pressure exerted on the dough compared to conventional pairs of rolls.

The width of doughs is sometimes adjusted through the use of cross rollers (Figure 12.23). The degree of adjustment in width that can be obtained is usually limited. These devices are also believed to reduce the tendency to develop stresses only in the longitudinal direction of sheeting.
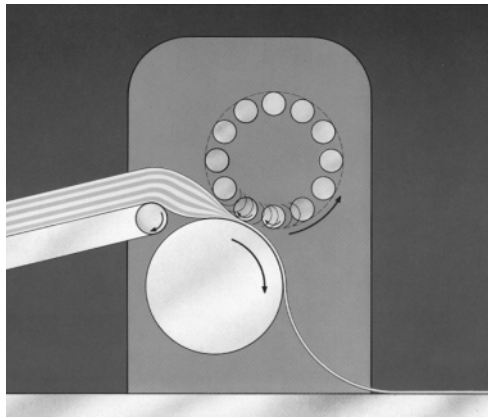
FIGURE 12.21   A stretcher. (Courtesy of Rheon, Irvine, CA.)
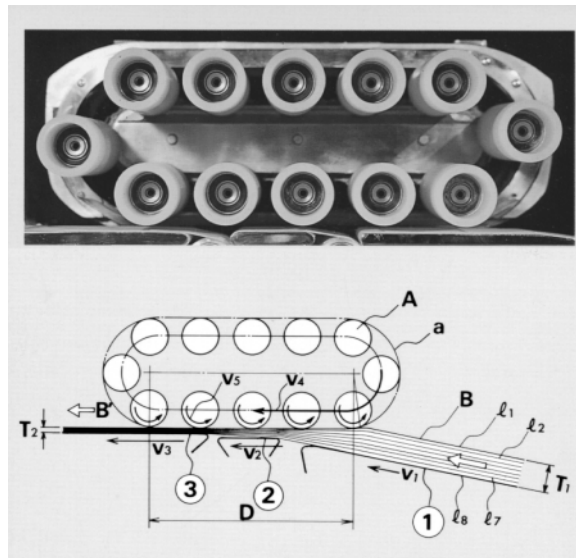
FIGURE 12.22   A multiroll sheeter. (Courtesy of Rykaart, Inc., Hamilton, OH.)

12.4.2 LAMINATING OF DOUGHS

In order to laminate doughs, one must provide a layer of the separating material (shortening). This is accomplished in several ways. One method is to "stuff" shortening, which is received in the form of blocks into a positive displacement pump with a slit die at its discharge. An example of a "stuffer" is illustrated in Figure 12.24. "Stuffers" usually incorporate extrusion screws to force the shortening into the pump's feed. A variation on this replaces the pump "stuffer" and pump with a hydraulic ram which forces the shortening blocks through a slit die.

Another method that is used to form a sheet of shortening is to feed blocks to a roll extruder (Figure 12.25). A roll extruder is composed of a pair of corrugated rolls that force the shortening into a slit die. The roll extruder is similar to the device known as a wire cut machine that is used for the production of cookies. The performance of these types of devices are discussed by Levine and Boehmer (1992).

There are a number of ways to begin the lamination process. One method is the sandwich method illustrated in Figure 12.26. Another method is through the coextrusion of shortening
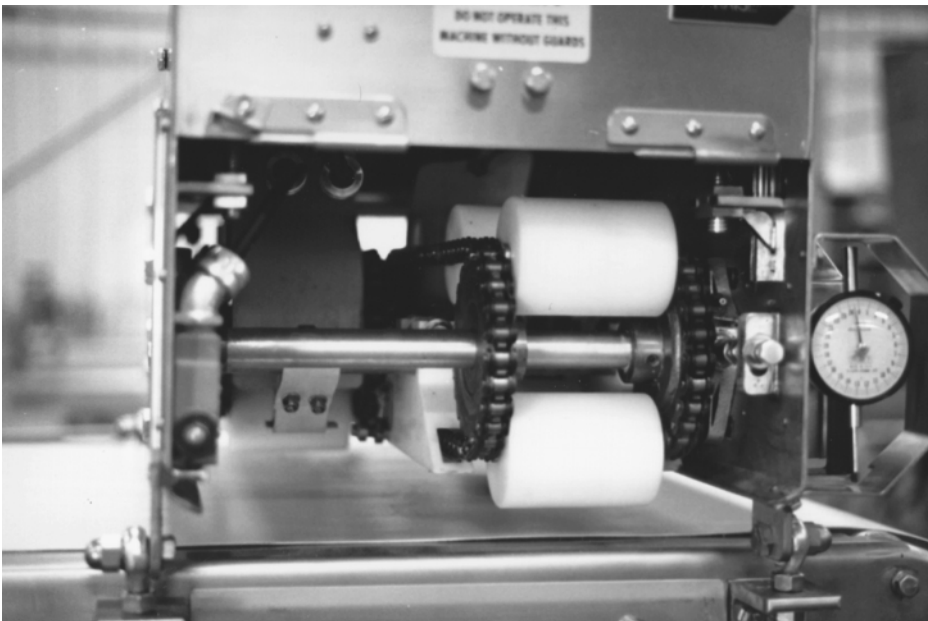
FIGURE 12.23 A cross roller. (Courtesy of Moline, Duluth, MN.)

into the center of a tube of dough. The other method is to lay a strip of extruded shortening onto a sheet of dough. The dough is then folded as illustrated in Figures 12.27 and 28. In order to form the multiple layers required for pastries and crackers, additional folding and reduction is then required.

The folding and laminating steps are eliminated by the roll-in method illustrated in Figure 12.29. The multilayered "rope" of dough that is formed by this method must be reduced by further rolling operations.

Laminating to produce multiple layers of dough and shortening from a sandwich of shortening in dough produced by the sandwich method, coextrusion, or folding methods is
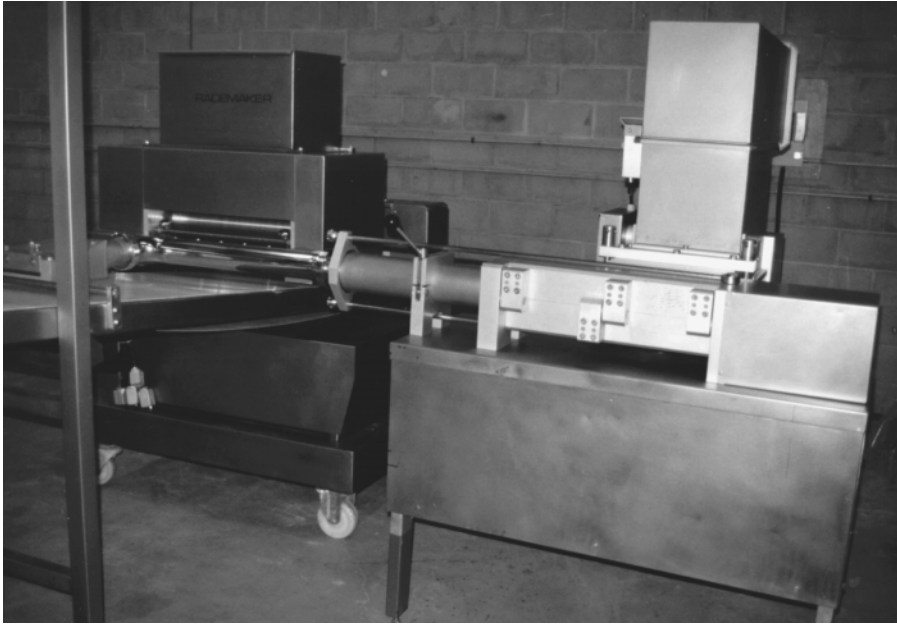
FIGURE 12.24   A pump stuffer. (Courtesy of Rademacher, Inc., Hudson, OH.)
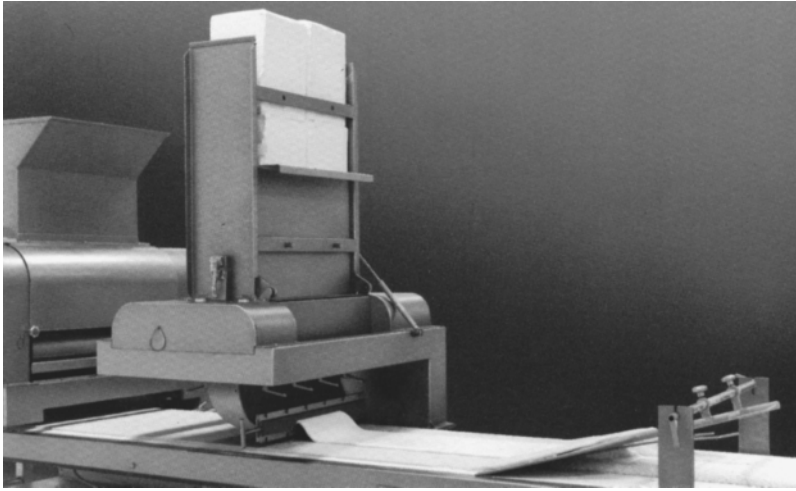
FIGURE 12.25   A shortening roll extruder. (Courtesy of Rykaart, Inc., Hamilton, OH.)

accomplished by lapping the dough (Figure 12.30) or by the cutting and stacking sections of dough (Figure 12.31). After laminating, the sheet is reduced to the desired final thickness by additional sheetings. Lapping is also used to adjust the width of the sheet and to distribute the stresses in the dough in both the crosswise and lengthwise directions.

There are a number of manufacturers of this sheeting and laminating equipment; among them are APV Baker Inc., Sasib Inc., Vickers Inc., Rykaart Inc., Rademacher Inc., T.L. Green Inc., Rheon Inc., and The Moline Company.
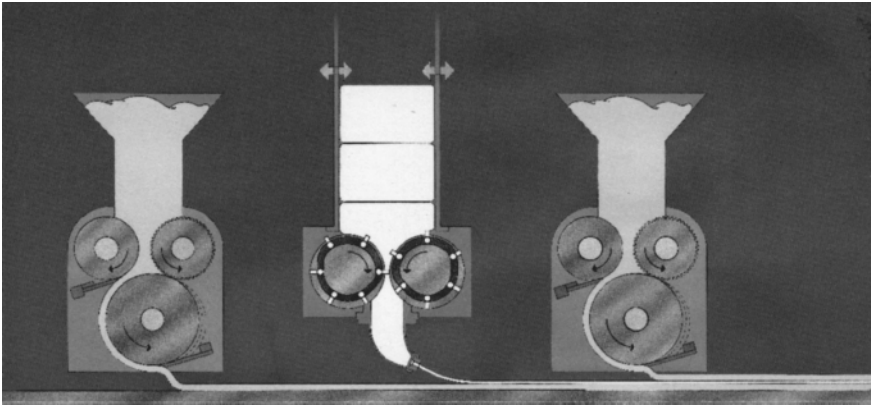
FIGURE 12.26 The sandwich method. (Courtesy of Rykaart, Inc., Hamilton, OH.)
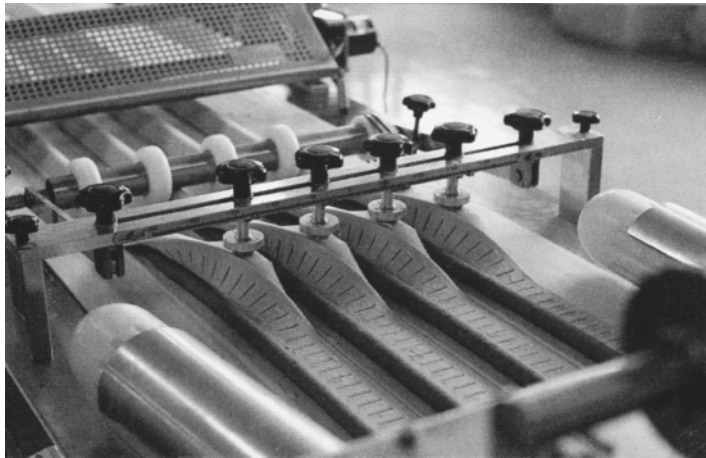
FIGURE 12.27 A single fold. (Courtesy of Rheon, Irvine, CA.)
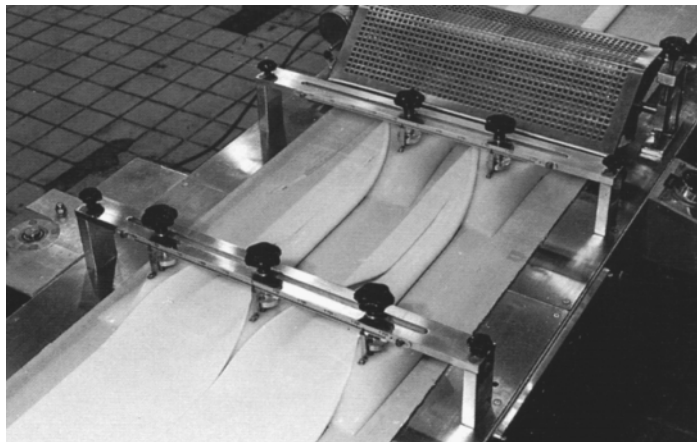
FIGURE 12.28 An envelope fold. (Courtesy of Rheon, Inc., Irvine, CA.)
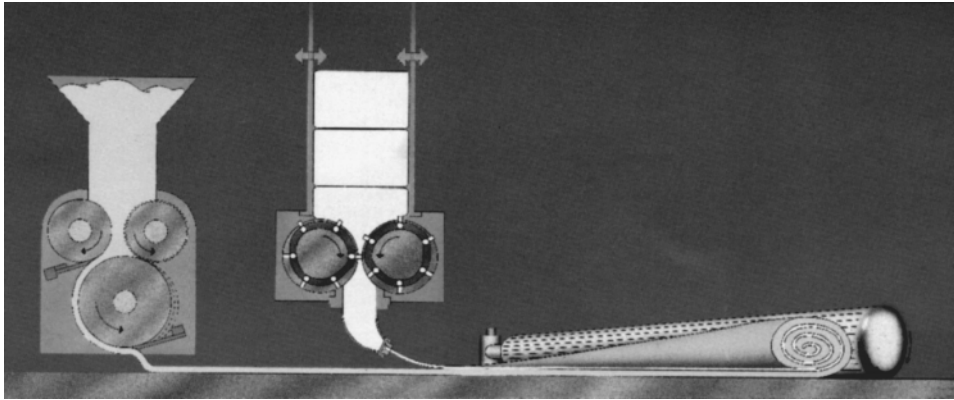
FIGURE 12.29 The roll-in method. (Courtesy of Rykaart, Inc., Hamilton, OH.)
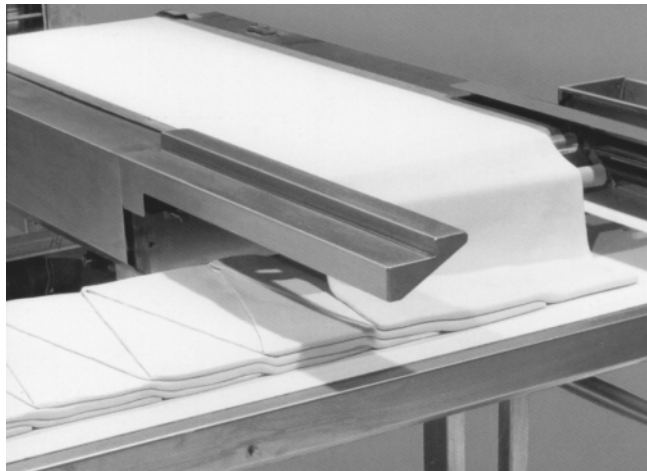
FIGURE 12.30 A lapping system. (Courtesy of Rykaart, Inc., Hamilton, OH.)

12.4.3 ENGINEERING ASPECTS OF SHEETING OPERATIONS

Sheeting of dough is analogous to the calendering process used in the polymer industries. Levine and Drew (1990) discuss the mathematical theories behind sheeting with rolls operating at equal speeds. This work is an extension of the polymer literature (e.g., Middleman, 1977; Brazinsky et al., 1970). Recently Levine (1995) extended the theory to unequal speed rolls. Although unequal speed sheeting is sometimes used with a pair of rolls, it is an essential part of the three roll system, such as illustrated in Figure 12.15, and in the stretcher and multiroll systems described in Figures 12.21 and 12.22. Rather than describing all the theoretical developments, this work will summarize the essential aspects of these efforts.

Motion of the dough through a pair of rolls is the result of the shear flow induced by the drag the rolls exert on the dough. As the dough passes through the rolls a pressure profile is developed. This profile reaches a maximum pressure just before the roll nip (point of smallest gap) and the pressure is zero at the point of first dough contact and the point of dough separation from the rolls. This pressure development is probably the source of the degassing that has been observed, so there would be an interest in controlling the level of pressure developed in a sheeting system.
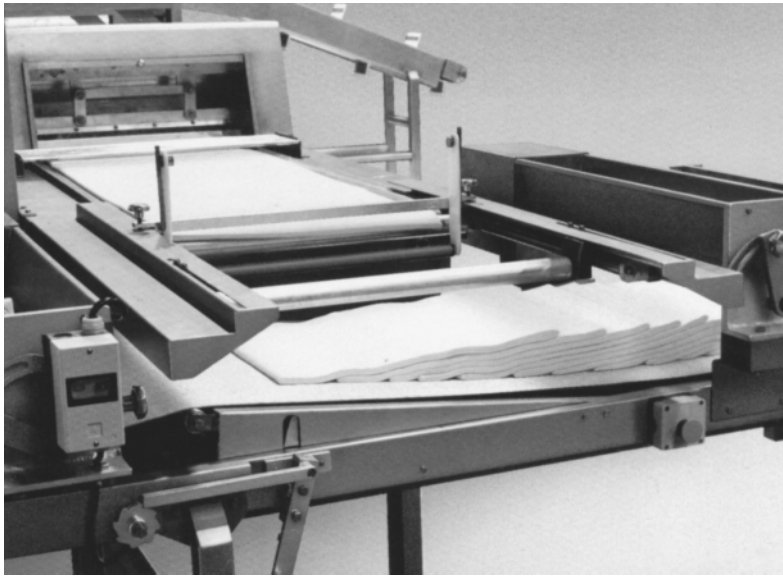
FIGURE 12.31 A cut and stack system (Courtesy of Rykaart, Inc., Hamilton, OH.)
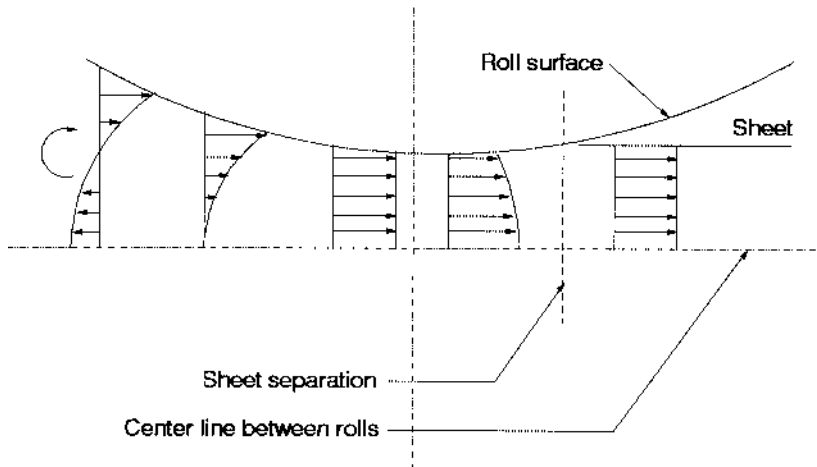
FIGURE 12.32 Flow pattern between rolls.

The pressure development causes the superposition of pressure flows upon the drag flow. This pressure flow affects the shear stresses observed, and causes back flows. Figure 12.32 illustrates the shape of the dough velocity profiles developed between equal speed rolls. Note that as one moves back from the nip, the back flow becomes more pronounced. At a far enough distance upstream of the nip, a circulation flow develops. Levine (1991) suggests that this circulation causes undesirable mixing that may be observable as a disruption of laminated structures. This phenomenon occurs when the reduction ratio (ratio of feed thickness to gap) exceeds a value of approximately three. Since the final dough produced is thicker than the nip (about 1.5 times the gap) this is probably the explanation of the bakers' rule of thumb that the thickness of a dough should never be reduced by more than a factor of two in a single pass between a pair of sheeting rolls.

The development of pressure between the rolls results in several mechanical engineering design issues. This pressure acts across the entire contact area of dough and rolls and results in the development of significant separating forces. These forces can reach levels of ≥100,000 N.

12.4.4 ESTIMATING CAPACITY, PRESSURE, FORCES, AND POWER OF SHEETERS

In analyzing sheeting rolls, it is generally assumed that the rheology of the dough can be described by a simple power law model.
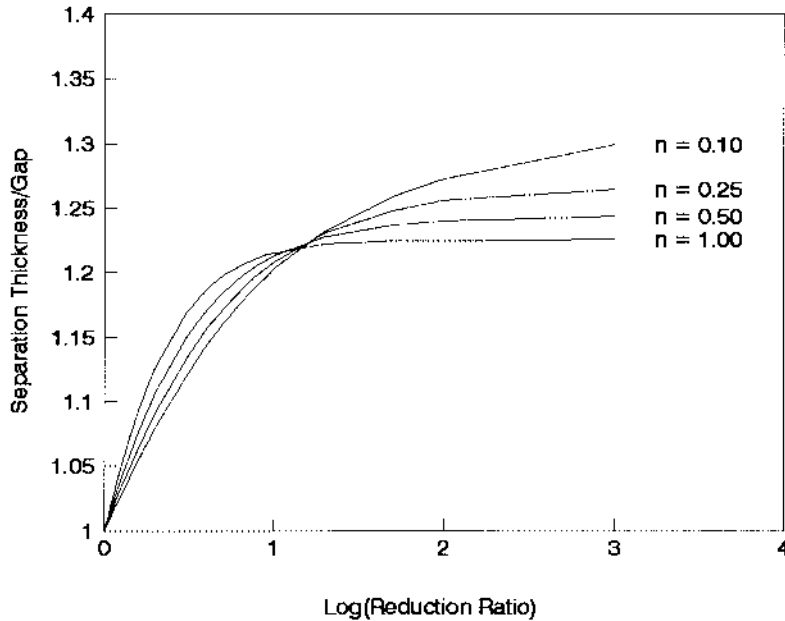
FIGURE 12.33 Separation thickness vs. reduction ratio (no speed differential).

$$\tau = m \cdot \left| \frac{dv}{dy} \right|^{(n-1)} \frac{dv}{dy} \qquad (12.13)$$

As discussed earlier, the value of the flow index, n, for dough seems to be in the range of 0.25 to 0.5. It is recognized that dough exhibits significant viscoelasticity and extensional viscosities, but there has been little, or no, success in analyzing the sheeting problem for these more complicated fluids.

The pumping capacity per unit width (Levine, 1985; Levine and Drew, 1990; Levine, 1995) of the rolls is given by

$$\frac{Q}{W} = UB \qquad (12.14)$$

The ratio of separation thickness to gap is a function of the flow index, reduction ratio, and roll speed differential. This ratio is presented in Figures 12.33 through 12.36. Levine and Drew suggest that over the normal range of sheeting operation that Equation 12.14 can reasonably be approximated by

$$\frac{Q}{W} = 1.1 \, UB_0 \qquad\qquad (12.15)$$
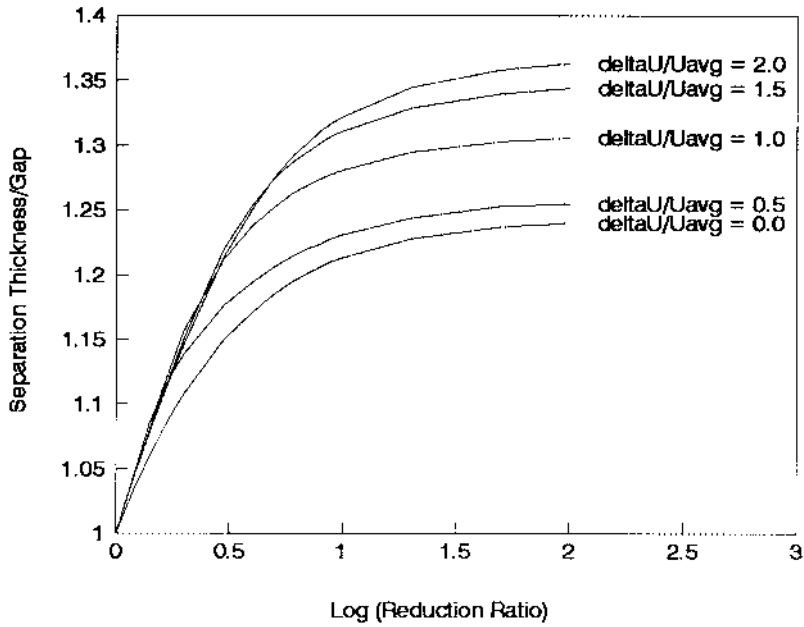
FIGURE 12.34 Separation thickness vs. reduction ratio (flow index = 0.5).
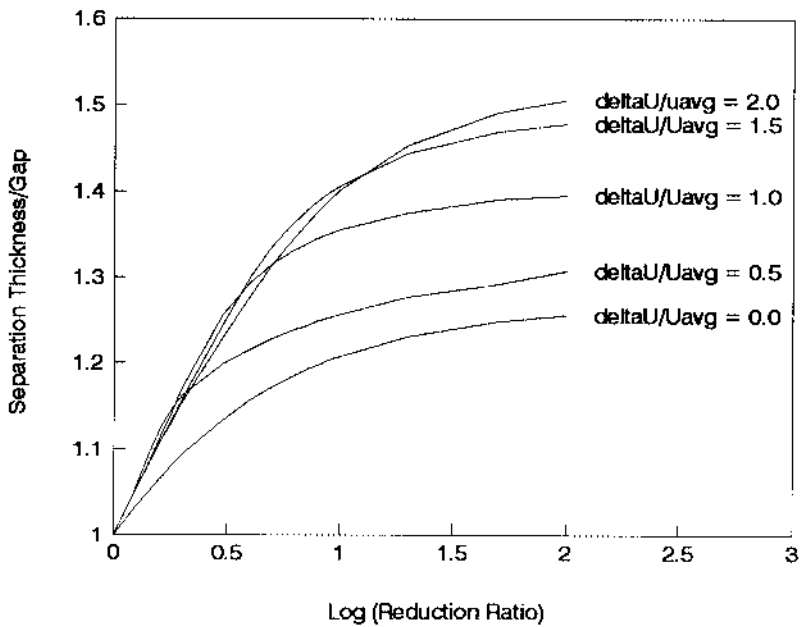
FIGURE 12.35 Separation thickness vs. reduction ratio (flow index = 0.25).

The data supporting Equation 12.15 are illustrated in Figure 12.37. Note that the pumping capacity is proportional to the average speed of the rolls and inversely proportional to the gap between the rolls.
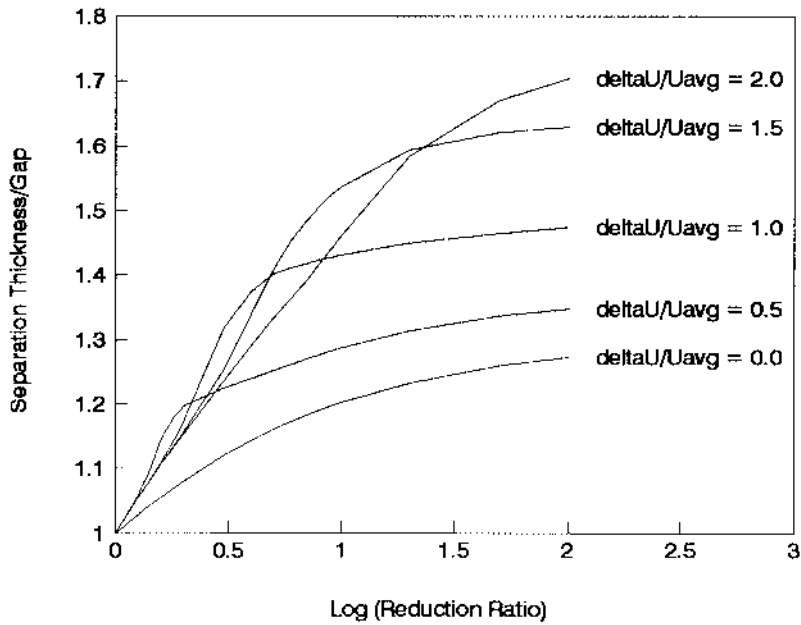
FIGURE 12.36 Separation thickness vs. reduction ratio (flow index = 0.1).
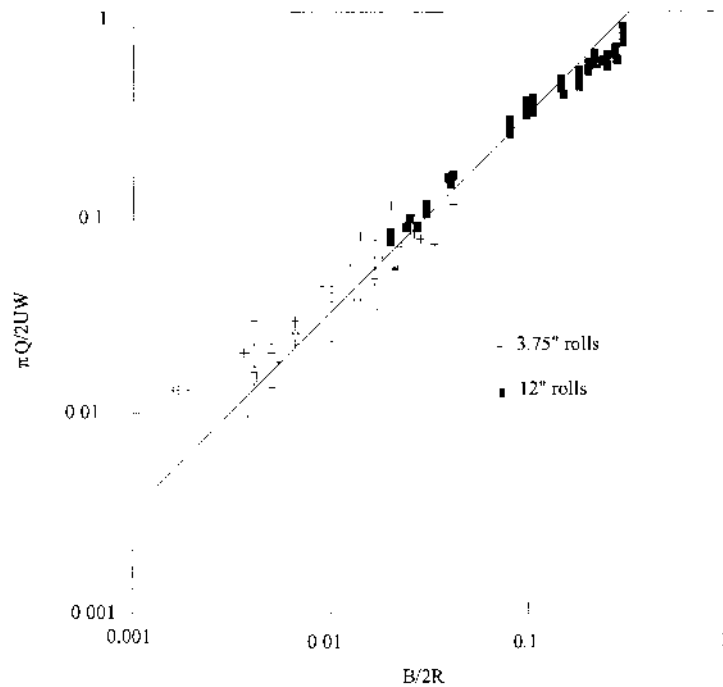
FIGURE 12.37 Sheeting capacity of rolls.

The maximum pressure development by the rolls is given by Equation 12.1*. There are two factors that are needed for using this equation. The leading coefficient is a function of flow index. This coefficient is found in Middleman (1977) and is presented in Figure 12.38.
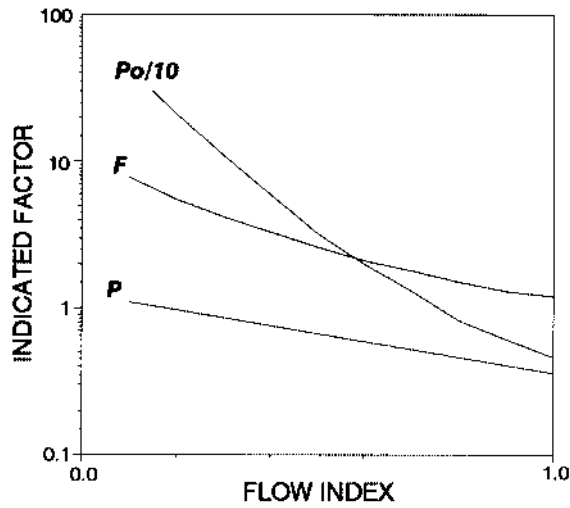
FIGURE 12.38 Pressure, force, and power factors vs. flow index.

The trailing coefficient is a function of the flow index, reduction ratio, and roll speed differential. The value for the trailing coefficient is given in Figures 12.39 through 12.42.
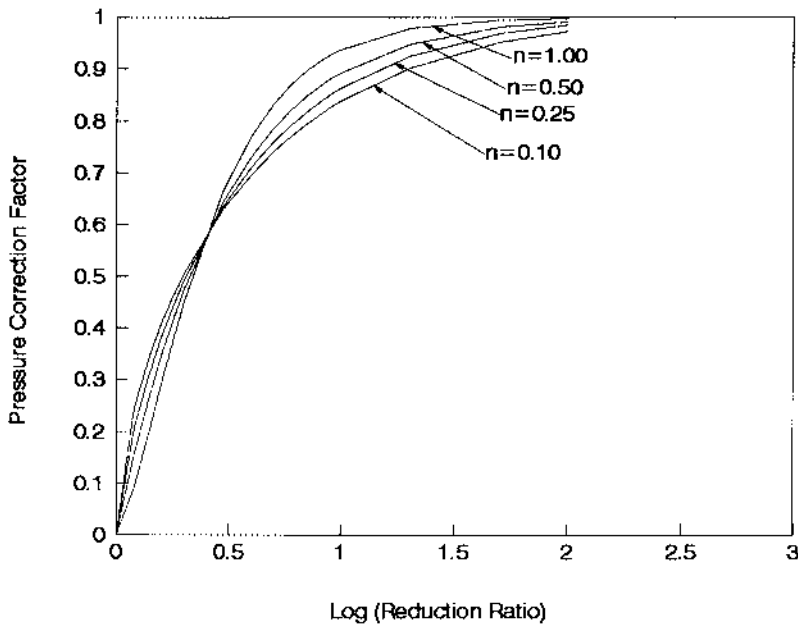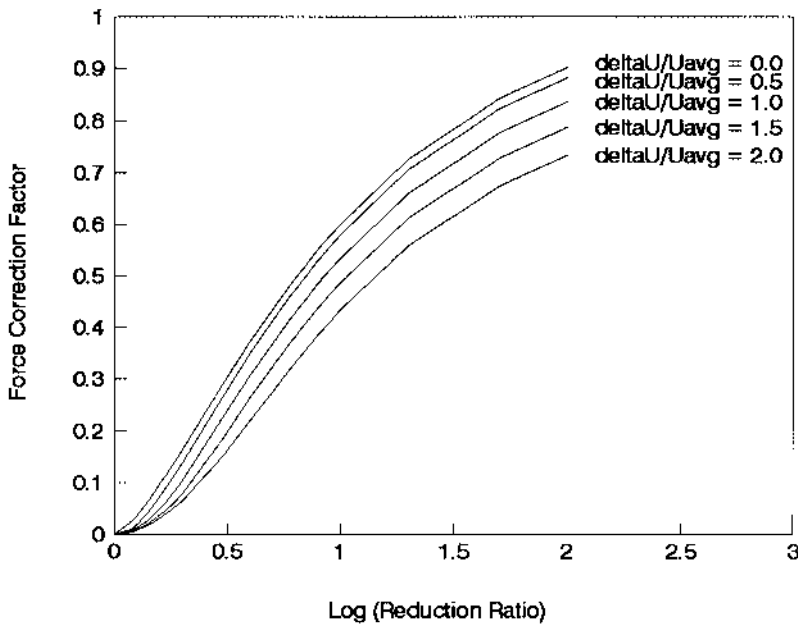

FIGURE 12.39 Pressure correction vs. reduction ratio (no speed differential).

---

* For Equations 12.16, 12.17, 12.18 the equations may be modified for unequal size rolls by using an equivalent

radius defined by, $\dfrac{1}{R_{eq}} = \dfrac{1}{2} \cdot \left(\dfrac{1}{R_1} + \dfrac{1}{R_2} \right)$
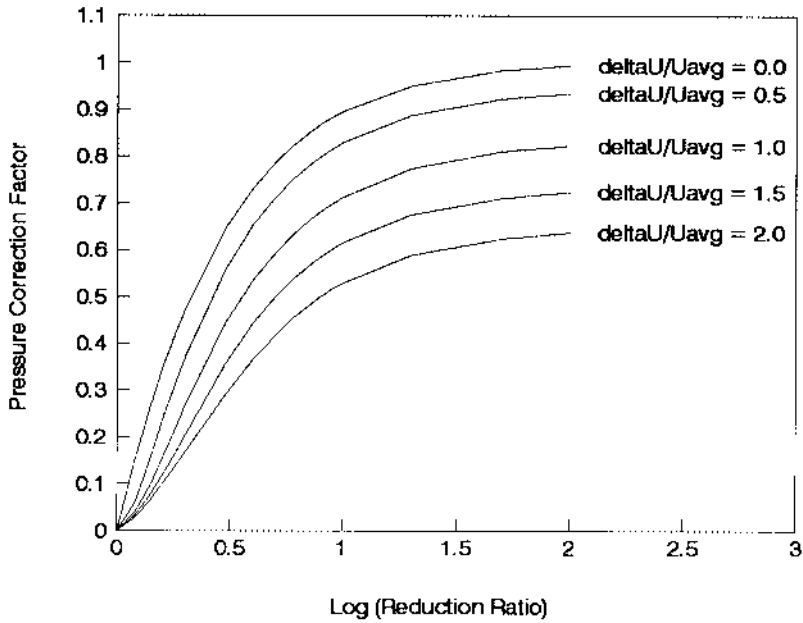
FIGURE 12.40 Pressure correction vs. reduction ratio (flow index = 0.5).
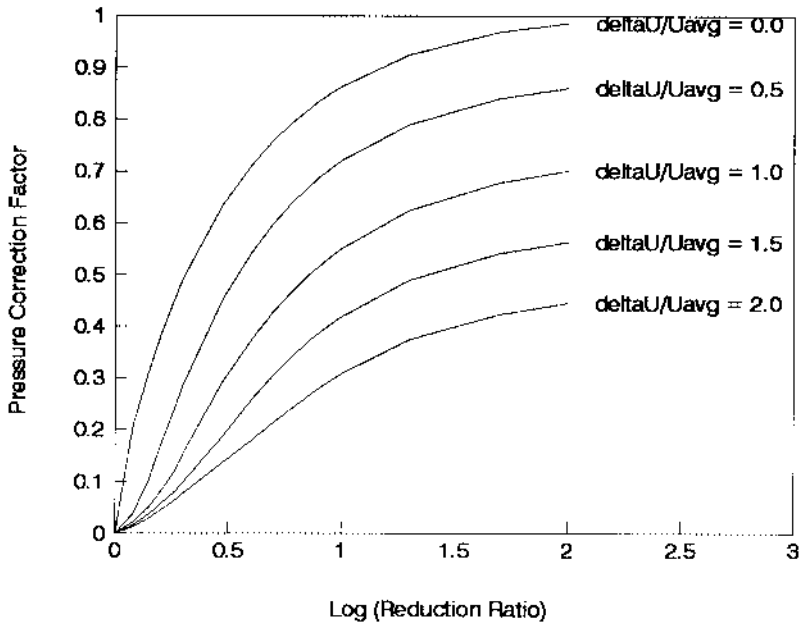
FIGURE 12.41 Pressure correction vs. reduction ratio (flow index = 0.25).

$$p_{max} = P(n) \cdot m \cdot \left(\frac{2U}{B_0} \right)^n \cdot \sqrt{\frac{4R}{B_0}} \cdot C_p \left(rr, n, \frac{\Delta U}{U} \right) \qquad (12.16)$$

The pressure developed by the rolls, and presumably the tendency to degas the dough, increases with the speed of the rolls, the roll diameter, reduction ratio, and decreasing gap.
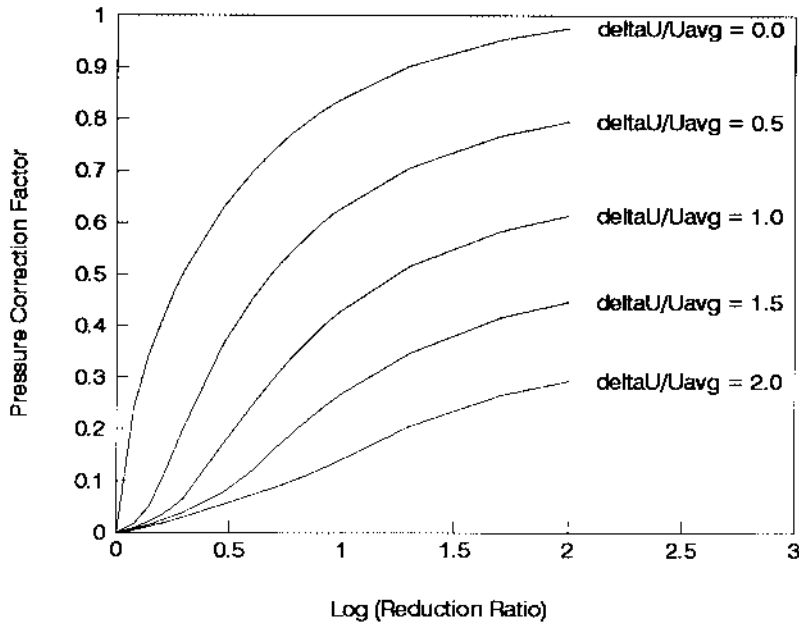
FIGURE 12.42   Pressure correction vs. reduction ratio (flow index = 0.1).

Note that the effect of roll speed differential can be very pronounced. In the range of normal reduction ratios, the introduction of speed differential can result in a pressure reduction by a factor of about three, at the same average roll speed (production rate). This, and the use of small rollers, is one of the benefits of the stretcher and multiroll systems, which use significant speed differences between the moving surfaces.

The separating force developed by the rolls is given by Equation 12.17. As with the pressure development equation, there are two factors that are needed for using the equation. The leading coefficient is a function of flow index. This is presented in Figure 12.38. As is the case for the pressure equation, the trailing coefficient is a function of the flow index, reduction ratio, and roll speed differential. The value for the trailing coefficients is given in Figures 12.43 through 12.46.

$$\frac{F}{W} = F(n) \cdot m \cdot \left(\frac{2U}{B_0}\right)^n \cdot R \cdot C_f\left(rr, n, \frac{\Delta U}{U}\right) \tag{12.17}$$

The separating force developed by the rolls, and the stresses on rolls, shafts, and bearings, increases with the speed of the rolls, the roll diameter, reduction ratio, and decreasing gap. Note that the effect of roll speed differential can be very pronounced. In the range of normal reduction ratios, the introduction of speed differential can result in a pressure reduction by a factor of two to three, at the same average roll speed (production rate). This is one factor that allows the stretcher and multiroll systems, which have significant speed differences between the moving surfaces, to incorporate smaller rollers in the design, without excessive deflection.

The power required to turn the rolls and dissipate in the dough is given by Equation 12.18. As is the case with the pressure and force equations, there are two factors that are needed for using the equation. The leading coefficient is a function of flow index. This is presented in Figure 12.38. The trailing coefficient is a function of the flow index, reduction ratio, and
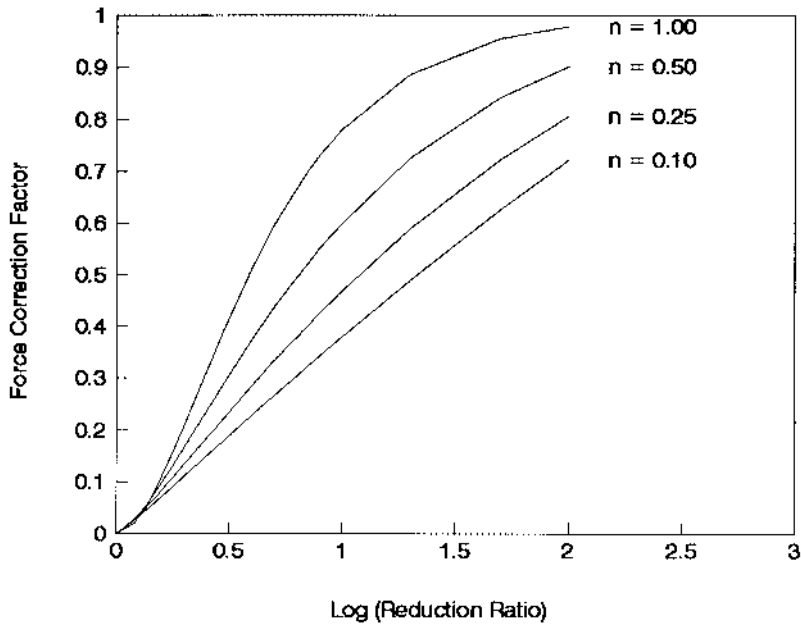
FIGURE 12.43   Force correction vs. reduction ratio (no speed differential).
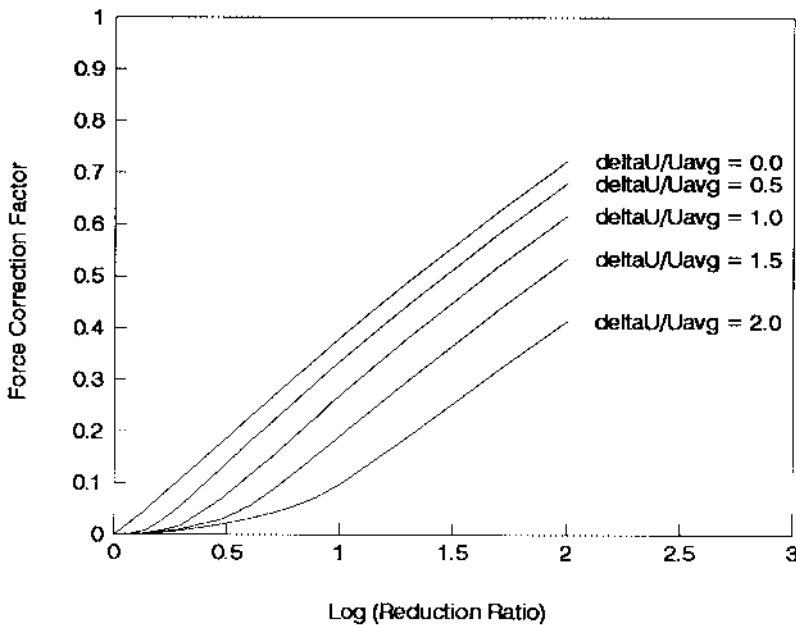

FIGURE 12.44   Force correction vs. reduction ratio (flow index = 0.5).

roll speed differential. The value for the trailing coefficients is given in Figures 12.47 through 12.51.

$$\frac{P}{W} = Po(n) \cdot m \cdot U^2 \cdot \left(\frac{2U}{B_0} \right)^{n-1} \cdot \sqrt{\frac{2R}{B_o}} \cdot C_w \left(rr, n, \frac{\Delta U}{U} \right) \qquad (12.18)$$
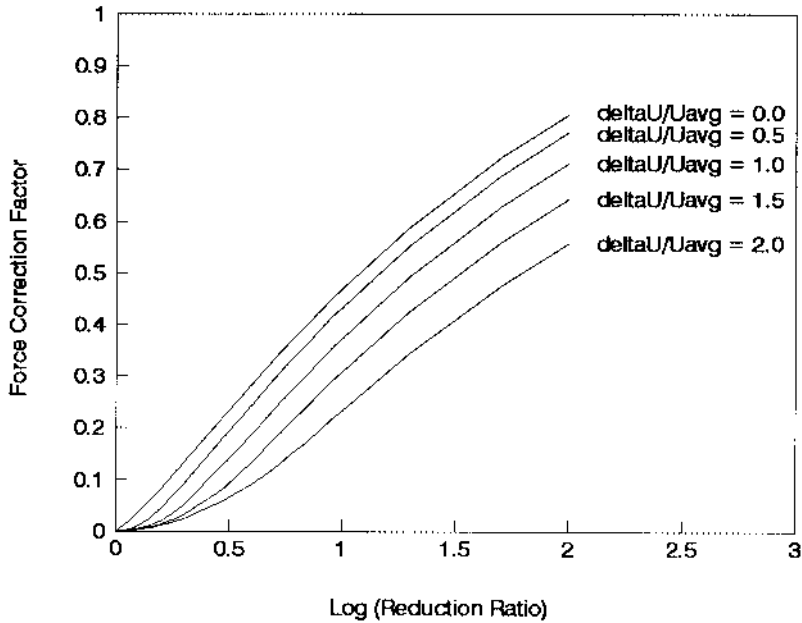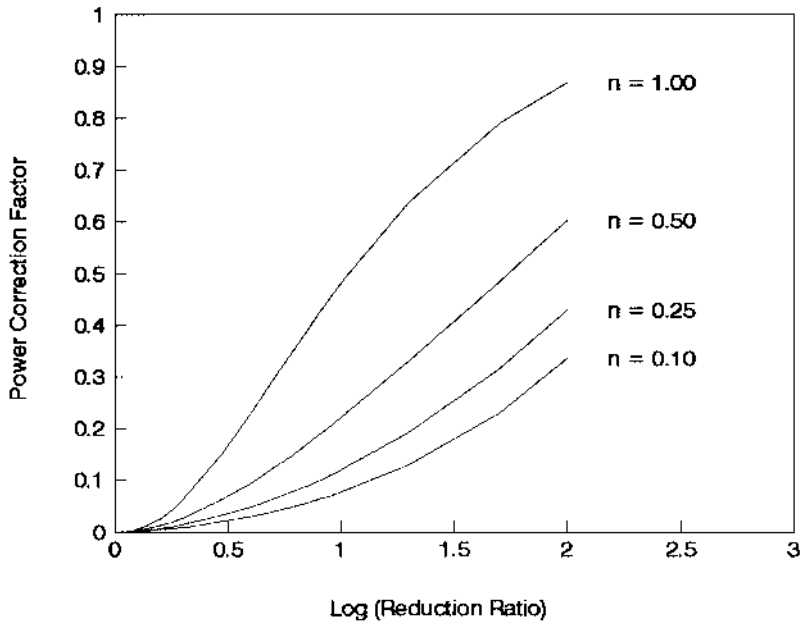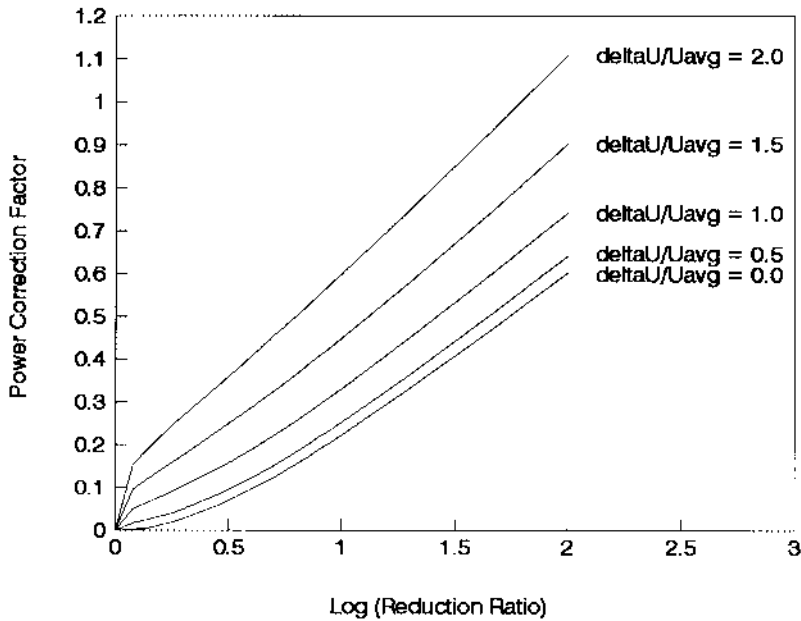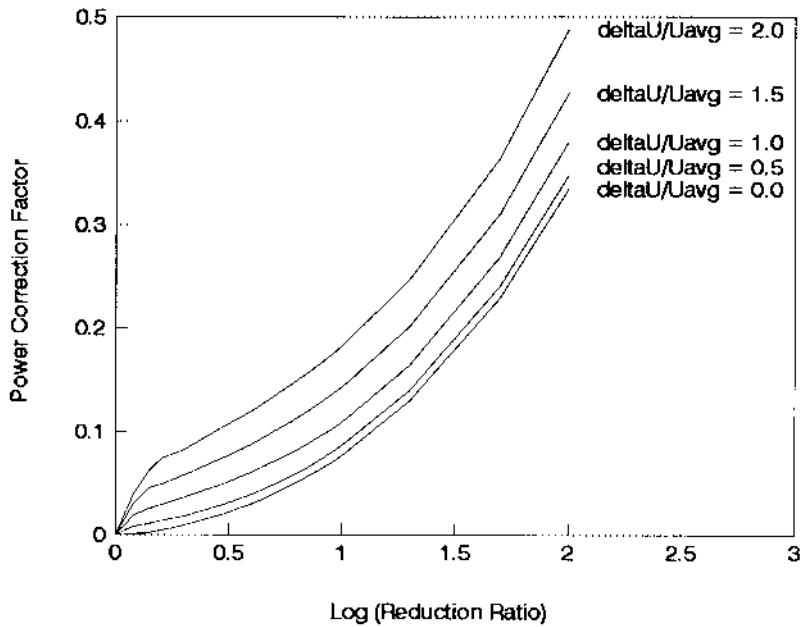
FIGURE 12.45 Force correction vs. reduction ratio (flow index = 0.25).

FIGURE 12.46 Force correction vs. reduction ratio (flow index = 0.1).

The power consumed by the rolls, and dissipated in the dough, increases with the speed of the rolls, the roll diameter, reduction ratio, and decreasing gap. Note that the effect of roll speed differential can be very pronounced. In the range of normal reduction ratios, the introduction of speed differential can result in a power consumption increase by a factor of about 10 at the same average roll speed (production rate). This is one potential disadvantage of stretcher and multiroll systems which use significant speed differences between the moving surfaces.

FIGURE 12.47 Power correction vs. reduction ratio (no speed differential).
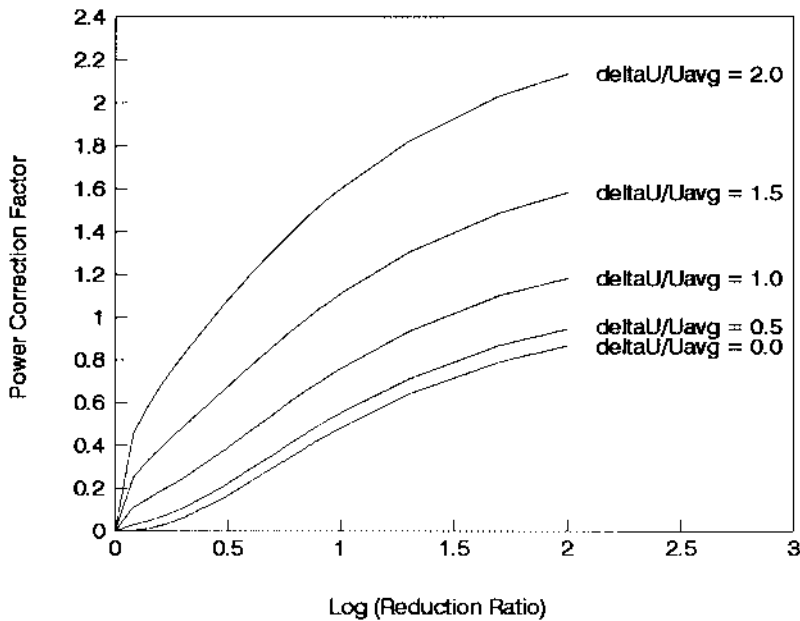
FIGURE 12.48 Power correction vs. reduction ratio (flow index = 1.0).

Work input is simply the power consumption divided by the pumping rate. Since pumping rate increases linearly with roll speed (Equation 12.14) and power increases with the $1 + n$ power of speed (Equation 12.18), work input must increase as line speed is increased. This suggests that even the simple act of increasing line speed to increase productivity can have an impact on product quality.

FIGURE 12.49   Power correction vs. reduction ratio (flow index = 0.5).
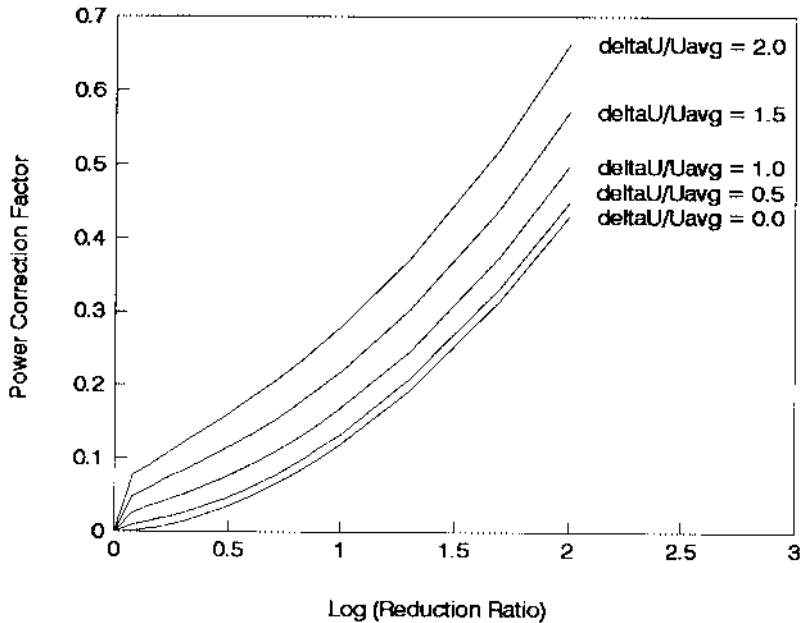
FIGURE 12.50   Power correction vs. reduction ratio (flow index = 0.25).

The concave shape of the trailing power coefficients (Figures 12.47 through 12.51) suggests that the path we choose (number of rolls, gap profile) to achieve a particular reduction defines the total work required to achieve a specified reduction. Levine and Drew (1990) illustrate the effect of the number of reductions required to achieve a given reduction. They assume a flow index of 0.5 and the geometric reduction ratio profiles given in Table 12.13.

FIGURE 12.51   Power correction vs. reduction ratio (flow index = 0.1).

TABLE 12.13
Reduction Profiles for Multiple Rolls

Number of reductions	Gap at indicated roll pair			
	#1	#2	#3	#4
1	2			
2	8	2		
3	13	5	2	
4	16	8	4	2

Note: Feed thickness = 32.

TABLE 12.14
Effect of Number of Reductions on Work and Maximum Pressure

Number of reductions	Total work	Maximum pressure
1	1.00	1.00
2	0.38	0.78
3	0.14	0.62
4	0.10	0.50

The effect of Table 12.13's reduction profiles on relative work input and maximum pressure development is given in Table 12.14.

Clearly, the process is becoming more "gentle", as the number of steps used to reduce the dough is increased. Note that this is another advantage of multiroll or stretcher systems over a *single* pair of rolls. The multiple rollers essentially create a system that employs a multitude of small reductions. The theory suggests that the "gentlest" process is one that incorporates an infinite number of infinitesimal reductions. Such a process, at least theoretically, would subject the dough to no work and no pressure.

The theory would suggest that no matter how fragile a dough one is dealing with, a sheeting system could be designed to successfully reduce the dough, provided the cost of the rolls is not a factor, which, unfortunately, it is. Another reason for discussing this theoretical approach to dough reduction is to alert the design engineer to a potential problem.

Bakers and food technologists are aware that multiple small reductions are a good way to preserve dough qualities. As a result, in order to produce the best possible laboratory prototype product, they will use a reversible sheeter and smallest gap step size available to maximize the number of reductions of the dough. This approaches the infinite number of reductions scenario, and as a result, is not commercially realizable. The problem is realized when the commercial product does not match the quality of the laboratory product.

TABLE 12.15
Different Four-Step
Reduction Profiles

	Gap at Indicated Roll Pair			
Style	#1	#2	#3	#4
Normal	16	8	4	2
Gentle	12	6	3	2
Severe	24	12	6	2

Note: Feed thickness = 32.

TABLE 12.16
Effect of Reduction Style on
Work and Maximum Pressure

Style	Total work	Maximum pressure
Normal	0.14	0.50
Gentle	0.08	0.33
Severe	0.25	0.60

The shape of the power vs. reduction ratio parameter given in Figures 12.47 through 12.51 also suggests that the choice of reduction profile for a given number of rolls may be optimized. For a four step reduction, Levine and Drew considered three different reduction profiles that they considered "normal", "gentle", and "severe". These profiles are described in Table 12.15.

For Table 12.15, the effect of reduction profiles on relative work input and maximum pressure development is given in Table 12.16.

Table 12.16 suggests that there is probably an optimum reduction profile for any given number of rolls. It also suggests that if one is going to take a large reduction in a pair of rolls, it is more "gentle" to do this when the dough is thick (early in the reducing process). Finally, a simple statement about the day to day operation of lines can be made. If the target final thickness of the dough is changed, the entire set of rolls should be adjusted, not just the gap of the last pair of rolls. Unfortunately, this is not normally done. This is simply explained. If the target thickness is increased, and just the last gap is increased, we can change a four roll stand into a three roll stand. Conversely, if the target thickness is decreased, and just the last gap is decreased, we turn a "gentle" reduction profile to a "severe" profile.

12.4.5 FINAL DOUGH THICKNESS

Because of the presence of residual stresses in the dough, the thickness of the dough at separation, as given in Figures 12.33 through 12.36, will not be the actual final thickness of the dough. The dough will always be thicker than the separation thickness because as these stresses are relaxed, the dough "snaps back" and increases its thickness. Levine (1985) suggests that the ratio of final thickness to gap can be estimated by

$$\frac{B_b}{B_0} = 0.06 \cdot \left(\frac{B_0}{2R}\right)^{-0.58} + 1 \tag{12.19}$$

This equation is subject to question, in that it does not include any factors accounting for rheology or the reduction ratio. This is partly due to the fact that only one dough (rheology) and only a small range of reduction ratios were tested. Recently, Raghavan, et al. (1995) demonstrated that the relaxed thickness can deviate significantly from the predictions of Equation 12.19. This work points out that an increasing reduction ratio does increase the relaxed dough thickness, and changing the dough formula, and presumably the rheology, changes the relaxed dough thickness. At the current time, there is no theoretical basis for predicting relaxed dough thickness, so prediction is problematic at best. Experience teaches that assuming a relaxed thickness of 1.5 to 2 times the gap gives a reasonable estimate of final dough thickness.

Final dough thickness can also be manipulated within a limited range by forcing relaxation or by stretching the dough by changing the speed of the belt that removes the dough from the rolls. The final dough thickness is simply calculated by mass balance (Equation 12.20).

$$B_b = \frac{UB}{U_b} \tag{12.20}$$

Lapping, or stacking, of the dough is intended to create laminations, force relaxation, or to alter the width of the dough. The final thickness for these situations is also determined by mass balance (Equation 12.21).

$$B_b = \frac{UBW}{U_b \cdot W_b} \tag{12.21}$$

12.4.6 DEFLECTIONS OF SHEETER SHAFTS AND BEARINGS

As previously stated the separating forces developed by the rolling process generate significant stress on the shafts, rolls, bearings, etc. Under the influence of the separating forces the rolls

can bend. This results in a nonuniform gap across the sheeter width. Although this changes the work input and pressure that the dough sees across the width of the roll, these effects will be ignored and instead, the concentration will be on the change in gap that results. This is readily observable as variable sheet thickness across the width of the sheet.

This is a straightforward problem in strength of materials. Details of the theory may be found in the literature (Shigley, 1977).

The maximum deflection occurs at the middle of the roll. The deflection at this point is given by

$$\delta = \frac{5\,FW^3}{284\,EI} \tag{12.22}$$

The modulus elasticity, E, is a property of the material of construction of the roll. For steels, a value of 3×10^9 kPa is normally used. The moment of inertia, I, for a hollow roll is given by

$$I = \frac{\pi}{4} \cdot \left[R^4 - \left(R_i\right)^4 \right] \tag{12.23}$$

Both rolls deflect, so the percent deviation of dough thickness between the center and the edges of the roll is given by,

$$d = \frac{5\,FW^3}{384\,EIB_0} \cdot 100\% \tag{12.24}$$

This deflection can cause many unexpected problems. As production capacity is increased by increases in roll width, deflection will increase significantly. According to Equation 12.22, deflection increases with the cube of width and the first power of force (Equation 12.17), which also increases with the first power of width, so, in total, deflection increases with the fourth power of roll width. All designers realize that the deflection may be minimized by increasing the moment of inertia of the roll. Although some increase can be obtained by increasing roll thickness, the most dramatic improvement in deflection is obtained by increasing roll radius.

Consider a roll operating at some arbitrary speed. Assume the deflection is 0.003 mm, a value that would not be noticeable even when producing very thin doughs. Now, consider increasing the roll width by a factor of five, to obtain a production rate increase of a factor of five. The deflection of the wider rolls would be about 1.88 mm. This would obviously be noticeable when sheeting thin products, such as tortillas. This deflection can be overcome by increasing the diameter of rolls. If the diameter of the rolls is increased by a factor of four, force developed will increase by a factor of four (see Equation 12.17), but the stiffness will increase by a factor of 256 (see Equation 12.23). The result would be a deflection of 0.03 mm, which is greater than the deflection observed on the smaller diameter, narrower, rolls, but is still insignificant compared to the sheet thickness.

The problem that the designer has created by the corrective action of increasing roll diameter is discovered by examining the effect of roll diameter on maximum pressure development and power (work input). This can be determined from examination of Equations 12.16 and 12.18. The larger diameter rolls will develop a maximum pressure and work input that is double the values obtained on the original, smaller diameter, rolls. Given the earlier discussion about the interaction of these variables with product quality it would

not be surprising if the products produced on the larger diameter system are different that those produced on the smaller diameter system.

These separation forces also act on the bearings and shafts. The deflection of the shafts is given by

$$\delta = \frac{FL^3}{6\,EI} \qquad (12.25)$$

The moment of inertia of the shafts is given by

$$I = \frac{\pi}{4} \cdot R^4 \qquad (12.26)$$

The shaft length is estimated as the distance from the center of the bearing to the side of the sheeting rolls. Obviously, Equation 12.25 indicates that this distance should be minimized by placing the bearing as close as possible to the rolls.

TABLE 12.17
Effect of Roll Diameter on
Relative Work Input and Pressure

Roll diameter (in)	Relative work or pressure
3	1
6	1.4
9	1.7
12	2

TABLE 12.18
Effect of Roll Speed
on Relative Power

Roll speed (m/min)	Relative work or pressure
5	1
10	1.4
15	1.7
20	2

Deflection of the shafts does not cause weight variations across the roll width, but can cause weight control problem. In poorly designed systems, the deflection of the shafts can be large enough to prevent producing the desired sheet thickness, because deflection can exceed target gap. The other way that shaft deflection causes weight control problems results from the fact that the rheology of the dough will vary from batch to batch as a result of formula variations, or changes in raw material source. This will cause variable separating forces, which results in varying shaft deflection and product thickness.

12.4.7 SCALE UP ISSUES

The scale up issues associated with sheeting systems have already been mentioned. Equations 12.16 and 12.18 illustrate the effect of roll diameter on pressure develpment and work input. At constant roll speed, Table 12.17 illustrates the effect of roll diameter at fixed roll speed (production rate).

When one considers that laboratory sheeters may have a diameter of three inches, or less, the consequences of increasing roll diameter on product quality may be significant.

The problem is further exacerbated by the fact that laboratory rolls usually run at slower speeds than plant rolls. Table 12.18 illustrates the effect of roll speed on relative pressure development and work input, assuming the dough exhibits a flow index of 0.5.

When one recognizes that both the effects of increased speed and diameter may be encountered on scale up, and the laboratory baker's tendency to use an "infinite" number of reduction steps, the effect of scale up on product quality may be very significant indeed.

The question remains as to what must be done to avoid such a potentially disastrous situation. One solution, which unfortunately is not usually possible, is to approve a formula, or product, for full scale production only after testing at full scale.

A more realistic approach is to perform the following tests:

- Insist that the laboratory baker does not use an "infinite" number of reductions. This alone is not sufficient to ensure success.
- Test the effects of increased work input by collecting the dough and resheeting it a sufficient number of times to emulate the work input of the full scale plant. Unfortunately, this will not produce the same maximum pressures that will be observed on the full scale.
- Operate the pilot plant, for short bursts of time, at speeds which will produce pressure development and work input characteristic of the full scale. Success with this test would provide reasonable certainty of success at full scale. An unsatisfactory result would indicate that the product be reformulated for increased tolerance to sheeting.
- Build a pilot plant that has full diameter rolls and operates at full operating speeds. Reasonable, pilot scale, production rates may be achieved by making the pilot plant rolls much narrower than the plant rolls. Unfortunately, although this is the best approach, it may not be a realistic one. The cost of such a pilot plant sheeting system will approach the cost of the full scale system. Even if the cost of the pilot plant is not an issue, there are still several other problems with this approach. If the product is large, for example, pizza crusts, the minimum width of the pilot plant will still require unacceptably high pilot plant production rates. Finally, operating the pilot plant at high linear speeds could cause considerable difficulties with pilot plant equipment feeding, or being fed by, the high speed sheeter. For example, if all the pilot plant sheeter production is fed to a continuous oven, the pilot oven would have to be as long as the full scale oven. Thus, it may be necessary to discard most of the product to avoid these peripheral scale issues.

NOMENCLATURE

A   Jacket area
B   The gap at separation
B_b Relaxed thickness
B_0 The gap

C_f	Force correction factor for finite feed sheet for equal speed rolls (Equation 12.17)
C_p	Pressure correction factor for finite feed sheet for equal speed rolls (Equation 12.16)
Cp	Heat capacity
C_w	Power correction factor for finite feed sheet for equal speed rolls (Equation 12.18)
d	Percent weight deviation
E	Roll modulus of elasticity
E_m	Energy input per unit mass
F	Separating force
F(n)	Flow index factor for force calculation (Figure 12.38)
I	Roll/shaft moment of inertia
m	Power law consistency
M	Mass of dough
M_i	Mass of component
n	Power-law flow index
p_{max}	Maximum pressure developed between rolls
P	Power
P(n)	Flow index factor for pressure calculation (Figure 12.38)
Po(n)	Flow index factor for power calculation (Figure 12.38)
Q	Volumetric flow
Q_j	Heat transferred through jacket
R	Roll radius
R_i	Inside radius of roll
rr	Reduction ratio, ratio of feed thickness to gap
t	Mixing time
U	Average roll speed
u	Overall heat transfer coefficient
U_b	Sheet speed after relaxation/lapping
W	Roll width
W_b	Sheet width after relaxation/lapping
v	Velocity
y	Direction normal to flow
δ	Roll/shaft deflection
Δh_i	Change in enthalpy of a component
Δh_w	Heat of flour wetting
ΔT_{LM}	Log mean temperature difference
ΔU	Roll speed differential
τ	Shear stress

REFERENCES

Andrews, G., Copeland, J., Fairburn, N., French, F., and Zielsdorf, R., 1989, High speed dough mixing and mixers, *Am. Inst. Baking Tech. Bull.* XI(12).

APV, 199x, *TBX-2500 mixer and SBX stationary bowl mixers,* Brochure, APV Baker, Goldsboro, North Carolina.

APV, 1995, *Tweedy Mixing Systems,* Catalogue #3/95/BP/384/385/386, APV Baker, Peterborough, England.

Bloksma, A.H. and Bushuk, W., 1988, Rheology and chemistry of dough, in *Wheat Chemistry and Technology,* Vol. 2, Pomeranz, Y., Ed., American Association of Cereal Chemists, St. Paul. MN.

Brazinsky, I., Cosway, H.F., Valle, C.F., Clark Jones, R., and Story, V., 1970, A theoretical study of liquid-film spread heights in the calendering of Newtonian and power law fluids, *J. Appl. Polym. Sci.* 2:2771–2784.

Bushuk, W., Kilborn, R.H., and Irvine, G.N., 1965, Studies on continuous-type bread using a laboratory mixer, *Cereal Sci. Today* 10(8):402–405.

CMC America, 1994a, *"Duo-Flex" Universal Double Arm Mixers,* Brochure #5a, Champion Machinery Co., Joliet, Illinois.

CMC America, 1994b, *Spiral Dough Mixers,* Brochure #5d, Champion Machinery Co., Joliet, Illinois.

Contamine, A.S., Abecassy, J., Morel, M.-H., Vergnes, B., and Verel, A., 1995, Effect of mixing conditions on the quality of dough and biscuits, *Cereal Chem.* 72(6):516–522.

Cooper, M., 1994, Personal correspondence with the Adamatic Division of the Hobart, Co., Eatontown, N.J., November.

D'Appolonia, B.L. and Kunerth, W.H., 1984, *The Farinograph Handbook,* American Association of Cereal Chemist, St. Paul, MN.

Doerry, W., 1955, *Baking Technology,* Vol. 1, Breadmaking. American Institute of Baking, Manhattan, KS.

Feillet, P., Fevre, E., and Kobrehel, K., 1977, Modification of durum wheat protein during pasta dough sheeting, *Cereal Chem.* 54(3):580–587.

Formo, M.W., 1979, Physical properties of fats and fatty acids, in *Bailey's Industrial Oil and Fat Products,* Swern, D., Ed., John Wiley & Sons, New York.

Fortman, K.L., Gerity, A.B., and Diachuk, V.R., 1964, Factors influencing work requirement for mixing white bread dough, *Cereal Science Today* 9(7):268–272.

French, F.D. and Fish, A.R., 1981, High speed mechanical dough development, *Bakers Digest.* 55(5):80–82.

Harper, J.M., 1981, *Extrusion of Foods,* Vol. 1, CRC Press, Boca Raton, FL.

Hazelton, J.L. and Walker, C.E., 1994, Changes in mixograms resulting from variations in shear caused by different bowl pin sizes, *Cereal Chem.* 71(6):632–634.

Hlynka, I., 1962, Influence of temperature, speed of mixing, and salt on some rheological properties of dough in the farinograph, *Cereal Chem.* 39:286.

Hobart, 199x, From manufacturer's brochure, Hobart mixers … choice of the food service and bakery industry, The Hobart Company, Troy, Ohio.

Kilborn, R.H. and Tipples, K.H., 1972a, Factors affecting mechanical dough development. I. Effect of mixing intensity and work input, *Cereal Chem.* 49(1):25–47.

Kilborn, R.H. and Tipples, K.H., 1972b, Factors affecting mechanical dough development. II. Implication of mixing at a constant of energy input, *Cereal Chem.* 49(1):48–53.

Kilborn, R.H. and Tipples, K.H., 1973, Factors affecting mechanical dough development. III. Mechanical efficiency of laboratory mixers, *Cereal Chem.* 50(1):50–69.

Kilborn, R.H. and Tipples, K.H., 1974, Implications of the mechanical development of bread dough by means of sheeting rolls, *Cereal Chem.* 51(5):648-657.

Kilborn, R.H. and Tipples, K.H., 1981, Device senses changes in dough consistency during dough mixing, *Bakers J.* 1981(April/May):16–19.

Launay, B. and Bure, J., 1973, Application of a viscometric method to the study of wheat dough, *J. Text. Stud.* 4(10):82–101.

Levine, L., 1983, Estimating output and power of food extruders, *J. Food Proc. Eng.* 6:1–13.

Levine, L., 1985, Throughput and power of dough sheeting rolls, *J. Food Proc. Eng.* 7:223–228.

Levine, L., 1991, Fundamentals of rolling and sheeting of doughs, *Activities Rep. R&D Assoc.* 44(1): 262–227.

Levine, L., 1995, A model for the sheeting of dough between rolls operating at different speeds. Paper presented at the Conference of Food Engineering (COFE), November, 1995, Chicago, IL.

Levine, L. and Boehmer, E., 1992, The fluid mechanics of cookie dough extruders, *J. Food Proc. Eng.* 15:169–186.

Levine, L. and Drew, B., 1990, Rheological and engineering aspects of the sheeting and laminating of dough, in *Dough Rheology and Baked Product Texture,* Faridi, H. and Faubion, J.M., Eds., Van Nostrand Reinhold, New York.

Levine, L. and Rokwood, J., 1986, A correlation of heat transfer coefficients in food extruders, *Biotechnol. Prog.* 2(3):105–108.

Manas-Zloczower, I. and Tadmor, Z., 1994, *Mixing and Compounding of Polymers, Theory and Practice,* Hanser Publishers, Cincinnati, OH.

Mani, K., Eliasson, A.-C., Lindahl, L., and Tragardh, C., 1992, Rheological properties and bread making quality of wheat flour doughs made with different dough mixers, *Cereal Chem.* 69(2):222–225.

Matz, S.A., 1992, *Bakery Technology and Engineering,* Van Nostrand Reinhold, New York.

Menjuivar, J.R., 1990a, Fundamental rheological properties of model cookie and cracker doughs. Paper read at the 75th Annual Meeting of American Assoc. of Cereal Chemists, Abstr. No. 33.

Menjuivar, J.R., 1990b, Fundamental aspects of dough rheology. in *Dough Rheology and Baked Product Texture,* Faridi, H. and Faubion, J.M., Eds., Van Nostrand Reinhold, New York.

Middleman, S., 1997, *Fundamentals of Polymer Processing,* Wiley, New York.

Mitchell, T.A., 1984, Dough mixer controls for the mechanical dough development process, *Proceedings of the International Symposium on Advances in Baking Science and Technology,* Kansas State University, Manhattan, KS.

Mohsenin, N.N., 1980, *Thermal Properties of Foods and Agricultural Materials,* Gordon and Breach Science Publishers, New York.

Moline, 199x, *Spiral Mixers,* Bulletin, 573, 574, The Moline Company, Duluth, MN.

Moss, H.J., 1980, Strength requirement of doughs destined for repeated sheeting compared with those of normal doughs, *Cereal Chem.* 57(3):195–197.

Oh, N.H., Seib, P.A., and Chung, D.S., 1985, Noodles. III. Effect of processing variables on quality characteristics of dry noodles, *Cereal Chem.* 62(6):437–440.

Okos, M.R. and Choi, Y., 1986, Thermal properties of liquid foods — review, in *Physical and Chemical Properties of Food,* Okos, M.R., Ed., American Society of Agricultural Engineers, St. Joseph, MI.

Peerless, 1985, *Stationary Bowl High Speed Mixer,* Brochure #SBHS-10-85-1000, Peerless Manufacturing Corp., Sydney, Ohio.

Pyler, E.J., 1988, *Baking Science and Technology,* Vol. 2, Soslund Publ., Meriam, KS.

Raghavan, C.V., Chand, N., Babu, R.S., and Rao, P.N.S., 1995, Modeling of the power consumption during sheeting of dough for traditional Indian Foods, *J. Food Proc. Eng.* 18:397–416.

Rask, C., 1989, Thermal properties of bakery products, a review of published data, *J. Food Eng.* 9:167–193.

Russell-Eggitt, P.W., 1975, Dough consistency control, *Bakers Dig.* 49:31–35.

Rykaart, 1994a, *High Speed Mixer*, Brochure, Rykaart Inc., Hamilton, Ohio.

Rykaart, 1994b, *Universal Mixer for the Bakery,* Brochure Rykaart Inc., Hamilton, Ohio.

Shigley, J.E., 1977, *Mechanical Engineering Design,* McGraw-Hill, New York.

Skeggs, P.K. and Kingswood, K., 1981, Mechanical dough development — pilot scale studies, *Cereal Chem* 58(4):256–260.

Stenvert, J.L., Moss, R., Pointing, G., Worthington, G., and Bond, E.E., 1979, Bread production by dough rollers, *Bakers Dig.* 53(4):22–27.

Uhl, V.W. and Gray, J.B., 1967, *Mixing Theory and Practice,* Vol. 2. Academic Press, New York.

Valentas, K.J., Levine, L., and Clark, J.P., 1991, *Food Processing Operations and Scale Up,* Marcel Dekker, New York.

Vidal-Quintanar, R.L. and Walker, C.E., 1994, Absorption and rpm effects on mixing parameters as determined by a prototype 2-gram direct-drive recording dough mixer, *Nat. Notes* 1(2):2–5.

VMI, 199x, *Twin spiral mixers,* Brochure, VMI Inc., Cranberry, New Jersey.

Watanabe, Y. and Nagasawa, S.J., 1968, A study of the rheological properties of noodles by means of relaxation testing, *J. Food Sci. Tech. Nihon Shokukin Kogyo Dakkai-Shi.* 15(10):466–468.

Werner and Pfleiderer, 1993, *ZPM Continuous Dough Mixing System,* Catalogue #03 080/2-2.0-VIII.93 KODO, Stuttgart, Germany.

White, J.L., 1990, *Twin Screw Extrusion, Technology and Principles,* Hanser Publishers, New York.

Wilson, A.J., 1992, Measurement of work input in industrial mixers, *Proc. 42nd RACI Cereal Chemistry Conference.*

Wooding, A.R., Martin, R.J., Wilson, A.J., and MacRitchie, F., 1994, Effect of sulphur-nitrogen treatments on work input requirements for dough mixing on second season, *Proc. 44th RACI Cereal Chemistry Conference.*

Wooding, A.R. and Walker, C.E., 1992, Comparison of alternative recording mechanism for the 35 and 10 gram mixographs, *Cereal Chem.* 69(3):249–253.

Yacu, W.A., 1985, Modeling of a twin screw extruder, *J. Food Eng.* 8:1–21.

13 Cost and Profitability Estimation

J. Peter Clark

CONTENTS

13.1 INTRODUCTION

Estimating capital and operating costs, and their impact on profitability, are probably among the most common tasks of the food engineer, yet often these tasks are performed in the relative absence of context. This chapter aims to provide practical techniques and information along with a discussion of the business context for such estimates and evaluations.

Much of the existing engineering economics literature, some of which is cited in the references, focuses on elaborate techniques for evaluating and comparing alternatives. Other texts, especially in chemical engineering plant design, provide methods for estimating capital costs of chemical and petrochemical plants, but little has been published on the estimation of food plants. There is a scarcity of relevant data and fewer commonalities among such plants, as compared with their chemical counterparts. Where generalizations can be made, this chapter will provide them, but usually the details of each case must be determined specifically.

One major intent of this chapter is to provide the practicing food engineer with an understanding of how his or her project will be evaluated by financial analysts so that he can anticipate the information required. Another objective is to provide some specific information that will aid in preparing preliminary estimates.

13.2 NATURE OF THE BUSINESS ENTERPRISE

The primary concern of the firm, private or public, is to survive. This means, in the simplest terms, that it must somehow generate enough money to pay its obligations in a timely manner, otherwise it will be dissolved and its assets sold. The most common way to generate money is to sell goods or services at prices that exceed their cost. Other sources of money include borrowing, selling shares of ownership, and selling assets. These are illustrated in Figure 13.1.

Expenses include the direct cost of goods, salaries, and wages of employees, interest on debt, taxes, rents and various other expenses. The difference between money flowing in from sales and money flowing out for expenses is profit, a portion of which may be shared with the owners (shareholders) as dividends and the balance retained for reinvestment in the business.

Depending on the business involved, some form of asset is usually required to generate the goods or services sold. This might include a manufacturing plant, a distribution center, a fleet of sales trucks, an inventory of seasonal raw material and finished goods, money in the bank, and intellectual property such as patents and trade marks. When the business was established, some investment was needed to acquire the initial assets before they could begin to produce sales. As the business operates, tangible assets wear out and need to be replaced. If the business is to grow, as most try to do, additional assets need to be acquired. Maintenance and growth require money, obtained from the retained earnings not distributed to the owners, when possible, or from other sources if necessary, including debt and selling additional equity (or ownership).

Modern corporations can be very complex in their financial structure, but at their core, this simple model describes them correctly. Money is needed to start; those who provide this investment expect to earn a profitable return. Their return can be in the form of an income stream from dividends and/or from an increase in the value of their ownership, often reflected in the increase in the price of a share of stock. Thus, once survival is assured, a very important secondary concern of any business is to enhance value.

Value may be reflected in the market price of publicly traded stock, in calculated book value or in cash flow, depending on the business and its ownership structure. In theory, stock prices reflect the present value of future cash flows to the owners, often estimated as earnings per share. In practice, the actual price of a stock is affected by supply and demand, by opinions about the economy, and by opinions about potential changes in future earnings of the firm.
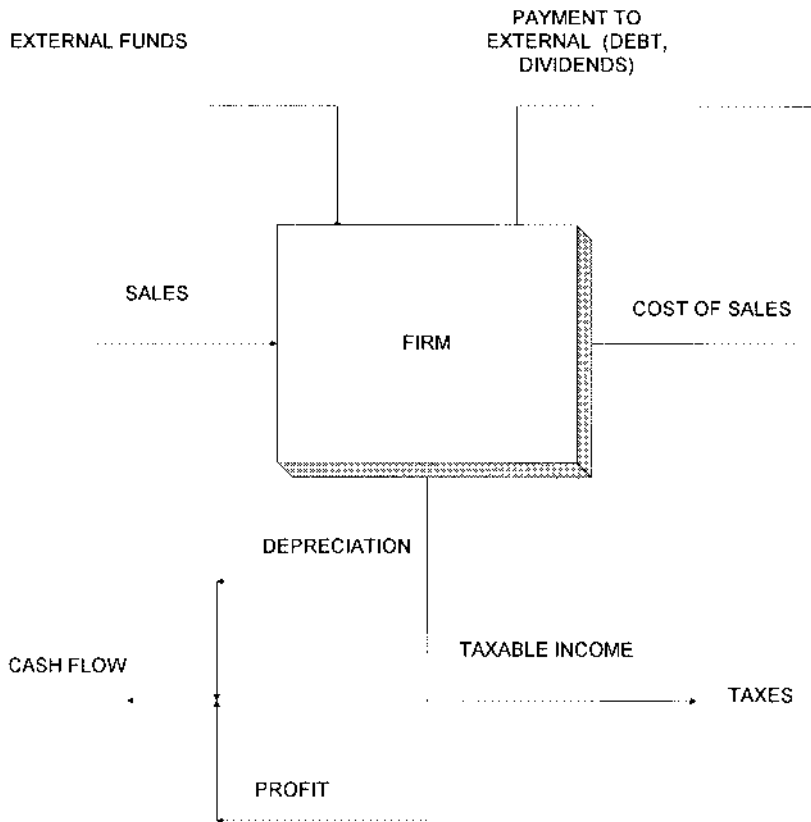
FIGURE 13.1 Flow of funds in a firm.

Companies which are believed to be capable of rapid growth often are valued more highly than those seen as more stable. Growth companies often achieve their results: by retaining a higher portion of earnings, sometimes paying no dividends at all; by assuming relatively high debt loads, thus acquiring assets more quickly than profits alone would permit; and by operating in relatively new fields, such as technologies and/or markets less well known and, therefore, riskier.

More stable corporations, such as most major food companies, have stocks which usually pay dividends, a reasonable balance between debt and equity in their financial structure, and reasonably predictable earnings, all of which lead to stock values which tend to grow steadily but reliably over time. The ultimate reason we care about capital and operating cost estimates is to help allocate the funds available for investment so as to increase the value of the firm, no matter how it is realized.

Cash is the lifeblood of business, hence it is critical to survival and value enhancement. Thus most evaluation techniques depend on estimating the cash impact of investments. Cash is defined as the net flow of money into the firm after taxes are paid; it is the difference between money received from sales and money paid out for expenses and taxes. Money received from financing (debt and equity) is not income and that paid for assets is not part of expenses. These are transactions that make it possible to generate cash, but they do not contribute directly to cash flow. One exception occurs when evaluating capital projects — cash paid out is included in computing net present value for comparison purposes.

Summarizing, cash flow is the most critical element in the health of a business and so all the techniques discussed in this chapter involve the estimation of cash flows and their

TABLE 13.1
Cost Distribution for Several Food Plants

Category	Plant A	Plant B	Plant C
Site	3.5	4.1	2.2
Building	25	30.8	29.8
Process Equipment	33.1	20.8	37.8
Equipment Installation	23.7	31.1	21.4
Other	2.5	2.8	2.4
Engineering	12.1	10.4	6.4
Total	100	100	100

Note: Costs presented are as percent of total cost. Plant A is a large pet food plant (1991). Plant B is a medium sized food ingredient plant (1992). Plant C is a large ice cream plant (1989).

proper comparison. Positive cash flow enables a company to survive and to enhance its value to its owners. Investments are made to generate positive cash flows or to avoid negative flows. Capital and operating cost estimates are made to help choose the best investments. The best investments, as we shall see, are those that generate the highest net cash flows when properly compared over time.

13.3 CAPITAL COST ESTIMATION

Capital cost estimation for food plants is an inexact art. This section will describe some of the techniques that can be used in the absence of complete data and, drawing upon several sources, will provide some rules and "sanity checks".

There are many systems for categorizing project cost, most of which have been developed for the convenience of contractors and builders. Because these systems are widely used among engineering and construction companies, there are data on the building portion of food plant projects collected in some detail. Unfortunately, the building portion of a project is rarely more than 30 to 40% of the total cost; the balance, as seen in Table 13.1, is process equipment, installation, engineering and other costs. Table 13.2 shows the range of building costs for food plants according to one standard code of accounts. These costs are calculated as dollars per square foot ($/ft^2) and were collected for the U.S. in the late 1980s. (Methods to adjust costs for changes in time and location are discussed later.)

Appendix 13.1 lists the data typically required in a food plant project. Rarely are all of these data available initially; often there are complex evaluations needed before certain decisions can be made, and these can impact cost significantly. Nonetheless, it is possible to describe a general approach to food plant design which permits early evaluation of feasibility and identification of critical elements.

13.3.1 COMPONENTS OF THE FOOD PLANT
TO BE INCLUDED IN THE ESTIMATE

The typical components of a food plant are included the following sections. Sections 13.3.1.1 through 13.3.1.10 are intended to be a form of checklist for preparation of a capital and operating cost estimate. Specific detail of the relevant process and packaging system must be added in each case and then costs should be assembled for every item.

TABLE 13.2
Building Costs for food Plants

	Plant A	Plant B	Plant C
Sitework	5.98	13.33	9.80
Concrete	17.40	6.44	37.03
Masonry	1.33	1.60	.94
Metals	24.98	11.27	4.35
Carpentry	.15	.42	.64
Moisture protection	4.71	7.38	2.65
Doors, windows	7.23	2.77	2.39
Finishes	1.66	3.73	3.39
Specialties	.35	.20	.28
Building equipment	.55	.89	3.58
Furnishings	.01	0.00	0.00
Special construction	16.14	3.66	1.19
Building transportation	.93	0.00	1.17
Mechanical	24.15	32.83	19.33
Electrical	11.32	19.82	10.90
Total	116.89	104.35	97.65

Note: Costs given in $/ft². Plant A is a large breakfast cereal plant (1990); Plant B is a large pet food plant (1989); and Plant C is a large breakfast cereal plant (1989).

13.3.1.1 Raw Material Receiving and Storage

Food raw materials are often perishable, usually are variable in properties, frequently are contaminated with soil and microorganisms because of their agricultural origin, and often are seasonal in supply. All of these characteristics distinguish food plants from other manufacturing and contribute to costs.

13.3.1.2 Packaging Material Receiving and Storage

Packaging materials including containers, such as cans and bottles, may be made on-site or purchased; in any event, they must be received, stored (sometimes in controlled environments), and delivered as required to a use point.

13.3.1.3 Processing Equipment and Facilities

Each food process is unique, but many have in common the elements of mixing, forming, cooking, and preserving. Mixing may involve solids with solids, solids and liquids, and liquids with liquids. Foods usually are non-Newtonian in their physical properties, often are viscous and sticky, and may be sensitive to shear. Forming may involve depositing by weight or volume, extruding, compressing, dicing, slicing, laminating, molding and other special operations. Cooking usually involves direct or indirect heating to change flavor, water content, color, and texture. Finally, preserving may involve heating before or after packaging, freezing, chilling, chemical sterilization, or irradiation.

13.3.1.4 Material Handling

Material handling is a significant cost in most food plants. While it is not a unit operation, it can have a significant impact on material properties. For example, many food solids are

fragile and can be broken by pneumatic conveying or transfer from one belt conveyor to another. Pneumatic conveying is used for many particulate solids, such as flour, sugar, salt and cereal grains. Dense phase conveying is more gentle than dilute phase, and permits the transfer of sugar without creation of fines. Belt conveyors are common in the food industry, but must use materials which can be easily cleaned. Screw conveyors and drag conveyors are more complex mechanical devices which can handle some sticky and pasty materials, such as ground meat, and cake mixes.

13.3.1.5 Packaging

Many food products are sold in relatively small consumer packages and so must be dispensed by weight or volume into some form of package. Primary packaging includes pouches, cans, bottles, and paper or film wrappers. Secondary packaging includes closures for containers, labels, and cartons. Tertiary packaging includes cases, paper wrapped bundles, and trays. Finally, most tertiary packages are stacked on wooden or plastic pallets and shrink or stretch wrapped for convenience in distribution.

13.3.1.6 Utilities

Food plants use all the usual factory utilities, but a few deserve special attention. The "usual" utilities include: electricity, steam, water (which must be potable), compressed air and fuel (often natural gas, because of its cleanliness).

Vacuum, refrigeration, and sanitizing chemicals are common in food plants and less so in other factories. Vacuum systems are often used for dry cleaning of plants in which dust is generated. Such dusts can harbor insects if the vacuum system is not designed correctly, and can also be explosion hazards. Vacuum is also used for pneumatic transport of food powders.

Refrigeration is common in food plants and may be based on ammonia, fluorocarbon, or another refrigerant. Costs, operating efficiencies, and ease of maintenance used to be the deciding factors in this choice, but the recent ban on manufacture of certain familiar refrigerants, because their release to the atmosphere is believed to damage the ozone layer, has complicated the issue. There are few good substitutes for the long-used fluorocarbons, and those that exist are expensive and unproven so far. Most new plants that need large amounts of refrigeration for freezing, chilling, and cold storage will probably use ammonia-based systems.

Finally, most food plants are designed with centralized clean-in-place (CIP) systems in which dilute caustic, dilute acid, detergent and sanitizer solutions are supplied to use points and returned to storage tanks. Concentrated cleaning materials are stored in special tanks, often of fiberglass because they can be corrosive, in special rooms equipped with alarms and special drains. The dilute solutions are made up in stainless steel tanks and heated and circulated as needed.

13.3.1.7 Environmental Controls

Food plants generate relatively large quantities of liquid and solid wastes which normally are biodegradable, but may be quite strong and may require special provisions for disposal. For example, many food wastes are useful as animal feeds and so may be given or sold to local farmers. This will require safe and sanitary storage facilities. Liquid wastes almost always will exceed fat, oil, and grease (FOG) levels set by local water treatment authorities (often as low as 100 mg/l) and so a food plant, at a minimum will need a grease trap or dissolved air flotation system. Biological oxygen demand (BOD) levels will also almost always be above "expected" levels, which usually are based on average sanitary sewage levels of about

200 mg/l. However, food wastes are usually easily treated and so, for the payment of a surcharge, most food plants can arrange for proper disposal of their liquid waste. In this case, flows and concentrations must still be monitored, for computation of the fee, and the plant should be designed and operated so as to minimize its liquid waste generation.

Air emissions control has not traditionally been a major concern for food plants, but is becoming more so. Examples include volatile organic carbon (VOC) standards imposed by the federal Clean Air Act in many areas which require bakeries to incinerate the stack gases from their ovens because of the ethanol content from bread and cracker fermentation. Odors of roasting coffee and cocoa have been found offensive, requiring special controls, in some areas. These issues are discussed to help make even a preliminary cost estimate more comprehensive and complete, because early oversight of one or two such cost factors can lead to very nasty surprises later.

13.3.1.8 Building

A food plant may require a new, expanded, or modified building, or some combination of all three. Modifying buildings is fraught with potential surprises and so more difficult to estimate accurately. Some of the issues in building cost include: demolition (an aspect of site preparation), special provisions for construction during on-going operation (especially relevant in an expansion or modification), the base building (floors, walls, ceiling, structural support, insulation), heating ventilation and air conditioning (HVAC) which usually includes any refrigeration, lighting, electrical system, plumbing, fire protection, and permitting. Permitting can become especially time consuming, especially in other countries and some parts of the U.S.

13.3.1.9 Engineering and Construction Fees

Some allowance for these fees must be included even if they are believed to be included in a "lump sum" or other arrangement. There are costs incurred by the owner for his own engineering and supervision which are properly attributed to a project for accounting and tax purposes, as will be discussed further. Outside engineering and construction firms charge fees under various contractual terms, but for estimating purposes, design fees of about 10% are common and construction fees are usually 3 to 5%.

13.3.1.10 Contingency

Contingency is a controversial topic in cost estimating. Part of the controversy involves differences of opinion over what is meant by contingency and, therefore, how much should be allowed for it. The position of this chapter is that contingency is a line item in a cost estimate (or budget, which is what often becomes of estimates!) which is intended to account for errors in the other elements of the estimate. It therefore reflects the precision of the estimate, which is generally a function of the engineering effort invested, the time allowed and the data available.

Contingency in an estimate or budget is *not* intended to cover changes in scope, "acts of God", or other extraordinary circumstances, such as the failure of a supplier. Because such events do occur, project managers often like to attempt some form of protection for their budgets. Such protection should not be confused with the contingency intended to protect the accuracy of the estimate. Sometimes it is called the owner's account, intended to allow some scope flexibility. To comply with internal practices and policies, portions of the "true" contingency and the owner's discretionary account may be buried (that is, not listed explicitly) in published estimates, but when this is done, it should be recognized what the real values are.

13.3.2 Procedures and Techniques for Estimates of Individual Items

There are various procedures and techniques for making estimates of the individual items. Which procedure or technique is appropriate depends on the time and money available, the level of detailed data available, and the purpose of the estimate. In declining order of both accuracy and effort, the various approaches are listed in Sections 13.3.2.1 through 13.3.2.5 which follow.

13.3.2.1 Firm Quotes from Suppliers, Vendors and Contractors

The biggest risk with this approach is the possibility of missing something in the estimate, e.g., freight or insurance on a piece of equipment, or having some error in the design, which requires a field change to correct. If one assumes a reasonably complete design, firm quotes from reputable suppliers and contractors, and no unusual surprises, then an estimate compiled from this data should be accurate within ±5% *as long as it includes a proper contingency*! (Contingency and risk are discussed again later.)

13.3.2.2 Quantity Take-Offs and Unit Costs

Many automated cost estimating systems make this approach appear simple, because they include standard models of time and material requirements for standard equipment installations, e.g., pumps and heat exchangers. However, comparable models do not exist for most specialized food processing equipment, and so the estimator's judgment is more critical. For building cost estimates, quantity take-offs depend solely on the accuracy of available drawings and their degree of detail. If the dimensions of the building are correct, then calculation of the wall, roof, and floor areas should be correct.

Unit costs are usually well known for any given geographic area and so building costs can be estimated fairly well *provided the location is specified*! Thus building costs based on a good drawing and a specified location can be estimated within ±10% from quantity take offs and unit costs. Equipment costs are more problematic and depend heavily on the estimator's skill and experience. Reliance on automated systems may be misleading, though they can help identify required data, such as labor rates by craft in a prospective geographic area.

13.3.2.3 Factored Estimates Based on Major Equipment and Correlations

It has long been a rule of thumb in the chemical process industry that chemical process plants are about 4 to 5 times the cost of the major pieces of equipment. This correlation arises because such plants involve much piping and instrumentation and relatively simple equipment. Food plants involve more complex equipment, often made from stainless steel, and relatively little piping and instrumentation (though that is changing somewhat). Thus there is no well-established factor to convert major equipment to total installed cost for food plants. Taking equipment alone, it appears to represent 20 to 30% of the total cost, which would imply a factor of three to five. This is too large a range to be very useful.

13.3.2.4 Square Foot Costs Based on Prior Experience

While factoring from major equipment has little basis for confidence, it turns out that there is a surprising agreement among many food plants in their average square foot costs. Roughly, large (over 100,000 ft^3), new food plants in the late 1980s and early 1990s cost about \$300/ft^3, of which about \$100 was for the building and \$200 was for installed equipment, with fees included. The actual range of costs experienced was about ±15% (\$250 to 350) and because of other uncertainties in any specific case, accuracy of an estimate based on size and these

values would be ±30%. However, it is one of the faster ways to make an estimate and, in many cases, the precision can be improved by applying proprietary information from similar facilities, when available.

13.3.2.5 Ratio Estimates Based on Sales or Production Volumes

It turns out that the sales to assets ratio of the food industry averages about two to five, depending somewhat on the segment of the industry and very much on the age of the plant. New plants in high margin segments can have ratios near 1.0; old facilities in low margin segments may be over 4.0. Another ratio that can be calculated from available data is the average cost per ton of annual capacity. This ranges from $400 to $2400, with the higher value for relatively dry products such as cereal, and the lower value for relatively wet products, such as ice cream. These few values have such large ranges that, in the absence of additional facts, they are useless for cost estimating. However, they can serve as "sanity checks" on estimates made other ways. Over time, an experienced estimator collects such ratios and learns how to apply them in his or her own area of expertise.

13.3.3 A RECOMMENDED APPROACH TO CAPITAL COST ESTIMATION

13.3.3.1 Define Components of Estimate

Thoroughly define the production capacity, process, raw materials, packaging, and growth philosophy. Each of these deserves discussion. The production capacity is heavily dependent on some forecast of market demand, usually made by the marketing department. In the case of a new product, this can be especially difficult to do accurately. Even in the case of existing products, demand can be so sensitive to price that a single projection is meaningless. An engineer responsible for preparing a cost estimate for a proposed plant or project must understand the basis for any volume assumptions and insist that the forecast include a range and not just a single number. Often plants will be described in terms such as cases per year, tons per day, bottles per minute or pounds per hour. It is important to distinguish between instantaneous and average rates. Each is important and needs to be specified, but they are distinctly different. In addition, both rates can be sensitive to product mix in a multiproduct plant, which most food plants are. Because costs can be sensitive to rate and scale, it is usually necessary to prepare more than one estimate for various extremes of the forecasted volume.

An important element of plant capacity is hours of operation. Many food plants operate three shifts per day, 5d/week, but some of this time is commonly lost to cleaning and sanitizing. Others operate for longer weeks, and some have learned to reduce lost time for cleaning through careful design and operation. The assumptions about operating time may be dictated by company policy or tradition, but the conscientious engineer will challenge any such assumptions which appear to increase costs unnecessarily. The most successful companies now say that 7 d/week and 24 h/d is 100% of time available; any reduction from this must be justified.

The process must be described in words and in process flow diagrams which is the fundamental language of the process engineer. Based on the previously established average and instantaneous rates, a material, energy, and pressure balance must be prepared. This requires that specific choices be made for most, if not all, pieces of equipment. There can be no "black boxes" and, preferably, few, if any "generic" pieces of equipment, because it is very difficult to accurately estimate costs for unspecified food processing equipment. This is in contrast with some other process industries where good correlations exist for the costs of heat exchangers and vessels based on their area, weight, or other easily calculated properties. Costs for food processing equipment can vary widely among suppliers and, more importantly, performance can vary even more.

Clearly, the procedure must be iterative — choices must be made, their consequences determined, and then new choices made until costs and performances have been thoroughly explored and conditions found that satisfy the requirements of the exercise.

Raw materials must be specified including: means of delivery, physical and chemical properties, sensitivity to storage conditions and time, costs, and any special requirements such as cleaning, fumigating, or variation in properties. As with several other key variables, ranges rather than single values must be provided to reflect the natural variability of most food raw materials. Yields need to be estimated on the basis that raw material as purchased is 100%. Allowances for losses made during estimating should not be confused with allowances created in typical standard cost accounting systems. In fact, it is the position of this chapter that there should be no allowances for losses in standard cost systems, because these tend to become crutches. When 100% is the ideal it is easier to see the relation between actual performance and costs. For estimating purposes, a material balance must be constructed and some yield assumed. Again, a range should be created so as to test sensitivity to extremes.

Packaging for the final product must be specified, along with the source, properties, and range of variability of all the materials used. Some packaging material is vulnerable to humidity and must be stored carefully; all food contact material must be treated as a potential food ingredient and protected from contamination. Conventional dry storage may not be adequate. The specific choice of packaging equipment can have significant impact on cost, performance, and rate of the entire facility.

Finally, assumptions need to be made about the growth philosophy of the proposed facility, including whether it will ever expand (most plants expect to, but some may be unable), how much preinvestment is appropriate and what constraints may apply. Appendix 13.1 lists some additional data that are useful, indeed essential eventually, but which can be deferred for a while.

13.3.3.2 Prepare Block Flow Diagrams

Prepare block flow diagrams of process and overall material flow. Material flow in a food plant dictates layout and, hence, space requirements. It also has a profound effect upon efficiency of operation, constructability (especially in an existing facility), sanitation and safety. All of these affect cost. From a block flow diagram and material flow diagram, a preliminary building layout can be prepared.

13.3.3.3 Prepare Block Building Layout

Prepare block building layout to establish space requirements, adjacencies, and to help define personnel and material flow. There is a distinction between a block building layout and a building design. As discussed previously, an adequate building cost estimate can be prepared so long as the size is approximately correct; a block building layout can provide that information. Space is one of the most useful characteristics of a food plant — allowances in the early stages should be generous because almost always the understanding of equipment requirements and sizes is inadequate. For some reason, equipment always seems to proliferate and grow in size as a project progresses, so it is best to make generous allowances for access and separations in equipment layouts.

13.3.3.4 Establish Equipment List

Establish an equipment list including utility requirements, status (new, existing, rebuilt, used), source, cost, installation cost, and identifying name or number. Conventional spread sheets and data bases work well for equipment lists. Some software packages link directly to computer aided design and drafting packages to create lists from layouts and maintain accurate information as changes are made. The exact format is less critical than the establishment of

TABLE 13.3
Typical Equipment List for Food Plant

Item	Description	Quantity	Cost	Source
T-3403	SS Tank, 375 Gal	1	$5000	Tri-City Fabricators
A-3402	Agitator, 10% solids suspension, .33 HP	1	4400	Chemineer
P-3403	Recycle pump, centrifugal 50 GPM, 3 HP	1	2500	Goulds
W-3401	Weigh belt feeder, 800-7800 lbs/hr .33 HP	1	17,590	CST Auto

TABLE 13.4
Capital Cost Estimate

Major equipment	
Process	$20,000
Packaging	6,000
Installation	10,000
Building	11,000
Site	2,000
Engineering	4,500
Contingency	13,400
Total	$66,900

the needed information and the maintenance of it consistently throughout a project. Table 13.3 is an example of a simple equipment list.

13.3.3.5 Prepare Preliminary Estimate

Prepare a preliminary capital cost estimate using the best data available and present in table form (See Table 13.4). Calculation of the percentage each major category represents of the total is another useful sanity check. It is risky to create the dollars from the percentages, as the ranges in actual cases can be quite broad.

13.4 OPERATING COST ESTIMATES

Operating cost estimates are dependent on the specifics of the product, process and corporate practices. The major elements of operating costs are

1. Raw materials
2. Packaging materials
3. Energy
4. Labor
5. Depreciation
6. Indirect costs

It is usually best to calculate operating cost on an annual basis and then relate it to other time periods and to units of product. One of the critical variables in any calculation of operating costs is yield of finished product against raw material and of finished packages against packaging

TABLE 13.5
Typical Operating Cost
($/year) Applesauce

Raw material	
Apples 5 ton/h	$750,000
Sugar 365 kg/h	49,640
Packaging materials	
Cans 8761	876,100
Boxes 365	54,750
Energy	
Fuel oil 300 l/h	120,000
Electricity 500 kW	50,000
Water 10 m³/h	10,000
Rented equipment	75,000
Labor, 15 people	150,000
Depreciation	94,000
Indirect costs	100,000
Total	2,329,490

For 8,761,000 cans/year, average cost is $0.266/can.

Based on data from Bartholomai, A., Ed., 1987, Food Factories — Processes, Equipment, Costs, VCH, Weinheim, Germany.

material. Labor and energy are typically small components of food processing operating costs, but they are always important. Depreciation is discussed in detail later. Briefly, it is an accounting allowance, treated as a cost for tax purposes, but representing a positive cash flow. In principle, it is allowed to permit recovery of the investment cost in capital assets, and thus is calculated as a fraction of the initial capital cost. An example of a relatively simple calculation of operating cost is shown in Table 13.5.

Operating costs are a major, but not the only, component of cash flow. Other components include:

1. Sales and distribution
2. Marketing
3. General administrative
4. Taxes
5. Insurance

Some of these costs can be very high in the food industry. For example, sales and distribution of route delivered products, such as bread, cake, and fried snacks may be 40% of the wholesale price, because of commissions paid to driver/sales people and the high costs of operating a large fleet of delivery vehicles. Other foods, delivered in trailer trucks to supermarket warehouses are much less expensive to distribute. Usually the values of these items are known or specified for a particular case, often as corporate averages.

A brief discussion on accounting is appropriate here. Traditionally, costs not directly associated with manufacture have been allocated by some formula, for example as a percentage of sales or on a per capita basis of direct labor. Thus if a company has a sales force that costs $10 million per year and total sales of $100 million per year, they would say that sales costs are 10% of product sales and use that figure in a new product estimate.

There also is the implication that the cost of selling is the same fraction of income for all products. In reality, this is not true, and the somewhat lazy assumption can be misleading. Most companies have products that represent a large fraction of volume and others that represent a small fraction. This unequal distribution is often described by the "80–20" rule, which says that 80% of sales volume comes from 20% of the products. For some food companies, the disparity in contribution is much greater — cases in which 50% of the products contributed 99% of sales are known. Salesmen often joke, with some wisdom, that it is just as easy to sell a trailer load as to sell a case. In other words, the actual cost to sell high volume products is certainly less than the corporate average (expressed as percent of sales) and the cost to sell low volume products is higher than the average. Correcting this simplification requires activity-based accounting of costs and relies on the improved information resources now available.

For the engineer doing a preliminary estimate, the recommendation is to try and generate realistic cost allowances for the indirect costs *as if activity based accounting were practiced.* This may provoke some controversy in some firms, and may not be permitted for formal estimates, but it will clearly show that the engineer is enlightened and might catalyze the transformation of the firm's thinking.

For example, in an estimate of cash flow from a new product, the engineer could assume that the incremental cost of the new product in the marketing department would be 50% of a product manager and the equivalent of one person in sales. Their annual salaries would be charged as costs to the new product, rather than some average percentage of sales. The difference is subtle, but important.

Between the price paid by consumers and the income realized by the manufacturer, there are some additional costs which do not affect the manufacturer's cash flow except to help define the net income. These include

1. Retailer's margin (often about 30% of wholesale)
2. Distributor's margin (if there is one)
3. Returns
4. Discounts and promotions, if not included elsewhere

Net profit after taxes is net income minus all costs. Cash flow is net profit after taxes plus depreciation. There are many other terms used in firms and the literature to describe various measures of business success (profit before tax (PBT), profit after tax (PAT), gross profit, net profit, gross income, net income, and many others) but most are confusing and ambiguous; as previously mentioned, cash flow is the most significant measure of health and is, therefore, the only measure that matters here.

An example of the unit cost elements for a typical food product is given in Table 13.6. In this case, the selling price is predetermined (by competition or some other means) and profit is found by difference. In other cases, the task may be to determine a selling price, given a desired unit profit. Other permutations are obviously possible.

13.5   COMPARISON OF ALTERNATIVES

Alternative investment opportunities are compared by putting them on a common basis of value, namely the net present value of all future cash flows. This involves adjusting future cash flows, whether income or expenses, to a common point in time using a discount rate. The calculations are relatively simple and are now performed routinely by spreadsheet programs for personal computers and even hand held calculators. The critical factor in the calculation is the selection of the discount rate. This is a strategic decision, usually made by the finance department of a corporation.

TABLE 13.6
Unit Cost Structure for a Typical Food
Product (Applesauce)

Raw material and packaging	74.3%
Energy	7.7
Labor	6.4
Indirect costs	4.3
Depreciation	4.0
Other	3.3
Total direct costs	100
Sales and distribution	15
General and administrative	10
Total plant cost	125
Selling price	137.5
Unit profit	12.5
Taxes (@43%)	5.4
Unit profit after tax	7.1
Cash flow	11.1 ($0.03/can)

Data from Table 13.5.

The fundamental concept is that money can earn more money by earning interest over time, for example by putting it in a common savings account, buying a bond from the U.S. government or investing it in some other vehicle. Thus a dollar today is equivalent to a dollar plus the interest it could earn a year from now and that sum plus additional interest in 2 years, and so forth. In equation form:

$$FV = PV * (1+i) ** n \qquad (13.1)$$

where, FV = future value; PV = present value; i = interest rate, expressed as fraction per unit time; n = time period, consistent units, e.g., years. This is the familiar concept of compounding of interest. The interest rate is replaced by a discount rate in computing present values of future cash flows, and the equation is rearranged:

$$PV = FV/(1+i) ** n \qquad (13.2)$$

Present values are additive, and so Equation 13.2 provides a way to compare projects in which future cash flows may vary with time. When comparing projects, those with the highest net present value, for any given discount rate, are best. Net present value is simply the sum of all future cash flows discounted to time zero. Time zero is usually taken to be when the initial capital investment is made, which is a negative cash flow. Future cash flows may be positive or negative. When the discount rate is selected correctly, any project providing a positive net present value is acceptable, *assuming funds are available.* The most common situation in a corporation is a limited supply of funds and the desire to maximize value. In this case, that combination of projects should be identified which yields the highest net present value at a given discount rate.

Factors which influence the discount rate include:

1. Return available from safe investments, such as Treasury bills and high grade corporate debt.
2. The cost of borrowed money, usually related to the prime rate, which is published as that rate which major banks charge their most creditworthy customers. The actual cost to most corporations is slightly higher.
3. Degree of perceived risk from various factors, such as inflation, uncertainty in the market, political stability, and competition. The higher the perceived risk, the higher the discount rate is set, so as to screen from consideration projects with insufficient potential reward to compensate for the risk.
4. Desired rate of return on investment, often called the hurdle rate.

In practice, the finance department will generally set, as a matter of strategy, a discount rate to be used for analysis of projects under various circumstances. In most cases, only projects with positive net present values, using the appropriate discount rate, are considered for investment. Those with the highest values generally have the highest priority.

Ironically, misuse of this analytical approach can have effects the opposite of those intended. Most corporations have a goal of maximizing value to the owners by maximizing growth in earnings and cash flow. When this goal is translated to too high a discount rate, emphasis in investing is focused on relatively short term, low risk projects at the expense of larger, potentially more valuable projects, from a long-term viewpoint. A counter argument can be made that the more valuable projects should show their value somehow, but often it is a matter of strategic judgment and even faith that induces a firm to invest for the long term. Thus selection of the discount rate (or rates) to be used in corporate analysis of investment opportunities is a serious task with profound implications.

Another measure of value often used for comparative purposes is the internal rate of return (IRR). This is the value of the discount rate for which the net present value of all cash flow is zero. It is found by trial and error calculation. The IRR permits the ranking of alternative projects by relative rates of return regardless of size (which can influence net present value because larger projects usually have larger cash flows), but it has several faults as an analytical technique. There are some, admittedly unusual, patterns of cash flow which give multiple values of the IRR. It can give rankings which are different from those using net present value. Since net present value represents accurately the contribution to value of the firm of a given project, rankings by it are correct, and so IRR is unreliable. Nonetheless, many firms still use it, so it may be prudent to calculate it when necessary.

There are other measures of return, including payback time and simple annual return on investment, which provide no new information and are overly simplistic. It is not recommended that they be used to evaluate alternative investments. For completeness, the usual definitions are noted. Payback time is found by dividing initial investment by annual cash flow to find the time at which the investment is repaid. If annual cash flow is variable, as it often is, this "simple" measure becomes more complex and still does not really help in ranking choices. Annual return on investment (ROI) has many variations (before or after tax, cash flow or profit, average or varying), which contributes to its ambiguity and reduces its usefulness. In general, ROI is found by dividing some measure of return, for example profit after tax, by initial investment and expressing the result as a percentage. In principle, this can be compared to other potential returns, as discussed with regard to the discount rate. However, since returns are rarely constant year to year, the number is relatively meaningless.

The exception to selecting projects on the basis of net present value concerns projects critical to survival but not directly contributing to enhancement of value, namely "nondiscretionary" projects, such as those required to conform to environmental, human safety, product safety, or quality requirements and regulations. These projects may not appear to contribute directly to profits (except in the form of avoided fines) and so will not normally

provide high net present values. However, the same techniques can be used to compare alternative solutions on a rigorous basis. In most cases, nondiscretionary projects have first call on available capital over the most attractive profit-making projects because failure to conform with environmental or safety regulations may mean the collapse of the firm.

13.6 ADJUSTMENTS OF ESTIMATES FOR TIME

There are a number of published cost indices which permit adjustment of estimates made at one point in time to another. These include the Engineering News Record, Marshall and Stevens, Nelson refinery and Chemical Engineering plant construction index. There also are several specialized cost indices. Jelen (1970) presents a good discussion. Each index is constructed of a weighted combination of material and labor costs thought to be representative of the overall cost of relevant projects. A given year is arbitrarily designated to have an index value of 100 and all other years are related to it as a ratio. Thus correction of an estimate accurate for 1 year to another is accomplished by multiplying by the ratio of the indices for the 2 years. There is no comparable index for food plant construction, and the indices that might be thought appropriate vary considerably among themselves. Thus an estimator must find by experience the adjustment that works best for his or her organization and experience. One suggestion is to use the Engineering News Record building index for the building and the Marshall and Stevens index for equipment, because it includes installation costs in its calculation.

13.7 DEPRECIATION

As previously mentioned, depreciation is a contributor to positive cash flow allowed by tax law to recover the cost of tangible and some intangible property used in business. It is calculated by spreading the initial cost across some allowable recovery period. A company may have a different strategy for treating depreciation for tax purposes and financial performance reporting. The correct approach to use in project evaluation will be specified by company policy. In the absence of direction to the contrary, straight line depreciation over 10 years will be close for comparative purposes.

There are accelerated means of depreciation, which, thanks to the time value of money, increase net present value, but reduce apparent profit. In practice, most companies will use these allowable means to reduce payment of taxes, but the complications do not significantly enhance project evaluation. If the difference in method of computing depreciation makes a difference between acceptance or rejection of a project, then it probably should be rejected, because the uncertainty in most estimates is larger than the small difference in net present value created by using accelerated depreciation.

13.8 COMPARING PROJECTS WITH UNEQUAL DURATIONS

The concept of a perpetuity is helpful in analyzing circumstances where service lives are different, or in comparing investments with different time spans. A perpetuity is a constant annual payment generated forever (in perpetuity) by a single investment at a given interest rate. For purposes of comparison, the interest rate chosen is the cost of money, or the specified discount rate, and the net present value of all future cash flows of the various cases is the investment, or present value. The equivalent annual payment is simply

$$A = PV * i \qquad\qquad (3)$$

The ratio of A to the initial investment gives the perpetuity rate of return (PRR) which can be used to rank alternative investment choices without the potential errors of the IRR (Howe 1991).

The capitalized annual cost is a closely related technique for choosing among alternative equipment with different service lives. The concept is to compare the amount of money that would be invested at a given rate of return to allow replacement at the end of the respective service lives. The choice with the lower capitalized cost is preferred, assuming no impact on operating cost and no effect of inflation. (These can be introduced if desired.) The equation is

$$S = W * \left((1+i) ** n\right) \Big/ \left(\left((1+i) ** n\right) - 1\right) \qquad (13.4)$$

where, S = capitalized cost; W = replacement cost; n = service life; and i = discount or interest rate. See Valle-Riestra (1983) for a more detailed discussion.

13.9   RISK AND CONTINGENCY

Risk and contingency deserve separate discussion because misunderstandings in these areas are responsible for more errors than any other aspect of cost and profitability estimating.

All projects and estimates involve some degree of risk. These include:

1. The risk of requesting too little capital and then requiring more, being unable to complete the project (because there is no more money), or suffering severe embarrassment and career jeopardy in the process of obtaining more funds.
2. The risk of estimating the cost of a good project so high that it fails to pass a financial hurdle and does not proceed, when in fact it should have. In this case, the firm misses an opportunity to earn cash.
3. The risk that in the course of construction, events occur that increase costs even though the original estimates were accurate, absent untoward events. This has the same effect as estimating too low, though perhaps with less onerous consequences for the parties involved (because it is understood that events were probably beyond control).
4. The risk that events will occur that lengthen the schedule, postponing the generation of income. In light of the time value of money, this can have severe effects on the net present value even if the costs and income are exactly as estimated (See Valentas et al. 1991). The delay of a project by 1 year, all else being equal, changes the net present value at 10% from $80,000 to $72,700, using the example in Valentas et al., page 40. In reality, costs will almost always escalate if a project is delayed, making the effect of schedule slippage even worse.
5. The risk that the process will not work as intended, for example that yields are lower than expected. Such events are departures from the assumptions made in the estimation of operating costs and profit.

To account for these risks, estimators use contingencies, as previously mentioned. Contingency is an allowance in a capital cost estimate to cover errors in the estimate and some, *small*, schedule slippage or untoward event. It is not meant to cover significant changes in scope, major schedule changes, or major untoward events. Properly prepared estimates need to define clearly what sort of contingency is included and what assumptions have been made. The less detailed information that is available, in the form of drawings, specifications, and process performance, the more likely errors will occur in the estimate and that a generous contingency will be absorbed. As detail becomes available, with further design effort, the contingency allowance can be reduced. No experienced estimator of capital costs will ever allow it to be zero. Studies have shown that even as projects are 95% complete there can be a 5% error in projections of final cost! (Merrow et al. 1981)

TABLE 13.7
Recommended Contingency Factors

Conceptual/Preliminary Design	25%
Basic Engineering Complete	
Building	10%
Process/Packaging	15%

A common error, leading to over-estimation of project costs is the compounding of contingencies. This can occur, for example, in computing unit product costs, when a contingency allowance appears in the capital cost estimate (which contributes to the depreciation account) and then another contingency is applied to the estimate of unit cost.

The components of a capital cost estimate are often estimated by individual disciplines, for example electrical engineering, process engineering, and mechanical engineering. Each may implicitly or explicitly include their own safety factor. These are contingencies. If another factor is applied to the overall estimate, it may inflate the cost unnecessarily.

Recommended contingency factors are given in Table 13.7 for different classes of projects encountered in the food industry.

13.10   SUMMARY

Cost and profitability estimating must be understood in the context of the corporation and its requirements for survival and growth of value. Capital costs are estimated and evaluated in order to select those best investments which will add the most to corporate value. Value is measured as the present value of future cash flows generated by the investment. This requires understanding of how sales or savings are generated, and making accurate assumptions about performance, efficiency, and productivity. It is critical to perform sensitivity analyses on any estimate, recognizing that most assumed values will fall within some range. The extremes as well as the "most likely" value should be tested.

Food plants cost about $300/ft^2 fully equipped (in the late 1980s and early 1990s). Food products, on the average, have about 70% of their cost in raw materials and packaging, and about 10% each in labor, energy, and other charges, including depreciation. Specific cases may vary widely, but these rules of thumb can serve as "sanity checks" for specific estimates.

FOR FURTHER INFORMATION

The Engineering Economist is an inexpensive journal which publishes scholarly research in the general area. It is published by the Institute of Industrial Engineers at 25 Technology Park, Norcross, Georgia 30092.

Bartholomai, A., Ed., 1987, *Food Factories — Processes, Equipment, Costs*, VCH Weinheim, Germany, is a compilation of food plant designs and cost estimates for a variety of mostly small installations. Some of the data are summarized in Appendix 13.2.

Several other texts on Engineering Economics which are good references but were not cited specifically include:

- Happel, J. and Jordan, D.G., 1975, *Chemical Process Economics* Marcel Dekker, New York.
- Holland, F.A., Watson, F.A., and Wilkinson, J.K., 1974, *Introduction to Process Economics*, John Wiley & Sons, New York.

Two references specifically on the economics of the food industry are:

- Connor, J.M. 1988, *Food Processing — An Industrial Powerhouse in Transition*, Lexington Books, Lexington, MA.
- McCorkle, C.O. Ed., 1988, *Economics of Food Processing in the United States*, Academic Press, San Diego, CA.

REFERENCES

Howe, K.M., 1991, Perpetuity rate of return analysis, *Eng. Econ.* 36(3):248-257.

Jelen, F.C., Ed., 1970, *Cost and Optimization Engineering*, McGraw-Hill, New York.

Merrow, E.W., Phillips, K.E., and Myers, C.W., 1981, *Understanding Cost Growth and Performance Shortfalls in Pioneer Process Plants*, RAND Corporation, Santa Monica, CA.

Moresi, M., 1984, Economic study of concentrated citrus juice production, in *Engineering and Food: Processing Applications,* Vol. 2, McKenna, B.M. Ed., Elsevier, England.

Valle-Riestra, J.F., 1983, *Project Evaluation in the Chemical Process Industries*, McGraw-Hill, New York.

Valentas, K.J., Levine, L., and Clark, J.P., 1991, *Food Processing Operations and Scale-Up*, Marcel Dekker, New York.

APPENDIX 13.1
BASIC DATA REQUIREMENTS

RAW MATERIALS

Listing of all raw materials
Composition of major raw ingredients
Form in which received — size, shape, volumes, weights
Anticipated yields for major raw ingredients
Delivery methods — truck, rail, other
Sourcing for major raw ingredients
Inventory control levels
Quality control requirements
Any special receiving, handling, or storage needs

CONTAINER AND PACKAGING MATERIALS

Containers

Listing of all finished product package descriptions
Listing of all container requirements by type, size, shape, volume, weight
Form in which containers are received — pallet, cased
Delivery method — truck, rail
Inventory control levels
Quality control requirements

Packaging Materials

Listing of all packaging materials including
Cartons
Cases
Films

    Overwraps
    Glues
    Labels
    Other

Provide data as indicated above for containers. Note any known special receiving, handling, or storage requirements for containers and packaging materials.

MANUFACTURING OPERATIONS

Listing of current and future manufacturing operations
Block flow diagrams of manufacturing operations
Annual production by manufacturing operation
Operating schedule by manufacturing operations — days per year, shifts per day, hours
    per shift
Line rates and efficiencies
Estimated times for
    Cleanup
    Changeover
Listing of equipment for each manufacturing operation with utilities
Line layout and equipment drawings and specifications, if available
Quality control requirements
Identification and description of waste streams

PACKAGING OPERATIONS

Listing of present and future packaging operations
Description of finished goods — size, form, weight, volume
Products per case
Case size and weight
Cases per pallet
Pallet size and weight
Quality control requirements
Identification and description of waste streams

WAREHOUSING

Inventory level by product
Physical inventory turns per year
Distribution of products
    Received from this facility
    Received from other facilities
Load stacking heights
Activity distribution per:
    Pallet
    Tier
    Case
Operating methods
    Number of operating shifts
    Unitization methods
    Rail and truck activity

APPENDIX 13.2
Summary of Cost Data for Food Plants

Process	Total cost ($)	Area (ft²)	Equipment cost ($)	Raw (TON/H)	Finished (TON/H)	Source[a]
Apple processing	2,923	20,000	2,006	5	4	
Cannery	204	1,500	123	5	4.8	
Fruit puree	1,100	5,000	782	4	3	
Multi purpose fruit		1,000	402	3	2.4	
Orange juice	2,057	20,000	1,116	20	1.6	
Baby food	200	3,000	184	6.6	5.5	
Tomato paste	1,837		1,087	15	2.5	
Frozen vegetable	1,350	30,000	852	4.8	2.2	
Mushroom farm	116	60,000	41		0.04	
Mozzarella cheese	842	15,000	350	5.6	0.7	
Blue cheese	4,093	113,000	2,908	11.5	2.1	
Dairy	13,530	70,000	6,400	20.8	18.1	
Modular dairy	1,210	10,000	760	2	2	
Powder milk	4,000	15,000	2,835	18	1.7	
Dried whole egg	2,287	12,000	1,357	2.5	0.25	
Yogurt	4,828	85,000	3,477	8	8	
Ice cream	2,515	17,000	1,530	2	2	
Parboiled rice	1,379	6,000	1,004	5	5	
Corn starch	30,298	24,000	14,169	8.3	5.3	
Pasta	2,353	20,000	1,760	0.73	0.71	
Precooked lasagna	3,261	11,500	2,305	0.7	0.67	
Tofu		1,440	350	0.38	1.32	
Baker's yeast	26,550	80,000	11,049	2.5	1.14	
Vinegar	750	3,750	525	0.033	0.31	
Quenelles	985	3,500	600	0.66	0.66	
Tortilla chip	1,688	9,500	1,270	0.5	0.55	
Corn snacks	310	5,000	131	0.18	0.27	
Catfish	2,400	12,000	1,040	3.2	1.8	
Shrimp	431	6,000	204	0.5	0.25	
Surimi	10,000	115,000	6,080	15	5.7	
Cattle slaughter	3,660	52,000	930	40	16	
Coextruded sausage	2,000	10,000	1,049	1	1	
Protein recovery	2,671	10,000	1,972	12	6	
Soybean oil extraction	24,900	25,000	6,200	42	42	
Vegetable oil refinery	2,359	10,000	1,456	2	1.8	
Pan bread	2,803	28,000	1,795	1.5	2.2	
Arabic bread	1,272	10,000	702	1.2	1.7	
Half-baked frozen baguette	1,953	10,560	1,228	0.48	0.54	
Seawater desalination	18,433	1,100	9,262	3,100	417	
Fruit juices	809	7,240	514	2	2	
Soymilk		3,150	910	0.15	1	
Orange juice concentrate	2,424		890	20	1.5	
Sausage	10,323		3,219	1	1	Clark (1982)[b]

Note: Total cost, building area, equipment cost, raw material rate, and finished product rate are provided for a number of case studies. Most are from Bartholomai 1987 and are said to represent costs in 1986.

[a] Bartholomai (1987) unless otherwise noted.
[b] Author's data from 1982 adjusted to 1986.

14 Simulation and Optimization

Enrique Rotstein, Julius Chu, and I. Sam Saguy

CONTENTS

14.1   INTRODUCTION

Simulation is short for mathematical simulation. It implies a mathematical model that behaves on paper as a reasonable approximation of the corresponding real-life system. Simulation is a powerful Food Engineering tool. It allows running different scenarios on paper, without consuming raw materials or wasting products. It does not operate on real time and it can use whatever time scale is appropriate to the objective of the simulation. While it is mathematically based, the engineer can select the appropriate level of approximation. In other words, the model requirement is that it works not that it is mathematically sophisticated.

Simulation may be used for many reasons: understanding the behavior of complex interactive systems, predicting operation results, developing process control systems or optimizing the performance of a system. Optimization is the process by which a set of operating parameters is found that will result in maximizing (or minimizing) the objective of the

optimization. For instance, one may want to minimize cost or maximize profit; reduce a certain undesirable impurity, or maximize content of a particular ingredient.

14.2 COMPUTER SIMULATION

Computers have empowered food engineers and made the mathematical contents of a simulation task readily available. It is now common to work in a PC environment, using tools that go from a spreadsheet where a model is built from scratch to software packages of various degrees of sophistication.

Computer simulation is widely used in the chemical and petrochemical industry, both to design processes and to improve existing operations (Dimian, 1994). The efforts to model processes using computational methods started in the late 1950s and evolved in comprehensive flowsheeting packages (Perkins, 1990). These packages are made of a block of generic models of unit operations and balance equations and a block of physical properties of chemical mixtures. The two blocks interact to describe changes along a flow description of the process being considered.

The application of the above packages to the food industry has been scarce. They provide at best a framework for modeling and simulation but they lack specific functionality. Most of the food processing unit operations are not included. With a few exceptions, *ASPEN PLUS* and *SPEEDUP* (Perkins, 1990), they do not allow for solid processing operations. Importantly, the state of the art in knowledge and mathematical representation of physical and equilibrium properties of food materials is well behind what one finds in materials that are the focus of the above packages.

14.3 FUNDAMENTALS

14.3.1 MODEL FORMULATION

Section 14.3.1.1 below outlines a generic approach to simulation model building. These steps include several recommended essential steps. Successful modeling has two resource requirements that parallel the two levels of iterations that make up the modeling. First, modeling requires applying an array of statistical techniques to a data set. This is directed toward finding the model that best fits a given set of data and often requires examining various relationships between data and potential models, before a best fit can be chosen. Second, experiments can be run either to explore the process space or to confirm the best model. It is worth noting that fitting a model to data does just that; it does not fit to the phenomena (Rand, 1983; Saguy and Karel, 1987).

General considerations for experimental designs and data gathering are the data should cover the region of interest evenly; appropriate distinct data points should be gathered so that the model of the system is over determined; there should be replicates of the data; and no systematic lack of fit (residuals) should be observed.

14.3.1.1 Building a Process Simulation Model

1. **Define the problems**
   Simulation is used for problem-solving. The first step to build a model is to find out what exactly is the problem. We need to address and define its physical boundaries. Are we concerned with a specific operation? Is the problem local or global?
2. **Identify the objectives**
   We need to state the objectives of the model. If there are multiple objectives, how do we approach them? For instance, can we assign different weighting factors to evaluate them at the same time?

3. **Understand the system and collect data**

   Understand the overall system including a process, a manufacturing plant, or a business activity. While you are trying to understand your system, identify, specify, and collect the data you need for the model. This includes finding not only numerical data values but also mathematical formulas such as distributions for random events.

   It is extremely useful to consult previously published information on the theory that governs the phenomena investigated. If such theory is not available, one should be postulated and its validity tested during the verification step.

4. **Select software**

   Knowing the system and the nature of your data, you can select from a wide variety of software tools. (See Software, in this chapter.)

5. **Draw process flow diagram**

   Determine where information flows from one part of the model to the next and which parts need information simultaneously. The information can be as varied as material, flows, or resources, or cash flow, depending on the nature of your problem.

6. **Create a rough-cut model**

   Build your model, using simulation software as appropriate. Start a small and rough sketch of your model. Keep in mind that you can always go back to enhance it as needed. Try to avoid randomness at this time, it is important to check if your model is logically correct at this time. Using averaged data input. it can be easier to validate the rough model results.

7. **Verify and validate your initial results**

   Compare the results from your simulation model to what you intended or expected. Confirm that the model meets expectations. Verification is essential to ensure the validity of the model and/or theory. It should be always carried out by comparing the simulation results to an additional experimental data set not used in the model building.

8. **Refine the model**

   At this time, you can add randomness and other degrees of complication to better represent reality. Rerun the model with the modifications and obtain the results. Compare these results with real data, to verify the model is functional.

9. **Modify your base model with alternatives**

   After you feel comfortable with the reliability of the base model, you can start adding alternative scenarios and options, as required by the problem.

10. **Analyze results and draw conclusions**

    Draw conclusions from the model's results and make recommendations on how the system can change.

14.3.2 SIMULATION

From the standpoint of the scope, simulation (and its corresponding use in optimization) can be local or global. The first refers to focusing the task in a piece of equipment or even a part within a piece of equipment. The second addresses a system made of a number of pieces of equipment.

For instance consider a potato-flakes drying plant. The engineer may want to model the whole plant, from raw potato input to packaged product output. The objective could be, for instance, to analyze material losses of the whole operation for different raw material qualities and operating conditions. On the other hand, the task may be to localize the analysis focusing on drum drier performance.

The mathematical tools more commonly used are expressions of the conservation principle or balances. These balances can be made around total mass, mass of individual components, total energy, and momentum. Depending on the application, all or some of these

balances are used, unsteady or steady state is considered and appropriate state variables are selected. Empirical correlations are frequently used to tie variables. When steady state is selected, the operations can be reduced to sets of algebraic equations. When unsteady state is considered the solution involves numerical integration of differential equations.

14.3.3 OPTIMIZATION

Once a manufacturing venture has reached acceptable safety and production operational goals, the next goal is how to make the operation of the plant more profitable. This requires defining an optimization objective and the strategy and tactics to accomplish it. The engineer may pursue single or multiple objectives. Typical single objectives may be safety, profit, cost, minimal consumption of a scarce resource, or minimal amounts of a given effluent. Multi-objectives address a set of single objectives simultaneously.

In general terms, optimization involves determining the structure and operating conditions resulting in a highest (or lowest) value of the predefined objective. It addresses one or more variables. There is a large number of mathematical procedures designed to optimize manu-facturing systems. The stepping stone of an optimization effort is, in many cases, a dependable model resulting from a previous simulation effort. The degree of mathematical formalism depends on a practical balance between time, effort, and value of the results.

When a formal mathematical procedure is followed, the elements are:

- Design variables — These will include temperature, pressure, flow rates and the like.
- Equality or inequality constraints — Equality constraints are the fixed values variables will assume at space or time boundaries. Inequality constraints refer to upper or lower values of the variables that the system may approach at boundaries.
- Feasible solutions — These are values of the design variables within the constraints.
- Objective function — A function of the design variables that quantifies the desired result.

14.4 OPTIMIZATION PROCEDURES

There is a large number of optimization procedures, which continue growing as more interest is focused on the application. The optimization problem is to determine what values of the independent variables will result in an optimal value of a dependent variable. Two types of problems result

- Problems where the functional dependence is not known
- Problems where a functional dependence can be posed mathematically

When the functional dependence is not known, we use search procedures. When the problem can be mathematically posed, we have procedures of optimization by differentiation and programming methods, depending on the nature of the mathematical problem.

14.4.1 SEARCH METHODS

Search methods are numerical procedures based on defining the objective function at a starting set of values of the independent variables. A second set is then selected and the new value of the objective function is compared with the initial one. Comparison between these two values indicates whether or not the objective function is improving toward an optimum. Searches are simultaneous, when all sets of evaluation values are preselected. They are sequential when new sets of data are selected based on information from the previous sets

of data. Well-established search procedures include the golden section, Fibonacci, Lattice, Hooke, and Jeeves' direct search (Carnahan and Wilkes, 1973; Fletcher, 1987; Gill et al., 1981; Saguy, 1983a; Beightler and Wilde, 1967).

To highlight some of the optimization methods, the Appendix highlights the utilization of the vast resources readily available on the Internet. The Appendix includes an optimization tree that allows the reader to focus on the specific problem and find its definition, search methods, algorithm, case studies, and available software.

14.4.2 RESPONSE SURFACE

The response surface method (RSM) is based on fitting the dependent variable behavior to a suitable polynomial in the independent variables. The RSM method is based on the assumption that for n independent variables, the response is a function of the levels at which these variables are combined. The resulting response surface provides insight into the overall behavior and shows the existence of optimal regions (Myers, 1971). RSM simplicity, ease of application, and wide acceptability made this method one of the most utilized in food applications. It has a special value in new product development. Where a number of variables are modified (e.g., salt, sugar, acidity, oil, spice), RSM locates the optimum combination furnishing the most acceptable organoleptic and/or sensory attributes (Joglekar and May, 1991).

14.4.3 OPTIMIZATION BY DIFFERENTIATION

When the objective function is continuous and continuously differentiable and it is not at the region limit, the optimization can be done analytically. This implies solving a set of differential equations made of the first derivatives of the objective function with respect to each independent variable and following the usual mathematical procedures for maxima and minima (Dennis and Schnabel, 1983, 1989). Additional mathematical procedures include the use of Lagrange multipliers and variational calculus (Bertsekas, 1982; Saguy, 1983a).

14.4.4 PROGRAMMING METHODS

When the problem can be posed mathematically but the conditions for an analytical solution by differentiation are not met, programming methods are an option. Linear programming is used when the constraints and objective function are linear in the design variables (Noble and Daniel, 1977; Schrijver, 1986). Linear programming is also useful when the problem is nonlinear but could be adapted to meet the requirements (Saguy, 1988). Dynamic programming does not have this restriction. It is a multistage decision process that exploits system or information flow structure. It is especially useful in dealing with multistage processes (Bellman, 1957; Bellman and Dreyfus, 1962; Hadley, 1964; Nemhauser, 1966; Saguy, 1983b). The reader is advised to consult the Appendix for further details.

14.5 NEURAL NETWORKS

A relatively new tool, neural networks, offers an exciting potential for modeling, simulation, and optimization. In simple terms a neural network is made of an array of units each one of which outputs f(x) when receiving an input x, through a functional relationship

$$f(x) = 1 / [1 + e^{-x}] \qquad (14.1)$$

The units are called neurons, organized into layers. Bhagat (1990) described a "backprop net" particularly relevant to process engineers. Connections are made between neurons of adjacent layers so that a neuron receives information from the preceding layer and transmits

TABLE 14.1
Software Categories more relevant to Food Engineering

Biochemical engineering, pharmaceuticals
CAD/CAM, drafting
Data acquisition/management
Drying
Environment control, waste management
Equipment design
Expert systems
Fluid dynamics, particle dynamics, flow analysis
Graphics
Mechanical engineering
Network optimization: heat exchanger, separation
Physical and chemical properties
Process control, system analysis, automatic control, process measurement
Process design/simulation
Process economics, costing, investment analysis
Project and production management, scheduling, inventory, maintenance
Safety, material safety data sheets
Separation: absorption, distillation, extraction
Thermodynamics

output to each neuron in the next layer. The networks "learn" the behavior of a system when supplied with sets of data made of input and output values. Connection weights are updated during this process of exposure to data until the learned behavior meets expectations. At this point, it can be used as a predictive tool.

The potential for this tool is significant in particular when the application involves empirical relationships, or poorly understood or complex operations.

14.6 SOFTWARE

Modeling and simulation have become increasingly easier with the availability of software options. In turn, software is growing exponentially. Available software goes all the way from spreadsheets that provide a framework for simulation to programs that integrate a unit operations library with property data banks and mathematical capabilities. Examples of the latter are *ASPEN PLUS* (Aspen Technology, Cambridge, MA), *BATCHES* (Batch Process Technologies, West Lafayette, IN), and *SPEEDUP* (Aspen Technology). The limitation in using these packages is that property data banks for foodstuffs are still scarce.

There are an increasing number of software packages focused on specific applications, such as equipment design, drying, environmental control and waste management, fluid dynamics applications, mechanical design, process control, economics, separation process, and others. Probably the best review is the yearly *Chemical Engineering Progress Software Directory* (Lutta Simpson, 1996), issued with the January issue of CEP. The Directory covers 32 categories. Table 14.1 lists those categories which are more relevant to food engineering. It provides a short description of the scope of each packet in its most current version, its cost and details of processor, operating system, RAM and hard disk requirements. etc. The 1996 issue covered over 1600 programs and on-line databases, from more than 510 vendors in the U.S. and abroad.

Finally, there are a number of programs using building block approaches to model building. Many of these software packages are developed for general-purpose applications

ranging from a specific scientific analysis to modeling of various types of industries such as banking, transportation, manufacturing, etc. Examples are *SLAMSYSTEM* (Pritsker Corporation, Indianapolis, IN), *EXTEND* (Imagine That, Inc., San Jose, CA), and *TAYLOR II* (F&H Simulations, Inc., Orem, UT). For food engineering applications, these programs can be used to study material and process flow, batch or continuous process control, scheduling, man and machine interface, production system control, etc. However, because of their complexity, a modeler will spend a significant learning time before he/she can take full advantage of these simulation programs.

14.7 APPLICATIONS AND EXAMPLES

We will discuss applications that have proved popular in food engineering practice. For more examples, see Saguy et al. (1990).

14.7.1 RESPONSE SURFACE METHODS

We show two illustrative applications. One optimizes a high protein snack making process. The other optimizes quality of dehydrated potatoes.

Batistuti et al. (l991) studied the optimization of extrusion cooking of chickpea defatted flour to produce a high protein snack. The process was optimized for maximum value of expansion ratio and sensory rating of extrudates and minimum value of shear strength. They used a five level design and fitted the results to a second order polynomial

$$y = B_0 + B_1 x_1 + B_2 x_2 + B_{12} x_1 x_2 + B_{11} x_1^2 + B_{22} x_2^2 + E \qquad (14.2)$$

Where y is either expansion ratio or shear strength or sensory preference, x_1 = feed moisture, x_2 = temperature at the central zone of the barrel, E = experimental error. As an example, the experimental data showed that the expansion ratio y_1, is correlated by

$$y_1 = 2.676 - 0.367\, x_1 - 0.135\, x_2 - 0.081\, x_2^2 \qquad (14.3)$$

indicating that the snack expansion ratio decreases linearly with increasing feed moisture while a maximum can be observed as barrel temperature increases, consistent with the second order effect. Conditions for maximum or minimum can be identified by mathematical analysis or by inspection.

Mudahar et al. (1990) used RSM to optimize dried potato cubes quality. The objective was to obtain maximum rehydration ratio, puffing and water holding capacity, and minimum nonenzymatic browning. The process included blanching in water containing pectin and polydextrose, followed by a two-step drying procedure. The blanched potatoes were first dried in a batch-type high-temperature fluidized bed drier (HTFB) at varying experimental conditions. They were then finished in a tunnel drier at standard conditions.

The independent variables were HTFB drying temperature (T) and time (t), blancher biopolymers concentration (c) and time (b). Ranges were 135 < T < 155°C, 5 < t < 15 min, 0.5 < c < 1.5% and 2 < b < 6 min.

For each response variable a second degree polynomial equation was used.

$$y_k = B_{ko} + \sum_{i=1}^{4} B_{ki} x_i + \sum_{i=1}^{4} B_{kiii} x_i^2 + \sum_{i=1}^{3} \sum_{j=i+1}^{4} B_{kij} x_i x_j \qquad (14.4)$$

$$y_k = y_k \ (T, t, c, b)$$

Find effect of each processing variable on each response variable through analysis of variance.

Find optimal values of processing variables and optimal region through contour plots.
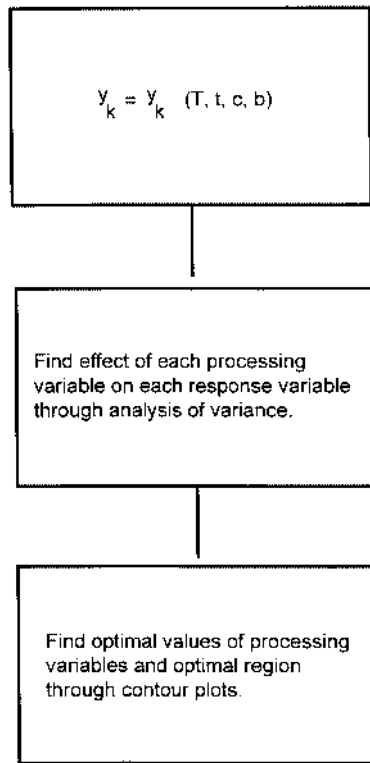
FIGURE 14.1 Searching for the optimal processing region.,,

TABLE 14.2
Effect of Processing Variables on Response Variables

Processing variables	Response variables			
	Rehydration ratio	Puffing	Water holding	Nonenzymatic browning
HTFB temperature	*			*
HTFB time	*	*		*
Blanching concentration			*	
Blanching time				

Note: * Indicates significant effect of processing variable on corresponding response variable.

where y_k is one of the above four response variables, x_i are the coded independent variables (T, t, c, and b) and B_{ko}, B_{ki}, B_{kii}, and B_{kij} are constant coefficients. Data were fit to the correlation using a statistical analysis computer package.

With the regression coefficients thus obtained, data were manipulated according to RSM as sketched in Figure 14.1. Analysis of variance indicated the effects shown in Table 14.2.

The values of processing variables determined to be optimum were T = 145°C, t = 10 min, c = 1.2%, and b = 4.5 min. Verification experiments confirmed optimality, although the actual value for nonenzymatic browning proved to be lower than predicted.

14.7.2 LINEAR PROGRAMMING AND QUALITY OPTIMIZATION

Reddy and Das (1993) showed an application of linear programming (LP) to quality optimization of potato chips. The objective function to be minimized was

$$\phi = M + O + \ln C \tag{14.5}$$

where M = weight percent of moisture content, O = weight percent of oil and C = the arithmetic summation of red, yellow, and blue color values.

LP can be used because the authors found linear regression equations describing the relationships between dependent and independent variables.

$$M = 192.42 - 0.426807\,\theta_f - 0.795\,T + 9.958\,b \tag{14.6}$$

$$O = 54.98 + 0.21156\,\theta_f + 0.398\,T - 4.904\,b \tag{14.7}$$

$$\ln C = 1.1619 + 0.00463\,\theta_f + 0.0178\,T - 0.1546\,b \tag{14.8}$$

Here, T = temperature, b = thickness, and θ_f = frying time. With constraints $145 < T < 185°C$, $1.5 \times 10^{-3} < b < 20 \times 10^{-3}$ m, $2 < M < 3$, $39 < O < 41$, $7 < C < 9$, $220 < \theta_f < 255$ s, they found that the optimal oil temperature should be 145 to 146°C and the frying time should be 220 to 222 s.

14.7.3 MAXIMIZING PROFIT IN APPLE JUICE MANUFACTURING

Bandoni et al. (1990) used inequality constrained LP to maximize profit in an apple juice concentrate manufacturing operation. The plant flowsheet is shown in Figure 14.2. The model variables are x_1, input of raw material, x_2, continuous presses disposed pomace, and x_h, amount of rehydrated water used in recovering juice from the continuous presses pomace. The soluble solids recovery shows a nonlinear dependence on x_h. The authors linearized this dependence by partitioning the equilibrium curve in eight linear segments, thereby replacing x_h by model variables x_3 through x_{10}. The objective function was

$$\phi = \sum_{j=1}^{10} s_j x_j - \sum_{j=1}^{10} c_j x_j \tag{14.9}$$

where s_j and c_j are sales prices and costs, respectively, associated with the corresponding variable x_j. The constraints of the problem were mathematical expressions resulting from mass balances, equipment capacities, and rehydrated pomace handling. The problem was posed allowing for parameters' uncertainty.

Solution of the problem indicates maximum profit for $x_1 = 4913$ ton/month and no disposal of pomace from continuous presses.

14.8   FOR FURTHER INFORMATION

Readers are encouraged to make use of computerized literature searches and the resources through their library resources and the vast capabilities of the Internet world-wide web (see Appendix). Usually an intersection of simulation, optimization, food product, and/or process yields rich and up-to-date applications. Do not hesitate to go beyond food products. The
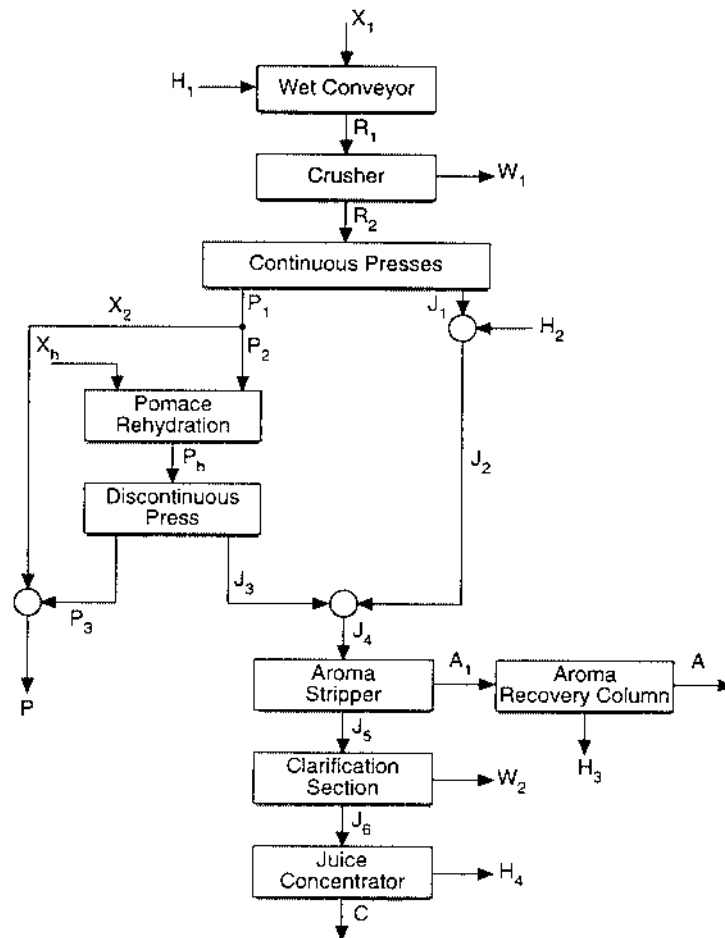
FIGURE 14.2 Flowsheet of the apple concentrate plant: A, aroma concentrate; A_1, head product from aroma stripper; C, juice concentrate (72 degree Brix); H_1, water absorbed in the wet conveyor; H_2, washing water of the continuous presses; H_3, water eliminated in the aroma recovery column; H_4, water elimated in the juice concentrator; J_1, juice from continuous presses; J_2, juice diluted from continuous presses; J_3, juice from discontinuous press; J_4, total juice from presses; J_5, juice stripped of its aroma; J_6, juice clarified; P, total pomace eliminated; P_1, pomace from continuous presses; P_2, pomace from continuous presses sent to re-hydration; P_3, pomace from discontinuous press; P_h, re-hydrated pomace; w_1, waste from mill; w_2, waste from clarification; x_1, processed apples; x_2, disposal pomace from continuous presses; x_h, re-hydration water.

literature of application to other industries, especially the chemical industry, in many cases can be applicable to the reader's problem.

In addition to the above-cited specific references, readers may want to expand their knowledge of linear and nonlinear programming techniques. These techniques have yet to be fully utilized in food engineering practice. Schrijver (1986) provides a good review of the theory of linear programming. Murtagh (1981), Palmer et al. (1984), and Saguy et al. (1990) review applications. Bazaraa and Shetty (1979) review the fundamentals on nonlinear programming. A good support reference is Minoux (1986).

On the general field of optimization, some good, thought-provoking discussions are found in Arora (1989), Biegler et al. (1988), Gill et al. (1981), and Morris (1982).

REFERENCES

Arora, J. S., 1989, *Introduction to Optimal Design*, McGraw-Hill, New York.

Bandoni, J. A., Romagnoli, J. A., and Rotstein, E., 1990, Optimization under uncertainty in inequality constrained linear programs, *Latin Am. Appl. Res.*, 20:189–202.

Batistuti, J. P., Cerdeira Barros, R. M., and Gomes Areas, J. A., 1991, Optimization of extrusion cooking process for chickpea (Cicer arietinum, L.) defatted flour by response surface methodology, *J. Food Sci.* 56(6):1695–1698.

Bazaraa, M. S. and Shetty, C. M., 1979, *Nonlinear Programming*, Wiley, New York.

Beightler, D. J. and Wilde, C. S., 1967, *Foundations of Optimization*, Prentice Hall, Englewood Cliffs, NJ.

Bellman, R. E., 1957, *Dynamic Programming*, Princeton University Press, Princeton, NJ.

Bellman, R. E. and Dreyfus, S., 1962, *Applied Dynamic Programming*, Princeton University Press, Princeton, NJ.

Bertsekas, D. P., 1982, *Constrained Optimization and Lagrange Multiplier Methods*, Academic Press, New York.

Bhagat, P., 1990, An introduction to neural networks, *Chem. Eng. Progress* 86(8):55–60.

Biegler, L. T., Grossman, L. E., and Reklaitis, 1988, Application of operation research techniques in chemical engineering, in *Engineering Design, Better Results through Operation Research Methods*, Levary, R., ed., North-Holland, New York.

Box, G. E. P. and Draper, N. R., 1987, *Empirical Model Building and Response Surface*, Wiley, New York.

Carnahan, B. and Wilkes, J. O., 1973, *Digital Computing and Numerical Methods*, Wiley, New York.

Dennis, J. E. and Schnabel, R. B., 1983, *Numerical Methods for Unconstrained Optimization and Nonlinear Equations*, Prentice Hall, Englewood Cliffs, NJ.

Dennis, J. E. and Schnabel, R. B., 1989, A view of unconstrained optimization, in *Optimization*, Nemhauser, G. L., Rinnooy Kan, A. H. G., and Todd, M. J., Eds., North-Holland, Amsterdam, 1–72.

Dimian, A., 1994, Use process simulation to improve plant operations, *Chem. Eng. Progress* 89:58–65.

Fletcher. R., 1987, *Practical Methods of Optimization*, 2nd ed., Wiley, New York.

Gill, P. E., Murray, W., and Wright, M. H., 1981, *Practical Optimization*, Academic Press, New York.

Hadley, G., 1964, *Nonlinear and Dynamic Programming*, Addison Wesley, Reading, MA.

Joglekar, A. M. and May, A. T., 1991, Product excellence through experimental design, in *New Product Development: From Concept to the Market Place*, Graf, E. and Saguy, I., Eds., Van Nostrand Reinhold (AVI), New York, 211–230.

Lutta Simpson, K., 1994, 1966 CEP Software Directory. A Supplement to *Chem Eng. Progress* 92:1.

Minoux, M., 1986, *Mathematical Programming*, Wiley, New York.

Montgomery, D. C., 1991, *Design and Analysis of Experiments*, Wiley, New York.

Morris, A. J., Ed., 1982, *Fundamentals of Structural Optimization: A Unified Approach*, Wiley, New York.

Mudahar, G. S., Toledo, R. T., and Jen, J. J., 1990, A response surface methodology approach to optimize potato dehydration process, *J. Food Process. Preserv.* 14(2):93–106.

Murtagh, B. A., 1981, *Advanced Linear Programming*, McGraw-Hill, New York.

Myers, R. H., 1971, *Response Surface Methodology*, 1st ed., Allyn and Bacon, Boston.

Nemhauser, G. L., 1966, *Introduction to Dynamic Programming*, Wiley, New York.

Noble and Daniel. 1977.

Palmer, K. H., Boudwin, N. K., Patton, H. A., Sammes, J. D., Rowland, A. J., and Smith, D. M., 1984, *A Model-Management Framework for Mathematical Programming*, An Exxon Monograph, Wiley, New York.

Perkins, J. D., 1990, Advanced computational methods for process modeling and simulation, in *Engineering and Food*, Vol. 1, *Physical Properties and Process Control*, Spiess, W. B. L., and Schuber, H., Eds., Elsevier, London.

Rand, W. M., 1983, Development and analysis of empirical mathematical kinetic models pertinent to food processing and storage, in *Computer-Aided Techniques in Food Technology*, Saguy, I., Ed., Marcel Dekker, New York, 71–90.

Reddy, G. V. and Das, H., 1993, Kinetics of deep fat frying of potato and optimization of process variables, *J. Food Sci. Technol. (India)* 30(2):105–108.

Saguy, I., 1983a, Optimization methods and applications, in *Computer-Aided Techniques in Food Technology*, Saguy, I., Ed., Marcel Dekker, New York, 263–320.

Saguy, I., 1983b, Optimization of dynamic system utilizing the maximum principle, in *Computer-Aided Techniques in Food Technology*, Saguy, I., Ed., Marcel Dekker, New York, 321–360.

Saguy, I., 1988, Constraints to quality optimization in aseptic processing, *J. Food Sci.* 53(1):306–307, 310.

Saguy, I. and Karel, M., 1987, Index of deterioration and prediction of quality losses, in *Objective Methods in Food Quality Assessment*, Kapsalis, J. G., Ed., CRC Press, Boca Raton, FL, 233–260.

Saguy, S., Levine, L., Symes, S., and Rotstein, E., 1990, Integration of computers in food processing, in *Biotechnology and Food Processing Engineering*, Schwartzberg, H. G. and Rao, M. A., Eds., Marcel Dekker, New York.

Schrijver, A., 1986, *Theory of Linear and Integer Programming*, Wiley, New York.

INTRODUCTION

The objective of this appendix is to illustrate by way of an example the wealth of optimization resources on the Internet. The step-by-step example will traverse through the NEOS-Network Enabled Optimization Center located at *http://www.mcs.anl.gov/home/otc*. A partial listing of internet resources including Usenet newsgroups pertaining to optimization is listed at the end of the appendix. The reader is encouraged to employ the varied internet search engines for specific optimization information.

NETWORK ENABLED OPTIMIZATION CENTER (NEOS)

The Optimization Technology Center (OTC) is a joint enterprise of Argonne National Laboratory and Northwestern University. The center is located at *http://www.mcs.anl.gov/home/otc*. The following are web pages at the NEOS site.
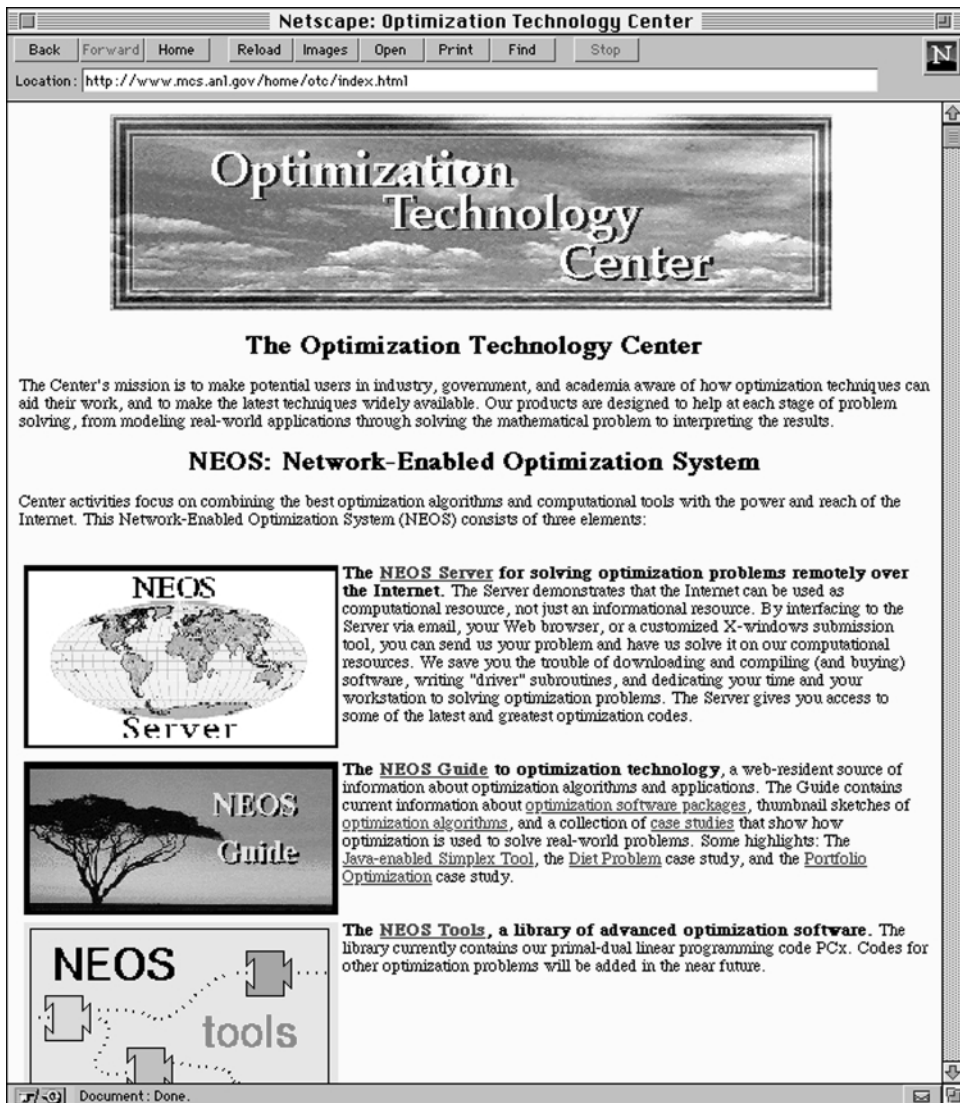
THE SERVER

Go to the *NEOS Server* if you have a problem ready to solve, or if you would just like to try it out and see how it works. The server uses a flexible combination of electronic mail, FTP, and web browser tools to allow you to remotely process your data on our computational resources. It relieves you of the burden of downloading and compiling software, writing "driver" subroutines, and dedicating your time and computational resources to solving the problems.

The NEOS Server uses the computational and algorithmic resources of OTC collaborators to solve optimization problems automatically with minimal input from the user. Users of the NEOS Server are able to solve optimization problems over the Internet with state-of-the-art optimization software without downloading and linking code.

The NEOS Server only needs a definition of the optimization problem; all additional information required by the optimization solver is determined automatically. Users with nonlinear problems, for example, can have derivatives and sparsity patterns determined automatically.

NEOS Server Information

- Current news and future developments
- NEOS submission tool
- Usage statistics
- Collaborators
- Funding

THE GUIDE

Go to the *NEOS Guide* (by clicking on the icon) if you have questions about optimization or its applications, or if you want information on the NEOS Library of software. This guide will help both novices and experienced users make informed decisions about how optimization technology can help you solve the problems that arise in your work. From simple examples to practical applications to straightforward explanations, it will guide you through the process of formulating your problems, selecting the appropriate software, and interfacing to it.

OTHER INFORMATION ABOUT THE OTC

The OTC is a joint enterprise of Argonne National Laboratory and Northwestern University. It was founded in 1994 with support from the U.S. Department of Energy and Northwestern University. You may reach this site by clicking on the OTC Home Page at the corner of the page.

The next step is reached by clicking on the NEOS Guide mark.

NEOS GUIDE TO OPTIMIZATION

Click on one of the Guide areas on the NEOS GUIDE or on the specific topic that includes

the *Optimization Tree*, the *Optimization Software Guide*, *Frequently Asked Questions, Case Studies, Test Problems, Search Utility, Applications of Optimization, Other Optimization-Related Web Sites,* or *Access Logs*.

...OR TRY ONE OF THESE OTHER OTC-AFFILIATED RESOURCES

The *NEOS Server* or the *Interior-Point Methods Online*.

CAN I START AGAIN IF I GET LOST?

Yes. You can get back to OTC home page or this page by clicking on one of the logos that appear at the bottom of the page.

Happy Searching!

Let us now move to the next site by *clicking on the Optimization Tree...*

Let us explore <u>What is Optimization</u>? by clicking on the last line.

Back | Forward | Home | Reload | Images | Open | Print | Find | Stop

Location: http://www.mcs.anl.gov/home/otc/Guide/OptWeb/opt.html

What is Optimization?

Optimization problems are made up of three basic ingredients:

- An **objective function** which we want to minimize or maximize. For instance, in a manufacturing process, we might want to *maximize the profit* or *minimize the cost*. In fitting experimental data to a user-defined model, we might *minimize the total deviation* of observed data from predictions based on the model. In designing an automobile panel, we might want to *maximize the strength*.
- A set of **unknowns** or **variables** which affect the value of the objective function. In the manufacturing problem, the variables might include the *amounts of different resources used* or the *time spent on each activity*. In fitting-the-data problem, the unknowns are the *parameters* that define the model. In the panel design problem, the variables used define the *shape and dimensions* of the panel.
- A set of **constraints** that allow the unknowns to take on certain values but exclude others. For the manufacturing problem, it does not make sense to spend a negative amount of time on any activity, so we constrain all the "time" variables to be non-negative. In the panel design problem, we would probably want to limit the *weight* of the product and to constrain its *shape*.

The optimization problem is then:

Find values of the variables that minimize or maximize the objective function while satisfying the constraints.

Are All these ingredients necessary?

Objective Function

Almost all optimization problems have a single objective function. (When they don't they can often be reformulated so that they do!) The two interesting exceptions are:

- *No objective function.* In some cases (for example, design of integrated circuit layouts), the goal is to find a set of variables that satisfies the constraints of the model. The user does not particularly want to optimize anything so there is no reason to define an objective function. This type of problems is usually called a *feasibility problem*.
- *Multiple objective functions.* Often, the user would actually like to optimize a number of different objectives at once. For instance, in the panel design problem, it would be nice to *minimize weight* and *maximize strength* simultaneously. Usually, the different objectives are not compatible --- the variables that optimize one objective may be far from optimal for the others. In practice, problems with multiple objectives are reformulated as single-objective problems by either forming a weighted combination of the different objectives or else replacing some of the objectives by constraints. These approaches and others are described in our section on multi-objective optimization.

Variables

These are essential. If there are no variables, we cannot define the obective function and the problem constraints.

Constraints

Constraints are not essential. In fact, the field of unconstrained optimization is a large and important one for which a lot of algorithms and software are available. It's been argued that almost all problems *really do* have constraints. For example, any variable denoting the "number of objects" in a system can only be useful if it is less than the number of elementary particles in the known universe! In practice though, answers that make good sense in terms of the underlying physical or economic problem can often be obtained without putting constraints on the variables.
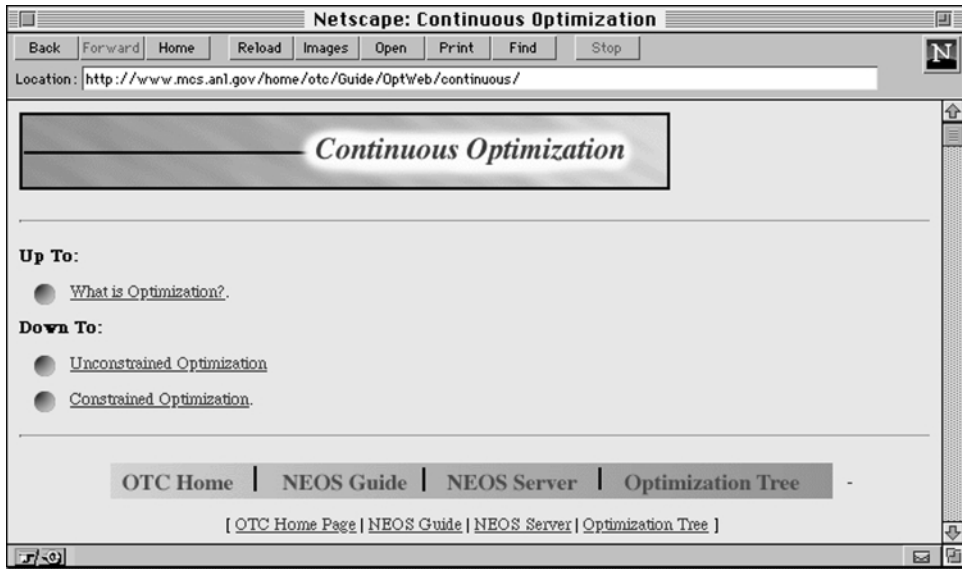

Up To:

- NEOS Guide Optimization Tree.

Down To:

- Continuous Optimization, in which all the variables are allowed to take values from subintervals of the real line;

- Discrete Optimization, in which you require some or all of the variables to have integer values.

Now, select Continuous Optimization.

Netscape: Continuous Optimization

Back | Forward | Home | Reload | Images | Open | Print | Find | Stop

Location: http://www.mcs.anl.gov/home/otc/Guide/OptWeb/continuous/

Continuous Optimization

Up To:

- What is Optimization?.

Down To:

- Unconstrained Optimization
- Constrained Optimization.

OTC Home | NEOS Guide | NEOS Server | **Optimization Tree** -

[OTC Home Page | NEOS Guide | NEOS Server | Optimization Tree]

Click on <u>Unconstrained Optimization</u>.

Back | Forward | Home | Reload | Images | Open | Print | Find | Stop

Location: http://www.mcs.anl.gov/home/otc/Guide/OptWeb/continuous/unconstrained/

Unconstrained Optimization

The unconstrained optimization problem is central to the development of optimization software. Constrained optimization algorithms are often extensions of unconstrained algorithms, while nonlinear least squares and nonlinear equation algorithms tend to be specializations. In the *unconstrained optimization problem*, we seek a local minimizer of a real-valued function, $f(x)$, where x is a vector of n real variables. In other words, we seek a vector, $x*$, such that
$f(x*) <= f(x)$ for all x close to $x*$.

Global optimization algorithms try to find an $x*$ that minimizes f over *all possible* vectors x. This is a much harder problem to solve. We do not discuss it here because, at present, no efficient algorithm is known for performing this task. For many applications, local minima are good enough, particularly when the user can draw on his/her own experience and provide a good starting point for the algorithm.

Newton's method gives rise to a wide and important class of algorithms that require computation of the *gradient vector*

$$\nabla f(x) = \begin{pmatrix} \partial_1 f(x) \\ \vdots \\ \partial_n f(x) \end{pmatrix},$$

and the *Hessian matrix,*

$$\nabla^2 f(x) = \left(\partial_j \partial_i f(x) \right).$$

Although the computation or approximation of the Hessian can be a time-consuming operation, there are many problems for which this computation is justified. We describe algorithms in which the user supplies the Hessian explicitly before moving on to a discussion of algorithms that don't require the Hessian.

Newton's method forms a quadratic model of the objective function around the current iterate x_k. The model function is defined by

$$q_k(s) = f(x_k) + \nabla f(x_k)^T s + \tfrac{1}{2} s^T \nabla^2 f(x_k) s$$

In the basic Newton method, the next iterate is obtained from the minimizer of q_k. When the Hessian matrix, $\nabla^2 f(x_k)$, is positive definite, the quadratic model has a unique minimizer that can be obtained by solving the symmetric $n \times n$ linear system:

$$\nabla^2 f(x_k) s_k = -\nabla f(x_k).$$

The next iterate is then

$$x_{k+1} = x_k + s_k$$

Convergence is guaranteed if the starting point is sufficiently close to a local minimizer $x*$ at which the Hessian is positive definite. Moreover, the rate of convergence is quadratic, that is,

$$\|x_{k+1} - x^*\| \leq \beta \|x_k - x^*\|^2,$$

for some positive constant β.

Unconstrained Optimization continues:

```
┌────────────────────────────────────────────────────────────────────────────┐
│ □          Netscape: Unconstrained Optimization                          ▣ │
├────────────────────────────────────────────────────────────────────────────┤
│ Back  Forward  Home   Reload  Images  Open  Print  Find   Stop          N  │
├────────────────────────────────────────────────────────────────────────────┤
│ Location: http://www.mcs.anl.gov/home/otc/Guide/OptWeb/continuous/unconstrained/ │
└────────────────────────────────────────────────────────────────────────────┘
```

In most circumstances, however, the basic Newton method has to be modified to achieve convergence.

Versions of Newton's method are implemented in the following software packages:

> BTN, GAUSS, IMSL, LANCELOT, NAG, OPTIMA, PORT 3, PROC NLP, TENMIN, TN, TNPACK, UNCMIN, and VE08.

The NEOS Server also has an unconstrained minimization facility to solve these problems remotely over the Internet.

These codes obtain convergence when the starting point is not close to a minimizer by using either a *line-search* or a *trust-region* approach.

> The line-search variant modifies the search direction to obtain another a downhill, or *descent* direction for f. It then tries different step lengths along this direction until it finds a step that not only decreases f, but also achieves at least a small fraction of this direction's potential.

> The trust-region variant uses the original quadratic model function, but they constrain the new iterate to stay in a local neighborhood of the current iterate. To find the step, then, we have to minimize the quadratic subject to staying in this neighborhood, which is generally ellipsoidal in shape.

Line-search and trust-region techniques are suitable if the number of variables n is not too large, because the cost per iteration is of order n^3. Codes for problems with a large number of variables tend to use truncated Newton methods, which usually settle for an approximate minimizer of the quadratic model.

So far, we have assumed that the Hessian matrix is available, but the algorithms are unchanged if the Hessian matrix is replaced by a reasonable approximation. Two kinds of methods use approximate Hessians in place of the real thing:

> The first possibility is to use difference approximations to the exact Hessian. We exploit the fact that each column of the Hessian can be approximated by taking the difference between two instances of the gradient vector evaluated at two nearby points. For sparse Hessians, we can often approximate many columns of the Hessian with a single gradient evaluation by choosing the evaluation points judiciously.

> Quasi-Newton Methods build up an approximation to the Hessian by keeping track of the gradient differences along each step taken by the algorithm. Various conditions are imposed on the approximate Hessian. For example, its behavior along the step just taken is forced to mimic the behavior of the exact Hessian, and it is usually kept positive definite.

Finally, we mention two other approaches for unconstrained problems that are not so closely related to Newton's method:

> Nonlinear conjugate gradient methods are motivated by the success of the linear conjugate gradient method in minimizing quadratic functions with positive definite Hessians. They use search directions that combine the negative gradient direction with another direction, chosen so that the search will take place along a direction not previously explored by the algorithm. At least, this property holds for the quadratic case, for which the minimizer is found exactly within just n iterations. For nonlinear problems, performance is problematic, but these methods do have the advantage that they require only gradient evaluations and do not use much storage.

> The nonlinear Simplex method (not to be confused with the simplex method for linear programming) requires neither gradient nor Hessian evaluations. Instead, it performs a pattern search based only on function values. Because it makes little use of information about f, it typically requires a great many iterations to find a solution that is even in the ballpark. It can be useful when f is nonsmooth or when derivatives are impossible to find, but it is unfortunately often used when one of the algorithms above would be more appropriate.

Up To:

  ● Continuous Optimization.

Down To:

  ● Nonlinear Least Squares
  ● Nonlinear Equations
  ● Global Optimization
  ● Nondifferentiable Optimization

The reader is invited to further explore the vast optimization reservoir available at the NEOS site.

OTHER INTERNET OPTIMIZATION RESOURCES

NEWSGROUPS

1. *sci.op-research* — general research newsgroup including optimization problems. Also available Brian's Digest, a sort by topic of newsgroup articles.
   htpp://www.maths.mu.oz.au/~worms/digest/digest.html#topics
2. *comp.graphics.algorithms* — some articles pertaining to optimization algorithms.
3. *sci. math.num-analysis* — optimization articles.

FAQ — FREQUENTLY ASKED QUESTIONS

1. Linear programming
   a. Posted monthly to Usenet newsgroup: *sci.op-research*
   b. WWW version:
      http://www.skypoint.com/subscribers/ashbury/linear-programming-faq.html
   c. Plain text version
      ftp://rtfm.mit.edu/pub/usenet/sci.answers/linear-programming-FAQ
2. Nonlinear programming
   a. Posted monthly to Usenet newsgroup: *sci.op-research*
   b. WWW version:
      htpp://www.skypoint.com/subscribers/ashbury/nonlinear-programming-faq.html
   c. Plain text version:
      ftp://rtfm.mit.edu/pub/usenet/sci.answers/nonlinear-programming-FAQ

WWW — WORLD WIDE WEB

1. An extensive list of optimization codes retrievable through the internet. Site maintained by Jiefeng Xu.
   http://ucsu.colorado.edu/~xu/software.html
2. NEOS guide optimizatin tree — An on-line guide to the field of numerical optimization.
   http://www.mcs.anl.gov/home/otc/Guide/OptWeb/
3. Exhaustive code and information pertaining to Global Optimization.
   http://solon.cma.univie.ac.at/~neum/glopt.html#intro
4. Mathematical Optimization — an electronic book
   http://csep1.phy.ornl.gov/mo/mo.html

SOFTWARE

1. GAMS, the Guide to available mathematical software.
   http://math.nist.gov/cgi-bin/gams-serve/class/G.html
2. Optimizationa and NETLIB (FORTRAN)
   http://www.netlib.org/opt/

ACKNOWLEDGMENT

15 CIP Sanitary Process Design

Dale A. Seiberling

CONTENTS

15.1   INTRODUCTION

Cleaned-in-place (CIP) technology began to evolve during the latter stages of World War II, when tinned-copper tubing and stainless steel tubing, the normal materials for construction of "sanitary" piping systems became relatively scarce. Some operators experimented with Pyrex glass lines which, due to the "breakage" hazard, were of necessity cleaned-in-place. The early successes reported by Thom (1949) and Fleischman et al. (1950) led to the development of special joints and gaskets for stainless steel piping systems which would permit them also to be recirculation cleaned. Havighorst (1951) reported the development of methods for installing stainless steel piping by gas welding and grinding to remove the filler metal.

The nation's universities began studies of the developing technology in the early 1950s and Sheuring and Henderson (1951) reported that more than 40 commercial dairies and college dairies were using permanent glass lines. In 1953 Parker et al. reported a study determining those factors which were most responsible for the effectiveness of the recirculation cleaning process. Velocity was found to be a significant factor and the early studies suggested a minimum flow rate equivalent to a velocity of 5 ft/s in the largest diameter tube in the circuit. The 3-A Standards committee serving the dairy industry (International Association of Milk, Food, and Environmental Sanitarians, 1986) also began evaluating this new development in the mid-1950s and began to develop recommendations for the design, installation, and operation of in-place cleaned piping systems. An early emphasis was placed on the need for a return line recording thermometer to provide a chart record showing the time at cleaning temperature as a means of documenting the application of a suitable CIP program.

The first application of automatic control to CIP operations was made in 1953–1954 and reported by Seiberling (1955). It was demonstrated that improved (more repetitive) results could be assured via this approach, as compared to dependency on the operator to control time, temperature, and concentration, and proper pre-flushing and final-rinsing operations. Seiberling and Harper subsequently reported the development of Ball Spray Cleaning and the radio-isotope evaluation of the cleanability of air operated valves. New dairy plants designed to combine welded pipelines, automated CIP, and automated flow control via CIP air-operated valves were placed into operation in 1960, one is described by Bonem (1960). Johnson (1960) described the improvement of dairy product quality attributed to automated CIP and at that time Kaufmann et al. (1960) reported on a study of the cleanability of different stainless steel surface finishes by ball spray procedures.

By 1964 substantial progress had been made in developing highly automated product piping systems and automated CIP. Automated control of product flow was accomplished initially via relay-logic control systems and automatic cleaning of the transportation tankers, all plant storage and processing tanks, and all interconnecting piping was being accomplished on a highly reliable basis. CIP was beginning to mean Clean-In-Place rather than "Clean-In-Part". By this time CIP cleanable equipment in the form of centrifugal machines, homogenizers, plate heat exchangers, and packaging machines was being introduced and by the late 1960s the design of liquids processing systems reduced the manual effort for cleaning to (a) disconnecting the process supply and discharge lines, (b) completing connections to several permanently installed CIP tie lines, and/or installing one or more CIP jumpers, and (c) initiating operation of an automated CIP system to clean the connected process under fully automatic control.

And, whereas the early development of this technology occurred in the dairy industry, by the mid-1960s CIP procedures attracted the interest of many processors of nondairy foods. Seiberling (1968) outlined equipment and process design factors desirable for satisfactory mechanical/chemical cleaning.

The early application of CIP to brewing vessels and lines was reported by Seiberling (1970) and by the late 1960s the concepts initially developed and applied in the dairy foods processing plant were equally applicable to systems designed to produce liquid dressings, dessert toppings, various soy-protein based food products, and for brewing and wine processing. Expansion of spray cleaning technology permitted CIP cleaning of belt-type conveyors used for continuous production of cheddar cheese, draining whey from Italian cheese, as well as a variety of rising-film and falling-film evaporators, and various types of spray dryers used primarily for dairy products including nonfat dry milk powder and whey powder. Several other types of food dryers were subsequently CIP cleaned. Similar applications of both process engineering and CIP cleaning have been incorporated in systems for producing soups, meat sauces, and the batter, fillings, and coatings for candy bars. The meat industry found the same basic concept applicable to the cleaning of the edible oil process, pet-food processes, and smoke houses. In the late 1970s the drug industry first applied the same concept to the design and installation of high-capacity systems for producing intravenous solutions. Subsequently it was applied to smaller, but totally sterile, systems for handling a variety of i.v. feeding products both lipid and protein based, and to the processing of fractions of whole blood.

The CIP recirculating unit, the associated supply-return piping, the spray devices, and the CIP return pumps were recognized as the "heart and veins" of the automated process. It was found that the quality of the finished product was dependent upon the proper performance of the complete system. Considerable attention must be given to proper engineering design and selection of the appropriate sprays and pumps to assure initial and continued optimum hydraulic performance. A piece of pipe in a CIP supply-return system, in addition to adding to capital cost, impacts performance in terms of: (a) its contribution to head loss; (b) its content in gallons, hence an impact on the quantity of water required for accomplishing the various steps of the program; and (c) its ability to drain. Return-side engineering is especially critical as this impacts the reliability of centrifugal pumps which must necessarily become "air-bound" frequently during the typical spray-cleaning program.

Experience has shown that CIP design provides the key to many other changes in technology. The ability to ensure controlled sanitation through mechanical/chemical cleaning has led to extensive development of all welded-product piping systems, application of air-operated valves, appreciable increases in the size of processing and storage tanks as compared to flow rates and packaging machinery capacity, and approaches to plant design and arrangement not previously feasible. The total cleaning problem involves far more than pumps, tanks, sprays, and controls. The design of a modern food processing plant requires consideration of materials and methods of construction, equipment layout, specialized cleaning equipment, design of the processing equipment, and finally design of the process. The ability for CIP, through application of mechanical/chemical procedures, permits design approaches which were not feasible when accessibility for manual cleaning was necessary.

The benefits have been substantial, and include

- Substantial increases in processing capacity
- Reduced losses through the application CIP cleanable automated valves and highly automated processes
- Improved quality of all products and significant improvement in the shelf-life of perishable products
- Reduced labor for both processing and cleaning

15.2 FUNDAMENTALS

15.2.1 CIP System Components

15.2.1.1 Typical Recirculating Equipment

CIP as applied today is essentially chemical in nature. Processing equipment and CIP appurtenances are designed to permit the cleaning solution to be brought into intimate contact with all soiled surfaces and to be continuously replenished. Since relatively high volumes of solution must be applied to soiled surfaces for periods of time ranging from as little as 5 min to as much as 1 h (or more), recirculation of the cleaning solution is essential to maintain economic operation.

CIP systems are available in two different forms (Figure 15.1). Multitank re-use recirculating units may utilize the same wash solution for a large number of cleaning operations during the production day. This solution can be added to as required to maintain strength and cleaning ability. Single-tank, single-use systems operate on the basis of creating smaller volumes of solution automatically to the required concentration. These systems use the solution once at the lowest possible strength and discharge it to the sewer at the end of each cycle.

The two systems are comparable with respect to program control equipment. Multi-tank systems require more space and utilize more parts in the form of tanks, valves, level controls, and temperature controls and require added attention during the operating day to check solution condition or to dump and recharge the tanks. The multi-tank systems also lack flexibility in that a single combination of temperature and concentration must be used for all equipment to be cleaned with the system. The single-tank system is small in size, simpler in design, lower in initial investment, and more flexible in application. All chemicals are fed automatically and in the proper proportions, from the shipping containers or from bulk storage. Olenfalk (1975a,b) and Richter et al. (1975) reported on comparative performance of the two basic types of systems. Tamplin (1980) provided a detailed analysis of the two concepts, including detergents, chemical feed, and control.

Single-tank single-use systems are relatively small in size and are generally supplied as "packaged" units. Several manufacturers supply shop fabricated re-use systems but more commonly these systems are field assembled from a bill of material including tanks, pipes, pumps, valves, steam injection mixers or shell and tube heaters, etc. as required.

Substantial experience has taught that it is "easier to get water into a tank" than to get it out, reliably, under automatic control and herein is a major source of trouble related to the operation of CIP systems on spray cleaning applications. The effective flushing, washing, and rinsing of a tank or tanker is dependent upon keeping the vessel properly evacuated, i.e., having minimal solution "stagnant" in the bottom of the vessel. The single-tank single-use recirculating unit is more effective in accomplishing this objective than the alternative approaches, namely because the return pump and the supply pump are physically connected in series for the recirculation periods of the cleaning program, eliminating the problem of "balancing supply and return flow". The only water in the system is that in the CIP supply–return (CIPS/R) piping, on the sidewalls of the vessel being cleaned, and as the "puddle" at the outlet of the vessel. If one pump becomes momentarily air-locked, the other will cause continued flow through the system and seldom do even momentary fluctuations in pressure occur. By comparison, cleaning the same vessel under the same circumstances with two pumps and two tanks in series is likely to result in one pump or the other frequently becoming air-bound for a prolonged period of time. The result is that all of the solution accumulates in the vessel from which the air-locked pump is pumping and flow soon stops, as does effective cleaning action.

Even a single-tank single-use system, however, cannot cope with the problem created by cleaning two or more tanks simultaneously and in parallel with both connected to a common
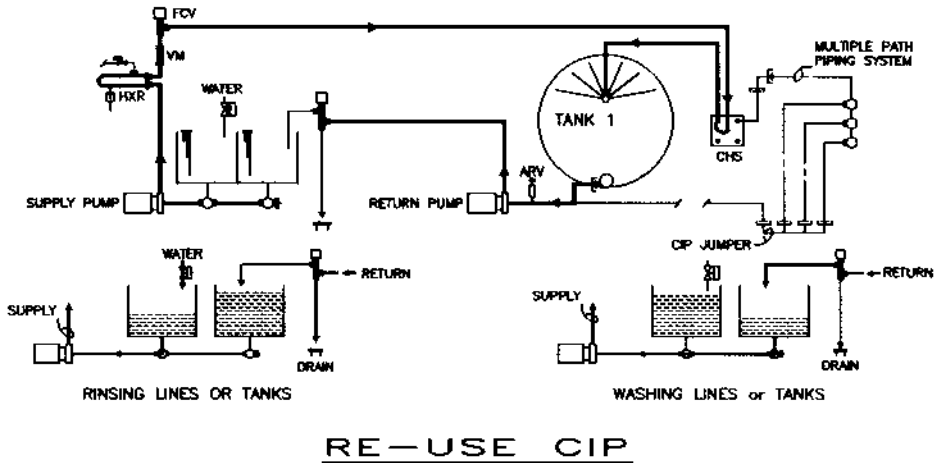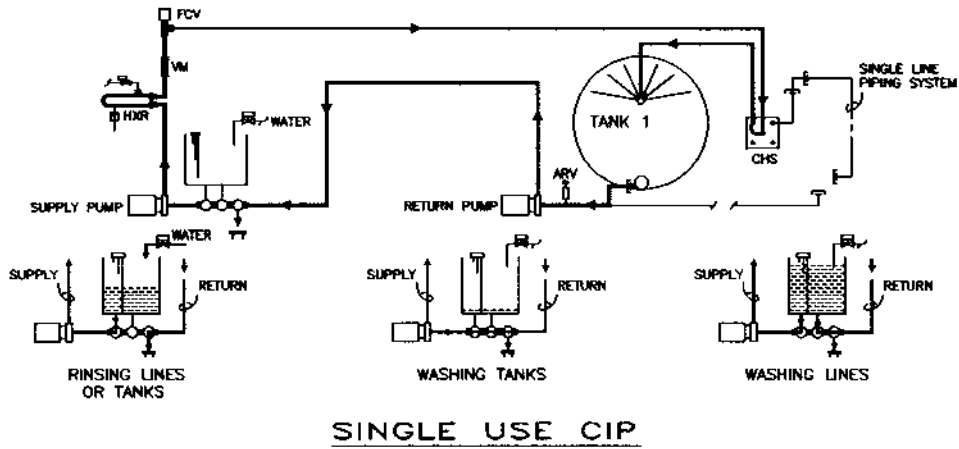
FIGURE 15.1 CIP Systems may use combinations of tanks, pumps, and valves to create many different configurations but most operate on either the single-use or re-use basis and are capable of spray washing tanks and pressure washing line circuits.

header on the inlet side of the return pump. Multiple return streams are best handled by designing for gravity flow of all streams to a return sump tank. The return tank serves as the air-elimination device and 3–4 in. of water in this tank replaces the solution in the vessel being cleaned, as the "puddle" on the return side of the system.

The cleaning circuits in most food plants include both tanks and lines. Tanks are fitted with permanently installed spray devices and supplied with flush, wash, and rinse solutions by CIPS/R piping systems from the CIP unit to the production area. Figure 15.1 illustrates how a cleaning hook-up station (CHS) may be used to supply spray devices in multiple tanks from a common line, and also, from different ports it may supply one or more line (piping) circuits. Line circuits may be supplied from any one of several CHS locations, and may return to any available CIPR header. The single-use system is shown connected to a simple single line circuit whereas the re-use system is connected to a line circuit containing multiple paths through which flush, wash, and rinse solutions would be sequenced on a repetitive basis.

Beginning in the early 1980s a major objective has been the accomplishment of effective CIP of ever larger systems with less and less water. This is the result of rapidly increasing costs for water, and for the discharge and treatment of the resultant waste. If and when zero

biological oxygen demand (BOD) in the effluent from food processing plants is required, then all cleaning solution must be separated and reused. That procedure, however accomplished, will be most economical if the volume of solution can be reduced to a minimum.

The Single-Use Eductor-Assisted (SUEA) CIP unit described in Figure 15.2 is one means of reducing water requirements. The unique air separation/recirculation tank serves also as the motive tank and the operating concept of the eductor-assisted system uses the vacuum produced by the eductor to continuously prime centrifugal return pumps located on the ends of CIP return headers supporting the tankage. A small diameter return line (as compared to eductor-based systems) is used and this return line is generally only about half full of liquid. The remainder of the volume is air being continuously pulled through the outlet of the vessel being cleaned, then through the centrifugal pump and back to the unit. The SUEA air separation/recirculation tank contains only 12–15 gal of solution during recirculation though the combined flow downwards through the vertical leg may reach 200 to 240 gal/min. A 60,000 gallon silo-type tank located approximately 100 ft from a SUEA CIP unit can be recirculation cleaned at a flow rate of 100 gal/min with as little as 40 to 50 gal of solution in the system.

When a SUEA system is equipped with a recovered solution tank, all of the water required for the cleaning operations is used twice, first in its fresh form for the postrinse and the recirculated acidified final rinse following which it is discharged to the recovered rinse tank, and then (in combination with the wash solution also discharged to this same tank) it is used again as the prerinse and wash fill for a subsequent operation.

15.2.1.2 Water Use Criteria

The volume of water required to rinse a piping circuit is normally found to be 1½ to 2 times the volume contained in that piping, including the CIPS/R system. That volume may need to be increased in automated systems which incorporate valve sequencing to clean branches or subcircuits as illustrated for the multipath line circuit on the re-use portion of Figure 15.1.

On this basis, the total water requirement for a complete program (prerinse, solution wash, postrinse, and recirculated acidified final rinse) would be 6 to 8 times the volume of the circuit for a single-use recirculating unit. This volume might be decreased by 15 to 20% for a re-use system which utilizes the same wash solution for a number of programs. However, this will be offset by the amount of controlled "waste" required to maintain the solution at an acceptable soil load, and the initial volume required to fill the solution tank.

### 15.2.1.3 Chemical Feed Equipment

In addition to pumps, tanks, valves, and heat exchangers, the CIP system must also include provisions for chemical feed and control of wash solution concentration. Most food processing equipment can be effectively cleaned with a solution which is 99.5 to 99.75% water, with stronger solutions being required only for extremely heavy or "burned-on" soils. The chemicals making up the remainder may be supplied in liquid or dry form, though liquids are the preferred source for automated CIP systems.

Air-operated piston or diaphragm-type chemical feed pumps are generally used to feed the required ingredients in proper quantities and ratios. For the single-use system, concentration control is accomplished by adding a *known quantity of the chemical ingredients to a known quantity of water* which is recirculating within the circuit being cleaned. Chemicals are generally fed directly to the solution tank(s) of re-use systems on an "on-demand" basis on a conductivity sensor signal.

Employee safety concerns have caused many operators to locate the chemical pumps in a remote area and use a "chemical feed loop" as illustrated on Figure 15.3 to convey full
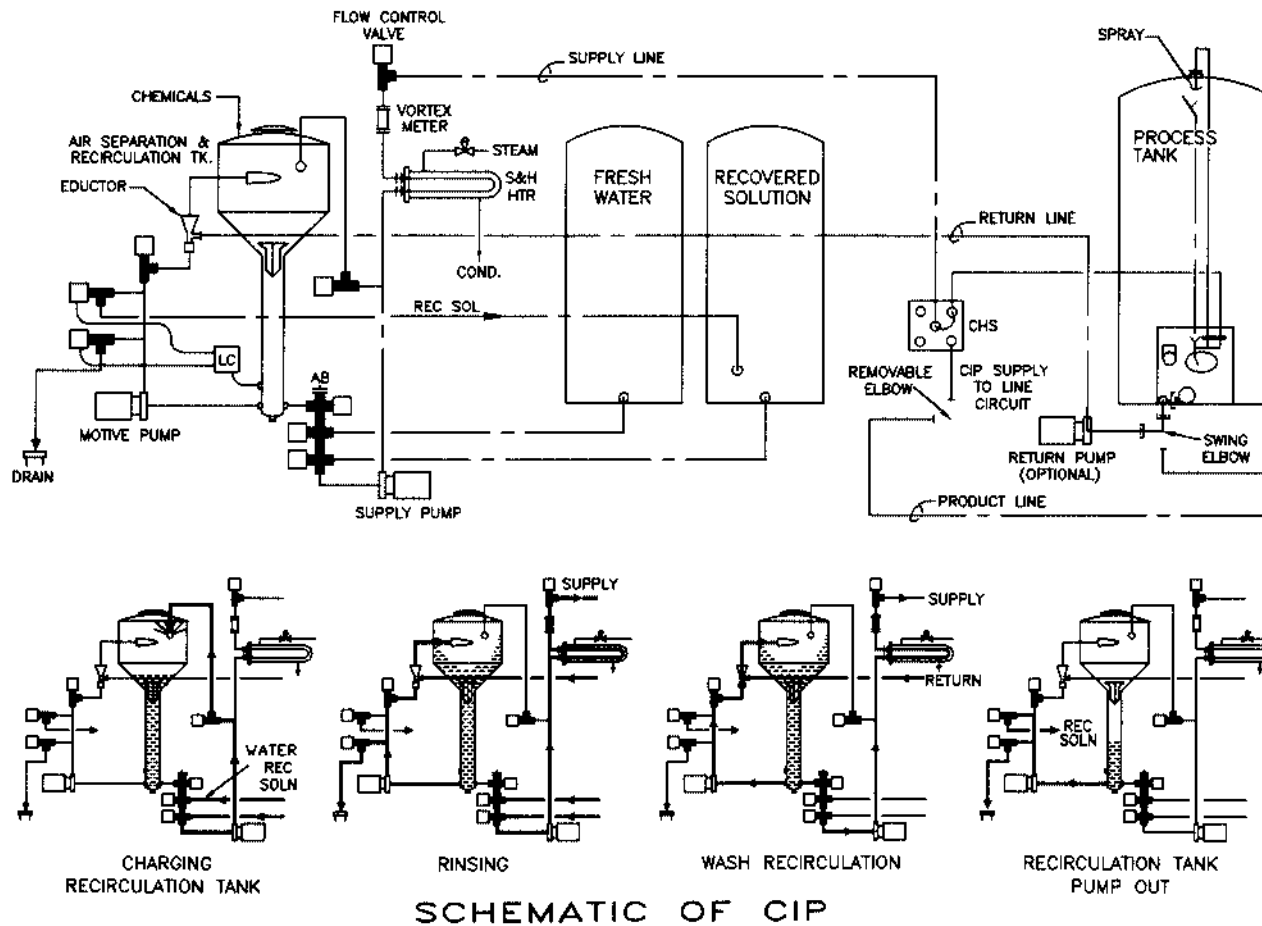
FIGURE 15.2 The SUEA (Single-Use Eductor Assisted) CIP System provides great reliability, minimizes water and chemical requirements for tank CIP operations, and is self cleaning.
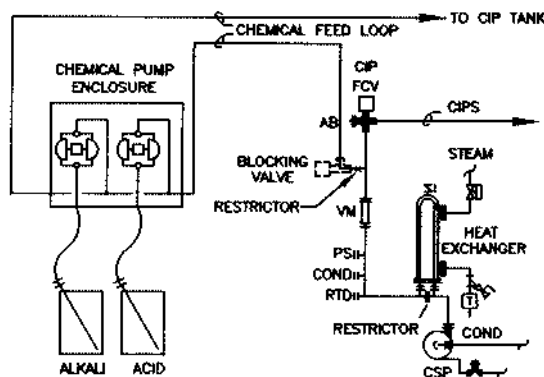
FIGURE 15.3 Chemicals are generally supplied to the CIP system directly from the shipping containers or day-use tanks. The provision of a chemical feed loop permits the chemicals and pumps to be located remotely from the CIP unit.

strength chemicals to the recirculating solution, thus restricting access to full strength chemicals to the chemical pump enclosure and drop pipes to the supply containers. The "loop" piping will generally be ¾ or 1 in. OD tubing and a restrictor at the CIPS connection will be sized to control flow through the loop at 3 to 5 gal/min at the maximum cleaning supply pump (CSP) discharge head. If the CIPS air-blow is located at the pump, rather than on the flow control valve (FCV), a blocking valve shown in dash line delineation is required to prevent air loss through the loop to the CIP tank. Figure 15.4 is a photograph of a large chemical pump enclosure which supports two CIP systems and a high-temperature short-time (HTST) CIP system, from barrels and bulk sources. Note the small diameter chemical loop piping to and from the enclosure and also the Occupational Safety and Health Administration (OSHA) required safety shower and eye wash fountain in the area where hazardous chemicals are handled.

Re-use systems are generally programmed to "waste" a small part of the solution at the end of each cleaning cycle to continuously remove soiled solution from the system. This is followed by the addition of fresh water to bring the solution tank to the normal operating level after which the conductivity-cell based chemical feed system will add more chemical.

15.2.1.4   CIP Program Control

CIP program control system may be simple or complex depending upon the nature of the application. Fully "automated" control of the cleaning program is preferable to manual control and should include variables of rinse, drain and recirculation times, temperature, concentration, and flow-rate, the latter via either instrumentation or engineering design.

There may be no automation required beyond the recirculating unit for a system applied to clean permanently installed or portable tanks or simple piping circuits. If, however, the process involves considerable air-operated valving or mechanics and requires the operation of pumps and other processing equipment, then the program control system selected must be capable of handling the entire requirement.

Through the mid-1970s CIP program controllers were generally cam-timers or drum-type stepping switches used in combination with relay-logic based control systems. The CIP program controller of the 1990s is more commonly a microprocessor-based system in the form of (a) dedicated CIP controllers, based on microprocessors, (b) off-the-shelf programmable logic controllers (PLC) configured and programmed to establish the desired operation, or (c) a portion of the hardware and software of a larger computer-based system or Distributed Control System (DCS).

FIGURE 15.4 Chemical pump enclosure — supply containers and safety shower in a dairy processing facility.

PLC and DCS based control systems have many capabilities not possible with hard-wired systems, including analog input and output, PID control, ASCII output to display messages, RS232 ports to allow communication with other PLC and computers, and many other modules available to increase application capabilities.

The CIP program control may be time-based, or flow-rate and volume based (with tank wash drain periods still time-based), via application of a flow meter, a flow control (throttling) valve, and the required software. Program variables to be controlled include time, volume, temperature (via Resistance Temperature Devices (RTD) inputs to a PLC or computer), pressure via P/I transducers and inputs to a PLC or computer, and conductivity and resistivity via the appropriate sensing devices and interface to the PLC or computer. Figure 15.5 illustrates typical sensors of sanitary design and construction.

Matrix programming is preferable for both the CIP program and the associated programs for sequential operation of process valves, pumps, agitators, and processing machinery, if required. The CIP program can be monitored from beginning to end and certain checkpoints may be established to verify specific operations. Some common "endpoint control" checks might include:
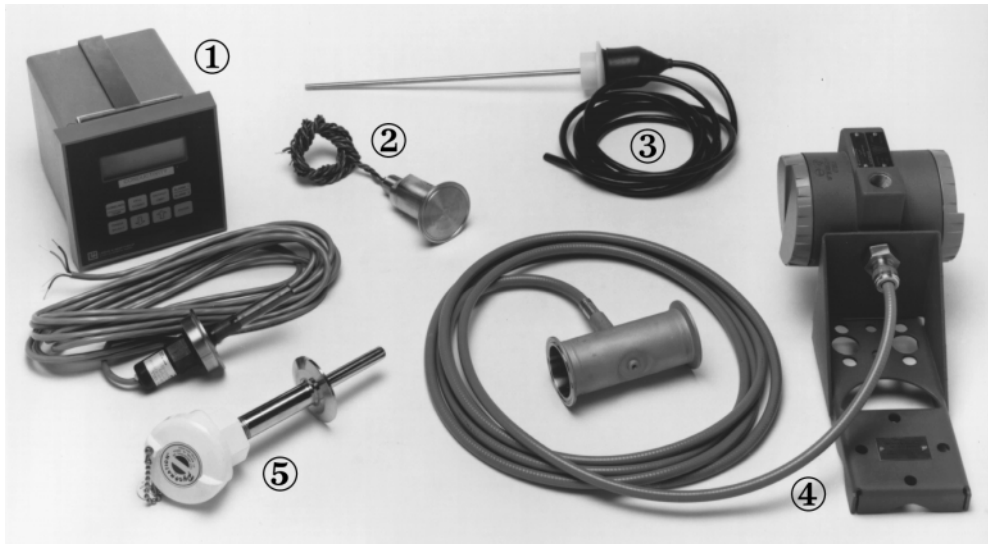
FIGURE 15.5 Sanitary design sensing devices include (1) conductivity probe with analyzer/transmitter, (2) pressure transducer, (3) liquid sensing probe, (4) flow transmitter with vortex meter, and (5) RTD (resistance temperature device).

1. *No Return flow* — A signal based on a probe in the return line checking for return flow immediately following the first portion of the prerinse. Failure to achieve return flow indicates improper connections or an inoperative pump or valve.
2. *Delay-to-temperature* control logic — A control that is arranged to stop program advance at the beginning of the wash cycle until all of the solution in the circuit reaches the desired cleaning temperature, assuring washing for the proper time at the desired temperature.
3. *Low chemical concentration* — A conductivity cell may be used to monitor a minimal "threshold level" to assure that chemical feed systems are operative and that chemicals are available in the source containers.

Interlocks are easily incorporated in the control logic to minimize product loss and equipment damage brought about by human error. Typical interlocks could include: (a) a *process to CIP* interlock to prevent the start of a CIP cycle on equipment that is in the process mode, i.e., a tank containing product as sensed by the gauging system or being filled or emptied; (b) a *CIP to process* interlock to prevent attempts to fill or empty a tank or use a system during the cleaning program; and (c) a *manual connection check*, an interlock generally accomplished via a proximity sensor used in combination with a magnet on a U-bend to verify proper position of all manual connections affecting the selected CIP circuit, and an *Over-temperature* shut-down (temperature sensor based) interlock to stop the program, place it on hold, and require manual intervention for correction of the cause. Such action may prevent the collapse of a tank as a result of rinsing with cold water after the tank (and the air contained) has been heated to an excessively high temperature.

The control system should make it possible for "process oriented personnel" in the form of production or quality control supervisors to monitor and adjust those variables which affect the performance of the CIP system. However, access to the means of adjusting these variables should be limited, and should not be available to the operator who need be concerned only with starting, stopping, and resetting the program.

15.2.1.5 CIP Program Data Acquisition

The 3-A accepted practice as applied in the dairy industry and often used as a guideline by other users of CIP technology states, "Solution temperature shall be automatically controlled by the use of a temperature regulator with a response range of plus or minus 5°F." This is loosely adhered to, if at all, as there is no requirement for a specific cleaning temperature for any application. This same standard requires a "recording thermometer having a scale range of 60 to 180°F with extension of scale on either side permitted. Graduated in time scale divisions of not more than 15 minutes. Between 110–180°F, the chart shall be graduated in temperature divisions of not more than 2°F, spaced not less than ¹⁄₁₆ in. apart, and be accurate within 2°F plus or minus. The sensor shall be protected against damage at 212°F, and the sensing element of the recording thermometer shall be located in the return solution line." The intent of this requirement is to provide a chart record of the cleaning time and temperature relationship, in recognition that the effectiveness of this *essentially chemical procedure* is determined by time, temperature, and solution concentration.

Hydraulic performance is equally important. Cleaning solution may remain stagnant in the return system at wash temperature while a return pump is air bound for prolonged periods of time. This condition ultimately impacts the performance of the supply pump. Whereas a temperature recorder alone may suggest a suitable recirculation period, a recorder chart and recording instrument which provides a temperature pen and a pump discharge pressure recording pen permits operating, maintenance, and quality control personnel to evaluate the hydraulic performance of the system, in addition to knowing the recirculating time and temperature.

Recent revisions of the FDA regulations for dairy CIP systems now permit the substitution of equivalent (and superior) recording devices. Figure 15.6 is a schematic representation of a CIP data logger comprised of "off-the-shelf" components applied in combination with special software. This system may be retro-fitted to any existing CIP recirculating unit as a *stand-alone system* or as an extension of a PLC based control system. Desirable data logging capabilities include:

1. Graphic print-out/screen display with operators initials or password.
2. Text description of circuit name and mode of operation (i.e., CIP, sanitize, etc.), date, start time, and CIP unit number.
3. Real-time screen display of a currently operating cycle should include numeric display of all plotted variables, with engineering units and scale, and current step description.
4. Listing of alarm messages that occurred during the program.

A color printer is desirable to produce hard copy in a large, easily readable, color line format. The system may be capable of printing the raw numeric data, and for storing data in accordance with management or regulatory agency requirements. It is desirable for data acquired for any circuit on any day during the current operating period to be selectively redisplayed for subsequent evaluation. Templates of proper programs can be stored for comparison to the chart for a program just completed.

15.2.1.6 CIP Supply–Return Piping

Permanently installed CIPS/R piping was an integral part of the earliest "automated" CIP installations. In dairy processes and some portions of food processes it is necessary to clean processing and storage vessels during the production period. A number of those vessels may also contain product when the process piping is subsequently CIP.
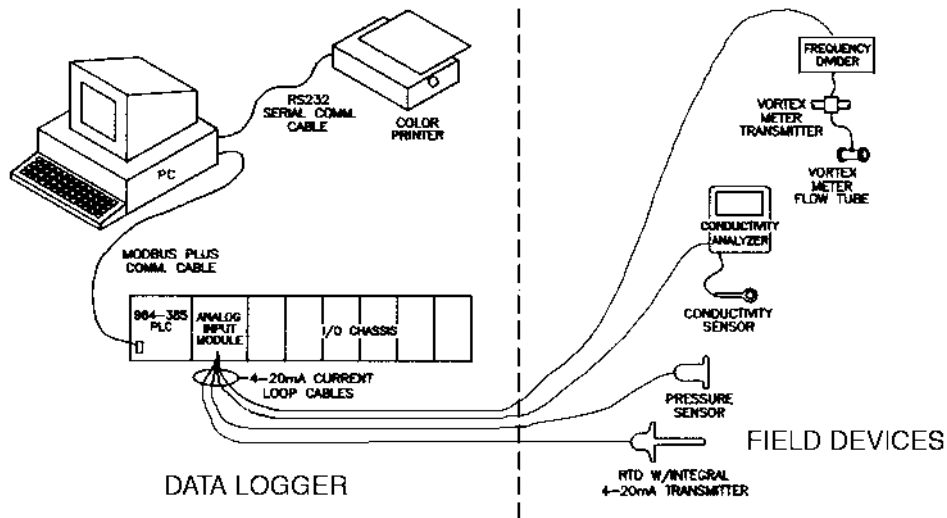
FIGURE 15.6 Components and connection diagram for a CIP program data logger for temperature, supply pressure, conductivity, and flow.

The *3-A Accepted Practices for Permanently Installed Sanitary Product Pipelines and Cleaning Systems (1986)* require "All connections between the solutions circuit and the product circuit shall be constructed as to positively prevent the commingling of the product and solution during processing." Compliance with this requirement is best accomplished via the installation of separate CIPS/R piping. The "make-break" connections between the product vessels, the process lines, and the CIPS/R lines generally consist of removable elbows, U-bends, or "goosenecks" (an elbow on a straight length of tubing) physically arranged to prevent improper connections, or simultaneous connection of a tank to product and CIP solution lines.

15.2.1.7 Return Flow Motivation

The CIP system schematics and CIPS/R piping shown in Figure 15.1 were based on "pumped return". Though pumped return is perhaps the most common method of return flow motivation, other methods may be used.

   Gravity Return Flow — Flush, wash, and rinse solutions may be continuously removed from a vessel being spray cleaned at a rate equal to the solution supply if tank outlet valves and return system piping is sufficiently large to accomplish this by gravity head alone. This is generally applicable only when the tank being cleaned is at one or more levels above the recirculating unit. However, gravity drainage is more effective than any other method for removing the final traces of liquid from a circuit. Return piping should be pitched continuously from the vessel being cleaned to the CIP recirculating unit with exception of the necessary vertical rises from low-level collector piping and pumps to high-level transfer lines.
   Eductor Assisted Return Flow — This concept described in Figure 15.2 permits reduction of water volume required to fill CIPR piping and provides extremely reliable operation and freedom of all pump balancing requirements.
   Eductor Based Return Flow — This method would be similar to the above except that no return pumps would be located in the process area. CIPR piping must

generally be 3 in. in diameter and runs must be limited to a headloss not exceeding 16 to 18 ft, equivalent to the 16 to 18 in. of vacuum produced by the eductor. This concept is enhanced by location of the CIP unit under the loads, thus eliminating any return side positive static head.

Top Pressure — When cleaning pressure vessels, top pressure may be used in place of gravity or a return pump to produce flow through CIPR piping to the CIP recirculating unit. The CIPR head loss should preferably be less than 12 to 15 psi to use this concept. A *hold back valve* may be required in the return line. This valve is controlled by the weight of the vessel being cleaned (if load-cell mounted) or by the CIP tank level to prevent loss of top pressure by blowing the puddle out of the vessel, except at the desired times following each major program step.

Return Pumps — Low-speed (1750 rpm) return pumps will provide effective and reliable return flow IF the return connection pitches continuously from the tank being cleaned to the pump inlet, and if static head of 18 to 24 in. is available on the pump inlet. On longer return lines, or on CIPR headers, an air-relief valve located at the pump inlet will provide improved performance. High-speed (3450 rpm) return pumps have a greater tendency to become "air-bound" than low-speed pumps. Return system engineering should limit return pump suction side losses to less than 10 ft of head, though a slight negative pressure is required on the pump inlet to close air relief valves (if used) during recirculation.

Return system engineering must give consideration to balancing solution flow, i.e., regulating the discharge of the return pump from each portion of the system so that it is approximately 1.5 times the capacity of the supply pump for multitank re-use systems and sufficient to "stuff" the supply pump at a positive 3 to 5 psi for single-tank single-use CIP systems. This is accomplished by sizing pump impellers and lines, and (when necessary) installing restrictors to control flow. A single return pump will generally support only five to seven tanks due to the suction side head loss limitation and difficulty of assuring continuous pitch from the tank outlets to the return pump inlet.

15.2.1.8 Spray Cleaning of Processing and Storage Vessels and Nonliquid Handling Processing Equipment

Successful spray cleaning of storage tanks and processing vats is dependent upon properly designed tanks and properly applied spray devices.

The permanently installed fixed-ball spray has gained favor over rotating and oscillating spray devices. Its advantages include

1. There are no moving parts.
2. It can be made completely of stainless steel.
3. Its performance is not affected greatly by minor variations in supply pressure.
4. A properly established installation will continue to provide satisfactory service.
5. It sprays all of the surface all of the time.

Fixed-ball sprays are available with a variety of characteristics in terms of flow rate, discharge pressure, and pattern of coverage. Experience has indicated that cylindrical and rectangular tanks can be adequately cleaned if sprayed at 0.2 to 0.3 gal/min/ft^2 of internal surface, with patterns designed to spray the upper one third of the tank (Figure 15.7). If considerable appurtenances exist in the tank, such as heating or cooling coils and complex agitators, some special patterns may be required to cover these surfaces with resultant increases in the total flow rate required.
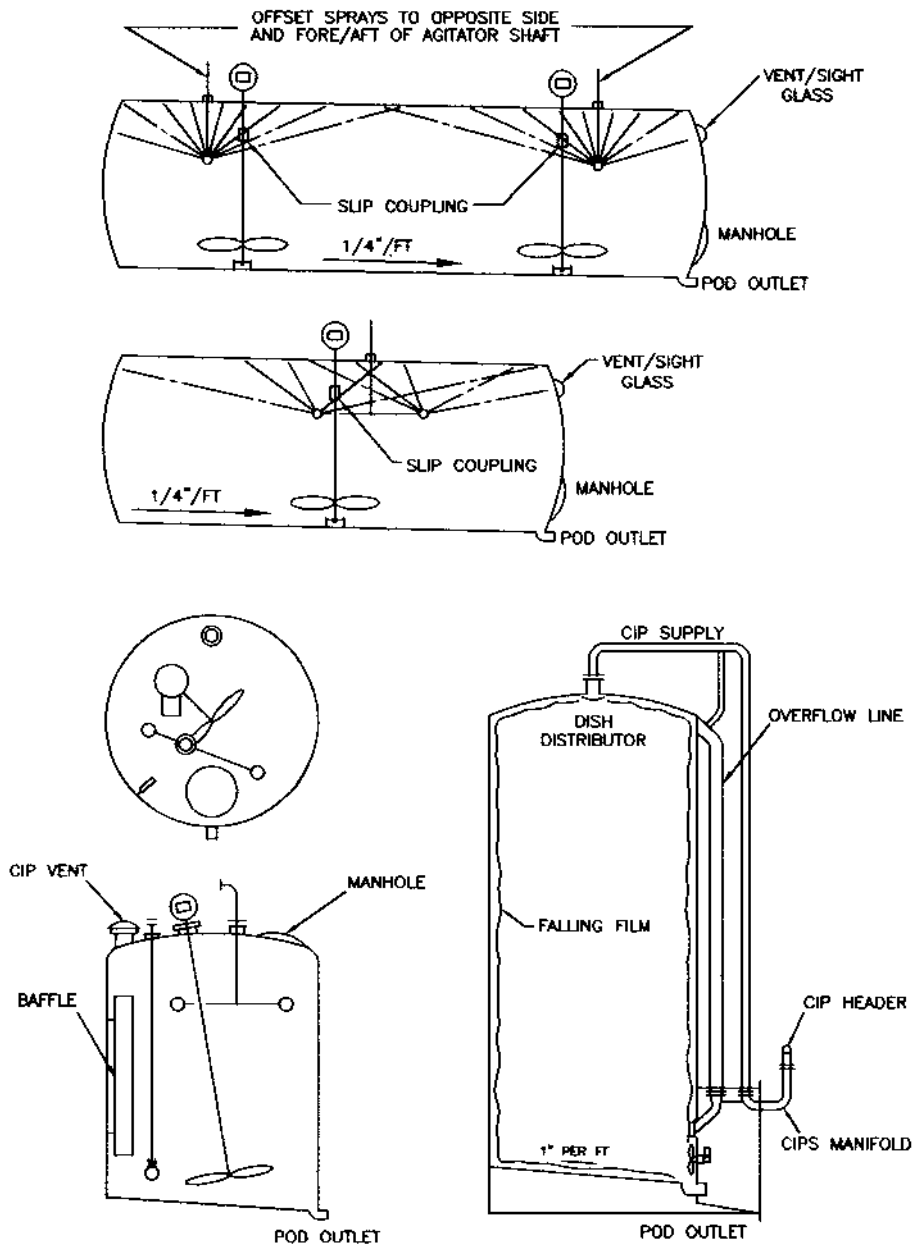
FIGURE 15.7 Fixed ball-type spray device locations are suggested in this photograph for cylindrical horizontal tanks and processing vessels. Silo type tanks are generally cleaned with disk or dish distributors of nonclogging design to permit the CIP supply line to be used as a re-vent line as part of the tank overflow protection system.

Vertical silo-type tanks (Figure 15.7) may be cleaned satisfactorily at flow rates of 2.0 to 2.5 gal/min/linear ft of tank circumference. Nonclogging disk sprays are used in vessels of this type because of the relative difficulty in reaching the spray devices for occasional inspection and cleaning. The 3-A criteria for installation of silo tanks on pads external to the building includes the requirement for all openings to the tank to be in the alcove area accessed
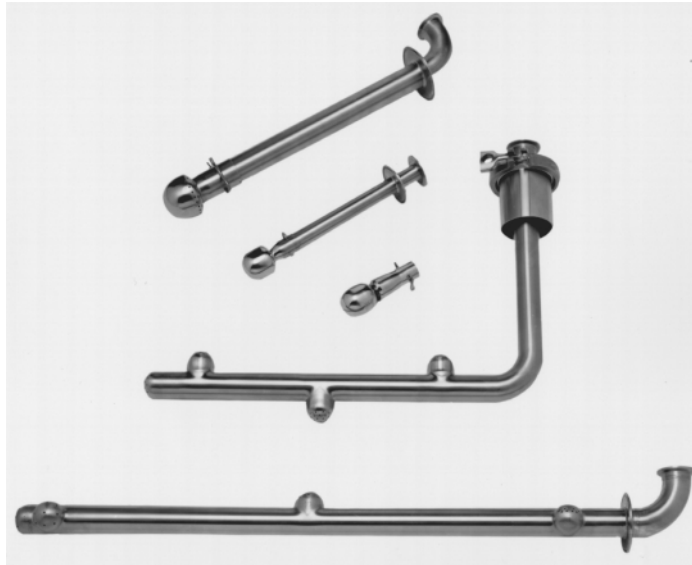
FIGURE 15.8 Fixed spray devices are available in the form of drilled ball-type sprays and tube sprays. A small water-driven rotating spray is in the center of this photograph. (Courtesy Electrol Specialties Company.)

from a sanitary process area, with the fill/discharge line(s) and vent/overflow line terminating within the building for sanitary reasons. The CIPS to the dish distributor generally serves as the overflow revent line.

Several fixed ball-type sprays and tube sprays are shown in Figure 15.8. An assortment of bubble sprays and installation fittings are shown in Figure 15.9 with a standard ball spray. The application of these sprays will be described in the subsequent section.

Tank cleaning programs involving the use of spray devices differ from lines cleaning programs. Prerinsing and postrinsing are generally accomplished by using a burst technique. Water will be discharged in three or more bursts of 20 to 45 s duration, and the tank will be drained completely between successive bursts. This procedure is more effective in removing sedimentation and foam than is continuous rinsing and can be accomplished with much less water.

15.2.1.9 Air-Operated Valves

Prior to 1960 the plug-type valve in either a 2- or 3-way configuration was the valve most commonly used in dairy and food plant piping systems. The plug-valve cannot be cleaned in position, and the plug must be removed following the prerinsing operation so that both the body and plug can be manually cleaned prior to reassembly. Afterwards, the remainder of the CIP operation is completed with the plug in a fixed position.

Diaphragm type valves have been used to eliminate the necessity for manual cleaning but have the disadvantage of being available only in 2-way shut-off configurations. Hence, it is necessary to use three individual valves to achieve the same degree of flow control as is possible with a single 3-way plug valve. And, these valves must be installed with the diaphragm in a near vertical position to achieve proper drainage of the body cavity.

Butterfly disk valves have become widely used in nondairy food processes during recent years. Karpinsky and Bradley (1988) found that none of six commercially available butterfly valves proved to be totally cleanable without maintenance within 1 year of simulated operation, with all but one failing within 6 months. They cited a 1986 USDA training memo that

FIGURE 15.9 This assortment of ball and bubble type sprays and installation fittings is typical of those required for cleaning dry product processing systems. (Courtesy Electrol Specialties Company.)

"dictated that butterfly valves are to be installed in such a manner as to be readily accessible and demountable for inspection and servicing" and reported that none of the valves in the study complied with this requirement.

Butterfly valves and conventional ball valves are not considered CIP and if included in process piping must be manually cleaned prior to completing the CIP program for the connected equipment. However, a caged-ball valve is acceptable for mechanical cleaning if designed and installed in accordance with 3-A Standard Number 66–00 (1995).

The most satisfactory valve for CIP application is the rising-stem compression type valve with a molded rubber valve plug or seal or a Teflon™ O-ring seal on a stainless steel disk (Figure 15.10). O-rings are used for the valve stem seal, and the piping system design must provide for inclusion of all ports of the valve in the CIP circuit. Then, valve sequencing procedures are used to operate the valves in proper combinations throughout the cleaning program, causing water to first pass through the piping system in various directions. Every valve will be operated two or three times during the prerinse, four or six times during the wash, and three or four times during the postrinse. All portions of every valve and every part of the piping system are exposed to equivalent mechanical/chemical treatment. The operation of the valve causes the stem O-ring to pump some cleaning and rinsing solutions into the gland area.

When air-operated valving is used in extensive food plant piping systems, the design must permit one functional system to be cleaned while other systems are being used for process operations.

15.2.1.10 Mixproof Valves

Air-operated CIP-cleanable compression-type valves have been applied to automate dairy processes since the early 1960s. However, FDA regulations and 3-A Standards have never permitted a valve of any type to be used to separate a product containing vessel or line from a vessel or line containing cleaning solutions. They require instead a design which provides "make-break" connections for such isolation purposes.
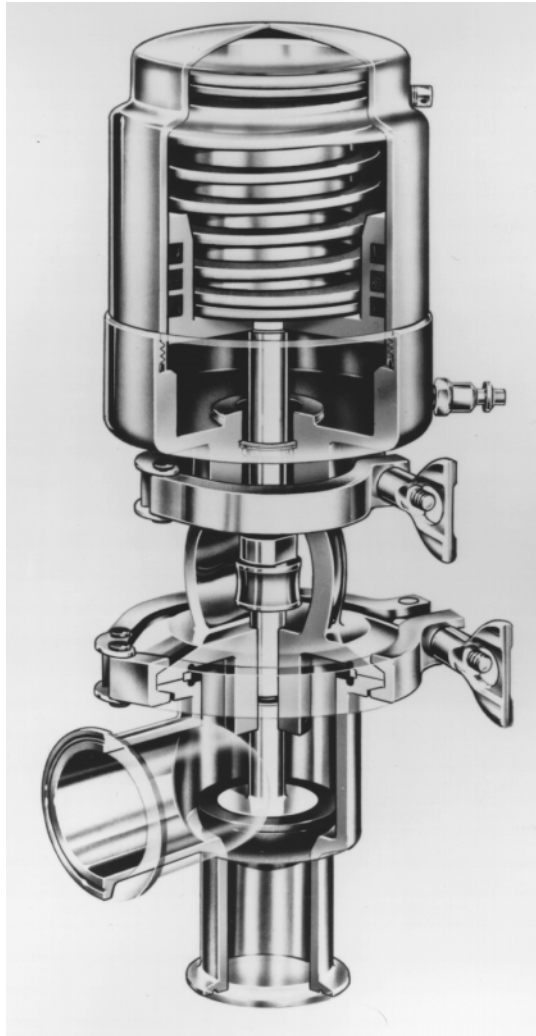
FIGURE 15.10 This compression-type sanitary valve is fitted with a reversible actuator. Valve stem must be "pulsed" during CIP operations to clean the stem O-Ring. (Courtesy Tri-Clover.)

More than two decades ago, several European manufacturers introduced the concept of mix-proof valves via the design and application of a *single* valve which provides the normal function of the well-known "double block-and-bleed" concept in reduced space, at lower cost, and in a fully CIP cleanable design. Mix-proof valves have been used extensively in the brewing industry and more recently in a variety of nondairy food processes and in pharmaceutical/biotech applications.

Figure 15.11 is a photograph of a mixproof valve recently introduced in the U.S. which has been designed to FDA and 3-A standards to include a full size leak port. This valve includes a seat lifter module on the actuator, a CIPS port which conveys CIP flush, wash, and rinse solutions to a passage between the inner and outer stems which control movement of the valve discs to a spray distributor located on the outer stem within the leak port area.

When this valve is closed the upper and lower discs and seals separate and provide a leak passage between both seats and any liquid in either body cavity to atmosphere via the large diameter leak port. When operating air is supplied to the actuator the top disc first contacts the seal on the leak port disc, closing the passages to the leak port. Continued

FIGURE 15.11 This mix-proof valve is equipped with a seat lifter module (top) and a vent cavity CIP supply (center). Any leakage due to failure of either of the valve sealing rings will be to atmosphere through the full size leak port, rather than from one fluid to the other. (Courtesy APV.)

movement to the open position permits flow between the upper and lower bodies, the moveable leak port being sealed to the lower body via the lip seals. During CIP cleaning of the associated piping CIP flush, wash, and rinse solutions may be applied to the leak port area and drain freely to the atmosphere (collection system generally provided) even when the upper body contains product, without subjecting the upper seat seal to pressure which might result in leakage and contamination of the product with cleaning solutions. The optional seat lifter module permits individual actuation of either disc seal to flush from the upper or lower body cavity to the leak port. Optional proximity sensors permit detection of the valve seat positions.

15.2.1.11 U-Bend Transfer Panels

U-bend transfer panels have been used in many dairy food plants to provide maximum flexibility for the production function, yet make it possible to assure controlled sanitation through mechanical/chemical cleaning and further guarantees the integrity of all individual product and cleaning and/or sterilizing flow paths. Such transfer panels are the result of continued modification and development of the component commonly referred to as a "flo-verter" or "cleaning hook-up station" used in the past primarily to control CIP solution distribution.

Four variations of small U-bend transfer panels are shown in Figure 15.12. With the exception of the two-port arrangement the others are based on some variation on the 120° triangle, the four-port diamond arrangement, or the more complex basic six-port hexagon which is widely used in many expanded forms to connect several primary ports to a multitude of others with a common length U-bend.
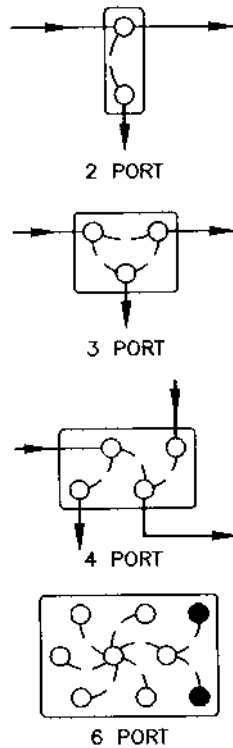
FIGURE 15.12 U-bend transfer panels of 2-port, 3-port (triangle), 4-port (diamond), and 6-port (hex) plus design may be used in these configurations, or as the basis of design of more complex panels.

Figure 15.13 is a photograph of a filler supply panel in a large fluid milk processing facility. This panel permits any of seven fillers to be connected to (a) a valve group which in turn controls flow from six high-volume product tanks, (b) any one of six byproduct tanks via the four upper headers, or (c) to a CIPS header. The lower headers include a CIPR header for cleaning individual byproduct tanks and a by-pass header to isolate a filler from the final circuit which includes six tanks, the valve group, all piping, and as many fillers as are available in a single circuit. Seiberling described the end result of this design concept as an "extended shelf-life fluid milk plant", i.e., a dairy capable of producing finished product with greater keeping quality by substantially improving the control of sanitation downstream of the pasteurization process, while using conventional heat treatment and packaging technology.

The Tank Connection Panel shown in Figure 15.14 was designed to connect a tank outlet valve to (a) a fill line port, (b) a filler supply line port, or (c) a CIPR port. A CIPS port was included to supply the filler supply line circuit. This panel included short internal headers.

The utilization of headers in transfer panels as described above requires special emphasis on the elimination of any dead ends. A branch of a tee (e.g., the port from the header to the skin of the transfer panel) must be limited to approximately 1½ pipe diameters to allow recirculation cleaning at normal velocities. Headers may be of double-tube construction or loop-type design as shown in Figure 15.15 to assure movement of solution in all portions of the system, at all times. The end portion of the transfer panel in Figure 15.15 is representative of the internal piping and construction of the loops as applied on the filler supply panel in Figure 15.13 and the double tube header in Figure 15.15 is representative of the headers in the tank panel shown in Figure 15.14.

The use of manually-positioned U-bends for establishing processing and CIP connections in a highly automated system may require some means of verifying the integrity of the
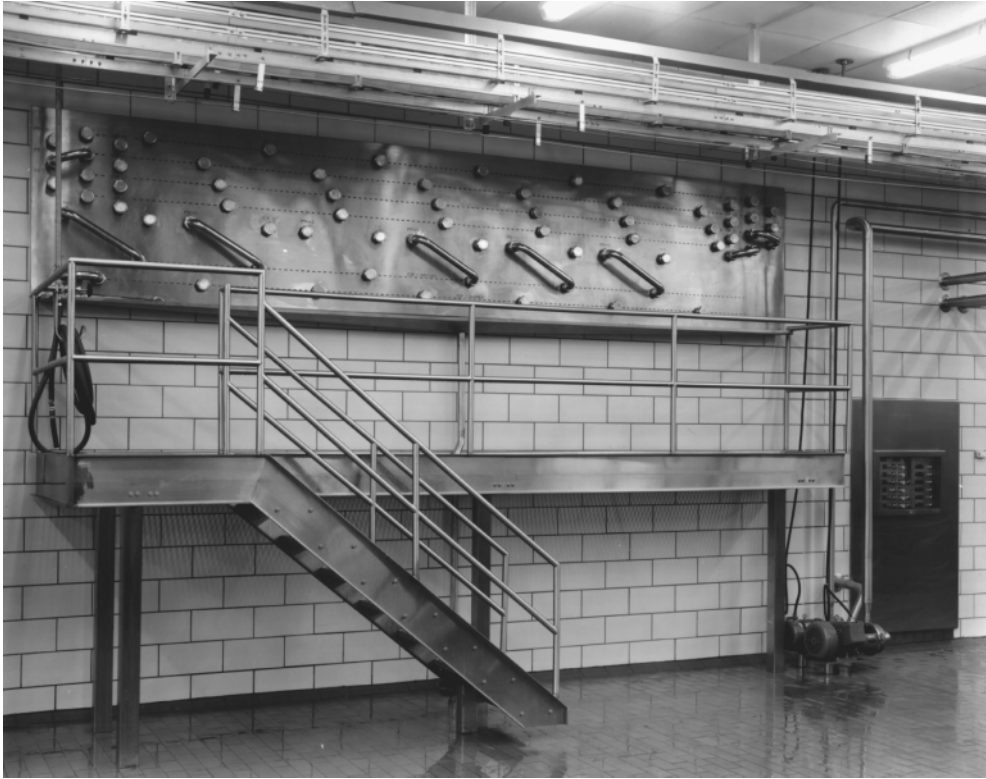
FIGURE 15.13 This filler supply transfer panel permits any or all of seven fillers to be supplied from any of four automated tanks, or by U-Bend connections to any of four byproduct tanks via four headers. There can be no mixing of products or products and CIP solutions in any operating configuration. (Courtesy Electrol Specialties Company.)
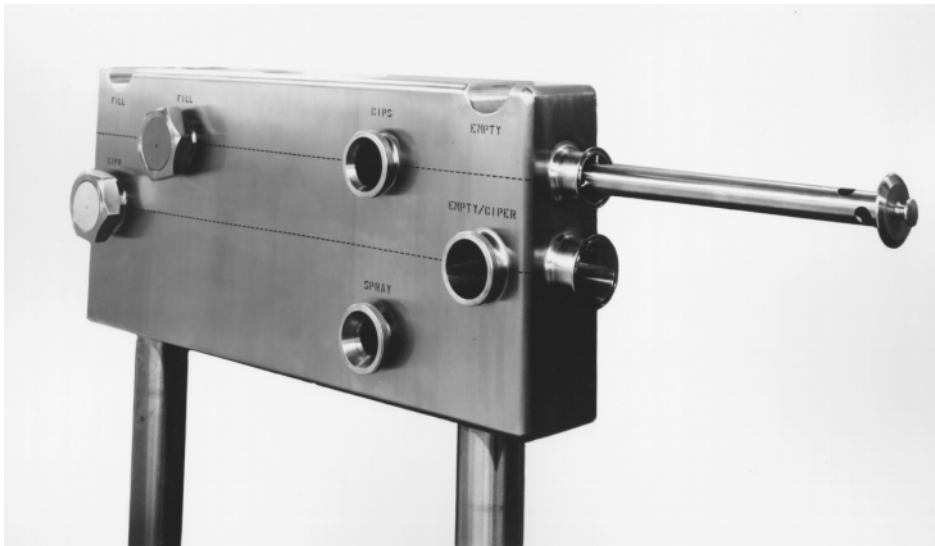
FIGURE 15.14 The headers in this tank outlet transfer panel are fitted with internal tubes (one partially withdrawn) to eliminate dead-ends. (Courtesy Electrol Specialties Company.)
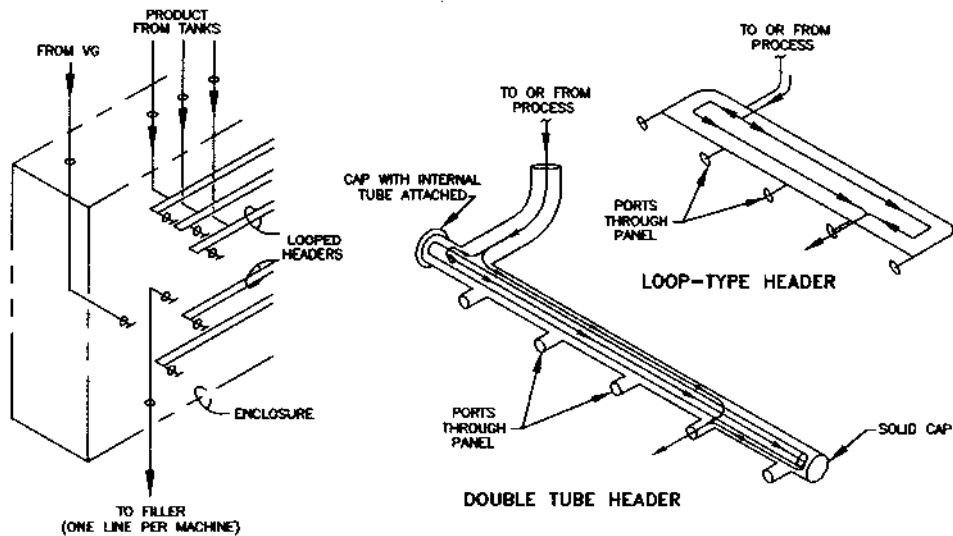
FIGURE 15.15 Transfer panel headers must be designed to eliminate header dead-ends. Loop-type and internal tube headers are illustrated on the right of this drawing which also shows a partial view of the internal piping of a panel similar to Figure 15.15.

required flow paths. This has been accomplished in practice by installing permanent magnets in stainless steel enclosures welded to the center of the U-bend connection. Proximity switches located behind the skin of the transfer panel may then be used to detect the presence or absence of a U-bend between any selected pair of ports. The computer or programmable controller database is developed to include the "allowed" or "required" connection for every established flow path necessary for processing, cleaning, or sterilizing procedures.

15.2.2 CRITERIA FOR CIP PROCESS EQUIPMENT DESIGN

CIP as applied today in those industries handling fluid and semifluid products is essentially chemical in nature. The processing equipment and all interconnecting piping is designed to permit the cleaning solution to be brought into intimate contact with all soiled surfaces and to be continuously replenished. Since the relatively high volumes of solution must be applied to soiled surfaces for periods of time ranging from as little as 5 min to as much as 1 h (or more), recirculation of the cleaning solution is essential to maintain economic operation. Flush and rinse water and cleaning solution may be pumped through piping systems at velocities ranging from 1.5 to 5 ft/s or more. Supply pressures to spray devices may vary from a minimum of 12 to 15 psi to a maximum of 60 psi.

Effective cleaning by this essentially "chemical" process requires maintenance of the cleaning solution at the required temperature and concentration throughout the recirculation period. This is easily accomplished in processing systems designed and operated for handling fluid and semi-fluid products but creates some special problems in cleaning the many types of equipment utilized in the dry cereal process.

Dairy processing equipment in the U.S. has, for many years, been constructed and installed in compliance with the 3-A Sanitary Standards or Accepted Practices formulated jointly by the International Association of Milk, Food and Environmental Sanitarian, U.S. Public Health Service, and the Dairy Industry Committee. On occasion, representatives of other food and beverage processing industries have viewed these standards as unnecessarily rigid. Perhaps some of the requirements such as inspectability, surface finish, and minimum radii are not as necessary with the advent of mechanical/chemical cleaning as when equipment

was being manually cleaned. Most of the design practices are based on long-term experience and will be reviewed here for the benefit of those concerned with the specification, purchase, and design of equipment for future nondairy food processes, with special attention to non-liquids processes.

15.2.2.1 Tank-Like Vessels

The criteria applicable to the design of horizontal tanks of both cylindrical and rectangular construction are, in many respects, equally applicable to the design and construction of mixers, bins, cyclones, and any other "vessels" involved in the process. Suggested criteria include:

1. Bottoms of flat vessels should pitch not less than ¼ in./ft from rear to front (or more specifically the high-point to the low-point) and ½ in./ft from side-to-center to provide reasonable flow across the surfaces for purposes of moving suspended solids.
2. Flat top surfaces should pitch approximately ½ in./ft from center to sidewalls to encourage the continual flow of water sprayed on these surfaces toward the side-walls.
3. A minimum radius of 1 in. is desirable at all corners, whether vertical or horizontal.
4. The vessel must be equipped with an adequate permanent vent to protect against all changes in pressure or vacuum resulting from the heating and cooling associated with the cleaning process.
5. Mechanical seals should be used for agitators, and if steady bearings are required, they should provide only line or point contact and serve mainly to provide guiding only, rather than support.
6. Projectile-type thermometer wells are acceptable for use with filled tube temperature indicating and recording systems. Thermocouples or RTDs are installed to sense only the temperature of the tank surface and provide an even more satisfactory installation from the standpoint of cleanability.

15.2.2.2 Dryers and Ovens

The modification of the design of dryers and ovens to improve CIP cleanability should include, in addition to the above, consideration of the following criteria:

1. Doors (and their associated gaskets) should be eliminated to the maximum extent possible.
2. Bolted-together assemblies (sections) are acceptable if the joint/gasket design provides a reasonably flush interior surface, free of crevices and/or protrusions.
3. Bottom and top surfaces should be pitched in accordance with the criteria previously established as should minimum radii wherever possible.
4. Provision should be made for installation of valves and CIP return line connections at all drain points.
5. The interconnecting ductwork to and from the fans, heaters, and cyclones should be as short as possible and included in the CIP system, requiring consideration of the same criteria to this part of the machine as subsequently described for *piping and ducts*.

15.2.2.3 Piping and Ducts

Some general recommendations regarding the design and installation of CIPS/R piping, and applicable to a substantial degree also to the design of ducts utilized for moving product with air or by gravity include the following

1. Inert-gas welded joints are the most suitable for all permanent connections in transfer systems constructed of stainless steel.
2. Clamp-type joints of CIP design are acceptable for semipermanent connections. In the broadest terms, CIP design infers (a) a joint and gasket assembly which will maintain the alignment of the interconnecting fittings, (b) a design which will position the gasket so as to maintain a flush interior surface, and (c) a design which assures pressure on each side of the gasket at the interior surface to avoid product buildup in crevices that might exist in joints which are otherwise "water tight".
3. All parts of the piping or ductwork should be pitched at $\frac{1}{16}$ to $\frac{1}{8}$ in./ft to drain points.
4. The support system, provided for the piping and ductwork, should be of rigid construction to maintain pitch and alignment under all operating and cleaning conditions.
5. Dead-ends and branches are undesirable and all mandatory branches or tees should be located in a horizontal position and should be limited in length to not more than 1.5 pipe diameters. Vertical dead-ends are undesirable in fluid processes because entrapped air prevents cleaning solution from reaching the upper portion of the fitting.
6. Piping or ductwork design should provide for inclusion of the maximum amount of the system in the CIP circuit(s). It is better to install one or two small jumpers than to remove and manually clean five or six short lengths of piping or ductwork. Mechanical/chemical cleaning is much more rigorous and is subject to better control than manual cleaning.

15.2.2.4 Conveyors

A variety of conveyors have been included in CIP cleaned food processes, including belt, screw, bucket, and pneumatic conveying systems. Belt, large screw, and bucket conveyors are generally shrouded or installed in housings to permit effective application of spray devices. The housings in turn must be constructed to the above-defined criteria for tank-like vessels. Examples of successful applications are included in the subsequent section.

Design practices and installation procedures which have been proven to produce satisfactory CIP results are illustrated on Figure 15.16. *Note:* (1) the center to end pitch of ¼ in./ft; (2) the center to side pitch of ½ in./ft; (top and bottom); (3) the radius corners; (4) the pod-type outlet to enhance CIP return pump operation; (5) the sump-type CIPR connection which will eliminate any quiescent puddle on the bottom of the vessel; and (6) the installation of bubble sprays in the attached ductwork. Details (A) and (B) illustrate methods of installing sprays in glass-lined tanks or Teflon®-lined piping and detail (C) illustrates the tri-clamp connection applicable to the sprays shown as item (6).

15.2.2.5 Materials and Surface Finish

Whereas other materials may ultimately find increased application in food processing systems, stainless steel is the most suitable material of fabrication at the present time. Dairy and beverage processing equipment and interconnecting piping has most commonly been made of Type 304 (18-8) material. Those processes which handle products high in chloride concentration are more commonly constructed of Type 316 stainless steel, or more recently Type 316L. Many pump heads and valve bodies are now fabricated of Type 316 as the "standard" material. Considerable experience has demonstrated that the high finishes required by the 3-A standards are not necessary in other food industries, but the basic principles of construction are beneficial in achieving a high degree of cleanliness. Zoltai et al. (1981) has reported on the cleanability of stainless steel surfaces with variations in surface finish.
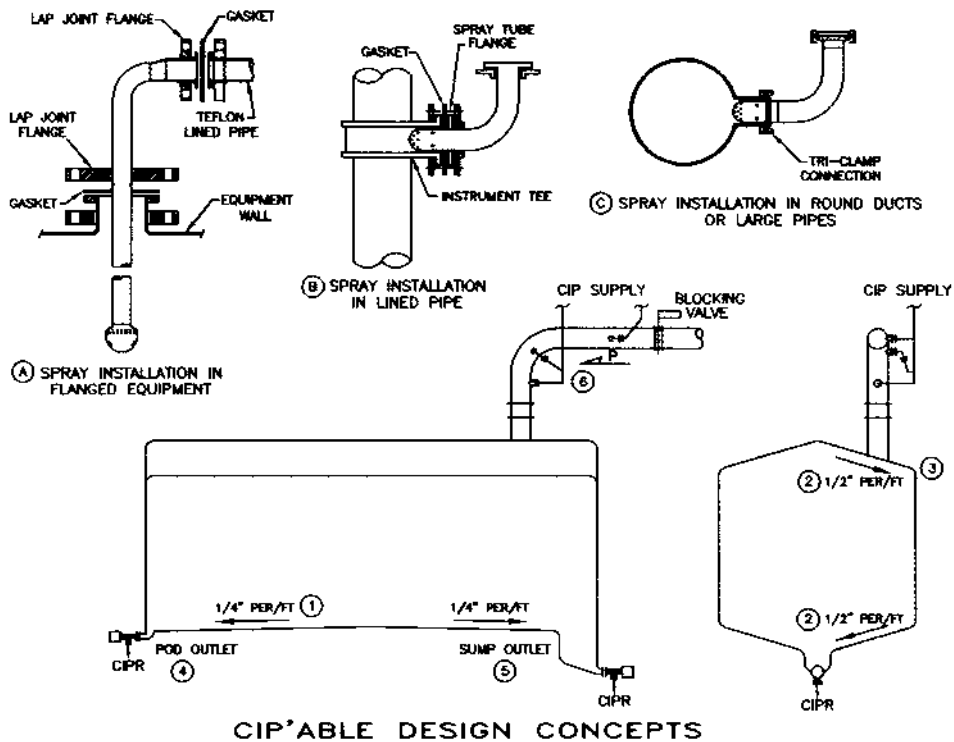
FIGURE 15.16 A dry material processing, transport, or storage vessel may be made CIP proficient by using construction details defined in this illustration.

The CIP process has been successfully applied to a substantial amount of equipment not of stainless steel construction, especially in the brewing industry, both in this nation and abroad. Fermentation and storage tanks constructed of epoxy-lined mild steel have provided excellent service if the design and application prevented any requirement for frequent personnel entry and the associated physical damage. In England, CIP systems have been successfully used to clean fermentation and storage tanks of both copper and Ebon-line concrete construction as well as glass-lined construction.

All processing equipment must be designed to permit cleaning solutions to be brought into contact with all product contact surfaces. And, the equipment should preferably confine these cleaning solutions to eliminate loss and to prevent damage to personnel or other equipment in the immediate area as a result of splashing, spilling, or leakage. The requirements of the cleaning operations must be given as much consideration during the system design as the requirements of the process itself.

15.3   APPLICATIONS

15.3.1   CIP CLEANING OF A LIQUID FOOD PROCESS

15.3.1.1   Automated Process Piping via Headers

A simple combination of three tanks, a small amount of receiving and process supply piping and a CIPS/R system designed to clean everything from a permanently installed CIP unit is delineated by Figure 15.17. This generic process provides for receiving oil and liquid sugar (or corn syrup) by tankers equipped with self-contained pumps capable of delivering all or part of the tanker's contents via a hose connection to a U-bend transfer panel PHS-1 (product

hook-up station 1), located through an exterior wall of the facility. Oil receiving would be through a single line to tank OIL1, via an elbow final connection to a top fill nozzle. Two different sugars may be received to SUG1 and SUG2 by a common line to two air-operated valves which control discharge to the selected tank.

The CIP unit is interfaced to the process piping and tanks by a CIPS to four distribution valves above the CHS (cleaning hook-up station). One valve supplies the CHS following which the positioning of the associated U-bend provides continuation of flow to the spray in the selected tank. The tank outlet connection is also by a U-bend to either the process supply pump or to the CIPR header.

A second CIPS valve is connected to the end of the CIPR at SUG1 and is a *CIPR Flush* line. To prevent the development of a dead-end in the CIPR header when washing SUG2 or OIL1, or the transfer line circuit AB, this valve would be pulsed, i.e., opened for 3 to 5 s once each minute throughout the CIP program to flush, wash, and rinse that portion of the CIPR header which would otherwise contain a mixture of the first product to be rinsed from the tank and the various CIP solutions on completion of the program. The small schematic *Tank Circuit TF* illustrates the continuous flow **T** through the CHS to the OIL1 spray and return flow from the tank to the CIPR header. The intermittent flow **F** would be controlled by the flush valve, with supply to the spray diminishing whenever this valve is opened, thus maintaining a constant recirculation rate controlled by the vortex meter VM and flow control valve FCV. Any one of the three tanks can be cleaned in this identical manner, whenever empty.

The process transfer is via an oil pump PP1 and a sugar pump PP2 for either sugar, with delivery through two parallel lines to the required point in the subsequent process. On completion of process supply, and with the tanks still containing ingredients, the transfer piping and pumps can be cleaned by disconnecting each tank from its discharge line and repositioning the U-bend to connect the supply port of the transfer header to the CIPR header. The two moveable elbows at the discharge control valves would be repositioned to the CIPS connections to provide reverse flow through the transfer lines and pumps to the CIPR header to use a common CIPR line. When cleaning the resulting *line circuit ABF* the CIPS flow **ABF** would be from the process line distribution valve as stream **AB** subsequently sequenced through the sugar line as **A** and the oil line as **B**. The CIPR flush valve would be pulsed as described previously to permit stream **F** to clean the end of the CIPR header and the permanent flush line connection.

The receiving line would be cleaned independently, after each use by supply at PHS1 and continued flow through the lines to the fill connections at the tanks, where moveable elbows would be positioned to CIP tielines to continue the flow to the CIPR header.

The simple concepts illustrated in Figure 15.17 may be applied to any combination of piping and tanks to (1) isolate the products in tanks and piping from any CIP flush, wash, and rinse solutions, and (2) assure absolute freedom of dead-ends in the process-CIPS/R piping runs as the common CIP unit is automatically controlled to (3) spray clean process vessels or (4) pressure wash transfer piping.

### 15.3.1.2 Automated Process Piping Design with Valve Groups

The traditional application of air-operated valves in a CIP cleanable piping system as applied to dairy, brewing, and many food processes is illustrated on Figure 15.18. The piping shown provides the means of filling, emptying and cleaning three tanks via a low-level valve group and product transfer pump PP1. The bottom fill/bottom empty configuration shown in Figure 15.18 would function as follows:

1. For the production run, the moveable elbow at each tank outlet valve would connect to the fill/discharge line from the tank to the valve group. The tank could be filled
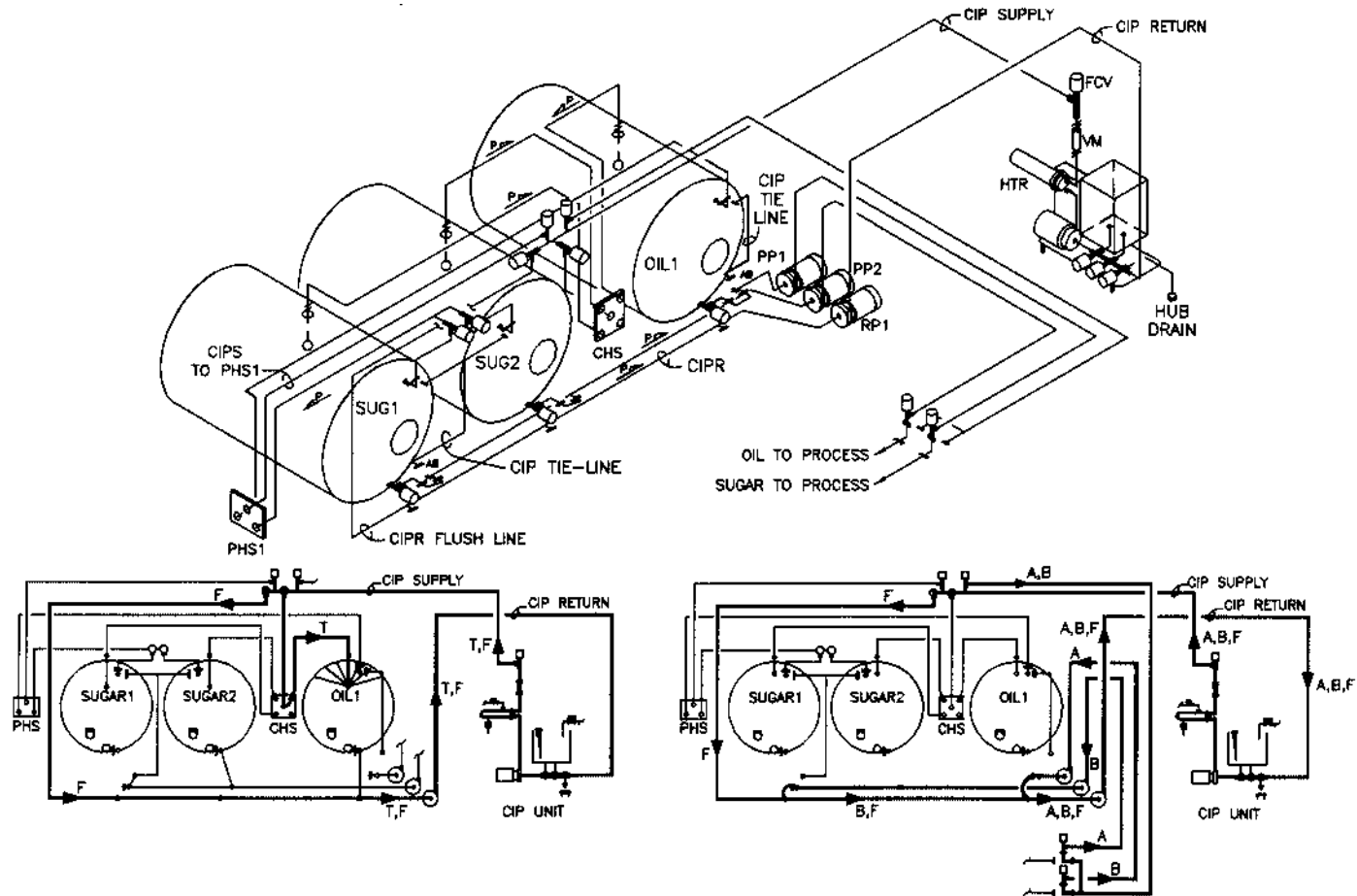
FIGURE 15.17 CIP systems are interfaced to the tanks and lines to be cleaned by installation of CIP supply/return piping. Typical CIP circuits are shown at the bottom of this figure.
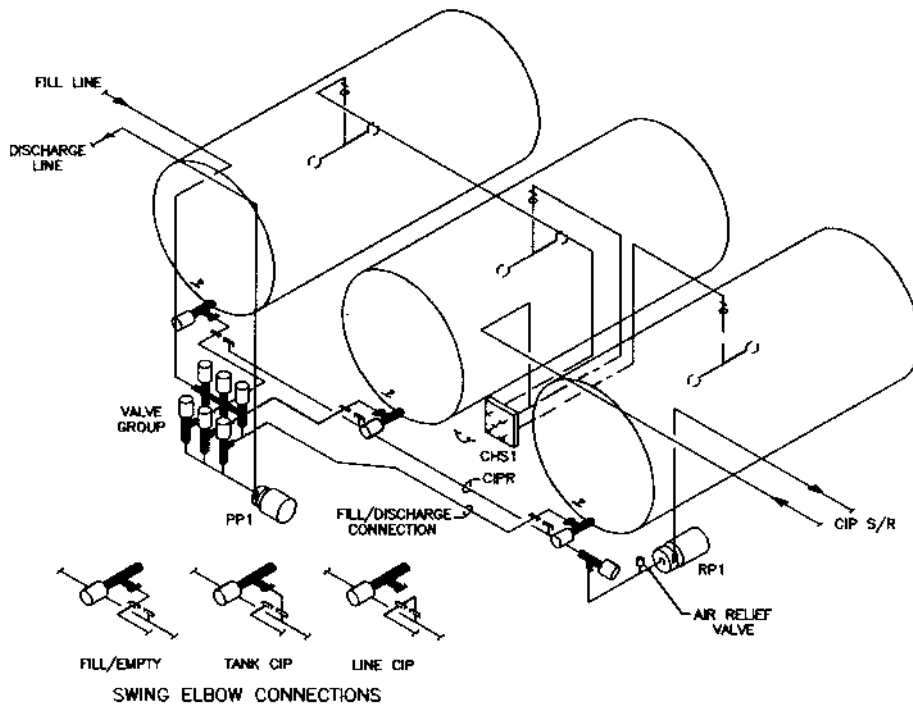
FIGURE 15.18 Compression type valves in manifolded assemblies for shop fabrication provide two fill paths and one discharge line for three tanks. Moveable elbows provide process/CIP separation.

or emptied under automatic control by proper operation of the process valves and pumps.

2. To clean a tank, (a) process flow would be terminated, (b) the moveable elbow would be reinstalled between the tank outlet valve and the tank CIP return line, and (c) the cap removed from the return line would be used to temporarily close the fill/empty line. These fittings must be rinsed and cleaned when making the connection change. In this configuration, the tank is isolated from the process piping via the swing-elbow. The U-bend on the cleaning hook-up station would be properly positioned to supply solution to the desired spray.

3. At the end of the production run, and with product possibly remaining in the tanks, the removable elbow would again be manually cleaned and repositioned to connect the fill/empty line to the tank CIP return line now used as a CIP tie line. The cap would be placed on the tank outlet valve, providing protection against contamination or inadvertent loss of product due to improper operation of that valve when the tank is not connected to the process piping system.

4. When cleaning the tanks, the tank outlet valve must be "pulsed" to clean the valve stem O-ring and this is generally accomplished during the drain period following the prerinse, solution wash, and postrinse.

5. When cleaning the lines, the fill/discharge valves in the valve group must be sequenced to provide controlled flow through each portion of the interconnecting piping and to clean the valve stem O-rings.

Experience has demonstrated that each valve should be moved three to four times during the prerinse, four to six times during the solution wash, and four to six times during the combination of the postrinse and acidified final rinse.

The arrangement shown in Figure 15.18 could be extended to include a separate fill valve group for separation of filling and emptying lines. The additional fill piping could connect to the CIPR header for cleaning by use of CIP tielines as described previously for Figure 15.17. Whereas the additional fill valves increase the capital cost, the operator workload, and the opportunity for recontamination following cleaning, such design practices are necessary if it is essential to clean piping which controls filling of tanks and emptying of tanks separately from piping which empties the tanks.

15.3.1.3   CIPS/R Piping Engineering and Installation

The installation of CIPS/R piping for applications as described by Figure 15.17 and Figure 15.18 should be in accordance with the following general design criteria

1. The CIPS distribution valves should be located at the highest point so that the piping will drain backwards to the CIP unit and forward to the low spot of the loop, then to the floor through CHS1.
2. The CIPS to CHS1 should pitch downwards, or if the CHS is at a higher level, it may *continue* to pitch upwards.
3. All spray supply lines should pitch from a point over the spray device backwards to drain to the CHS ports which are opened on completion of the CIP operation.
4. All CIPR headers must pitch continuously towards the pumps and generally the risers from the pumps will become the high points of the system and the CIPR piping will pitch continuously from that point toward the CIP unit.
5. Primary and secondary CIP supply lines would generally be 2 in. in size for CIP flow rates of 40 to 80 gal/min.

15.3.1.4   CIP Pump and Control Valve Sizing

The flow control valve (FCV) should be provided as a throttling-type valve with a Cv which enables the valve to produce 20 to 25% of the total CIPS system headloss for good sensitivity, quick response for flow-rate adjustment, and prevention of "wire-drawing" due to operation too close to the seat. The use of vortex meters and flow control valves in the CIPS system permits software control of all CIP flow and is a major improvement over the use of restrictors to balance flow as applied from the beginning of CIP until the mid-1970s.

15.3.1.5   CIP as an Integral Part of the Process

It is not always necessary to purchase and install CIP recirculating units and supply-return piping to accomplish highly effective CIP cleaning. Figure 15.19 shows a HTST pasteurizer used in the dairy industry, a combination of a three-section plate heat exchanger, constant-level tank, holding tube, flow diversion valve, and interconnecting piping which can be engineered to meet the production requirement *and* provide highly effective automatically controlled cleaning. The system is physically isolated from the supply and discharge piping and connections are made to provide for automatic addition of acid and alkali to the constant-level tank (CLT). The latter tank then serves as the solution tank, a two-speed centrifugal pump (SP) provides the motive force required to achieve the desired recirculation flow rate and the HTST recycle valve becomes the drain valve, controlling discharge to either the constant-level tank for recirculation or to the drain for flushing and rinsing. The regenerator bypass valve, flow diversion valves (FDV), and HTST discharge valves will all be "pulsed" under automatic control to assure proper cleaning of the associated piping and the valve stem O-rings. Figure 15.20 is a photograph of a system similar in design which includes a CHS at the constant level tanks to organize the piping connections for the production run, CIP of the HTST, and CIP of the supply piping from the source tanks and a milk recovery system.
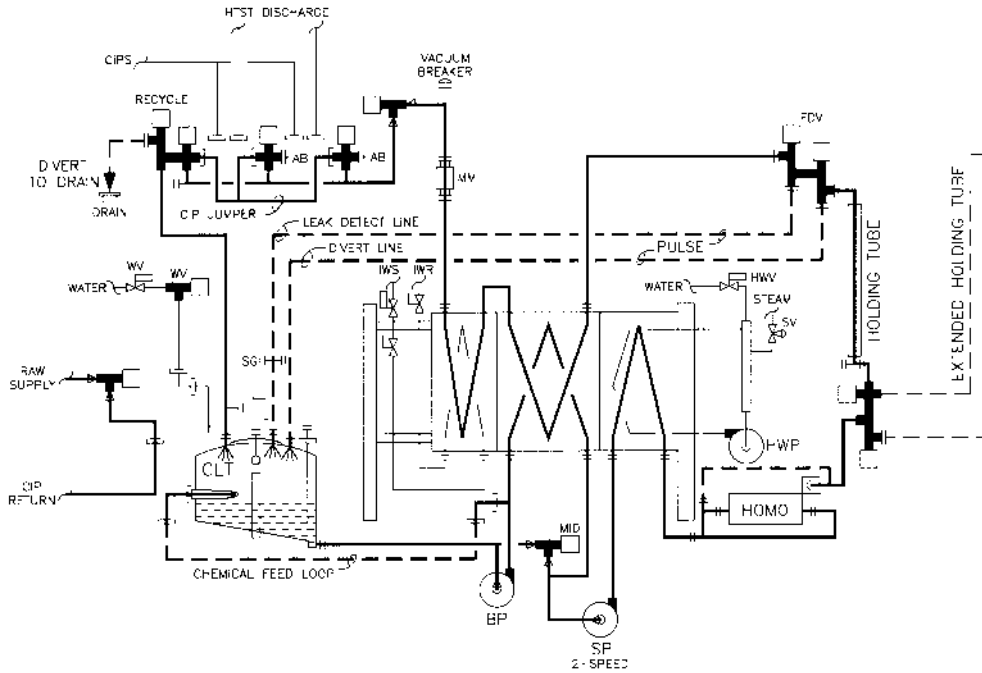
FIGURE 15.19 Some processing systems, like this dairy HTST system, can be modified to accomplish CIP as an integrated process by use of process pumps, valves, heat exchange, and control equipment.

15.3.2 CIP Cleaning of the Dry Food Process

Prior to about 1963 the dairymen considered the milk spray dryer to be trouble-free from the sanitation standpoint in that it was always dry, and always hot, and would therefore not support bacteriological growth. Several food poisoning outbreaks provided the impetus to develop CIP systems to clean dryers more effectively than the manual procedures then in use. Since the major soil was in the main chamber it was often decided to install CIP equipment for that part of the system alone. It was quickly learned, however, that the labor and physical requirement to separate the main chamber from the continuing ductwork, cyclones, vent stack, etc. was difficult and time consuming. Further, the migration of moisture into these areas during the cleaning process resulted in the partial wetting of the solid residues, subsequent caking, and ultimate discharge of this unsatisfactory material to the finished product. Within a period of several years it was determined that the most effective way to clean a milk spray dryer was to clean the complete system, as an entity, and design it accordingly.

The basic concepts and criteria applicable to the CIP cleaning of milk spray dryers, and the applicable 3-A Standards, have been applied during the last two decades to the design and installation of many items of equipment and complete processes, which in the final analysis, were comparable to the problems faced in cleaning one or more spray dryers, in a single system, simultaneously. The 3-A Standards accept only welded pipelines and silo tanks as CIP without provisions for inspection. Adherence to the basic 3-A criteria, however, has enabled the design of many satisfactory CIP systems for snack food, dry cereal, and drug processes, and a high potency agricultural chemical process. In each application it was mandatory to reduce the openings for inspection or manual cleaning to the minimum, as the ability to *inspect and CIP are not mutually compatible.* These projects required a much greater level of confidentiality than the normal dairy project and the experiences of the past 20 years

FIGURE 15.20 This HTST is equipped with a CIP constant level tank supplied through a U-bend transfer panel.

were reported by Stewart and Seiberling (1996) only recently. Some generic extractions of the designs of typical processing equipment follow.

Figure 15.21 shows an application of permanently installed spray devices to clean stainless steel conveyor belts in a continuous cheese cheddaring machine. The entire assembly of belts, rollers, and sprays was mounted in a stainless steel frame with removable stainless steel covers designed and installed to confine solution and cause it to ultimately drain to the CIPR return pan at the bottom of the machine which was approximately 3 ft wide × 60 ft long. The CIP unit shown on this drawing incorporates a powered rotary strainer in the CIPR line to remove undissolved cheese curd from the return line and prevent its recirculation through the system and, ultimately, plugging of the spray devices.

Some years ago meat smokehouses were made of mild steel since they were always hot and dry, and the presence of natural fats prevented rusting. They were cleaned only occasionally by scraping. Then contamination of the product with residual material became a greater concern and the smokehouses were subsequently constructed of stainless steel but to the prior designs. High-pressure spray cleaning and foam cleaning proved to be very labor intensive and substantially less than 100% effective. When a major meat processor provided the initial opportunity to CIP a smokehouse, it was quickly determined that the smokehouse was analogous to the milk and whey dryer in that it was a combination of large chambers, ductwork, vent stacks, air handling equipment, and air distribution equipment within the structure. The soils found on these surfaces included creosote, charred protein material and fat, and represented the most rugged soil ever attacked via CIP procedures. It was found that high-volume recirculation of a chelated caustic at perhaps 3% concentration and 175–180°F would remove all of the soil from all of the surfaces of a system which required 18 man h
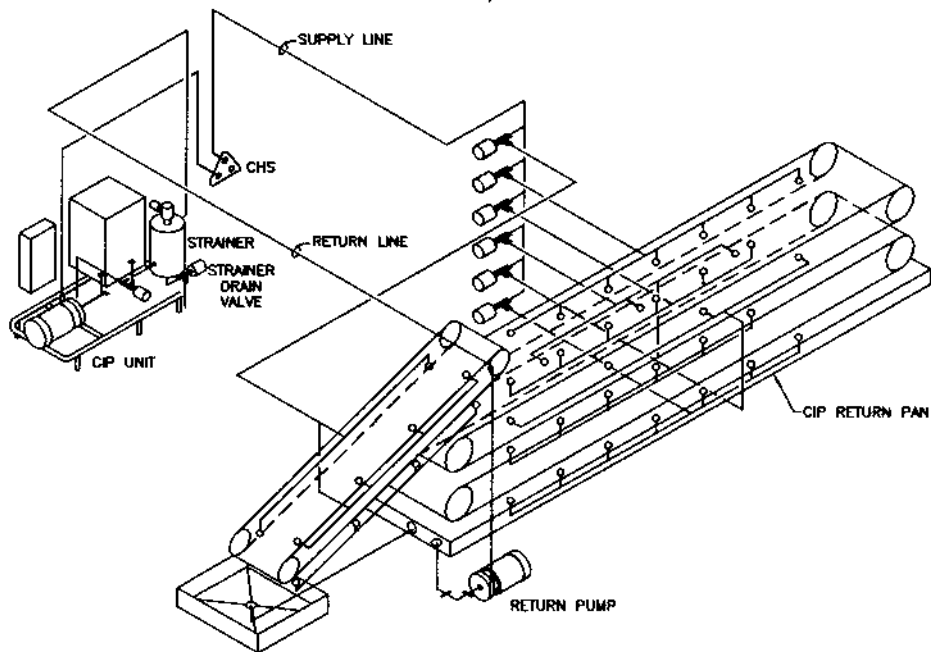
FIGURE 15.21 This continuous cheddaring machine includes perforated stainless steel belts on support rollers and guides in a stainless steel housing approximately 40 ft × 4 ft × 8 ft in overall dimensions and is an example of how permanently installed ball and bubble sprays may be used to apply flush, wash and rinse solutions in a top-to-bottom sequence. Nonsoluble material must be removed from the return flow by a powered strainer in the CIP return line.

to clean to a lesser degree with either foam or high-pressure low-volume systems. A schematic diagram of a typical smokehouse system is shown in Figure 15.22. Since smokehouse soil was also high in nonsoluble particulate material, the CIP system for this application was also fitted with a CIPR powered rotary strainer.

15.3.2.1 CIP of Dry Granular Product Processes

This generic definition applies to any system which (1) processes a nonliquid product, and (2) will not fully contain (or confine) water, due to (a) the nature of the equipment and (b) the machine-to-machine interface requirements involving food transfer between fixed, vibrating, rotating, or otherwise moving parts. More simply put, it is very easy to CIP clean a piping system via pressure recirculation, or to spray a tank with a single outlet for return solution flow. The equipment used for drying milk or whey, cheddaring cheese, smoking meats, drying yeast, making snack foods, and making a variety of cereals creates a considerably greater challenge. The design criteria, however, and the basic approach, are very similar.

15.3.2.2 Example of Dry Granular Process CIP Application

The powder dumping, de-lumping, screening, and blending system shown in Figure 15.23 will introduce the concepts applicable to complete processes. This basic system is common to many dry product processes, sometimes being installed in multiples to handle different ingredients simultaneously.

The powder dumping/dust control system at the top of this figure requires access to remove the bags before CIP and a gasketed cover to close the dump hopper. The exhaust line is fitted with a butterfly valve below the elbow. A single ball-type spray on an elbow above
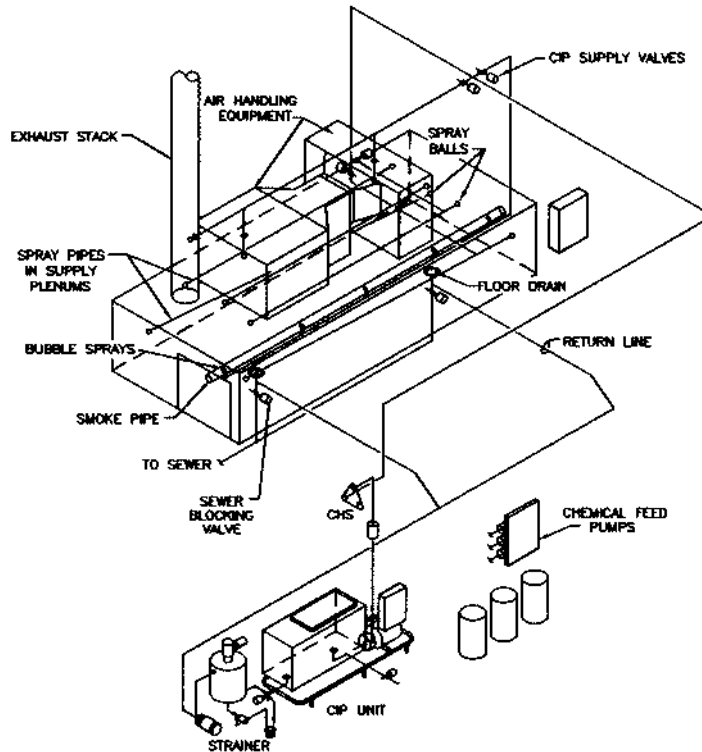
FIGURE 15.22 A stainless steel smokehouse approximately 30 ft × 8 ft × 10 ft plus air heating and recirculation equipment and smoke generators is an example of how the application of permanently installed tube and ball sprays may permit cleaning large surface areas in complex, inaccessible locations.

the bag area will provide downwards coverage of the bag retainers and will spray up to the face of the valve. A better design would place the valve in the horizontal run beyond the elbow, and add a spray at the elbow to wash the face of the valve. This would eliminate the possibility of dry material downstream of the valve falling back into the clean system when the valve was opened after CIP.

An elbow mounted ball spray above the de-lumping grate would provide coverage of the bottom of the bag retainers and the top of the de-lumper grate. A multiple bubble tube spray would adequately cover the bottom of the de-lumper grate, the hopper area, and the chute to the feed screw to the screen. Ball or bubble sprays would be installed to clean the screw conveyor per a subsequent figure. The screen is most effectively cleaned by installation of a tube spray within the screen and the housing is covered by the ball spray below the screen. For CIP a removable CIP collector is manually installed to divert solution discharged through the large particle chute at the end of the screen to a nozzle in the subsequent Mixer.

The mixer is fitted with paddles shown only on the end view, with the discharge screw in the center. A tube spray with multiple bubbles provides adequate coverage of the mixer body, the rotating paddles, and the rotating screw. Supplementary bubble sprays are required in the screw feeder discharge tube as shown. The large CIP collector pan would be manually installed to receive *all* return flow. The sprays in the various portions would be supplied through separate CIPS distribution valves for the dumper, screen, and mixer and flush, wash, and rinse solutions would be continuously sequenced downwards through the stack throughout the CIP program. Proper selection and application of sprays would permit this total system to be cleaned at a flow rate of 80 to 100 gal/min maximum.
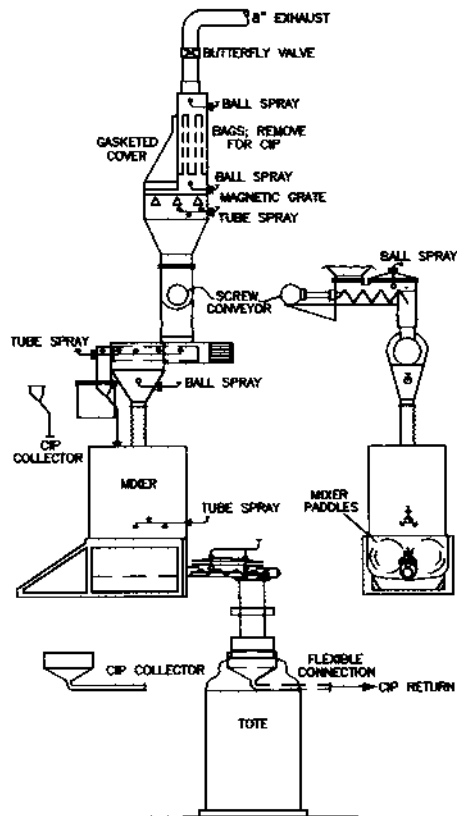
FIGURE 15.23 The dry material dumping, de-lumping, screening, and blending equipment on this illustration is fitted with fixed ball, bubble and tube type sprays illustrated on Figure 15.8 and Figure 15.9. Note the two *CIP collector* devices and dash-lined installation positions.

15.3.2.3 Dry Cereal Process CIP Application

A large dry cereal process was designed as CIP by mounting all of the equipment on three space frames similar to the generic example on Figure 15.24. The process could not be made water-tight as many transitions of the product from one item of equipment to the next occurred between rotating or vibrating components which could not be sealed to one another. The process was therefore a dust producer and during a production run of 5 to 12 d both fines and product would escape to and deposit on the surfaces of the space frames and the external surfaces of the equipment. A major design decision was to incorporate an *external CIP system* as the means of removing both accumulated solid waste and flush, wash, and rinse solutions which escaped from the *internal CIP system* during the cleaning programs, each of which were designed to clean an entire module inside and outside simultaneously.

To handle solution return from the external CIP system the space frames were located above a dairy brick floor set in chemical resistant grout to serve as the CIP return collector. Large diameter PVC pipe conveyed liquids from the floor area to four external CIP units each of which was fitted with static screen strainers capable of removing any solid material which would plug sprays during recirculation. The solids were conveyed to a solids collection tank for removal from the site by tanker.

The process included cookers specially designed for spray cleaning on an individual basis after each period of use, much like a dairy tank, via a conventional CIPS/R piping system fitted with automated return collector pans to replace similar components in the example
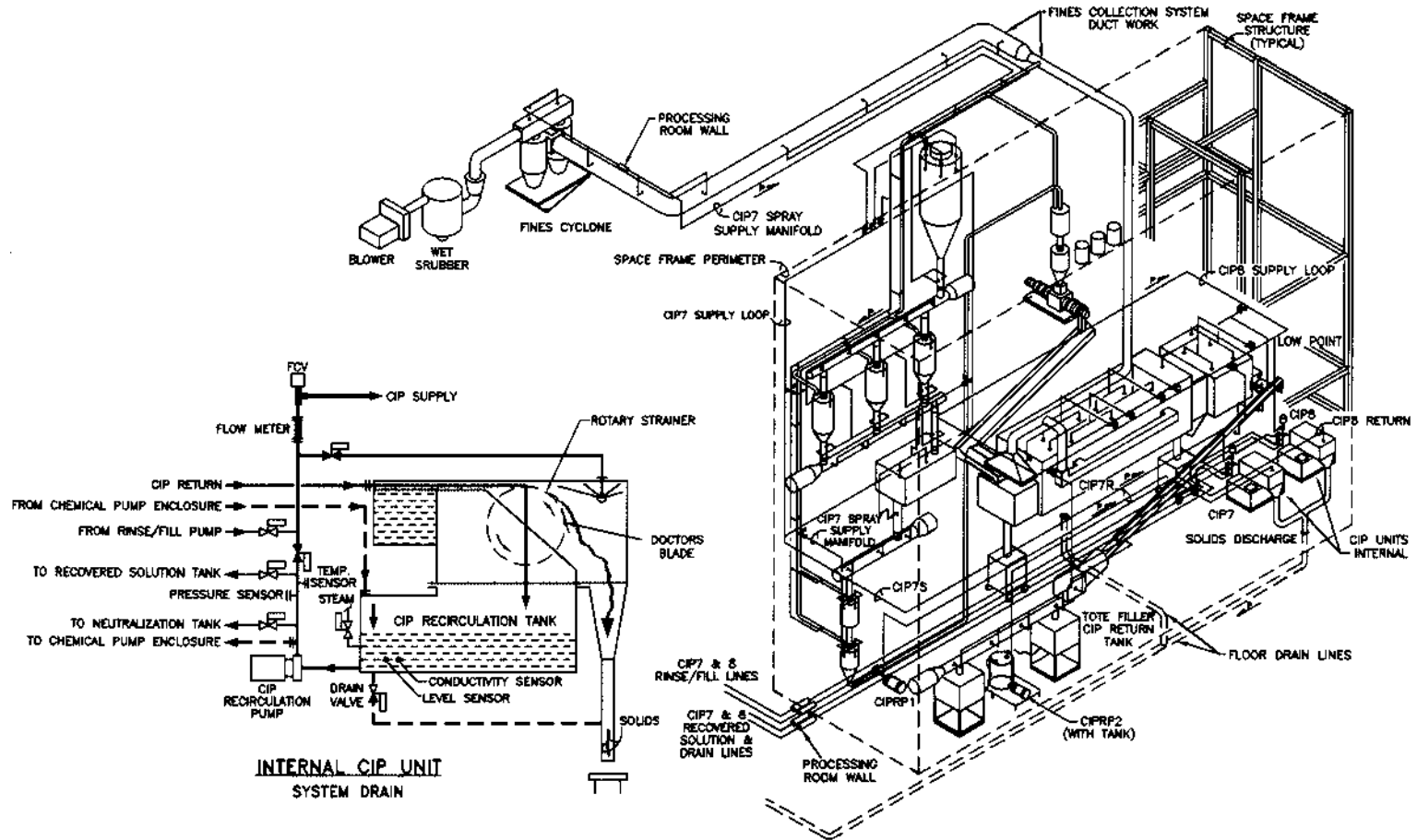
FIGURE 15.24 This isometric illustration shows the routing of CIP supply piping to sprays in a variety of machines required to process a dry granular food product and to fines collecting ductwork. The process was arranged on multiple space frames located on a dairy brick floor and was cleaned internally and externally, simultaneously, by separate CIP systems. The primary CIP support equipment is shown in Figure 15.30.

shown in Figure 15.23. And, the process included a number of horizontal tanks for liquid ingredients which were also supported by conventional CIPS/R piping which permitted any tank or the associated receiving and transfer lines to be cleaned whenever not in use, in a manner similar to that shown in Figure 15.17.

The remainder of the process, however, was cleaned in one or more circuits running simultaneously from *internal CIP units* located at the lowest point of each module (but above the floor) as shown in Figure 15.24, supported by large tanks, high capacity CIP pumps, the required CIPS/R distribution valves, and the external CIP units located at the lowest level of the facility (Figure 15.30).

Each of the CIP circuits was designed to be cleaned with a recirculation volume of approximately 300 gal, this amount of water consisting of (a) that water required to fill the CIPS piping from the CSP to the sprays, (b) the water actually running down the surfaces of the area being sprayed at 300 gal/min at any given moment, (c) that water which occurs in puddles draining from the equipment previously sprayed (little holdup, however), and (d) the volume of water in the strainer hopper and CIP unit tank necessary to supply the CSP.

The detail schematic of the internal CIP unit shows solution flow paths during the recirculation wash step of the CIP program and will aid understanding of the following description of the system operation:

1. *Prerinse* — Recovered Solution (when available) or water from the support tanks via the rinse/fill pumps (Figure 15.30) will be delivered through the flow meter to the FCV and then to the sprays by a CIPS loop, i.e., one of the CIPS7 or CIPS8 loops defined on Figure 15.24, from which individual CIPS distribution valves control flow to the various groups of sprays. The loop eliminates any dead-end possibility on the supply side of the system.

   Rinse solutions sprayed sequentially into the various portions of the circuits above the Internal CIP units will all drain by gravity to the collection tank of the rotary strainer mounted above the CIP recirculation tank. Those portions of the circuits which terminated below the Internal CIP units were provided with CIP return pumps, i.e., CIPR1 for the stack of cyclones, vibratory tube conveyors and surge bins to the left of the illustration and CIPR2 with a collection tank to receive the discharge from tote filler CIP return tanks placed beneath the covers for the CIP operation. Both return pumps discharged to the internal CIP unit rotary strainer.

   Solids in the return flow will be removed by the doctor blade and dropped through the chute to the external CIPR piping. A spray in the strainer enclosure continuously flushes the strainer discharge chute area to fluidize the solids and move them to CIPR.

   On completion of the prerinse the drain valve would open to drain the tank of final rinse water.

2. *Solution Wash* — The first step is a system fill; the delivery of the required quantity of water through the sprays and via the return system to the CIP recirculation tank to a software controlled volume. At that time the rinse/fill pump operation will be terminated and the CPS will start to establish recirculation from the CIP unit through the circuit and back, via the rotary strainer. The steam valve would open to inject steam to heat the solution and the chemical pumps would deliver alkaline solution through a chemical loop as previously described in Figure 15.4. The recirculated wash time would start when the entire circuit was at temperature and would continue for the required volume to sequence solution through the various sub-circuits the required number of times. The wash times for the various subcircuits were individually adjustable on the basis of soil load in each circuit.

3. *Postrinse* — Potable water from the support tank via the rinse/fill pump will be delivered through the flow meter to the FCV and then to the sprays as described above for the prerinse. However, CIPR flow continues through the rotary strainer to the CIP recirculation tank, and then via the CSP to the recovered solution tank, for use as the prerinse for a subsequent circuit. If the recovered solution tank reaches a high level, discharge is diverted to the neutralization tank. On completion of the postrinse, the drain valve would open to drain the tank of final rinse water.

4. *Acidified Final Rinse* — The first step is a system fill as described for the solution wash. When the CPS starts to establish recirculation from the CIP unit through the circuit and back, via the rotary strainer, the steam valve again opens to inject steam to heat the solution and the chemical pumps would deliver acid solution through a chemical loop as previously described in Figure 15.3. The recirculated acidified rinse time would start when the entire circuit was at temperature and would continue for the required volume to sequence solution through the various subcircuits the required number of times. On completion of the acidified final rinse (a) the CIPS piping would be cleared of solution to all sprays via an air-blow and (b) the drain valve would open to drain the tank of final rinse water.

5. *Equipment Drain and Dry* — The program would be completed with hot lightly acidified water on all surfaces, which drains and dries very rapidly. When all programs are complete, the fines collection blowers are turned on to aid in moving temperature and humidity controlled air through all of the equipment thus removing the last traces of moisture.

6. *Concurrent External CIP* — During the above, fresh water is continuously recirculated over the structure, service piping, and external equipment surfaces. Whenever the concentration of chemical reaches a minimum set-point, due to loss of strong solutions from the internal circuits to the external solution, the external solution is discharged to the neutralization tank and replenished with additional fresh water.

The application of the above internal/external CIP concept required that all of the processing equipment and interconnecting conveyors, chutes, and spouts be designed (a) in accordance with the previously defined criteria for CIP, (b) to confine internal CIP solutions to the maximum extent possible at all transition points, (c) to assure that any mixing of internal and external solutions was from the former to the latter, and (d) to provide for gravity return flow and drainage from the process equipment to the low-level CIP units, or to a few CIP return collector tanks below the units for pumped return to one level above. The equipment on the various modules included the following major items, and everything else required to run and control the production operations, all designed to be cleaned in the appropriate CIP circuits.

Belt-Type Conveyors — The belts were installed in stainless steel tunnels, built like a small rectangular tank, with roller supports through sidewall openings to external bearings, as shown in Figure 15.25. The enclosure was to sanitary design criteria regarding gasketing, radius corners, pitch-to-drain, accessibility for inspection and maintenance, etc., and the entire interior was vigorously sprayed by permanent installation of multiple tube sprays as one step of a multistep program including associated equipment, in the in-feed discharge lines. A typical conveyor would require a CIPS flow of 80 to 120 gal/min, intermittently, throughout the program.

Vibratory Pan Conveyor — A cross section of this item is also shown in Figure 15.25. A fixed cover is recommended to be permanently mounted several inches above the conveyor pan and the upper edge of the sidewalls of the conveyor should be rolled
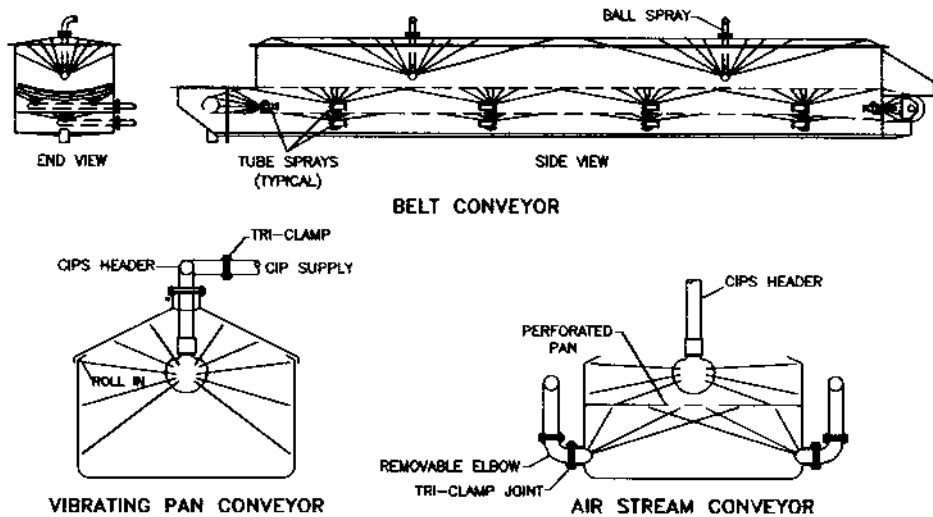
FIGURE 15.25 Belt-type conveyors, vibratory pan conveyors and air stream conveyors can all be modified to respond fully to CIP procedures.

slightly inward to aid in confining solution to the pan. Ball-type sprays can be slip-joint mounted through installation nozzles in the fixed cover at approximately 12-ft intervals on center, starting 6 ft from one end and supplied by a common header for each length of cover section. This conveyor should be pitched at $\frac{1}{16}$ to $\frac{1}{8}$ in./ft from the feed end to the discharge end, providing for major discharge of solution through the vertical duct to subsequent equipment.

Fluid Bed Conveyors — A cross section of this type conveyor is also shown in Figure 15.25. The sides of this type of conveyor should extend sufficiently high to permit a spray device to be located at a level below the top edge, well above the air stream. Sprays would be located approximately 12 ft on center, being supported from the 1½ in. supply header above. The sprays are custom-drilled for an essentially horizontal pattern and water will ricochet from the sidewalls and drain to the perforated pan.

If it is desired to clean the plenum area, bubble-sprays welded through the side-walls and staggered at 8-ft intervals on opposite sides would suffice. A 1½ in. supply header would be required on each side and tri-clamp elbows would be required between this header and the sprays to permit access for inspection and/or cleaning. Space permitting, an acceptable alternative would be to install the bubble-type sprays through the bottom of the plenum, reducing the cost by approximately one-half.

Screw Conveyors — Depending on size and type, these may be either sprayed via permanently installed sprays in the sidewalls and/or covers, flooded, or pressure washed in reverse flow. Figure 15.26 shows how ball sprays can be utilized to handle a trough/auger (or paddle) combination with a raised cover (Type A). The cover must provide a minimum of 5 in. clearance between the top of the auger and the upper surface of the cover and a 3 in. nozzle would be welded through the cover to receive the ball spray supply tube. A removable supply connection with Tri-clamp connections is required between the spray supply tube and the CIP supply header to facilitate removal of the entire cover assembly.

If product discharge from the screw conveyor is from any level above the bottom, an auxiliary drain connection will be required with a valve and connection to the CIPR system. A single ball spray installed as shown would handle a screw conveyor
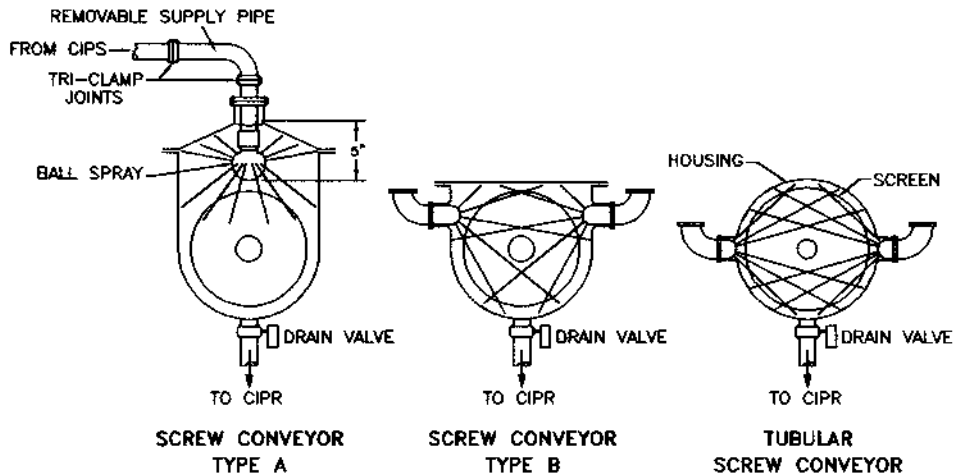
FIGURE 15.26 The installation of spray devices in screw conveyors, blanchers, and similar equipment items must give consideration to headspace and clearance requirements.

of 4 to 6 ft total length. Ricochet off of the top and ends will cover the ends of the screw which will be operated during the cleaning process to assure solution coverage of all surfaces. If the screw conveyor requires a tight flat cover, ball sprays and the associated ricochet cannot be utilized. As shown in Figure 15.26 (Type B) this configuration may be cleaned by installing bubble sprays through the sidewall several inches below the cover, spaced at twice the pitch of the screw, alternately, on each side of the conveyor trough. As for the above type, the screw must be operated throughout the CIP program.

Tubular screw conveyors of large diameters (12 to 16 in.) may be fitted with bubble sprays also, and if the clearance between the tube and screw is minimal, the Bubble Spray can be recessed as shown in Figure 15.26. Small diameter screw feeders originating at hoppers are best cleaned by pressure washing in reverse flow via a suitable CIPS connection. A restrictor in the CIPS line may be designed to control flow to a velocity of 1 to 2 ft/s based on tube diameter. A spray will be provided also for the feed hopper. A CIPR connection will be required through the hopper sidewall at an elevation slightly above the screw to discharge all flow through the screw and from the hopper spray to CIPR.

Storage Bins/Cyclone Separators — Figure 15.27 describes a vessel which could be a collection bin for a pneumatic conveying system, or a cyclone separator. The bin or cyclone is generally cleaned effectively by installing three Ball Sprays at 120° spacing and designing for a total flow based on the vessel or chamber diameter. The supply and exhaust ductwork, including chutes and spouts, must generally be included in the circuit in its entirety. It is impossible to separate one item of processing equipment from another. Bubble sprays are used exclusively for this application to minimize the protrusion into the cross-section of the duct. A common supply header in the form of a vertical run central to a number of spray supply points will feed a multiplicity of sprays so as to clean a substantial path during one step of the CIP sequence.

The ductwork may include diverter valves. Figure 15.28 shows typical locations of bubble spray devices with relation to a diverter valve in vertical and sloped ducts of 6 to 8 diameter. Two sprays would be used in the vertical duct directly beneath the diverter valve and would be directionally drilled to spray upwards into the valve
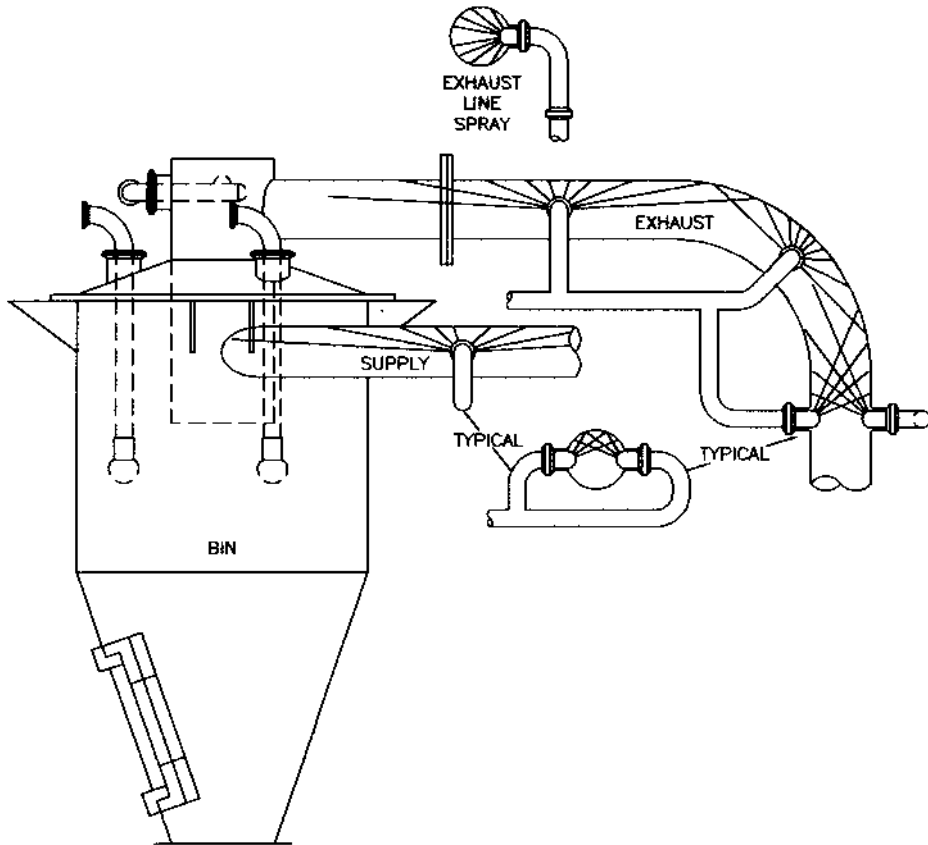
FIGURE 15.27 Bins, cyclones, and the associated ductwork are easily cleaned via the installation of multiple ball or bubble sprays.
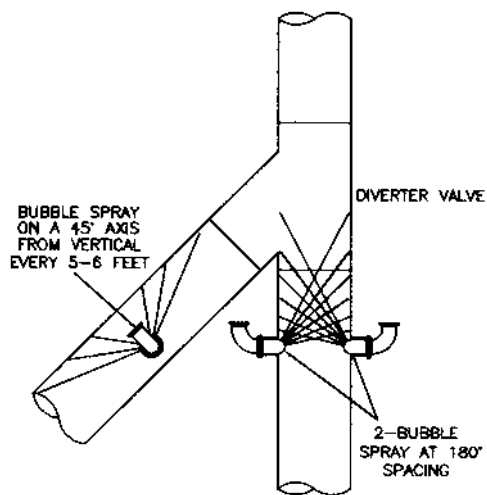
FIGURE 15.28 Vertical ductwork is easily cleaned by spraying at the top only. Sloped ductwork, however, requires spacing sprays at distances determined by duct diameter and cone of coverage.
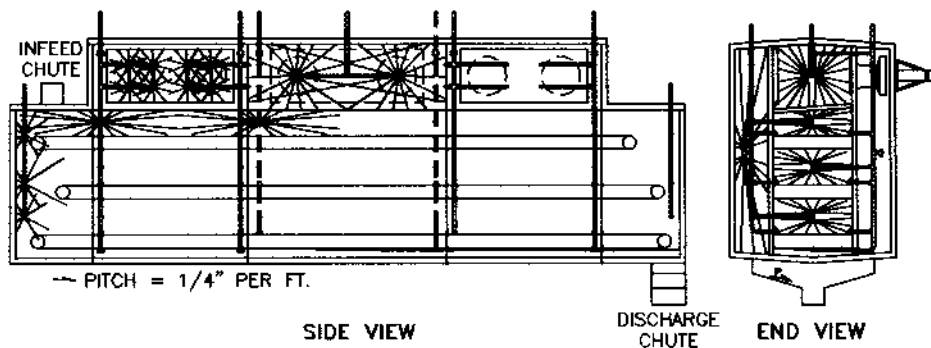
FIGURE 15.29 Multiple belt dryers must be designed to minimize door gaskets, preferably by placing the belt system, drives, support shafts, coils, and fans all in essentially an insulated rectangular tank.

mechanism. The subsequent run-down will handle a minimum of 20 ft of vertical duct beneath. One spray on a ±45° from the vertical would be required every 5 to 6 ft in the sloped portion of the duct, and in any horizontal portions. This concept would apply to the full run of the fines collection system shown in Figure 15.24.

Dryers and Ovens — A multibelt dryer shown in side- and end-view in Figure 15.29 is used as the example for this type of equipment. Many variations of the basic concept have been applied. Essentially, all belts, support and drive rollers, fans, and heating coils have been installed in large stainless steel tanks with two access doors at the ends for servicing the components. Ovens, using higher temperature external heaters, are handled otherwise in a similar manner.

Pneumatic Conveyors — Various methods of pressure washing both conventional and dense-phase pneumatic conveying systems and the associated cyclones, have been applied. A significant problem is isolation of the blowers during CIP.

Chutes, Spouts, Diverters and Rotary Valves — All of the interconnecting product transfer and flow control devices were redesigned to be CIP, successfully.

Fines Collection System — Early experience with partial CIP of dairy dryers in the early 60s provided convincing proof that any noncleaned surface must be fully isolated and maintained dry, or else included in the CIP circuits, which is the easiest, the least costly, and the *best* for sanitation and product quality purposes. The fines collection system shown in Figures 15.24 and 15.30 was of all stainless steel construction, fully fitted with bubble sprays, and cleaned to and through the wet-collectors. It was used to dry the process following CIP by finishing the program with a recirculated hot acid rinse, then draining and drying.

Other Equipment — The materials of construction for the mills were used to permit wet cleaning with chemicals. CIP flush, wash, and rinse solutions pass through the mills, with supplemental sprays as required to clean noncontact surfaces. Screw-type extruders with a variety of dies, hopper fed, and providing for the continuous addition of additive agents, were redesigned to be CIP cleanable, fitted with shrouds at the discharge end, and incorporated in CIP circuits with all supply and discharge side equipment.

Other equipment included weight belts, sizing screens, and de-lumpers (Figure 15.23), coating drums, magnetic traps, tote dumping stations, tote filling stations, and in total, every item of processing equipment required to produce the product. All of the above major components were combined in three different modules to produce and coat cereal products. In addition to eight internal CIP
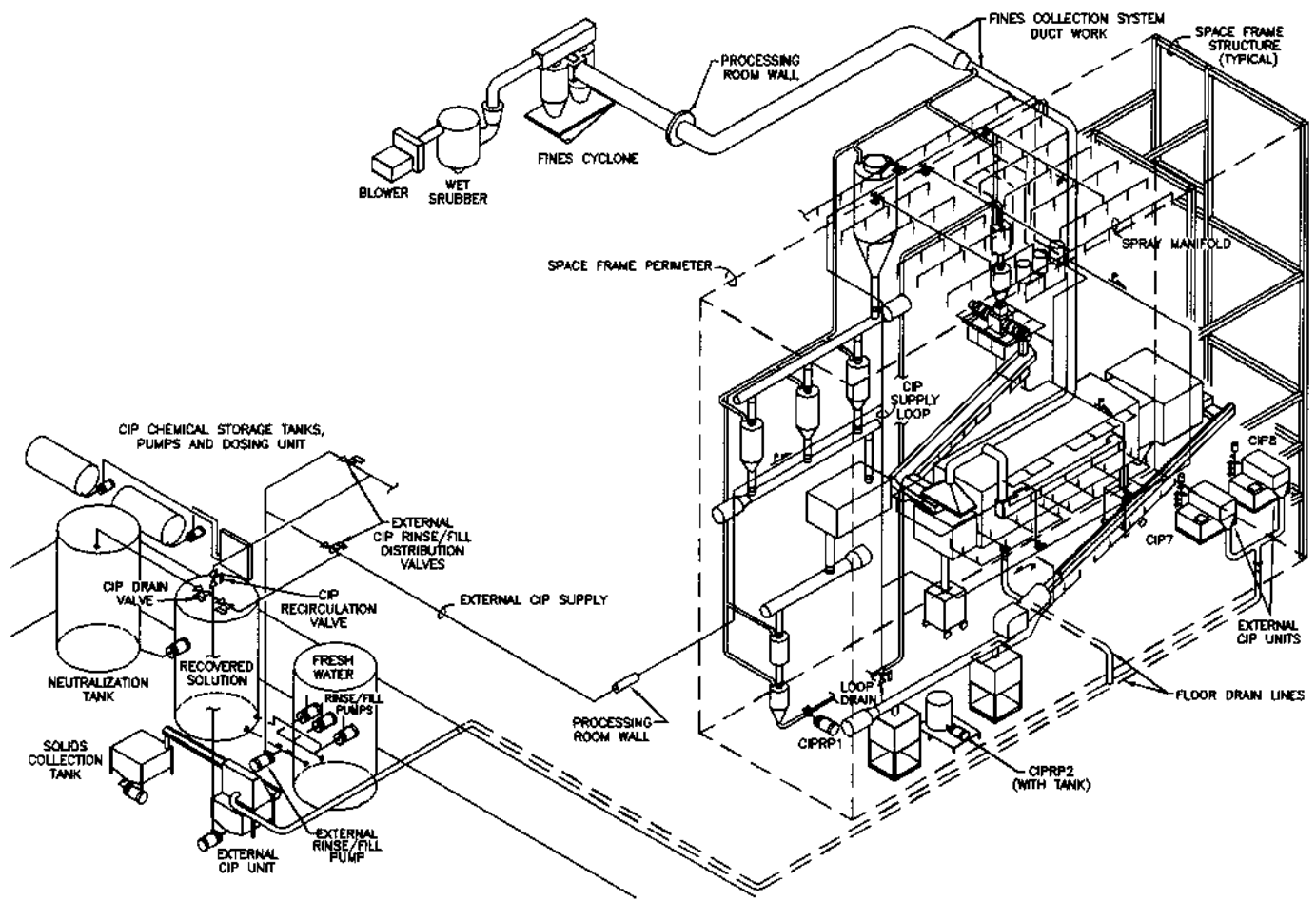
FIGURE 15.30 This isometric illustration of the same space frame shown in Figure 15.24 shows the routing of CIP supply piping to external sprays provided to continuously flush cleaning chemicals from both non-watertight equipment and non-stainless steel surfaces.

systems (see internal CIP unit in Figure 15.24) operating at 300 gal/min., the installation included four external CIP systems operating at 400 gal/min by distribution of warm potable water through the permanently installed external sprays as illustrated in Figure 15.30. The external CIP systems supplied more than 1500 sprays which continuously flushed all external equipment surfaces to remove the dust and solids which accumulated during the production period and to flush the high strength caustic and acid chemicals (which escaped from the product transition points, bearing openings, etc. during internal CIP) from the painted, aluminum, copper, or mild steel components.

The internal and external recirculating units were in turn supplied by high-head and volume rinse/fill pumps drawing from 30,000 gal potable water and recovered solution tanks located at the CIP support equipment level. The 12 CIP units were capable of cleaning the entire array of processing equipment (all three modules) in approximately 5.5 hours, followed by 2.5 h for drying, in accord with production schedule requirements, under full automation, with minimal manual preparation, and no personnel in the process area during CIP.

This technology is most applicable to new processes, where the machinery has not already been built and installed. Successful implementation requires considerable forward planning and a commitment to do all that is necessary to exploit the power and reliability of CIP to the maximum.

15.3.3 TYPICAL CLEANING PROGRAMS AND PROCEDURES

15.3.3.1 General Sequence of Treatment

Nearly all CIP cleaning of food processing equipment is accomplished with water-based solutions by a program consisting of (a) a prerinse with potable water or recovered solution until the effluent is clear, (b) an alkaline solution wash under a variety of time and temperature combinations, (c) a post-rinse with potable water, and (d) a recirculated acidified rinse, generally at ambient temperature, to neutralize final traces of the alkaline solution, which is not easily rinsed from stainless steel surfaces. A chemical or heat-based sanitizing operation may precede use of the equipment for a subsequent production operation.

To achieve consistently acceptable cleaning results in food operations, it is necessary to give consideration to the following:

1. The composition of the available water.
2. Selection of cleaning compound(s) best suited for the job.
3. Determination of concentrations needed to most economically accomplish the desired cleaning.
4. Establishment of the external energy factors to enhance the chemical cleaning procedure.
5. Determination of the method of application of the cleaning compound.

15.3.3.1.1 Water quality

This factor cannot be overemphasized when planning cleaning procedures. If the water is heavily loaded with scale forming minerals (calcium, magnesium, iron, or sulfate) the cleaning compound must be adjusted to eliminate the deposition of minerals or the water must be treated to reduce the mineral content prior to use for cleaning. The efficacy of postcleaning rinses is directly related to water quality. Magnesium, calcium, iron, and manganese salts in rinse water will precipitate more readily from alkaline solutions than from acid solution. The

conditioning of final rinse water with acid (to pH of 6.5 or less) will aid in controlling the deposition of mineral water salts on cleaned equipment surfaces.

15.3.3.1.2   Cleaning compound selection

The choices depend upon several interrelated factors, which include:

1. The type and amount of soil on the surface
2. The nature of surface to be cleaned
3. The physical nature of the cleaning compound
4. Method of cleaning available
5. Cost
6. Service

In some instances, the amount of soil on the surface is controlled by more frequent cleaning of the equipment. Generally, however, the cleaning solution should be of a type and concentration to handle the highest anticipated soil loads and provide some reserve capability.

Under normal food plant operations the variations in the surface finish of stainless steel has little influence on cleaning efficiency under practical conditions. The presence of non-stainless materials; i.e., gaskets and rubber or plastic parts, must also be considered.

Automated CIP is generally accomplished with liquid chemicals, which though more hazardous to handle, lend themselves to better and more uniform concentration control through liquid feed devices. This discussion is limited to CIP applications. The cleaning operation will be largely chemical in nature as a result of spray application or pressure recirculation through lines and equipment. The amount, quality, and reliability of the service provided by the manufacturer and/or supplier of cleaning materials is extremely important. However, knowledge of the fundamentals of cleaning on the part of food plant personnel is useful in evaluation of reliability of available services.

Tamplin (1980) has provided a detailed analysis of *Cleaning and Disinfection: A Chemical and Microbiological Approach*. For purposes of this handbook consideration will be given to three decades of practical experience which have demonstrated that the product soil encountered in all fluid and semifluid processes for food products can be removed by one or a combination of several of the following treatments:

Chlorinated Alkalies — In its simplest form this chemical solution may be nothing more than a mild solution of caustic soda supplemented with liquid sodium hypochlorite. More commonly a chelated caustic is used to provide some control of water hardness. Chemical concentrations may vary from as low as 800 to 1200 ppm of alkalinity for lightly soiled equipment to a maximum of 5000 ppm. Cleaning temperatures are normally in the range of 135 to 160°F, and exposure time (recirculation at temperature) may vary from 5 to 20 min.

Acid Rinse — A minimum postrinse using fresh water to drain will be used to remove the major portion of the chlorinated alkaline solutions from the equipment surfaces. Then, to minimize water requirements for rinsing, the final treatment will be a recirculated solution lightly acidified with food-grade phosphoric acid to produce a pH of 5.5 to 6.0 (just slightly on the acid side of neutral). This solution recirculated at the water supply temperature will *neutralize* all traces of alkali residual films on the equipment surfaces. It has the further benefit of providing an equipment surface which will drain and dry free of spots. Finally, though not a sanitizing agent, a mild acid solution is bacteriostatic and its use as the final treatment reduces or slows down the growth of any bacteria that may be present as a result of the water supply or that may remain due to improper cleaning.

Strong Alkalies — Chelated caustic may be used alone at higher concentrations and temperatures to handle heavy fat and protein soils. Chemical concentrations may range from 0.5% (5,000 ppm) to as much as 50,000 ppm. Recirculating temperatures may be increased to 180 to 190°F and the recirculating period may be extended to 45 to 60 min. This is typical of the treatment used for cleaning a milk HTST pasteurizing system, a beer kettle, or a whey evaporator.

Strong Acids — The above treatment may be either preceded or followed by recirculation of a strong acid solution, phosphoric acid being the most common. Acid will be added to produce a pH as low as 2.0 and the recirculating temperatures may be in the 170 to 190°F. range though the time will generally be shorter than for the caustic product (20 to 30 minutes maximum). The decision as to which to use first will depend upon the predominance of fat or protein in the soil. High-fat soils are most easily attacked by strong alkaline products, followed by the acid to handle the remaining mineral deposits and the deposition of any hardness from the water used for preparing the cleaning solution. Soils which are heavy in mineral will be more responsive to the acid first, followed by caustic.

Sanitizing — All equipment used in producing products sold in the "fresh" form (such as fluid milk, cottage cheese, and ice cream) must, by regulation, be sanitized following the cleaning and before processing. Sodium hypochlorite is the most common sanitizing agent, being applied in cold solutions at concentrations ranging from 55 to 200 ppm for periods of only a couple of minutes.

15.3.3.1.3   External energy factors

The cleaning process can be improved by increasing the "external energy" applied, either by increasing the temperature or the force applied. In this discussion the effective time will be considered as an external factor. Each of these can be varied independently to adjust a cleaning operation to a particular problem or plant operating practice. The conditions generally are selected so as to permit the best cleaning job at the least cost. The significance of the various factors will vary with the method of cleaning used or with the type of condition of the soil to be removed.

Temperature — Temperature is extremely significant in cleaning operations. Increasing the temperature has the following effects: (a) decreases the strength of bonds between the soil and the surface, (b) decreases viscosity and increases turbulent action, (c) increases the solubility of soluble materials, and (d) increases chemical reaction rates. For milk products within a temperature range from 90 to 185°F, an increase in temperature of 18°F, will approximately double the efficiency of the cleaning operation. Below 90°F, milk fat remains in a solid state and above 185°F. heat-induced interactions bind the protein more tightly to the surface and decrease cleaning efficiency. For any food soil, the minimum effective temperature will be approximately 5° higher than the melting point of the fat. The maximum temperature will depend upon the temperature at which the protein in the system is denatured. Temperatures above the denaturation point can increase the adhesion of the protein to the surface faster than the cleaning efficiency is increased.

Time — All other factors remaining constant, the cleaning can be increased by utilizing longer times. However, increasing the time beyond a given value provides little additional increase in effectiveness. As previously discussed for concentration, there is only minimum time for effective cleaning and a practical maximum time for achieving desired results economically.

Physical Action — In hand-cleaning, force is applied by "elbow-grease", whereas fluid-flow is utilized in the application of force in CIP or CIP systems. Originally, the utilization of velocity as a means of measuring the fluid flow force was employed

with the "thumbrule" of 5 ft/second being employed by Regulatory Agencies. Although this value is still suggested in the regulations, effective cleaning can be achieved by velocities lower than 5 ft/second. This is because velocity and turbulence, which is the actual cleaning force, are not equally related under all conditions of flow. To be effective, fluid flow must be turbulent (Reynold's number greater than 4000 in pipeline systems). Generally, the values above 4000 (for pipeline systems) give greatest effectiveness and are achieved easily.

15.3.3.2 Standard Cleaning Programs

There is no single "best way" to handle any particular cleaning program, for as observed in the previous section, the effectiveness of mechanical/chemical cleaning is related to a number of variables including time, temperature, concentration, and physical action. More importantly, exact or specific numbers (as part of the recommendation) are of no value if the equipment is still dirty upon completion of a cleaning cycle. The first objective must be to "do what is necessary to get the equipment clean" after which further adjustments giving consideration to limitations of temperature, time, or cleaning chemical cost may be completed.

In the final analysis, however, the true test in cleaning compound selection is a measure of its effectiveness in actual application under the commercial conditions being used. Emphasis is placed on the need to make sure that any surface to be tested is "technically clean" before initiating the evaluation of a cleaning compound. The surface should be dried to visualize any mineral "stone" deposits and heated to visualize protein films. A 150-W exterior floodlight held 12 to 15 in. away from the surface will dry the surface and help to visualize deposits. Protein films give the appearance of aluminum that has been exposed to weather. Protein films can be differentiated from mineral "stone" deposits by scrubbing adjacent dried surfaces with undiluted milk stone remover or a fourfold concentrated solution of chlorinated alkali. Acid will remove the mineral stone and the chlorinated alkali will remove the protein film. This method is effective unless the buildup is massive or consists of alternating layers of protein and mineral.

15.3.3.3 Controlled Discharge of Effluent to Pretreatment Processes

The discharge from the CIP units and from processing systems which are designed to provide a CIP capability is especially high in inorganic material and in chemical content. When planning new facilities it is well to consider the segregation of the drains receiving such discharge from the drains serving large floor areas and other sanitary facilities. Ultimately, treatment of the cleaning solutions may be required prior to permitting their discharge to waste treatment facilities whether privately or municipally owned. The well engineered application of "Single-Use" CIP systems equipped with solution recovery tanks has provided an interim solution to the problem of controlling chemical and BOD discharge for the end result of such procedures is (a) to dilute the small volume of strong wash solution, and high BOD load, with two to three times as much water from the subsequent rinses, following which the diluted mixture is sent to the sewer in small doses as part of a "burst" prerinse program. Some food processing facilities are now being required to install neutralization tanks between the CIP units and the discharge to local treatment facilities (Figure 15.30).

15.3.3.3.1 Evaluation of results

It is possible to design and apply equipment and programs which can produce food contact surfaces that are physically clean and nearly free of all bacterial contamination. There are many new and rigorous methods of determining the effectiveness of CIP procedures, but the most simple will often be the best. On completion of a CIP program the equipment should (a) look clean, (b) feel clean, and (c) smell clean. Shelf-life tests are also an excellent means

of providing long-term evaluation of cleaning and sanitizing practices for products which undergo continuing microbiological degradation.

Standard bacteriological swab tests on CIP cleaned equipment should yield sterile plates (no growth) in 75 to 80% of all samples and plates showing not more than 2 to 10 colonies for the remaining samples when swab sampling is done immediately following cleaning and before sanitizing. If equipment is properly handled, there will be no positive coliform counts on any swab taken from surfaces cleaned by in-place cleaning procedures.

Other methods of evaluating the effectiveness of CIP cleaning include:

Black Light Evaluation — A high intensity fluorescent light will enable the detection of very minute organic residues. Both protein and fat soils will fluoresce under black light. This method was used during the early development and evaluation of both spray balls and CIP programs in general. Cultured buttermilk was used to paint or spray tank surfaces, following which the soil was dried with an infrared light. Black light inspection followed the subsequent CIP program. The application of this procedure with the following modifications will contribute to an understanding of the power of time, concentration, and temperature in the cleaning regimen by performing the evaluation after the first rinse, after the third rinse, then after recirculation of water with no heat or chemicals for the normal wash time, and then finally add first the chemicals but no heat, and then the whole program. This approach will make it possible to discern the difference in the removal of the proteinaceous (organic) material. The suggested procedure would also illustrate that when running on water alone, the soil would probably only be removed from the spots where the streams hit, whereas once chemicals are added and time and temperature are involved, cleaning will occur in the other areas by chemical action alone, rather than by impact.

Micro Assay — Some pharmaceutical processors are applying trace elements which can be measured instrumentally in very minute quantities. Swabbing is a prerequisite, however, and to use this approach it would first be necessary to identify the suspected trouble areas and then use swabs to remove residual soils (if any) which could then be detected via the instrumental analysis procedure.

Chlorine Degradation — This is probably more applicable to piping then to tanks for if (a) all surfaces or critical surfaces of a tank are soiled, and (b) these critical surfaces are not contacted by the spray coverage, then (c) there would be no impact of the soil on the degradation of the chlorine. The principle is very simple, organic material will be oxidized by a weak chlorine solution which in turn will be rapidly reduced in concentration. The contact of 55 ppm cold chlorine with minute portions of organic matter will result in a degradation of the chlorine level and changes of, e.g., 55 to 50 or 45 ppm following brief recirculation of chlorinated pure water through a pipeline or vessel would be an indication that some organic material not removed by the previous CIP procedure had been contacted by the chlorine.

15.4 ECONOMIC CONSIDERATIONS

The effective integration of automated CIP technology in the food processing system can provide many benefits, including

1. The elimination of human error and assurance of uniformity of cleaning, rinsing, and sanitizing which is not possible with manually applied cleaning procedures.
2. It improves safety for production and cleaning personnel.
3. Increases productivity by reducing the production operation down time required for cleaning. CIP cleaned equipment generally requires less maintenance, thus maintenance downtime is reduced, also.

4. The automated CIP procedure enables modern computer-based control technology to be applied to document the cleaning process and assure compliance with all required parameters.

5. Properly engineered CIP cleaned processes permit the application of controls and sub-systems, i.e., automated air-blow systems, which enhance reduction of processing losses.

6. Careful design of the CIP cleaned process may reduce accidental product damage as a result of operator error, indirectly reducing product loss.

It is seldom possible to assign a "cost vs. profit" factor to any combination of the above. However, in combination, the listed advantages often contribute to making a specific process possible by effectively dealing with factors of size, speed and complexity not easily handled via manual control, or manual cleaning. In addition to the above benefits, the best recognized economic forces for CIP are generally reduced cleaning labor and reduced water and chemical utilization.

The final cost of process/CIP automation is related to complexity, and in fluids processing operations complexity in turn is related to the size and number of the vessels involved. Each vessel, whether capable of holding 500, 5,000, or 50,000 gal requires its proportionate share of those components required to control and clean the process. The cost of installing and maintaining highly automated systems can be substantially reduced by (a) simplifying the process in terms of the number of product/package combinations to be produced on a daily basis and (b) utilizing processing and storage vessels of the maximum possible size and in a minimal number. Recognition of this fact by dairy food processors and brewers has resulted in the widespread application of very large tanks, most commonly of "silo-type" construction, as experience has demonstrated that it is better to spend the money on tanks to minimize the expenditure for valves, instruments, and controls and subsequent maintenance of the more complex systems.

When planning renovation of existing liquids processing facilities CIP technology may permit substitution of fewer and larger tanks external to the sanitary area, and sometimes remote or overhead, thus permitting the more costly sanitary construction to house higher capacity processing and packaging systems. The nature of the engineering design of the CIP system is inclusive of the cost of conventional systems incorporating substantial separate CIPS/R piping vs. integrated design which maximizes the use of process piping, valves, and pumps as the means of moving flush, wash and rinse solutions. Although the cost of adding CIP to an existing process can be considerable, when it is properly implemented in the design of a new process the actual CIP components may often be only 2 to 3% of the total project budget. Several large dairy food processes of recent vintage have yielded the following ratios of CIP vs. total process cost:

Example 1 — A cultured product facility major renovation and expansion requiring no added land produced a CIP cost of $22,400, a total automated process piping cost of $76,000, and a major equipment cost of $150,000 per $1,000,000 of budgeted capital cost. Therefore, CIP represented about 10% of the cost of the processing equipment and piping.

Example 2 — A new cultured product facility which included land produced a CIP cost of $6,000, a total automated process piping cost of $44,000, and a major equipment cost of $70,000 per $1,000,000 of budgeted capital cost.

Example 3 — A new ice cream facility requiring no land produced a CIP cost of $7,000, a total automated process piping cost of $60,000, and a major equipment cost of $100,000 per $1,000,000 of budgeted capital cost.

Similar results have been achieved when applying CIP to nonfood processes. A very large and complex biotech facility in which integrated CIP/process piping design was used to the maximum produced a budgeted cost for CIP of less than 2% of the project cost, even though the components were entirely fabricated of 316 stainless steel and electropolished.

Another example involved a complex process designed to campaign seven highly potent compounds with low parts per million cross-contamination limits as described by Stewart and Seiberling (1996). The design objectives for the plant cleaning system were developed via comparison to an existing "sister" plant which accomplished changeovers between products by "manually" cleaning equipment and included:

- Controlled cross-contamination to <10 ppm. The "sister" plant could only achieve 200 ppm cross-contamination.
- Achieved a turnaround in <3 d. The "sister" plant required 14 d.
- Improved safety by eliminating
  - Water blasting
  - Vessel entry
  - Extensive dismantling of equipment
- Reduced aqueous and organic waste by 80% (vs. "sister" plant changeover waste generation).
- Reduced labor required for changeover.

A major portion of the process piping was Teflon lined, or hastelloy. Process valves were hastelloy. CIPS/R piping was 316 stainless steel tubing with Tri-Clamp connections to a final flange connection to a hastelloy valve with final connections by either Teflon-lined pipe or hastelloy tubing to hastelloy spray supply tubes and sprays.

The total CIP-related costs, which included direct CIP costs plus costs such as equipment modifications to make it more cleanable, were 3.3% of the total investment. This includes engineering, equipment, piping, the DCS expansion, instrumentation, programming, labor, and construction supervision. The CIP-related engineering and construction supervision costs were 6% of the total engineering and construction supervision costs for the project.

Whereas the above projects are not directly comparable due to major variations in scope and the cost of the major equipment, they suggest that the cost of CIP is a small part of the total budget for a new facility, just as the cost of the sprays for a tank are a small part of the tank cost. The above are all liquids handling processes which utilize equipment already designed to be CIP proficient. The CIP cost for a dry product process would include some escalation of major equipment cost to make it cleanable.

15.5 SUMMARY

A modern food processing facility, whether designed to handle fluid or semifluid products, or nonliquid foods should encompass in the design the results of considerable evolution in process and facility design achieved during the last 40 years. During the decade beginning in 1965, CIP was recognized as the key which would open the door to many other changes in dairy *and* food processing technology. This procedure led to the extensive development of all-welded product piping systems, extensive application of air-operated CIP cleanable sanitary valves, and appreciable increases in the sizes of processing and storage tanks as compared with vessels that had to be manually cleaned. During this period, CIP procedures were applied extensively in many nondairy food and beverage industries, including brewing, wine processing, meat processing, and some processes which handled dry or semifluid products in stainless steel equipment. The effective integration of major equipment and interconnecting piping in a manner which reduces the need for manual labor for both

production and cleaning also contributes to improvement and greater consistency of product quality and reduction in processing losses.

Since the automated process requires the capability of being CIP due to the complexity of the piping systems and air-operated valves, the technology is commonly referred to as process/CIP automation. This terminology is not limited to new facility construction. Adherence to the proper design concepts and principles has enabled renovation of many existing dairy food operations to increase production capacity three- to fivefold over a period of 30 years by adding primarily to the support areas required for case handling, and refrigerated and dry storage. Processing and packaging capacity increases can occur via replacement of the original equipment with higher speed equipment often in the same space and using the same controls.

Existing meat, cereal, and snack food processes are, for the most part, manually cleaned and inspected prior to being placed back into production. Only welded pipelines and silo tanks are accepted as CIP proficient without provisions for inspection under the 3-A Standards applicable to all dairy processes and followed in many other segments of the food industry. However, the openings normally required for manual cleaning and inspection of the equipment are the first major obstacle to overcome in designing a CIP process. Inspectability and CIP are not mutually compatible and design criteria for each unique process must reconcile these factors.

GLOSSARY

Clean-in-place: Also in-place or recirculation cleaning; The removal of process equipment and piping soil by recirculation or spray application of flush, wash, and rinse solutions.

Single-use CIP: A system designed to use the smallest possible volume of fresh solution once, followed by discharge to waste or a recovered solution tank.

Re-use CIP: A system designed to use large tanks of chemical solution repetitively, by wasting and replenishing a small portion following or during each subsequent CIP cycle.

Spray wash: Cleaning by continuously spraying the upper areas of a tank, bin, or enclosure and removing the soil by chemical action.

Pressure wash: Cleaning by pumping solutions through piping and equipment at sufficient velocity, normally 5 feet/second, to assure filling all areas of the piping.

CIP cleanable: An individual item of equipment or a complete process designed to facilitate spray or pressure recirculation as the means of contacting all soiled surfaces with flush, wash and rinse solutions.

CIP unit: The combination of tanks, valves and pump(s) installed to deliver flush, wash and rinse solutions

CIP supply/return piping: Piping installed to convey cleaning solutions from the CIP unit to the cleaning circuit and back.

Ball spray device: A spherical shaped stainless steel ball drilled to produce a specific pattern of spray coverage.

Tube spray device: A stainless steel tube, straight or formed, fitted with half drilled spherical sections for multiple source spray patterns.

Mixproof valve: A single valve with double seats to provide a break to atmosphere between to process streams, to prevent accidental mixing due to component failure.

NOMENCLATURE

BOD   Biological Oxygen Demand
CHS   Cleaning Hook-up Station. A stainless steel panel with ports for U-bend connection of cleaning supply or return piping
CIP   Clean-In-Place
CIPS   Clean-In-Place Supply piping system
CIPR   Clean-In-Place Return piping system

CIPS/R	The combined CIP supply and return piping system, piping required for conveying flush, wash, and rinse solution to and from the process equipment
CSP	Cleaning Supply Pump
DCS	Distrubuted Control System
FCV	Flow Control Valuve with reference to CIP supply flow rate control
HTST	High-Temperature Short-Time. The common dairy product pasteurization system
PHS	Product Hook-up Station A U-bend connection panel used for product piping connections and cleaning connections
PID	Proportional Integral Derivate Control
P/D	Pressure to contant transducer
PLC	Programmable Logic Controller
PVC	PolyVinyl Chloride
RP	Return Pump
RTD	Resistance Temperature Device
SUEA	Single Use Eductor Assisted

FURTHER REFERENCES FOR SUGGESTED READING

Seiberling, D.A., 1976, Typical variations in automated CIP system design, control and application, *N.Z. J. Sci. Technol.*, 11(3): and 11(4).

Seiberling D.A., 1976, Fluid flow processes, in *Dairy Technology and Engineering,* Harper, W.J. and Hall, C.W., Eds., AVI Publishing, Westport, CT, 403.

Seiberling, D.A., 1985, Recirculation cleaning of HTST systems, *Milk Pasteurization Controls and Tests*, 2nd edition, 159.

Seiberling, D.A., 1992, Alternatives to conventional process/CIP design — for improved cleanability, *Pharm. Eng.* 12(2): 16–26.

REFERENCES

Bonem, F.L., 1960, Single operator controls complex operation, *Food Processing*, 2(July):36–38

Fleischman, F.F., Jr., White, J.C., and Holland, R.F., 1950, Glass lines: do A-1 job; no take-down to clean, *Food Ind.* 22(10):1686.

Havighorst, C.R., 1951, Revolutionary advance in dairy engineering: permanent welded pipelines, *Food Eng.* 23(9):74–79.

International Association of Milk, Food and Environmental Sanitarians, 1986, 3-A Accepted practices for permanently installed sanitary product pipelines and cleaning systems, no. 605-02, Int. Assoc. Milk Food Env. San., Ames, Iowa.

International Association of Milk, Food and Environmental Sanitarians, 1995, 3-A Sanitary standards for caged-ball valves for milk and milk products, no. 66-00, Int. Assoc. Milk Food Env. San., Des Moines, IA.

Johnson, C.R., 1960, Automated CIP improves quality of product, *Food Processing*, 1(June):36.

Karpinsky, K.L. and Bradley, R.L., Jr., 1988, Assessment of the cleanability of air-actuated butterfly valves, *J. Food Protect.*, 51(May), 364–368.

Kaufmann, O.W., Hedrick, T.I., Pflug, I.J., Pheil, C.G., and Keppeler, R.A., 1960, Relative cleanability of various stainless steel finishes after soiling with inoculated milk solids, *J. Dairy Sci.*, 43(1):28–41.

Olenfalk, L.O., 1975a, Personal correspondence regarding internal report.

Olenfalk, L.O., 1975b, Detailed economical and technical study of various cleaning systems, *Mjolk-centralen Internal Rep.*, (personal communication).

Parker, R.B., Elliker, P.R., Nelson, G.T., Richardson, G.A., Wilster, G.H., 1953, Cleaning pipelines in-place, *Food Eng.* 25(Jan) 82–86, 176–178.

Richter, R.L., Bailey, J., and Frye, D.D., 1975, A field study of bulk milk transport washing systems, *J. Milk Food Technol.* 38(9):527–531.

Seiberling, D.A., 1955, An Ohio plant applies automation to the cleaning-in-place operation, *Am. Milk Rev.*, 17(Feb):32–34.

Seiberling, D.A., 1968, Equipment and process design related to mechanical/chemical cleaning procedures, *Proc. Chem. Eng. Progr. Symp.* 64(68):94–104.

Seiberling, D.A., 1970, Automated cleaning of brewing vessels and lines, *Master Brewers Assoc. Am. Tech. Q.*, 7(1):73–80.

Seiberling, D.A., 1979, Process/CIP engineering for shelf-life improvement, *Am. Dairy Rev.*, 41(10):14–22, 64–67.

Seiberling, D.A. and Harper, W.J., 1957a, Ball spray cleaning of storage tanks and pick-up tankers, *Milk Dealer*, 46(4):40–41, 48.

Seiberling, D.A. and Harper, W.J., 1957b, Automatic sanitary valves for dairy plants, *American Milk Rev.*, 19(1):30–31, 34.

Sheuring, J.J. and Henderson, H.B., 1951, *South. Dairy Prod. J.*, 49, 52–53, 64-65.

Stewart, J.C. and Seiberling, D.A., 1996, CLEAN in Place: Are you ready? *Chem. Eng.*, 103(1):72–79.

Tamplin, T.C., 1980, CIP technology, detergents and sanitizers in *Hygienic Design and Operation of Food Plant,* Jowitt, R., Ed., AVI Publishing, Westport, CT, 183.

Thom, E., 1949, Glass sanitary piping in dairy plants, *The Milk Dealer*, 39(1): 42.

Zoltai, P.T., Zottola, E.A. and McKay, L.L., 1981, Scanning electron microscopy of microbial attachment to milk contact surfaces, *J. Food Protect.*, 44(3):204–208.

16 Process Control

David Bresnahan

CONTENTS

16.1 INTRODUCTION

16.1.1 DEFINITION

Process control* is the manipulation of process variables to achieve desired product attributes.

The above definition is not all inclusive, but does cover the aspects of automatic control covered in this chapter. Process control has many facets, from the control of process variables on the plant floor to the handling of information from plant or corporate manufacturing information systems. This discussion will focus on the former. Plant floor control involves both *digital* or *machine control* as well as *analog* or *continuous control*. Continuous control will receive most of the attention here although digital control will enter into some control techniques.

16.1.2 WHY AUTOMATIC PROCESS CONTROL?

Technology has made significant strides since the beginning of the industrial revolution. The introduction and proliferation of computer technology have allowed for greater automation of manufacturing operations.

Automatic control provides greater consistency of operation, reduced production costs, and improved safety. A process that is vulnerable to upsets is going to have a more consistent output if the process variables are adjusted constantly by an automatic control system. Human variability can be taken out of an operation with a properly implemented automatic control system.

Improved consistency of operation can produce products with attributes closer to specification targets, thereby increasing overall quality. Closer control can also lead to less out-of-specification product and therefore increase productivity.

The constant vigilance of an automatic control system can improve safety by reacting more quickly to unsafe conditions. Automatic shutdown procedures can be implemented. Some of these procedures can protect workers while others can prevent unsafe product from passing through to the consumer.

16.2 THE PROCESS MODEL

A process model depicting negative *feedback control* is shown in Figure 16.1. The process variable to be controlled is measured. The *process measurement* is compared to a *set point* to generate an *error signal*. The error signal is used by an algorithm to determine the control response. The control response is then used to manipulate a final control element that affects the control variable and the loop is repeated.

An example of negative feedback control is the manual temperature control of a fluid passing through a steam heat exchanger. The fluid temperature is the control parameter. A

---

* Italicized words throughout chapter can be found in the Glossary at the end of the chapter.
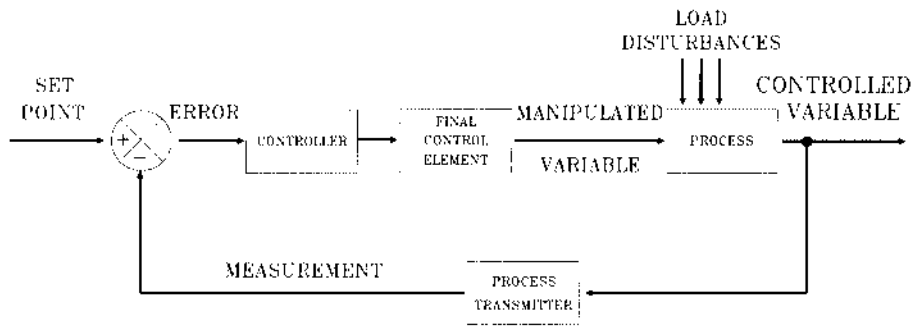
FIGURE 16.1 Feedback process model.

temperature indicator is used as the measurement device. Judgment of whether the temperature is too high or low is made by the operator. The steam valve is used to make appropriate adjustments. If the fluid is too hot then the steam valve is adjusted towards the closed position; thus the concept of negative feedback control. A positive error requires a negative response for correction. At first the operator adjustments are large. As the desired set point is approached, the operator makes finer and finer adjustments.

This adjustment sequence is typical of many automatic control algorithms; as the error becomes smaller so too does the control response. The adjustments by some automatic *controllers* are continuous (as in the case of pneumatic controllers). Digital controllers repeatedly perform the calculations so rapidly that the adjustments are essentially continuous.

16.3 CONTROL LOOP ELEMENTS

The diagram in Figure 16.1 shows the information flow in a feedback control loop configuration. The elements within the loop can vary but are often similar.

The process variable is detected with a *sensing element*. In automatic control the sensing element is a *transducer*. A transducer is a device that produces an output in some relationship to the measured parameter. Most often the output of a transducer is an electrical signal.

The output signal of the sensing element is not always linear with respect to the measured variable, nor is it always in a state that makes it practicable for use in a control system. The signal could be a low level millivolt signal that is difficult to transmit long distances without interference or extraneous noise being incorporated into the signal, rendering it useless. The signal from one sensing element may be volts, another may be frequency, and yet another may be current variation. Many controllers today have the capability to handle a variety of input types. However, it is sometimes more practical and cost effective to limit the number of different types of input signals that will be handled by a control system in order to limit the number of input conversion devices needed to be purchased.

Transmitters are transducers used to convert the sensing element signal into a more robust and standardized signal, often linearized to the measured variable, that is output to the controller. The most common output of a transmitter is 4 to 20 mA. This current signal is powered by a low level (~24 V) direct current source. The transmitter manipulates the current of this loop. Extraneous electrical noise can induce a voltage on top of this signal. However, within limits, the extra voltage does not affect the reading device since it is responding to the changing current. The 4 to 20 mA loop can be used to drive several devices by wiring them in a series loop, providing that the resistance of all the devices in the loop does not exceed the capabilities of the power source driving it.

The transmitted signal is read by the controller. The controller is able to interpret the signal and relate it to a set point. Controllers will often have the capability of interpreting

many input signals; millivolts, volts, milliamps, frequency, and so on. Some controllers are completely pneumatic; that is, the controller is fed an air signal, manipulates the signal vs. a set point, and outputs an air signal. Pneumatic controllers are useful in environments where electrical equipment is undesirable, such as in rooms where explosive ingredients are handled.

Most controllers today have a digital computer that compares the input to the set point and does the calculations to determine the output. A digital controller takes the input electrical signal and converts it to a digital signal in an analog to digital converter (A/D). The computer provides a digital output that is then converted back to an analog signal; again quite often in the form of 4 to 20 mA, although a variety of outputs can be provided.

The output signal is used to adjust the final control element. Often times the signal is converted once again. Many control valves are driven pneumatically and therefore a current to pneumatic (I/P) converter is needed. One common pneumatic signal used by control valves is 3 to 15 psig (pounds per square inch gauge). Quite often the I/P converter takes a 4 to 20 mA input and outputs 3 to 15 psig.

There are other types of final control devices in addition to valves. Pumps can be used for flow or pressure control. A pump can have its output varied by adjusting the speed of the motor driving it. A *variable frequency drive* takes in the controller output and varies the frequency to the pump motor. It therefore acts as another example of a signal converter before the final control element.

The way communication happens between devices in a control loop is evolving. Application of the ISA/IEC Fieldbus Standard, now under development, will provide networking between the control system components. This will allow greater access to more information with less wiring. Digital information will be superimposed on the normal analog signals providing information at remote sites that was previously only available at the particular control component. Many manufacturers are already providing digital communication capability to their remote devices allowing for easier setup and diagnostics.

16.3.1 SENSORS

Table 16.1 is a list of some sensor types that may be found in food process control applications. For each process variable there are many measuring techniques available. It is important to consider the range, accuracy, and cost for each application.

For sensors in contact with the product it is required that the contact surfaces be constructed of approved food contact materials. All liquid applications do not require 3A approval, but this certification indicates that this sensor can be used in clean-in-place (CIP) applications without much extra consideration by the design engineer. Sensors in a process that will be CIP should be mounted to minimize any dead volume and be self draining.

Sensor installation is important for proper functioning. A temperature sensor should make good contact with the material being measured. Flow sensors often require certain lengths of straight piping runs up and down stream of the flow element. Some sensors are vibration sensitive while others are susceptible to electrical noise.

Consideration of the mounting environment is also important. In the food industry, washdown and dust tolerance are very often required for the sensor enclosures. National Electrical Manufacturers Association (NEMA) ratings of 3 (weatherproof), 4 (watertight), or 5 (dusttight) are often specified.

16.3.2 CONTROL VALVE SIZING

Proper sizing of the control valve is critical to the performance of the control loop utilizing it. Too small a valve will not allow enough flow to reach the upper operating range of the control parameter, while too large a valve (which is the more common case) will reach the high end of the operating range while only opening a small percentage of the total. Generally

TABLE 16.1
Common Sensors List

Parameter	Sensor	Application range	Comment/special considerations
Temperature	Resistance temperature detector (RTD)	–430 to 1200°F	100-Ω Platinum most widely used; good accuracy — 3 or 4 wire models recommended for improved accuracy
Temperature	Thermocouple		Moderate accuracy — long runs of thermocouple wire not recommended due to low signal level
	Type J	–320–1400°F	
	Type T	–310–750°F	
	Type K	–310–2500°F	
Volumetric flow	Magnetic	Down to 0.01 gal/min	Some minimal conductivity required; good accuracy for most control applications
Volumetric flow	Vortex — shedding	Down to 10 gal/min	High Reynolds required; can be used for steam; often used in CIP circuits
Mass flow	Coriolis	Down to 0.1 lb/min	Highly accurate, pressure drop can be a concern; density also measured independently; good for metering applications (e.g., batching)
Mass flow	Heat loss	Down to 0.5 cc/min	Commonly used for gasses
Density	Vibration	Down to 0.2 g/cc	Coriolis meters generally include independent density measurement; two phase flow can cause unreliable readings
Density	Nuclear	Down to 0.1 g/cc	Very accurate; subject to radioactive materials' handling regulations
Pressure	Strain gauge	Down to 2 psi	High temperature applications (>250°F), usually require isolation mounting.
Level	Differential pressure	Down to <1 in. of water column	Widely used for tank gauging; height calibration is density dependent
Level	Capacitance	Point level to >20 ft	Susceptible to product coating
Level	RF impedance	Point level to >20 ft	Reduced effects of coating
Level	Ultrasonic	Several inches to 100 ft	Noncontact, surface perturbations can be problematic; can detect liquid/liquid interfaces
Moisture	Infrared	1 to 100%	Surface measurement
Moisture	Microwave	0 to >35%	Density dependent (density independent models are becoming available)
Viscosity	Vibration	0.1 to 106 cP	Read kinematic viscosity; air build up can be a problem

the operating range of the valve should be from 5 to 85% to achieve the minimum and maximum operating conditions of the controlled parameter (Bauman, 1994).

Valve sizing is usually expressed in a valve coefficient (C_v). In its simplest form for liquids, C_v is expressed as follows

$$c_b = Q \times \sqrt{\frac{P_s}{\Delta P}} \qquad (16.1)$$

where Q = flow rate (gal/min), P_s = specific gravity, and ΔP = pressure drop (psi).

Thus a valve with a C_v of 1 will allow 1 gal/min of water at a specific gravity of 1 to flow across the valve with a 1 psi pressure drop. Flow will increase with the square root of the pressure increase up to a point where a critical flow is reached.

Critical flow occurs at the point where the pressure at the vena contracta after the valve is lower than the vapor pressure of the liquid causing the liquid to vaporize. At some point
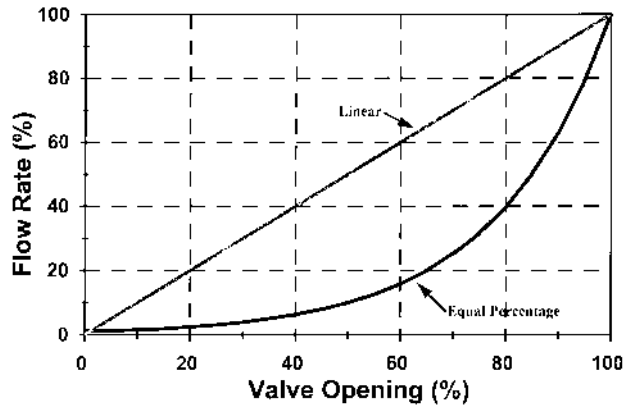
FIGURE 16.2 Control valve characteristics.

downstream where the pressure is recovered to a value between the *vena contracta* pressure and the upstream pressure, the vapor will collapse back to liquid. This is a phenomenon known as cavitation and will be damaging to the valve.

There are many more variations of this basic equation to take into account, such as viscosity and gas flow. More complete sizing equations are available in ANSI/ISA S75.01-1985 — *Flow Equations for Sizing Control Valves*. These equations are also available in program form. Sizing programs are also offered by most valve vendors.

Control valves vary the flow through them by varying their opening. Different valve characteristics provide different relationships between valve opening and flow. Figure 16.2 shows linear and equal percentage valve characteristics. The equal percentage valve has an exponential relationship between valve opening and flow.

A rule of thumb is to use an equal percentage characteristic if the pressure drop across the valve varies by more than 2:1 for minimum and maximum duties. Otherwise a linear characteristic will due, although equal percentage will probably also provide acceptable performance (Bauman, 1994).

16.4 PROCESS DYNAMICS

Processes are often in need of adjustment due to many factors. The output of a process may have to fluctuate to match the needs of downstream operations and efficiencies. The process demands will also vary depending on the current phase of the process, for instance: heating, cooling, and mixing for batch systems, and sterilization, product startup, continuous processing, shutdown, and cleaning for a pasteurizer. Even during one phase of a process where throughput is being held constant, there can be various upsets that subsequently require a compensating adjustment.

There are process dynamics that will delay the response time of a system. The delaying effects are characterized as being one or more of the following; inertia, lag, and *dead time*.

The inertia of a system is described by Newton's second law

$$F = m \times a \tag{16.2}$$

where F = the force acting on a mass, m = the mass, and a = the acceleration of the mass.

Inertia is mostly associated with mechanical systems. It can have some bearing on fluid systems although most fluid control systems have, in essence, instantaneous responses due to the incompressible nature of most fluid food products and the proper selection of a control
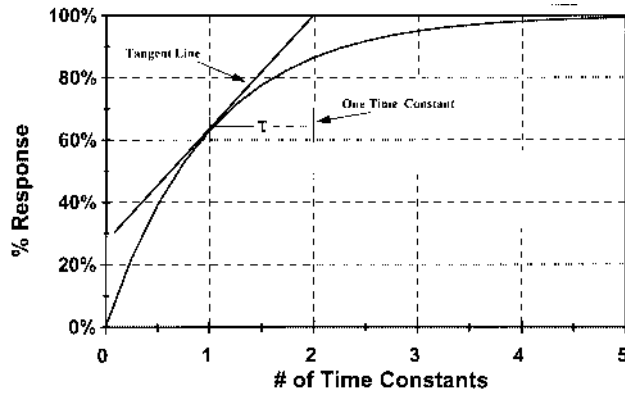
FIGURE 16.3 First order response.

device. Even the response of compressible gases with pressure waves traveling at the speed of sound can be considered instantaneous in most applications.

Capacitance is the ability of a system component to store energy. At the same time system components can impede the rate of energy transfer. The capacitance and resistance of energy transfer result in control system response lags. If in the heating of a batch tank the steam flow is suddenly increased, the system lags due to the amounts of materials that need to be heated (the vessel and its contents) and the rate of heat transfer as determined by the cumulative resistances. A lag of this type can be described by a first order response equation.

$$Y = A \times \left(1 - e^{\frac{-t}{\tau}} \right) \qquad (16.3)$$

where Y = the system response, A = the amplitude of the input change, e = Euler's number (2.718…), τ = time since the step change, and t = the system first order time constant.

Dead time is a delay in the response of a system usually due to a transport phenomenon. If the material in the tank above is being sent through a pipe to a temperature detector, part of the delay in the temperature rise detection will be due to the time it takes for the heated fluid to reach the temperature probe.

16.4.1 FIRST ORDER PROCESS

One model to characterize some processes is the first order model as described in Equation 16.3. Equation 16.3 describes the first order response to a step change in the input. As Figure 16.3 shows, the process response approaches the new steady state value asymptotically.

A tangent line anywhere along the response curve will intersect the 100% response curve one *time constant* (τ) away from the point where the tangent originated (see Figure 16.3). One time constant after the step change the response is 63.2% of the final value. After five time constants the response is essentially complete by being 99.3% of the final value. The time constant of a system is an important consideration in the design of a control loop.

16.5 MODES OF CONTROL

16.5.1 ON/OFF CONTROL

The *on/off control* algorithm is trivial in terms of its mathematical expression, however it is applicable to many control situations. On/off control works by completely turning on or off
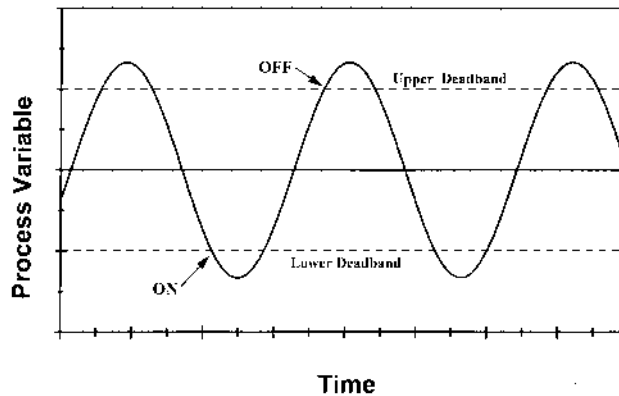
FIGURE 16.4 On/off control (with dead bands).

the control element in response to a change in sign of the error. For instance when heating a batch of product, once the temperature crosses the set point, the valve on the heating medium supply is turned off. After the batch subsequently cools back down below the set point, the heating media supply valve is turned back on.

On/off control will approximately maintain the average temperature as the set point; however there can be substantial excursions above and below the set point depending on the dynamics of the system involved. This type of control is typically applied to batch heating or cooling and large ingredient or product holding tanks. If the vessel is well agitated, promoting good heat transfer, control within ±2 to 5°F can be achieved. Poor agitation/heat transfer will cause slow response of the measurement and large fluctuations can result.

On/off control can result in rapid cycling of the control valve if the control parameter is oscillating quickly around the set point. *Dead bands* are often used in on/off control to prevent this. A point below the set point will be used to turn on the valve in heating applications. Another point above the set point will be used to turn the valve off (Figure 16.4).

16.5.2 PROPORTIONAL CONTROL

The process control model in Figure 16.1 has the error between the set point and the measured variable being manipulated by an algorithm to determine the control response. A *proportional controller* uses a calculation as follows;

$$O = E \times G + M \tag{16.4}$$

$$E = (SP - P) \quad [\text{for reverse acting}] \tag{16.5}$$

$$E = (P - SP) \quad [\text{for direct acting}] \tag{16.6}$$

where O = the *controller output*, E = the *error*, G = the controller *proportional gain*, M = the controller *bias*, SP = the process set point, and P = the process measurement,

From Equation 16.4 it can be seen that the change in controller output is inversely or directly proportional, depending on how the error is calculated, to the change in the error. A reverse acting controller will have a decreasing output in response to an increasingly positive error. A direct acting controller will have the opposite effect by increasing the output as the error increases in a positive direction.
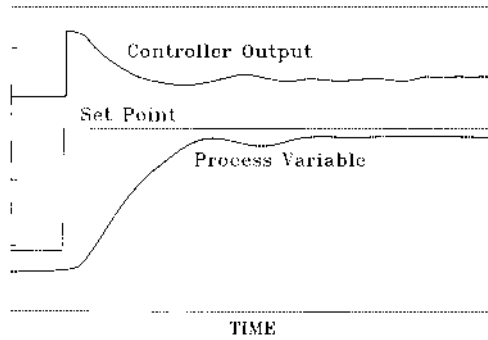
FIGURE 16.5 Proportional control.

The response of a proportional only controller in relationship to the error is a simple straight line with a slope equal to the gain and a y-intercept equal to the bias.

Many controllers use *proportional band* (PB) instead of gain. The relationship between PB and gain is as follows

$$PB = \frac{100}{G}; \tag{16.7}$$

or

$$G = \frac{100}{PB}. \tag{16.8}$$

Thus the equation for a proportional only controller using PB is as follows;

$$O = E \times \frac{100}{PB} + M. \tag{16.9}$$

Since gain and PB are inversely proportional to each other, then the effect of increasing one vs. the other will have an opposite effect on controller response. Increasing the gain will increase controller response, while increasing PB will decrease controller response.

A proportional only controller will generally have an offset between the set point and the measurement. Figure 16.5 shows the response of a proportional only controller to a change in set point. The first response of the controller is a step change as a result of the step change in error. As the system controlled variable responds, the error decreases and so does the controller output. Eventually an equilibrium is reached at which point the error term no longer changes. Since the controller output is only a function of the error times the gain plus the bias, there is nothing to cause a change in response and a constant error or offset will persist.

One means to reduce the offset of proportional only controllers is to set the gain to a high value. For processes with any sort of response lag the maximum gain is limited. The response of proportional control is instantaneous to any error that occurs. When the gain is too high, the process lag will result in constant over correction by the controller and oscillation of the controlled variable. The extent of this over correction can be so severe that the controller is constantly fully opening and fully closing the control valve, acting in essence as an on/off controller. This can result in the control value oscillating around the desired set point. However, the amount of oscillation around the set point is generally more than desired and the constant movement of the control valve will decrease its service life.

Control variables that do have very fast responses can be controlled by high gain proportional only controllers. One variable that this applies to is pressure. In fact pressure regulators are generally this type of controller. Flow is another variable that has a very fast response to a controller output change. High gain proportional only controllers are generally not used for flow control, however.

Flow measurements generally are corrupted by a significant amount of noise. The controller will respond to the noise as well as to any real change in the flow signal. This can result in erratic control. One way to reduce the noise is to apply a filter to the flow transmitter signal. This then is the same as having lag in the process response and therefore high gain proportional only control still does not apply.

16.5.3 INTEGRAL CONTROL

In order to eliminate the offset from a proportional only controller one needs to adjust the bias term for each set point. *Integral (or reset) action* does exactly this by adjusting the controller output based on a cumulative error in addition to the instantaneous action of the proportional part of the controller.

A *proportional and integral (PI) action controller* may have the following equation to calculate the output

$$O = G \times \left(E + \frac{1}{t_i} \times \int E \, dt \right) \tag{16.10}$$

where t_i = the reset time tuning parameter.

The units on the reset time are time per repeat; often minutes per repeat. Some controllers will use the inverse of this and have an integral tuning parameter with the units of repeats per unit of time. It is important to know which integral term is being applied since the two types have opposite effects on controller response similar to the differences between gain and PB.

Since many controllers work with discreet time steps between calculations the PI control output can be calculated as follows

$$O = G \times \left(E + \frac{1}{t_i} \times \sum (E \times \Delta t) \right) \tag{16.11}$$

The reset time, t_i, in the above equations represents, for a given error, the amount of time for the integral action to provide a change in output signal equal to that provided by the proportional control mode. So for a t_i equal to 1 min and if the error at time zero goes from 0 to 1, the output instantaneously has magnitude G from the proportional part of the equation. If the error stays constant, after 1 min the output will have magnitude $2 \times G$, with G contributed by the proportional component and the additional G coming from the accumulation of the error over the 1 min. After a second minute, another G will be added to the controller output magnitude from the integral component. This will continue until the error goes away or the controller reaches a saturation point of either 0 or 100% output (Figure 16.6).

Saturation as a result of integral action is known as reset windup. Reset windup can cause sluggish controller response since the accumulated error must reach zero to eliminate the integral response. It can cause large overshoots or undershoots in response to large errors or in the response of sluggish systems. For this reason, most modern controllers provide anti-reset windup capabilities.
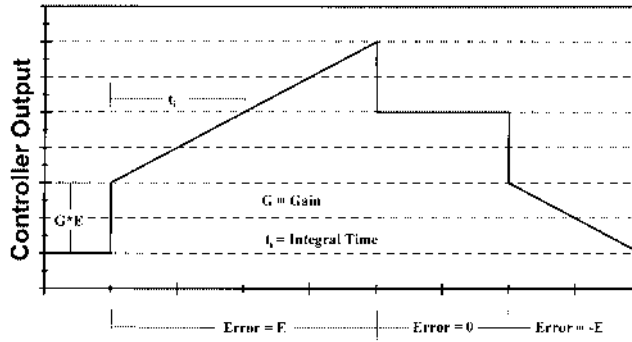
FIGURE 16.6 Proportional and integral control.

16.5.4 DERIVATIVE CONTROL

The *derivative or rate action* of a controller provides a contribution to the controller output in proportion to the rate of change in error with respect to time. One controller output calculation utilizing *proportional, integral, and derivative control (PID)* action is as follows

$$O = G \times \left(E + \frac{1}{t_i} \times \sum (E \times \Delta t) + t_d \times \frac{dE}{dt} \right) \tag{16.12}$$

where t_d = the derivative time tuning parameter.

The slope of the error vs. time curve times the derivative tuning parameter provides additional corrective action in a PID controller. Derivative action provides a type of antici-patory control (McMillan, 1994). Another way to calculate a derivative term is to modify the process variable (P) by using the slope of its change with time to project a new value in the future. This predicted future process value is then used in the error calculation instead of the actual process variable.

$$P_d = P + t_d \times \frac{dP}{dt} \tag{16.13}$$

$$E_d = \left(SP = P_d \right) \quad \left[\text{for reverse acting} \right] \tag{16.14}$$

$$E_d = \left(P_d - SP \right) \quad \left[\text{for direct acting} \right] \tag{16.15}$$

The error term E_d is then used in the PI control algorithm (Equation 16.10) to provide PID control.

Derivative action is very useful in systems where large excursions from set point are encountered or where significant lag exists. One common example of large excursion from set point is when a batch or continuous cooking system is started up.

At startup the deviation from set point is often very large. This can cause a controller to saturate very quickly. Without derivative, the error will have to change signs for some period of time to unwind the integral portion of the control algorithm. This can result in significant overshoot past the process set point. High overshoot cannot always be tolerated. Burn on of product can occur resulting in fouled heat exchangers and/or poor quality product.
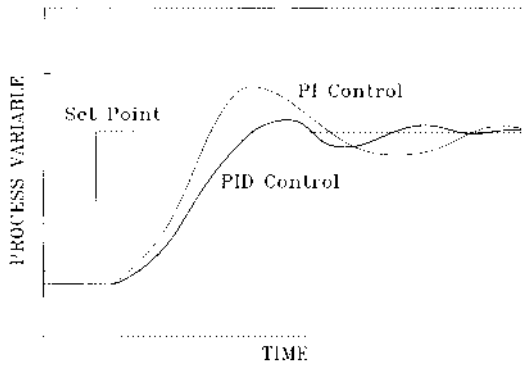
FIGURE 16.7 Proportional, integral, and derivative (PID) control.

TABLE 16.2
PID Parameter Applications

Controlled variable	Proportional	Integral	Derivative
Temperature	Medium to high	Low to medium	Low to medium
Flow	Medium to high	Medium to high	None to low
Pressure	High	Medium to high	None to low
Level	Low to high	None	None to low

Note: PID = proportional, integral, derivative.

A comparison of startup curves with PI vs. PID control is shown in Figure 16.7. While the derivative control reduces or eliminates the overshoot it also increases the time it takes for the process to reach the set point.

For systems with very fast responses derivative control is not used. In these instances, derivative control is not only not necessary, but can also be detrimental. Process variables that have noisy signals will also be difficult to control with derivative action since the derivative algorithm will react to error created by noise as well as to real process deviations from set point. Again, proper sensor installation and/or signal filters can be used to reduce the noise and enhance the ability of the controller to regulate the process.

16.5.5 COMBINED CONTROL MODES

The equations for PID control presented thus far have each control mode dependent on the proportional gain (G). Some controllers offer a control algorithm with independent gains for each mode. Independent gains provide isolation of each control mode effect. This may be useful in some situations, however it can create confusion if the dependent gains equation is expected. Difficulties may also be encountered since more parameters are required.

The PID modes can be used in many different combinations. Table 16.2 shows common combinations for some commonly controlled variables. It is even possible to combine on/off control with derivative control in order to minimize overshoot with a simple "combined" control algorithm.

On/off and PID control are not the only control algorithms, but they are the most common. Many enhancements are available that may be useful for certain control problems. Some of
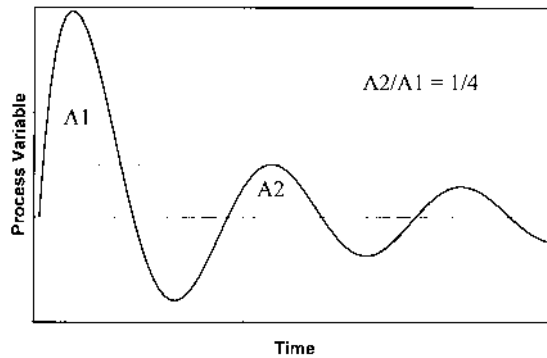
FIGURE 16.8 One quarter decay tuning.

these enhancements are used as supervisory controllers, providing set points to standard PID controllers.

Fuzzy logic and neural networks are two techniques gaining prominence in control applications. These techniques can provide control based on experience or knowledge of a particular system without requiring a rigorous model.

There are advantages to utilizing these techniques or, for that matter, any other sophisticated techniques, in a supervisory fashion. One advantage is that the burden of the vagrancies of the process and control system components can be handled by the conventional controllers, lessening the load on the supervisory system. Another advantage is that if a problem exists in the supervisory control system, then the process can be temporarily run in a conventional fashion.
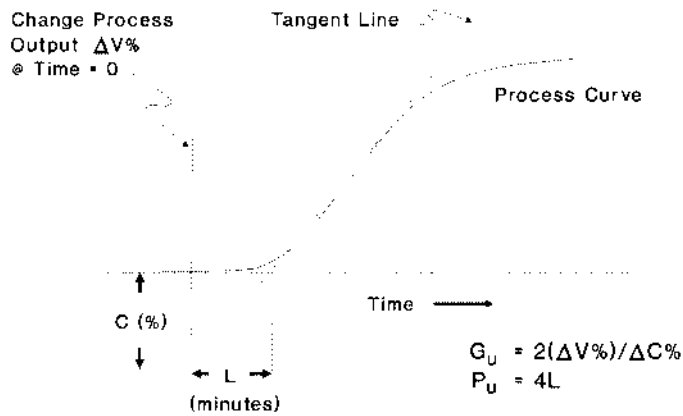
16.6 CONTROLLER TUNING

A PID controller is a very useful tool. However, proper setting of the PID parameters is required to get the desired results. The type of response desired will vary depending on the application. In some applications the desire to get to the set point as fast as possible may be the predominant desire while in others it may be very important to minimize the amount of overshoot or undershoot. Sometimes a combination of different characteristics is desired such that either compromises are made to get some of each characteristic or changes in the control loop are made for different circumstances.

Even when a controller is tuned, the response cannot be expected to be the same over 100% of the range of the controlled variable and the various upsets. For instance, the gain of a heating loop at high flow rate may be fairly low. When the flow is slowed, the amount of valve opening per degree change in product temperature will be less and thus the loop gain is higher. This increased response may cause poor or even unstable control response.

Some components of the control loop are not linear in their response and thus the gain of the loop will change in these areas. Control valves can have many different responses (see Figure 16.2). If a valve is grossly oversized the upper range of the controlled variable may be reached with a small valve opening. Control becomes difficult since a large portion of the control response is useless.

One common type of control response is the quarter decay response as first described by Ziegler and Nichols (1942). Quarter decay is defined as having the area under the response curve reduced by a quarter for each subsequent excursion on the same side of the set point (Figure 16.8). This type of response is designed to provide a fast response while also keeping the total error small.

FIGURE 16.9 Ziegler-Nichols open loop tuning. Ziegler, J.G. and Nichols, N.B., 1942, *Trans. ASME,* 64:759. With permission.

TABLE 16.3
Tuning Parameter Estimates

Controller modes	Controller parameter
Proportional	$G = 0.5 \times Gu$
Proportional	$G = 0.45 \times Gu$
Integral	$t_i = Pu/1.2$
Proportional[a]	$G = 0.71 \times Gu$
Derivative	$t_d = Pu \times .15$
Proportional +	$G = 0.6 \times Gu$
Integral +	$t_i = Pu/2$
Derivative	$td = Pu/8$

[a] Moore Products Co., 1990, *Digital Controller Tuning AM-35*, Issue 3, Moore Products Co., Springhouse, PA.

Ziegler, J.G. and Nichols, N.B., 1942, *Trans. ASME*, 64:759. With permission.

Again this may not be the most desired response, particularly if undershoot or overshoot cannot be tolerated. Other tuning objectives and more detail on tuning methodologies can be found in McMillan (1994), Corripio (1990), and Liptak and Venczel (1985).

Two common tuning techniques are the *open* and *closed loop* methods (Ziegler and Nichols, 1942). Each method has its advantages depending on the circumstances.

Open loop tuning is accomplished by placing the loop in manual and changing the output. Typically the output change is on the order of 5 to 10%. The control variable response with time is plotted from the inception of the output change. A graphical analysis is made (Figure 16.9) to determine parameters that are substituted into equations for the different controller modes depending on the modes employed (Table 16.3).

The open loop method is difficult with fast responding loops such as pressure or flow. The dead time will appear nonexistent unless great pains are taken in recording the response curve. The fact that the loop is no longer in automatic during the test means that care should be exercised when performing this test in order to avoid creating a safety or product quality problem.
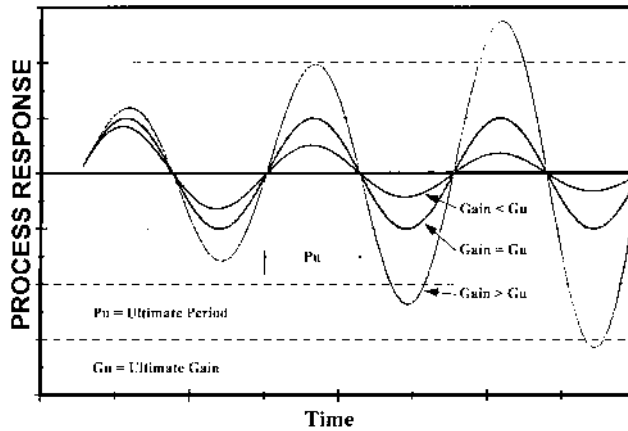
FIGURE 16.10 Closed loop tuning.

Closed loop methods keep the controller in automatic. All modes of control except proportional are disabled. One method has the proportional action increased until sustained equal amplitude oscillations result (Figure 16.10). The gain to get sustained oscillation is called the ultimate gain (G_u) while the time for one cycle of the loop is the ultimate period (P_u). G_u and P_u are used in equations to estimate the control mode parameters (Table 16.3).

Since the controller response can vary over the range of control, the optimal tuning parameters will also vary. The objective of tuning then is to get the best response in the normal operation range while achieving acceptable response in other areas. Often experience and considerable patience are required to get acceptable performance from a control loop. Applying more sophisticated control techniques can help to overcome the problems of some loops. However, from an operation and maintenance perspective, control schemes should be kept as simple as possible.

16.6.1 AUTOMATIC TUNING

Controllers with self tuning capability are widely available. This feature can be a great aid in the startup and long-term operation of a process. However, they are not a panacea. Their mode of operation must be understood and applied properly in order to get value from the self tuning ability.
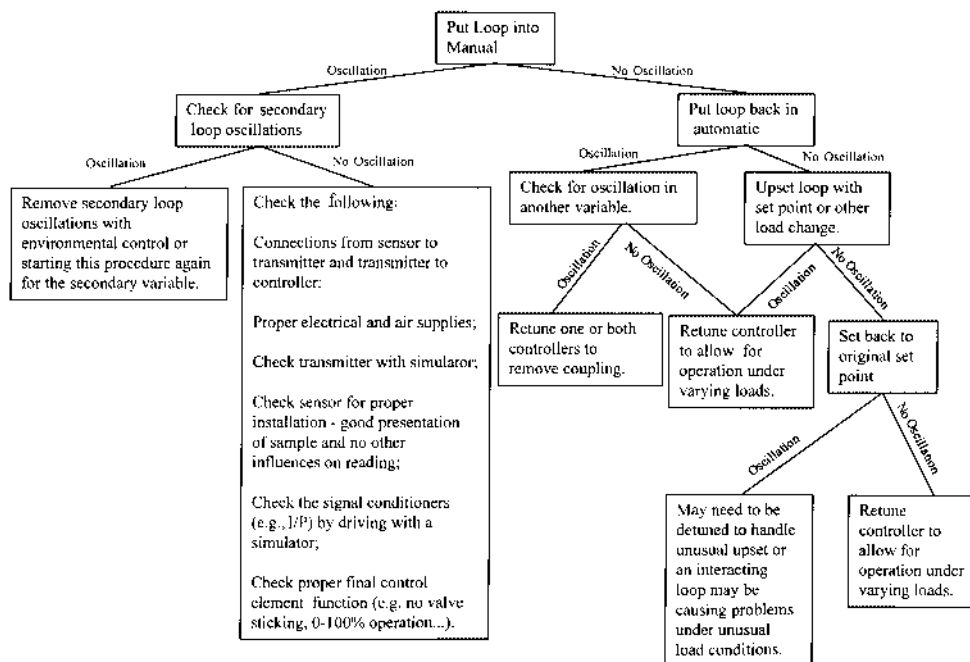
The two major classes of self tuning controllers are deterministic and stoichastic (McMillan, 1994). A deterministic self tuner causes set point changes to provide control loop upsets. The response to the upset is used in the calculation of new tuning parameters. The operator can adjust the magnitude and frequency of the set point changes.

A stoichastic self tuner does not cause upsets to the control loop. Rather, it uses normal process upsets to determine the best tuning constants to apply. The operator can adjust the frequency of checking control loop performance as well as an exponential forgetting rate. The forgetting rate determines how much the recent disturbances determine the controller settings.

Self tuning algorithms are particularly useful when commissioning a new control loop, provided the disturbances are representative of those that will occur once normal production begins. Utilizing the self tuning feature to compare current settings to suggested new settings can be a helpful ongoing practice in order to help identify control loop problems.

The continuous use of self tuning controllers can have its problems. The constant upsets caused by a deterministic self tuner could produce undesirable fluctuations in the control variable. If the control loop sits at one set of conditions for a long period, the self tuner will tend to optimize performance around those conditions. A subsequent abrupt change in load may not be handled well due to the optimization at the previous load.

SCHEME 16.1 Control loop troubleshooting.

Put Loop into Manual

— Oscillation → **Check for secondary loop oscillations**
- Oscillation → Remove secondary loop oscillations with environmental control or starting this procedure again for the secondary variable.
- No Oscillation → Check the following:

  Connections from sensor to transmitter and transmitter to controller;

  Proper electrical and air supplies;

  Check transmitter with simulator;

  Check sensor for proper installation - good presentation of sample and no other influences on reading;

  Check the signal conditioners (e.g., I/P) by driving with a simulator;

  Check proper final control element function (e.g. no valve sticking, 0-100% operation...).

— No Oscillation → **Put loop back in automatic**
- Oscillation → **Check for oscillation in another variable.**
  - Oscillation → Retune one or both controllers to remove coupling.
  - No Oscillation → Retune controller to allow for operation under varying loads.
- No Oscillation → **Upset loop with set point or other load change.**
  - Oscillation → Retune controller to allow for operation under varying loads.
  - No Oscillation → Set back to original set point
    - Oscillation → May need to be detuned to handle unusual upset or an interacting loop may be causing problems under unusual load conditions.
    - No Oscillation → Retune controller to allow for operation under varying loads.

An average set of tuning parameters is usually used to give the best performance over the range of operating conditions. Often, it is possible to download tuning parameters at discrete load conditions. Startups, shutdowns, and changes in product represent some load varying conditions that can offer difficulties for self tuning control algorithms. In the application of self tuning controllers, the use of override control, and returning loops to the manual mode when they are not in use, such as when the process is shut down, can help prevent some of the unexpected results.

16.6.2 CONTROL LOOP TROUBLESHOOTING

Very often when a control loop is performing poorly, the first reaction is to adjust tuning parameters to fix the problem. For a previously working loop, adjusting the tuning may make it perform better, but most likely it will only be fixing a symptom without finding the cause.

Before changing the tuning on a loop that starts to perform poorly, a systematic investigation of each loop component needs to take place. Scheme 16.1 provides a troubleshooting guide. Following is an expansion on some of the key areas of troubleshooting. Troubleshooting should only be done by those knowledgeable of safe process operation.

If the problem persists after putting the loop into manual, then there may be another, secondary variable that is the actual cause of the problem. Try to see if any other variable that may affect the controlled variable is oscillating in kind. For instance the oscillation in a temperature loop could be caused by an oscillating flow of the product or an oscillation of a utility. If a secondary variable is interacting with the variable of interest, then that disturbance should be removed before going back to the original variable.

The procedure for removing the fluctuation in the secondary variable could be to start this procedure over with this variable. If there is a utility fluctuation, then it may require some *environmental control* such as a regulator. If it is not possible to control the variable causing the upset, then either the variable of interest will have to tolerate the oscillations or it can be tuned faster to negate the effects of the upsets. Faster tuning refers to increasing

the gain (decreasing the proportional band) and decreasing the reset time (repeats per minute). Caution should be employed with this approach as instability in the loop may result. Remember that loop performance will generally vary as the load varies.

If other system variables have been removed as causes of the problematic fluctuations and the fluctuations persist, then the next step is to make sure that the sensor signal is being received properly. Be sure to check whether the disconnection of this sensor will cause alarms, interlocks, or unsafe conditions to result.

Check the sensor connections to the transmitter to make sure that they are tight and that there is good contact with the wire and the terminals. With good sensor connections, the use of a transducer simulator can indicate whether the transducer itself is bad. Even though there is no oscillation with the simulator connected and oscillation again occurs when reconnected to the transducer, there could still be a process variable interaction or installation problem causing the disturbances.

Consider the following examples of process installations that can cause process variable reading disturbances. A low flow rate of coolant in a plate and frame heat exchanger will result in uneven cooling and nonuniform product temperature (this is why the *feed and bleed design* should be employed for these exchangers as shown in the cooling loop in Figure 16.12). Inadequate mix time or poor mixing after a steam injector will result in fluctuating temperatures. Flow or pressure measurements may be disturbed after a pipe size change or change in flow direction by the perturbations caused by these changes. A positive displacement pump can cause the flow to pulsate.

Some of these disturbances can be removed with proper system design and proper sensor installation. Double check the actual sensor installation vs. the manufacturer's suggestions. A signal filter is an alternative means of removing some fluctuations. Many transmitters offer filtering as a standard feature. The filter acts as a time averaging signal conditioner. Filtering may reduce the noise of the sensor, but it will add lag to the response of the control loop. A fast control loop may require some detuning to compensate for the lag added by the filter.

16.7 CONTROL TECHNIQUES

There are many possible combinations of control elements. The different combinations are called control techniques. A few of the techniques are described below.

16.7.1 PROCESS AND INSTRUMENT DRAWING (P&ID) SYMBOLOGY

The representation of control schemes is generally done on P&ID. These drawings show the relationship of the sensing elements to the process equipment, although not to scale. The connections of the different control elements are also shown. P&ID's are used for design, installation, and troubleshooting of control schemes and as such there can be different versions with different levels of detail.

Figure 16.11 shows a simple control scheme with explanations for the symbols used in this text. The ANSI/ISA-S5.1-1984 *Instrumentation Symbols and Identification* standard has an extensive list of symbols. This resource should be primary when developing P&IDs in order to easily convey the design to the many parties involved.

16.7.2 NEGATIVE FEEDBACK CONTROL

Negative feedback control is the most common control technique. The term feedback comes from the fact that the controlled variable is measured after being influenced by the final control element. This does not mean that the controlled variable transducer is always located downstream of the final control element. Rather, the feedback refers to the flow of information in a backward loop as shown in Figure 16.1. The feedback information is used
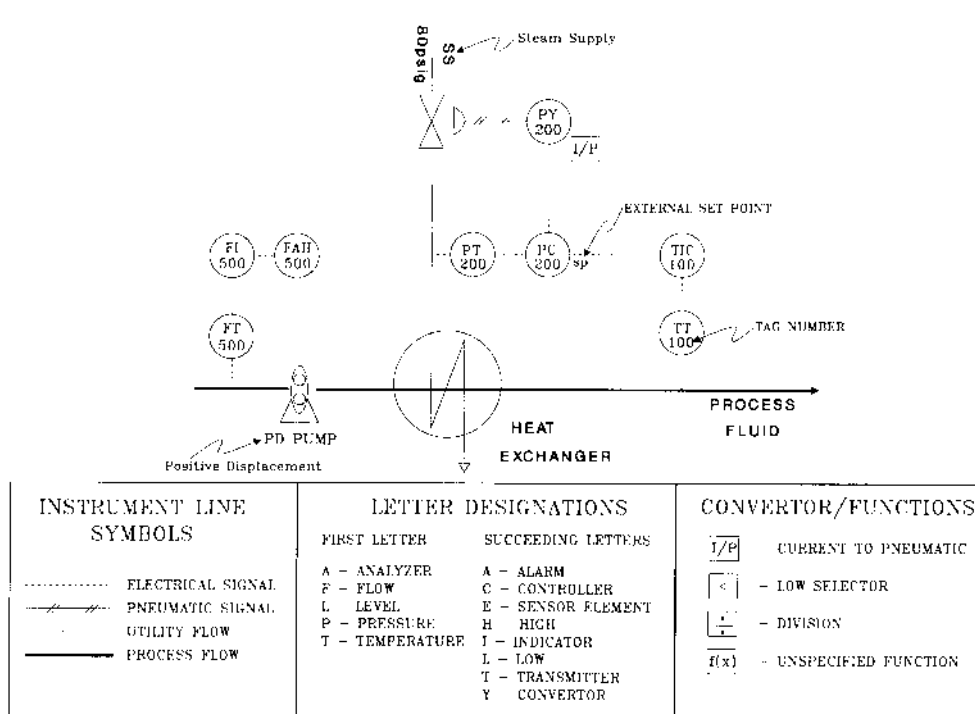
FIGURE 16.11 Process and instrument diagram (P&ID) key.

by the controller to attenuate the effects of disturbances and to bring the process variable back to set point. The negative refers to the change in sign that information must make in the loop to bring the error towards a value of zero. Figure 16.12 shows schematics of three feedback control loops.

Feedback control can be either reverse or direct acting. Reverse acting refers to the direction of the control action. Most feedback loops will take action in the direction opposite to the error. For instance, in the Figure 16.12 heating loop, if the error is positive (that is the actual temperature is above the set point) then the reaction is negative (that is the valve is closed by some increment) reducing the amount of steam supply.

The heating temperature control loop in Figure 16.12 will be direct acting if the valve is normally open, air to close. The controller will have to increase its output in order to close the valve. While the whole loop remains reverse acting, the controller action needs to be reversed since the valve action has been switched.

The cooling control in Figure 16.12 is an example of direct acting control. If the temperature is above the set point resulting in a positive error, then the reaction is also positive: opening the valve to allow more coolant flow.

The direction of each control component must be taken into account in order to determine the setting of the controller as either direct or reverse acting. Most controllers will provide the capability of switching between these modes.

Feedback control is simple to implement and therefore is widely used. One drawback is that the controller is always reacting to events that have already happened. The sensor measures the effects of an upset and then responds. For control loops with long lags or dead times, this type of control may not be able to handle large upsets.

Feedback control is oscillatory in nature. Improper setting of the controller gain can lead to instability. Nonlinearities in the control loop components will lead to an inconsistent response across the total range of control. Feedback control loops often have a lag between
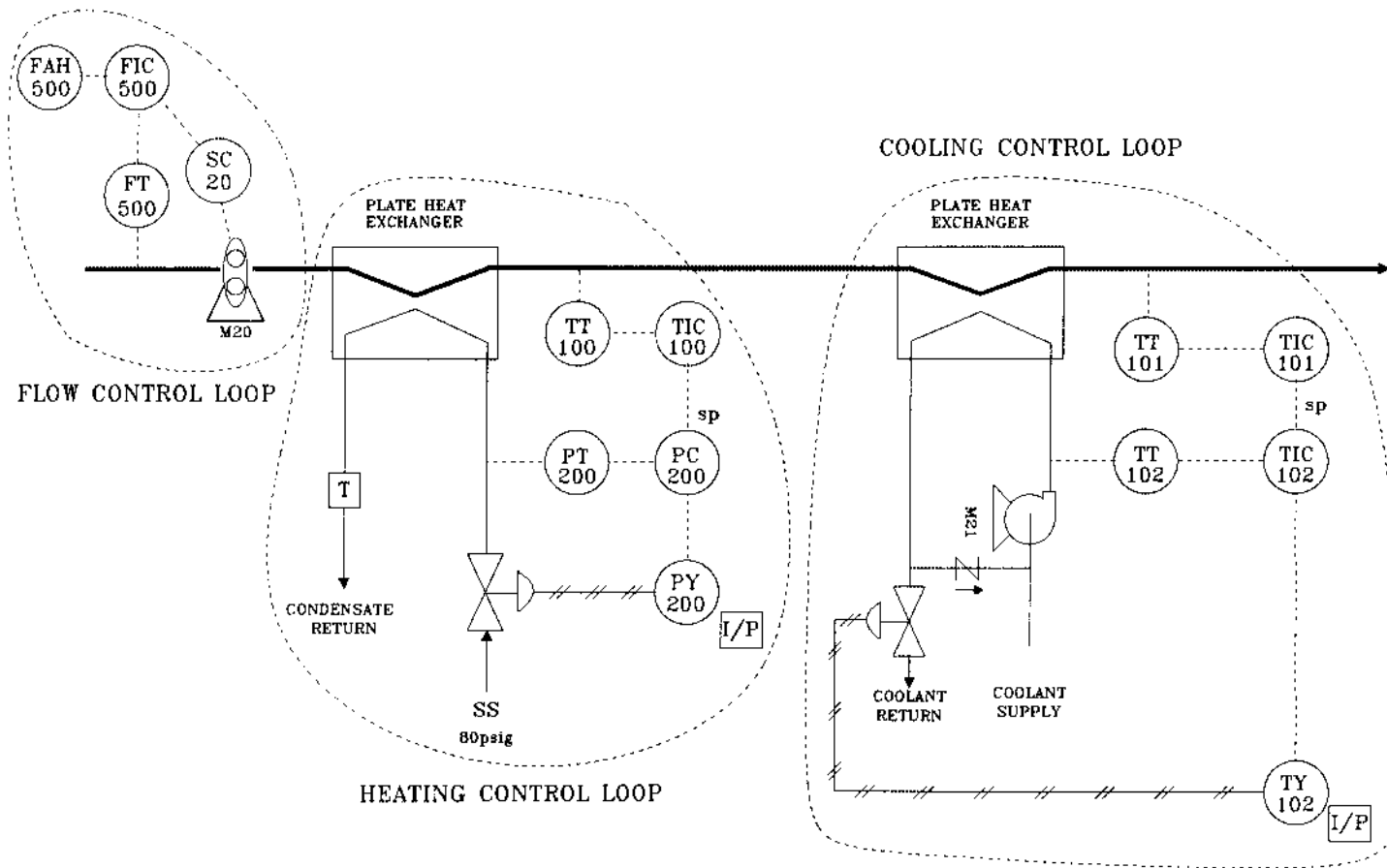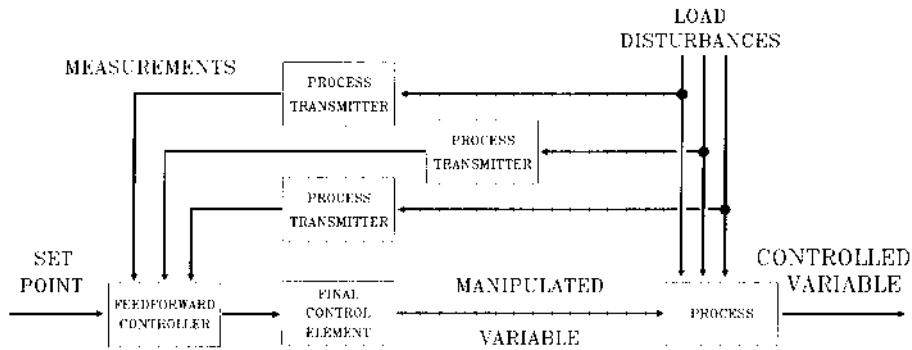
FIGURE 16.12 Control loop examples.

FIGURE 16.13   Feedforward process model.

when a correction is made and when the effects of that correction are measured. This can cause overshoot of the set point or make the control unstable due to constant over correction.

Even with some disadvantages, feedback control is often the heart of a control system design. Combining other techniques with feedback control can usually overcome the deficiencies while keeping the overall system easy to understand and maintain.

16.7.3 FEEDFORWARD CONTROL

Feedforward control measures disturbances and adjusts the final control element in advance of the upset affecting the controlled variable. This is not closed loop control (Figure 16.13) and therefore is not subject to some of the disturbances that effect feedback control.

Not closing the loop means that confirmation of the adjustment affects is not made. The control adjustments are determined by a model of the disturbances vs. the control variables. Some process models are simple, but in most cases trying to model all disturbances related to a desired outcome is very complex.

Many more measurements may be required for feedforward control to ensure that all the disturbances are accounted for. Figure 16.14a shows a feedforward solution to water temperature control by blending hot and cold water. Feedback control is very simple, but is susceptible to disturbances in hot and cold water flows and temperatures. The feedforward control measures these disturbance variables and uses an enthalpy model to calculate the required hot water flow. The model then sends a set point signal to a hot water flow feedback control loop.

The hot water flow feedback control could also be replaced by feedforward control by measuring the valve position and the up- and downstream water pressures. A model of flow vs. these additional parameters would be used to adjust the valve position. The hot water flow would no longer need to be measured.

Feedforward control can eliminate the effects of disturbances very quickly. However, a price is paid in having added components and the dependence on a model to provide the control. Even in the simple example of the water temperature control, disturbances due to varying heat losses through the pipes are not taken into consideration. A comprehensive model can be very complicated leaving unforeseen disturbances unaccounted. The benefits from the extra cost and complexity need to be weighed against the improved control.

The lack of cross checking the result of the control action vs. the controlled variable is a drawback to most forms of feedforward control. Combining feedforward and feedback can overcome this and some of the complexity issues of feedforward control alone.

For instance in the blended water temperature control example, if the hot and cold water stream temperatures hold relatively constant, then the cold water flow becomes the only input to the model. The model becomes a simple ratioing of flows. A temperature feedback loop
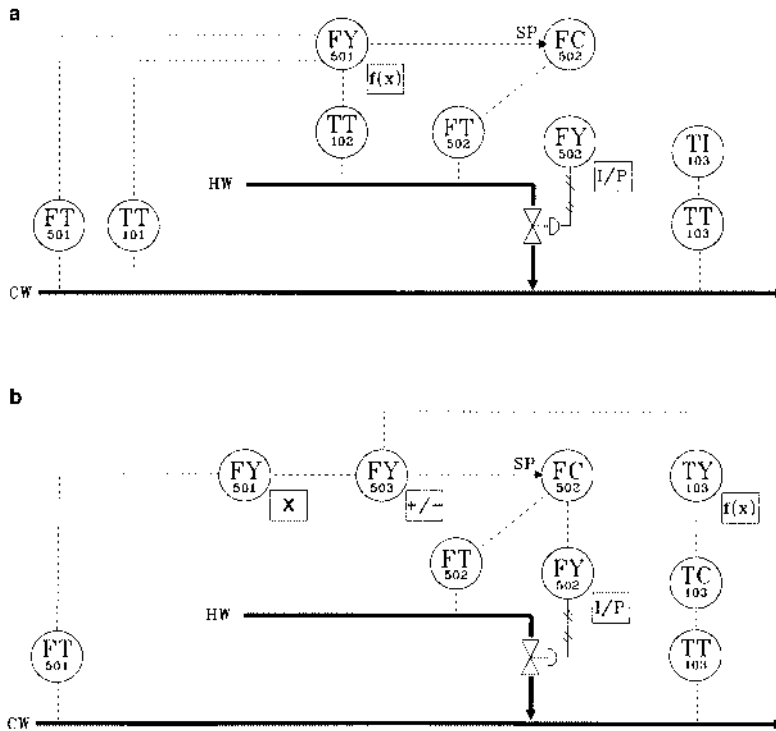
FIGURE 16.14 (a) Feedforward control; (b) feedforward with feedback trim.

can then be used to adjust the output of the model to compensate for the not-accounted-for disturbances. The output of the temperature control loop can be adjusted to be plus or minus some percentage of the total output to act as a trim. To have the temperature loop provide a ±25% trim of the 0 to 100% flow signal, then the output of the temperature controller is divided by two and has 25% subtracted from the result. This calculation and the addition of the trim to the model output are represented by the TY-103 and FY-503 bubbles, respectively, in Figure 16.14b.
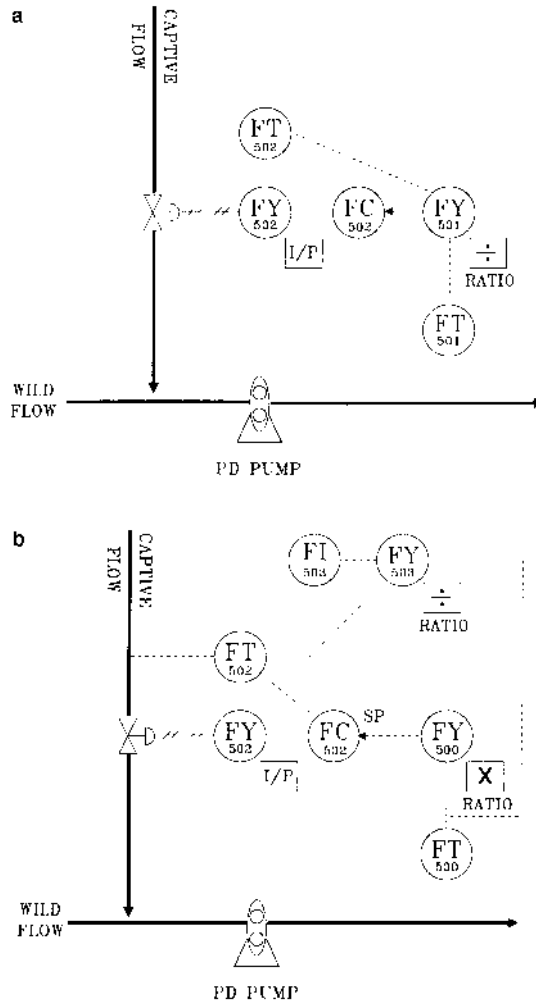
16.7.4 RATIO CONTROL

Ratio control is the simplest form of feedforward control. Blending of various feed streams is the most common application of ratio control. The model for this control is very simple in that the total flow must equal the sum of the parts. One complication arises from the desire for a mass ratio when measuring the volumetric flow. In this instance fluctuating densities are not taken into account.

Two different methods of setting up ratio control are shown in Figure 16.15. Figure 16.15a shows the ratio computed method. Here the flows are ratioed and fed to the controller as the measured value. The controller set point is the desired ratio. The controller adjusts the flow of the captive stream while the other stream, the wild stream, is not controlled by this part of the control scheme.

Ratio computed control has the advantage that the ratio is the set point of the controller and the ratio is calculated by the controller. The ratio is therefore available to the operator as a part of the controller.

The disadvantage of the ratio computed method is that the gain of the controller will vary as the flow of the wild stream varies. The loop gain is the ratio of the change in output to the corresponding change in process variable. The process variable is the ratio of the captive

FIGURE 16.15 Two methods of ratio control: (a) ratio computed and (b) flow computed.

to the wild flow. With an increase in wild flow, the same change in output and therefore in the captive flow, will have a correspondingly smaller effect on the ratio. Therefore, an increase in the wild flow decreases the gain of the loop. This can result in instabilities in different parts of the loop operating range.

Another ratio control method is called the flow computed method. In this method the wild flow is multiplied by the ratio to calculate a set point for the captive flow feedback controller (Figure 16.15b).

The flow computed loop gain is not affected by the wild flow since the gain is merely the ratio of a change in controller output to the corresponding change in captive flow. The disadvantage of this method is that the ratio is not calculated and displayed without additional control components as indicated by the FY-503 and FI-503 bubbles in Figure 16.15b.

Figures 16.15a and b show valves as the final control elements for fluid flow control. Upstream and downstream pressure fluctuations can affect the gain of these control loops as it will affect the total flow for a given valve opening. The use of variable speed drives with positive displacement pumps can decrease the effects of varying line pressures on loop gain. The use of pumps as the flow control elements should be considered in processes where there is a pump providing the flow.

An alternative to the ratio control schemes in Figures 16.15a and b is to use positive displacement piston pumps with variable stroke lengths ganged to a common drive. Once the ratios of the various components are set by adjusting the stroke lengths, there is no need for further control adjustment. Changes in the main flow rate are accomplished by adjusting the main drive speed which likewise adjusts the speed of the ganged pump heads by the same amount. Proportions are automatically maintained since the stroke lengths are not affected by the speed changes.

With the ganged pump heads there are no measurements required. The lack of measurements also means that there is no confirmation of proper dosing. Flow and level switches should be incorporated to provide some level of assurance of proper system operation.

16.7.5 ENVIRONMENTAL CONTROL

Feedback and feedforward control are meant to react to disturbances and keep the controlled variable close to the set point. Environmental control removes disturbances by controlling them.

The heating control in Figure 16.12 can have many disturbances; the steam supply pressure and product flow rate are examples. Adding a steam supply regulator and the flow controller provides some control of these variables. While this removes some of the disturbances, others such as heat exchanger fouling and room temperature and humidity may still affect the heating control.

Appropriate use of environmental control can greatly improve the performance of other control loops. Often a disturbance variable cannot practically be held constant. In the heating loop, if the product flow rate needs to change to meet downstream demands, the rate of change of the flow rate set point should be limited in order that the heater can keep up with the changing demand.

16.7.6 CASCADE CONTROL

Cascade control is a technique that can be used to improve the performance of some control loops and to help overcome some system disturbances. The control is split into two parts; a secondary (inner) loop and a primary (outer) loop. The primary loop output is used as the set point for the secondary loop.

Both the heating and cooling control loops in Figure 16.12 are set up as cascade control loops. The heating loop has TC-100 as the primary loop and steam pressure controller PC-200 as the secondary. In the cooling control, TC-101 is the primary loop, while TC-102 controlling the temperature of the recirculating cooling media, is the secondary loop.

The secondary loop can take care of upsets in the manipulated variable before they impact the primary variable. With the manipulated variable already under feedback control, the primary control loop may be more linear. The primary loop controller adjusts a set point that is more linearly related to the primary variable than is the position of the final control element.

The primary variable speed of response will be improved through the application of cascade control if a lag exists in the secondary control loop.

The response speed of the secondary loop needs to be faster than that of the primary loop. Otherwise the primary loop will always be making set point changes to the secondary loop without enough time passing for the effects of those changes to be realized. Loops interacting in this fashion result in constant oscillations of the primary loop. Oscillation elimination is accomplished by making the secondary loop faster by a factor of three or more than the primary loop.

Note that making the secondary loop three times faster than the primary loop does not mean taking the tuning parameters of the primary loop and multiplying or dividing them by three. Rather, this implies that the correction of a given error by the secondary loop be three times faster than the correction to the same percent error in the primary loop. The tuning

constants for the two loops will generally bear no relationship to each other due to the differences in the individual loop gains.

If a valve positioner is used on a secondary loop then a double cascade loop will exist. The valve positioner is useful in that it will help remove valve hysteresis and make the loop more linear.

There are often several choices of variables to use in the secondary control loop. The variable that represents the greatest disturbance to the primary loop and is the fastest to respond should be selected. Pressure, flow, and valve position are typical fast loops that are used as secondary loops.

The secondary or inner loop should be tuned first when tuning cascaded loops. Since the primary controller is constantly providing a set point correction to the secondary controller, offset in the secondary controller can be tolerated. Allowing offset means that reset action is not necessary. Reset action may not be desirable since it has the potential to slow down control loop response.

16.7.7 INTERLOCKS

Interlocks are discrete signals that are generated in response to certain process conditions. Often interlocks are used to initiate an event or series of events that prevent an unsafe or otherwise undesirable process state from being reached. An example is a surge tank high level switch that is used to tell the system to stop sending product to the tank thereby preventing an overflow. In high temperature short time (HTST) processing systems, high flow and low temperature alarms are used to divert under processed product away from downstream operations, preventing it from ultimately reaching the consumer.

Interlocks can be used to put control loops in manual and force the outputs to the closed or off positions. This will act as a secondary safety for utility shutoff when the loop is inactive. Another benefit for placing a control loop's output to zero when not in use is that the controller will have to rampup its output when put back into automatic, thereby reducing spikes that may have affected the equipment if the output had been left at a high value. Turning a loop from the manual to automatic mode will start the loop with no accumulated reset action. If the reset action is allowed to saturate (windup or winddown) with the control loop inactive, upon start up control action may be sluggish due to the accumulated reset action.

Digital signals for interlocks can come from a variety of sources. Alarms configured in PID controllers and various sensor activated switches installed in the process are common sources. Temperature, pressure, flow, and level are some of the sensor activated switches often used as interlocks. Motors are installed with current switches to shut them off if the load gets too high. This prevents damage to the motor and other dangerous situations that may occur.

16.7.8 OVERRIDE CONTROL

Override control is a technique that will transfer control to an alternate controller when certain process conditions occur, preventing other undesirable conditions from occurring. Override controls differ from interlocks, in that they take analog control action to prevent unsafe operating conditions, or out of specification production, instead of discreet actions. Override controls may result in the continuation of normal production whereas interlocks usually stop or change production modes.

Figure 16.16 shows the addition of override control to a heating control to help prevent the low temperature interlock (TAL-100) from activating. The added override control takes the form of a flow controller with the output of the pressure controller as the input. A high value of pressure controller output indicates a problem with supplying enough heat. The override controller will slow the flowdown allowing the temperature to be maintained.
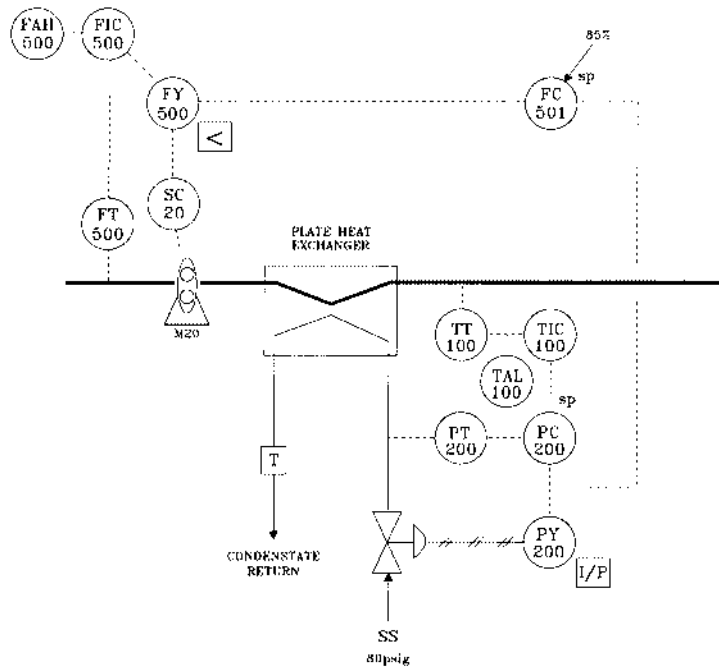
FIGURE 16.16 Override control. FC-501 is an override controller, slowing the flow rate whenever the steam control valve is open more than 85%.

If the output of the pressure controller (0–100% valve position) is below the set point of the override controller, the output of this PI controller saturates at 100%. A *low selector* is used to choose the lowest value signal to feed to the speed controller. In this instance the low selector will pass on the output of the flow controller.

Once the override controller's input exceeds its set point, the output of the override controller will be reduced until it is eventually below that of the flow controller. The low selector will then choose the output of the override controller rather than the output of the flow controller. Flow will be reduced until the output of the pressure controller is below the override controller set point or a low limit or *clamp* is reached.

As the system recovers, the override controller will raise the flow rate set point up to a value where the flow controller will again take control as determined by the low selector. The feedback parameter for both flow controllers should be configured to be the output after the low selector to ensure smooth transitions between the controllers.

Override controllers are not meant to replace interlocks. Rather they are meant to help prevent their activation.

16.8 CONTROL EQUIPMENT

There are many different types of control equipment. Digital computing technology has greatly enhanced the variety and capabilities of available equipment. Control action can be classified as occurring mostly in three major types of devices; the *single loop controller (SLC)*, the *programmable logic controller (PLC)*, and the *distributed control system (DCS)*. The boundaries between these classes of equipment are being blurred as further increases in technology provide more options within each equipment category.

16.8.1 Single Loop Controller

SLC, as its name implies, generally is dedicated to a single control loop. The variety of types and capabilities is extensive. Low end controllers with a single input and output and rudimentary user interface for set point and PID parameter adjustment are available, as are high end, multiple loop controllers with multiple analog and digital inputs and outputs and sophisticated user interface.

Communication capabilities are available in some SLCs. This allows for more sophisticated control schemes than what is available with a single unit. This also allows for centralized monitoring and adjustment and a more sophisticated user interface. This combination of SLCs networked to a central monitor becomes in essence a DCS.

16.8.2 Distribute Control System

The DCS grew out of the need to have more sophisticated centralized design, monitoring, and user interface capabilities, while not depending on a single complicated computer to perform all the functions. In a DCS the functions and computing power are spread out among several processors creating a more powerful, yet relatively simple, system.

Typically a central control console will be used to program and/or configure modules that are connected to the field devices as well as to provide the operator interface. The field device modules will have the sensors and final control elements wired into them. The analog to digital (A/D) conversion, the control algorithm calculation, and the digital to analog conversion (D/A) can all be done in the field device module.

Multiple field device modules can be attached to a single central control station and several control stations can be linked together to form a single control system. Modularity allows these systems to fit the application without requiring special systems that are dependent on the size of the job to be done.

A field device module can control from one to several dozen control loops. Other capabilities such as digital logic control are also available. The trend for DCS manufacturers is to increase the modularity by having each module responsible for fewer items, but to provide more capabilities in terms of options and self diagnostics for each module.

Initially DCS utilized proprietary hardware and software making communication to other systems difficult at best. Increasing demand for networking capabilities by customers is forcing the DCS vendors to write code in standard program languages, utilize familiar computer platforms, and provide communications utilizing standardized protocols.

16.8.3 Programmable Logic Controllers

PLC were originally developed to provide programmable devices that replaced inflexible and complicated relay panels. Their original function was to provide sequence and other discrete control. Math and other computational capabilities were very limited.

Digital computer advances have increased the capabilities of the PLC such that PID control and other computational abilities are now common. Even though communication between the various components of a PLC is generally accomplished on a proprietary network, interfacing to other protocols and systems is available. Incorporation of personal or work station computers into the backplane of the PLC is even available through some manufacturers.

PLCs generally do not come with a standard operator interface. In their traditional implementation, push buttons were the only interface necessary. Programming was accomplished through the use of specialized programming terminals.

The proliferation of personal and other computers has provided a platform for a PLC user interface. Linking the personal computer with the enhanced capabilities of PLCs can provide the functionality of a DCS.

16.9 ECONOMICS OF PROCESS CONTROL

It is often difficult to decide upon the appropriate level of automation for a given project. However, many factors can provide economic justification for applying process control. Some of them are reviewed below.

Proper control system design should consider applying the appropriate amount of technology. Superfluous technology can be distracting. Simplicity is a key for a successful implementation. Long term success is dependent on useful functionality for the operator and ease of maintenance. Fancy graphics may look nice for touring management but can be distracting to operators and may make updates more cumbersome. Sophisticated programming techniques may provide elegant solutions to the programmer and save a few bytes of memory, but can be confusing for maintenance personnel.

Labor savings is usually the area where the most potential for cost savings can be found. Automated controls can result in simplifying the operators' job such that fewer operators are required in a given process area. However, labor reduction through mechanization is often easier than through the application of process control. While process controls provide improved performance, they do not always eliminate the need for an operator to start, stop, and supervise the system.

Consistency of operation can provide economic justification for automated controls. More consistent operation can mean a reduction in the amount of product that is out of specification and that must be either scrapped, reworked, or sold at a lower cost.

Consistent operation can increase production time by reducing shutdown incidences that result from running out of specification. In a process with a heating kill step, for example, incidences of dropping below the minimum required temperature can be reduced by adding controls to variables affecting temperature such as the steam supply and product flow rate.

Reducing the product attribute variability can allow the shifting of the targets to those that are more economical. Decreasing the moisture variability of a baked or dried product can allow raising the moisture target while not compromising product safety or quality.

More consistent operation will usually result in an overall increase in the quality of the product. Quality is often difficult to quantify as an economic justification by itself. Nevertheless, it is an important objective. Sometimes the economics of quality are clear. For example, if a product is sold according to grades, then controls can help provide a more economical split between grades.

16.9.1 CONTROL SYSTEM COSTS

Control system equipment types (single loop controller, programmable logic controller, and distributed control system) vary dramatically in their cost. Single loop controllers are by far the least expensive for implementation of only a few loops. However, when many loops and more complex functionality are needed this price advantage will disappear. Control systems' capabilities are constantly being upgraded as are their abilities to conform to individual project needs. The decision on which system to purchase depends first on the capabilities required, and then on the ability to implement and maintain the hardware and software.

Hardware costs used to be the predominant cost of a system. Advances in digital computer technology have brought the costs down while increasing capabilities. The added capabilities and reduced costs have allowed for the installation of more and more complex systems. These factors have led to rising software costs that can range anywhere from one to five times the purchase price of the hardware.

Providing detailed process descriptions to the programmers will significantly reduce the number of modifications that are required during commissioning and startup. Applying structured programming techniques will make troubleshooting easier and reduce the costs of maintenance and future modifications.

Training is another significant cost of a process control system implementation. Larger systems may require that operators be trained on full-scale simulators to ensure safe and economical operation after installation.

16.9.2 Control System Cost Estimating

One way to estimate the process control equipment cost is to calculate this cost as a percentage of the total capital expenditure. A factor of 2.5 to 7% with 3% as a median is suggested by Peters and Timmerhaus (1968) for "normal" capital projects. A "normal" project may be defined as one in which the bulk of the capital is allocated to processing and packaging equipment, buildings, and utilities.

Projects vary greatly in their process control content. Projects with much or very little amounts of control equipment are better estimated with actual quotes from vendors. A typical control loop will cost from $2000 to $8000 installed. Unusual sensors, such as many analyzers (e.g., color, moisture, density), can have purchase prices many times those normally encountered (e.g., temperature, pressure, and flow).

Engineering for process control equipment is often estimated based on the number of input and output (I/O) points. For each I/O point (either digital or analog), 2 h of engineering is a frequently used estimate. An hour of engineering can cost from $50 to $100 depending on the firm being used and the engineering detail required.

16.10 CONTROL SYSTEM DESIGN

The most important consideration in control system design is to know the process that is to be controlled. Cause and effect relationships between product attributes and process variables should be known in some quantitative fashion. The limits and precision required of each process variable will determine the type of control that should be applied. If a product has little tolerance for variation of a certain process variable, that variable will require an accurate sensor, a carefully tuned controller, and proper sizing of the final control element. Careful control of other variables affecting the critical variable may also be required.

Most control is inferential; that is the product attributes (taste, texture, appearance, microbial load reduction) are not directly measured but are controlled inferentially by controlling other easier to measure variables (e.g., temperature, flow, pressure). Often these inferences assume certain consistencies in raw materials as well as in mixing operations. Raw material variations generally occur infrequently. Set points and other operating parameters can be adjusted in a feed forward based on laboratory checks of raw material attributes.

More sophisticated sensors to measure product attributes such as gas chromatographs, mass spectrometers, and spectrophotometers are being offered for on-line use. However, these devices require an increase in sophistication of users and increased maintenance. Cost justification for these sensors should include not only their purchase price but also any additional maintenance and service contracts.

Simplicity is an important design goal. Complexity should only be added where justified. Keeping the number of devices to a minimum reduces the number of components that can potentially fail and eases the overall maintenance requirements.

Control system design needs to consider the transitory conditions that may occur in a process. Startup, shutdown, and transitions between products are examples of transitory states. Proper consideration to these states can help reduce product waste and promote better steady state operation. For example, a dryer or oven may have a substantial load change when changing products. Altering the temperatures and flows in a systematic way to accommodate the load change can help reduce the amount of product that either has too much or too little heat transfer. In heating a liquid product, providing the proper amount of heat as the production

line comes up to temperature will avoid scorching the product onto the heat transfer surface, promoting better heat transfer efficiency for the duration of the run.

16.11 CONTROL LOOP EXAMPLES

16.11.1 Heat Exchangers

Examples of liquid temperature controls are shown in Figure 16.12. The heating control has a steam heated exchanger with a temperature to steam pressure cascade loop.

The cooling is accomplished with a liquid to liquid heat exchanger. The primary loop of the cascade may not be necessary if excess heat transfer surface area is provided and the circulating utility temperature is controlled close to that desired for the product.

Temperature control loops have dead time due to the transport time from the point of heat transfer to the sensor and lag due to equilibration times of the heat exchanger and the sensor. It is desirable to reduce both of these to improve control.

Dead time can be minimized by locating the sensor close to the outlet of the heat exchanger. In some cases such as with direct steam injection heating, some minimum distance is required to allow a uniform product temperature to be reached.

Lag can be reduced by utilizing small diameter temperature probes. Maintaining high flow rates of heat transfer media in systems such as shown in the cooling loop in Figure 16.12 is important in order to maintain the heat transfer rate and to avoid variations in lag time. The high flow rate will also keep the entire heat exchanger flooded, preventing channeling and inconsistent heat transfer over the surface area.

16.11.2 Batch Heaters and Coolers

Very often batches of materials are heated or cooled in the vessel in which they were mixed. The temperature of the mix will be very slow to respond due to the large mass of product affected. Recirculation through a heat exchanger will provide faster and more efficient heat exchange at the expense of the extra equipment: a pump, heat exchanger, and piping. Another option is to heat or cool the individual ingredients close to the desired final temperature prior to adding them to the batching vessel.

If large temperature changes are to be achieved utilizing a jacketed vessel, the product should be well mixed to facilitate heat transfer. Poor agitation/heat transfer will cause slow measurement response and large fluctuations in temperature can result. In some applications product damage can result if the heating or cooling media is not somehow restricted. With poor agitation or too high a media temperature in a heating application, scorching of product on the vessel walls can occur. In a cooling application selective crystallization of components can occur resulting in a batch that does not contain the expected balance of materials.

16.11.3 Storage Vessel Temperature

Ingredient or product storage vessels often required to hold their contents within certain temperature limits. On/off control is usually adequate to maintain the product within the specified limits. However, precautions should be taken to ensure that the media temperatures are within limits to prevent abuse by overheating or crystallizing the stored material.

An alternative to on/off control for storage vessels that maintain product temperatures is to control the jacket media temperature at the set point desired for the stored product. This avoids product degradation due to extremes of temperatures at the walls, but does not allow for fast compensation for temperature upsets such as may happen when new ingredients are added to the vessel. The temperature of the product in the vessel is no longer used as the control variable. Rather, the product temperature is controlled inferentially by controlling the

media temperature. This method can be used with some confidence since the laws of thermodynamics state that the product temperature will asymptotically approach the media temperature. Given enough time, it can be considered to be in a steady state condition. This is especially useful for storage vessels where the incoming material is close to the desired holding temperature. Even though the product temperature is not used as a control signal, alarms should still be used to indicate system problems.

16.11.4 OVENS AND DRYERS

Proper placement of temperature probes in ovens and dryers is critical. The temperature probes should be placed where the air is well mixed and representative of the effect of the temperature on the product.

For drying, the air inlet and exit temperatures are indicative of the heat load of the system and are most often used for control. Air flow rate control is often achieved with manually adjusted dampers. Each product will vary in the required drying and/or heat transfer rate to achieve the desired moisture and other product quality attributes.

For drying, the inlet air temperature profile with time will generally decrease with time. At the beginning, high temperatures can be used since moisture is constantly being supplied to the surface. As the mass transfer of moisture from the interior of the product to the surface becomes limiting, the temperatures are usually lowered to prevent temperature abuse of the product. Drying the surface too quickly can result in case hardening; severely limiting further drying of the interior.

Final product moisture measurement is generally difficult at best. However, inferential control is often possible. During the falling rate period of drying, the moisture content is related to air temperatures as follows

$$M = C \times \ln\left(\frac{T_i - T_w}{T_o - T_w}\right), \qquad (16.16)$$

where M = product moisture content, C = system dependent constant, $\ln$ = natural log, T_i = inlet air temperature, T_o = outlet air temperature, and T_w = inlet-air wet-bulb temperature.

For certain drying situations then, the product moisture can be controlled by monitoring and controlling the system temperatures.

16.11.5 FLOW

The final control element in Figure 16.12 is a pump, while in Figure 16.15 the final control element is a valve. Note that the flow sensors are upstream of the control elements. This is done because the flow disturbances caused by the control elements could affect the accuracy and stability of the flow measurement. In general each flow sensor has particular installation requirements to which careful attention that should be paid for reliable flow measurement.

A flow sensor may be of a smaller diameter than the rest of the piping. This may require that a bypass be installed to get sufficient flow for CIP operations.

16.11.6 BACK PRESSURE

In many heating applications, the product pressure must be controlled to keep the product from vaporizing. A back pressure controller is implemented to prevent product flashing. This type of control is similar to flow control. Most often the final control element is a valve, but it can be a positive displacement pump.

The back pressure loop is often the fastest loop in a heating system. Since the back pressure may affect the flow, even when it is controlled by a pump (positive displacement pumps may still have some slippage), the flow loop will have to be tuned in a manner to prevent the two loops from interacting.

16.12 SUMMARY

The food industry has not been a leader in process control implementation. Industries such as the petrochemical and automotive with higher profit margins, longer production runs of single products and high global competitive pressures, have led the way. The food industry has taken advantage of improvements in process control technology as it has become less expensive and easier to use. An increase in global competition and in demands to reduce production costs will force an increase in the use of process control. An increase in new food product introductions and shorter product lifetimes will require the process development engineer to design systems that shorten startup times and are adaptable to new products. Process control is not an end unto itself, but is an important tool to allow companies to remain competitive.

GLOSSARY

Analog control: Control of a variable over a continuous range of control action (e.g., 0 to 100% valve position).

Bias: A constant added to result of a calculation.

Cascade control: Control in which the output of one controller is the set point for another controller.*

Clamp: A controller setting that limits the output from going above, for a high clamp, or below, for a low clamp the set value.

Closed loop: A signal path that includes a forward path, a feedback path and a summing point and forms a closed circuit.*

Continuous control: Control of a variable over a continuous range of control action (e.g., 0 to 100% valve position).

Controller: A device that operates automatically to regulate a controlled variable.*

Controller output: A signal sent from the controller in proportion to the control algorithm result.

Dead band: The range through an input signal may be varied, upon reversal of direction, without initiating an observable change in output signal.*

Dead time: The interval of time between initiation of an input change or stimulus and the start of the observable response.*

Derivative or rate action: Control action in which the output is proportional to the rate of change of the input.*

Digital control: Control in which devices are turned either on or off in a specific sequence or in response to certain conditions.

Direct acting controller: A controller in which the value of the output signal increases as the measured value increases.*

Distributed control system (DCS): A group of devices performing control functions connected together via a communications network.

Environmental control: Control of variables that are not the main influence of the manipulated variable.

Error: The algebraic difference between the ideal value (set point) and the measured signal.*

Feed and bleed temperature control: An equipment configuration where liquid heat exchange media is circulated at a high rate through the heat exchanger. New media is introduced into the loop by bleeding off some of the media from the loop in order to control the loop temperature.

---

* ANSI/ISA, 1979, ANSI/ISA-S51.1-1979, *Process Instrumentation Terminology*, Instrument Society of America, Research Triangle Park, NC.

Feedback control: Control in which a measured variable is compared to its desired value to produce an actuating error signal which is acted upon in such a way as to reduce the magnitude of the error.*

Feedforward control: Control in which information concerning one or more conditions that can disturb the controlled variable is converted, outside of any feedback loop, into corrective action to minimize deviations of the controlled variable.*

Integral or reset action: Control action in which the output is proportional to the time integral of the input.*

Interlocks: Discrete signals that are used by the control system to change the mode of the process operation.

Low selector: A mathematical transformation of two inputs where the output is equal to the lesser of the two input values.

Machine control: Control in which devices are turned either on or off in a specific sequence or in response to certain conditions.

On/off controller: A two position controller for which one of the two discrete values is zero.*

Open loop: A signal path without feedback.*

Override control: A control scheme where one controller will take control of another controller's final control element under certain configured conditions.

Process control: The regulation or manipulation of variables influencing the conduct of a process in such a way as to obtain a product of desired quality and quantity in an efficient manner.*

Process measurement: The acquisition of information that establishes the magnitude of process quantities.*

Programmable logic controller (PLC): A programmable control device invented to replace electrical relay panels performing machine sequencing. Capabilities have increased substantially to include analog control as well as other features.

Proportional band: The change in input required to produce a full range change in output due to proportional control action.*

Proportional controller: A controller that produces proportional only control action.*

Proportional gain: The ratio of the change in output due to proportional control action to the change in input.*

Proportional and integral (PI) controller: A controller that produces proportional plus integral (reset) control action.*

Proportional, integral, and derivative controller (PID): A controller that produces proportional plus integral (reset) plus derivative (rate) control action.*

Ratio control: A control scheme that uses the controller to maintain a predetermined ratio between two variables.*

Reverse acting: A controller response in which the value of the output signal decreases as the value of the input (measured variable) increases.*

Sensing element: The element directly responsive to the value of the measured variable.*

Set point: An input variable that sets the desired value of the controlled variable.*

Single loop controller (SLC): A control device that has as its primary function the control of a single controlled variable at its set point.

Time constant: The time required to complete 63.2% of the total rise or decay for the output of a first order system forced by a step or an impulse.*

Transducer: An element or device that receives information in the form of one quantity and converts it to information in the form of the same or another quantity.*

Transmitter: A transducer that responds to a measured variable by means of a sensing element, and converts it to a standardized transmission signal that is a function only of the measured variable.*

Variable frequency drive: A device used to control motor speed by altering the motor's electric power frequency.

Vena contracta: The point along a flow stream after an orifice in which the lowest pressure is reached. This is one of the desired measuring points for an orifice plate differential pressure flow meter.

NOMENCLATURE

a	Acceleration of the mass
A	Amplitude of the input change
A/D	Analog to digital converter
C	System dependent constant
CIP	Clean in place
DCS	Distributed control system
°F	Degrees Fahrenheit
ΔP	Pressure drop (psi)
e	Euler's number (2.718…)
E	The error
F	The force acting on a mass
G	The controller proportional gain
G_u	Ultimate gain
HTST	High temperature, short time
I/O	Input/output
I/P	Current to pneumatic converter
ln	Natural log
m	The mass
M	Product moisture content
M	The controller bias
mA	Milliamps
O	The controller output
P	The process measurement
P&ID	Process and instrumentation diagram
PB	Proportional band
PID	Proportional, integral, and derivative
PLC	Programmable logic controller
P_s	Specific gravity
psig	Pounds per square inch gauge
P_u	Ultimate period
Q	Flow rate (gal/min)
SLC	Single loop controller
SP	The process set point
τ	The system first order time constant
t	Time since the step change
t_d	The derivative time tuning parameter
T_i	Inlet air temperature
t_i	The reset or integral time tuning parameter
T_o	Outlet air temperature
T_w	Inlet air wet bulb temperature
Y	The system response

FURTHER READING

ASAE, 1990, *Food Processing Automation, Proceedings of the 1990 Conference,* ASAE, St. Joseph, MI.

ASAE, 1992, *Food Processing Automation, Proceedings of the FPAC II Conference,* ASAE, St. Joseph, MI.

ASAE, 1994, *Food Processing Automation, Proceedings of the FPAC III Conference,* ASAE, St. Joseph, MI.

ASAE, 1995, *Food Processing Automation, Proceedings of the FPAC IV Conference,* ASAE, St. Joseph, MI.

Bimbenet, J.J., Dumoulin, E., and Trystram, G., Eds., 1994, *Automatic Control of Food and Biological Processes, Proceedings of the ACoFoP III Symposium,* Elsevier, Amsterdam.

Hughes, T.A., 1988, *Measurement and Control Basics,* Instrument Society of America, Research Triangle Park, NC.

Liptak, B.G. and Venczel, K., 1985, *Instrument Engineers' Handbook — Process Measurement,* rev. ed., Chilton, Randor, PA.

Morris, R.L., 1982, *Controller Tuning EM-50-14,* Issue 1, Moore Products Co., Springhouse, PA.

Murrill, P.W., 1988, *Application Concepts in Process Control,* Instrument Society of America, Research Triangle Park, NC.

Murrill, P.W., 1991, *Fundamentals of Process Control Theory,* 2nd ed., Instrument Society of America, Research Triangle Park, NC.

St. Clair, D.W. and Freuhauf, P.S., 1994, PID tuning: it's the method, not the rules, *INTECH,* 41(12):26-30.

REFERENCES

ANSI/ISA, 1985, ANSI/ISA-S75-1985, Flow Equations for Sizing Control Valves, Instrument Society of America, Research Triangle Park, NC.

ANSI/ISA, 1992, ANSI/ISA-S5.1-1984 (R1992), *Instrument Symbols and Identification*, Instrument Society of America, Research Triangle Park, NC.

ANSI/ISA, 1979, ANSI/ISA-S51.1-1979, *Process Instrumentation Terminology*, Instrument Society of America, Research Triangle Park, NC.

Bauman, H.D., 1994, *Control Valve Primer*, 2nd ed., Instrument Society of America, Research Triangle Park, NC.

Corripio, A.B., 1990, *Tuning of Industrial Control Systems*, Instrument Society of America, Research Triangle Park, NC.

Liptak, B.G. and Venczel, K., 1985, *Instrument Engineers' Handbook — Process Control*, rev. ed., Chilton, Radnor, PA.

McMillan, G.K., 1994, *Tuning and Control Loop Performance*, 3rd ed., Instrument Society of America, Research Triangle Park, NC.

Moore Products Co., 1990. *Digital Controller Tuning AM-35*, Issue 3, Moore Products Co., Springhouse, PA.

Peters, M.S. and Timmerhaus, K.D., 1968, *Plant Design and Economics for Chemical Engineers*, McGraw Hill, New York.

Ziegler, J.G. and Nichols, N.B., 1942, Optimum settings for automatic controllers, *Trans. ASME*, (64):759.

17 Food Chemistry for Engineers

Joseph Warthesen and Martha Muehlenkamp

CONTENTS

17.1   INTRODUCTION

This chapter will describe the most significant chemical reactions that occur during food processing and distribution. While food products vary greatly in characteristics and composition, most foods share common chemical components. Many of the chemical reactions that occur will take place to differing degrees in a variety of food products. Yet a given food system will be known for key reactions that are affected by formulation and processing and result in specific quality attributes.

For the engineer, these principle chemical properties and reactions must be understood and controlled to optimize the manufacture of foods. When changes are made in equipment, processing conditions, formulation, or food product characteristics, it becomes even more critical to know and control the chemical reactions involved.

To address the need for general knowledge in food chemistry, the chemical reactions that occur in most foods will be described by each class of chemical component, starting with water. Emphasis will be placed on the effects of heat because of its central role in processing. High temperatures change chemical properties and accentuate reactions. Indeed, the goal of any thermal process is to cause chemical change. Almost always, the processing parameters for time and temperature are designed to bring about one or more reactions.

Within the chemistry section, four unique and influential reactions in food processing will be emphasized. These key reactions are Maillard browning, starch gelatinization, protein denaturation, and lipid oxidation. The role of chemical properties in food dispersions will be addressed by looking at physicochemical traits.

The applications section summarizes chemical reactions taking place in eight selected food systems. The applications have been chosen to show connections between the isolated chemical reactions and the chemical changes that occur in practice. The food systems have been chosen to illustrate food chemistry in a variety of products. For the engineer, the food systems will provide practice in analyzing the full range of chemical changes that are associated with complex food products.

TABLE 17.1
Water Content and Activity of Some Foods

Food	Water (%)	a_w
Peaches	87	0.99–1.0
Chocolate milk	82	0.99
Figs	79	0.97
Eggs	78	0.97–0.98
Meat	70	0.97–0.99
Canned ham	61	0.95–0.91
Cream cheese	54	0.87–0.91
Bread	40	0.95–0.98
Dried fruits	20	0.75–0.80
Honey	17	0.60–0.75
Pasta, dry	12	0.50
Crackers	5	0.1–0.3
Whole egg powder	5	0.4

Note: Water contents (percent by weight) from USDA. a_w values estimated from Fennema, 1985.

17.2 THE CHEMISTRY OF FOOD COMPONENTS

17.2.1 WATER

17.2.1.1 Occurrence

Water is one of the smallest and simplest molecules found in foods. Yet water and water content are considered to be some of the most influential forces in food chemistry. Water has many roles in food processing and, while the chemistry is simple, the impact on food reactions and food quality is greater than any other chemical component.

When the chemical composition of food is considered in the aggregate, there is more water than any other component. Fruits, vegetables, beverages, sauces, puddings, frozen desserts, meats and prepared foods all have high water contents. Beside the obvious quality parameters of being too dry or too wet, the amount of water has a tremendous economic impact because most foods are sold on the basis of weight.

Even apparently "dry" foods have water and the moisture content is usually critical to quality characteristics. Dry breakfast cereals, crackers, and powdered ingredients such as flour and salt, all have measurable moisture of a few percent. Edible oil is one of the few food ingredients that has no significant or measurable water. Table 17.1 lists the typical water content of selected foods.

17.2.1.2 Water as an Ingredient

Water is an ingredient in many processed foods. Ironically, water is often added at some early stage in the processing and then later removed by drying. This suggests a temporary function for water at some intermediate point in the processing scheme. Otherwise, the bother of adding and the expense of drying could be eliminated.

When water is used as an ingredient, it comes with much more than just the H_2O molecules associated with water. Depending on the source, water will contain various minerals which
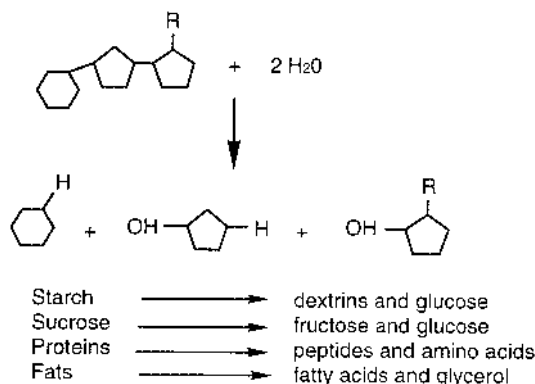
FIGURE 17.1 Representation of hydrolysis of food components.

can influence functionality and interactions with the food components. Processing plants in different locations sometimes seem to produce subtly different products when the only apparent differences are the local water. Water can also contain chlorine, fluoride, microorganisms, parasites, off-flavors, color, acidity or alkalinity, environmental contaminants, and particulates. In-plant water filtration and other treatments may be needed to take the variability out of the local water supply.

17.2.1.3 Water Properties and Reactions

Water is a polar molecule and therefore serves as a dissolving solvent for many different polar compounds in food. Water is a dipolar molecule with a negative area near the oxygen atom and positive areas near the hydrogen atoms. This is part of the reason why water heats so well in a microwave field. When exposed to microwaves, water molecules vibrate and flip, creating frictional heat (Potter, 1986). This dipole nature also allows water molecules to form hydrogen bonds with each other and with other polar molecules in food, such as carbohydrates and proteins. One of the effects of heat, especially mild heat, on foods is the disruption of the hydrogen bonds. These changes will be described in more detail in later sections.

Ice, liquid water, water vapor, and steam are prevalent in food processing. The chemical reactivity and physical properties differ greatly from one form of water to another. Liquid water is fairly inert in foods. It is not typically degraded but more likely, will simply change state and evaporate during processing.

One reaction that causes the water molecule to break apart is hydrolysis. The more significant part of hydrolysis is that other molecules in foods such as protein, starch, or lipids will break apart as well. These hydrolysis reactions usually bring about changes in functional properties because polymers may be shortened in length or flavor compounds may be produced. Figure 17.1 illustrates some of these hydrolysis reactions.

17.2.1.4 Water Activity

While the actual content of water in a food can be used to estimate whether certain water-controlled chemical reactions will occur, the multiple chemical components in food make the system too complex to use percent composition of water as an accurate predictor of reactions. Water activity (a_w) is considered a more powerful tool in looking at how water will influence chemical reactions in food. a_w in foods can be represented by the following equations

$$a_w = P/P_o$$
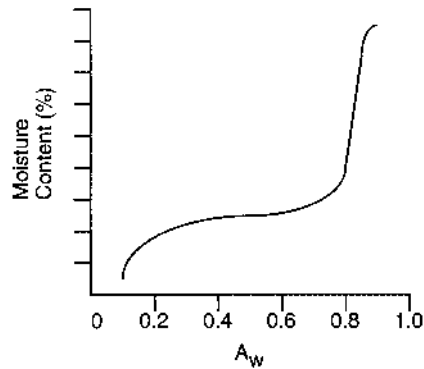
FIGURE 17.2   Typical sorption isotherm for a food product.

where P = vapor pressure of water in the food, and P_o = vapor pressure of pure water under the same conditions or

$$a_w = \text{relative humidity of a food}/100$$

or

$$a_w = \text{moles of water/moles of water} + \text{moles of solute}$$

a_w varies between the theoretical values of 0 and 1.0. In principle, a food will move to an equilibrium with the relative humidity of its surroundings. This explains why, if left in a room of 50% relative humidity, a slice of bread (a_w about 0.96) will lose moisture and a cracker (a_w about 0.10) will gain moisture. The quality of both products would be lost because of the equilibration with the surrounding humidity. This also means that in a packaged food, mixed components such as dried fruit and breakfast cereal flakes will move toward equilibration of a_w with each other. Moisture uptake or loss due to relative humidity differences of the food and its environment will often result in quality changes. Packaging that is impermeable to water vapor is used to protect the food from the humidity of its environment. In certain breakfast cereals, the moisture content and a_w must be in a narrow range. Physical fracturing of the structure and undesirable chemical reactions will occur if the product is too dry. Loss of crispness will become obvious if the product is too moist.

The relationship of a_w to water content in a given food system is illustrated by a sorption isotherm in Figure 17.2. At low a_w and low water content, water molecules are thought to be spread out in a monolayer referred to by chemists as the BET layer (Fenemma, 1986). Water in this state is tightly bound by food components and not easily removed by drying. These water molecules have a low vapor pressure, do not form ice at freezing temperatures, and do not dissolve food components that would otherwise be water soluble.

As a dry food is exposed to higher relative humidities it adds more moisture and the additional water molecules are called multilayer water. At even higher moisture and a_w, the water becomes more reactive and is called free water. Its chemical reactivity and properties would be similar to pure water. In frozen foods, the proportion of ice vs. liquid water is temperature dependent. Since liquid water is responsible for the vapor pressure a_w is controlled primarily by temperature.

Not only are chemical reactions controlled by a_w, the growth of microorganisms for spoilage or fermentations is influenced by a_w. To illustrate how a_w can influence the reactions in food, Labuza (1971) has summarized some key chemical reactions and general growth of microorganisms as shown in
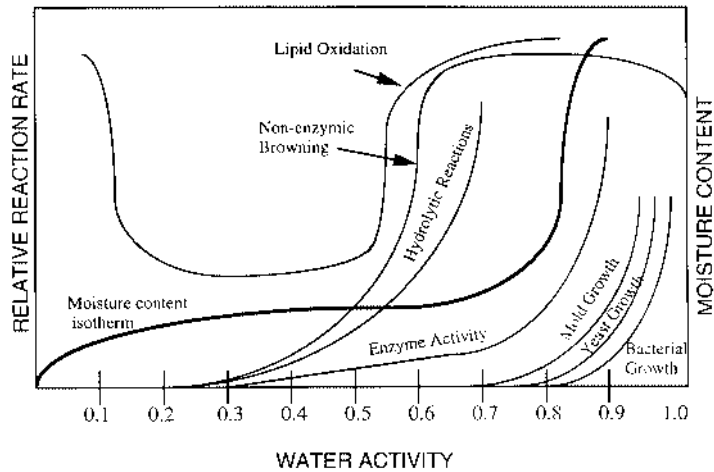
FIGURE 17.3 Estimated relationships between water activity and reaction rate of food chemical reactions in comparison to the sorption isotherm. (From Labuza, T.P., 1971, *Proceedings SOS/70 Third International Congress of Food Science and Technology,* Institute of Food Technologists, Chicago, 633. With permission.

17.2.1.5 Glass Transition

Another way of explaining how water affects the texture of food components is glass transition. Proteins and starch are polymers that have glass transition temperatures (T_g). Below the T_g, the polymers will be in the glassy state and above the T_g they will be in the rubbery state. When a polymer goes through the T_g, there is a large change in modulus. As water content is increased or decreased, the T_g can shift and foods can move from the glassy (crystalline) state to the rubbery (limp or flow) stage without a change in temperature. Therefore, moisture can control how proteins and complex carbohydrates behave particularly with respect to texture.

Cereal products with their protein and starch polymers are good examples of the effects of temperature and moisture content on glassy or rubbery texture. Figure 17.4 illustrates this for a product that starts with flour in the glassy state. As water and heat are added in an extruder, the polymers become rubbery and flexible. Drying after the extrusion step allows the return of the glassy (crisp) state. Additionally, if the dry cereal product takes up moisture, crispness is lost and the cereal converts to the rubbery state. For further discussion of glass transition in cereals see Slade and Levine (1992) and Hoseney (1994).

17.2.2 PHYSICOCHEMISTRY OF DISPERSIONS

17.2.2.1 Colloidal Dispersions

Food systems frequently exist as colloidal dispersions where a liquid, solid, or gas phase is dispersed in another phase. A solid dispersed in liquid is called a sol; skim would be an example where the milk proteins are dispersed in water. A liquid such as an oil dispersed in water would be an emulsion; a salad dressing would be an example. A gas dispersed in a liquid is a foam. Whipped egg whites are an example.

A goal during food processing and distribution is to maintain these dispersions so the phases do not separate. For most types of salad dressing, separating into an oil layer and a water layer is unattractive and undesirable. Whether this happens during processing (such as during filling of the bottles) or during storage (on the grocery store shelf), the end result of the separation is an unacceptable product.
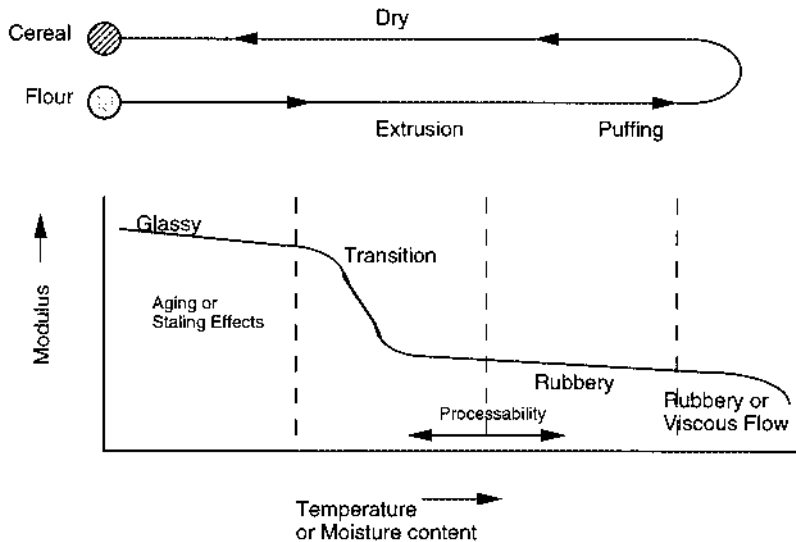
FIGURE 17.4 An example for the conversion of flour to ready-to-eat cereals using T_g vs. moisture content to show what happens during a complex food manufacturing process. (From Mulvaney, S.J., 1994, Personal communication.)

In food dispersions, the forces that separate the phases are natural and numerous. If the dispersed particles are too large, they will float to the top or settle to the bottom due to gravity and density differences between the phases. Homogenization of milk is used to decrease the size of the fat droplets to slow gravity separation. Surface tension or interfacial tension is a driving force for separation because of the dissimilarity of the dispersed and continuous phases.

Electrostatic charge of the dispersed particles can also be a factor in stabilizing food dispersions. If all particles have a net positive or net negative charge, they will repel each other and stay dispersed. However, if the charge on the particles is converted to no net charge by a change in acidity, the charge repulsion is no longer a factor and the dispersed phase particles can lose the ability to stay dispersed. This is the reason why certain protein suspensions will precipitate at a specific pH.

Viscosity is another force that affects the stability of dispersions. If the continuous phase can be made thicker, the dispersed particles will have trouble moving toward each other and separation is less likely. Adding a thickening gum to a salad dressing will make it more difficult for the fat to separate. When butter is cold, the continuous fat phase prevents the dispersed water droplets from separating. When the butter is heated, the fat melts, becoming much thinner and readily allowing the water in the butter to separate.

17.2.2.2 Gels

Gels are formed when dispersed solid polymers in a sol form a network of interconnected strands that trap water and take on a semisolid appearance (Schwartzberg and Hartel, 1992). Gelatin desserts, yogurt, puddings, and jelly are examples of gels formed from widely differing polymers. Only certain food polymers are capable of forming gels. Water binding properties and polymer-polymer interactions are key to gel formation.

If the connected polymer molecules over associate, entrapped water is expelled and liquid accumulates external to the gel. This separation is called syneresis, weeping or "wheying off" and is a major defect in stored gels. Yogurt, cottage cheese, and puddings that have
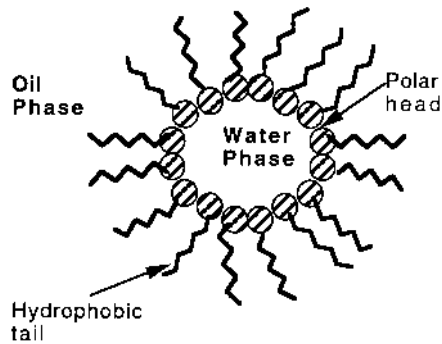
FIGURE 17.5 Representation of the orientation of an emulsifier in a biphasic system.

syneresis are objectionable. Freeze thaw cycles are known to promote syneresis. Syneresis in gels can be inhibited by the addition of water binding gums and increasing the solids content.

17.2.2.3 Emulsions

Emulsions are dispersions of oil-in-water or water-in-oil. For a more extensive treatment see Larsson and Friberg, 1990. Since these two phases have a high interfacial tension, separation is almost immediate after mixing oil and water. Any chance for stability of the fat and water dispersion requires the addition of an emulsifier; a chemical that is able to lower the interfacial tension and promote a longer term dispersion.

Emulsifiers (or surfactants) occur naturally in foods but they can also be added as food ingredients. The major molecular characteristics of emulsifiers are that they have nonpolar regions and polar regions to interact with the fat and water portions, respectively. By orienting at the interface of the fat and water, emulsifiers are able to lower interfacial tension and therefore provide some measure of emulsion stability. See Figure 17.5.
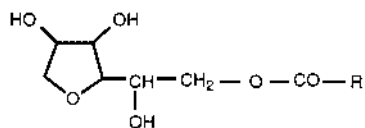
Naturally occurring emulsifiers are found in the membrane surrounding fat in milk and in egg yolk in the form of lecithin and lipid-containing proteins. Emulsifiers that can be added to emulsions include mono- and diglycerides, polysorbates, isolated proteins, phospholipids, sucrose esters, and many other compounds. Examples of chemical structures are given in Figure 17.6. Often used at levels of ¼ to ½%, choosing an emulsifier depends on whether the emulsion to be formed is a water-in-oil or oil-in-water.

Some emulsifiers are positively charged. They help to prevent fat droplets from coalescing with each other by decreasing surface tension between the fat and water phases. Charged emulsifiers also impart a charge to the oil droplet which results in repulsion from other positively charged droplets.

Besides the use of emulsifiers, emulsions can be stabilized by making the size of the dispersed particles small enough to resist gravity separation (Rao and Steffe, 1992). Increasing the viscosity of the continuous phase with gums or other thickeners will also inhibit separation. Avoiding freezing and freeze thaw cycles can also keep emulsions stable.

17.2.2.4 Foams

In foods, foams are usually air dispersed in water although occasionally other gases such as carbon dioxide and other liquids or semisolids such as plastic shortening may be involved. As with emulsions, the phases of a foam are inherently unstable because of density differences and surface tension. Separation is the natural tendency and stabilization is achieved by increasing the viscosity of the continuous phase and lowering the surface tension.

HO   OH

CH—CH$_2$—O—CO—R
|
OH

(O in ring)

1,4-Sorbitan ester

CH$_2$—O—CO—R$_1$
|
R$_2$—CO—O—CH   O   CH$_3$
| ‖ |
CH$_2$—O—P—O—CH$_2$—CH$_2$—$\overset{+}{N}$—CH$_3$
| |
O$^-$ CH$_3$

Lecithin

O   CH$_3$ CH$_3$
‖ | |
C$_{17}$H$_{35}$—C—O—C—C—O—C—COONa
| ‖ |
H   O   H
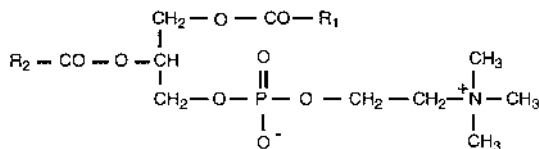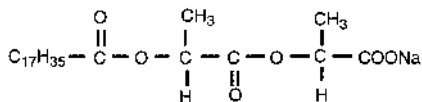
Sodium Steroyl-2-Lactylate

FIGURE 17.6 Structures of three common emulsifiers used in food products.

Water soluble proteins, emulsifiers, and soaps (sodium salts of fatty acids) are used as foaming agents. Egg white proteins are especially good foaming agents because, during whipping, they partially denature, stretch around the air bubbles, and increase the viscosity of the water phase. When egg white foams are heated, they coagulate and permanently trap the air bubbles in a solid structure. When foam formation is undesirable in processing, a small amount of oil or a commercial food grade antifoam can be used to inhibit foaming.

17.2.3 CARBOHYDRATES

Carbohydrates come in a variety of forms but the major differences in chemical properties and functions divide them into sugars and polysaccharides. While some molecular aspects are in common to both groups, the sugars and the polysaccharides have vastly different functional properties.

17.2.3.1 Sugars

Sugars commonly found in foods are the monosaccharides glucose and fructose and the disaccharides sucrose, lactose, and maltose. All are found naturally and are frequently added as ingredients either in relatively pure form or as a part of some other ingredient. The most obvious contribution of sugars to foods is sweetness although they are not uniformly sweet. Sucrose is used as the reference point for sweetness and is assigned a relative sweetness of 1.0. On an equal weight basis, fructose is 1.1 to 1.5 times more sweet, glucose is 0.7, maltose is 0.5 and lactose is 0.3 (Belitz and Grosch, 1986). One sugar may be used as a substitute for another when formulating to a given level of sweetness, but different amounts of sugar are required. Even then, due to synergy and context effects, a sensory panel is the final gauge of sweetness intensity.

Sugars, particularly those other than sucrose, can be hygroscopic (water attracting). This means sugary foods tend to retain moisture and are difficult to take to dryness by evaporation. Sugars vary in their solubility and tendency to form crystals when cooled or concentrated. In confectionery products sugars form crystals or amorphous structures resulting in hard and soft candies. The crystallinity of sucrose is responsible for texture in sugar cookies and fudge. Concentrated sugar solutions are viscous and provide some body to sweetened soft drinks compared to water or soft drinks sweetened with high intensity sweeteners.

Glucose and fructose are widely occurring in natural products like honey, fruits, and fruit juices. When used as more refined ingredients, glucose and fructose are derived from corn and typically used in the liquid syrup form. Maltose, composed of two glucose units, is found in products where there has been starch degradation. Sucrose is glucose and fructose combined into a nonreactive nonreducing sugar. When used as a refined ingredient, sucrose is obtained from sugar beets or sugar cane. Distinguishing features of crystalline sucrose are more a matter of particle size than source of the sucrose.

Lactose, composed of glucose and galactose, is found only in milk and dairy products. Lactose intolerant individuals are unable to digest lactose and therefore may experience digestive discomfort when large quantities of lactose are consumed. This is because the lactose splitting enzyme is missing or not active in their digestive systems. In dairy fermentations lactose is converted by bacteria to lactic acid.

Sugar alcohols are sugar derivatives that are found naturally but are more commonly manufactured from sugars and added as pure ingredients. Sugar alcohols provide sweetness but are not fermented by oral bacteria and therefore do not contribute to tooth decay. Examples of these sugar alcohols are sorbitol, mannitol, and xylitol. Compared to sugars, sugar alcohols are chemically less reactive and digested more slowly. If consumed in high levels they may cause digestive discomfort. Sugar alcohols are used as sweeteners in sugarless gum and candy although they contain a caloric density of 4 cal/g, the same as sugars.

17.2.3.2 Sugar Reactions

A key feature for sugar reactivity is the availability of a ketone or aldehyde group making it a reducing sugar. Most sugars are reducing sugars except sucrose and sugar alcohols. See Figure 17.7. Even then, sucrose can hydrolyze to its component sugars glucose and fructose. The hydrolysis of disaccharides to monosaccharides occurs with heat and acid or enzymes. The acid environment in a soft drink can convert sucrose to glucose and fructose during storage. The effects of sucrose hydrolysis on sweet taste are not great because the two component sugars result in a similar overall level of sweetness. However, the reactivity of the component sugars is much greater because both are reducing sugars. When lactose hydrolyzes to galactose and glucose there is an overall increase in sweetness.

When heated to high temperatures, sugars, whether reducing or not, degrade by carmelization. The series of reactions involved leads to the formation of flavor compounds, brown colors, and polymers with limited water solubility.

17.2.3.3 Maillard Browning

The Maillard browning reaction occurs between a carbonyl (aldehyde or ketone group) found in a reducing sugar and an amine found in proteins and amino acids (Finot et al., 1990). The results of the reaction are the flavor and color development of bread crust, cooked meats, coffee, cocoa, potato chips, and brown beans. While the products of Maillard reaction are often desirable, they may be undesirable or over produced leading to negative attributes in the products. Maillard browning includes a series of reactions where development of the color is the last step of the process. A simplified flow of the reaction is given in Figure 17.8.
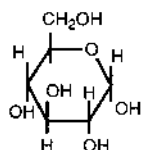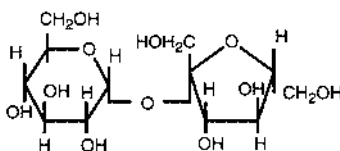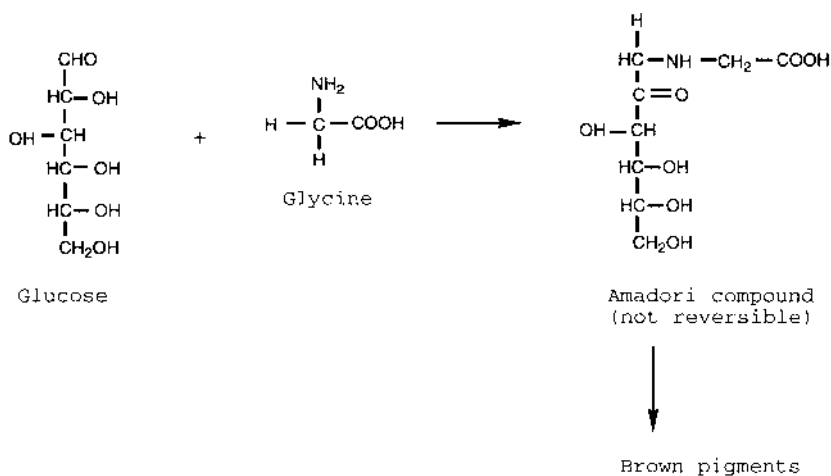
FIGURE 17.7 Comparison of the reducing sugar, glucose, to a nonreducing sugar, sucrose — table sugar.

FIGURE 17.8 Simplified Maillard reaction. The carbonyl compound, glucose, reacts with the amino acid, glycine, to form brown pigments.

The Maillard reaction usually occurs during thermal processing and is common at low moisture levels such as during baking and toasting. The surface of products baked in a microwave oven do not show the surface Maillard browning that their conventional oven counterparts do. This is because the surface of products heated in the microwave tends to be more moist and at temperatures not exceeding 100°C.

Another major factor affecting the extent of the Maillard reaction is the presence of a reducing sugar or a nonreducing sugar such as sucrose that undergoes hydrolysis. Reducing sugars may be added to a formulation containing high levels of sucrose, not to enhance sweetness, but to enhance the Maillard browning reaction. There are no practical ways to inhibit the Maillard reaction except to minimize heat, keep the product moist and acidic (low pH tends to slow the reaction) and eliminate reducing sugars. It is less practical to eliminate amino groups.
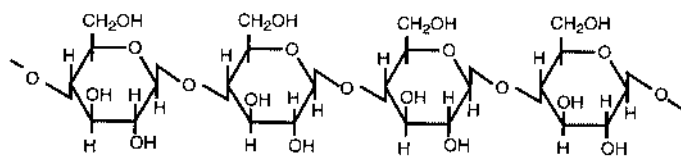
FIGURE 17.9 Structure of the β-(1,4) linkage between glucose units found in cellulose.
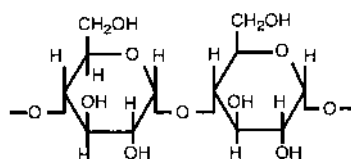
FIGURE 17.10 Structures of the α-(1,4) linkage between glucose units in amylose and the α-(1,4) and α-(1,6) linkages in amylopectin.

17.2.3.4 Cellulose
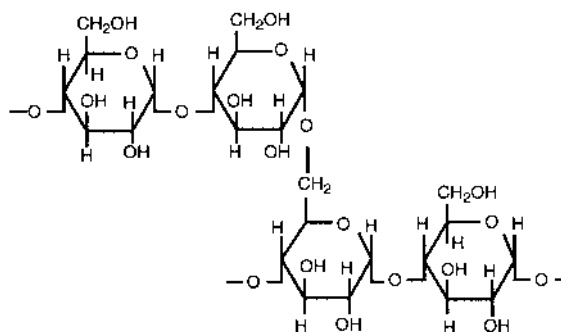
Polysaccharides are carbohydrates that have ≥10 saccharide units linked together. Glucose is the most common unit in polysaccharides but when tied up in linkages, glucose loses its sweetness and reactivity as a reducing sugar. Cellulose is a polymer of glucose where the units are linked by a β1–4 linkage (Figure 17.9). The specific linkage between glucose units creates a polymer that is not affected by heat, moderate acid, alkali, or enzymes normally used in food processing and the human digestive tract.

Cellulose as a food component or an ingredient is considered an insoluble dietary fiber and has no caloric value. Zero calories and water binding are the attributes of cellulose in food. The palatability and functionality can be improved through physical disruption and particle size reduction.

17.2.3.5 Starch

Another glucose polymer is starch. The subunits are linked α1–4 and α1–6. These linkages create polymers that are digestible and much more functional than cellulose. When the glucose units are mostly 1–4, the form is called amylose while the form that has both 1–4 and 1–6 linkages is called amylopectin. Structures of these are shown in Figure 17.10.
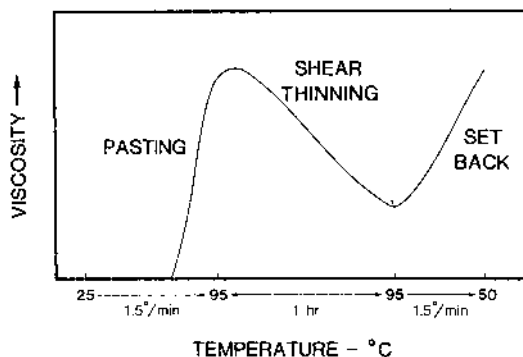
FIGURE 17.11 Stylized amylogram for a starch-water system, showing pasting, shear thinning, and set back with cooling. (From Hoseney, R.C., 1994, *Principles of Cereal Science and Technology,* 2nd Ed., American Association of Cereal Chemists, St. Paul, MN, 48.

Starch is found in plant material in the form of organized structures called granules. These granules are compact starch storage units with areas of crystallinity and amorphous areas. When heated in the presence of excess water, these granules swell and eventually rupture to discharge the amylose and amylopectin molecules. This process is called gelatinization. The swelling is accompanied by a dramatic increase in viscosity and water uptake. Gelatinization is temperature dependent starting as low as 50°C and not being totally completed until temperatures reach 120°C (Hoseney, 1994). The relationship of gelatinization to increased viscosity can be measured in an amylograph where heating, holding, and stirring are used to control the process. Figure 17.11 shows the viscosity increases in a heated starch-water system. The initial gelatinization results in pasting and upon reaching 95°C viscosity is maximized. When held at 95°C with stirring, the viscosity of a starch paste will decrease due to sheer thinning. The gelatinized starch, while cooling, shows increases in viscosity, and can form a gel.

Not all starches gelatinize in the same way. Starches from different sources such as corn, waxy corn, wheat, potato, and tapioca will vary in gelatinization time, temperature, viscosity, and gel characteristics.

Uniformity of starch gelatinization is a key to successful viscosity development and uneven gelatinization can lead to lumping. When in lumps, the outside layers take up water and become more viscous preventing additional water from reaching the interior where the granules are in need of more water for further gelatinization. Water and stirring or mixing with some other separating agent (such as sugar or fat) are required to keep the granules separated and promote uniform gelatinization.

In fully cooked sauces and puddings there is sufficient heating and ample water so gelatinization is nearly complete. In many cereal products, the amount of starch in the form of granules is high but the gelatinization may not reach its full development because of limitations in the amount of available water or the amount of heating.

Starch molecules that have gone through gelatinization may undergo a partial reversal of the gelatinization during storage in a reaction called retrogradation. Starch molecules reassociate by hydrogen bonding with each other or with proteins, if present, to become more firm. This reaction is the cause of staling in stored baked products, the loss of water holding in starch gels, and the formation of enzyme-resistant starch. The results of this reassociation of starch molecules means a firming of the structure of foods and some indigestibility of the normally digestible starch.

17.2.3.6 Modified Starches

Starches in their natural form provide water binding, viscosity, mouthfeel, and texture to foods. Natural starches have some disadvantages because of the time and care needed for

gelatinization. The tendency to thicken with heat may be a problem for pumping and heat exchangers. Starches degrade and thin due to acid and heat and retrograde with storage. Alteration of these undesirable characteristics can be achieved with selection of starches from other plant sources that may behave differently, selection of varieties that may have altered ratios of amylose and amylopectin, or even the development of newer varieties of corn that produce a unique starch property.

Modified starches are altered starches that are designed to overcome some of the short-comings of natural starch functionality. Pregelatinized starch is a starch ingredient that has been fully cooked (gelatinized) and then dried. When cold water is added, the product becomes thick without the need to heat and stir for long periods. This type of starch is the basis for instant puddings. Viscosity development and gel formation are achieved with the addition of cold water and heat is not needed.

Other starches may be modified by partial hydrolysis to give a thinner starch (acid thinned). This type of starch would be easier to pump and run through heating equipment without the problems of high viscosity. In other forms of modified starch chemical groups such as hydroxy propyl are covalently bonded to the starch to slow the reassociation of the starch molecules during cooling and storage. This modification would minimize the effects of retrogradation. Starch molecules are also cross-linked with other starch molecules to prevent thinning during acidic heating. The cross-links make the starch more resistant to the effects of hydrolysis, e.g., in an acidic thermally processed fruit sauce.

17.2.3.7   Conversion of Starch to Sugars

Corn syrups are a family of food ingredients derived from corn starch. The starch is degraded by acid, heat, and enzymes to convert the starch polymers into shorter units with glucose being the eventual end product if the reaction were taken to completion. The varied extents of hydrolysis result in a series of corn syrups that are characterized by their dextrose equivalent (DE). If entirely degraded to the monosaccharide glucose (also called dextrose) the DE is 100 while starch has a theoretical DE of nearly zero. As starches are degraded to higher levels of DE, the product takes on the characteristics closer to glucose and maltose such as increased sweetness, increased hygroscopicity, and increased reactivity in the Maillard reaction. Starch hydrolyzates below 20 DE are called maltodextrins and are more starch like in their properties.

Another step in corn syrup processing is the treatment of high glucose corn syrups with glucose isomerase, an enzyme that converts glucose to fructose. The product is called high-fructose corn syrup and contains both fructose and unconverted glucose. Forms of these syrups can be produced where the fructose level can be increased to even higher concentrations to give an overall sweetness similar to sucrose. The main advantage of high-fructose corn syrups is an increased level of sweetness over glucose-maltose syrups. Since the development of high-fructose corn syrup processing, many applications formerly served by sucrose have been replaced by high-fructose corn syrup.

17.2.3.8   Heteropolysaccharides and Gums

Another class of carbohydrates are the polymers made up of various monosaccharide subunits linked in various ways that are not degraded by the human digestive process. These carbo-hydrates are relatively inert chemically although they bind water develop significant viscosity and/or form gels. Some heteropolysaccharides have a negative charge and can bind to posi-tively charged food components. Carrageenan, guar gum, pectin, alginate, locust bean gum, xanthan gum, modified cellulose, and β-glucan are examples of these types of heteropolysac-charides (Figure 17.12). From a functionality perspective these carbohydrates are stabilizers and water binders. Because the sugar subunits and linkages differ, these polymers differ in their rheological properties, gel forming ability, and effects of heat and pH.
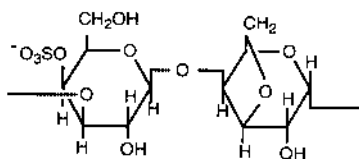
FIGURE 17.12 Structure of the repeating unit found in a common food gum, κ-carrageenan.

TABLE 17.2
Protein Content of Some Foods

Food	Protein %
Peaches	1
Mayonnaise	1
Banana	1
Potatoes	2
Mushrooms	2
Broccoli	3
Spinach	3
Whole milk	3.3
Skim milk	3.4
Wild rice, cooked	4
Corn Flakes®, Kellogg's	8
Grape Nuts®	12
Egg, raw	13
Pepperoni	21
Blue cheese	21
Cheddar cheese	25
Salmon, cooked	25
Fried chicken	50
Turkey franks	63

Note: Percent by weight and wet basis of edible portion.

From USDA, Agriculture Handbook 8, U.S. Department of Agriculture, Washington, DC.

One difficulty in handling these gums as dry ingredients is that they thicken quickly in water. Completely hydrating and dispersing the powdered gums become a problem. Because the outside of a clump is thick, the interior may not get enough water to hydrate. The end result is an incomplete dispersion with the appearance of "fish eyes" which are unhydrated gums.

17.2.4 PROTEINS

Proteins are found in plant and animal foods in a variety of concentrations (Table 17.2). Some generalizations can be made about food protein reactions, but protein behavior during thermal processing can vary greatly. While the protein content of foods can be nutritionally significant, more recently emphasis has been placed on the roles that proteins play in functionality such as texture, water binding, emulsification, gel formation, and foam formation.

17.2.4.1 Structure and Functionality

Proteins are polymers of amino acids linked together in the same type of amide bond called a peptide bond. The unique features of proteins depend on their chain length and the mix of amino acids that make up the sequence. Even though the amino acid composition varies, the amount of nitrogen in food proteins is fairly constant at about 16%. This allows protein quantitation to be done on the basis of nitrogen analysis. When the nitrogen is quantified, the value is multiplied by a factor of 6.25 to determine the estimated protein concentration. With some protein sources the factor might vary such as 6.38 for dairy and 5.7 for wheat.

The amino acid components differ in reactivity, polarity, charge, and functional groups. The characteristics of proteins take on some of the properties of the amino acid components. Proteins, in their native state, fold on themselves and create a very specific three-dimensional structure. This unique shape is key to the functionality of the proteins in their indigenous state and impacts how the protein behaves in food.

Food proteins have a variety of functional properties depending on the amino acid composition which, in turn, depends on the source of the protein. A number of proteins will develop foams with agitation. Egg white proteins are the prime example of agitation and air incorporation resulting in foam formation. When mixed with water, the gliadin and glutenin proteins in wheat flour form gluten which is an extensible, cohesive, and elastic structure that is key to the texture of dough products.

Several types of proteins will form gels because they possess the polymer characteristic that forms a network and traps water. Whey proteins, gelatin, casein proteins, and soy proteins can be manipulated to form products like yogurt, cottage cheese, gelatin desserts, and tofu. Other proteins are known for their ability to emulsify fat and stabilize emulsions. Dairy, meat, and egg yolk proteins are known for their emulsification abilities (Walstra and Jenness, 1984). Food proteins are also used as thickening agents although their ability to do this is often affected by heat and pH.

17.2.4.2 Heat Denaturation

When the three-dimensional structure is altered, protein properties irreversibly change. There are a variety of factors that cause denaturation but heat is the most common denaturing agent in food processing. Other denaturing agents include agitation, solvents, and salts. The three-dimensional structure of proteins changes with heat because the bonds and forces holding the polymer in a spacial arrangement are disrupted.

Hydrogen and disulfide bonds are heat sensitive and are disrupted resulting in denaturation of some food proteins. Functionality of proteins often changes dramatically with denaturation because of changes in solubility, altered chemical reactivity because of exposure of reactive sites on the protein molecule, or increases in protein-protein interaction. One of the most heat sensitive proteins, egg white, denatures at 65°C and forms a gel. Other proteins, such as the caseins found in milk, are not affected by heat and do not denature under typical food processing conditions. In thermally processed products, proteins such as egg white, egg yolk, wheat, meat, whey, and soy become heat denatured resulting in thickening, a loss of solubility, the formation of structures such as gels, and the solid textures found in cereal products. The influence of heat on collagen (connective tissue in muscle) results in conversion to gelatin. This means solubilization and tenderization of the meat and the formation of a protein structure capable of forming gelatin gels.

17.2.4.3 Effects of pH

Proteins are ionic and the charges on the amino acid side chains are influenced by pH. At higher pH levels proteins are negatively charged while at low pH levels they are positively charged. At some intermediate pH called the isoelectric point, the protein molecule, has no

net charge. This can lead to attraction of protein molecules to each other resulting in loss of solubility, coagulation, and precipitation. When milk proteins are acidified to pH 4.6, the casein proteins precipitate while whey proteins still remain in solution. A combination of denaturing heat and pH 4 to 5 is needed to precipitate the whey proteins. In the manufacture of soy protein fiber for meat analogues, alkali-soluble soy proteins are pumped through an orifice into an acid bath that sets up strands of precipitated protein. These strands are packed together to simulate meat fibers.

17.2.4.4 Effects of Salt

Salts can affect the charge on proteins and change solubility. Meat myofibrillar proteins are solubilized by salt. In the preparation of meat emulsions, the muscle proteins must be solubilized by added salt in order to emulsify the fat and prevent separation of the emulsion during cooking. Salt also affects how wheat proteins function in baked products with a stronger dough resulting from the added salt. The salts neutralize the charge repulsion between proteins, thus allowing better protein-protein interaction and gluten formation.

17.2.4.5 Enzymes

Enzymes are proteins that catalyze chemical reactions. Foods naturally contain a host of enzymes that bring about a series of chemical changes. In some situations, the action of indigenous enzymes is essential to develop the final flavor and texture in products such as fruits and vegetables, tenderizing of meat, ripening of cheese, and conversion of starch into fermentable sugar. Enzymes are also responsible for the deterioration of quality of products such as frozen vegetables that are not blanched, browning of a bruised apple or cut raw potato, rancid flavors from fats in milk and in cereals, and the mushiness in over-ripe fruits.

Undesirable enzymes are often inactivated (denatured) by thermal processing. Most enzymes will denature with heat and lose their catalytic ability at temperatures around 50 to 90°C. For fresh foods where thermal inactivation is not an option, enzymes can be inhibited by limiting their substrate availability, changing pH, or adding salt. Oxidative enzymes, such as polyphenolase, cause enzymatic browning and can be inhibited with oxygen deprivation. Ascorbic acid, as a reducing agent, is effective in limiting the oxidative enzymatic browning reaction in fresh fruits and vegetables.

Enzymes also play key roles in food processing where they may be added as ingredients. Rennin added to milk to form cheese, amylase added to dough to make fermentable sugars from starch, and brewing where barley malt is added to degrade both the proteins and starch. Yeasts, molds, and bacteria can also be sources of enzymes in foods. Whether intentionally added for fermentations or present as contamination, microorganisms can contribute a variety of enzyme activities to foods.

17.2.5 Lipids

Defined loosely, lipids are a class of compounds that are soluble in organic solvents. Fats are solid at room temperature and oils are liquid. In practice, lipids, fats, and oils mean essentially the same thing in food systems. Fat provides some unique functionalities to foods that cannot be replaced or duplicated by other food components. Yet fats are a concern because they have a high caloric density (9 cal/g), are dietary components frequently associated with chronic diseases, and can lead to oxidative off-flavors in foods. The fat content of various foods is given in Table 17.3.

There are reasons to minimize the amount of fat in natural or formulated foods and a great deal of product development and processing development has been devoted to decreasing the fat content of foods. Generally, elimination of the fat is not the challenge; the resultant changes in product quality characteristics are the concern. A simplified approach of lowering

TABLE 17.3
Fat Content of Some Foods

Food	Fat %
Skim milk	0.2
Apple	0.4
Macaroni, cooked	0.7
Cod, cooked	1
Tomato soup	2
Total®	2
Whole milk	3
Yogurt, plain	3
French dressing, low cal	6
Salmon, cooked	8
Turkey, roasted	9
Chicken, fried	17
Nature Valley®, granola	17
Snickers®	22
French dressing, regular	41
Pepperoni	44
Margarine, corn	80
Butter	81
Canola oil	100

Note: Percent of edible portion.

Data from USDA, Agriculture Handbook 8.
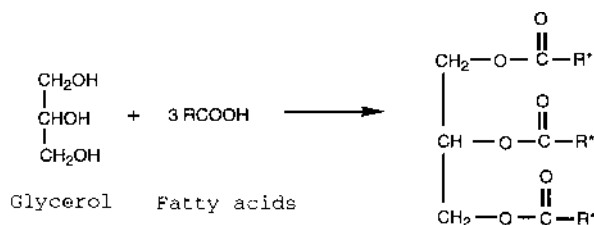
FIGURE 17.13 Formation of a triglyceride from glycerol and three fatty acids. R* represents any fatty acid.

the fat content without compensations in processing and formulation does not usually result in an acceptable product.

17.2.5.1 Chemical Structure

The lipids in foods are mostly in the form of triglycerides. These structures consist of three fatty acids linked by ester bonds to a glycerol molecule as shown in Figure 17.13. Other less predominant forms of lipids in foods are fat-soluble vitamins (A, D, E, and K), fat soluble pigments (such as chlorophyll and carotenoids), mono-and diglycerides, cholesterol, waxes, and phospholipids.

TABLE 17.4
Melting Temperature of Some Fatty Acids

Fatty acid	Melting temperature (°C)
Butanoic acid (C4)	–7.9
Caproic acid (C6)	–3.9
Caprylic acid (C8)	16.3
Capric acid (C10)	31.3
Lauric acid (C12)	44.0
Myristic acid (C14)	54.4
Palmitic acid (C16)	62.9
Stearic acid (C18)	69.6
Oleic acid (C18:1)	13.4
Linoleic acid (C18:2)	–5.0
Arachidonic acid (C20:4)	–49.5

Adapted from Belitz and Grosch, 1987.

The fatty acids on triglycerides vary in chain length and number of double bonds. Differences in chemical reactivity and fat functionality are highly dependent on the fatty acid characteristics. Some of the most common fatty acids and their melting points are shown in Table 17.4. The longer-chain fatty acids cause the triglycerides to be more solid at room temperature. Shorter chains and more double bonds in the fatty acid means the fat is more likely to be liquid at room temperature.

The length of fatty acid chains is a function of the source of the fat while the number of double bonds (unsaturation) is a function of the source of the fat as well as the process of hydrogenation. Animal fats (lard, tallow, butter) tend to have less unsaturation and are therefore harder fats. Fish oils are the exception in that they contain long chain fatty acids with many double bonds. Plant sources of fat tend to contain more unsaturation and therefore are liquid rather than solid at room temperature. Exceptions are coconut and palm kernel oil (the tropical fats) which have short to medium chain length highly saturated fatty acids causing these sources to be solid at room temperature.

Hydrogenation involves the addition of catalysts and hydrogen gas to oils converting the double bonds of fatty acids to single bonds. The net effect of hydrogenation is decreasing the number of double bonds and increasing the melting temperature. Hydrogenated oils also have less chemical reactivity than those at higher levels of unsaturation. Hydrogenation results in fats that are more solid than the unhydrogenated form and less reactive than the higher unsaturation levels. Margarine is a solid at room temperature while the starting material it is made from is liquid. The softness of the margarine can be controlled by the extent of hydrogenation.

A side reaction of the hydrogenation is the conversion of the naturally occurring *cis* form of double bonds to the *trans* form (Figure 17.14). While still contributing to unsaturation, the *trans* double bond contributes to a higher melting point (more solid) fat. These *trans* forms are a byproduct of the hydrogenation process and some questions have been raised about their metabolism in humans.

17.2.5.2 Functionality

Fats and oils are multifunctional components in foods that make their reduction or elimination a challenge. Fats are a medium of heat transfer and are used to thermally process a large
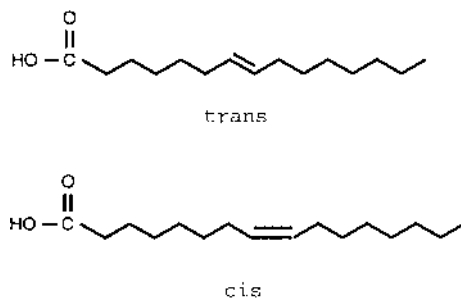
FIGURE 17.14 Structures of *cis* and *trans* fatty acids.

number of products in commercial and food service fryers. There are no nonfat substitutes for frying oils although fat uptake during frying can be regulated by various factors. Fats are lubricants that prevent sticking and permit the release of product from surfaces.

Fats provide the sensory characteristics of mouth feel, juiciness and flavor. Flavor compounds are often preferentially solubilized in the lipid portion of food. Not only do fats trap and deliver flavor compounds in foods but the fats themselves may degrade during heating to provide desirable flavors. The flavor of meats is due in part to the decomposition of fat during cooking.

In cereal-based products, fats contribute to product tenderness by coating flour particles during mixing. This minimizes the interaction of water with the flour proteins and limits the interaction of proteins with each other. The end result is reduced gluten formation and a more tender product. Oils, because of their low viscosity, are more effective on a weight basis at tenderizing than are harder fats. Historically this tenderizing function in baked products was called shortness which led to the fats being called shortening. Fats also provide flakiness to pastry products by serving as a barrier between gluten layers.

Fats contribute to the opacity or whiteness of foods, particularly when emulsified. For example, skim milk has a less white appearance than whole milk at 3.25% fat because of the way the fat particles refract light. Low or no fat salad dressings may not have the opacity of the fat-containing counterparts.

Fats may be used in foods as solids, liquids, or a soft semisolid form called a plastic fat. The plasticity characteristic is controlled by temperature and the mix of fat sources. When converting from liquid to solid forms, triglycerides can form different types of crystalline structures. Depending on the cooling process, the crystal forms can have different melting characteristics. In a process called interesterification, the fatty acids are released from their triglyceride structure and then reattached in a sometimes different position. This process results in a redistribution of the fatty acids on the triglycerides and is used to improve the melting or plastic characteristics of the fat source.

17.2.5.3 Lipid Oxidation

The oxidation of fatty acids results in the development of undesirable flavors that can lead to unacceptable food quality. Lipid oxidation and loss of flavor quality is probably the most frequent cause of deterioration in foods that are not otherwise subjected to microbial spoilage. The shelf-life of products like breakfast cereals, frozen meats, potato chips, and edible oils themselves, is limited by oxidation. Besides producing off flavors, lipid oxidation can cause the loss of essential fatty acids needed for human nutrition, fading of pigments, destruction of fat soluble vitamins, and the production of potentially harmful compounds from the oxidized fat (Fennema, 1986).

The number of double bonds in a fatty acid or fat source is a good indication of the potential for lipid oxidation. Any oil source that is high in unsaturation should be viewed as

very susceptible to degradation. Fish oil is an extreme example of a highly unsaturated oil that is very unstable in a food system.

The oxidation reaction involves the formation of highly reactive free radical compounds that develop as a result of the double bond. Lipid oxidation in foods has an induction period where the reaction may seem slow or nonexistent. But with time, the speed of the reaction increases and efforts to stop or slow the progress at this point are futile. Oxygen becomes involved in the reaction by forming peroxides and hydroperoxides on the affected fatty acids. The next step is the decomposition of the fatty acid into lower molecular weight compounds such as aldehydes and acids. These compounds may have potent flavors themselves or further react to cause other flavor problems. A final step in the reaction is that free radical fatty acids may react with each other to form larger molecular weight compounds. The oil may become more viscous and discolored. At this stage in the reaction, the flavor compounds are likely to be so objectionable that the product is inedible.

A variety of means are used to inhibit lipid oxidation. The use of more saturated fats and more hydrogenation of unsaturated fats will decrease the susceptibility to oxidation. However, more unsaturated fats are desired for health reasons, lipid oxidation problems have to be solved by other means such as packaging, storage conditions, antioxidants, and processing parameters. While there are exceptions, lipid oxidation can be thought of as a storage reaction rather than a heat-induced reaction. Nonetheless, temperature plays a role and cool, as opposed to warm temperatures, are recommended for storage of oxidation-sensitive foods. Light promotes lipid oxidation, so opaque or colored packaging and protection from visible and ultraviolet light are preventative measures. Mixing oxidized oil, even in small amounts, with fresh oil will allow the reaction to skip past much of the induction period and therefore take place at an accelerated rate. The peroxides and free radicals in the old oil will expedite the formation of off-flavors.

Oxygen is one of the reactants and is a strong promoter of the reaction. Any measures to eliminate air or oxygen from the food will slow lipid oxidation. The nature of most foods will not allow complete expulsion of air, but vacuum packaging (for roasted peanuts), nitrogen flushing (for potato chips), and oxygen impermeable packaging (foil lining for some snack foods) can all be helpful in inhibiting the reaction. The effects of water content on lipid oxidation are mixed because in dry foods such as powders and dried cereal products, lowering the moisture even further will promote oxidation. Under other circumstances, increases in water content or a_w can increase the extent of oxidation. The generalized effects of a_w on lipid oxidation are given in Figure 17.3.

Metal ions such as iron and copper are catalysts for lipid oxidation. The presence of these metals in processing equipment, water, oils, or other food ingredients should be looked upon as sources of pro-oxidants. Some antioxidants such as citric acid are used to bind or chelate metal ions, thereby destroying the catalytic activity. Naturally occurring antioxidants such as vitamin E and β-carotene can slow the rate of oxidation as will the addition of synthetic antioxidants such as TBHQ (tertiary butyl hydroquinone), BHA (butylated hydroxy anisole) and BHT (butylated hydroxy toluene). The power of these antioxidants is limited and they can only be used in low levels. Normally, a combination of preventative measures must be used against lipid oxidation in foods containing unsaturated fats and even then, the products will have a limited shelf-life because of the reaction.

17.2.5.4   Frying oils

Frying oils are used as a medium of heat transfer, are a source of flavor and also end up as a component of the fried food. While frying oils may be saturated or unsaturated to varying degrees, the high temperature conditions of frying lead to breakdown of the triglycerides. Heat-induced hydrolysis of the fatty acids from the triglyceride creates free fatty acids which
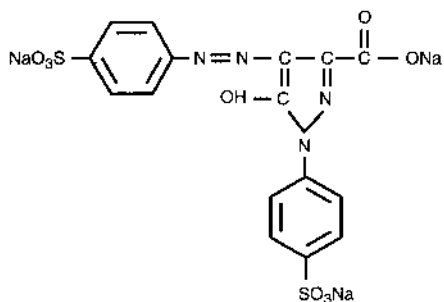
FIGURE 17.15 Structure of a food colorant, yellow No. 5.

may have a flavor. They are also susceptible to further chemical degradation to acrolein which has a pungent odor and to smoke which is undesirable in frying.

Most frying is done around 175°C because lower temperatures tend to cause excessive oil uptake in the food and higher oil temperatures can lead to rapid oil breakdown. Even under normal frying temperatures, triglycerides degrade to create smoke, darker colors and higher viscosity (due to polymerization), and various off flavors. In most frying operations, replenishing the oil removed with the product occurs on a regular basis. In other situations, the old oil is extensively degraded and must be discarded because its presence in the fried food can cause off-flavors and short shelf-life.

The positive flavor contributions of frying are due to the high temperature causing Maillard browning. The oil itself also degrades to flavor compounds and these are transferred into the product being fried. It is well known in fryer processing that all fresh oil does not make the best tasting product nor would oil that has been darkened or polymerized. The optimum flavor results are achieved by a steady state of fresh replacement oil being added to the used oil.

17.2.6 PIGMENTS AND COLORS

The color of foods is a key factor in acceptability. Poor color or inconsistent color, as judged by the consumer, suggests over processing, spoilage, low quality, or inferior ingredients. Food color, in some cases, is produced by processing (such as the color of baked products) and production of a uniform color is associated with having the process under control. In other cases, food color can be destroyed by processing (such as the color of canned green beans) and minimizing the impact of processing on color change becomes a factor in process development. The color of formulated foods will also be a function of colorant ingredients (such as added caramel color or yellow No. 5) or ingredients that may react to form colors (for example, addition of glucose to enhance Maillard browning). See Figure 17.15 for examples of structures.

17.2.6.1 Fat Soluble

Naturally occurring colors are most noticeable in plant materials. Chlorophyll, a fat soluble green pigment in plants, is chemically unstable. The structure of chlorophyll is complex but the two features that affect stability are a magnesium ion and an attached fatty acid that provides fat solubility. In the presence of acid and heat, chlorophyll will degrade to pheophytin which is an olive-green color. This occurs because the magnesium ions are replaced by hydrogen ions. The slightly acidic and prolonged heating conditions during vegetable canning are devastating to chlorophyll and little of the original bright green color found in vegetables remains after thermal processing. This loss of color is irreversible although some special can linings release metal ions and partially restore some of the green color. An increase in water
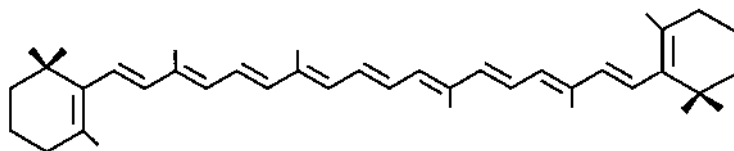
FIGURE 17.16 Structure of a natural food pigment, β-carotene.

solubility can occur when the fatty acid, called phytol, is cleaved by processing conditions or the enzyme chlorophyllase.

Carotenoids are fat-soluble orange-red pigments found in carrots, squash, tomatoes, pineapple, oranges, corn, and other plant material. Animals do not produce carotenoids but extract them from their diet and deposit them in fat tissue. The yellow color of chicken fat, egg yolks, and milkfat is due to carotenoids in the diet of the animal. Carotenoids have received recent attention for the role they may play as dietary components that can inhibit chronic diseases such as cancer.

There are many carotenoids in foods and some of the most common ones are α- and β-carotene, lycopene, lutein, and canthaxanthin. Their chemical stability to processing is very good although slight color changes occur due to isomerization of the naturally occurring *trans* bonds to the *cis* forms. Like lipids with double bonds that react with oxygen, carotenoids are also sensitive to oxidation Figure 17.16. Because of this, carotenoids can be unstable in dried foods that are exposed to air. In contrast to some of the other plant pigments, carotenoids have been successfully used as food colorants. The color of orange Cheddar cheese and butter are due to added carotenoids which come from the annatto bean. Water dispersible forms are available so fat solubility is not a limiting factor. Certain carotenoids such as β-carotene have vitamin A activity so they may be added for nutritional value as well as color.

17.2.6.2 Water Soluble

The red to blue colors in products such as berries, apples, grapes, red cabbage, and cherries are from the anthocyanin family. These pigments are water soluble and will change color dramatically with shifts in pH. When taken to alkali conditions, the typically red anthocyanins turn more pale, blue, or gray. They are also sensitive to metal ions and will discolor in the presence of such ions as aluminum, tin, or iron. Beet colors are similar in properties but come from compounds called betalains. Extracts of grape skins, beets, or other anthocyanin-containing plant materials have been used as color concentrates for other foods. They are somewhat unstable to prolonged heating, can undergo fading due to oxidation during storage, and change color with changes in pH.

A related family of pigments are the anthoxanthins. These are white pigments found in wheat flour, potatoes, and onions. The color is not noticeable except in alkaline conditions where, due to alkaline water supplies or alkaline ingredients, anthoxanthins turn yellow. In the presence of aluminum they turn yellow and with iron they can turn black or brown.

17.2.6.3 Meat Pigments

The color of meat products is a result of the presence of myoglobin which, in raw meat, can be bright red to brown depending on the exposure to oxygen. Essential features of the molecules are that it contains iron and is attached to a protein. During the cooking of meat, the reddish pink color is replaced by a brown color. This pigment, hemichrome, forms irreversibly from the myoglobin molecule and results from the denaturation of the protein. Since brown color is often the indicator of doneness in meats, hemichrome is called the cooked meat pigment. In cured meat products such as ham, sausage, bacon, and hot dogs, nitrite is added as part of the curing process. The nitrite reacts with the myoglobin to give a

pink color. When heated, this color becomes set and is known as nitrosohemichrome. It does not change color with further heating so the reheating of hams and hot dogs does not necessarily give a change in color and the brown cooked meat color does not develop.

17.2.6.4   Color Ingredients

A number of colorants are available as food ingredients. Some are from natural sources and are termed uncertified colors. Some of these colorants have been mentioned. Caramel is created from the thermal reaction of reducing sugars with or without amines and comes in a variety of brown colors and caramel flavors. Caramel colors are the end result of sugar degradation or Maillard browning and they are used in products such as dark breads and cola beverages. Cochineal and carmine are red pigments extracted from insects. Titanium dioxide is a white pigment used for whitening and icings.

The artificial colors, sometimes referred to as certified colors, are water soluble in the form of dyes. They can also be attached to aluminum salts in an insoluble form called "lakes". There are six dyes approved for liquid applications and these have common names as well as numbers such as yellow No. 5. The dyes are tested and certified by the Food and Drug Administration as safe for use in foods. Compared to the natural colorants, certified dyes are more potent, more stable during processing and storage, and more consistent in coloration. The "lake" form of the dyes, color by dispersion rather than by being dissolving. "Lakes" are used for powders and other dry mixes where water solubility is not necessary.

17.2.7   VITAMINS AND MINERALS

A continual concern in food processing is the decrease of nutritional value due to loss of vitamins and minerals. Losses can occur at various stages but often overlooked are the losses that occur due to washing and or fractionation of the raw food material. For example, the milling of cereal grains removes the bran and the germ where vitamins and mineral are concentrated. If these components are not used for food or are not recombined to make whole wheat flour, there is a loss of nutrients. This has led to enrichment guidelines for the addition of niacin, riboflavin, iron, and thiamin to refined flour to compensate for the loss of nutrients when the bran and the germ are not used in the final food product. Peeling and washing can also lead to the separation of vitamins from the edible portion of the food.

Many of the vitamins and unbound minerals are water soluble. If water is lost by being squeezed out or if the tissue is washed or mixed with the cooking liquid, leaching of the nutrients can occur. Minerals are not heat sensitive and are generally not lost during processing except by fractionation leaching into the water. Certain food components like fiber and phytate can bind minerals and make them nutritionally unavailable for uptake in the digestive process.

Chemical degradation is also a mechanism of loss for some vitamins but not minerals. Vitamins most sensitive to heat are vitamin C and thiamin. Losses during baking or canning can be significant. The fat soluble vitamins A and E can be lost during lipid oxidation. Riboflavin and vitamin A are known to be light sensitive and can undergo chemical degradation. For example, milk packaged in transparent containers exposed to light will show significant riboflavin loss with storage.

17.2.8   FLAVOR

Flavor in foods is much like color in that it is an essential quality component. Flavors may be formed during processing and may be desirable or undesirable. With a few exceptions such as selected wines and certain cheeses, flavor deteriorates with time and frequently causes an end to the shelf-life. Flavors may also be added as ingredients which can be either natural or artificial.

17.2.8.1 Taste

A comprehensive definition of flavor includes taste and aroma. Taste is divided into salty, sweet, sour, and bitter. Salty taste comes only from sodium chloride. Other combinations of ions, while contributing to some saltiness, do not give an acceptable salty flavor of their own. Sweet taste can be furnished by a variety of chemicals including sugars and a group of compounds called high intensity sweeteners. These sweeteners share some common chemical features but are not closely related in overall structure. The sweetness perceived on a molecular basis varies with the sweetener and the food system it is used in. Sour is primarily a function of pH with acidic foods perceived as more sour. Bitter is a sensation produced by several chemicals such as certain peptides and alkaloids such as caffeine. The harsh effects of sour and bitter in a food can be mitigated by sweeteners.

Other taste sensations are the heat of peppers (due either to capsaicin or piperine) and the cooling sensation of menthol. Another group of chemicals are known as flavor enhancers. While not contributing their own taste in the levels used, they tend to bring out the better flavor components in complex food systems. These flavor enhancers include monosodium glutamate and the disodium salts of 5′ nucleotides such as inosine monophosphate and guanosine monophosphate.

17.2.8.2 Aroma

The aroma of foods is far more complex, subtle, and distinguishing for a given food product. So important is aroma that it is frequently used interchangeably with food flavor. Chemicals contributing to aroma are low molecular weight, volatile, and usually perceived at low concentrations. Plant materials develop their own flavor systems due to metabolic processes. As examples, vegetables produce sulfur-containing compounds, some of which are not released as flavor until the product tissue is disrupted or until heated. Onion and garlic are an example of the former and cabbage and broccoli are examples of the latter.

Fruits get their characteristic flavor by combining alcohols and acids to produce esters. Spicy flavors come from the conversion of aromatic amino acids to aromatic aldehydes. Terpenes are another class of flavor compounds found in fruits which are produced by the plant's metabolism. Short chain fatty acids can also be flavor compounds, especially in animal products.

The majority of flavors produced during processing can be attributed to three types of reactions: Maillard browning, lipid degradation, and fermentation. The classes of flavor compounds produced by Maillard browning include aldehydes, alcohols, pyrazines, and acids. Lipid degradation products provide some of the flavors in dairy products (lactones) and in fried products (certain aldehydes in french fries). Meat flavor is produced by Maillard browning and heat-induced lipid degradation.

Fermentation contributes to flavor as microorganisms convert fermentable sugars to primary products such acids, aldehydes, and alcohols and secondary products such as ketones, esters, and amino acids. Cheese, yogurt, wine, beer, pickles, and bread are examples of products where the fermentation has a major impact on flavor. Optimization of the flavor production requires careful control of the fermentation parameters of organisms, substrate, temperature, pH, and time.

Flavorings are ingredients that are either extracted from natural sources or produced chemically. From a regulatory basis the distinction between natural and artificial has more to do with source and processing and less to do with chemical composition. The combination of chemicals used in flavorings provide or enhance the flavor of foods. In general, flavorings are sensitive to chemical reactions such as oxidation during processing and storage. They are volatile and can be lost during heating.

17.2.8.3 Undesirable Flavors

Off-flavor development is an equally important chemical reaction. Not surprisingly, off flavors can result from loss of control of the same chemical pathways that produce the desirable flavor. As an example, roasting can produce the needed Maillard browning flavors in a snack food but excessive roasting can lead to flavor loss and the development of burned or charred flavors and bitterness. Potato chips benefit from the flavor of the slightly degraded frying oil but if the oil were oxidized to a more advanced stage, shorter shelf-life and stale flavor would be a major quality defect in the product.

Unwanted enzymatic activity can cause off-flavors especially with the lipid component of foods. Lipase is an enzyme that will cause the release of free fatty acids and lipoxygenase can cause an acceleration of lipid oxidation.

Light catalyzed off flavors can be a problem caused by a combination of transparent or translucent packaging and exposure to sunlight or retail display lights. The bottles used for beer are usually brown or green to prevent the "skunkiness" flavor caused by the formation of a mercaptan compound. Milk is especially sensitive to light and develops a cardboard-like flavor when exposed during storage. In general, lipid oxidation is catalyzed by light. While slower to develop than other light catalyzed reactions, the flavors produced by this reaction can be detrimental. Opaque packaging or other protective measures are needed in some products to protect against the development of off-flavors.

Microbial growth is also a source of off-flavor causing sour, musty, fruity, or other detectable flavors. Contamination of foods by external odors can also be a problem during food processing and distribution. This can come from the air (e.g., diesel or paint fumes), water (e.g., chlorine or algae growth), disinfectants (e.g., a medicinal smell), detergents (e.g., perfume or soapy smell), and packaging (e.g., chemicals used in plastics or lamination).

17.3 APPLICATIONS — CHEMICAL REACTIONS IN FOOD PROCESSING

The chemical functions and reactions taking place in a given food are multiple and complex. These chemical changes influence process optimization and quality characteristics. By looking at specific food systems, the set of reactions involved can be integrated and understood in the context of the end product.

17.3.1 BREAD

The chemistry of bread production involves mixing, fermentation, baking, and post-baking changes (Eliasson and Larsson, 1993; Pomeranz, 1988). Key bread ingredients wheat flour, and water are mixed with the yeast, salt, sugar, and shortening. During the mixing stage the gliadin and the glutenin proteins in flour are hydrated with water and interact with each other to form gluten. Shortly after that the yeast start to convert sugars into carbon dioxide, ethanol, acid, and may produce other flavor compounds. The fermentable sugars may be added as ingredients or converted by yeast enzymes from sucrose or maltose to monosaccharides. If there are no added sugars, the amylase enzymes in the flour or added as an ingredient slowly degrade starch to maltose.

Carbon dioxide is produced more rapidly under warm conditions because yeast grow and ferment fastest at 25 to 30°C. The gas is retained in the dough because of the ability of the gluten to stretch and expand. As the volume increases, the dough may be punched down to redistribute the yeast food and the gas. Once adequate fermentation has occurred based on a specified time or volume increase during a step called proofing, the bread goes into an oven at about 200°C.

During the first stages of baking there is an increase in volume of the loaf due to gas expansion. The yeast soon are inactivated by the high temperature and fermentation stops. Gluten proteins heat denature and contribute to the bread texture. Starch granules, which make up the bulk of the dough, undergo gelatinization although the degree of gelatinization is restricted because of the limited amount of water. The heating causes evaporative moisture and ethanol loss, thus a weight reduction during baking of about 10% can be expected.

Since the outer layer of the bread is at a high temperature and a low moisture level, the Maillard browning reaction takes place predominantly at that location. The amine groups of the proteins are reacting with any residual reducing sugars to cause browning of the crust and production of flavor compounds. As the bread cools, some of the starch molecules reassociate to cause crumb firming.

With additional time of storage, the starch will hydrogen bond with itself or proteins to cause undesirable firming as part of the staling process. This can be partially reversed with warming which causes hydrogen bonds to break and restores a softer texture. Other storage reactions include the softening of the crust due to equilibration of the moisture content with the crumb or ambient humidity. Growth of mold can be a problem due to the high a_w of bread although the presence of mold is due to environmental contamination with mold spores after baking because any mold in the ingredients or equipment would get destroyed by the heat of baking.

17.3.2 Process Cheese

The chemistry of cheese production includes coagulation of milk, fermentation, aging, and conversion into process cheese (Walstra and Jenness, 1984). Milk is treated with the enzyme rennin which cleaves a bond in one of the casein proteins, causing the clotting of the casein micelle complex. At the same time, starter culture bacteria are added to the milk to convert lactose into lactic acid. The decrease in pH changes the charge of the casein proteins so they are nearer the "no net charge" pH and the proteins will attract each other and form a semisolid structure. As the coagulation occurs, the casein traps water and milkfat but not the lactose or the whey proteins.

Curds that are formed are further dehydrated by salting and pressing to expel more water. The cheese then undergoes a period of ripening where the small amount of remaining lactose is converted to lactic acid, and the proteins are further degraded by residual rennin and proteolytic enzymes from the bacteria. Protein degradation results in a softening of the cheese texture and the development of flavor. There is some degradation of the milkfat triglycerides to give free fatty acids which also contribute to flavor.

While some cheese may be consumed after short or long periods of aging, a great deal of cheese is further converted to a process cheese product. This is done by blending various natural cheeses at a high temperature. The blended cheese becomes liquid during cooking because the fat is melted and the proteins become more soluble. Phosphate salts are added to the mixture to help the cheese proteins emulsify the fat. The phosphate salts are called emulsifying salts although their effect is through making the proteins more effective as surfactants. The hot cheese is then put in packages and the structure sets upon cooling.

17.3.3 Hot Dog

Hot dogs are emulsions formed by mixing lean muscle and fatty tissue with water and then cooking (Price and Schweigert, 1978; Girand, 1992). The key physicochemical reaction is the formation of the emulsion. Water and salt form the brine which dissolves the muscle proteins so that they function as emulsifiers. Salt also serves as a preservative by retarding bacterial growth. When the emulsion is being formed, the comminuted meat can also be mixed with flavorings and nitrites. The emulsion is kept cool so the fat stays in the solid form.

Upon smoking and cooking, the myoglobin pigment reacts with the added nitrite to give a stable pink color. While heating causes some protein denaturation, the process is carefully controlled to limit the amount of heating in order to maintain the ability of the proteins to bind fat and water. The cooking develops flavor from the degradation of fat although the major flavor contribution in a hot dog comes from the added ingredients.

17.3.4 CANNED GREEN BEANS

The major chemical changes in canning green beans are the degradation of the chlorophyll, softening of the texture and flavor development. Green beans are likely to be blanched prior to filling cans. Blanching, which is a mild heat treatment, eliminates air from the tissue, partially softens the texture, and inactivates enzymes like peroxidase. The continued heating of the can in a retort is a more severe heat treatment which extends the effects of heat further. While the heat treatment is designed to inactivate the spores of *Clostridium botulinum,* the build up of acid in the closed container also contributes to the conversion of chlorophyll to pheophytin, the olive-green color of canned beans.

Texture changes are caused primarily by the solubilization of pectic substances that hold the cell structure of the green beans together. The heating conditions are such that tissue softening is extensive. Softening of the texture can be somewhat prevented by the addition of calcium ions that react with pectic substances and firm the texture. Further heating of the beans after the can is opened does little more to damage either color or texture.

Flavor development mechanisms in green beans are not well characterized, but the cooked green bean has a more intense flavor than the raw product. Nutrient losses during canning amount to those vitamins that are heat labile and those that leach into the liquid during heating and subsequent storage. Losses of vitamin C are substantial.

17.3.5 MAYONNAISE

Mayonnaise is a white semisolid deriving both its texture and appearance from an emulsified oil-in-water emulsion. The dispersed oil particles are homogenized to a very small particle size in order to stabilize the emulsion and develop viscosity. Key to the emulsification is the addition of egg yolk which is an excellent emulsifying ingredient because it contains phospholipids and lipoproteins. Emulsifiers prevent the undesirable creaming, flocculation, and coalescence of the oil. The phospholipids and lipoproteins of the egg yolk are dispersed around the oil droplets to lower interfacial tension and form a stable emulsion. The mayonnaise emulsion is stable unless heated or frozen. Heating causes denaturation of the emulsifying protein. Freezing creates ice crystals which, upon thawing, form pools of water and cause total separation of the oil and water phases.

17.3.6 FRYING POTATO CHIPS

The reactions during frying of potato chips include extensive dehydration of the potato tissue and uptake of fat to replace the lost water. Color, flavor, and texture development also occur during heating. Potato tissue is about 78% water and less than 1% fat. Potato chips are about 1% water and have about 40% fat. The reversal in fat and water composition takes place as the high temperature oil causes rapid moisture loss, allowing frying oil to fill the void left by the escaping steam.

The light golden brown color of potato chips is a result of Maillard browning. The sugar level in potato tissue is dependent on the storage conditions of the potato. When held at low temperatures, potatoes reversibly accumulate sugars and when held at warmer temperatures, the sugars are converted to starch. The reducing sugar content must therefore be controlled

by storage temperature in order to get an appropriate and uniform amount of browning. Potatoes are low in protein but have a significant amount of free amino acids which contribute to the Maillard reaction. Care must also be taken to limit air exposure of sliced potatoes for long periods of time prior to heating. Exposure would result in enzymatic browning which is an unacceptable color in the finished product.

Potato chips are then packaged with a nitrogen gas flush in an opaque container to minimize lipid oxidation. Even then, the product will usually lose its freshness after several months.

17.3.7 BREAKFAST CEREAL

The manufacture of a breakfast cereal involves texture, flavor, and color changes (Fast and Caldwell, 1990). Several different processes can be used but the chemistry of the reactions is much the same. The cereal flour is first cooked to gelatinize the starch. At this point the proteins also become denatured and relatively nonfunctional. This is why breakfast cereals can be made with various sources of grain without much consideration whether the proteins are able to form a structure.

After cooking, the cereal is flaked or puffed to give shape and texture. Extrusion can be considered a combination of the cooking and puffing steps because the extruder is heated and upon exiting there is a pressure drop, water flashes off, and the shape is formed. Sugars, both reducing and nonreducing, can be part of the cereal formula to improve sweetness. After flaking, puffing, or extruding, the product is dried and then toasted to develop flavor and color via the Maillard reaction. Sugar coating after toasting may be used as a barrier to moisture uptake during storage. If the cereal is fortified with vitamins and if antioxidants are added, they are usually sprayed on the product after the heat treatment. To add them earlier in the process would subject them to high temperatures and partial chemical degradation.

The final moisture content of the cereal is controlled so as to maintain the crisp texture and yet not so dry that lipid oxidation will be strongly favored. As it is, most cereals will lose texture due to moisture uptake and lose flavor due to oxidation. Shelf-life is usually between 6 and 12 months.

17.3.8 SHORTENED CAKE

A shortened cake batter is complex both physically and chemically. The flour, sugar, fat, salt, leavening, and eggs are mixed with water or milk to form a batter which is a sol, a foam, a solution and an emulsion (Charley, 1982). Surfactants such as monoglycerides and egg yolk stabilize the emulsion of oil (or shortening) in water. Various thickening agents such as gums stabilize the emulsion as well as the foam. The foam is formed by mixing air bubbles into the batter. Carbon dioxide released by the chemical leavening system during mixing also contributes to the foam formation. Egg whites stabilize the foam.

Although there is significant mixing of the flour proteins, gluten does not develop to any great extent because of the high water and fat content and low protein concentration. The fat and sugar ingredients tenderize the cake by minimizing the amount of gluten that can form.

During heating, more carbon dioxide produced by the chemical leavening is released to increase the size of the gas bubbles and increase the volume of the cake. Starch gelatinization is extensive and the structure of the cake is developed by the uptake of water during this process. The wheat and egg proteins heat denature to further contribute to the structure. The crust of the cake will turn golden brown due more to sugar carmelization than Maillard browning. Flavor development during baking is not extensive and some flavoring ingredients such as vanilla, may be partially lost during the heating process. With storage, the cake will become stale (tougher) because of starch reassociation.

GLOSSARY

Colloidal dispersion: One phase (gas, liquid, or solid) dispersed in another phase. Gels, foams, and emulsions are colloidal dispersions.

Gel: A semisolid structure where polymers such as pectin, starch, or gelatin have trapped large amounts of water.

Glass transition: The shift of food polymers such as starch and proteins between a glassy and a rubbery texture state. This shift is caused by changing temperature or water content.

Lipid oxidation: The reaction of double bonds in lipids with oxygen resulting in the formation of off flavors usually during storage.

Maillard browning: The reaction of proteins with certain sugars to cause the formation of thermally induced flavors and brown color.

Protein denaturation: An irreversible change in the spacial arrangement of a native protein molecule which results in altered chemical and physical protein properties.

Starch gelatinization: The irreversible heat-induced change in a starch granule characterized by water uptake, swelling, and viscosity increases.

Water activity: The partial pressure of water in a food divided by the partial pressure of pure water under the same conditions. It is measured by a hygrometer and has a scale of 0 to 1.

NOMENCLATURE

a_w Water activity defined as the partial pressure of water in a food divided by the partial pressure of pure water under the same conditions.

cis   A carbon-carbon double bond where the hydrogen atoms are on the same side of carbon chain. In nature, fatty acids occur in the cis form.

DE   Dextrose equivalent; a measurement of the degree of conversion of starch to smaller glucose chains. On a scale of 0 to 100, a high DE means more extensively degraded with properties more similar to glucose and a low DE means less degraded and more starch-like.

T_g Glass transition temperature; for polymers that exhibit glassy and rubbery states, above this temperature the polymer is in the rubber state and below this temperature it is in the glassy state.

trans   A carbon-carbon bond where the hydrogen atoms are on opposite sides of the carbon chain. *trans* Fatty acids are not usually found in nature but are converted from *cis* double bonds as a byproduct of the hydrogenation process.

FURTHER INFORMATION

BOOKS

A book that emphasizes chemical structures and reactions in foods is *Food Chemistry* by H.-D. Belitz and W. Grosch, Springer-Verlag, 1987.

A reference book that emphasizes the physical chemistry part of food science is *Food Chemistry,* edited by O. Fennema, Marcel Dekker, New York, 1985.

A reference that combines processing and food chemistry is *Food Science*, fifth edition, by N. Potter and J. Hotchkiss, Chapman and Hall, 1995.

ASSOCIATIONS

The American Association of Cereal Chemists (AACC) is a professional scientific organization headquartered in St. Paul, MN (phone 612-454-7250). AACC publishes the scholarly journal *Cereal Chemistry and Cereal Foods World*. AACC sponsors short courses, publishes books in cereal and food science, and sponsors an Annual Meeting. There is an Engineering and Processing Division for those members interested in the food engineering discipline.

The American Chemical Society (ACS) is a professional scientific organization headquartered in Washington, D.C. (phone 202-872-4600). ACS publishes numerous scientific journals and *Chemical & Engineering News* magazine. ACS sponsors two national meetings annually and has a Division of Agricultural and Food Chemistry.

The Institute of Food Technologists (IFT) is a professional scientific organization headquartered in Chicago, IL (phone 312-782-8424). IFT publishes the *Journal of Food Science* and *Food Technology* magazine. It sponsors an Annual Meeting and Expo and has a Food Engineering Division.

REFERENCES

Belitz, H.-D. and Grosch, W., 1987, *Food Chemistry,* Springer-Verlag, 201–256.

Charley, H., 1982, *Food Science,* 2nd ed., Macmillan, New York, 252–371.

Eliasson, A.-C. and Larsson, K., 1993, *Cereals in Breadmaking: A Molecular Colloidal Approach,* Marcel Dekker, New York, 261–361.

Fast, R.B. and Caldwell, E.F., 1990, *Breakfast Cereals and How They Are Made,* American Association of Cereal Chemists, St. Paul, MN, 15–42.

Fellows, P.J., 1988, *Food Processing Technology Principles and Practice,* Ellis Horwood, 1985, 221–235.

Fennema, O.R., 1985, *Food Chemistry,* Marcel Dekker, New York, 24–237.

Finot, P.A., Aeschbacher, H.U., Hurrell, R.F., and Liardon, R., 1990, *The Maillard Reaction in Food Processing, Human Nutrition and Physiology,* Birhauser-Verlag, 19–40.

Girand, J.-P., 1992, *Technology of Meat Products,* Ellis Horwood, 206–262.

Hoseney, R.C., 1994, *Principles of Cereal Science and Technology,* American Association of Cereal Chemists, St. Paul, MN, 47–48, 301–333.

Labuza, T.P., 1971, *Proceedings SOS/70 Third International Congress of Food Science and Technology,* Institute of Food Technologists, Chicago, 633.

Larsson, K. and Friberg, S., 1990, *Food Emulsions,* 2nd ed., Marcel Dekker, New York, 1–40.

Mulvaney, S.J., 1994, Personal communication.

Pomeranz, Y., 1988, *Wheat Chemistry and Technology,* 3rd ed., (American Association of Cereal Chemists, St. Paul, MN, 131–201.

Potter, N.N., 1986, *Food Science,* 4th ed., AVI, Van Nostrand Reinhold, Westport, CT, 320–325.

Price, J.F. and Schweigert, B.S., 1978, *The Science of Meat and Meat Products,* Food and Nutrition Press, 435-512.

Rao, M.A. and Steffe, J.F., 1992, *Viscoelastic Properties of Food,* Elsevier, 335–349.

Reineccius, G.A., *Source Book of Flavors,* 2nd ed., Chapman & Hall.

Schwatzberg, H.G. and Hartel, R.W., 1992, *Physical Chemistry of Foods,* Marcel Dekker, New York, 263–306.

Slade, L. and Levine, H., 1991, Beyond water activity: recent advances based on an alternative approach to the assessment of food quality and safety, *CRC Crit. Rev. Food Sci. Nutr.,* 30(2,3):115–360.

USDA, Human Nutrition Information Service, Agriculture Handbook 8, U.S. Department of Agriculture, Washington, DC.

Walstra, P. and Jenness, R., 1984, *Dairy Chemistry and Physics,* John Wiley, New York, 211–228.